The Atlas of Chick Development

Third Edition

Ruth Bellairs and **Mark Osmond**

Department of Cell and Developmental Biology,
University College London, UK

ELSEVIER

Amsterdam • Boston • Heidelberg • London • New York • Oxford
Paris • San Diego • San Francisco • Singapore • Sydney • Tokyo

Academic Press is an Imprint of Elsevier

Academic Press is an imprint of Elsevier
The Boulevard, Langford Lane, Kidlington, Oxford, OX5 1GB, UK
225 Wyman Street, Waltham, MA 02451, USA

Copyright © 2014, 2005, 1998 Elsevier Ltd. All rights reserved.

No part of this publication may be reproduced or transmitted in any form or by any means, electronic or mechanical, including photocopying, recording, or any information storage and retrieval system, without permission in writing from the publisher. Details on how to seek permission, further information about the Publisher's permissions policies and our arrangement with organizations such as the Copyright Clearance Center and the Copyright Licensing Agency, can be found at our website: www.elsevier.com/permissions

This book and the individual contributions contained in it are protected under copyright by the Publisher (other than as may be noted herein).

Notices
Knowledge and best practice in this field are constantly changing. As new research and experience broaden our understanding, changes in research methods, professional practices, or medical treatment may become necessary.

Practitioners and researchers must always rely on their own experience and knowledge in evaluating and using any information, methods, compounds, or experiments described herein. In using such information or methods they should be mindful of their own safety and the safety of others, including parties for whom they have a professional responsibility.

To the fullest extent of the law, neither the Publisher nor the authors, contributors, or editors, assume any liability for any injury and/or damage to persons or property as a matter of products liability, negligence or otherwise, or from any use or operation of any methods, products, instructions, or ideas contained in the material herein.

British Library Cataloguing in Publication Data
A catalogue record for this book is available from the British Library

Library of Congress Catalog Number
A catalogue record for this book is available from the Library of Congress

For information on all Academic Press publications visit our website at store.elsevier.com

ISBN 978-0-12-384951-9
Printed and bound in Poland

14 15 16 17 10 9 8 7 6 5 4 3 2 1

Preface to First Edition

The study of the chick embryo reaches back into antiquity but continues to this day. Indeed, the chick embryo has for long been one of the most widely used laboratory animals for both teaching and research, and the reasons are clear to see: fertilized eggs are cheap and available in large numbers all the year round; development is fast in comparison with most mammalian embryos and similar to that of the mouse, lasting a mere 21 days; perhaps more important, the physiology of the embryo is not complicated by the presence of a placenta nor, once the egg has been laid, by events taking place within the mother hen; the genetics are well known, both for the normal embryo and for many mutant forms; and lastly, being an amniote, the chick's development resembles that of a mammal in its broad outline. For these reasons it has found favour in many molecular biological and biochemical laboratories.

There has long been a need for an atlas of chick development, especially since a knowledge of developmental anatomy is less general in the scientific population than in former days. Most of the available textbooks of embryology pay little attention to stages of the chick embryo later than day 3, whilst the detailed accounts of Lillie (1952) and Romanoff (1960) give few illustrations of sectioned material.

In this atlas, we have provided labelled photographs of sections up to day 13, almost two-thirds of the incubation period. By this time, the major significant events have already taken place and the embryo has become so large that further sections through the whole body are inappropriate. In addition to the photographs, we have thought it valuable to include text on the development of the different systems, since many users of the book will be coming to the chick embryo for the first time and will probably be more familar with mammalian embryos. Not all the structures mentioned in the text can be found in the plates selected for this book, nor are all the structures that are illustrated discussed in the text. The plates follow a chronological sequence of sections through whole embryos whilst the text is based on the anatomical development of different organ systems. References to the plates made in the text are, therefore, not necessarily in sequential order. In identifying the structures in the later stages (days 9–13) we have had recourse to works on the anatomy of the adult fowl, particularly Ede (1964), King and McLelland (1979) and Baumel *et al.* (1993). Throughout this book we have used the Normal Table of Hamburger and Hamilton (1951) (see Appendix II) to indicate the developmental stage of an embryo during the first 3 days of incubation (i.e. up to stage 18), but have considered it more convenient to describe the older embryos in terms of days of incubation. We have tried to be consistent in terminology, and where possible have favoured the anglicized rather than the latinized versions but, when in doubt, have followed the guidelines in Baumel *et al.* (1993).

We owe a particular debt of gratitude to Professor M. Kaufmann, who not only helped with his valuable advice on the preparation of the book, but generously gave us an essential supply of black and white label lines, otherwise unobtainable, to Dr. Jeremy Cook, who photographed the alizarin preparations, and to A.J. Lee, who prepared many of the text figures. We are deeply grateful to other colleagues and friends who have most kindly read through sections of the book: Dave Becker, Ann Burgess, Donald Ede, Marjorie England, Jay Lash, Pamela Lear, Paul Maderson, Drew Noden, Esmond Sanders and Willie Vorster. Their comments have helped us greatly, but we alone can be held responsible for any errors that may still be present.

We wish to acknowledge the generosity of the Leverhulme Trust, who provided a grant to R.B. to enable the expenses of microscopy and photography to be met. We would also like to thank the authors and publishers who have kindly given permission for reproduction of certain text figures.

Preface to Second Edition

In the second edition we have supplemented all sections of the original version. The text, as before, does not claim to give an all-embracing account of the development of the chick embryo, but to provide an outline of the more important aspects. Some of these, such as the development of the coelomic cavities, have not attracted attention in recent years so that there has been little to add to the first edition. By contrast, others, such as the process of neurulation or the segmentation of somites, have provoked such extensive modern programmes of research that we have had to be more selective in our references than we would have liked. In mitigation, we can only plead that the text is intended as an introduction to the chick embryo and not as a total review of every known aspect of its development.

The number of plates has been increased, largely by the inclusion of many scanning electron micrographs. Some of the new plates have been generously supplied by other authors (the source duly acknowledged in each case) to whom we are most grateful. We are indebted to those authors and publishers who gave permission for the reprinting of text figures and plates, or advised us on particular points of fact, all of which have enabled us to extend the scope of the atlas. We are especially grateful to M. Bakst, M. Bancroft, A. Carretero, V.G. Djonov, D.A. Ede, H. Eyal-Giladi, R. Hirakow, T. Hiruma, M. Jacob, S. Matsuda, J. Ruberte, E.J. Sanders, C. Tickle, D.J. Wilson and G. Wishart. In addition, we thank those colleagues and friends who have given their time to help and advise us on technical aspects of the work, especially Alan Boyde, Claudio Stern and Ian Todd. We are grateful to the Samuel Sharpe Foundation for a grant to help in the preparation of the book.

Preface to Third Edition

Since the last edition of this book was published, there has been a great increase in our knowledge of development of the chick embryo. Molecular biologists continue to provide ever better insights into the events involved in the differentiation of organs and tissues, and the possibilities have been greatly enhanced since the entire genetic sequence of the chick became available. All of this has attracted many investigators, some of whom have little basic knowledge of morphogenesis. Our aim, as before, has been to provide a picture of the changing events in the chick embryo during its formation.

We have retained the same layout in this book as previously, though the main sections have been expanded and, hopefully, improved. The first and smaller part, the text, is intended to provide a background to some of the more critical events in chick development. We do not attempt a complete coverage of all the literature but, where possible, refer the reader to the most important reviews on the subject. In such a rapidly moving field, those with specialist knowledge may regret the absence of specific features but will, we hope, realise the impossibility of covering every aspect.

As in previous editions, the major part of the book is devoted to labelled plates illustrating the structure of the chick embryo in a sequence of stages up to 13 days of incubation, by which time all the major tissues and organs are in place. In this edition, we have included several important stages that were absent previously, whilst some of the original specimens have been rephotographed to provide more detail. Where appropriate, we have supplemented existing plates with enlargements of regions of special interest or complexity. In addition, the number of coloured images has been increased.

Once again we are indebted to colleagues who have helped us in various ways. At University College London, Claudio Stern and members of his laboratory guided us through preparation of much of the new material, whilst Tim Arnett expertly photographed some of the larger sections, and Susan Evans kindly checked the labelling of certain structures. Jeremy Cook helped us recover essential image files from the previous editions, which were thought to be lost forever. At the Technical University of Dresden, Hans Epperlein and his colleagues Yuka Taniguchi, Thomas Kurthe, Susanne Weiche and Anja Menge prepared frozen, sectioned material. Monika Jacob from the University of Bochum helped with the presentation of *Plate 52*. Ian Lindsley gave us invaluable advice on the use of Photoshop, Emma St. Joseph sorted out computer problems and Heather Coltman advised on aspects of photography. All these colleagues and friends gave generously of their time and expertise, and we greatly appreciate their kindness. Nevertheless, such faults as may remain must be attributed to ourselves only.

We have attempted to contact all authors of images that are new to this edition, but have not always been successful. We apologise for this and also regret that we have failed to track down the copyright holder of *Plate 59b*, despite extensive searches. Acknowledgements of permission granted for the use of copyright material are given where appropriate.

We acknowledge the generosity of the Samuel Sharpe Foundation for a grant which smoothed our path financially during the preparation of the book.

Downloaded from Vet-eBooks.com

Note on Plates

All but a few of the embryos illustrated in this atlas are staged according to the Table of Hamburger and Hamilton (Appendix II), the exception being the very early embryos in eggs which have yet to be laid (see Appendix I).

There are three main types of photographic plates: light micrographs showing whole embryos; scanning electron micrographs demonstrating surface or internal features, usually at higher magnifications; and light micrographs of histological sections through embryos of different stages.

The diagrams accompanying many of the plates showing sectioned material provide an indication of the level and angle at which the sections are taken through the whole embryo, but do not necessarily include all the structures shown in the photographs. Sections through embryos usually pass in either the transverse plane, or longitudinally (sagittal or coronal planes). In transverse sections through the embryo after the head has become bent ventral to the body (cervical flexure), the dorsal side of the head lies towards the bottom of the page, and the ventral side towards the top. As the series of sections progresses into the neck and trunk regions, the dorsal side of the embryo lies towards the top of the page (e.g. *Plates 126 and 127*). In embryos that have already developed flexures (see p. 45) the transverse sections may give way to longitudinal ones in the curved region (e.g. *Plates 144 and 145*).

Plates 230–232 are photographs of whole embryos stained with alizarin red and alcian blue to show skeletal development.

Downloaded from Vet-eBooks.com

Glossary

Achondroplasia several mutant types of dwarfism in which ossification of bones is premature, reducing growth, e.g. *nanomelia* in birds (Greek: *a* = not: *chondro* = cartilage; *plasia* = plastic).

Acrosome vesicular structure at the anterior end of the sperm containing hydrolytic enzymes (Greek: *akron* = extremity, top).

Activation of the egg the stimulation of an egg cell, normally by fusion with a sperm, resulting in the onset of development (Latin: *activus* = active).

Activation of the sperm the acquisition of motility by a sperm.

Agenesis failure of part of the body to develop (Greek: *a* = not; *genesis* = to come into being).

Air space the space between the two shell membranes at the blunt end of the egg. The chick pushes its beak into this space shortly before hatching and takes its first breath of air.

Albumen the egg-white of a bird's egg (Latin: *albus* = white).

Allantoic stalk the base of the allantois, which connects it to the hindgut.

Allantois sac-like outgrowth from the hindgut consisting of endoderm covered with **splanchnic mesoderm**. It becomes highly vascularized and fuses with the **chorion** (*see* **Chorioallantois**). Excretory products are stored in its lumen (Greek: *allas* = sausage; *eidos* = form). N.B.: the chick allantois is balloon-like, not sausage-shaped.

Amniocardiac vesicle bilaterally situated spaces forming in the mesoderm on either side of the head process. The dorsal wall of each cavity is composed of ectoderm and somatic mesoderm and gives rise to the **amnion**. The cavities become continuous medially with the cardiac cavity (becoming the pericardial coelum) and with the coelomic cavity laterally.

Amnion the sac that envelops the embryo from about 3 days of incubation (Greek: *amnos* = a lamb).

Amniotes the three classes of truly terrestrial vertebrates, reptiles, birds and mammals, all of which possess a true **amnion**.

Amniotic fluid the proteinaceous fluid contained within the **amnion** and whose main function is to prevent dehydration and adhesions between the limbs and other regions of the body prior to cornification of the epidermis.

Amniotic folds the folds of ectoderm, together with adherent somatic mesoderm, which fuse with one another to form the **amnion** and **chorion**.

Angiogenesis development of certain parts of the vascular system (e.g. in the area vasculosa) by the formation of **blood islands**, which then join together by sprouting (but *see also* **Vasculogenesis**) (Greek: *angeion* = vessel; *genesis* = generation, development).

Animal pole the uppermost surface of the fertilized egg, as opposed to the vegetal pole, the lowermost side.

Anlagen (German) *see* **Primordium**.

Anterior **cranial**, **rostral** towards the head end (Latin: *ante* = in front of).

Anterior intestinal portal the opening of the foregut in the early embryo into the lumen of the

Downloaded from Vet-eBooks.com

yolk sac (Latin: *ante* = before; *intus* = within; *porta* = door).

Anterior necrotic zone (ANZ) a patch of dead cells that appears on the anterior surface of the limb bud at stage 22 (about 3.5–4 days) (Latin: *ante* = before; Greek: *nekros* = dead body).

Anterior neuropore the gap left between the unfused region of the neural folds at their most anterior end (*see Plate 18*). This pore becomes lost when the neural folds fuse at about stage 11 (*see also* **Posterior neuropore**).

Apical ectodermal ridge the thickened epithelium at the tip of a limb bud, which is essential for limb development (*see Plate 30*).

Apoptosis *see* **Programmed cell death** (Latin: *ap* = before; Greek: *ptosis* from *piptein* = to fall).

Area centralis the central area of a bird's blastoderm before the establishment of the area pellucida and area opaca.

Area opaca the peripheral region of a young blastoderm, encircling the **area pellucida**. When removed from the yolk mass and viewed by transmitted light, the tissue appears opaque because of the large amount of intracellular yolk droplets.

Area pellucida the central area of a young blastoderm, which possesses little intracellular yolk and is therefore relatively transparent compared with the **area opaca**.

Area vasculosa the proximal part of the **area opaca** after it has become vascularized.

Area vitellina the distal part of the **area opaca** that remains unvascularized.

Atresia the reduction or elimination of the lumen of an organ, or the failure of a duct to canalize (Greek: *a* = not; *tresio* = perforate, passage).

Atrio-ventricular canal the constriction between the initial atrium and ventricle in the developing heart, which becomes divided into left and right sides by the growth of the atrio-ventricular cushions (Latin: *atrium* = vestibule; *ventriculus* = small belly; *canalis* = channel).

Atrophy the wasting away of an organ or tissue. Although the term implies that this results from a lack of sufficient nourishment, this is not necessarily the case (Greek: *a* = not, *trophe* = food).

Auditory (otic) vesicle *see* **Otic vesicle** (Latin: *auditus* = *hearing*).

Autopodium the distal, flattened end of a limb bud that will give rise to a foot or hand (Greek: *autos* = self; *podium* = foot).

Axial mesoderm mesoderm lying in the midline (notochord) or immediately on either side of it (somitic mesoderm), which will take part in the formation of the axial structures, i.e. tissues arranged along the anterior–posterior axis of the body.

Axis in a bilaterally symmetrical embryo there are three body axes, antero-posterior (head–tail, cranio-caudal), dorso-ventral (back–belly) and left–right (Greek: *axis* = axis).

Balbiani body a region of the early oocyte rich in Golgi apparatus and mitochondria.

Bilaminar embryo a blastoderm consisting of two layers only, **epiblast** and a lower layer, the **hypoblast**.

Blastoderm, blastodisc, germinal disc, embryonic disc the flattened disc of cells that forms during cleavage in the early embryo and persists until the end of gastrulation. By the time of laying two major regions are visible, the centrally situated **area pellucida** and the peripherally located **area opaca** (Greek: *blastos* = bud; *derma* = skin).

Blastodisc *see* **Blastoderm**.

Blastomeres cleavage stage cells, each completely enclosed by a cell membrane (*see also* **Open cells**) (Greek: *blastos* = bud; *meros* = part).

Blastula an embryo during cleavage (*see also* **Blastoderm**).

Blood islands isolated clusters of mesoderm cells in the **area vasculosa** (developing yolk sac), each consisting of a vesicle of endothelial cells surrounding the earliest red blood corpuscles.

Body folds head, lateral and tail folds that raise the embryo above, and eventually separate it from, the extra-embryonic region of the blastoderm.

Downloaded from Vet-eBooks.com

Bucco-pharyngeal membrane, oral plate, stomatodaeal plate membrane formed by fused ectoderm of the mouth (buccal cavity) and the most anterior part of the foregut endoderm. This becomes broken down at about stage 30, which results in the mouth and pharynx coming into communication (Latin: *bucca* = cheek; *oris* = mouth; Greek: *stoma* = mouth).

Candling technique for determining whether an incubated hen's egg contains a developing embryo. A bright light is shone through an egg of at least 9 days incubation, and the embryo can be seen as a dark mass.

Cell cycle the sequence of events through which a mitotic cell passes from its own formation until its division into two new cells.

Cell lineage the history of a differentiated cell, with an emphasis on the cell types of its forebears.

Chalaza one of the two spring-like structures projecting from the equatorial region of the vitelline membrane of the laid egg. The chalazae are thought to act as 'balancers', helping the yolk to float in the albumen (Greek: *chalaza* = lump).

Chimera an organism derived from two genetically different individuals other than by fertilization, e.g. by **xenoplastic grafting** (Latin from Greek: *chimaira* = she goat).

Chondrogenesis the process of cartilage formation (Greek: *chondros* = cartilage).

Chorioallantois, allantochorion the composite membrane formed by the fusion of the **allantois** with the **chorion**. Pressed beneath the shell membranes, it acts like a lung, exchanging oxygen and carbon dioxide through the pores in the shell.

Chorion (serosa) an extra-embryonic membrane formed, together with the **amnion,** from **ectoderm** and **somatic mesoderm**. After separating from the **amnion**, the chorion comes to lie close beneath the shell membranes and fuses with the **allantois** to form the **chorioallantois** (Greek: *chorion* = enclosed space).

Cleavage the stage of development, after fertilization, during which many cells are formed by repeated cell division (German: *Kleben* = to adhere).

Cleidoic egg the type of egg typical of birds and reptiles, possessing an almost impervious shell (Greek: *kleidoun* = to lock).

Cloacal bursa, bursa of Fabricius a diverticulum on the dorsal side of the cloaca (Latin: *bursa* = purse).

Coelom the space between the two layers of lateral plate mesoderm (**somatic and splanchnic**). The internal coelom becomes the body cavity of the embryo.

Commitment (also known as Determination) a state of commitment (determination) is reached when a cell is no longer capable of changing its developmental path (i.e. no longer capable of **regulation**).

Compaction the process by which a group of loosely associated cells becomes more compact, mainly as the result of increased cell adhesion. An example is the compaction of mesoderm cells to form a **somite**.

Congenital anomaly an anomaly present in the individual from (and probably before) hatching (Latin: *con* = with; *gignere, genitum* = to beget).

Coturnix coturnix japonica the Japanese quail.

Cranial end head end, anterior end (Greek: *cranium* = skull).

Creeper fowl a mutant fowl with short limbs, a form of **achondroplasia**, which is lethal in the homozygous state.

Cuverian veins another name for the Common Cardinal veins.

Cytodifferentiation the development of specialized structures and functions in embryonic cells.

Delamination the separation of a primordial layer of cells into two layers by a process of cell migration (Latin: *laminatus* = plated).

Dermamyotome, dermomyotome the dorsolateral side of a somite, which will contribute to the dermis **(dermatome)** and muscle **(myotome)** (Greek: *derma* = skin; *myos* = muscle).

Downloaded from Vet-eBooks.com

Dermis the deeper layer of the skin, lying beneath the **epidermis** (Greek: *derma* = skin).

Determination the process by which a cell or tissue becomes determined **(committed)** to follow a specific line of development rather than any other.

Developmental anatomy the anatomical changes occurring during development.

Differential gene expression *see* **Gene expression**.

Differentiation the increasing complexity of the developing tissues in an embryo. Cells that are initially undifferentiated gradually acquire the molecular and histological characteristics of specialized cells.

Diploid possessing the full complement of chromosomes as found in a somatic (body) cell (*see* **Haploid**).

Distal that part of an organ or tissue lying furthest from the midline (*see also* **Proximal**).

Diverticulum a blind-ended extension from an organ, e.g. the caecum (Latin: *diverticulum* = byway).

Dorsal the back aspect of the body (Latin: *dorsum* = back).

Dorsal mesentery the mesentery that suspends organs in the body cavity from the dorsal body wall. In some regions the dorsal mesentery is renamed to indicate the organ it is serving, e.g. the dorsal mesentery that suspends the heart is known as the dorsal mesocardium.

Down feathers the fluffy, earliest feathers of the newly hatched chick.

Ductus arteriosus the remnant of the right sixth aortic arch artery which connects the ventral and dorsal aortae and enables blood to bypass the lungs during embryonic development. It closes on hatching (N.B. in mammals it is formed from the left aortic arch artery).

Ductus venosus a complex series of venous channels in the embryonic liver through which blood from the yolk sac and the posterior part of the body pass before entering the posterior vena cava.

Ectoderm the outermost (upper) layer of a blastoderm (Greek: *ektos* = outside; *derma* = skin).

Ecto-mesenchyme obsolete term for the **neural crest**.

Egg tooth a protruberance on the tip of the beak used for breaking through the shell membranes and shell at hatching. It is not a true tooth and does not possess dentine and enamel.

Embryonic disc alternative term for **blastodisc/ blastoderm**.

Endoblast a term sometimes used for the lower layer of a bilaminar embryo, the equivalent of **hypoblast** (Greek: *endo* = within; *blastos* = bud).

Endoderm the lowest layer of a trilaminar embryo (Greek: *endo* = within; *derma* = skin).

Endophyll some of the earliest cells to form in the **lower layer** or **endoblast** (Greek: *endo* = within; *phyllon* = leaf).

Ependyma the epithelial layer of cells of the neural tube that surrounds the lumen.

Epiblast the upper layer of a bilaminar embryo (Greek: *epi* = on, over; *blastos* = bud).

Epiboly the flattening of an epithelial sheet of cells, and its consequent expansion. It is an integral component of the gastrulation movements.

Epithelial–mesenchymal interactions the interactions that take place between adjacent epithelia and mesenchyme tissues during some types of **embryonic induction**, e.g. in the feather bud.

Epimere the dorsal part of the myotome.

Epithelium an histological term to describe a sheet of cells, in contrast to loosely arranged cells **(mesenchyme)**. An epithelium may be of ectodermal, mesodermal or endodermal origin (Greek: *epi* = upon; *thele* = *nipple*).

Experimental embryology analysis of an embryonic process by experimental means, e.g. extirpation or transplantation of part of the embryo to investigate the effect on development.

Downloaded from Vet-eBooks.com

Extracellular material material lying between cells consisting of fibres (e.g. collagen) and glycosamino-glycans, such as hyaluronic acid.

Extra-embryonic membranes tissues formed along with the embryonic tissues. They play an essential role in supporting the embryo but do not form part of it (e.g. *see* **Allantois, Amnion, Chorion, Yolk sac**).

Fabricius, bursa of *see* **Cloacal bursa**.

Falciform ligament a remnant in the adult of the embryonic **ventral mesentery** (Latin: *falcis* = sickle).

Fate maps (prospective, presumptive fate maps) maps showing the expected developmental fate of the different regions in an early embryo where the tissues are not yet determined.

Feather buds/germs the rudiment of a developing feather formed from a localized thickening of the epidermis underlain by a concentration of cells in the **dermis**, the dermal papilla.

Feather follicle just before hatching the base of the **feather bud** sinks into a depression, the feather follicle.

Feather tract the **feather buds** form in tracts (rows), the first appearing at about 5 days of incubation.

Fibroblast connective tissue cell. Fibroblasts secrete fibronectin and pro-collagen. Confusingly, the term is used also for cells growing in **tissue culture** that have lost their specialized morphological characteristics and acquired a fibroblast-like appearance. Even cells of very different origins may be fibroblast-like and no longer distinguishable from one another, but they do not necessarily correspond in behavioural and physiological aspects to true fibroblasts. Care should therefore be taken in drawing conclusions about the behaviour of fibroblasts in culture from morphological characteristics alone (Latin: *fibra* = fibre; Greek: *blastos* = bud).

Fields, embryonic fields, individuation fields field is an imprecise and almost obsolete term introduced in the early part of the twentieth century to indicate an area of an embryo that forms a particular organ or tissue, and it included the events involved in the formation of that tissue even if these were not known. The emphasis was on the coordination of many complex processes necessary for the differentiation of that organ or tissue. The term was also used to indicate the entire area throughout which the cells were capable of forming that organ or tissue, even though this ability was suppressed over much of it. This second usage of the term was, therefore, for a larger area than the first, e.g. the limb bud normally forms from a small, well-defined area on the flank of the embryo, but if that area is extirpated, a much wider area of flank is capable of forming a limb, and this wider area was sometimes called the limb field.

Flexures a vertebrate embryo becomes curved into a C-shape during development. The following bends (flexures) are recognised (*see also Text-Figure 30*):

a. **Cervical:** the flexure of the head on the trunk at the junction of the rhombencephalon and the spinal cord.
b. **Ventral mesencephalic:** a ventral bend in the midbrain.
c. **Pontine:** a ventral bend in the region of the rhombencephalon.
d. **Telencephalic:** a further bend in the forebrain.

Floor plate a distinctive group of cells in the midline of the floor of the neural tube.

Follicle, ovarian the epithelial layer (granulosa) surrounding each oocyte in the ovary.

Foramen an aperture or hole.

Foregut in the early embryo the anterior end acquires a floor and becomes a tube that is no longer open to the yolk sac except at its posterior end. This is the embryonic foregut. Its posterior end is marked by the **anterior intestinal portal**. The distinction between the foregut and the midgut is that the former possesses a floor whereas the midgut does not. Eventually, the entire gut acquires a floor and the term foregut is then confined to the region extending from the mouth to the umbilicus.

Forelimb bud, wing bud a bulge of mesoderm covered with epithelium that will develop into a wing.

Frontal section, coronal a longitudinal section at a right angle to the sagittal plane, which includes both left and right sides of the body.

Downloaded from Vet-eBooks.com

Gamete the **haploid** male or female **germ cell** (Greek: *gameein* = to marry).

Gastrula an embryo undergoing **Gastrulation** (Latin: *gastrula* = little stomach).

Gastrulation the period, after cleavage, when the cells that will form the future embryo migrate into their appropriate positions, forming **endoderm** and **mesoderm** ready to start to **differentiate**. It results in the **bilaminar** embryo becoming **trilaminar**.

Genes the hereditary elements, formed from DNA, which pass from one generation to another (Greek: *genes* = born).

Gene expression a gene acts (expresses itself) by producing **transcripts** which lead to the formation of specific proteins. Different genes act in different regions of the body and at different times (differential gene expression).

Genetic engineering the production of a new genetic make-up by experimental means.

Genome the entire complement of genes in any cell or organism.

Genotype the genetic constitution of each cell in an organism. Not all genes are expressed in the **phenotype**.

Genital folds/urethral folds paired swellings to the right and left of the cloaca, which will form part of the external genitalia.

Genital ridge *see* **Nephrogenic ridge**.

Genital tubercle protrusion that forms at the anterior end of the genital folds and gives rise to the penis.

Germ cells the mature germ cells **(gametes)** are the ova and sperm, formed from the immature germ cells, the **oocytes** and **spermatocytes**, respectively, by the process of gametogenesis (Latin: *germen* = sprout, bud). *See also* **Primordial germ cells.**

Germ layers **ectoderm**, **mesoderm** and **endoderm**.

Germ wall the edge of a cleavage or gastrula stage embryo, which lies on the surface of a large yolk (as in a bird). The germ wall is the expanding edge of the **blastoderm**.

Germinal crescent a region in the **area opaca** at the cranial (anterior) end of the avian **blastoderm** to which the primordial germ cells migrate prior to entering the blood stream and being transferred to the developing gonad.

Germinal disc, germ anlage that part of a **blastoderm** of a yolky egg that contains the cytoplasm from which the embryo will develop.

Germinal epithelium the mesothelial layer covering the gonad of the embryo, strands of which ingress to form the primary and secondary sex cords. The **primordial germ cells** become carried into the gonad during the ingression. Formerly, it was thought that cells of the germinal epithelium itself differentiated into germ cells, hence the terminology, but this idea is no longer accepted.

Germinal vesicle the enlarged nucleus of the **oocyte** during **prophase**.

Gonadal ridge *see* **Nephrogenic ridge**.

Granulosa ovarian **follicle** cells (Latin: *granulum* = dim. *Of granum* = grain).

Haematopoiesis the process of red blood cell formation (Greek: *haema* = blood; *poieen* = to make).

Haploid a **germ cell** possessing half of the somatic complement of chromosomes (*see* **Diploid**).

Head fold a fold in the three germ layers that forms anterior to the head process (*see* **Body folds**).

Head mesenchyme mesenchymal cells in the earliest stages of head formation. They may be of **mesodermal** or **neural crest** origin.

Head process that part of the **notochord** that is formed by cells migrating anteriorly from **Hensen's node**.

Hensen's node the anterior end of the **primitive streak**.

Heterogametic sex the sex (gender) that produces two types of gametes, as opposed to the

Downloaded from Vet-eBooks.com

homogametic sex, which produces one type. The sex of the offspring is determined by the heterogametic sex, which is the male in mammals, and the female in birds (Greek: *heteros* = other).

Heteroplastic grafting *see* **Quail**.

Hindgut the simple gut tube at the posterior end of the early embryo. It extends into the tail region as the **tail gut,** and its anterior boundary is the **posterior intestinal portal** (*see also* **Anterior intestinal portal**).

***Hox* genes** certain homeobox-containing genes important in establishing and maintaining the antero-posterior axis of the embryo.

Hypoblast the lower layer of a **bilaminar embryo** (Greek: *hypo* = under; *blastos* = bud).

Hypomere the ventro-lateral part of the somitic myotome, which gives rise to the muscles of the body wall and limbs.

Indifferent gonad the gonad prior to its **differentiation** into ovary or testis.

Induction, embryonic the interaction between two cells or tissues in which one, the inducer, affects the **differentiation** of the other.

Infundibulum (a) **primordium** of the neurohypophysis (posterior pituitary), which arises from the floor of the diencephalon; (b) the funnel-shaped opening at the cranial end of the oviduct (Latin: a funnel, from *in* = in and *funder* = to pour).

Ingression the process in bird embryos by which cells pass through the primitive **streak** to form the **endoderm** and **mesoderm** layers.

Intermediate cell mass, intermediate mesoderm the **mesoderm** lying between the **somites** and the lateral plate, which gives rise to most of the urino-genital system.

Invagination the remoulding of a region of **epithelium** so that it sinks into the substance of the embryo, forming a cavity, e.g. the **optic cup** (Latin: *in* = in; *vagina* = sheath).

In vitro tissues removed from an organism and then grown away from the body are described as being grown *in vitro* (Latin: *in* = in; *vitro* = glass), or in culture (e.g. **tissue culture**).

In vivo in living tissues or animal (Latin: *in* = in; *vivo* = the living).

Koller's sickle (Rauber's sickle) crescentic region at the posterior end of the **area pellucida** that gives rise to the **primitive streak**.

Labile determination *see* **Specification**.

Latebra column of white yolk extending from the centre of the (yellow) yolk of a hen's egg to the periphery, just beneath the **ooplasm**.

Lateral side, away from midline (Latin: *lateris* = side).

Lateral plate mesoderm the unsegmented **mesoderm** lying lateral to the **somites** in the early embryo. The upper **(somatic)** layer and the lower **(splanchnic)** layer are separated by a **coelom**.

Lecithin a component of the yolk (Greek: *lekithos* = yolk).

Limb bud the bulge on the side of the body that is the first stage in the formation of a limb.

Lipovitellins lipoproteins forming the major component of the yolk granules (Greek: *lipos* = fat; Latin: *vitellus* = yolk).

Lower layer the ventral layer of the **bilaminar embryo**, which consists of various populations of cells (*see* **Hypoblast, Endoblast, Endophyll**).

L.S. longitudinal section; may be either **sagittal**, in which the plane of section passes from the ventral to the dorsal side, or **frontal** (**coronal**), in which the plane of section passes from left to right (Latin: *sagitta* = arrow).

Mammillary knobs projections on the inner surface of the egg shell that act as anchor points for the shell membranes (Latin: *mammilla* = diminuitive of *mamma* = breast).

Margin of overgrowth the periphery of the **blastoderm**, consisting of specialized **area opaca** cells.

Downloaded from Vet-eBooks.com

Marginal layer the major part of the wall of the neural tube in the early embryo.

Marginal sinus *see* **Sinus terminalis**.

Medial in or towards the midline, as opposed to **parietal** or **lateral**.

Medullary plate *see* **Neural plate**.

Melanocyte a cell of **neural crest** origin that produces melanin (Greek: *melas* = black; *kytos* = vessel, cell).

Mesenchyme an histological term describing cells that are irregular in shape and arrangement (as opposed to **epithelial** cells, which are regular and arranged in sheets).

Mesendoderm cells that become either **mesoderm** or **endoderm**.

Mesoderm the middle layer of a **trilaminar embryo** (Greek: *mesos* = middle; *derma* = skin).

Mesonephros the second (intermediate) kidney to develop (*see also* **Pronephros** and **Metanephros**).

Metamerism repetition of a structure several times, e.g. the paired **somites** are repeated about 50 times in the chick (Greek: *meta* = among; *merism* = repetition).

Metanephros the third and final kidney to develop (*see also* **Pronephros** and **Mesonephros**).

Midgut in the early embryo, that part of the simple gut tube that lacks a floor and is, therefore, open to the yolk sac (*see also* **Foregut** and **Hindgut**).

Morphogenesis the development of form (Greek: *morph* = form; *genesis* = birth).

Morphogens chemical substances (e.g. retinoic acid) that may be necessary for the correct development of a tissue.

Müllerian duct the developing oviduct.

Multipotentiality the ability of most cells in an early embryo to develop along many different and alternative pathways. Most multipotent cells eventually become unipotent during development, becoming restricted to development into a single cell line, though others remain as **stem cells**.

Muscle mass the early stage in the development of certain muscles.

Myogenesis muscle formation (Greek: *myos* = muscle; *genesis* = birth).

Myotome the portion of a differentiating somite, which contributes to skeletal muscle (Greek: *myos* = muscle).

Nasal (olfactory) placodes thickened patches of **epithelium** that **invaginate** to form the nasal pits (Greek: *plax* = anything flat).

Nephric duct the duct that serves the **pronephros** and, later, the **mesonephros**. It subsequently becomes the vas deferens in males.

Nephrogenic ridges the paired ridges, left and right, formed on either side of the gut, which will give rise to the kidneys and their ducts, as well as to the gonads and genital ducts. (*see also* **Urogenital ridge**).

Neural arch the dorsal part of a vertebra.

Neural crest cells initially located at the dorsal side of the neural tube that migrate to form a range of tissues.

Neural plate that portion of the **ectoderm** that will become the **neural tube**.

Neural tube the precursor of the spinal cord and most of the nervous system.

Node/primitive node *see* **Hensen's node**.

Normal Table *see* **Appendices**.

Notochord a rod of cells formed from **Hensen's node** and which lies beneath the **neural tube**. One of the few truly midline structures in the body (Greek: *notos* = back; *chorde* = a cord).

Notochordal sheath a thick band of connective tissue that wraps around the **notochord** after about stage 11.

Notoplate the **notochord** together with the base of the **neural** tube.

Downloaded from Vet-eBooks.com

Omphalo-mesenteric blood vessels *see* **Vitelline blood vessels** (Greek: *omphalos* = navel; *enteron* = gut).

Oocyte the female **germ cell** prior to **gamete** formation.

Ooplasm egg cytoplasm.

Open cells some of the earliest cells of the cleavage stage embryo are incompletely surrounded by a cell membrane and are continuous with the yolk. Ultimately, they become fully enclosed by cell membranes and are then known as **blastomeres**.

Optic cup primordium of the eye formed as an outgrowth from the forebrain.

Organiser the dominant region of the early embryo that controls the development of the body axis. The term was introduced to describe the dorsal lip of the amphibian blastopore, but is also applied to **Hensen's node** in birds.

Otic (auditory) placode thickened region of **ectoderm** that invaginates to become the otic vesicle.

Otic (auditory) vesicle primordium of the inner ear.

Otocyst *see* **Otic vesicle**.

Overgrowth, margin of the periphery of the young **blastoderm** as it expands over the yolk by **epiboly**.

Ovulation release of an ovum from the ovary.

Pander, nucleus of white disc of yolk that lies beneath the early **blastoderm** at the surface of the **latebra**.

Paracrine factors signalling molecules involved in cell–cell communication (as opposed to endocrine factors), e.g. TGFβ, FGF.

Paraxial regions immediately to either side of the midline axis (i.e. of the **notochord**). The paraxial **mesoderm** gives rise to the **somites** (Greek: *para* = beside; *axis* = axis).

Parietal the position in the body of an organ or tissue relative to the walls of the organism. This tends to be the furthest from the midline (Latin: *parietis* = wall).

Pattern formation the formation of an orderly arrangement of tissues and organs in an embryo.

Periblast an acellular region of mixed yolk and cytoplasm associated with the cleavage stage of large-yolked eggs (Greek: *peri* = around; *blastos* = bud).

Periderm a temporary layer of squamous epithelial cells covering the simple epidermis in the early stages of skin development.

Perivitelline layer *see* **Vitelline membrane**.

Pharyngeal (visceral) arches segmental region of the pharynx corresponding to gill arches of fishes. They are separated from one another by **pharyngeal pouches** internally and by **pharyngeal grooves** externally.

Pharyngeal (visceral) grooves *see* **Pharyngeal arches**.

Pharyngeal (visceral) pouches *see* **Pharyngeal arches**.

Phenotype the morphological expression of the **genotype** (Greek: *phainen* = to show).

Phosvitin a component of yolk.

Placode a thickened region of **ectoderm** that **invaginates** to form certain organs of special sense or certain cranial ganglia (Greek: *plax* = flat).

Polarity the presence in an organism of a head and tail end, and dorsal and ventral sides (Greek: *polos* = axis).

Polarizing zone the posterior region of the limb bud, which specifies position along the antero-posterior axis.

Positional information a concept of development that supposes that the **differentiation** of a cell or group of cells is largely determined by their position in the embryo.

Posterior or caudal tail end.

Downloaded from Vet-eBooks.com

Posterior intestinal portal the opening of the **hindgut** in the early embryo into the lumen of the yolk sac.

Posterior marginal zone the posterior margin of the border between the **area pellucida** and **area opaca**. Cells migrate from here to form the **primitive streak**. *See also* **Koller's sickle**.

Posterior neuropore an opening remaining at the posterior end of the neural tube in the final stages of neural tube closure. It becomes obliterated at about stage 11–12 (*see also* **Anterior neuropore**).

Prechordal mesoderm mesoderm lying anterior to the **primitive streak** and head process.

Presumptive fate *see* **Specification**.

Primitive foot plate the flattened end of a leg bud that will become the foot.

Primitive hand plate the flattened end of a wing bud that will become the avian equivalent of a hand.

Primitive node *see* **Hensen's node**.

Primitive streak the midline region of the early embryo where **ingression** of cells occurs during **gastrulation**.

Primordial germ cells precursors of the **germ cells**, proper. In birds, they arise in the early **epiblast** and later migrate to the gonad to become either **spermatocytes** or **oocytes**.

Primordium/Anlagen the rudiment of an organ, e.g. the **optic cup** is the rudiment of the eye.

Proepicardial serosa a specialized region of the heart that forms from the pericardium.

Programmed cell death death of a group of cells that occurs as a normal event in the development of certain tissues in the embryo (*see also* **Apoptosis**).

Progress zone cells at the tip of a limb that proliferate.

Proliferation increase in the mass of a tissue by mitosis.

Pronephric duct *see* **Nephric duct**.

Pronephros the first kidney to develop (*see also* **Mesonephros** and **Metanephros**).

Prophase the first phase of mitosis.

Prospective/presumptive fate the fate that can be expected for a particular tissue, but is not yet fixed **(determined)** and may still change under experimental or adverse conditions.

Proximal the part of an organ or tissue lying nearest the midline (*cf.* **Distal**).

Pyknosis shrinkage and increased staining of the nuclei in dying cells; it is, therefore, a measure of cell death (Greek: *pyknos* = dense).

Quail *Coturnix coturnix* japonica, the Japanese quail, whose nucleoli possess a distinctive appearance, which enables them to be recognized easily after **xenoplastic grafting**.

Rauber's sickle *see* **Koller's sickle**.

Regression the gradual disappearance of the **primitive streak**, from its anterior to its posterior end, as the cells **ingress** to become converted into axial tissues.

Regulation the ability of a group of cells in the early embryo to switch from developing according to their **prospective fate** (as shown in the **fate maps**) and form into different tissues.

Roof plate the mid-dorsal region of the **neural tube**.

Sagittal section a **longitudinal** section passing through the body from dorsal to ventral sides (as opposed to a **frontal** or **coronal** section) (Latin: *sagitta* = arrow).

Sclerotome that part of a **somite** that will form vertebral cartilage (Greek: *skleros* = hard).

Segmental plate the band of **paraxial mesoderm** posterior to the newly formed **somites** that will form more somites.

Segmentation the division of an initially continuous mass of tissue into segments (repeating units). **Somites** are the first segmental structures to form.

Downloaded from Vet-eBooks.com

Serial sections sections, whether **transverse** or **longitudinal**, passing systematically through an organism and mounted in correct sequence.

Sero-amniotic connections the points at which the **amniotic folds** fuse over the embryo before separating to form the **chorion** (**serosa**) and **amnion**.

Serosa *see* **Chorion**.

Shell membranes two specialized membranes lining the shell.

Sinus terminalis/marginal sinus a blood vessel that encircles the entire **area vasculosa**.

Somatic cells body cells that are not **germ cells** (Greek: *soma* = body).

Somatic mesoderm that part of the lateral plate **mesoderm** that lies beneath the **ectoderm** (*cf.* **Splanchnic mesoderm**).

Somatopleure somatic ectoderm together with the underlying somatic mesoderm.

Somites paired blocks of **mesoderm** that form on either side of the neural tube and give rise to dermis, muscle and cartilage.

Somitomere primordium of a **somite**, visible as a group of cells in the **segmental plate** that gradually become more and more adherent to one another. Best seen by scanning electron microscopy.

Specification the first stage in the **differentiation** of an organ or tissue. Formerly known as **labile determination** to emphasize that the course of future development is not completely fixed (not yet **determined**); the term 'specification' is equivalent to **presumptive fate**.

Sperm nests diverticula in the oviduct where sperm are stored awaiting the eggs to ovulate.

Spermatocyte the male **germ cell** prior to **gamete** formation.

Splanchnic mesoderm that part of the **lateral plate mesoderm** associated with **endoderm** (Greek: *splanchnic* = gut).

Splanchnopleure the composite tissue formed by **splanchnic mesoderm** and **endoderm**.

Staging *see* **Normal Tables** (Appendices I and II).

Stem cells specialized undifferentiated cells that undergo repeated mitosis but remain able to differentiate if the conditions are favourable.

Stomatodaeal plate the anterior tip of the early **foregut** where it is fused to the **ectoderm** (Greek: *stoma* = mouth).

Sub-blastodermal cavity the fluid-filled space in the yolk immediately beneath the **blastoderm**.

Sub-germinal cavity *see* ***S*ub-blastodermal cavity**.

Sub-germinal fluid fluid in the **Sub-germinal (sub-blastodermal) cavity**.

Syndrome multiple effects of a disorder.

Tail bud the remnant of **Hensen's node**, after its **regression**, which forms the rudiment of the tail.

Tail fold *see* **Body folds**.

Tail gut extension of the hindgut into the tail.

Talpid a genetic mutant of the domestic fowl, whose main characteristic is short broad limbs that superficially resemble those *of Talpa,* the European mole.

Time-lapse cinematography/videography a method of visualizing aspects of development, such as **gastrulation,** by taking a sequence of photographs of the same tissue but separated from one another by a selected interval of time. This has the effect of showing the process in a speeded-up form.

Tissue culture see ***In vitro***.

Totipotency the ability of a cell to **differentiate** into any cell type.

Trilaminar embryo a three-layered embryo possessing **ectoderm**, **mesoderm** and **endoderm**.

Urogenital ridge *see* **Nephrogenic ridge**.

Downloaded from Vet-eBooks.com

Ureteric duct also known as the metanephric duct. The future ureter.

T.S. transverse section across the embryo.

Vasculogenesis blood vessel formation (*see also* **Angiogenesis**).

Ventral belly side, as opposed to **dorsal** side.

Ventral aorta the main artery extending cranially from the heart in the early embryo.

Visceral arches *see* **Pharyngeal arches**.

Vital dyes dyes that are tolerated by living tissues with little or no toxicity.

Vitelline blood vessels blood vessels of the yolk sac (Latin: *vitellus* = yolk).

Vitelline membrane/perivitelline layer transparent elastic layer surrounding the yolk of a bird's egg.

Vitello-intestinal duct *see* **Yolk sac**.

Wolffian duct *see* **Nephric duct**.

Wolffian ridges precursors of limb buds.

Xenoplastic grafting grafting of tissues from one species to another, e.g. quail to chick (*see* **Quail**) (Greek: *xenos* = foreign; *plassein* = to mould).

Yolk granules, spheres, white all components of the egg yolk.

Yolk sac derived from the area opaca, the yolk sac absorbs yolk and transports it to the embryo via the **vitelline blood vessels** in the yolk sac stalk.

Zone of polarizing activity (ZPA) *see* **Polarizing zone**.

Zygote the cell that is formed after the fusion of the male and female **gametes**, i.e. a fertilized egg.

Downloaded from Vet-eBooks.com

Some Highlights in the History of Chick Embryology

In many ways the history of chick embryology is the history of embryology itself because the great accessibility of the chick has always made it a favourite subject to study. All the great advances and discoveries in chick development have relevance for other vertebrates, including mammals, and some have brought about dramatic changes in the fundamental understanding of development itself. There are several excellent reviews on the subject (e.g. Needham, 1934; Oppenheimer, 1955; Mayer, 1939; Horder *et al.*, 1986), and these deal with the growth in our general understanding of the processes involved, encompassing a range of species. This present account is restricted to the most significant events in the history of chick embryology.

The first clear-cut account of chick embryology was given by Hippocrates (460–377 B.C.). He is quoted by Needham as follows: 'Take 20 eggs or more and give them to 2 or 3 hens to incubate, then each day from the second onwards till the time of hatching take an egg, break it, and examine it….' This orderly and systematic approach is meaningful even today. Aristotle (382–322 B.C.), who also followed this system, appears to have been the first to dissect the chick embryo.

During succeeding centuries many others were curious enough to open partially incubated eggs and often record their findings. The seventeenth-century English physician and anatomist, William Harvey, based some of his discoveries and theories pertaining to the formation and function of the heart and circulation partly on his observations of chick development *in ovo*. He opened hens' eggs at various lengths of incubation and observed with magnifying lenses the different stages of heart formation and the commencement of beating. He also noted the formation of blood islands and their gradual incorporation into the circulation. Before this, it was generally believed that the heart and circulation were idle until hatching, or birth in the case of mammals. Harvey observed the formation of other organs in the chick embryo and also described how the yolk was used as nourishment during development.

It was not until the invention of the microscope that it became possible to acquire some understanding of what was happening in the earliest stages. The Italian, Malpighi (1628–94), using the microscope, was the first to describe the blastoderm of the chick, the neural folds and groove, the optic vesicles, the early stages of heart development and the somites (see Needham, 1934).

More descriptions of chick embryos were made during the seventeenth and eighteenth centuries, but the most valuable achievement during this period was the resolving of one of the great controversies, that of **preformation** versus **epigenesis**; this was settled primarily by reference to chick development. The preformationists thought that the entire individual was present in miniature in the egg or, alternatively, within the sperm and that it simply grew until it hatched; there was thought to be no differentiation, merely growth. The epigeneticists considered that both growth and differentiation were involved and were necessary. Today, we are all epigeneticists. The argument was settled by Caspar Friedrich Wolff (1753–94), who was born in Berlin but spent most of his research life in St. Petersburg. He not only argued philosophically against preformation, but clinched his arguments by providing two clear examples from the chick embryo. First, he pointed out that the blood vessels of the area opaca were not present from the beginning of incubation, but that they developed from blood islands that joined up together. However, sceptics argued that perhaps the blood vessels were there all the time, although not visible to the human eye. Wolff countered that by searching for a tissue

Downloaded from Vet-eBooks.com

where this argument could not hold and, once again, found an excellent example in the chick. He pointed out that the gut is formed from a flat sheet of tissue that folds into a tube, the different stages being clearly visible. This cleverly chosen example was ultimately accepted and destroyed the case for preformation, not only in the chick but in all embryos.

The first description of the germ layers (ectoderm, mesoderm and endoderm) was made in the chick by the Russian embryologist, Pander (1794–1865), who was a follower of Wolff. However, it was an Estonian, Von Baer (1792–1876) who, with meticulous analysis of many embryos and the use of the light microscope, was able to show that the three layers were not merely a feature of the chick but were universal in vertebrates. Von Baer, himself, was opposed to the misleading ideas of recapitulation, popular in the early nineteenth century, whereby the stages of development were thought to represent progressive stages of evolution. He discovered the notochord and studied the asymmetry in the chick, as well as the passage of materials from the yolk and the egg white into the embryo. Jane Oppenheimer (1955) described Von Baer as the 'most distinguished and influential of the *early nineteenth century* embryologists', and his work is said to have influenced Darwin.

The nineteenth century produced other great scientists, and among these was Roux (1850–1924), who might be described as the most influential of the *late nineteenth century* embryologists, and whose name is commemorated in the journal Wilhelm Roux's Archives. He is often called the father of experimental embryology (*Entwickelungsmechanik*). Roux realized that the answers to many of the questions that were being asked about development could be obtained only by carrying out experiments directly on the embryo. He was also the first to pose many of those questions that still fascinate us today, such as the ways in which the planes of symmetry are established in the early embryo. His introduction of the experimental approach to embryology was a great step forward, both conceptually and technically, and during the first half of the twentieth century descriptive accounts of development became superseded by the experimental approach.

The effects of various changes in the physical or chemical environment on the chick embryo were investigated and simple experiments were performed on it *in ovo.* For example, Peebles (1898) inserted small pieces of sable hair into the anterior end of the primitive streak and found that they were carried posteriorly as Hensen's node regressed. More detailed studies on the morphogenetic movements were carried out by others, using spots of vital dyes to mark different areas whose shifting positions could then be followed closely. Gräper (1929) is especially noteworthy because he introduced the technique of recording the gastrulation movements of the chick by cinematography. Experiments of this type provided evidence toward the production of the early fate maps which, although they have been refined and modified in recent years by modern techniques, nevertheless were reliable enough to provide a basis for much of the experimental work that came afterwards.

During all these centuries, the chick was not the only embryo whose basic development had been studied, and other species later proved to be easier subjects for some experimental studies. Many of these new experiments were carried out on amphibian embryos whose tissues were often easier to manipulate than those of the chick, so it is perhaps not surprising that the most famous experiment on embryos of the twentieth century was carried out on amphibians, resulting in the concept of the 'organiser' as a major controller of development (reviewed by Spemann (1938), and discussed in greater detail in Chapter 4). Inevitably, the question arose whether a similar 'organiser' existed in other animals, and especially in amniotes. Experiments of this type on early mammalian embryos were technically not possible then and, consequently, attention became refocused on the chick. However, the large yolk and the fragility of the early blastoderm made the transplanting of tissues within the chick embryo extremely difficult. It was not until Waddington (1932) developed a procedure for removing the blastoderm from the egg and growing it *in vitro,* using a modification of a culture technique devised by bacteriologists, that it became possible. This technique was later modified and greatly improved by New (1955) and has since been the basis for much of the experimental work on the early blastoderm.

From our twenty-first century perspective, the latest most significant advances in the history of the development of the chick are twofold. First, increasingly advanced imaging techniques have revolutionized the way developing tissues are visualized from the cellular to gross anatomical level, enabling details and relationships to be dramatically displayed. Second, the completion of the sequencing of the chick genome has opened up, often in combination with other new molecular techniques, novel avenues of discovery for many of the controlling events of development.

Downloaded from Vet-eBooks.com

Chapter 1

The Hen's Egg and its Formation

Birds of all species lay eggs and none is viviparous. Although this might seem to be a disadvantage, nevertheless birds have established themselves successfully in all types of terrain, due not only to their highly developed brooding behaviour and parental care, but also to the structure and composition of their eggs.

A bird's egg contains all the raw materials for the formation of the embryo apart from the oxygen, which enters through small pores in the shell. If these pores are experimentally clogged with wax, then no development occurs.

Text-Figure 1 shows the structure of an unincubated but fertilized egg of the domestic fowl. The yolk is about 2–3 cm in diameter and is enclosed by a thin transparent membrane, the vitelline membrane. The main components of the yolk are lipids and proteins, and they are not alive. The embryo itself is a tiny blob of cytoplasm that floats to the uppermost surface of the yolk, coming to lie close beneath the vitelline membrane (which is sometimes called the perivitelline layer), and is the only part which is living. The egg white or albumen lies around the yolk and is in turn enclosed by two tough shell membranes that are fused together, except at the blunt end, where they are separated by an air space that is important in hatching. The inner surface of the calcareous shell is elaborated into little projections, the mammillary knobs, and strands from the shell membranes are attached to them.

Birds' eggs vary in size, shape and surface pigmentation according to the species, though there is considerable individual variation. Even in the same strain of domestic fowl, some hens lay more elongated or more pointed eggs than others, whilst the pigment patterns of quail eggs vary greatly even within the same flock. The general morphology of the egg, however, remains the same throughout the avian species, and is related to the activities of the different regions of the reproductive tract in the hen.

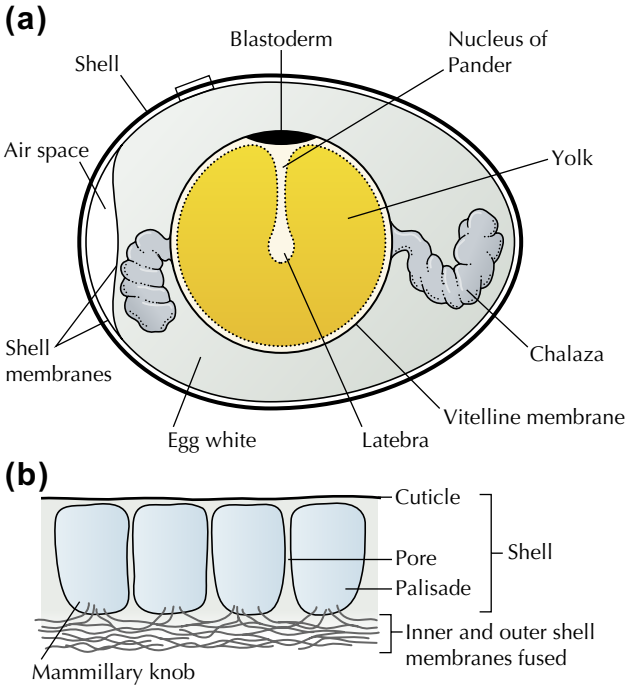

Text-Figure 1. *(a) Sagittal section through a hen's egg. The latebra and the Nucleus of Pander are regions of white yolk. The blastoderm lies over the Nucleus of Pander and below the vitelline membrane. The chalazae are balancers that support the yolk. The two shell membranes are separated by an air space at the blunt end. (b) Enlargement of the portion of the shell shown in (a). (From Bellairs (1971), with permission of Elsevier.)*

THE REPRODUCTIVE TRACT OF THE HEN

The formation of a bird's egg takes place step-by-step along the oviduct in a way that is often compared to the assembly of man-made articles along a factory belt. Although both left and right ovaries and oviducts are formed in the embryo, the right degenerate and only the left remain.

The Atlas of Chick Development. http://dx.doi.org/10.1016/B978-0-12-384951-9.00001-0
Copyright © 2014 Elsevier Ltd. All rights reserved.

Downloaded from Vet-eBooks.com

Many egg yolks are visible in the body of the laying hen, the largest being of comparable diameter to those in laid eggs (*Text-Figure 2*). Inexperienced investigators tend to assume, wrongly, that these are ovulated (and so perhaps fertilized) eggs lying along the genital tract. Normally, however, only one egg is present at a time in the oviduct, and the remainder of the yolks are still oocytes, each with its own follicle (*Plate 1a,b* and *Text-Figure 3*). The ovary of a laying hen contains many follicles, and these vary in size according to whether they yet possess any yolk or to the amount of yolk already deposited in them. The largest oocyte usually measures about 3 cm in diameter and is almost ready to ovulate.

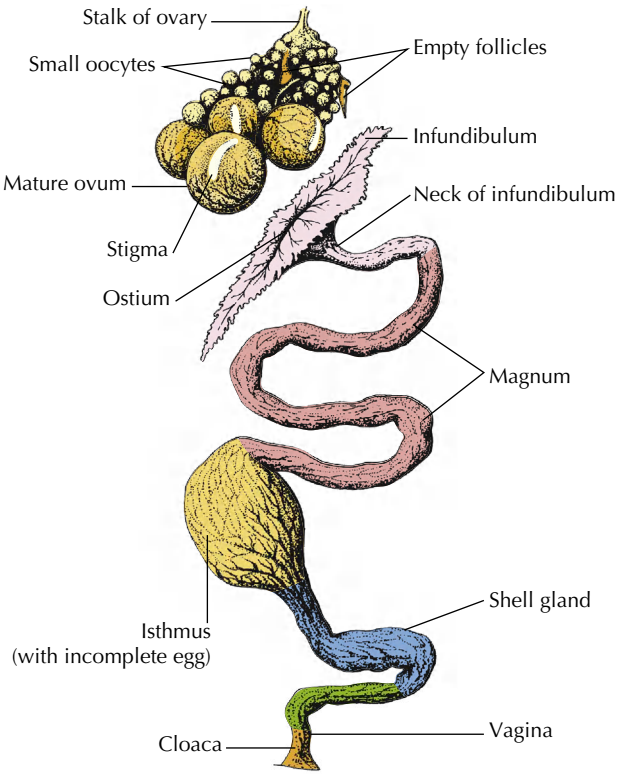

Text-Figure 2. *Ovary and left oviduct of the domestic fowl. (After Duval, 1889.)*

In a hen that has been laying regularly, several empty (discharged) follicles are visible in the ovary (*Text-Figures 2, 3*). These are the vascularised sacs that have been ruptured by the ovum during ovulation, and they may vary in diameter from about 2 cm down to 2 mm or less. The size is an indication of the time that has elapsed since ovulation took place from that particular follicle, since they become progressively smaller as they are absorbed. In a hen that has gone 'off-lay', no large oocytes are visible, though small ones are still plentiful and measure up to about 5 mm in diameter.

The raw materials from which yolk is manufactured are formed in the liver of the laying hen and pass from there in the blood plasma to the ovary. Large quantities of lipids and proteins are present in the blood of the laying hen, and these closely resemble and are often identical with similar substances in the yolk. They are not present in the blood plasma of male or juvenile birds, nor of hens that have gone 'off-lay'. Labelled serum proteins injected into the blood stream of laying hens have been subsequently found in the yolk.

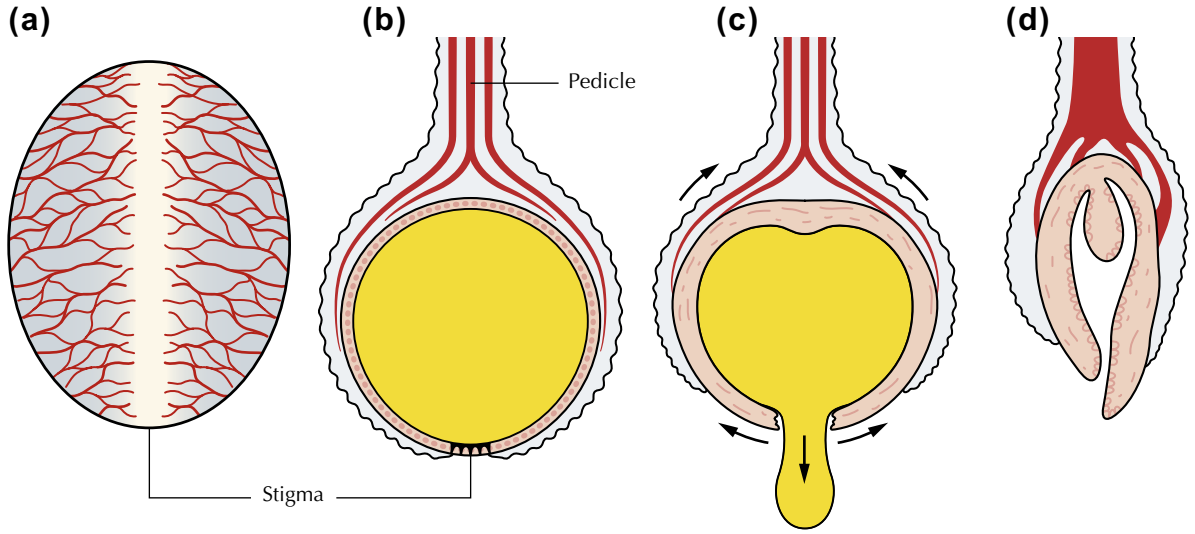

Text-Figure 3. *(a) Distal surface of an oocyte shortly before ovulation. The follicle tissue is highly vascularised except in a narrow band, the stigma, along which the follicle will split at ovulation. (b) Section passing through an oocyte at right angles to (a). It is suspended from the ovary by the pedicle. (c) Section showing the same region as (b) with the oocyte/ovum undergoing ovulation. (d) Discharged follicle.*

Downloaded from Vet-eBooks.com

The substances that pass through the capsule of follicle cells into the oocyte are the definitive proteins and lipids from which the yolk is formed; there is no real synthesis of yolk in the oocyte, but merely a rearrangement of materials. The yolk precursors are probably taken into the oocytes in the many coated vesicles which lie beneath the surface of the oocyte and possess receptors for the lipoproteins (Shen *et al.*, 1993). The smallest oocytes are probably incapable of utilizing these materials.

When the oocyte is about 2.5 mm in diameter, the inner layer of the vitelline membrane (see below) becomes laid down, but the outer layer is not formed until after ovulation. By the time the oocyte is about 2.5 cm in diameter, the inner layer has reached its maximum thickness of about 2.5 µm. In the final stage of oocyte growth, large vacuoles appear beneath its cell membrane (oolemma), and the number of villi at the surface decreases. When the oocyte has become about 3 mm in diameter, yolk spheres become visible.

THE OVIDUCT

The regions of the oviduct are shown in *Text-Figure 2*. The most cranial region, the infundibulum, consists of a funnel about 9 cm wide at its opening immediately posterior to the ovary, leading into a narrower, tubular region. The magnum follows and, at about 30 cm, is the longest part of the oviduct. The isthmus is about 10 cm long and is succeeded by the shell gland (which, confusingly, is known also as the uterus) and the vagina, which leads into the cloaca. Each region is modified for a particular secretory function, which is best understood by following the egg down the oviduct. For an account of the anatomy, histology and fine structure of the avian oviduct, see Bakst (1998). During this period, the embryo embarks on the earliest stages of development. The events are indicated in *Table 1*.

Fertilization takes place as the egg is ovulated, in the funnel of the infundibulum, which contains no glandular tissue. It occurs before the laying down of the outer layer of the vitelline membrane, which happens at the junction of the funnel and tubular regions. The 'thick' albumen that immediately surrounds the yolk is secreted by the tubular region of the infundibulum, and immediately blocks further sperm contact with the ovum (Wishart and Horrocks, 2000). The 'thin', watery, albumen is added in the magnum, which is rich in a mucus-secreting epithelium. The shell membranes are deposited in the isthmus; they are composed mainly of type X collagen (Sparks, 2009).

Table 1 Passage of the egg down the oviduct

Oviduct	Time spent	Event
Ovary	0 h	Ovulation
Infundibulum	15 min	Fertilization/thin albumen
Magnum	3 h	Albumen added
Isthmus	15 min	Shell membranes added
Shell gland	20 h	Shell added
Vagina	Negligible	Egg laid

Shortly after the egg enters the shell gland, fluid passes into the albumen so that it expands to its full size. This 'plumping' fluid, which is derived from the blood of the laying hen, carries with it the inorganic ions for the shell and deposits them on the outer side of the shell membrane.

The shell gland is about 5 cm long and highly muscular. Calcium ions pass from the blood of the hen to the shell membranes where they form columns of calcite (i.e. crystals of calcium carbonate) separated by pores *(Text-Figure 1B*) which will later allow the exchange of gases between the embryo and the outside environment. A small amount of organic material is secreted at the same time and forms a web that plays a role in the calcification. During its sojourn in the shell gland, the egg slowly rotates; this probably helps to ensure an even distribution of the calcium ions, but is also important in establishing the orientation of the embryo.

Detailed accounts of the egg and its components are given by Burley and Vadehra (1989) and Board and Sparks (1991).

THE OVULATION CYCLE IN THE LAYING HEN

Egg laying in wild birds is usually limited to one or two clutches a year, the eggs in a batch being laid one after the other over the space of a few days and then incubated together. The mature domestic fowl is capable of laying throughout the year. Nevertheless, the eggs are still laid in batches at the rate of about one per day (about every 26 to 28 hours) for a period of between four and six days. There is then a rest, which may be as short as one day in a good layer, followed by another period of egg-laying days, and so on. The increased egg-laying in domestic birds has been brought about by a reduction in the length of time between clutches.

The process is under complex hormonal control from gonadotrophins produced by the anterior

Downloaded from Vet-eBooks.com

pituitary gland. An ovulation-inducing hormone (OIH), which corresponds in many ways to the luteinising hormone of mammals, is released by the pituitary and, if there is a sufficiently mature follicle available, responds to the OIH by ovulating within about 4 to 8 hours (Gilbert, 1971). If the hormone is injected into a laying hen, it can provoke premature ovulation. Progesterone also plays a role, probably acting through the hypothalamus and thus controlling the release of the OIH by the pituitary. For a further account see King and McLelland (1981) and Etches (1996).

THE VITELLINE MEMBRANE (PERIVITELLINE LAYER)

The vitelline membrane is the transparent casing that encloses the yolk of the hen's egg and separates it from the albumen. It consists of two major layers, the inner layer, which is laid down in the ovary, and the outer layer, which is secreted in the oviduct. Bellairs *et al.* (1963) described the fine structure by transmission electron microscopy, and their findings have since been confirmed by others. The fibres of both layers are rich in glycoproteins (reviewed by Wishart and Horrocks, 2000).

The inner layer is about 1–3.5 μm thick, and consists of a meshwork of solid cylindrical fibres that mainly run parallel to the surface of the yolk and vary in thickness from about 0.2 to 0.6 μm (*Plate 2c).* The outer layer varies in thickness from about 0.3 to 9 μm and is composed of a variable number of sublayers lying one above the other. It also contains fibres, but these are thinner than those of the inner layer; strands of the outer fibres are extended out into the chalazae *(Text-Figure 1* and see below*)*, where they are spirally arranged and coated with thick albumen. The material between the sublayers of the outer layer of vitelline membrane is probably albumen, and it is likely that there is a penetration of the outer layer by albumen, or that the secretion of the albumen starts to take place before the entire thickness of the outer layer has been laid down.

Each layer of the vitelline membrane consists of proteins, though the amino acid composition differs. The principal components of the outer layer are ovomucin, lysozyme and vitelline membrane outer proteins I and II (Burley and Vadehra, 1989). The ovomucin makes up the fibrous framework on which the outer layer is built, whilst lysozyme forms an electrostatic complex with the ovomucin that provides the bulk and strength.

The principal components of the inner layer are glycoproteins, five having now been identified (Rodler *et al.*, 2011). ZPc is a glycoprotein homologue analogous to ZP3 found in the mammalian zona pallucida, and is present in the inner layer of the chick vitelline membrane (Han *et al.*, 2010). It is thought that the glycoprotein homologous II is concerned with the structural integrity of the inner layer. There is also a carbohydrate-containing fraction (Kido *et al.* 1976), which includes lectins (Cook *et al.,* 1985). See Wishart and Horrocks (2000) for a fuller discussion of the biochemistry of the vitelline membrane.

TRANSPORT OF MATERIALS ACROSS THE VITELLINE MEMBRANE

During the first week of incubation, the albumen loses more water than could be attributed to evaporation and, at the same time, the yolk acquires more water (New, 1956). It is therefore assumed that water is passed through the vitelline membrane into the yolk, and it has been calculated that about 16 g of fluid is drawn through the vitelline membrane during the first week of incubation (Romanoff and Romanoff, 1949) and collects as the sub-blastodermal fluid. When the chick blastoderm is grown in culture fluid appears to be drawn through the membrane and to collect at the ventral side of the embryo. If the washed vitelline membrane is used like a 'dialysis' membrane, water-soluble proteins obtained from the egg are able to pass through it (Jordanov *et al.* 1966).

Callebaut (1987) labelled albumen by injecting laying Japanese quail hens with tritiated tyrosine and harvesting the eggs. Non-radioactive yolks, still in their own vitelline membranes, were then obtained from non-injected laying hens. The labelled albumen and the unlabelled yolk, together with its vitelline membrane, were assembled in an unlabelled egg shell and incubated. Autoradiographs showed that during the first two days of incubation, albumen penetrated through the vitelline membrane and accumulated distal to the margin of overgrowth, the outer area of the blastoderm.

Sodium transport across the vitelline membrane from the albumen into the yolk appears to be controlled by the ectoderm of the embryo, since removal of the endoderm and mesoderm have been found to have little effect on it (Kucera *et al.*, 1994).

The possibility that the vitelline membrane itself selectively controls the passage of materials through

Downloaded from Vet-eBooks.com

it has frequently been investigated, but no clear evidence has been found (see discussion by Burley and Vadehra, 1989).

ALBUMEN AND THE CHALAZAE

The chalazae are a pair of spring-like structures that project from the equatorial region of the vitelline membrane into the albumen and are considered to act as balancers, maintaining the yolk in a steady position in the laid egg. Each chalaza contains fibres that appear to be identical with the fibres in the outer layer of the vitelline membrane, but are spirally coiled and embedded in albumen. Typically, they are illustrated as passing to the blunt and pointed ends of the egg (*Text-Figure 1*). If an egg is placed in an upright position, however, the yolk rotates so that the cytoplasm remains at the uppermost side, and the chalazae shift their position accordingly.

The albumen (egg white) is not of the same consistency throughout (see above). This can be seen by emptying a fresh egg into a dish, the thinner, more watery, albumen spreading further than the thicker albumen which remains around the yolk. Within the unbroken egg, the same relationship occurs, the thicker albumen adhering to the vitelline membrane.

The albumen has been the subject of a considerable amount of research, and its protein composition is well-documented (see Table 4.3 of Burley and Vadehra, 1989). The principal proteins are ovalbumin (54% of total protein), ovotransferrin (12%), ovomucoid (11%) and lysozyme (3.4%).

THE EGG SHELL AND ITS FORMATION

About 91% of the weight of the hen's egg shell consists of inorganic matter, and about 98% of this is calcite (calcium carbonate crystals) (Burley and Vadehra, 1989), the remaining 2% of inorganic material being composed of small amounts of magnesium carbonate and tricalcium phosphate. The remainder of the weight of the shell as a whole is made up of about 6% protein and some water.

The calcite crystals are arranged in columns, or palisades (*Text-Figure 1B*), which extend through almost the entire thickness of the shell and are closely packed together (Simkiss and Taylor, 1971). Morphologically, the shell is divided into two regions, the inner mammillary layer and the much thicker outer, spongy, layer. Gaps between the pallisades act as pores and enable gases to be exchanged (Sparks, 2009; Ar and Deeming, 2009). There are variations in the structure of the pores in different species of birds, which may reflect adaptations to the nesting environments (Board, 1982). Each crystal is rounded on the inside of the shell and attached to the outer surface of the shell membrane by a mammillary knob. These knobs mark the sites at which calcification begins, each starting as a small centre of crystallization on the outer shell membrane. Fibres from the shell membrane become encapsulated in the mammillary knobs. The outer shell membrane is so adherent to the knobs that in the unincubated egg it is impossible to separate them without damage. During the later stages of incubation, the embryo obtains calcium from the shell, which leads to a partial demineralisation of the shell (for a recent account of the effect of demineralization on the shell, see Chien *et al.*, 2009). It then becomes possible to separate the shell from the shell membranes (*Plate 2b*).

The outside of the egg shell of the domestic hen is covered by a thin cuticle (about 10 μm thick) which is thought to act as a barrier to the passage of non-gaseous materials.

THE LAID EGG

The Egg Yolk

The yolk of the laid egg is enclosed in the vitelline membrane. Despite its apparently homogeneous appearance to the naked eye, the egg yolk possesses a well-defined structure (*Text figure 1a*). Its centre is marked by a ball of white yolk, the latebra, and from this a column of white yolk, the neck of the latebra, extends upwards to join with a disc of white yolk, the nucleus of Pander, which lies beneath the blastoderm. The latebra is surrounded by predominantly yellow yolk. When the blastoderm is dissected from the yolk, the nucleus of Pander is left behind and can be mistaken by the inexperienced worker for the blastoderm itself.

Sections through a hard-boiled egg often show the yolk to be arranged in a series of concentric rings around the latebra. Similar bands are visible in stained sections of yolks which have been fixed. It has sometimes been suggested that these alternating bands are of yellow and white yolk, the broader being laid down during the day and the narrower at night. However, in hens that have been fed on a uniform diet *ad libitum*, this banded pattern is not seen, so that it seems more likely that the pattern reflects the fact that the hen has eaten foods of differing pigmentation.

Downloaded from Vet-eBooks.com

Physically, the yolk is an aqueous fluid in which float yolk spheres (also known as globules or yolk droplets) and lipid droplets (known also as yolk granules). Individual yolk spheres enclose a number of glistening lipid droplets, those taken from the yellow yolk possessing many small droplets, whilst those from the white yolk possess fewer but larger droplets (Bellairs, 1964).

Chemically, the yolk consists mainly of proteins and lipids in an aqueous solution. Methods for fractionation are discussed by Burley and Vadehra (1989).

The major chemical components of the yolk are the following:

- **α and β Lipovitellins.** These are lipoproteins, and the two forms differ from one another principally in the amount of protein-bound phosphorus they contain and in their amino acid composition. The relative proportion of α and β lipovitellins differs according to the breed of the hen. The lipovitellins constitute the main non-aqueous constituent of the yolk and are therefore an important component of the yolk granules.
- **Phosvitin**. This is the second-most plentiful constituent of the yolk granules. It is a phosphoprotein and has many of the physical properties of a polyelectrolyte. It binds iron and so is used as an iron store for the developing embryo.
- **Low-density lipoproteins.** The low-density lipoprotein found in the yolk granules appears to be similar to that in the aqueous phase. This is sometimes called lipovitellenin (but incorrectly so, according to Burley and Vadehra, 1989). The main proteins in this class are the apovitellenins, AI and AII. These have been extensively studied, and certain variations have been found in their composition between different species (e.g. between hens and geese). Apovitellenin I is as yet known only in the blood and yolk of laying birds; one of its characteristics is that it lacks the amino acid histidine. Apovitellenin II is present in the domestic hen and geese, but not in certain other species. Apovitellenins III, IV, V, VI have received less attention.
- **Livetins.** The α, β and τ livetins are a major component of the aqueous phase and appear to be identical to the serum globulin in the blood of the laying hen. Other livetins have also been reported, as well as some vitamin-binding proteins.
- **Inorganic ions** and some **enzymes.**

Vitellogenin is the name given to a stable protein precursor, a phosphoglycolipoprotein, that is synthesised in the liver of the laying hen and passes in the blood to the ovary. On entering the oocyte it become split to form phosvitin and the lipovitellin apoproteins (Burley and Vadehra, 1989).

Downloaded from Vet-eBooks.com

Chapter 2
Techniques

This chapter is concerned with certain techniques that have been devised especially for avian embryos. It does not deal with methods that are standard for other biological tissues unless modifications are needed; many of these are described by Stern and Holland (1993) and Darnell and Schoenwolf (1997). Additionally, an excellent compilation (edited by Bronner-Fraser, 2008) describes in detail many of the newer techniques used in the study of chick development; they include methods designed or modified for the study of specialized tissues and organs and will not be dealt with here.

'MILKING' HENS

A traditional technique in the pigeon fancy has been that of removing an egg from the shell gland to reduce the weight of the bird before flight. The process, known as 'milking' the pigeon, involves firm stroking down the abdomen towards the cloaca. It is a useful means for obtaining cleavage stage embryos without sacrificing the hen, but is easier to perform with quail hens than domestic fowls.

STORAGE OF EGGS

Laboratories that do not have easy access to farms or hatcheries usually arrange to receive their eggs once a week. If carefully packed and handled the eggs should arrive in good condition whether they have travelled by road or rail. During transport, however, they may have been subjected to various hazards. If the boxes have been roughly handled, breakages may have occurred. If they have been subjected to abnormally low temperatures in winter, or abnormally high ones in summer, they may have suffered. The most common ill-effect is ageing, brought about by delay in reaching the laboratory. It is important to inform the supplier if this is the case as he may be unaware that it is important to you. If you then see no improvement, change your supplier.

If the eggs are not to be used immediately on arrival they should be stored in a cool room. The ideal temperature is about 12°C, and if necessary, this can be achieved by adapting a domestic refrigerator. Under these conditions, eggs which were no more than 2–3 days old upon arrival will remain usable for up to a further week. It must be emphasized, however, that ageing eggs are unlikely to give such reliable results as fresher ones.

The changes that occur in eggs as they age include a decrease in the strength of the vitelline membrane, a higher albumen and yolk pH and decreased viscosity compared with a freshly laid egg (Kirunda and McKee, 2000). The strain of poultry also has an effect on the quality of the stored eggs (Lapao *et al.,* 1999). There is some indication that if eggs are to be stored for up to 14 days before use they are more likely to remain viable if they have been incubated briefly before storage, so as to have reached complete hypoblast formation (Fasenko *et al.,* 2001).

INCUBATION

The ideal temperature is about 37–38°C. There are several types of incubators available commercially. Ideally, an incubator should possess the following characteristics:

- The temperature should remain constant, not only throughout incubation, but also within the incubator, i.e. it should not be hotter at the top of the incubator than at the bottom. In a 'forced draft' incubator this is accomplished by an internal fan.
- There must be some arrangement to prevent dehydration of the eggs. This is usually a reservoir of

The Atlas of Chick Development. http://dx.doi.org/10.1016/B978-0-12-384951-9.00002-2
Copyright © 2014 Elsevier Ltd. All rights reserved.

Downloaded from Vet-eBooks.com

water at the bottom of the incubator, which ensures that there is a high humidity.

- There should be a method for 'turning' the eggs, anything between about 30° and 180°. This is usually accomplished by a slow tipping of the racks containing the eggs, first one way then the other, though some incubators are fitted with rollers which roll the eggs through 180° every hour. The most critical period is from 4 to 7 days (New, 1966). In eggs that are not turned, the young embryo tends to become stuck to the shell membranes, especially if there is some dehydration. Another ill-effect of not turning is that the albumen adjacent to the yolk sac becomes depleted of sodium (Latter and Baggott, 1996), which interferes with the passage of ion and water transport across the blastoderm into the yolk (see p. 4). Deeming (1989) reported that in unturned eggs there was a retardation in the formation of the allantoic and amniotic fluids, restricted albumen uptake and retarded growth. He suggested (Deeming, 2009) that egg turning is necessary for the complete utilization of the proteins and fluids of the albumen.

Commercial incubators are usually designed to hold several hundred eggs, but many smaller models designed for about two dozen eggs or less are now available. These are usually supplied with special racks to make them suitable for other species (e.g. quail, duck or turkey eggs). It is not always necessary to use commercial incubators, however, especially if the requirements for incubating eggs are for a limited period only. Tissue culture incubators may also be used, provided care is taken to maintain a reservoir of water in the base and either to turn the eggs manually by about 180° each day or, less satisfactorily, to stand them vertically with the blunt end uppermost. Eggs should not be introduced into an incubator that is regularly used for cell or tissue cultures, since the outside of an egg shell is non-sterile. It is not advisable to use histological slide incubators for incubating eggs, since they are often contaminated with fumes from toxic mountants. Eggs should be removed from their packaging on arrival and should not be placed directly on top of one another in the incubator; it is important for them to have space for gaseous exchange.

STAGES OF DEVELOPMENT

Normal stages for the chick are given in Appendices I and II, respectively. Those for other avian species are listed in Appendix III.

LABELLING TECHNIQUES

Traditional methods, such as the dabbing of Nile Blue sulphate or carbon particles onto the surface of the embryo, have long since been replaced by more reliable and sensitive procedures. New vital dyes (e.g. DiI, DiO) remain on and within the cell and its progeny for many generations and may, especially if fluorescently labeled, be followed with confidence (Stern and Canning, 1988). Other markers continue to become available (discussed by Kulesa, 2004) as do more and more sensitive ways of applying them. Foremost is the technique of electroporation, which enables materials such as genes to be introduced into specific cells by temporarily disrupting the cell membrane with a high voltage pulse. *In ovo* electroporation has become a widely used technique in the chick embryo. See protocols of Sauka-Spengler and Barembaum (2008) for use with embryos older than stage 3, and Voiculescu *et al.* (2008) for younger embryos. For a 'primer' on using electroporation in chick embryos *in ovo* for analysing gene function see Krull (2004).

One of the most important methods of labeling developing tissues, however, is to replace a chosen region of an early embryo with an identical part from another embryo which bears a specific label. It is then possible after further development to discover the fate of the selected region of the early embryo.

In carrying out transplants it is essential to be able to distinguish host from graft cells after development has taken place. This is possible by using two species, chick and quail, one for host and the other for graft. Grafting between two species is called xenoplastic grafting. The cells of the Japanese quail, *Coturnix coturnix japonica,* possess a large single nucleolus with dense heterochromatin, whereas those of the chick usually have two or more small nucleoli (Le Douarin, 1969). The difference is clearly shown by staining with Feulgen's technique or by a modified method of Harris' haematoxylin (Hutson and Donahoe, 1984). It is usual to use the chick as host and the quail as the donor of the graft, but ideally the converse experiment, with the quail as host and the chick as donor, should be performed also to test for the possibility of the species differences affecting the results. Quail embryos have a shorter period of incubation than the chick – 19 days as opposed to 21. Chick–quail chimeras may also be obtained by injecting dissociated cells of quail blastoderms into the subgerminal cavities of chicks (Naito *et al.,* 1991b). Detailed accounts of chick–quail transplantation techniques are described by Le Douarin *et al.* (2008). For an account of techniques for preparing

Downloaded from Vet-eBooks.com

quail–duck and mouse–quail chimeras (see Lwigale and Scheider, 2008).

CULTURE TECHNIQUES

One of the major drawbacks of working with the chick embryo is that it rests on yolk so that even the slightest pressure causes it to shift around on its fluid bed. Injection into the embryo of carefully measured doses of drugs or other chemicals can result in erratic or misleading results if the substances leak into the yolk. A further problem is that by about 5 days of development the embryo has become so vascularized that some forms of microsurgery can lead to haemorrhage and death. Further difficulties are imposed by the shell, which makes access a problem.

To some extent these difficulties can be overcome by ingenious *in ovo* experiments, but in many cases it may be necessary to carry out experiments on embryos that have been removed from the shell.

There are three main approaches:

- removing the early embryo from the yolk, after which it is grown in culture; see 'Explantation of the Blastoderm' (below).
- removing the early embryo from the yolk, carrying out microsurgery on it *in vitro,* and then grafting it back into another egg; see 'Grafting in Ovo' (below).
- transferring the contents of the entire yolk into an artificial container; see 'Shell-less Culture' (below).

The saline solution of Pannett and Compton (1924) has been used traditionally in preparing cultures of early chick embryos, but this is time-consuming to prepare, and equally good results can be obtained by using commercially available saline buffer pellets (pH 7.0) dissolved in sterile water.

Explantation of the Blastoderm

The classical method was devised by New (1955) and procedural details are given by Stern (1993a). The technique is designed to maintain *in vitro* the same relationships between blastoderm, vitelline membrane and albumen as exist in the egg. It has been the basic technique for over half a century for experimental analysis of the young blastoderm, whether by microsurgery or by its use in various types of imaging. A piece of vitelline membrane, with the blastoderm still attached to it, is removed from the yolk and placed embryo side upwards in a watch-glass. A glass ring is laid on the vitelline membrane so that it surrounds the embryo and the vitelline membrane is stretched taut by pulling its edges over the ring. Albumen is then introduced beneath the vitelline membrane and the whole is enclosed in a moist chamber (*Text-Figure 4*). Although the procedure is traditionally carried out using sterile glassware and instruments, sterility is not essential (unless the albumen is supplemented by agar or other vulnerable materials), since the bactericidal properties of albumen prevent infection except under grossly squalid laboratory conditions. Fungicidal infections are also unlikely to occur since these cultures are not normally maintained for more than 36 h. The technique is suitable for explanting embryos that have been previously incubated *in ovo* for periods up to about 48 h, and then for maintaining them in culture for up to about 36 h. It has been successfully used for filming morphogenetic movements (Bortier *et al.,* 1996). Development is usually slightly slower than in controls growing *in ovo*. Nevertheless, in successful explants the blastoderm expands to the glass ring and the embryo undergoes extensive differentiation. The success of development may be as high as 100% during the first 24 h for embryos explanted at stages between about 4 and 6 of Hamburger and Hamilton (Appendix II), but is likely to be much less for embryos explanted at younger stages. The success rate drops again with older embryos, partially because the diameter of the blastoderm is already so great at explantation that there is little space available for expansion. Furthermore, the vitelline membrane of the older embryos has less elasticity, though this difficulty can be circumvented to some extent by explanting the older embryos on vitelline membranes taken from unincubated eggs. It is usually possible to obtain some development during the second day after explantation, but it is seldom normal after the first 36 h.

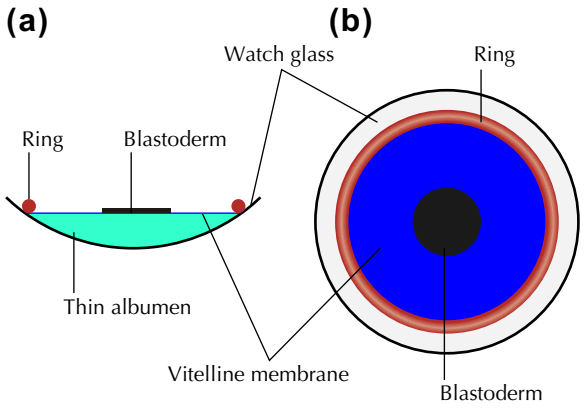

Text-Figure 4. *The culture technique of New. (a) Side view. (b). Seen from above. (From New, 1955.) The albumen (green) lies beneath the vitelline membrane (blue).*

Downloaded from Vet-eBooks.com

Modifications of the New Technique

Plastic Petri dishes

The original glass Petri dish and watch glass may be replaced by a standard 35 mm plastic Petri dish (Streit and Stern, 2008). A layer of thick albumen, 2–3 mm deep, is poured on to the base of the plastic dish and the ring with its attached vitelline membrane and embryo is then slid onto it. The plastic Petri dish is placed in a box containing wet tissue or cotton wool and transferred to the incubator.

Albumen–agar technique

The purpose of this modification is to provide a semi-solid base beneath the vitelline membrane that is helpful when carrying out microsurgery. The addition of agar to the albumen, however, raises the risk of bacterial infection, so that strict sterility should be maintained. A few drops of Indian ink may be incorporated if a dark background is required. Chapman *et al.* (2001) recommend substituting a disc of filter paper for the glass ring so that the vitelline membrane adheres to the paper. This adaptation is not suitable for embryos younger than stage 3 because of a high death rate and microcephaly (Voiculescu *et al.,* 2008). More recently, El-Ghali *et al.* (2010) reported better results by replacing the filter paper with rings made from nitrocellulose or PVDF membranes.

Inversion technique

In the traditional New technique the endodermal side of the embryo is uppermost, so that access to the ectoderm is difficult. Nicolet and Gallera (1963) solved the problem by adding an additional ring, which fits snugly inside the standard one so that the edge of the vitelline membrane is gripped tightly between the two. It is then possible to invert the paired unit of rings so that the vitelline membrane is uppermost and the ectoderm may be reached by making a small slit in it.

Special culture chambers

Czirók *et al.* (2002) described a ‘compact microscope-attached incubator’ suitable for maintaining young chick embryos during time-lapse filming. Kucera and Burnand (1987a) devised a dish that was thought to increase gas exchange.

GRAFTING AND TRANSPLANTS

In Explanted Embryos

In embryos explanted in New or similar cultures, the tissues are under tension and any small hole left in the blastoderm will become pulled into a larger one as it expands. The blastoderm is inverted, so the endoderm is uppermost.

- To remove a piece of tissue through the entire thickness of the blastoderm and replace it with a graft from a donor: First, prepare the graft by cutting through the endoderm only; this will ensure that clean outlines are obtained. Now cut through the remaining tissues, mesoderm and ectoderm, and move the graft to the host using a broad-mouthed pipette. Using the same technique, cut a hole in the host slightly smaller than the graft so that a tight fit results when the graft is inserted. Draw off as much fluid as possible.
- To insert a graft between the germ layers (e.g. the classical organizer graft): Before stage 4, the germ layers are easily separated. A slit is made in the area opaca endoderm close to the border with the area pellucida. A blunt knife is inserted and pushed gently into the area pellucida to make a pocket in the mesoderm. A graft may now be introduced into the pocket and positioned where required. Grafts may be pushed into the area opaca using the same procedure.

Shell-less Culture

Dunn (1991) reviewed methods for shell-less and semi-shell-less culture of avian embryos. In completely shell-less culture, the contents of the egg are tipped into a glass or plastic container, which is then incubated. The main advantage is that the embryo and its membranes are readily accessible for experiments. The main disadvantage is that the major source of calcium is lost to the embryo, which consequently suffers skeletal and other anomalies, reduced growth and failure to hatch. This ‘disadvantage’ is useful, however, for studying aspects of calcium transport and skeletal development (Tuan *et al.,* 1991).

The technique recommended by Dunn is as follows: After 3 days of normal incubation, the egg contents are tipped into hemispherical hammocks made from sheets of the plastic normally used for wrapping food. These hammocks are supported on tripods and are covered with a sterile Petri dish lid. The whole arrangement is then placed in a forced draft incubator

Downloaded from Vet-eBooks.com

in 1% carbon dioxide. Embryos younger than 3 days are apparently in greatest danger of desiccation and consequently show less satisfactory survival rates. An improvement in the technique would probably be to stand the tripod in sterile water in a plastic box which has been sterilized. The lid should then be placed on the box and sealed with masking tape. If two small holes have been made in the lid, the appropriate amount of carbon dioxide and air mixture may now be introduced by means of a hypodermic syringe and the holes sealed. In this way greater humidity as well as sterility will be retained.

In semi-shell-less cultures, the egg contents are transferred to a glass or plastic receptacle for carrying out the experiment. After this, they are transferred back into a true shell, which need not necessarily be from the same species. The chorioallantoic membrane develops in association with the foster shell, permitting resorption of calcium, though the embryos tend to be retarded in comparison with normal controls.

The semi-shell-less technique of Rowlett and Simkiss (1987) involves transferring the contents of an egg which has been incubated for 3 days to the empty shell of another fowl or even turkey egg. Approximately 55% of such embryos are likely to survive until day 17 of culture, and the authors reported that some had hatched and been reared to maturity. Unfortunately, this technique is not always suitable, since many important changes have occurred by 3 days of incubation. Perry (1988) and Naito *et al.* (1991b), therefore, introduced an additional technique for raising newly fertilized eggs taken directly from the oviduct. The eggs are initially immersed in a solution of albumen and saline in a glass beaker for 24 h. During this period they absorb fluid and 'plump up' as they would in the oviduct. Afterwards they are transferred to foster egg shells (*Text-Figure 5*).

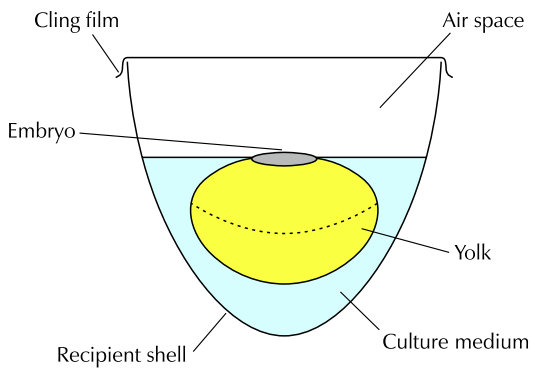

Text-Figure 5. *The final stage of the three-stage culture technique. (From Perry (1988), with permission of The Company of Biologists Ltd.)*

IN OVO TECHNIQUES

Preparation

The ideal approach must always be to disturb the environment as little as possible by carrying out experiments *in ovo* rather than *in vitro*. With young embryos the blastoderm rises to the top of the yolk, so the eggs should be allowed to settle on their sides for some minutes after removing them from the incubator.

Procedure

Wipe the shell with 70% methanol, and using a vial saw or a sharp scalpel, outline an area about 2–3 cm square by scratching the upper surface of the shell. Now gently saw or cut through the shell, but leave the shell membranes intact until the shell has been removed. The shell membranes may then be picked away with fine forceps. The embryo should be visible but, if not, pick away more shell and shell membranes with the forceps. Sometimes it is advantageous to lower the yolk away from the shell at this stage. Using a sharp knife or a mounted needle, make a small incision through the blunt end of the shell into the outer air sac. The air is then released and the yolk drops down. After the operation has been performed, both holes are sealed with clear plastic tape, care being taken that it is pressed down firmly so that no air can enter, or albumen escape.

From about 8 days of incubation, the position of the embryo in the shell can be established by candling the unopened egg, which enables the experimenter to position the window in the most suitable site. The egg is held against a bright light: a 60 W bulb is adequate, but it is important to cover the sides of the egg to shut out excess light. The embryo can be seen as a dark patch with the highly pigmented eyes showing most strongly. With unfertilized eggs, no patch is visible.

Grafting *In Ovo*

Small pieces of tissue (e.g. somites) may be extirpated and replaced with grafts of similar size, although if the experiment is carried out after about 3 days of incubation the embryo is so vascularized that heavy bleeding may prevent success. It is often helpful to inject an Indian ink solution beneath the embryo to give a high-contrast background, although this may have mild toxic effects. Bagnall (1988) recommended

Downloaded from Vet-eBooks.com

dilution of the Indian ink with yolk spun on a bench centrifuge. To operate, a small hole is made in the vitelline membrane over the appropriate region of the embryo, the ectoderm above the selected tissue (e.g. somite) is peeled away and the tissue removed with a fine needle, taking care not to damage the underlying endoderm, as this can result in yolk flooding through the gap. A graft may now be inserted into the space; a tight fit is desirable. As much fluid as possible is removed from above the embryo so that the graft does not float out of position. The shell is then sealed with adhesive tape and incubation is resumed with the window uppermost.

Intracoelomic grafting is a method for maintaining tissues within the coelomic cavity of a host embryo. A graft is inserted into the extra-embryonic coelom at about stage 6 and pushed gently through into the embryonic coelom. After the body becomes folded off from the yolk sac, communication between the extra-embryonic and embryonic coeloms is lost but the graft may survive not only until hatching but throughout the life of the adult bird. This useful technique is seldom utilized these days. For a full description consult Hamburger (1947) or Wilt and Wessels (1967).

The **technique of Martin** (1972) is not easy but can provide excellent results. The entire area pellucida of the experimental embryo, together with a surrounding circle of area opaca (but not the entire area opaca), is removed from its own yolk, operated upon in a Petri dish and then grafted back into another egg. The host egg having been incubated for the same length of time, a slit is made in the vitelline membrane over its embryo and the vitelline membrane is trimmed away until a large part of the area opaca is exposed but the periphery remains intact and still adherent to the vitelline membrane. The area pellucida is cut out of the host and discarded. The operated embryo is now laid over the hole and its area opaca fused onto that of the host. This is done using fine ophthalmological scissors, which slowly pinch the host and graft tissues together in such a way that the cut edges become fused and the discarded portions can be removed. The endoderm of the area opaca of the host embryo becomes fused to the endoderm of the area opaca of the grafted embryo. The secret of this technique is to proceed slowly, taking very small 'bites' with the scissors and allowing the blades to remain pressed together for several seconds after each cut. Gradually, by progressing around the circumference of the join, the two tissues become 'stitched' together.

An additional procedure for transplanting tissues *in ovo* is described by Stern (1993a,b) and techniques for grafting pieces of limb buds by Tickle (1993).

Injection and Other Techniques

Avian chimeras can be formed by injecting quail cells at stages X (Etches *et al.,* 1993) and XI–XIII (Watanabe *et al.,* 1992) into chicks of a similar age. Petitte *et al.* (1990) described a technique for producing chimeras by injecting cells from stage X embryos into the subgerminal cavity of a different strain. Albazerchi *et al.* (2007) describe a technique to transfect the chick hypoblast, carried out gene transfer using viral vectors.

Localized electroporation methods developed for use with avian embryos are described by Atkins *et al.* (2000) and Cui *et al.* (2006). A system for injecting stem cells into chick embryos is supplemented by a video on-line Boulland *et al*. (2010).

Techniques for making corrosion casts of blood vessels are described by Carretero *et al.* (1993) and Hiruma and Hirakow (1995). Examples supplied by these authors are shown in *Plates 45-47.*

PREPARATION OF SERIAL SECTIONS

Older embryos (from about 3 days of incubation) are prepared using standard histological methods. Difficulties may arise with the younger stages, however, because of the delicacy of the material and the need to prevent the blastoderm from curling at the time of fixation. Removal of the blastoderm from the yolk may be accomplished in at least three ways.

- A thin paper disc is laid over the blastoderm so that it adheres to the vitelline membrane. Using a circular cut through the vitelline membrane, the disc is removed, together with the embryo, and washed briefly in saline to remove any yolk adhering to it. It may then be placed in the fixative and the paper removed later.
- One end of a piece of nickel–chrome wire (about 22 gauge) is bent into a ring about 15 mm in diameter and the other end is fashioned into a handle at right angles to it. The ring is heated to red heat in a flame and quickly applied to the vitelline membrane and the area opaca. The vitelline membrane and area opaca stick to the ring, and if a fine sharp blade is passed around the outer side of the ring, they may be lifted cleanly from the yolk (Daniel, 1955). The blastoderm is still fixed to the wire to keep it flat.
- The procedure used for preparing New cultures may also be employed. The blastoderm, together with the vitelline membrane, is peeled off the yolk in a saline bath. The vitelline membrane is then stretched

Downloaded from Vet-eBooks.com

around a ring and fixative is dropped gently on to the embryo.

A variety of fixatives may be used when preparing material for paraffin sections, but that of Schoenwolf and Watterson (1989) gives good results. Carnoy's, Bouin's, formal buffered saline (made with paraformaldehyde) and Zenker's are all satisfactory. For embryos up to about 4 days, fixation need not last longer than 2 h, though it can be extended overnight provided that the pots are covered to guard against evaporation. After fixation the specimens are dehydrated in a series of increasing concentrations of alcohol. The time spent in each grade of alcohol can be as short as 10 min for young embryos. Transferring embryos from pot to pot is to be avoided because of their fragility. When passing through the final stage of dehydration, it is advantageous to add a few drops of a stain, such as 1% light green in absolute ethanol, so that the specimens will subsequently be visible in the wax block. After a quick rinse in xylene, the embryos are transferred to the paraffin wax at about 50°C. A common fault is to leave these delicate young specimens for too long in the wax; two consecutive periods of 30 min each are adequate. Longer periods are needed for older embryos.

Most of the sections illustrated in this book were embedded in paraffin wax and cut at 10 µm. If frozen sections are to be made, the material should be fixed in paraformaldehyde and not passed through ethanols. The staining procedures for avian embryos were standard. Most of the sections illustrated were stained with haematoxylin and eosin or with Masson's trichrome. The whole mount embryos in which both cartilaginous and ossified tissues were stained blue and red, respectively (*Plates 30–32*), were prepared according to the method of Dingerkus and Uhler (1977).

Plastic Sections

Superior histological detail is generally obtained by embedding material in plastic (e.g. araldite or modern methacrylate) instead of paraffin wax, though thinner sections must be cut.

Preparation for Scanning Electron Microscopy

The techniques are basically the same as those used for preparing adult tissues for scanning electron microscopy. The major difficulties lie in the fragility of the early embryo so that extreme care must be taken, especially during the mounting of the specimens.

INSTRUMENTS

No instruments peculiar to the chick are necessary. Operations are generally carried out using tungsten needles (Stern, 1993a,b), ophthalmological knives and scissors, sharpened steel sewing needles or sharpened Borradaile knives.

Imaging

Recent imaging techniques combined with modern labelling and culture methods have proved among the most valuable tools in advancing our understanding of development in the chick. These include not only refined video time-lapse cinematography, but also optical projection tomography, which allows three-dimensional high-resolution of the anatomy of small developing organs (Sharpe, 2003; Kim *et al.*, 2011). Other imaging methods are high-frequency ultrasound, magnetic resonance imaging (MRI) scanning, and position emission tomography (PET) scanning. Techniques using optical coherence tomography (OCT) to measure strains, stresses and tissue deformations are described by Varner *et al.* (2010).

A technique for the imaging of embryos *in ovo* is described by Kulesa *et al.* (2010). For a review of imaging methods especially suitable for studying cell migration, see Dorman and Weijer (2006).

Three-dimensional reconstructions can be made from non-paraffinized sections of embryos using confocal and fluorescent microscopy (Jirkovská *et al.*, 2005).

COMMON ABNORMALITIES

Abnormal embryos occur infrequently among commercially supplied eggs, the most common being Siamese twins formed from a duplication of the primitive streak (see Newman, 1917) followed by an interaction between the two axes. Similar Siamese twins can be produced experimentally (*Plate 3*). Micropthalmia of one or both eyes, cyclopia and anopthalmia present infrequently. A well-documented range of mutations exists, maintained in various research centres (e.g. Storrs Agricultural Experiment

Downloaded from Vet-eBooks.com

Station, The University of Storrs, Connecticut, USA and the Department of Avian Sciences, University of California, Davis, California, USA). A list of gene banks of both mutants and various pure-bred lines was published by Delaney (2004).

The individual names of the mutants have usually been chosen because of their most obvious anomaly, though frequently there are additional malformations; for example, the **Talpid** mutants (*Plate 29*) are so-called because of their short, broad mole-like limbs which superficially resemble the limbs of the mole, *Talpa,* although they have, in addition, abnormalities of the face and a short vertebral column. These anomalies are all brought about by a single recessive gene (Landauer, 1967). Talpid mutants have appeared spontaneously several times and all are not necessarily the result of the same mutation. The **Creeper** mutant is characterized by shortness of the extremities, especially the legs, and is an achondroplastic, lethal mutation (Landauer, 1967).

The study of the development of mutants has proved valuable in understanding aspects of normal development; for example, the discovery of the essential role played by the apical ectodermal ridge in normal limb development was made by Zwilling (1949) when studying the early embryology of the **Wingless** mutant. These results stimulated an extensive series of experiments in which the apical ectodermal ridge of a normal embryo was separated from its underlying mesenchyme and then recombined with tissues from the Creeper mutant. More recently, the study of the molecular basis of mutations has opened up new approaches (see Abbott and Pisenti, 1993).

Downloaded from Vet-eBooks.com

Chapter 3
Early Stages

FERTILIZATION AND PRE-LAYING

There is a tendency to think of the development of the chick embryo as starting at incubation and lasting 21 days, but not only does fertilization take place before the egg is laid, some of the most critical events occur during this period. They have attracted little attention compared with those of the older stages, largely because of the practical difficulties involved in their study.

The structure of the **avian sperm** resembles that of other vertebrate species in that there is a head, consisting mainly of the nucleus and acrosome, a mid-piece with mitochondria, and a long flagellum. In the domestic fowl, however, the nucleus is so long and slender that the head does not bulge out (*Text-Figure 6; Plate 1*) in the way characteristic of most vertebrate sperm. Sperm of this type are typical of non-passerine birds and are described as fusiform or vermiform because of their slender shape. The fowl sperm nucleus is about 12 μm long and 0.6 μm in diameter (Wishart and Horrocks, 2000). For a full description by transmission electron microscopy see Bakst and Howarth (1975) and Thurston and Hess (1987). Avian sperm, unlike those of mammals, develop their fertilizing ability whilst still in the testes and, as there are no accessory glands corresponding to those in mammals, the semen passes directly into the genital tract of the hen (Wishart and Horrocks, 2000). Fertilization takes place in the infundibulum of the oviduct (*Text-Figure 2*).

After mating some, but not all, of the sperm are transported to the (lower) sperm storage tubules that lie at the junction of the vagina and the shell gland (uterus, see *Text-Figure 2*). (For a detailed accont of the sperm storage sites see Bakst, 1998). It is not clear what factors determine which sperm are transported and which are not, though differences in sperm motility (Froman, 2003) or in sperm selection by the vaginal environment have both been suggested. There are additional sperm storage tubules at the upper end of the infundibulum. If sperm are present there they may fertilize the egg (Bakst and Vinyard, 2002). The sperm storage tubules do not appear from their histology to be secretory and probably act merely as receptacles, the sperm lining up in an orderly manner with their heads to the epithelium of the tube and their tails hanging in the lumen. As many as 100 sperm may be stored in one tubule (Bakst *et al.,* 1994). The main significance of the sperm storage tubules is that they enable fertilization of a clutch of eggs to take place without the need for synchronized copulation. This is important since fertilization must occur immediately after ovulation in the brief period, perhaps only 15 min (Wishart and Horrocks, 2000), before the outer layer of the vitelline membrane is laid down and blocks sperm entry. The sperm are probably metabolically quiescent whilst in the tubes, the concentration of calcium in the tubular fluid apparently inhibiting sperm motility (Holm *et al.,* 2000), but become activated upon leaving. The mechanism of sperm storage and survivability is discussed by Das *et al.* (2008). The length of time in which sperm remain fertile varies according to the hen, but 18–21 days is common (Liu *et al.*, 2008). There is some evidence that a neural stimulus may bring about the release of the sperm from the storage tubules, since individual tubules are separately innervated (Freedman *et al.,* 2001). The sperm appear to be released continuously and not necessarily as the result of any event in the oviduct. Once the egg enters the infundibulum, many sperm rapidly contact the surface of the inner layer of the vitelline membrane and pass through it, apparently dissolving the granular material lying between the fibres with hydrolytic enzymes released from the acrosome (Wishart and Horrocks, 2000).

The Atlas of Chick Development. http://dx.doi.org/10.1016/B978-0-12-384951-9.00003-4
Copyright © 2014 Elsevier Ltd. All rights reserved.

Downloaded from Vet-eBooks.com

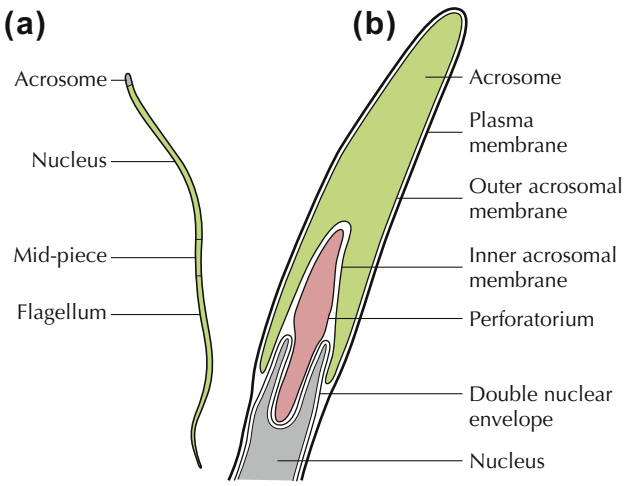

Text-Figure 6. *Morphological features of the sperm of the domestic fowl. (a) The entire spermatozoan. (b) The acrosomal region. See also Plate 1c. (After Wishart and Horrocks (2000), with permission of Springer-Verlag, Heidelberg.)*

In penetrating through the inner layer, each sperm first binds to receptors on it, which appear to be carbohydrate based (Robertson *et al.,* 2000). There is evidence that the breakdown of the acrosome membrane (acrosome reaction) at this time is induced by an *N*-linked oligosaccharide with terminal *N*-acetyl-glucosamine residues (Horrocks *et al.,* 2000). This appears to trigger the rupture of the membrane around the acrosome, resulting in the release of hydrolytic enzymes, which digest away a small area of the inner layer of the vitelline membrane so that the sperm is able to pass through it.

One of the problems for species with large-yolked eggs is that of how the sperm nucleus finds and fuses with the female nucleus. In some small-yolked eggs (e.g. sea urchins and mammals) there are mechanisms to prevent the entry of more than one sperm, but in birds many sperm pass into the egg, which presumably increases the chance of success. However, only one successfully fertilizes it, the male and female haploid nuclei fusing to form a zygote possessing the diploid number of chromosomes about 3 h after ovulation (Waddington *et al.,* 1998). The first mitotic division occurs after about a further hour (Wishart and Horrocks, 2000). The remaining (supernumerary) sperm may undergo division, before breaking down.

Spontaneous parthenogenesis occurs in some birds. Olsen (1962), using an inbred strain of Beltsville White turkeys, obtained an incidence of nearly 40% parthenogenetic embryos, of which a few survived into adulthood; they are thought to have doubled their chromosomes by retention of the second polar body. Such a biological solution to the problems of fertilization is, however, an abnormal one. In birds (and probably all reptiles) the male is the homogametic sex, the female is the heterogametic one, producing two types of eggs, called ZZ and ZW, so that parthenogenetic embryos may be either male or female. This is the reverse situation of that in mammals, where the female is homogametic, producing only one type of egg, so that all parthenogenetic offspring are female. Some parthenogenesis has been reported in quail embryos, but development appears to be restricted to the formation of area opaca- and area pellucida-like tissue (e.g. Parker and McDaniel, 2009).

Even before ovulation the egg cytoplasm has almost separated from the yolk and, because it is lighter, has come to lie on the uppermost side of the egg, the animal pole, and is known as the germinal disc. Components of the germinal disc include the metaphase II meiotic nucleus and discarded first polar body, mitochondria and glycogen granules (see Bakst and Howarth (1977) for a full description). As the large egg yolk (with its embryo), enclosed in its vitelline membrane, passes down the oviduct it becomes covered first by the albumen, then by the shell membranes and finally by the shell (see Chapter 1). During this time the embryo undergoes cleavage, this process differing greatly in birds from that found in mammals. Cleavage furrows are visible in fertilized eggs taken from the oviduct (*Text-Figure 7; Plate 5*), although the first 16 cleavage cells are not completely enclosed in their own cell membranes but are open ventrally to the yolk mass; they are known as 'open cells'. With each mitotic division the cell membrane becomes completed around one of the daughter 'cells', whilst the other migrates into the adjacent yolky cytoplasm, carrying some cytoplasm with it, so that a new open cell is formed. By the 64-cell stage the most centrally situated cells have each become completely surrounded by a cell membrane, but there is still a region of mixed yolk and cytoplasm (ooplasm) beneath and around the embryo known as the subgerminal and marginal periblast, respectively (*Text-Figure 7*). During this time fluid is drawn from the albumen through the vitelline membrane and accumulates beneath the embryo in the subgerminal cavity (*Plate 6a*).

The most important event for the cleaving embryo is to acquire differences among its cells. If this did not occur the embryo would continue to grow in size but lack any form or pattern to its body. Differences begin to appear with the establishment of the axes of polarity. First, the dorsal and ventral sides become apparent (the dorso-ventral axis) and then the antero-posterior (the cranio-caudal axis). With the interaction of these two axes the embryo achieves a left and a right side.

Downloaded from Vet-eBooks.com

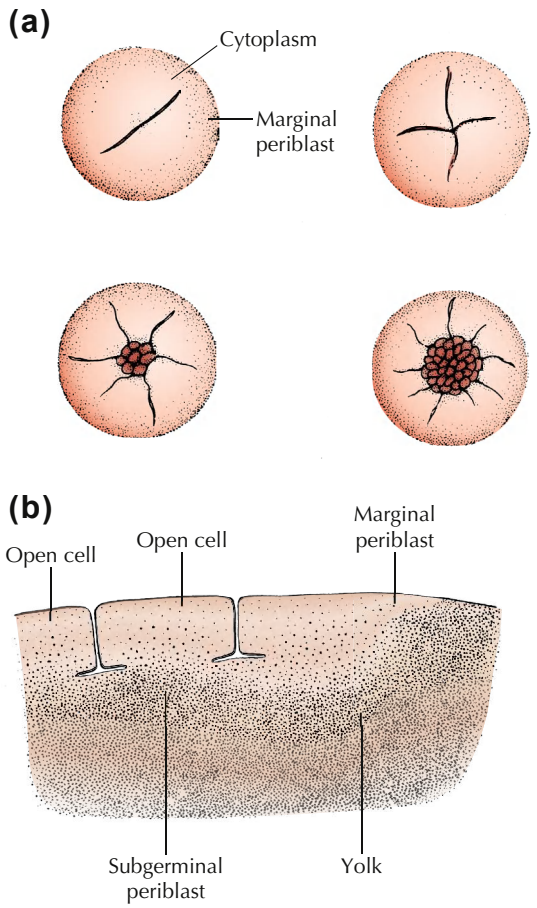

Text-Figure 7. *Early cleavage showing the 'open cells'. (a) Four stages seen from the dorsal side of the embryo. The yolk is not illustrated, but the marginal periblast is visible. (b) Vertical section through the edge of an early cleavage stage embryo. (From Bellairs et al. (1978), with permission of The Company of Biologists Ltd.)*

The establishment of the dorso-ventral axis is directly associated with the relationship between the yolk and the cytoplasm. During its early stages the chick embryo is a flat disc, the blastoderm. Its lower surface rests on the yolk and becomes the ventral side of the embryo, while the cells at the upper side lie immediately beneath the vitelline membrane and become the dorsal side. There is a potential difference of 25 mV across the blastoderm between the acidic ventral side and the basic dorsal side (Stern and Canning, 1988), though it is not known if the same situation applies before laying. It seems probable, that the differing environments at the two sides of the blastoderm play a role in bringing about the dorso-ventral polarity.

The establishment of the antero-posterior axis results from a shifting of the ooplasmic components by gravity. This takes place during the 20 or so hours spent in the shell gland (uterus) when the entire egg rotates at about 10–12 turns per hour as the shell is

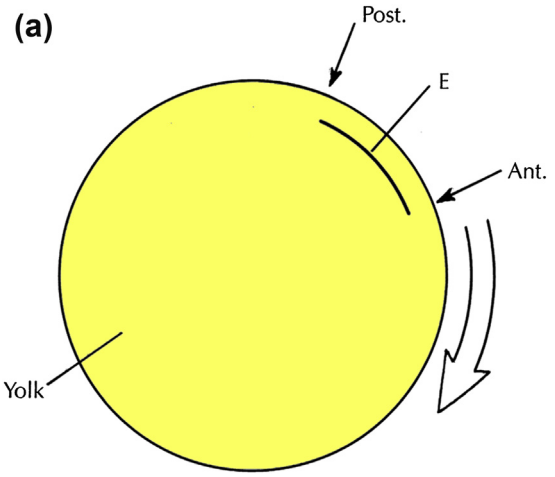

Text-Figure 8. *Rotation of the yolk which occurs in the shell gland. After rotation, the embryo no longer lies uppermost on the yolk, but has been tipped to one side. Ant = future anterior end of embryo. E = embryo Post = future posterior end.*

laid down; during this process the blastoderm becomes tipped from its original position on top of the yolk. The future anterior (head) end forms in the region that has been tipped lowest (*Text-Figure 8*), whereas the future posterior (tail) end forms from the highest region (Eyal-Giladi and Fabian, 1980). Callebaut (1987) suggested that this tilting is accompanied by a shifting of the yolky ooplasm beneath the oocyte so that the more lightweight of its components, especially the so-called β-ooplasm, come to lie beneath one side of the blastoderm which, probably as a result, becomes the future posterior end. The nature of the interaction between the periblast and the blastoderm is not understood. It is clear, however, that the antero-posterior axis is not yet completely determined at this stage, since it can be experimentally changed even after laying; if the blastoderm of a laid egg is bisected before incubation it may form twinned axes (*Plate 3b*) and these do not necessarily have the same orientation as one another. Normally, however, a range of *Homeobox* and other genes that are associated with the establishment and maintenance of antero-posterior polarity begins to be expressed soon after laying (see Chapter 5).

Repeated cell divisions occur during cleavage so that by the time the egg is laid the chick embryo possesses several thousand cells. Estimates range from 32,000–42,000 cells (Stepinska and Olszanska, 1983) to as many as 60,000 (Spratt, 1963).

NORMAL TABLES

A Normal Table is a convenient way of describing the stage of development reached by any normal embryo

Downloaded from Vet-eBooks.com

(see page 597 for a general account). The Normal Table of Hamburger and Hamilton (1951, 1992) is the standard one for describing post-laying stages (Appendix II), whilst that of Eyal-Giladi and Kochav (1975) is concerned with the pre-laying stages (Appendix I). There is some overlap between the two tables, stages X–XI of Eyal-Giladi and Kochav roughly corresponding to stage 1 of Hamburger and Hamilton so, where necessary, the suffixes EG&K and H&H are used to indicate which Normal Table is being referred to. Throughout this book the Hamburger and Hamilton tables are used for all the later stages unless otherwise indicated.

Normal Tables exist for specialized regions of the embryo and for other species of birds (Appendix III).

THE EARLY POST-LAYING STAGES

The transformation of a group of unspecialized cells into a basic embryonic body occurs during the first 2 days of incubation and at this time the embryo is at its most vulnerable to disturbances. Many of the abnormalities seen in late embryos or hatchlings have their origins in mishaps at these early stages.

When the egg is laid its temperature falls from that of the hen's body (about 40°C) to that of its surroundings, which is normally well below the incubation temperature of 37–38°C. The result is that the development of the embryo slows dramatically and virtually ceases below about 25°C, remaining arrested until incubation begins. In the wild, a hen may take several days to complete the laying of a clutch of eggs and only then begin to incubate them, the result being that all the chicks hatch at much the same time.

The morphological changes occurring during the first 24 h are best seen by dissecting the embryo from the surface of the yolk and examining it by transmitted light. The most striking feature is the division into the **area pellucida,** the almost transparent central region, and the **area opaca,** the more opaque peripheral ring (*Text-Figure 9a*). *Plate 8a* illustrates these regions by scanning electron microscopy, though the technique has made them no longer transparent. Sections show that there are two layers, the upper (epiblast) and the lower, throughout the area opaca and in the posterior part of the area pellucida (*Text-Figure 9b* and *Plate 9).* The opacity of the area opaca is due to the presence of large numbers of intracellular yolk droplets in the lower layer. Intracellular yolk droplets are present in the area pellucida also, but they are much smaller and fewer than those in the area opaca so that the tissue

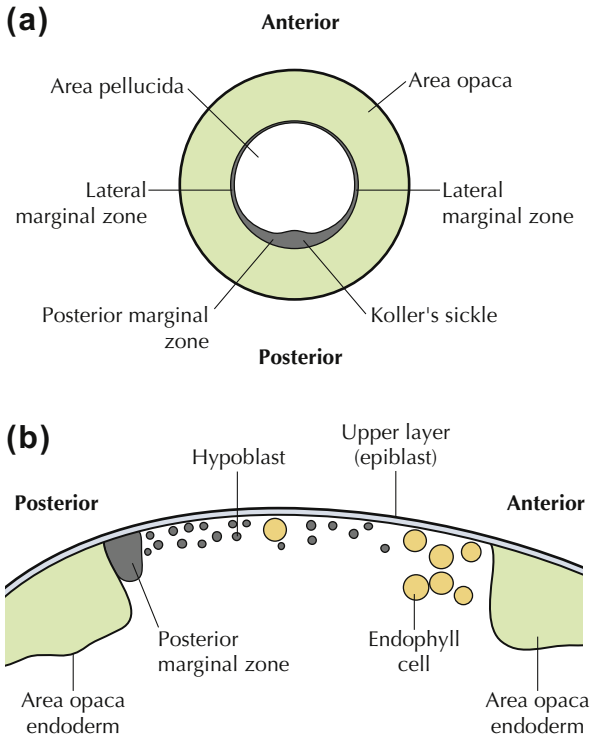

Text-Figure 9. *(a) Lower surface of an unincubated chick embryo. (b) Section through the same embryo passing along the anterior-posterior axis.*

is relatively transparent. The area pellucida gives rise mainly to embryonic tissues, although the lateral borders of the area pellucida together with the entire area opaca form extra-embryonic tissues (see Chapter 13 for more details of the area opaca).

The primitive streak starts to be visible in the area pellucida at about the 6th–7th hour of incubation (stage 2 of Hamburger and Hamilton, 1951; stage XIV of Eyal-Giladi and Kochav, 1975). It appears in the living embryo as a dark triangular region in the upper layer, its apex lying in the area pellucida and its base along the border with the area opaca. By about 18 h of incubation (stage 2 of Hamburger and Hamilton) it has reached its full length, extending about two-thirds of the way across the area pellucida and its most important region, Hensen's node, is visible as the swollen tip at the anterior end (*Plates 8b, 9a*).

Two key structures involved in the formation of the primitive streak are the posterior marginal zone and Koller's sickle.

The Posterior Marginal Zone and Koller's Sickle

The marginal zone lies at the border between the area opaca and the area pellucida and is already visible at

Downloaded from Vet-eBooks.com

the time of laying, Its widest part, the multilayered posterior marginal zone, lies at the posterior end of the area pellucida, and becomes progressively thinner in its lateral and anterior regions. Koller's sickle is a crescent-shaped area at the anterior edge of the posterior marginal zone (*Text-Figure 9*) and is also known as Rauber's sickle, since it was described initially by Rauber in 1876 (Callebaut *et al.,* 2000b). The significance of the posterior marginal zone and Koller's sickle lie not only in the role they play in the formation of the primitive streak, but also in establishing, albeit tentatively, the antero-posterior and medio-lateral polarity of the embryo (see p. 16).

The cells of the posterior marginal zone and of Koller's sickle are in direct contact with the underlying yolk, whilst the area pellucida, which is anterior to them, lies over the fluid-filled sub-germinal cavity. This close association with the yolk is of great significance since there is evidence that the ooplasm may contribute to the posterior marginal zone and Koller's sickle (Callebaut, 1987). There has been some disagreement about the number of cell layers present in this region and the precise relationship of Koller's sickle to the posterior marginal zone. This is not surprising since it is difficult to distinguish the different types of cells by traditional staining, though the situation is easier in the quail than in the chick. It should be noted that some authors (e.g. Eyal-Giladi, 1991) regard Koller's sickle and the posterior marginal zone as being one tissue. According to Zehavi *et al.* (1998) there is a high level of cell proliferation in both the posterior marginal zone and Koller's sickle.

Fate Maps

There is no visible sign in the early embryo of the tissues and organs that will form from it. Yet the future development (fate) of each region is now known, so that we can say that the fate of a specific area is to give rise to a particular tissue (e.g. neural tissue, somites, gut). These fates have been discovered by attaching labels to groups of cells and following them to their destinations (see Chapter 2 for labelling techniques). A fate map is a diagram of the early embryo, or part of it, showing the fates of different regions. Fate maps are sometimes called presumptive or prospective fate maps to emphasise the fact that the fates portrayed are not yet fully established and, under unusual circumstances, may be changed. For example, when assessing the effects of surgical interference or of the relationship of specific molecular activity to aspects of differentiation, the investigator needs to know the normal fate of a particular region of the early embryo. The more recently introduced term 'specification map' refers to the arrangements of areas that are already partially labiley determined (specified) but not yet totally determined. In practice they are usually much the same as an ordinary presumptive fate map.

The Lower Layer

Four types of cells contribute ultimately to the lower layer (see *Text-Figure 12*). At the time of laying, usually about stage X of Eyal-Giladi and Kochav (Appendix I), the area pellucida consists of an upper layer, the epiblast, underlain by scattered clumps of cells each about 30–50 μm in diameter (*Plate 6*). These clumps are the first indication of a developing lower layer and were named **endophyll** by Vakaet (1962). Alternative names are polyinvaginated cells (Eyal-Giladi and Kochav, 1975) and primary hypoblast (Stern, 1990). They are situated in the anterior (cranial) extension of Koller's sickle (Callebaut *et al.,* 1998) and are thought to arise by ingression from the upper layer, though the evidence is based mainly on the staining of fixed material (Fabian and Eyal-Giladi, 1981). Most, if not all, of the endophyll cells are thought to give rise to the primordial germ cells and they may also contribute to the yolk sac stalk (Stern, 1990).

Shortly after the start of incubation the second component of the lower layer, the **hypoblast** proper, arises at the posterior end of the area pellucida. It appears to form principally by migration of cells from Koller's sickle, and by about 12 h of incubation (stages XIII–IV) has come to lie beneath the entire area pellucida. As it spreads from the posterior to the anterior end of the area pellucida it forms a loose sheet in which some of the endophyll cells are caught and carried anteriorly. Ultimately, they become located in the germinal crescent (see page 75). The hypoblast cells, individually about 15–20 μm in diameter and yolky, are attached to one another loosely. There is no basal lamina associated with them and no apparent dorso-ventral specialization, so the sheet cannot be said to be a true epithelium. Hypoblast cells have been studied by time-lapse cinematography in tissue culture (Sanders *et al.,* 1978) and have been found to settle and migrate readily, even on untreated glass, laying down a thick layer of fibronectin. According to Rosenquist (1971) the hypoblast cells give rise to the endoderm of the yolk sac stalk (but see below). Several markers of the hypoblast are now available, e.g. *Otx2,* HNF3β, *gsc* and cCer/caronte (discussed

Downloaded from Vet-eBooks.com

by Foley *et al.,* 2000), the most significant being Cerberus, which prevents the formation of Hensen's node at the posterior end of the primitive streak (Bertocchini and Stern, 2002, 2008).

At about stage 2–3 H&H the posterior hypoblast becomes replaced by the third component of the lower layer, the **endoblast,** which is sometimes considered to consist of two types of cells, the **sickle endoblast** (Vakaet, 1970) lying beneath Koller's sickle, and the **junctional** endblast situated further laterally (Callebaut *et al.,* 2001). The endoblast is derived partially from Koller's sickle (Callebaut and Van Neuten, 1994) and partially from the lateral posterior marginal zone (Stern and Ireland, 1981). The sickle endoblast has been found to form the yolk sac endoderm and to influence the formation of the yolk sac blood vessels (Callebaut *et al.,* 2000a); this finding does not necessarily contradict that of Rosenquist (mentioned above), but reflects the fact that Rosenquist did not distinguish between hypoblast and sickle endoblast.

Bachvarova *et al.* (1998) produced a fate map by staining selected groups of cells in and around Koller's sickle with DiI/DiO (*Text-Figure 10*). Using goosecoid *(gsc)* as a marker, which is expressed in the hypoblast but not the endoblast, they concluded that the two tissues are derived from different locations in the deep layers of the sickle endoblast. Elaborating on this map, Kimura *et al.* (2006) showed that the first endoderm cells to ingress gave rise to the mid- and hind-gut, the next to the dorsal foregut, and the final lot to the ventral foregut (*Text-Figure 11*).

The fourth and final component of the lower layer is the **definitive endoderm** which consists of cells that have ingressed through the anterior end of the primitive streak after it has fully formed, and becomes the endoderm of the developing gut. These four components of the lower layer are illustrated in *Text-Figure 12*. According to Lawson and Schoenwolf (2003) the definitive endoderm originates in the lateral epiblast and then migrates to the primitive streak.

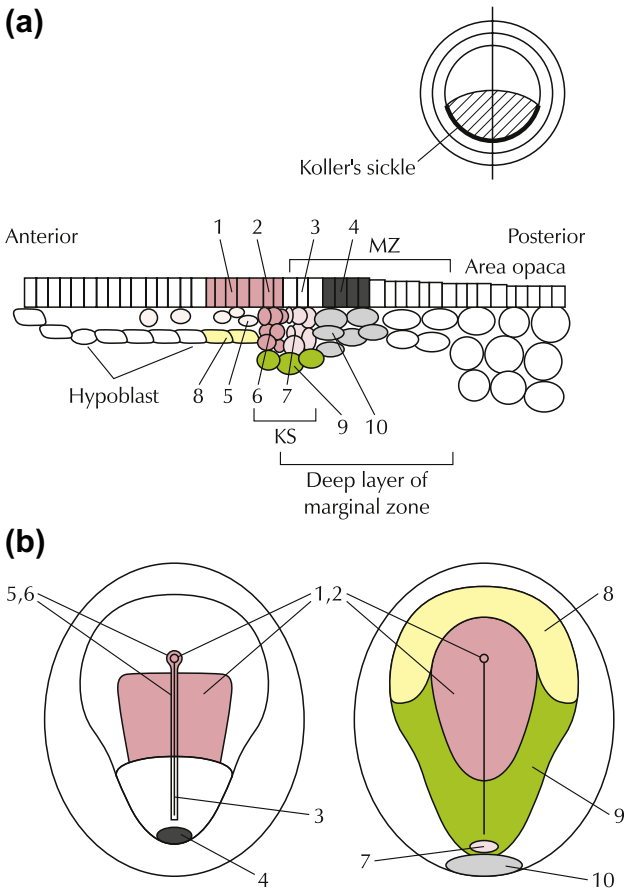

Text-Figure 10. *(a) Midsagittal section of a prestreak embryo at about stage XII (see Appendix I) showing the various structures at sites of labelling with DiI/DiO. (b) Positions of cells at stage 4 (see (Appendix II) derived from the labelled sites. The fates of the upper layers (ectoderm and mesoderm) are shown in the left diagram, and of the lower layers in the right diagram. Upper sites: 1, 2, 5 and 6 contribute to Hensen's node, the anterior streak and the embryonic mesoderm. Site 3 contributes to the posterior streak and the embryonic mesoderm. Site 4 remains in the posterior area opaca. Lower sites: 1 and 2 contribute to the embryonic endoderm. Site 8 is found in the hypoblast of the germinal crescent. Site 9 is found in the endoblast, whilst 7 and 10 remain posterior to the primitive streak. (After Bachvarova et al. (1998), with permission of The Company of Biologists Ltd.)*

The Upper Layer (Epiblast)

During this period when activity is taking place in the lower layer the embryo is expanding over the yolk, and the upper layer becomes thinned from about four to six cells deep to one cell, probably by intercalation and changes in cell shape. Canning and Stern (1988) showed by staining with the monoclonal antibody HNK-1 that there is a pepper-and-salt pattern in chick embryos at stages XII and XIII, indicating that the epiblast cells are not identical throughout. A similar conclusion was previously drawn by Bancroft and Bellairs (1974), who showed that the pattern and distribution of the microvilli on the dorsal surface of the epiblast varied according to the region (*Plate 7*). Later, Stern and Canning (1990) found that the HNK-1 positive cells are precursors of the mesoderm and definitive endoderm of the primitive streak.

Between stages X EG and 3HH there is a convergence of cells to the posterior midline, followed by anteriorward movements along the midline (Vakaet,

Downloaded from Vet-eBooks.com

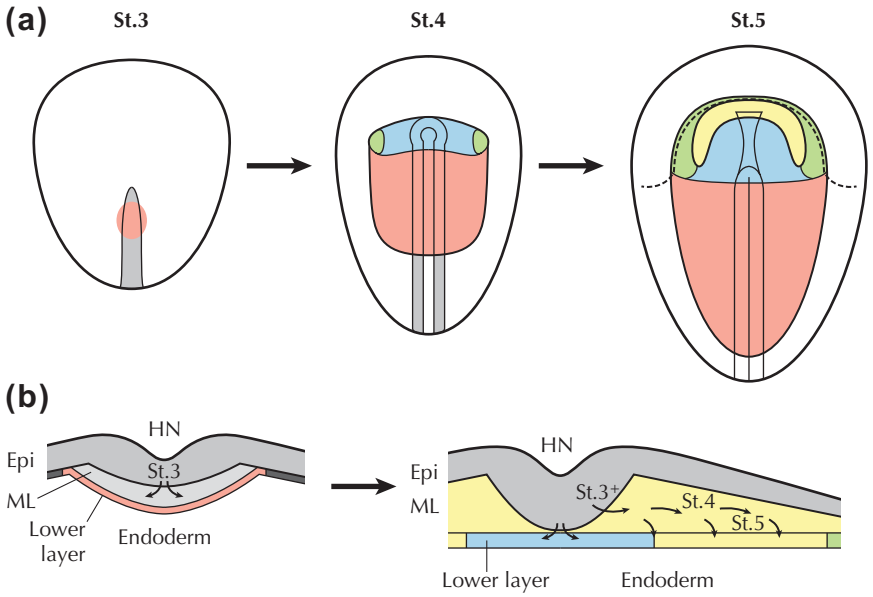

Text-Figure 11. *Fate map of the lower layer at stages 3–5. Cells that ingress early give rise to the midgut endoderm (light red) followed by dorsal foregut endoderm (light blue) and lateral foregut endoderm (green). Finally the presumptive ventral foregut territory extends to the peripheral area of the head process (yellow). (From Kimura et al. (2006), with permission of Elsevier.)*

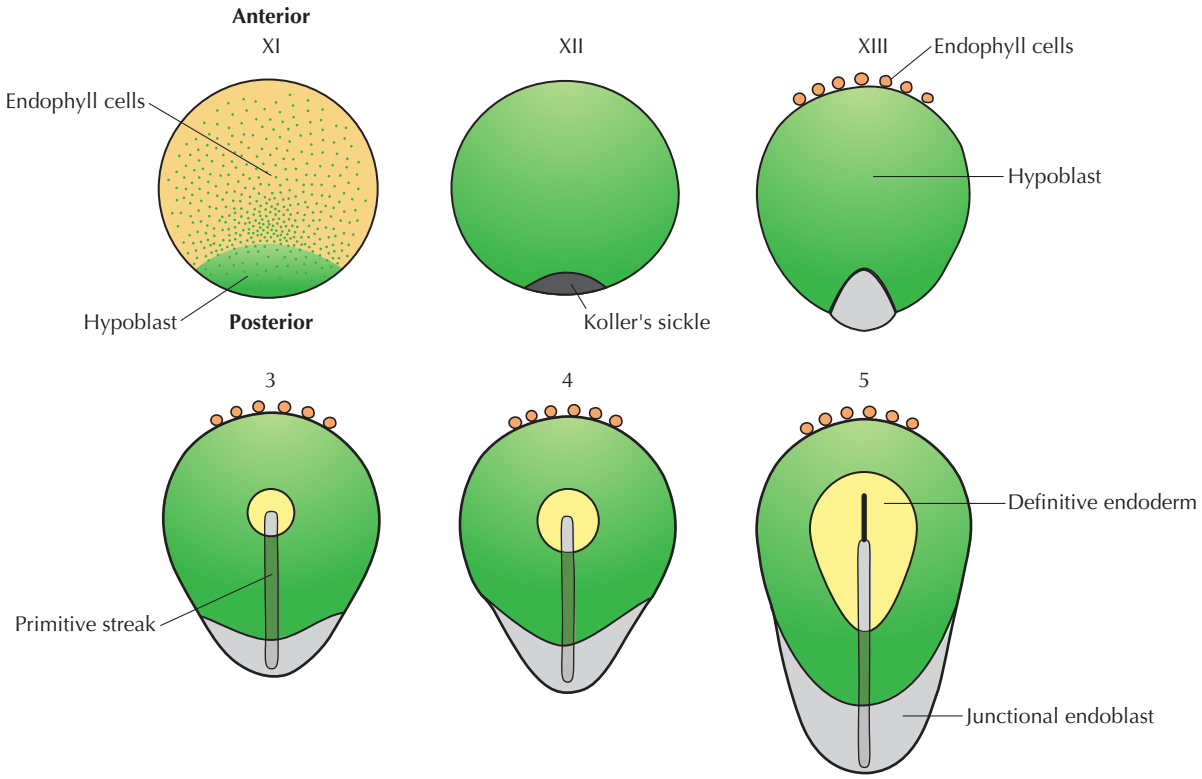

Text-Figure 12. *The relations of the four tissues that form the lower layer of the area pellucida. Initially the hypoblast spreads from the posterior end and forms a continuous sheet (stages XI, XII and XIII of Eyal-Giladi and Kochav). The junctional endoblast (future yolk sac endoderm) then spreads from the posterior end and the definitive endoderm ingresses through the anterior end of the primitive streak (stages 3, 4 and 5 of Hamburger and Hamilton). Other components of the lower layer are the endophyll cells (future primordial germ cells). (After Sanders et al.(1978); Adapted with permission of The Company of Biologists Ltd.)*

Downloaded from Vet-eBooks.com

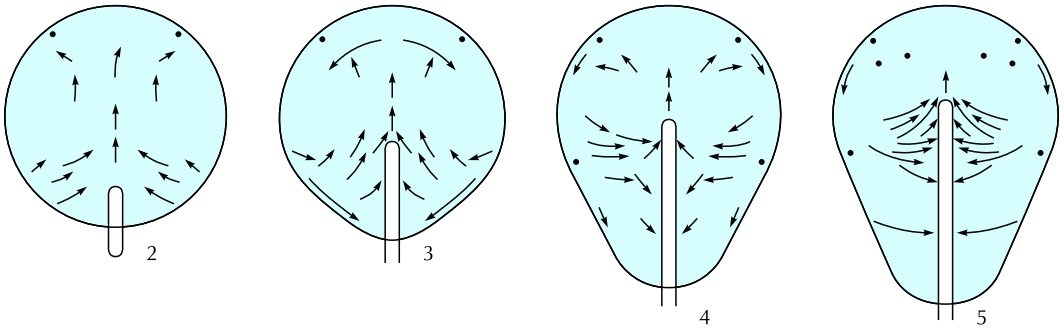

Text-Figure 13. *Gastrulation movements in the upper layer of the area pellucida during formation of the primitive streak and the onset of regression (stages 2–5). (After Vakaet et al. (1980), with permission of Academic Press (Elsevier).)*

1984; *Text-Figure 13*). Modern maps indicate that there is considerable overlap of the prospective fates in these early stages (Hatada and Stern, 1994). This is possible because most, and possibly all, of the cells are not completely determined as yet. They are merely **specified** (labilely determined), as can be shown by transferring small pieces of tissue from a particular region to a foreign environment (e.g. by grafting to the chorioallantoic membrane, or explanting into tissue culture). For example, gut endoderm is capable of developing in explants taken from almost the entire area pellucida of a stage XI to XIII embryo, though normally it forms only from cells of the posterior third of the area pellucida. Hatada and Stern concluded that the cells in the anterior region of the area pellucida are normally prevented from developing into gut endoderm because of influences from neighbouring cells.

By stage 3 the epiblast, now more properly called **the ectoderm,** is a well-defined epithelium, its cells fixed to one another by tight junctions, and underlain by a basal membrane which possesses a 'full range' of basement membrane components (Nakaya *et al.*, 2011).

The Primitive Streak

The formation of the embryonic tissues is dependent on the development of the primitive streak (see *Plates 8b, 9, 10, 11*). It is first visible at about 6–7 h of incubation as a triangular-shaped dark shadow at the posterior end of the area pellucida (stage 2) (Appendix II), or stage IV (Appendix I). It gradually extends further anteriorly until about 13 h of incubation (stage 3+) when it reaches the centre of the area pellucida, and during the next 2 h it achieves its final length. (This is not shown in the Hamburger and Hamilton table in Appendix II, their stage 4 already illustrating the beginning of the next, the head process, stage). The primitive streak is so-called because it appears as a dark double line across the relatively translucent area pellucida. The darkness is due to the large number of cells which have piled up there, waiting to ingress (*Plates 10 and 11*). All the tissues of the embryo will form from these cells, and as they begin to appear, the primitive streak itself disappears (see **Regression**, below).

In a classical experiment, Waddington (1932) showed that if the upper layer (epiblast) of a prestreak embryo was explanted in culture on its own, it failed to form a primitive streak and consequently an embryo. If the lower layer (hypoblast) was present, then a primitive streak could develop. The traditional view, then, was that the primitive streak was induced in the epiblast by the underlying hypoblast. Eyal-Giladi (1991) and her colleagues (e.g. Khaner, 1995), who carried out a series of extirpation and transplantation experiments to test this concept, considered that the hypoblast was derived, at least in part, from the posterior marginal zone (*Text-Figure 9*) and so investigated which regions of the posterior marginal zone were capable of inducing a primitive streak. They found that there was a gradient of potential along the marginal zone in this ability to induce a primitive streak, the posterior part having the highest. If this region is extirpated, then the two lateral marginal regions on either side act as high points and two primitive streaks form. Eyal-Giladi suggested that the formation of a single primitive streak in normal development depends on an interaction between inductive action from the medial posterior marginal zone and inhibitory effects from the lateral marginal zone.

Many investigators have sought to discover the precise source of the supposed inductive region, but the hypothesis that the hypoblast itself is the inductor has now been abandoned. Experiments (Khaner, 1998) implicated Koller's sickle as the critical region in addition to the posterior marginal zone. This is of particular interest because Koller's sickle in birds is thought to be comparable to the Nieuwkoop centre

Downloaded from Vet-eBooks.com

in amphibians. The Nieuwkoop centre is a region of vegetal cells in the amphibian blastula, which lies beneath the mesoderm of the dorsal lip of the blastopore and induces it to become the amphibian organizer of Spemann.

The posterior marginal zone of the chick has many similarities to the Nieuwkoop centre in that it is associated with the induction of the principal organizer region (i.e. Hensen's node), and it expresses genes homologous to those implicated in the Nieuwkoop centre (viz. *Vg1* and *Wn8c;* Bachvarova *et al.,* 1998) and can induce a complete axis from the upper layer (Callebaut *et al.,* 1998; Bachvarova *et al.,* 1998). The ability to carry out this induction is greatest in the region of Koller's sickle, but can occur in the area just posterior to the sickle (Bachavarova *et al.,* 1998; Zehavi *et al.*, 1998).

cVg1 (the chick version of the amphibian *Vg1* gene) is a member of the transforming growth factor (TGFβ) family of signalling molecules. An ectopic primitive streak can be induced in the marginal zone by *cVg1* (Shah *et al.,* 1997), and this is related to the fact that the marginal zone expresses *Wnt8c* (Hume and Dodd, 1993). Skromne and Stern (2001) showed that the area pellucida can also form an ectopic primitive streak in response to *cVg1* provided that *Wnt* is also supplied. Moreover, inhibition of endogenous *Wnt* activity with *Crescent* or *Dkk1* in the marginal zone blocks the axis-forming ability of the *cVg1*.

Other genes that are expressed in the region of the posterior marginal zone and/or Koller's sickle include *goosecoid (gsc), GSX, CNOT1, CNOT2, HNF3*β*, Otx2* and *chordin,* all of which originally have sickle-shaped domains but, as the primitive streak forms, become elongated along it.

Koller's sickle, therefore, contains precursor cells of Hensen's node and of its derivative, the prechordal plate which express characteristic organizer markers. The posterior marginal zone and Koller's sickle do not, however, possess the same ability as the amphibian organizer to induce a complete axis, although they are able to induce a primitive streak.

Formation of the Primitive Streak

Where do the cells of the primitive streak itself come from? Principally, they arise from a population of epiblast cells in the posterior midline (Lawson and Schoenwolf, 2001). Time-lapse cinematography shows that there is a convergence of epiblast cells at the posterior end of the area pellucida towards the midline and then a forward migration (*Text-Figure 13*), and this is supported by transplant studies (Eyal-Giladi, 1991). Further evidence comes from DiI cell labelling experiments (e.g. Hatada and Stern, 1994) between stages X EG and 3HH.

GASTRULATION MOVEMENTS

Gastrulation is the period during which mass migrations of cells take place so that they come to lie in the appropriate positions to embark on the formation of organs and tissues. It begins shortly after the start of incubation with the convergence movements and formation of the primitive streak and includes **Regression** (see below). It continues at the posterior end of the embryo when differentiation has already begun at the anterior end and ceases gradually.

Many experiments have shown that most cells at the primitive streak stages are still able to change their fate and form different tissues. As the mass migrations of the cells take place, the spatial arrangements of the presumptive tissues also change. Therefore, investigations that tell us about the fate maps (see page 19) also reveal the changing patterns of cell migrations. These have been discovered by labelling small areas of their new positions during the following hours. When the results from many experiments of this type are collated, the overall sequences in migration become apparent and, more significantly, the shapes and positions of the presumptive areas at different stages are revealed.

The routes taken by the migrating cells as the primitive streak forms were initially described by Gräper (1929), who labelled small patches of the surface of the blastoderm with vital dyes and followed their movements by time-lapse cinematography. This introduction of cinematography was a significant step in the study of cell migration and has remained the basis for all future work. Filming experiments of this type have been repeated with modifications, sometimes *in ovo* like Gräper's, but usually on embryos transplanted *in vitro* and with increasingly sophisticated labelling techniques. For example, Vakaet (1984) based their findings on the careful analysis of xenoplastic grafts of quail cells (see Chapter 2) followed by time-lapse cinematography and a histological analysis of the fate of the quail cells. The maps obtained were very similar to those of earlier authors (e.g. Pasteels, 1937) who used vital dyes to label their cells. A criticism of the technique, however, is that Vakaet's grafts may have included cells from several layers, and so the movements may have reflected more than just the superficial layers.

Downloaded from Vet-eBooks.com

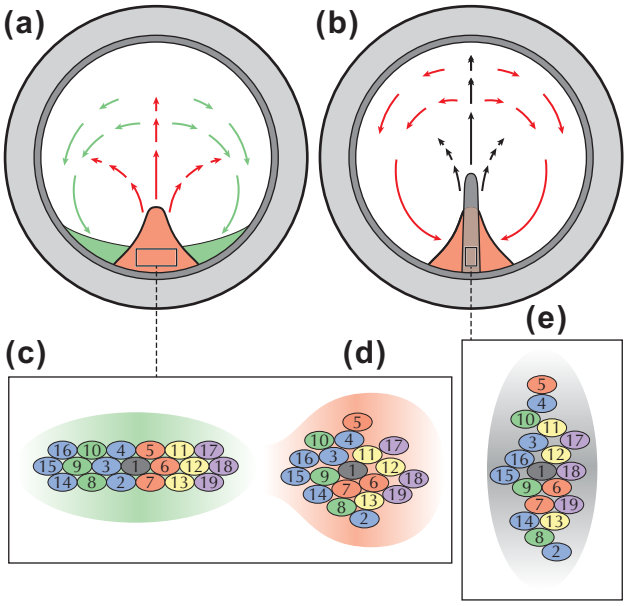

Text-Figure 14. *Cell rearrangements driving primitive streak formation. (a) Stage XII. (b) Stage 2. (c, d, e) enlargements of the regions illustrated in colour in (a) and (b) showing the intercalation of the cells in these regions. (From Voiculescu et al. (2007), with permission of Nature Publishing.)*

Nevertheless, they provide us with a general picture of the pattern of the cell migrations at this time.

The results of the different authors have not always been identical in detail, but throughout there has been a general agreement that there is a convergence of cells from both the left and right lateral borders of the area pellucida toward the mid-posterior region (the region of Koller's sickle), and that from here the cells move anteriorly to form the primitive streak (*Text-Figure 14*). There is also some movement of cells from the anterior end of the area pellucida towards its lateral borders, so that the general effect is of a swirling pattern, this being known as a 'Polonaise' movement, a charming reminder of the popular Victorian dance (Gräper, 1929; Voiculescu *et al.,* 2007). Yanagawa *et al.* (2011) found that if they inhibited *Nodal* in the early embryo, the morphogenetic migrations in the epiblast, including the Polonaise movement, were disturbed.

The cell migrations not only lead to the formation of the primitive streak, but they also are the cause of its structure. Its typical appearance is as two darkened lines extending at full length three quarters of the way across the area pellucida (*Text-Figure 15*). In transverse section the lines can be seen as two ridges, the primitive ridges, each made up of many cells (*Text-Figure 16*; these are cells that are waiting to ingress (see below). Between the ridges is a less dense region, the primitive groove.

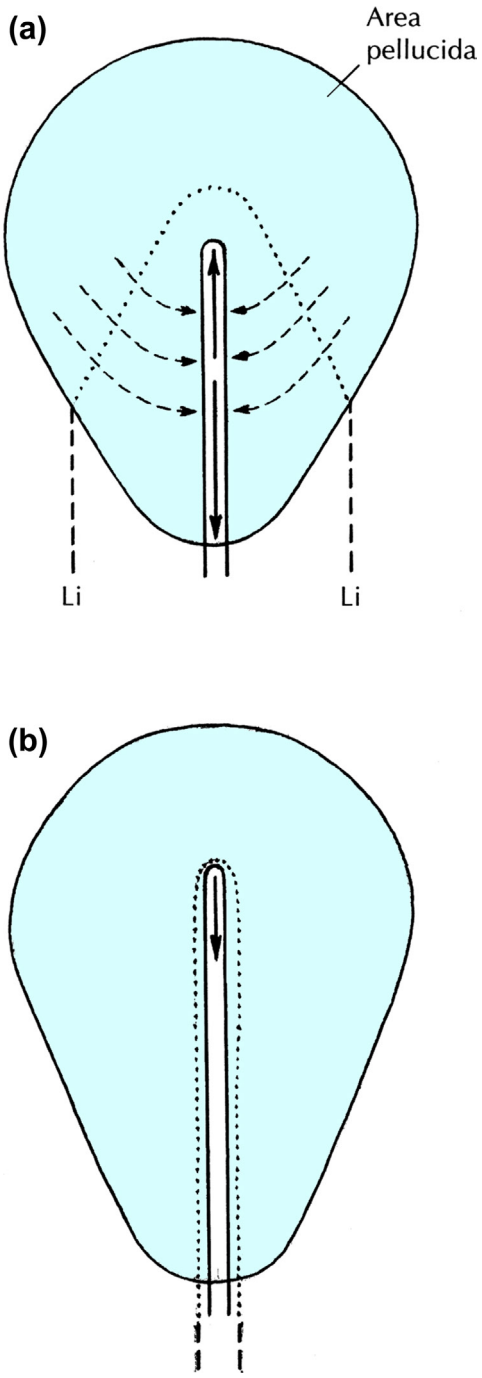

Text-Figure 15. *Gastrulation movements in the area pellucida of the chick embryo. (a) During formation of the primitive streak: convergence movements in the upper layer are shown as curved broken arrows. Their action results in the cells moving towards the midline where they pile up as paired primitive ridges. Li = limit of the area that will ingress. The area pellucida has become pear-shaped because of the stretching of the primitive streak along its length (shown by arrow on the primitive streak). (b) During regression: the major movement is from anterior to posterior. (After Vakaet (1984), with permission of Academic Press (Elsevier).)*

Downloaded from Vet-eBooks.com

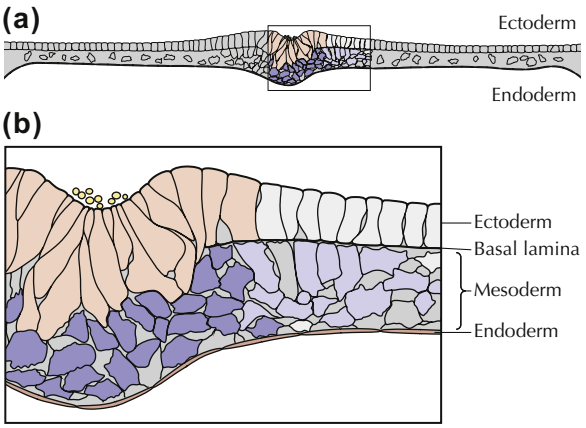

Text-Figure 16. *Transverse section through the anterior end of the primitive streak. (a) The entire width of the area pellucida. (b) Enlargement of the rectangle indicated in (a). The basal lamina in the area of ingression (pink) has begun to disappear. Some of the cells have lost their epithelial structure and become mesenchymal (blue). The earliest cells to have ingressed have migrated further laterally and formed mesoderm (mauve).*

We have seen (see page 22) that when the primitive streak starts to form it appears as a dark triangle at the posterior end of the area pellucida (see stage 2 of Appendix II), but as the convergence movements gather momentum, the left and right sides of the triangle become pushed closer together, forcing the cells into the two primitive ridges. Meanwhile the apex of the triangle moves further and further anteriorly in the epiblast so that the streak acquires its characteristic appearance. Its anterior tip, Hensen's node (alternatively known as the primitive node or knot) marks the culmination of the convergence movements. Many of the presumptive areas come to lie around Hensen's node (*Text-Figures 17, 18,* and *19*).

Initially, there is no clear groove in the primitive streak, though, as the migrating cells continue to converge and pile up, the developing streak becomes narrower and the groove deeper (*Plates 10 and 11*). According to Hatada and Stern (1994), the convergence begins between stages XI and XIII in the epiblast and some of the cells that will contribute to Hensen's node have reached the centre of the blastoderm before the primitive streak starts to form. A second migration of cells is then initiated at stage 2 when the lower layer moves forward. The first population of cells is destined to give rise to the prechordal mesendoderm, the notochord and some somite cells, whereas the second gives rise mainly to definitive endoderm. By stages 3+/4 most cells of Hensen's node express the organizer markers, *chordin,* HNF3β and *goosecoid.*

The primitive streak elongates by extending not only anteriorly, but also posteriorly (Harrisson *et al.,* 1988) so that the posterior end eventually moves into the area opaca, causing the area pellucida as a whole to become pear-shaped.

Much work has been centred on the mechanisms by which the orderly sequences of migration are controlled, especially during the formation of the primitive streak. One possibility is that there is a morphological gradient perhaps of the extracellular materials, and that the migrating cells are attracted away from Koller's sickle, whilst a second idea is that there is a high level of mitosis in Koller's sickle, forcing cells forward. Cui *et al.* (2005) found there was no good evidence to support either of these theories, but there was instead a higher level of cell division at the lateral borders of the area opaca and concluded that this was the source of the cells that ultimately formed the primitive streak, though 'it does not drive it'. It should be remembered, however, that this region of greater proliferation may also help to feed the expanding area opaca.

There is evidence that changes in the shapes of the cells as well as their relation to one another may play a role. In particular, the cells become spindle-shaped. Films by Voiculescu *et al.* (2007) show that at stage XIII the epiblast cells in, and adjacent to, the site where the primitive streak will begin to form (the central posterior region of the area pellucida) become spindle-shaped and are oriented at right angles to the future primitive streak. Once the streak starts to appear, the cells in this region re-orientate so that they now lie along the antero-posterior axis of the blastoderm; films show that intercalation occurs (i.e. the cells become inserted between one another) so that gradually the epiblast cells in this region become rearranged. They have proposed that local intercalation is responsible for, and shapes, the primitive streak. Labelling of individual cells or small groups of cells with dyes such as DiI (see Chapter 2) has provided evidence that many of the cells do not necessarily remain in the same relationship to one another during gastrulation. Moreover, the clear-cut boundaries between the different presumptive areas illustrated in the fate maps of earlier investigators are no longer acceptable

The formation of the primitive streak depends, at least in part, on the underlying hypoblast, a tissue that emits large amounts of fibronectin (Sanders *et al.* 1978). There is evidence from many investigators (e.g. Hardy *et al.,* 2008*)* that Wnt may also have an essential role. Voiculescu *et al.* (2007) found that rotating the hypoblast affected the polonaise movements and that this was associated with an increase in the expression

Downloaded from Vet-eBooks.com

of Wnt planar cell polarity (Wnt-PLC). But, although the routes followed during the cell migrations have been consistently mapped, we still do not know how the cells are driven to follow their characteristic polonaise pattern.

Once the posterior marginal zone and Koller's sickle have become established, the antero-posterior and left–right polarities of the embryo are apparent. As the primitive streak develops, the left and right sides become more clearly visible, although they will not be fully determined until a sequence of molecular differences become active on the two sides. These appear to be set in train as Hensen's node develops. Up to this point, the *sonic hedgehog* gene has been active on both sides, but now it ceases to be expressed on the right side. The basic features are that the left side expresses *sonic hedgehog* and *lefty-1*, but the right side is prevented from doing so by activin signalling. A cascade of molecular events on the left side results in the activation of the *pitx2* gene and the suppression of *snail,* whilst a different cascade on the right side leads to the activation of *snail.* Intracellular calcium enrichment on the left side of Hensen's node may also play a role (Garic-Stankovic *et al.*, 2008). Recently, however, Dathe *et al.* (2003) have reported that by the time that the asymmetric expression of these molecules is apparent, Hensen's node already shows some morphological differences between the left and right sides. It seems likely, therefore, that the critical events occur before Hensen's node is visible.

By the time the primitive streak is fully formed, at about 18 hours of incubation, it has reached the stage shown in (*Plate 9a*). This stage was ommitted from the table of Hamburger and Hamilton and is intermediate between their stages 3+ and 4. It is usually designated as 4–, the definitive streak stage. Hensen's node is the thickened tip of the primitive streak. Migration of the epiblast cells toward the primitive streak has now ceased and ingression is about to begin. This is the process in which the cells leave the primitive streak and migrate away from it to give rise to the definitive endoderm and the mesoderm

INGRESSION AND CELL MIGRATION AWAY FROM THE PRIMITIVE STREAK

We can now consider the morphogenetic events in the primitive streak itself. All the presumptive areas, apart from the definitive endoderm, are arranged in the epiblast before they ingress through the primitive streak. **Ingression** is the process by which the cells leave the epiblast and become part of the primitive streak before migrating away from it to give rise to the definitive endoderm and mesoderm. (The term 'invagination' is no longer considered appropriate to describe the passage of cells through the primitive streak since it implies the formation of a cavity, such as the archenteron of the amphibian embryo. No cavity is associated with the primitive streak). The cells lose their epithelial character and become mesenchymal as they enter the primitive streak, and this appears to be largely due to a change in cell surface carbohydrates (Sanders, 1991). *Plate 10* shows sections through the primitive streak and the region lateral to it viewed by light microscopy, whilst *Plate 11* illustrates similar regions by scanning electron microscopy. Subsequently, most of the cells become arranged in epithelia again as they are transformed into specific tissues. These tissues are: (1) the definitive **endoderm,** which will form the lining of the gut and the respiratory system; (2) the head process and **notochord;** (3) the paraxial **mesoderm** (somites), the intermediate mesoderm (which forms the urino-genital system) and the lateral plate mesoderm (which becomes the lining of the coelom and contributes to the extra-embryonic membranes. Thus, there is a sequence of morphological changes in most cells as they pass through the primitive streak from epithelial to mesenchymal and back to epithelial. Some of the processes involved are outlined by Chuai and Weijer (2009). A further derivative of the ectoderm is the neural crest (see page 40).

Before ingression the epiblast is an epithelium, its identity being maintained by tight junctions and a basal lamina, but these both become disrupted as the cells ingress (Nakaya and Sheng, 2009). The basal lamina disappears from the epiblast in the region of the primitive streak, and the individual cells lose their epithelial character (*Text-Figure 16*). The microtubules become rearranged and changes occur in gene expression (Chuai and Weijer, 2009).

A number of fate maps have been produced for the endoderm, the earlier ones being based on simple labelling of the early tissues with carbon particles (Bellairs, 1953), or grafts of tritiated thymidine (Rosenquist, 1971), or chick–quail transplants (Fontaine and Le Douarin, 1977), which, although differing in detail, agree in placing the presumptive endoderm around Hensen's node.

Recently, more sophisticated approaches have expanded our knowledge. Chapman *et al.* (2007), using mainly *in situ* hybridization techniques of putative endoderm marker genes, especially Sox 17, Gata 5 and 6, were able to map the origin of the endoderm from Koller's sickle up to stage 4.

Downloaded from Vet-eBooks.com

Fate maps of different regions of the future gut were published by Lawson and Schoenwolf (2003) and by Kimura *et al.* (2006). The two sets of maps do not cover precisely the same time periods, but although there is a general agreement on the major finding that the endoderm ingresses through the anterior end of the primitive streak, they differ in that those of Lawson and Schoenwolf include the origin of the mesodermal tissues, whilst those of Kimura *et al.* are concerned with the migrations of cells to form the individual regions of the gut (i.e. foregut, midgut and hindgut) as well as the dorsal, medial and lateral regions.

Whilst the primitive streak is still forming, and before ingression begins, the blastoderm is still two-layered, the lower layer being principally the hypoblast. As the cells ingress from the primitive streak into the lower layer, they intercalate with the hypoblast cells (Lawson and Schoenwolf, 2003). Those hypoblast cells that lie beneath the anterior tip of the extending primitive streak at stages 2/3 become displaced laterally, and eventually give rise to the extraembryonic endoderm (Sanders *et al.*, 1978; Kimura *et al.*, 2006).

The first of the definitive endoderm cells to enter the lower layer directly at stage 3 contribute to the mid- and hind gut, and at stage 3+ to the dorsal foregut; cells that contribute to the ventral foregut, however, pass through the middle layer of Hensen's node and then migrate laterally before entering the lower layer at a point between the dorsal and lateral foregut (*Text-Figure 10*). The ingression of the mesoderm cells does not take place until after that of the endoderm, and is related to the process of regression (see Chapter 4).

One of the immediate consequences of gastrulation is that the initially two-layered embryo (consisting of the upper (epiblast) and lower layers) has become converted into a three-layered one, composed of ectoderm, mesoderm and endoderm. This is the result of cell migration, and there is no evidence to suggest that it is due to any high level of cell proliferation in the primitive streak or in the cells that migrate from it (Sanders *et al.,* 1993).

There is some disagreement whether the paths taken after ingression are controlled by the cells themselves or by their environment. According to Garcia-Martinez and Schoenwolf (1992), cells migrating out from pieces of anterior primitive streak which have been grafted into a posterior position follow a more lateral pathway than if they had been left *in situ,* whereas cells from grafts that had been implanted into a more anterior position follow a more medial pathway. They concluded, therefore, that the extent of migration depended on the position of the cells within the primitive streak. By contrast, Psychoyos and Stern (1996) found that the migrating cells followed pathways that depended more on the tissue that they would form rather than on their position within the streak; they plotted the migration routes for the major tissues.

With the expansion of our knowledge of the genes that are active during this period, there has been an extensive reworking of many of the older experiments in an attempt to relate molecular changes to distribution and differentiation of individual tissues. For example, the gene *chordin* is associated only with the notochord and may therefore be used as a marker for it. Some genes are expressed widely throughout the early blastoderm but then 'disappear' or become restricted to a specific region; for example, *cGata2* is strongly expressed in the epiblast at stages X–XIII but disappears abruptly at stage 3+ and a new domain subsequently appears at stage 4 in the prospective non-neural ectoderm (Sheng and Stern, 1999). Others appear faintly at first in the region that will become a specific tissue and then slowly increase in intensity as the tissue differentiates. In such cases it may be difficult to determine whether the gene is responsible for the differentiation of the tissue or is merely expressed as the tissue differentiates, and it is important under these circumstances to try to remove the gene product to see if the tissue is able to differentiate without it.

Now that the whole chick genome has been sequenced, many genes are being found to be active during gastrulation and it is not always clear what role they play in development. There can be little doubt that few, if any, of them act alone. Most, if not all, probably have antagonists that suppress them, and it seems likely that many need to act synergistically with other genes to bring about differentiation.

There is much evidence that changes in **cell surface receptors** and their relationships to the extracellular materials play an essential role in cell migration. The most important glycosaminoglycan (GAG) in the extracellular material is hyaluronic acid, accounting for 80–90% of the total GAG (Sanders, 1989). Collagen type IV is present in the basement membrane of the epiblast, but the interstitial collagens (II, III and IV) do not appear to play a role at this time. It is possible that after leaving the primitive streak at least some of the migrating cells use the basal lamina beneath the ectoderm as a guide. This does not appear to be so in the earlier stages as the primitive streak is forming since, according to

Downloaded from Vet-eBooks.com

Zamir *et al.* (2008) who studied early quail embryos by time-lapse cinematography, both the epiblast and its associated extra-cellular matrix migrate together. Similarly, after ingression, when a more substantial extracellular matrix has formed, it appears to remain as a 'composite meshwork' carried along by the associated cells. Other cells seem to crawl over one another, and it is therefore not surprising that the extracellular matrix glycoprotein, fibronectin, plays an important role. The peptide of fibronectin that is most concerned with cell adhesion is the RGD sequence, which binds to receptors on the cell surface and will do this even if the remainder of the fibronectin molecule is absent, but not if the sequence of the amino acids is changed (e.g. to GRD). When GRD or antibodies to the fibronectin receptor were applied to the gastrulating embryo, the adhesive qualities of the fibronectin were seriously decreased or eliminated and the migration of the mesoderm cells was greatly reduced (Brown and Sanders, 1991). FGF (Lunn *et al.*, 2007; Chuai and Weijer, 2009) and PDF signalling (Yang *et al.*, 2008) also play a role in the migration of mesoderm cells.

Growth factors are also involved in the transition from epithelial to mesenchymal morphologies. TGFβ1 becomes increasingly expressed in the mesoderm cells as they migrate laterally away from the primitive streak, and appears to reinforce the factors responsible for the conversion from epithelium to mesenchyme (Sanders and Prasad, 1991).

Specification, Determination and Commitment of the Germ Layers

Traditionally, the way to discover whether a tissue can develop only according to its presumptive fate is to transplant it to another region of the embryo or to explant it to a different environment. If it does develop according to its original presumptive fate, we say it is now **determined** (or **committed**). If it does not, we say it is merely **specified** (or to use an older term, labilely determined). Within the last few decades, however, the process has been supplemented and refined by investigating whether it continues to express the same genes. Once the definitive endoderm cells have ingressed, they appear to be committed to remain as endoderm (Chapman *et al.*, 2007). They therefore owe their fate to their position in the blastoderm, only those that lie around the anterior end of the primitive streak forming definitive endoderm. Until they ingress, they are not determined, and perhaps not even specified.

Expansion of the Blastoderm

At the time of laying, the chick blastoderm measures about 5–8 mm in diameter and has embarked on the process of **epiboly**, the spreading of an epithelial sheet in which the cells become flattened and increase their surface area. In birds, the blastoderm eventually comes to cover almost the entire yolk, and most of the active migration is by cells at the edge of the blastoderm.

In the unincubated egg the blastoderm lies freely on the surface of the yolk, but after about 12 h of incubation it has become attached to the inner surface of the vitelline membrane. Under normal circumstances, however, the attachment is limited to the periphery of the blastoderm, and a special relationship appears to exist between the edge cells (also known as the margin of overgrowth) and the inner surface of the vitelline membrane (*Plate 2*). New (1959) showed that the young blastoderm is unable to expand if its edge is detached from the vitelline membrane, although if it is allowed to reattach, migration continues. Some migration can take place if the edge cells are explanted onto other substrates, such as glass, but expansion is slower. The edge cells are largely responsible for exercising a degree of tension throughout the blastoderm and if this is not maintained, abnormal or stunted embryos develop (Bellairs *et al.,* 1967). Kucera and Burnand (1987b) have calculated that the tension is of 1–1.2 × 10^4 dyn/cm^2 and is generated by radial contraction of the cells of the area opaca.

The edge cells are a specialized extension of the area opaca ectoderm and are therefore epithelial. The extreme tips of these cells consist of filopodia and, when studied by time-lapse filming, they can be seen to undergo ruffled membrane activity as they move across the inner surface of the vitelline membrane (Bellairs *et al.,* 1969). They are rich in microtubules, and if treated with Nocadazole, a microtubule inhibitor, these become disassembled and migration ceases (Mareel *et al.,* 1984). Microfilaments also play a role since, if these are disrupted by treatment with cytochalasin B, migration ceases (Chernoff and Overton, 1979). Fibronectin too is important in the relationship between the edge cells and the vitelline membrane (Lash *et al.,* 1990). Although the diameter of the blastoderm increases as it expands over the upper half of the yolk, the edge cells do not undergo cell division (Monnet-Tschudi and Kucera, 1988); rather, there is a band of rapidly mitosing cells lying proximally to them (Flamme, 1987), which may contribute to the population of edge cells.

Downloaded from Vet-eBooks.com

Chapter 4

Establishment of the Embryonic Body

When the primitive streak is fully formed (stage 4, *Plate 9*), the first stages of gastrulation are complete and the tissues that will develop into the body are arranged around its anterior end. During the next 12 h they will be transformed into a basic embryonic axis consisting of ectoderm, including neural plate and neural crest, notochord, somites, lateral plate and intermediate mesoderm, and endoderm. Steps in these changes are illustrated in:

- Normal Tables in Appendix II.
- selected stages of whole-mounted embryos (e.g. *Plates 9, 13, 14*).
- selected stages of whole-mounted embryos seen by scanning electron microscopy (*Plates 15–59*).
- histological sections (*Plate 60 et seq.*).

The key structure in the primitive streak stages is **Hensen's node** (alternative names are primitive node or primitive knot and, more recently, chordoneural hinge by Charrier *et al.,* 1999), the anterior tip of the primitive streak, where the primitive groove ends in the primitive pit and is enclosed anteriorly and laterally by the swollen primitive folds (*Plates 9, 10*). It corresponds in many ways to the dorsal lip of the blastopore in amphibians. One of the most famous and influential experiments ever performed on an embryo was that of Spemann (1938), who grafted a piece of tissue from the dorsal lip of an amphibian blastopore into the flank of a similar embryo of the same stage of development, which resulted in a second axis forming in the host embryo. It became apparent that the graft had influenced the host tissues adjacent to it to form an embryo, and Spemann concluded that the dorsal lip of the blastopore possessed special properties which enabled it to 'organize' the other tissues around it to form an embryonic axis. The dorsal lip of the gastrula therefore became known as the 'organizer'. Subsequently, it was shown by Waddington (1932 and later, summarized by Waddington, 1952) that the same sort of activity occurred in birds. He demonstrated that if Hensen's node was extirpated, stripped free of any adherent lower layer and implanted beneath the ectoderm at the edge of the area pellucida of another embryo, it was able to induce a secondary axis consisting of neural tube, gut and somites. It soon became apparent, moreover, that the ability to induce a secondary axis was not restricted to Hensen's node, but was present also in at least the anterior third of the primitive streak (Waddington and Schmidt, 1933), although the power to bring about an induction of neural tube was found to be greater in Hensen's node than in any other part of the primitive streak (see below for neural induction). A major characteristic of Hensen's node is that it expresses the chick homeobox-containing gene, *goosecoid* (*gsc*) (Izpisúa-Belmonte *et al.,* 1993). This gene was initially derived from a *Xenopus* blastopore dorsal lip cDNA library, and is therefore considered as a marker for the organizer region. Its presence in Hensen's node emphasizes the analogous organizer roles of the amphibian dorsal lip and chick Hensen's node. An important finding of Izpisúa-Belmonte *et al.* was that *goosecoid* is first expressed in a restricted region of middle layer cells in Koller's sickle, implying that these cells are the precursors of Hensen's node.

By the time the primitive streak is fully formed, the main presumptive areas lie clustered around its anterior end and it now expresses a range of markers. For example, in addition to *goosecoid,* it expresses HNF3β, *Otx2,* ADMP, FGF8 and *chordin*, though some (e.g. *goosecoid, Otx2,* ADMP and FGF8) are no longer expressed after stage 4. At later stages Hensen's node expresses other genes, such as *sonic hedgehog*, *noggin* and *nodal.*

Detailed fate maps for stages 3–4 have been published by Selleck and Stern (1991) and Garcia-Martinez *et al.* (1993). Selleck and Stern's (1991) fate maps of Hensen's node were based on DiI labelling of

The Atlas of Chick Development. http://dx.doi.org/10.1016/B978-0-12-384951-9.00004-6
Copyright © 2014 Elsevier Ltd. All rights reserved.

Downloaded from Vet-eBooks.com

small groups of cells and lysine–rhodamine–dextran labelling of single cells. They concluded that the node consists of several clearly defined regions (*Text-Figure 17*), each possessing its own presumptive fate. By stage 4 all the definitive endoderm has ingressed (*Text-Figure 11*) and the node contains only the mesoderm and that part of the presumptive neural plate that will form the floor plate. By stage 5 the presumptive notochord region has become narrower in the midline, since many cells have ingressed to form the head process and the notochord.

The lateral folds of Hensen's node give rise to the medial halves of the somites, whilst a separate region of primitive folds posterior to the node forms the lateral half of each somite. The fate map of Selleck and Stern was limited to the primitive streak, but Garcia-Martinez *et al.* (1993) published a map of the entire area pellucida ectoderm at stage 4, based on the results of chick–quail transplantation experiments (*Text-Figure 18*).

Other maps include:

- the location of the presumptive heart rudiments in the primitive streak at stages 3–4 (Garcia-Martinez and Schoenwolf, 1993);
- the early neural plate (Bortier and Vakaet, 1992);
- the primitive streak (Psychoyos and Stern, 1996) (*Text-Figure 19*) and the mesoderm (Sawada and Aoyama, 1999 (*Text-Figure 20*); Lopez-Sanchez *et al.* (2001);
- a spinal cord fate map at regression stages (Catala *et al.*, 1996);
- tail bud (Le Douarin, 2001) (*Text-Figure 21*).

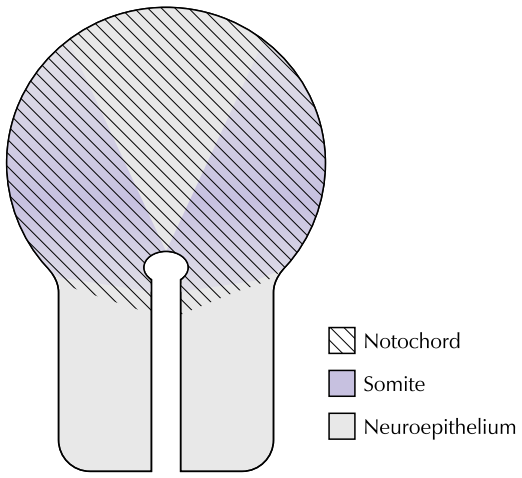

Text-Figure 17. *Fate map of the tissues in Hensen's node at the fully grown primitive streak stage (stage 4-). (After Selleck and Stern (1991), with permission of The Company of Biologists Ltd.)*

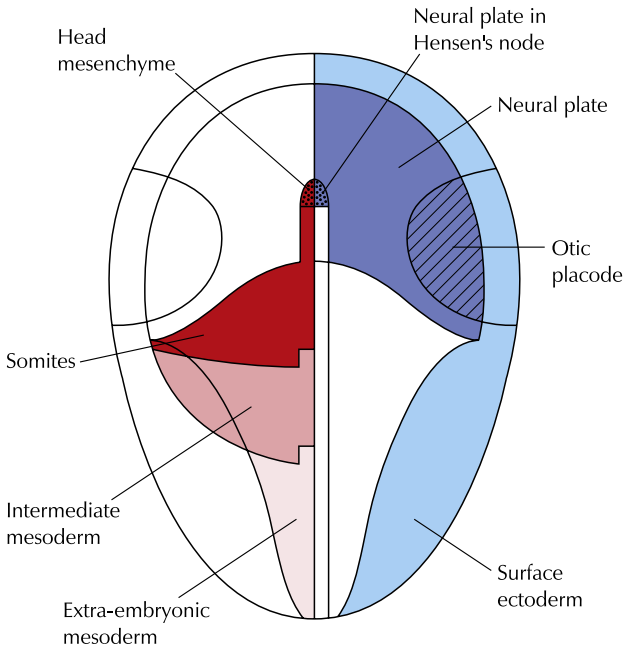

Text-Figure 18. *Fate map of the ectoderm and primitive streak at about stage 4 to show the layout of the presumptive areas. (After Garcia-Martinez et al., 1993; reprinted by permission of Wiley-Liss, Inc., a subsidiary of John Wiley and Sons, Inc.).*

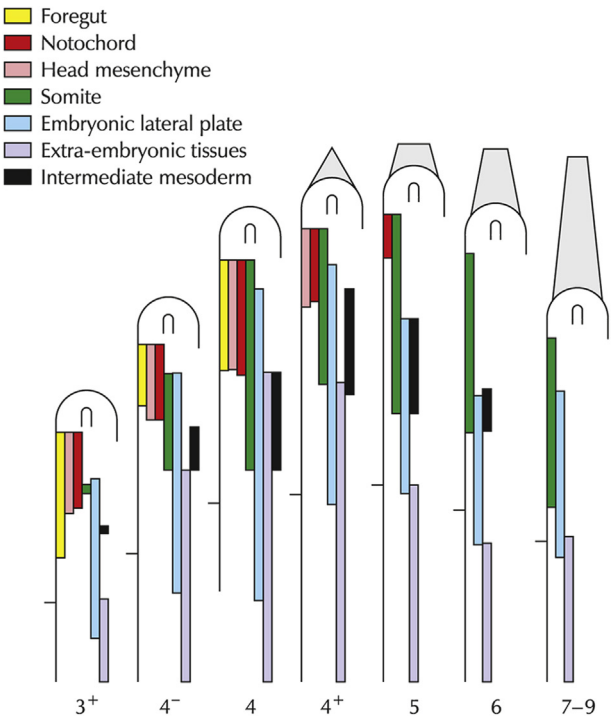

Text-Figure 19. *Fate maps of the primitive streak, summarising the relative antero-posterior positions of the precursors of the main tissue types along the axis. The prospective cell types are shown side-by-side for clarity, but this should not be taken to imply any defined medio-lateral position in the diagram. (After Psychoyos and Stern (1996), which should be consulted for further details. Reprinted with permission of The Company of Biologists Ltd.)*

Downloaded from Vet-eBooks.com

Until about stage 4– most of the mesoderm cells are as yet uncommitted to their individual fates, but the presumptive notochord cells, situated in Hensen's node and the anterior end of the primitive streak, appear to be totally committed to form notochord. The evidence comes from a wealth of experiments in which tissues are transplanted from one region to another of the embryo (e.g. Selleck and Stern, 1992; Garcia-Martinez and Schoenwolf, 1993). The cells in most of the grafts were able to ignore their presumptive fate and develop according to their new position, but the presumptive notochord cells appeared to be able to form only notochord.

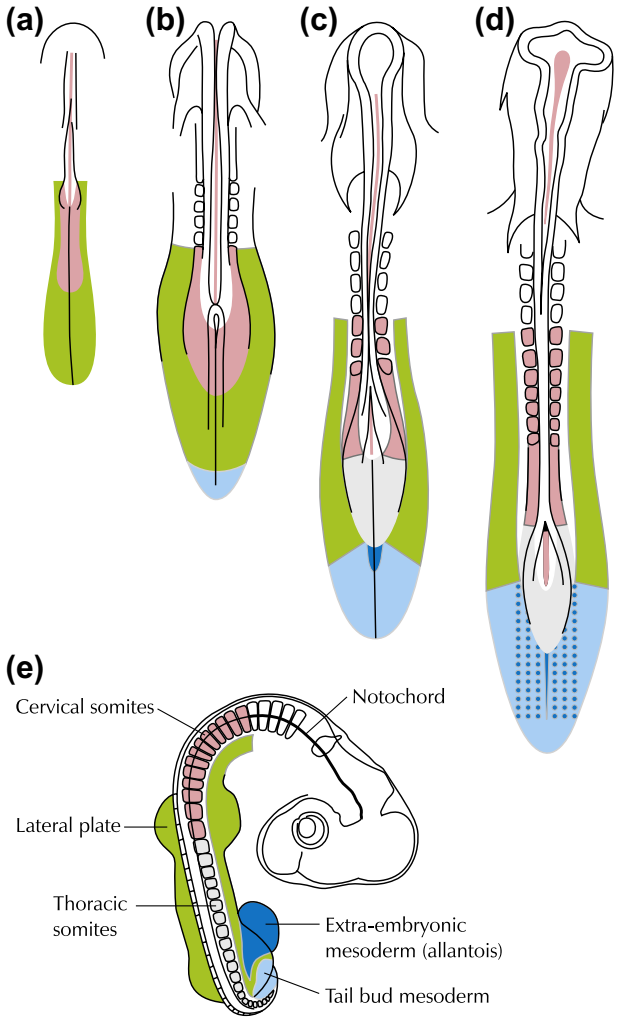

Text-Figure 20. *Fate maps of the mesodermal cells of the primitive streak between stages 6 and 20. (a) Stage 6; (b) Stage 8; (c) Stage 9; (d) Stage 10; (e) Stage 20. (After Sawada and Aoyama (1999), with permission of UBC Press.)*

HEAD PROCESS AND REGRESSION

In the fully formed primitive streak (stage 4) ingression has ceased and the presumptive areas are grouped around its cranial end (see above). As regression occurs, they become rearranged to lie along the future body axis (*Text-Figure 22*). The presumptive notochord cells in Hensen's node and the anterior primitive streak give rise to the **notochord** proper, a rod of cells running along the length of the embryo. The most anterior part of this rod is the **head process** (*Plate 13*); it is formed by the anteriorward migration of cells from Hensen's node, whereas the trunk notochord is formed by the caudalward movement of cells during the process of regression. The first appearance of the head process is as a small dark triangle anterior to Hensen's node at stage 4 (Appendix II). The onset of regression initiates the start of the disappearance of the primitive streak. Differentiation of the tissues takes place gradually from anterior to posterior as regression occurs, so that the development of the anterior tissues is always in advance of the posterior ones. Wnt5a appears to promote the migration of cells from the posterior end of the primitive streak, which will form lateral plate mesoderm, whilst Wnt3a opposes this action at the anterior end of the primitive streak in the cells that will become somites (Sweetman *et al.*, 2008).

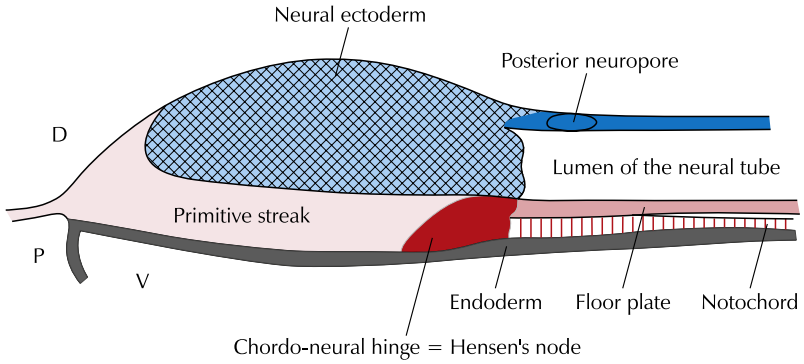

Text-Figure 21. *Fate map of the tail bud of the quail at a stage of about 26 somites (corresponding to about stages 15–16 of the chick). D = dorsal; P = posterior; V = ventral. (From Le Douarin (2001), with permission of UBC Press.)*

Downloaded from Vet-eBooks.com

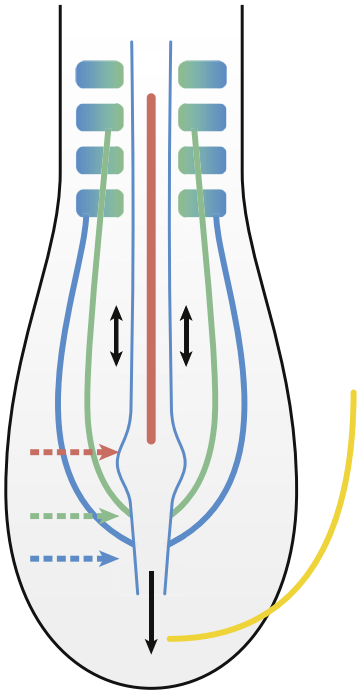

Text-Figure 22. *Cell migration patterns during regression. Anterior primitive streak cells migrate to form the medial part of each somite (pale green), whilst posterior streak cells migrate out to become the lateral part of each somite (blue). The yellow line indicates the origin of the cells that migrate into the extra-embryonic area to become blood islands. The regression of Hensen's node is indicated by the black arrow, the trail of notochord that has been left by this process is shown in red. (After Chuai and Weijer (2009), with permission of Elsevier.)*

The **head process** is more clearly visible at stage 5 (*Plates 13, 14* and Appendix II). It must be distinguished from the **prechordal mesoderm**, which lies anterior to it and does not form notochord. Like the head process it is derived from Hensen's node, but there is evidence to suggest that TGFPs from the underlying endoderm repress the notochord characteristics (Vesque *et al.,* 2000). The loose mesenchyme which later appears on either side of the head process is known as the **head mesenchyme**, and is critical in the formation of the head muscles and skull (see Chapter 10).

A major event in development is the conversion of the flat, almost 2-dimensional, embryo into a rounded, 3-dimensional one. The first visible event is the appearance of the **headfold**. This is a tuck in the ectoderm which pushes beneath the head process and prechordal mesoderm and lifts the head above the area pellucida. It begins to form at about stage 6 and has become clearly visible by stage 7 (see *Text-Figures 50 and 52*). Varner *et al.* (2010) provided experimental and computational evidence that shape changes in the neural plate, active cell shape changes at the anterior border of the neural plate, as well as shape changes in the non-neural plate ectoderm all played a role in the formation of the headfold.

There has been much confusion over the term **regression**. Essentially, it describes the gradual disappearance of the primitive streak, which shortens from anterior to posterior as the presumptive mesodermal tissues ingress and leave it, but it is also used to describe a series of morphogenetic movements that take place at this time. The main feature is that most of the presumptive notochord cells leave Hensen's node and become deposited as a trail of notochord cells down the body (*Text-Figure 19*). There is recent evidence to indicate that the floor plate of the neural tube and a longitudinal strip of endoderm are deposited at the same time (Catala *et al.,* 1996; Le Douarin, 2001) (*Text-Figure 21*). The individual cells of the notochord become greatly elongated by the stretching and extension of the area pellucida, which occurs at this time. It is, however, not only the presumptive notochord and floor plate tissues that are affected by the regression movements. Other presumptive tissues that are still within the primitive streak (*Text-Figures 19 and 20*) also become extended. The morphogenetic movements involved in node regression also take place to a lesser extent in the regions lateral to the primitive streak, so that all the presumptive areas become elongated along the body axis.

THE TAILBUD

By about stage 11 the remnants of Hensen's node and the primitive streak lie at the posterior end of the area pellucida, and by stages 13–14 have become a clump of cells, the *tailbud,* which lengthens until about stage 25 (4–5 days) (Griffith *et al.*, 1992). The tailbud becomes undercut by the *tail fold* (*Text-Figure 51*). Examination of the tail bud at these stages show a mass of mesoderm enveloped by ectoderm (*Plates 31b, 72*). This mesoderm is not a homogeneous collection of cells. Using grafts from transgenic chick embryos, McGrew *et al.* (2008) showed that a population of mesodermal progenitor cells is present in the tailbud, the descendants of which contribute to the somitic mesoderm, the notochord, and the neural tube. Their destination seems to depend on their position within the tailbud.

The tailgut, which is continuous with the hindgut, also forms from the tailbud mesenchyme (Griffith *et al.*, 1992).

Downloaded from Vet-eBooks.com

With the formation of the tailfold the remnant of the primitive streak and Hensen's node becomes shifted to the ventral side of the tailbud where it forms a thickened ridge, the *ventral ectodermal ridge.* It is thought that the cells probably continue to ingress (Ohta *et al.*, 2007) since there is no basal lamina beneath the ventral epidermal ridge to enable it to remain as an epithelium, and this may be due, at least in part, to the inhibition of BMP signaling, which is normally associated with epithelial/mesenchymal transformations as the cells pass through the primitive streak (Ohta *et al.*, 2010). Ingression ceases at about stages 21 to 24 (Ohta *et al.*, 2007).

There has recently been much consideration whether the tailbud is a secondary organizer (i.e. a signaling centre) comparable with the primary organizer (i.e. Hensen's node) or the apical epidermal ridge of the limb bud (Griffith and Sanders, 1991). Knezevic *et al.* (1998) demonstrated by means of tail grafting experiments that the tip of the tailbud has residual organizer-like properties, being able to recruit cells to overcome their presumptive fate and become neural. Ohta *et al.* (2007, 2010) proposed that the ventral ectodermal ridge is the signaling centre for the tailbud and that it regulates that part of the ectoderm that is not, at least initially, underlain by a basal lamina, and so regulates the tail length. They suggested that the expression of *Nog* genes adjacent to the ventral ectodermal ridge inhibits Bmp signaling in the tailbud, which in turn suppresses the ridge and leaves to a formation of basal lamina, and so regulates the tail length. They concluded that the expression of *Nog* genes adjacent to the ventral ectodermal ridge inhibits Bmp signaling in the tailbud, which in turn suppresses the ridge and leads to formation of the basal lamina.

The structures that develop from the tailbud are continuous with those that form in the main part of the body, though some of the developmental processes differ. The tail neural tube does not form by a rolling up of the ectoderm into a tube, but by cavitation of a solid mass of mesenchyme (secondary neurulation). Similarly, although the foregut and hindgut both form by folding, the tail gut develops by cavitation of the mesenchyme. By the time the tailbud starts to regress the neural tube and notochord have reached the tip of the tail, but the somites never do so; the terminal tailbud mesoderm never becoming segmented (Sanders *et al.*, 1986; Bellairs and Sanders, 1986). Eventually, the tail gut and the tail somites are overcome by cell death and disappear. According to Le Douarin (2001) cell death in the tail is due to the absence of adjacent structures secreting *sonic hedgehog* protein, and the tissues can be rescued if *sonic hedgehog-secreting* tissues are implanted. Fate maps of the tail bud are illustrated in *Text-Figures 21 and 24*.

NEURAL INDUCTION

The presumptive neural plate at stage 3+ to 4− is an extensive area of epiblast lying over and around Hensen's node (*Text-Figures 17 and 18*), anteriorly, posteriorly and laterally. The evidence comes from experiments of many authors in which small areas of the ectoderm have been labelled and traced to their destinations (e.g. Pasteels, 1937; Rosenquist, 1966; Garcia-Martinez *et el.* 1993). According to Garcia-Martinez *et al.* it extends 0.5 mm posterior to Hensen's node. Before the primitive streak has formed the presumptive neural plate region lies at the posterior end of the area pellucida either within Koller's sickle (*Text-Figure 9*).

By the time the primitive streak is fully formed the ability of the ectoderm to form neural plate extends beyond the presumptive neural plate region. There is ample evidence that if a small piece of ectoderm, together with its underlying mesoderm, is taken from almost anywhere in the anterior half of the area pellucida at stage 3 and isolated (even on the chorioallantoic membrane; see page 129), it can give rise to neural tissue.The underlying cells are necessary for this to happen, so we say that they induce the neural tissue.

For many years after the organizer region was discovered in amphibians, attempts were made to identify the supposed chemical nature of a signalling molecule, but it was not until about 70 years later that molecular biological techniques began to make possible an understanding of a very complex process involving a cascade of interacting molecular events. The earliest signals appear to originate in the hypoblast (reviewed by Streit and Stern, 1999; Wilson *et al.*, 2009). A body of information began to be acquired about the interacting genes and their products in early vertebrate embryos. The sequencing of the entire chick genome opened up a new range of molecular markers (especially the definitive neural markers, *SOX3,* and *ERI*) in stage 3 embryos. It had long been suspected that the hypoblast was the source of neural induction, but Albazerchi and Stern (2007) and Bertocchini and Stern (2008) found that although the hypoblast could indeed induce a group of markers (especially the definitive neural markers, *SOX* and ER1) in stage 3 embryos they were transitory in nature, and that there was no real evidence that they were responsible

Downloaded from Vet-eBooks.com

for neurulation. By contrast, there is considerable evidence that FGF signalling plays a major role in neural induction (Albazerchi and Stern, 2007; Karabagli *et al.*, 2002). The problem has proved to be a highly complex one, not least because of the difficulty of identifying the first critical steps in the process and deciphering the important reactions occurring both within the inducing tissue and the induced. For further clear reviews see Wittler and Kessel (2004) and Stern (2005). The epiblast loses its ability to respond to induction between stages 4 and 4+ (Darnell *et al.,* 1995), the three main signalling molecules, FGF, Wnt, BMP apparently playing significant roles. FGF does not act directly but has an essential role (as an antagonist for BMP), and can induce the transcription factor SOX2, which is expressed throughout the neural plate. The region where BMP4 and two of its antagonists, *chordin* and *noggin*, are active appears to be the boundary between neural and non-neural ectoderm. Streit and Stern suggested that the main functions of *noggin* at this stage may be in somite formation, by protecting the prospective somite cells from the inhibitory actions of BMPs, whilst *chordin* is primarily involved in axis formation. Two markers, *ERNI* (early response gene for neural induction) and *Sox3* (a similar early response gene), are induced by Hensen's node (as well as other neural inducters such as head process mesoderm), and each may, therefore, be used as an early marker for neuralising activity. Streit and Stern (1999) found that when cells from the middle layer of Koller's sickle were grafted into the area opaca of a primitive streak stage embryo, which is a region that would not normally form neural tissue, both *ERNI* and *Sox3* were induced. Markers for later development of the neural tissue were, however, not induced unless epiblast from the centre of the area pellucida was also included. These authors, therefore, suggested that neural induction is initiated before the start of gastrulation by signals (FGF signals) from a small population of organizer precursor cells in Koller's sickle, and that when these cells spread anteriorly and make contact with a second precursor population centre (in the middle of the area pellucida epiblast), the two groups of cells interact with one another to produce a functional organizer; this then leads to a cascade of reactions, including the sensitisation of the epiblast to the BMP antagonists. Interestingly, transplantation experiments indicate that the inducing ability is restricted to the medial region of Hensen's node, and is not present in the deep portion of the posterior-lateral part (Storey *et al.,* 1995).

By the time that the neural tube has formed it already possesses a dorso-ventral polarity (see below).

FORMATION OF THE NEURAL PLATE AND NEURAL TUBE

At the end of neural induction the embryo possesses a thickened region, the neural plate, which subsequently rolls up to form the neural tube. The individual cells of the neural plate become narrower at the apical surface; evidence from transmission electron microscopy suggests that this is due, at least in part, to the contraction of microfilaments (see *Text-Figure 23*) which appear to act like purse strings drawing the apices together. At about the same time the neural plate cells elongate, an event which is associated with a reorientation of the microtubules.

Initially there is no sharp morphological border between the cells of the neural plate and the adjacent ectoderm, the height of the epithelium changing gradually in the transitional zone. If this transitional zone is removed, the neural plate is unable to form neural folds (*Plates 10 and 13)* and remains flat (Moury and Schoenwolf, 1995). The traditional view is that the neural plate is induced from Hensen's node, even though some neural plate formation can take place in its absence. The inducing ability of the various subpopulations of the node was investigated by Storey *et al.* (1995). After grafting carefully selected small populations of cells into an extra-embryonic

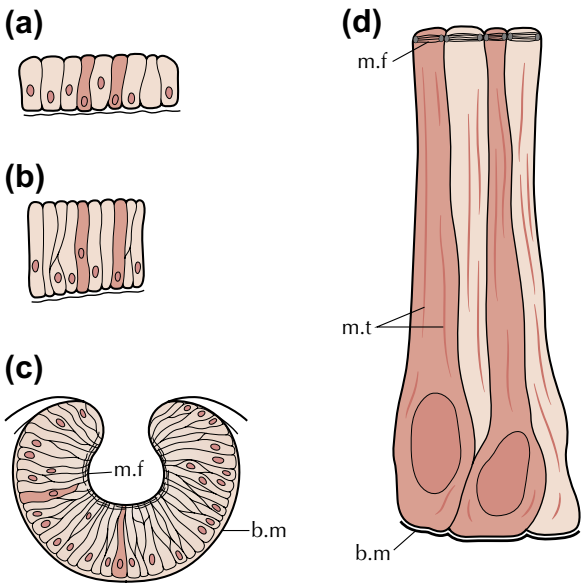

Text-Figure 23. *A: Transverse section through ectoderm prior to neurulation. B: Cells have become elongated. C: Microfilaments have contracted at the apical surfaces of the cells resulting in the rolling up of the neural plate. D: Enlargement of part of C. To show the nuclei at the basal side of the neural tube, the microtubules which play a role in the elongation of the cells, and the microfilaments. bm: basal membrane; mf: microfilaments; mt: microtubules.*

Downloaded from Vet-eBooks.com

site beneath ectoderm that would not normally form neural plate, they concluded that the neural inducing ability was associated not only with specific regions of Hensen's node, but also with certain types of cells.

After the neural plate has formed, the morphogenetic movements of **regression** lead to a narrowing and posterior extension of the trunk region, and about this time there is a widening of the brain area. These regression movements are accompanied by dramatic changes in the shapes and arrangements of the cells, the epidermal cells becoming flatter and the neural cells deeper. The notochord is attached to the floor plate (the floor of the neural plate) (*Plate 71)* and acts as a hinge about which the neural plate folds and bends to form a tube (Schoenwolf and Smith, 1990). The floor plate expresses HNF3β and is probably induced by the notochord, since grafts of notochord can induce an ectopic floor plate which expresses HNF3β (Ruiz I Altaba *et al.,* 1995). According to Catala *et al.* (1995), the notochord and floor plate express so many genes in common that they should be considered as the same tissue.

Theories about the possible mechanisms involved in the process of neural folding are discussed by Moury and Schoenwolf (1995) and by Lawson and Schoenwolf (2001), who emphasise that neurulation, especially neural plate formation, is a multifactorial process resulting from forces both intrinsic and extrinsic to the neural plate. Changes in the tenascin component of the cells are associated with changes in cell shape, whereas changes in the cell membranes are involved in the increasing adhesion of the cells to one another.

Fusion of the neural folds begins at about stage 8 at the level of the midbrain, and is rapidly followed by fusion throughout the entire brain and the anterior regions of the trunk. The final point of fusion in the brain is the anterior neuropore (*Plate 14),* which is obliterated at about stage 12. The neural tube closes progressively down the trunk until by about stage 9 or 10 the process is almost complete and an opening remains only at the posterior end, the sinus rhomboidalis or the neural crest, which by stage 13 has become the posterior neuropore. As the neural folds fuse, the cells of the neural crest (see below) come to lie at its dorsal side. The ectoderm that is not enclosed within the neural tube subsequently becomes the epidermis.

The dorsoventral patterning of the neural tube is brought about by the interaction of at least two major gene products, ventralization by *sonic hedgehog* protein from the notochord, and the dorsalizing influence results from BMPs probably secreted by the ectoderm (Patten and Placzek, 2002).

The way that the neural tube forms in the tail bud (see page 33) is designated **secondary neurulation** to distinguish it from the rolling up of the neural plate described above, which is sometimes called **primary neurulation.** In secondary neurulation, mesenchyme cells on the dorsal side of the tail bud become condensed into an epithelial-like rod, which then separates off from the remaining tissues and becomes hollowed out. This mesenchyme lies in the epiblast caudo-medially to Hensen's node at stage 8, but becomes drawn further posteriorly into the tailbud during further development) (*Text-Figure 24*). A region of overlap occurs where the so-called **primary neural tube** of the trunk gives way to the secondary neural tube of the tail (*Plate 87*). The secondary neural tube forms the lumbo-sacral and coccygeal region of the spinal cord (Griffith *et al.*, 1992).

Transverse sections through the early neural tube of the trunk region show that it possesses thick walls (*Text-Figure 25; Plates 17, 19*); these will give rise to both the neurones and glia. The dorsal and ventral regions of the tube, the roof plate and floor plate, respectively, become narrower than the lateral walls with wedge-shaped cells, and form neuroglia only.

REGIONALIZATION OF THE NEURAL TISSUE

We have seen that in addition to the cells forming the notochord and head process, several other types of cells originate in Hensen's node. These are the **definitive endoderm,** which gives rise to the gut, the **mesendoderm** cells, which pass anteriorly to lie beneath the anterior-most end of the node and contribute to the gut and prechordal plate mesoderm, and the lateral cells, which contribute to the somites. Initially, it is difficult to identify the types of cells as they leave the node since, morphologically, they are indistinguishable from one another. For this reason they are often collectively, but confusingly, called mesendoderm cells. The ability of Hensen's node to induce neural tissue is lost when the mesendoderm cells have left it (Storey *et al.,* 1992).

Markers for the forebrain are *GANF*, *CNOT1* or *Nkx2.1*, which are normally expressed in the neural plate as it forms (Boettger *et al.,* 2001), though they can be induced experimentally by grafts of the mesendoderm. Grafts taken from the region of

Downloaded from Vet-eBooks.com

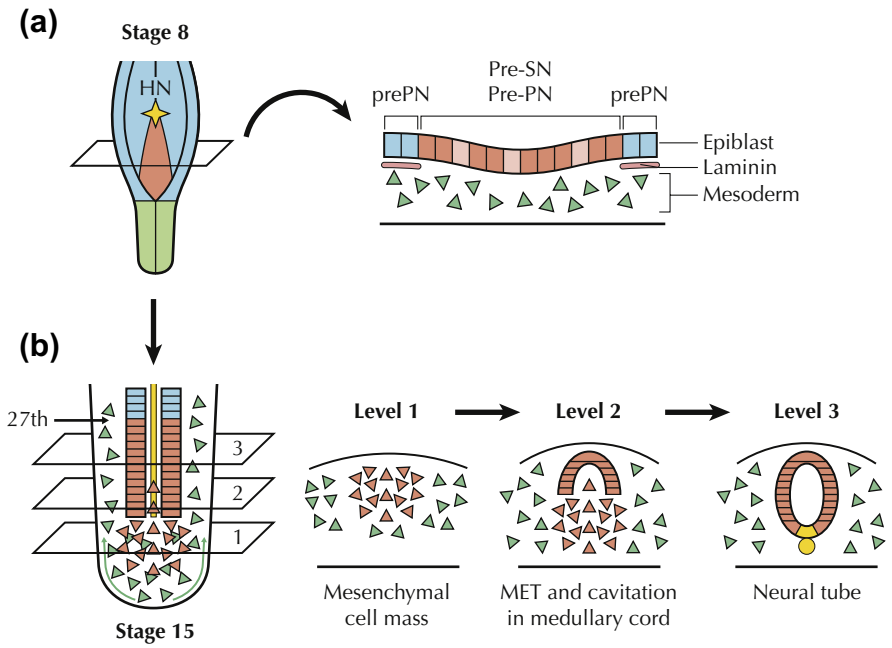

Text-Figure 24. *Fate maps of precursors of secondary neurulation.* ***Stage 8:*** *The ectoderm (red) posterior to Hensen's node gives rise to secondary neural tissue (SN); the primary neural tissue (PN) is shown in light blue. The primitive streak (green) gives rise exclusively to mesoderm.* ***Stage 15:*** *Cells that have ingressed from the pre-SN region form a mesenchymal cell mass at the posterior tip of the neural tube. These cells progressively undergo epithelialisation. (From Shimokita and Takahashi (2011); reproduced with permission of John Wiley and Sons.)*

the primitive streak just posterior to Hensen's node are still able to induce neural plate, though not forebrain. It appears therefore that the forebrain is not established at the time of neural induction, but is probably induced at the anterior end of the neural plate when it becomes underlain by the underlying mesendoderm.

Foley *et al.* (2000) put forward a model to explain forebrain patterning. They found that the migrating hypoblast induced the expression of early forebrain markers (*Sox3* and *Otx2*) but was unable to induce forebrain. They suggested that a role of the hypoblast was to direct the cell movements in the overlying epiblast so that the prospective forebrain was removed from the caudalizing effects of the node.

There are a large number of other genes involved in regionalization of the neural tube. For example, the homeobox gene *cDix* is restricted to the presumptive ventral forebrain region of the neural plate that ultimately gives rise to the hypothalamus and adenohypophysis (Borghjid and Siddiqui, 2000). By the time that the neural tube has formed it already possesses a dorso-ventral polarity. *Sonic hedgehog* secreted by the notochord and floor plate is important in specifying ventral telencephalic cells (Gunhaga *et al.,* 2000). The response of the neural cells to *sonic hedgehog* can be altered *in vitro* by BMP signals causing cells that would have become ventral to change into dorsal-type cells (Liem *et al.,* 2000).

FORMATION OF THE NOTOCHORD AND SOMITES

The notochord and somites are structures that are found only in the early embryo and are not present at later stages.

The **notochord** (*Plate 19, 20*) plays a critical role in development. As we have seen above, it is derived from Hensen's node and is formed as regression takes place. It occupies a central position running down the length of the body and during its early stages is closely adherent to both the floor plate of the neural tube and to the underlying endoderm. The notochord is important in the dorso-ventral patterning of the neural tube. We have seen above that the notochord expresses *sonic hedgehog* protein, which has a ventralizing effect on the neural tube. But it also has a ventralizing effect on the somites. Subsequently, the neural tube and notochord become encased in the vertebrae (see Chapter 10), and the remnants of the notochord survive as the nucleus pulposus in the intervertebral discs.

The *somites* (*Plates 21, 22*) are paired blocks of mesoderm that form in a row on either side of the

Downloaded from Vet-eBooks.com

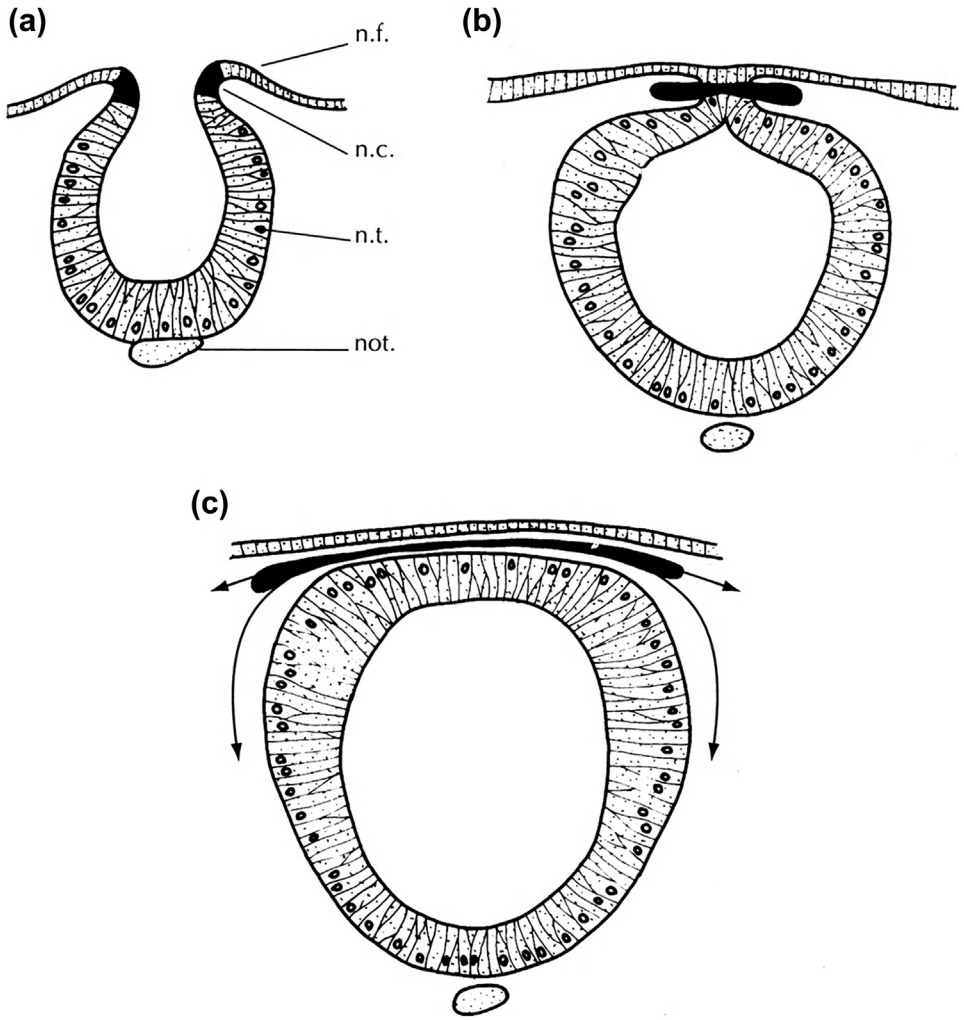

Text-Figure 25. *Sections through the neural tube at three consecutive stages to illustrate the origin of the neural crest. Arrows show the paths taken by the migrating neural crest cells. n.c.: neural crest; n.f.: neural fold; n.t.neural tube; not: notochord.*

notochord. They are the first segmented structures to develop in the embryo, and their layout influences that of all the other segmental structures that form subsequently; these are the vertebrae and ribs, the cranial and spinal nerves, the vertebral arteries and the skeletal muscles and ligaments.

The mesoderm that will give rise to the somites lies around the anterior end of the primitive streak at about stages 3–4 (*Text-Figures 18, 19*), including the lateral edges of Hensen's node, and probably starts to ingress soon afterwards. Cells pass into and through the primitive streak and then migrate laterally, passing between the ectoderm and the endoderm, usually keeping to the same side of the embryo, although occasionally individual cells may enter the primitive streak on one side and then leave on the contra-lateral side. Some of the ingressing cells become lateral plate mesoderm, others intermediate mesoderm and the remainder (nearest the neural plate) give rise to the segmental plate (sometimes called pre-segmental plate or even unsegmented paraxial mesoderm) mesoderm (*Plates 8, 17, 62*) from which the somites will form. The term paraxial mesoderm is sometimes applied as a joint description of the somites and segmental plate. The fate of any cell is determined (committed) soon after leaving the primitive streak and appears to be brought about by the relative concentration of several signals. There is a high concentration of TGFβ-like molecules, especially BMP4, in the lateral plate. (This region corresponds to the ventral region of amphibian embryos and so the effect of BMP4 is said to be a ventralizing one.) The node, meanwhile, produces *noggin* protein, which is an antagonist of BMP4 and so plays a role in preventing the pre-somitic mesoderm from developing into lateral plate (Streit and Stern, 1999). The interplay of these and other signals is discussed by Pourquié (2001). Aulehla and Pourquié (2008) suggest that oscillations may also be important in the development of limb outgrowth and neural progenitor maintenance, though they are

Downloaded from Vet-eBooks.com

careful to point out that no underlying core oscillator has yet been identified.

As the cells leave the primitive streak, two major morphogenetic movements are occurring in the mesoderm. These are the medio-lateral migration of the newly ingressed cells and the antero-posterior movements associated with regression, and it seems likely that these two streams of migrating cells interact with one another (discussed by Ooi *et al.,* 1986).

The first pair of somites appears at about stage 7, and succeeding pairs are laid down sequentially further and further posteriorly (*Plate 60*). The cells that will become somitic mesoderm enter the segmental plate as they leave the primitive streak. The left and right segmental plates lie on either side of the neural tube (*Plate 72*), and each consists of a strip of condensed mesoderm. They are easy to dissect from other tissues, especially if the embryo is treated for about 15 min with 1% trypsin in calcium- and magnesium-free saline. The cells at the posterior end of the segmental plate are mesenchymal, whereas those at its anterior end are arranged as an epithelial ball. Groups of cells at the anterior end of the two segmental plates become separated off simultaneously to form the left and the right of a pair of somites. Each newly formed somite is a ball of columnar epithelium, the walls consisting of a single layer of cells (*Plate 22*) surrounding a cavity, the **somatocoele**, which contains mesenchyme cells. Iimura *et al.* (2007) have suggested that the lateral part of each somite is formed from cells that ingress during the process of regression.

A new pair of somites forms from the anterior end of each segmental plate about every 90–100 min, but meanwhile a steady stream of mesenchyme cells is being added to the posterior end of the segmental plate. As a result the segmental plate remains visible, although there is a continual turnover of the individual cells which constitute its population. Between stages 10 and 18 it possesses the equivalent of about 10 pairs of somites (Packard and Meier, 1983). Once the cells have entered the segmental plate they are committed to becoming part of a somite. Differentiation into somites takes place gradually along the segmental plate as the original mesenchyme cells become arranged into an epithelium and, in appropriate preparations, it is possible to see part-formed somites (named **somitomeres** by Meier (1979)). Although best seen by scanning electron microscopy, the somitomeres are also visible in segmental plates that have been dissected from the embryo and viewed by light microscopy. The order in which the somites form establishes the order in which they lie in the body, the first formed giving rise to anterior structures, such as thoracic vertebrae and head muscles, whilst the somites formed later develop into more posterior structures.

Two genes that have been implicated in initiating epithelialization of the somites are *paraxis* (Sosic *et al.,* 1997) and *Epha-4* (Schmidt *et al.,* 2001), the latter gene, at least, being probably induced by signals from the adjacent ectoderm. More recently, mathematical modelling has been applied to the problem of how cells become rearranged during epithelialisation (Kulesa *et al.,* 2007).

As the cells gradually become arranged into epithelia, their cell-to-cell adhesiveness increases, the most anterior somite compacting immediately before segmenting off from the segmental plate. This increased adhesiveness appears to be brought about, at least in part, by the action of the glycoprotein, fibronectin (Lash *et al.,* 1984) (*Text-Figure 26*), which increases in concentration as the somitomeres mature along the segmental plate. This can also be brought about experimentally by the synthetic peptide, GRGDS, which corresponds to the adhesive segment of fibronectin (Lash *et al.,* 1987). Protogenin, an immunoglobulin protein, has been shown to be expressed on the surface of the future somatic mesoderm cells as they ingress (Ito *et al.* 2011); an over-expression of protogenin delayed the mesoderm migration by increasing cell-to-cell adhesion. Each newly segmented somite contains about 2,500 cells (Christ and Ordahl, 1995).

Before molecular biological experiments were possible, one of the greatest problems in embryology was that of explaining the underlying causes of segmentation. What causes a strip of tissue, the segmental plate, to become broken up into a repeating series of somites? Another way of looking at the same problem is to ask, 'What causes the boundaries between somites to be established?' And why does

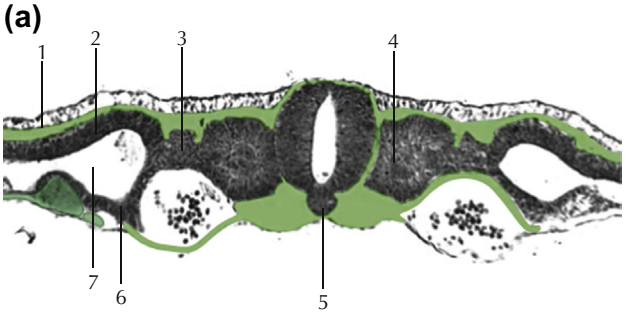

Text-Figure 26. *Transverse section of a 13-somite embryo through somites to show extracellular material, mainly fibronectin (coloured green). 1. Ectoderm; 2. Somatic lateral plate mesoderm; 3.intermediate mesoderm; 4. Somite; 5. Notochord; 6. Splanchnic mesoderm; 7. Coelomic cavity.*

Downloaded from Vet-eBooks.com

this take place step-by-step from the anterior to the posterior end of the developing embryo? Although a number of alternative theories were proposed in the past, the concept that oscillating genes control the process is now widely accepted. This idea was first put forward in a theoretical paper by Cooke and Zeeman (1976) and is now supported by modern molecular evidence (Pourquié, 2001). Members of the *Notch* signalling cascade, especially *lunatic fringe,* appear to be essential components in setting up the oscillatory clock as well as Wnt and FGF (Gomez and Pourqié, 2009). For recent reviews of other molecules involved in segmentation, see Stockdale *et al.* (2000) and Pourquié (2011).

Traditionally, the somites are numbered sequentially from the anterior to the posterior end of the embryo, which corresponds to the sequence in which they form. An alternative scheme for the numbering of somitomeres and somites was devised by Ordahl (1993), the aim being to provide a standard description of the developmental state of each somitomere and when comparing different stages. For example, the most recently formed somite of a 13-somite embryo (stage 11) and that of a 26-somite embryo may be considered comparable. Although there are certain advantages to this scheme, they are probably overshadowed by the possibilities for confusion generated, especially as it involves the numbering of the somites from posterior to anterior. In general, therefore, it is probably best to use this scheme only under very specialized circumstances.

The number of somites that develop depends on the species. In the chick it is about 52. The most caudal somites form in the tail, but somite formation ceases at about stage 24 before all the available mesoderm is exhausted, a small amount remaining at the tip of the tail arranged in two bands, which correspond topologically and morphologically to the segmental plate in the trunk (Mills *et al.*, 1990). It appears that the somite oscillator ceases about this time, at least partially due to a restriction of *Notch* activity, but according to Tenin *et al.* (2010) may also be due to endogenous retinoic acid in this region suppressing the oscillators Wnt3a and FGF8). This is unlikely to be the whole story, however, since other changes occur at this time; in particular, a patch of cell death appears in the tail bud (Schoenwolf, 1981; Mills and Bellairs, 1989), which may be of significance.

Individual somites appear to be rectangular or globular (*Plates 21, 22*) in shape when seen from the dorsal or the ventral side, but transverse sections show them to be wedge-shaped, the medial wall being curved to the shape of the neural tube. Their shape is largely dependent on the tension exerted by the collagen fibrils in the extracellular matrix that surrounds them and attaches them to the adjacent epithelia, the ectoderm, endoderm, notochord and neural tube (Veini and Bellairs, 1990; Chernoff *et al.,* 2001). A mass of extracellular material, including fibronectin (*Text-Figure 26*), is now conspicuous. The earliest somites are formed before the neural tube has rolled up completely, and have a flattened shape (*Text-Figure 45a*). As the neural tube closes, the somites apparently become drawn upwards and acquire the more familiar shape seen in transverse sections (*Text-Figure 45b*). Longitudinal sections show each somite as an epithelial ball of cells with walls one cell thick and centred around a lumen (*Plate 22*). Mesenchymal cells are present in the lumen.

Each newly formed somite consists of two main regions, the medial and lateral, each divided anterior and posterior (*Text-Figure 72*). The medial portion is derived from a stem cell population in Hensen's node, which is drawn posteriorly during regression, and the most anterior part of the primitive streak, whilst the lateral part originates in cells that ingress through the primitive streak during regression (Chuai and Wejer, 2009; Iimura *et al.*, 2007). Experiments in which regions of the chick segmental plate have been replaced with the corresponding tissue from quail embryos have shown that the fates of the cells, or groups of cells, depend on their position along the segmental plate.

One of the first visible changes in the mature somite is that the basement membrane in the medio-ventral region breaks down and the cells lose their epithelial character and become mesenchymal (*Plate 71*). They are the **sclerotome** cells. The change in the ventral wall of the somite releases the cells within the somitocoele, and these also become part of the sclerotome.

A further change follows as the epithelium at the dorso-lateral side increases in height and is then known as the **derma-myotome** (often spelled dermomyotome). In longitudinal sections it can be seen as a cap with its edges curved inwards (*Plates 23b, 71*); it gives rise to the dermatome and myotome. The sclerotome and the derma-myotome are formed almost exclusively from the cells of the medial half of each new somite, the derma-myotome from the dorsal part, the sclerotome from the ventral region. The cells of the lateral part of the somite migrate away to form the muscles of the limbs and probably of the ventral body wall (see Chapter 10). There is evidence that this medio-lateral patterning of the somites is the result of a cascade of molecular signals. The neural tube

Downloaded from Vet-eBooks.com

produces *Wntl,* which promotes *noggin* expression in the medial part of each somite, and this antagonizes the BMP4 which is produced by the lateral plate mesoderm (Hirsinger *et al.,* 1998). The patterning of the somites as they segregate into different regions involves many more molecular changes (reviewed by Stockdale *et al.,* 2000). The dorso-ventral patterning appears to be brought about principally by *sonic hedgehog* and *Wnt* signalling, whilst antero-posterior polarity is due to *notch.*

The anterior and posterior regions of the somite are separated from one another by a distinct gap, **von Ebner's fissure** The spinal nerves are able to enter the anterior half of each somite but not the posterior half.

The first myotome cells form in the anterior-medial region of the somite from the edge cells of the derma-myotome. By the time they have extended into the posterior half of the somite they have already begun to produce muscle proteins and are, therefore, probably already determined, though experiments have shown that the sclerotome cells are not (Dockter and Ordahl, 2000). Once the myotome has formed it becomes separated from the dermatomal component of the somite by a basement membrane. Later in development, dermatome cells migrate dorsally to become the dermis.

THE LATERAL PLATE MESODERM AND THE INTERMEDIATE MESODERM

The **lateral plate mesoderm** arises from the posterior region of the area pellucida and ingresses through the primitive streak, eventually spreading out to reach the edge of the area opaca and then continuing into this region as extra-embryonic mesoderm. As the lateral plate mesoderm migrates away from the primitive streak it becomes replaced by the ingressing somitic mesoderm. Similarly, as Hensen's node regresses caudally it comes to lie in the site formerly occupied by the presumptive lateral plate mesoderm, which now shifts laterally. Sweetman *et al.* (2008) suggested thatWnt3a and Wnt5a are involved in promoting and/or inhibiting these movements. The contribution from the primitive streak to the lateral plate ceases at about stage 10/11 (Knezevic *et al.*, 1998). Unlike the somitic mesoderm, the lateral plate is not segmented, but by stage 4 is present as two sheets, the somatic layer, which lies beneath the ectoderm (together forming the bilaminar sheet, the somatopleure) and the splanchnic layer, which lies over the endoderm (together forming the bilaminar layer, the splanchnopleure) (Text- Figure 35 and at a later stage *Plates 65, 72*). They are separated by a space, the future coelom (see Chapter 8). The development of the lateral plate appears to be linked in some ways to the somites. For example, *Epha-4* is expressed both in the lateral edge of the somites and in the lateral plate mesoderm and, as discussed above, the BMP4 produced by the lateral plate affects somite development. The lateral plate mesoderm subsequently forms the mesenteries, the lining of the pleural, cardiac and abdominal cavities, and the major substance of the heart, as well as contributing to the extra-embryonic membranes.

The **intermediate mesoderm** lies between the somites and the lateral plate mesoderm, to both of which it is initially attached (*Plate 65*). It appears at the same time as the somites and develops simultaneously with them from anterior to posterior down the trunk, but it differs from the somites in that it is not overtly segmented and does not extend into the postcloacal tail. It later forms most of the urino-genital system (see Chapter 7).

THE NEURAL CREST

Like the notochord and somites, the neural crest is found only in the early embryo and is not present at later stages. It is, as its name implies, a strip of cells situated along the dorsal side of the early neural tube, forming a 'crest' down its entire length (*Plate 24a,b*). Its former name, ectomesenchyme, is descriptive of its origin and fate rather than of its position, in that it is an ectodermal derivative that gives rise to a wide range of mesenchymal structures. There is extensive literature on the neural crest, including excellent reviews by Gammill and Bronner-Fraser (2002), with emphasis on the migration of specific neural crest cells, and Harris and Erickson (2007) and Kuo and Erickson (2010), with especial attention to gene profiles.

The neural crest arises from a broad crescent-shaped area in the gastrula ectoderm which is characterized by BMP4 expression (Ezin *et al.*, 2009). It originates from the ectoderm at the junction of the non-neural ectoderm and the presumptive neural ectoderm (Selleck and Bronner-Fraser, 1995) and there is evidence that the two tissues interact to induce it. Dickinson *et al.* (1995) found that neural crest could be induced from neural plate in culture either by ectoderm or by two proteins secreted by the ectoderm (BMP4 and 7). These two proteins induce the expression of *slug* protein and *Rhob* protein in the cells which become neural crest, and in the absence

Downloaded from Vet-eBooks.com

of either one of them the neural crest cells fail to leave the neural tube. Even the extra-embryonic ectoderm can be induced to form neural crest (Ruffins and Bronner-Fraser, 2000). *Rhob* is involved in the production of cytoskeletal elements that are needed for migration (Hall, 1999). The non-neural ectoderm remains able to induce neural crest from the neural ectoderm until about stage 10, though the neural plate loses its ability to respond after about this time (Basch *et al.,* 2000). These authors found that the marker, *slug,* was present in the neural folds even by the end of gastrulation, and suggested, therefore, that neural crest induction involves a series of stages. The gene, *lunatic fringe,* which is expressed in the neural tube but not in the neural crest cells, also plays a role, since excess *lunatic fringe* results in excess proliferation of neural crest cells at least in the cranial region (Nellemann *et al.,* 2001).

The neural crest is first visible as a thickened region just before the neural tube closes (*Text-Figure 25*). Its formation and subsequent development follow the normal anterior to posterior sequence. Three major regions of the neural crest (*Text-Figure 27*) are usually recognized:

1. **Cranial neural crest**, which lies anterior to the somites and gives rise to skeletal structures of the face, melanocytes, neurons, ganglia and glial cells.
2. **Vagal neural crest**, which is associated with somites 1–7, and includes the **Cardiac neural crest**, at somite levels 1–3, gives rise to enteric neurons of the gut, melanocytes, etc., as well as components of the heart.
3. **Trunk and tail neural crest**, which lies posterior to somite 8 and includes the **Adrenal neural crest** at somite levels 16–24.

There are differences in the behavior of neural crest cells from, and within, these different regions as they migrate, as well as in their eventual differentiation.

As the neural tube closes, the neural crest becomes lodged between it and the overlying ectoderm (*Text-Figure 25*), and as the three tissues separate from one another the neural crest cells settle down onto the dorsal surface of the neural tube (*Plates 24, 25*). Shortly before they leave the neural tube they flatten and reorientate so that the longest axis of each cell is arranged at right angles to that of the embryo, and there is a reduction in the intercellular spaces (Bancroft and Bellairs, 1976). The emigration from the neural tube takes place in a wave from anterior to posterior down the body. An important aspect is that it follows on closely after the wave of somite segmentation, and there is evidence that each pair of somites influences the release of the neural crest in its vicinity by affecting the BMP4 and *noggin* interrelationship. BMP4 appears to play a major role in releasing the neural crest cells from the neural tube. Sela-Donenfeld and Kalcheim (2000) found that in regions of the embryo where *noggin* expression is high in the neural tube, BMP4 is inactive and neural crest cells fail to emigrate, but progressive reduction in *noggin* activity coincides with activation of BMP4 and the emigration of neural crest cells. The authors suggested, as a result of a series of experimental ablations, that an inhibition of *noggin* was produced by the dorso-medial part of the epithelial somites. This would explain why neural crest delamination follows somite segmentation.

Once the neural crest cells have left the neural tube, they follow well-defined pathways through the body until they reach their target tissues. What are the controls that guide the cells as they migrate? And are the cells destined to differentiate into their appropriate tissues when they finally reach their destinations, or are their fates determined at an earlier stage? The answers to these questions seem to depend on the particular crest cells we are considering. For example, those cells in the trunk destined to become melanoblasts become specified (determined) soon after leaving the neural tube (Harris and Erickson, 2007), whereas others remain more flexible, even if not totally pluripotent, until they reach their destination. The major cues that direct their migration are provided by the surrounding environment: e.g. the neural crest cells pass through the anterior half of each somite but never through the posterior half. This rule is followed even in experimental situations where the somites are rotated or inverted so that their relationship to the emigrating neural crest cells is altered. *F-spondin,* which is expressed in the posterior region only of the somites, appears to play a role in inhibiting the crest cells from entering this region (Debby-Brafman *et al.,* 1999). Similarly, *ephrin* proteins inhibit the passage of crest cells through this region (Newgreen *et al.,* 1986). The neural tube also influences the direction in which the neural crest cells migrate, since if it is inverted in its dorso-ventral axis the crest cells that were destined to migrate down the side of the neural tube continue to do so, even though that leads them toward the ectoderm instead of the endoderm.

In the trunk, two major routes are apparent. The first cells migrate down the lateral side of the neural tube and into the anterior part of adjacent somites, following the basal lamina of the dermamyatome (*Text-Figures 28, 29*). This is the **ventral route** and

Downloaded from Vet-eBooks.com

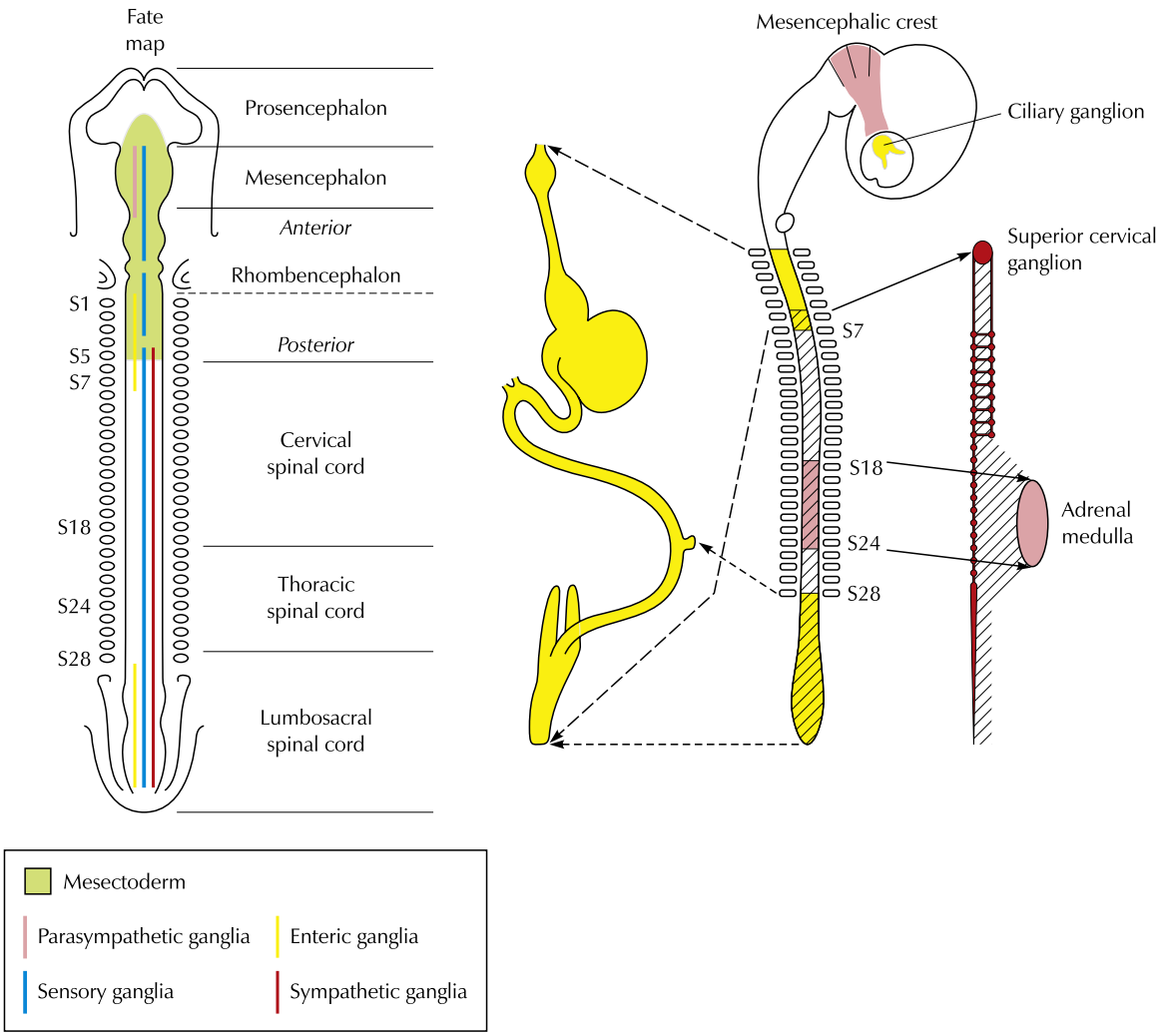

Text-Figure 27. *Regions of the neural crest and their contributions to the autonomic nervous system; the* ***cranial neural crest*** *gives rise to the cranial nerves and ganglia; the* ***vagal neural crest*** *(level somites 1-7) and the* ***sacral neural crest*** *(posterior to somite 28) form the nerves of the gut; the* ***cardiac neural crest*** *(level somites 1–3) contribute to the heart; the* ***trunk neural crest*** *give rise to the sympathetic neurons, those between somite levels 18–24 forming the adrenal medulla. (After Le Douarin and Kalcheim (1999); reproduced with permission of Cambridge University Press.)*

is repeated at one somite level after another down the trunk. It is succeeded by the **dorso-lateral route** (*Text-Figure 29*) where the cells migrate beneath the dermis.

The neighbouring tissues exert much of their influence on the neural crest through the medium of the extracellular matrix which surrounds them, the most important components being fibronectin, laminin, tenascin, collagen and various proteoglycans. Integrins and other adhesion molecules enable the neural crest cells to interact with the extracellular matrix. It is likely that the differing concentrations in which these materials are present in different regions of the body play a role in directing migration. The environment also plays a role in the final differentiation of the neural crest cells. Most neural crest cells appear to be pluripotent at the time they leave the neural tube in that they can often be made to abandon their presumptive fate and differentiate according to a new environment if transplanted. The major exception is that the trunk neural crest, which does not form cartilage or bone in the trunk, appears to be unable to do so even when transplanted into the head.

Neural crest which arises in the head region (cephalic neural crest), and forms cartilage and bone of much of the head and face skeleton, also gives rise to connective tissue as well as Schwann cells and cranial sensory ganglia (see Chapter 9). Neural crest in the vagal (just posterior to the head) and sacral regions forms the entire enteric (gut) nervous system. The neural crest in the trunk migrates as two separate streams; the dorsal one passes laterally beneath the ectoderm until it

Downloaded from Vet-eBooks.com

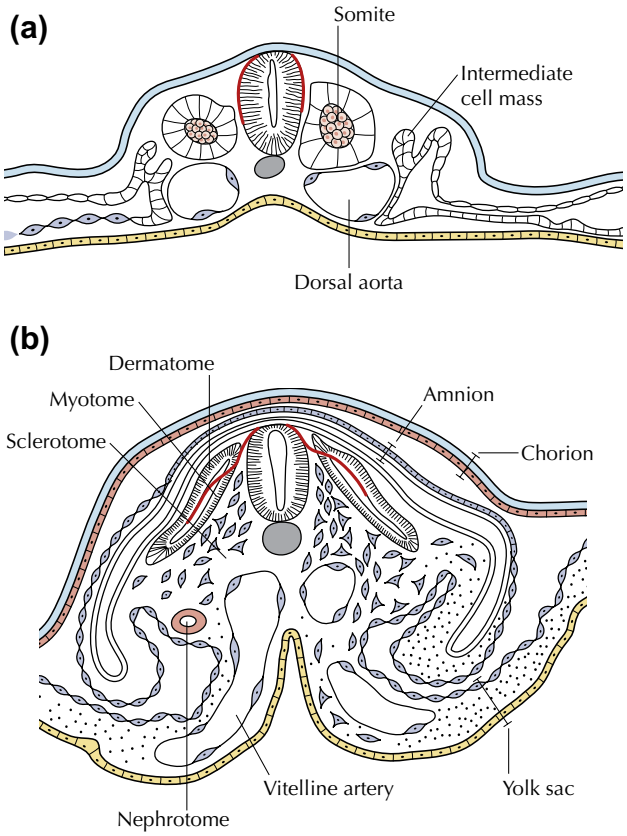

Text-Figure 28. *The trunk level neural crest cells (red) migrate ventrally between the neural tube and somites, some subsequently passing through the anterior part of each somite, moving along the basal lamina of the sclerotome.*

reaches the mid-ventral body wall. Eventually, it migrates into the substance of the dermis and forms the pigment cells. As the ventro-lateral stream passes through the anterior halves of the somites, some cells remain there and differentiate into dorsal root ganglia, whilst others give rise to sympathetic ganglia, Schwann cells and adrenomedullary cells. The cardiac neural crest extends from the first to the third somites, between the cranial and the trunk neural crests (*Text-Figure 27*). There have been fewer studies on neural crest development during secondary neurulation (i.e. in the tail region), but recent evidence suggests that the molecular aspects are similar to those in the trunk neural crest (Osório *et al.* 2009).

Some interesting parallels exist between the neural crest and the primitive streak (see Bellairs, 1987). In each case cells leave an epithelium and migrate to another part of the body; they move from the outer layer to the inside of the embryo and upon reaching their destination become arranged into new structures. The cells that leave the primitive streak inevitably differ from those of the neural crest in that they give rise to a different range of tissues. There is, however, an additional difference. The cells that arise from the primitive streak all give rise to epithelial tissues on reaching their destination (somites, lateral plate, pronephric duct, endoderm), but in birds the cells that arise from the neural crest seldom become rearranged as epithelia.

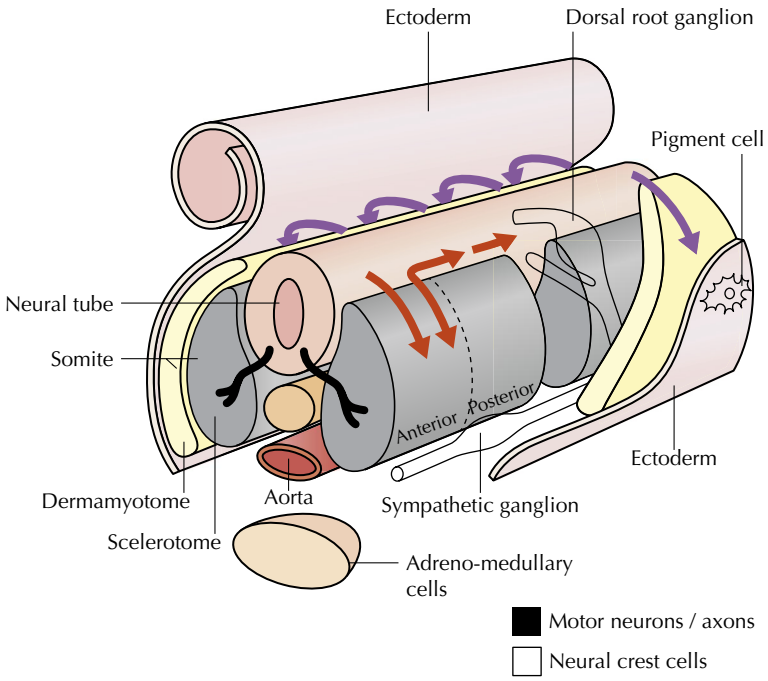

Text-Figure 29. *Schematic diagram showing the two pathways taken by the neural crest cells as they pass to their target tissues.* ***Purple:*** *the dorso-ventral pathway between the ectoderm and somites by cells that give rise to pigment cells.* ***Red:*** *the ventro-medial pathway, passing through the anterior, but not the posterior, parts of somites. (After Krull (2010), with permission of Landes Bioscience.)*

Downloaded from Vet-eBooks.com

Chapter 5

External Appearance and Polarity

We have seen in previous chapters that in the early stages the chick embryo is a flat disc, the blastoderm, the centre of which is destined to form the embryonic body, whilst the periphery will give rise to the yolk sac and amnion. The first indication of the body proper is at the anterior end at about stage 6 (about 24 h of incubation). Anterior to the tip of the head process a crescent-shaped groove appears in the entire thickness of the blastoderm. This is the head fold (*Text-Figures 34, 50; Plate 15*). The result is that the region of the future head, together with the developing foregut, becomes raised above the flat blastoderm (*Plate 61*). Sections show that the head is covered with ectoderm and is separated at its tip from the blastoderm. The folds continue to expand posteriorly and at the same time the growing head extends further anteriorly, becoming more and more defined. The lateral body folds (*Text-Figure 35*), which start to form as longitudinal grooves of the ectoderm and somatic mesoderm on either side of the embryo, are continuous with the posterior extensions of the head fold. There is a high level of cell division in the ectoderm of the folds (Miller, 1982); by stage 15 the lateral folds extend to the anterior wing level (somites 15–17) and by stage 16 have reached the level of somites 17–20. Meanwhile, the tail fold has begun to form at the posterior end (*Text-Figure 51*). By stage 17 the head fold (*Text-Figure 50*), lateral body folds (*Text-Figure 35*) and the tail fold have met to form a continuous groove around the periphery of the body, lifting it up above the surface of the yolk sac. By stage 20 the body is no longer continuous with the extra-embryonic tissues except in the region of the umbilicus where the head, tail and lateral body folds converge.

Although the foldings are most conspicuous in the ectoderm and somatic mesoderm, they also include the endoderm and the splanchnic mesoderm, so that they lead to the early stages in the formation of the gut. The foregut (*Plate 61*) forms as the head fold develops and the hindgut is initiated by the tail fold (see Chapter 8).

Once the body starts to become raised above the blastoderm, changes in the external appearance begin. The cranial flexure (*Text-Figure 30*) is visible from about stage 12 or 13 (*Plate 77*), though measurements of the cranial angle show that it begins as early as stage 10 (Goodrum and Jacobson, 1981; Pikalow *et al.,* 1994). It starts with the head bending ventrally toward the yolk sac, and there is evidence that this is correlated with the ventral bulging and elongation of the prosencephalon (Goodrum and Jacobson, 1981). The infundibulum at the anterior end of the neural tube is anchored to the foregut by Rathke's pouch (*Plate 105*) so that as the brain elongates, it has to bend around the foregut. Meanwhile, the head has begun to rotate also so that its left side comes to lie against the yolk sac and its right side to lie uppermost (see Appendix II; *Plate 88*). At this stage the trunk region has not yet turned and its ventral side still lies against the yolk sac with its dorsal side uppermost, but gradually the rotation spreads down the body until at about stage 20 the entire embryo has rotated and lies on its left side.

Two other flexures occur that affect the shape of the body. In the cervical flexure (*Text-Figure 30b*), which forms between about stages 14 and 23 (2–4 days), the head bends round in the neck region so that it comes to lie at right angles to the trunk, its ventral side lying against the ventral side of the pharynx. Experimental evidence suggests that the cervical flexure is related to looping of the heart, though whether the contraction of the heart from a straight tube to a looped one is responsible for pulling the head around in an arc (Flynn *et al.,* 1991) or, conversely, whether the head flexures are responsible, at least in part, for cardiac looping (Männer *et al.,* 1993), is not yet clear. Meanwhile the trunk itself becomes curled

The Atlas of Chick Development. http://dx.doi.org/10.1016/B978-0-12-384951-9.00005-8
Copyright © 2014 Elsevier Ltd. All rights reserved.

Downloaded from Vet-eBooks.com

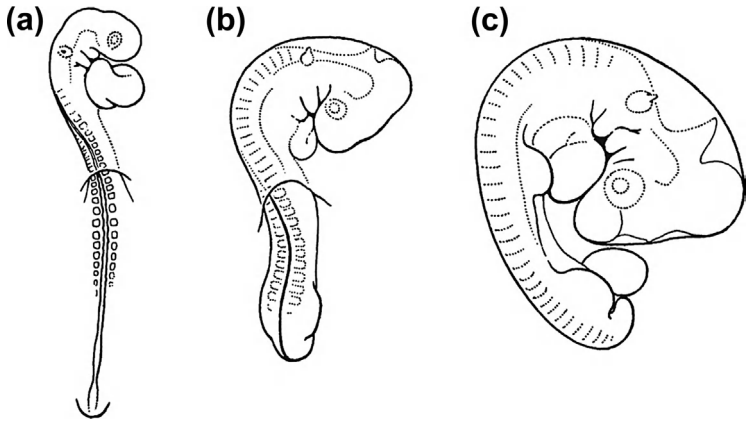

Text-Figure 30. Body flexures. (a) ***Cranial flexure****, about stage 14: the head has turned to the right but the trunk has not. (b)* ***Cervical flexure****, about stage 18: the head now lies at right angles to the trunk. (c)* ***Trunk curvature****, about stage 22: the trunk has now turned so that the whole embryo lies on its side and the tail bud is close to the head.*

around so that the tail bud comes to lie close to the head (*Text-Figure 30c*).

From this stage onwards the body shape is an indicator of many of the events taking place beneath the surface. These include the formation of the limb buds (*Plates 29, 30*), starting at about stage 17, with their enlargement and elaboration until the major features of the wing or leg have formed at about 10 days. The tail bud (*Plate 31*), the developing eyes, the beak and the pharyngeal pouches are all conspicuous aspects of the developing embryo, as is the bulge caused by the increasing size of the heart. These and other external features are categorized in the Normal Tables of Hamburger and Hamilton (1951; see Appendix II).

FACE

Before the face starts to form, the anterior part of the head consists of an ectodermal layer over the forebrain with a few scattered mesenchyme cells. The facial structures are derived from neural crest cells which migrate between the forebrain and the ectoderm during day 4, or earlier, of incubation (after the stomatodaeal plate has ruptured; see Chapter 8), and form a group of outgrowths. These are the left and right **maxillary** and **mandibular** processes of the first pair of pharyngeal arches which lie on either side of the stomatodaeal opening, and the medial **fronto-nasal process** which lies above it. The nasal placodes (*Plate 27*) become visible as shallow pits at stages 15–16 and indent further by stage 18 on either side of the fronto-nasal process. The maxillary processes grow towards the midline of the face during days 4 and 5 and fuse with the sides of the fronto-nasal process. The fronto-nasal process itself becomes extended forward to form the upper jaw, whilst the two mandibular processes also fuse in the midline and become extended forward to form the lower jaw (*Text-Figure 79*). The maxillary processes meet in the midline and form the palate and, together with the fronto-nasal process, the upper lip (beak). The expansion of these processes is largely due to cell proliferation, especially at the tips of the maxillary and mandibular processes, but also at the base of the fronto-nasal process (McGonnell *et al.*, 1998). Apoptosis takes place in the **periderm** (see Chapter 11, p. 120) at the site of fusion and the epithelial cells proper break down to form mesenchyme at the region of junction (Sun *et al.,* 2000).

The facial outgrowths form as a result of an interaction between the overlying epithelium and the neural crest mesenchyme. The bone morphogenetic proteins BMP2 and BMP4 appear to play a role in the outgrowth of these structures (Francis-West *et al.,* 1994) as well as FGF signals emitted from the nasal pits (Szabo-Rogers *et al.*, 2008). High levels of *Msx* gene transcripts have been correlated with regions of outgrowth (Brown *et al.,* 1997). The presence of the epithelium is essential, since without it the neural crest mesenchyme cells will not form the primordia (Saber *et al.,* 1989) but the type of facial prominence that does develop is determined by the mesenchyme. The evidence comes from recombinant experiments in which the epithelium has been separated from the mesoderm of one primordium and been replaced by the epithelium of another (Richman and Tickle, 1989), and is supported by molecular studies showing that signals from the ectoderm of the fronto-nasal process regulate the BMP proteins in the neural crest-derived cells (Hu and Marcucio, 2009a,b).

The site at which a particular primordium forms, however, appears to be dependent on events in the

Downloaded from Vet-eBooks.com

ectoderm. For example, before the cranial neural crest cells have arrived in the facial region, the ventral head ectoderm expresses FGF8 in two domains that correspond to the future mandibular processes, and BMP4 at the site of the future maxillary processes. The spatial relationship between the forebrain and the facial features appears to be coordinated by local retinoid signalling that maintains the expression of FGF8 and *sonic hedgehog* (Schneider *et al.,* 2001; Le *et al.,* 2001). A region of the fronto-nasal process, the fronto-nasal ectodermal zone (FEZ), has been identified as a signaling centre expressing SHH controlling the dital tip of the upper jaw (Hu and Marcucio, 2009b); it is expressed in the forebrain prior to the outgrowth, but then becomes activated in the adjacent epithelium of the FEZ.

A morphometric analysis of changes within the fronto-nasal process was published by Patterson and Minkoff (1985). The development of the primary palate was described by Yee and Abbott (1978). Extirpation of the fronto-nasal process leads to the reduction of the upper beak, agenesis of the primary palate and impaired development of the maxillary processes and the palatal shelves (McCann *et al.,* 1991).

ORIGIN OF THE LIMBS

The potential limb regions become visible from about stage 15 (50–55 h) (Appendix II) as slightly thickened ridges of the somatic lateral plate mesoderm, though, according to Stephens *et al.* (1992) a limb-forming region can be recognized as early as stage 11. The wing buds (*Plates 94, 107d*) form at the level of somites 15–20 and the leg buds (*Plate 96*) at the level of somites 26–32, these levels apparently being determined by the distribution expression of various *Hox* genes. For example, the forelimb buds form at the most anterior level of expression of *Hox-6* (Burke *et al.,* 1995; Burke, 2000).

As the lateral body folds form, the limbs come to lie along the sides of the body wall. At 3 days of incubation each limb bud is about 1 mm in length by about 1 mm in width (*Plate 5* of Appendix II). Each consists of an envelope of ectoderm enclosing a core of mesoderm; the ectoderm is derived from the ectoderm of the lateral body wall and the mesoderm is formed from the somatic lateral plate, although this subsequently becomes supplemented by cells migrating in from the somites. The somatic mesoderm gives rise to the tendons, skeleton, dermis and connective tissues of the limbs, whilst the somitic cells form the muscles.

The first morphological step in the formation of the limb bud is the proliferation of the lateral plate mesoderm cells, and this appears to be brought about by the production of the paracrine factor FGF10 by the lateral plate mesoderm itself. When beads soaked in FGF10 were inserted under ectopic ectoderm supplementary limb buds were induced (Sekine *et al.,* 1999). The FGFs themelves appear to be induced by members of the *Wnt* family of growth factors. In particular, *Wnt2b* is expressed in the wing region and *Wnt8c* in the leg (discussed by Tickle and Munsterberg, 2001). The mesenchyme cells become polarised along the proximo-distal axis of the limb bud as they migrate (Wyngaarden *et al.,* 2010; Gros *et al.,* 2010).

In their early stages of development, the wing and leg buds are similar to one another morphologically, but by about stage 24 they have begun to acquire their individual characteristics. These events are controlled, at least in part, by the transcription factors TBX5, which is present in the wing buds, and TBX4, which is found in the leg buds. Experimental introduction of these factors into a developing limb bud has been shown to influence its future development into either a wing bud or a leg bud.

At the tip of the limb the ectoderm becomes thickened and is then known as the **apical ectodermal ridge** (*Plates 141, 142*). Important interactions take place between the ridge and the underlying mesoderm. The ridge itself is induced to form by the mesenchyme cells, largely through the secretion of FGF10, and possibly also FGF8 (Johnson and Tabin, 1997), but the mesenchyme is subsequently dependent on the presence of the ridge. If the ridge is removed, the limb fails to differentiate further, whereas if an additional apical ectodermal ridge is grafted onto the limb bud a supernumerary limb structure develops (Saunders *et al.,* 1957). The development of the ridge and the signalling pathways involved are reviewed by Fernandez-Teran and Ros (2008).

The mesenchyme immediately beneath the **apical ectodermal ridge** is a region of high mitotic activity, being the source of the additional cells that are needed as the limb bud elongates. It is known as the **progress zone** and consists entirely of cells that are as yet undifferentiated. It appears to be maintained by FGF8 secreted by the apical ectodermal ridge. There is also evidence that *Wnt* signalling is involved (Kawakami *et al.,* 2001). Gradually, the most proximal cells in the progress zone leave it, being replaced by more cells distally as mitosis continues. The first cells to leave the progress zone form the most proximal structures of the limb, and successively, as more and more

Downloaded from Vet-eBooks.com

cells leave the progress zone, they become destined to form progressively more distal structures. The specification of the tissues that form along the limb bud is due to the activity of a sequence of *Hox* genes. In the wing bud the humerus forms first, apparently under the influence of *Hox-d9* and *10,* which is expressed at the time throughout the limb bud. This first phase is followed by the formation of the radius and ulna (middle phase) and then by the metacarpals and digits (third phase), and during these periods there is a rearrangement of the expression of these genes and the expression of additional *Hox* genes. These skeletal structures are formed initially in cartilage and become ossified later (see Chapter 10). Once the regions of the limb have become laid down, the apical ectodermal ridge disappears (Wolpert, 2002). During this period when the proximo-distal axis is already present, two further axes become established. The first is that of the anterior-posterior axis. This has been shown by a series of experiments to be controlled by the so-called ZPA (zone of polarizing activity), a region of mesenchyme at the posterior border of the early limb bud near its junction with the body wall (*Text-Figure 31*). If this region is transplanted to the anterior border of another, intact limb bud it leads to the formation of additional, duplicated limb skeletal elements with a polarity defined by the graft usually in mirror image to that of the host limb. Similar duplications were seen in which beads soaked in retinoic acid were implanted in the same region, the degree of duplication being dose dependent (Tickle, 1991). It appears that retinoic acid is synthesized in the proximal mesenchyme and then passes distally along the limb bud forming a gradient of concentration, the higher levels initiating more proximal structures whilst the lower levels cause more distal ones (Bénazet and Zeller, 2009).

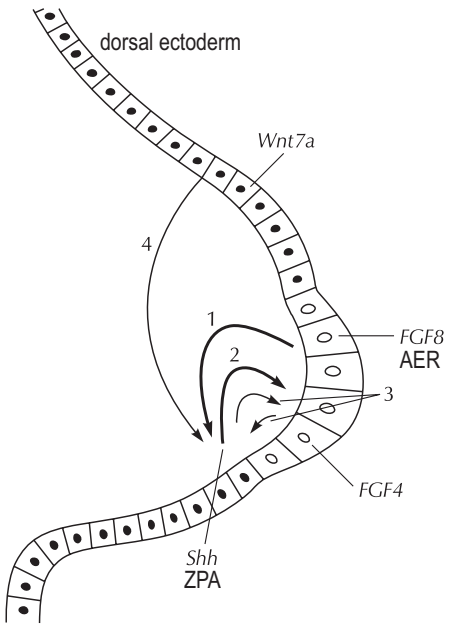

Text-Figure 31. *Some of the molecular interactions at the apical ectodermal ridge which are involved in the initiation and maintenance of the limb bud. Stage 1: the apical ectodermal ridge (AER) expresses FGF8, which induces sonic hedgehog (Shh) in the zone of polarizing activity (ZPA). Stage 2: ZPA expresses Shh, which induces FGF4 in the posterior apical ectodermal ridge. Stage 3: Shh and FGF4 reciprocally maintain each other. Stage 4: the dorsal ectoderm expresses Wnt7a which helps maintain Shh in the ZPA.*

Riddle *et al.* (1993) demonstrated that the ZPA was characterized by the gene *sonic hedgehog* and that similar duplications could be obtained when cells that were capable of secreting *sonic hedgehog* protein were grafted into a chick limb bud. In the normal limb bud the *sonic hedgehog* also controls the level of FGF4 in the posterior region of the apical ectodermal ridge. The role of *sonic hedgehog* in controlling the antero-posterior axis is not, however, a straightforward one, as BMP2 and BMP4, as well as retinoic acid, play a part. Moreover, SHH is expressed not only in the mesenchyme, but also in the overlying ectoderm (Harfe, 2011).

Each limb also develops a dorso-ventral axis so that, for example, the dorsal (upper) side of the foot differs from the ventral (plantar) side. This appears to be due mainly to the activity of events in the ectoderm. In particular, *Wnt7a* is active in the dorsal ectoderm and is responsible for a cascade of events.

The autopod (hand or foot) is the final region of each limb to be laid down. TGF32 and activin signalling are involved in the skeletogenesis of the digits (Merino *et al.,* 1999a). (For a recent review of digital development see Sanz-Ezquerro and Tickle, 2003). The 'hand' of the wing is highly modified in birds, and it is generally considered that the digits of the avian wing develop in positions 2, 3 and 4, though there is some evidence that these three digits should be reclassified as 1, 2 and 3 (discussed by Young *et al.,* 2011). The patterns of gene action in the development of individual digits have been mapped by Fisher *et al.* (2011).

By contrast, the foot retains the characteristic vertebrate plan of five digits. It initially forms as a flattened paddle-like structure (Appendix II) in which the cartilaginous elements are clearly distinguishable yet still connected by mesenchyme (*Plate 174*). In the duck and other web-footed birds this interdigital region remains as a web, but in the chick it is removed by apoptosis except at the base, so that the toes become separated.

Downloaded from Vet-eBooks.com

Other specialized areas of the limb bud, in addition to the ZPA, are the **anterior necrotic zone** (ANZ) and the **posterior necrotic zone** (PNZ), which not only play a role in the shaping of the limbs, but are centres from which morphogens appear to diffuse and interact with other tissues, playing an essential role in the patterning of the limbs. There is evidence that retinoic acid is an active principle secreted by these zones (reviewed by Paulsen, 1994). The relationship between SHH and FGF has attracted much attention (see Harfe, 2011). The development of the limb in the chick and other vertebrates has attracted many investigations, perhaps largely because of its ease of access compared with that of internal organs. But the complexity of limb development with its interacting axes (dorso-ventral, antertior-posterior and proximo-distal) and its eventual differentiation into sharply distinct regions has led to many theoretical attempts to provide an over-arching concept. Earlier ones were based on the idea of simple gradients of diffusing substances, but with the ever-increasing molecular evidence now available, new ideas embracing modern knowledge of the genes involved and their interacting products (e.g. Bénazet and Zeller, 2009; Cooper *et al.*, 2011; Fisher *et al.*, 2011), more sophisticated concepts are being put forward.

These changes in the external appearance of the limbs are illustrated and described in the Normal Table of Hamburger and Hamilton 1951 (see Appendix II).

GROWTH OF THE EMBRYO

Growth, a process usually defined as the increase in mass of an organism, is brought about mainly by the continual rise in the population of cells present in the embryo.

Changes in cell shape and size, as well as the accumulation of extracellular materials, also affect the shape and size of developing organs. Some regions undergo a more rapid rate of cell division than their neighbours, leading to a build-up of tissue. Growth factors, such as FGF, play an important controlling role. Schellpffer *et al.* (2005), using high-frequency ultrasound imaging, published charts and tables of the normal growth *in ovo* of purebred White Leghorn chick embryos. Seven morphological structures were measured (e.g. crown-rump length, femur length). Kim *et al.* (2011), using microcomputered tomography to study 3D aspects of chick growth between 4 and 12 days of incubation, found that whereas some organs showed constant growth (e.g. eye and heart), others grew in spurts (e.g. forebrain and limbs).

APOPTOSIS

As well as regions of high proliferation, there are also areas that have a high rate of cell death. Probably in all embryonic tissues there is a continuous loss of cells through death, but in certain parts of the developing body the death rate outstrips the proliferative rate. This means that just as some regions become enlarged by rapid cell division, others become eroded away. The dying cells undergo a process of breakdown and gradually become phagocytosed by other cells. Apoptosis is also known as 'programmed cell death' because in many cases the patches of cells die in a particular location of the embryo at a specific time in development and play an important role in morphogenesis. Two classical examples in the chick occur in the shaping of the wing bud and of the toes. Apoptotic cells are, however, found in normal embryos even as early as gastrulation (Bellairs, 1961), and after that in many well-defined sites in the differentiating tissues, e.g. in the mesonephros (Chapter 7), in the heart (Chapter 6), in the sclerotome (Sanders *et al.* 1997), in the nervous system (Oppenheim *et al.,* 1999), in the neural crest (Jeffs and Osmond, 1992) and in the tail bud (Sanders *et al.,* 1986), branchial arches and lateral body wall (Hirata and Hall, 2000). In most of these examples, cell death is focused on a highly localized region and occurs within a restricted period of time, e.g. cell death within the endocardial cushions of the developing heart occurs only between about days 5.5–7.5 (Keyes and Sanders, 1999).

Regions of cell death play a specific role in the shaping and patterning of organs, though they can sometimes be 'rescued' from death if treated with an appropriate growth or differentiation factor. For example, regions of programmed cell death in the early nervous system of the chick embryo can be counteracted by the application of *sonic hedgehog* protein (Charrier *et al.,* 2001). Hirata and Hall (2000), who have reviewed the temporo-spatial patterns of cell death from stages 1 to 25, have concluded that cell death is a feature of development at all these stages, but that there are changing patterns, depending on the specific stages of growth, differentiation and morphogenesis.

POLARITY: SYMMETRY AND ASYMMETRY

We have already seen that the embryonic axes (dorso-ventral and antero-posterior) begin to be established even before the egg is laid, but the finalization of this

Downloaded from Vet-eBooks.com

polarity does not take place until later. Although the antero-posterior polarity is initiated by the effects of gravity during cleavage, it is still possible to overcome it until the primitive streak has begun to develop. At that time a series of *Hox* genes comes into play which interact with one another so that each level of the body becomes categorized in a unique way. It acquires its own 'positional information' (Wolpert, 2002). There are a number of markers of antero-posterior polarity, e.g. *Gata2* protein is expressed in the area opaca epiblast prior to primitive streak formation as a gradient along the antero-posterior axis, being highest anteriorly (Sheng and Stern, 1999) and disappears at stage 3+ (though it reappears later in other regions, such as the lateral part of the somites).

With the establishment of antero-posterior polarity, the embryo acquires a left and a right side. The two sides are asymmetrical, being mirror images of one another (e.g. a left wing and a right wing), which essentially remain so throughout development. With the differentiation of the internal organs, however, the two sides diverge and certain regions become more highly asymmetrical, as shown by the heart, liver and gut.

The first signs of left–right asymmetry appear to be associated with Hensen's node and involve a molecular cascade. Sonic hedgehog produced by Hensen's node plays a critical role in establishing the left cascade, which includes *Nodal–Lefty–Pitx* (Levin *et al.,* 1995). By contrast, *sonic hedgehog* ceases to be produced on the right side where actin, FGF and BMP play major roles. The establishment of asymmetry between left and right is dependent on a sharp boundary along the midline, and it has been suggested that the individual cells are themselves orientated in respect to that boundary. This is supported by evidence that Vangl2, a core planar cell polarity protein, is 'consistently polarised', giving cells in the blastoderm a vector pointing toward the primitive streak (Zhang and Levin, 2009). It is possible to disrupt the left–right arrangement of the body by interfering with the cascade. For example, if cells secreting *sonic hedgehog* are transplanted to the right of the node, nodal is induced symmetrically and the looping of the heart may occur randomly to the left or right (Levin *et al.,* 1997). BMP signaling also plays a role in left–right asymmetry in Hensen's node by inhibiting DAN, which is normally expressed on the left side (Katsu *et al.*, 2011). Nodal plays a significant role in the essential communication that occurs between the left and right sides; this process is a complex one (discussed by Katsu *et al.*, 2013). Many genes have been implicated in the establishment and maintenance of asymmetry, many of which propagate signals in small populations of cells that subsequently result in left- or right-sidedness in the future organs (Levin, 2005).

Downloaded from Vet-eBooks.com

Chapter 6

Heart, Blood Vessels and Lymphatics

HEART

The heart proper begins to develop at about stage 9 or 10 and is initially present as a simple tube which then loops into an S-shape (*Plates 32–34*). Even as it forms, the basic regions become apparent, first the truncus and ventricle, then the atrium and lastly the sinus venosus. The first beats are at about stage 10 and the circulation has become well established by about stage 16. Division into left and right sides takes place during days 3–5.

PRIMARY AND SECONDARY HEART FIELDS

The main part of the heart is formed from two regions of the early embryo, the primary and secondary heart fields.The term primary heart field is given to two patches of splanchnic mesoderm, left and right, lying one on either side of the head process at stages 5–6 after ingression (Rawles, 1943) (*Text-Figure 32*). They are derived from progenitor mesoderm cells that are present in the primitive streak at stage 4 (Selleck and Stern, 1991) and have then migrated away from it in an antero-lateral direction, possibly as the result of the action of Wnt3a in the primitive streak (Münsterberg and Yue, 2008; Lopez-Sanchez *et al.*, 2009

A secondary heart field has been identified more recently as a result of modern labelling experiments (e.g. Mjaatvedt *et al.,* 2001; Waldo *et al.,* 2005b; Kelly and Buckingham, 2002). It is formed partially from splanchnic mesoderm which lies in the midline anterior to the simple heart tube at about stage 10, and its cells subsequently become incorporated into the myocardium of the truncus (see below). But the secondary heart field also contains neural crest cells which have migrated from the pharyngeal arches III, IV and VI. The paths taken by the cardiac neural crest cells are shown in *Text-Figure 33*. The secondary heart field also includes cells that eventually become part of the muscles at the base of the pulmonary trunk (Waldo *et al.*, 2005a, b).

Single-cell analysis of isolated presumptive heart cells taken from stage 4 embryos and grown *in vitro* has established that they are capable of forming muscle-specific myosin heavy chains, though they do not appear to be able to express chains specific for atrial or ventricular muscle unless grown at high density (Gonzalez-Sanchez and Bader, 1990). The cells are, however, not yet determined, and if transplanted elsewhere can still give rise to other tissues (Veini and Bellairs, 1990; Climent *et al.,* 1995); conversely, tissues taken from outside the primary heart field area are still capable of becoming incorporated into the heart (Orts-Llorca and Collado, 1970). Nevertheless, there is evidence that the primary heart field mesoderm generates a subpopulation of cells, cardiomyocytes and endocardial endothelial cells, and that their precursors are already established by stage 3 (Wei and Mikawa, 2000).

After the precardiac cells have migrated into the anterior lateral plate they come under the influence of signals from the underlying endoderm (reviewed by Lough and Sugi, 2000). The paracrine factors required to allow cardiac myocytes to form include fibroblast growth factors (FGFs), especially FGF8, and bone morphogenetic proteins (BMPs). Repressors of cardiogenesis, which include *Wnt8c,* are expressed in the posterior lateral mesoderm but not in the primary cardiac fields (Marvin *et al.,* 2001; Yutzey and Kirby, 2002).

When the lateral plate mesoderm splits into two layers, somatic and splanchnic (*Plate 61*), the splanchnic layer becomes closely associated with the endoderm. Initially, the space between the two layers, which will become the **coelomic cavity**, is

The Atlas of Chick Development. http://dx.doi.org/10.1016/B978-0-12-384951-9.00006-X
Copyright © 2014 Elsevier Ltd. All rights reserved.

Downloaded from Vet-eBooks.com

present only in the future trunk region of the embryo, but intercellular spaces gradually join up together and extend the coelom cranially. By stages 7–8 this newly formed coelomic cavity is now arranged as a crescent-shaped space extending either side of the head process and known as the amnio-cardiac vesicle (*Text-Figure 34*) because it takes part in the formation of the amnion (see Chapter 13, p. 128) as well as the pericardial cavity. It has a tendency to swell up in embryos under unsuitable osmotic conditions. By the time the amnio-cardiac vesicle has formed, the precardiac mesoderm of the primary heart field has become localized in the left and right splanchnic mesoderm. Organized myofibrils are already present in the precardiac mesoderm of the primary heart field at the time that the two sides fuse together (*Text-Figure 35*) and rhythmic contractions occur at the time of fusion (Colas *et al.*, 2000).

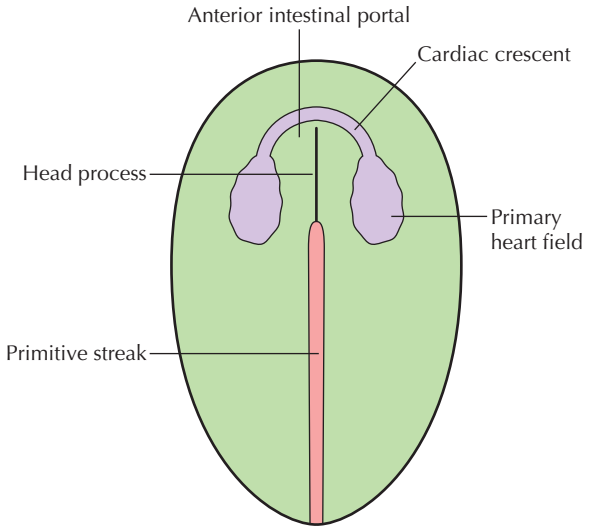

Text-Figure 32. *Chick embryo at stage 5 to show the location of the left and right primary heart fields and cardiac crescent. (After DeHaan (1965), with permission of John Wiley and Sons.)*

The Migration of the Precardiac Mesoderm

From about stage 5 the left and right primary heart fields migrate anteriorly to become united by a crescent-shaped band (the cardiac crescent or cardiogenic plate, *Text-Figure 32*) which by stage 8 passes anterior to the anterior intestinal portal (Redkar *et al.*, 2001; Cui *et al.* 2009). Abu-Issa and Kirby (2007) found that the distal regions of the primary heart field at stage 7 were precursors of the inflow parts of the heart whilst the proximal parts became the outflow tract.

The precardiac mesoderm adheres so closely to the underlying endoderm that it is difficult to separate the two layers cleanly without the use of enzymes. This is because the interface between the endoderm and mesoderm is richly coated with fibronectin. If the endoderm is removed, the precardiac mesoderm does not migrate. Formerly, it was thought that the

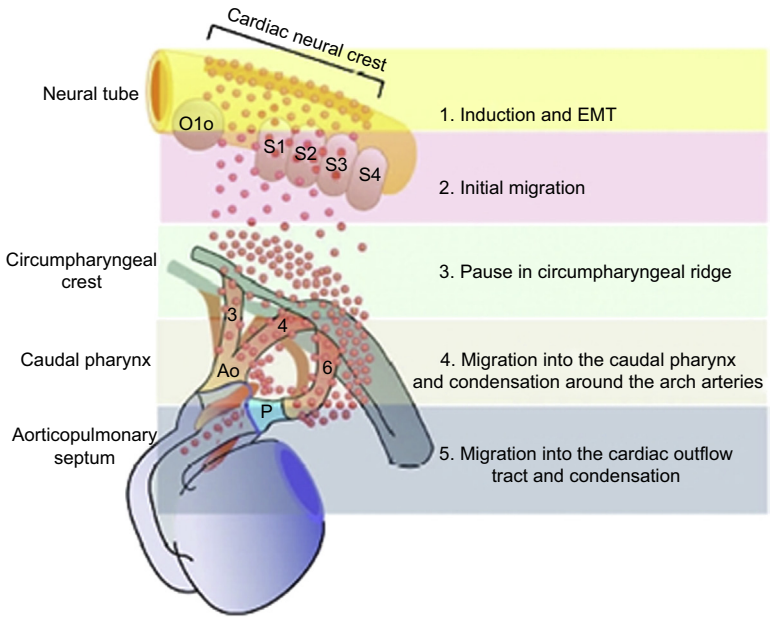

Text-Figure 33. *Phases in the migration of the cardiac neural crest cells to the heart. (From Kirby and Hutson (2010), with permission of Landes Bioscience.)*

Downloaded from Vet-eBooks.com

mesoderm cells were carried passively into the midline by the folding of the foregut endoderm, but time-lapse studies have shown that they migrate independently of it (DeHaan, 1965). Linask and Lash (1986) and Easton *et al.* (1990) concluded that the precardiac mesoderm selectively migrated up a gradient of fibronectin and, with the use of synthetic peptides, were able to show that the fibronectin was an essential component of the endoderm substratum. If migration of the precardiac mesoderm on the substratum is disrupted, either surgically or chemically, the resulting heart will be deficient in its anterior portion, or even divided into two separate hearts (Osmond *et al.,* 1991).

As the foregut forms, the left and right precardiac cells are moved into the midline and each begins to condense into an endocardial tube. The developing foregut loses contact with the yolk sac and the two tubes of the heart fuse in the midline to form a single tube, starting anteriorly and progressing posteriorly. The process can best be seen by studying a sequence of sections from progressively older embryos (*Text-Figure 35*). Fusion of the two endocardial tubes begins, anterior and ventral to the anterior intestinal portal, at about stage 8 (Coffin and Poole, 1988). At the same time, the two sides of the foregut join medially, forming the characteristically V-shaped pharynx (*Plate 64*). The left and right sheets of splanchnic mesoderm ventral to the pharynx combine to form the dorsal and ventral mesocardia (*Text-Figure 35; Plate 32*). The latter is so transient, however, as to be seldom visible, rupturing at about stage 10. The

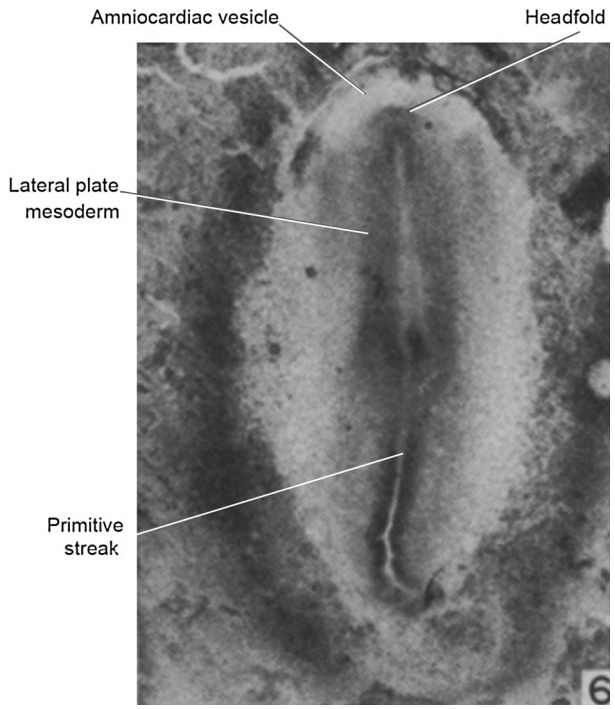

Text-Figure 34. *Stage 6 embryo from Normal Table of Hamburger and Hamilton (see Appendix II), seen in transmitted light. The amniocardiac vesicle is visible as a clear area anterior to the headfold.*

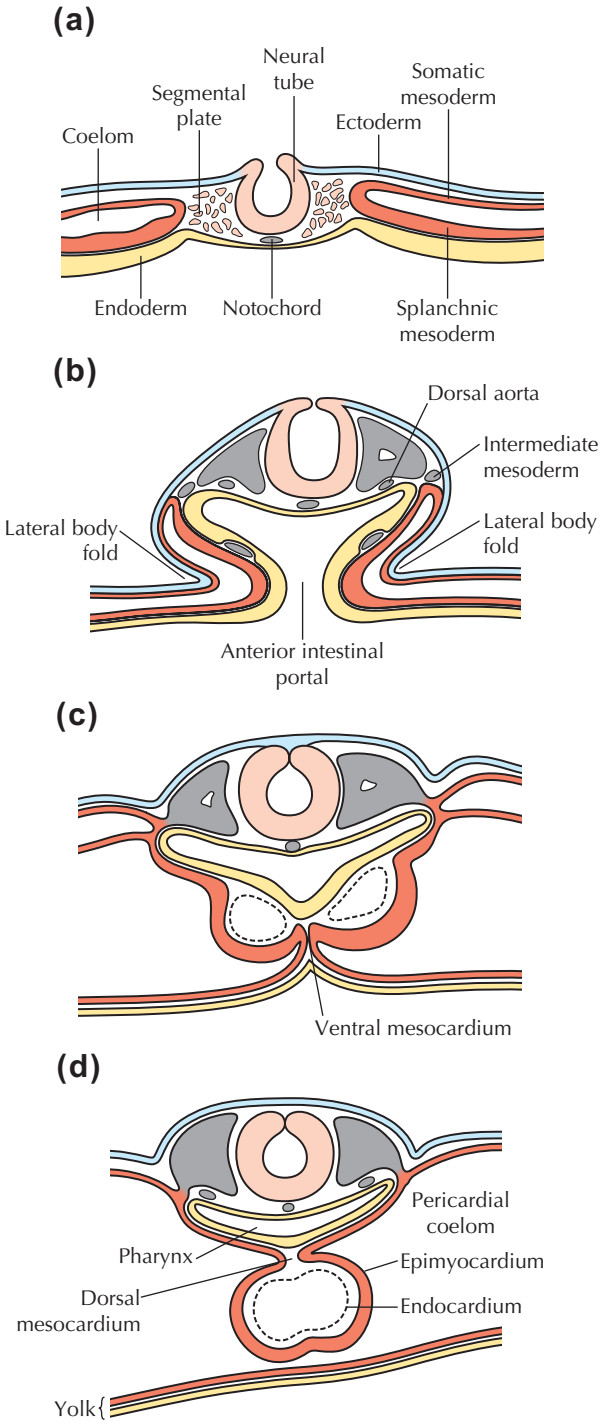

Text-Figure 35. *A series of transverse sections through an embryo at stage 8 to illustrate the lateral body folds and early stages of heart formation, (a) being the most posterior and (c) the most anterior. (d) Transverse section across the heart at stage 10 to illustrate the loss of the ventral mesocardium.*

Downloaded from Vet-eBooks.com

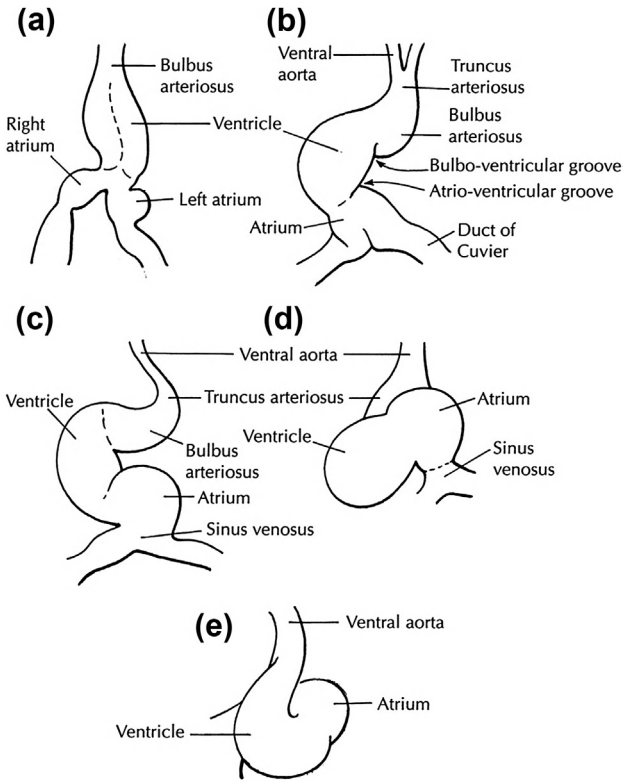

Text-Figure 36. *Looping of the heart seen from the ventral aspect. (a) Stage10; (b) Stage 12; (c) Stage 13. The fully looped heart at stage 16 is seen from the left side (d) and the right side (e).*

simple tube is initially suspended into the coelom beneath the pharynx by the dorsal mesocardium, but this structure is also transient, persisting only until about stages 12–13. As the lateral body folds form (see p. 45), the coelom surrounding the heart becomes isolated from the more posterior coelom and is henceforth known as the pericardial coelom or cavity (*Plates 35, 81*).

The foregut develops in an antero-posterior sequence and its development is paralleled by the anterior to posterior formation of the heart. The most anterior part of the heart, the future truncus arteriosus (*Plates 33a, 81*), forms first (from the secondary heart field) and is then succeeded by the ventricle (*Plates 33, 79, 81*), the common atrium (*Plate 33*) and the sinus venosus (*Text-Figure 36*), in that order. The additions of these new regions result in an elongation of the heart tube. The part where the ventricle narrows to form the truncus is known as the conus (bulbus) arteriosus. Development of the heart and foregut are closely associated with the head fold formation (*Text-Figure 50*) and with the lateral body folds (*Text-Figure 35*). These folds can be considered separately in longitudinal and transverse sections, but they are continuous with one another, and the effect is that of a horseshoe-shaped trench undercutting the future head region (*Text-Figure 50*).

The posterior extension of the foregut can be prevented experimentally by cutting through the anterior intestinal portal (DeHaan, 1959) or by inserting a mechanical obstacle such as a lump of thick albumen. In either case the result is that the two sides fail to fuse and diplocardia results. Each side then forms a small but perfect heart which begins to beat independently and at the appropriate time.

Once the heart has formed into a simple tube (*Plates 32, 33*), two distinct layers are visible (*Plate 85*): the thin inner layer, the endocardium, and the thicker outer layer, commonly known as the epimyocardium. Subsequently, the heart becomes three-layered, these layers being the **endocardium,** the **myocardium** and the thin enveloping **epicardium.** The traditional view has been that the precardiac mesoderm gives rise to all three layers of the heart, but several authors using transmission or scanning electron microscopy (e.g. Shimade and Ho, 1980), or experimental techniques (Männer, 1993), have concluded that the epicardium arises from the pericardium (i.e. from the splanchnic mesoderm of the pericardial wall), and the traditional view has now been modified. The relevant part of the pericardial wall, now known as the **pro-epicardial serosa** (*Plate 36*), surrounds the entire region near the sinus venosus, and contributes primarily extracardiac cells to the developing heart (Männer *et al.,* 2001). As the pro-epicardial serosa starts to develop at stages 13–14, bleb-like protrusions form at the ventral wall of the left and right horns of the sinus venosus. Cells from the pro-epicardial serosa are then transferred across the pericardial cavity to the surface of the developing ventricles, either as free-floating aggregates or by the formation of bridges across the lumen. The primordial epicardium then spreads as a continuous epithelial sheet over the myocardium (Männer *et al.* 2001). The pro-epicardial serosa also gives rise to the coronary blood vessels as well as to a small number of endocardial cells (Männer, 2001). For more information on the origin of the pro-epicardial serosa in the quail, see Virágh *et al.* (1993) or Männer *et al.* (2001).

Looping

Looping is the process that converts the single straight heart tube into a helically wound loop (Männer, 2009). It determines the left/right position of the future ventricles and also results in the confluence

Downloaded from Vet-eBooks.com

of the heart with the great vessels. Looping begins at about stage 10 and normally occurs to the right (*Plates 33, 34, 38*). The right ventricular wall bulges outwards and becomes convex at the same time as the left wall becomes concave (*Text-Figure 36*). Coincidentally, the heart rotates to the right. There is no well-proven explanation how this is brought about, nor why the initial loop is to the right though, as we have seen, molecular differences between the right and left sides of the embryo have become established before the heart begins to form. The homeobox gene, *Pitx2,* has been found to play a crucial role, *Pitx2c* being present in the left lateral plate as well as in the left side of the heart tube and head mesoderm. Ectopic expression of this gene resulted in random looping (Yu *et al.,* 2001). Nowadays, most authorities believe that many factors are involved, and the idea that the heart is forced into a loop because it is in a confined space has long been abandoned. There is some evidence that heart looping and cranial flexure are related (see Chapter 5), but although the cranial flexure may depend on heart looping, heart looping can occur in the absence of cranial flexure (Männer *et al.*, 1989).

The simple tube is capable of looping as soon as it has formed. The work of Butler (1952) is much quoted though not easy of access. Butler isolated newly formed chick hearts *in vitro* and found that although they bent they did not rotate to the right. Castro-Quezada *et al.* (1972) showed that if parts of the simple heart tube were removed, looping occurred in the remaining sections. It seems likely that in both these experiments the initiation of the process had begun at the molecular level before extirpation of the tissue. Indeed the pre-loop heart is already slightly asymmetrical (Stalsberg, 1969).

There is evidence that an important role in looping is played by the actin bundles. These become arranged in a circumferential pattern as the tube forms, but are more prominent on the right than on the left side. When small crystals of cytochalasin B were inserted into the right side of the heart, bundles at that side were disrupted and looping took place to the left. By contrast, when crystals were inserted into the left side, looping took place as normally, to the right (Itasaki *et al.,* 1991). These authors have suggested, therefore, that the bundles in the right side of the heart normally generate tension and lead to dextro-looping. This explanation, however, fails to account for the difference in distribution of the actin bundles on the two sides of the heart, and for the reversal of looping in the right-hand side in diplocardia.

There is a possibility that the actin bundles are influenced by the cardiac jelly, which fills the lumen of the early heart and consists of a complex matrix of glycosaminoglycans, collagen and non-collagenous glycoproteins, with hyaluronic acid as the principal constituent. It was suggested that the cardiac jelly produces an outward pressure so that the walls in the heart are under tension and become deformed (Nakamura *et al.,* 1980). This concept was questioned, however, by Baldwin and Solursh (1989) who cultured rat embryos in the presence of hyaluronidase, which digested away the cardiac jelly, but found that normal looping took place. So, although the cardiac jelly may play a role in looping, it does not appear to be an essential one.

After the dorsal mesocardium breaks down, the heart is anchored only at its anterior end (to the developing aorta) and at its posterior end (where it is still attached to the endoderm at the anterior intestinal portal) (*Plate 33a*). It therefore lies freely in the future pericardial cavity (*Text-Figure 35*). The result is that looping is now possible and the ventricular region moves posteriorly, whilst the anterior-most region moves into a more ventral position. During the time that the looping is taking place, cells from the secondary heart field become added to the ventricular outflow tract, forming the conus (bulbus) arteriosus, between stages 12 and 22 (2–4 days) (*Plate 34*). FGFs and BMPs are expressed in the pharyngeal endoderm at this time and appear to be necessary for the differentiation of the muscle and the conotruncal cells from the secondary field. Further refinements in the looping and rotation of the heart have been described in detail by Patten (1922), Coffin and Poole (1988), Männer (2009) and Van den Berg and Moorman (2011).

Septation of the Heart

The divisions of the heart into the major regions, conus, ventricle, atrium and sinus venosus, are enhanced by the development of grooves, the bulbo-ventricular and atrio-ventricular grooves, between stages 16 and 20 (*Text-Figure 36*). The simple tube is subsequently divided into left and right channels by the growth of a series of septa, so that after hatching, the two sides of the heart are completely separate. The septa are derived from the endothelial cells that line the heart, under the influence of TGFβ (Darland and D'Amore, 2001). The process of septation is comparable to that in the human heart, which is extensively described in textbooks of human embryology, though there are certain differences.

Downloaded from Vet-eBooks.com

At stages 16–17 two apposed ridges, the atrio-ventricular cushions, project into the lumen of the atrio-ventricular canal from its dorsal and ventral walls. The cushions are initially formed from acellular cardiac jelly, which then becomes invaded by cells from the endocardium (see Icardo (1989) for a morphological description of the cushions). The transcription factor, *slug,* is expressed in this region and is necessary for the initiation and conversion of epithelium to mesenchyme (Romano and Runyan, 2000). The cushions meet and fuse in the midline toward the end of day 5, leaving a channel, the atrio-ventricular canal, on either side (*Plate 128*). Many authors have now shown that BMPs and TGFβs play a critical role in the epithelio-mesenchymal transformation of the endothelial cells during the formation of the atrio-ventricular cushions (e.g. Boyer and Runyon, 2001; Keyes *et al.,* 2003). Meanwhile a septum, the interatrial septum (*Plate 90*), which begins to form at about stage 14 as a small ridge at the cranio-dorsal end of the single atrium, grows down to meet the atrio-ventricular cushions. By 4 days (about stage 24) the interatrial septum has begun to fuse with the cushions at about the same time as the cushions are fusing with one another. The result is to divide the atrium into left and right compartments, but the two sides do not become completely separated because many small holes, the interatrial foramina, break through the septum and allow communication between the left and right atria. This is important because, in the embryo, most of the venous blood returns to the right side of the heart, only a trickle from the pulmonary vein returning to the left. The passage of blood through the foramina into the left atrium enables the pressure in the two sides of the heart to be balanced, which is necessary for their equivalent growth. Strands of tissue overlap the holes so that they open only when the right atrium becomes expanded during diastole, and blood then passes from the right to the left atrium. When the atrial wall contracts during systole, equal pressure is re-established in the two atria and the foramina close.

In birds, there is development of neither a single large foramen corresponding to the foramen ovale of mammalian embryos, nor of a secondary septum corresponding to the septum secundum of the mammalian heart.

At the time of hatching there are important changes in the circulation that lead to an equalization of pressure in the two sides of the heart and which in turn results in the closure of the foramina. In the domestic fowl, though apparently not in all birds, both the pulmonary vein and part of the left atrial tissue become absorbed into the interatrial septum, and in this respect also the development of the chick heart differs from that of mammalian hearts (Quiring, 1933). During the period of separation of the left and right sides, changes occur in the histology of the heart. By 5 days of incubation bands of muscles have begun to form in the atria, and between days 7 and 11 these become the ‘muscular arches’, which are characteristic of the avian atria and play an important role in systole.

The conversion of the single ventricle into right and left components starts during day 3 as the left ventricle bulges, and during day 4 as the right ventricle bulges. These bulges are thought to be due to the force of the blood streams. Part of the original wall of the single ventricle remains between the two bulges and is the source of the interventricular septum. This septum (*Plates 40, 128, 152*), which lies initially at the apex of the ventricles, extends towards the atrio-ventricular cushions and fuses with them by day 6, leaving only a small gap, the interventricular canal.

During day 5, the proximal part of the truncus arteriosus becomes incorporated into the right atrium, whilst the distal part becomes divided into the aorta and the pulmonary arteries by the growth of the aortico-pulmonary septum (*Plates 35, 152*). This forms from two endocardial ridges which arise from opposite sides of the truncus and meet in the middle. The position in which they arise is apparently determined by the spiral course taken by the two blood streams leaving the ventricles. The result is that the aortico-pulmonary septum develops in a spiral manner and separates the truncus into its two channels, the aorta and the pulmonary artery. (For a full discussion of the process, see Icardo (1990).) Between days 6 and 7 (stages 30, 31) extensive apoptosis occurs in the myocardium of the outflow tract and, since this coincides with extensive remodelling of this region, its function is thought to enable the great vessels to align properly over their respective ventricles (Rothenberg *et al.,* 2003). By the end of day 7, the septum has extended back into the interventricular canal and become continuous with the interventricular septum, so that the right ventricle now opens directly into the pulmonary artery whilst the left ventricle opens into the aorta. (For a discussion of some of the differences in this aspect of development between chick and mouse embryos, see Icardo, 1990.) The aortico-pulmonary septa are patches of condensed mesenchyme formed principally by neural crest cells (see Chapter 4) which arise from between the region of the otic placode and the posterior level of somite 3. The migration of these neural crest cells into the

Downloaded from Vet-eBooks.com

developing outflow tract depends on the action of BMP2-4, and if this is inhibited by *noggin* before septation, the endocardial cushions fail to form properly (Allen *et al.,* 2001). Extirpation of this region of neural crest results in failure of the trunco-bulbus septum to form, whilst partial removal leads to defects such as tetralogy of Fallot (Kirby, 1990); replacement with neural crest from other regions fails to repair the defects. It appears, therefore, that the 'cardiac' neural crest cells are already committed to form cardiac cells (Kuratani and Kirby, 1991). Removal of the nodose ganglion at the same time as these 'cardiac' neural crest cells results in even greater anomalies.

During days 4–5 the valvulae venosae and the sinu-atrial valves develop from the wall of the right atrium at its junction with the sinus venosus. The valves in the atrioventricular canal (*Plate 127*) are formed partially from the endocardial cushions and partially from the atrial and ventricular muscles. The ventricular walls become greatly thickened (*Plates 40, 41, 136*) and muscular with extensive trabeculae carnae. The sinus venosus and the sinu-atrial valves are retained as definitive structures in the adult bird heart (Quiring, 1933), whereas in mammals the sinus venosus is absorbed into the right atrium.

During the period of separation of left and right sides of the heart changes occur in their histology. By 5 days of incubation, bands of muscles have begun to form in the atria, and between days 7 and 11 these become the 'muscular arches' which are a characteristic of the avian atria and appear to play an important role in systole.

Change in Relative Position of the Heart

In its initial stages as a simple tube, the heart lies at the level of the rhombencephalon, but by day 4 of incubation, when all the main chambers have been formed, it is situated at the level of the wing buds. The 'descent' of the heart is largely the result of an increase in the length of the neck and brain, which therefore shift forward in relation to the heart.

The Heart Beat

The hearts of birds differ from those of mammals in that they have heavier workloads because of the requirements for flight: very large volumes of blood passing to the wings and flight muscles. A review of the adult heart and circulation is given by West *et al.* (1981).

If isolated cells from the precardiac mesoderm at stage 7 are maintained *in vitro,* they will begin to pulsate, though each at its own rhythm. If they come into contact with one another, then they beat in synchrony. According to DeHaan (1990), who exchanged pieces of tissue within the precardiac mesoderm area, the heart mesoderm is not yet stably coded for its future intrinsic beat rate, and local cues from the surrounding tissues can alter it as it differentiates.

Action potentials in the cardiac mesoderm can be recorded at stage 9, first appearing in the left caudal region of the ventricle (Hirota *et al.,* 1987) before either the atrium or the sinus venosus have formed. This indicates the first sign of the pacemaker. Contractility is visible in the heart from about stage 10. By about stage 12 waves of excitation sweep forward from the caudal pacemaker and lead to a rhythmical contraction of the muscles, an event which causes the blood to start circulating (DeHaan, 1990). The beat rate is higher at the posterior (sinu-atrial) end than at the cono/anterior end. The heart rate increases from about 78 beats per minute at stage 12 to about 162 at stage 24 (Keller *et al.*, 1990). As with other tissues, gap junctions play an essential role in the electrical conductivity of the heart. Overall junctional resistance depends on the number of channels in a junction, their single channel conductance and the probability that the channels are open. Interestingly, although the size of the heart increases by more than a thousand times during the embryonic period, the time for the spread of excitation remains relatively constant because the conduction velocity increases rapidly in the ventricles (DeHaan, 1990). The atrio-ventricular node and the upper part of the atrio-ventricular bundle (conducting tissue) develop in the interatrial septum at 5.5 to 6 days (Argüello *et al.,* 1988).

Circulation

The first blood vessels are extra-embryonic and are formed by the process of angiogenesis (sprouting). Blood islands (*Text-Figure 37*) become visible in the proximal region of the yolk sac, the area vasculosa, from about stage 6. They develop from isolated clumps of cells in the splanchnic mesoderm. The peripheral cells of each blood island become the endothelium, whilst the remaining cells become the haematopoietic (primitive) blood cells. Columns of cells sprout from each blood island and become

Downloaded from Vet-eBooks.com

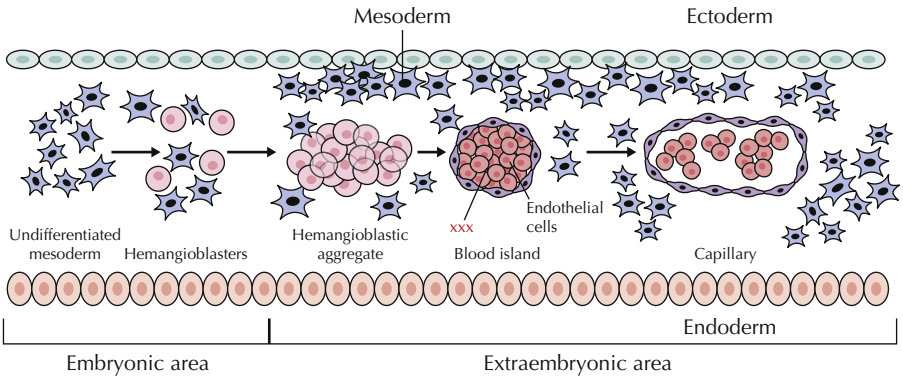

Text-Figure 37. *Yolk sac blood islands. The major types of cells arise from undifferentiated cells, the future haemangiopoietic cells and the endothelial cells. As the early cells aggregate into blood islands, the central ones (pink) become haemangioblasts, whilst the surrounding ones (blue) form the endoblasts. (From Eichmann et al. (2005), with permission of The International Journal of Developmental Biology.)*

canalized and fuse with those from adjacent blood islands to form angioblastic plexuses. In this way a network of branching and intercommunicating vessels is formed (*Plate 43*). The largest vessels, which develop in the distal part of the area vasculosa, generate both blood cells and endotheleial cells, whereas the smaller ones, which arise in the proximal regions, give rise to endothelial cells only (Sheng, 2010). The first erythrocytes, identified by the presence of a haemoglobin gene, are found at about stage 7 (Nakazawa *et al.*, 2006). The erythrocytes of birds, unlike those of mammals, remain nucleated throughout life but, like the mammalian one, they undergo a sequence of changes in their haemoglobin during embryogenesis (see Sheng (2010) for a clear discussion of chick erythropoiesis).

Most of the embryonic blood vessels are formed *in situ* by the development of endothelial precursor cells, angioblasts, which then fuse together to form vesicles, but without forming haematopoietic cells, except in a small region of the aorta (Risau and Flamme, 1995). This process is often called **vasculogenesis** to distinguish it from angiogenesis, though in each case an angioblastic plexus is formed. The endothelial precursor cells are mainly derived from the splanchnic mesoderm by undergoing a transition from epithelium to mesenchyme. This is due to an induction from the underlying endoderm, though it can be experimentally initiated by treatment with FGF2 (Poole *et al.*, 2001) so that it is thought that the angioblasts are induced by FGF2. The vascular endothelial growth factor, VEGFR2, and its receptor, do not appear to be involved in angioblast induction, though they may play a role in the growth and arrangement of the early blood vessels into a vascular pattern (Poole *et al.*, 2001). Even somatic mesoderm is able to form angioblasts if cultured in the presence of endoderm (Pardenaud and Dieterlen-Lièvre, 1999). The vesicles accumulate along the future pathways of some of the earliest blood vessels, such as the dorsal aorta, and may fuse either to each other or to existing vessels. Experiments in which labelled tissues have been transplanted to other regions of the early embryo (Pardenaud and Dieterlen-Lièvre, 1993) have shown that most mesodermal populations, but especially those of the splanchnopleure, contain cells that have the ability to form the endothelium of blood vessels. Not all the embryonic blood vessels form *in situ*, however; for example, the intersomitic arteries are formed at stage 9 by sprouting from the dorsal aorta (Coffin and Poole, 1988).

Once the main vessels have been laid down, refinements of the pattern take place with the formation of extra vessels by angiogenesis (Pardenaud and Dieterlen-Lièvre (1999). The question as to why some vessels become arteries and others veins has not yet been elucidated. Some role appears to be played by the circulation at later stages, but there is evidence of differences in expression of neuropilins, which are receptors for class 3 semaphorins. Both np-1 and np-2 are expressed in the blood islands of 24 h-old chick embryos, but by 48–72 h np-1 is confined mainly to the arteries and np-2 to the veins (Herzog *et al.*, 2001).

Analysis of several signalling molecules in other vertebrates (e.g. in both zebra fish and mice) suggest that the individual parts of the vascular system may be predetermined for an arterial or venous fate from an early stage, though it remains possible to convert arteries into veins, and *vice versa*, by ligating vessels so that the blood flow is diverted (Eichmann *et al.*, 2005). The blood begins to circulate at about stage 12 or 13).

Downloaded from Vet-eBooks.com

THE BLOOD VESSELS

The Extraembryonic Blood Vessels

The extraembryonic blood vessels serve the tissues that develop in the extraembryonic membranes; the first are the omphalo-mesenteric (vitelline) vessels. These carry blood from the embryo to the yolk sac and back again, and their function is to transport partly digested yolk to the embryo. The second are the chorioallantoic blood vessels which carry respiratory gasses to and from the chorioallantois (see Chapter 13).

The sequencing of the pattern of the vessels of the yolk sac is a complex one, and a detailed account is given by Romanoff (1960). Small vessels consist initially of a single-layered endothelium. The pattern begins from about stage 9 with the blood islands in the splanchnic mesoderm of the proximal part of the area opaca joining those in the distal part of the area pellucida to form a meshwork of capillaries. By the time that circulation begins (about stage 12), a series of channels of varying size has formed. By about stage 16 the vascular area of the yolk sac has become surrounded by the sinus terminalis (*Text-Figure 38*), a vein that sharply delineates the area vasculosa from the non-vascular area vitellina, which lies more peripherally. The capillaries that form near the body are relatively large and gradually become transformed into a major pair of vessels, the left and right omphalo-mesenteric (vitelline) arteries. As the circulation begins in the embryo itself, blood passes from the dorsal aorta at about the level of the 18th pair of somites, into the right and left omphalo-mesenteric arteries and then into the area vasculosa. It enters a series of smaller and smaller branching arteries, eventually moving through a meshwork of fine capillaries that extends over the proximal part of the area vasculosa (the developing yolk sac). It is then collected up into the anterior or posterior **omphalo-mesenteric (vitelline) veins**, either directly or by way of the sinus terminalis. Blood returns from these veins to the heart. Initially, a left and right pair of anterior omphalo-mesenteric veins develop, but by about 3.5 days the two begin to anastomose, and by the end of day 4 only one remains (*Text Figure 38*), the unfused remnant of the other one having atrophied. There is some disagreement in the literature as to whether it is the left or the right which survives, but it is possible that there is some individual variation. The posterior omphalo-mesenteric vein also appears to be paired in some cases, but eventually becomes single. The haemodynamics of blood flow in the omphalo-mesenteric arteries at stage 16 are described by Lee and Lee (2010). Although the pattern

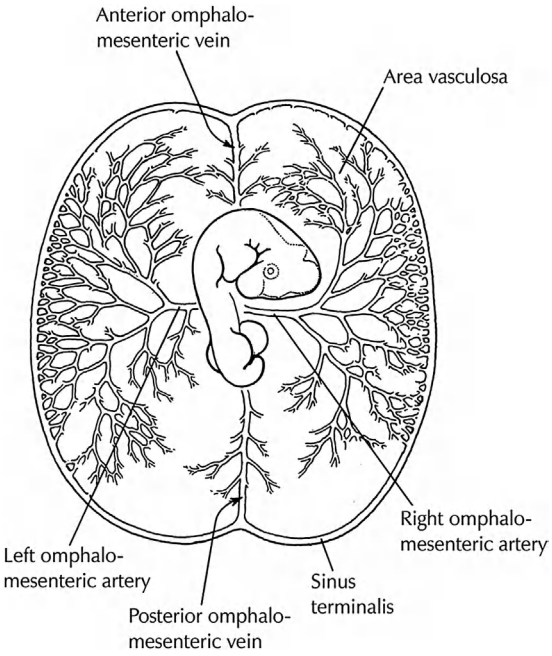

Text-Figure 38. *Vitelline circulation in the area vasculosa at 4 days, seen from the dorsal side. The vitelline vessels become the omphalo-mesenteric vessels in the embryo.*

of the omphalo-mesenteric bood vessels is similar in different individuals, the details of the network show many variations. Using an optical imaging technique Davis *et al.* (2008) showed that the early heart tube structure influences the dynamics of blood flow.

Those capillaries through which blood flows most rapidly become the largest vessels (Hughes, 1937). According to Romanoff (1960), changes in the circulation during day 3 cause some of the capillaries that were originally arterial to become transformed into veins, and the sinus terminalis to begin to regress from about stage 20 (4 days). By the end of day 5, however, a dense network of blood vessels has formed. By stage 16 the two omphalo-mesenteric arteries have fused into a single vessel which lies between the fifth and tenth somites. The omphalo-mesenteric vessels continue to branch and extend into the endodermal folds on the inner side of the yolk sac through most of the incubation period. The yolk sac is withdrawn into the body at hatching, and the omphalo-mesenteric vessels continue to absorb yolk for the first day, after which they begin to degenerate.

The Allantoic and Chorioallantoic Circulations

The allantois starts to develop from about stage 18 (3 days), though in some individuals it may not appear until 4 days. Shortly after its appearance it forms a

Downloaded from Vet-eBooks.com

ramifying network of capillaries that receive blood via the allantoic (umbilical) arteries and return it to the body via the allantoic (umbilical) veins.

Fusion of the allantois with the chorion to form the chorioallantois begins during days 6–7. The pattern of vascularity in the chorioallantois begins now to differ from that in the inner layer of the allantois. The capillaries of the outer layer of the allantois proper become highly modified (*Plate 44*) and penetrate not only into the chorion, but even pass through it and come to lie between the shell and the shell membranes. Here they are well placed to take part in the exchange of gases. Romanoff (1960) reported that the capillary vessels are of such a narrow bore that blood corpuscles can pass through only in single file.

EMBRYONIC BLOOD VESSELS

Paired **dorsal aortae** are visible beneath the somites (*Plates 17, 71*) by about stage 8. At about stage 15 the right and left dorsal aortae begin to fuse together. They are brought into proximity by the enlargement of the coelom and the formation of the dorsal mesentery. This process is related to the folding of the body wall (*Text-Figure 35*). The fusion remains incomplete in the extensions of the aortae anterior to the heart, which subsequently become the internal carotids (*Text-Figure 39*; *Plate 100*). At the most posterior end the dorsal aorta extends into the tail as a small vessel, the caudal artery (*Text-Figure 43; Plate 47*).

The pattern of development of the embryonic arterial system is comparable to that of mammalian embryos, the major difference being that in adult birds the aorta loops to the right, whereas in mammals it loops to the left. In order to understand how these differences are brought about, we must consider the development of the aortic arches.

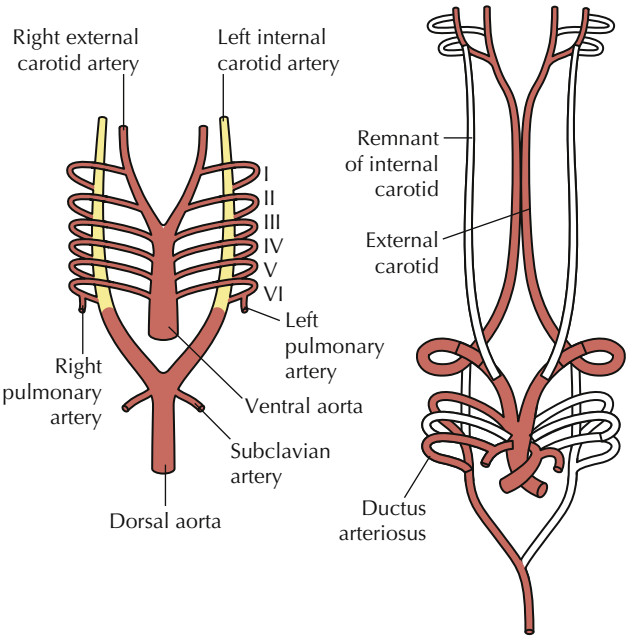

Text-Figure 39. *The relationship between the dorsal aorta, ventral aorta and aortic arches. (a) Basic pattern in vertebrate embryos; not all vessels are present simultaneously. (b) Pattern in late bird embryo and adult. (After Kerr, 1919.)*

The Aortic Arches (Arterial Arches)

The aortic arches (*Plates 45, 46, 108–110, 119*) are the blood vessels that supply the pharyngeal arches (Chapter 8), and they serve as a communication between the ventral and dorsal aortae. They are formed mainly from neural crest cells (Brockman *et al.,* 1990). A splanchnic plexus forms around the foregut and gives rise to the pharyngeal arch arteries as well as the pulmonary and bronchial vessels (DeRuiter *et al.,* 1993). The ventral aorta is the main artery into which the truncus arteriosus leads (*Text-Figure 39; Plates 45, 46*). It bifurcates into left and right vessels which extend forward as the paired external carotids, whilst the paired dorsal aortae extend forward as the internal carotids. The aortic arches do not all develop at once, and some are of a transitory nature, disappearing before others have even begun to form. They are paired, serving the left and right pharyngeal regions. A morphological study of their formation was published by Hiruma and Hirakow (1995) using corrosion casts analysed by scanning electron microscopy (*Plates 45, 46*). The first pair forms at about stage 9 (Coffin and Poole, 1988) and passes through the left and right first pharyngeal (mandibular) arches, respectively. The remaining arterial arches form sequentially over the next 3 days of incubation (*Table 3*, p. 81). The basic pattern is characteristic of all amniotes and is indicated diagrammatically in *Text-Figure 39*. The aortic arches are formed, like the dorsal and ventral aortae, from solid angioblastic cords which develop *in situ* from mesoderm and subsequently become canalized. As the pharyngeal arches differentiate into other structures, the individual arterial arches either disappear or become converted. The cranial extensions of the dorsal aortae become the internal carotids in all young amniote embryos, whilst the cranial extensions of the ventral aortae become the external carotids. They are retained as such in mammals, but in birds the internal carotids in the head anastomose with the external carotids at about

Downloaded from Vet-eBooks.com

6.5 days (Hughes, 1934), and the remnants of the internal carotids in the neck region disappear. The paired external carotids come to lie in close proximity to one another, fusing into a single vessel in some species (e.g. herons), though not in the fowl. The carotids branch to supply all the arteries of the head; the main branches have formed by 7.5 days and are illustrated in *Text-Figure 40*. A number of other anastomoses occur between the arteries of the head, forming structures that are sometimes compared to the circle of Willis of mammals. Some anastomoses take place also between arteries and veins. There is evidence that *sonic hedgehog* plays an important role in the formation and modelling of the aortic arches (Kolesova *et al.*, 2008).

Another important way in which birds differ from mammals is that in birds (*Text-Figure 39*), the communication of the fourth arterial arch with the dorsal aorta is retained on the right and lost on the left (about days 6–7), whereas in mammals the the left is retained and the right lost. In amphibians and reptiles both sides are retained, resulting in a double 'systemic' arch.

In the chick it has been possible to induce experimentally the mammalian pattern by ligaturing the fourth arch on the right side (Stéphan, 1949), so that the blood is then diverted through the left aortic arch, which

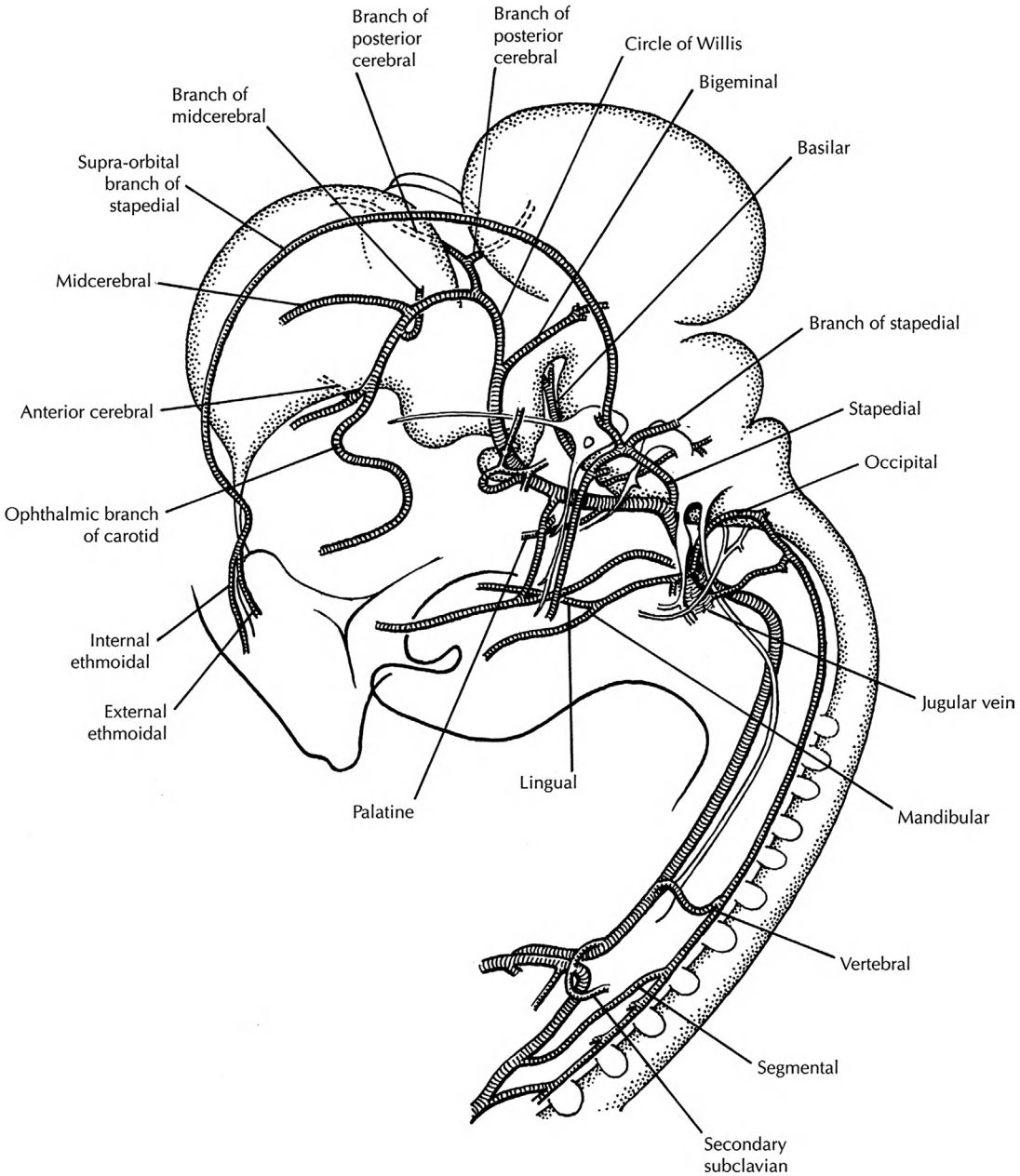

Text-Figure 40. *Arteries of the head and neck at 7.5 days. (After Hughes, 1934.)*

Downloaded from Vet-eBooks.com

therefore fails to become obliterated. Experiments of this sort (e.g. ligation experiments by Wang *et al.* (2009)) provide further evidence of the importance of the blood flow in modifying the vascular pattern, but have little to tell us about the factors that provoke the normal closure and disappearance of blood vessels during embryogenesis. Hughes (1937) suggested that the 'posteriorward shift' in the position of the chick heart and aortic arches as the heart 'descends', together with the torsion and elongation of the truncus arteriosus, lead to mechanical tension which obliterates the lumina of the aortic arches (but see p. 57).

The fifth arch is transitory and disappears on both sides soon after formation. Although it is traditionally considered that the pulmonary arteries in amniotes are derived from branches of the sixth aortic arches (as in *Text-Figure 40*), there is now evidence that they develop as branches of the fourth aortic arch which connect with the endothelial vesicles in the pulmonary mesenchyme (Noden, 1990), and that only later does a communication arise with the sixth aortic arch.

On the right side the connection with the aorta remains as the ductus arteriosus. The distal part of the ductus is very muscular, whereas the proximal region is more elastic, and it is the lumen of the proximal part that becomes occluded at the time of hatching, though it may remain patent for several days (Belanger *et al.,* 2008).

The two dorsal aortae unite posterior to the heart (*Plate 90*) to form a single median vessel which gives rise to:

- The arteries supplying the limbs.
- The segmental (intersegmental) arteries (*Text-Figure 40; Plates 43, 155*), which are branches of the dorsal aorta and extend out between the somites. They contribute to the formation of the vertebral and subclavian arteries, and by stage 11 have formed between all existing somites.
- The omphalo-mesenteric (vitelline) arteries (*Plates 154, 174*).
- The primary mesonephric arteries (*Plate 48*) from which the secondary and tertiary mesonephric arteries are formed, the latter becoming the afferent glomerular arteries (Carretero *et al.,* 1995).
- The allantoic (umbilical) arteries.
- The caudal artery, which is the most posterior end of the dorsal aorta.

THE VENOUS SYSTEM

The embryonic venous system of birds is similar to that of mammals. It forms as an H-shaped structure which subsequently undergoes extensive modification. The

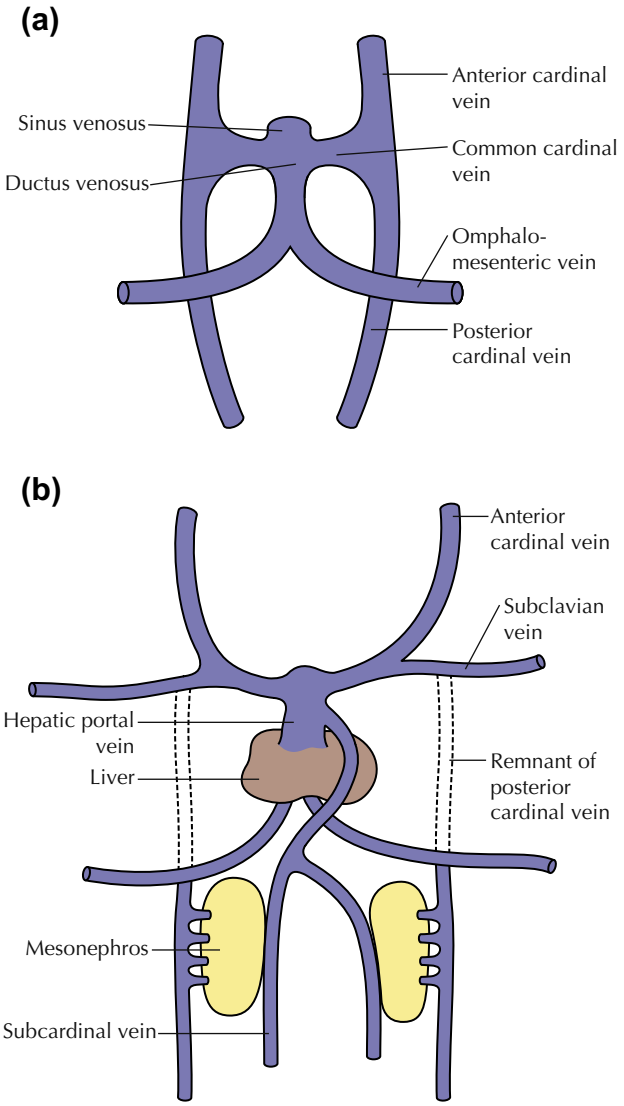

Text-Figure 41. *(a) The cardinal venous system at 3 days. (b) Modifications that have occurred by 4 days.*

sides of the H are derived from the left anterior and posterior cardinal veins and from the right anterior and posterior cardinal veins, whilst the crossbar is formed by the left and right common cardinals (ducts of Cuvier) which bring blood to the sinus venosus. *Text-Figure 41* is a simplified diagram, but *Text-Figure 42* indicates the curving of the sides of the H. The common cardinals begin to form at about stage 11 and by about stage 12 have fused with the omphalo-mesenteric (vitelline) veins, and the circulation has started. The cardinal veins arise *in situ* by the segregation of endothelial cells from the mesoderm (Coffin and Poole, 1988).

The anterior cardinal vessels (*Plate 99*) begin to develop at about stage 8 and are formed by the fusion of a number of vascular spaces which include the left and right head veins (vena capitis), which lie

Downloaded from Vet-eBooks.com

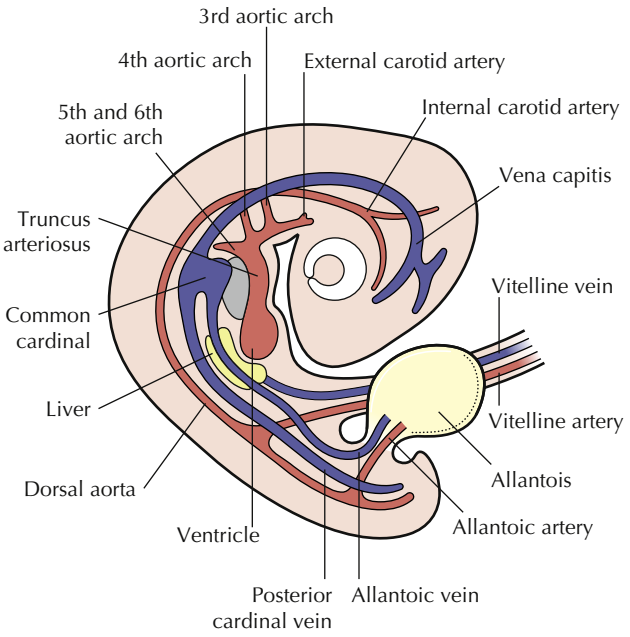

Text-Figure 42. *The main blood vessels of a 4-day old chick embryo prior to modification of the carotid arteries. (After Patten, 1950.)*

on either side of the rhombencephalon. The anterior cardinal vein and the **vena capitis medialis** (median head vein) subsequently give rise to the main venous vessels of the head and neck. A network of vessels, the primary capillary plexus of the head, develops simultaneously. It becomes supplied with blood by the aorta in the forebrain and midbrain and is drained by the vena capitis medialis in the hindbrain region. Further veins, the left and right **vena capitis lateralis** (lateral head vein), have formed by about stage 17 and taken over the drainage of the forebrain. There are many changes in the patterning of the blood vessels of the head during the first half of incubation, vessels forming, anastomosing and often degenerating. They are described by Hughes (1934) and will not be considered here.

The anterior cardinal veins give rise to the jugular veins and the ventral veins of the neck region. Birds differ from mammals in that they do not form a true innominate vein, but instead retain both anterior cardinals, although a small cross-connection, the **interjugular anastomosis** (anastomotic vein), forms at about 7 days and the right anterior vena cava becomes longer than the left. The pulmonary veins are formed from the blood vessels that develop in the splanchnic mesoderm surrounding the foregut (DeRuiter *et al.,* 1993), and they extend into the heart via the remnant of the dorsal mesocardium (Webb *et al.,* 2000). The left and right subcardinal veins (*Plate 149*) are derived as branches from the posterior cardinals (*Plates 112, 114*). By day 6, however, much of the posterior cardinal system has disappeared and the subclavians have formed connections with the anterior cardinals (*Text-Figures 41,43*). The jugular veins on each side join the vertebral and subclavian veins near the heart to form the **anterior vena cava**.

The Omphalo-Mesenteric (Vitelline) Veins

These bring blood back to the body from the yolk sac (*Text-Figure 41, 42*), entering the body at the level of the anterior intestinal portal and merging into a single channel, the **ductus venosus** (*Plate 136*), which empties into the sinus venosus. During subsequent development, the ductus venosus becomes enveloped by the developing liver and breaks up into many channels, though its anterior end remains intact and contributes to the **posterior vena cava** (*Text-Figure 43*). The situation is similar to that in mammalian embryos where the ductus venosus is usually described as a shunt passing through the liver. By day 5 the hepatic portal vein has formed from the omphalo-mesenteric vein.

The Posterior Vena Cava

The formation of the posterior vena cava involves the formation and destruction of a series of vessels. The posterior cardinals (*Text-Figures 41, 43*) are fully formed by about stage 17, sprouts from them becoming the segmental (intersegmental) veins which pass into the inter-somitic spaces along with the segmental arteries. Additional sprouts extend from the posterior cardinals and anastomose to form a new series of veins, the left and right subcardinals (*Text-Figures 41, 43; Plate 48*), which lie close to the left and right posterior cardinals, respectively, on the medial side of the mesonephroi and lateral to the aortae. Branches from the subcardinals collect blood from the hindlimbs and tail as well as from the intestines, and pass it via the mesonephric veins on to the posterior cardinals. The mesonephric veins are therefore renal portal vessels (see Chapter 7). (See Arcalis *et al.* (2002) for a detailed description of the vasculogenesis and angiogenesis of the quail mesonephros.) The posterior vena cava (*Plate 141*) begins to form at about 3.5 to 4 days. Both the posterior cardinals and the subcardinals contribute to it. The subcardinals fuse just caudal to the

Downloaded from Vet-eBooks.com

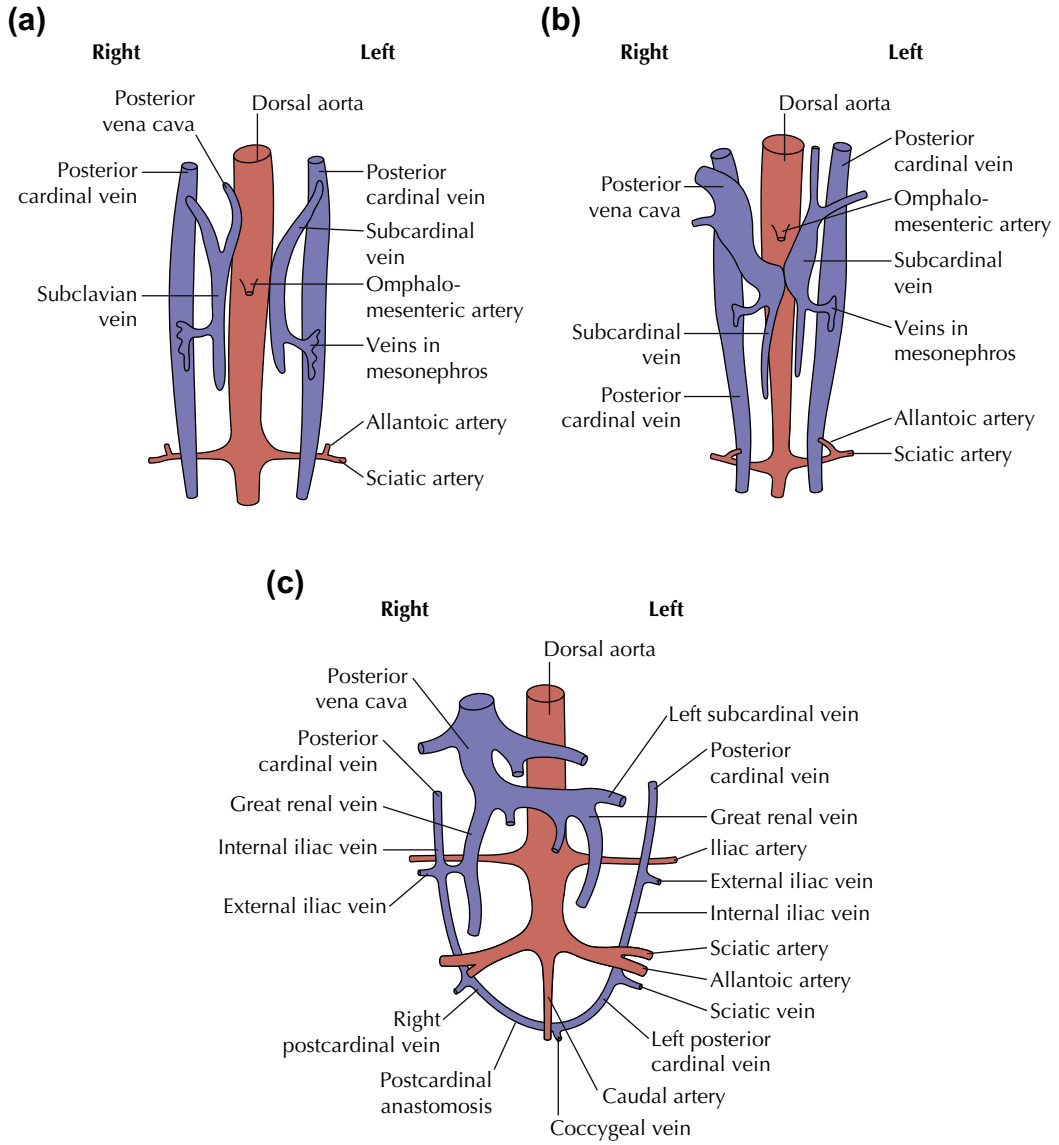

Text-Figure 43. *Development of the posterior vena cava and the renal portal system at (a) 60h; (b) 5 days; (c) 14 days. (After Lillie, 1952.)*

omphalomesenteric artery by day 5 (*Text-Figure 43*), and the anterior part of the posterior vena cava subsequently fuses with the right subcardinal vein. By day 6 the anterior ends of the posterior cardinals have disappeared so that all the blood from the posterior end of the body must now pass through the mesonephric kidneys (*Plates 47, 48, 142*) on its way to the subcardinals. The subcardinals, therefore, become the efferent vessels of the mesonephros. Using scanning electron microscopy of vascular erosion casts, Carretero *et al.* (1997) discovered that an additional blood supply reaches the anterior part of the mesonephros by a hitherto undescribed vessel, the anterior mesonephric portal vein (*Plate 48*). Later, the mesonephric kidneys become replaced by the metanephric kidneys (*Plate 175*; see Chapter 7) and the posterior parts of the subcardinals disappear and are succeeded by the renal veins. The metanephros possesses both an anterior and a posterior portal vein. The posterior metanephric portal vein forms from the mesonephric portal vein, itself a derivative of the posterior cardinal vein, whilst the anterior metanephric portal vein is formed from a new vessel unconnected with the mesonephros. It connects with the vertebral venous sinus. The posterior part of the posterior cardinals fuse together on day 6 (*Text-Figure 43c, Plate 47*) and send a branch, the **coccygeal (caudal) vein,** into the tail. Further anteriorly, the posterior cardinals give rise to the **sciatic** and **iliac veins.** The internal iliac is also known as the posterior mesonephric portal vein (Carretero *et al.,* 1997).

Downloaded from Vet-eBooks.com

THE ENDOTHELIAL AND HAEMOPOIETIC STEM CELLS

The formation of the blood cells is closely linked with the development of the endothelium, the layer of cells lining the blood vesels. The **first endothelial stem cells** arise in the splanchnic mesoderm of the yolk sac and give rise not only to more endothelial cells but also to the first erythrocytes. The factors responsible for the selection of one route rather than the other are not clearly understood, though recent findings implicate GATA transcription factors (Kamei *et al.* 2011).

The first **erythrocytes** (the primary lineage) in amniotes arise from stem cells in the yolk sac and possess a specific haemoglobin (Dieterlen-Lièvre, 1984), though eventually these stem cells die out (Dieterlen-Lièvre, 1997). This author suggested that there is an early haemoblastic rudiment consisting of common ancestors for endothelial cells and haemangiopoietic cells, and that for cells to become committed to the haemangioblastic line they need to be induced by the underlying endoderm. Thus, mesoderm that lies against ectoderm (somatopleuric mesoderm) never becomes vascularized and, as Dieterlen-Lièvre points out, this correlates with the lack of vascularity of the amnion, which is composed of ectoderm and mesoderm. By contrast, the splanchnopleural mesoderm does become vascularized, and this includes the rich vascularization of the allantois (endoderm plus splanchnic mesoderm). Eichmann *et al.* (2005) found that the haemangioblastic aggregates were positive for VEGFR2 but that expression became reduced in the blood islands and capillaries whilst being maintained in the endothelial cells. In the dorsal aorta endothelial cells become haematopoietic cells by downgrading epithelio-specific genes and upgrading haematopoietic ones (Jaffredo *et al.*, 2005). The second generation stem cells subsequently colonise other organs, including liver, bone marrow, spleen, thymus and Bursa of Fabricius (reviewed by Moore, 2004) and even the allantois. New lines of stem cells may be produced in these organs. Dieterlein-Lièvre (2005) emphasized that the emergence of haematopoiesis 'moves from one site to another and is an event spread out over a long period of development'.

Haematopoiesis begins in the spleen at about 10 days, though haematopoietic cells are present from day 4. Lymphocytic homing in the spleen begins just before hatching (Yassine *et al.,* 1989); Nakazawa *et al.* (2011), who analysed chick embryo tissue between 2 and 4 days of incubation, found that the yolk sac endoderm was the major, possibly the only, source of lipids and proteins in the serum.

THE LYMPHATICS

Until recently, the lymphatic system was thought to be formed by sprouting from the venous system but new, highly specific, markers for lymphatic endothelium have shown that lymph angioblasts are present in the mesoderm a considerable time before the lymph sacs develop. Lymph angioblasts migrate from the somites into the somatopleure and contribute to the lymphatics of the limb (Wilting *et al.,* 2001). A series of lymphatic capillaries forms a plexus. Lymph 'hearts' are muscular swellings which pulse and help the lymph to flow, and are thought to be a modification of the lymph vessels. They form along the jugular, subclavian and auxillary veins and subsequently along the posterior cardinals followed by sacs in the lumbar region. (Wilting *et al.*, 2001). Apart from the thymus, the Bursa of Fabricius is the main lymphoid organ in birds, producing B cells (Nagy *et al.*, 2004; Nagy and Olán, 2010). It is difficult to see the lymph vessels in histological sections because of their small size in the embryo; even in the adult they seldom exceed 1 mm in diameter. A detailed account of the adult lymphatic system is given by Rautenfeld (1993).

Downloaded from Vet-eBooks.com

Chapter 7

Urino-Genital System

The development of the urino-genital system follows the usual amniotic pattern, but it includes certain differences that are related to the production of large-yolked eggs, one of the most important being the reduction and loss of function of the right ovary and oviduct. The kidneys of birds differ from those of mammals in certain respects and birds possess a renal-portal system (see Chapter 6) that is not present in mammals.

THE URINARY SYSTEM

With the exception of the cloaca and the primordial germ cells, the urino-genital system is derived from the intermediate mesoderm which lies between the somites and the lateral plate, to both of which it is initially attached (*Plate 65*). It appears at the same time as the somites and develops simultaneously with them, from anterior to posterior down the trunk, but it differs from the somites in that it is not overtly segmented and does not extend into the region of the post-cloacal tail. The intermediate mesoderm becomes a thick band, the so-called **nephrogenous mesenchyme** or nephrogenic cord (*Text-Figure 44; Plate 103*) extending down the trunk on either side of the gut. By 3 days of incubation they have each formed a ridge, the **urinogenital (nephric) ridge.** It gives rise initially to the anteriorly situated **pronephros** (pronephric kidney), then to the more posteriorly located **mesonephros** (mesonephric kidney) (*Plate 48a,b*), which is active throughout much of embryonic life, and finally to the **metanephros** (metanephric kidney) (*Plate 48c*), which is fully functional by day 15 of incubation. At each stage the kidneys are arranged in pairs, left and right. The pro- and mesonephric kidneys are continuous with one another (*Text-Figure 44*) and initially there is not always a clear division between where one ends and the next begins so that they are sometimes called together the nephric kidney to distinguish them from the metanephric kidney. Each kidney is supplied with an excretory duct. The duct that serves the pronephros and subsequently the mesonephros has commonly been known in its early stages as the pronephric duct and in its later stages as the mesonephric duct. However, many authorities now prefer to call it the nephric duct throughout its entire period as a urinary structure. When the nephric duct is no longer needed as a urinary duct it becomes the **Wolffian duct,** and ultimately the **vas deferens** in males. Prior to the development of the metanephros, a new duct forms, the **metanephric (ureteric) duct,** which later becomes the ureter. The development and remodeling of the blood supply of the developing kidneys are described by Makanaya *et al.* (2005).

The pronephric region of the nephric kidney begins to form at about 36 h of incubation (about stage 10) (Abdel-Malek, 1950) and is visible as a solid cord of cells from the level of the sixth to the twelfth somite. By about stage 15 the dorsal part has become tubular, forming the nephric duct (*Text-Figure 45*), and a series of small apertures now open into the coelomic cavity. The openings, the nephrostomes, are visible by scanning electron microscopy (Hiruma and Nakamura, 2003). The ventral part of the kidney forms the tubules (Hiruma and Nakamura, 2003). The pronephric kidney is generally considered to be non-functional, but Hiruma and Nakamura suggested that initially it might have some function since they found that not only were there some glomeruli, but these were connected by thin strands to the nephrostomes. Beginning at about stage 13, it degenerates from anterior to posterior, and has completely disappeared by day 8 of incubation (Romanoff, 1960). The mesonephros (*Plates 48a, 49–51*) overlaps the pronephric region and extends from about the level of the 9th to the 15th somites and, like the pronephric kidney, it forms sequentially

The Atlas of Chick Development. http://dx.doi.org/10.1016/B978-0-12-384951-9.00007-1
Copyright © 2014 Elsevier Ltd. All rights reserved.

Downloaded from Vet-eBooks.com

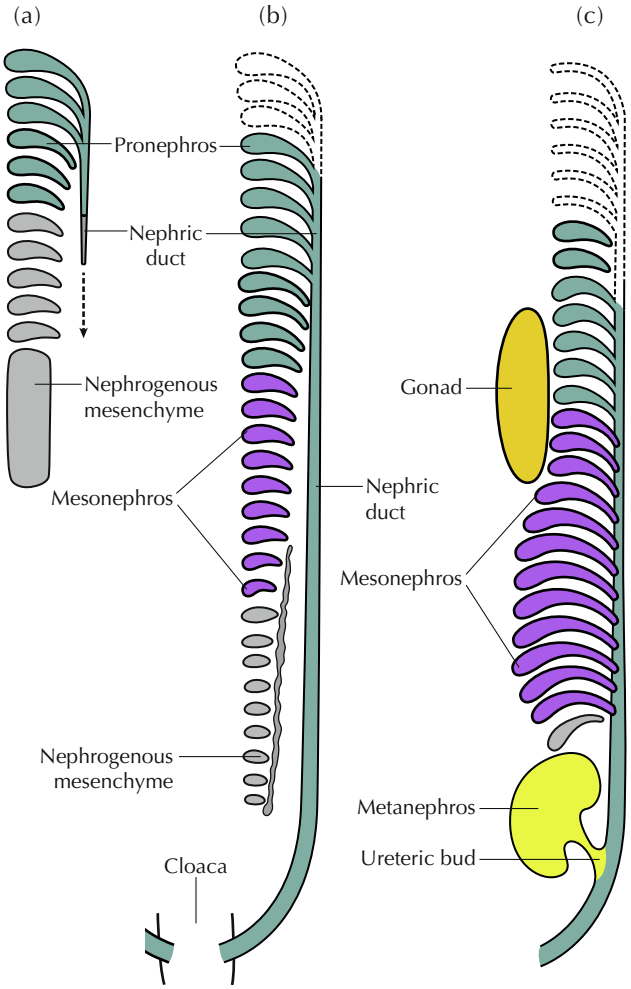

Text-Figure 44. *Plan of the relationship of (a) the pronephros, (b) the mesonephros and (c) the metanephros. (After Burns (1956), with permission from Elsevier Press.)*

from anterior to posterior. It functions from about day 5 to day 11 of incubation. A vascular cast of the mesonephros of a 6-day quail embryo is shown in *Plate 48e*. There is some discrepancy in the literature as to when the mesonephros starts to degenerate, but it has probably ceased to function in the chick by about day 15 of incubation. For a description of mesonephric degeneration, see Carretero *et al.* (1995).

The first-formed (pronephric) region of the nephric kidney appears to be induced before stage 8 by signals from the adjacent paraxial segmental plate mesoderm, although the growth and survival of the lateral plate mesoderm itself depends on contact with the ectoderm (James and Schultheiss, 2003). Mauch *et al.* (2000), using *Pax-2* mRNA expression and Liml/2 antibody staining as markers for the conversion of intermediate mesoderm into pronephric tissue, showed that if the intermediate mesoderm was surgically separated from the somitic mesoderm the pronephros failed to develop. By contrast, the presence or absence of the neural tube, or the notochord or the lateral plate, did not affect its development of the pronephric region.

The prospective pronephric region of the intermediate lateral plate mesoderm was shown by James and Schultheiss to be capable of expressing kidney genes even at stage 6. These authors proposed a model for patterning of the pronephros in which it is repressed by signals from the lateral plate, but these are overcome at stage 9 by signals from the axial tissues.

The gene *Frizzled-4* (*cFz-4*), which is characteristic of the metanephric kidney, is first expressed in the pronephric region posterior to the third somite at stage 10, its expression increasing with development, though gradually becoming restricted to the newly formed glomeruli and tubules of the mesonephros and metanephros (Stark *et al.,* 2000).

The mesonephric nephrons are probably induced by the nephric duct. After experiments in which parts of the nephric duct were ablated, or in which migration of the duct was interrupted (e.g. Gruenwald, 1941; Bishop-Calame, 1965), no further differentiation of the mesonephros took place. Not all experimental evidence supports the idea of induction of the mesonephric kidney by the nephric duct, however, some favouring the possibility of induction by other tissues (e.g. by the gut endoderm, Croisille *et al.,* 1976).

The histological structure of a vertebrate nephron is shown in *Text-Figure 46*. A major component is the glomerulus, a tuft of capillaries that carries afferent blood and is formed as an outgrowth from the dorsal aorta. Vascular casts of encapsulated **glomeruli** from mesonephric and metanephric kidneys are illustrated in *Plates 48b and 48c*, respectively, and sections through mesonephric glomeruli are shown in *Plate 51*. The proximal and distal tubules of each nephron unite to form a collecting duct that communicates with the nephric (or metanephric) duct. This basic structure undergoes modification in later stages. The nephric tubule of the mesonephros, which extends from the glomerulus to the nephric duct, elongates to form a highly coiled structure consisting of proximal and distal regions, together with several intermediate (or transitional) 'segments'. Zemanova and Ujec (2002), who examined the potential difference across the tubular epithelium in embryos of 7 days incubation (stage 30–31), concluded that the distal nephron, unlike the proximal, is capable of active transport at this stage. Excretory products from the blood are filtered through the glomerulus and pass into the nephric duct.

Downloaded from Vet-eBooks.com

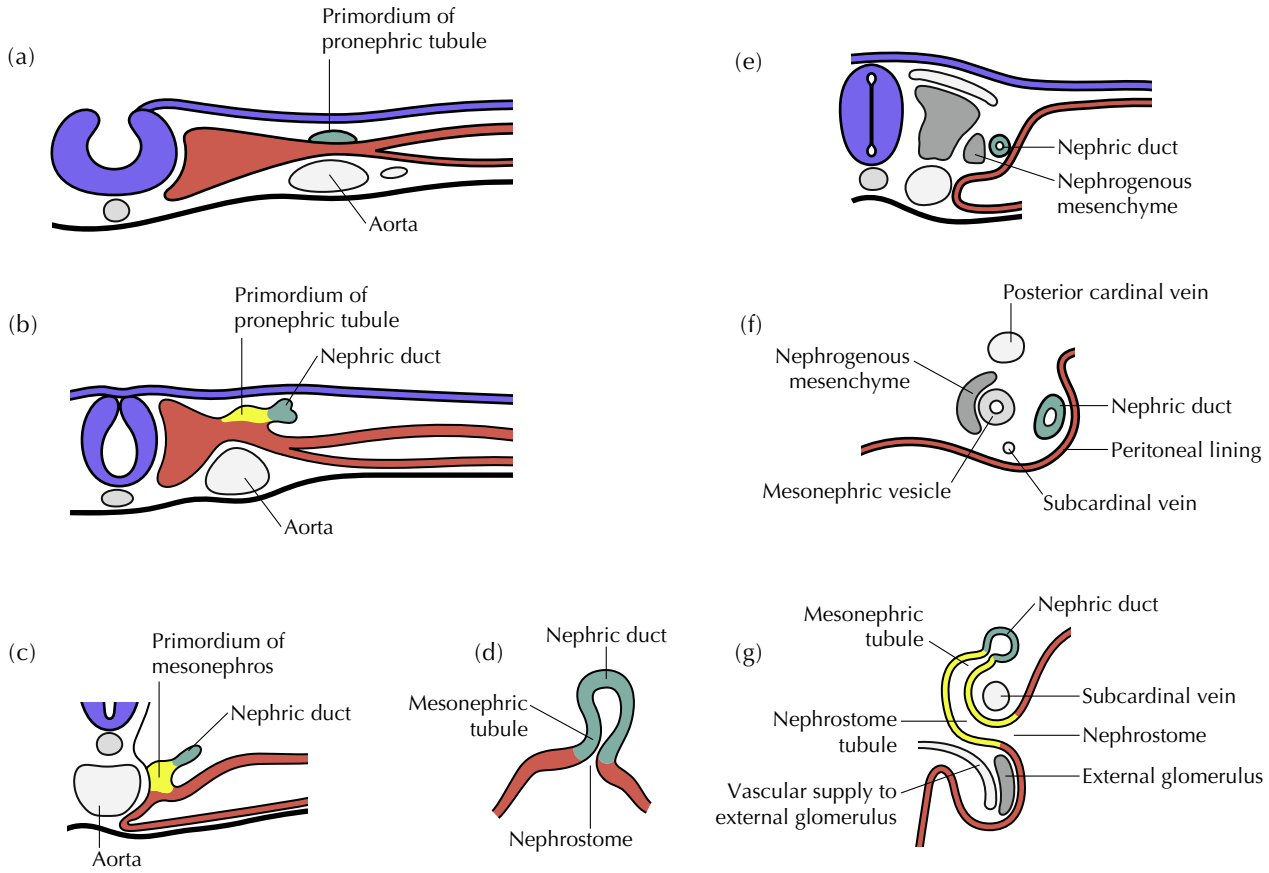

Text-Figure 45. *Transverse sections to show stages in the formation of the nephric duct and kidney. (a,b) The primordium of the nephric duct and a pronephric tubule at about stage 10, at about the level of somites 11 or 12. (c,d) The primordium of the mesonephros at about stage 11 at the level of somite 11. (e) About stage 16 at about the level of somites 22. (f) At about stage 17 at the level of somite 15 to show the nephric duct alongside the nephrogenous mesenchyme. The increased mass of tissue now bulges into the coelomic cavity and is known as the nephrogenic ridge. (g) At about stage 18 at the level of somite 12, showing a mesonephric tubule and an external glomerulus with its blood supply. (All adapted from Abdel-Malek (1950); reprinted by permission of Wiley-Liss. Inc., a subsidiary of John Wiley and Sons, Inc.)*

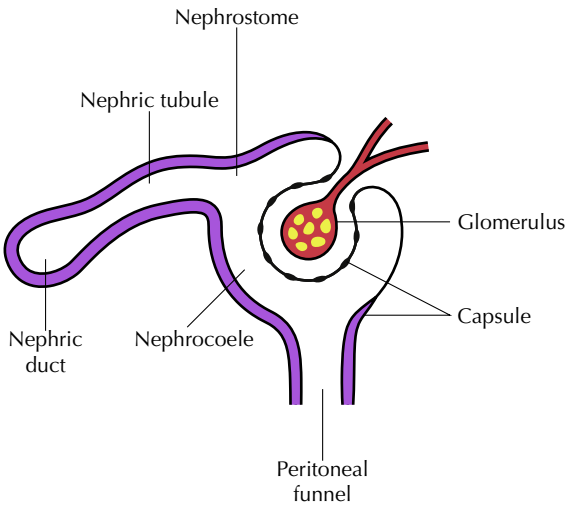

Text-Figure 46. *Diagram of a vertebrate nephron. (After Torrey, 1965 with permission of Academic Press.)*

By 8 days of incubation and until day 20, transforming growth factor α (TGFα) becomes expressed in the distal nephric tubules, and from day 14 of incubation, and continuously thereafter into the adult, is found in the distal nephric tubules of the metanephros (Diaz-Ruiz *et al.*, 1993).

A distinction between internal and external glomeruli is sometimes made (*Text-Figure 48*). External glomeruli, which are the first to form, are nephrogenic masses hanging freely in the body cavity, forming the nephrogenic ridge (*Text-Figures 45, 48*). Internal glomeruli, which develop later, lie within the nephrogenic ridge and are individually enclosed within a capsule, an internal glomerulus together with its capsule constituting a Malpighian corpuscle. External glomeruli are characteristic of the most anterior (pronephric) region, whereas internal glomeruli are characteristic of the mesonephric and metanephric regions.

Downloaded from Vet-eBooks.com

Each nephric duct (*Text-Figure 44; Plate 50*), like its kidneys, develops from the intermediate mesoderm and is visible at about 30 h of incubation (stage 9). During the next 30 h it lengthens steadily and fuses with the cloaca (*Plate 104*) at about stage 17.

There are several possible, though not mutually exclusive, ways in which the duct might lengthen. They include differentiation of intermediate mesoderm *in situ,* addition of cells from the lateral plate, a high level of mitosis and/or cell elongation, and finally the migration of mesodermal cells at the caudal end. The evidence strongly supports the idea that migration plays a significant role (discussed by Bellairs *et al.,* 1995) and is based mainly on the results of transection experiments (Bishop-Calame, 1965), of the effects of destruction of the caudal end (Boyden, 1927; Jacob and Christ, 1978), and of the composition of the duct in experimentally produced chick–quail chimeras (Martin, 1971). As it lengthens, the duct becomes epithelial, but at its posterior (i.e. undifferentiated) end it remains mesenchymal (*Plate 50*). In amphibian embryos, the nephric duct has been shown experimentally to migrate actively toward the cloaca, apparently up an adhesive (haptotactic) substrate gradient (Poole and Steinberg, 1982), though the nature of the gradient material is unknown, and to recruit cells *en route* (Cornish and Etkin, 1993). The substrate probably includes fibronectin (Bellairs *et al.,* 1995).

An important controversy, extending back for more than a hundred years, surrounds the early stages of development, that of whether the first nephric ducts form before (e.g. Jarzem and Meier, 1987) or after (e.g. Abdel-Malek, 1950) the first nephrons in the pronephric kidney. Related to this is another question, that of whether the ducts form from the nephrons or the nephrons from the ducts. The evidence is largely morphological. Lear (1993), who used both scanning electron microscopy and immunocytochemistry, concluded that the duct begins to form just before the nephrons, whilst Hiruma and Nakmura (2003) found that the nephric duct and tubules formed simultaneously.

The metanephric diverticulum (the future ureter) arises from the posterior end of the nephric duct just short of its junction with the cloaca and begins to form at the end of day 4. It extends first dorsally and then anteriorly, passing close to and parallel with the nephric duct (*Text-Figure 47a*), though separated from it by the posterior cardinal vein. The question of how the metanephric duct is guided to its destination is an intriguing one, since unlike the nephric duct, which travels towards the posterior end, the metanephric travels away from it. It seems likely

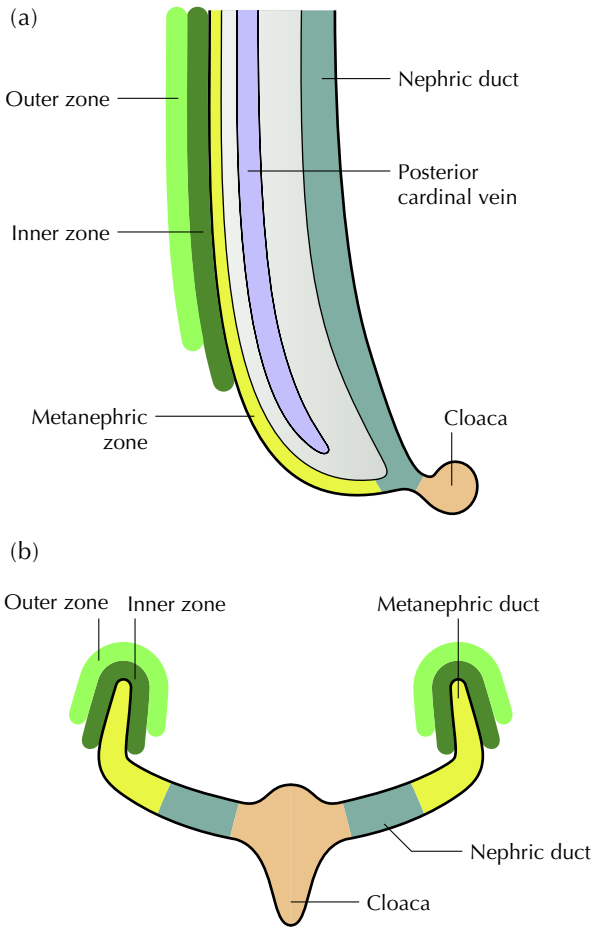

Text-Figure 47. *Relationship of the nephric (Wolffian) duct and metanephric duct at about 4 days. The metanephric mesoderm consists of an inner and an outer zone. (a) Lateral view. (b) Ventral view. (After Abdel-Malek (1950); reprinted by permission of Wiley-Liss, Inc., a subsidiary of John Wiley and Sons, Inc.)*

therefore that the nephric and metanephric ducts are either responding to different cues in the environment, or that there is a significant change in the distribution of environmental cues in the time interval between the completion of migration of the nephric duct and the start of that of the metanephric duct.

The metanephric kidney begins to develop after the metanephric duct has contacted the most posterior region of the nephrogenous mesoderm, which has not been incorporated into the mesonephros. The procedure appears to be similar to that in mammals; if the nephric duct is experimentally prevented from making contact with the cloaca, then no metanephric duct develops and no metanephric kidney is formed. This, and many other experiments, provide compelling evidence that the metanephros is induced by the metanephric (ureteric) diverticulum.

Although the nephrogenic tissue of the metanephros is originally continuous with that of

Downloaded from Vet-eBooks.com

the mesonephros, the two sets of kidneys become separated by the degeneration of the junctional region on days 4–5. Some of the mesonephric veins that supply the mesonephros degenerate, along with the mesonephros itself, whilst others colonize the developing metanephros (Carretero *et al.,* 1997). An account of the process of degeneration of the pronephros is given by Nacher *et al.* (2006).

The metanephric kidney is formed partly from the most caudal (metanephric) end of the nephrogenous mesenchyme and partly from the metanephric duct. The mesenchyme gives rise to the renal corpuscles and the cortical tubules as well as the capsule and stroma of the kidney; the metanephric duct forms the medullary (collecting) tubules and ureter. It is vascularized by branches of the dorsal aorta. Our understanding of the interactions between the epithelial metanephric duct and the metanephric mesenchyme is based mainly on the mouse and is reviewed by Gilbert (2000). By the time it reaches the metanephric mesenchyme, the metanephric duct has begun to branch and, contrary to the usual pattern of organ development, the posterior branches form first, followed progressively by more and more anterior ones; this may be related to the fact that the duct itself contacts the posterior region first. The metanephric mesenchyme consists of two zones, the inner lying between the outer zone and the metanephric duct (*Text-Figure 47a,b, 48*). The primary capsule of the kidney is formed from the outer zone. At about 7 days, each branch of the metanephric duct induces adjacent to it the formation of a cluster of cells formed from the inner region. A lumen develops within each cluster, which then transforms into an epithelial vesicle. Each vesicle elongates into an S-shape, a secretory tubule, the proximal portion of which fuses with the collecting tubule, whilst the distal portion becomes the renal corpuscle. Further elaboration takes place and by day 11 the entire metanephric kidney has formed secreting tubules, and has begun to excrete. The glomeruli are supplied by segmental branches of the dorsal aorta.

At about days 5–6 of incubation, the cloacal wall expands to engulf the posterior end of the nephric duct so that its junction with the metanephric duct becomes absorbed, the result being that the metanephric duct acquires a separate opening into the cloaca from the nephric duct. The metanephric duct will become the ureter. The process is similar to that in mammals except that birds retain the cloaca and do not form a bladder.

The metanephric kidney of adult birds is three-lobed and elongated and does not possess the 'kidney-shape' characteristic of mammals. The left and right kidneys lie at the same antero-posterior level and are not staggered as in mammals. The loop of Henle is less well developed than that of mammals.

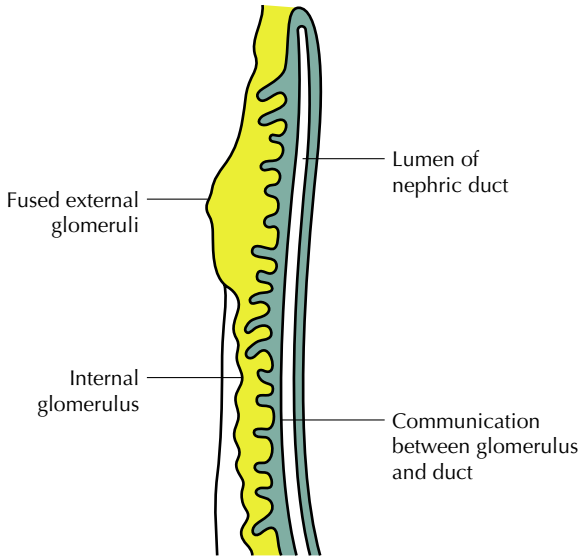

Text-Figure 48. *Longitudinal section to illustrate the relationship between the external and internal glomeruli. (After Abdel-Malek (1950); reprinted by permission of Wiley-Liss, Inc., a subsidiary of John Wiley and Sons, Inc.)*

In the adult kidney there are three types of nephrons, mammalian type I (juxtamedullary) with long loops of Henle, mammalian type II with short loops of Henle, and reptilian type. These differentiate after day 14, but maturation is not complete until after hatching (Gambaryan, 1992). In the mammalian kidney the cortex and medulla are clearly defined, but in the avian metanephric kidney the two are intermingled.

THE GENITAL SYSTEM

Like the urinary system, the genital system forms from the intermediate mesoderm, the two sets of organs being closely linked. By day 3, the nephrogenous mesenchyme has enlarged and given rise to a pair of ridges that hang down from the body wall into the peritoneal cavity on either side of the gut (*Plate 49b*). As the genital components develop, each ridge becomes known as a uro-genital, nephrogenic or **genital ridge** (*Plate 102*). It is covered by the peritoneal epithelium derived from the splanchnic mesoderm. Although an inspection of the chromosomes will disclose the sex of the embryo, it is not possible in the early stages of gonad development to determine from its histology or gross

Downloaded from Vet-eBooks.com

morphology whether it will become a testis or an ovary. This is, therefore, called the **indifferent stage**. There is a large body of literature to show that further differentiation is affected by hormonal activity. For example, female embryos develop testes if implanted at 3 days of incubation with testes from 13-day-old male embryos (Stoll *et al.,* 1993) and early treatment of males with oestradiol leads to feminization of the gonads and retention of the Müllerian duct (Faucounau *et al.,* 1995). In birds the **heterogametic sex** (ZW) is the female, whereas the homogametic sex (ZZ) is the male. This is the reverse of the situation in mammals, where the heterogametic sex (XY) is the male and the homogametic (XX) is the female. It is thought that the sex chromosomes of birds may have developed during evolution from a different set of autosomal chromosomes from those of mammals (Smith, 2007). Until recently the genetic basis for sex determination in birds has been obscure, theories alternating between the effects of specific genes on the W or the Z chromosomes. The problem appears to have been solved, however, by Smith *et al.* (2009), who demonstrated that the conserved Z-linked gene DMRT1 (double sex and mab-3-related transcription factor1) is essential, in double dosage, for testis determination in the chick.

By 3.5 days **the primordial germ cells** have begun to colonize the gonad and initially lie in the peritoneal epithelium. They can be distinguished morphologically from the peritoneal cells by their size, about 10 μm in diameter, as opposed to the peritoneal cells, which are about 5 μm, but more reliably by specific staining (see below). The primordial germ cells enter both the right and left gonads and undergo proliferation from 10 days, but the degree of cell death is greater in the right than in the left (Ukeshima and Fujimoto, 1991), and the right ovary has itself undergone considerable atrophy by the time of hatching.

There are two further components of the indifferent gonad, the **rete cords** and the **primary sex cords.** The rete cords are solid columns of epithelial cells that appear on day 5 among the mesenchymal stroma, and form a meshwork in the anterior region of the gonad by branching and anastomosing. At a later stage they become canalized in the male and form a connection between the primary sex cords and the modified Wolffian tubules, thus forming the rete testis. In the female this connection is not made.

The primary sex cords appear toward the end of day 5. They differentiate into the seminal tubules in the male and the medullary cords in the female. They form by proliferation of the epithelial cells that invade the mesenchymal stroma and they carry the primordial germ cells with them into the substance of the gonad. As both the rete cords and the sex cords proliferate, the indifferent gonad increases greatly in size, causing the genital ridge to bulge further into the coelomic cavity. In both sexes the left gonad is larger than the right and contains more primordial germ cells. The oestrogen receptor mRNA is present in both males and females at stage 26 before any morphological differentiation has taken place between males and females (Andrews *et al.,* 1997). Once the sex differentiation of the gonads has begun, however, the expression of the *aromatose* gene (*cAROM*), which is essential for the synthesis of oestrogen, is restricted to the female. At the time that the morphological differences between the left and the right ovary start to become apparent, the expression of the *aromatose* gene in the left ovary becomes much greater than that in the right (Villalpando *et al.,* 2000). Administration of an *aromatose* inhibitor induces testis development in a genetic female (Nakabayashi *et al.,* 1998) and masculine type genitalia (Burke and Henry, 1999). Conversely, the administration of oestrogen induced an ovo-testis in genetically male embryos (Nakabayashi *et al.,* 1998). The normal development of the male is characterized by the production of anti-Müllerian hormone (Oreal *et al.,* 1998) and the expression of Sox9 in the genital ridges (Kent *et al.,* 1996; Morais da Silva *et al.,* 1996).

Sexual Differentiation

The Testis (Plate 186)

By the end of day 7 the sex cords have proliferated so much that the rete cords have become confined to the hilum. The primary sex cords, which will differentiate into the seminiferous tubules, continue to branch and proliferate and anastomose, but do not become canalized until about day 20. The **primordial germ cells** begin to divide and differentiate about day 13 into spermatogonia. The Sertoli cells and steroidogenic cells have been shown by fate mapping studies to originate from mesonephric mesoderm (Sekido and Lovell-Badge, 2007) and not from coelomic epithelium as traditionally thought; this is in contrast to the situation in the mouse embryo. Administration of FSH stimulates proliferation of the seiminiferous and peritubular cells (Mendez *et al.*, 2003).

We have seen that as the rete cords become canalized they provide a passage for the sperm from the seminiferous tubules to the mesonephros. These mesonephric tubules become the vasa efferentia and

Downloaded From Vet-eBooks.com

their glomeruli disappear. The nephric (Wolffian) duct is no longer an excretory duct and becomes the vas deferens, subsequently carrying the sperm to the cloaca.

The Ovary (Plates 204, 205)

Only the left ovary is functional in adult birds. The indifferent gonad becomes recognizable as an ovary at about 7–8 days by the expansion of the primary sex cords, which individually increase in cross-section and length at about 9–11 days. Subsequently, a second set of cords, the **secondary sex cords,** are formed from the epithelium. The primary sex cords become the medulla of the ovary, whilst the secondary sex cords become the cortex.

The primordial germ cells lie in the secondary sex cords and differentiate into oogonia during day 7. The right gonad fails to form a cortex and remains rudimentary unless the left ovary is removed, when the right undergoes compensatory growth (Groenendijk-Huijbers, 1967). It is capable of differentiation, however, if the left ovary is extirpated, though it forms a testis and not an ovary. It is usually considered that a gonad is incapable of becoming a true ovary without the cortex. Guioli and Lovell-Badge (2007a,b) were able to rescue the right ovary from degeneration by experimentally increasing the expression of Pitx2 (a bicoid type homeobox gene) so that the right and left gonads became indistinguishable from one another. During development, *pitx2c* mRNA transcripts become restricted to the cortex of the left ovary (Rodriguez-Leon *et al.*, 2008). There is also evidence that Pitx2 plays a role in controlling the size and shape of the gonad (Ishimaru *et al.*, 2008). Possible biological reasons why most birds have adopted a single-ovary system are discussed by Guioli *et al.* (2014).

Unlike the situation in the testis, no communication is made between the ovary and the mesonephros, and the latter then degenerates, apart from the region that corresponds to the rete testis in the male. This is found as a rudiment, the epio-ophorum, in the female.

The Sex Ducts

The potential to form either male or female structures is not confined to the gonads, but is also a feature of the sex ducts and the external genitalia. Each individual initially possesses paired male **(Wolffian, nephric)** and paired female **(Mullerian** or **paramesonephric)** ducts (*Plate 49*), but by day 8 of incubation there is a higher density of progesterone receptor-containing cells in the epithelium of the urino-genital sinus of the female than of the male (Gasc, 1991).

We have seen that the male (Wolffian) duct is used in the early stages for excretion by the mesonephros (and is then known as the mesonephric or nephric duct) but is subsequently converted into the male genital duct. This duct undergoes degeneration in the female though remnants may persist in the adult.

The female (Müllerian) ducts (*Plates 52, 204*) develop adjacent to the Wolffian ducts but at a later stage, and according to Gruenwald (1941), are induced by them. Both of the Müllerian ducts of the male and the right Müllerian duct of the female begin to degenerate about day 8. In the male, the degeneration involves extensive cell death, and there is some evidence that this is related to the secretion of the male hormones by the testis (Wolff, 1953). The Müllerian ducts have usually disappeared in the male by about day 12, whereas in the female the right Müllerian duct persists until about day 18.

Our understanding of the way in which the Müllerian duct forms has recently been revised. The traditional concept has been that the Müllerian duct develops first as a groove that appears on the dorso-lateral surface of the nephrogenic ridge and rolls up into a tube, which then sinks beneath the surface of the genital ridge. Jacob *et al.* (1999), however, using scanning electron microscopy, have shown that it begins as a placode-like thickening in close contact with the Wolffian duct at stage 19, and subsequently becomes canalized, the process being almost completed by about stage 28. The Müllerian duct extends by means of groups of cells which detach from the solid cord and move posteriorly, using the basal lamina of the Wolffian duct as a substrate (Gruenwald, 1941). There is a high level of cell proliferation at this stage (Jacob *et al.,* 1999). The blind posterior end meanwhile extends by cell elongation and rearrangement and partially by active migration. These results were supported by Guioli *et al.* (2007), who carried out image tracing experiments and showed that a discrete population of coelomic epithelial overlying the pro-mesonephros was a primary source of all the Müllerian duct apart from the epithelium cells. According to Gruenwald (1941), if the nephric duct is interrupted, the Müllerian duct does not migrate beyond the break, and it seems likely, therefore, that the Müllerian duct uses the Wolffian (nephric) duct as a guide. The ducts in the female fuse with the cloaca about day 11. The left duct then undergoes modification into ostium, glandular regions and the shell gland (*Text-Figure 2*). The opening of the duct into the cloaca does not, however, occur until after hatching.

Downloaded from Vet-eBooks.com

The External Genitalia

In both sexes genital folds and swellings (*Plates 54, 206*) arise at about 6 days of incubation around the cloaca, and a genital tubercle forms at the anterior end. In the mouse, the development of the external genitalia is, in part at least, dependent on *sonic hedgehog* signalling from the urethral epithelium (Perriton *et al.,* 2002), but it is not clear whether the same processes are involved in birds. The appearance of the external genitalia varies considerably in different species (discussed by Romanoff, 1960). In the goose and the male mallard duck the genital tubercle is highly developed even in the embryo, whereas in the domestic fowl it is rudimentary until after hatching.

The appearance of the external genitalia is affected by the hormonal activity of the embryo. Treatment with 17β-oestradiol leads to an increase in the proportion of embryos exhibiting phenotypically female external genitalia (Coco *et al.,* 1992).

The development of the external genitalia has been described by Bakst (1986) (*Plates 54, 55*). Paired 'genital eminences' have formed in the cloacal membrane by day 5 (*Plate 54a*) and have fused together to form the genital tubercle by day 5.5 (*Plate 54b*). Meanwhile, paired 'genital swellings' have formed at the base of the tail, and by day 6 they have not only merged with each other, but have grown to overhang the genital tubercle (*Plate 54c*). By day 7 the enlarged genital tubercle has acquired a bi-lobed appearance (*Plate 54d*), and by day 8 the genital swellings have fused with each other and extended like a collar around the genital tubercle (*Plates 54e,f*). The phallus is formed from the genital tubercle (now the median phallic body) with contributions from two (left and right) lateral phallic bodies. The phallus enlarges and rotates towards the floor of the proctodaeum so that it is visible only after dissection. Meanwhile, radial folds arise around the periphery of the cloaca, and by day 16 the cloacal aperture has become transversely oriented with the smaller, dorsal lip overhanging the ventral one.

The genital tubercle is initially a solid mass of mesenchyme covered with epithelium, but in the male chick a groove develops along its length, the edges of which come together and convert it into a tube, the external seminiferous duct. This gives rise to the penis, which shows remarkable morphological variation in different species, e.g. in the mallard duck the penis is a conical organ with a triple spiral. The male tubercle in the 1-day-old hatched chick is slightly bigger than that of the female and can be used by experienced operators for sexing. Commercially, however, this procedure has been largely superseded by the introduction of breeds of fowl in which the colour or patterning of the down is sex-linked.

The Primordial Germ Cells

The primordial germ cells are the cells that give rise to the germ cells in the gonads from which the gametes are ultimately derived. They begin to differentiate in the early embryo long before the gonads, or indeed any other organs, have started to form, and subsequently migrate through the body to the germinal ridge to colonize the developing gonads (*Text-Figure 49*).

One of the classical problems of embryology has been that of the origin of the primordial germ cells. Weismann (1885) proposed that a specific region of cytoplasm, the so-called **germ plasm,** was set aside in the fertilized *egg* and that this was the forerunner of the entire lineage of the germ line. This theory, usually called the 'continuity of the germ plasm', supposed that the cytoplasm of the germ line was always kept separate from that of the somatic cells from generation to generation. The alternative concept is that the germ cells arise *de novo* in each individual from somatic cells. Nieuwkoop and Satasurya (1979), who reviewed the situation throughout the animal kingdom, concluded that the idea of a continuity of the germ plasm is an out-of-date and unneccessary concept and that the differentiation of germ cells and of somatic cells is much the same. Similarly, McLaren (1981) assembled evidence to suggest that all cells

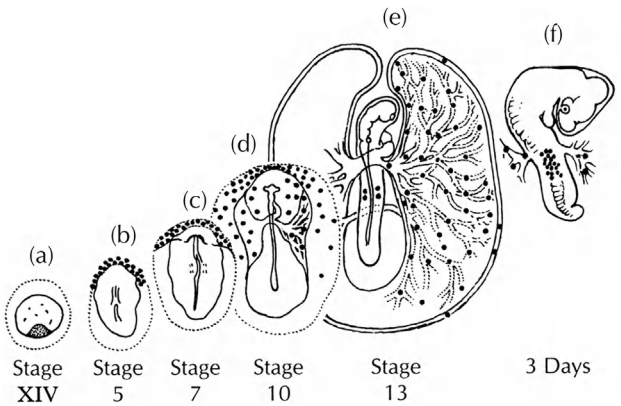

Text-Figure 49. *The primordial germ cells, shown as black dots, arise in the early area pellucida from endophyll cells (a) and migrate to the germinal crescent at the anterior end of the area pellucida (b–d). They enter the circulation (e), and eventually pass into the gonads (f). (After Nieuwkoop and Satasurya (1979), with permission of Elsevier.)*

Downloaded from Vet-eBooks.com

are initially totipotent and that their development into germ cells or somatic cells is dependent on the position in which they find themselves in the embryo during the crucial early stages. This totipotency has been since confirmed by many investigators.

An important component of the developing germ cells is the *vasa* gene protein, which is expressed in the germ layer of several species and is therefore considered to be a characteristic of germ cells. Tsuneakawa *et al.* (2000), using an antibody to the chick *vasa* homologue protein, traced it from the first cleavage stage until it eventually became part of the germ cells. It was associated with the Balbiani body (mitochondrial cloud) of the oocyte and subsequently with the primordial germ cells, and then with the germ cells proper until the formation of the **spermatids** and oocytes in the adult. The function of the *vasa* protein is not yet clear. There are indications that the germ cell is capable of altering its fate under suitable experimental conditions; for example, Kagami *et al.* (1995) found that genetically male primordial germ cells could differentiate into functional ova, and genetically female germ cells into male sperm.

Interestingly, a chick gene, *crescent*, which is first found at stage X (see Appendix I) in the centre of the area pellucida (where the primordial germ cells arise) subsequently becomes localized to the **germinal crescent** (Pfeffer *et al.,* 1997), though it is not clear whether it is associated with the primordial germ cells.

The main reason why this has been such a difficult problem is a technical one. Until modern markers became available, it was not possible to identify the primordial germ cells of birds with confidence before about stage 4 when they started to arrive in the anterior germinal crescent (*Text-Figure 49*), which is located at the anterior end of the area pellucida at its junction with the area opaca. They did not appear to arise in that region, but it was not known how they came to be there. Modern work, which has provided answers to this problem, falls into two categories, specific labelling and microsurgical experiments.

The primordial germ cells from the primitive streak stages onwards stain strongly with periodic Schiff stain (Meyer, 1964), but cannot be stained in this way at earlier stages. A number of specific markers have been reported that not only pick out the primordial germ cells in the germinal crescent, but also identify them at earlier stages. Their major characteristic is that they indicate a strong carbohydrate component at the surface of the primordial germ cells (e.g. Pardenaud *et al.,* 1987; Loveless *et al.,* 1990; Didier *et al.,* 1990). For a review, see D'Costa *et al.* (2001).

Although some differences exist between the results of different workers, nevertheless they are in agreement that primordial germ cells are present from the time of laying (unincubated stage) and are initially in the epiblast. Evidence from a series of experiments (Eyal-Giladi, 1991; Karagenc *et al.,* 1996) in which pieces of the early blastoderm were isolated and allowed to develop *in vitro* suggests that the primordial germ cells arise from the central (i.e. embryonic) region of the area pellucida. These cells are also known as the **endophyll cells** (Vakaet, 1970), or the primary hypoblast by others (e.g. Stern, 1990) (see Chapter 3). With the forward extension of the main hypoblastic sheet from the posterior to the anterior end of the area pellucida, the primordial germ cells become displaced anteriorly, though it is not known whether they are carried passively by the hypoblast or whether they migrate actively along with it. By stage 5, the primordial germ cells that leave the hypoblast land among the mesoderm cells, which have spread out from the primitive streak and then probably migrate actively toward the **germinal crescent.** The numbers of primordial germ cells at stages IX to XIII were found to be about 150 (Karagenc *et al.,* 1996), whilst Nakamura *et al.* (2007) reported that the numbers increased from about 130 at stage X to about 440 at stage 10. When chick embryos were subjected to simulated microgravity in a clinostat, there was a significant reduction in the numbers of primordial germ cells (Li *et al.,* 2002). Further experiments will be needed, however, to decide whether gravity plays a role in the formation or mitosis of primordial germ cells. For a recent review of differentiation and development of germ cells see Nakamura *et al.* (2013).

If the germinal crescent is extirpated, the gonads that subsequently develop possess no germ cells and are, therefore, sterile (Willier, 1937). The size of the germinal crescent varies not only in individual chick embryos, but also among different species of birds (Nieuwkoop and Satasurya, 1979). In the chick and turkey it extends around the anterior half of the area pellucida, whereas in the quail it reaches as far posteriorly as Hensen's node, and even further posteriorly in the duck (D'Costa *et al.,* 2001).

The primordial germ cells arrive in the germinal crescent at stages 4–5, and remain there until the region becomes vascularized at about stage 10. They then enter some of the blood vessels, probably by an active migration, and are carried through the body. Vascular dissemination is found in birds and some reptiles, but not in mammals. Estimates of the numbers of primordial germ cells present at any given stage vary not only according to the investigator, but

Downloaded from Vet-eBooks.com

also to the individual embryo. The greatest number of primordial germ cells in the circulating blood was reported as about 13 per 10 µl at stage 14, though this was followed by a reduction in succeeding stages as the cells entered the gonad (Tajima *et al.,* 1999).

There have been many attempts to explain how the primordial germ cells leave the blood stream and enter the gonad. One possibility is that they become trapped by narrow-bore capillaries in the developing gonad (Kuwana and Rogulska, 1999), though Nieuwkoop and Satasurya (1979) argued against this idea. There is some evidence that primordial germ cells may be specifically attracted to the genital ridges, perhaps by some chemotactic effect (Kuwana *et al.,* 1986). It appears that they leave the blood stream at about stage 16–17 in a region just posterior to the omphalo-mesenteric (vitelline) artery and enter the splanchnopleure. The splanchnic epithelium shifts with the body folding (see p. 53) to become part of the coelomic lining at the site of the future gonad (Ukeshima *et al.,* 1987). Initially, the numbers of primordial germ cells entering the left and right gonads are similar, but by stage 24 greater numbers are present in the left ovary than the right, and by stage 27 more are present in the left testis than in the right (Zaccanti *et al.,* 1990). (For reviews of primordial germ cells see Gomperts *et al.,* 1994; Ginsburg, 1997.)

Petitte *et al.* (1990) produced chick/chick chimeras by injecting blastoderm cells from a darkly pigmented strain (Barred Plymouth Rock) into the subgerminal cavity of an unpigmented strain (White Leghorn). The cells were subsequently found to have become somatic cells (neural crest, erythrocytes) and germ cells. Interspecies chimeras have been similarly produced, e.g. quail/chick (Naito *et al.*, 1991a,b) and quail/duck (Gao, 2011).

The ability to produce chick somatic and germ line chimeras has opened up new approaches to analyzing development in the chick, just as it has in the mouse. For example, Lavial and Pai (2010) have derived embryonic stem cells by culturing chick blastoderm cells *in vitro*. Continual modifications of procedures have led to increasingly sophisticated experiments, and a growing literature.

Downloaded from Vet-eBooks.com

Chapter 8

Gut, Coelom and Respiratory System

EARLY STAGES

The gut of adult birds differs from that of mammals in some important ways. Although birds possess salivary glands, they lack teeth and so are unable to crush and break up food in the mouth. The food passes directly down the oesophagus and collects at its lower end, the **crop.** From here it enters the anterior part of the stomach, the **proventriculus,** where it is subjected to digestive enzymes. It then moves into the gizzard, the highly muscular part of the stomach, where it is ground up. At its posterior end too, the gut of birds differs from that of mammals in that it is not separate from the urinary and genital ducts, but shares with them a common cloaca and cloacal aperture. As in all vertebrates, the entire gut, apart from the stomatodael and proctodael regions, is formed from a lining of endoderm and a covering of mesoderm.

We have seen (Chapter 3) that the definitive endoderm, which becomes the gut endoderm, arises by ingressing from the upper layer through the anterior end of the primitive streak and then spreading to form a disc which becomes drawn posteriorly into a pearshape. The simple tubular embryonic gut is formed by the folding of the body (see Chapter 5; *Text-Figures 35, 50*), and by day 3 consists of the **foregut, midgut** and **hindgut.** The foregut, which starts to appear at about stage 8, is composed of endoderm with closely associated mesoderm. The first part of it to form lies anteriorly, ending blindly at the stomatodaeal plate (see below) where it is fused to the ectoderm (*Plate 64*). In the head the gut is surrounded by head mesenchyme, but throughout the greater part of its length the gut endoderm is associated with splanchnic mesoderm.

The endoderm forms the epithelial lining of the gut and the ducts of the mucous glands, whilst the mesoderm gives rise to the muscular wall and associated structures. The shape of the walls and the lumen vary greatly along the gut. In the oesophageal region the foregut has a uniform structure with a round lumen and thick walls (*Plates 99, 100, 127*), but in the more posterior regions the shape of the lumen and the thickness of the walls vary. For example, see sections of the gizzard (*Plates 141,155*) and colon (*155, 156*). The open, posterior end of the foregut diverticulum is the anterior intestinal portal (*Text-Figure 50, 52; Plate 33a*); it is not a fixed point but an opening into the foregut. Matsushita (1995, 1996) and Matsushita *et al.* (2002) have traced the fates of different regions of the endoderm and the splanchnic mesoderm of embryos of 1.5 days incubation (approximately stages 9–11) using DiI labelling. Although there is some overlap between areas, nevertheless, the cells for each presumptive organ are already 'roughly' segregated. Those endoderm cells located anteriorly and medially contribute to the anterior end of the gut, whilst cells located posteriorly become part of the posterior regions of the gut, though they are situated more laterally at this stage than the anterior cells. As the gut tube continues to form, these lateral cells become drawn medially. The endodermal cells between the first and tenth somites contribute to the gut from the level of the posterior pharynx to the jejunum, and also to the yolk sac. Metzger *et al.* (2011) have recently provided a scanning electron microscope study of the foregut.

The morphogenetic movements that bring about the formation of the foregut extend further and further posteriorly so that there is a gradual movement of cells toward the anterior intestinal portal and through it. As a consequence, the foregut increases in length and the anterior intestinal portal is displaced further and further posteriorly, the population of the cells in its walls continually changing as the cells become incorporated into the foregut. Between stages 7 and 10, the anterior intestinal portal is displaced

The Atlas of Chick Development. http://dx.doi.org/10.1016/B978-0-12-384951-9.00008-3
Copyright © 2014 Elsevier Ltd. All rights reserved.

Downloaded from Vet-eBooks.com

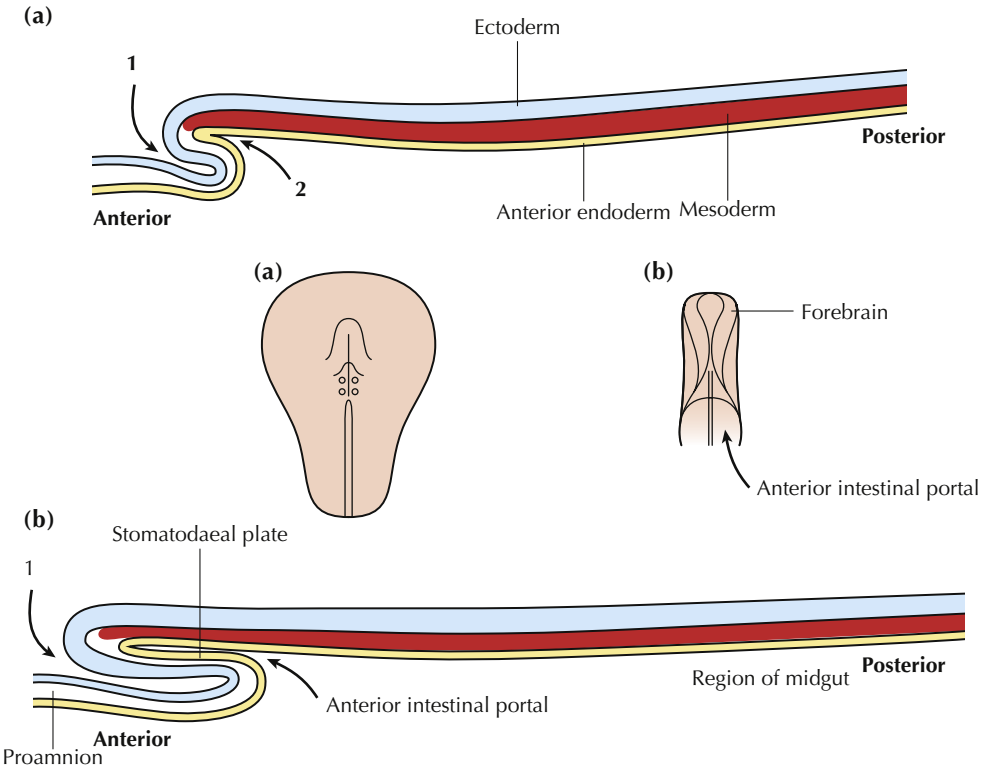

Text-Figure 50. *Formation of head fold and foregut. (a, a) embryo at stage 7 in surface view (a) and sagittal section (a). Arrow 1: head fold; arrow 2: foregut. (b, b) embryo at stage 8, showing surface view of anterior end (b) and sagittal section (b). The head fold has deepened and, as the foregut has lengthened, the posterior end of the foregut, the anterior intestinal portal, has shifted posteriorly.*

posteriorly at the rate of about 0.1 mm h^{-1}, but by stage 12 has slowed to less than 0.02 mm h^{-1} (Seidl and Steding, 1978).

The hindgut, which forms in a comparable manner to the foregut, is present as a simple tube by about stage 14, its anterior border being the posterior intestinal portal (*Plate 83*). A small section of the posterior gut extends into the tail region (*Text-Figure 51*) and is known as the tailgut. The **allantoic diverticulum** (see Chapter 13) starts to arise from the hindgut in embryos at about stage 18, though there is considerable individual variation.

The midgut differs from the foregut and hindgut in that, although it possesses lateral body walls, it lacks a ventral wall and is in communication with the yolk sac (*Text-Figures 50, 52; Plate 79*). By the end of day 5 the foregut and hindgut have extended greatly, whilst the midgut has been reduced to a narrow region, only about 150 μm in diameter, the **yolk sac stalk** (*Plate 176*). Meanwhile, both the foregut and hindgut extend in length. (It should be noted here that in the later embryo and adult the term foregut refers only to that region which lies anterior to the liver, and hindgut to the region posterior to the caecum; the midgut is represented by the intervening portion of gut.)

The differentiation of the simple gut tube into specific regions along its length appears to be associated with localized differences in gene expression. An example given by Smith *et al.* (2000b) is that BMP4 is expressed throughout the hindgut and midgut but not in the early gizzard, and this is correlated with differences in the expression of BMP receptors. *Hox* genes are also associated with differentiation of the various regions of the gut (Sakiyama *et al.,* 2000). Both BMP4 and the specific *Hox* genes appear to be induced by the endodermal signal *sonic hedgehog* (Roberts *et al.,* 1995).

Sonic hedgehog gene also acts as a morphogen, being involved in the morphogenesis and cyto-differentiation of the gut (Fukuda and Yasugi, 2002). Smith and Tabin (2000), who have analysed the lineage relationships of cells derived from the original gut, have found that clonally related cells have become restricted to a single organ by stage 12. They reported that from day 4 to at least day 6 the proventriculus was characterized by *Wnt5a,* the gizzard by *BMPR1B,* the pyloric sphincter by *Nkx2.5* and the small intestine by *Nkx2.5.*

Endo-mesodermal (i.e. epithelio-mesenchymal) interactions play an essential role in the development

Downloaded from Vet-eBooks.com

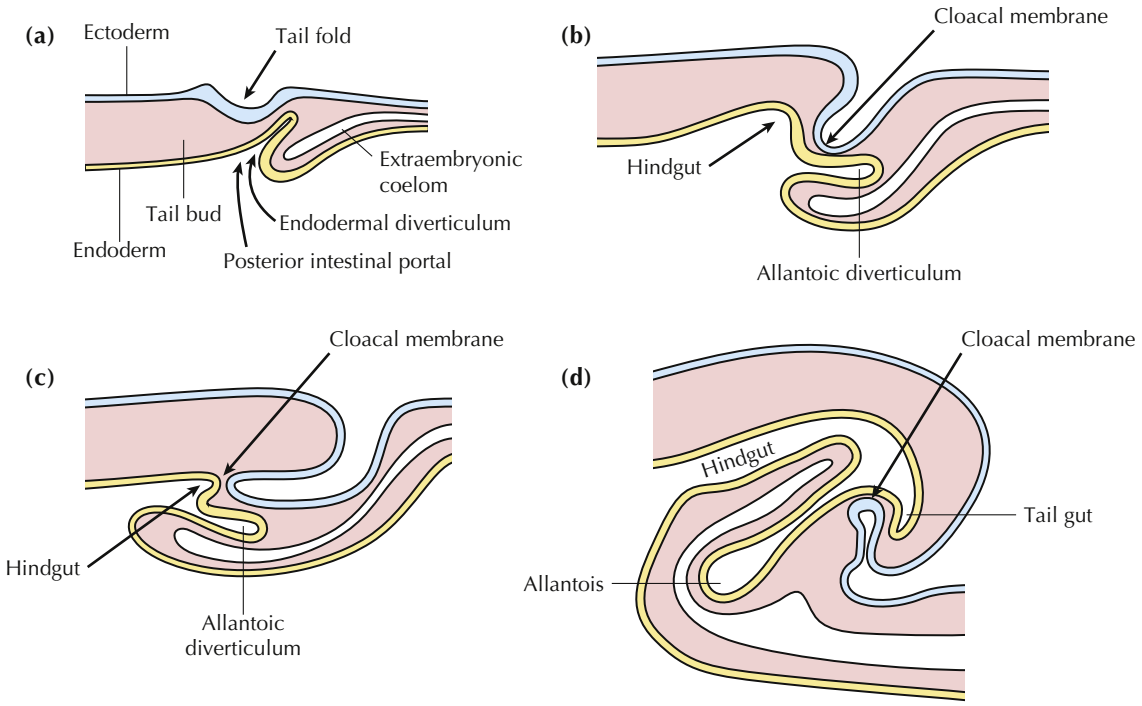

Text-Figure 51. *Formation of tail fold, allantoic diverticulum and hindgut shown in sagittal section at stages 12–13 (a); 13–14 (b); 18 (c); and 20 (d). With the formation of the tail fold, the cloacal membrane becomes drawn ventrally.*

of the gut. Interestingly, the presumptive endoderm cells for the individual regions of the gut were found by Matsushita (1996) to lie anterior to the corresponding mesoderm cells. He suggested, therefore, that the epithelial–mesenchymal interactions that take place as the organs develop may not begin until the two tissues become aligned with each other as the result of morphogenetic movements. Nevertheless, each of these regions of presumptive gut endoderm of stage 10 embryos appears to be already regionally committed, since if each region is individually cultured with flank somatic mesoderm with which it would normally not come into contact, it forms tissues expressing its own appropriate genes (Matsushita *et al.,* 2002). Kimura *et al.* (2007) found that specification begins between stages 8–10 for the foregut but as early as stages 5–8 for the hindgut, and concluded that the differences in timing may be due to differences in the times when the endoderm cells ingress through Hensen's node (Grapin-Botton, 2005). Another possibility is that FGF signaling promotes development of the cells at the posterior end whilst inhibiting those in the anterior regions (Dessimov *et al.*, 2006). Kimura *et al.* (2007) concluded that the endoderm has a regional specification for the foregut, but that strong influences from adjacent tissues are needed for final differentiation. A similar conclusion was reached for other regions of the gut (Yasugi and Mizuno, 2008). There is evidence that the signals include bone morphogenetic proteins (BMPs) that are expressed by the mesoderm. In particular, BMP-2, -4 and -7 are expressed by the mesenchyme of the proventriculus prior to the formation of the proventricular glands (Narita *et al.,* 2000).

The Beak

See Chapter 11.

The Oral Cavity

The mouth is formed partly from the stomatodaeum (*Plates 64, 70*), an ectodermal depression that appears beneath the forebrain at the end of day 2, and partly from the most anterior part of the foregut itself. The stomatodaeum is specified by signals from the endoderm (Withington *et al.,* 2001). **The stomatodaeal (oral) plate** is the region where the endoderm of the foregut fuses with an ectodermal depression of the head, no mesoderm intervening (*Text-Figure 52*). The stomatodaeal plate breaks down in the chick at the end of day 3 so that the anterior (ectodermal) and posterior (endodermal) parts of the oral cavity are now continuous with one another, and the lumen of the foregut comes into communication with the amniotic cavity. The former position of the

Downloaded from Vet-eBooks.com

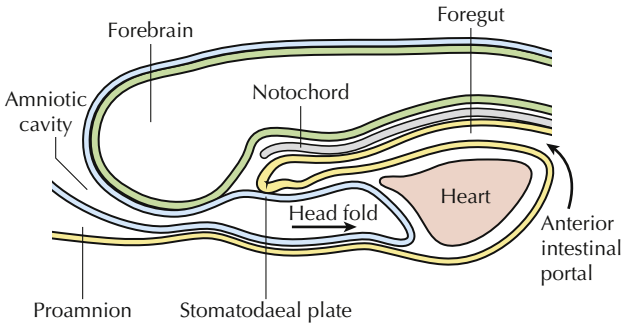

Text-Figure 52. *Sagittal section to show head of embryo at about stage 9. The anterior end lies to the left and the posterior to the right.*

stomatodaeal plate is visible in later embryos by the position of Rathke's pouch (*Plate 96*), which arises immediately anterior to it. Further development of the mouth includes the formation of the jaws from the first pair of pharyngeal arches (see Chapter 10).

The tongue develops principally, as in mammals, from two swellings in the floor of the pharynx in the region of the foramen caecum (the point of origin of the thyroglossal duct) (*Plate 99*) (see Chapter 12 for thyroid development), the **tuberculum impar,** which forms during day 4 at the junction of the first and second pharyngeal arches, and the **copula** (hypobranchial swelling), formed from the basihyal and basibranchial cartilages. Further contributions to the tongue are made by the lateral lingual ridges after the fusion of the main rudiments (see also Chapter 10 for tongue muscles, which are derived from the dermomyotomes). The entire organ is covered with an epithelium. Huang *et al.* (2001) found that the growth of the tongue occurred throughout the tissue and was not associated with any distally located growth zone of the type found in limb bud development. They reported also that the epithelial and mesenchymal components of the tongue were controlled by different genes. There was a high expression of *sonic hedgehog* and *patched* in the dorsal epidermis until about 8 days of incubation, after which the intensity declined and cornification began. These genes were not expressed in the mesenchyme (see also *Text-Figure 83*, which shows the skeleton of the tongue). A scanning electron microscopical study of the chick tongue was published by Bryk *et al.* (1992), and of the goose tongue by Skieresz-Szewczyk *et al.* (2012).

The Pharynx

The first-formed and most anterior part of the foregut tube is the pharynx, which lies immediately posterior

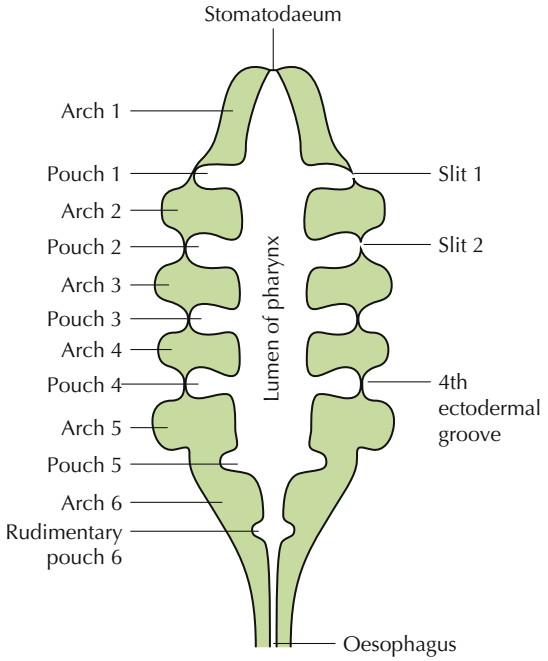

Text-Figure 53. *Stylized diagram of a section along the pharynx to show the relationship between the arches and pouches. On the right side the first pouch has perforated where it has contacted the associated ectodermal groove.*

to the mouth. Its central lumen is initially round in transverse section, but a series of paired pouches extends laterally, the pharyngeal (visceral) pouches (*Plate 80*), so that it becomes trough-shaped in transverse section. The dorsal wall, which lies beneath the notochord and somites, is thinner than the ventral one, which is underlain by splanchnic lateral plate mesoderm (*Plate 61*). In the chick there are four well-developed pairs of pharyngeal pouches, together with a fifth which is smaller. Remnants of a sixth have been described in some birds and may be present in the chick. Cells of the pharyngeal pouch endoderm are rich in cables of actin, which have been shown to play a role in the maintenance of the morphology of the pouches (Quinlan *et al.*, 2004). These pouches form sequentially between stages 10 and 22 and coincide with a series of grooves, the **ectodermal grooves**, that indent the ectoderm. At these points the ectoderm and endoderm fuse and in the case of the first three pouches a temporary perforation is formed (*Text-Figure 53*). The first arch, the maxillary-mandibular, is a major contributor to the facial structures, the maxillary part being traditionally considered to give rise to the maxillary process of the upper jaw, whilst the mandibular process forms the lower jaw. Recent evidence has indicated that interactions with the fronto-nasal process, involving both *Fgf8* and *sonic hedgehog,* may also be important. This

Downloaded from Vet-eBooks.com

communication of the pouches with the outside (i.e. with the amniotic cavity) resembles the gill slits of fishes. Similar perforations are unusual in mammals, but can occur as an abnormality (e.g. as branchial fistulae in humans).

The slits corresponding to pouches 1 and 2 are visible at stage 14, and to pouch 3 at stage 15. The fusion of the endoderm of the pouch and the ectoderm of the groove is possible because the mesoderm is lacking in those regions, although it is present in the remainder of the pharyngeal wall and forms the pharyngeal arches (e.g. *Plate 99*). Each arch consists of a band of mesoderm that passes ventral to the pharynx, and each becomes continuous with the mesoderm of the arch on the other side of the body and is covered externally by ectoderm and internally by endoderm. Pouches and arches alternate (*Text-Figure 53*), the nomenclature being that arch 1 lies anterior to pouch 1, which is followed by arch 2 and then by pouch 2 and so on. The position in which the pouches and arches form appears to be due to an interacting series of signals, *Sonic hedgehog* produced by the pharyngeal endoderm affects the production of *FGF8* in the endoderm of the first pharyngeal arch, which is needed for the development of the cartilages (Haworth *et al.*, 2007). By contrast, *Shh* signaling, whilst remaining high in the anterior pouches, is greatly reduced in the posterior ones where the parathyroid marker, *Gcm2,* is expressed (Grevellec *et al.,* 2011).

The arches and pouches give rise to much the same structures as in mammals (see *Table 2*). The changes begin to take place during the fourth day, and the perforations of the first three pouches close during days 4–5. Each of the three pouches is subdivided into a dorsal and a ventral diverticulum, and these give rise to different tissues.

The **thymus** and **parathyroids** begin to develop about day 4.5, starting as endodermal buds on the 3rd and 4th pouches, the thymic rudiments dorsally and the parathyroids more medio-anteriorly (Le Douarin and Jotereau, 1975; Neves *et al.*, 2012). BMP4 is essential for the development of the early stages (Neves *et al.*,2012). The early development of the thymus and parathryoids is dependent on epithelio-mesenchymal reciprocal interactions between the gut endoderm and neural crest-derived mesenchyme (Neves *et al.*, 2012). The rudiments separate from the pharynx at about day 5 (stage 26) and lymphoid progenitor cells begin to colonise the organ about day 6.5. The entire population of lymphoid cells in the thymus is derived from stem cells, possibly from the yolk sac, carried through the blood vessels, whilst the thymic mesenchyme and the thymic associated blood vessels are derived from neural crest cells that colonise the organs (Le Douarin and Jotereau, 1975). Subsequently, T-lymphocytes emigrate from the thymus and colonise the peripheral lymphoid organs.

Table 2 Pharyngeal derivatives

Arches	Pouches	Derivatives
I Maxilla		Palato-quadrate
I Mandibular	I	Meckel's cartilage Part of tubo-tympanic recess
II Hyoid		Median: copula I and basihyals Lateral: columella and ceratohyals
	II	Thymus II from wall
III		Median: copula II; lateral: Ceratohyal II and epibranchials
	III	Dorsal: thymus III Ventral: parathyroid III
IV		No skeletal contribution?
	IV	Dorsal: thymus IV Ventral: parathyroid IV
V		No skeletal contribution?
	V	Ultimo-branchial body

The **ultimo-branchial bodies** develop from the fifth pouches and become the ultimo-branchial glands of the adult (Dudley, 1942; Kameda, 1984, 1993), which are involved in calcium metabolism (Simkiss, 1967). Their endocrine cells, the C cells, are responsible for the production of calcitonin.

The **pharyngeal arches** give rise primarily to cartilages and muscles (see *Table 2* and Chapter 10). Each arch is served by an aortic arch artery (*Plates 45, 46*), which acts as a link between the ventral and dorsal aortae (see Chapter 6), and by a cranial nerve (see Chapter 9).

The primordium of the thyroid, the **thyroglossal duct,** develops as an invagination (foramen caecum) in the floor of the pharynx at the level of the second pair of pouches (*Plate 99*).

The larynx, trachea and lungs form from an invagination in the floor of the posterior part of the pharynx (see below).

The Oesophagus and Crop

The oesophagus of birds differs from that of mammals in that ridges (plicae) run along its length and protrude into the lumen. They are larger in the domestic fowl, which tends to eat hard food, than

Downloaded from Vet-eBooks.com

in birds which feed on small insects. In the early embryo, the oesophageal region of the foregut has a more uniform structure than the pharynx, with a round lumen and thick walls (*Plates 83, 111*). The lumen becomes reduced from about day 5 to day 6 (*Plate 130*), proceeding from anterior to posterior, ultimately becoming obliterated, apparently due to the rapid growth of the epithelial lining. It starts to re-open during days 6–8, but now proceeding from posterior to anterior. A morphometric analysis was published by Gheri-Bryk *et al.* (1993).

The oesophagus becomes innervated about day 5 by the invasion of fibres from the vagus nerve, and by day 8 **Auerbach's plexus**; by day 13 the **Meissner's plexus** is visible in suitably stained specimens. Solid epithelial buds grow into the tunica propria of the associated mesoderm from day 16, giving rise to the mucous glands.

The **crop** (*Plates 146*) begins to form during days 5 and 6 as a swelling at the posterior end of the oesophagus at about the level of the seventh vertebra. By the end of day 7 it bends to the right and has acquired a lumen about 0.25 mm wide, as opposed to that of the oesophagus proper, which is about 0.16 mm. The crop continues to grow in size as a diverticulum at the right side of the oesophagus (*Plate 166*), its walls and plicae (*Plate 212*) being thinner than those of the main part of the oesophagus.

The Spleen

The spleen starts to be visible during the 4th day of incubation as a condensation of mesodermal cells in the dorsal mesentery. For a recent account of its growth and histology, see Khalil *et al.* (2009).

The Stomach

The region of the foregut which will form the stomach has begun to swell by the end of day 3 and to shift toward the left of the midline. Shortly afterwards the division into the **proventriculus,** the glandular region of the stomach (*Plates 173, 174*) and the **gizzard** where grinding of the food takes place. Epithelial–mesenchymal interactions play an important role in further development. *FGF10* is an early mesenchyme signal necessary for the cell proliferation and formation of the glands in the proventriculus (Shin *et al.,* 2006) which begin to form about day 7. Endodermal invaginations invade the mesoderm layers and undergo budding, and by day 11 have become multilobed. Further modifications take place during the remainder of the incubation period. The shift of the stomach leftwards continues, and by day 7 the gizzard has swollen into a thick-walled sac that points posteriorly (*Plate 153*). The gizzard of the adult is highly muscular and is innervated by Auerbach's plexus, formed partially from neural crest cells (Le Douarin and Kalcheim, 1999) and partially by derivatives of the vagus nerve (Zimmerman *et al.,* 1995). The development of this thickened region is apparent in gross sections from about day 6, but becomes more marked as development proceeds, with the formation of circular muscles. The smooth muscle regulatory proteins, caldesmon and myosin, are, however, expressed before this, as early as day 5 (Paul *et al.,* 1995). Although the secretory glands begin to form about day 12, mucosubstances have been reported to be present as early as day 3 by Matsushita (1998), who examined the gizzard by means of antimucus antibodies. Stimulation of the nerve supply to the gizzard elicited little response, whether intramural or vagal, until after hatching (Ohashi *et al.,* 1993).

The pyloric sphincter appears to be induced at the caudal end of the developing gizzard by *BMP4* signalling from mesoderm of the small intestine from about day 2.5 (Smith and Tabin, 1999). *Nkx2.5* is a marker for the sphincter (Smith *et al.,* 2000b).

The Liver and Gall Bladder

The presumptive liver areas are closely associated with those of the heart, and together are known as the cardio-hepatic regions. They lie on either side of Hensen's node at stages 4–5. But whereas the heart is an entirely mesodermal structure, the liver is formed from both mesoderm and endoderm (*Text-Figure 54*). At stage 12 the endodermal component is located in the floor of the anterior intestinal portal and is derived from a diverticulum of the gut, and by stage 14 it invades the mesoderm that will form the matrix of the liver. The mesodermal component is part of the ventral mesentery, itself derived from the splanchnic mesoderm, and is present as two bilateral patches extending to about the level of the 15th somite (*Text-Figure 54*). The endodermal component becomes split into two diverticula around the ductus venosus, an anterior and a posterior part (sometimes called the left and right diverticula, respectively). By stages 15–16 the anterior diverticulum has extended over the ductus venosus as far as the common cardinal veins. By stage 17 the anterior diverticulum

Downloaded from Vet-eBooks.com

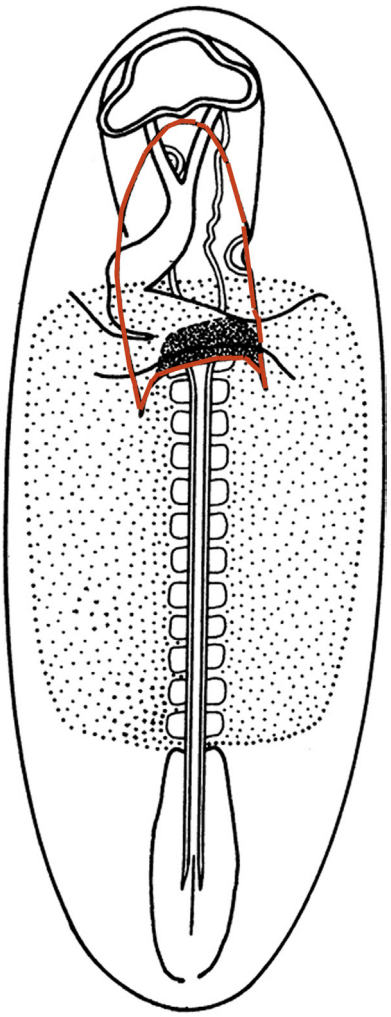

Text-Figure 54. *Distribution of hepatic endoderm (dark shading) and mesodermal areas (light shading) in a stage 12 embryo. The foregut and anterior intestinal portal are indicated in red. (Modified from Croisille and Le Douarin, 1964.)*

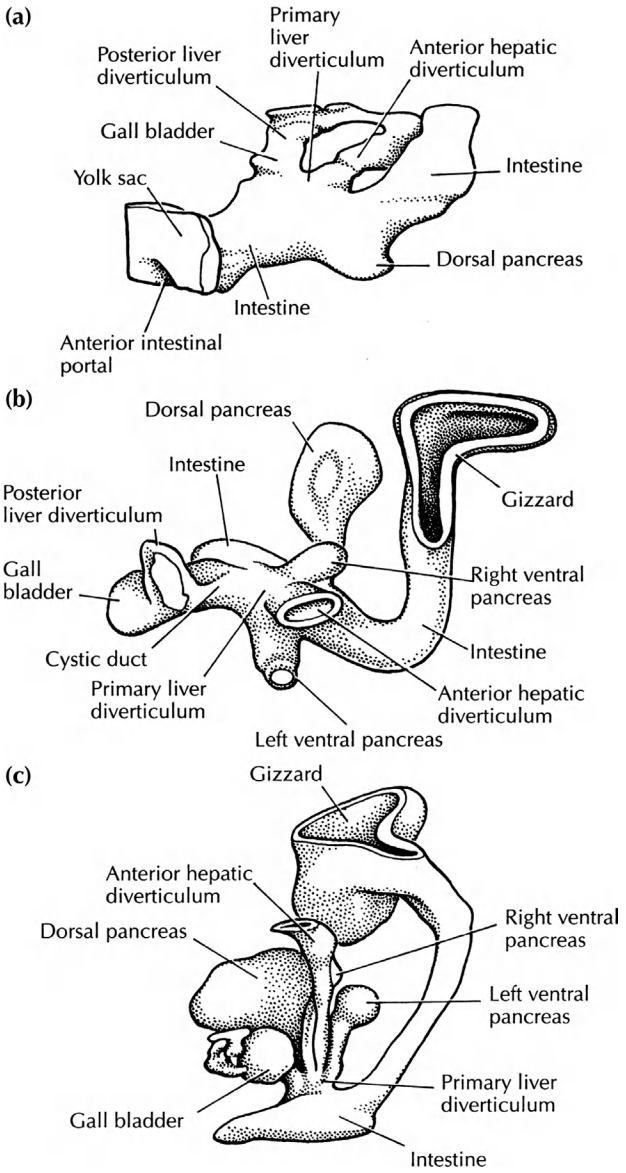

Text-Figure 55. *Development of the biliary and pancreatic ducts and of the gall bladder, (a) stage 18 (3 days); (b) 4 days; (c) 5 days. (Modified after Romanoff, 1960.)*

lies to the left of the ductus venosus and the posterior to the right. The gall bladder and bile duct (*Plate 174*), the **ductus choledochus,** form at about stage 18 as an appendage of the right diverticulum. From about 11 days, the lining cells of the gall bladder undergo dramatic changes (Gheri-Bryk *et al.,* 1990). Experiments in which the endodermal and mesodermal components have been separated from one another or recombined with other tissues have shown that until about stage 8 the endoderm is not determined to form liver. After this, the endoderm is induced by the mesoderm of the hepato-cardiac area. A secondary induction, now from the hepatic mesenchyme, leads to the formation of hepatic cords (Croisille and Le Douarin, 1964).

The liver primordium is visible at the end of day 2. As it grows, it comes into contact with the body wall (*Plate 174*). The veins that pass through the liver are discussed in Chapter 6 (e.g. allantoic vein, hepatic vein, subcardinal vein).

The Pancreas

The pancreas (*Plate 174*) of birds develops from three rudiments, one dorsal and two ventral (*Text-Figure 55*). The dorsal pancreas forms at about stages 17–18 as an outgrowth from the dorsal wall of the gut, and its formation is associated with signals from the notochord (which repress the expression of *sonic hedgehog* in that region (Hebrock *et al.,* 1998), the lateral plate (Kumar *et al.*, 2003) and the somatic

Downloaded from Vet-eBooks.com

mesoderm (Katsumoto *et al.*, 2009). The left and right ventral pancreatic rudiments evaginate from the base of the hepatic diverticulum and are clearly visible toward the end of day 4 (Patten, 1950). Their formation appears to be the result of induction from the splanchnic mesoderm. The initial budding of the pancreatic rudiments from the gut epithelium is associated with the transcription factors *Pdx-1* and *ngn3* (Grapin-Botton *et al.,* 2001). Fate maps of the stomach, pancreas and intestine were published for stages 5–10 by Katsumoto *et al.* (2009).

The three rudiments of the pancreas start to fuse together during day 6, although the process is not completed until about day 9. The number of pancreatic ducts that are retained depends on the species of bird, but usually all three are present in the adult domestic fowl, and open near the end of the duodenum, close to the two bile ducts (for a discussion of the variation in species, see McLelland, 1979). Cell differentiation of the pancreas begins on day 6.

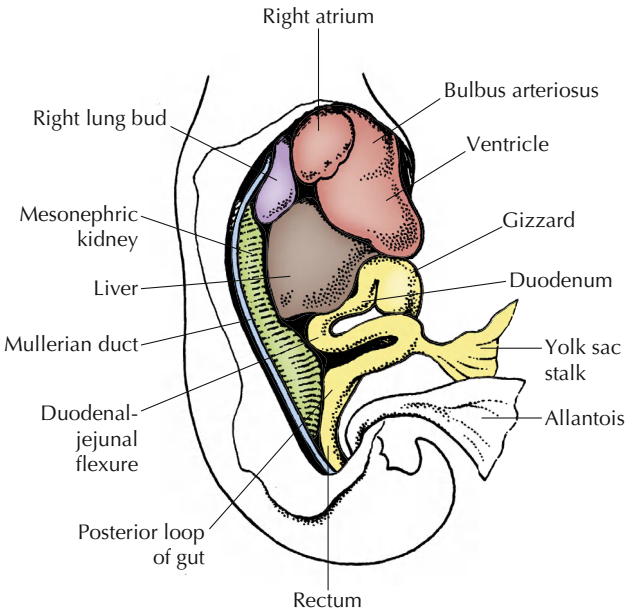

Text-Figure 56. *View of the dissected trunk of an embryo of 6 days to show the gut and other internal organs. (Modified after Duval, 1889.)*

THE INTESTINES

Southwell (2006) published descriptions of the intestines at stages corresponding to Hamburger and Hamilton stages 16–36 (2.5–10 days), though it is not clear how much individual variation exists at each stage.

The Small Intestine

The future divisions of the intestine can be recognized by day 6. A small duodenal loop, which lies beneath the right lobe of the liver, is followed by the duodenal–jejunal flexure (*Text-Figure 57*) and a further loop connecting it to the yolk sac stalk. The caecum, which is present as a small bulge, lies at the junction of the small and large intestines. In later stages the pancreas forms within the duodenal loop. The small intestine, particularly the ileum, grows extensively and, as in other amniotes, is herniated into the umbilical cord (*Text-Figures 56, 57; Plate 187*). This is possible because both the internal and external coeloms, which were in communication in the early embryo, remain so through the umbilical cord. The apex of the loop is continuous with the yolk sac (*Plate 206*). By day 6, the intestinal loop has begun to rotate through 90°, the anterior section moving to the right and the posterior section to the left, a process that is completed by day 11. Further convolutions take place (see Romanoff, 1960), and the gut is gradually drawn back into the abdomen from about day 17, though the process is not completed until about day 19 when the remnant of the yolk sac stalk is also withdrawn. A morphometric analysis of the ileum was carried out by Gheri and Gheri-Bryk (1987). The utilization of the yolk in the newly hatched chick is described by Noy and Sklan (1998).

The Caeca

Although most mammals have only one caecum, birds have two. They begin to form during day 4 as bilateral swellings approximately midway between the umbilical wall and the base of the allantois. By day 7 they have grown to 2–4 mm in length, and by the time of hatching to about 30 mm. A morphometric analysis was carried out by Gheri *et al.* (1992).

The Large Intestine

The large intestines lie posterior to the caeca and begin to elongate after day 4, though they are still only about 20 mm at the time of hatching. At about day 6 the lumen of the large intestine occludes, but has recanalized by about day 12. A morphometric analysis of the ileum was carried out by Gheri and Gheri-Bryk (1987).

Downloaded from Vet-eBooks.com

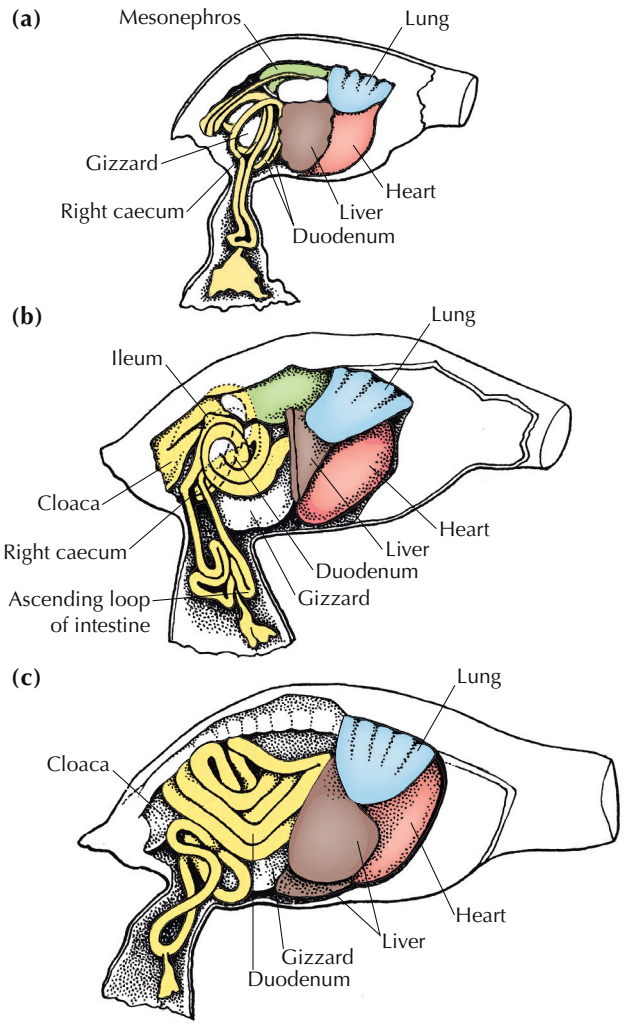

Text-Figure 57. *Development of the intestinal loops herniated into the umbilical cord, seen from right side after removal of body wall, (a) 11 days, 21 h; (b) 12 days, 22 h; (c) 15 days, 22 h. (Modified after Romanoff, 1960.)*

The Hindgut and Tail Gut

The endoderm that will form the hindgut lies posterior to the last somite at 1.5 days of incubation (about stage 10) and becomes greatly elongated antero-posteriorly during gut formation (Matsushita, 1999).

The hindgut begins to appear at about stage 13, and its development is closely associated with that of the tail bud (*Plates 83, 104*). (For a review of the tail bud, see Griffith *et al.*, 1992.) The most posterior section of the hindgut becomes an integral part of the tail and is there known as the tail gut (*Plate 105a*). Both the mesoderm and the endoderm of the tail gut express *Hox-a13*, which appears to be involved in the epithelial–mesenchymal interactions that take place during tail growth and patterning (De Santa Barbara and Roberts, 2002). The tail gut becomes obliterated, largely as a result of cell death (Miller and Briglin, 1996), and has usually disappeared by about 3.5 days (stage 21).

The development of three important structures is closely associated with that of the hindgut, viz. the **cloacal membrane** (also known as the anal plate, **cloacal plate** or proctodaeal membrane) (*Plate 177*), the **allantois** (*Plate 112*) and the cloacal bursa (**Bursa of Fabricius**) (*Plate 207*).

The Cloaca

The cloaca is the enlarged end of the hindgut (*Text-Figure 51d*), which by about stage 10 has become divided into the three main regions, the **urodaeum**, into which the nephric ducts and the Müllerian ducts empty, the **coprodaeum**, which is the collecting point for the hindgut, and the **proctodaeum,** which is associated with the cloacal membrane. The **cloacal membrane** becomes visible at about stages 12–14 as a region just posterior to the tail bud, where an indentation of the ectoderm fuses with the posterior end of the gut endoderm (*Text-Figure 51*). As the tail fold forms, the cloacal membrane becomes shifted relatively anteriorly, its position marking the junction between the trunk and tail. The cloacal membrane perforates just before hatching, and its ectodermally derived part becomes incorporated as the proctodaeum into the cloaca, as opposed to the endodermally derived components coprodaeum (*Plates 208, 209*) and the urodaeum.

The Allantois

Like the gut, the allantois is formed essentially from endodermal epithelium with associated mesoderm. It begins to arise about stage 15 and is usually considered to form as an outgrowth from the hindgut, though some investigators have maintained that it develops before the hindgut. According to Matsushita (1999), pre-allantoic endoderm cells are confined to a small area at the posterior end of the primitive streak. It is only as the tail fold forms that it becomes relocated as a diverticulum of the hindgut. For further development of the allantois, see Chapter 13.

The Cloacal Bursa (Bursa of Fabricius)

During day 4 the Bursa of Fabricius (cloacal bursa) (*Plates 207, 208*) forms as a diverticulum from the

Downloaded from Vet-eBooks.com

proctodaeum, and interacts with the surrounding mesenchyme (Le Douarin *et al.,* 1984a; Nagy and Olah, 2010) and soon becomes highly plicated. By 10 days it has become extensively vascularised (Schoenwolf *et al.*,1981). Its role is related to that of the thymus (Schoenwolf and Singh, 1981) and the spleen (Glick and Olah, 1993). Lymphoid tissue develops in the Bursa of Fabricius on days 12–13 (Goldschneider and Barton, 1976). Cells migrate from liver, spleen, bone marrow and yolk sac blood islands to colonise the Bursa of Fabricius, and the synthesis of immunoglobulins begins soon afterwards. Mature B cells then pass throughout the body to all other lymphoid tissues, where they undergo further differentiation (discussed by Narabara *et al.*, 2009). Other lymphoid tissues include **Peyer's Patches,** which are found only near Meckel's diverticulum, and the **Cecal Tonsil** (Kajiwara *et al.*, 2003).

THE COELOM, MESENTERIES AND RESPIRATORY SYSTEM

The coelom, or body cavity, begins to develop as the lateral plate mesoderm forms (*Plate 61*). We have seen (Chapter 4) that by stage 8 the mesoderm on either side of the midline posterior to the head is starting to form into somites and lateral plate (*Plate 71*). The lateral plate mesoderm remains unsegmented but becomes arranged as two separate sheets, the upper, somatic, layer lying close beneath the ectoderm, and the lower, splanchnic, layer, which adheres to the endoderm (Chapter 5). The space between the two sheets is the coelom or body cavity (*Text-Figures 35, 58*). The splitting of the two sheets follows the usual anterior-to-posterior pattern, though it is not synchronized with the adjacent antero-posterior segmentation of the somatic mesoderm (Funayama *et al.*, 1999). Before the embryonic body begins to fold, the coelom is arranged as two separate regions, the left and the right coeloms, and each of these extends distally beyond the tissues that will contribute to the embryonic body and into the extra-embryonic region. The embryonic and extra-embryonic coeloms are, therefore, in communication, a situation that enables intracoelomic grafting to be carried out at this time (see Chapter 2). As the head fold forms, each lateral coelom extends anteriorly, forming the amnio-cardiac vesicles (*Text-Figure 34; Plate 60*), and the two sides unite anterior to the head at about stage 7. The lateral regions subsequently join to form the heart, whilst the more anterior part, the proamnion, gives rise only to the amnion. By stage 8 the lateral body folds have begun to form, which will eventually lead to the closing off of the ventral body wall, not only bringing the two lateral coeloms into communication with one another, but separating off the embryonic from the extra-embryonic coeloms, as well as playing a role in the formation of the gut and the mesenteries (*Text-Figures 35, 58*). The gut endoderm becomes folded initially into a trough that is open ventrally, but gradually separates from the extra-embryonic endoderm of the yolk sac, except in the region of the midgut, the splanchnic mesoderm of the lateral plate remaining closely adherent to the gut endoderm during this process (*Plate 61*). The left and right sheets of splanchnic mesoderm meet and fuse with one another both dorsally and ventrally to the post-pharyngeal gut as it forms (*Text-Figures 58a,b*). The dorsal fused sheet is the **dorsal mesentery**, and the ventral fused sheet is the **ventral mesentery** (*Text-Figure 58*). In this way the left and right coelomic cavities come into communication with one another and the gut hangs down in the dorsal mesentery. The ventral mesentery survives only in the region of the heart, liver and cloaca.

Throughout its length the coelomic cavity is lined by an epithelial sheet, the **peritoneum**, derived from the splanchnic mesoderm, and any organ or tissue which may appear to protrude into the coelomic cavity does not normally penetrate this sheet but merely invaginates it.

In adult birds, as in mammals, the coelom is divided into three basic compartments, pericardial (*Plate 127*), pleural (*Plate 170*) and peritoneal (*Plate 128*), but there are important differences between the two classes of vertebrates. The first stages are comparable, but differences develop in the relative position of the organs since in birds the heart 'shifts', (though see p. 57) further caudally than it does in mammals. A major difference, however, is that the air sacs, developing from the lungs, penetrate between the mesenteries, further dividing the coelom. McLelland and King (1970, 1975) identified eight coelomic cavities in adult birds. They are the pericardial cavity, the left and right pleural cavities, and five peritoneal cavities (the left and right dorsal hepatic cavities, the left and right ventral hepatic cavities and the intestinal cavity; *Text-Figure 59*). These are all there by 5 days. No true diaphragm is present in birds.

Division of the Initial Coelom

The **pericardial cavity** (*Plates 35, 127*), or pericardial coelom, is formed from the most anterior part of the

Downloaded from Vet-eBooks.com

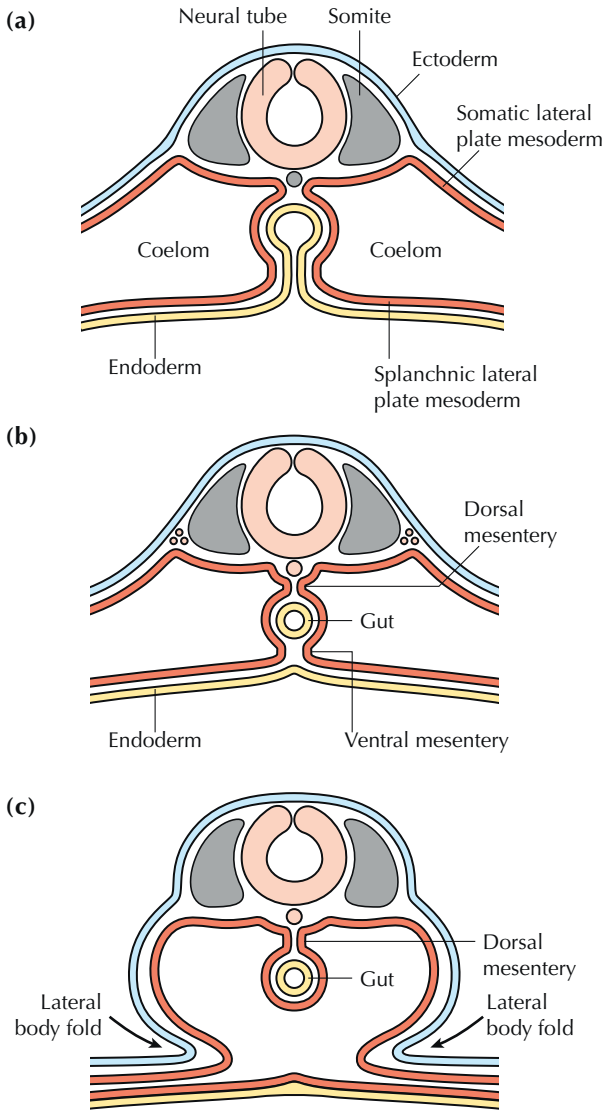

Text-Figure 58. *Transverse sections to show right and left coeloms (a, b) fusing to form a single coelom (c). The dorsal and ventral mesenteries (a, b) form from splanchnic mesoderm, the ventral mesentery breaking down (c) over much of the length of the gut, whilst the dorsal mesentery persists.*

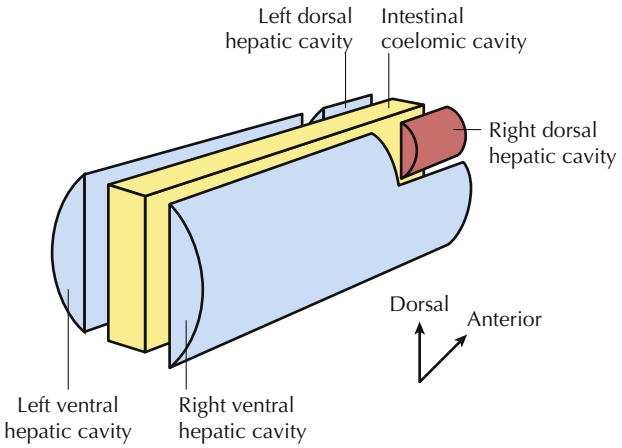

Text-Figure 59. *Highly schematic diagram of the five peritoneal cavities in an adult fowl. (After McLelland and King (1970), with permission of Elsevier GmbH.)*

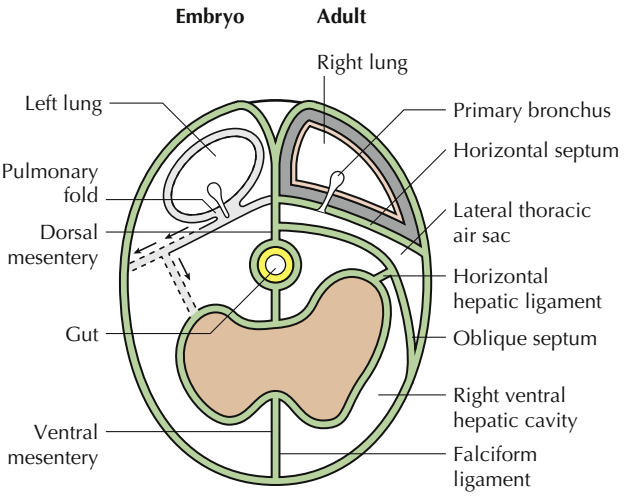

Text-Figure 60. *Transverse section through the pleural region of an embryo (left) and an adult (right). Each pulmonary fold grows ventro-laterally to fuse with the peritoneal lining of the body wall and the liver (indicated on the left by dotted lines and arrows). Later, the lateral thoracic air sac penetrates between the two layers of the pulmonary fold, separating it into the horizontal septum and the oblique septum (shown on right). (After McLelland and King (1970), with permission of Elsevier GmbH.)*

coelom (see amnio-cardiac vesicles in *Text-Figure 34*), and is visible at about 22 h in whole-mounted embryos. As we have seen, the heart develops from thickened splanchnic mesoderm and is initially supported by dorsal and ventral mesenteries (also known as the dorsal and ventral mesocardia), though these break down later, leaving the tubular heart attached to the walls of the pericardial cavity at its anterior and posterior ends only (*Plate 74a*). Shortly after its formation, the pericardial cavity is still in communication with the left and right coelomic regions (*Text-Figure 35*), which themselves extend further posteriorly. It then becomes separated from them by the formation of the lateral mesocardial folds. These arise dorso-laterally from the splanchnic epithelium over the **omphalo-mesenteric veins**.Searls (1986) ascribed the relationship between the pericardial and pleural coeloms to caudal movement of the aortic arches.

The **pleural cavities** become divided from the abdominal cavities by the pulmonary folds (*Plate 128*), each of which arises medially from a lung bud and extend laterally, left or right (*Text-Figure 60; Plate 65*). (In mammals the corresponding folds arise laterally and extend medially.) Each

Downloaded from Vet-eBooks.com

pulmonary fold fuses with the peritoneal lining of the body wall to form the **pleuro-peritoneal membrane**, with the pericardium to form the **pleuro-pericardial membrane**, and with the peritoneum covering the liver to form eventually, the **lateral hepatic ligament** (*Plate 204*). During development the lateral thoracic air sacs on each side invade the pulmonary fold (*Text-Figure 60; Plate 204*), splitting apart the two layers so that two separate septa are formed, the horizontal septum (also known as pulmonary aponeurosis, sacco-pleural membrane (*Plate 204*), or pulmonary diaphragm) and the oblique septum (also known as thoraco-abdominal diaphragm or sacco-peritoneal membrane). (Note: these are not true diaphragms, as found in mammals, so this term is best avoided.) The ventral mesentery persists as the falciform ligament (*Plate 204*), a transverse sheet connecting the ventral body wall (inner face of the sternum) with the ventral surface of the liver. It thus corresponds with the falciform ligament of mammals. The post-hepatic septum is an extension of the mesentery arising at the level of the gizzard.

The **dorsal** and **ventral hepatic cavities** (abdominal coeloms) (*Plate 204; Text-Figures 59, 60*) lie on either side of the midline. Their mode of formation is not clearly understood, and no recent investigation appears to have been carried out.

The **intestinal coelomic cavity** (*Text-Figure 59*) contains all of the intestinal tract from the proventriculus to the rectum, including the pancreas and liver, as well as the gonads, the spleen and the abdominal air sacs.

THE RESPIRATORY TRACT

The lungs of birds differ markedly from those of mammals and other vertebrates, their unique modifications being related to the higher metabolic rate of birds. These modifications include the absence of alveoli and the anastomosis of branches of the bronchi so that the lung resembles a sponge in structure (*Plates 56, 57, 170*). The air is thus able to pass quickly throughout the organ. The avian lung differs also from the mammalian one in that it is not elastic and expandable, and that air sacs extend posteriorly from it. These air sacs, which are poorly vascularized, expand during inspiration and contract during expiration, like bellows, so that the air is continually passing through the lungs, where blood gas exchange occurs. The motive force for this activity is provided by the abdominal muscles.

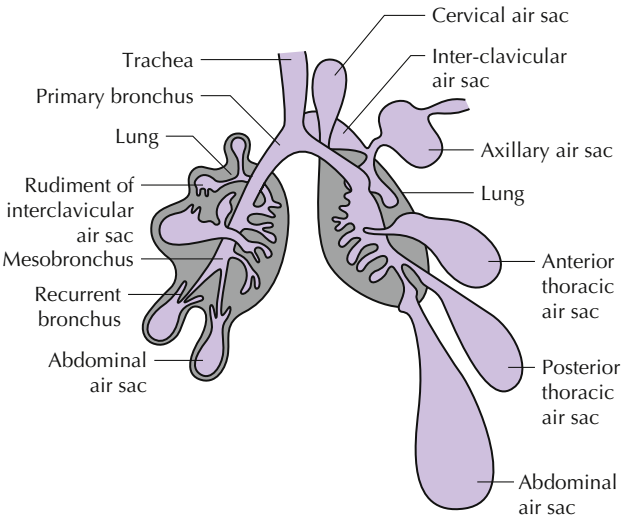

Text-Figure 61. *The lungs and air sacs at about day 4 (left) and in the adult (right).*

In the adult bird the air is taken into the respiratory system through the **external nares** and nasal sacs and enters the mouth through a V-shaped slit, the **internal naris** (*Plate 163*). The glottis (*Plate 192*), the opening into the trachea, lies posterior to the tongue. The tracheal wall is modified to become the larynx and is supported by tracheal cartilages. The trachea bifurcates into two primitive bronchi, one passing to each lung, giving rise not only to the air passages within the lung, but also to the air sacs which extend to different parts of the body (*Text-Figure 61*).

The larynx, trachea and lungs are derivatives of the gut and, like the gut, are formed from a thin lining of endoderm and a thicker covering of mesoderm. As with the gut, epithelial–mesenchymal interactions play an important role in the differentiation of the various regions. The pharyngeal endoderm gives rise to the epithelium of the bronchial tree, whilst the mesenchyme forms the muscles and connective tissue of the lungs as well as the blood vessels and the lymphatic vessels. The pulmonary and bronchial vasculature are both derived from a splanchnic plexus that forms around the foregut before the lung buds develop (DeRuiter *et al.,* 1993). As the two lung buds grow, they extend in a posterior direction. *Hox-b* genes appear to play a critical role in demarcating different regions. *Hox-b5* and *Hox-b6* expression characterizes the trachea, bronchial tree and airsacs (Sakiyama *et al.,* 2000).

The first morphological signs of the development of the respiratory tract are the **laryngo-tracheal groove** (*Plate 110*), which becomes visible in the midline of the floor of the pharynx during days 3 or 4 of incubation, arising posterior to the fourth pharyngeal

Downloaded from Vet-eBooks.com

pouches, and **rudiments of the lung** which begin as bilateral swellings in the foregut (Metzger *et al.*, 2011). As it extends posteriorly, it becomes closed off from the pharynx along most of its length, forming a tube, the trachea, although it remains open to the pharynx at 4–5 days, its most anterior end, this opening constituting the glottis (*Plate 192*). There is a temporary closure of the lumen of the trachea during day 4 (Romanoff, 1960). By day 6 the trachea has lengthened and its anterior end has expanded to form the larynx, the lumen of which becomes temporarily obliterated between days 8 and 11 of incubation. The development of the larynx and trachea was studied by transmission electron microscopy between days 10 and 21 of incubation (Walsh and McLelland, 1978). The **syrinx** (*Plate 216*), the vocal organ of birds equivalent to the mammalian larynx, forms at the junction of the trachea and bronchi.

During day 3, **cartilaginous rings** begin to form in the mesoderm surrounding the trachea and bronchi and, during day 9, syringeal cartilages and muscles start to develop. By day 11, the syrinx of the male is larger than that of the female. (For a fuller description of the development of the trachea and syrinx, see Romanoff, 1960.)

The **lungs** start to arise during day 3 as paired evaginations from the laryngo-tracheal groove. The distal part of each evagination forms the lung and the proximal part of the bronchus (*Plate 167*). Each bronchus may be further subdivided into two regions: the mesobronchus, which is the part that becomes partly enclosed in the lung, and the primary (or extrapulmonary) bronchus, the part outside the lung (*Text-Figure 61*). The mesobronchus gives rise to a series of secondary bronchi (parabronchi, *Plate 57*) (see Makanya and Djonov 2008 for detailed description). Epithelial–mesenchymal interactions are involved in lung branching (Stabellini *et al.,* 2001). By about the end of day 4 the lungs have become small, smooth-surfaced, sacs lying on either side of the oesophagus (*Plate 38*). By day 5 the distal end of the mesobronchus has swollen to become the abdominal sac. The pulmonary veins and pulmonary arteries become visible about days 5–6. For a description of the pulmonary vascular system between stages 23 and 40 (days 4 and 14 of incubation), see Anderson-Berry *et al.* (2005). It follows that of the air conduits and is moulded by them (Makanaya and Djonov, 2009). Surfactant protein mRNA has been detected in the lungs as early as day 14 (Johnston *et al.,* 2000), and appears to be formed by similar cellular pathways to those used by mammalian embryos, despite the differences in lung structure and function (Sullivan and Orgeig, 2001).

The **air sacs**, which have all formed by outpushings of the mesobronchi, develop their own bronchial tubes after hatching. Apart from those in the cervical air sac, the bronchi each form a loop which passes back into the lung proper, and for this reason are known as the recurrent bronchi or sacobronchi (Makanaya and Djonov, 2008). The abdominal air sacs (*Plates 204, 206*) start to migrate into the abdomen about day 9, penetrating the pleuro-peritoneal septum (*Plate 169*), and from day 10 they expand, reaching the posterior end of the coelom by day 15. The other air sacs possess a similar history, forming as dilatations of the bronchi and then penetrating to other regions of the body (Locy and Larsell, 1916). Considerable development takes place after hatching. For a recent study of the post-hatching lungs by scanning electron microscopy, see Maina (2003).

Respiration begins via the chorioallantoic membrane about 1 day before hatching. For an account of the respiratory rhythms just before and after hatching, see Chiba *et al.* (2002). The growth rate of heart and lungs from 15 days of incubation to 5 days post-hatching are considered by Yang and Siegel (1997).

Hatching

Gas exchange takes place via both the chorioallantoic membrane and the lungs (Menna and Mortola, 2002), though, as the circulation in the chorioallantoic membrane gradually ceases, the exchange becomes restricted to the lungs. About a day before hatching, the chick pierces the inner shell membrane with the egg tooth (*Text-Figure 88*) and begins to draw air into its lungs from the air space (*Text-Figure 1*). After a further 8–9 h, the beak breaks through the shell over the air space (pipping) and, after a further 3–4 h and a complex series of hatching movements, the chick emerges from the shell. Cheeping begins while the chick is still in the egg, and there is some evidence that it can play a role in the synchronization of hatching in a batch of eggs (Freeman and Vince, 1974).

Downloaded from Vet-eBooks.com

Chapter 9

Nervous System

The nervous system is formed from the neural plate and the neural crest (see Chapter 4), and in the head region there are significant contributions from the ectodermal placodes.

THE BRAIN

The anterior end of the neural tube enlarges to form the brain. *Text-Figure 62* shows a fate map of the most anterior region of the neural plate based on the results of chick–quail transplants. By stage 9, the primary optic vesicles (see below) have begun to form, and by stage 10 the brain has become divided into three primary regions, the **prosencephalon** (forebrain), the **mesencephalon** (midbrain) and the **rhombencephalon** (hindbrain) (*Plate 66*). By stage 11 the rhombencephalon has become subdivided into the **metencephalon** (cerebellum and pons) and the **myelencephalon** (medulla oblongata), which enclose the metacoele and the myelocoele, respectively (*Text-Figure 64*).

The division of the prosencephalon into telencephalon and diencephalon (thalamus) has begun to take place by stages 12–13. Paired swellings appear just anterior to the optic vesicles and form the telencephalic vesicles, each of which contains a lateral telocoele communicating with the median telocoele (the central lumen of the brain in that region) by the foramen of Monro. Fate maps of the developing forebrain have been published for stage 8 by Cobos *et al.* (2001) and Le Douarin *et al.* (2012) (*Text-Figure 63*), and for stage 10 by Pombero and Martinez (2008). At about the same time the cranial flexure has begun to appear as a bend at the anterior end of the mesencephalon; the cervical flexure begins at about stage 18 (day 3) (*Text-Figure 30*; Chapter 5). By stage 36 (10 days) the cranial flexure has almost gone, and the cervical flexure has become reduced so that the neck is less convex and the head no longer tucked against the thorax (see Normal Table in Appendix II). The walls of the telencephalic vesicles begin to thicken at about stage 13 (2 days) and will form the cerebral hemispheres, their lumina becoming the lateral ventricles. The cerebral hemispheres have expanded so much that by stage 37 (11 days) they overlap the diencephalon, and by stage 44 (18 days) the mesencephalon (*Text-Figure 65*).

The communication between the optic vesicles and the anterior end of the diencephalon has become reduced to a stalk by about stages 13–14 (*Plate 81*). The wall of the optic recess (*Plate 96*), a depression in the floor of the diencephalon between the optic vesicles, becomes very thin by stage 18 (3 days), but a thickened region immediately posterior to it marks the development of the optic chiasma (*Text-Figure 64; Plate 182*). The pineal organ begins to form at about stage 19 as an evagination from the median part of the roof of the diencephalon (*Text-Figure 64, Plate 108*). A description of its development is given by Calvo and Boya (1979). The infundibulum (see Chapter 12 and *Plates 108, 144*) develops posterior to the chiasma and combines with Rathke's pouch (*Plate 96*) to form the pituitary.

The mesencephalon has increased greatly in size by about stage 18 (3 days) and becomes clearly marked off posteriorly from the rhombencephalon by a narrower region, the isthmus (*Text-Figure 64*) located in the meso-metencephalic fold. By about stage 22 (3.5–4 days) the mesencephalon has grown so large that it projects over the metencephalon. The differentiation of the optic lobes from the mesencephalon begins to occur at about stage 27 (5–5.5 days), but even as early as 3 days, the surface of the mesencephalon is covered with fibres, foreshadowing the enormous size of the optic lobes in the adult, which itself is correlated with the importance of vision in birds.

The Atlas of Chick Development. http://dx.doi.org/10.1016/B978-0-12-384951-9.00009-5
Copyright © 2014 Elsevier Ltd. All rights reserved.

Downloaded from Vet-eBooks.com

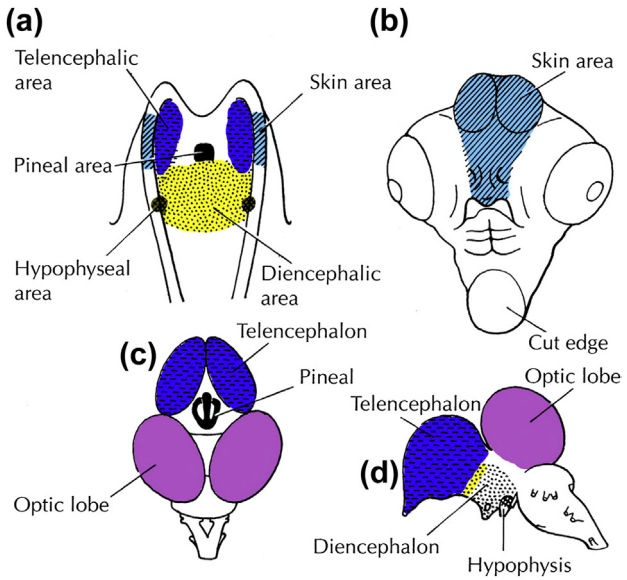

Text-Figure 62. *Origin of the different tissues of the head. (a) Fate map of the anterior end of the neural tube at stage 7 (24 h). (b) Skin area of the face at stage 34 (8 days), which has originated from the lateral neural folds. (c,d) The telencephalic and diencephalic regions at stage 34 (8 days), including the hypophysis. (After Couly and Le Douarin 1988 with permission of Company of Biologists Ltd.)*

The rhombencephalon is characterized by a thin-walled roof in the early stages, though by about 4 days this becomes thicker in the anterior region as the metencephalon develops (*Plate 108*). A striking feature of the newly formed rhombencephalon is the development of a series of seven pairs of segmental bulges, each of which is known as a **rhombomere**. They extend from the anterior border of the rhombencephalon to its posterior end where they abut the first pair of somites. There is good evidence to suggest that each rhombomere is a 'compartment', that is to say that although the cells are able to mingle freely within their own rhombomere and form localized clones, they are unable to pass into adjacent rhombomeres. Young neurons migrate from the brain between the rhombomeres. This segmental pattern of the rhombomeres is subsequently lost, but is thought to be of significance in generating the neuronal patterns of the hindbrain (Lumsden, 2004).

The walls of the metencephalon also become thicker as the two halves of the cerebellum begin to form. During the following days they enlarge, and by about stage 36 (9–10 days) they have fused together in the midline. During the remainder of the incubation period, the cerebellum increases in size and complexity, and by day 16 almost abuts the cerebral

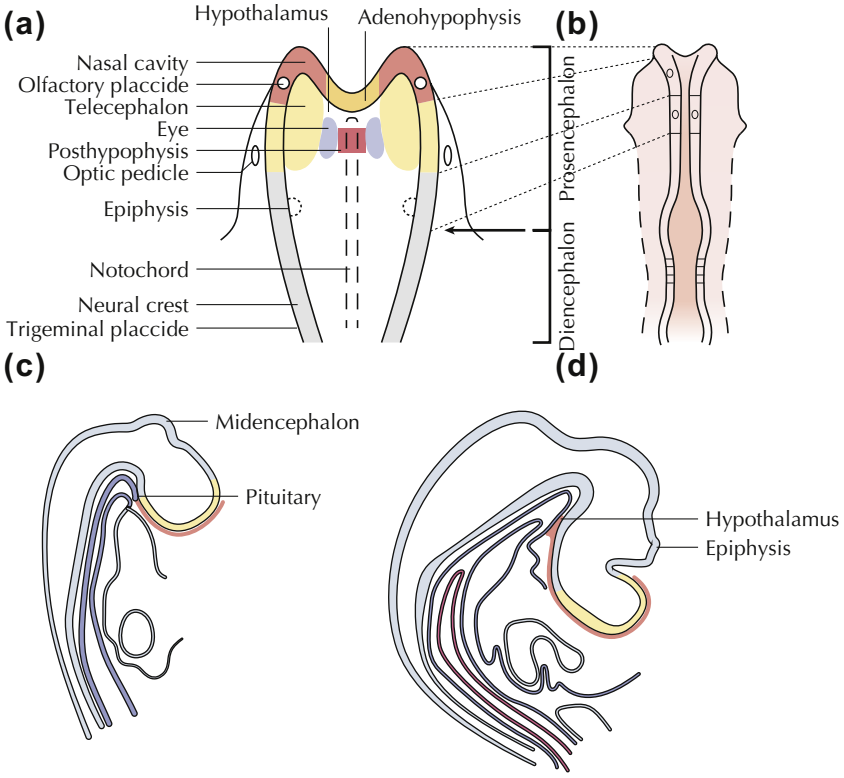

Text-Figure 63. *Fate map of the pre-otic region of the brain. The telencephalon is formed by the lateral-most regions of the anterior neural plate which develops between the two optic vesicles and in front of the notochord. (After Le Douarin and Kalcheim (1999) with permission of Cambridge University Press.)*

Downloaded from Vet-eBooks.com

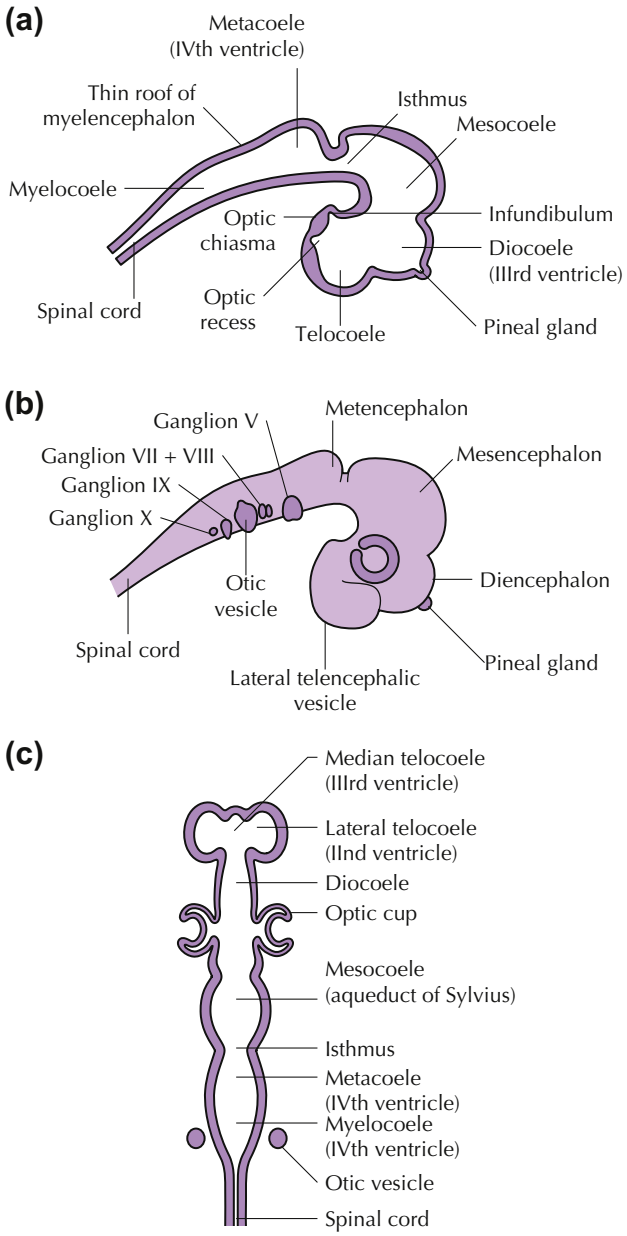

Text-Figure 64. *Diagrams of the brain to show the topography of a 4-day (about stage 22) embryo. (a) Sagittal section. (b) View of brain from right side showing some of the cranial nerve ganglia. (c) Schematic frontal section plan with flexures straightened. (Modified after Patten, 1950.)*

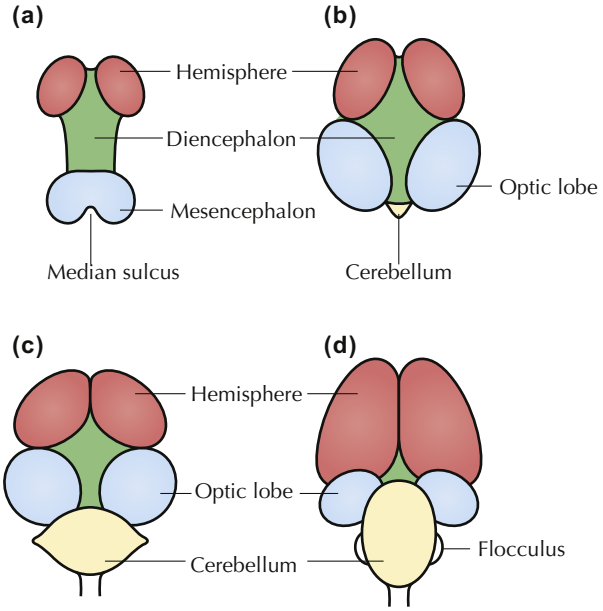

Text-Figure 65. *Dorsal view of the brain to show how the cerebral hemispheres formed from the telencephalic vesicles expand and overlap the diencephalon. (a) Stage 18 (3 days); (b) stage 33 (7–8 days); (c) stage 38 (12 days); (d) stage 44 (18 days). (After Miller, 1903.)*

hemispheres (day 18 shown in *Text-Figure 65a*). The myelencephalon has acquired the characteristic shape of the medulla oblongata by about stage 36 (9–10 days; *Plates 160, 191*). Many fibre tracts have developed in the brain by 5 days (stage 26). These are often visible in sections stained with haematoxylin and eosin, but better in silver preparations or after labelling with specific antibodies. The patterning of the developing axons in the chick brain appears to be organized in a way comparable to that in the mouse (Ware and Schubert, 2011).

We have seen (Chapter 4) that a range of genes play a role in patterning of the brain and spinal cord. Expression of *Wnt8b* and *Wnt7b* are of importance in the patterning of the forebrain (Garda *et al.,* 2002), while *Wnt1* and *Wnt3a* may be implicated in the specification of the dorsal spinal cord (Muroyama *et al.,* 2002). The dorso-ventral patterning of the spinal cord is also dependent on *sonic hedgehog*; cells in chick neural plate explants differentiate into ventral cell types under the influence of *sonic hedgehog* (Robertson *et al.*, 2001).

HISTOLOGY OF THE SPINAL CORD AND DEVELOPMENT OF THE FIBRE TRACTS

A fate map of the spinal cord in the thoracic, lumbar and caudal regions was published by Catala *et al.* (1996). At the time of its formation from the ectoderm, the neural tube consists of a thickened columnar epithelium, but changes soon take place in its shape and histology. All the cells of the neural tube are elongated with their long axes radiating out from the ependyma to the periphery. By stage 16 (2.5 days) the neural tube possesses two layers, the **ependyma,** which lines the neural canal and contains a large number of mitotic cells, and the **marginal**

Downloaded from Vet-eBooks.com

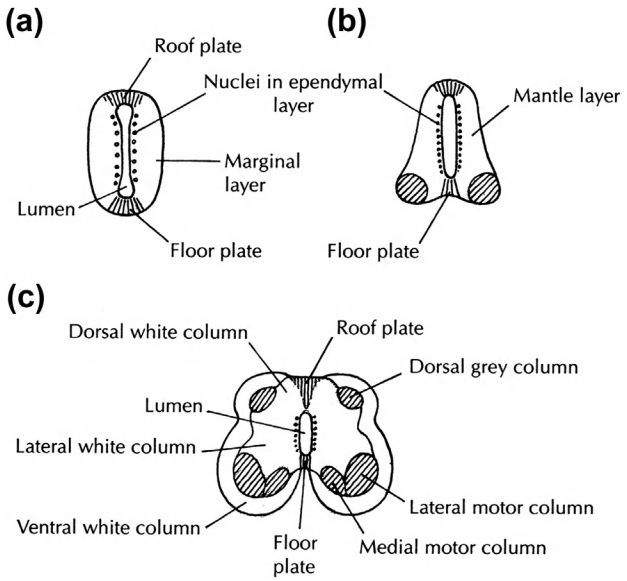

Text-Figure 66. *Development of the spinal cord at stage 16 (2.5 days); (b) stage 24 (4.5 days); (c) stage 34 (8 days). (After Romanoff, 1960.)*

layer (*Text-Figure 66*), and by stage 18 (3 days) the **mantle layer** is also recognizable. Neuroblasts are visible from about stage 15 (2 days) in the ventro-lateral part of the tube; this region is about six cells deep, whereas in the floor plate (the keel) there is only a single layer of cells.

By stage 16 spinal nerves have developed, and by stage 22 (3.5–4 days) regions of 'grey' and 'white' matter are recognizable. Nissl substance is visible in embryos of this stage stained with basic dyes. Dorsal and ventral horns can be seen in the grey matter from about stage 31 (day 7) and glial cells in the white matter. During the following days the spinal cord becomes larger in transverse section and there is a change in shape of the lumen from a longitudinal slit to an almost square or round shape. This is accompanied by the development of dorsal and ventral fissures. With the outgrowth of the spinal nerves the size and shape of the spinal cord varies along its length.

SPINAL NERVES

Each spinal nerve has both a somatic and a splanchnic component, the former serving the somatopleure and the body axis and the latter the viscera, and each part has both motor and sensory components. By about stage 34 (8 days) there are 38 pairs of spinal nerves. The spinal ganglia are of neural crest origin (see Chapter 4).

The segmentation of the spinal nerves is associated with that of the adjacent somites so that eventually each spinal nerve emerges between two vertebrae. After leaving the neural tube, each axon passes through the anterior half of the sclerotome and is inhibited from going through the posterior half. The neural crest cells are similarly constrained to migrate through the anterior and not the posterior half (Keynes and Stern, 1984).

The ventral roots of the spinal nerves have emerged in the cervical region by about stage 13 and appear progressively in the more posterior regions during the following day. The spinal ganglia begin to appear early in day 3 and the dorsal roots that arise from them develop during days 3–4. The neurons in the dorsal root ganglia vary in structure. The size of the dorsal root ganglia themselves also varies, being especially large for the nerves innervating the limbs. By stage 20 (3–3.5 days), the ganglia of the brachial segments 14–15 are more than 80% larger than those in the cervical segments 5 and 6, and this has been correlated with the colonization of the brachial region by a larger number of neural crest cells (Goldstein *et al.,* 1995).

The motor axons of the spinal nerves innervate the myotomes to which they attach and become transported by the developing muscle. The sensory fibres subsequently migrate along the motor nerves. Lance-Jones (1988), who studied the somitic level of origin of the hindlimb muscles, found that the motor neurons supplying them arose from the same somitic level and, subsequently (Lance-Jones, 1990), that the axons were guided by the limb somatopleure. The dorsal root ganglia are derived from the neural crest cells, which differentiate into many subpopulations of sensory neurons as well as glial cells. The development of these sensory neurons has been analysed by George *et al.* (2010).

Spinal nerve plexuses develop in the brachial and lumbo-sacral regions from the 13th to 16th and the 23rd to 29th spinal nerve, respectively. Chick spinal nerves have been found to undergo a transient period of spontaneous activity during their development, with regularly occurring episodes interspersed with quiescent periods (Wenner and O'Donovan, 2001).

The meningeal layers of the spinal cord, and the endoneurium of the peripheral nerves are all formed from mesenchyme cells of non-neural crest origin, whereas the Schwann cells are of neural crest origin (Halata *et al.*, 1990).

Oligodendrocytes first appear in the ventral region of both the spinal cord and the metencephalon (Davies and Miller, 2001) under the influence of *sonic hedgehog*. Conversely, the specification of oligodendrocyte precursors is inhibited by bone morphogenetic proteins (BMPs) (Mekki-Dauriac *et al.*, 2002).

Downloaded from Vet-eBooks.com

Cranial Ectodermal Placodes

Cranial ectodermal placodes are thickened patches of ectoderm which invaginate. They each break away from the ectoderm and contribute to a specific special sense organ (see below) or to one of the cranial nerves (V, VI, IX or X). The precursors of these placodes are arranged in 'a horse-shoe shaped region around the anterior neural plate, at the border of the neural plate and non-neural ectoderm' (McCabe and Bronner-Fraser, 2009). Initially there is some overlap between the precursors of the different placodes, though eventually they become established in a clear linear arrangement (*Text-Figure 67*). Specific inductions from adjacent tissues appear to play an important role in their differentiation (reviewed by McCabe and Bronner-Fraser, 2009). For example, Wnt signals derived from the isthmus act together with FGF in the development of the trigeminal placode (Canning *et al.*, 2008).

THE CRANIAL NERVES AND GANGLIA

The development of each of the cranial nerves is closely associated with that of fibre tracts and nuclei in the brain. The following cranial sensory nerve ganglia are partially derived from the neural crest and partially from epidermal placodes: the trigeminal (V), geniculate (VII), vestibular acoustic (VIII), and the proximal ganglionic components of the petrosal (IX) and the nodose (X). The head neural crest cells migrate between stages 9 and 11, and some condense lateral to the brain and join with cells from the epidermal placodes which will become neuroblasts. McCabe and Fraser (2009) have mapped the position of the neural crest and placodal anlagen (*Text-Figure 67*) from stages 7–15, and the position of the cranial ganglia at 12 days.

Cranial Nerve I (Olfactory Nerve) (*Plates 163, 193*)

The sense of smell is poor in birds, and this is reflected in the small size of the olfactory nerve. It forms by the growth of cells from the nasal placode (*Plate 27c,d*) to the olfactory lobes, which begins about stages 17–18 (3 days). Fibres become visible at about 3–4 days.

Cranial Nerve II (Optic Nerve)

Vision is highly developed in birds, and this is indicated by the large optic nerves and optic lobes. The optic nerves grow from the retina toward the ventral region of the diencephalon, where they cross to form the optic chiasma (*Plates 182, 192*) and terminate on the contralateral side of the brain. The retinal fibres enter the optic stalk at about stage 18 (3 days) and cross through the optic chiasma at about the beginning of day 4, reaching the surface of the optic lobes on day 5. By day 7 many fibres have spread over the surface of the optic lobes.

Cranial Nerve III (Oculomotor Nerve) (*Plate 113*)

This is the main nerve to the extra-ocular muscles and is especially large in birds because of the great size of

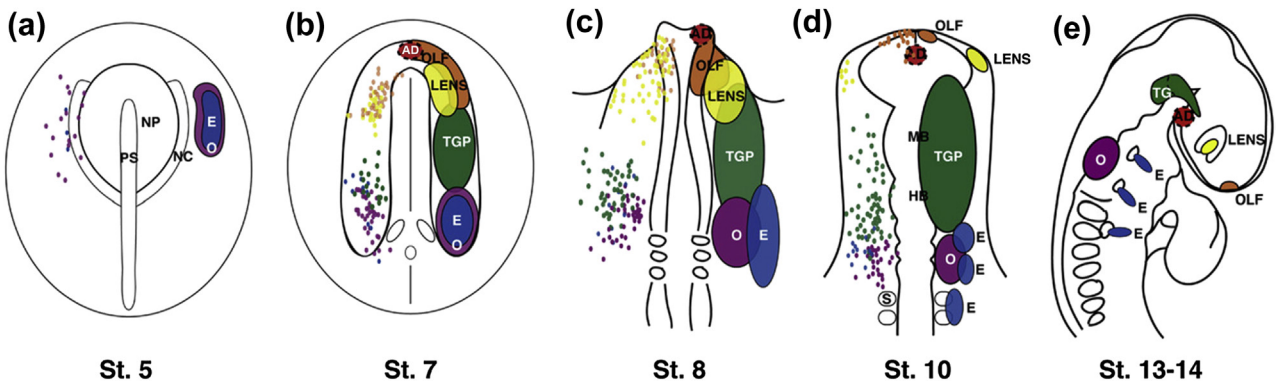

Text-Figure 67. Placode development. The right side of each diagram shows the placodes which form by stage 13–14, whilst the left indicates the overlapping areas that give rise to them. AD: adenohypophysis (red); E: epibranchial (blue); Lens (yellow); OLF: olfactory (orange); O:otic (purple); TGP: trigeminal placode (green); HB: hindbrain; NP: neural plate; PS: primitive streak; NC: neural crest. (From McCabe and Bronner-Fraser (2009), with permission of Elsevier.)

Downloaded from Vet-eBooks.com

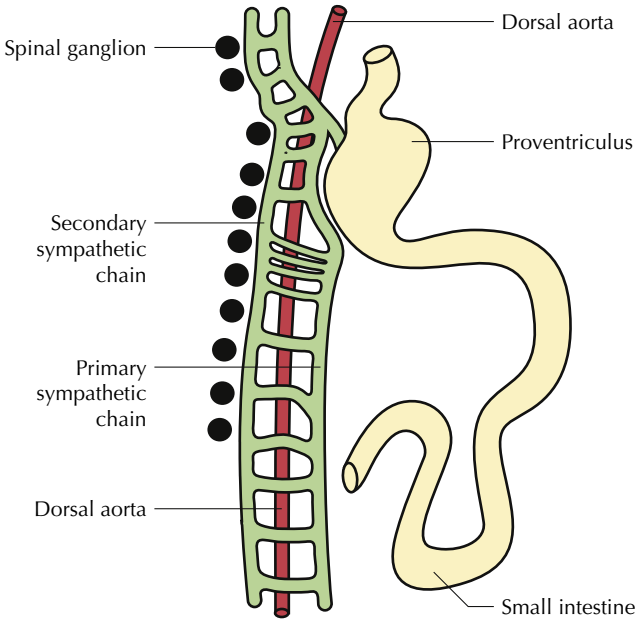

Text-Figure 68. *Autonomic nervous system showing primary and secondary sympathetic chains at 10 days. (Modified after Romanoff, 1960.)*

the eyes. The left and right oculomotor nerves grow from the ventral side of the midbrain immediately posterior to the hypophysis and innervate the superior and inferior rectus muscles of the eye. The ciliary ganglia appear at about stage 10, and each is situated two-thirds of the distance from the proximal to the distal end of the oculomotor nerve. The ciliary nerve, which runs from the ganglion to the iris, is visible according to some authors at 4 days (stage 23).

Cranial Nerve IV (Trochlear Nerve)

This special somatic nerve arises at about 3–3.5 days (stage 20) at the dorsal surface of the midbrain posterior to the oculomotor nerve, and innervates the superior oblique muscle of the contralateral eye. The left and right nerves cross at about 3.5 days (stage 21) at the dorsal surface of the midbrain, and then start to grow ventrally over the lateral face of the mesencephalon.

Cranial Nerve V (Trigeminal Nerve)

The various branches of the trigeminal nerve appear at about stages 13–14 together with the neural crest-derived trigeminal (Gasserian/semilunar) ganglion, and is easily recognizable (shown at later stages *Plate 108*) by its large size and its situation at the widest part of the mesencephalon. The sensory parts of the nerve are formed from the ganglion, and the motor components are derived from the rhombencephalon. The major branches of the trigeminal nerve are the ophthalmic (*Plate 107*) and the maxillary-mandibular, the latter subdividing into its maxillary and mandibular branches (*Plates 109*) during day 4.

Cranial Nerve VI (Abducens Nerve)

This cranial nerve (*Plate 192*) arises during day 3 in the midline from the ventral side of the myelencephalon, and has migrated to the primordium of the lateral rectus muscle by stage 24 (4.5 days). There is no ganglion associated with it. The main nucleus, which is situated ventral to the floor of the fourth ventricle, appears at 5 days. The accessory nucleus, which lies between the descending root of the trigeminal and superior olive nerve, is derived from cells which have left the main nucleus.

Cranial Nerve VII (Facial) and Cranial Nerve VIII (Acoustic or Vestibulocochlearis Nerve)

The development of these two nerves is closely associated. The facial nerve, which becomes recognizable at about stage 11, is formed partially from neural crest and partially from the epibranchial placode of the first pharyngeal groove. A branch from the facial ganglion has reached the upper end of the hyoid arch by stage 13, and has extended into the third rhombomere by stage 15. Cells leave the auditory epithelium at about stage 18 to form the acoustic ganglion (shown at stage 37 in *Plate 192*) and at about the same time the facial and acoustic ganglion columns fuse with one another (shown at stage 23 in *Plate 109*). Meanwhile cells bud from the placode over the hyoid arch and fuse with the facial and acoustic columns to form the geniculate ganglion (shown at stage 23 in *Plate 108* and stage 26 in *Plate 118*). By about 3.5–4 days (stage 22) the geniculate ganglion is attached to the rhombencephalon.

Early on day 4 the acoustic ganglion is present as two parts and has become independent of the facial nerve, but by day 5 it is a large bilobed structure, closely applied to the auditory epithelium. The vestibular ganglion is derived almost entirely from the epibranchial placode. At 5 days the motor nucleus of the facial nerve is a single group of cells, but by day 7 this has become divided into a dorso-medial and a ventro-lateral group.

Downloaded from Vet-eBooks.com

Cranial Nerves IX and X (Glossopharyngeal and Vagus Nerves)

The glossopharyngeal nerve (*Plate 109*) innervates the pharyngeal muscles and the salivary glands. The vagus nerve (*Plate 118*) supplies the cervical and thoracic regions and much of the abdominal viscera. The peripheral differentiation of the vagus nerve was described by Kuratani and Tanaka (1990). Sato *et al.* (2002) found that electrical stimulation of these nerves between days 4 and 8 of incubation elicited a pattern of optical recordings which changed with advancing development.

A large ganglionic complex begins to form at about stage 13 at the root of the two nerves, the most rostral part being the superior ganglion of the glossopharyngeal nerve (shown at stage 23 in *Plate 108*), and the more caudal part the jugular ganglion of the vagus (shown at stage 23 in *Plate 110*). In addition, a ganglion develops on the trunk of each nerve a short distance from the brain, the **petrosal ganglion** on the glossopharyngeal and the **nodose** on the vagus. The nodose ganglion provides sensory innervation to the heart and other viscera (Harrison *et al.,* 1995).

Both the petrosal and the nodose ganglia receive a contribution of cells from the ectoderm (the nodose from the ectoderm dorsal to the fourth pharyngeal cleft and the petrosal from a more anterior region), in addition to that from the neural crest. The nodose ganglion begins to appear at stage 18 (3 days) as a group of cells lateral to the dorsal aorta, where it is joined by the anterior cardinal vein (D'Amico-Martel and Noden, 1983), but it subsequently shifts posteriorly.

By stage 13 the cells of the glossopharyngeal–vagus part of the neural crest have already migrated under the ectoderm and over the first and second somites. By stage 15 the distal part of the migrating column of cells has started to bifurcate, the anterior part going to the third visceral arch and the posterior part to the fourth visceral arch.

The ganglia of the IXth and Xth cranial nerves form just posterior to the auditory vesicle at the dorsal side of the second and third visceral furrows.

Cranial Nerve XI (Spinal Accessory Nerve)

This nerve supplies the pharynx and shoulder muscles. In the 4–5 day embryo the strand runs from the ganglion and dorsal root of the third cervical nerve to the root of the vagus.

Cranial Nerve XII (Hypoglossal Nerve)

This nerve supplies the muscles at the base of the tongue. It leaves the ventral side of the rhombencephalon by several roots opposite the third and fourth somites, which unite to form a single trunk. The first axons appear at about stages 17–18 (3 days). During days 4–5 the nerves extend posteriorly and enter the pharynx.

THE AUTONOMIC NERVOUS SYSTEM

This is of neural crest origin. The levels of the neural crest that give rise to the various autonomic ganglia as well as to the adreno-medullary cells were determined experimentally by exchanging strips of neural tube, together with the associated neural crest, between chick and quail embryos (Le Douarin *et al.,* 1984a, b). All the sympathetic ganglia arise from the neural crest posterior to the level of the fifth somite. The adreno-medullary cells form from the neural crest between levels of the 18th and 24th somites. All the parasympathetic enteric ganglia receive neural crest cells from somite levels 1–7, but those parasympathetic ganglia that lie posterior to the yolk sac stalk receive additional neural crest cells from the sacro–lumbar region. The ganglion of Remak is derived from the lumbro–sacral crest posterior to the level of the 28th somite.

The first signs of the primary sympathetic chain are visible at the end of day 3 as two rows of cells lying one on either side of the neural tube, ventral to the somites and immediately lateral to the aorta. Ganglia form on the chains about days 4–5. The secondary sympathetic chains, which start to appear early on day 5, grow out as sprouts from the primary chain and then become connected with one another to form the secondary chain, which runs close to the spinal ganglia (*Text-Figure 68*). The primary chain then becomes reduced in size and it eventually disappears. There are about 38–39 secondary sympathetic ganglia (*Plate 166*), consisting of 13 cervical, 7 thoracic, 14 lumbro-sacral and 4–5 coccygeal. The rami communicantes are visible in silver preparations by 5–7 days, and pass from the secondary sympathetic ganglia to the roots of the spinal nerves.

The secondary chain (*Text-Figure 68*) becomes a continuous nerve cord (the paravertebral) between days 4 and 8, running from the superior cervical ganglion to the coccyx. It bifurcates around each rib, but remains as a single structure between the ribs. It connects with the plexuses in the following regions: the aortic plexus

Downloaded from Vet-eBooks.com

(which becomes modified further into the coeliac plexus around the coeliac artery, as well as the pelvic and hypogastric plexuses), the medullary plexus of the adrenal gland, the splanchnic plexus and Remak's ganglion in the rectal region.

The times at which enteric neurons first appear in different regions of the gut have been plotted by Fairman *et al.* (1995). Most of the enteric nervous system is formed from neural crest cells of the vagal region, though there is also a contribution from the sacral neural crest (Burns and Le Douarin, 2001).

ORGANS OF SPECIAL SENSE

The Eye

The first sign of the development of the eyes is a bulging at the lateral sides of the prosencephalon at about stage 9 (*Plate 64*). These are the rudiments of the optic vesicles which lie beneath the head ectoderm. By stage 10 each vesicle has begun to constrict at its base (*Plate 68*) until by stages 12–14 its connection to the brain has been reduced to a narrow stalk (*Plates 74, 81*); but the lumen of the optic vesicle is still in communication with the prosencephalon via the stalk.

Meanwhile, the distal part of each optic vesicle (the future sensory layer) invaginates and presses against the proximal part (the future pigment layer of the retina, iris and ciliary body). This results in the formation of the **optic cup** *(Text-Figure 69, Plate 81*), the elimination of the original lumen of the optic vesicle and the formation of a new lumen, the future **vitreous chamber.** The invagination of the optic cup does not start at the extreme lateral border of the optic vesicle, but from a more ventral position. The wall of the cup is therefore lacking on the ventral side and the invagination is thus able to continue along the inferior (ventral) side of the optic stalk, so that a groove forms, along which the optic nerves and blood vessels subsequently pass. The gap in the ventral wall of the optic cup is the **choroid fissure** (*Text-Figure 69, Plate 107*). By the time the optic cup has formed, regional differences are already marked within it.

The lens is formed from the lens placode (*Plate 28*), a thickening of the ectoderm formed in response to an inductive signal from the optic cup. It is first visible at about stage 12 (Bancroft and Bellairs, 1977) and invaginates at about stage 14 to form the lens vesicle (*Plates 81, 100*), which sinks beneath the surface of the ectoderm, the latter becoming the cornea. By about stage 18 (3 days) the wall of the proximal side of the lens vesicle has greatly thickened, whereas the wall at the distal side has become thinner. The thickening is brought about by an increase in the length of the individual cells that stretch across the entire thickness of the walls, a band of nuclei being visible within the thickening (seen as a dark band in *Plate 145b*). A high mitotic rate at the periphery of the lens results in its continuing growth. By day 4 the lens cavity has been obliterated and at the same time the lens has begun to acquire its characteristic, lentoid, shape. Both the lens and the optic cup require the function of the gene Pax6 to develop (Canto-Solev and Adler, 2006).

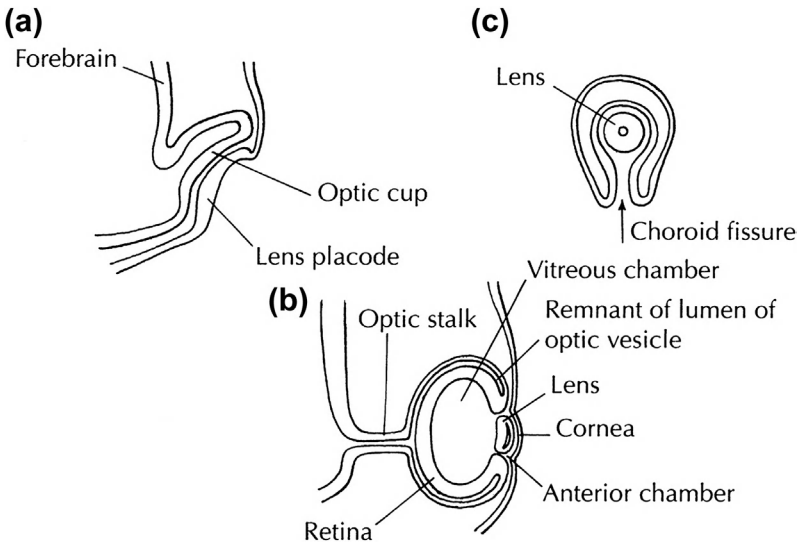

Text-Figure 69. *Development of the optic cup and lens. (a) Stage 14, longitudinal section through the developing lens and retina. (b) Stage 18, transverse section through the eye to show retina and developing lens. (c) Stage 18, frontal section through the eye to show the choroid fissure.*

Downloaded from Vet-eBooks.com

As the lens continues to grow, the cells in the thickened region lose their ability to divide and become converted into fibres that will become the core of the adult lens. Fibroblast growth factor (FGF) signals appear to play a role in the conversion to fibres (Le and Musil, 2001). New fibres are formed from the cells at the periphery of the lens which divide rapidly and become arranged in concentric circles around the original core. By the time of hatching there are three concentric layers of fibres, the core (0.8 mm in diameter), the intermediate layer of irregularly arranged fibres, and the radial layers which continue to grow after hatching. The major lens protein is Δ-crystallin (not δ-crystallins as in mammals), though α- and β-crystallins can be detected when the lens placode has only just begun to form (Zwaan and Ikeda, 1966). The lens capsule, which is an extracellular material with a high collagenous component, starts to form about day 7. The ciliary body develops close to the lens, its role being to secrete the fluid of the vitreous chamber. It appears to be induced by lens FGF and BMP, each playing a critical role (Dias da Silva *et al.*, 2007).

As the lens loses contact with the ectoderm a space is formed, the **anterior chamber of the eye** (*Text-Figure 69*). Neural crest cells, which have reached the margin of the optic cup by stage 18, have migrated into the anterior chamber by stage 23 (Beebe and Coates, 2000). The corneal epithelium develops from the ectoderm covering the anterior chamber, whilst the corneal stroma forms from the mesenchyme and becomes visible on day 4 as a thin layer beneath the epithelium. It becomes thicker as mesenchyme cells migrate into it during day 7, and by the formation of Bowman's membrane from 11 days, followed by Decemet's membrane from about 13 days.

The **iris** arises from cells at the margin of the anterior chamber at about day 7. Removal of the lens results in disorganization of the components of the anterior chamber (Beebe and Coates, 2000).

The **retina** is formed from the optic cup. Its inner layer becomes the neural retina and its outer layer the pigmented retina. FGF8 is associated with the differentiation of the neural retina, and BMP7 with that of the pigmented retina (Vogel-Hopker *et al.*, 2000).

The **choroid** and **sclera** differentiate from the mesenchyme around the optic cup, forming the inner pigmented vascular layer, and the outer, fibrous layer, respectively. The melanophores of the choroid are derived from cells of the neural crest that reach the eye during day 2 and develop pigment on day 7. Cartilage starts to form in the sclera on day 8. On day 9 (stage 35–46), 14 papillae become visible on the conjunctival sclera; each is composed of a solid cord of epithelium and becomes associated with a condensation in the underlying mesenchyme, which is derived from the neural crest. By 13 days the papillae have disappeared and the condensations have become 14 scleral ossicles (*Plate 232*). Jourdeuil and Franz-Odendaal (2012), who produced a detailed map of the blood vessels of the eye, concluded that there was no correlation between blood vessel development and the patterning of the conjunctival papillae. The development of the sclera ossicles is described by Zhang *et al.* (2012).

The **eyelids** start to form at about 7 days (stage 31) from a circular fold of skin surrounding the eye which becomes modified to form the upper and lower eyelids. A semicircular fold within this circular fold becomes the nictitating membrane. The Harderian gland begins to develop on day 11 (stage 37) from epithelial cones on the conjunctiva (Niedorf and Wolters, 1978).

The **choroid fissure** usually begins to close in the region near the lens about day 4 (stage 23), though accounts vary. At this time a ridge of mesoderm, carrying with it a blood vessel, migrates along the choroid fissure into the posterior chamber of the eye and enlarges during day 5 (about stage 26) to form the **pecten** (seen at stage 29 in *Plates 160, 165*). Subsequently it becomes wrapped around by the ridges of the choroid fissure in the optic stalk and is totally covered by day 8. The pigment cells of the pecten are derived from the pigmented retina (Yew, 1978). The pecten is a structure characteristic of birds, and it is thought that it acts not only by bringing oxygen and nutritive materials to the eye but that it may also play a role in vision. Its development has been described by Uehara *et al.* (1990) (not seen).

The development of the pecten, the neural retina and the retinal pigment epithelium are all influenced by retinoic acid and *sonic hedgehog*. BMPs also play a role in the development of these structures. Adler and Belecky-Adams (2002) showed that overexpression of *noggin,* which binds several BMPs at the optic vesicle stages, led to microphthalmia, together with abnormalities of the retinal pigment epithelium and lens. Similar treatment at the optic cup stages resulted in extensive anomalies, including coloboma and pecten agenesis. BMP4 is expressed in the developing neural retina, where it appears to be responsible for apoptosis (Trousse *et al.*, 2001). The **optic nerve** is derived principally from the retina, its axons growing along the choroid fissure on their way to the brain (see p. 98).

The vitreous humour is secreted by the cells of the optic cup. For a general review of the molecular

Downloaded from Vet-eBooks.com

events in the development of the vertebrate eye, including that of the chick, see Graw (2010).

The Ear

The **inner ear** is derived from the otic placode (*Plates 26, 27, 85*). The **middle ear** is formed from the first pharyngeal pouch, and the **outer ear** from the adjacent ectodermal groove. The ectodermal groove becomes the external auditory meatus (Eustachian tube) (*Text-Figures 53, 70*). The tissue between these two regions develops into the tympanic membrane.

The left and right **otic placodes** are visible in embryos at about stage 10 (Bancroft and Bellairs, 1977) as thickened regions on either side of the head just anterior to the somites. Precursors for vestibular and auditory cells are already regionally segregated (Bell *et al.*, 2008). By stage 12 each has invaginated to form an otic pit, probably as a result of induction by FGF3 (Vendrell *et al.,* 2000), and by stage 14 the opening of the pit has become greatly restricted and the whole structure now becomes known as the **otic vesicle** or otocyst (*Plates 79, 89*). If the basal lamina associated with the otic placode is enzymatically disrupted, the placode fails to invaginate properly (Moro-Balbás *et al.,* 2000). The otic vesicle loses its communication with the outside of the embryo at about stage 18. The endolymphatic duct is a blind-ended outgrowth from the dorsal wall of the otic vesicle. The precursors of both the vestibular and auditory cells occupy different regions of the otic placode. The otic neurons are formed from the anterior medial region of the placode (Alsina *et al.*, 2004) and give rise to the cochlear vestibular ganglion (d'Amico-Martel and Noden, 1983). Bell *et al.* (2008) showed by the use of labelling experiments that the sensory organs and their nerves each formed from the same region of the otic placode and that the development of the neurons preceded that of the sense organs. Similarly, the differentiation of the vestibular system took place before that of the cochlea.

During days 5–7 the distal end of the endolymphatic duct (*Plate 119*) enlarges to form the **endolymphatic sac** (*Plate 157*), which grows above the brain and comes to lie at the dorso-lateral side of the myelencephalon. The remainder of the otic vesicle meanwhile has become loosely divided into a **superior chamber**, which will form the semicircular canals and utricle, and an **inferior chamber**, which will give rise to the saccule and cochlea. The development of the cochlea duct is, at least partly, controlled by rhombomeres 5 and 6 (Liang *et al.*, 2010).

The **semicircular canals** (*Text-Figure 71*) start to develop on days 4–5 as three grooves in the wall of the superior chamber, which each invaginate and close over to form a tube. The lumen of each tube is continuous

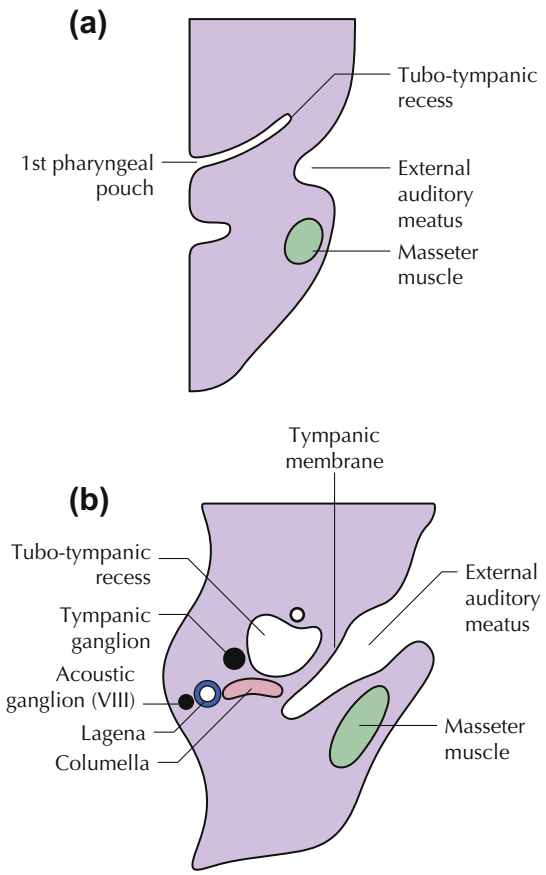

Text-Figure 70. *Transverse section through the right middle and outer ear at (a) 4 days, (b) 12 days. (After Romanoff, 1960.)*

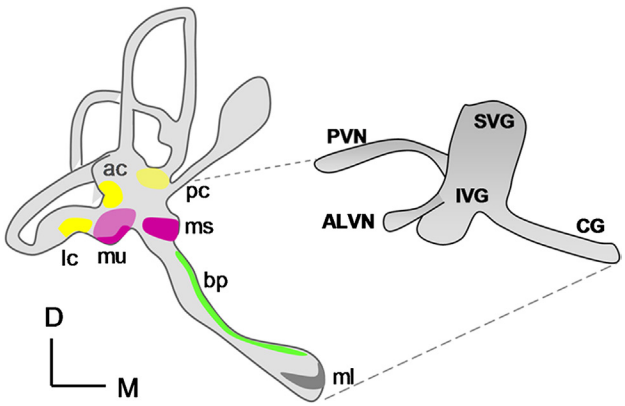

Text-Figure 71. *Schematic diagram of the inner ear and its innervations at stages 30–31 (day 7). ac: anterior crista (yellow); bp: basilar papilla; lc: lateral crista (orange); mu and ms: utricular and saccular maculae (purple); pc: posterior crista. The anterior vestibular nerve (ALVN) innervates ac and lc; the inferior vestibular ganglion (IVG) projects to the maculae; the posterior vestibular nerve (PVN) to the pc; and the cochlear ganglion (CG) to the bp. SVG = superior vestibular ganglion. (From Bell et al. (2008), with permission of Elsevier.)*

Downloaded from Vet-eBooks.com

with that of the superior chamber of the otic vesicle, which itself will become the utriculus. The anterior semicircular canal (which lies in the sagittal plane) forms first, followed by the external semicircular canal (which lies in the horizontal plane) and finally by the posterior canal (which lies in the frontal plane). The canals then move out from the main body of the otic vesicle, each carrying with it a thin fold of otic wall. By days 7–8 this thin sheet has perforated so that the canals remain attached to the otocyst only at the ends. Swellings which form along the canals during days 5–6 form the ampullae. There is some evidence that BMP2, secreted by the epithelium of the otocyst, is involved in the early stages of the formation of the semicircular canals and may affect the chondrogenesis of the otic capsule around the canals (Chang *et al.,* 2002). BMP4 is essential for normal development of the semicircular canals (Gerlach *et al.,* 2000).

The **saccule** begins to appear on day 7 as a swelling on the dorso-medial wall of the inferior chamber. The cochlea and the cochlear duct start to form during day 6 by growing out from the ventral region of the inferior chamber.

The **middle and outer ear** are formed from the first pharyngeal pouch and the surrounding wall of the pharynx (see Jaskoll and Maderson, 1978). The dorsal part of the first pharyngeal pouch gives rise to the tubo-tympanic recess, which later becomes the auditory (Eustachian) tube (*Text-Figure 71*). The **external auditory meatus**, which forms from the first ectodermal groove, is apparent by day 6 and further elaborated by day 12 when it then lies in juxtaposition to the tympanic cavity. The thickened region of the wall which separates them is the primordium of the tympanic membrane. Birds possess a single auditory ossicle, not three as in mammals. The cartilaginous predecessor of this bone, the **columella** (*Plate 161*), is present by 6 days and lies between the tympanic membrane and the cochlea, and the tubo-tympanic recess is directed towards it. Wood *et al.* (2010) have provided a detailed account of the columella at different stages. For a full description of the development of the middle ear and tympanum see Jaskoll and Maderson (1978).

The maturation of the tympanum layers is discussed by Chin *et al.* (1997). For a report on the changing sizes of the individual components of the inner ear between 10 days of incubation and adulthood see Cohen *et al.* (1992), and on patterns of chondrification and ossification see Cohen and Hersing (1993).

For an atlas on the gross anatomy of the chick inner ear see Bissonette and Fekete (1996). The neural relationships in the vestibular region of the 11-day-old chick embryo are described by Diaz *et al.* (2003).

The Nose

The nasal (olfactory) placode (*Plates 27, 110*) becomes visible at stage 16 (Bancroft and Bellairs, 1977) as two thickened regions anterior to the eyes. Like the optic and otic placodes, each nasal placode invaginates, and it forms the **nasal pit** on days 3–4. A slight depression on the medial wall of each pit at about 4–5 days is thought to be the **organ of Jacobson**. Each nasal pit remains open to the surface of the head during its earliest stages of development, this opening eventually becoming the **external naris** (see Chapter 5). It becomes closed from about day 6, however, by the proliferation of epithelial cells forming a plug, and does not reopen until hatching, by which time the epithelial plug has degenerated.

The pits deepen, partly due to the bulging up of the ectoderm around the opening, forming the lateral and median fronto-nasal processes. The cavities of the nasal pits initially open into the oral cavity, but when the palate forms between days 5 and 7, the upper (nasal) part of the oral cavity becomes partly separated off from the lower part, and as a consequence the internal nares (*Plate 151*) become displaced to the posterior end of the mouth. In birds, however, the palatine processes do not fuse completely along the length of the **median palatine fissure** (*Plate 193*), even though they meet in the midline on day 4. Birds are therefore said to have a split palate.

Three **conchae** (turbinals) (*Plate 193*), the superior, middle and inferior, develop from the lateral wall of the nasal cavity and project into the lumen, the middle appearing on day 5, the superior at days 5–6 and the inferior (or vestibular) during day 7. The inferior turbinal is found only in birds, although not in all birds.

The lateral nasal glands form between days 8 and 14, starting as a solid mass in the septal wall of the nasal cavity as designated.

Downloaded from Vet-eBooks.com

Chapter 10

Skeleton and Muscles

The development of the skeleton and muscles are closely linked, not only in their dependence on each other for functioning, but also during development. Nevertheless, it is convenient to consider the two systems separately here.

SKELETON

Birds resemble other amniotes in that most of the skeleton is initially laid down in cartilage which subsequently becomes ossified. Bones formed in this way are known as **cartilaginous bones,** as opposed to **membrane bones,** which are ossified directly from mesodermal tissues and do not go through a cartilaginous phase. Birds differ from other amniotes, however, in possessing air-sacs, which form as outgrowths from the lungs (see Chapter 8) and extend into the bones and even replace the marrow of the long bones. This process, known as **pneumatization,** leads to a reduction in weight and is helpful for flight, but does not take place until after hatching (Schepelmann, 1990). Fusion of some of the vertebrae to form the **synsacrum** (see below) occurs during embryonic development and is an adaptation to reduce the shock of landing after flight.

The Vertebral Column

The vertebrae develop from the sclerotomes and the notochord. The first pair of somites forms at stage 7 (about 23–26 h of incubation) and succeeding pairs continue to be laid down until about 50 pairs have formed, by stage 22 (3.5–4 days). As we have seen (Chapter 4), each somite gives rise to three major components, the dermatome, the myotome and the ventrally located sclerotome, as well as to the cavity within the somite, the somitocoele. In the same way as the segmentation of the somites proceeds from anterior to posterior, so the differentiation of individual somites into the three components takes place in a chronological sequence down the body; this is followed by the formation of the vertebrae in the same order. A useful consequence is that the maturation of the somitic tissues may be studied not only by comparing embryos of different ages, but also by comparing somites in different positions along the body of the same embryo. *Plates 86 and 87* illustrate a series of transverse sections through the somites of the same embryo at the levels indicated.

The origin of the **notochord** has been described on p. 26. It extends from the level of Rathke's pouch to the tip of the tail bud by about stages 20–21 and is one of the few medial structures in the body. It is round or oval in transverse section, and until about stage 16 it measures about 30 μm in diameter. After that its diameter increases, reaching about 115–160 μm by about stage 23 (4 days). This increase is due to the development of vacuoles (*Plate 20*) which subsequently secrete material that supplements the notochordal sheath (peri-notochordal tube) and are visible from about stage 11.

We discussed in Chapter 4 that the secretion of *sonic hedgehog* protein by the notochord and floor plate leads to the formation of sclerotomal cells (which are mesenchymal) from the medio-ventral part of the somite which, until then, has been epithelial. Some, though not all, of the sclerotomal cells now express *Pax-1* and *Pax-9* and migrate toward the notochord to form the notochordal sheath (Ebensperger *et al.,* 1995). *Pax-1* and *Pax-9* are considered to be among the markers of sclerotome cells, others being *twist* and *scleraxis* (Christ *et al.,* 2000). *Sonic hedgehog (Shh),* and possibly *noggin,* are essential for the survival and maintenance of these *Pax-1*-expressing cells (Dockter, 2000). *Sonic hedgehog* is considered to act as a ventralizing signal since it is present in

The Atlas of Chick Development. http://dx.doi.org/10.1016/B978-0-12-384951-9.00010-1
Copyright © 2014 Elsevier Ltd. All rights reserved.

Downloaded from Vet-eBooks.com

the notochord and the ventral region of the neural tube (floor plate), whereas its antagonist, BMP4, has a dorsalizing effect, as do members of the *Wnt* family (produced by the ectoderm and neural tube). It appears that *Shh* signalling from the notochordal sheath actively attracts the migrating sclerotome cells. About day 10 of incubation, the diameter of the notochord starts to be reduced, and by day 14 the vacuoles have disappeared. The size of the sclerotome depends, at least in part, on the balance between the dorsal and ventral signalling, but may also be affected by adjacent tissues (reviewed by Christ *et al.,* 2000).

The anterior half of each sclerotome becomes partially separated from the posterior half by a discontinuity, the **fissure of von Ebne**, the cells being more densely packed in the posterior half. The fates of the different regions have been traced mainly by immunostaining (Christ and Ordahl, 1995; Ebensperger *et al.,* 1995). (The mesenchyme cells, which initially lie in the somitocoele, contribute to the sclerotome). Most of the skeleton is formed by the sclerotome cells, though the clavicle, coracoid, sternum and pelvic girdle are derived from somatic mesoderm. The lateral part of the posterior region of each sclerotome (*Text-Figure 72*) gives rise to the neural arches and pedicles of the vertebrae and, in the thorax, to the ribs. The medial part of the sclerotome forms the perinotochordal sheath and the vertebral body, and contributes to the vertebral disc. In addition, the sclerotome cells form the ligaments and the periosteum, as well as contributing to the endothelium of certain blood vessels (Huang *et al.,* 1994).

The vertebrae are cartilaginous at 5 days and ossification begins at about 11–13 days (*Plates 230–232*). Until recently, a controversy existed whether the segmentation of the vertebrae is 'intersegmental'. The traditional concept holds that, as the sclerotomal component of each vertebra is derived from the posterior half of one pair of somites and the anterior half of the succeeding pair, the position of each vertebra is not identical with that of either of the two pairs of somites from which it arose but with the intersomitic clefts that separate them. Traditionally, therefore, the vertebrae are considered to be 'intersegmental', in that they alternate in position with the somites.

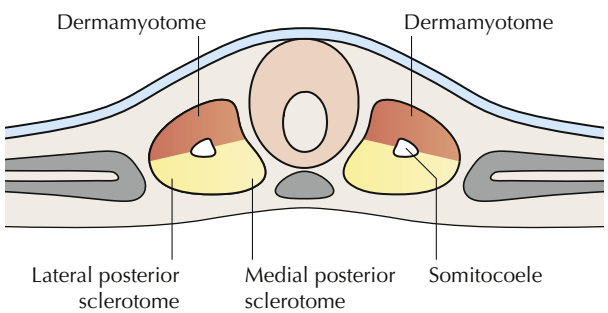

Text-Figure 72. *A pair of somites illustrating regions as described by Christ and Ordahl (1995).*

This concept was challenged by Verbout (1985), who suggested that the sclerotomal components of each vertebra were derived exclusively from one pair of somites only. Attempts to settle the problem by extirpating either one or two somites and studying the effect on the relevant vertebrae (e.g. Bagnall *et al.,* 1988) did not give clear-cut results. More recent work, based on immunohistochemical studies (Christ and Wilting, 1992) and on the grafting of one-and-a-half somites, to eliminate the possibility of a wrong orientation of the graft (Huang *et al.,* 2000a), concluded that the resegmentation theory was in essence correct. Interestingly, the spinous process of each vertebra has been found to have a different origin from that of the rest of the vertebra (Monsoro-Burq *et al.,* 1994; Aoyama and Asamoto, 2000) and appears to be formed as a result of the influence of BMP4 secreted by the dorsal side of the neural tube (Dockter, 2000).

The individual vertebrae of birds possess the typical structure found in all vertebrates: ventral to the spinal cord is the vertebral body or centrum; dorsal and lateral to the spinal cord are the neural arches. Each adult vertebra possesses articulating surfaces at the anterior and posterior aspect of each vertebral body, and paired articulating processes, the prezygapophyses at the anterior end and the postzygapophyses at the posterior end. It is thus able to articulate with the preceding and succeeding vertebrae. There are over 40 vertebrae in the hatched domestic fowl, of which 14 are cervical, 7 thoracic, 5 lumbar, 2 sacral and 10 caudal, whilst several fused vertebrae form the pygostyle (*Text-Figure 73*). These figures do not apply to all birds, variations existing between species not only in the numbers in each region, but also in the total number present. The atlas and axis are formed from somites 6–8. Each thoracic vertebra articulates with a pair of dorsal ribs (dorsal costa). Except for the first two pairs, each dorsal rib articulates also with a ventral (or sternal) rib, and each bears a posteriorly projecting process, the uncinate process (*Text-Figure 73; Plate 231*), to strengthen the rib cage. The most anterior four of the five ventral ribs also articulate with the sternum.

After the sclerotome cells have migrated around the neural tube and notochord, they form membranous structures, the **arcualia,** the forerunners

Downloaded from Vet-eBooks.com

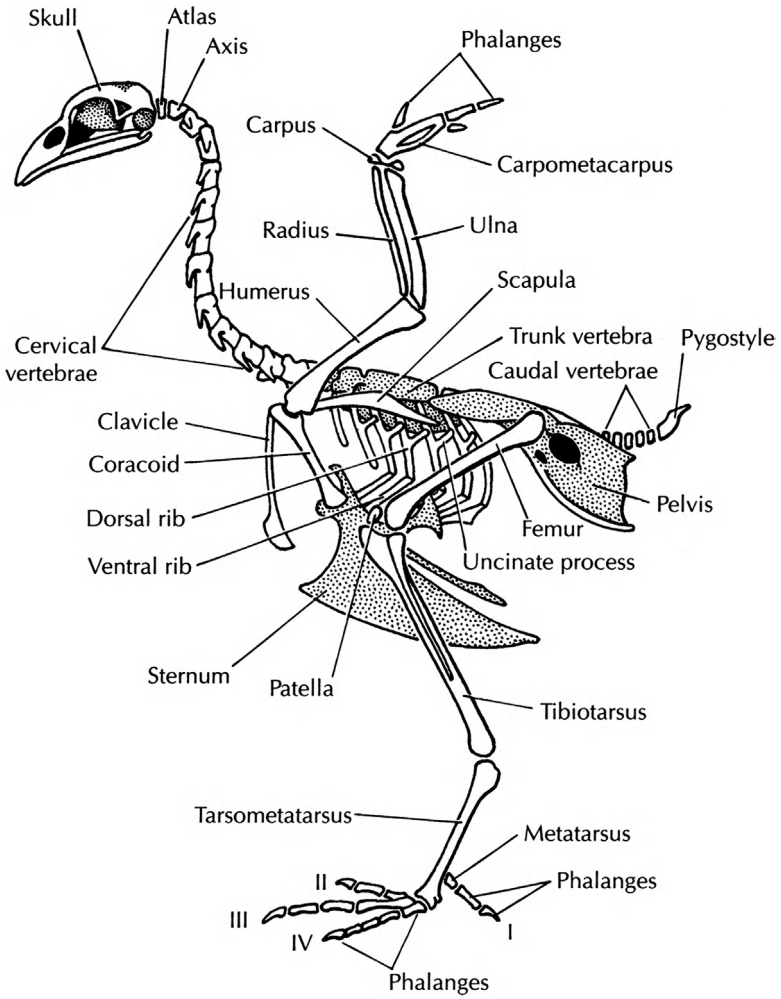

Text-Figure 73. *Components of the skeleton of an adult fowl. (After Ede (1964).)*

of the cartilaginous (later bony) vertebrae and the ligaments and periosteum. Chondrification begins in each vertebra at certain well-defined centres. The vertebral bodies are cartilaginous at 5 days and the dorsal spines at 6.5 days (Shapiro, 1992), and by day 8 almost every part of the vertebra has become cartilaginous. As the membranous vertebrae form, some mesenchyme remains between them, and this, together with remnants of the notochord, forms the intervertebral discs. The three primary centres of ossification in each vertebra are located in the vertebral body and the two sides of the neural arch, respectively. Ossification begins in the vertebral body about days 12–13 but is not completed, even in the cervical vertebrae, by the time of hatching.

The **type of vertebra** which develops (i.e. cervical, thoracic, lumbar, sacral or coccygeal) is determined by the position of the cells, even before segmentation, along the body axis. This was shown by transplanting regions of segmental plate mesoderm to other locations in the chick embryo by Kieny *et al.* (1972), who found that the graft formed a vertebra corresponding to its original position and not to its new one. The development of the different regions along the spine appears to be controlled by the activation of specific *Hox* genes (Burke, 2000; Iimura *et al.*, 2009).

A characteristic of the bird's skeleton is that extensive fusion occurs between certain vertebrae. The synsacrum is formed by the fusion of the most posterior (seventh) thoracic, the five lumbar, the two sacral and the five most anterior of the caudal vertebrae (*Plate 207*). This rigid structure is itself fused to the ilia of the pelvic girdle, the entire lot being immovable. Ossification in the synsacral vertebrae is not completed until just before hatching. Ossification of the last caudal vertebrae begins on day 19 and has been completed by hatching.

The intervertebral discs are formed mainly from the densely packed fibrous tissue which surrounds the remnant of the notochord, the nucleus pulposus (Christ and Wilting, 1992). The peripheral parts are

Downloaded from Vet-eBooks.com

derived from the mesenchyme cells that originated in the somatocoele (Mittapalli *et al.*, 2005), as are the articular surfaces of the intervertebral joints.

Ribs

The components of the avian ribs are illustrated in *Text-Figure 73*. Vertebral (dorsal) and sternal (ventral) ribs, together with the trunk and intercostal muscles, are derived from somites, the ribs from the sclerotomes and the intercostal muscles from the derma-myotomes. The evidence comes from the results of experimental ablation and transplantation experiments (Chevallier, 1975; Huang *et al.,* 2000d) and from separating the tissues from one another by inserting strips of aluminium foil (Aoyama *et al.*, 2005). The proximal part of each rib forms from the medial part of the thoracic sclerotome, whilst the distal part forms from the lateral region (Olivera-Martinez *et al.,* 2000). The development of the proximal region depends on signals from the notochord (Sudo *et al.*, 2001) and ventral neural tube (Aoyama *et al.*, 2005), whereas that of the distal region is dependent on signals from the somatopleure, of which bone morphogenetic protein 4 (BMP4) is an important component (Sudo *et al.,* 2001), or possibly from the surface ectoderm (Aoyama *et al.*, 2005). Suggestions that the derma-myotome might contribute cells to the ribs (Kato and Aoyama, 1998) have been discounted by others (Huang *et al.,* 2000d; Sudo *et al.,* 2001).

The only somites capable of forming ribs are those of the thoracic region, and they are already specified to do so by the time they have segmented. Even that part of the segmental plate from which they form is capable of developing ribs if explanted to a region of the body where ribs do not normally form (Nowicki and Burke, 1999). The specificity for ribs in this region appears to be due to the action of the *Hox* genes at that level.

Outgrowth of sclerotome and somitocoele cells begins at about stages 14–15 (Pinot, 1969). Initially, all the neck and trunk vertebrae bear rudiments of ribs, and these are derived as outgrowths from the vertebrae. The cervical ribs of the adult are small, apart from the last two pairs, and each chondrifies from a single centre. In the thorax the rudiments of the ribs migrate ventrally and contact the sternum. They chondrify from two centres, one close to the vertebra and the other near the sternum. The ribs begin to appear in membrane from about the end of day 6, become cartilaginous about 7–7.5 days, and ossify at 10–12 days.

Although processes comparable to ribs form from the lumbar and sacral vertebrae they do not separate from the vertebrae. In the chick, no ribs develop in association with the atlas vertebra.

Sternum

The sternum and the ventral muscles are derived from the somatopleural mesoderm (Chevallier, 1975, 1977) at the level of somites 12–26. The sternum, which develops independently of the ribs (Valasek *et al.*, 2011), begins to form at about 8 days as a bilateral pair of mesodermal condensations lying in the dorso-lateral wall of the thorax immediately posterior to the pericardial cavity. These **'sternal plates'** migrate ventrally and fuse together progressively from the anterior to the posterior end on day 9 (*Text-Figure 74*), forming not only the main body of the sternum but also the keel. Chondrification is completed by 9 days, and ossification begins in the chick at about the time of hatching. There are five centres of ossification.

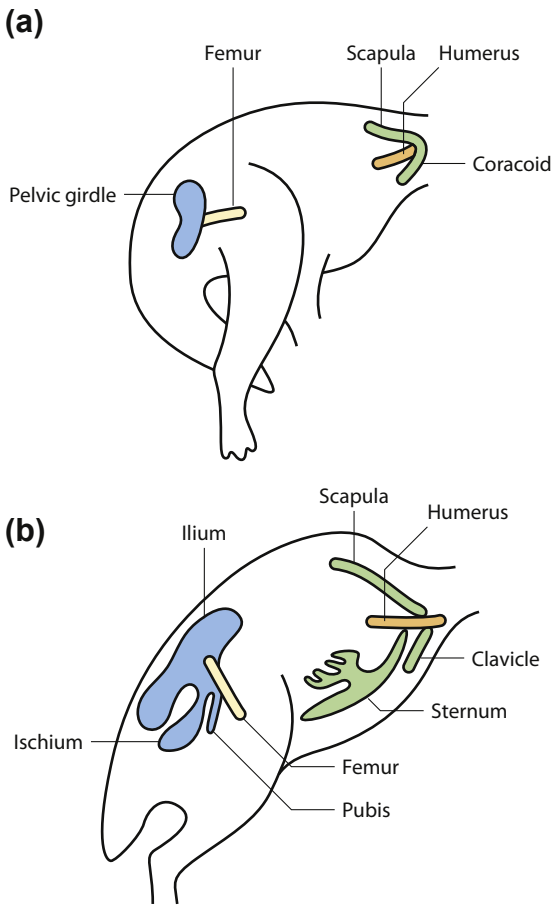

Text-Figure 74. *Developing pectoral and pelvic girdles (a) at 7 days and (b) 9 days, seen from the right side. (Modified after Chevallier (1977), with permission of the Company of Biologists Ltd.)*

Downloaded from Vet-eBooks.com

The Pectoral Girdle

The pectoral girdle consists of three components, the **scapula,** the **coracoid** (alternatively called the procoracoid, see Huang *et al.,* 2000b) and the **clavicle,** each of which is present as a pair of bones on the left and right, respectively (*Text-Figure 75*). In the adult bird the scapula is firmly attached to the rib cage by muscles and ligaments, whilst the coracoid and clavicle act as supports for the wing (*Text-Figure 73*). According to Chevallier (1977), using chick–quail grafting experiments, the scapula is derived from somitic mesoderm of levels 15–24. However, Huang *et al.* (2000b), also using chick–quail grafts, found that the scapula had a dual origin; the scapula blade was formed from cells derived from derma-myotome of somites 17–24, whilst its neck and head developed from the lateral plate (somatopleural) mesoderm; however, all the cells that formed the scapula expressed *Pax-1*. According to Shearman *et al.* (2011), six somites contribute to the distal end of the blade, and approximately two-thirds of the scapula is derived from the lateral plate. Signals from the ectoderm, together with BMPs from the lateral plate control the fate of the scapula precursors, but the dermomyotome compartment does not become committed to chondrogenesis until its cells have undergone epithelio-mesenchymal transition (Wang *et al.* 2010).

The coracoid and clavicle are formed from the somatopleural mesoderm at levels 10–15 and 15–17, respectively (Gumpel-Pinot, 1984). However, long-term fate mapping shows that the clavicle also receives some cells migrating from the cranial neural crest (McGonnell *et al.,* 2001). Both the scapula and the coracoid have become established in membranous bone by day 5, and chondrification begins at about the end of day 6. Ossification starts on day 12, although the junctional region of the two bones remains permanently cartilaginous.

The clavicle (furculum, wishbone) is essentially a membrane bone and ossifies directly from membrane. It begins as a condensation of mesenchyme at stages 31–32 (7.5 days) and starts to become ossified at stage 33 (8 days). There is then a brief appearance of secondary cartilage, though this lasts merely from about stages 35–36 (Hall, 2001). The left and right clavicles meet and fuse about days 12–13, forming the wishbone (furculum or merrythought). Defects of the shoulder girdle have been produced by treating embryos with signalling molecules that lead to the expression of BMPs, which in turn suppress *Pax-1* in the limb (Hofmann *et al.,* 1998).

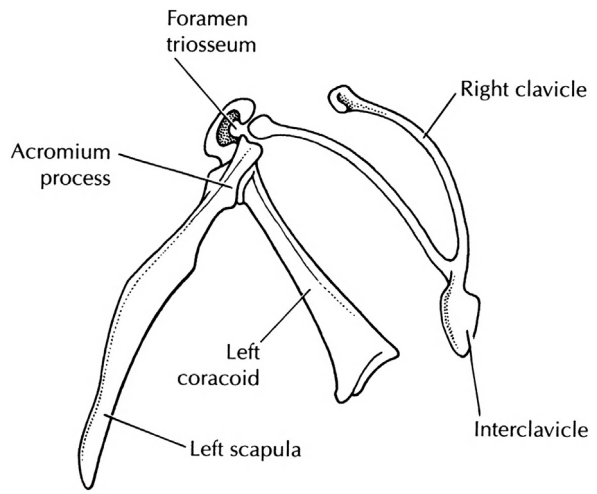

Text-Figure 75. *Components of the left half of the pectoral girdle of an adult fowl. (After Ede (1964).)*

The Pelvic Girdle

The pelvic girdle (*Text-Figure 74*) is formed from somatopleural mesoderm (Chevallier, 1977). On day 4 a mesenchymal condensation begins to separate into the three components of the pelvic girdle, the dorsally situated **ilium,** the laterally situated **ischium** and the latero-ventrally situated **pubis.** Chondrogenesis begins on day 6. The ilium begins to ossify on day 12, the pubis about day 13 and the ischium about day 14. The ilium fuses with the synsacrum, the ischium fuses with the ventral part of the ilium and the pubis fuses with the border of the ischium. The acetabular region is still chondrogenic at hatching, and fusion of the pelvic girdle with the sacral vertebrae has still not occurred.

The Wing and Leg Skeletons

See Chapter 5 for early stages in limb development. Like all pentadactyl limbs, the **wing** of the fowl consists of proximally, the **humerus**, followed by the **radius** and **ulna**, and distally by the carpals, metacarpals and phalanges (*Text-Figure 76; Plate 29*), the digits being the last part of the wing to form. These structures are clearly visible in the young embryo, but the distal ones have undergone considerable modification by hatching. After the humerus, radius and ulna have formed in membrane from the mesenchyme of the wing bud, chondrogenesis takes place at about 6 days, and ossification starts at about 7 days. The carpal and

Downloaded from Vet-eBooks.com

metacarpal bones begin to appear between 6 and 8 days (carpal at 9 days in *Plate 167*). Thirteen separate carpal bones have been described, but by day 13 most have lost their individuality, having fused either with each other or with the metacarpals, thus forming the carpo-metacarpus. By day 8 the metacarpals have been reduced to four cartilages, the first having disappeared, and metacarpals 3 and 4 become fused distally (*Text-Figure 76*). The first of the phalanges does not extend out as a digit, but is thought to be one of the 13 carpal bones. Digits II–V become modified, II and III being the longest, whereas IV remains short and fuses with V (*Plate 29*). As the wing develops, its position relative to the pectoral girdle changes (Yander and Searle, 1980).

The **hindlimb skeleton** develops from the same mesoderm as the pelvic girdle. The precartilaginous precursors of the **femur**, **tibia** and **fibula** are laid down by day 5, whereas those of the **tibiotarsus** and **metatarsus** (shown at 11 days in *Plate 206*) appear during the early part of day 6. The femur becomes chondrified during day 5 and ossification starts on day 6. The bone marrow cavity begins to form on day 8.

The tibia and fibula become chondrified during day 6 and ossification begins shortly afterwards. The patella forms in membrane between days 8 and 9 and starts to chondrify on day 10; ossification does not take place until about 11 weeks after hatching.

The foot and ankle region of birds is greatly modified from the basic pentadactyl plan. The embryo possesses a group of cartilaginous structures which fuse with either the distal end of the tibia or with the second, third or fourth metatarsal, and so are lost as separate entities. Of the five digits that form, the fifth disappears, the second, third and fourth extend, and after being ossified they fuse at their proximal ends, not only with each other, but also with the distal tarsals, to form the tarso-metatarsus. The first digit remains short, and the number of phalanges differs in different toes, e.g. toe 1 has two phalanges, whereas toe 4 has five (see *Plate 29*).

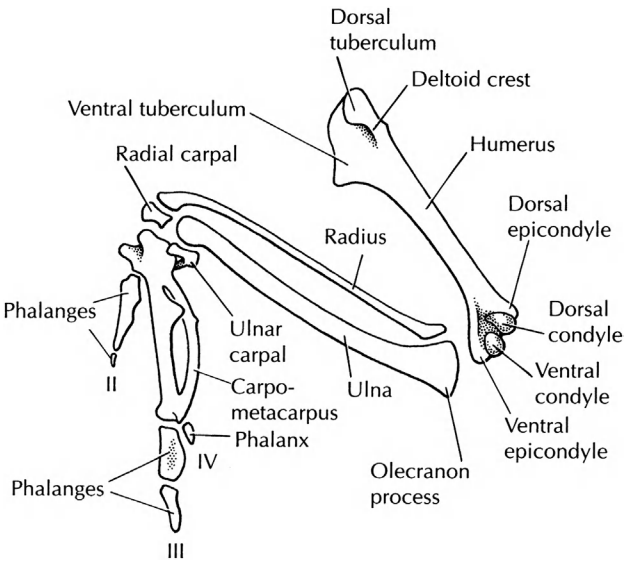

Text-Figure 76. *Components of wing skeleton of adult fowl. (After Ede (1964).)*

The cartilaginous elements of both the wing and the leg appear about stages 27–28 (5 days). They initially form as a number of chondrogenic rays in the flat **handplate** or **footplate.** The number of digits, as well as the type of each digit (e.g. second or fourth toe), is determined by signalling from the **polarizing zone** (Panman and Zeller, 2003). Several naturally occurring mutants have contributed to our knowledge of chick limb development. Most of them were identified and maintained at Storrs Agricultural Experimental Station and catalogues by Landauer (1967). They include the *Creeper*, which is achondroplastic and characterized by shortened longbones; it is due to a dominant mutation and is lethal in the homozygous. *Micromelia*, another achondroplastic, suffers from short extremities and defects to the beak.

The *talpid* mutant is an extreme example of polydactylism, affecting both wings and legs as well as other abnormalities, especially of the face. The *talpid 3* gene (KIAA0586) has been identified as the critical fator, being ubiquitously expressed and encoding a centrosomal protein essential for cilia formation (Davey *et al.*, 2006; Yin *et al.*, 2009). Experiments in which grafts of polarizing tissue have been inserted into abnormal places in a host embryo have produced additional digits, the type of each digit depending on its distance from the polarizing region. For example, the digit that forms nearest to the polarizing region differentiates into the most posterior digit, toe 4, whereas the digit furthest from the polarizing region becomes toe 1.

Chondrogenesis appears to be associated with transforming growth factor beta (TGFβ), and apoptosis between the digits is associated with signals of BMP4. For a review of digit formation see Sanz-Ezquerro and Tickle (2003).

The Skull

The skull is formed from three tissues whose respective origins in the early embryo are discussed in Chapter 4: the cranial neural crest, the unsegmented paraxial head mesenchyme (*Text Figure 77*) and the first five pairs of somites (*Table 3*). The evidence

Downloaded from Vet-eBooks.com

comes principally from transplantation experiments involving chick–quail chimeras, but in recent years has been supplemented by molecular studies. BMPs, FGFs and other molecules have been shown to play essential roles, not only in directing mesoderm cells into osteogenic or muscle pathways, but in controlling the development of specific bones and muscles . For reviews see Haworth *et al.* (2004), Noden and Trainor (2005), and Bothe *et al.* (2011).

Table 3 Origin of head skeleton

I. BONES OF NEURAL CREST ORIGIN[a]	
Membrane bones	
of face:	*of skull:*
Nasal	Frontal
Maxilla	Parietal
Vomer	Squamosal
Palatine	Columella
Quadrato-jugal	
Mandible	
Cartilaginous bones	
Interorbital septum	
Basipresphenoid	
Scleral ossicles	
Ethmoid, pterygoid	
Meckel's	
Quadrato-articular	
Hyoid	
Pars cochlearis of otic capsule (partly)	
II. BONES OF PARAXIAL HEAD MESODERM ORIGIN	
Cartilaginous bones	
Supra-occipital	
Sphenoid	
Pars canalicularis and cochlearis of otic capsule	
III. BONE OF SOMITIC ORIGIN	
Cartilaginous bones	
Basi- and exo-occipital	
Pars canalicularis of otic capsule (partly)	

[a]Based on data from Couly *et al.* (1993).

The paraxial head mesoderm has formed by stages 5–7 and the first five pairs of somites by stage 8, by which time the head has started to lift from the surface of the yolk sac. The cranial neural crest does not form over the brain until about stage 11. The most anterior cells of the neural crest migrate over the prosencephalon and around the optic vesicles; they form the maxillary and fronto-nasal processes and are essential in the formation of the beak (Schneider, 2005: *Text-Figure 79*) and also contribute to the cornea (Noden, 1983b) (*Text-Figure 79*; see Face, p. 46). The neural crest cells arising posterior to the optic vesicle move ventrally to form the pharyngeal arches (*Text-Figure 77*). The two regions of the cranial neural crest differ in that the anterior one does not express *Hox* genes, whilst the posterior one does (Creuzet *et al.*, 2005). Mesenchyme derived from the neural crest needs to be subjected to BMP proteins to become committed to the osteogenic pathway (Abzhanov *et al.*, 2007). The differentiation of the cranial neural crest into skeletal structures frequently depends on an interaction with adjacent tissues, though the precise elements which form are probably inherent in the cranial neural crest cells themselves.

The paraxial head mesenchyme migrates anteriorly to form bones associated with the most anterior regions of the skull, the supra-occipital, sphenoid, pars canicularis and cochlearis of the otic capsule (Couly *et al.,* 1993; Noden, 1983b). The contribution of the anterior somites to the skull is shown in *Text-Figure 80*, which is based on the chick–quail grafts

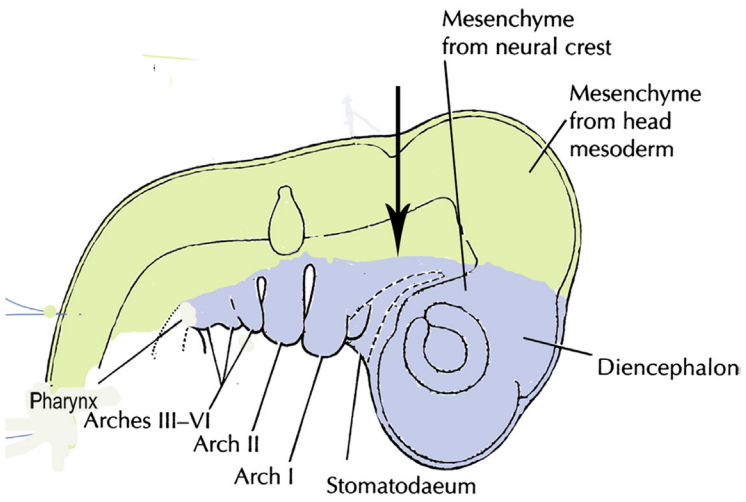

Text-Figure 77. *Distribution of the cells derived from the head mesenchyme and neural crest, respectively. Arrow shows interface between the two regions. (After Noden (1987); reprinted by permission of John Wiley and Sons. Inc.)*

Downloaded from Vet-eBooks.com

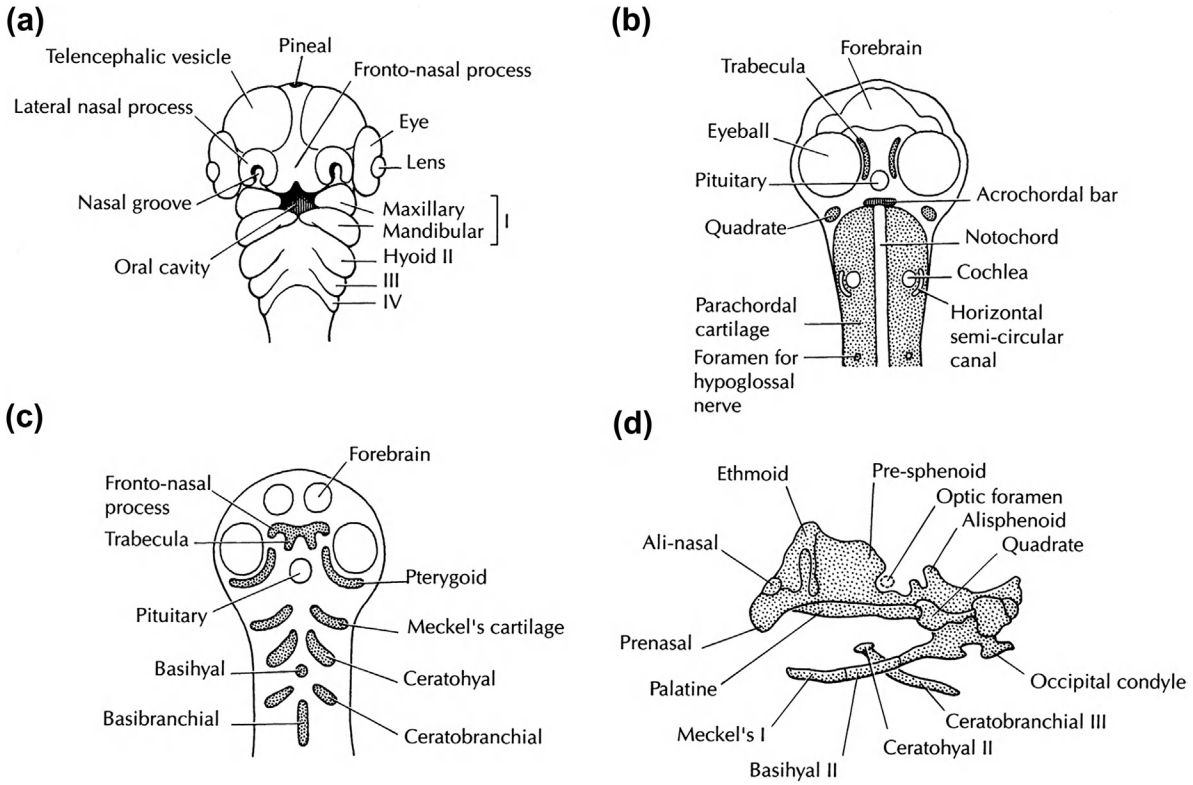

Text-Figure 78. *Developing head structures: (a) Day 4, viewed from below.* (b) Day 5, after removal of dorsal structures, viewed from above.† (c) Day 5, after removal of lower jaw, viewed from below.† (d) Day 7, lateral view of chondrocranium.† Stippled regions represent cartilages. I–IV = pharyngeal arch origins. (*After Patten (1950). †After Parker and Bettany (1877).)*

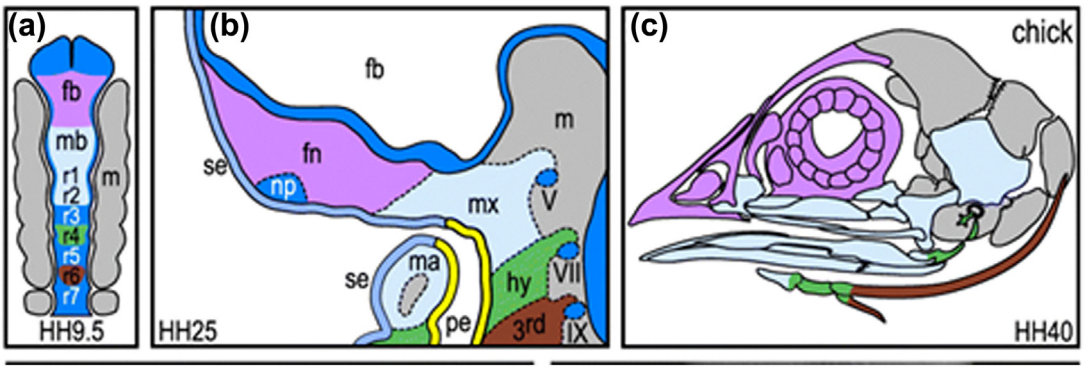

Text-Figure 79. *Development of the beak. **A**. Neural crest cells migrate from the caudal forebrain (b) and midbrain (mb) and give rise to the fronto-nasal structures (pink). Cells from the caudal midbrain and the first two rhombomeres® of the hind brain give rise to maxillary and mandibular derivatives (light blue). The hyoid arch forms fromr4 (green) and the third arch from r6 (brown). Neural cells migrate through and around mesodermal mesenchyme (m.grey). **B**. By stage 25 the fronto-nasal (fn), maxillary (mx), mandibular (ma) and hyoid (hy) primordial are surrounded by surface ectoderm (se:light blue) and contain contributions from the neural crest, nasal placode (np:dark blue) and cranial ganflia (V, VII, IX: dark blue). Mesoderm (m)produces muscles, vascular endothelial cells and some skeletal tissues. **C**. By stage 40 the neural crest cells have formed cartilaginous and bony elements in the face and jaw. Note the circle of bony plates, the scleral ossicles, in the eye. (From Schneider (2005), with permission of John Wiley and Sons, Inc.)*

of Huang *et al.* (2000c). These authors point out that the border between head and neck is in the centre of somite 5, and this corresponds with the expression boundary *of Choxb-3.*

The controversial idea that the vertebrate skull has been derived during evolution from segments corresponding to the somites of the trunk and tail received some support from the claim of Meier (1981) that somitomeres, which are a feature of the trunk (see p. 38), were also visible in the head mesoderm. Computer-assisted reconstructions of the head mesenchyme, however, failed to substantiate

Downloaded from Vet-eBooks.com

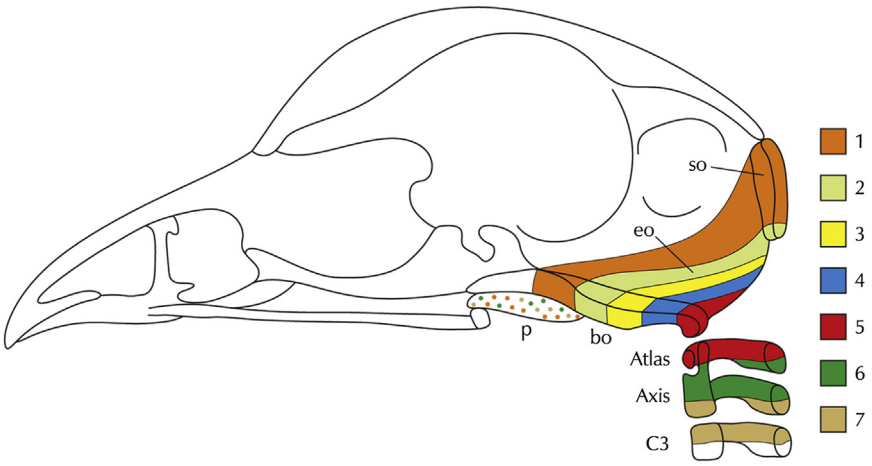

Text-Figure 80. *Distribution of somite-derived cells to the neurocranium. Somites are labeled consecutively from cranial to caudal. C3 =third cervical vertebra; bo = basioccipital bone; eo = exoccipital bone; p = parasphenoid bone; so = supraoccipital bone. (From Huang et al. (2000c), with permission of Springer-Verlag).*

this claim (Freund *et al.,* 1996), and the concept is probably best avoided.

The skull is formed from both cartilage and membrane bones. The cartilages form most of the base of the skull, the capsules of the ear and nose, the inner wall of the orbit, the jaw articulation and the hyoid skeleton, whilst the membrane bones provide most of the vault and sides of the skull, the jaws and palate. For a detailed description of the development of the chondrocranium see Vorster (1989).

The development of the skull inevitably reflects that of the underlying brain. By day 5 the cranial flexure (see p. 39) is clearly established and the cerebral hemispheres and eyes are prominent. The nasal pits are visible, whilst the oral cavity, which lies beneath the forebrain, is bordered above by the fronto-nasal process (which separates the two nasal pits), and laterally by the maxillary processes. The pharyngeal arches are well defined. The anterior end of the notochord lies just posterior to the developing pituitary (*Text-Figure 78*) and the **parachordal** cartilages lie on either side of it, whilst the acrochordal cartilage has formed at about 4.5 days as a small transverse bar anterior to it. Each parachordal lies beneath the midbrain and hindbrain and is continuous laterally with the chondrified wall of the otic vesicle, the **pars cochlearis**. The cochlea and semicircular canals are already present within the otic vesicle. The paired **trabeculae** develop anterior to the notochord and lie beneath the diencephalon and cerebral hemispheres, extending through the interorbital region to the nasal sacs.

Posterior to the parachordals the notochord becomes surrounded by three cartilaginous rings, which correspond with the first three occipital vertebrae. The first two fuse with the parachordals, whilst the third becomes the atlas vertebra (*Plate 182*). During day 7 the paired trabeculae become a single structure, the trabecula communis. Traditionally this has been thought to be due to fusion of the two components, but recent investigations using molecular markers has suggested that a cartilaginous component, the intertrabecular, derived from the neural crest, is inserted between the left and tight trabeculae (Wada *et al.*, 2011). The term **basal plate** (*Plate 187*) is applied to the collection of cartilages lying beneath the brain, extending from the trabeculae to the occipital vertebrae. Its posterior border is the ventral edge of the foramen magnum.

By days 6 and 7 of incubation, the trabecular region has become longer than the parachordal region. The trabeculae fuse together during day 7 and are then considered as two regions, the **interorbital** (shown at day 9 in *Plate 163*) and the **ethmoidal** regions, the whole structure extending from the pituitary fossa to the tip of the head. The ethmoidal region itself is divided into the **pre-nasal cartilage** from which the beak will form, and the **ali-nasal cartilage.** The preotic region of the basal plate grows both dorsally and laterally and forms the **alisphenoid**, which extends from the posterior edge of the orbit to the anterior border of the cranial cavity (*Text-Figure 78*). The cartilages of the tongue are discussed on p. 115.

The Pharyngeal Arch Cartilages

The formation and development of the pharyngeal arches is discussed in Chapter 8. The fate of the cartilages only is considered here.

Downloaded from Vet-eBooks.com

By the end of day 2, three to four pairs of pharyngeal arches are present, and by day 4 the first and second have become much bigger than the rest. During day 6 the first arch (the maxillary-mandibular) is considered to give rise to the palato-quadrate in the upper jaw and to Meckel's cartilage in the lower jaw (*Plate 150*), which articulates with the articular process of the palato-quadrate. Meckel's cartilage elongates greatly and its tips fuse at about 16 days. Recent experiments, however, have indicated that most, if not all, of the maxillary cells and skeletal derivatives are formed from the mesenchyme that condenses between the eye and the maxillary-mandibular region (Lee *et al.*, 2004). Meanwhile, the palate has begun to form as a roof to the oral cavity. Its development resembles that of the mammalian palate in that a shelf, the **palatine process** (*Plates 148, 193*), grows medially from the lingual surface of each maxillary process, but differs from that of mammals in that the two shelves do not meet in the midline but remain separated by a slit that is the **internal naris**.

The second arch, the **hyoid**, forms a median ventral structure and paired lateral cartilages. The median structure gives rise to the **basihyal** (or copula I), which forms part of the **basi-branchial** (see below). The lateral cartilages develop into the **columella** of the ear (*Plate 161*) and the **ceratohyals,** which give rise to the **entoglossal cartilage** and part of the **cornua** of the hyoid.

The third pharyngeal arch gives rise centrally to the basibranchial (or copula II) and laterally to the paired **ceratobranchial** and **epibranchial cartilages.**

The Face

See Chapter 5.

Ossification of the Skull

The membrane bones begin to be ossified from about day 9, though there are discrepancies in the exact times given by different authors. Most of the skull bones have undergone at least some ossification by day 14 (see Table 22 of Romanoff, 1960).

The **scleral ossicles** (*Plate 178*) are a ring of 14 overlapping bony plates in the sclera around the margin of the cornea. Their future position is indicated on day 8 by a series of conjunctival (scleral) papillae which disappear on day 12 as ossification occurs (Coulombre *et al.,* 1962). Each scleral papilla induces a scleral ossicle between 6.5 and 10 days (Hall, 1981). *Sonic hedgehog* (*Shh*) is expressed in the conjunctival papillae and may play a role in the induction process (Franz-Odendaal, 2008).

THE MUSCLES

The interdependence of the bones and muscles during development is especially apparent in the head and neck region where the neural crest, which provides most of the material for the face, is also important in the differentiation of the head muscles (Grenier *et al.*, 2009) and of the extra-ocular muscles (Bohnsac *et al.*, 2011). The patterning of the head involves a complex interplay between BMP and FGF signaling, promoting myosin expansion, which is in turn limited by retinoic acid (discussed by Noden and Trainor (2005) and Bothe *et al.* (2011)).

Most of the muscles in the body are formed from somites, particularly the skeletal muscles of the dorsal and dorso-lateral regions of the trunk and of the limbs. The lateral plate mesoderm, by contrast, gives rise to the muscles of the lateral and ventral body wall and to the tendons of the limbs. The muscle sheaths are also derived from the lateral plate mesoderm (Ordahl and Le Douarin, 1992), while the extra-embryonic lateral plate mesoderm gives rise to the muscles of the amnion and allantois. The neural crest, prechordal mesoderm, paraxial head mesenchyme and the most anterior somites all contribute to the muscles of the head (Noden, 1983a). The precursors of these muscles are arranged in an antero-posterior sequence which corresponds with the future location of the motor nerves.

As discussed in Chapter 4, the dorsal region of each somite develops into the derma-myotome, which then gives rise to both dermis and myotome. The skeletal muscles form from the myotome. The most important part of the derma-myotome is the **dorsal medial region** (*Text-Figure 72*), since if this extirpated no further myotome cells develop (Ordahl *et al.,* 2001). Cells from this region have, traditionally, been thought to migrate around the curved epithelium of the derma-myotome. However, the results of recent labelling experiments using DiI suggest that they do not do this, but rather join the other cells of the myotome and migrate directly (Denetclaw *et al.,* 2001). The cells of the myotome are orientated longitudinally along the body axis,

Downloaded from Vet-eBooks.com

in contrast to those of the derma-myotome, whose orientation is at right angles to it.

The most medial cells of the myotome form the **epaxial** muscles, while the lateral edge of the myotome forms the **hypaxial** muscles. These lateral cells lose their epithelial nature and become mesenchymal, migrating to form the abdominal body wall and the limb muscles (Ordahl and Le Douarin, 1992). The connective tissue of the epaxial muscles is formed from the somites, but that of the hypaxial muscles is derived from the somatic lateral plate mesoderm (Christ and Ordahl, 1995). *Myf5* and *MyoD* transcripts have been detected in the epaxial region of occipital somites even before stage 12, although there was an interval of 2 to 3 days before they began to produce myosin (Noden *et al.*, 1999). These authors suggested that the delay was probably due to the influence of neural crest cells on the head myoblasts, especially as such delays did not occur with other muscles.

We have seen in Chapter 4 that the newly formed somite is not yet determined as to the future of its cells. If the somite is experimentally inverted, the myotomes develop from cells that would normally have given rise to sclerotome, while the sclerotome develops from cells that would have formed myotome. See Borycki and Emerson (2000) for a review.

The factors controlling the development of muscles from the somites and other muscle-forming cells include a large group of genes, of which the **myogenic regulatory factor** (*MRF*) genes are the most important (Brand-Saberi and Christ, 1999). The timing of expression for these different genes was found to be similar in different mesoderm populations, i.e. *Myf4* was expressed first, followed by *MyoD* and then *myogenin* (Hacker and Guthrie, 1998). Two of these genes, *MyoD* and *Myf5,* which are expressed in both somitic epaxial (back) and hypaxial (intercostal) muscle progenitor cells, are activated simultaneously in the dorsomedial cells of the epithelial somite (reviewed by Borycki and Emerson, 2000).

The activation of *MyoD* and *Myf5* in the epaxial cells is brought about by influences from the notochord and neural tube on the newly formed somites (Pownall *et al.,* 1996). If these tissues are separated from the somites at this time, the epaxial muscles fail to form and the somite cells become apoptotic (Sanders and Parker, 2001).

There are other genes involved in the development of these tissues. For example, *sonic hedgehog (Shh)* is needed for development of both the myogenic and chondrogenic lines *Wnt*-signalling molecules, which are expressed by the dorsal neural tube and the ectoderm, appear to be involved in the formation of the myogenic cells in the somite (Wagner *et al.,* 2000). The gene *Lbx1* is expressed in the migrating hypaxial muscle precursors at occipital, cervical and limb levels from stage 14 (Dietrich *et al.,* 1998).

General Morphology and Nomenclature of Muscles

No single monograph appears to exist on the development of muscles in the domestic fowl, though accounts of specialized regions are available (e.g. limb muscles). Most of the body muscles are laid down between about days 5 and 9, and the adult pattern is well established by day 10. Identification of muscles from about 9 days of incubation is therefore usually based on the pattern of the muscles in the adult, though lack of uniformity in the terminology can be confusing. Muscles have been given different names by various investigators, and although some of these names correspond to those used for mammalian muscles, they are not necessarily identical in function. The names given in this book are based principally on those used by Berger (1960) and Vanden Berge and Zweers (1993). Where suitable, alternatives are shown in parentheses.

Limb and Girdle Muscles and Tendons

The early development of the limbs is discussed in Chapter 5.

Limb muscles form from somites, and their associated tendons and connective tissue develop from somatic mesoderm (Chevallier *et al.,* 1978).

For detailed morphogenesis of the wing muscles see Sullivan (1962), Beresford (1983) and Zhi *et al.* (1996), of the thigh muscles see Romer (1927) and Drushel and Caplan (1991), and of the lower leg muscles see Wortham (1948). The wing muscles are formed from somites 16–21, those of 18–20 giving rise to most of the muscles of the hand (Zhi *et al.,* 1996). These authors found that anteriorly located somites contributed to muscles on the ulnar side, but the hand muscles were derived from both anterior and posterior somites. Cells from these somites actively migrate into the wing bud between stages 15 and 18 (Schramm and Solursh, 1990). The leg muscles form from somites 26–32 (Gumpel-Pinot, 1984; Lance-Jones, 1988); cells from these somites migrate into

Downloaded from Vet-eBooks.com

the leg bud mainly during stages 17 and 18 (Jacob *et al.,* 1979). The somites which give rise to limb muscles also supply endothelial cells for the limb buds, though the migrating cells do not follow the same route (Huang *et al.,* 2003).

Traditionally, all the muscles of the pectoral and pelvic girdles have been thought to be derived exclusively from the somites, but some of the chick–quail transplant experiments have shown that the superficial muscles of the pectoral girdle (latissimus dorsi) are formed from cells which originate in the somites, then pass into the developing wingbuds where they stay briefly and then return to the mani body axis (Valasek *et al.*, 2011). A similar process, called the 'in-out' mechanism, has been reported for the pelvic girdle together with the cloacal sphincter (Valasek *et al.*, 2011).

The first indication of muscle development in a limb bud is the formation of two pre-muscle masses which form close to the girdle. They become visible in the wing bud at about stages 24–26 (4.5–5 days) lying dorsal and ventral to the condensation of cartilage that will form the wing skeleton (*Plate 147*). Lobulations in the ventral mass indicate some of the future muscles. Each dorsal and ventral mass undergoes a sequence of divisions, giving rise to the series of muscles (Sullivan, 1962).

Differentiation takes place in a proximo-distal direction. *Text-Figure 81* shows a reconstruction of the wing at 6–6.5 days (stage 29). A scanning electron microscopic study of normal wing development has been prepared by Murray and Wilson (1994) as a supplement to the table of Hamburger and Hamilton (1951).

Development of the leg muscles takes place between 6–8 days (*Text-Figure 82*). The dorsal and ventral pre-muscle masses are well defined by 6 days. Each then undergoes a series of subdivisions comparable to those of the pre-muscle masses of the wing bud. The dorsal mass of the thigh region forms a superficial group and a deeper group of muscles. Both the dorsal and the ventral pre-muscle masses divide at the knee into proximal and distal components, the proximal ultimately forming the muscles of the lower leg and the distal the muscles of the foot.

The tendons of the limbs also form from the dorsal and ventral pre-muscle masses, though they develop from different populations with different cell lineages. The tendons are derived from the somatopleure, whereas the muscles are formed from cells that have migrated from the somites (Christ *et al.,* 1977; Chevallier *et al.,* 1978). However, absence of a specific muscle is accompanied by absence of the

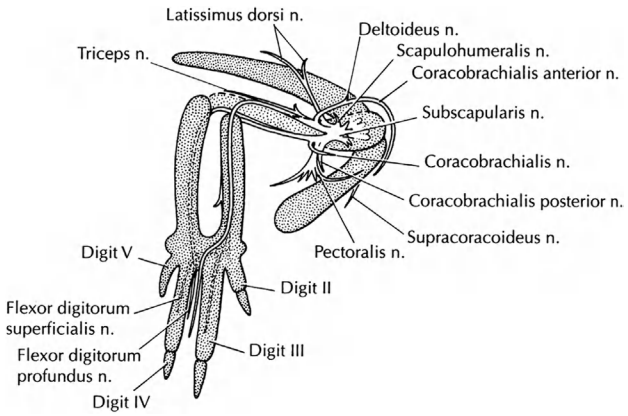

Text-Figure 81. *Pre-muscle masses (stippled) of right wing bud together with nerves at about 6–6.5 days. (After Sullivan (1962), with permission from CSIRO Publishing: http://www.publish.csiro.au/journal/ajz.)*

corresponding tendon (Chevallier *et al.,* 1978). The tendons begin to form in the lower leg at the end of day 6 or the start of day 7 (Wortham, 1948). Schweitzer *et al.* (2001), using a specific marker, *Scleraxis,* showed that they are derived from a population of cells in the mesenchyme induced by ectodermal signals. As each muscle forms from the pre-muscle mass, the tendon grows forward from it to its place of insertion. Each tendon grows along a digital ray, which is essentially a band of collagen around which the tendon condenses (Ros *et al.,* 1995). All the leg tendons are defined by 9 days, apart from those of the toes, which are unable to complete their insertions until day 11 when the final skeletal cartilages are formed. Like the muscles, the tendons continue to enlarge and differentiate during the succeeding days of incubation. For further information on tendon development in the avian limb, see Oldfield and Evans (2003).

Muscles of the Thorax and Abdomen

The thoracic and abdominal muscles are formed from the somitic myotomes, which become divided into a dorsal part (the **epimere**, which gives rise to the epaxial muscles) and a ventral part (the **hypomere**, which forms the hypaxial muscles). The myoblasts of these layers migrate laterally and ventrally, passing through the substance of the somatic mesoderm immediately beneath the ectoderm. The epimeres form the extensor muscles of the vertebral column, whilst the hypomeres form the flexor muscles of the vertebrae, the limb muscles and the intercostal muscles. The hypomeres give rise also to the muscles of the abdominal wall.

Downloaded from Vet-eBooks.com

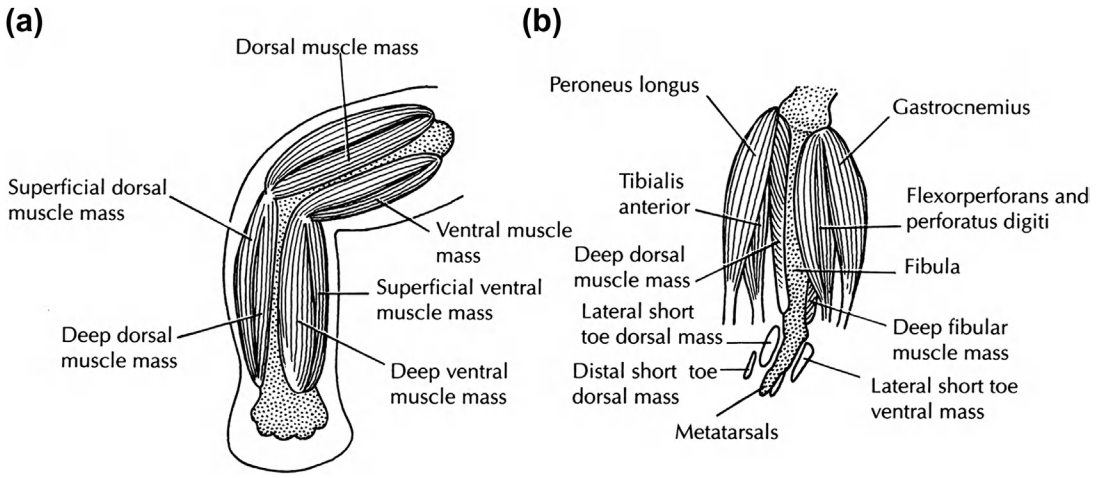

Text-Figure 82. *(a) Longitudinal division of pre-muscle masses of the thigh at 6.5 days into superficial and deep layers, with incomplete separation in the region of the knee; (b) Differentiation of peroneus longus and tibialis anterior muscles from the superficial dorsal pre-muscle mass, at about 6.75 days. There is incomplete separation of the flexor perforans et perforatus digiti group of muscles from the lateral portion of the superficial ventral muscle mass and complete separation of the short toe muscles masses from the leg muscle masses. (After Wortham (1948), with permission of John Wiley and Sons.)*

Muscles and Cartilages of the Tongue

The deep muscles of the tongue are formed from anterior somites, though the precise somites and their individual contributions remain controversial, despite modern chick–quail grafting experiments. For example, the glossal muscles have been reported to receive cells from somites 2–5 (Noden, 1983a), 1–5 (Couly *et al.,* 1992) or 2–6 (Huang *et al.,* 1999, 2001). The skeleton of the tongue consists of the **basibranchial** cartilage, which supports the base of the tongue, and the **paraglossum** (entoglossum), which supports the body of the tongue. In addition, paired lateral wings are formed by the **ceratobranchials** and the **epibranchials** (*Text-Figure 83*). Huang *et al.* (1999, 2000a) have classified the tongue muscles according to their origins and insertions into **glossal** (attached to the entoglossal cartilage), **suprahyoid** or hypobranchial (extending from the mandible to the hypobranchial skeleton) and **infrahyoid** muscles (which originate from the larynx, tracheal cartilage, sternum and clavicle, and are attached to the hypobranchial skeleton). They conclude from their experiments that somites 2–6 give rise to all the glossal and infrahyoid muscles but not the suprahyoid muscles. Huang *et al.* (1999, 2000a) found that myoblasts from different somites intermingled during their migration to the tongue, apparently streaming to a focal point and then migrating in a stream. The migrating muscle cells carry with them the hypoglossal nerve. The signalling cascades involved in the development of the tongue are described by Huang *et al.* (2001). The more superficial muscles are derived from the

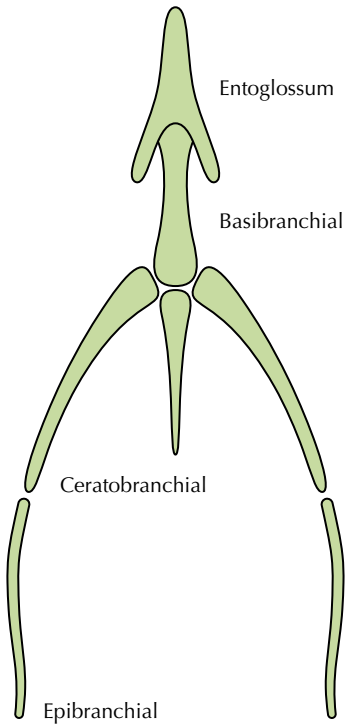

Text-Figure 83. *Schematic drawing of the tongue skeleton.*

mesoderm of the first, second and third pharyngeal arches and are innervated by the trigeminal, facial and glossopharyngeal cranial nerves, respectively.

Head and Neck Muscles and Connective Tissue

Those muscles formed from the fronto-nasal process have been traced back to the neural crest. The

Downloaded from Vet-eBooks.com

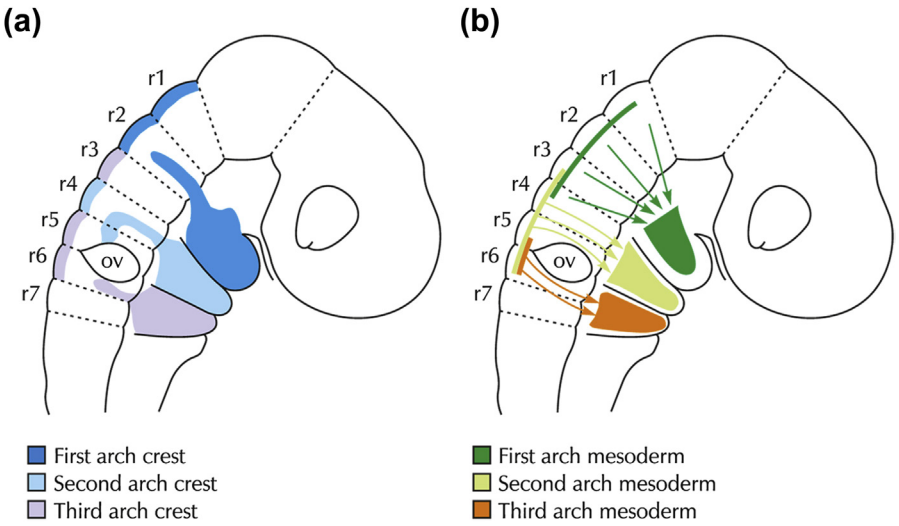

Text-Figure 84. *Migration of (a) the cranial neural crest, and (b) the cranial paraxial mesoderm. r1 – r7 = rhombomere position of populations of cells; ov = otic vesicle. (Reprinted from Hacker and Guthrie (1998), with permission from The Company of Biologists Ltd.)*

remainder of the head muscles, including the external eye muscles, as well as all the voluntary muscles of the face, are formed from the paraxial head mesenchyme (Noden, 1983a,b; Hacker and Guthrie, 1998), which is the unsegmented mesoderm situated anterior to the somites in the early embryo and lying on either side of the neural tube. Its cells migrate to the first, second and third branchial arches and colonize the core of each arch, forming a muscle mass (*Text-Figure 84*). At much the same time neural crest streams to line the periphery of each of these branchial arches, though recent findings (Grenier *et al.*, 2009) suggest that there may be mingling of the two types of cells at the interface.

The prechordal mesoderm, which lies anterior to the notochord and medial to the paraxial mesenchyme, is found subsequently beneath the anterior region of the midbrain and the prosencephalon, and gives rise to the oculorotatory muscles innervated by the oculomotor nerve (Jacob *et al.,* 1984). The tip of the notochord lies beneath the caudal midbrain and the hindbrain (Noden, 1992).

According to Noden (1983a), somites 3–7 only contribute to the formation of the cranio-cervical muscles, but Huang *et al.* (2000c) found that somites 2–8 are involved. The origin of the neck muscles is of particular interest since they have been considered to arise from occipital somites (Couly *et al.*, 1993), but have recently been found to be derived mainly from the lateral plate mesoderm (Theis *et al.*, 2010). The connective tissues of the head also have differing origins. Those of the midfacial, peri-ocular, glossal and visceral arch regions are derived from neural crest. The laryngeal and tracheal connective tissues develop from the lateral plate mesoderm of the level of the first two pairs of somites (Noden, 1986). The connective tissues for the head elevator and depressor muscles are formed from somites (see Noden and DeLahunta, 1985).

Heart Muscle

See Chapter 6.

Downloaded from Vet-eBooks.com

Chapter 11

The Integument

The term 'integument' includes not only the skin and feathers but also the beak, claws, scales, comb and wattle and the uropygial gland. Its morphology has been studied since the nineteenth century (Lucas and Stettenheim, 1972; Bereiter-Hahn *et al.,* 1986) and, because of its diversity, ease of access and amenability to experimental manipulation, it has been important in the study of cell and tissue interactions. Each specialized structure is formed from an interaction between its two components, the dermis and the epidermis. Much research has been focused on analysing these interactions by experimentally separating and then recombining them (reviewed by Sengel, 1976; Dhouailly *et al.*, 2004) and, more recently, on the cytological and molecular changes involved (reviewed by Chuong, 1993, Noveen *et al.*, 1995).

The **dermis** is formed mainly from neural crest mesenchyme in the facial region, from prechordal mesoderm over the cranium and from the dermatome or the lateral plate in the trunk region. The dermis of the epaxial (dorsal) region is derived from the dermatome, but of the hypaxial (lateral) region is from the somatic layer of the lateral plate mesoderm (Christ *et al.,* 1983). In the early stages the dermis is mesenchymal and is not present as a distinctive tissue until about 5 days of incubation (Sengel, 1976). Olivera-Martinez *et al.* (2001), who carried out a series of grafting experiments, demonstrated that the specification of the dermis to produce feathers was the result of a signal from the neural tube, probably *Wnt1*.

The **epidermis** forms from the ectoderm, which is initially a single layer but starts to become two layered at about stage 12. The outer layer is the **periderm**, a temporary layer of squamous epithelial cells that forms at about the time that the neural tube closes and acts as a barrier between the internal tissues and the amniotic fluid (Sengel, 1976). It becomes sloughed off at about 18 days of incubation.

Classical studies have shown that the rate of integumentary differentiation varies significantly in different regions of the body. Mayerson and Fallon (1985) reported that not only can early feather primordia be recognized at any stage between early 31 and 39 (7–13 days), but that there are important differences between the pterylae. Studies of scale differentiation in the legs (Sawyer *et al.,* 1986) provide a similar picture. Consequently, it can be misleading when discussing the differentiation of avian integument to give precise timing for specific developmental events.

THE FEATHERS

Adult feathers do not cover the body uniformly, but are arranged in tracts (**pterylae**) separated by regions where few, or no, feathers occur (**apterylae**). The feathers, as well as the scales, are formed from β-keratins, and the apteria express α-keratins (Prin and Dhouailly, 2004). There is considerable morphological variation between species, and the domestic fowl is exceptional in two respects (Lucas and Stettenheim, 1972). First, the embryonic apterylae are still recognizable in the adult. Second, whilst the major body feathers (including those of the wings and the tail) consist of **contour** feathers, the **plumules** (downy feathers) and **filoplumes** (fine, thread-like structures) that lie beneath them are relatively sparse in comparison with the situation in a duck or a goose.

The hatching plumage, consisting of **down feathers**, is soon replaced by the juvenile plumage, and this in turn gives way to the adult plumage, which is characterized by various forms of contour feather. The precise relationship between the widely studied 'embryonic feather germs', which form the hatching plumage, and the juvenile and adult plumage does not appear to have been investigated, and it is not known if the feather follicles of the adult bird are formed before hatching.

The Atlas of Chick Development. http://dx.doi.org/10.1016/B978-0-12-384951-9.00011-3
Copyright © 2014 Elsevier Ltd. All rights reserved.

Downloaded from Vet-eBooks.com

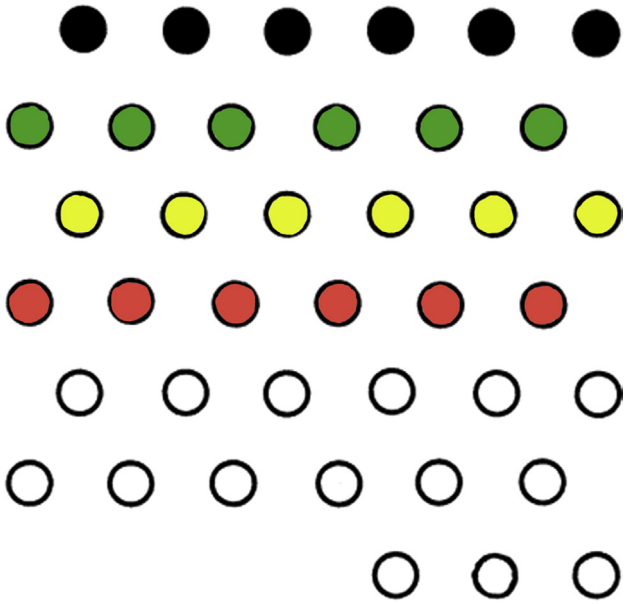

Text-Figure 85. *Diagram to show the sequence of patterning of feather rudiments on the right side of the lumbar region of the back. Row 1 (black dots) develops first, followed by row 2 (green), row 3 (yellow) and so on. The result is that the feathers come to lie in a pattern of oblique and longitudinal rows.*

The first visible sign of an individual feather rudiment is a white spot on the surface of the body: this is an epidermal placode, a localized thickening in the epidermis which then becomes underlain by a condensation of cells in the dermis, the **dermal papilla**. *Fgf10* signalling is needed for induction of a feather placode by the dermis (Mandler and Neubüser (2004). BMP and β-catenin signaling pathways also play a significant role in induction (Jiang *et al.*, 2011). The first feather rudiments appear at about 5 days as a single row in the lumbar region, separated by spaces where no feathers develop. As additional rows are laid down, the new rudiments are always opposite the spaces between the rudiments in the preceding row. The sequence of the patterning was described by Mayerson and Fallon (1985), each row, or tract, being established in precise relation to the preceding row so that the feathers become arranged in a hexagonal pattern of oblique and longitudinal rows (*Text-Figure 85*). This is brought about by the interaction of BMPs, follistatin and the receptor tyrosine kinase Eph-A4 (Patel *et al.*, 1999).

Each dermal papilla and the ectoderm above it proliferate, and the entire structure becomes extended into an elevated epidermal cylinder with a dermal core (*Text-Figure 86, Plate 224*), the feather bud. The two sides grow unequally so that the apex moves posteriorly and the entire structure lies almost flat on the surface of the skin. There is a region at the base of the feather bud, the **epidermal collar**, which has a high mitotic rate. The melanophores become arranged in rows along the feather. By day 11 a series of longitudinal ridges have appeared in the stratum corneum of the epidermal walls, and between 12 and 18 days they form the barbs and their associated barbules. The **calamus** is a hollow region at the base of the feather where the barbed ridges remain fused. About day 20 the base of the feather germ sinks into a depression, the **feather follicle**. A thin sheath of epidermal cells, the **periderm**, remains around the feather germ until after hatching, but splits as the chick dries and so releases the barbs and barbules. The down feathers are pushed out of the follicle by the apices of the **juvenile feathers**, which are similar in structure to the adult feathers. For a morphological description of the embryonic down feathers, see Matulionis (1970). Adult feathers are of three types:

- the **contour feathers**, which are the main body feathers including a wide variety of wing and tail feathers;
- the **plumules** or downy feathers, which lie beneath the contour feathers;
- the **filoplumes**, which are fine thread-like feathers closely associated with contour feathers.

All these definitive feathers are formed from the dermal papillae laid down in the embryo. All parts of each feather shaft are derived from the embryonic epidermal cells, the collar, which surrounds the dermal papilla. The pulp is formed entirely from the papilla.

The development of the feathers is an example of epithelial–mesenchymal interactions. The ectodermal epithelium is incapable of forming a feather unless induced by the underlying mesoderm; if the papilla is removed, no more feathers develop. Nevertheless, it is the epidermis that determines where the feather will eventually develop. A series of thickenings (placodes) appears in the epidermis, and each of these promotes a condensation of the mesoderm immediately beneath it. These condensations do not form in the absence of the epidermis (Sengel, 1976), and they do not form in the mutant *Scaleless,* which does not develop feathers (Goetinck and Sekellic, 1972). Each dermal condensation then induces the epidermis to form a feather bud. Interestingly, although the feathers are formed almost entirely from the epidermis, their future adult form is determined by the mesoderm. This has been shown by experiments in which epidermis from one region of the body has been

Downloaded from Vet-eBooks.com

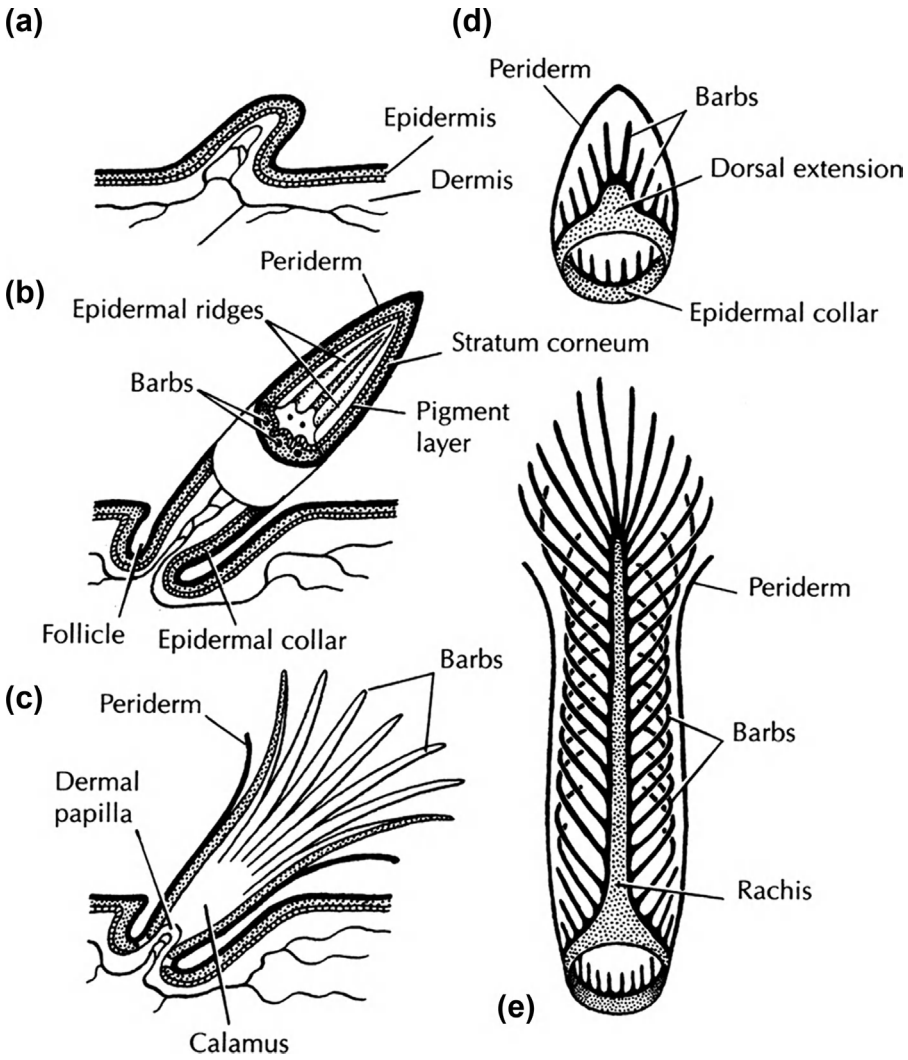

Text-Figure 86. *Stages in the formation of the down feather (a–c) and an adult contour feather (d,e). (After Ede (1964).)*

stripped of its associated dermis, recombined with dermis from another part of the body, and then grown in tissue culture. For example, if the dermis beneath wing bud epidermis is removed and replaced with dermis from the back of the embryo, the feathers that develop are characteristic of the back and not of the wing (Sengel, 1986). The inductive signals involved in these interactions are complex and not yet fully understood. Among the factors that have been implicated are: from epidermis to dermis, BMPs (Scaal *et al.,* 2002); and from dermis to epidermis, *FGF10* (Tao *et al.,* 2002), *cDermo-1* (Scaal *et al.,* 2002), *Wnt6* (Chodankar *et al.,* 2003), *sonic hedgehog* and BMP2 (Harris *et al.,* 2002), and *Sox 18* (Olsson *et al.,* 2001). For a recent series of reviews on further development, see Yu *et al.* (2004).

The regular hexagonal arrangement of the feather buds (see above) appears to be the result of an individual action of each developing epidermal placode which inhibits the formation of a similar placode in its immediate vicinity. The homeobox gene, *HB9,* is expressed in the epidermal placodes and feathers as well as in the dermal condensations, but not in the interplacode regions (Kosaka *et al.,* 2000). Conversely, the *c-Delta-1* gene is widely expressed in the dermis of the Scaleless mutant and its experimental overexpression in dermis from a non-mutant embryo inhibits feather formation (Viallet *et al.,* 1998). The morphogenesis of the induced feathers has been analysed by transgenic experiments which have shown that BMP enhances the size of the rachis, *noggin* increases branching and *sonic hedgehog* (*Shh*) causes webbing of the branches (Yu *et al.,* 2004). A fast, and inexpensive technique for commercial sex-typing of ostrich chicks has been devised by Malago *et al.* (2002) using DNA extracted from feathers.

Downloaded from Vet-eBooks.com

Pigmentation of the Feathers

See Pigmentation, below.

Feather Muscles

Four small smooth muscles form in the dermis around the feather follicle, and these are used for erecting and depressing the formed feather.

THE PERIDERM

The diversity of form of the integument covering the avian leg and foot, and the regional distribution in keratins (only some of which closely resemble the feather keratins) have stimulated the study of epithelial–mesenchymal interactions that produce patterns and control differential gene expression (Sawyer *et al.,* 1986; Barnes and Sawyer, 1995). The broad, overlapping scutate and scutellate **scales** on the anterior and posterior surfaces of the tarso-metatarsus are best known for their similarity to scales of archosaurian reptiles (Maderson, 1985). They arise as a series of placodes (*Text-Figure 87*) during days 10–11, form scale ridges by day 12, and elongate distally until the end of day 17, by which time the typical epidermal proteins are detectable. All types of avian scale lack the pronounced dermal condensations characteristic of feather primordia, although a transient increase in mesenchymal density is detectable at the scale ridge stage. Epidermal placodes are absent from the tubular, reticular scales on the plantar surface.

The ptilopodous ('feather-feet') phenotype seen in various breeds of the domestic fowl, as well as in some other galliformes and owls (Lucas and Stettenheim, 1972), and the possibility of its experimental induction, is often cited as supporting evidence for the evolutionary origin of feathers from scales. But, since small feathers can be induced to form on all types of scales by *in ovo* application of retinoids (Sengel, 1986; Sawyer *et al.,* 1986), it is more likely that these feathers result from the upsetting of regulatory genes (Michaille *et al.,* 1995; Noveen *et al.,* 1995) that are usually suppressed over the legs and feet.

The first rudiments of the scutellate scales (*Text-Figure 87*), which appear on the dorsal side of the foot, have formed placodes by day 11 and scale ridges by day 12; distal outgrowth of the scale ridges takes place between 12 and 17 days (Sawyer, 1972). Each tiny scale increases in size and becomes keratinized

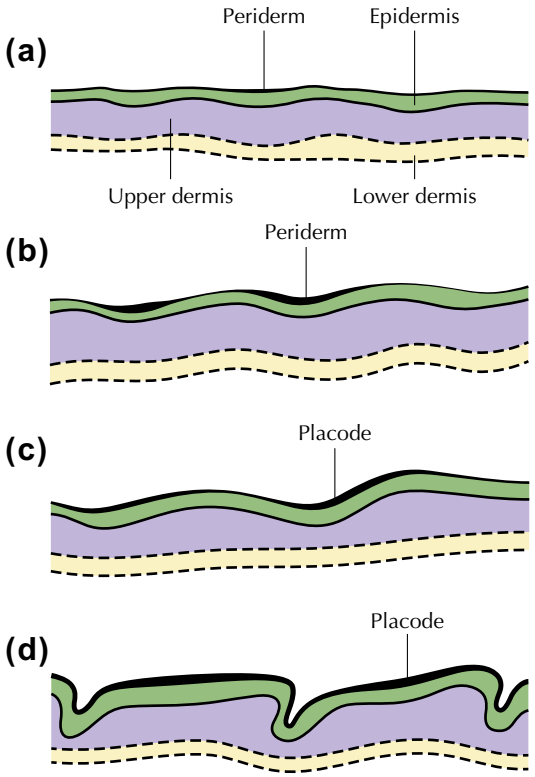

Text-Figure 87. *The development of two metatarsal scales. (a) Late stage 35 with symmetrical placodes. (b) Stage 36, the placodes are becoming asymmetrical. (c) Stage 37, the scale ridges have formed. (After Sawyer (1972), with permission of Wiley-Liss, Inc, a subsidiary of John Wiley and Sons Inc.)*

and overlaps the neighbouring scale, and blood vessels penetrate into the papilla.

BEAK AND CLAWS

The upper beak is formed from the maxillary process together with the fronto-nasal and latero-nasal processes (see Chapter 5). The lower beak is from the mandibular processes.

The ectoderm of the beak region has started to thicken by day 6 along the upper and lower jaws. By day 7 the egg tooth has begun to develop as a projection from the tip of the upper jaw (*Text-Figure 88*); it grows rapidly from about 3 mm in length at 10 days to about 3.5 mm at 14 days. Its role is to break through the shell at hatching, after which it is shed.

The beak starts to become cornified on day 10 and has hardened by day 14. The periderm of the beak is not sloughed off until about days 19–20. The size and shape of the beak differ markedly in the many species of birds, depending on their food-gathering habits. Wu *et al.* (2006), who compared the beak development of chickens, ducks and

Downloaded from Vet-eBooks.com

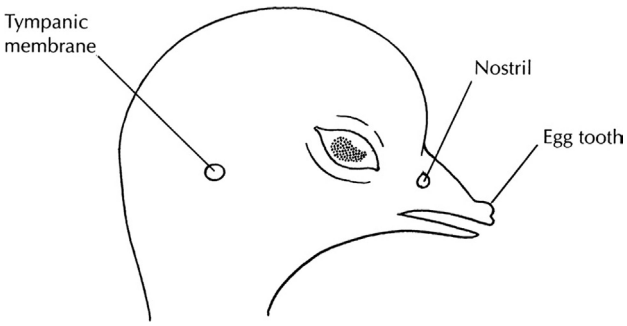

Text-Figure 88. *The beak of a chick embryo at about 12 days to show the egg tooth.*

cockatiel, found that different patterns of localized growth could account for the diversity. Moreover, the localized growth zones were each characterized by a high level of BMP4, which had previously been found to play a critical role in the morphogenesis of the face. Wu *et al.* demonstrated that when BMP4 was experimentally altered the beak size and shape were altered too.

Claws, which are modified scales, are visible at about 10 days (stage 36) on the toes and have started to become cornified by 14 days (stage 40, see Normal Tables, Appendices II, III). A transitory thumb-like claw is visible on the first digit of the wing at 10 days.

THE COMB

The comb is first visible as a ridge along the head at about days 6–7. It originates as a thickened and vascularized dermal thickening beneath the ectoderm (Menon *et al.,* 1981). Small papillae develop along the posterior two-thirds of the region, and are the forerunners of the adult serrated comb. As it enlarges during the following days, it becomes highly vascularized. Wattles start to appear at 11 days and develop in a similar way to the comb.

THE UROPYGIAL GLAND

Birds possess no integumentary glands apart from the uropygial (preen) gland, which forms on the dorsal side of the body at the base of the tail. It starts as a bilobed structure that arises on day 10 from a pair of ectodermal invaginations, one on either side of the vertebrae. These become paired ducts and each buds off further sacs. The two structures unite on day 14, but secretion does not begin until after hatching. For further details see Lucas and Stettenheim (1972), Quay (1986) and Fukui (1988, 1989).

PIGMENTATION

The yellow of the beak, skin and legs is due to lipochromes, which are carotenoid pigments. They appear at the time of keratinization and are derived from the carotenoids of the yolk. The melanin pigments are all derived from those neural crest cells that migrate beneath the ectoderm and above the somites. These cells are already specified to become melanocytes by the time they begin to migrate, and there is evidence to suggest that this is due, at least in part, to *Wnt* signalling from the dorsal neural tube (Jin *et al.,* 2001). These authors found that as the *Wnt* signalling increased, BMP4 decreased, suggesting that *Wnt* and BMP4 signalling had antagonistic functions, *Wnt* promoting melanocytes and BMP4 neuronal and glial cell lineages.

The premigratory neural crest cells express the endothelin receptor B (ETRB), and if they migrate along the dorsal pathway they continue to do so, whereas those that pass along the ventro-medial pathway express a different endothelial receptor (Dupin *et al.,* 2000). Only those neural crest cells that are specified as melanocytes are able to take the dorsal path (Erickson and Goins, 1995). In the normal embryo these dorsally migrating cells are unable to enter the ventral pathway. By contrast, in the development of the Silkie fowl they pass not only along the dorsal route but also along the ventral one, so that eventually most of the connective tissues become pigmented. Faraco *et al.* (2001) have provided experimental evidence that in the normal embryo environmental barriers, such as lectins, prevent the migrating melanoblasts from taking the ventral route, but that these barriers are not present in the Silkie embryo.

Those melanocytes that enter the wing bud of the normal embryo migrate in a proximo-distal direction under the influence of fibroblast growth factors FGF2 and FGF4, produced by the apical ectodermal ectodermal ridge (Schöfer *et al.,* 2001).

The melanocytes that lodge in the feather buds undergo extensive mitosis and enlarge and begin to secrete melanin from about days 8–9 (for a discussion see Le Douarin and Kalcheim, 1999). In breeds such as the White Leghorn, the melanophores differentiate as in the darker-feathered breeds but die before depositing pigment, so that the feathers are non-pigmented.

Downloaded from Vet-eBooks.com

INNERVATION AND SENSORY RECEPTORS IN THE INTEGUMENT

The innervation of the skin is restricted to the dermis and to a ring of skin around the base of each feather. Sensory receptors develop only when nerve endings are present in the dermis (Saxod, 1996).

Merkel Cells

Halata *et al.* (1990), using chick–quail chimeras, showed that the Merkel cells are essentially of neural crest origin and that in the limb they migrate along with the Schwann cells. The outer capsule of each Merkel cell is formed from the local mesenchyme (Saxod, 1996). They are found not only in the dermis (Grim and Halata, 2000), but also in other epithelial-derived structures such as the hard palate (Nafstad, 1986), the tongue (Toyoshima *et al.,* 1993) and the beak (Saxod, 1980; Halata and Grim, 1993). Their function is unknown.

Herbst Corpuscles

Herbst corpuscles are found in the skin and beak and consist of an inner core of cells derived from the neural crest and an outer capsule from the adjacent mesoderm (Halata *et al.,* 1990). Temperature receptors have been described in adult skin, but their development does not appear to have been described.

Downloaded from Vet-eBooks.com

Chapter 12
Endocrine Glands

The endocrine glands are the pituitary, thyroid, parathyroids, adrenals, pancreas and gonads. All become fully formed and functional, as endocrine glands, in the embryo. The question of when a particular endocrine organ begins to secrete has been approached in several ways. Traditionally, it was decided on morphological grounds; for example, the onset of activity of the thyroid gland was linked to the first appearance of colloid droplets. Recently this approach has been supplemented, or replaced by analyzing gene expression (Ellestad *et al.*, 2011), the genes investigated and the techniques used varying widely according to the investigators. The evidence of activity within an endocrine gland does not necessarily indicate full functioning, especially as this must be related to the ability of the target tissue to respond, though it has been suggested (De Groeff *et al.*, 2008) that many of the target tissues of the hypothalamic–pituitary axis become sensitive to their controlling factors even before the hypothalamic–pituitary system is fully functional.

General reviews and their physiological activity in birds are given by Höhn (1961), whilst certain aspects of endocrinological activity are covered by Scanes *et al.* (1987). Here we deal mainly with their morphological development.

THE PITUITARY GLAND

The pituitary (hypophysis) is formed partly from the **infundibulum** (*Plate 81*), a depression in the floor of the diencephalon, and partly from **Rathke's pouch** (*Plate 96*), an ectodermal invagination from the roof of the mouth. It is possible that the ventral diencephalon induces the formation of Rathke's pouch, and this supposition is supported by transplantation experiments (Gleiberman *et al.,* 1999). Rathke's pouch expresses *Sonic hedgehog* (Takagi *et al.*, 2008) and *Pitx2* and *Pitx6* (Sjödal *et al., 2008).* The infundibulum, which forms the neural or posterior lobe of the pituitary (the neurohypophysis) starts to appear at about stage 14, according to Jacobson *et al.* (1979), and during the following 2 days it increases and extends both anteriorly and posteriorly. Pearson *et al.* (2011) concluded that the chick infundibulum is formed from two separate cell populations in the floor plate of the prosencephalon at stage 9. The more anterior one subsequently expressed *Fgf3* but not *Fgf10*, whilst the posterior one expressed both. Further differences in gene expression and behavior emerged with further development.

Rathke's pouch, which is destined to become the anterior lobe of the hypophysis and the pars tuberalis, arises at about stage 17, and its anterior end fuses with the infundibulum. Its posterior end breaks away from the roof of the mouth at about 7 days of incubation. Birds differ from mammals in that they do not form a pars intermedia.

The term **adenohypophysis** is used for the pituitary lobes derived from Rathke's pouch. They are the pars distalis or larger lobe, and the pars tuberalis or smaller lobe, which is formed by two outgrowths from the pars distalis that fuse together. The pituitary is encapsulated by the dura mater.

The ectoderm which is destined to form Rathke's pouch is situated at stages 4–5 in the midline anterior to Hensen's node. With the formation of the head fold and head it becomes shifted so that by stage 14 it lies in the roof of the mouth, just anterior to the stomatodeal membrane. (For a detailed account see Jacobson *et al.,* 1979). Even as early as stage 20 (day 3 of incubation) distinct areas can be recognized histologically in Rathke's pouch that will give rise to the distinct regions of the pars distalis and pars tuberalis (Sasaki *et al.,* 2003). By 4.5 days the α-subunit mRNA of glycoprotein hormones can be found, and luteinizing hormone may be detected by immunoreactivity in the cephalic lobe by day 6 (Kameda *et al.,* 2000).

The Atlas of Chick Development. http://dx.doi.org/10.1016/B978-0-12-384951-9.00012-5
Copyright © 2014 Elsevier Ltd. All rights reserved.

Downloaded from Vet-eBooks.com

The pituitary growth hormone plays an essential role in post-hatching growth and development, but the pituitary itself does not begin to secrete it until about halfway through incubation, despite the fact that the growth rate of this organ is highest in the early embryo. It appears therefore that the early stages are independent of pituitary growth hormone, although there is accumulating evidence that immunoreactive growth hormone is present in many early embryonic tissues as early as day 3 of incubation, especially the neural tube, notochord, limb bud, somites, heart, stomach, liver and kidney. The problem is reviewed by Harvey *et al.* (2000), who conclude that the hormone acts locally at this time in a paracrine or autocrine fashion.

The pars distalis has appeared by day 5 (stage 26) at the tip of Rathke's pouch (Jacobson *et al.,* 1979). A capsule of connective tissue starts to form around the pars distalis at 13 days and has enveloped the whole pituitary by 16 days. The lumen of the pituitary is apparent at 6 days but has disappeared by 11 days. Investigations involving immunocytochemistry and immunoassays detected cells producing the following hormones: ACTH at 7 days, growth hormones at 12 days, prolactin at 6 days, LH and FSH at 4.5 days, thyrotropin at 6.5 days, and mesotropin and vasotocin at 8.5 days (Scanes *et al.,* 1987). For a recent account of the development of the main hypothalamic-pituitary hormones see Ellestad *et al.* (2011).

THE THYROID GLAND

The thyroid forms during days 2–3 from a median invagination from the floor of the pharynx into the underlying mesoderm at the level of the second pair of pharyngeal pouches (*Plate 99*). During day 3 it becomes a sac still open to the lumen of the pharynx, but on day 4 this connection is reduced to a solid stalk, the **thyroglossal duct** (*Plate 130*), and the organ itself becomes bilobed. According to Knospe *et al.* (1991) this is due to the enlarging oesophagus pressing the trachea on to the rudiment of the thyroid. During day 6, the thyroglossal duct degenerates and each lobe becomes further lobulated and extensively vascularized by vessels from the subclavian arteries (derivatives from the third aortic arches). The thyroid increases in size throughout this period from a length of 167 μm and a depth of 83 μm to a length of 209 μm and a depth of 250 μm by day 5 (Romanoff, 1960).

The thyroid consists entirely of an epithelium of endodermal origin until day 6, when it becomes invaded by mesenchyme. The epithelial cells now become arranged into cords, and sinusoids develop from the mesenchyme. By day 8 the organ measures about 0.4 mm and by day 12 a lumen has formed in each cord, which then dilates. The first appearance of colloid droplets is on day 7 (Hilfer, 1964), but it is not until about days 10–13 that the adenohypophysis–thyroid interactions become established (reviewed by Thommes, 1987; and see also McNabb, 2006; De Groef *et al.*, 2008). Before this, the function of the thyroid is apparently independent of the adenohypophysis, but after this it becomes dependent on it (Thommes, 1987). T4 and T3 have been found in the chick brain from as early as day 4 (Darras *et al.*, 2009. The growth of the embryo, as measured by body weight, skeletal size, muscle growth and growth of cartilages and bone, is greatly influenced by thyroid hormones in late embryonic development (King and May, 1984).

THE PARATHYROID GLANDS

The parathyroids are traditionally considered to be formed from the ventral parts of the third and fourth pharyngeal pouches (i.e. endoderm), as in mammals, though Merido-Velasco *et al.* (1996) concluded from chick–quail grafting experiments that parathyroid III is of ectodermal origin. The associated mesenchyme forms the stroma. The parathyroid rudiments are characterized by the expression of transcription factor Gcm2 (glial cell missing 2) (Gordon *et al.*, 2001), which begins in pharyngeal pouch 3 at 2.5 days (Okabe and Graham, 2004). Evidence that BMP4, produced by the mesenchyme, sustains Gcm2 expression in the presumptive parathyroid epithelium was shown in a range of experiments based on the exchange of chick and quail tissues by Neves *et al.* (2012). These authors demonstrated, moreover, that pharyngeal endoderm produces the first signal for parathyroid (and indeed thymic) development by recruiting the somatopleural mesenchyme to become glandular.

The parathyroids become innervated by branches of the vagus nerve (Egawa and Kameda, 1995). By 9.5 days the anterior lobe has become semicircular and contains epithelial cords separated by mesenchyme in which capillaries run. The parathyroids, which are supplied by branches of the carotid body artery (Kameda, 1990), become vascularized during the second half of incubation and have become fully differentiated by day 17 (Simkiss, 1967). It is thought that the parathyroid hormones are probably

Downloaded from Vet-eBooks.com

not necessary for calcium uptake during the greater part of embryonic life (Simkiss, 1991), as they are later on.

THE ADRENAL GLANDS

As in other amniotes the adrenal glands are formed from two sources, the cortex and the medulla. The adrenals of birds differ from those of mammals in that the cortex does not encapsulate the medulla but is intermingled with it, and in this respect resembles the adrenals of amphibians and reptiles.

The cells that will form the cortex (or inter-renal tissue) arise from the peritoneal epithelium of the urinogenital (nephric) ridge (see p. 67). During day 4 a groove becomes visible immediately posterior to the pronephric glomeruli, extending from about the level of the 17th to the 22nd somites. Cells that leave the epithelium of this groove proliferate rapidly and invade the underlying mesoderm. By the end of day 4 they have formed solid nodular structures lying between the mesonephros and the dorsal aorta, and are no longer attached to the peritoneal epithelium.

During the following days there is extensive proliferation, and by day 7 the cells have become arranged in cords. Each adrenal mass is in contact with the ventral side of the mesonephros. By day 8 the size of each adrenal mass, as seen in transverse sections, is approximately twice that of the dorsal aorta.

The adrenal medulla (or chromaffin tissues) is derived from cells of the sympathetic chain, which in turn have been formed from the neural crest. These cells migrate individually during days 4 and 5 from the sympathetic chain toward the mesentery and pass between the aorta and the cortical nodules. They then cluster around and penetrate into the cortical nodules. By day 7, the chromaffin cells have started to differentiate and become arranged in cords between the cortical cords. During the following 2 days the tissues continue to intermingle and by day 8 a meshwork of nerve fibres has formed. After day 9 development consists principally of further growth (*Plate 204* at day 11). By day 14 the adrenal function is under hypophyseal–pituitary control (De Groef *et al.*, 2008).

THE PANCREAS

The development of the pancreas has been described in Chapter 8. The endocrine cells are formed from the endoderm (Le Douarin, 1988). Insulin starts to be secreted by the β cells of the pancreas on day 4, but is not produced in large amounts until about day 12. Glucagon begins to be secreted from day 3 (see Freeman and Vince, 1974).

The insulin and glucagon islets are anatomically separate in birds, and production of the enzymes responsible for processing the prohormones occurs soon after the islet cells first appear (Rawdon, 1998; Rawdon and Larsson, 2000).

THE GONADS

The development of the gonads has been described in Chapter 7. Both female and male hormones are produced by the indifferent gonad. Oestrogenic hormones are secreted by the interstitial cells of the medulla from about day 4, whereas testosterone is produced by the cord cells. The pituitary–gonadal axis is established from about day 13 (see discussion by Freeman and Vince, 1974). Luteinizing hormone (LH) is present in the blood early in development, but does not reach a high enough level to stimulate steroidogenesis in the gonads until 13.5–14.5 days (Woods, 1987). Nevertheless, steroidogenic factor-1, which regulates steroidogenic enzyme expression, was detected by *in situ* hybridization in the undifferentiated genital ridge of both sexes as early as stage 21–22 (3.5 days). By stages 30–35 it had become higher in the ovaries than in the testes, and eventually was highest of all in the left (functional) ovary (Smith *et al.,* 1999). There was a reduced response in the right ovary as it regressed, and a comparable reduction was noted by Pedernera *et al.* (1999) in gonads treated with follicle-stimulating hormone (FSH). Both the left and right ovaries of 8-day embryos responded to FSH by secreting steroids, but in embryos older than 13 days the right ovary failed to respond.

GUT ENDOCRINE CELLS

There are many endocrine cell types in the gut that produce serotonin and a range of regulatory peptides. Most appear between 10 and 12 days of incubation and have been shown by chick–quail grafting experiments to be derived from the endoderm and not, as previously thought, from the neural crest. The gut mesenchyme plays a significant role in promoting their development. For a review of gut endocrine cells in birds, see Rawdon and Andrew (1999).

Downloaded from Vet-eBooks.com

Chapter 13

Extra-Embryonic Membranes

The embryo not only grows and differentiates, but undergoes those physiological processes that are necessary for life, some of which are possible only with the aid of the extra-embryonic membranes. These structures are continuous with the embryonic tissues, but are not part of the embryonic body proper and are discarded at hatching. They are the following:

- the **yolk sac,** which encloses the yolk and is so constructed that the partially digested yolk is passed into the embryonic blood stream;
- the **chorioallantois,** which has three functions, respiratory exchange, calcium transport and storage of nitrogenous wastes produced by the embryo;
- the **amnion,** which is a sac surrounding the embryo and which secretes fluid that cushions the embryo and prevents it from becoming dehydrated.

THE YOLK SAC

The yolk sac (*Plate 79*) is formed from the area opaca (see Chapter 3), which consists initially of a thin epithelial ectoderm underlain by a layer of tall endodermal cells containing many intracellular yolk droplets, these layers being continuous with the area pellucida upper and lower layers, respectively (*Text-Figure 9*). By about 12 h of incubation the periphery of the area opaca has become attached to the inner surface of the vitelline membrane (*Plate 2c*). At this stage the vitelline membrane is taut around the yolk and is used as a substratum by the peripheral cells of the area opaca migrating under it. The result is that the blastoderm itself is under tension, and if that tension is released, abnormal development follows (Bellairs *et al.,* 1967). Gil *et al.* (1992) devised a computer model to obtain measurements of the mechanical forces involved in the tension. The migration takes place all round the periphery of the area opaca, the so-called 'margin of overgrowth', so that the entire blastoderm gradually expands, the region showing the greatest increase in area being the area opaca. Mesoderm cells, which have ingressed through the primitive streak and migrated laterally, colonize the area opaca at about stage 5 (Kessel and Fabian, 1985). They are continuous with the lateral plate mesoderm of the embryo and are similarly arranged into somatic and splanchnic layers. Blood islands begin to form in the proximal part of the splanchnic mesoderm, and by about 48 h they have joined up to form a series of blood vessels that is in communication with the vascular system of the embryo. About this time it is usual to substitute the term yolk sac for that of area opaca. The vascularized region of the yolk sac is known as the **area vasculosa** and is to be distinguished from the distal part, which is known as the **area vitellina.** The two regions are clearly demarcated by a blood vessel at the periphery of the area vasculosa, the **sinus terminalis,** which also indicates the lateral extent of the splanchnic mesoderm (*Text-Figure 77*). It is likely that the mesoderm continues to invade the area vitellina. The vitelline membrane breaks down over the embryo during day 3 and its value as a substratum is lost. The edge cells of the yolk sac pass over the equator of the yolk between 5 and 7 days.

Before the area opaca has become vascularized, the embryo is nourished by intracellular yolk droplets. They are most conspicuous in the large yolky endoderm cells of the area opaca, but smaller ones are present in the ectoderm, mesoderm and endoderm cells of the embryo itself. The intracellular yolk drops in the embryo have become used up by about 48 h, the embryonic circulation has become established and the intracellular yolk of the area opaca has become available. By the time these new stores have become depleted, the yolk sac circulation has developed further and is so modified that the embryo

The Atlas of Chick Development. http://dx.doi.org/10.1016/B978-0-12-384951-9.00013-7
Copyright © 2014 Elsevier Ltd. All rights reserved.

Downloaded from Vet-eBooks.com

is able to tap the entire contents of the yolk sac. The development of the yolk sac circulation is considered in Chapter 6 and begins at about stage 9.

The extra-embryonic coelom (*Plate 79*), which is the space between the extraembryonic somatic and splanchnic lateral plate mesoderm, is continuous with the embryonic coelom for about 3 days, the communication being lost as the body folds (see Chapter 5). The blood islands form in the splanchnic mesoderm (see Chapter 6 and reviews by Sharp (2003) and Nagai and Sheng (2008)). Mesoderm cells surrounding them become arranged as vesicles which then fuse to form vessels (Kessel and Fabian, 1985). No mesoderm is present in the area vitellina. Meanwhile, the chorion (see below) begins to form from the somatopleure. The endodermal layer of the yolk sac undergoes extreme elaboration. By day 4 its inner surface consists of ridges and folds of endoderm which become highly vascularized and hang loosely into the yolk. The ridges become more and more elaborate as incubation proceeds. Digestive enzymes are secreted by the endoderm into the yolk and the partially digested material is then absorbed into the cells (Mobbs and McMillan, 1981; Lambson, 1970) and passes from there into the blood vessels and back to the embryo (see Chapter 6). There is evidence that glucose may be synthesised in the yolk sac, stored as glycogen and transferred to the embryo about the time of hatching (Yadgary and Uni, 2012).

The embryo becomes lifted above the yolk sac by the formation of the head, tail and lateral body folds (see Chapter 5), but remains connected to it by the yolk sac stalk, which becomes narrower and narrower during incubation. By day 19 most of the yolk has been absorbed and the remnants of the yolk sac and its contents (including albumen; see below) start to be drawn up into the body by contraction of the abdominal muscles and serve to nourish the hatchling during its first day. For a review of the nutrition of the developing embryo and hatchling, see Moran (2007). Day-old chicks may therefore be transported without needing to be fed.

THE AMNION AND CHORION

These two tissues are formed together. The first indication is a crescentic fold of ectoderm, together with its underlying somatic mesoderm, which starts to overlap the forebrain at about stage 12. The inner part of the fold will become the amnion, whilst the outer will form the chorion (*Text-Figure 28; Plates 83, 84*). The arms of the fold extend further and further posteriorly so that by stage 16 they have reached as far as somites 10–18 (see Normal Table, Appendix II). The growth of the lateral amniotic folds is characterized by increased cell proliferation (Miller *et al.*, 1994). As the lateral amniotic folds rise up (*Plate 59a*) they meet in the midline and fuse, the inner and outer layers becoming separated from each other (Overton, 1989). A similar crescentic fold begins to form immediately posterior to the tail bud at about stage 17, though there is great variation among embryos in the exact timing. This fold extends anteriorly. By about stage 18, the anterior, lateral and posterior regions of the amniotic fold have united above the region of the hind limbs, forming initially a small oval opening, the **amniotic umbilicus**. There is morphological and experimental evidence that the opening becomes closed mainly, perhaps entirely, by the contraction of actin cables in surrounding cells drawing the folds together in a 'purse-string' mechanism (Tipping and Wilson, 2011). After closure the inner and outer layers remain attached to one another at this point, the so-called **sero-amniotic connection,** though elsewhere the two membranes, amnion and chorion, are separate. By the end of day 3 the embryo is totally enclosed by the amnion (Sheng, 2010) (*Plate 59b*). The cells of the amnion now secrete fluid into the amniotic cavity around the embryo. During the last seven days of incubation the sero-amniotic connection breaks down and albumen passes into the amniotic cavity, mingling with amniotic fluid; this is swallowed by the embryo, absorbed into the small intestine, and so helps to increase the glycogen reserves in the body (Moran, 2007).

A characteristic of the amnion is that it lacks blood vessels. According to Pardenaud and Dieterlen-Lièvre (1993), this may be due to the fact that it has no contact with endoderm when it is forming, unlike the yolk sac and allantois, which are both vascularized. Another important feature of the amnion is that the muscular component is not innervated. Despite this, vigorous muscular contractions take place between days 5 and 9 (Müller *et al.,* 1983, Nechaeva and Turpaev, 2002), and these help to prevent adhesions of the amnion to the embryo until day 12, or between different parts of the embryo. After this period, the skin has undergone differentiation and the danger is lessened. The contractions have been found to last from 15 to 60 s with a frequency of about 11–18 per 10 min, depending on the temperature (Nechaeva and Turpaev, 2002).

THE CHORIOALLANTOIC MEMBRANE

The chorioallantoic membrane is formed by the fusion of the chorion (see above) and the allantois.

Downloaded from Vet-eBooks.com

The chorion, which consists of ectoderm underlain by splanchnic mesoderm, remains continuous at its lateral edges with the somatopleure covering the yolk sac, but elsewhere it becomes associated with the allantois. Additionally, from about day 7 the amnion fuses with that part of the chorion where the two tissues come into contact, forming the amnio-chorion (Sheng, 2010).

The allantois has begun to form from the hindgut by about stage 18 as an endodermal diverticulum with a covering of mesoderm (see Chapter 8). Although its speed of development varies between individuals, it has usually become a balloon-like structure outside the body by 4 days (*Text-Figure 30c, 89; Plate 106* at 6 days) and has begun to fuse with the inner layer of the chorion by about 6–7 days, forming the chorioallantoic membrane (also known as the allantochorion). When this has happened, the chorioallantoic membrane consists of three layers, **ectoderm** (from the chorion), **mesoderm** (fused somatic mesoderm from the chorion and splanchnic mesoderm from the allantois) and **endoderm** (from the allantois). The chorioallantoic membrane has a rich vascular system that develops within the mesodermal layer and is served by paired allantoic (umbilical) arteries and paired allantoic (umbilical) veins (*Plates 153, 154*) (see Chapter 6). The pattern of the blood vessels in the allantois and chorioallantois is the subject of many studies (e.g. DeFouw *et al.,* 1989).

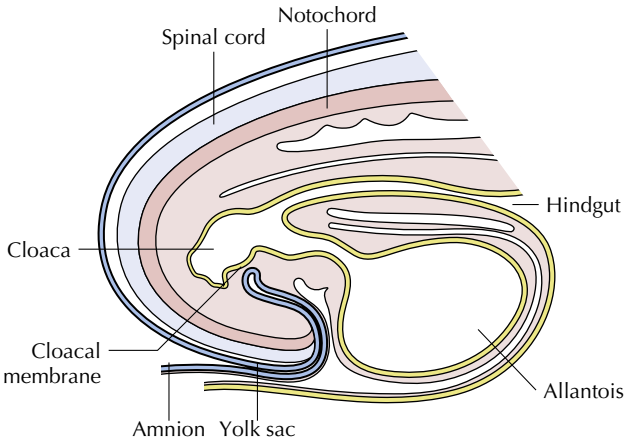

Text-Figure 89. *Diagram of a sagittal section through the posterior end of a chick embryo at stage 23 showing the allantois.*

The network is extended and elaborated by continual intussusceptive growth. Djonov *et al.* (2000), using methyl methacryalate casting (*Plate 44*), found the intussusceptive growth was also significant in the formation of vascular trees, especially between days 10 and 11. It is, perhaps, not surprising that the allantois has been found to be a site capable of producing both haemopoietic and endothelial cells (Caprioli *et al.,* 2001). By 16 days the chorioallantoic membrane has become so large that it covers most of the yolk sac and adheres to it in places, although the two circulations remain separate (Romanoff, 1960).

The chorioallantoic membrane becomes closely pressed against the shell membranes, which, together with its extensive system of blood vessels, enables it to act as a gas-exchange organ (Freeman and Vince, 1974; Paganelli, 1991), receiving oxygen and eliminating carbon dioxide through the pores in the shell. Reizis *et al.* (2005) found that the density of the blood vessels was greater beneath the pores in the shell than beneath the non-pore regions. This proximity has the additional benefit of enabling calcium ions to be absorbed from the shell and transported in the blood stream to the embryo. During the first 10 days, the embryo obtains its calcium from the yolk sac, but the requirements are greatly increased during the last 11 days as the bones begin to ossify, and calcium is then obtained mainly from the shell. The physiology of calcium mobilization has been studied extensively, using culture methods that eliminate the shell and so provide for calcium deficiency (Tuan *et al.,* 1991).

The third role of the chorioallantoic membrane is to store the excretory products. The mesonephros begins to excrete into the allantois during day 4, mainly as urea, ammonia and uric acid (Fisher and Eakin, 1957; Freeman and Vince, 1974). At hatching, the chorioallantoic membrane is left attached to the inside of the discarded shell.

Downloaded from Vet-eBooks.com

Photographic Plates

All staging of embryos, unless stated otherwise, is according to the table of Hamburger and Hamilton (see Appendix II). Pre-laying stages are indicated according to the table of Eyal-Giladi and Kochav (Appendix I). Magnifications are shown as bars for most of the scanning electron micrographs, and as direct magnifications for sectioned material. The latter are accompanied by thumbnail diagrams with magnification bars in the legends to show the appearance and approximate size of the embryo at each given stage, along with the orientation of the histological sections.

Downloaded from Vet-eBooks.com

Plate 1 Oocytes and sperm

(a) Light micrograph of an oocyte at the Balbiani stage with the nucleus lying centrally. Diameter of oocyte = 10 μm.

(b) Light micrograph of an oocyte at a later stage in which the cytoplasm has become vacuolated prior to yolk deposition. The Balbiani body has disappeared and its components lie at the periphery. The nucleus has shifted to one side, the future animal (dorsal) pole. Diameter of oocyte = 2 mm.

(c) Scanning electron micrograph of sperm from a domestic fowl. Note the small diameter (10 μm) of the head of each sperm.

1. nucleus
2. Balbiani body
3. follicle cells

(b) Reprinted from Bellairs (1967), with permission of the Company of Biologists Ltd.

(c) Kindly supplied by M. Bakst.

Downloaded from Vet-eBooks.com

Plate 1

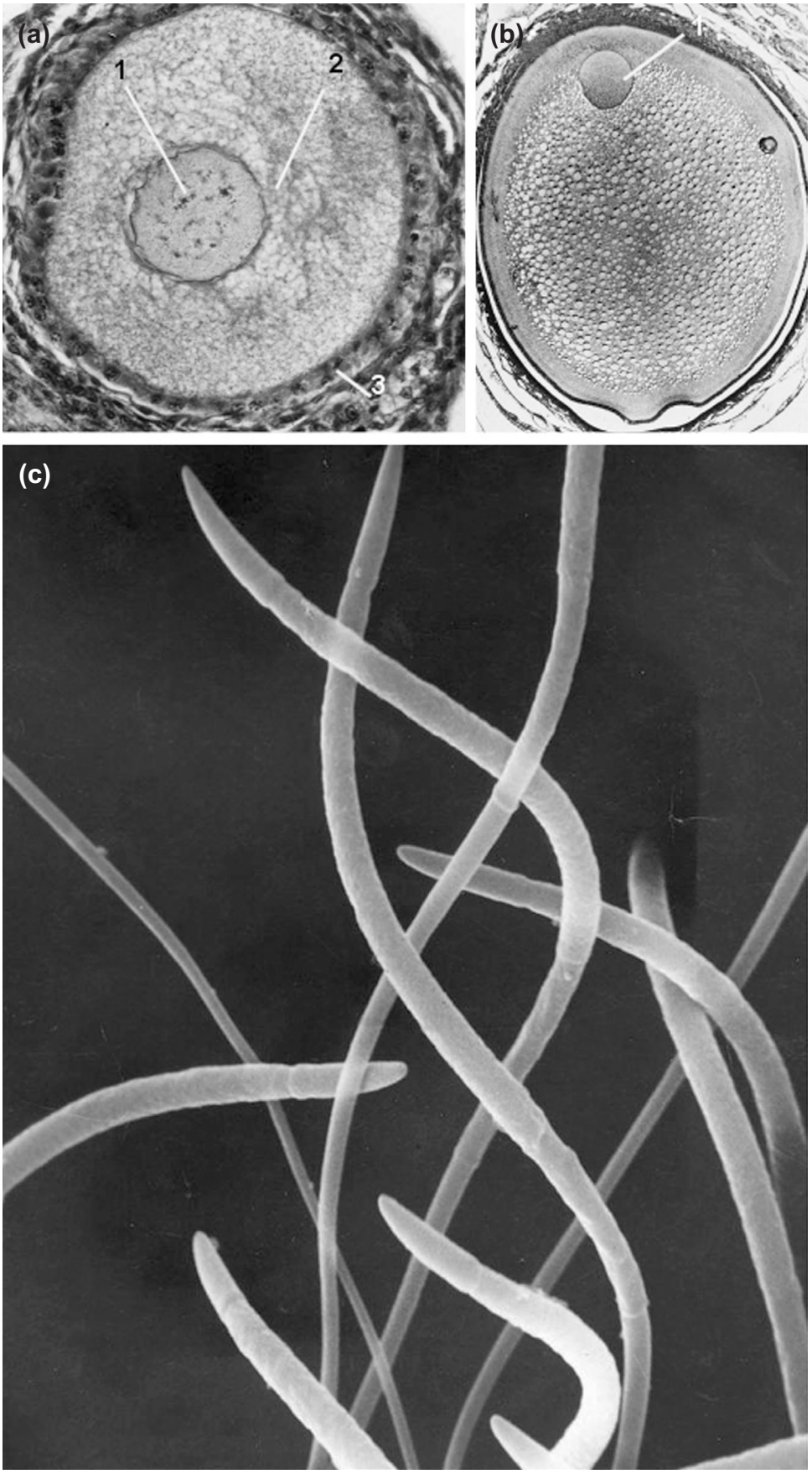

Downloaded from Vet-eBooks.com

Plate 2 Shell, shell membranes and vitelline membrane

(a) Scanning electron micrograph of the outer shell membrane from an egg incubated for 18 days: × 3000.

(b) Scanning electron micrograph of the inner surface of a shell from an egg incubated for 18 days. The mammillary knobs have been eroded away as the calcium has been removed during incubation: × 2000.

(c) Transmission electron micrograph through the edge of the area opaca of a stage 4 embryo. The leading cell process is firmly attached to the inner surface of the vitelline membrane (top of picture): × 60,000.

(a) Reprinted from Bellairs and Boyde (1969), with permission of Springer-Verlag.

Downloaded from Vet-eBooks.com

Plate 2

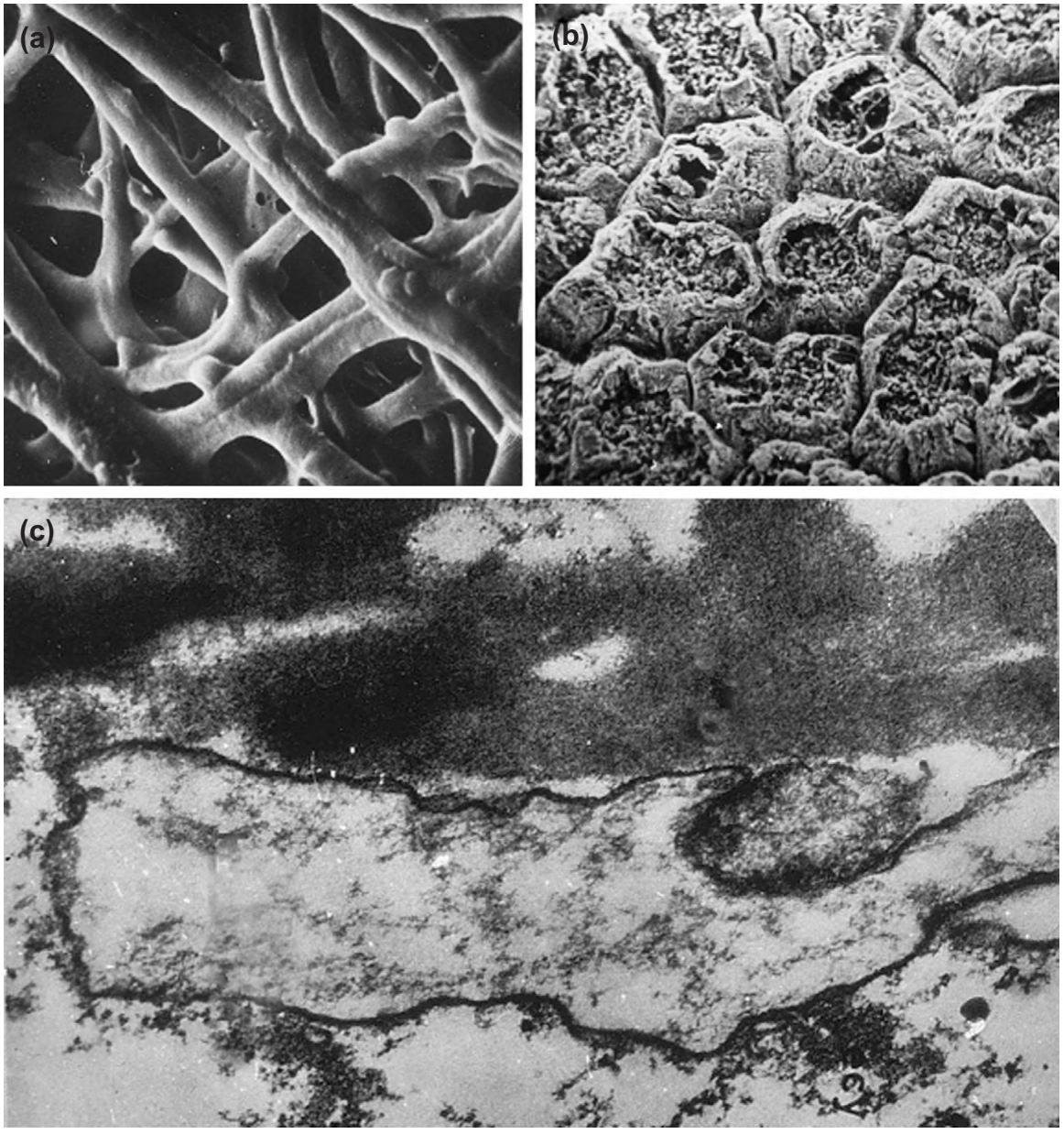

Downloaded from Vet-eBooks.com

Plate 3 Light micrographs of whole-mounted twin embryos

(a) Naturally-occurring *duplicitas anterior*. This anomaly appears to have developed from a single primitive streak that split into two at its anterior end, so that two Hensen's nodes were formed. As they regressed they were brought into contact by the gastrulation movements. Bar = 1 mm.

(b) Experimentally produced *duplicitas posterior*, formed by bisecting a pre-primitive streak stage quail blastoderm. Two primitive streaks developed and their anterior ends collided, as in (c). Bar = 2 mm.

(c) Naturally occurring *duplicitas posterior*. This appears to have resulted from two primitive streaks having developed in the same blastoderm. The head processes probably collided at about stage 5. Regression of Hensen's node appears to have taken place normally since two segmented trunks have formed. Bar = 3 mm.

Downloaded from Vet-eBooks.com

Plate 3

Downloaded from Vet-eBooks.com

Plate 4 Extra-embryonic blood vessels

Hen's egg incubated for 58 h and opened to show embryo at stage 16 together with the omphalo-mesenteric (vitelline) vessels spreading out over the yolk.

1. heart
2. anterior omphalo-mesenteric vein
3. right omphalo-mesenteric artery
4. posterior omphalo-mesenteric vein
5. left omphalo-mesenteric artery
6. fragments of shell membrane attached to inner surface of shell

Downloaded from Vet-eBooks.com

Plate 4

Downloaded from Vet-eBooks.com

Plate 5 Light micrographs showing Cleavage

(a) Vertical section through a 12 cell embryo (stage I – II, Appendix I), taken from the oviduct, showing open cells: × 210.

(b) Cleavage furrows and open cells: × 400.

1. cleavage furrows
2. junction of open cell and periblast
3. mitotic spindle
4. cytoplasm
5. vitelline membrane
6. subgerminal cavity
7. periblast

Reprinted from Bellairs *et al.* (1978), with permission of the Company of Biologists Ltd.

Downloaded from Vet-eBooks.com

Plate 5

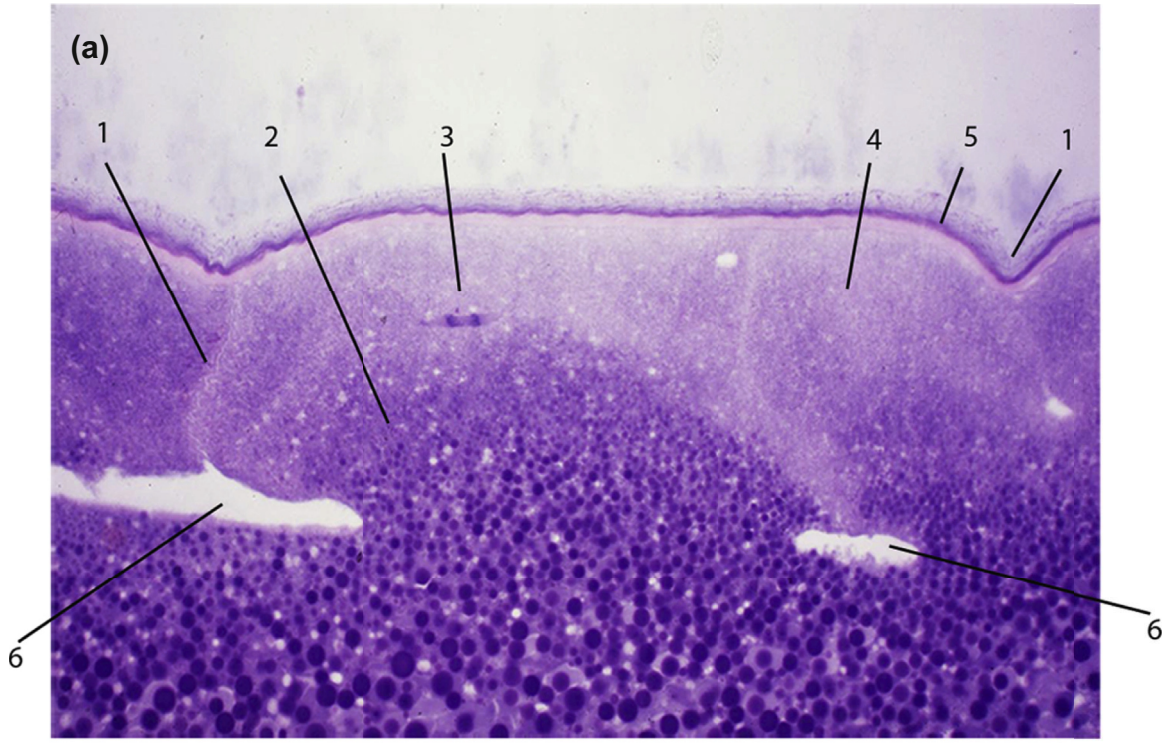

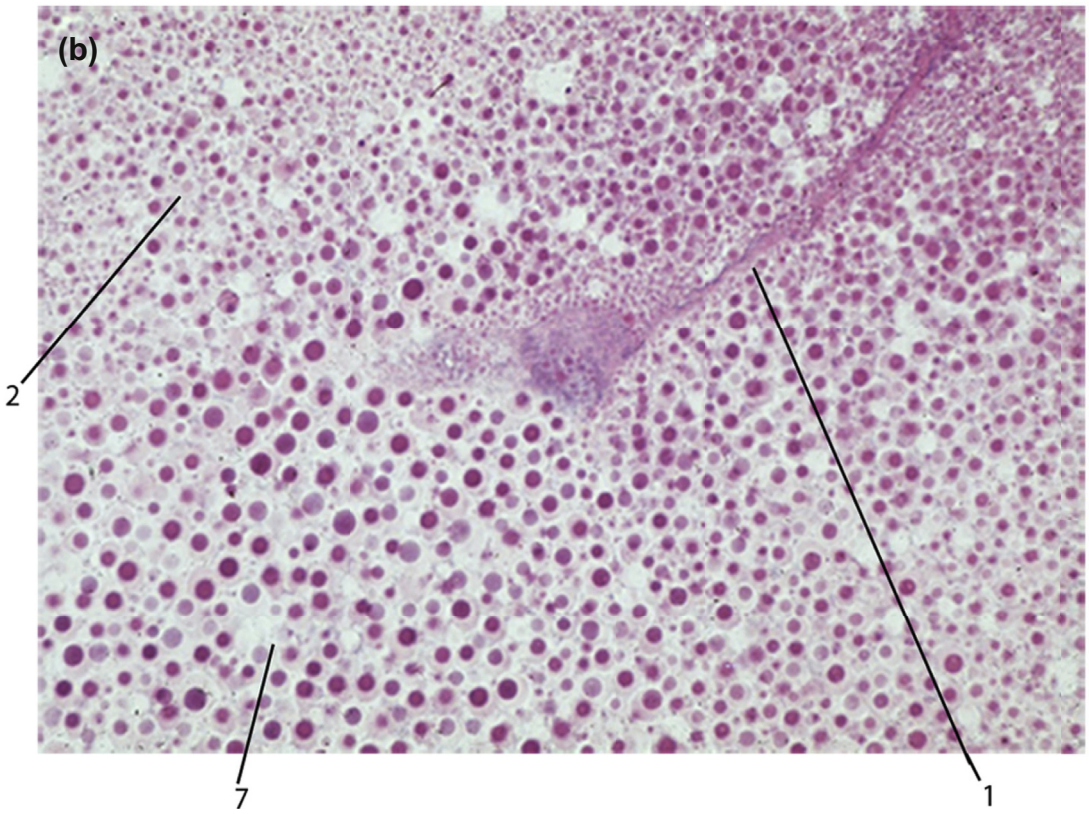

Downloaded from Vet-eBooks.com

Plate 6 Subgerminal layer

(a) Vertical section through a stage X embryo (see Appendix I), after laying but just before incubation: × 80.

(b) Enlargement of region shown in (a): × 250.

1. subgerminal cavity
2. upper cell layer
3. vitelline membrane
4. nucleus of Pander (white yolk)
5. endophyll cell of lower layer

Reprinted from Bellairs *et al.* (1978), with permission of the Company of Biologists Ltd.

Downloaded from Vet-eBooks.com

Plate 6

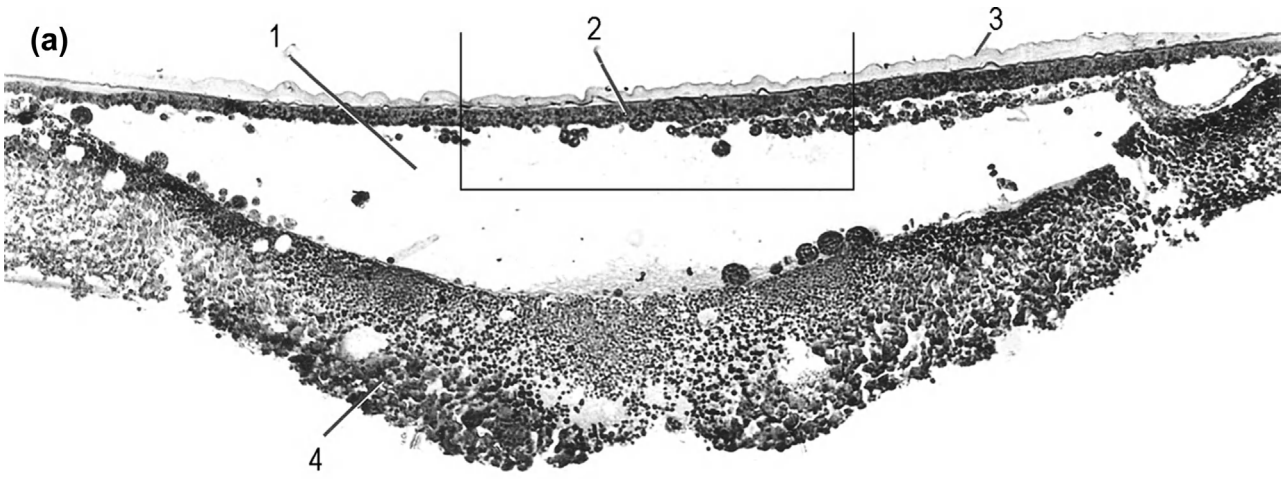

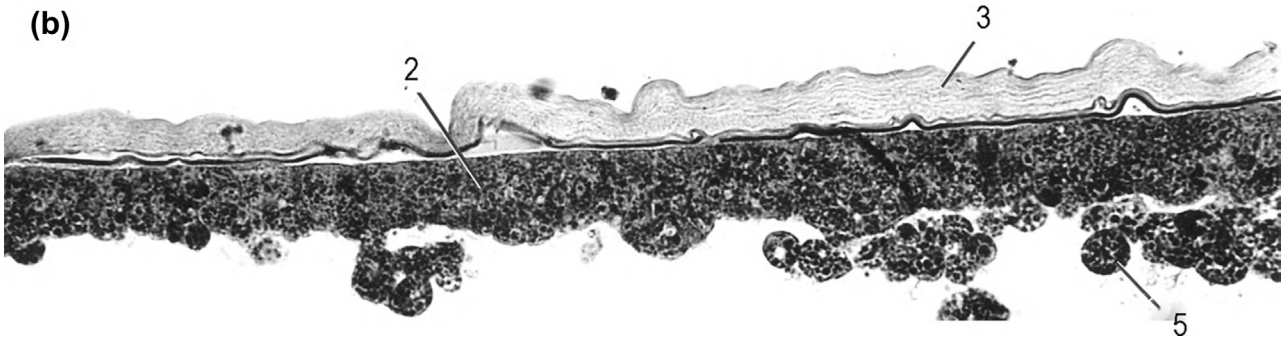

Downloaded from Vet-eBooks.com

Plate 7 Dorsal side of early embryos

Scanning electron micrographs of the dorsal surface of the epiblast. This upper layer is covered with microvilli, the pattern and distribution of which vary according to the region.

(a) Epiblast cells at the lateral side of the area pellucida of an unincubated embryo (stage XII: see Appendix I). Small globular microvilli and crypts between the cells are frequent. Bar = 100 µm.

The remaining images (b-e) are all taken from a single embryo at stage 5 (about 20 hours of incubation).

(b) Lateral to Hensen's node. Bar = 5 µm.

(c) Lateral to the primitive streak, about half way along its length. Bar = 5 µm.

(d) Posterior end of the area pellucida, especially rich in microvilli. Bar = 5 µm.

(e) Telophase bridge. Bar = 2.5 µm.

Downloaded from Vet-eBooks.com

Plate 7

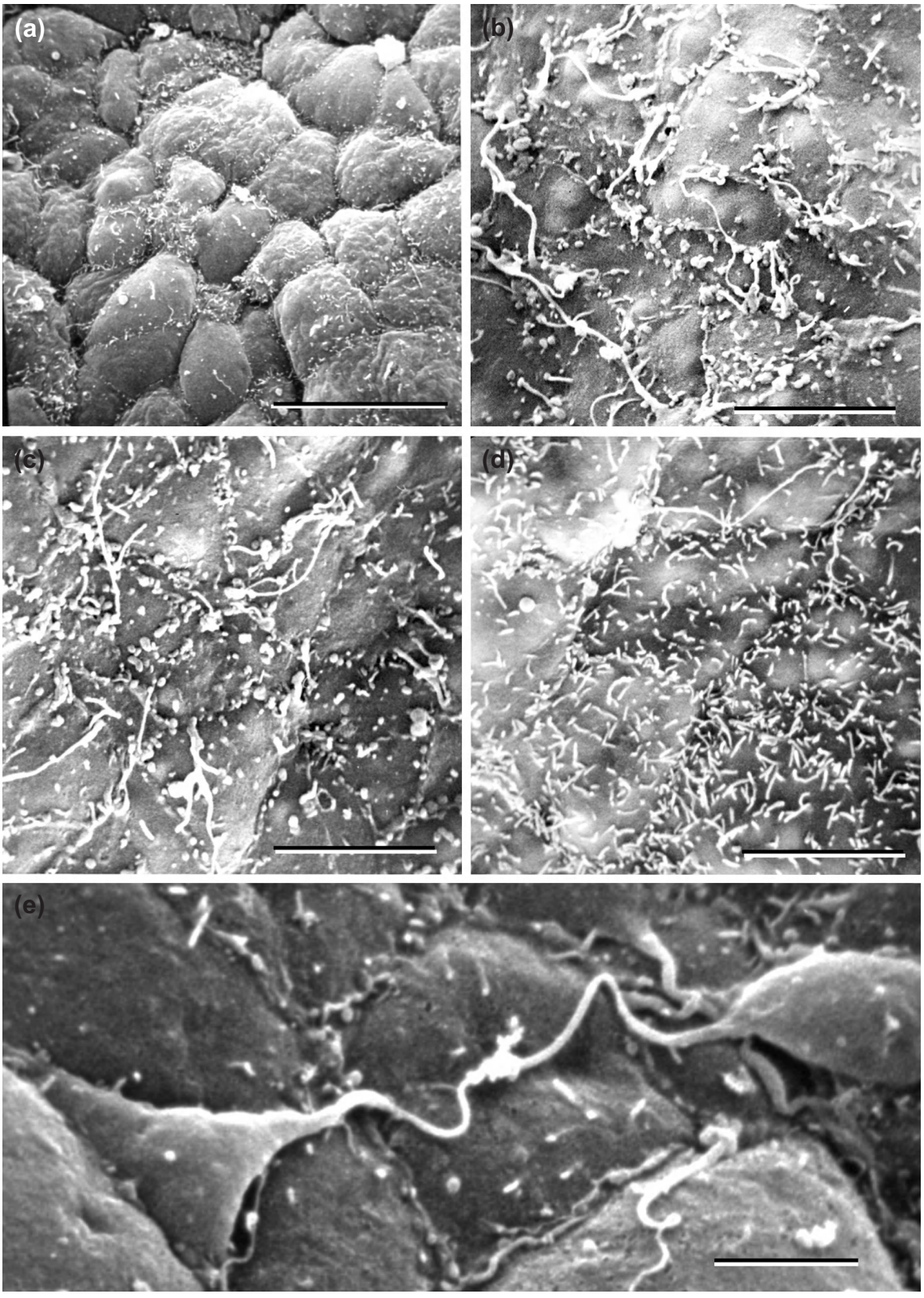

Downloaded from Vet-eBooks.com

Plate 8 Dorsal side: primitive streak and neural folds

Scanning electron micrographs of early embryos from the dorsal side.

(a) Stage XII (see Appendix I). This embryo was incubated for about 6 hours. The region of Koller's sickle is not visible. The rolled back edge of the area opaca shows the yolky cells of the ventral side. The fold in the centre is artifactual. Bar = 600 μm.

(b) Stage 5. This embryo was incubated for about 20 hours and regression had started at the time of fixation. The area pellucida is now pear-shaped and bisected by the primitive streak. The area opaca is not shown. Bar = 350 μm.

(c) Stage 8. This embryo was incubated for about 26 hours. The neural folds have almost met in the midbrain region and appear to have begun to fuse. The headfold extends beneath the forebrain. Bar = 300 μm.

(d) Stage 8. This embryo was incubated for about 30 hours and the undercutting of the head by the head fold has become more pronounced. The neural folds have now met and fused over a longer distance than in (c) but the brain remains slightly open at the anterior neuropore. Bar = 110 μm.

1. endodermal side of the area opaca
2. dorsal side of the area pellucida
3. border between area opaca and area pellucida
4. head process
5. Hensen's node
6. primitive streak
7. head fold
8. anterior neuropore
9. neural fold
10. neural folds at region of first fusion
11. unfused neural folds
12. fused neural folds

(b) Reprinted from Bancroft and Bellairs (1974) with permission of Springer-Verlag.

(c) Reprinted from Bancroft and Bellairs (1975) with permission of Springer-Verlag.

Downloaded from Vet-eBooks.com

Plate 8

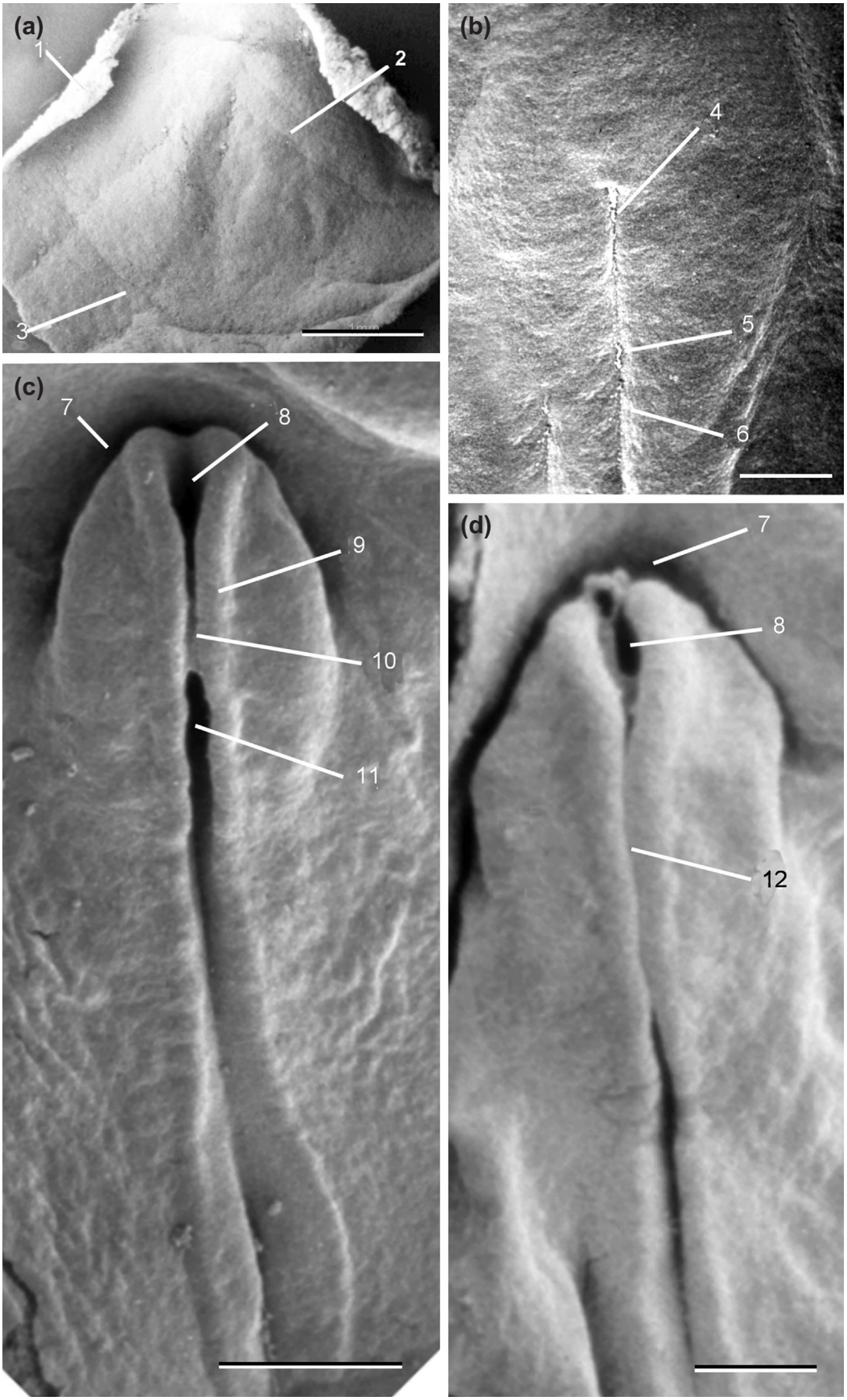

Downloaded from Vet-eBooks.com

Plate 9 Primitive streak

(a) Whole-mount dorsal view of a full length primitive streak at stage 4- (× 35). Note: this is a stage between stages 3+ and 4 of Hamilton and Hamburger (see Appendix II) and is reached after about 18 hours of incubation.

(b) Transverse section through the primitive streak of a stage 4- embryo (× 145).

1. germinal crescent
2. Hensen's node
3. primitive pit in Hensen's node
4. primitive fold
5. primitive groove
6. area opaca
7. area pellucida
8. limit of migration of mesoderm
9. ectoderm
10. endoderm
11. mesoderm

Downloaded from Vet-eBooks.com

Plate 9

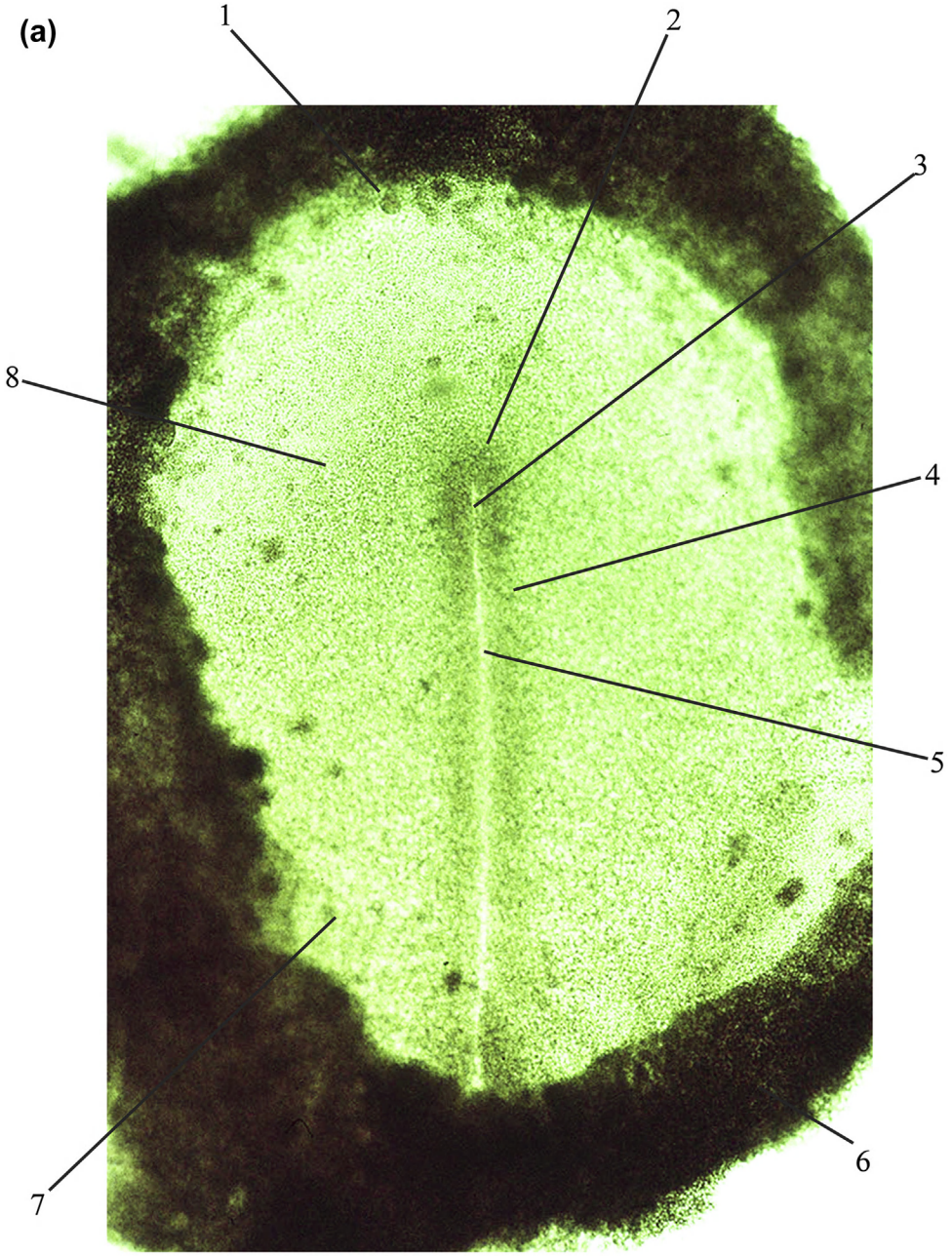

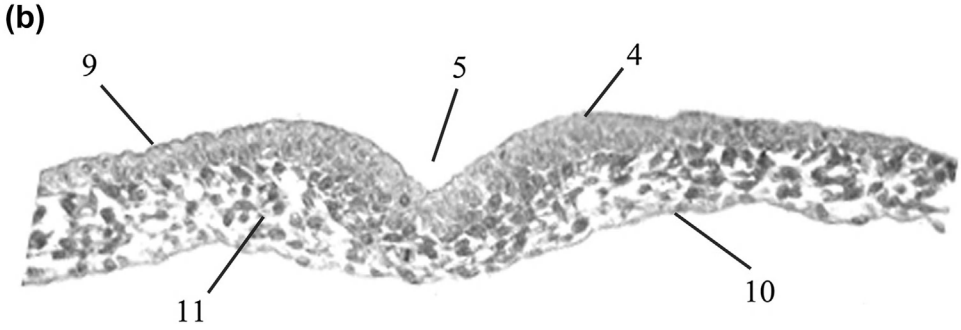

Downloaded from Vet-eBooks.com

Plate 10 Primitive streak sections: medial and lateral

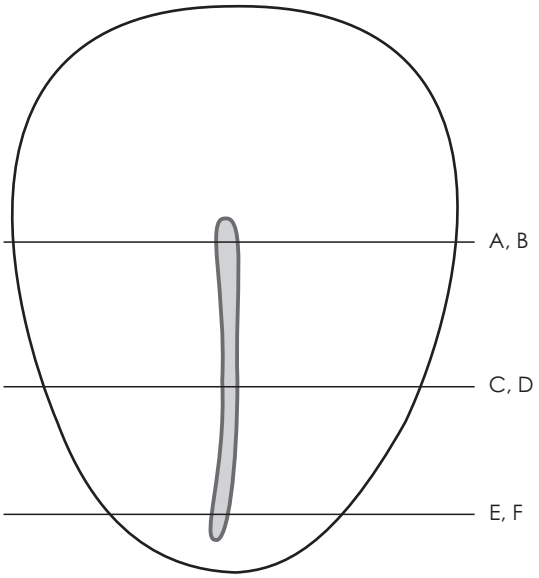

A full length primitive streak stage (4-) embryo before the head process has begun to form. Light micrographs of 4 μm frozen sections stained with toluidine blue.

(a), (c) and (e) are through the primitive streak at approximate levels shown.

(b), (d) and (f) are through regions lateral to the primitive streak.

(a-e) × 225. (f) × 290.

1. primitive fold
2. primitive groove
3. ectoderm
4. mesoderm
5. endoderm
6. mesoderm cells in primitive streak

Downloaded from Vet-eBooks.com

Plate 10

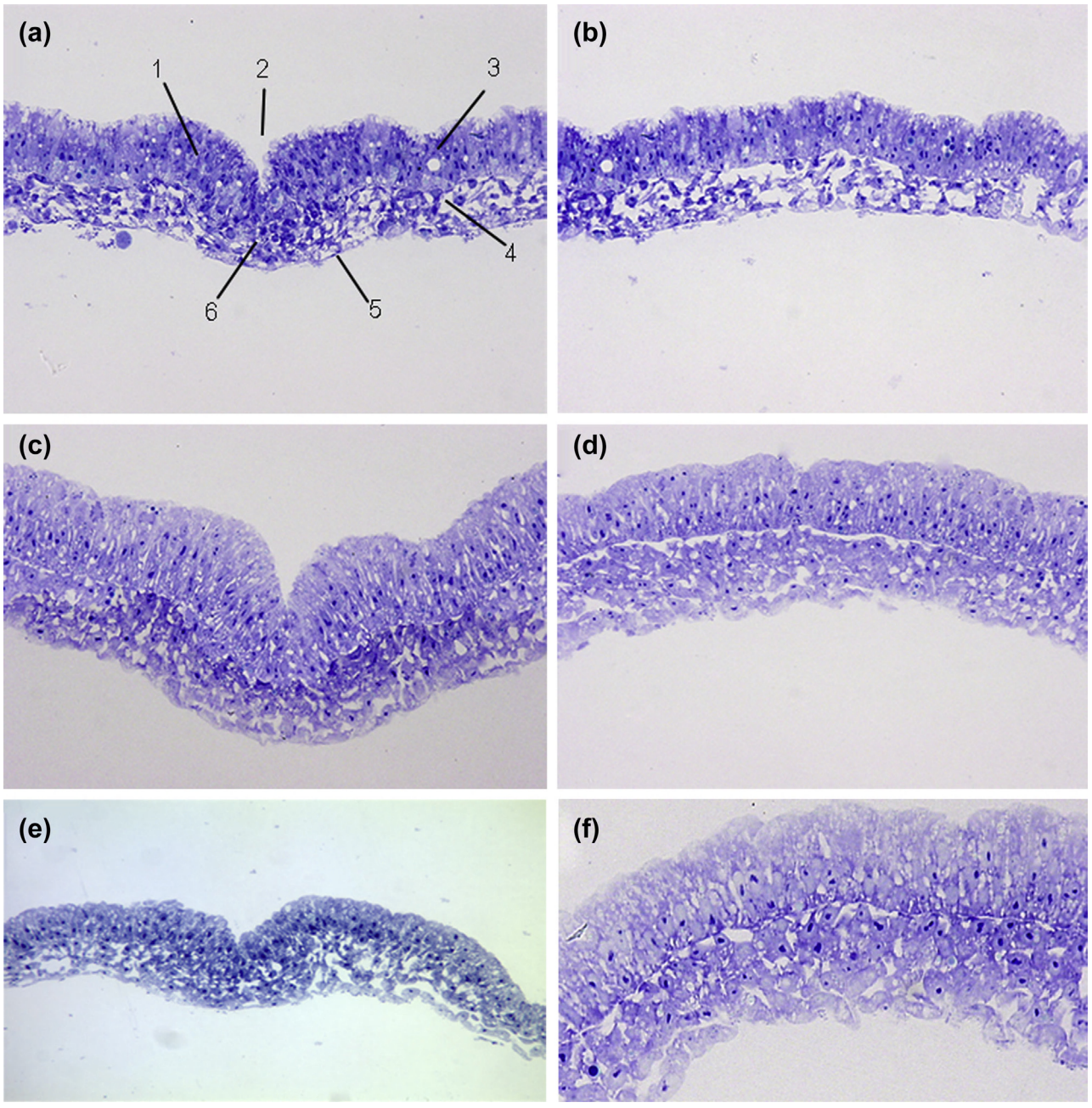

Downloaded from Vet-eBooks.com

Plate 11 Scanning electron micrographs of the primitive streak

(a) Anterior end of the primitive streak (Hensen's node) of a stage 3+/4- embryo at 16 hours of incubation. Bar = 500 μm.

(b) Detail of the primitive streak (running from bottom left to top right) of a stage 4- embryo at 18 hours of incubation. Bar = 40 μm.

(c) Transverse section through the primitive streak of a stage 4- embryo. Bar = 20 μm.

(d) Enlargement of part of (c) above. Bar = 10 μm.

(e) Transverse section lateral to the primitive streak of a stage 4- embryo. Bar = 15 μm.

1. primitive fold
2. primitive groove
3. mesoderm cells emerging from the primitive streak
4. cellular debris in primitive groove
5. bottle-shaped cell in primitive streak
6. endoderm
7. mesoderm cell
8. ectoderm

Downloaded from Vet-eBooks.com

Plate 11

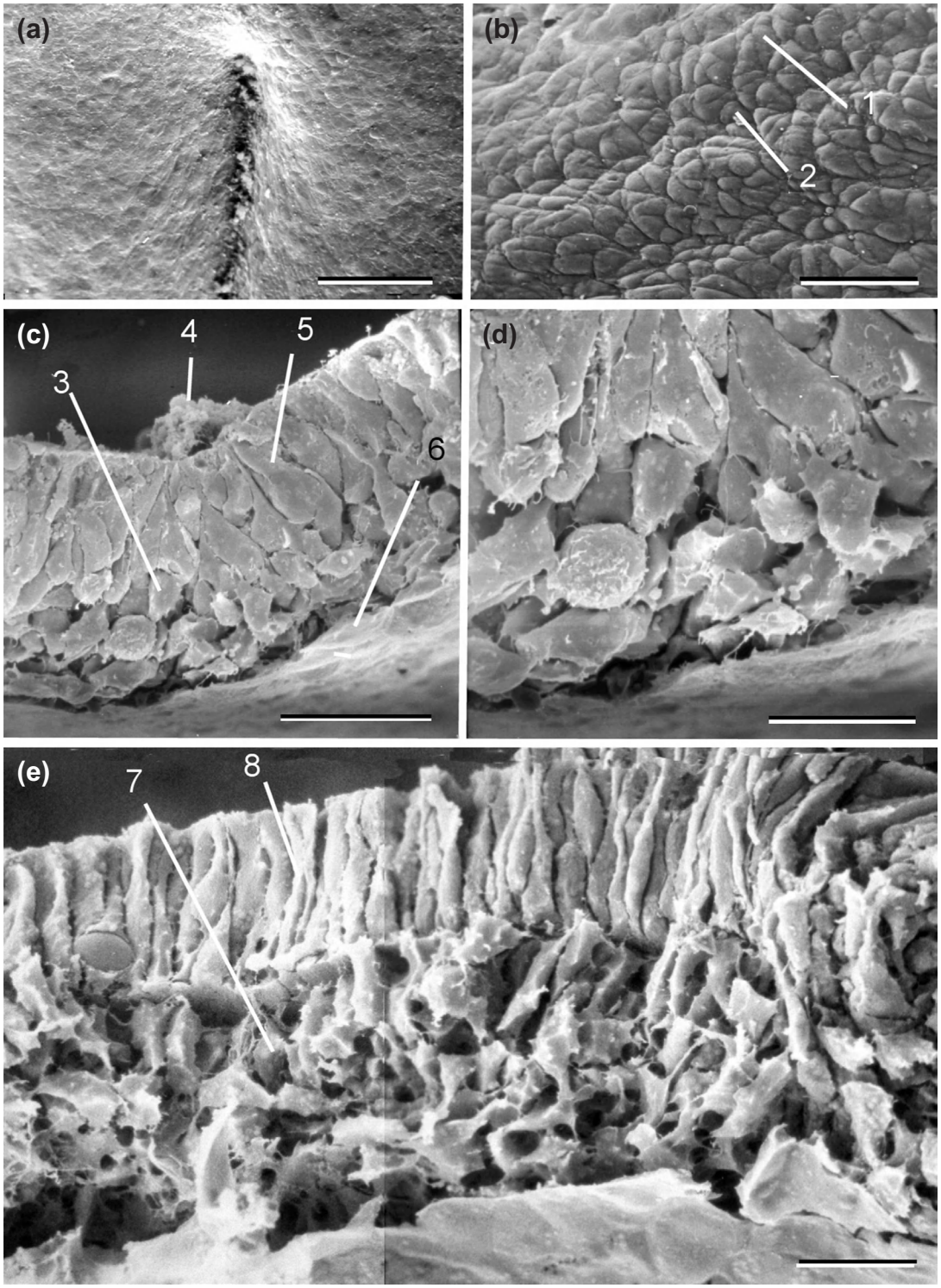

Downloaded from Vet-eBooks.com

Plate 12 Stage 4 (19–20 h) transverse sections (TS)

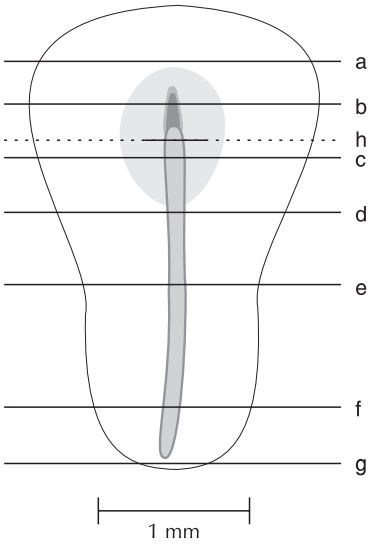

Light micrographs of sections through the primitive streak, from anterior to posterior, at approximately 19–20 hours of incubation.

(a) × 35

(b) – (g) × 150

(h) Enlargement through Hensen's node × 400

1. amnio-cardiac vesicle
2. ectoderm
3. endoderm
4. head process
5. primitive folds
6. primitive groove
7. primitive streak mesoderm
8. mesoderm

Downloaded from Vet-eBooks.com

Plate 12

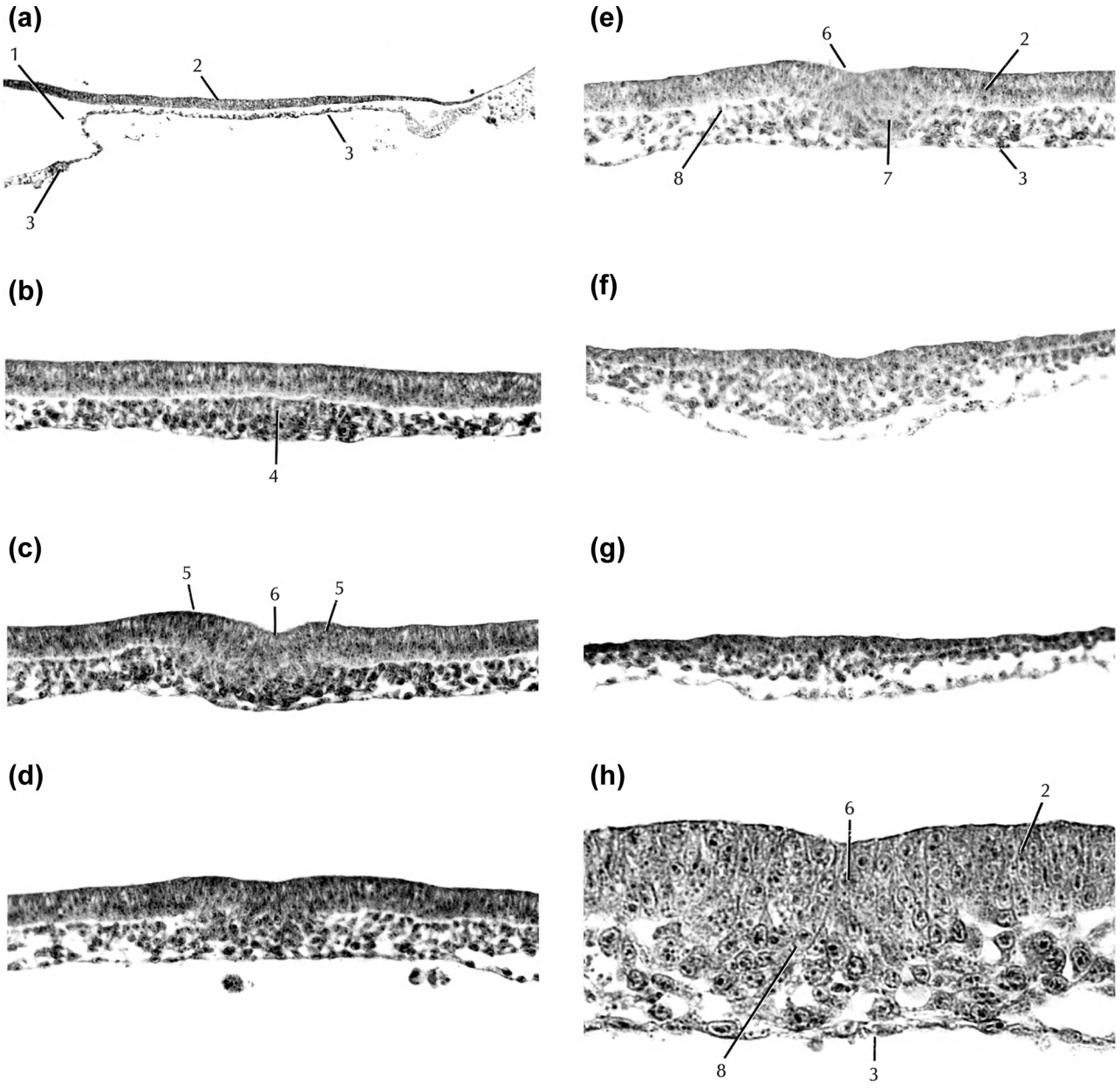

Downloaded from Vet-eBooks.com

Plate 13 Stage 5 (20–22 h)

Dorsal view of a whole-mounted embryo after 20–22 hours of incubation (× 45).

1. head process
2. anterior limit of head process mesoderm
3. germinal crescent
4. proamnion
5. Hensen's node (primitive node)
6. primitive streak
7. area opaca
8. area pellucida
9. presumptive cardiac mesoderm

Downloaded from Vet-eBooks.com

Plate 13

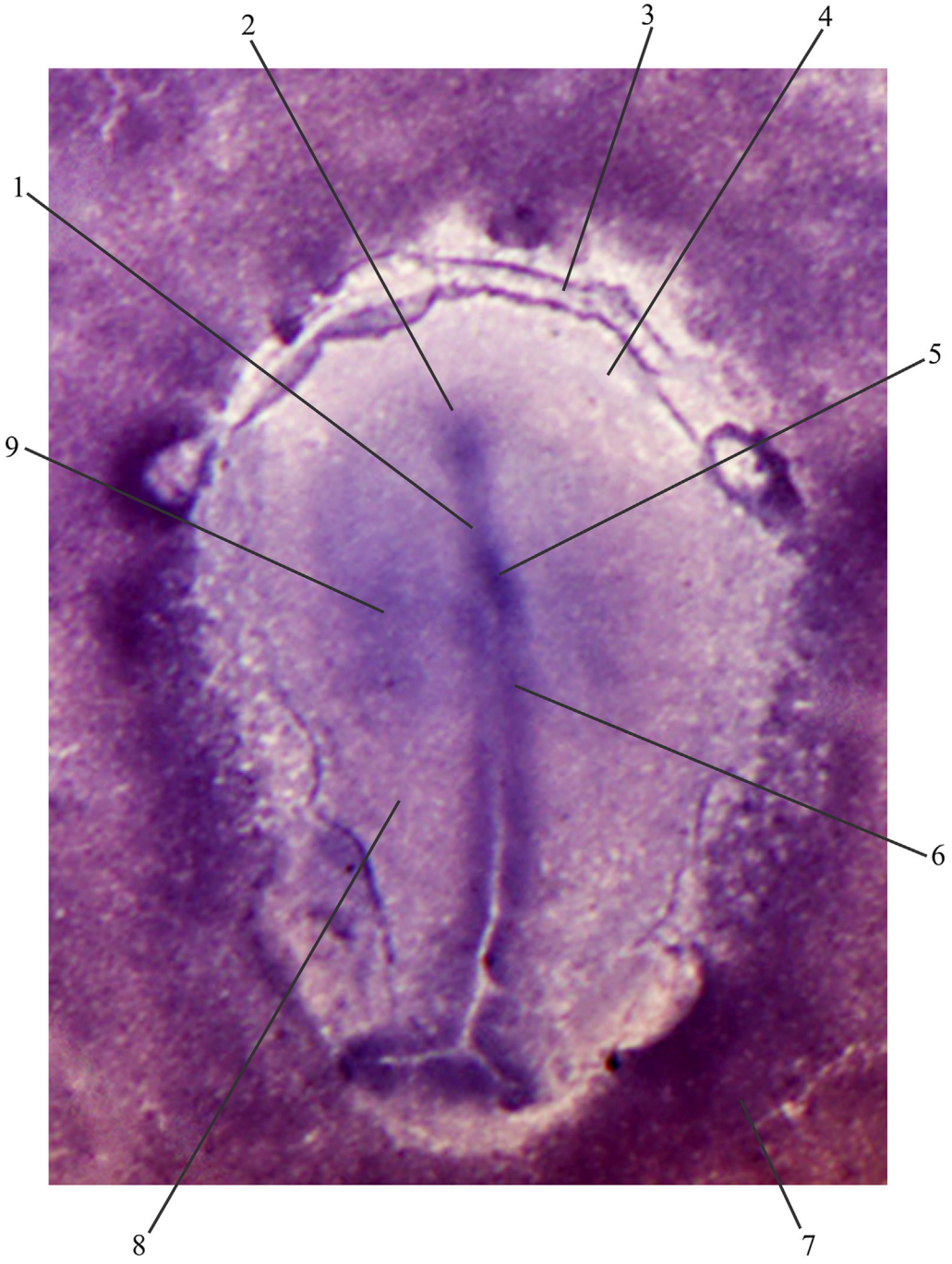

Downloaded from Vet-eBooks.com

Plate 14 Stage 6 (23–25 h)

Dorsal view of a whole-mounted embryo at stage 5+/6 after about 24 hours incubation (× 40).

1. head process
2. first sign of head fold
3. germinal crescent
4. proamnion
5. Hensen's node (primitive node)
6. primitive streak
7. primitive fold
8. area opaca
9. primitive groove
10. area pellucida
11. right presumptive cardiac area

Downloaded from Vet-eBooks.com

Plate 14

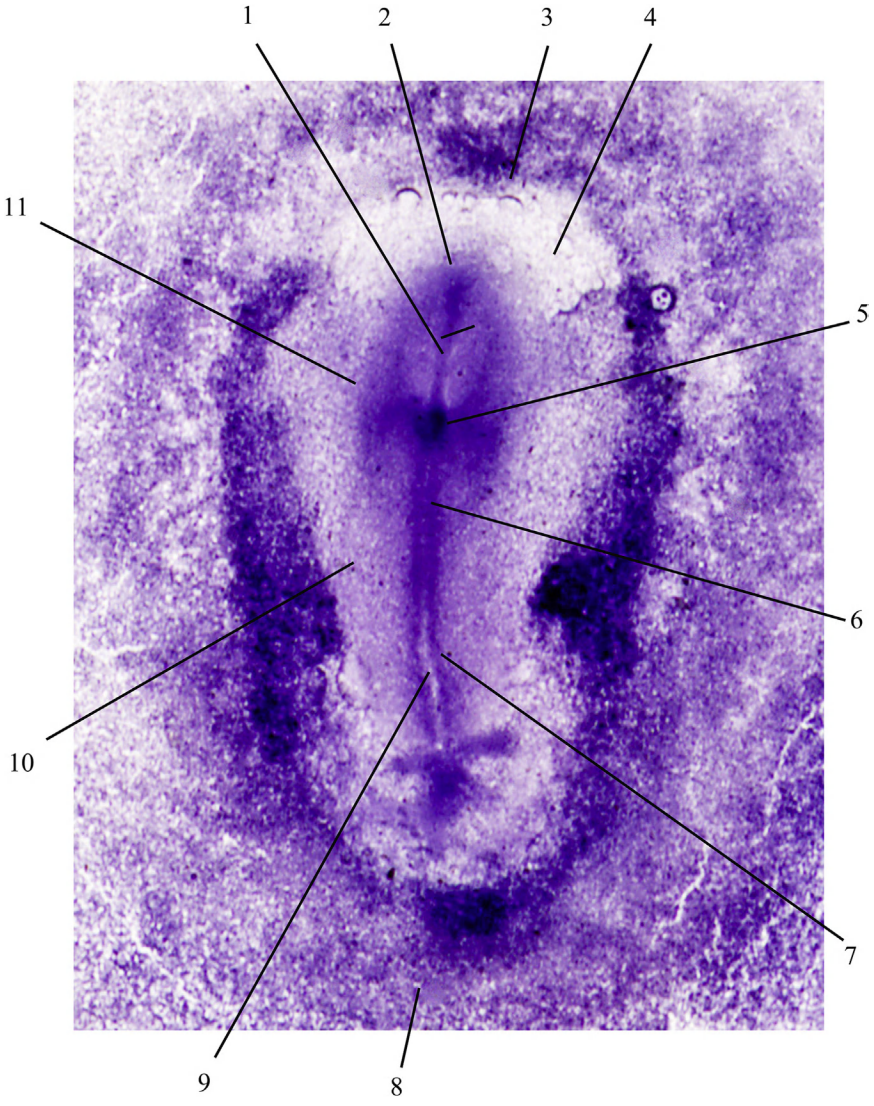

Downloaded from Vet-eBooks.com

Plate 15 Head region

Scanning electron micrographs showing dorsal views of the head region.

(a) and (b) Embryos at stage 6 (about 24 hours incubation). The head fold has begun to develop and the anterior end of the head process and the neural folds are now visible. Hensen's node has retreated some distance along the primitive streak. No somites have yet formed. In (a) the ectoderm has been dissected from the regions lateral to the neural folds. Bar in (a) = 300 μm. Bar in (b) = 500 μm.

(c) An enlargement of Hensen's node shown from the lower right corner of (a). Bar = 110 μm.

(d) Stage 13+ (about 50 hours incubation). The ectoderm has been dissected from the anterior end of the trunk (posterior end not shown) revealing 6 pairs of somites. The head has turned to the right and is partially submerged. Bar = 200 μm.

1. head fold
2. head process
3. Hensen's node
4. otic pit (see also *plate 26*)
5. somites

Downloaded from Vet-eBooks.com

Plate 15

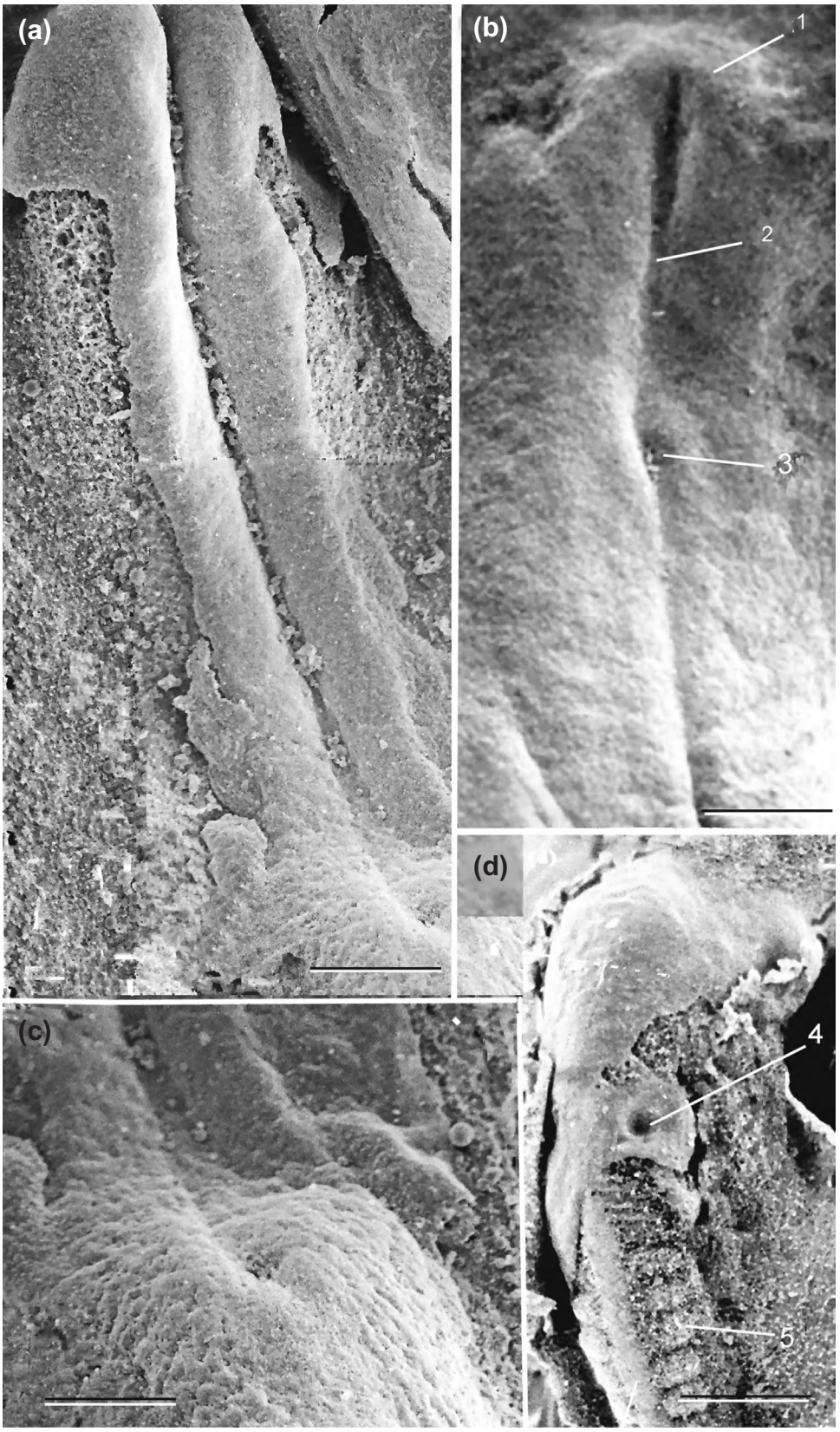

Downloaded from Vet-eBooks.com

Plate 16 Body flexures and area opaca

Scanning electron micrographs showing body flexures and area opaca at different stages.

(a) Stage 18 (about 68 h incubation). The embryo lies on its left side on top of the yolk and has undergone both cranial and cervical flexure. The amnion has been largely dissected from the embryo but remnants are visible. Bar = 1 mm.

(b) Stage 27–28 (5.5 days incubation). The right wing bud is seen from the ventro-lateral aspect showing the interdigital grooves. Bar = 250 μm.

(c) Area opaca from a stage 7 embryo (24 h). The specimen has been broken across the tissue to show the large yolky cells, the dorsal (ectodermal) surface being in the upper left of the image. Bar = 150 μm.

(d) Stage 27–28 (5.5 days). Hind limb buds and tail of specimen shown in (b). Interdigital grooves are visible. The distal edge of the right leg bud has been dissected to show the underlying mesoderm. Bar = 250 μm.

1. atrium
2. ventricle
3. myelencephalon
4. hyoid arch
5. metencephalon
6. mesencephalon
7. eye
8. nasal pit
9. remnant of amnion
10. right leg bud
11. tail bud
12. right wing bud
13. somites
14. right elbow
15. interdigital groove
16. right knee

Downloaded from Vet-eBooks.com

Plate 16

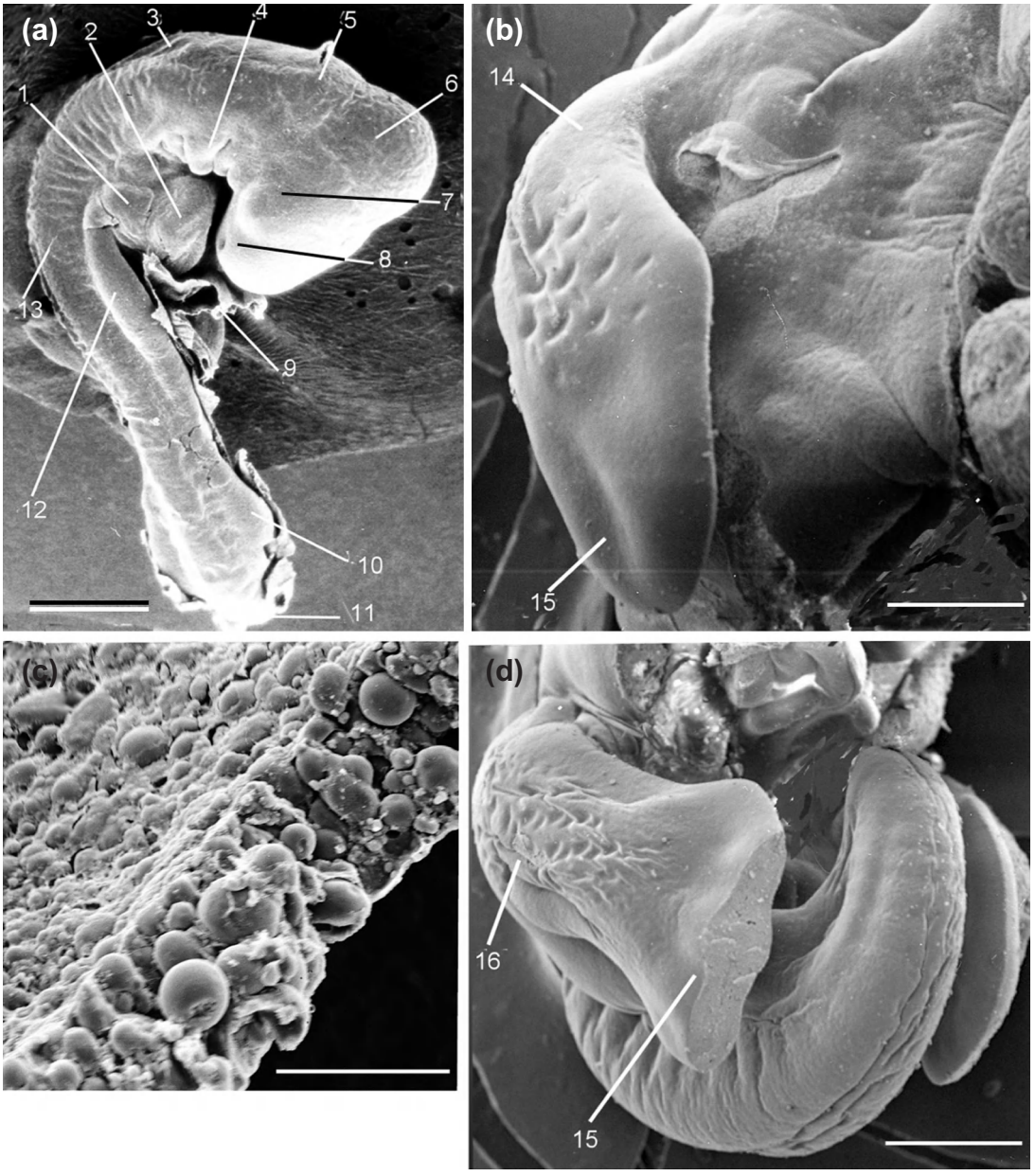

Downloaded from Vet-eBooks.com

Plate 17 Neural folds and neural tube

Scanning electron micrographs of the neural folds and neural tube at different stages.

(a) Stage 8 (about 28 h incubation). Neural folds seen from the dorsal side. Bar = 100 μm.

(b) Stage 9 (30 h). Transverse section across the trunk region to show the open neural plate. Bar = 50 μm.

(c) Stage 14 (52 h). Transverse section across the anterior trunk. Bar = 100 μm.

(d) Stage 10 (35 h). Transverse section at the level of the heart. Bar = 100 μm.

1. ectoderm
2. neural fold
3. neural groove
4. neural plate
5. notochord
6. neural tube
7. left dorsal aorta
8. gut
9. ventral mesentery
10. omphalo-mesenteric vein
11. coelom
12. anterior cardinal vein
13. lumen of neural tube
14. pharynx
15. left atrium
16. interatrial septum
17. wall of atrium
18. pericardial cavity
19. splanchnic mesoderm

Downloaded from Vet-eBooks.com

Plate 17

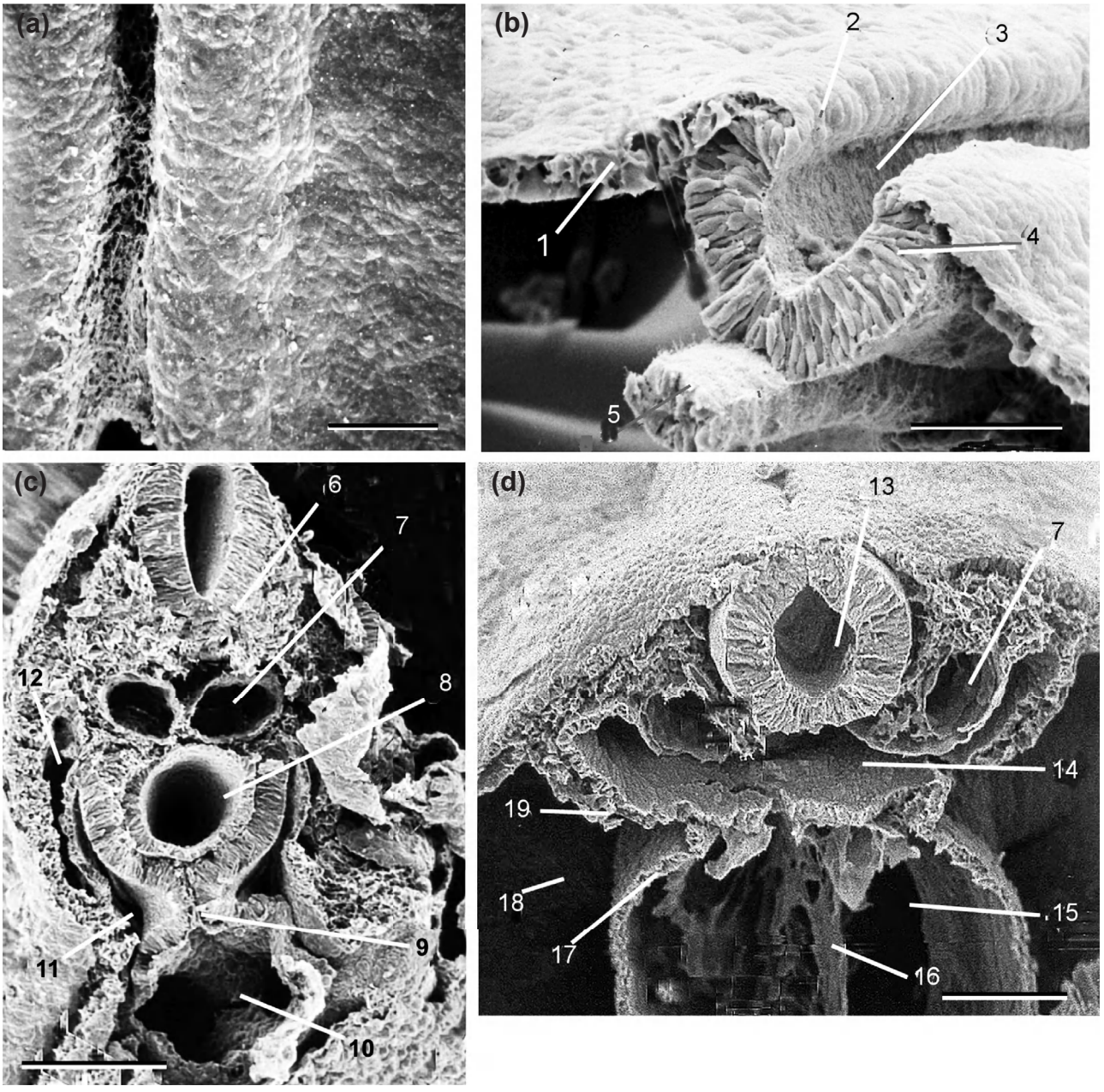

Downloaded From Vet-eBooks.com

Plate 18 Closure of the anterior neuropore

Scanning electron micrographs showing closure of the anterior neuropore at different stages.

(a) Stage 8 (about 28 h incubation) showing the open anterior neuropore at the tip of the forebrain. Bar = 1 mm.

(b) Stage 10 (34 h). The dorsal side of the forebrain with the neural folds almost closed. Bar = 200 μm.

(c) Enlargement of part of (b). Bar = 50 μm.

(d) Stage 10 (35 h) showing final point of closure of the anterior neuropore, much enlarged.

1. neural fold
2. anterior neuropore
3. amniotic ectoderm
4. ectoderm covering optic vesicle
5. final remnant of anterior neuropore

Downloaded from Vet-eBooks.com

Plate 18

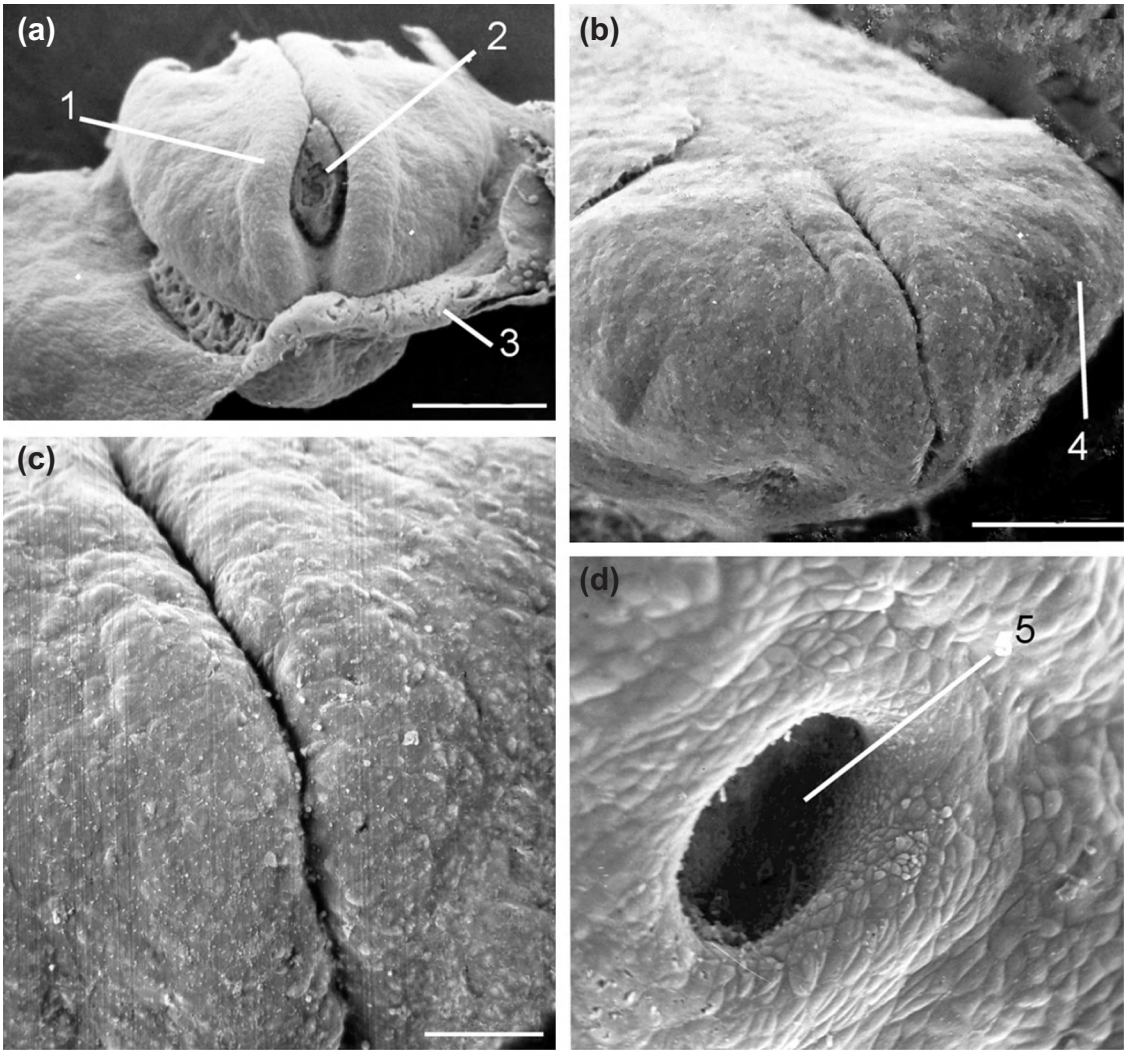

Downloaded from Vet-eBooks.com

Plate 19 Neural tube

Scanning electron micrographs of transverse sections in four embryos of different stages showing the neural tube in the anterior trunk region.

(a) Stage 10 (about 36 h incubation). The lumen is widely open. Bar = 30 µm.

(b) Stage 12 (48 h). The lumen is almost closed and the lateral walls have become thicker, whilst the basal plate is more distinct. Bar = 50 µm.

(c) Stage 14 (55 h). Bar = 30 µm.

(d) Stage 15 (54 h). The mesoderm has spread around the notochord. Bar = 25 µm.

1. lumen of neural tube
2. neural tube
3. notochord
4. basal plate
5. sclerotome
6. wall of neural tube, now thicker
7. blood vessels

Downloaded from Vet-eBooks.com

Plate 19

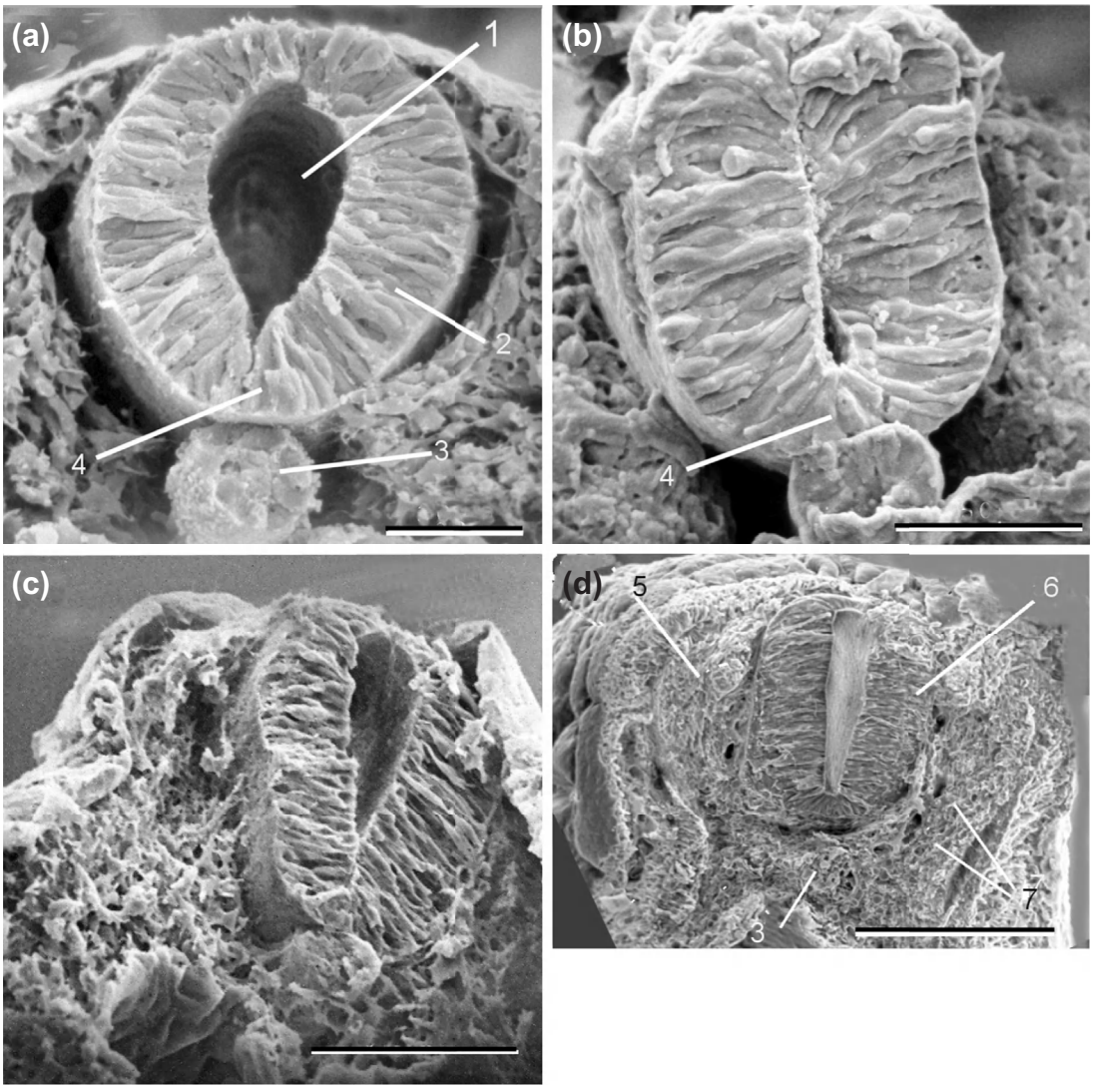

Downloaded from Vet-eBooks.com

Plate 20 Scanning electron micrographs of notochord

(a) Stage 11 (about 44 h incubation). Ventral view of the notochord after removal of endoderm and somites. Bar = 30 μm.

(b) Stage 6 (24 h). Transverse section across the notochord. Each cell is wedge-shaped with its widest (basal) end at the periphery, giving a radial arrangement to the tissue. The apical ends surround a small lumen containing cells. Bar = 5 μm.

(c) Stage 10 (34 h). Longitudinal broken section through the notochord. The extracellular materials are apparent on both dorsal and ventral surfaces. Bar = 10μm.

(d) Stage 23 (about 4 days incubation). Transverse section across the notochord. Each cell is highly vacuolated. Bar = 7.5 μm.

1. notochord
2. neural tube
3. wedge-shaped cell
4. lumen with cells
5. extracellular material
6. vacuolated cell

(b, d) Reprinted from Bancroft and Bellairs (1976) with permission of the Company of Biologists Ltd.

Downloaded from Vet-eBooks.com

Plate 20

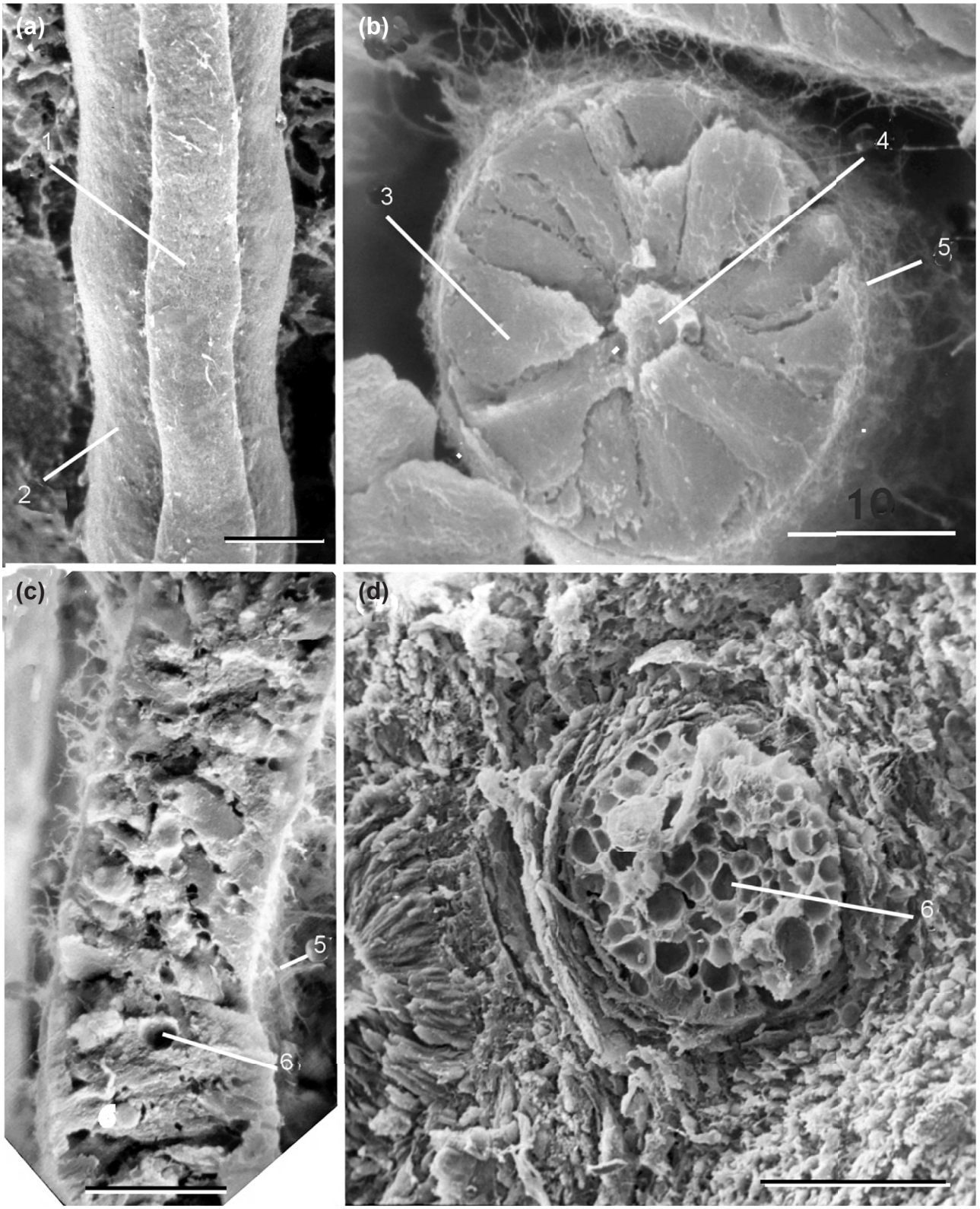

Downloaded from Vet-eBooks.com

Plate 21 Somites and segmental plate

Scanning electron micrographs of segmented and unsegmented mesoderm.

(a) Anterior end of a stage 11 (about 42 h incubation) after removal of much of the ectoderm.

(b) Posterior end of the same embryo at same magnification.

Bar = 200 μm

1. otic placode (see also otic pit *plate 26*)
2. ectoderm covering head
3. neural tube
4. intermediate mesoderm
5. somite
6. segmental plate mesoderm (pre-segmented mesoderm)
7. lateral plate mesoderm
8. ectoderm

Downloaded from Vet-eBooks.com

Plate 21

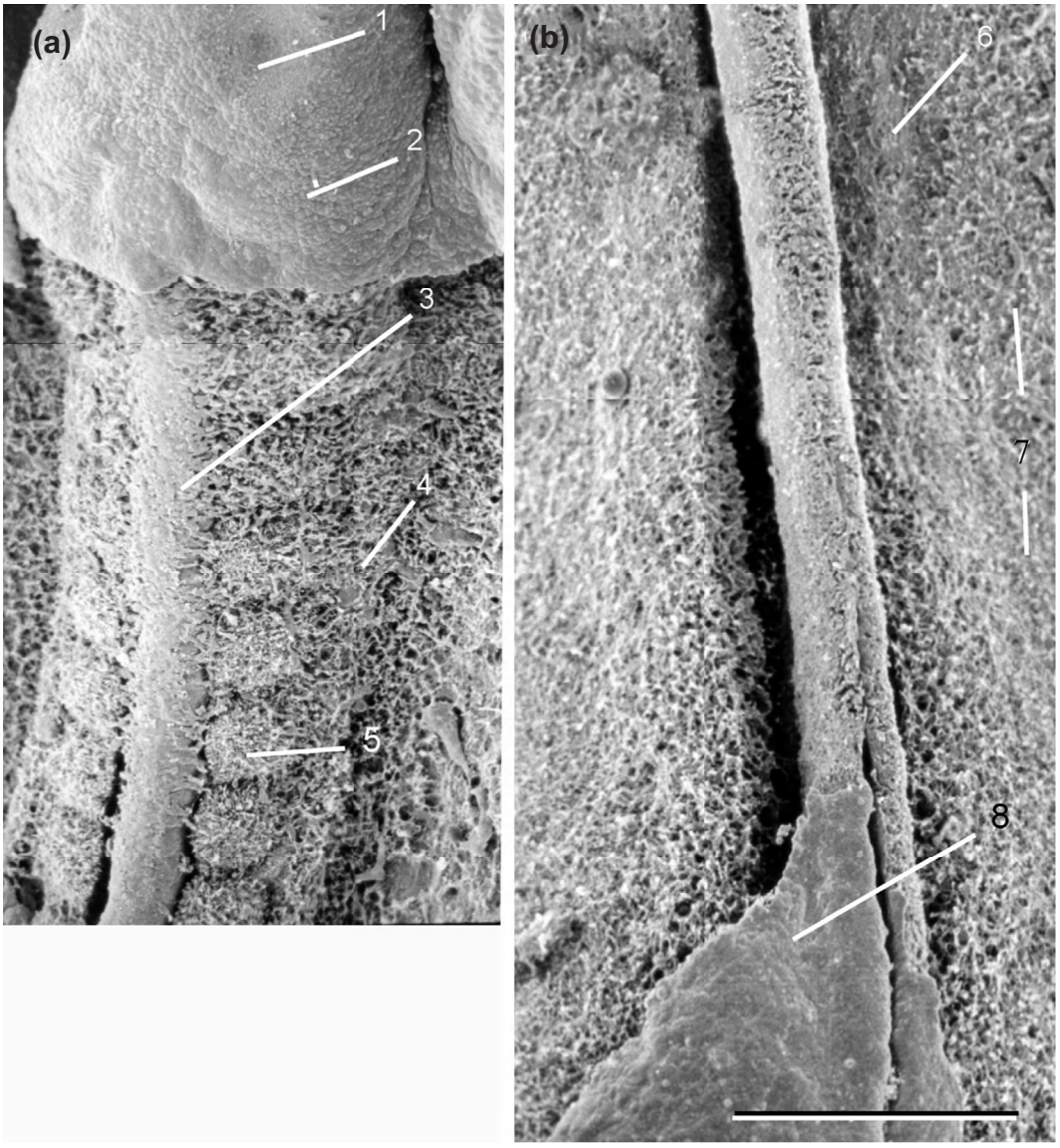

Downloaded From Vet-eBooks.com

Plate 22 Scanning electron micrographs of somites and nephric duct

(a) Somite from a stage 11 embryo (about 42 h incubation) broken open in a sagittal plane, lying against the notochord (left) and the neural tube (right). The walls of the somite are composed of a single layer of epithelial cells surrounding a central cavity, the somitocoele. The adjacent anterior and posterior somites have been removed. Bar = 75 μm.

(b) Enlargement of central region of (a) showing the cells in the lumen and the apical borders of the cells bordering it. Bar = 10 μm.

(c) Somite, nephric duct and lateral plate mesoderm of a stage 14 embryo (about 52 h incubation) seen from the dorsal side after removal of the ectoderm and neural tube. Bar = 100 μm.

(d) Nephric duct of a stage 14 embryo, showing the fine fibrils and filopodia passing over it, between the adjacent somite and lateral plate mesoderm. Bar = 50 μm.

1. notochord
2. intersegmental angioblastic cords which will contribute to the right cardinal vein
3. right nephric duct
4. left nephric duct
5. enlargement of a nephric duct to show filopodia

(a, b) Reprinted from Bellairs (1979) by permission of the Company of Biologists Ltd.

Downloaded from Vet-eBooks.com

Plate 22

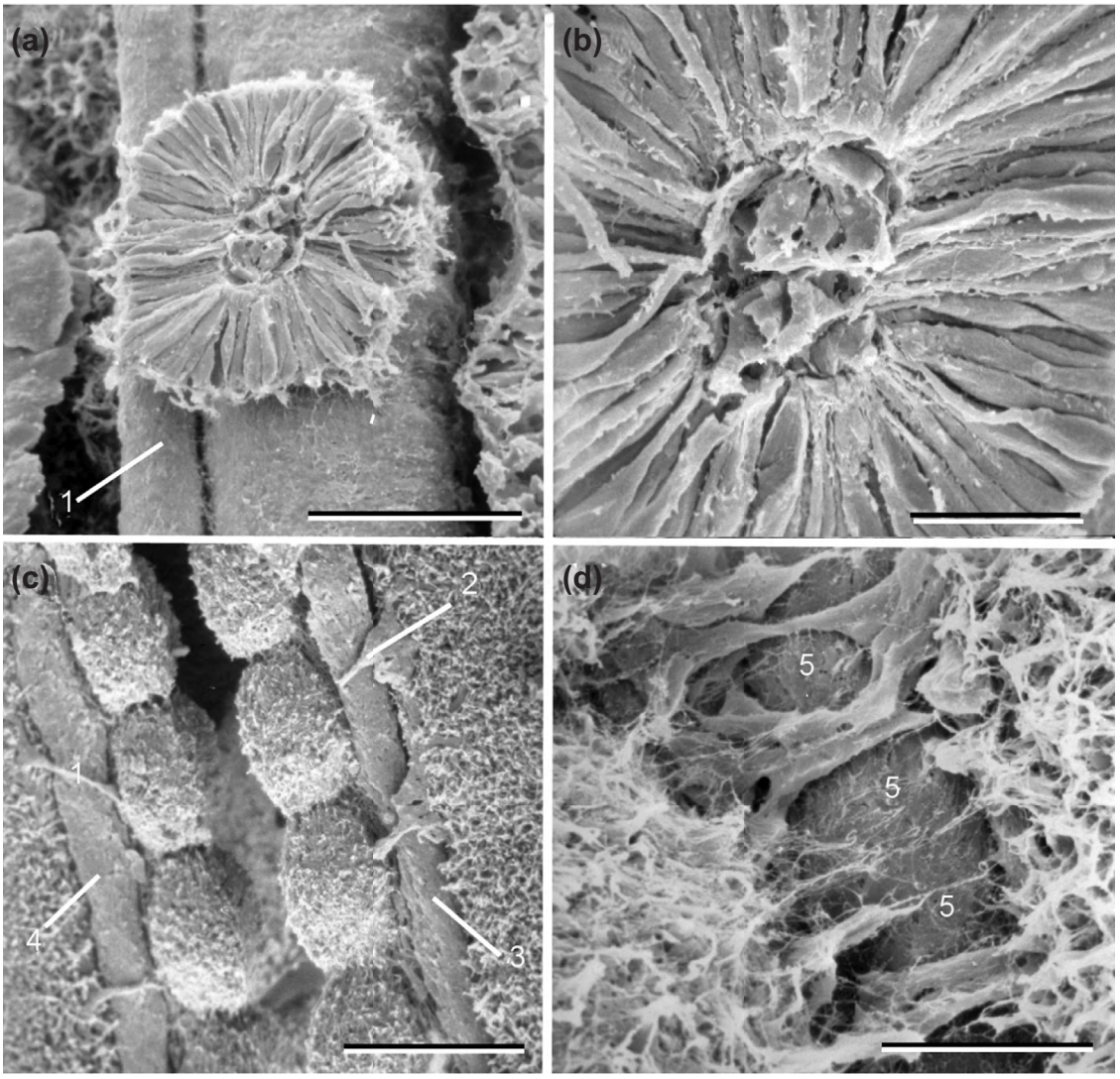

Downloaded From Vet-eBooks.com

Plate 23 Somite differentiation

Scanning electron micrographs of the dermatome, myotome and sclerotome at different stages.

(a) Part of the stage 15 (54 h) specimen shown in plate 19 (d). The ectoderm has been partially removed from over the dermamyotome. Bar = 28 μm.

(b) Section through a differentiating somite of a stage 14 embryo (about 52 h incubation), showing the simple columnar epithelium of the dermatome and the mesenchymatous cells of the sclerotome. Bar = 24 μm.

(c) Dermatome of a stage 16 embryo (about 55 h incubation) to show its relationship to the neural tube. Bar = 40 μm.

(d) Dermatome and myotome in a stage 17 embryo (about 60 h incubation), showing the many contacts between the dermatome cells. Bar = 10 μm.

1. ectoderm
2. dermatome
3. sclerotome
4. neural tube
5. fractured myotome cells

Downloaded from Vet-eBooks.com

Plate 23

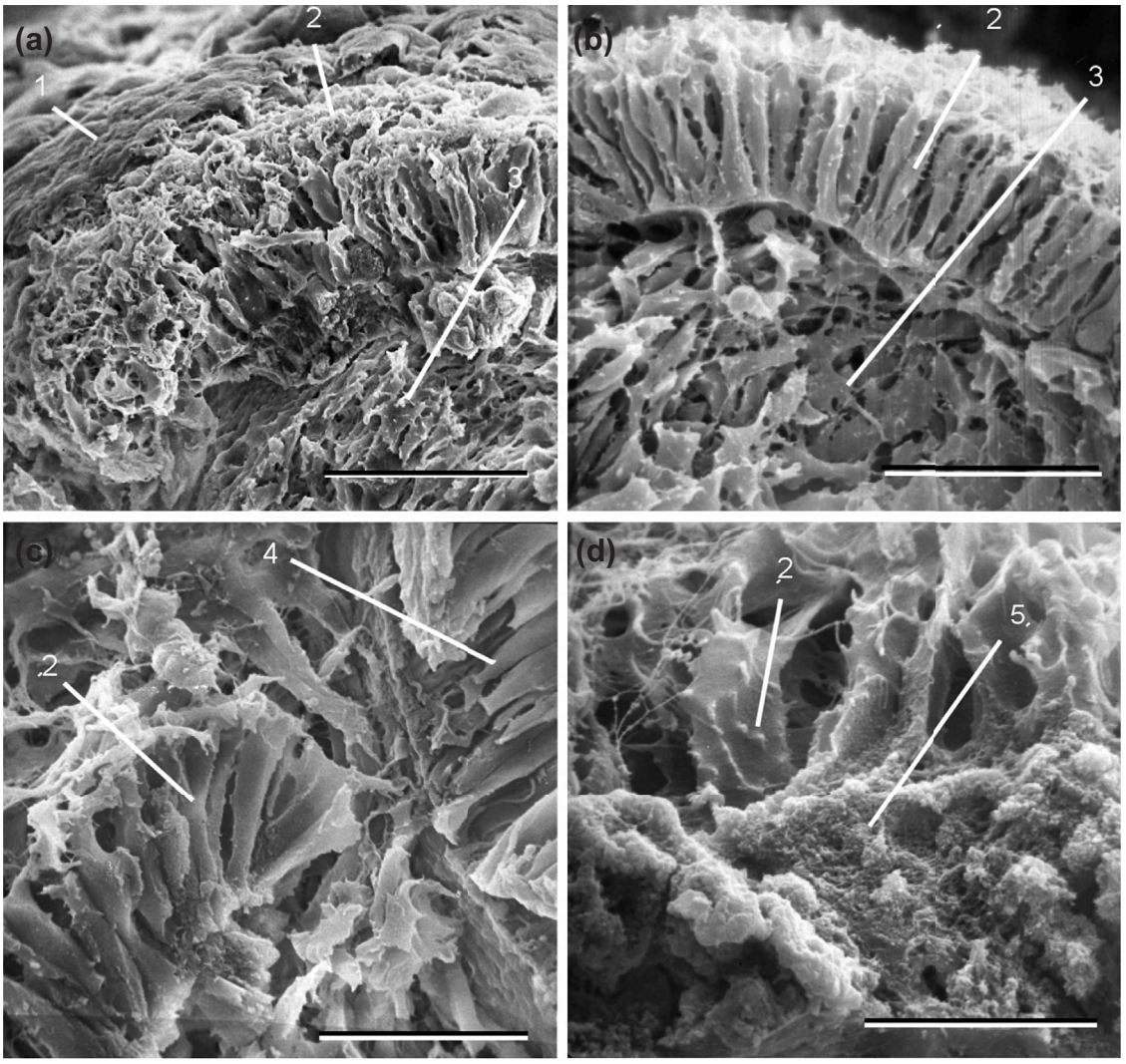

Downloaded From Vet-eBooks.com

Plate 24 Neural crest I

Scanning electron micrographs of neural crest at different stages and levels (a-d after removal of overlying ectoderm).

(a) Surface view of the neural crest in the unsegmented region of a stage 11 embryo (about 43 h incubation). Bar = 30 μm.

(b) Enlargement of part of (a). The cells are not yet flattened and the intercellular spaces are conspicuous. Note the filament-like strands of extracellular materials. Bar = 10 μm.

(c) Surface view of the neural crest overlying the dorsal side of the neural tube and somites at the level of the 13th somite of a stage 14 (50–53 h) embryo. Bar = 100 μm.

(d) Surface view of the neural crest at a level anterior to (c). The cells are flatter than in (c). Bar = 50 μm.

(e) Transverse section across the edge of a neural tube showing the migrating neural crest cells of a stage 14 embryo. Bar = 3 μm.

(f) Enlargement of part of (e). Group of neural crest cells caught in the act of migration down the lateral edge of the neural tube. Bar = 1.5 μm.

1. neural crest cell
2. neural tube
3. somite
4. flattened neural crest cells on the surface of the neural tube
5. ectoderm
6. neural crest cell fixed in transit
7. neural tube cells

Reprinted from Bancroft and Bellairs (1976), with permission of Blackwell Publishing Ltd.

Downloaded from Vet-eBooks.com

Plate 24

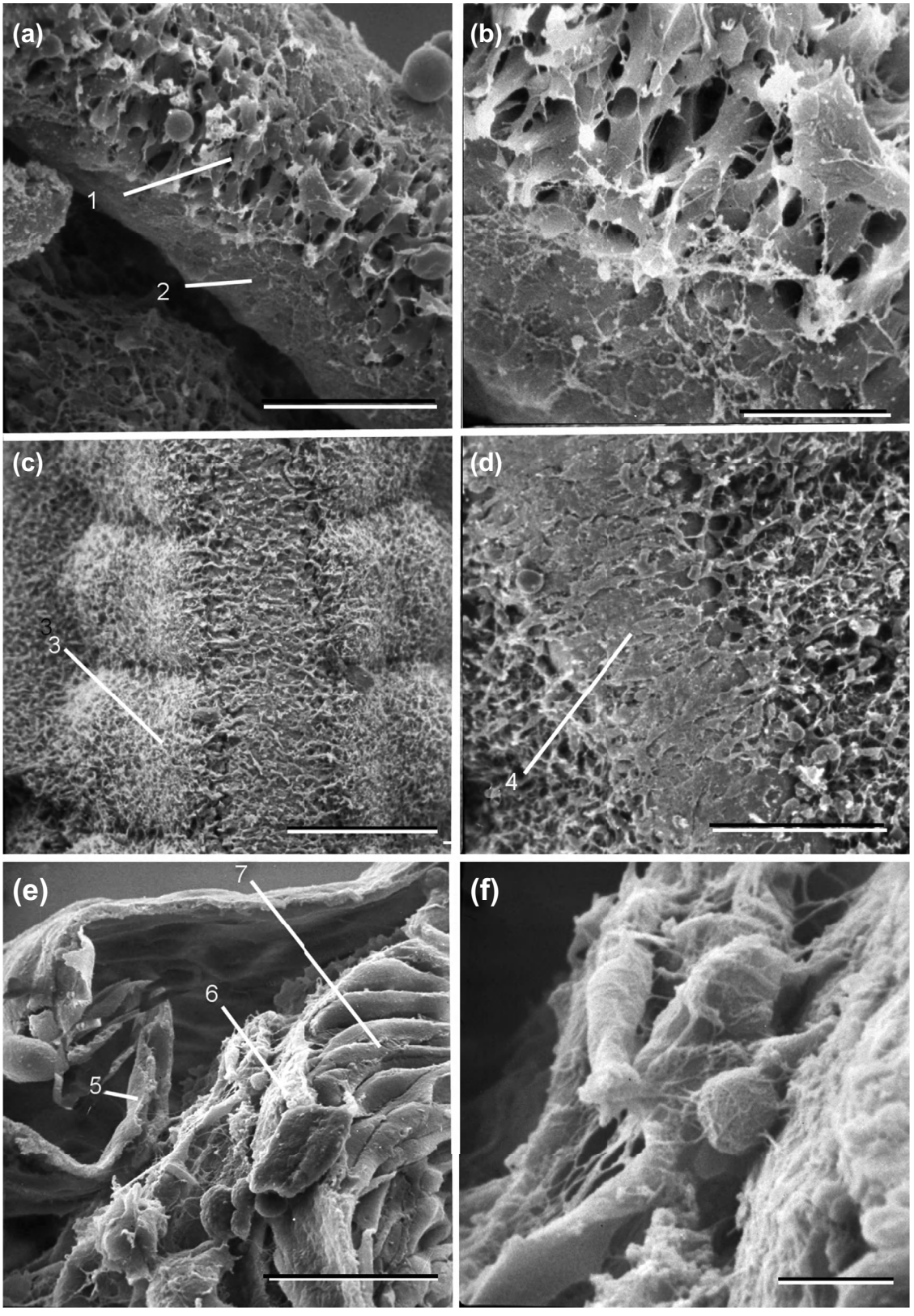

Downloaded from Vet-eBooks.com

Plate 25 Neural crest II

Scanning electron micrographs showing the neural crest at different levels of stage 14 embryos: (a–c) Dorsal views of neural crest cells all taken from the same stage 14 embryo, after removal of the ectoderm, illustrating stages in the maturation of the neural crest cells. In each case, the anterior end of the embryo is at the top of the photograph.

(a) The least mature neural crest, from the posterior end of the embryo. Bar = 20 μm.

(b) Neural crest from the middle of the trunk at the level of the 13th somite. Bar = 20 μm.

(c) The most mature neural crest from the anterior end of the trunk at the level of the first somite. With increasing maturity the cells become flattened onto the surface of the neural tube and reorientated from an antero-posterior direction to a medio-lateral one. Bar =15 μm.

(d) Fully flattened and reorientated neural crest from the level of the first somite of a different stage 14 embryo. Bar = 10 μm.

Reprinted from Bancroft and Bellairs (1976), with permission of Blackwell Publishing Ltd.

Downloaded from Vet-eBooks.com

Plate 25

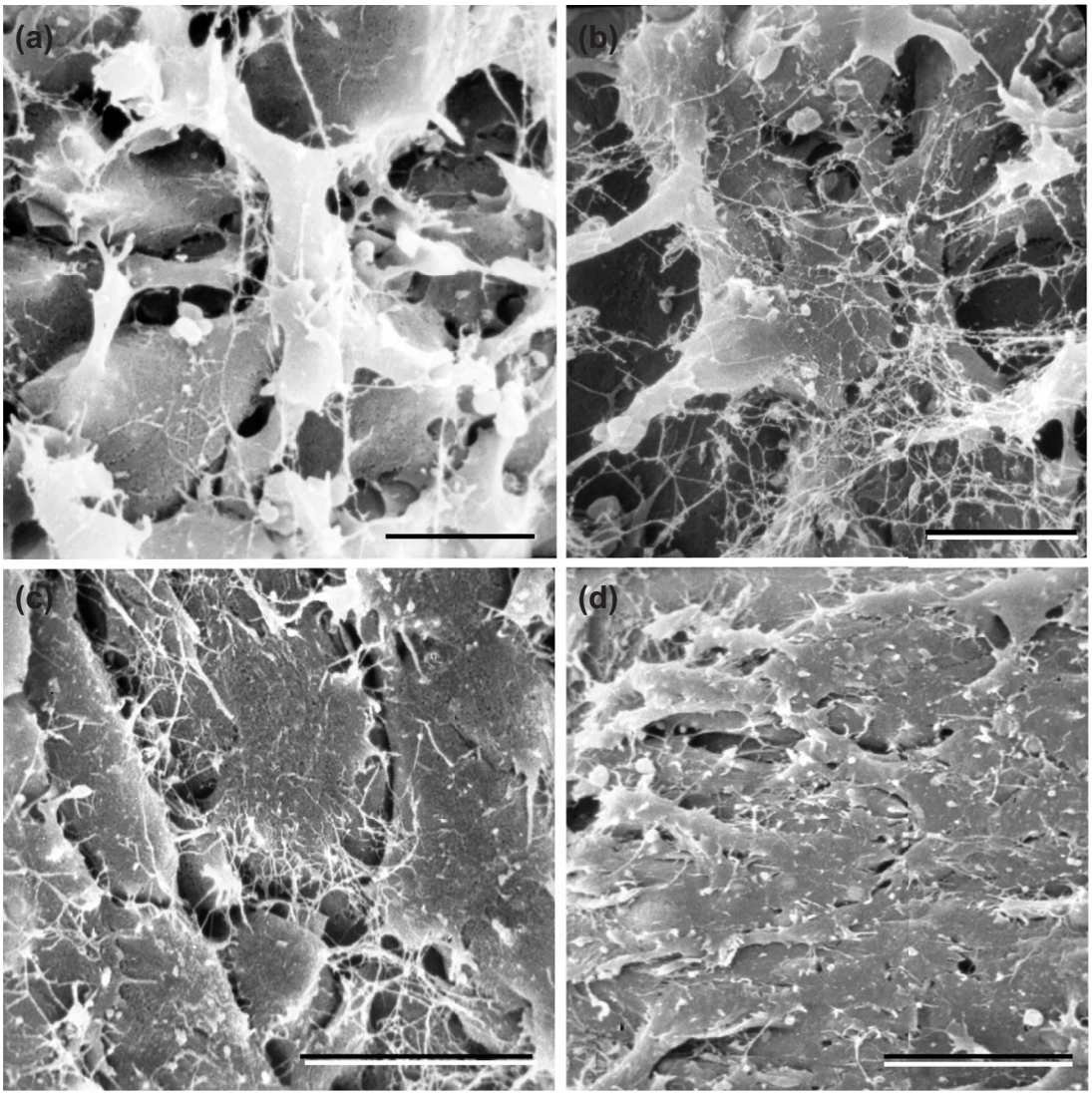

Downloaded from Vet-eBooks.com

Plate 26 Scanning electron micrographs of otic placodes and pits

(a) Otic placodes of a stage 11 embryo (about 40–45 h incubation), seen from the dorsal side – see also *plate 21a.* Bar =140 μm.

(b) Otic placode at stage 12 (45–49 h). Bar = 30 μm.

(c) Otic pit at stage 13 (48–52 h) – see also *plate 15d.* Bar = 30 μm.

(d) Otic pit at stage 14 (50–53 h). Bar = 50 μm.

All figures reprinted from Bancroft and Bellairs (1977), with permission of Springer-Verlag.

Downloaded from Vet-eBooks.com

Plate 26

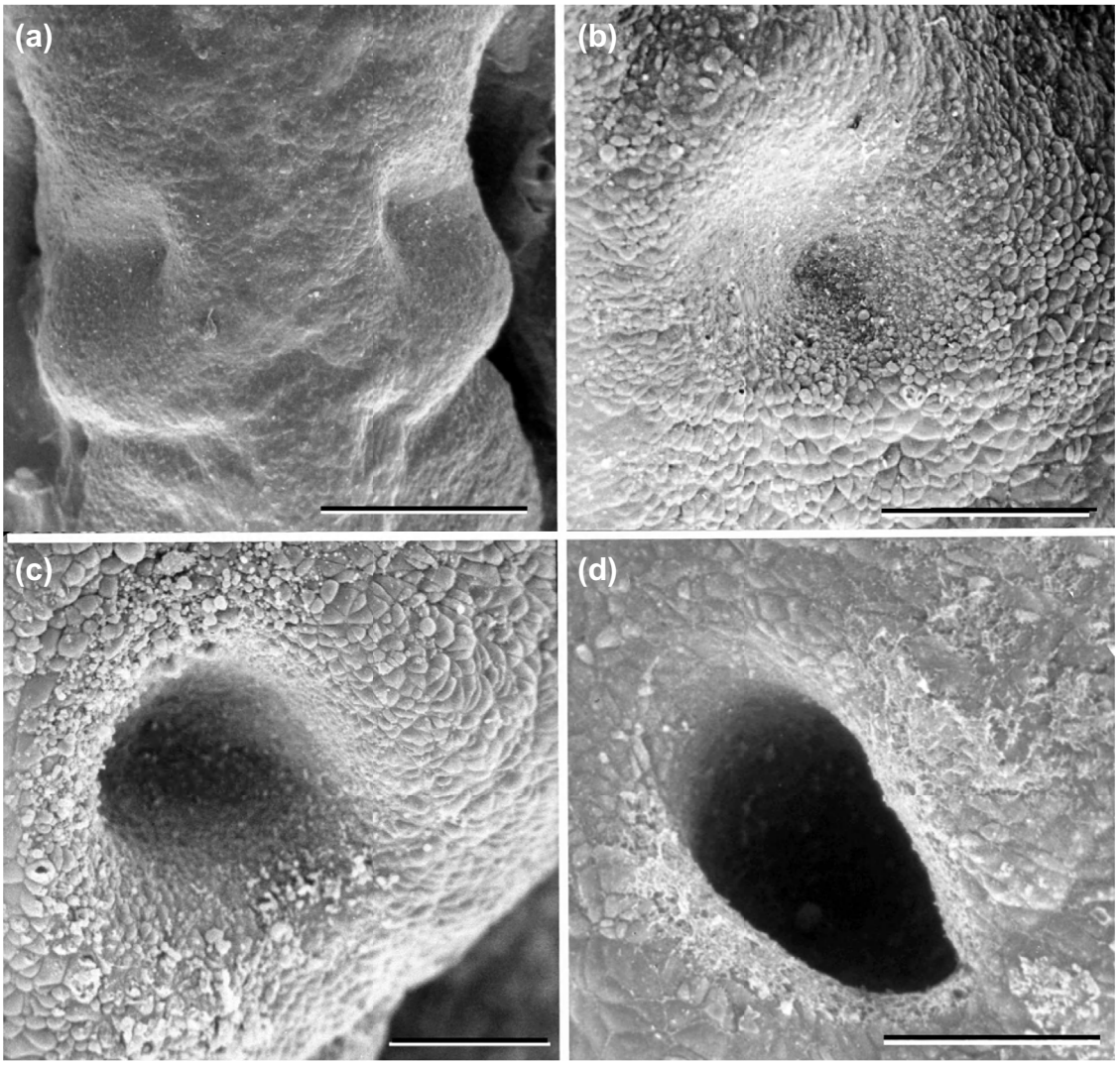

Downloaded From Vet-eBooks.com

Plate 27 Scanning electron micrographs of otic pits and nasal placodes

(a) Otic pit at stage 16 (51–56 h). Bar = 20 μm.

(b) Otic pit at stage 17 (52–64 h). Bar =10 μm.

(c) Nasal placode at stage 16. Bar = 85 μm.

(d) Nasal pit at stage 18 (65–69 h). Bar = 85 μm.

All figures reprinted from Bancroft and Bellairs (1977), with permission of Springer-Verlag.

Downloaded from Vet-eBooks.com

Plate 27

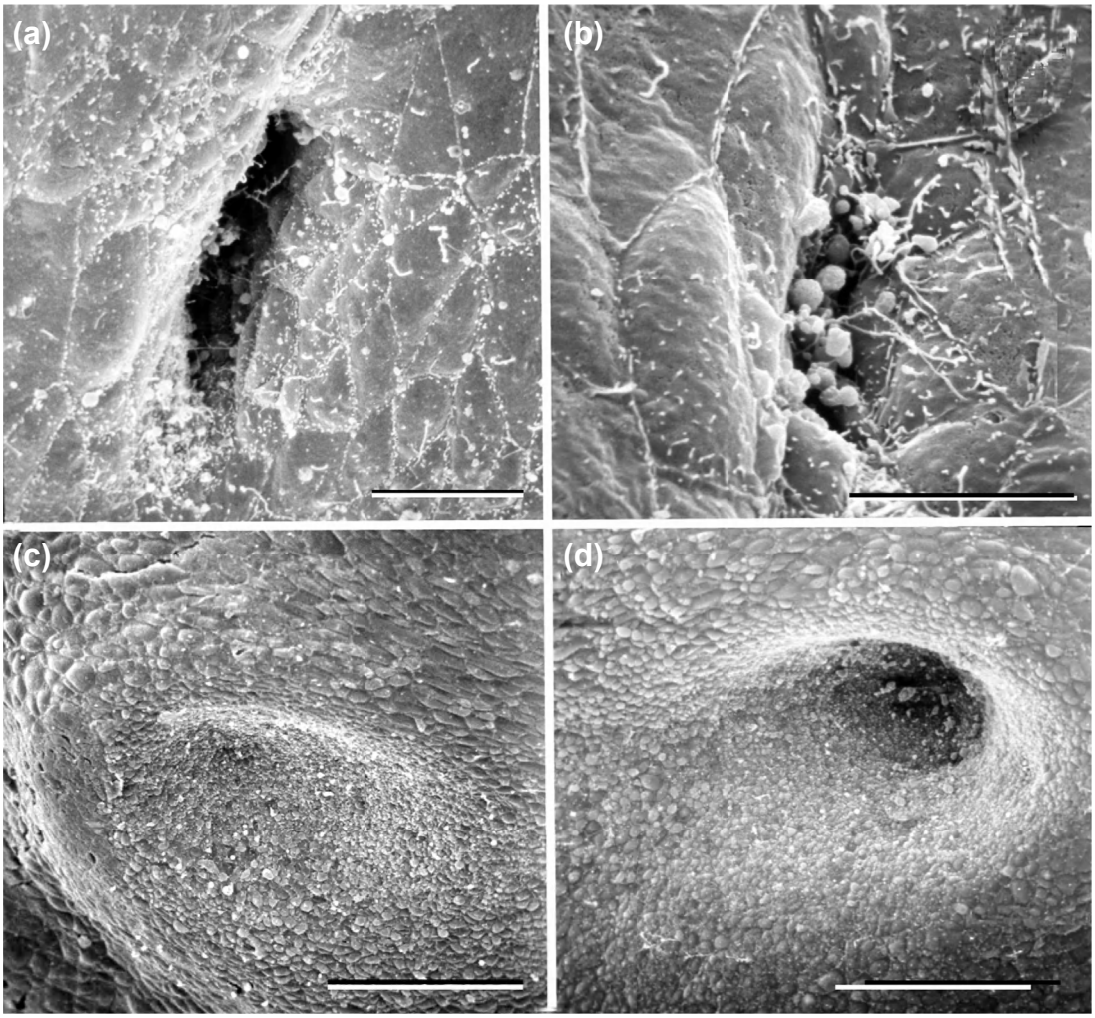

Downloaded From Vet-eBooks.com

Plate 28 Scanning electron micrographs of the lens placode

(a) Lens placode at stage 13 (48–52 h incubation). Bar = 50 μm.

(b) Lens placode at stage 14 (50–53 h), beginning to invaginate. Bar = 25 μm.

(c) Lens placode at stage 15 (50–55 h), almost completely invaginated. Bar = 100 μm.

(d) Remnant of invaginating lens placode at stage 17 (52–64 h), only a small cavity now remaining. Bar = 25 μm.

(a) Reprinted from Bancroft and Bellairs (1977), with permission of Springer-Verlag.

Downloaded from Vet-eBooks.com

Plate 28

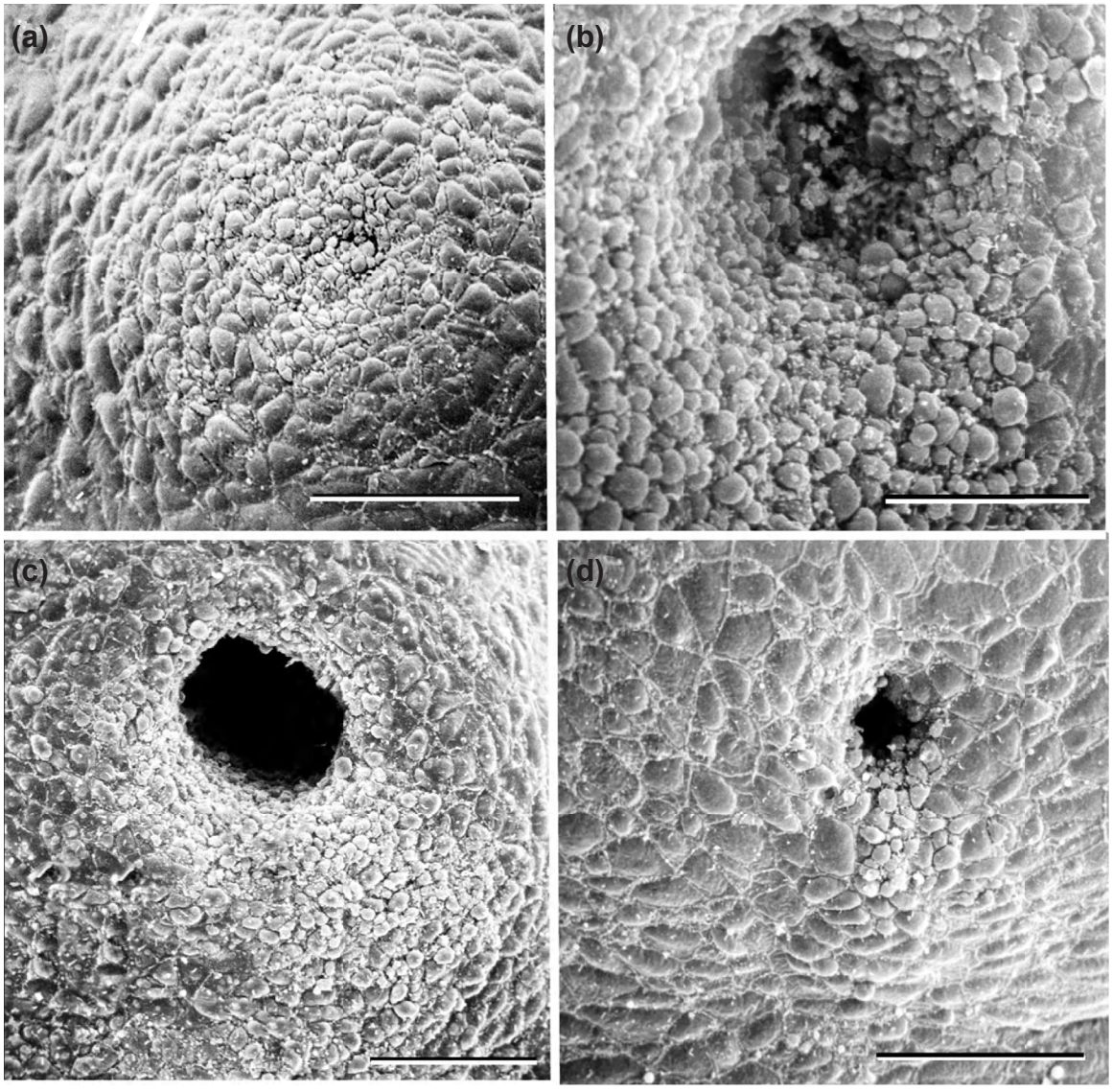

Downloaded from Vet-eBooks.com

Plate 29 Light micrographs of whole embryos and skeletally stained feet

(a) Normal (left) and talpid mutant (right) embryos at about stage 29 (6–6.5 days) to show the differences in the limb buds and the head.

(b) Right feet of normal embryos, stained with Alcian blue, between stages 29 and 34 (between 6 and 8 days).

(a) Courtesy of C. Tickle.

(b) Reprinted from Sanz-Ezquierro and Tickle (2003), with permission of John Wiley and Sons Inc.

Downloaded from Vet-eBooks.com

Plate 29

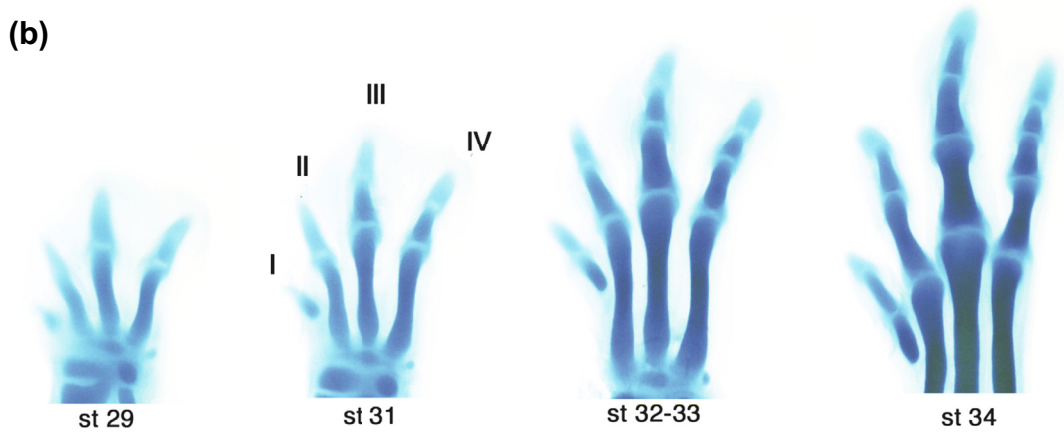

Downloaded from Vet-eBooks.com

Plate 30 Scanning electron and light micrographs of limbs

(a) Scanning electron micrograph showing a section through the apical ectodermal ridge of the wing bud in a stage 26 embryo (5 days of incubation). Bar = 17 μm.

(b) Light micrographs of a skeletally stained (with Alcian blue) normal wing skeleton (left), and duplicated wing skeleton (right) produced by grafting a polarizing region to the anterior margin of a stage 20 (70–72 h) wing bud.

(b) Courtesy of C. Tickle.

Downloaded from Vet-eBooks.com

Plate 30

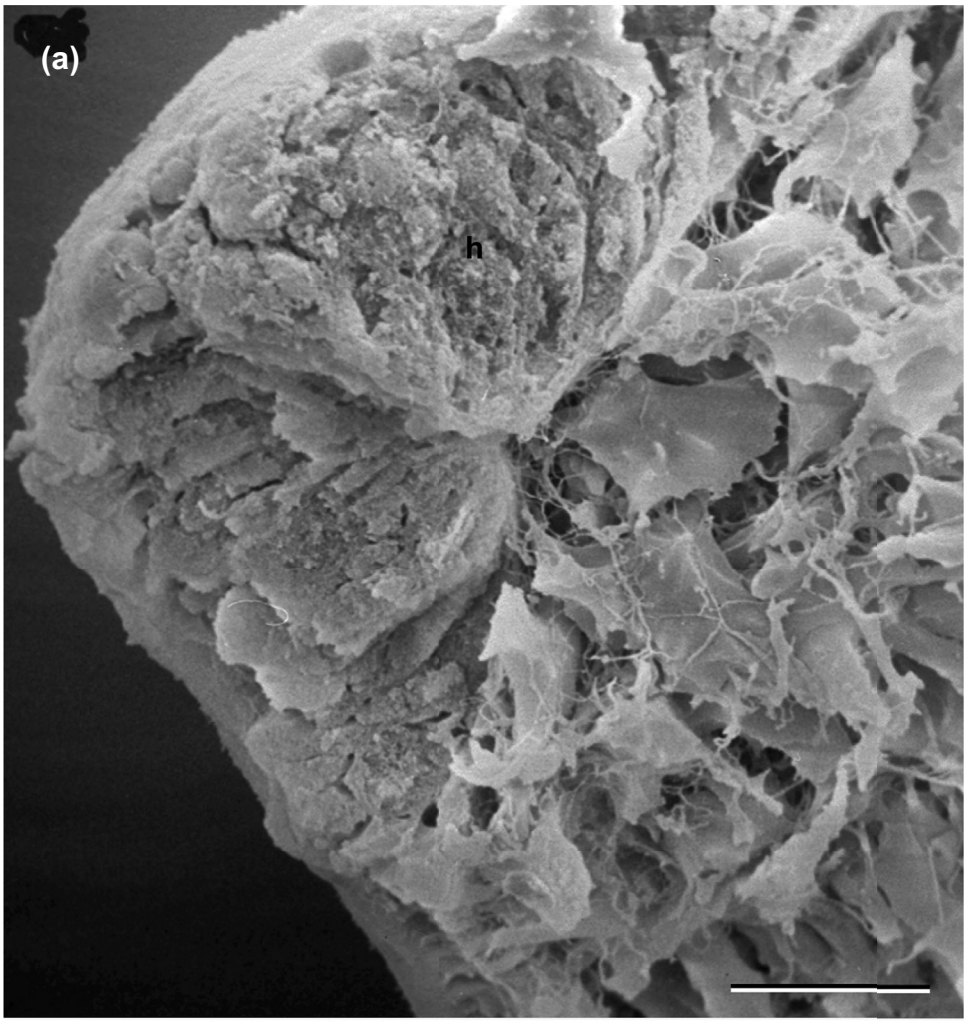

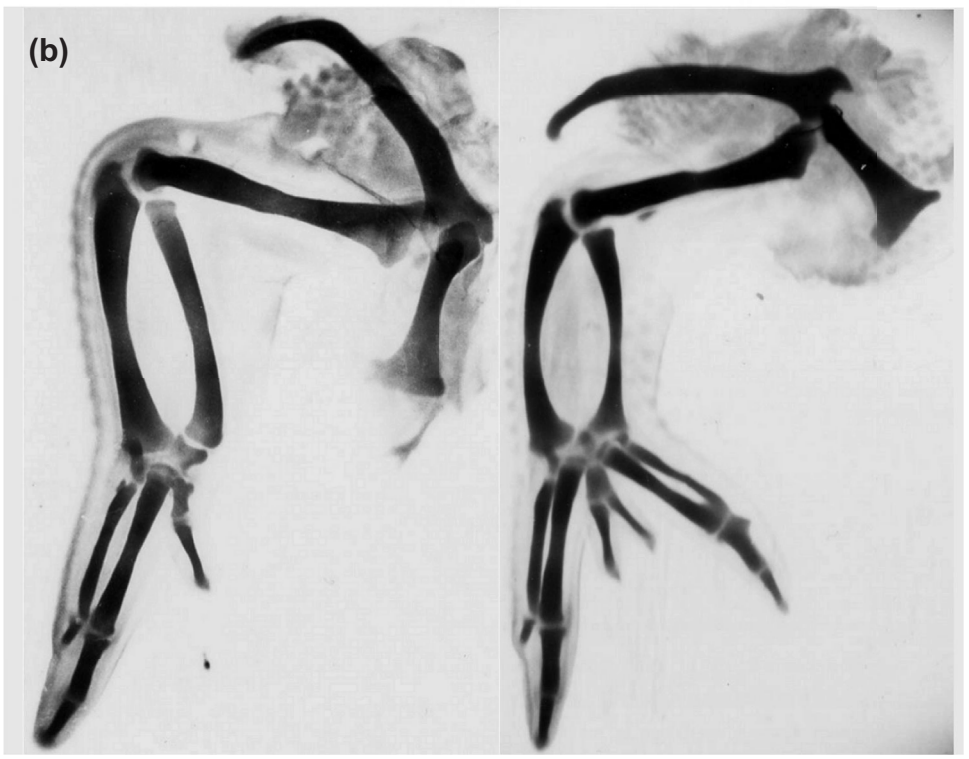

Downloaded from Vet-eBooks.com

Plate 31 Scanning electron micrographs of the tail bud

(a) Dorsal view of the tail bud of a stage 16 (52 h of incubation) embryo after removal of the ectoderm. Bar = 50 μm.

(b) Tail bud of a stage 22 (3.5 days) embryo. A block of mesoderm has been dissected from the left side. Bar = 20 μm.

(c) Tail bud of a stage 21 (3.5 days) embryo after removal of the ectoderm. Bar = 20 μm.

(d) Tail bud of an embryo at stage 22 after removal of the ectoderm. Bar = 11 μm.

1. neural tube
2. unsegmented mesoderm
3. blood vessel
4. somite
5. ectoderm
6. neural crest cells on surface of neural tube

(a) Reprinted from Bellairs and Sanders (1986), with permission of Springer-Verlag.

Downloaded from Vet-eBooks.com

Plate 31

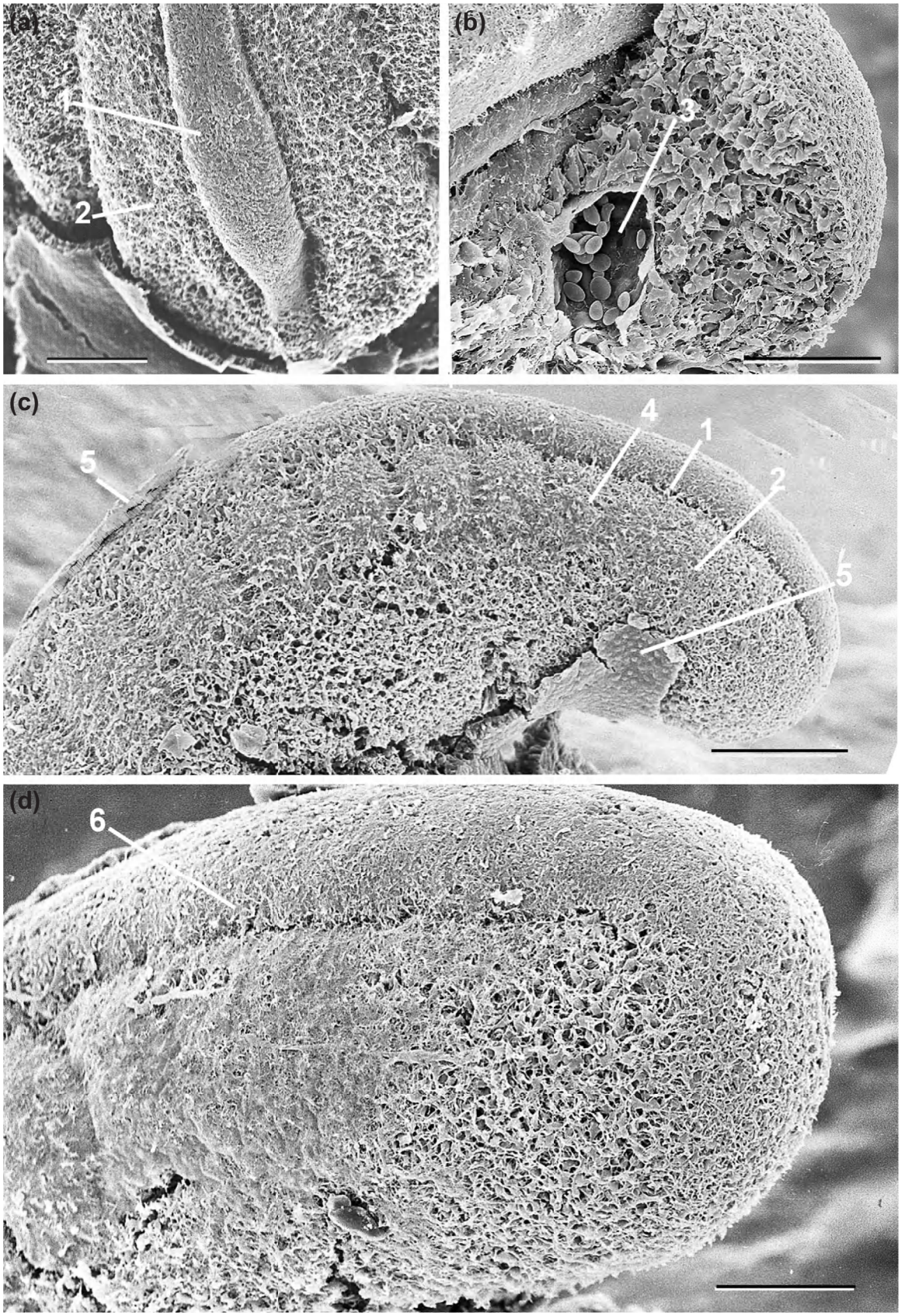

Downloaded from Vet-eBooks.com

Plate 32 Heart development I

Scanning electron micrographs showing ventral views of the early heart tube between stages 9 and 10 (between 29 and 38 hours incubation). In (a) and (b) the left and right sides are not yet completely fused.

(a) 8 somite stage (early stage 9). Bar = 50 μm.

(b) 9 somite stage (late stage 9). Bar = 50 μm.

(c) 10 somite stage (stage 10). Bar = 50 μm.

1. ventral aorta
2. ventral mesocardium
3. cardiac tube
4. developing bulbus cordis
5. developing ventricle

Reprinted from Hiruma and Hirakow (1985), with permission of Springer-Verlag.

Downloaded from Vet-eBooks.com

Plate 32

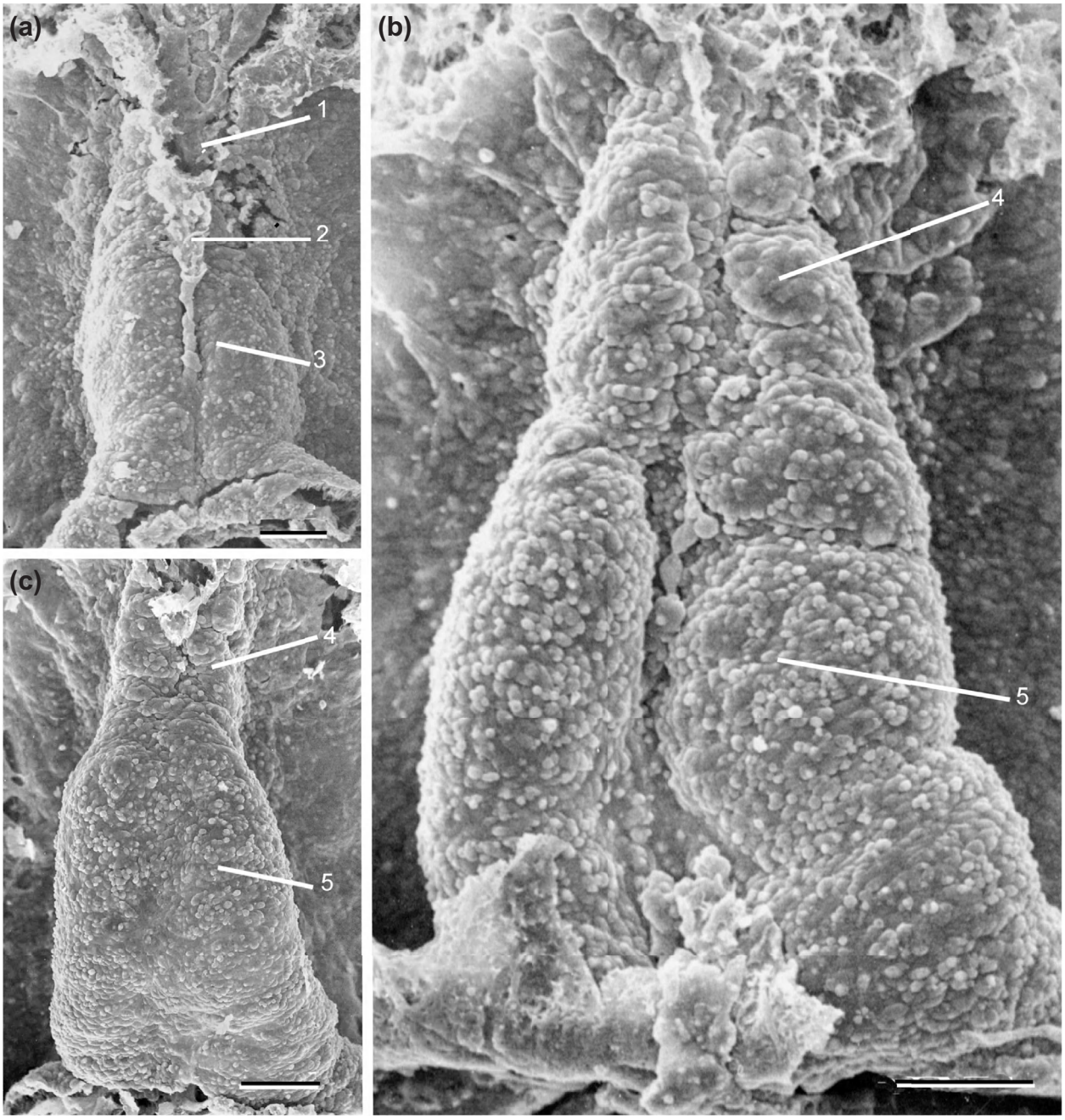

Downloaded From Vet-eBooks.com

Plate 33 Heart development II

Scanning electron micrographs of the developing heart at different stages.

(a) Ventral view of the developing heart of a stage 12 embryo (about 48 h incubation) from which most of the endoderm has been removed. Bar = 200 μm.

(b) Ventral view of the heart of a stage 22 embryo (3.5 days). Bar = 200 μm.

(c) Enlargement of part of (a). Bar = 40 μm.

(d) Enlargement of part of (b). Bar = 100 μm.

1. truncus arteriosus
2. pharynx
3. cut edge of splanchnopleure
4. anterior intestinal portal
5. atrium
6. ventricle
7. left dorsal aorta
8. left anterior cardinal vein
9. left aortic arch

Downloaded from Vet-eBooks.com

Plate 33

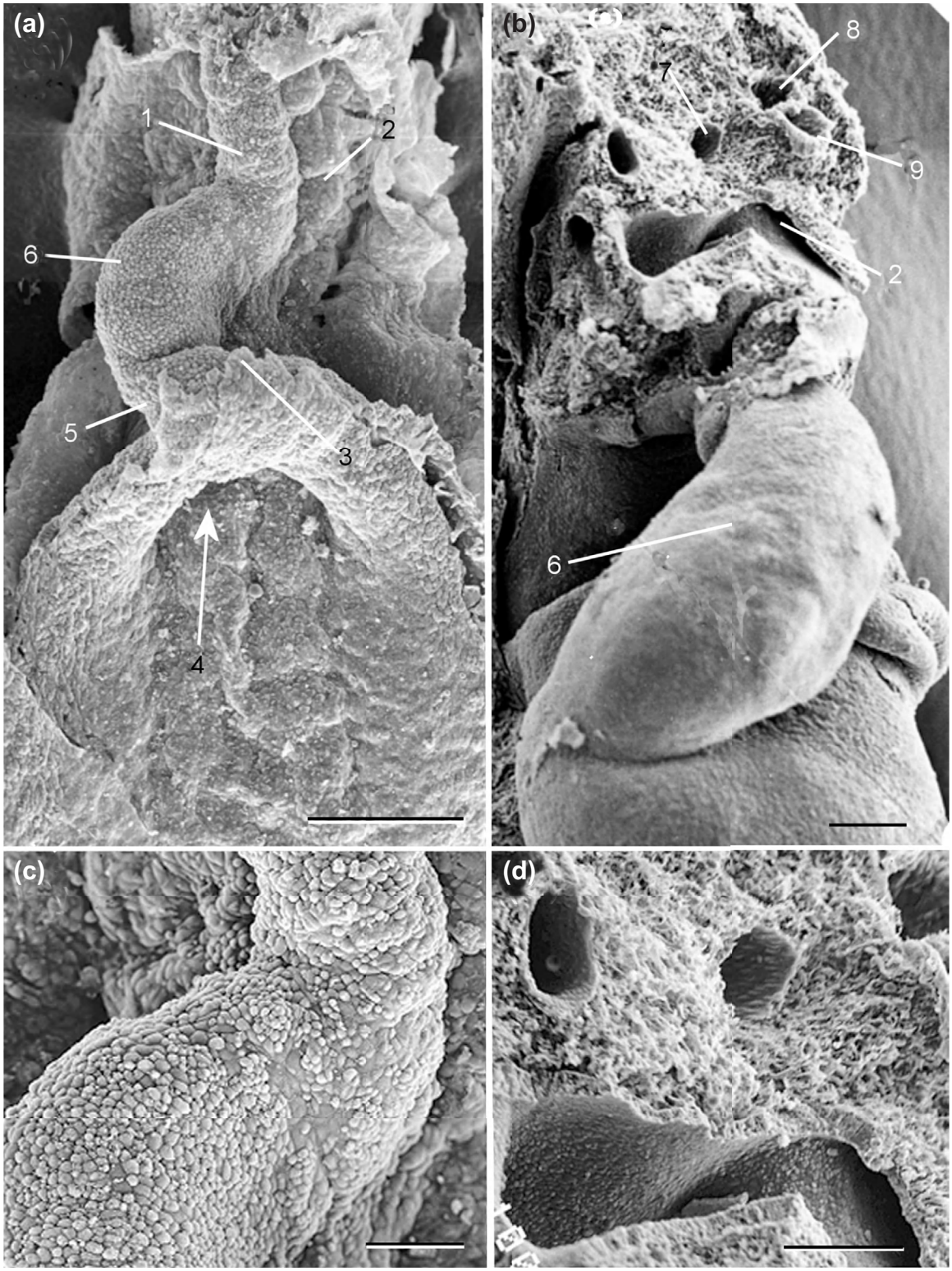

Downloaded from Vet-eBooks.com

Plate 34 Heart development III

Scanning electron micrographs of the developing heart at different stages.

(a) Stage 18 embryo (about 3 days incubation) showing the head and trunk with heart exposed. Bar = 400 μm.

(b) Enlargement of heart in (a). Bar = 100 μm.

(c) Stage 18 embryo with heart partially dissected (see also *plates 35* and *36)*. Bar = 300 μm.

(d) Heart of an embryo at stage 27 (5–5.5 days). Bar = 400 μm.

1. atrium
2. truncus arteriosus
3. conus (bulbus) arteriosus
4. ventricle

Downloaded from Vet-eBooks.com

Plate 34

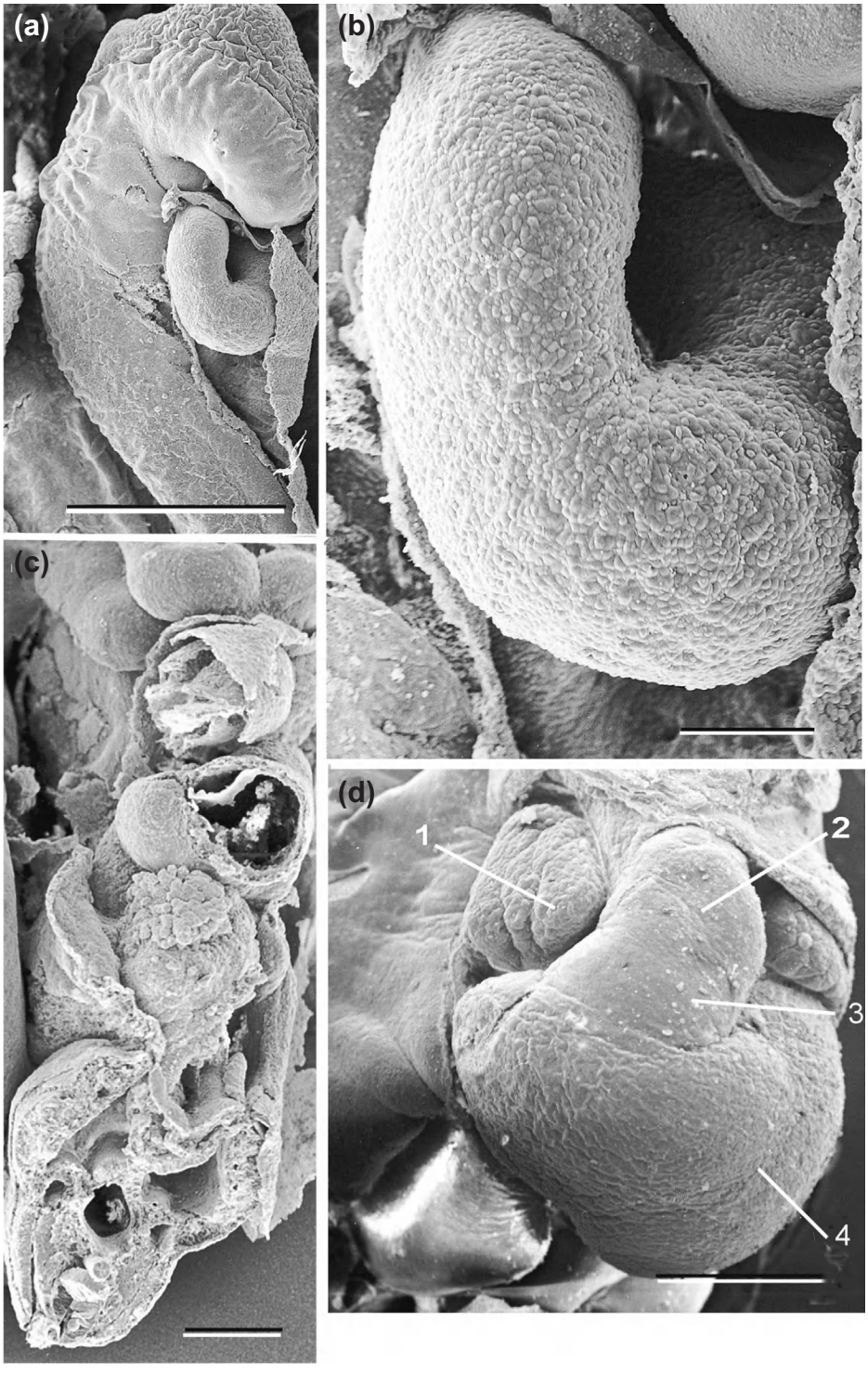

Downloaded from Vet-eBooks.com

Plate 35 Heart development IV

Scanning electron micrograph showing enlargement of heart area in *plate 34c*. The walls of the atrium and ventricle have been partially removed. Bar = 200 μm.

1. pharynx
2. mandibular arch
3. ectoderm of ventral body wall
4. wall of truncus arteriosus
5. wall of ventricle
6. lumen of ventricle
7. pericardial coelom
8. aortico-pulmonary septum
9. epicardium

Downloaded from Vet-eBooks.com

Plate 35

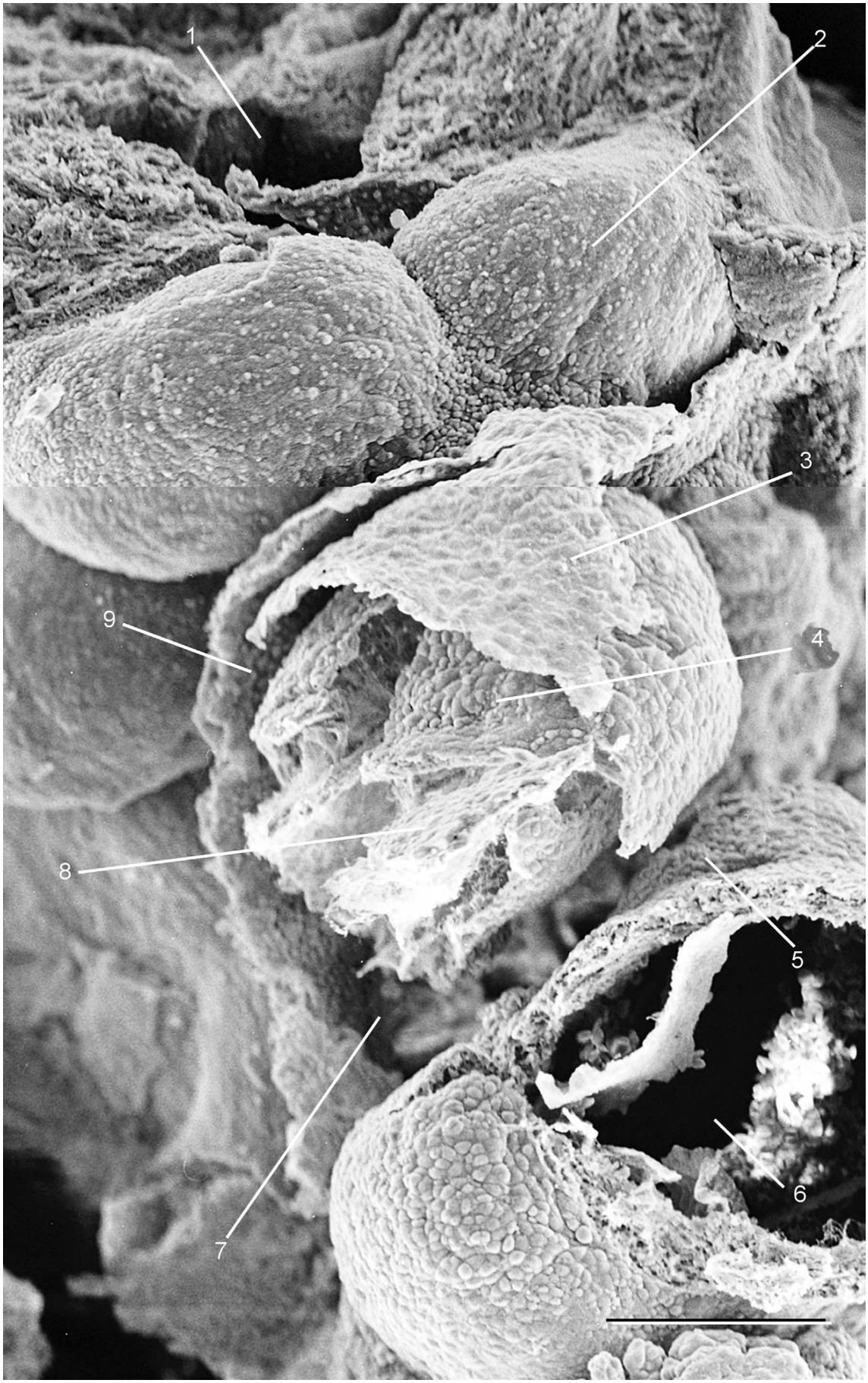

Downloaded from Vet-eBooks.com

Plate 36 Heart development V

Scanning electron micrograph showing enlargement of heart area in *plate 34c* just below region shown in *plate 35*. Bar = 150 µm.

1. ventricle
2. pro-epicardial serosa (also known as pericardial villi) covering sinus venosus
3. atrium
4. sinus venosus
5. posterior vena cava
6. hindlimb bud

Downloaded from Vet-eBooks.com

Plate 36

Downloaded from Vet-eBooks.com

Plate 37 Heart development VI

Scanning electron micrographs showing the developing atrium.

(a) Section across atrium at 5 days of incubation (Stage 26). Bar = 500 μm.

(b) Enlargement of part of (a) showing the developing sinu-atrial valves. Bar = 130 μm.

1. lumen of atrium
2. interatrial septum
3. sinu-atrial opening
4. wall of sinus venosus
5. ventricle

Downloaded from Vet-eBooks.com

Plate 37

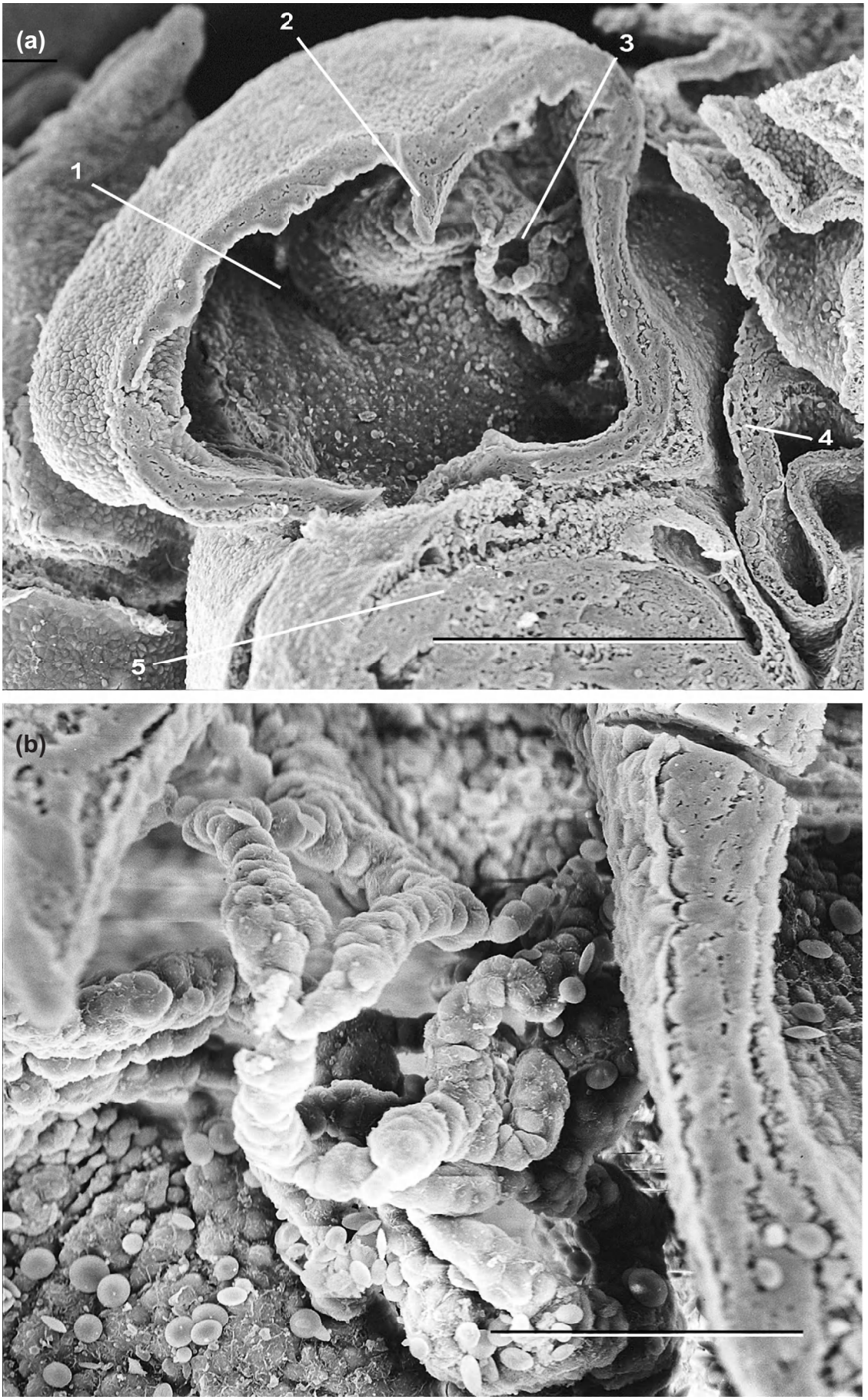

Downloaded from Vet-eBooks.com

Plate 38 Internal organs: heart and lungs

Scanning electron micrograph of a stage 29 embryo (6 days of incubation) dissected to show the heart and lungs. Bar = 500 μm.

1. truncus arteriosus
2. left atrium
3. remnant of left subclavian vein
4. left lung
5. mesentery
6. gizzard
7. right lung
8. pericardial cavity
9. ventricle

Downloaded from Vet-eBooks.com

Plate 38

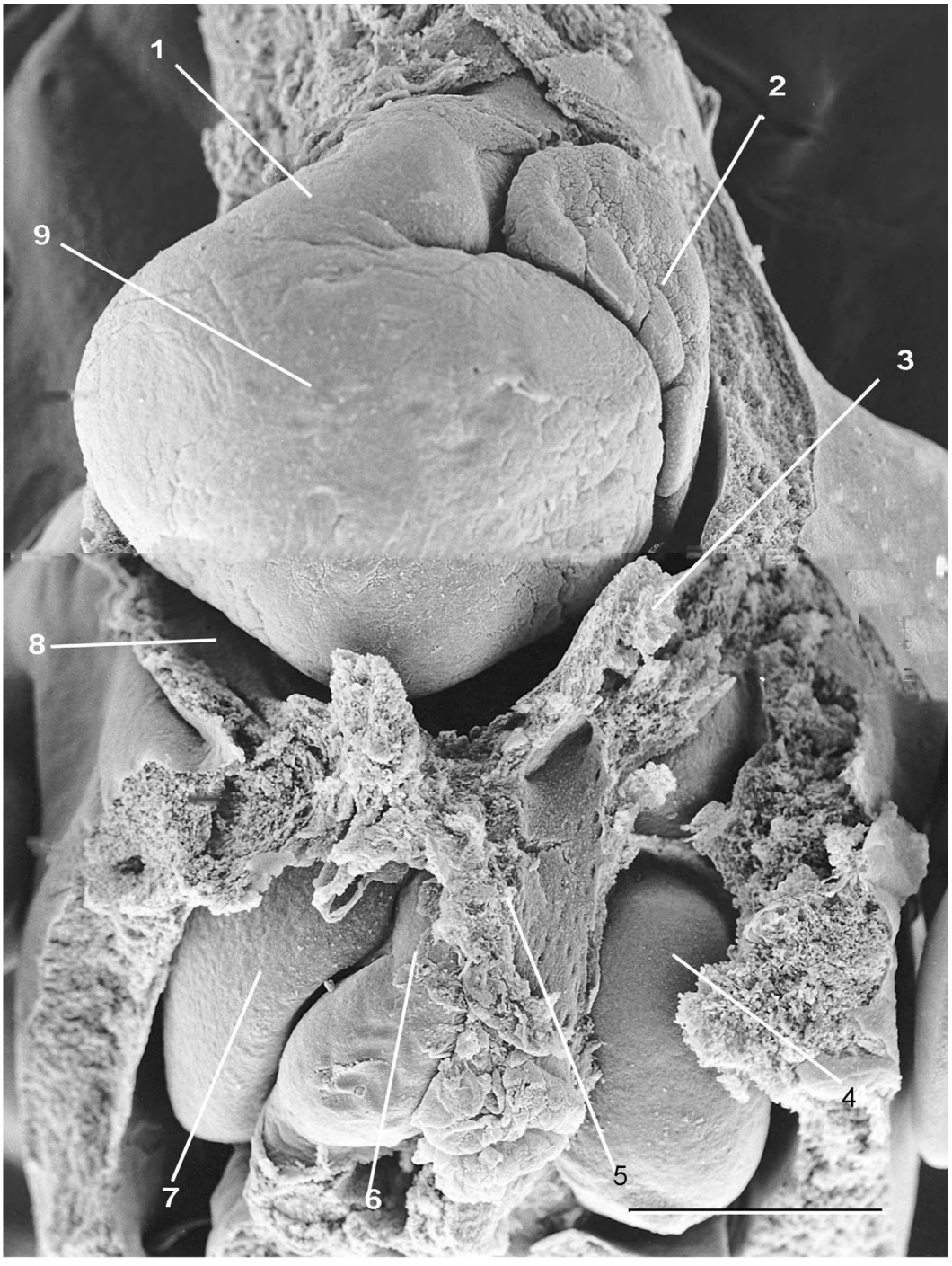

Downloaded from Vet-eBooks.com

Plate 39 Internal organs: intestinal and urogenital systems

Scanning electron micrographs showing the developing gut, kidneys and gonads.

(a) Abdominal cavity of an embryo at stage 35 (9 days incubation). Bar = 1 mm.

(b) Enlargement of colon seen in (a). Bar = 500 μm.

1. duodenum
2. gizzard
3. right ovary
4. metanephric duct
5. dorsal mesentery
6. mesonephros
7. left Mullerian duct
8. colon
9. mesentery
10. rectum

Downloaded from Vet-eBooks.com

Plate 39

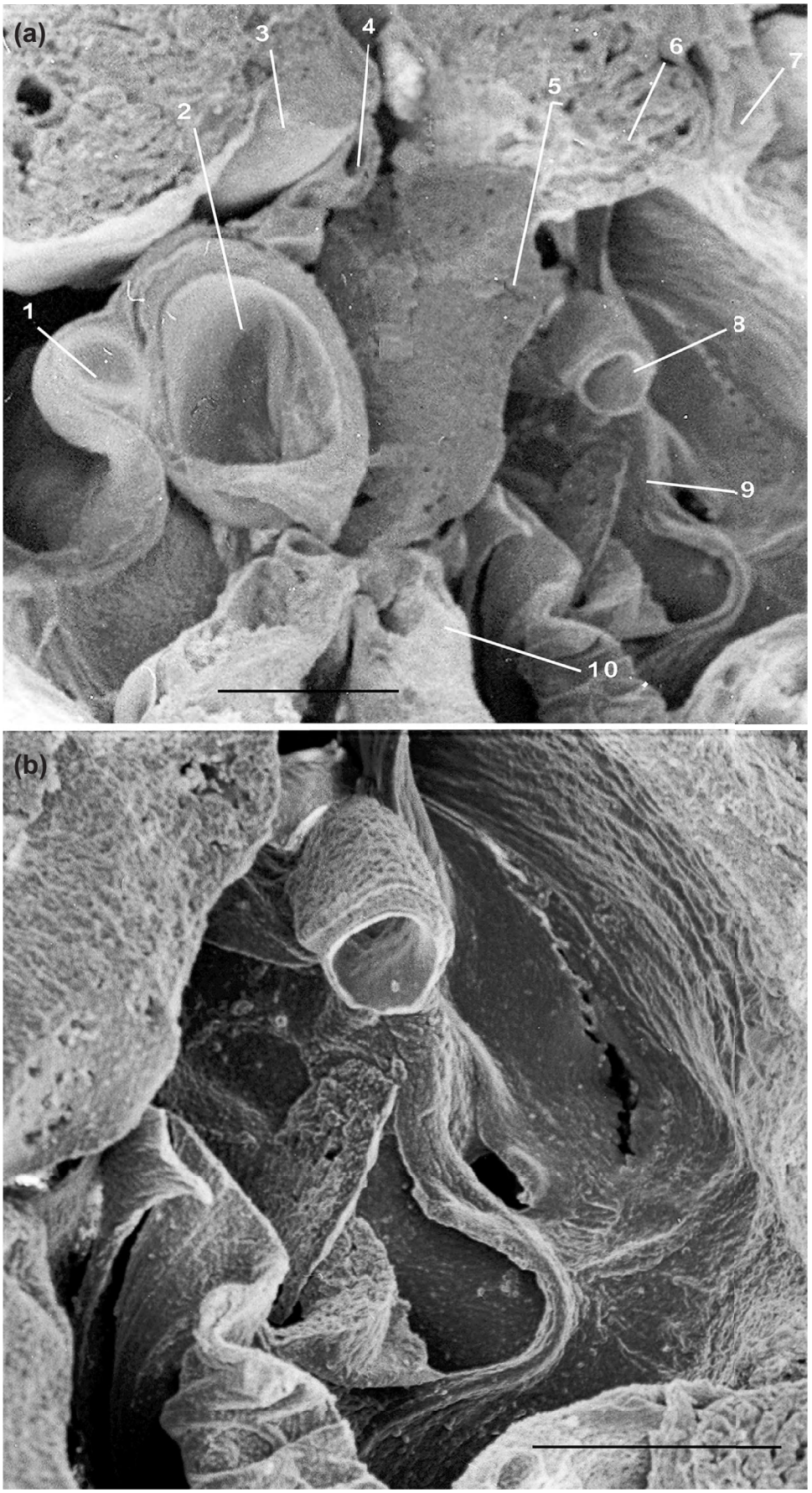

Downloaded from Vet-eBooks.com

Plate 40 Internal organs: heart and gizzard

Scanning electron micrographs showing the thoracic region of a stage 39 embryo (13 days incubation).

(a) The ventral body wall has been removed to reveal the liver, heart and gizzard. Bar = 3 mm.

(b) Enlargement of the gizzard in (a). Bar = 750 μm.

(c) Enlargement of the heart in (a). Due to the angle of section, both the interatrial and interventricular septa are visible as frontal sections. Bar = 500 μm.

1. liver
2. gizzard
3. sinus venosus
4. interatrial septum
5. pericardial cavity
6. coronary artery
7. left atrium
8. sinus venosus
9. left atrioventricular canal
10. interventricular septum
11. right atrio-ventricular canal
12. lumen of right ventricle

Downloaded from Vet-eBooks.com

Plate 40

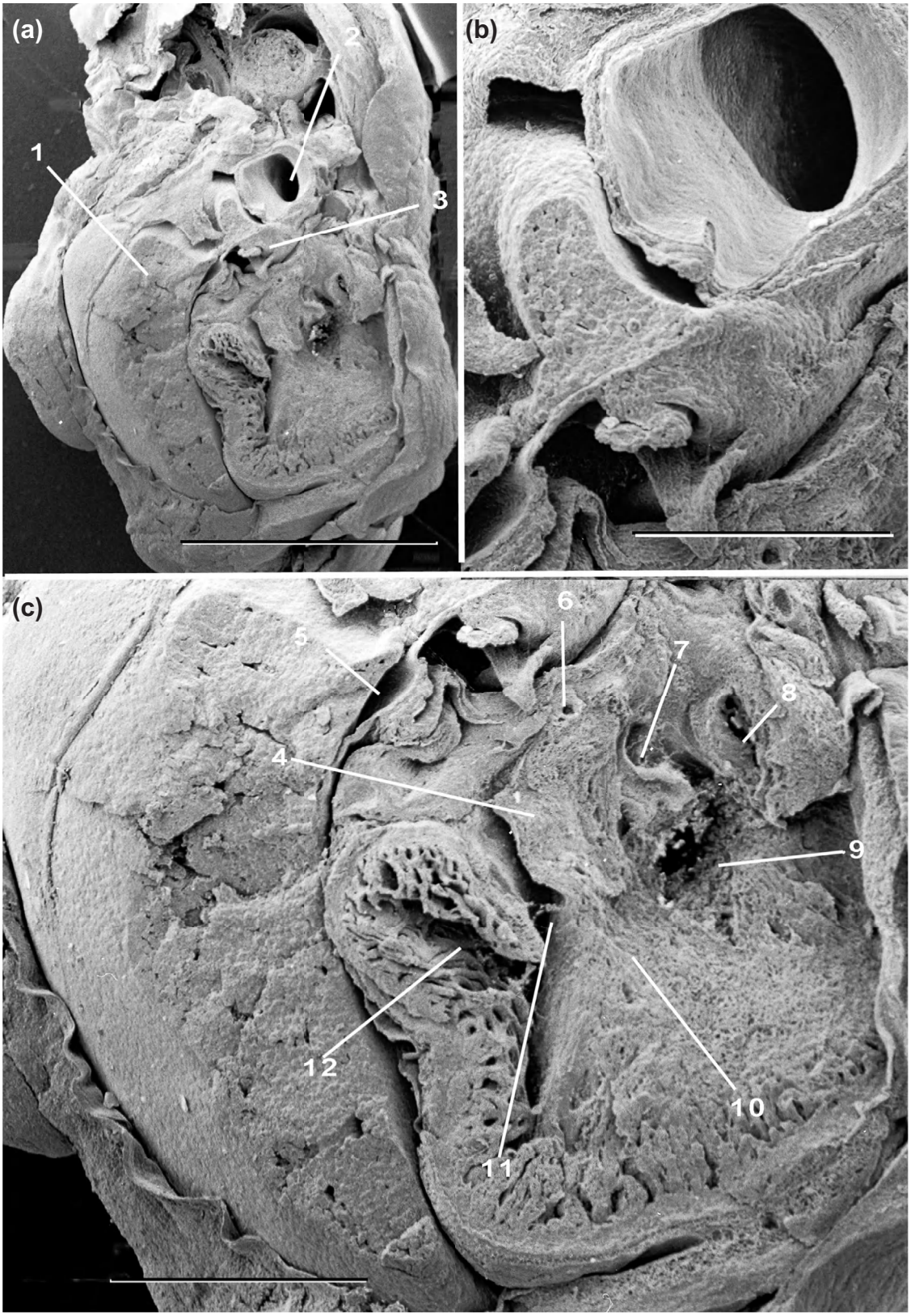

Downloaded from Vet-eBooks.com

Plate 41 Internal organs: liver and ventricle

Scanning electron micrographs of a section through a 5 day embryo (stage 26–27).

(a) Section through liver in (e) below. Bar = 500 μm.

(b) Enlargement of part of liver in (e). Bar = 50 μm.

(c) Section through ventricle in (e). Bar = 500 μm.

(d) Section through ventricle adjacent to that in (c). Bar = 500 μm.

(e) Section through liver and ventricle at 5 days.

1. liver sinus
2. parenchyma
3. myocardium
4. red blood corpuscles (avian red blood corpuscles retain their nuclei and so are not biconcave like those of mammals)
5. ventricle
6. wall of atrium
7. liver

Downloaded from Vet-eBooks.com

Plate 41

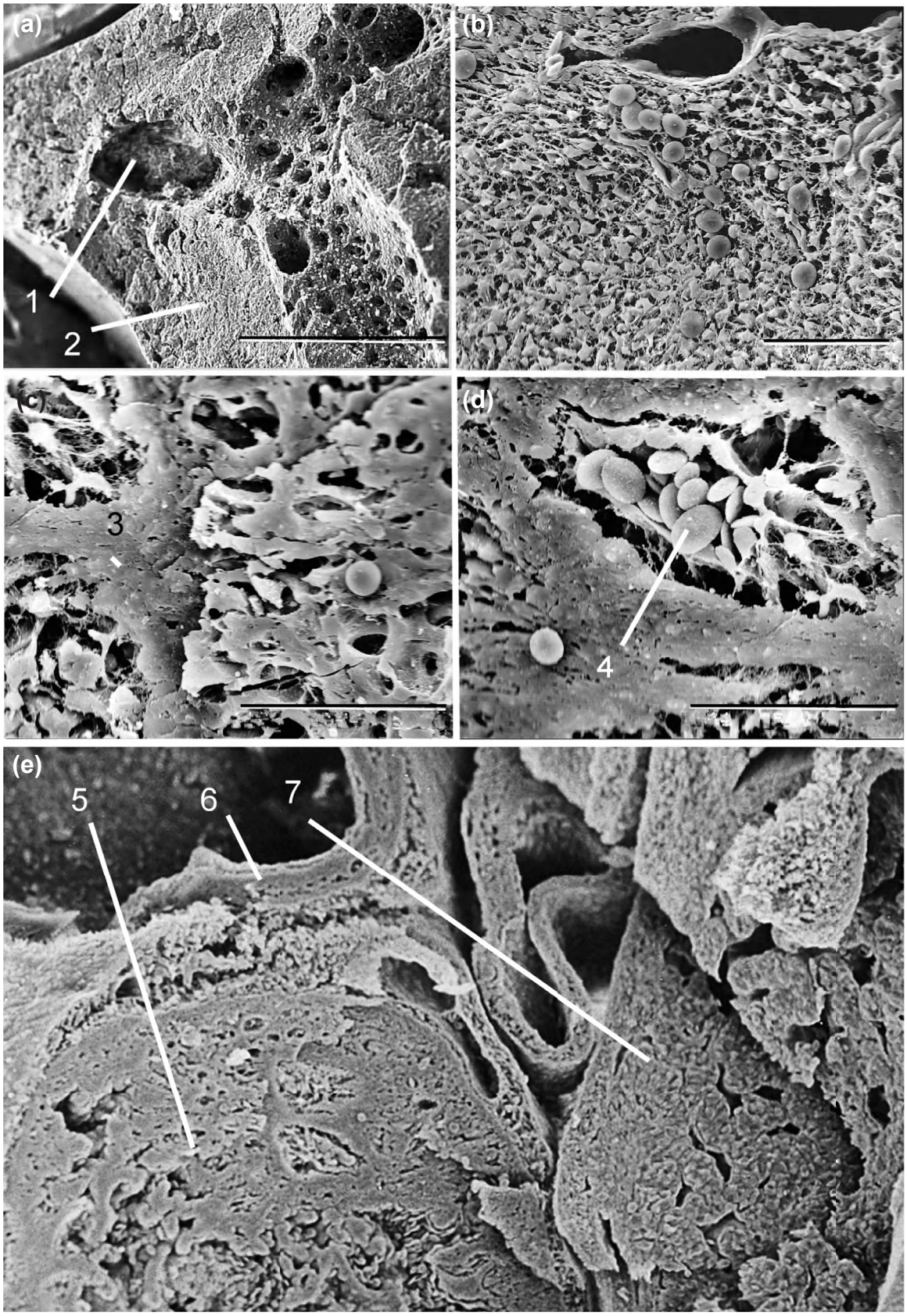

Downloaded From Vet-eBooks.com

Plate 42 Aortic arches

(a) Anterior right oblique view of the cardiovascular system from a μ-CT-scan of a stage 27 (5.5 days) embryo showing the third, fourth and sixth aortic arches.

(b) Frontal view of the heart in a stage 34 (8 days) normal embryo. A portion of the right ventricular wall has been cut open to show the interventricular septum.

AA: allantoic artery

Ao: aortic arch

Atr: atrium

B: right brachio-cephalic vessel

B': left brachiocephalic vessel

Ct: conotruncus

DA: dorsal aorta

IVS: interventricular septum

LA: left atrium

LV: left ventricle

OMP: fused omphalomesenteric veins

PA: pulmonary artery.

RA: right atrium

RV: right ventricle

From Hu *et al.* (2009), with permission of John Wiley and Sons Inc.

Downloaded from Vet-eBooks.com

Plate 42

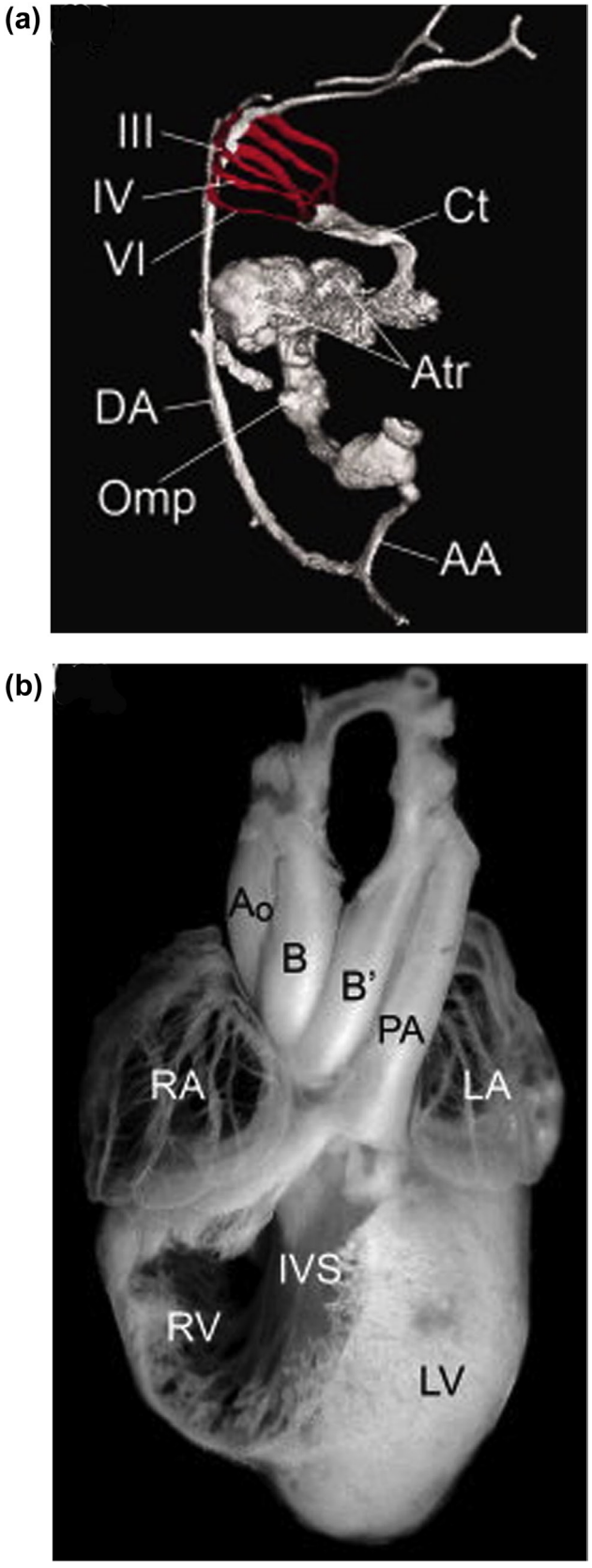

Downloaded from Vet-eBooks.com

Plate 43 Blood vessel formation

Scanning electron micrographs showing early stages of blood vessel formation. All specimens are viewed from the ventral side after removal of the endoderm.

(a) Angioblastic plexus in the area vasculosa of a stage 8 embryo (26–29 h incubation). Bar = 50 μm.

(b) Angioblastic plexus in a stage 9 embryo (29–33 h) in the process of forming the dorsal aorta. Bar = 50 μm.

(c) Angioblastic plexus at a slightly more advanced stage (stage 9–10) during the formation of the dorsal aorta. Bar = 50 μm.

(d) Developing left vena cava and intersegmental veins of a stage 10 embryo (33–38 h). Bar = 50 μm.

1. angioblastic plexus
2. mesoderm cell
3. dorsal aorta
4. pores between as yet incompletely fused angioblasts
5. left anterior cardinal vein forming
6. developing intersegmental artery
7. somite
8. neural tube
9. lateral plate mesoderm

Reprinted from Hirakow and Hiruma (1981), with permission from Springer-Verlag.

Downloaded from Vet-eBooks.com

Plate 43

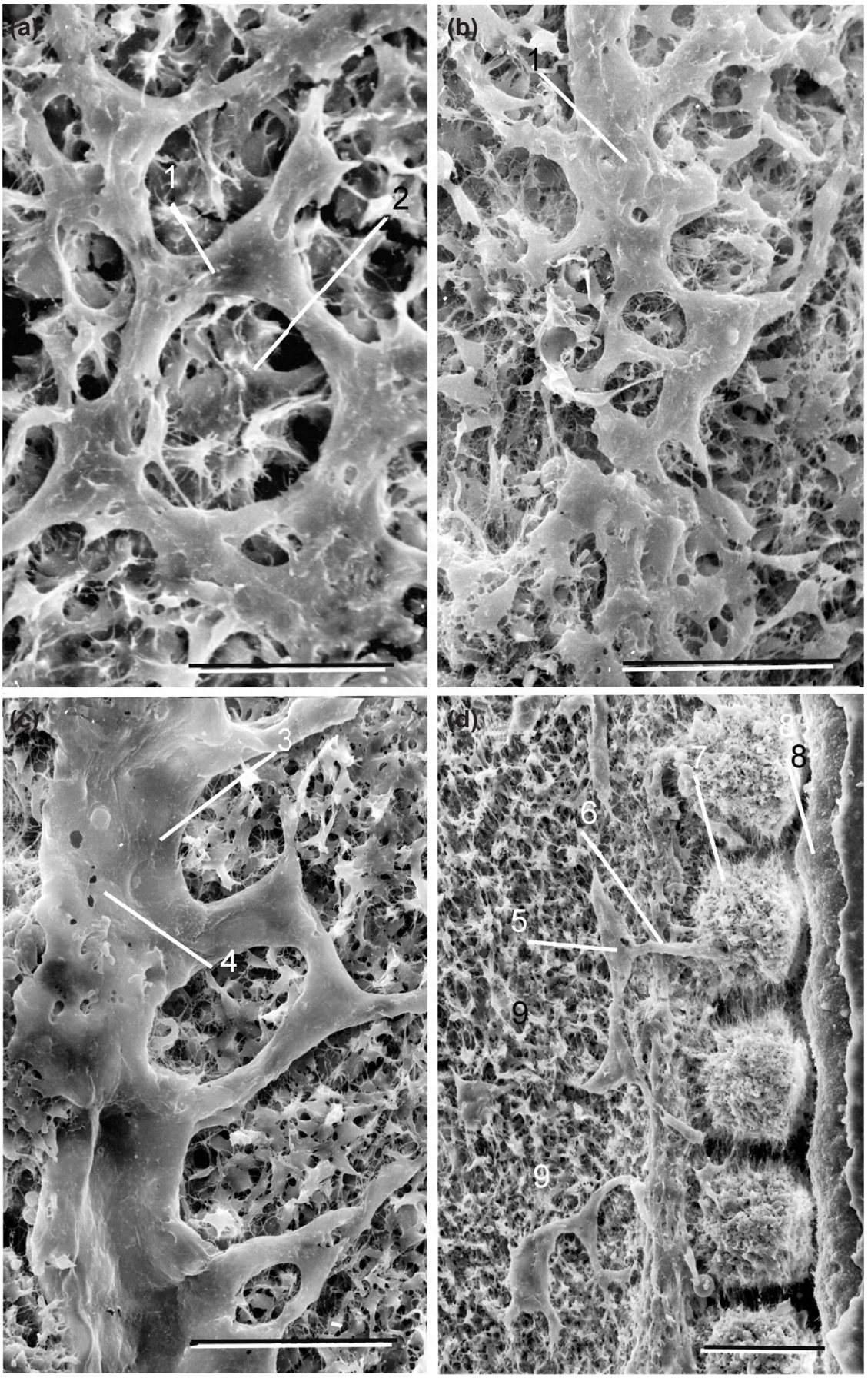

Downloaded from Vet-eBooks.com

Plate 44 Vascularization of the chorioallantoic membrane

Scanning electron micrographs showing vascularization of the chorioallantoic membrane at different stages. Arrows indicate where 'feed vessels' merge with the capillary network.

(a) 11 days of incubation (stage 37). Bar = 300 μm.

(b) 14 days of incubation (stage 40). There is a marked increase in the number of branches in the capillary network. Bar = 300 μm.

Reprinted from Djonov *et al.* (2000), with permission of Springer-Verlag.

Downloaded from Vet-eBooks.com

Plate 44

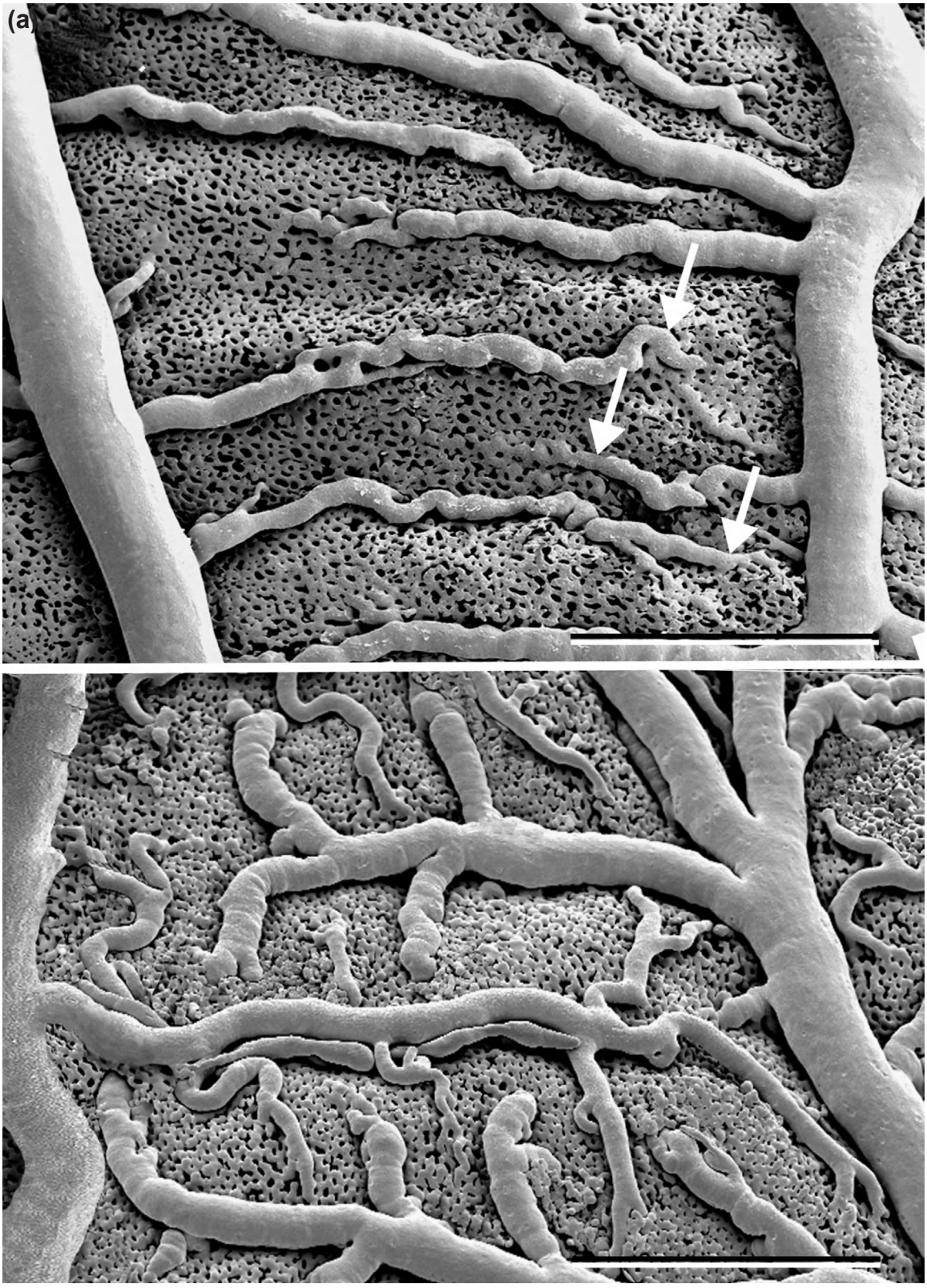

Downloaded from Vet-eBooks.com

Plate 45 Pharyngeal arch arteries I

Scanning electron micrographs showing a left side view of casts of the pharyngeal arch arteries. The individual pharyngeal arteries are labeled I–VI. The leg plexus, the tail bud plexus and the intersegmental arteries are also visible in (b), but not labeled.

(a) Stage 19 (68–72 h incubation). Bar = 250 μm.

(b) Stage 20 (70–72 h), general view. Bar = 250 μm.

(c) Stage 20. Bar = 250 μm.

(d) Stage 23 (4 days). Bar = 250 μm.

(e) Stage 24 (4.5 days). Bar = 250 μm.

1. dorsal aorta
2. ventral aorta
3. anterior cardinal vein
4. superficial capillary plexus of the mandibular arch
5. superficial capillary plexus of the hyoid arch
6. aortic root
7. plexus of wing bud
8. omphalo-mesenteric (vitelline) artery
9. blood vessels in allantois
10. truncus arteriosus
11. heart
12. eye
13. pulmonary artery
14. primary external carotid artery
15. stapedial artery

Reprinted from Hiruma and Hirakow (1995), with permission of Springer-Verlag.

Downloaded from Vet-eBooks.com

Plate 45

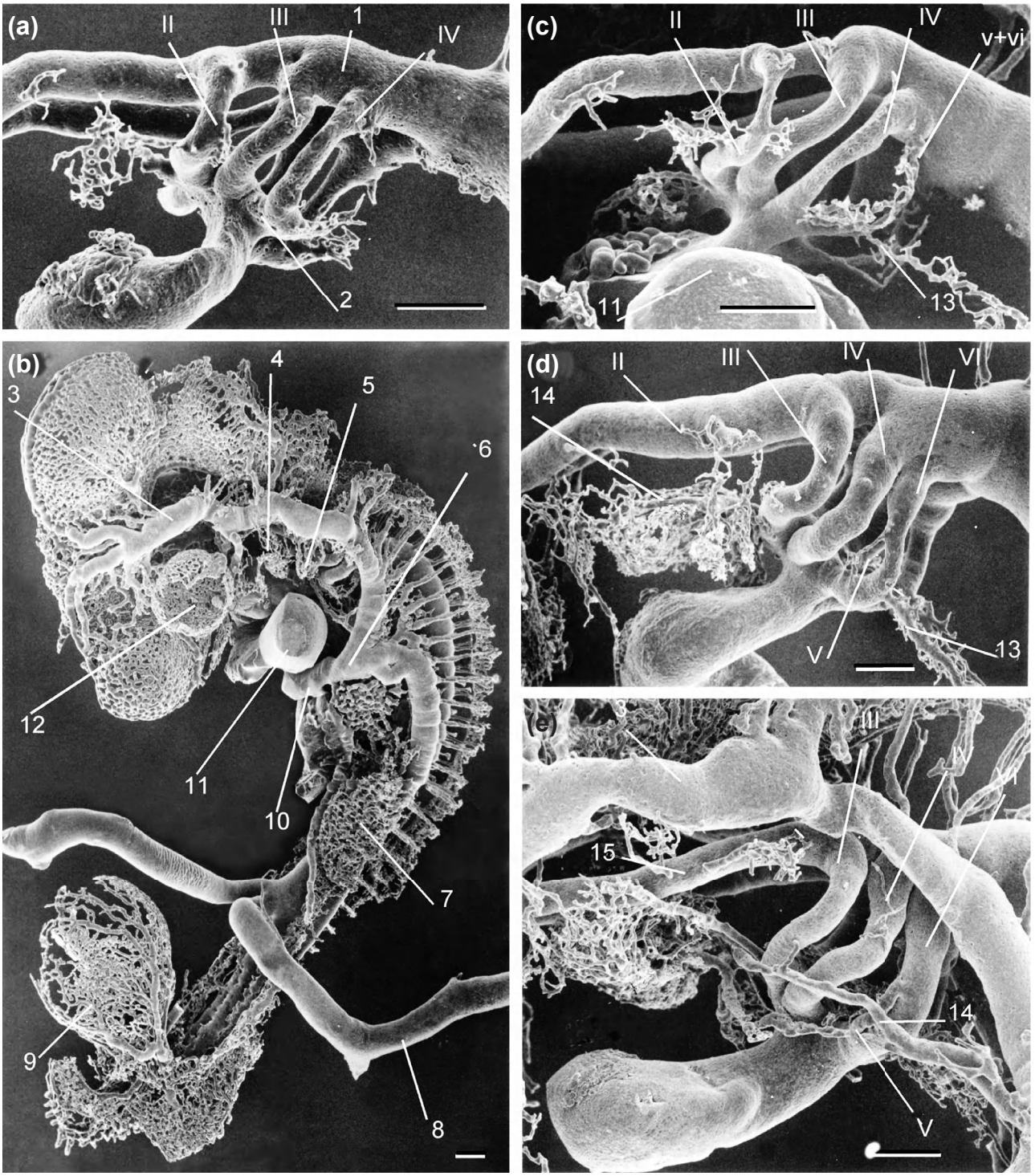

Downloaded from Vet-eBooks.com

Plate 46 Pharyngeal arch arteries II

Scanning electron micrographs showing casts of the pharyngeal arch arteries at later stages. The individual pharyngeal arteries are labeled I–VI.

(a) Stage 25 (4.5–5 days incubation). Bar = 0.5 mm.

(b) Stage 25. Bar = 0.5 mm.

(c) Stage 26 (5 days). Bar = 0.7 mm.

(d) Stage 27 (5–5.5 days). Bar = 0.5 mm.

(e) Stage 28 (5.5–6 days). Bar = 0.7 mm.

1. supraorbital branch of stapedial artery
2. stapedial artery
3. capillary plexus draining into supraorbital vein
4. secondary external carotid artery
5. primary external carotid artery
6. carotid duct
7. pulmonary artery
8. secondary subclavian artery
9. primary subclavian artery
10. anterior mesenteric artery
11. coeliac artery

Reprinted from Hiruma and Hiakow (1995), with permission of Springer-Verlag.

Downloaded from Vet-eBooks.com

Plate 46

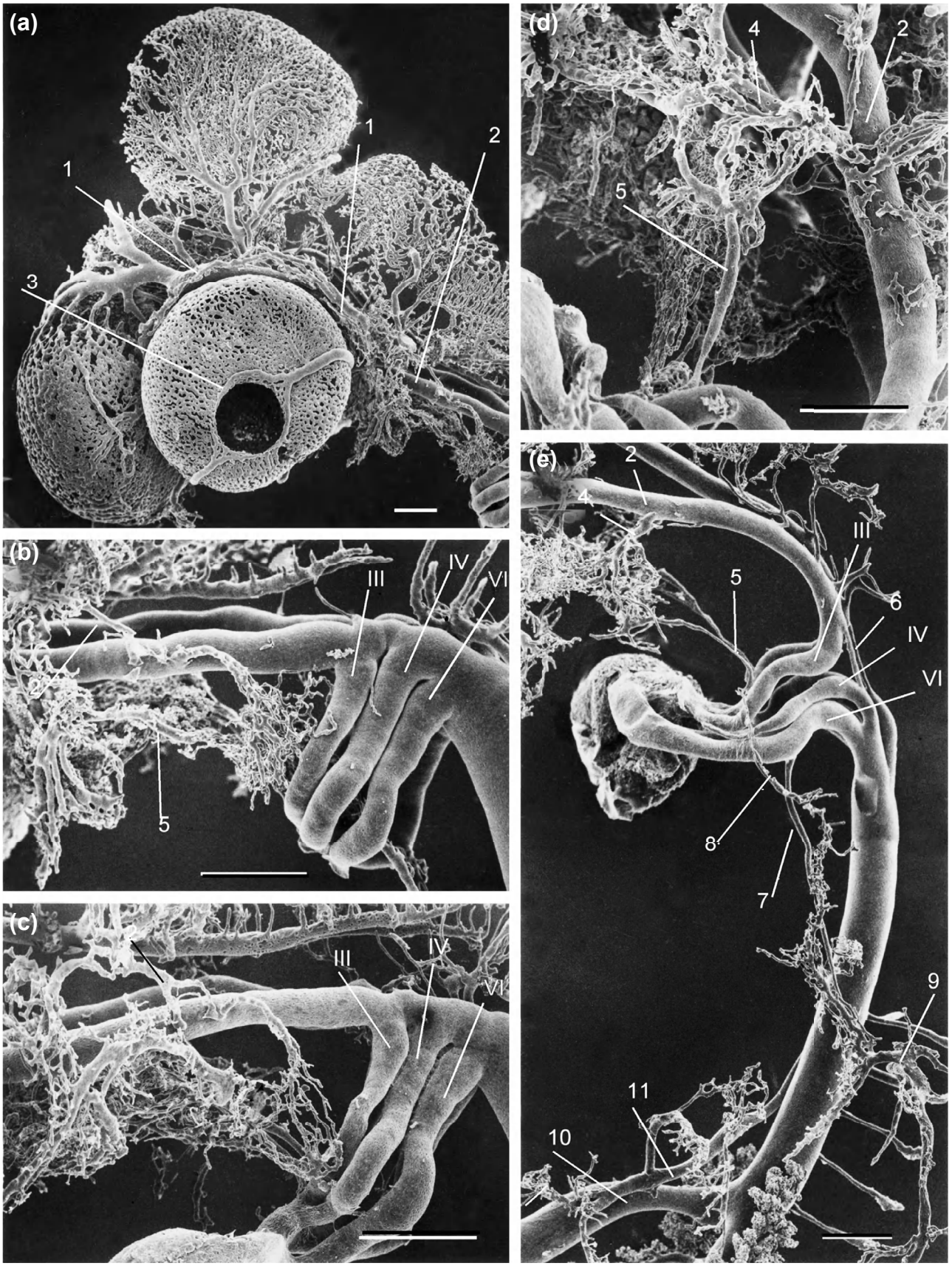

Downloaded from Vet-e-Books.com

Plate 47 Blood vessels in the trunk I

Scanning electron micrograph of a vascular cast showing a dorsal view of the mesonephric region in an embryo at stage 32 (7.5 days). Bar = 400 μm.

1. dorsal aorta
2. external iliac artery
3. great renal vein (future metanephric venous system)
4. posterior mesonephric portal vein (formed from posterior cardinal vein)
5. sciatic artery
6. allantoic artery
7. caudal artery
8. mesonephros

Modified from Carretero *et al.* (1993), with permission of *Scanning Electron Microscopy.*

Downloaded from Vet-eBooks.com

Plate 47

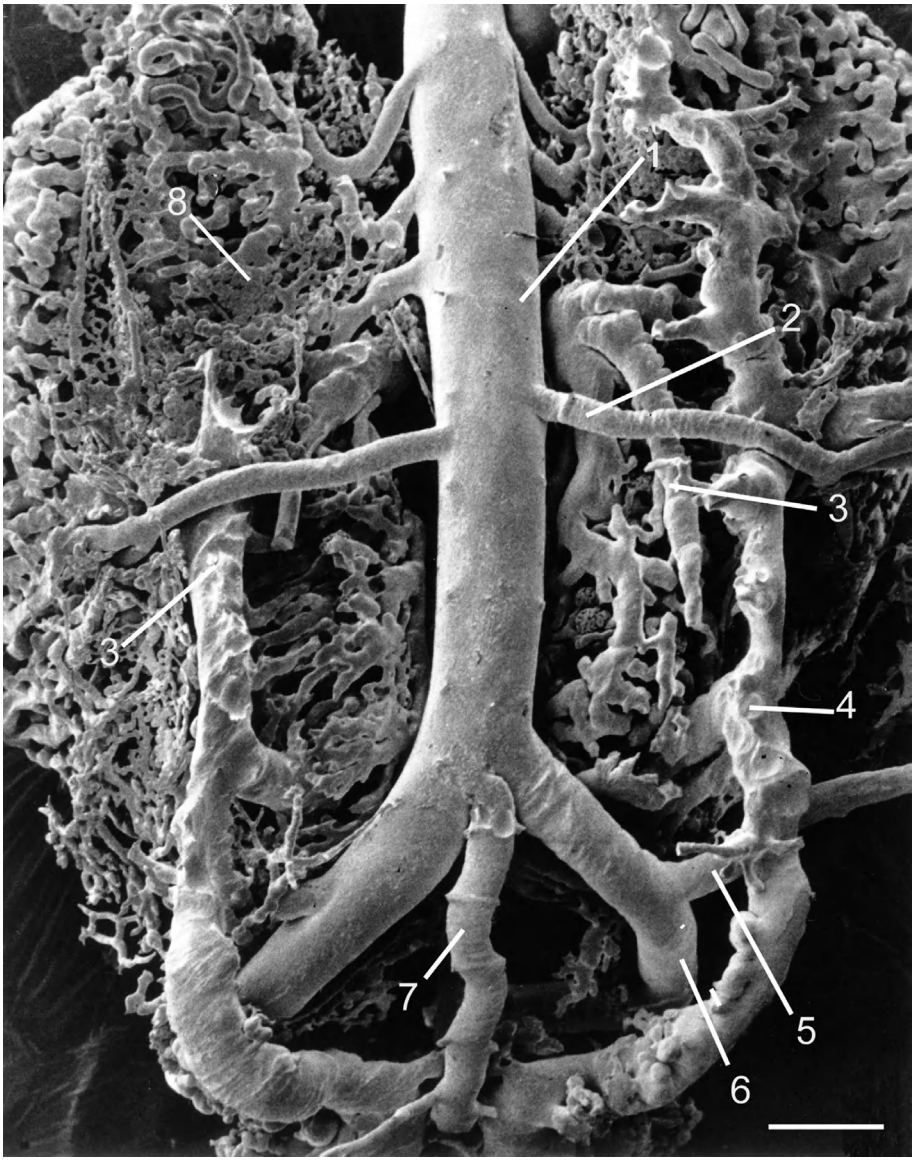

Downloaded From Vet-eBooks.com

Plate 48 Blood vessels in the trunk II

Scanning electron micrographs of vascular casts of the trunk at different stages.

(a) Ventral aspect of a vascular cast of the mesonephros in a quail embryo incubated for 6 days. Bar = 500 μm.

(b) Mesonephric glomerulus of a chick embryo at stage 22 (3.5 days). Bar = 12 μm.

(c) Metanephric glomerulus of a chick embryo at stage 37 (11 days). Bar = 3 μm.

(d) Dorsal aspect of the dorsal aorta in a chick embryo at stage 32 (7.5 days) to show the origin of the primary mesonephric arteries. Bar = 400 μm.

(e) Dorsal view of a vascular cast in a stage 40 chick embryo (14 days). Part of the metanephros has been removed to allow observation of the anterior metanephric portal vein. Bar = 600 μm.

1. dorsal aorta
2. subcardinal venous plexus
3. subcardinal veins
4. posterior vena cava
5. anterior mesenteric artery
6. primary mesonephric arteries
7. external iliac artery
8. origins of intersegmental arteries
9. anterior metanephric portal vein
10. branches to middle renal division of the metanephros
11. posterior metanephric portal vein
12. external iliac vein
13. common iliac vein

(a) Reprinted from Arcalis *et al.* (2002), with permission of Springer-Verlag.

(b–e) Reprinted from Carretero *et al.* (1995), with permission of John Wiley and Sons Inc.

Downloaded from Vet-eBooks.com

Plate 48

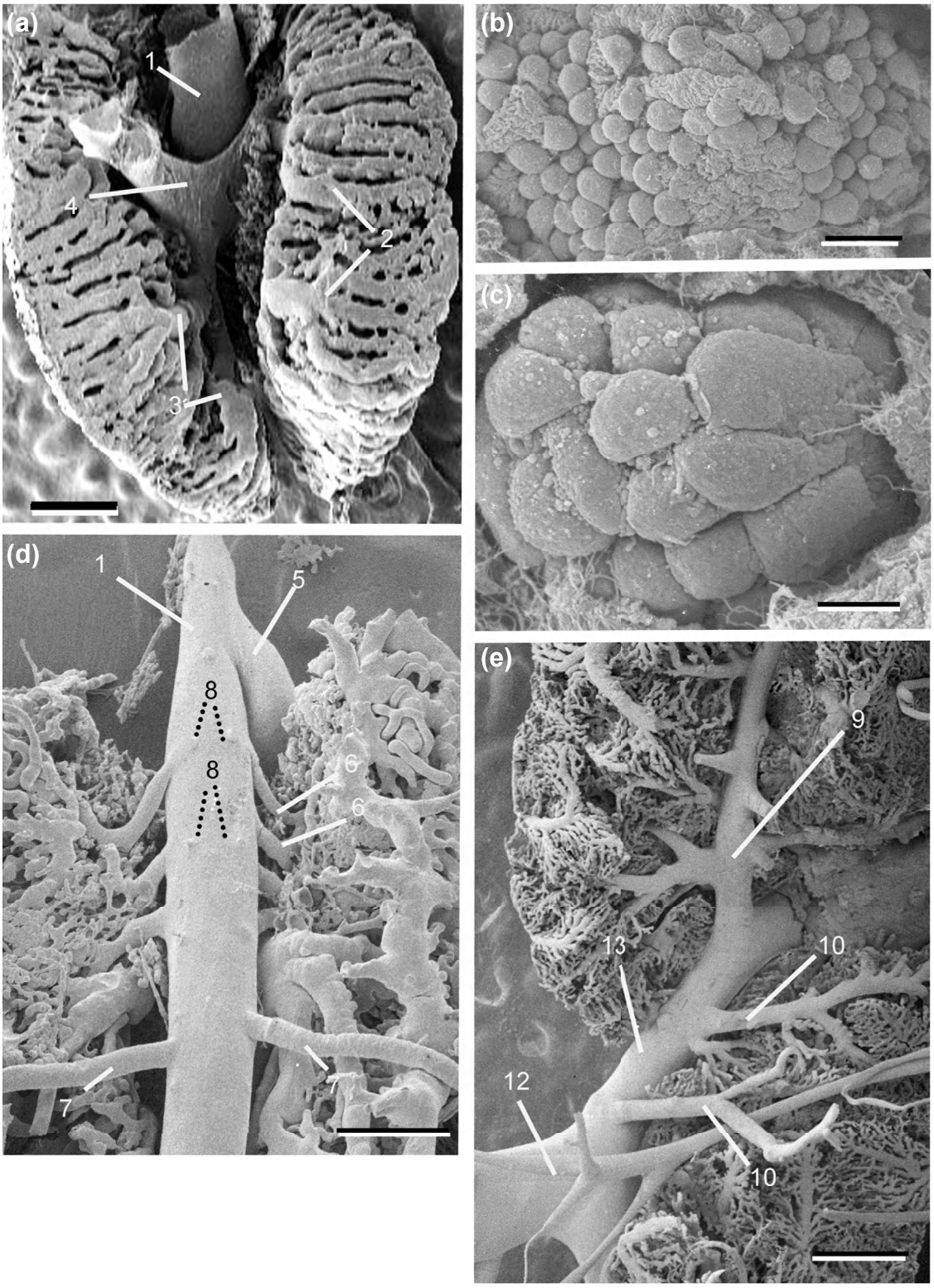

Downloaded from Vet-eBooks.com

Plate 49 Intestinal and urogenital systems

Scanning electron micrographs of abdominal structures at different stages.

(a) Small intestine of a stage 31 embryo (7 days). Bar = 200 μm.

(b) Enlargement of (a) to show left nephric duct and left subclavian vein in genital (nephrogenic) ridge. Bar = 100 μm.

(c) Mesonephros and oviduct of a stage 35 embryo (9 days). Bar = 130 μm.

1. lumen of intestine
2. subclavian vein
3. nephric duct
4. Mullerian duct (oviduct)

Downloaded from Vet-eBooks.com

Plate 49

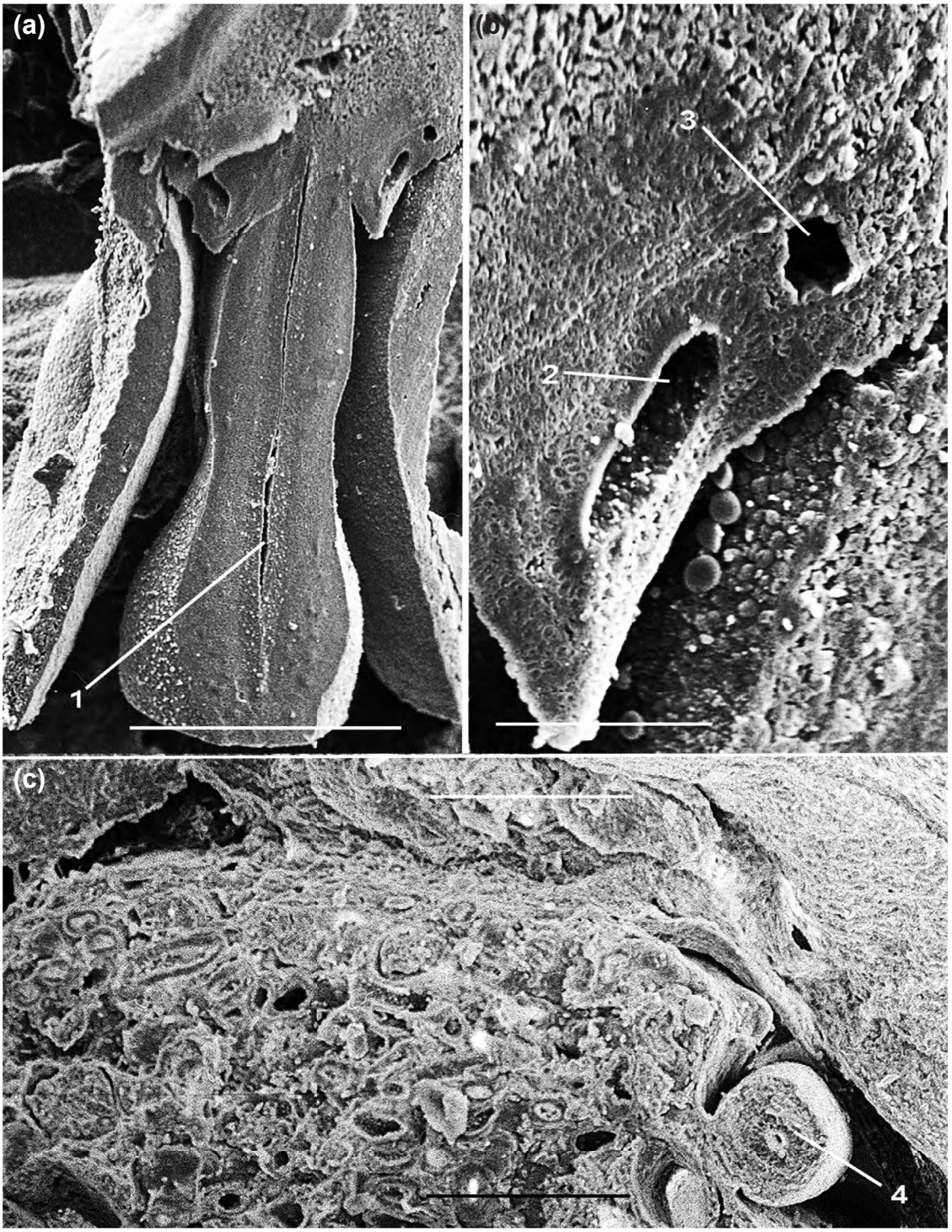

Downloaded From Vet-eBooks.com

Plate 50 Nephric duct

Scanning electron micrographs showing the nephric duct in a stage 14 embryo (50–53 hours incubation).

(a) Left lateral view after removal of the ectoderm. Bar = 500 μm.

(b, c) Enlargements at the posterior end of the mesonephros to show the posterior tip of the nephric duct. Bar of (b) = 130 μm; bar of (c) = 50 μm.

1. mesonephros
2. neural tube
3. somite
4. unsegmented mesoderm
5. tip of nephric duct

(c) Reprinted from Bellairs *et al.* (1995), with permission of John Wiley and Sons Inc.

Downloaded from Vet-eBooks.com

Plate 50

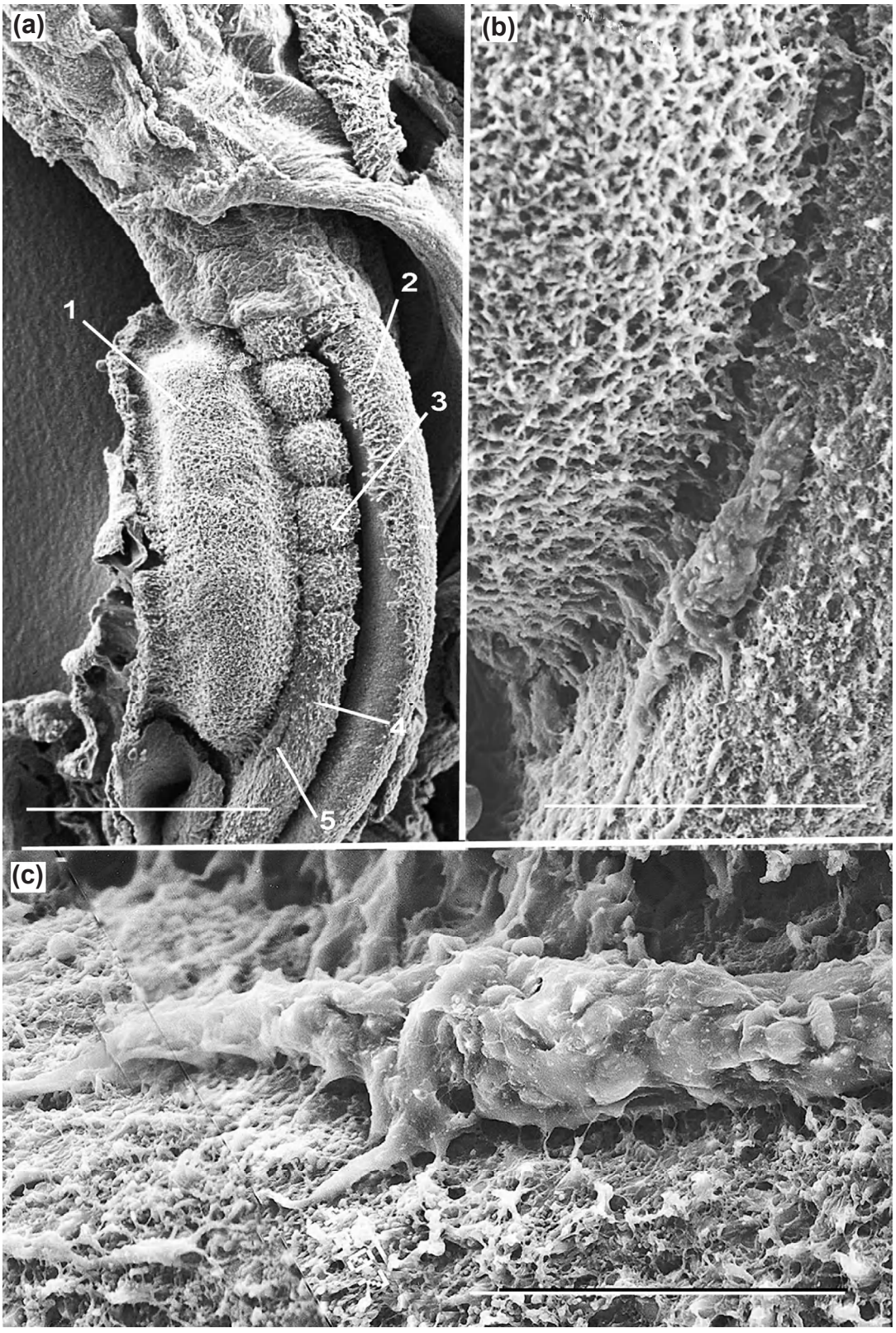

Downloaded from Vet-eBooks.com

Plate 51 Mesonephros

Scanning electron micrographs of the mesonephros.

(a) Section across the mesonephros of a 5 day embryo (stage 26–27). Bar = 25 μm.

(b) Enlargement of part of (a) to show a glomerulus. Bar = 15 μm.

1. nephric duct
2. red blood corpuscles in subcardinal vein

Downloaded from Vet-eBooks.com

Plate 51

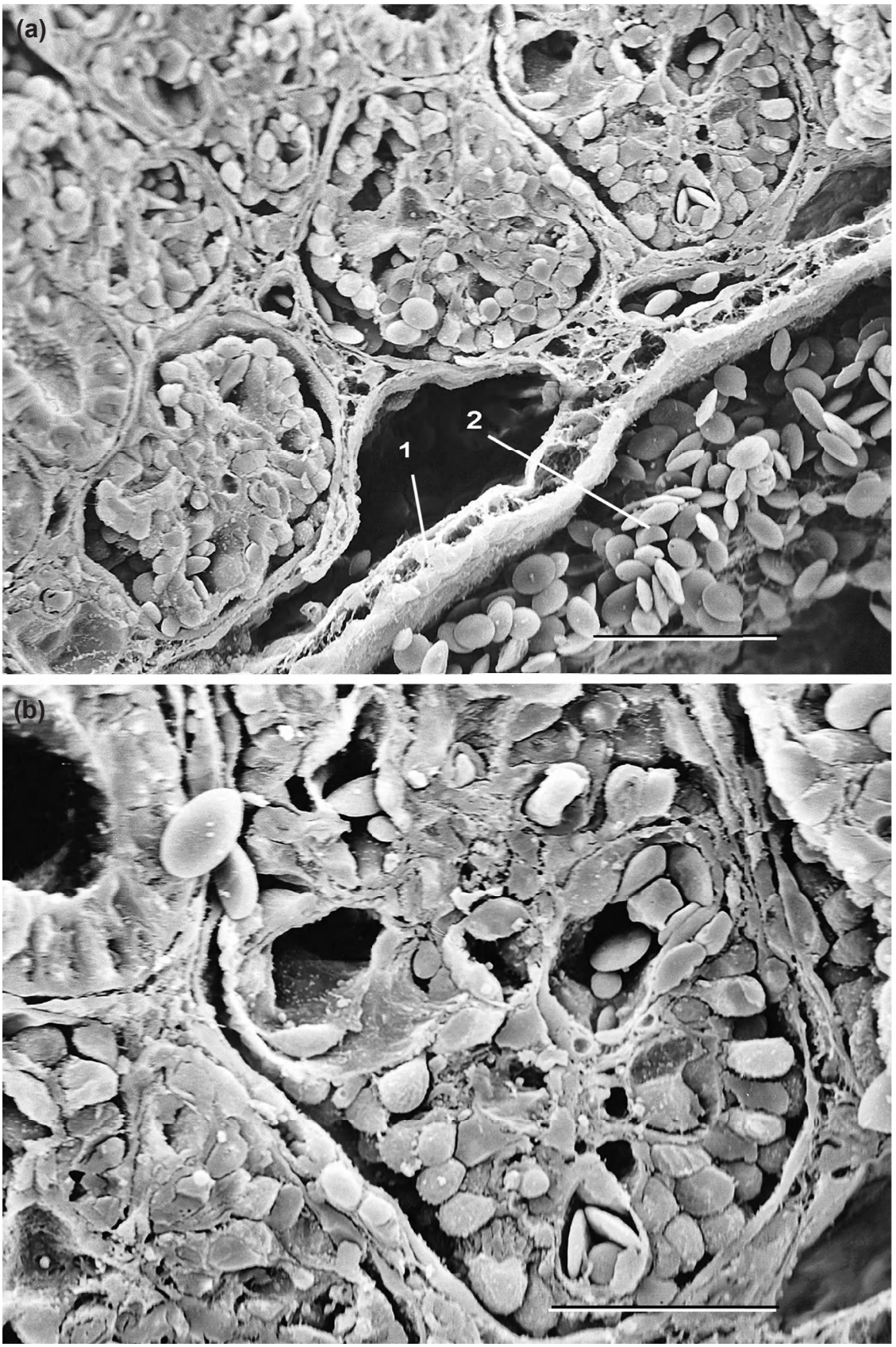

Downloaded From Vet-eBooks.com

Plate 52 Mullerian duct and mesonephros

Scanning electron micrographs of the Mullerian duct and mesonephros at different stages.

(a) Mullerian duct at stage 24 (4.5 days incubation) after removal of thoracic and abdominal organs. A row of nephrostomes is visible at the lateral side of the mesonephros. Bar = 100 μm.

(b) Enlargement of one of the nephrostomes in (a). Bar = 10 μm.

(c) Mullerian duct at stage 30 (6.5-7 days) to show the funnel opening. Bar = 10 μm.

1. external glomeruli
2. mesonephros
3. dorsal mesentery
4. gonad
5. Mullerian duct

Reprinted from Jacob *et al.* (1999), copyright Karger Publishers, Basel.

Downloaded from Vet-eBooks.com

Plate 52

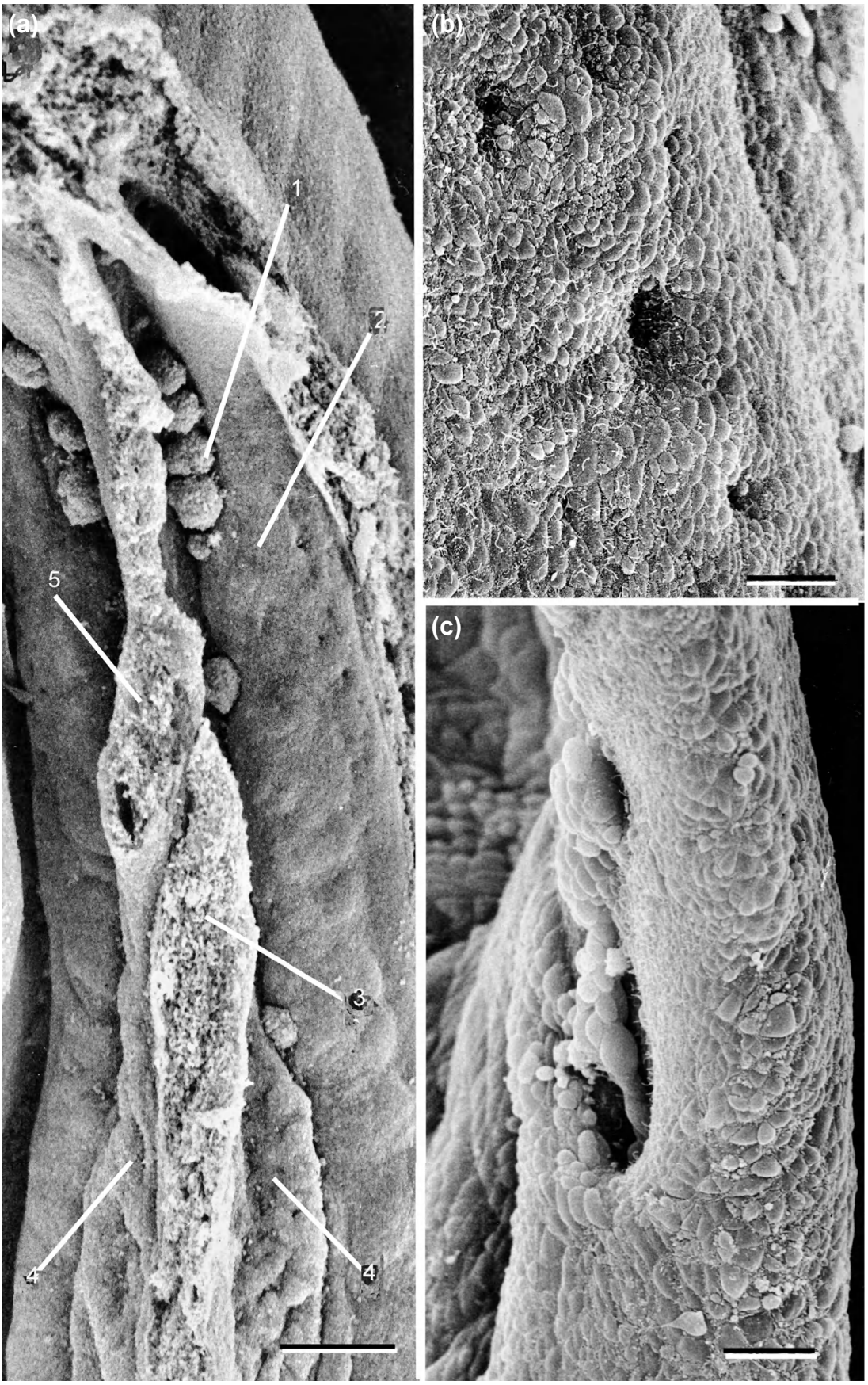

Downloaded from Vet-eBooks.com

Plate 53 Head and face

Scanning electron (a, b) and light (c) micrographs of the head and face at different stages.

(a) Stage 20 (70–72 h incubation).

(b) Stage 28 (5.5–6 days).

(c) Stage 36 (10 days).

1. frontonasal process
2. nasal placode
3. maxillary process
4. oral cavity
5. mandibular process
6. second pharyngeal arch
7. cut surface of pharynx
8. eye
9. egg tooth
10. external ear cavity

(a) Reprinted with alterations from McGonnell *et al.* (1998), with permission of John Wiley and Sons Inc.

(b) Reprinted from Hu and Marcucio (2009a), with permission of the Company of Biologists Ltd.

Downloaded from Vet-eBooks.com

Plate 53

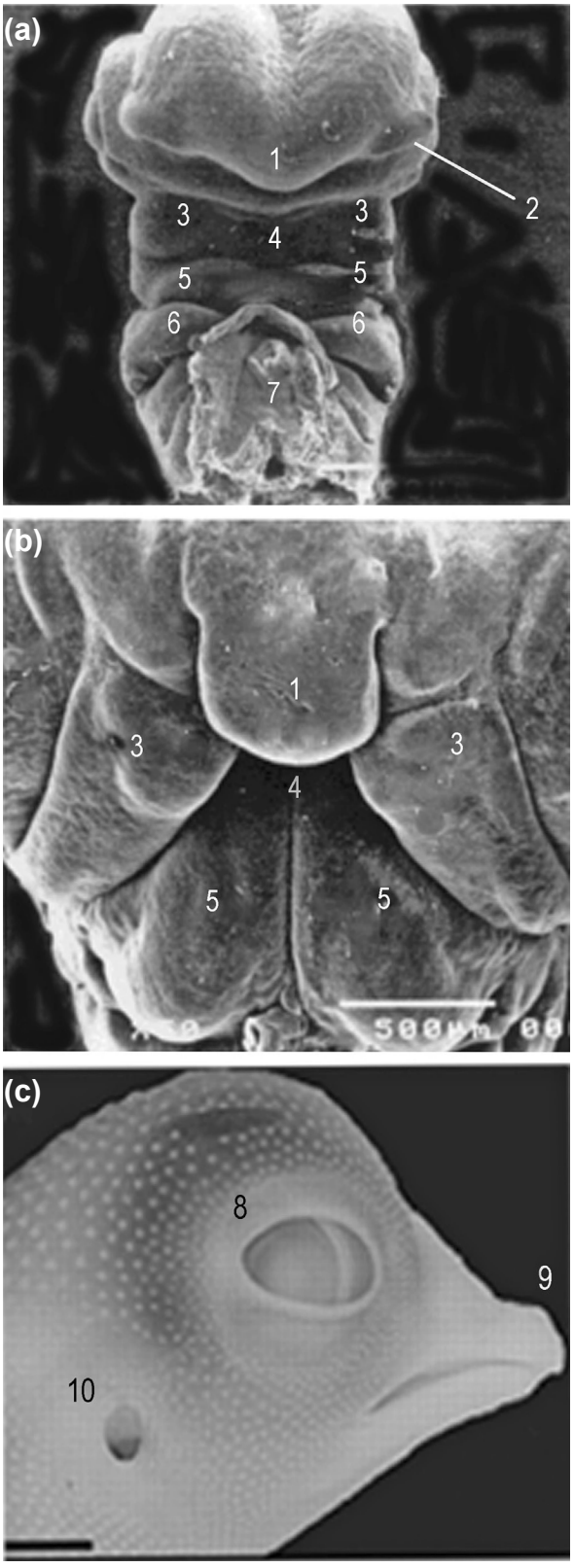

Downloaded from Vet-eBooks.com

Plate 54 External genitalia I

Scanning electron micrographs of a sequence of stages in the development of the external genitalia. Apart from (e) these are all seen in frontal view. The tail, or its cut edge, lies at the top of each image and the amnion at the bottom.

(a) 5 days incubation (about stage 26) showing genital eminences.

(b) 5.5 days incubation (about stage 27). The genital eminences have merged in the midline to become the genital tubercle. The genital crest lies between the genital tubercle and the tail bud. Divergent arrows indicate genital swelling; horizontal arrow points to genital crest.

(c) 6 days incubation (about stage 29). The genital crest has merged with the genital tubercle. Genital swellings overhang the genital tubercle. Arrow indicates phallic sulcus.

(d) 7 days incubation (about stage 31). The apex of the genital tubercle is now bilobed and its apical diameter is 350 μm.

(e) 8 days incubation (about stage 34) shown in lateral view. The genital swellings are now confluent with one another and have formed a collar around the genital tubercle.

(f) 9 days incubation (about stage 35). The collar now totally encloses the genital tubercle.

1. cut section across tail bud
2. left genital eminence
3. amnion
4. wall of tail bud
5. left genital swelling
6. genital tubercle
7. median phallic body (genital tubercle)
8. tip of genital tubercle
9. inner border of collar
10. phallic sulcus

All bars = 500 μm

Reprinted from Bakst (1986), with permission of *Scanning Electron Microscopy.*

Downloaded from Vet-eBooks.com

Plate 54

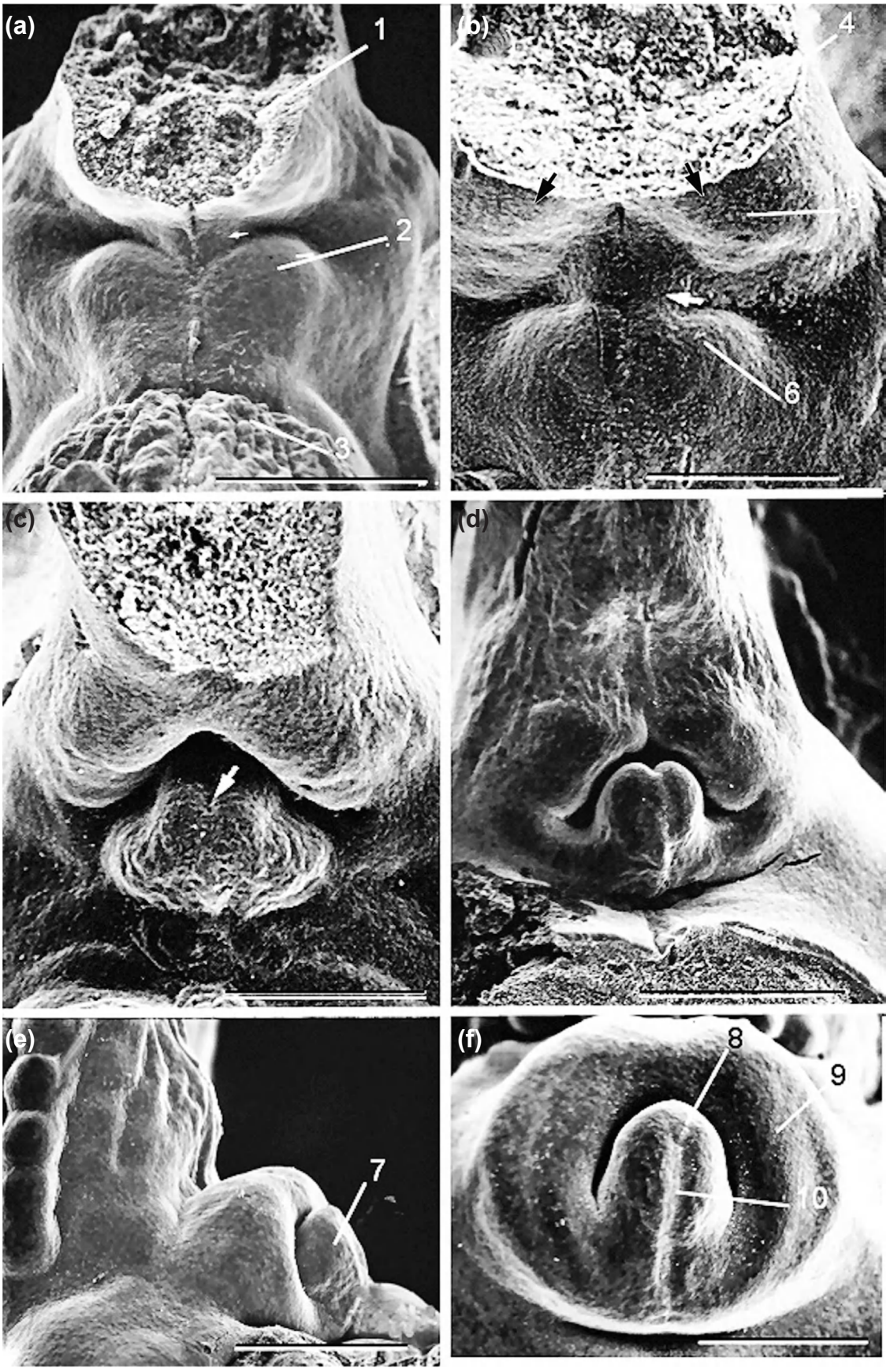

Downloaded from Vet-eBooks.com

Plate 55 External genitalia II

Scanning electron micrographs showing sequential development of the external genitalia at later stages.

(a) 12 days incubation (about stage 38): arrows indicate where the primordia for the lateral phallic bodies will arise.

(b) 15 days incubation (stage 40-41): the external cloaca has now developed folds (small arrows) around its periphery.

(c) 16 days incubation (stage 42): radially orientated folds are now present on both upper and lower cloacal lips. The dorsal lip now projects over the lower lip, giving the vent a slit-like appearance. The phallus is no longer visible externally.

All bars = 500 μm

Reprinted from Bakst (1986), with permission of *Scanning Electron Microscopy.*

Downloaded from Vet-eBooks.com

Plate 55

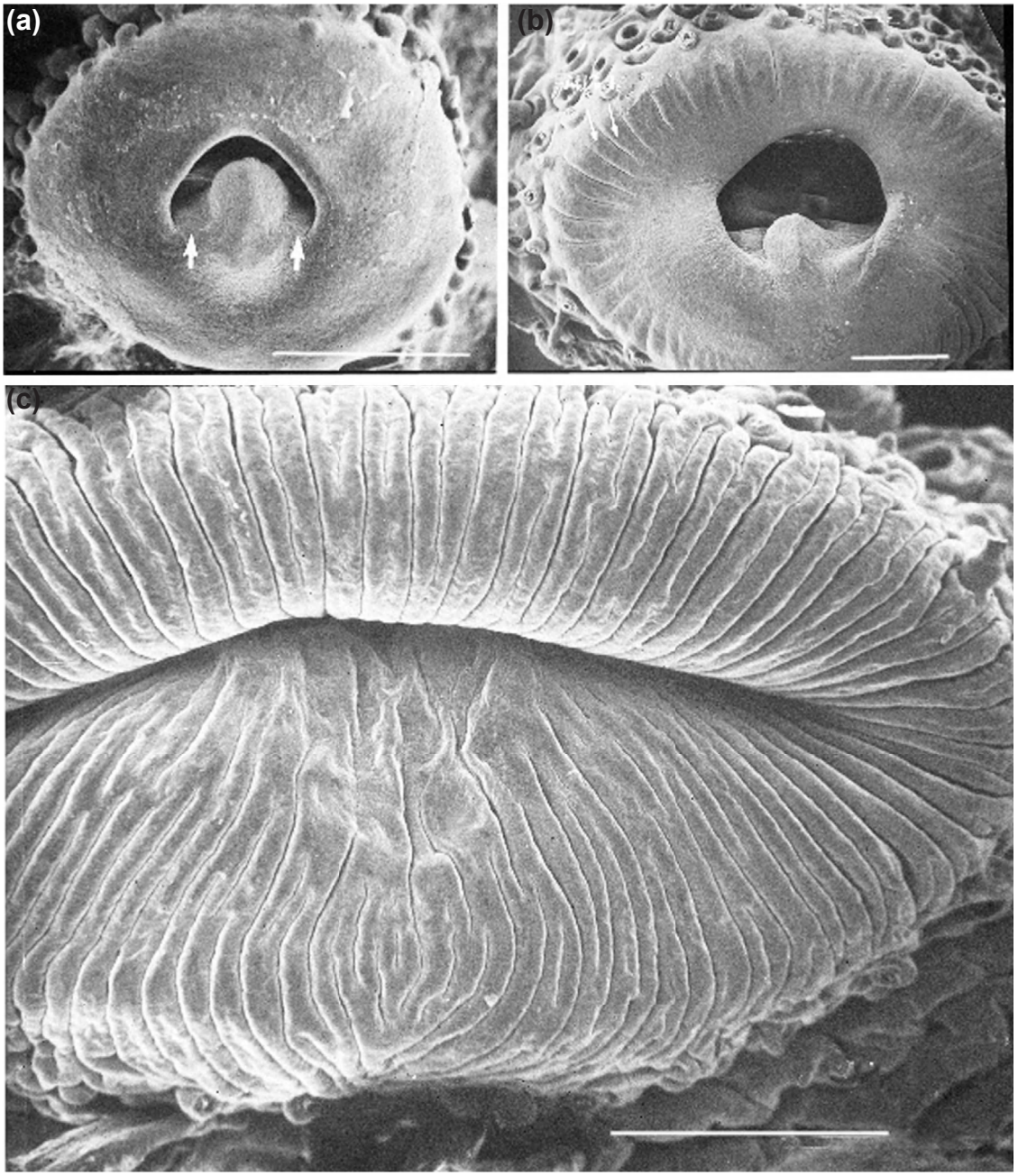

Downloaded From Vet-eBooks.com

Plate 56 Scanning electron micrographs of the lung

(a) Fracture through the lung of an 8-day (stage 34) embryo. Bar = 200 μm.

(b) Enlargement of a portion of (a). Bar = 100 μm.

Downloaded from Vet-eBooks.com

Plate 56

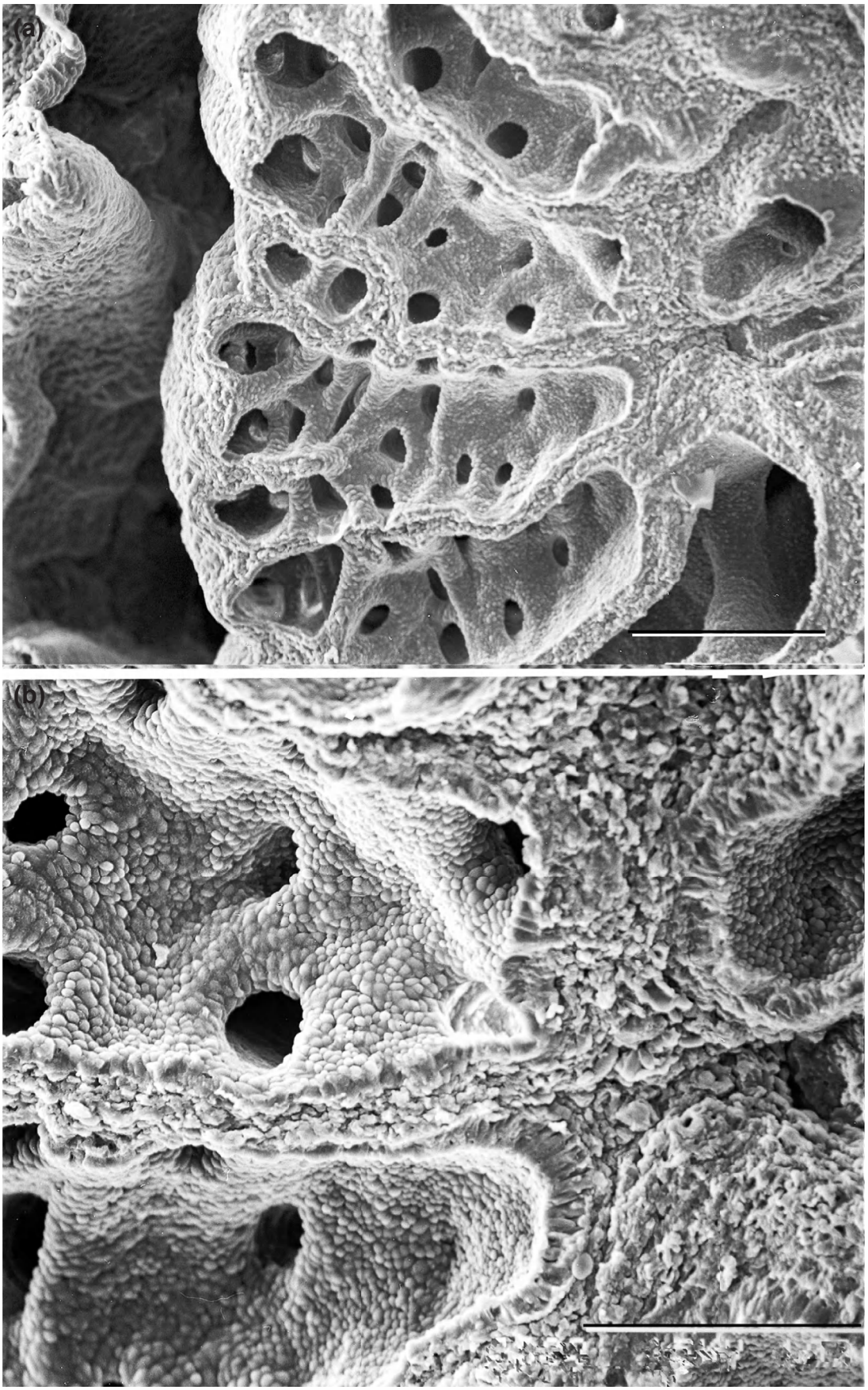

Downloaded from Vet-eBooks.com

Plate 57 Parabronchial architecture

Scanning electron micrographs of intravascular casts showing the arrangement of the parabronchial (PB) vessels in a 20 day (stage 45) embryo.

(a) 20 days incubation (stage 45). The capillary meshwork consists of hexagonal tubes surrounding the parabronchial lumina. The interparabronchial arteries and veins (A1 and V1) lie in the interparabronchial septa (arrowheads).

(b) Enlargement of (a) to show the interparabronchial artery (A1) running parallel to the long axis of the parabronchus.

(c) The interparabronchial vein runs parallel to the artery.

(d) The parabronchial arteries give rise to a meshwork of capillaries (*) surrounding the air capillaries in the parabronchial wall.

(e) The large interparabronchial vein (V1) receives the the parabronchial vein (V2).

(f) An enlargement of (e) to show vessels delineating the lung atria (circles).

A1, A2, A3: interparabronchial arteries

PB: parabronchium

V1, V2, V3, V4, V5: interparabronchial veins

From Makanya and Djonov (2009), with permission of John Wiley and Sons Inc.

Downloaded from Vet-eBooks.com

Plate 57

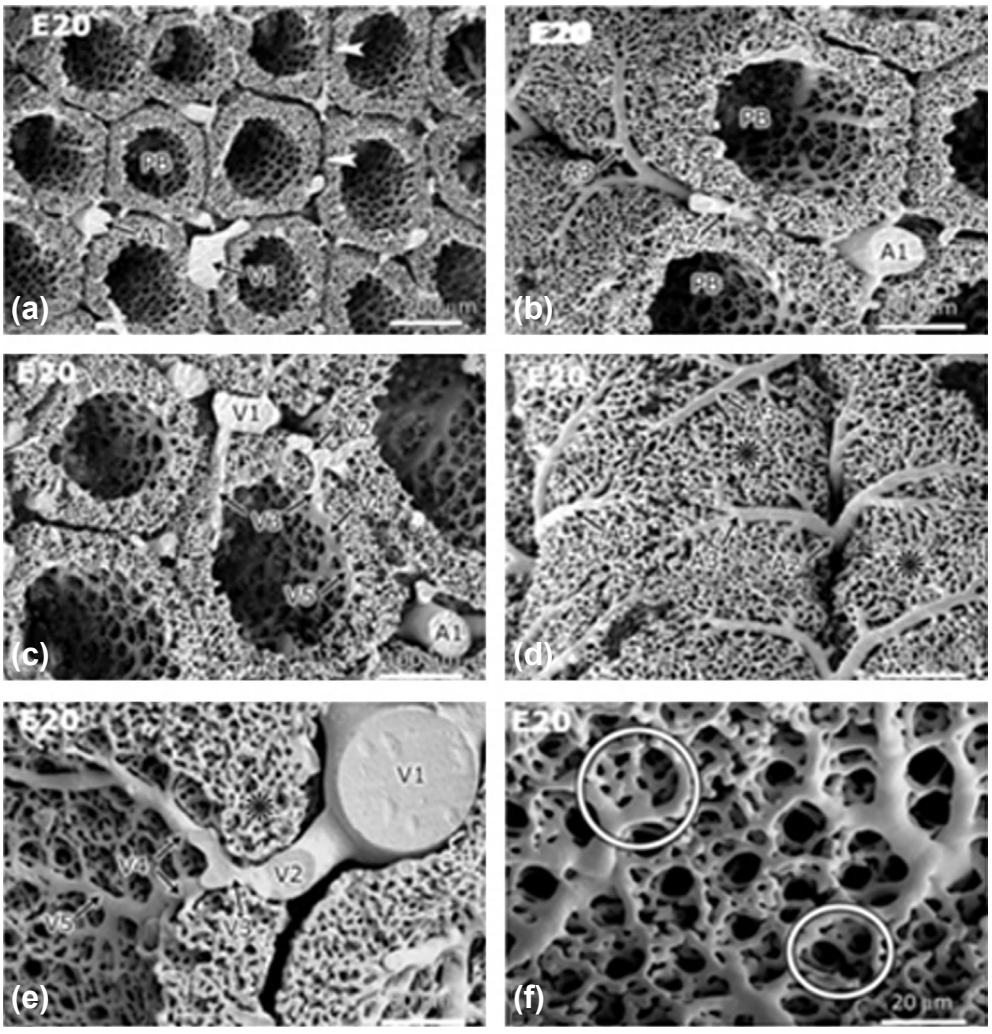

Downloaded from Vet-eBooks.com

Plate 58 Central nervous system

Scanning electron micrographs of neurons and dorsal root ganglion.

(a) Bipolar neuron at 8 days of incubation (stage 33–34).

(b) Bell-shaped neuron at 13 days of incubation (stage 39).

(c) Unipolar, long-stemmed dorsal root ganglion at 13 days.

All bars = 5 μm

Reprinted from Matsuda *et al.* (1996), with permission from Springer-Verlag.

Downloaded from Vet-eBooks.com

Plate 58

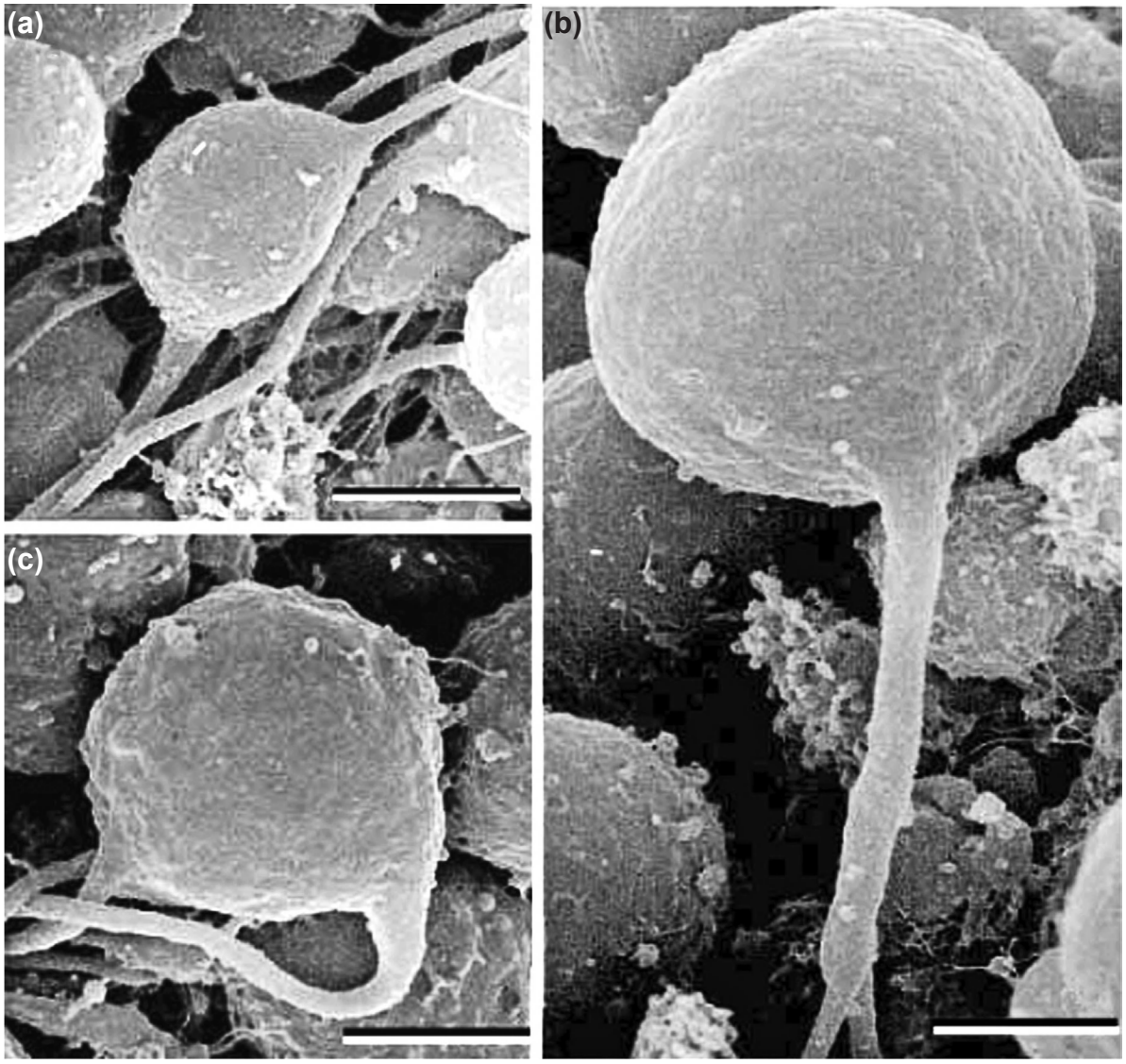

Downloaded from Vet-eBooks.com

Plate 59 Amnion

(a) Scanning electron micrograph showing the dorsal side of a stage 18 embryo (65–69 hours incubation). The amniotic folds have risen up all round the embryo.

(b) An embryo at about stage 33–34 (8 days incu bation).

(a) From Tipping and Wilson (2011,) with permission of John Wiley and Sons Inc.

(b) Source unknown.

Downloaded from Vet-eBooks.com

Plate 59

(a)

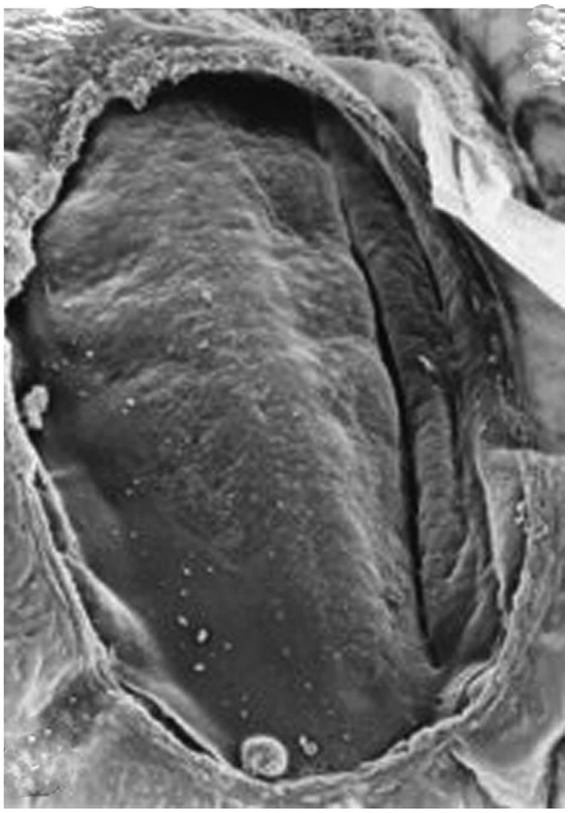

(b)

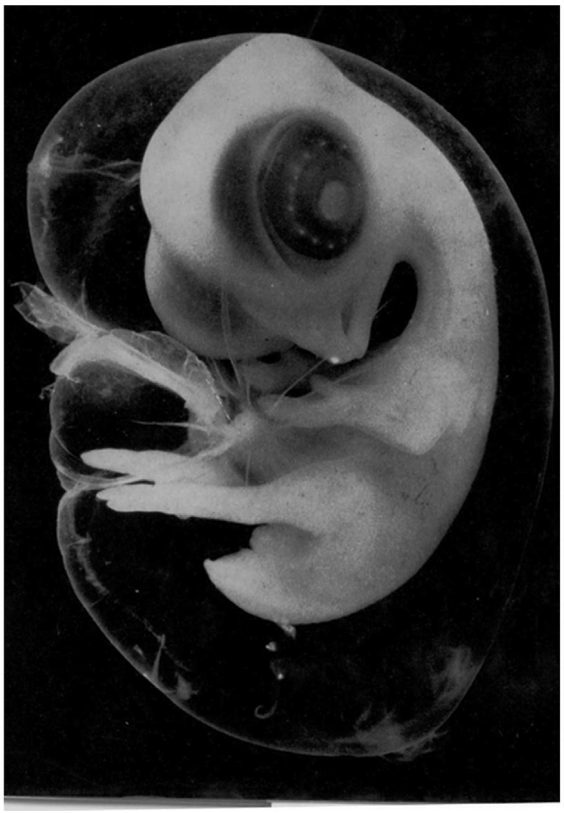

Downloaded from Vet-eBooks.com

Plate 60 Stage 8 (26–29 h)

Light micrograph of a whole-mounted embryo at stage 8 (26–29 h incubation) × 30.

1. head fold
2. anterior intestinal portal
3. anterior neuropore
4. forebrain
5. amnion
6. amniocardiac vesicle
7. somite
8. unsegmented mesoderm (segmental plate)
9. lateral plate mesoderm
10. area opaca
11. area pellucida
12. area vasculosa
13. primitive streak
14. Hensen's node
15. notochord seen through neural plate
16. limit of amniotic fold

Downloaded from Vet-eBooks.com

Plate 60

Downloaded from Vet-eBooks.com

Plate 61 Stage 8 (26–29 h) TS

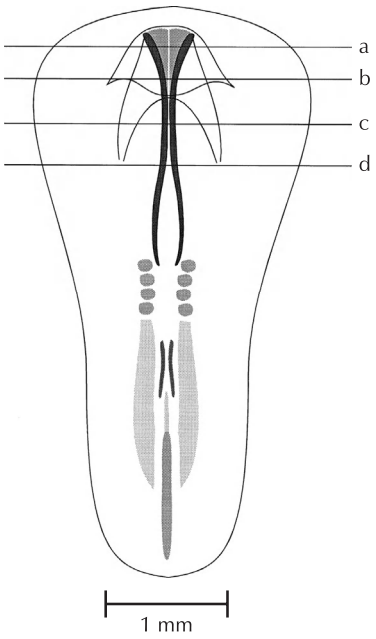

Transverse sections (TS): (a–d) × 160

1. head ectoderm
2. prechordal plate mesoderm
3. neural plate of future forebrain
4. anterior end of foregut
5. extra-embryonic endoderm
6. extra-embryonic ectoderm
7. space created by head fold
8. floor of pharynx
9. anterior neuropore
10. neural fold
11. thin roof of pharynx
12. head mesenchyme
13. point of fusion of neural folds
14. lumen of neural tube
15. anterior intestinal portal
16. lateral border of anterior intestinal portal
17. ectoderm
18. future neural crest
19. somatic lateral plate mesoderm
20. splanchnic lateral plate mesoderm
21. anterior tip of notochord
22. endoderm
23. embryonic coelom

Downloaded from Vet-eBooks.com

Plate 61

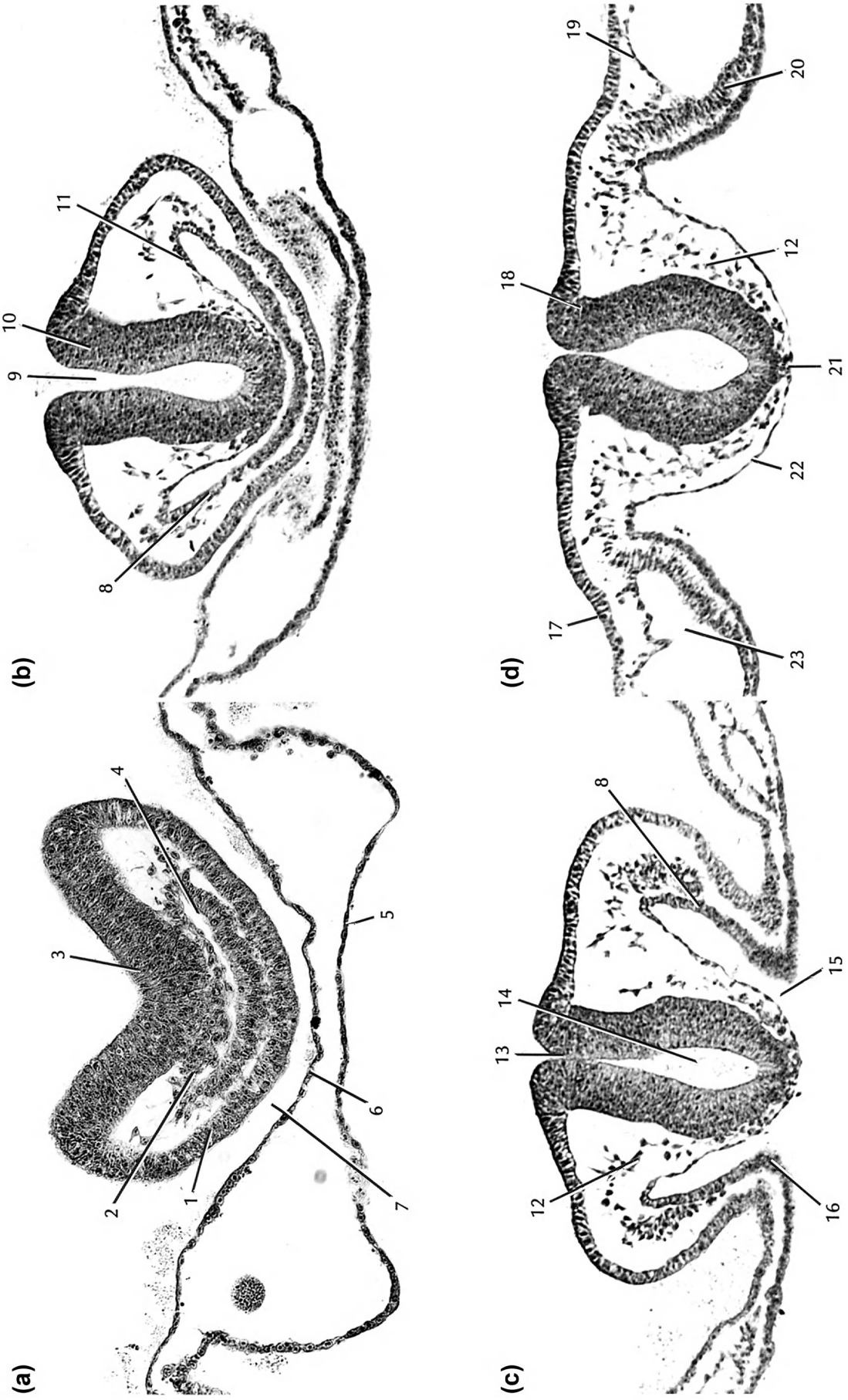

Downloaded from Vet-eBooks.com

Plate 62 Stage 8 (26–29 h) TS

Transverse sections (TS): (a–d) × 160

1. ectoderm
2. second somite
3. open neural plate
4. endoderm
5. notochord
6. lateral plate mesoderm
7. segmental plate mesoderm
8. primitive streak

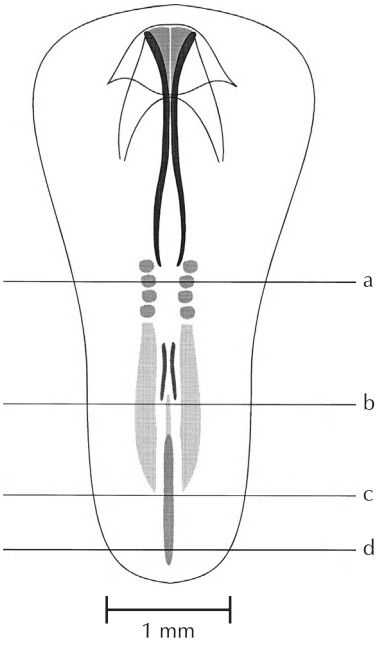

Downloaded from Vet-eBooks.com

Plate 62

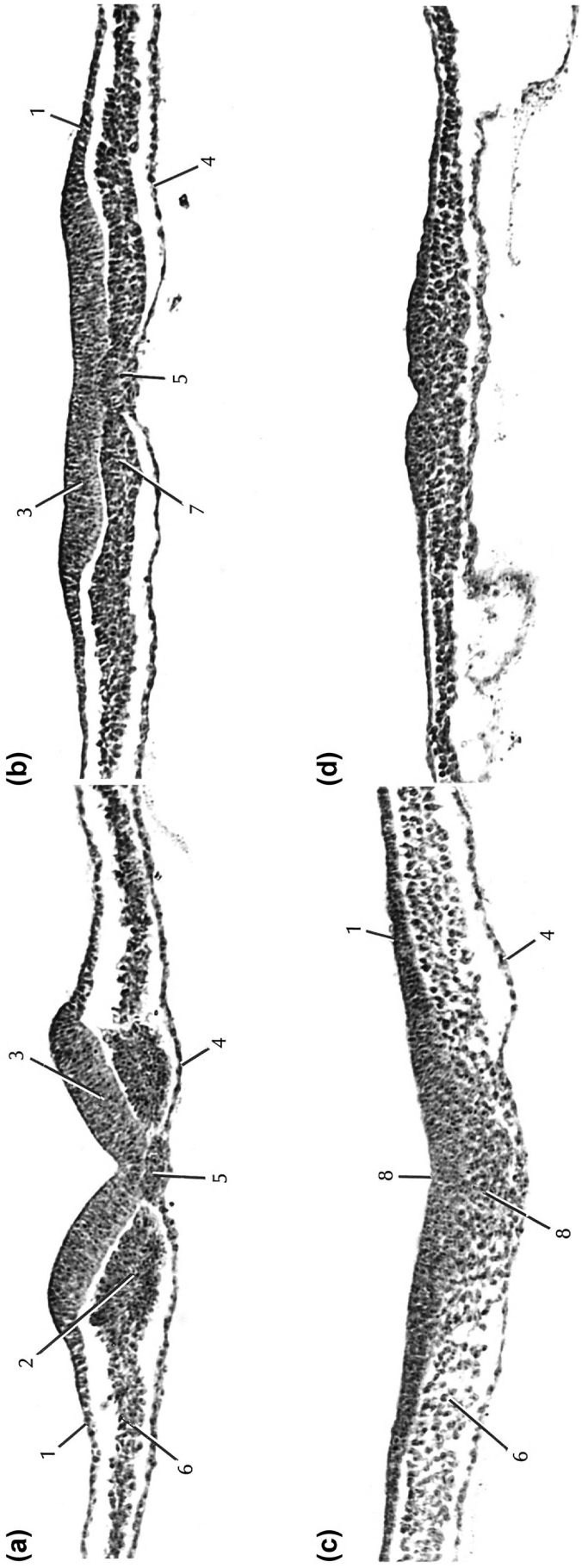

Downloaded from Vet-eBooks.com

Plate 63 Stage 9 (29–33 h)

Dorsal view of a whole-mounted embryo at stage 9 (29–33 h incubation) × 30.

1. anterior neuropore
2. neural fold
3. posterior limit of headfold
4. endodermal border of anterior intestinal portal
5. anterior intestinal portal
6. third right somite
7. right segmental plate mesoderm
8. Hensen's node
9. undifferentiated mesoderm seen through ectoderm
10. border between area pellucida and area opaca
11. primitive streak
12. area pellucida
13. left segmental plate mesoderm
14. notochord
15. third left somite
16. heart-forming region

Downloaded from Vet-eBooks.com

Plate 63

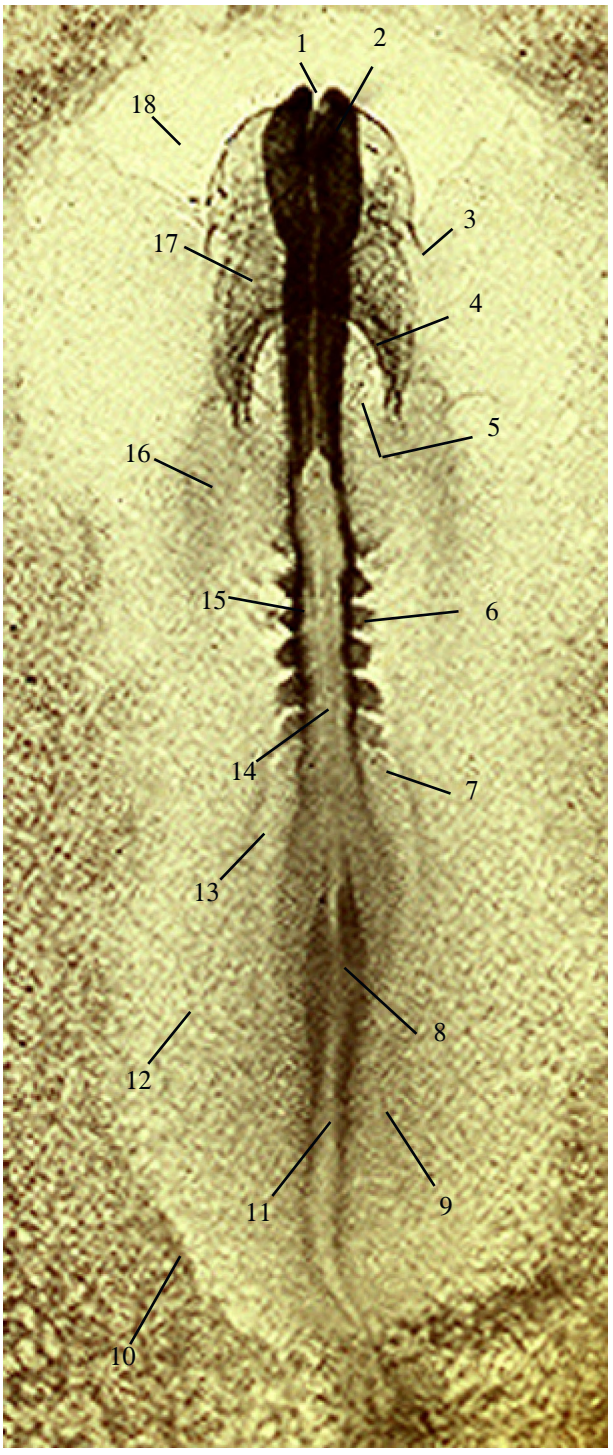

Downloaded from Vet-eBooks.com

Plate 64 Stage 9 (29–33 h) TS

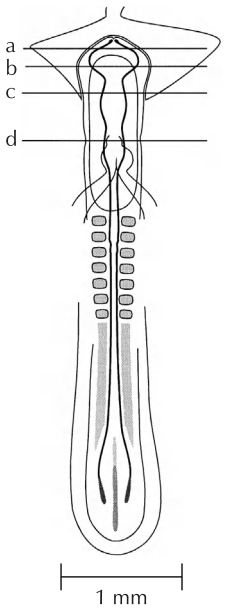

Transverse sections (TS): (a–d) × 100

1. edge of right optic vesicle
2. forebrain (a), midbrain (c)
3. left dorsal aorta
4. oral cavity
5. splanchnopleure
6. somatopleure
7. lumen of forebrain
8. head mesenchyme
9. notochord
10. pharynx
11. right ventral aorta
12. right dorsal aorta
13. ectoderm of head
14. stomatodaeum (stomatodaeal plate)
15. mesoderm
16. bulbus cordis

Downloaded from Vet-eBooks.com

Plate 64

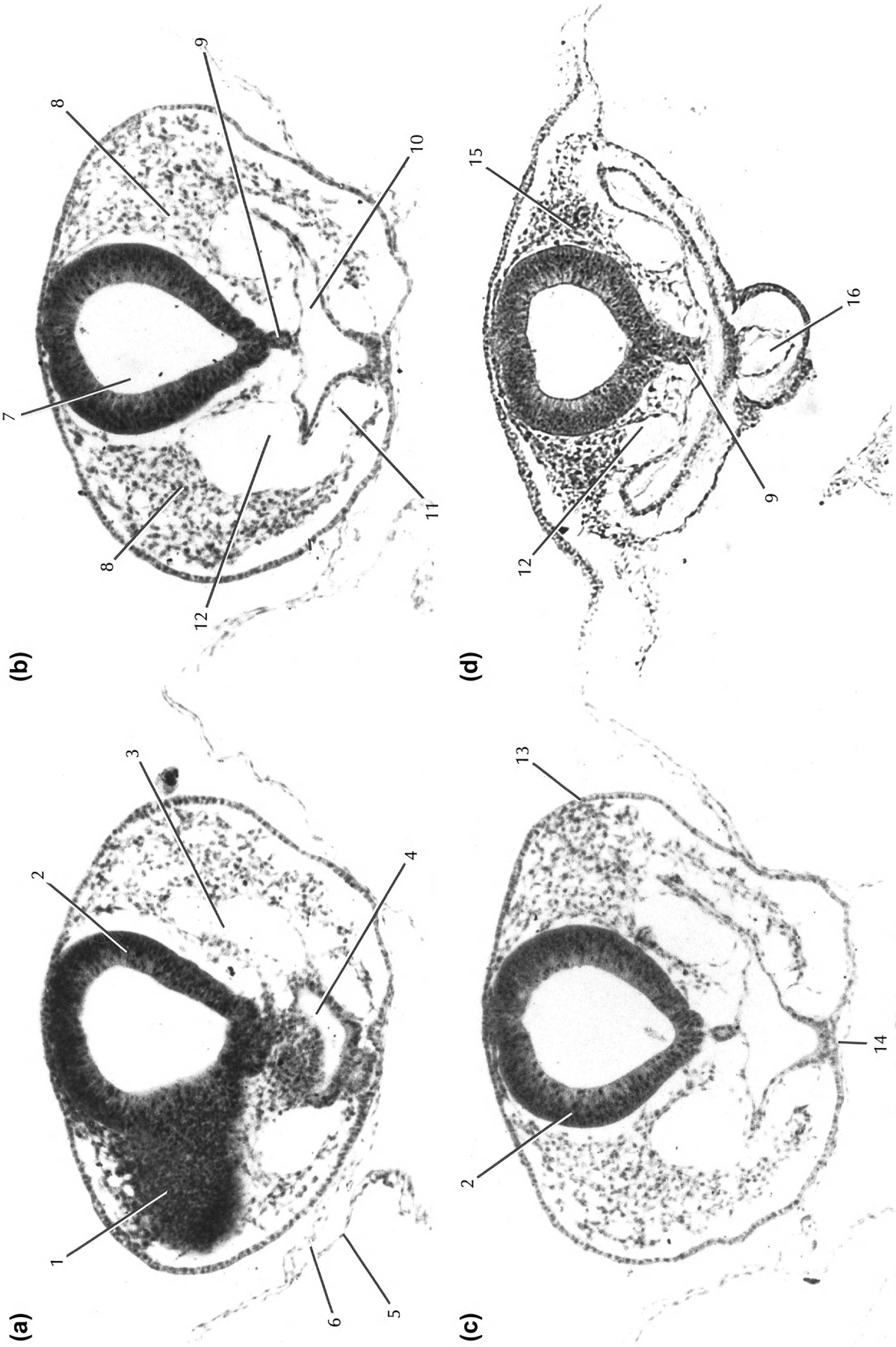

Downloaded from Vet-eBooks.com

Plate 65 Stage 9 (29–33 h) TS

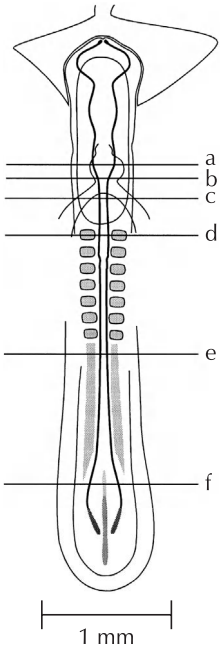

Transverse sections (TS): (a–f) × 100

1. mesenchyme
2. hindbrain
3. unclosed region of neural tube
4. notochord
5. wall of atrium
6. lumen of ventricle
7. wall of ventricle
8. coelom
9. right dorsal aorta
10. ectoderm
11. thin roof of pharynx
12. parachordal mesoderm
13. left dorsal aorta
14. endoderm
15. ventral mesentery (ventral mesocardium)
16. dorsal mesentery (dorsal mesocardium)
17. neural plate
18. anterior intestinal portal
19. right sinu-atrial region
20. wall of sinus venosus
21. right intermediate mesoderm
22. left intermediate mesoderm
23. somatic lateral plate mesoderm
24. splanchnic mesoderm of lateral plate
25. somite
26. segmental plate mesoderm
27. Hensen's (primitive) node

Downloaded from Vet-eBooks.com

Plate 65

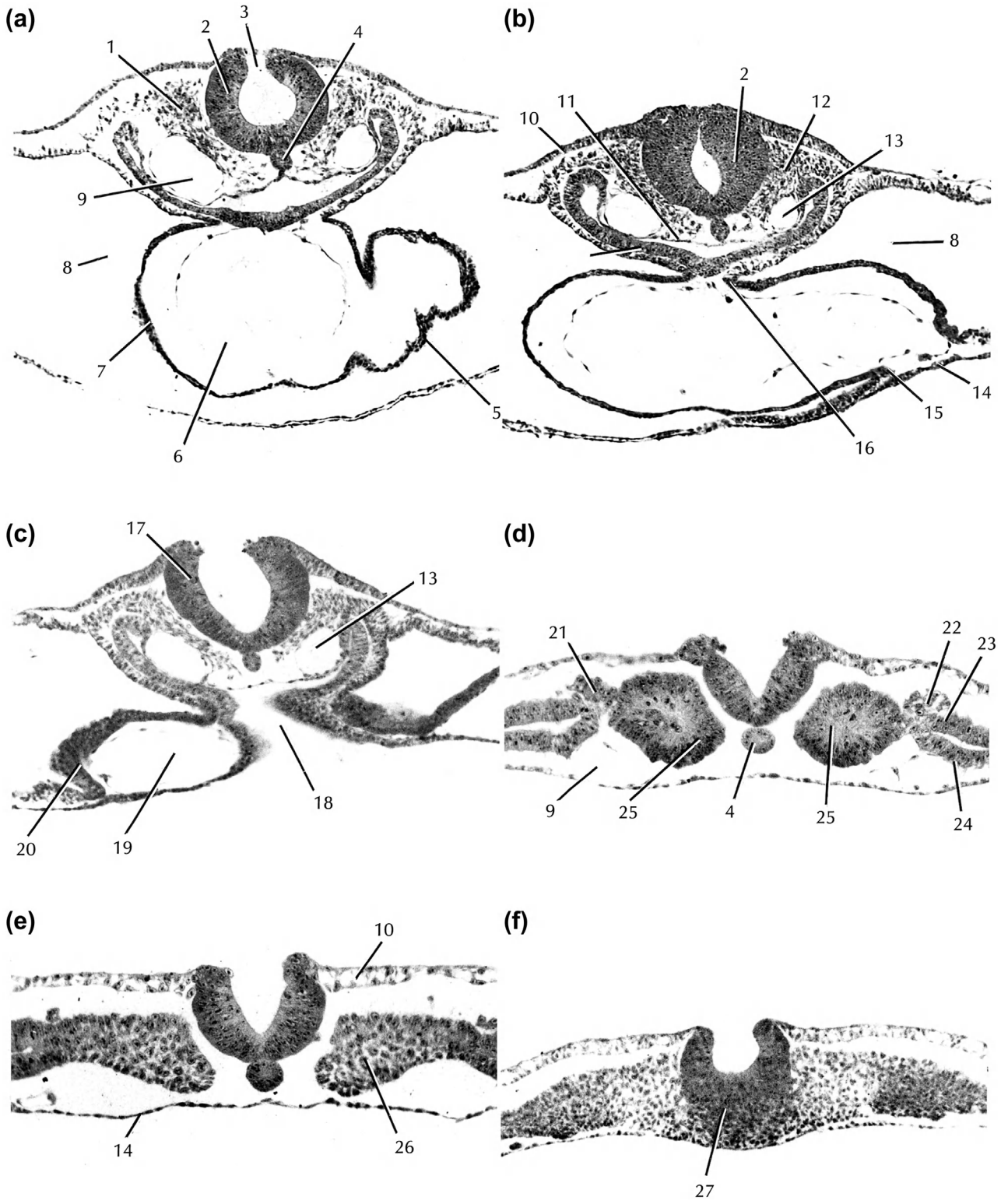

Downloaded from Vet-eBooks.com

Plate 66 Stage 10 (33–38 h)

Light micrograph of a whole-mounted embryo at stage 10 (33–38 h incubation) × 25.

1. optic vesicle in prosencephalon (forebrain)
2. mesencephalon (midbrain)
3. rhombencephalon (hindbrain)
4. posterior limit of headfold
5. right 4th somite
6. segmental plate mesoderm
7. lateral plate mesoderm
8. primitive streak
9. Hensen's node
10. neural tube
11. endodermal border of anterior intestinal portal
12. lateral limit of headfold

Downloaded from Vet-eBooks.com

Plate 66

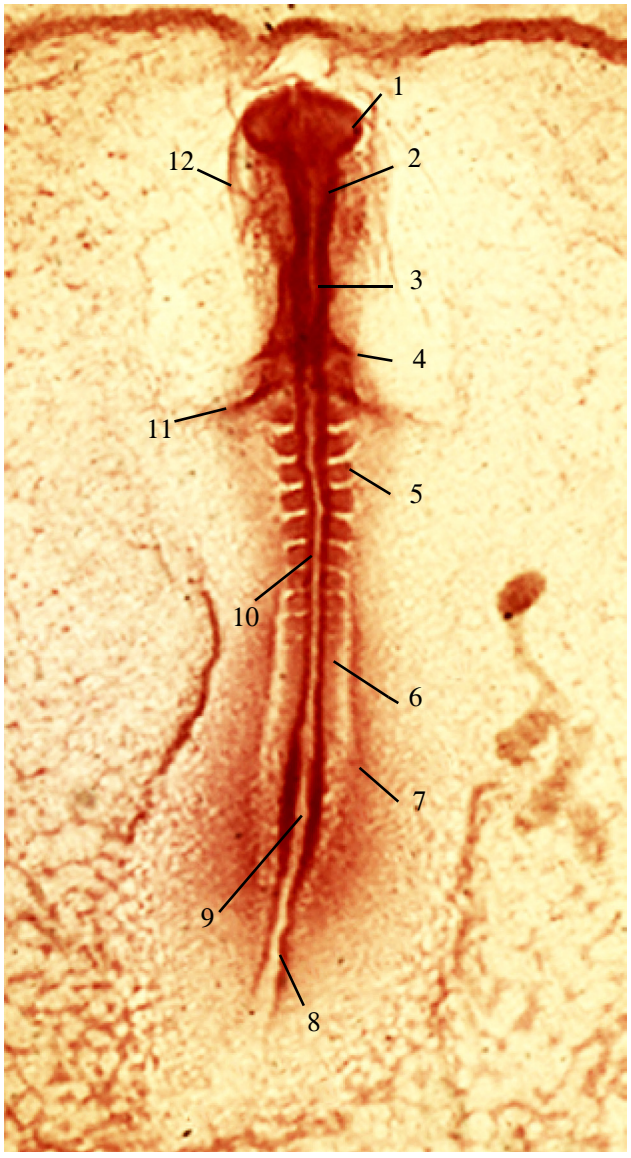

Downloaded from Vet-eBooks.com

Plate 67 Stage 10 (33–38 h) LS: sagittal

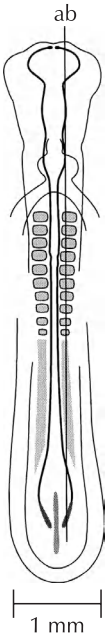

Longitudinal (sagittal) sections (LS):

(a) Anterior end of embryo × 120

(b) Posterior end of same embryo × 120

(c) Enlargement of two newly formed somites × 360

1. embryonic dorsal ectoderm
2. prosencephalon (forebrain)
3. extra-embryonic ectoderm and endoderm
4. ventral ectoderm of head
5. head mesenchyme
6. head fold
7. embryonic endoderm
8. foregut
9. pericardial cavity
10. cardiac primordium
11. anterior intestinal portal
12. sclerotome of an anterior somite
13. derma-myotome
14. dorsal aorta
15. neural plate
16. newly formed (posterior) somite
17. segmental plate mesoderm
18. cells in somitocoele of somite

Downloaded from Vet-eBooks.com

Plate 67

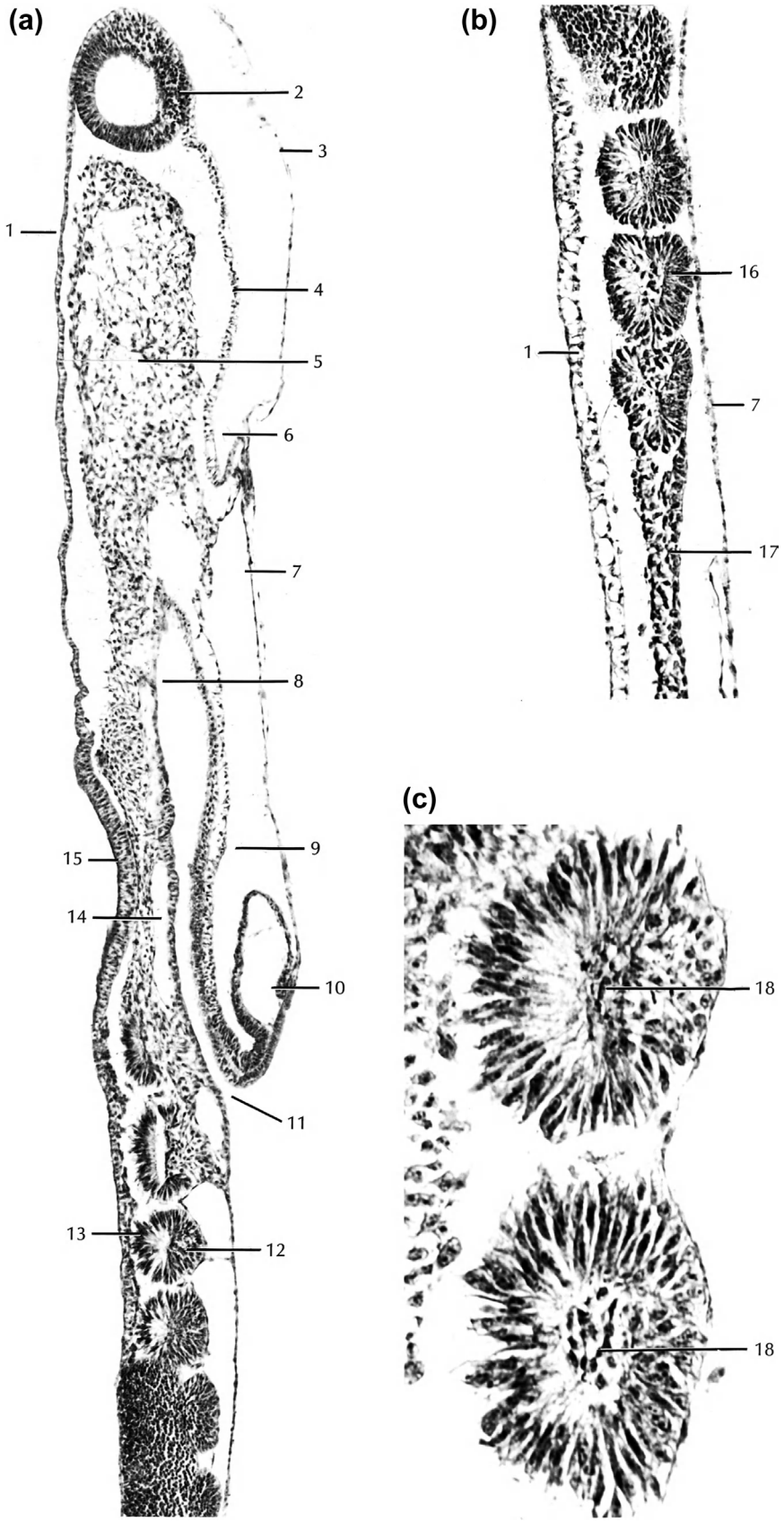

Downloaded from Vet-eBooks.com

Plate 68 Stage 10 (33–38 h) TS

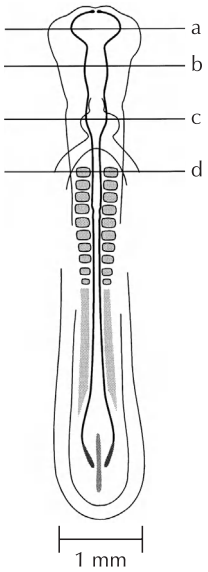

Transverse sections (TS): (a–d) × 150

1. ectoderm of head
2. prosencephalon
3. head mesenchyme
4. lumen of optic vesicle
5. right dorsal aorta
6. left dorsal aorta
7. pharynx
8. extra-embryonic somatic mesoderm
9. notochord
10. cardiac primordia (left and right)
11. stomatodaeum (stomatodaeal plate)
12. lateral head fold
13. otic placode
14. embryonic splanchnic (lateral plate) mesoderm
15. dorsal mesocardium
16. endoderm
17. epimyocardium
18. endocardium
19. sclerotome
20. neural tube
21. derma-myotome
22. embryonic somatic (lateral plate) mesoderm
23. embryonic coelom
24. lip of anterior intestinal portal

Downloaded from Vet-eBooks.com

Plate 68

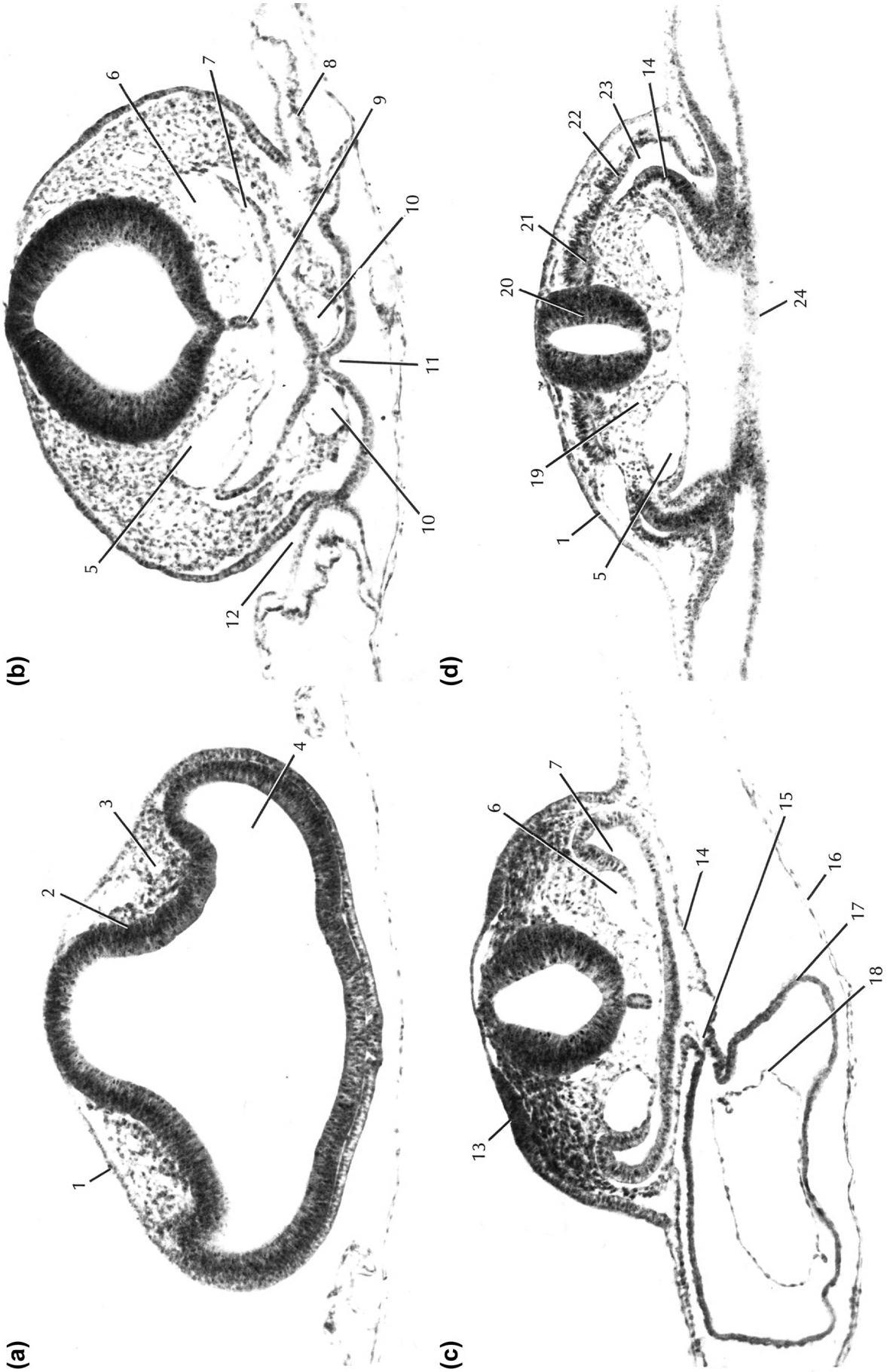

Downloaded from Vet-eBooks.com

Plate 69 Stage 10 (33–38 h) TS

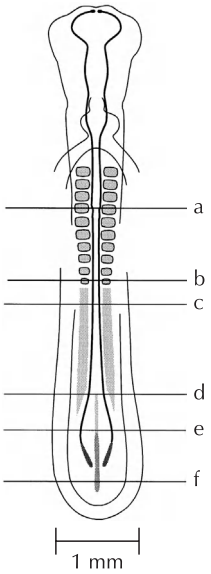

Transverse sections (TS): (a–f) × 170

1. intermediate mesoderm (nephric rudiment)
2. embryonic ectoderm
3. neural tube
4. left somite
5. notochord
6. endoderm
7. left segmental plate mesoderm
8. right segmental plate mesoderm
9. lateral plate mesoderm
10. unclosed neural plate
11. Hensen's node
12. primitive streak
13. mesoderm lateral to primitive streak

Downloaded from Vet-eBooks.com

Plate 69

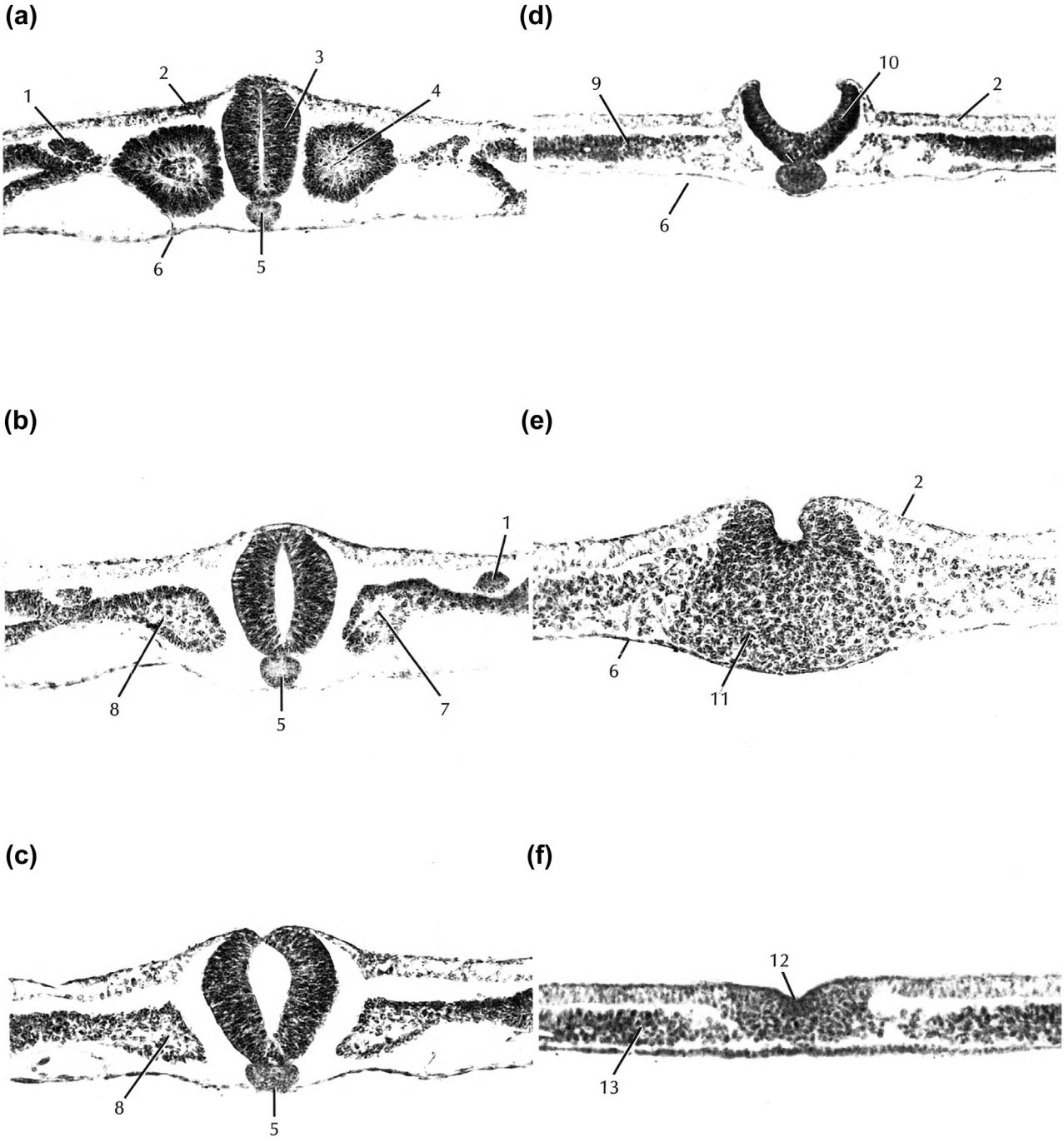

Downloaded from Vet-eBooks.com

Plate 70 Stage 11 (40–45 h) TS

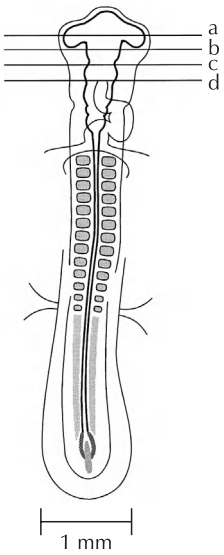

Transverse sections (TS): (a–d) × 133

1. head mesenchyme
2. lumen of prosencephalon
3. left optic vesicle
4. pre-notochordal mesenchyme
5. sub-cephalic pocket formed by head fold
6. right ventral aorta
7. ectoderm of head
8. mesencephalon
9. left dorsal aorta
10. left ventral aorta
11. anterior tip of foregut
12. communication of right ventral and dorsal aortae
13. extra-embryonic ectoderm
14. stomatodaeum (stomatodaeal plate)
15. oral cavity
16. tip of notochord
17. lumen of pharynx
18. extra-embryonic endoderm
19. pro-amnion

Downloaded from Vet-eBooks.com

Plate 70

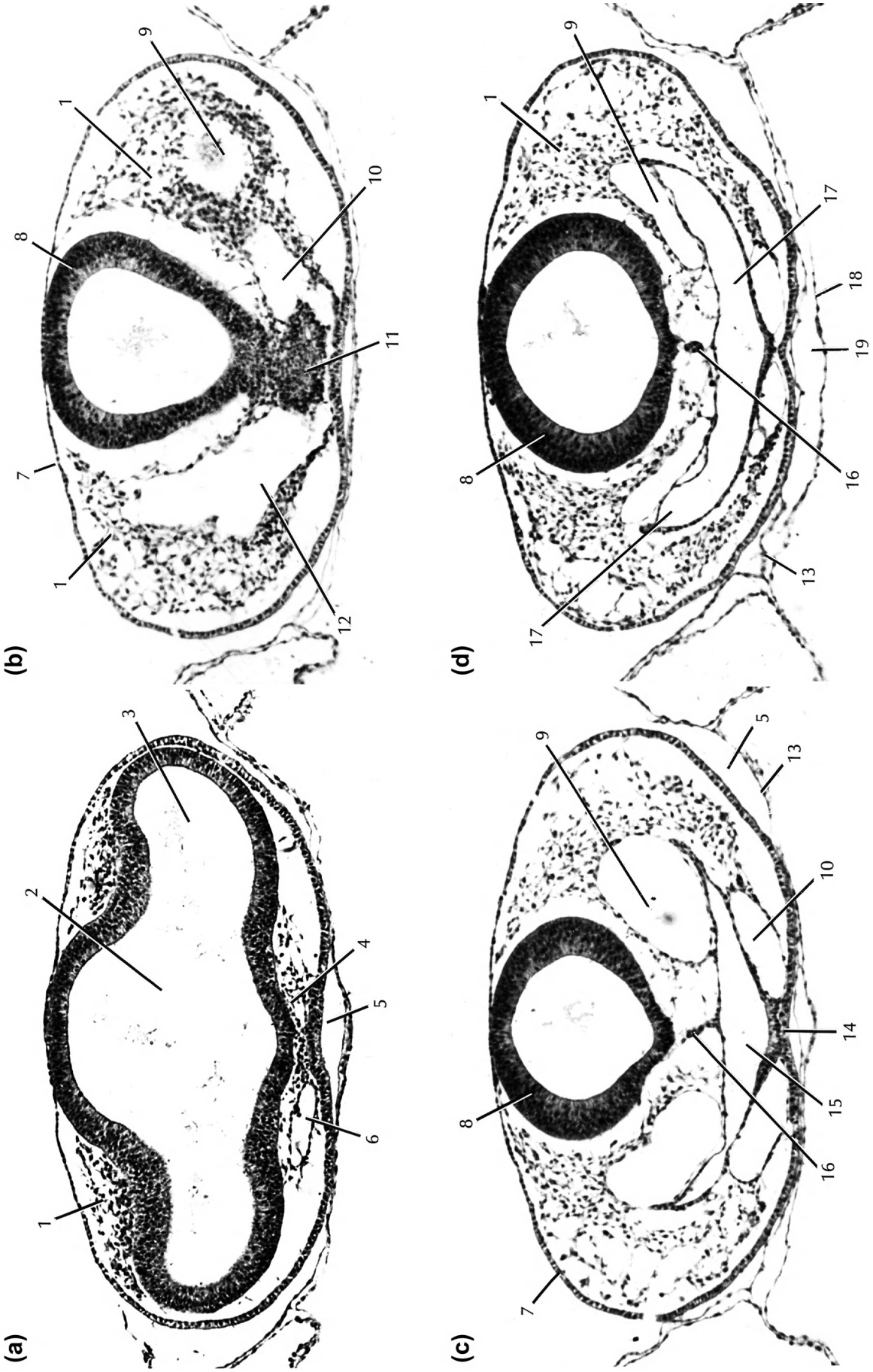

Downloaded from Vet-eBooks.com

Plate 71 Stage 11 (40–45 h) TS

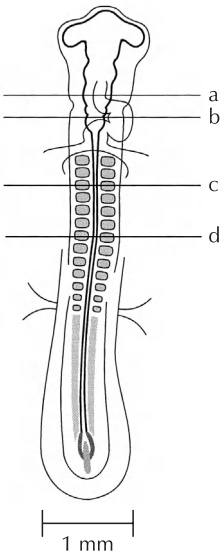

Transverse sections (TS): (a–d) × 175

1. ectoderm
2. mesencephalon
3. head mesenchyme
4. left dorsal aorta
5. lumen of pharynx
6. notochord
7. truncus arteriosus
8. splanchnic lateral plate mesoderm
9. right dorsal aorta
10. neural crest
11. keel of pharynx
12. dorsal mesocardium
13. endocardium
14. lumen of ventricle
15. epimyocardium
16. pericardial cavity
17. derma-myotome
18. left edge of midgut
19. sclerotome
20. midgut
21. right coelom
22. right somatic lateral plate mesoderm
23. lumen of neural tube
24. left coelom
25. endoderm

Downloaded from Vet-eBooks.com

Plate 71

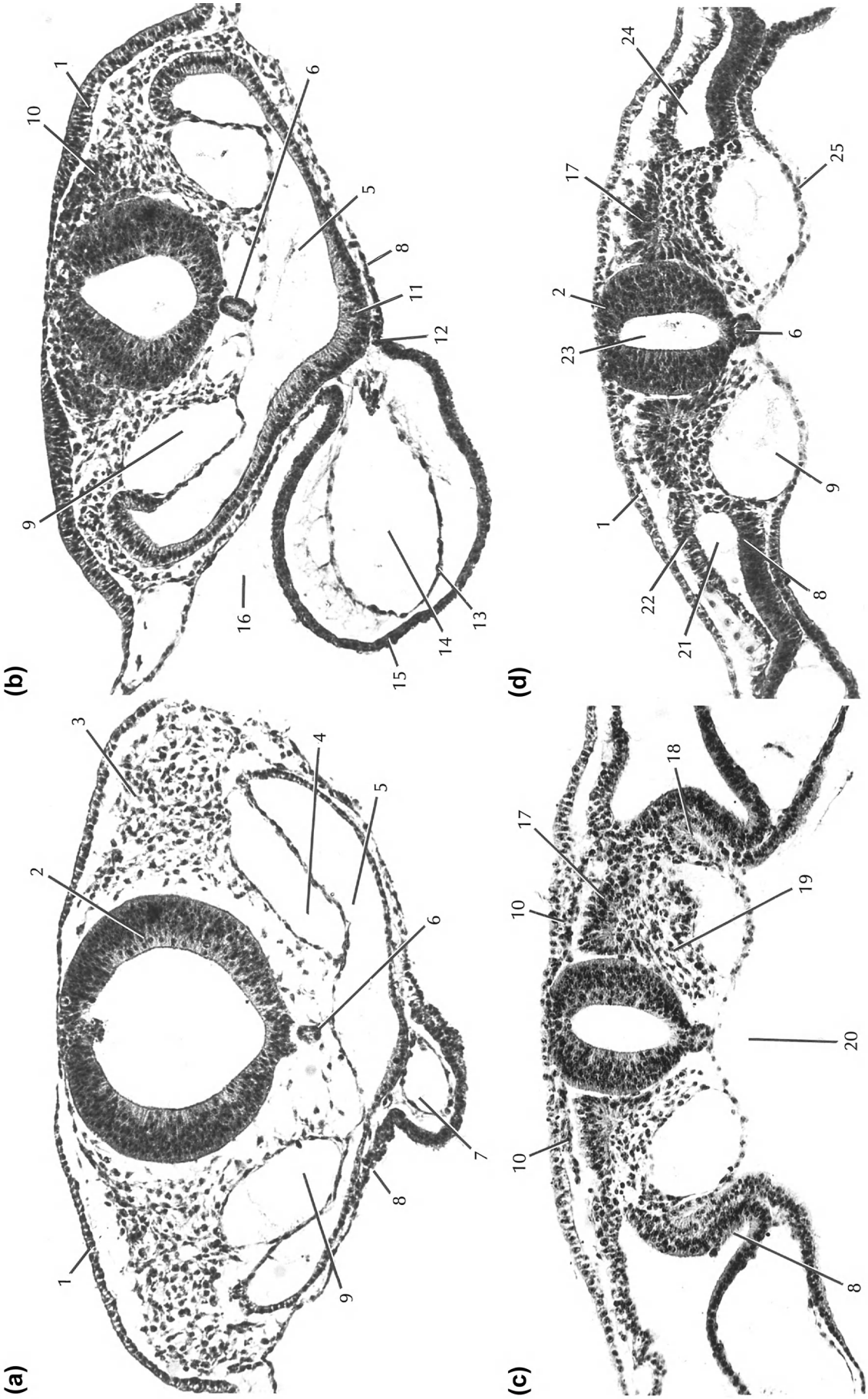

Downloaded from Vet-eBooks.com

Plate 72 Stage 11 (40–45 h) TS

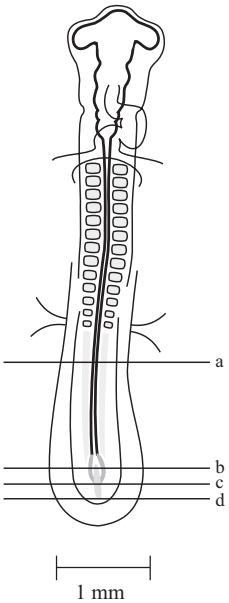

Transverse sections (TS): (a–d) × 200

(a) Segmental plate

(b) Posterior end of neural tube

(c) Tail bud

(d) Posterior end of area pellucida

1. right somatic layer of lateral plate mesoderm
2. right segmental plate mesoderm
3. neural tube
4. ectoderm
5. left segmental plate mesoderm
6. left somatic layer of lateral plate mesoderm
7. left coelomic cavity
8. left splanchnic layer of lateral plate mesoderm
9. left dorsal aorta
10. endoderm
11. notochord
12. right dorsal aorta
13. remnant of neural tube in tail bud region
14. secondary mesoderm in tail bud region
15. tail bud mesoderm

Downloaded from Vet-eBooks.com

Plate 72

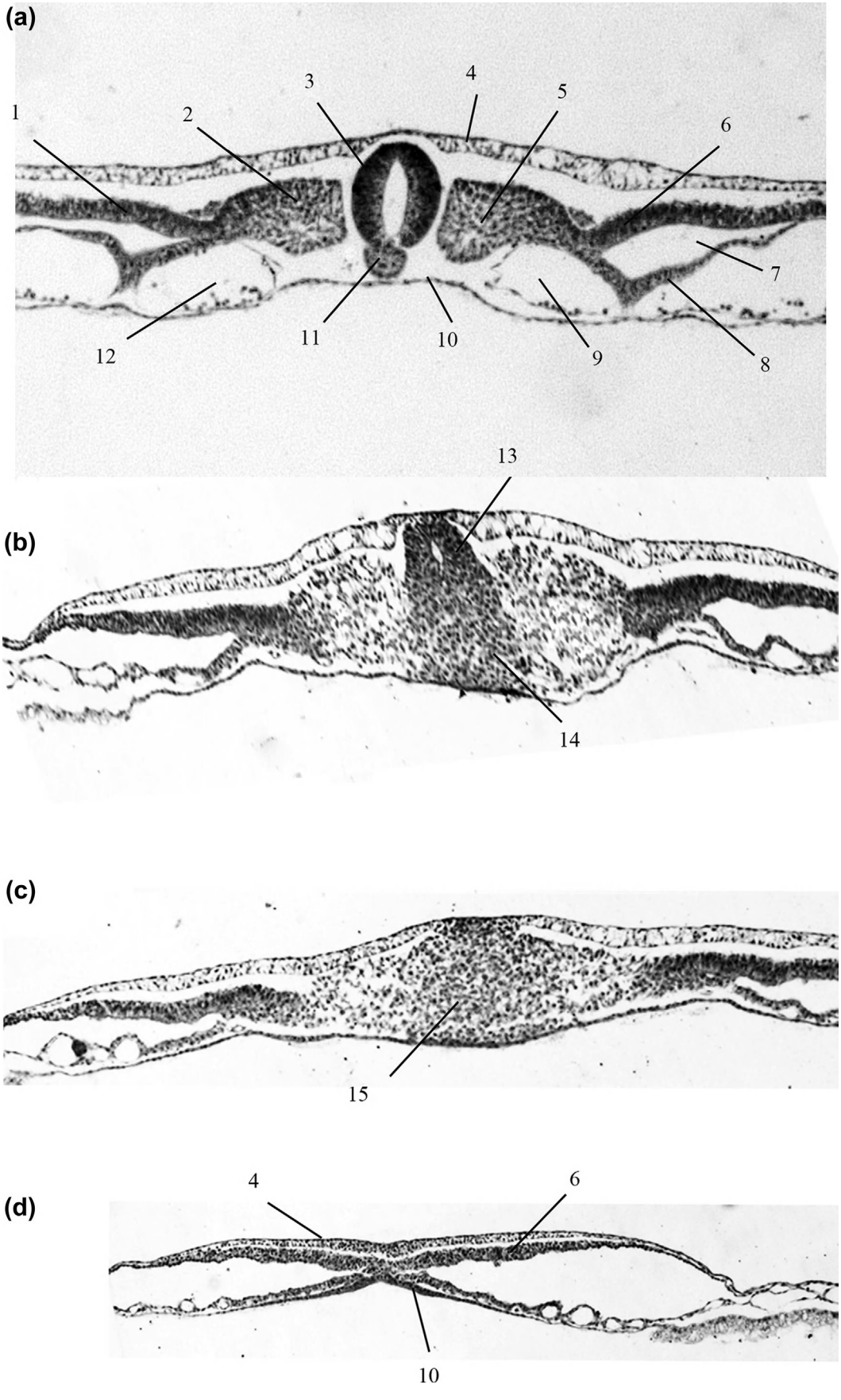

Downloaded from Vet-eBooks.com

Plate 73 Stage 12 (45–49 h) LS

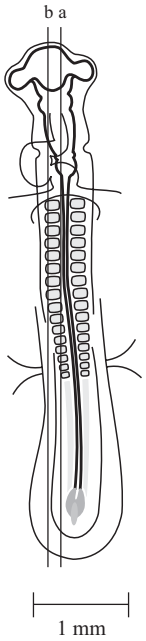

Longitudinal (sagittal) sections through a stage 12 embryo: (a, b) × 20

1. yolk sac
2. wall of mesencephalon
3. wall of myelencephalon
4. wall of neural tube in trunk region
5. somite
6. ectoderm
7. segmental plate mesoderm
8. tail bud mesenchyme
9. endoderm
10. heart
11. foregut
12. prosencephalon
13. vena capitis (head vein)
14. otic placode

Downloaded from Vet-eBooks.com

Plate 73

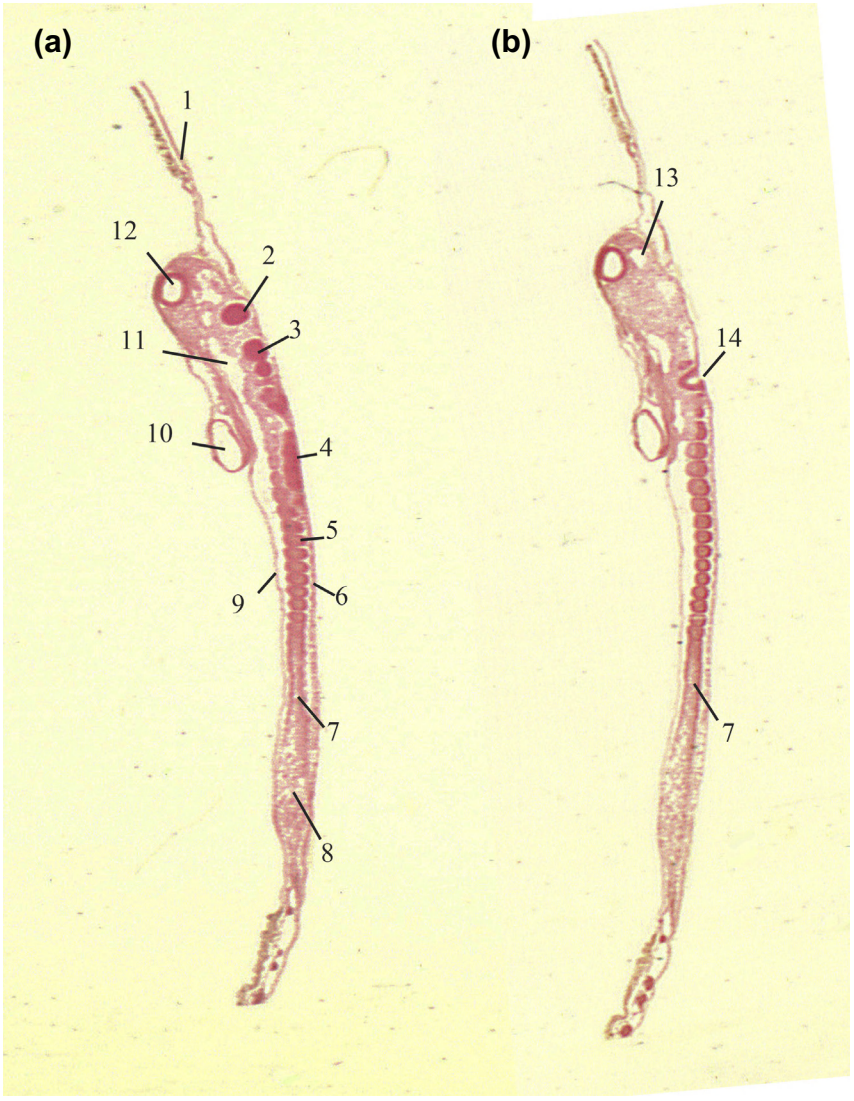

Downloaded from Vet-eBooks.com

Plate 74 Stage 12 (45–49 h) LS: coronal

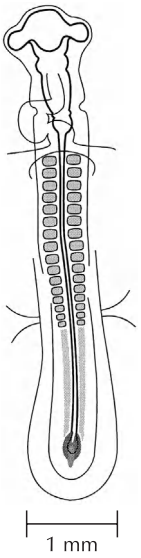

Longitudinal sections in the coronal plane. Diagram shows a ventral view of the embryo. Sections are taken through the plane of the page.

(a–c) × 50 (d) × 200

(a) Enlarged on *plate 75*

(d) Enlargement of part of (c)

1. amniotic ectoderm
2. left optic vesicle
3. amniotic cavity
4. left anterior cardinal vein
5. pericardial cavity
6. wall of neural tube
7. somite
8. ventricle
9. common cardinal vein
10. right anterior cardinal vein
11. gut in region of anterior intestinal portal
12. notochord
13. left omphalo-mesenteric (vitelline) vein
14. yolk sac
15. segmental plate mesoderm
16. Hensen's node
17. intermediate mesoderm

Downloaded from Vet-eBooks.com

Plate 74

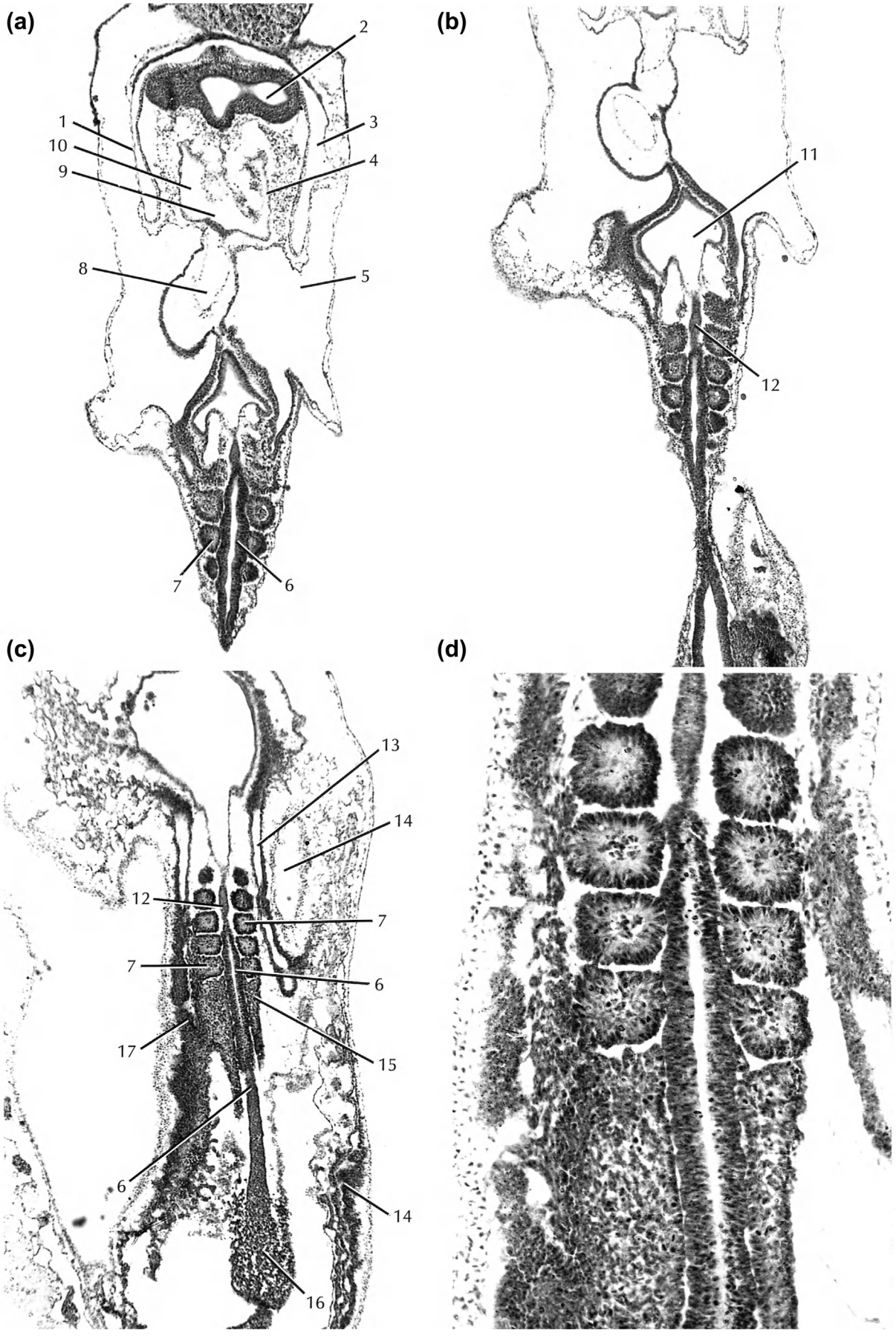

Downloaded from Vet-eBooks.com

Plate 75 Stage 12 (45–49 h) LS: coronal

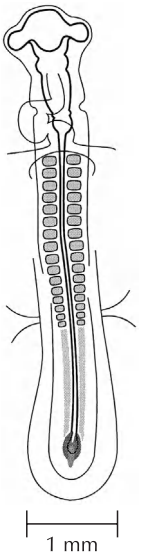

Enlargement of part of *plate 74a*: × 200

Longitudinal section in the coronal plane. Diagram shows a ventral view of the embryo. Section is taken through the plane of the page.

1. left anterior cardinal vein
2. ventricle
3. splanchnic lateral plate mesoderm
4. embryonic coelom
5. notochord
6. central cells of somite
7. epithelial wall of somite
8. lumen of neural tube
9. wall of neural tube
10. right dorsal aorta
11. gut in region of anterior intestinal portal
12. cardiac jelly
13. endocardium

Downloaded from Vet-eBooks.com

Plate 75

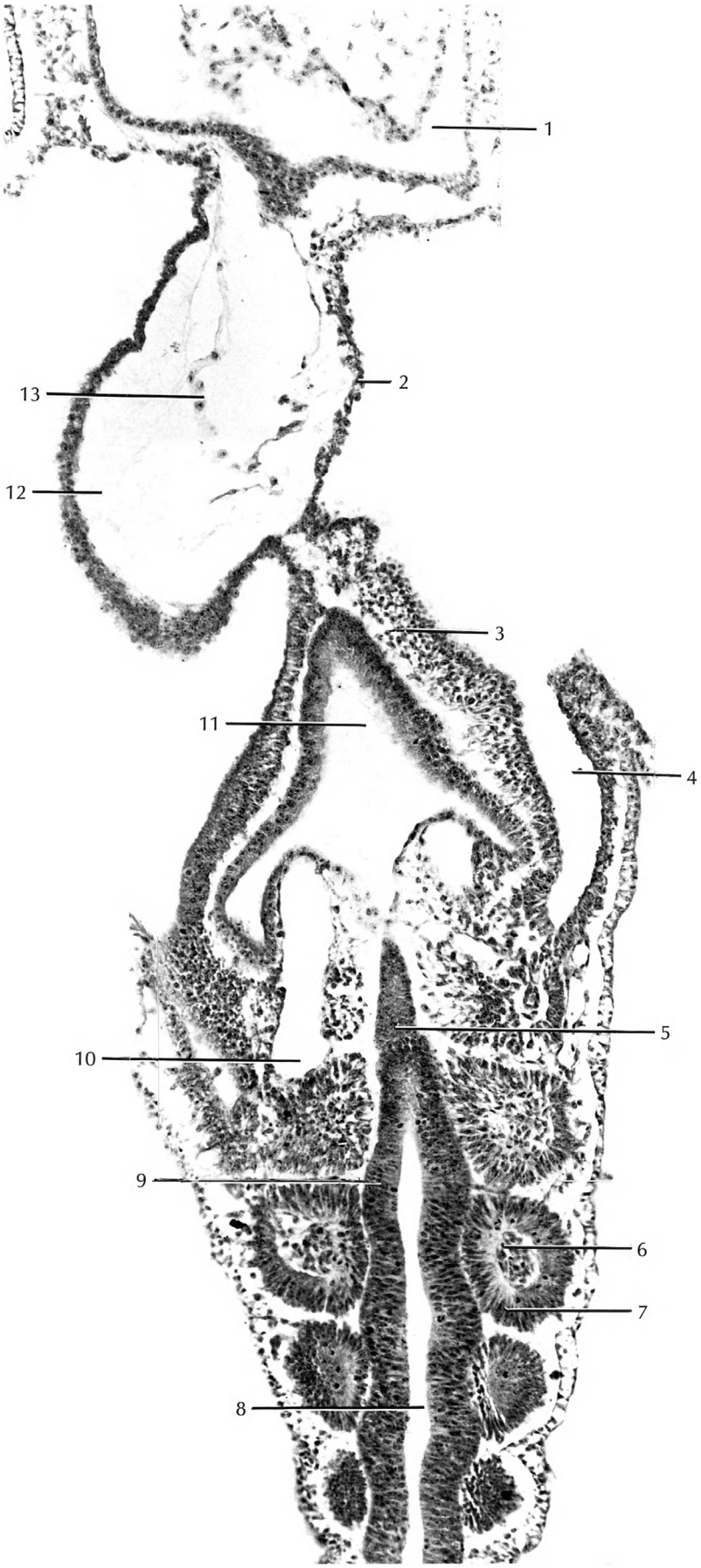

Downloaded from Vet-eBooks.com

Plate 76 Stage 13 (48–52 h)

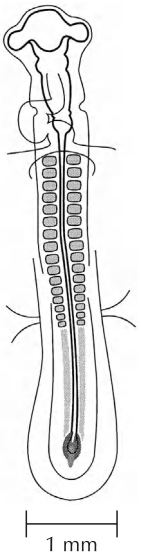

Ventral view of a whole-mounted stage 13 embryo. See *plate 77* for a dorsal view of a slightly older stage 13. Magnification × 13

1. border of area opaca
2. prosencephalon
3. optic cup
4. mesencephalon
5. metencephalon
6. myelencephalon
7. otic vesicle
8. neural tube
9. eighth left somite
10. left segmental plate mesoderm
11. remains of primitive streak
12. blood islands in area vasculosa
13. area vitellina
14. Hensen's node
15. right lateral plate mesoderm
16. right intermediate mesoderm
17. anterior intestinal portal
18. heart

Downloaded from Vet-eBooks.com

Plate 76

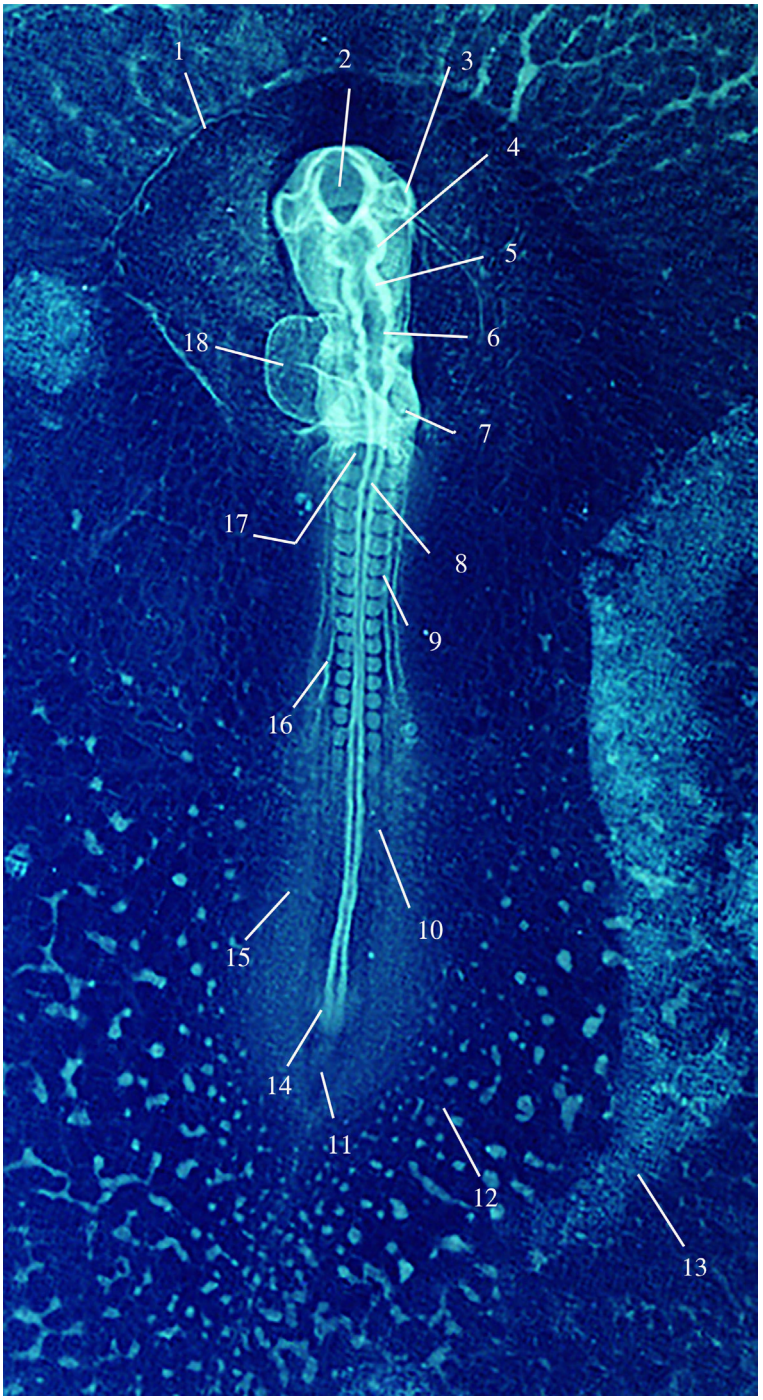

Downloaded from Vet-eBooks.com

Plate 77 Stage 13+ (52 h)

Dorsal view of a whole-mounted older stage 13 embryo. See *plate 76* for a ventral view of a slightly younger stage 13. Magnification × 10

1. edge of amnion
2. brain
3. anterior vitelline (omphalo-mesenteric) vein
4. S-shaped heart
5. right vitelline (omphalo-mesenteric) artery
6. area pellucida
7. area vitellina
8. sinus terminalis
9. area vasculosa

Downloaded from Vet-eBooks.com

Plate 77

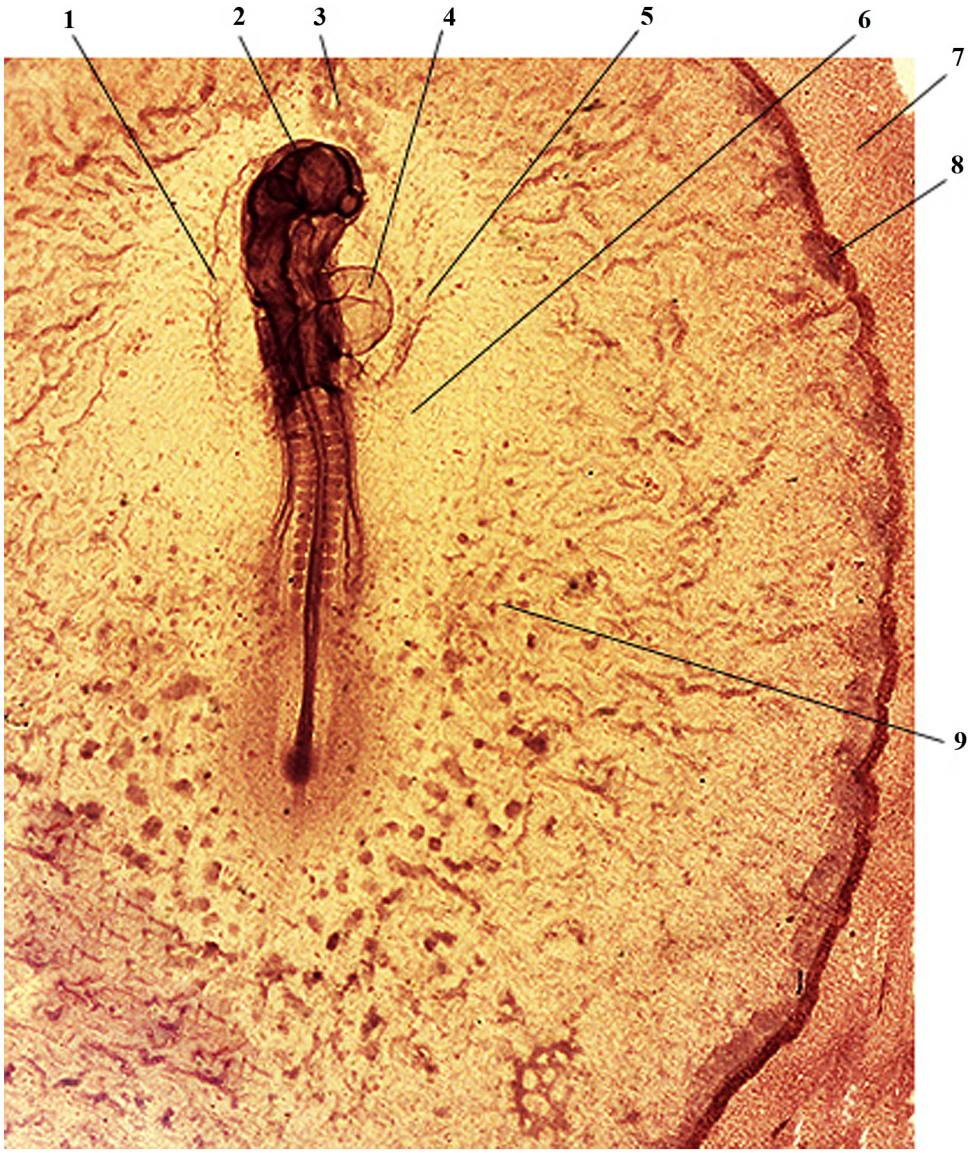

Downloaded from Vet-eBooks.com

Plate 78 Stage 13 (48–52 h) LS: coronal

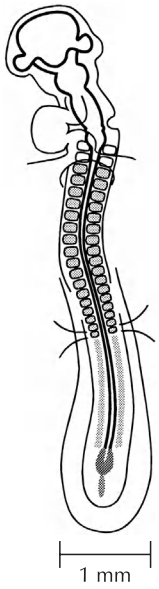

Longitudinal sections in the coronal plane. Diagram shows a ventral view of the embryo. Sections are taken through the plane of the page: (a–d) × 25

1. head mesenchyme
2. left otic vesicle
3. myelencephalon
4. somite
5. lumen of ventricle
6. right eye
7. mesocoele
8. first pharyngeal pouch
9. second pharyngeal pouch
10. myelocoele
11. embryonic coelom
12. 17th somite
13. wall of neural tube
14. nephric duct
15. lateral body wall
16. splanchnic lateral plate mesoderm
17. somatic lateral plate mesoderm
18. anterior cardinal vein
19. myotome
20. roof of neural tube
21. segmental plate mesoderm
22. last formed somite
23. gut
24. right common cardinal vein
25. pharynx
26. prosencephalon
27. left eye
28. left otic placode
29. left common cardinal vein
30. sinus venosus
31. atrium
32. pericardial cavity
33. ventral aorta
34. blood vessels in yolk sac

Downloaded from Vet-eBooks.com

Plate 78

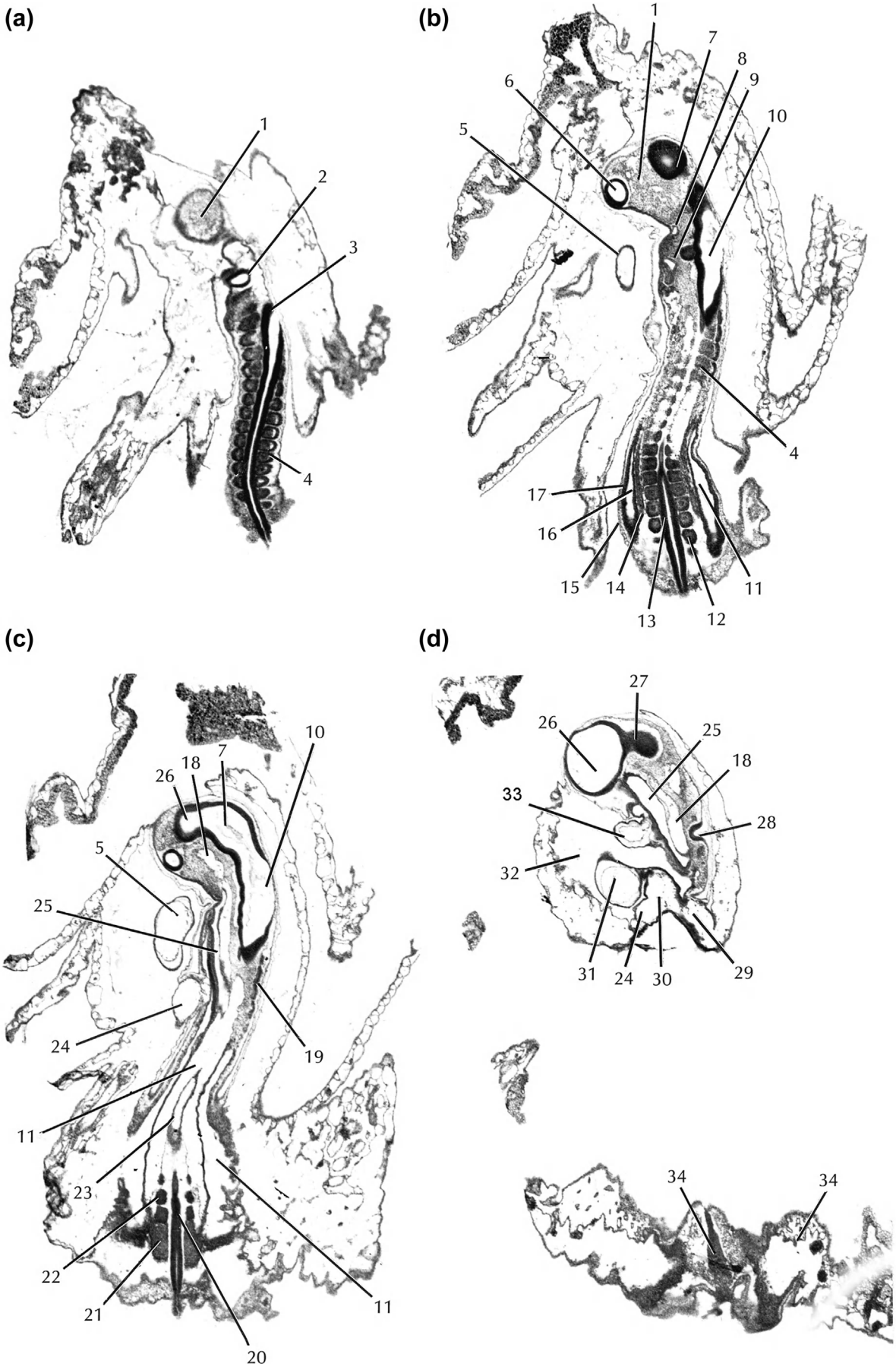

Downloaded from Vet-eBooks.com

Plate 79 Stage 13 (48–52 h) TS

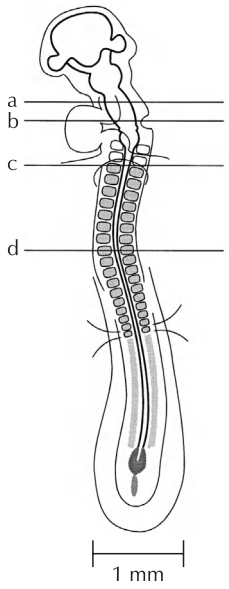

Transverse sections (TS): (a–d) × 100

Diagram shows view of embryo from the ventral side.

1. amniotic fold
2. myelencephalon
3. left dorsal aorta
4. notochord
5. truncus arteriosus
6. splanchnic lateral plate mesoderm of yolk sac
7. pharynx
8. sclerotome
9. left otic vesicle
10. thick-walled floor of pharynx
11. left ventral aorta
12. ventricle
13. right dorsal aorta
14. right otic vesicle
15. neural tube
16. derma-myotome
17. left anterior cardinal vein
18. amnion
19. left lateral body fold
20. endodermal layer of yolk sac
21. extra-embryonic coelom
22. embryonic coelom
23. left omphalo-mesenteric vein
24. endoderm
25. splanchnic lateral plate mesoderm of gut
26. midgut

Downloaded from Vet-eBooks.com

Plate 79

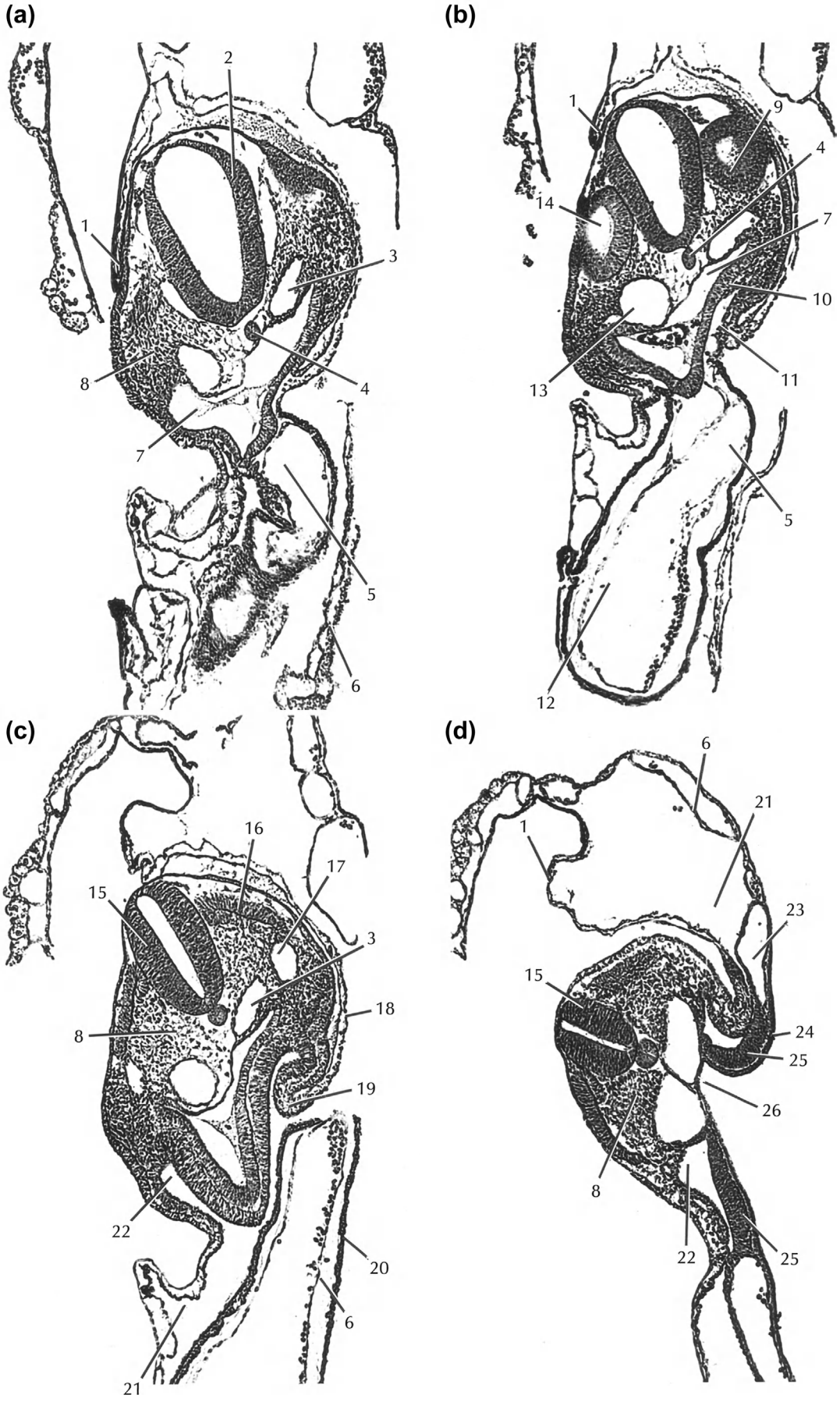

Downloaded from Vet-eBooks.com

Plate 80 Stage 14 (50–53 h)

Light micrographs of a whole-mounted stage 14 embryo (50–53 hours incubation).

(a) Shows relationship to area vasculosa: × 5.

(b) Image has been adjusted to show the major blood vessels: × 20.

1. trimmed edge of area vasculosa
2. amnio-chorion visible as a lighter area
3. blood islands in area vasculosa
4. left omphalo-mesenteric artery
5. dorsal aorta
6. vascular network around eye
7. ventral aorta
8. S-shaped heart
9. vascular network in liver
10. right omphalo-mesenteric (vitelline) artery

Downloaded from Vet-eBooks.com

Plate 80

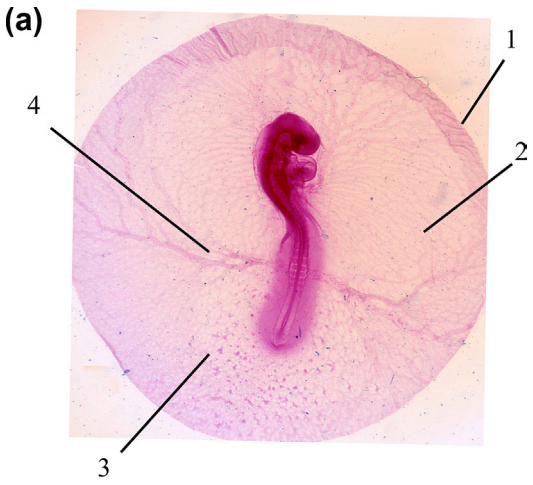

Downloaded from Vet-eBooks.com

Plate 81 Stage 14 (50–53 h) LS: coronal

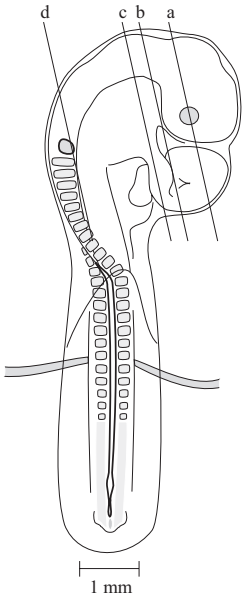

Longitudinal sections in the coronal plane: (a–d) × 125

1. optic stalk
2. amnion
3. diocoele (third ventricle)
4. optic cup
5. lens vesicle
6. head mesenchyme
7. diencephalon
8. left dorsal aorta
9. left anterior cardinal vein
10. first aortic arch
11. Rathke's pouch
12. infundibulum
13. aortic sac
14. pericardial cavity
15. ventricle
16. truncus arteriosus
17. amniotic cavity
18. right first (mandibular) pharyngeal arch
19. oral cavity
20. myelencephalon
21. otic vesicle
22. coelom
23. endoderm of gut
24. splanchnic mesoderm of gut
25. notochord

Downloaded from Vet-eBooks.com

Plate 81

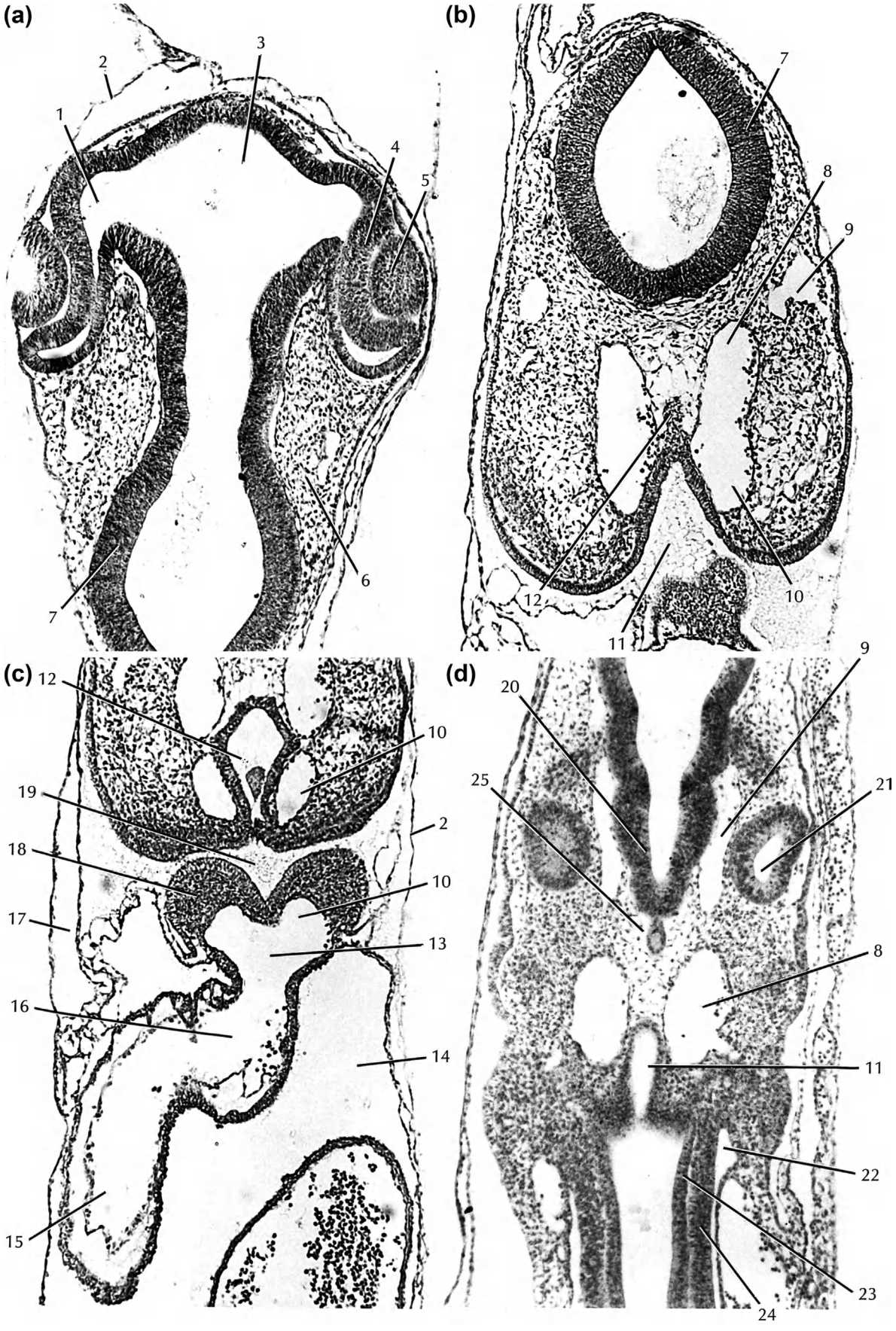

Downloaded from Vet-eBooks.com

Plate 82 Stage 14 (50–53 h) LS: coronal and sagittal

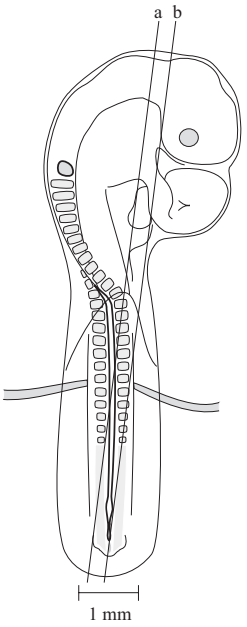

The cervical flexure (see chapter 5 page 46) is incomplete, so the sections pass coronally through the anterior end of the embryo and sagittally through the posterior end.

(a, b) × 45

1. left anterior cardinal vein
2. left dorsal aorta
3. second aortic arch
4. second pharyngeal pouch
5. pharynx
6. atrium
7. sinus venosus
8. left posterior cardinal vein
9. endoderm
10. lateral plate mesoderm
11. somite
12. third aortic arch
13. second pharyngeal groove
14. amniotic cavity
15. diencephalon
16. right dorsal aorta
17. left first (mandibular) pharyngeal arch
18. amnion
19. ventricle
20. coelom
21. notochord
22. segmental plate mesoderm
23. Hensen's (primitive) node
24. neural tube
25. right anterior cardinal vein
26. third pharyngeal arch
27. Rathke's pouch

Downloaded from Vet-eBooks.com

Plate 82

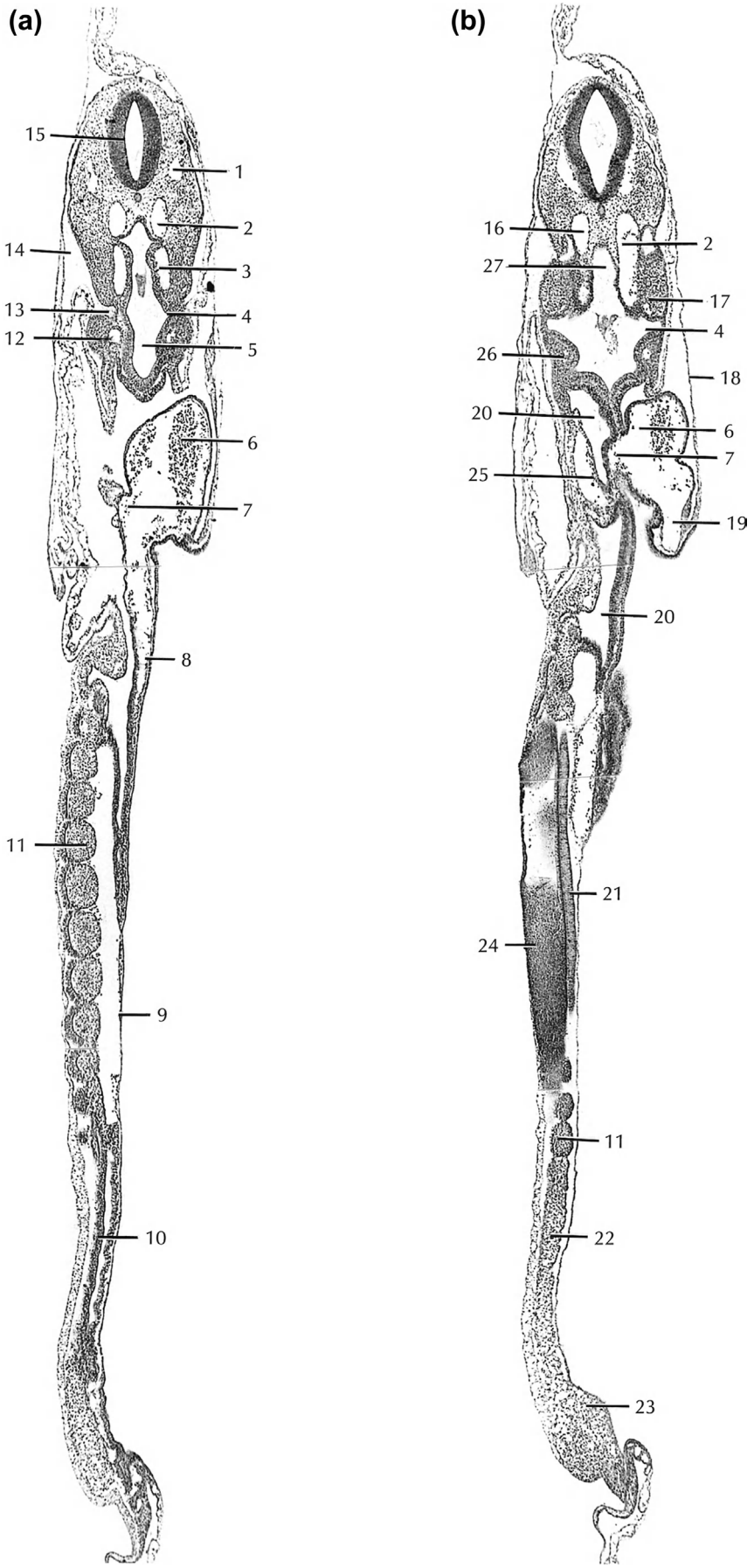

Downloaded from Vet-eBooks.com

Plate 83 Stage 14 (50–53 h) LS: coronal and sagittal

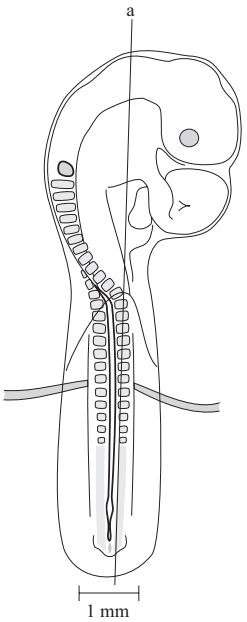

The cervical flexure (see chapter 5 page 46) is incomplete, so that the sections pass coronally through the anterior end and sagittally through the posterior end.

(a) × 45 (b) × 85 (c) × 135

1. yolk sac
2. notochord
3. third pharyngeal pouch
4. fourth pharyngeal arch
5. lumen of pharynx
6. oesophagus
7. right dorsal aorta
8. endoderm
9. somite
10. ectoderm
11. neural tube
12. posterior tip of amniotic fold
13. fourth pharyngeal pouch
14. right dorsal aorta
15. myelencephalon
16. wall of pharynx
17. coelom
18. tail bud mesoderm
19. posterior intestinal portal
20. hindgut
21. posterior amniotic fold
22. ectoderm of tail bud

Downloaded from Vet-eBooks.com

Plate 83

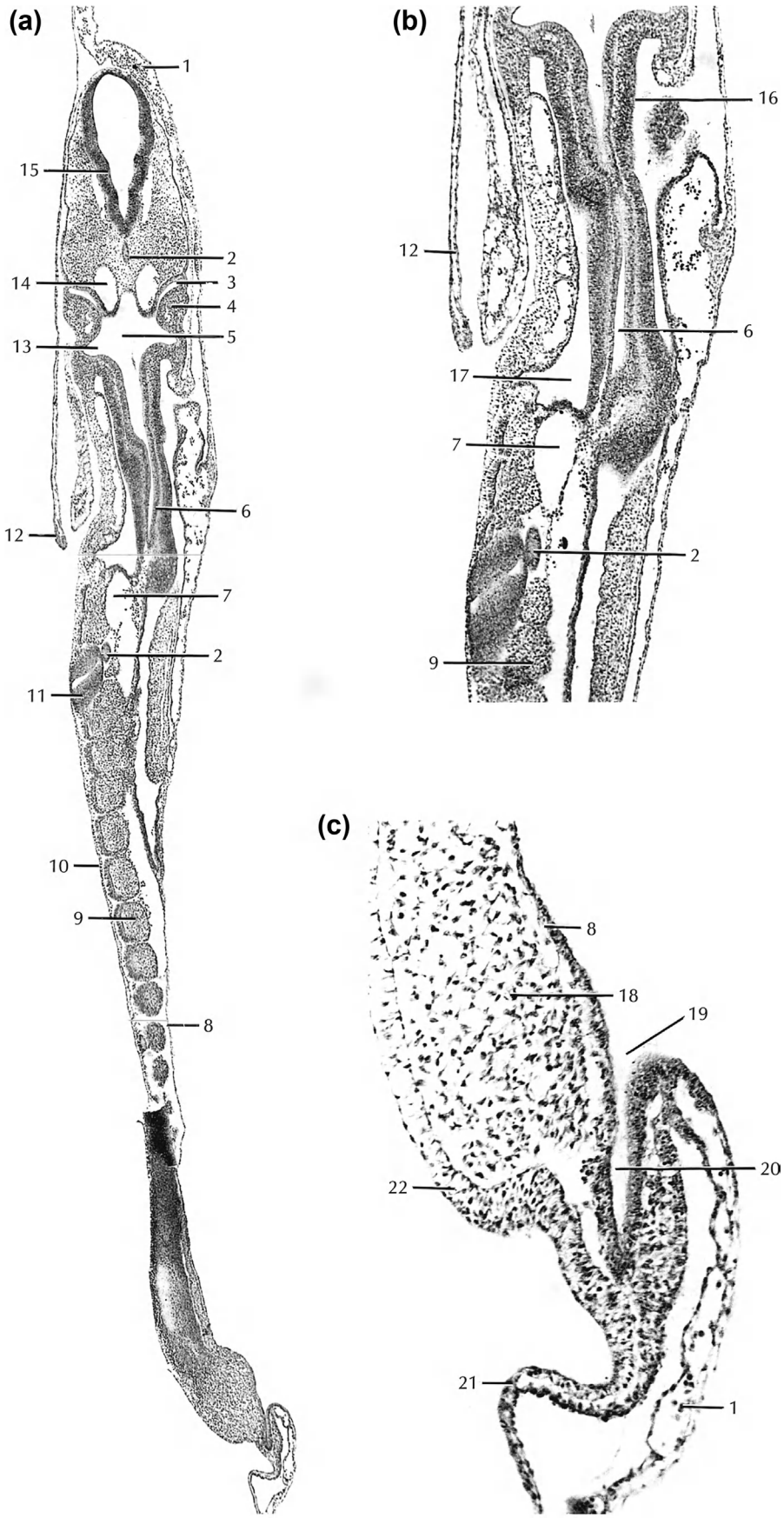

Downloaded from Vet-eBooks.com

Plate 84 Stage 14 (50–53 h) TS

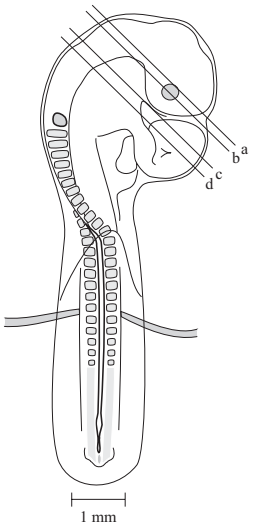

Transverse sections (TS): (a–d) × 85

1. mesencephalon
2. head mesenchyme
3. tip of optic evagination
4. diocoele
5. wall of diencephalon
6. yolk sac
7. left optic evagination
8. left optic stalk
9. mesocoele
10. left anterior cardinal vein
11. left dorsal aorta
12. left ventral aorta
13. stomatodaeum (stomatodaeal plate)
14. pharynx
15. notochord
16. right dorsal aorta
17. chorion
18. amnion
19. aortic sac

Downloaded from Vet-eBooks.com

Plate 84

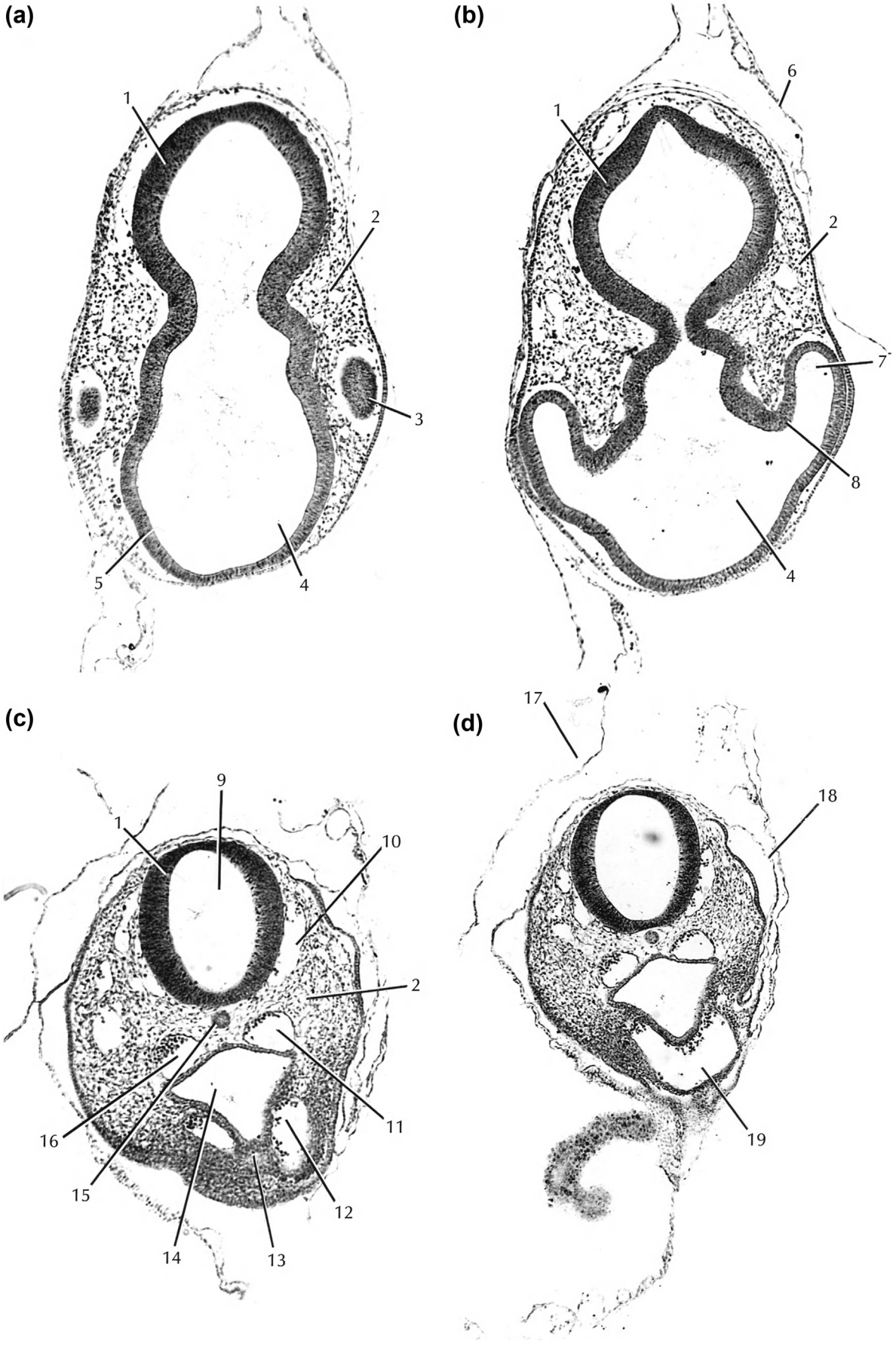

Downloaded from Vet-eBooks.com

Plate 85 Stage 14 (50–53 h) TS

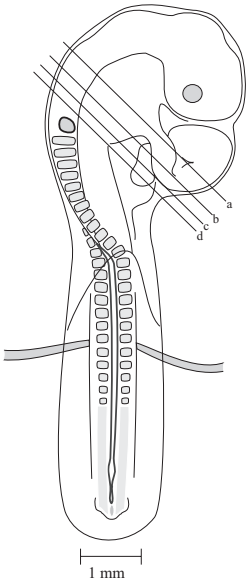

Transverse sections (TS): (a–d) × 85

1. thick wall of myelencephalon
2. thin roof of myelencephalon
3. left dorsal aorta
4. pharynx
5. lumen of truncus arteriosus
6. junction of truncus arteriosus and ventricle
7. ventricle
8. notochord
9. right anterior cardinal vein
10. fourth ventricle
11. left anterior cardinal vein
12. epimyocardium
13. atrium
14. right dorsal aorta
15. gap between the amniotic folds posterior to their fusion
16. left amniotic fold
17. chorion
18. amnion
19. left otic placode
20. right amniotic fold
21. fused dorsal aortae
22. derma-myotome
23. lateral body fold
24. extra-embryonic coelom
25. communication between embryonic and extra-embryonic coeloms
26. embryonic coelom

Downloaded from Vet-eBooks.com

Plate 85

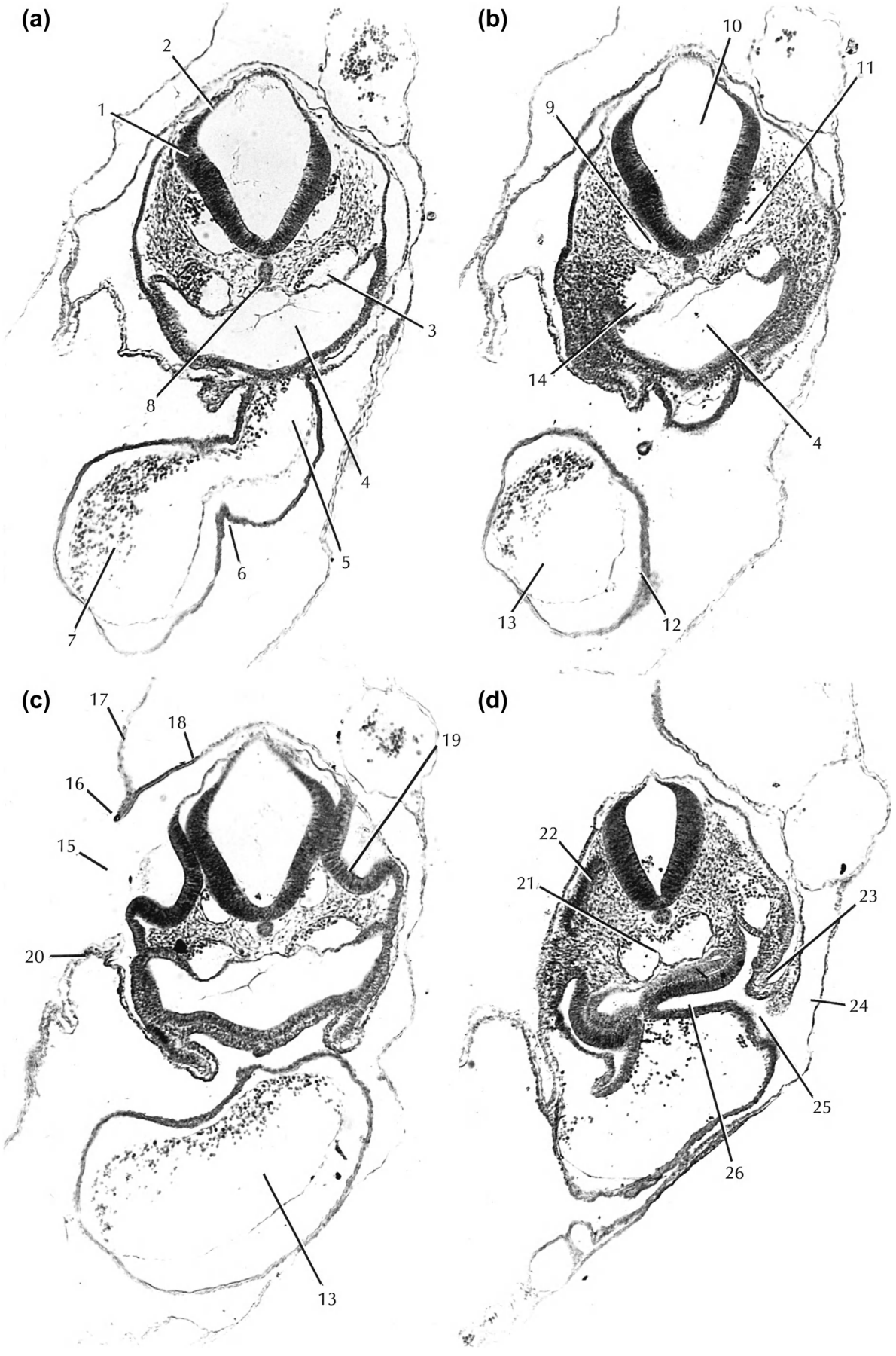

Downloaded from Vet-eBooks.com

Plate 86 Stage 14 (50–53 h) TS

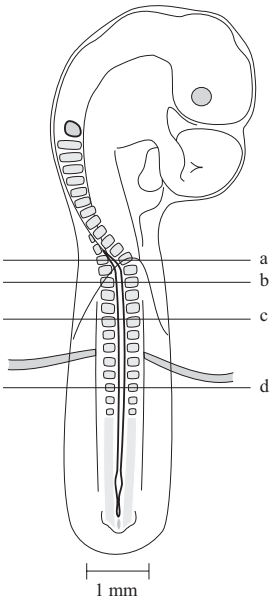

Transverse sections (TS): (a, b) × 85 (c, d) × 100

1. lateral plate mesoderm
2. derma-myotome
3. left omphalo-mesenteric vein
4. anterior intestinal portal
5. splanchnopleure
6. right embryonic coelom
7. left amniotic fold
8. left extra-embryonic coelom
9. left embryonic coelom
10. notochord
11. right nephric primordium
12. sclerotome
13. neural tube
14. ectoderm
15. left nephric primordium
16. somatic lateral plate mesoderm
17. left dorsal aorta
18. endoderm of midgut
19. right dorsal aorta
20. splanchnic lateral plate mesoderm
21. right newly formed somite
22. roof of neural tube
23. left newly formed somite
24. floor plate of neural tube

Downloaded from Vet-eBooks.com

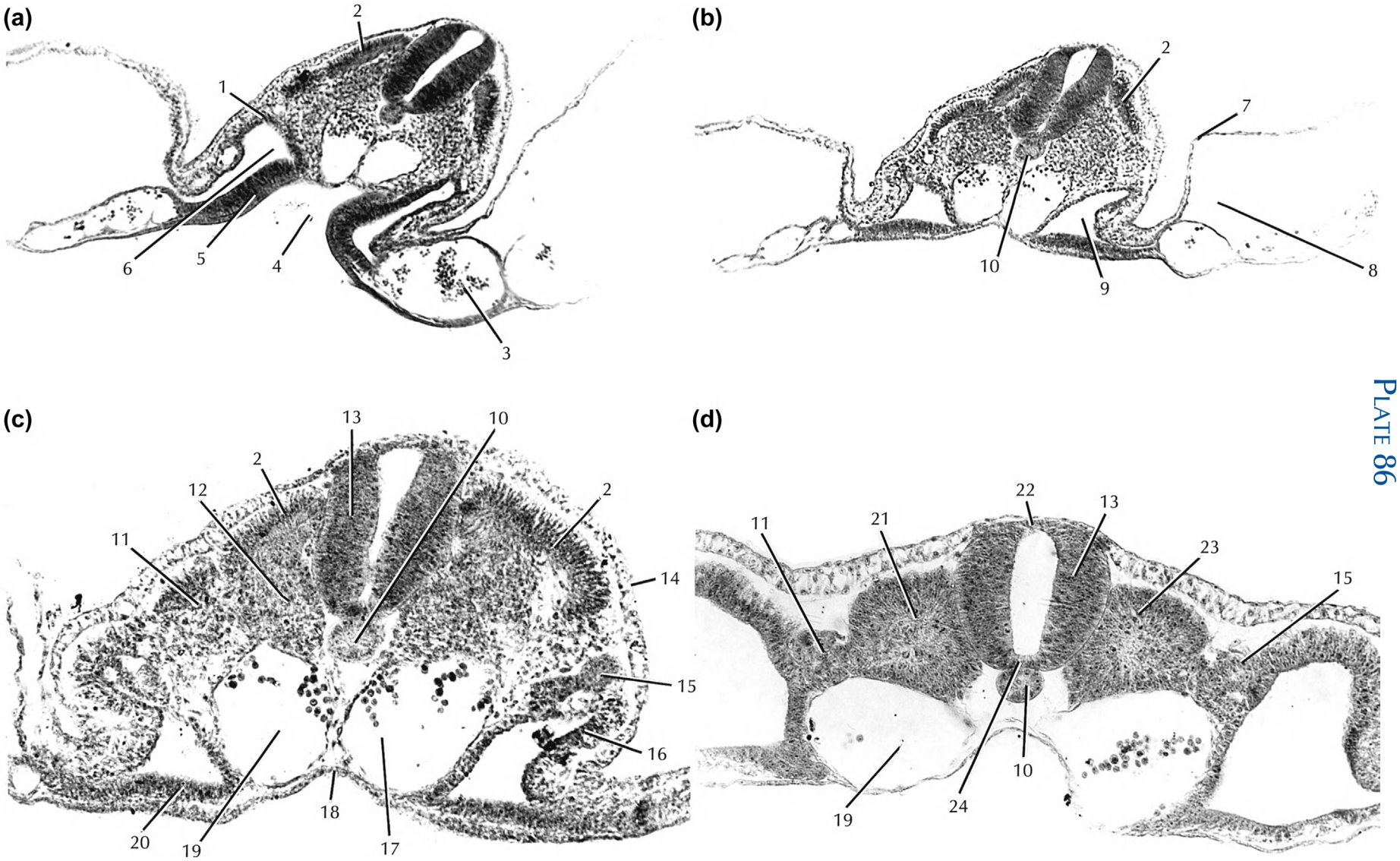

PLATE 86

Downloaded from Vet eBooks.com

Plate 87 Stage 14 (50–53 h) TS

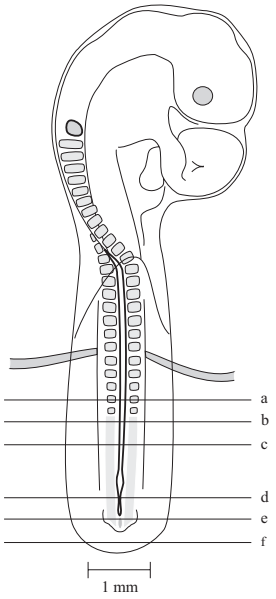

Transverse sections (TS): (a–f) × 100

1. ectoderm
2. somatic lateral plate mesoderm
3. nephric primordium
4. somite
5. notochord
6. splanchnic lateral plate mesoderm
7. embryonic coelom
8. posterior end of primary neural tube showing several lumina
9. segmental plate mesoderm
10. endoderm
11. left dorsal aorta
12. region of overlap of primary and secondary neural tube
13. secondary neural tube
14. tail bud mesoderm

Downloaded from Vet-eBooks.com

Plate 87

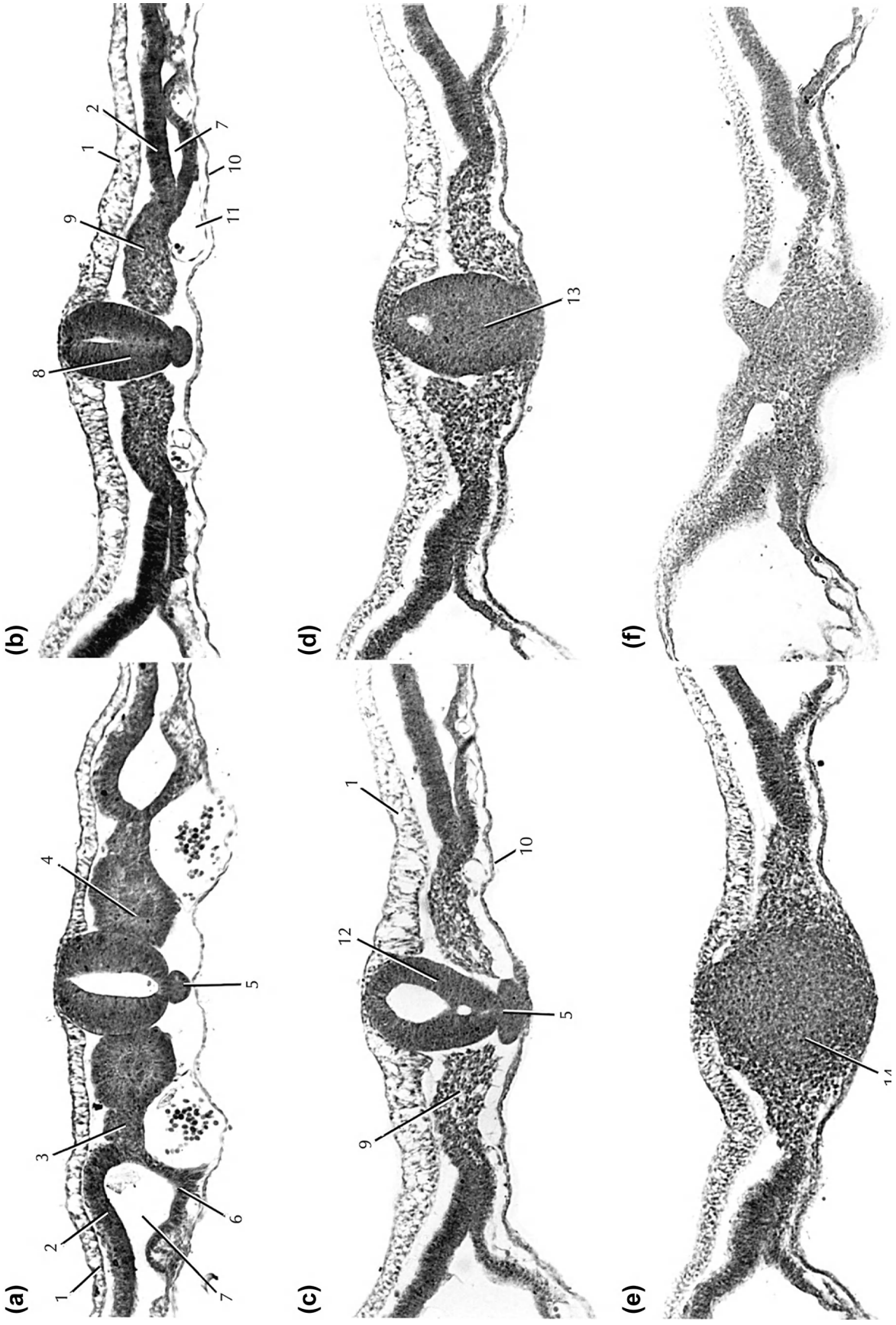

Downloaded from Vet-eBooks.com

Plate 88 Stage 16 (52–64 h)

Whole-mounted embryo viewed from the right side at the head end and dorsally at the caudal end: × 10

1. metencephalon
2. isthmus
3. amnion
4. mesencephalon
5. telencephalon
6. optic cup
7. pineal organ
8. diencephalon
9. ventricle
10. lateral body wall
11. right omphalo-mesenteric artery
12. somite
13. border of anterior amniotic fold
14. right leg bud
15. segmental plate
16. border of posterior amniotic fold
17. tail bud
18. neural tube
19. left leg bud
20. somite differentiated into myotome, sclerotome, dermatome
21. truncus arteriosus
22. otic vesicle

Downloaded from Vet-eBooks.com

Plate 88

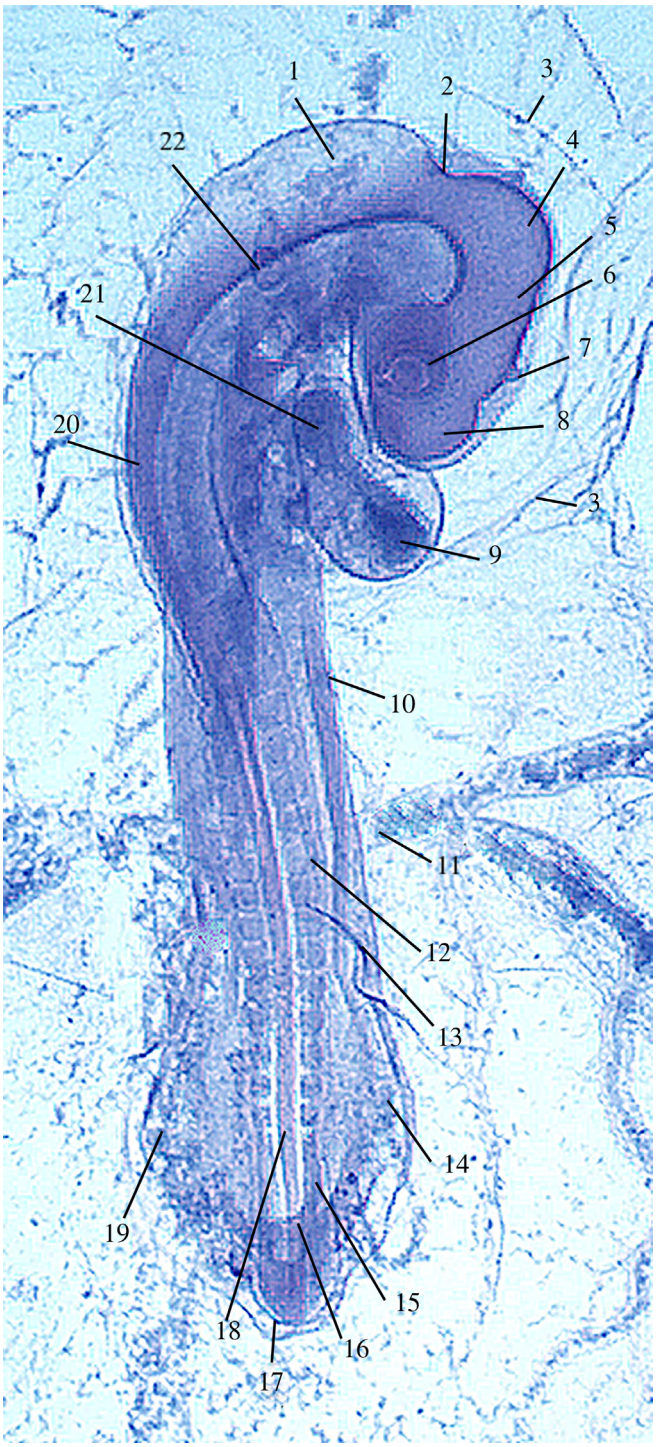

Downloaded from Vet-eBooks.com

Plate 89 Stage 17 (52–64 h) TS

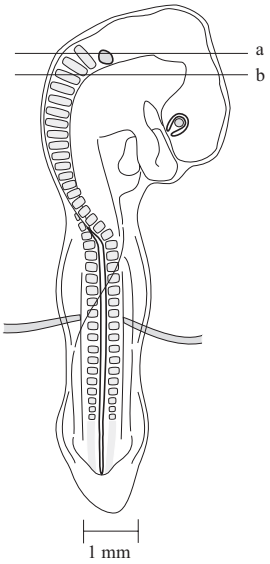

Transverse sections (TS): × 30

1. myelencephalon
2. left otic vesicle
3. left acoustic-facial (cranial nerves VII and VIII) ganglion
4. left trigeminal (cranial nerve V) ganglion
5. tip of mesencephalon
6. head mesenchyme
7. right acoustic-facial (cranial nerves VII and VIII) ganglion
8. right otic vesicle
9. neural tube
10. notochord
11. dorsal aorta
12. left anterior cardinal vein
13. left fourth aortic arch
14. left third aortic arch
15. left second aortic arch
16. left first aortic arch
17. Rathke's pouch
18. right head vein
19. head mesenchyme
20. right second pharyngeal arch
21. right second ectodermal groove
22. right third aortic arch
23. pharynx
24. right anterior cardinal vein
25. myotome
26. ectoderm

Downloaded from Vet-eBooks.com

Plate 89

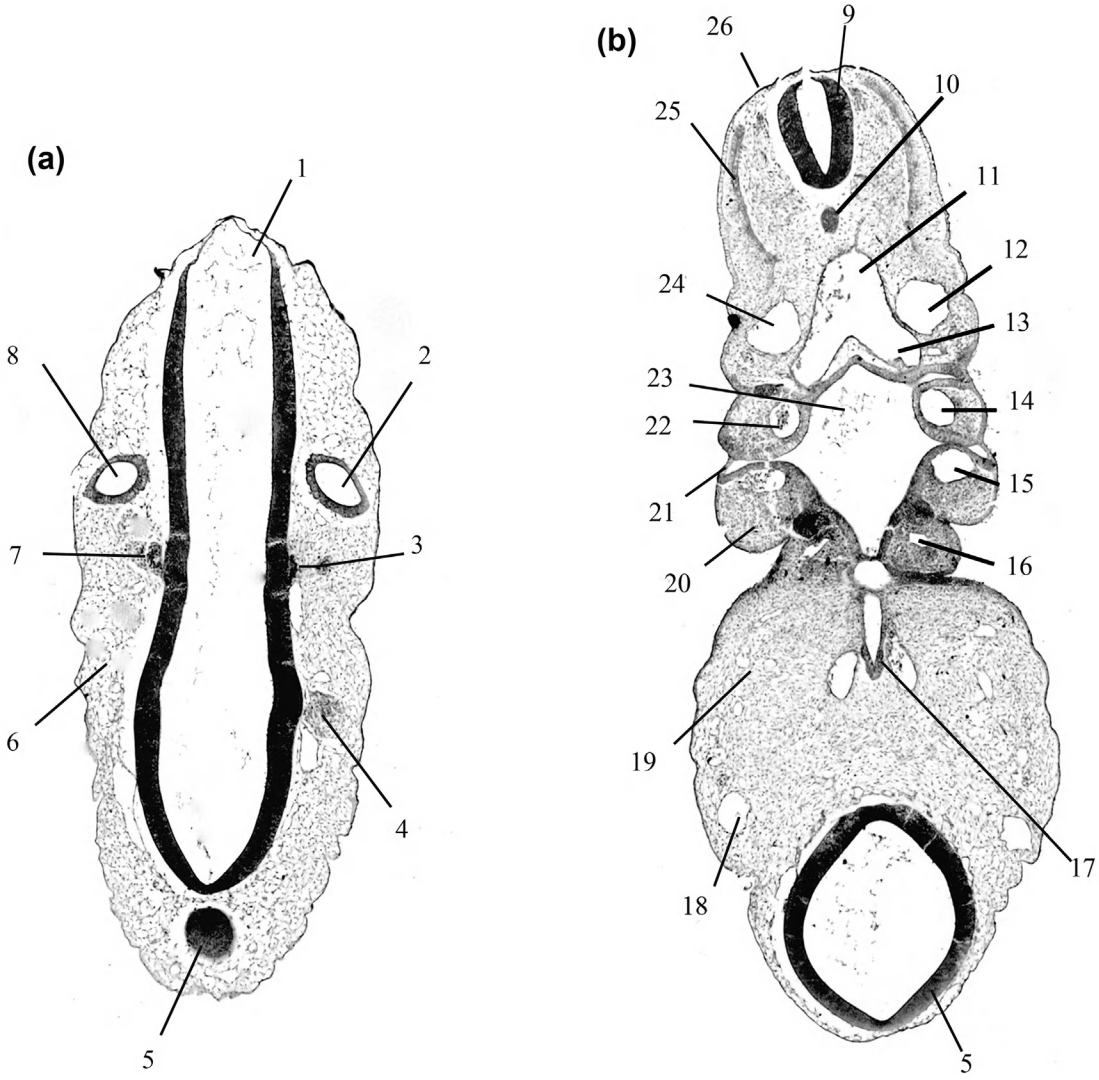

Downloaded From Vet-eBooks.com

Plate 90 Stage 17 (52–64 h) TS

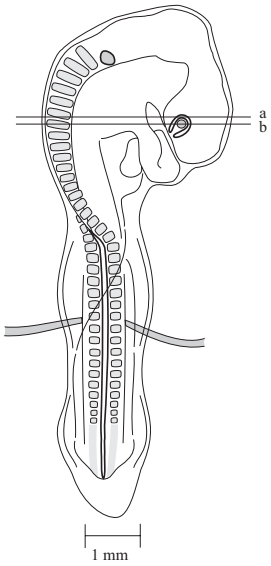

Transverse sections (TS): × 30

1. neural tube
2. notochord
3. dorsal aorta
4. left anterior cardinal vein
5. fourth pharyngeal pouch
6. third ectodermal groove
7. third aortic arch
8. mesenchymal condensations
9. left lens
10. left retina
11. diencephalon
12. head mesenchyme
13. mandibular arch
14. pharynx
15. thyroglossal duct
16. floor of pharynx
17. right anterior cardinal vein
18. myotome
19. left atrium
20. left optic stalk
21. right lens
22. truncus arteriosus
23. embryonic coelom
24. laryngo-tracheal groove
25. oesophagus
26. remnant of amnion after dissection

Downloaded from Vet-eBooks.com

Plate 90

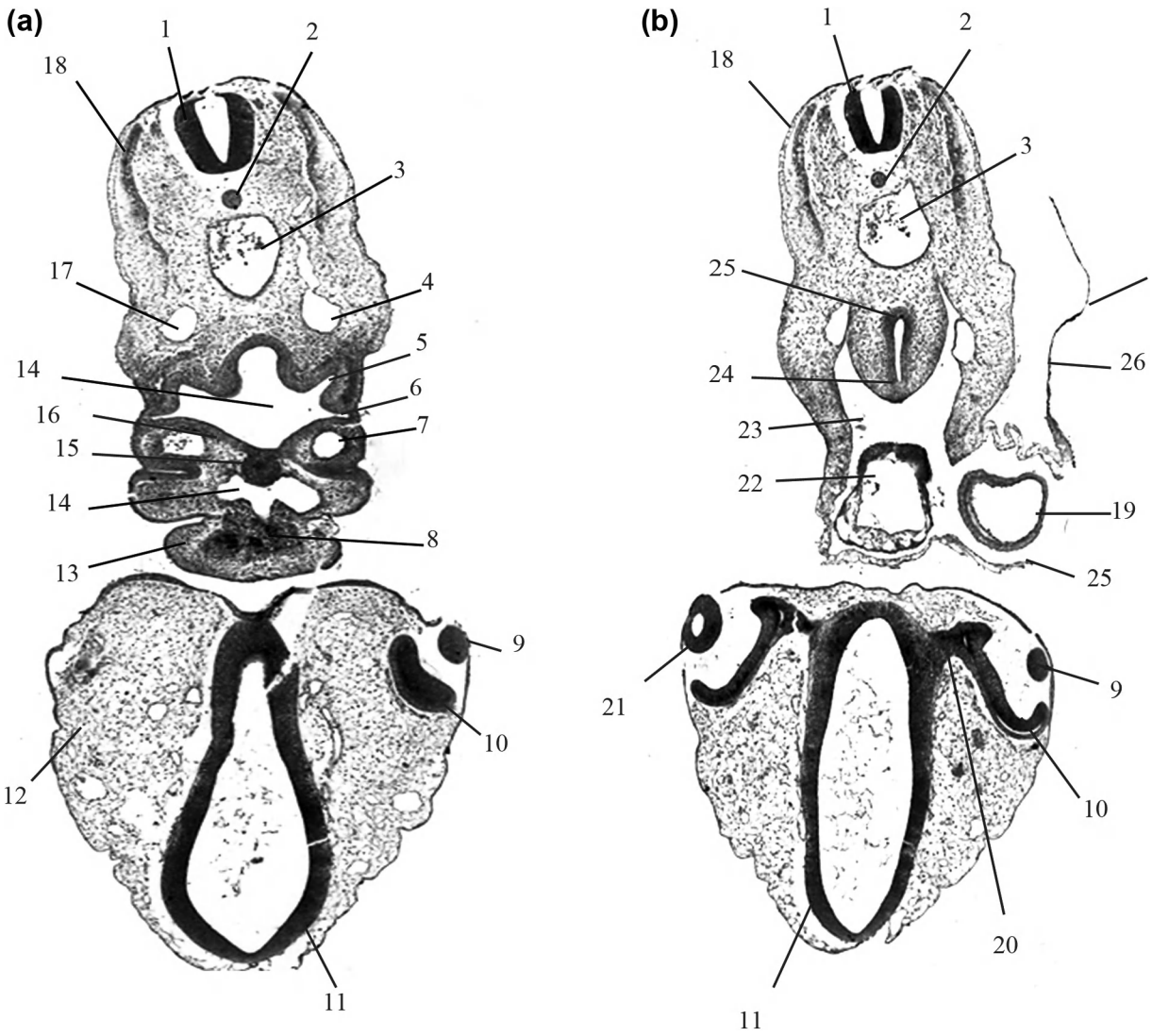

Downloaded from Vet-eBooks.com

Plate 91 Stage 17 (52–64 h) TS

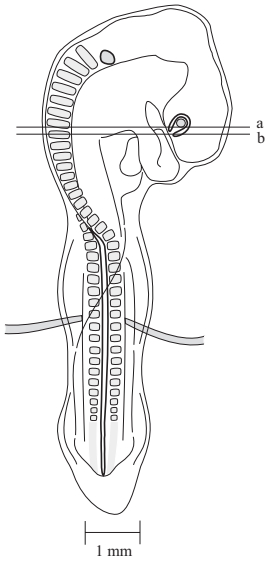

Transverse sections (TS): × 30

1. neural tube
2. notochord
3. dorsal aorta
4. left anterior cardinal vein
5. dorsal mesentery
6. left internal coelom
7. gut
8. ventral mesentery
9. atrium
10. ventricle
11. left optic cup
12. diencephalon
13. right optic cup
14. right lens
15. right optic stalk
16. truncus arteriosus
17. right internal coelom
18. dermatome
19. nasal placode
20. atrio-ventricular canal

Downloaded from Vet-eBooks.com

Plate 91

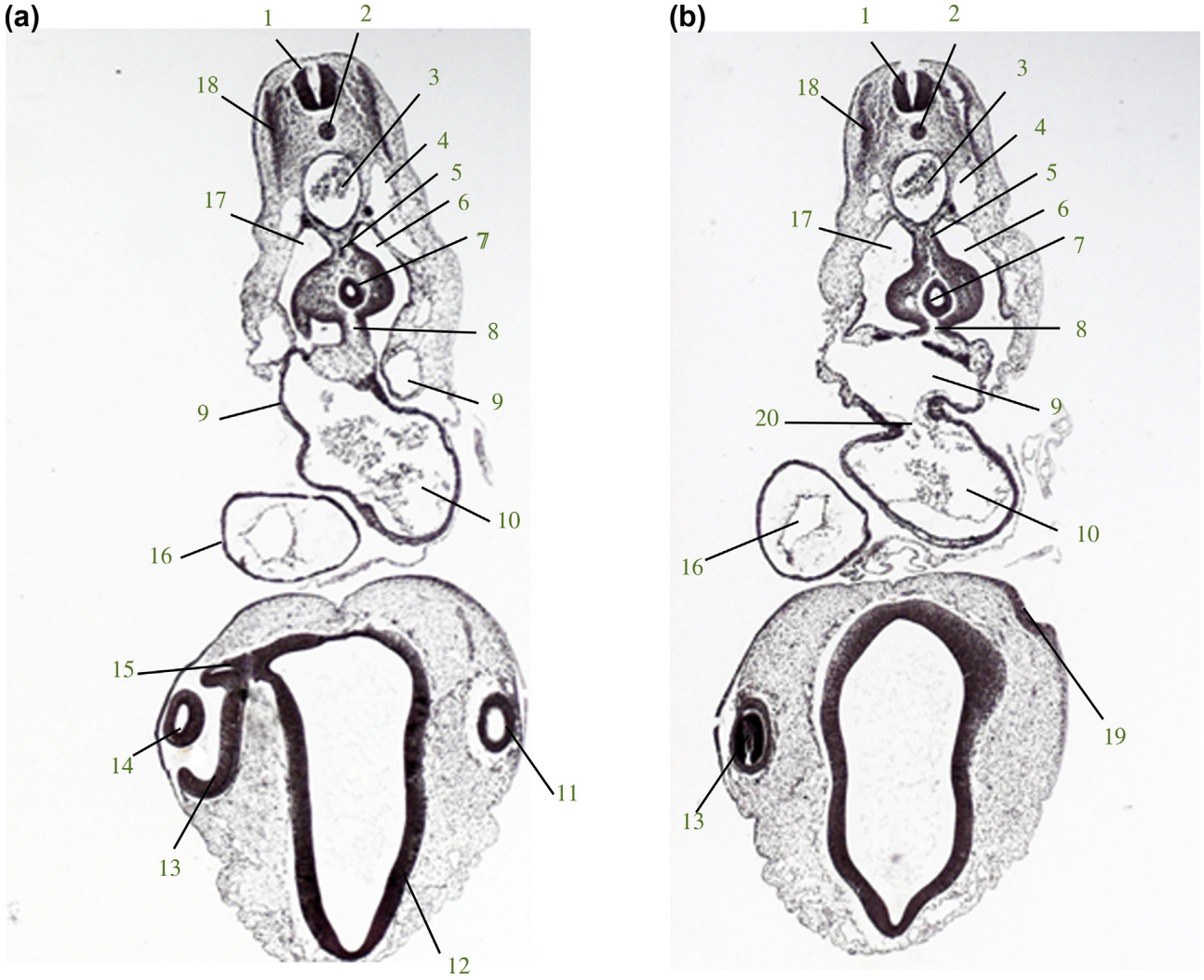

Downloaded from Vet-eBooks.com

Plate 92 Stage 17 (52–64 h) TS

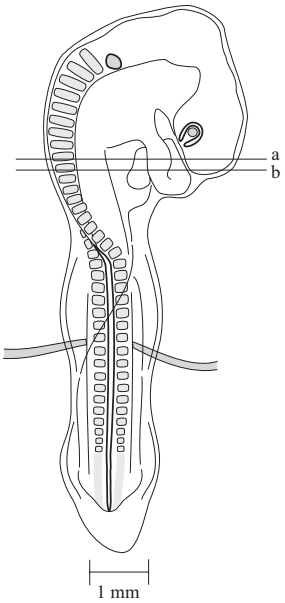

Transverse sections (TS): × 30

1. neural tube
2. notochord
3. dorsal aorta
4. left anterior cardinal vein
5. dorsal mesentery
6. gut
7. ventral mesentery
8. ventricle
9. left nasal placode
10. diocoele
11. truncus arteriosus
12. atrium
13. right internal coelom
14. dermatome
15. yolk sac wall
16. telocoele
17. right nasal placode

Downloaded from Vet-eBooks.com

Plate 92

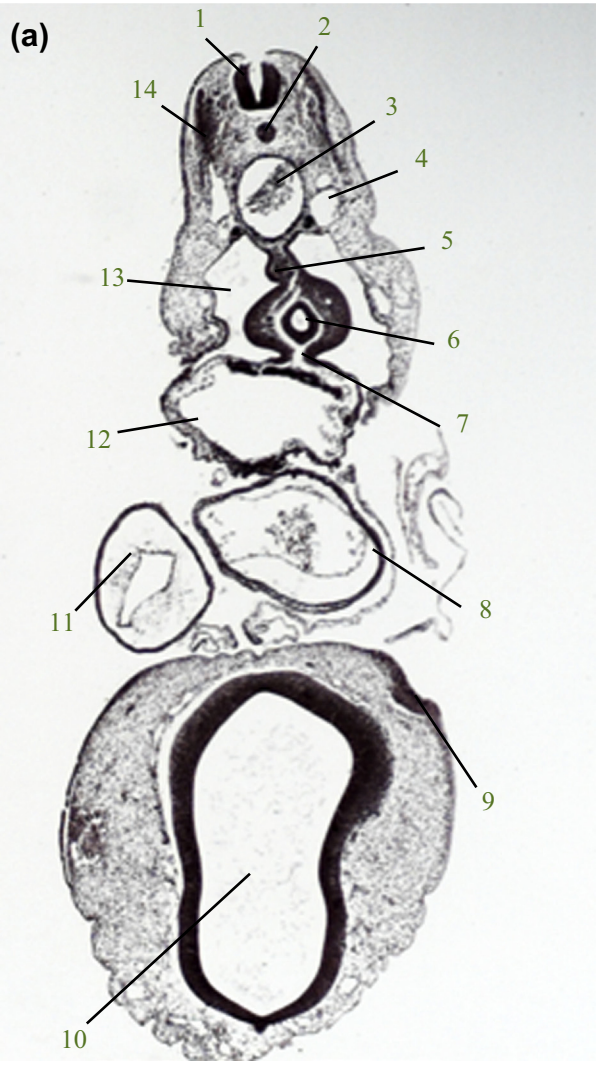

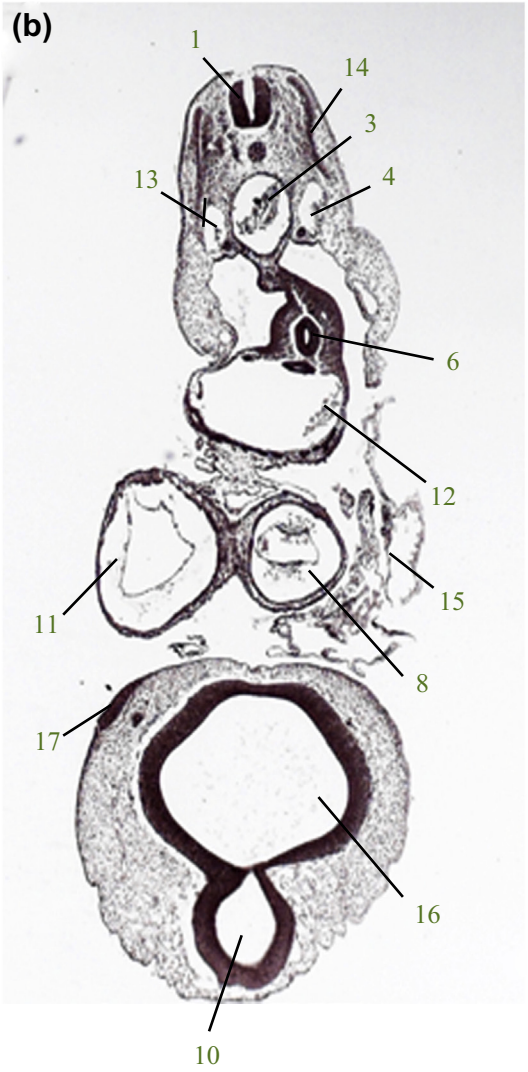

Downloaded from Vet-eBooks.com

Plate 93 Stage 17 (52–64 h) TS

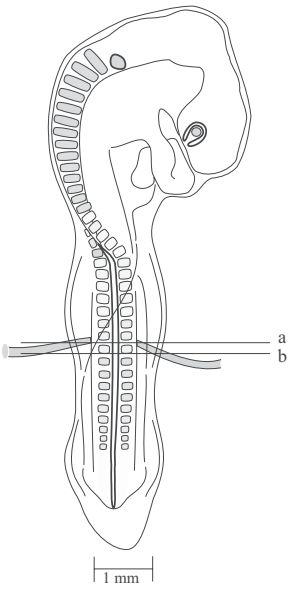

Transverse sections (TS): × 30

1. neural tube
2. notochord
3. dermatome
4. myotome
5. right anterior cardinal vein
6. left mesonephros
7. left internal coelom
8. communication between internal and external coeloms
9. left omphalo-mesenteric vein
10. midgut
11. bulge of yolk sac
12. right internal coelom
13. right anterior cardinal vein
14. dorsal aorta
15. sclerotome
16. opening of midgut
17. right omphalo-mesenteric vein
18. right mesonephros

Downloaded from Vet-eBooks.com

Plate 93

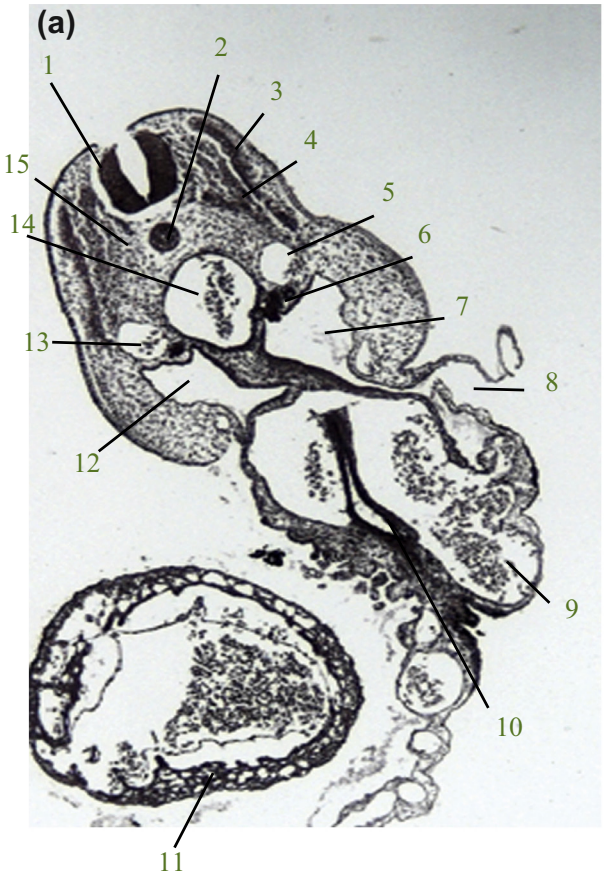

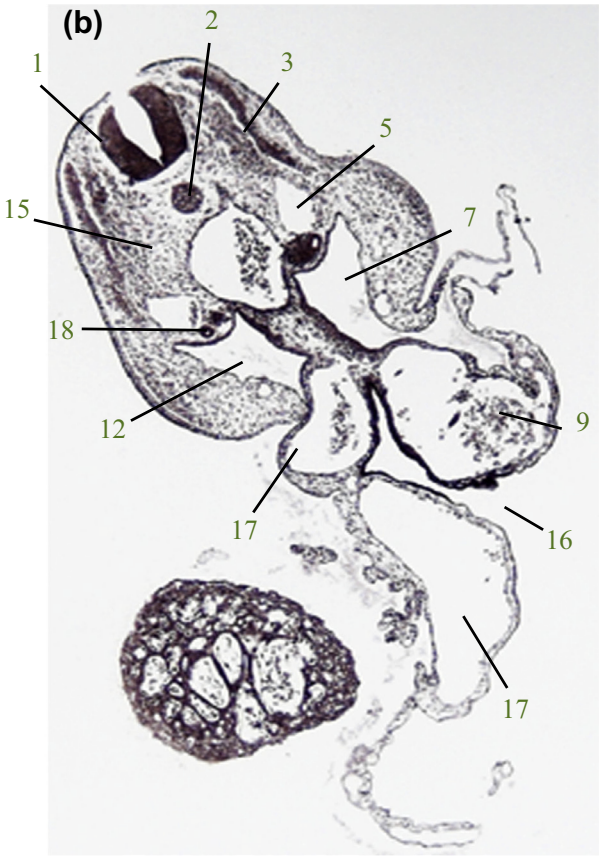

Downloaded From Vet-eBooks.com

Plate 94 Stage 18 (65–69 h)

Whole-mounted embryo viewed from the left side: × 30

1. mesencephalon
2. isthmus in meso-metencephalic fold
3. eye
4. pharynx
5. sclero-myotomes
6. right wing bud
7. right leg bud
8. left leg bud
9. allantois
10. heart
11. telocoele

Downloaded from Vet-eBooks.com

Plate 94

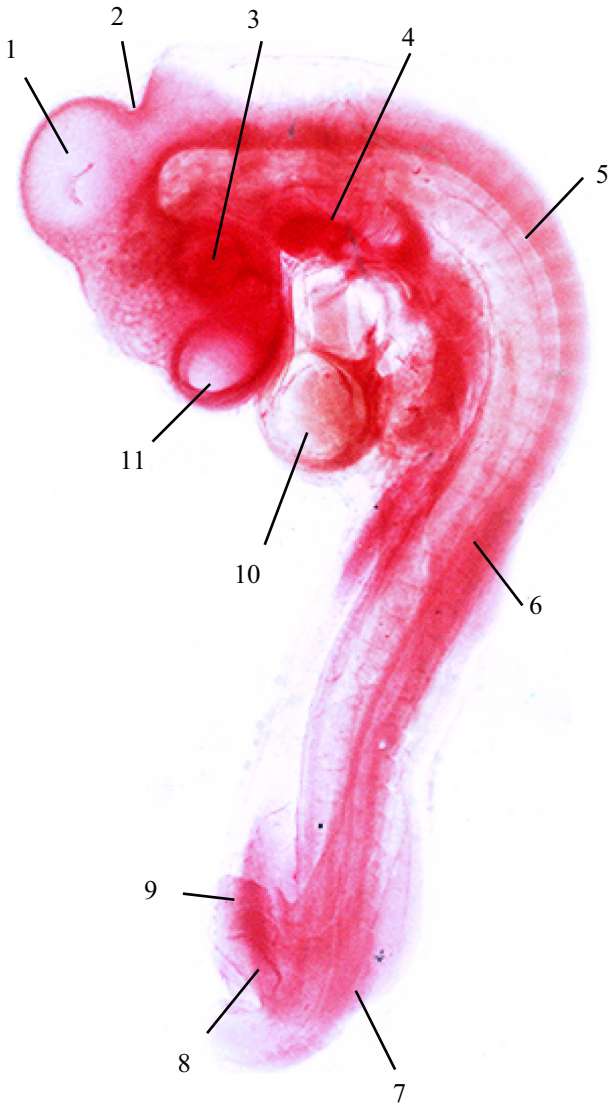

Downloaded from Vet-eBooks.com

Plate 95 Stage 18 (65–69 h) LS

Longitudinal (sagittal) section viewed from the left side, as shown in *plate 94*: × 24

1. first pharyngeal arch (mandibular part)
2. second aortic arch
3. second pharyngeal arch
4. third pharyngeal arch
5. left head vein
6. amnion
7. myotome
8. pharynx
9. truncus arteriosus
10. dorsal aorta
11. ventricle wall
12. lumen of ventricle
13. eye
14. mesencephalon
15. left anterior cardinal vein

Downloaded from Vet-eBooks.com

Plate 95

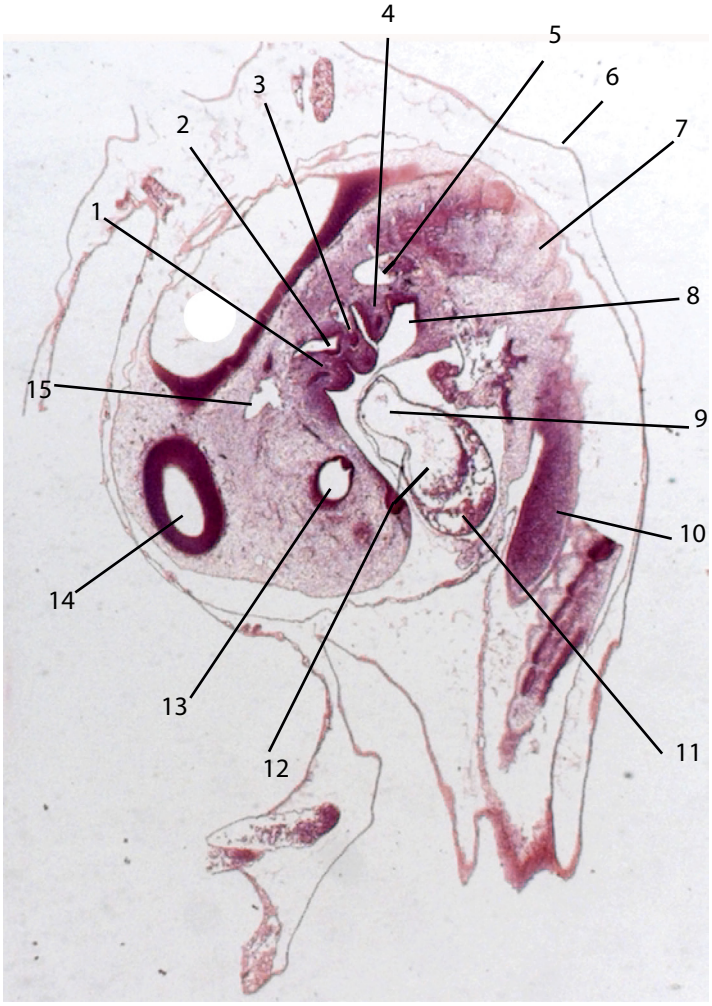

Downloaded from Vet-eBooks.com

Plate 96 Stage 18 (65–69 h) LS

Longitudinal (sagittal) section viewed from the left side, as shown in *plate 94*: × 24

1. notochord
2. truncus arteriosus
3. epidermis
4. atrium
5. lung bud
6. sinus venosus
7. ventricle
8. neural tube
9. body wall
10. dorsal aorta
11. sero-amniotic connection
12. mesonephros
13. left leg bud
14. lumen of neural tube
15. dermatome
16. hindgut
17. optic recess, which marks the original anterior tip of the neural plate
18. Rathke's pouch
19. isthmus
20. metacoele

Downloaded from Vet-eBooks.com

Plate 96

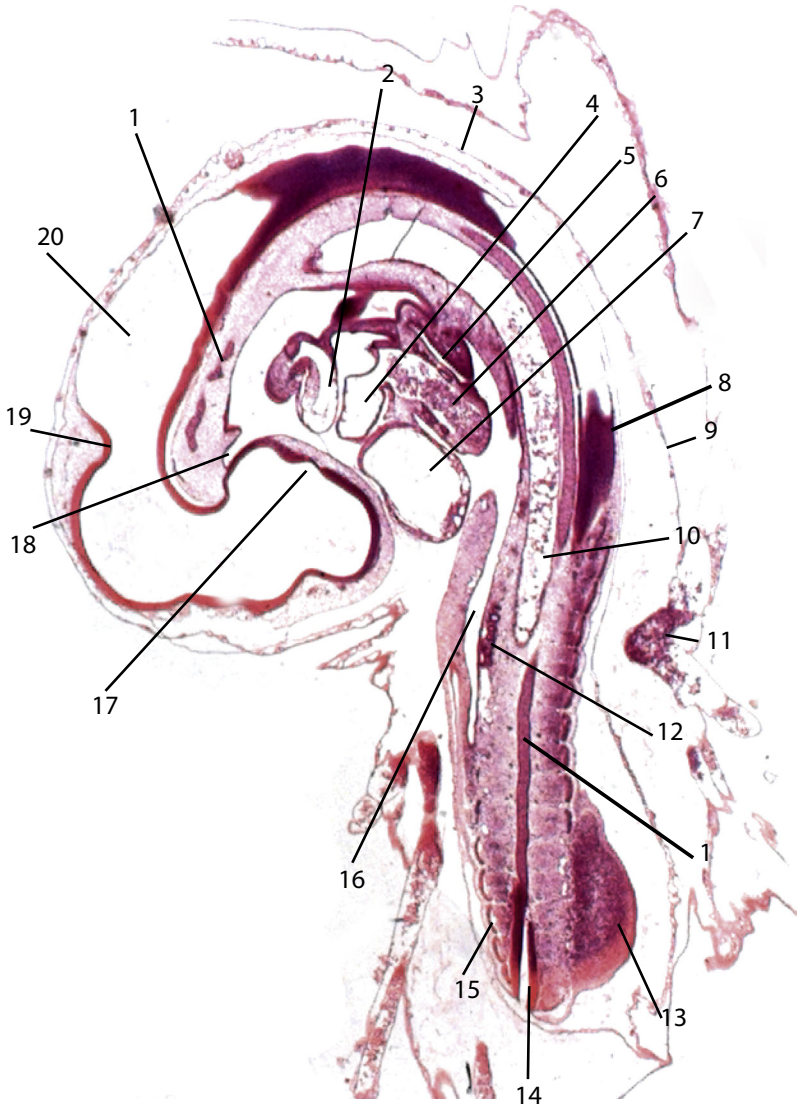

Downloaded from Vet-eBooks.com

Plate 97 Stage 18 (65–69 h) LS

Longitudinal (sagittal) section viewed from the left side, as shown in *plate 94*: × 24

1. first pharyngeal arch (mandibular part)
2. second aortic arch
3. trigeminal (cranial nerve V) ganglion
4. second pharyngeal arch
5. acoustic (cranial nerve VIII) ganglion
6. otic vesicle
7. fourth pharyngeal arch
8. glossopharyngeal (cranial IX) nerve
9. internal carotid artery
10. fourth aortic arch
11. pharynx
12. base of internal carotid artery
13. aortic arch
14. dorsal aorta
15. gut in mesentery
16. ventricle
17. mesonephros
18. ventral mesentery
19. dorsal mesentery
20. coelom
21. lumen of hindgut
22. neural tube
23. leg bud
24. wall of hindgut
25. umbilical vein
26. diencephalon
27. meso-metencephalic fold
28. mesencephalon

Downloaded from Vet-eBooks.com

Plate 97

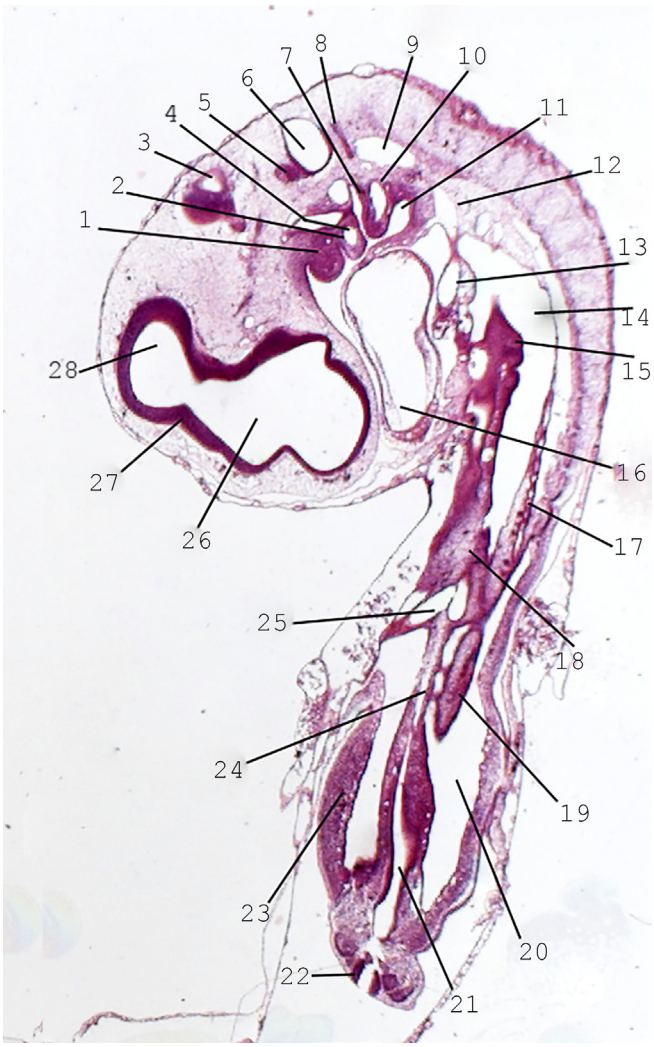

Downloaded from Vet-eBooks.com

Plate 98 Stage 18 (65–69 h)

Longitudinal (sagittal) section viewed from the left side, as shown in *plate 94*: × 24

1. floor of forebrain
2. dorsal aorta
3. wall of myelencephalon
4. pharynx
5. myotome
6. atrium
7. sinus venosus
8. ventricle
9. neural tube
10. tip of leg bud
11. somite
12. hindgut
13. omphalo-mesenteric vein
14. telencephalon
15. diencephalon
16. mesencephalon
17. meso-metencephalic fold
18. conus arteriosus
19. first aortic arch
20. second aortic arch

Downloaded from Vet-eBooks.com

Plate 98

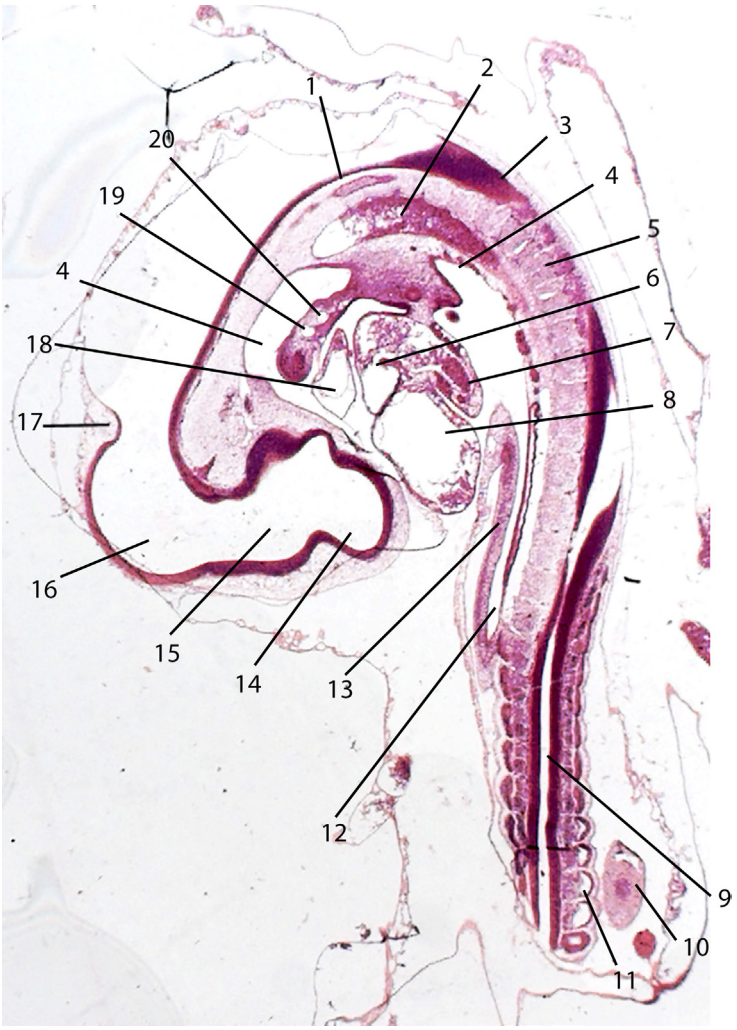

Downloaded from Vet-eBooks.com

Plate 99 Stage 18 (65–69 h) TS

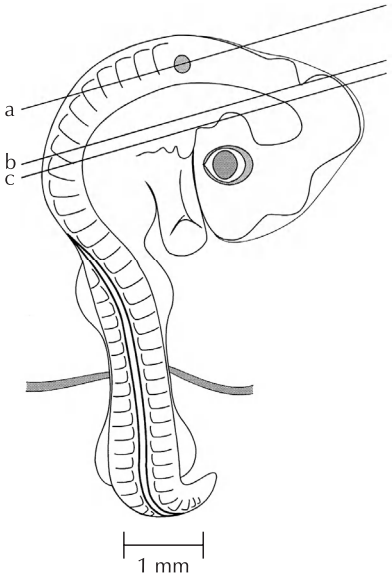

Transverse sections (TS): (a–c) × 45

1. dorsal aorta
2. notochord
3. neural tube
4. yolk sac
5. left third pharyngeal pouch
6. left third aortic arch
7. left second pharyngeal pouch
8. right otic vesicle
9. right second aortic arch
10. right third aortic arch
11. right fourth aortic arch
12. right anterior cardinal vein
13. thick wall of pharynx
14. coelom
15. left internal carotid artery
16. mesencephalon
17. left anterior cardinal vein
18. oesophagus
19. lung bud
20. left atrium
21. second (hyoid) pharyngeal arch
22. myotome
23. ophthalmic branch of trigeminal (cranial V) nerve
24. right internal carotid artery
25. pharynx
26. thyroid invagination – foramen caecum

Downloaded from Vet-eBooks.com

Plate 99

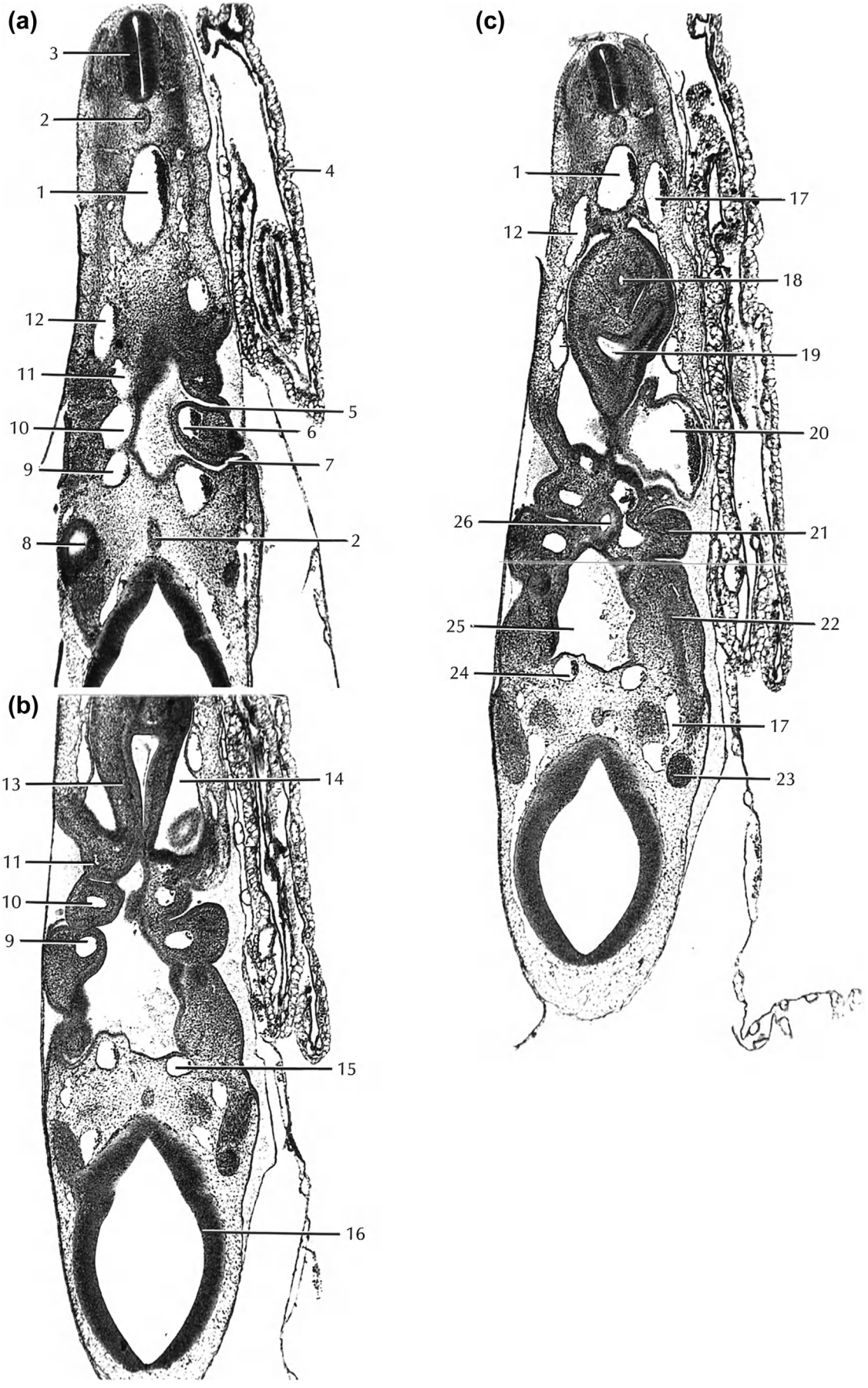

Downloaded From Vet-eBooks.com

Plate 100 Stage 18 (65–69 h) TS

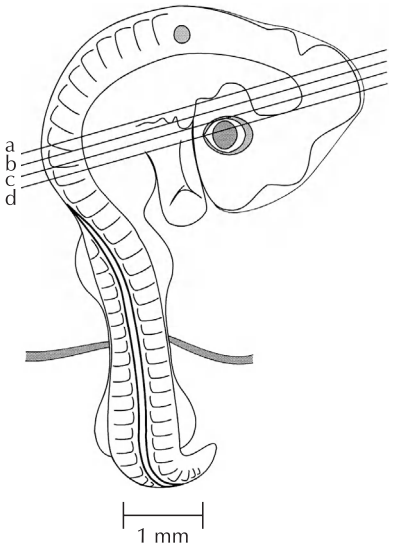

Transverse sections (TS): (a–d) × 45

1. dorsal mesentery
2. ventral mesentery
3. left atrium
4. oral cavity
5. ophthalmic branch of trigeminal (cranial V) nerve
6. right anterior cardinal vein
7. right internal carotid artery
8. right first (maxillary) pharyngeal arch
9. right first (mandibular) pharyngeal arch
10. truncus arteriosus
11. sinus venosus
12. right anterior cardinal vein
13. coelom
14. dorsal aorta
15. left anterior cardinal vein
16. left first (maxillary) pharyngeal arch
17. Rathke's pouch
18. oesophagus
19. bulbus cordis
20. ventricle
21. neural tube
22. left optic stalk
23. left lens vesicle
24. left retina
25. head vein
26. right eye
27. prosencephalon

Downloaded from Vet-eBooks.com

Plate 100

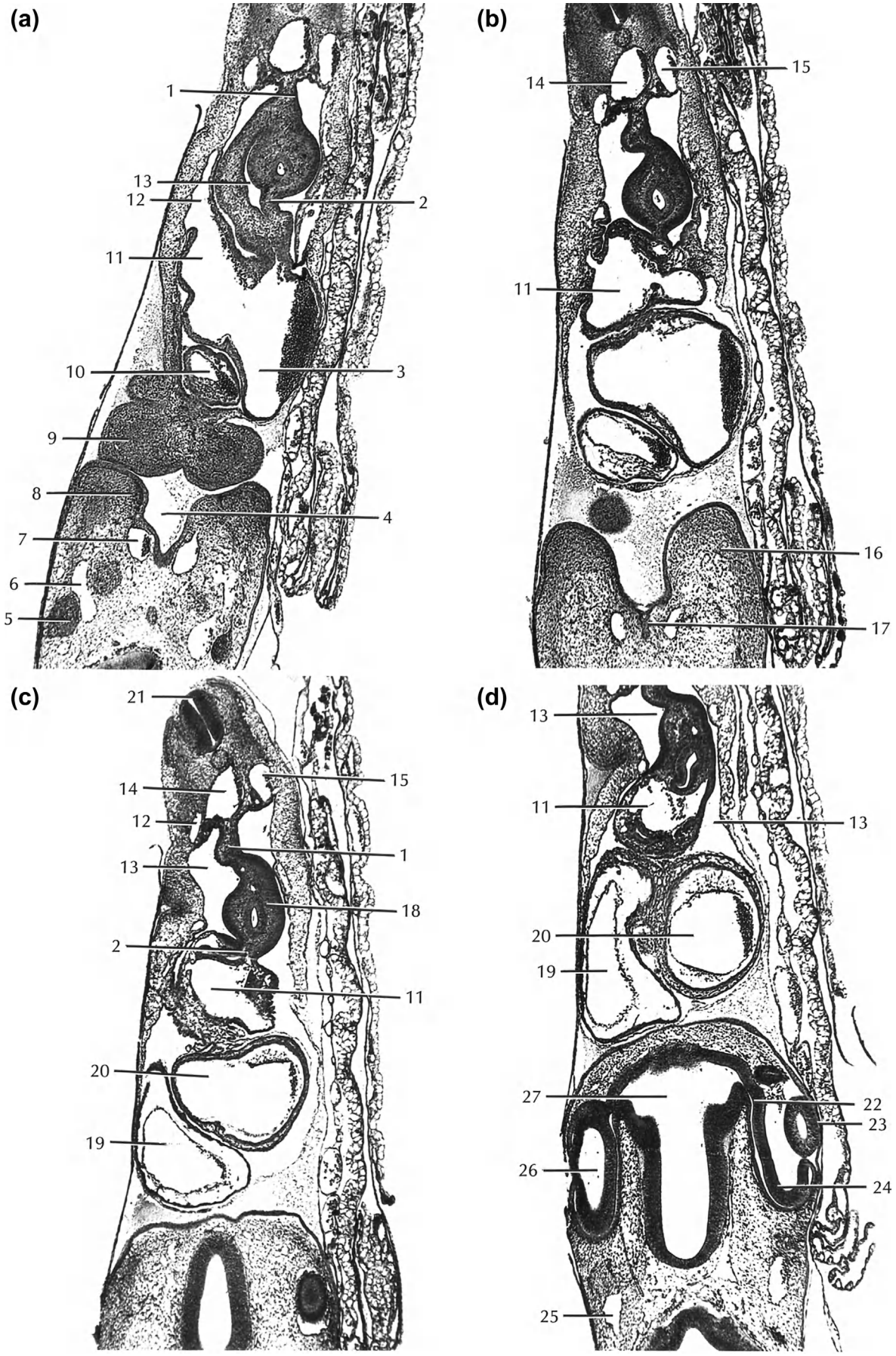

Downloaded from Vet-eBooks.com

Plate 101 Stage 18 (65–69 h) TS

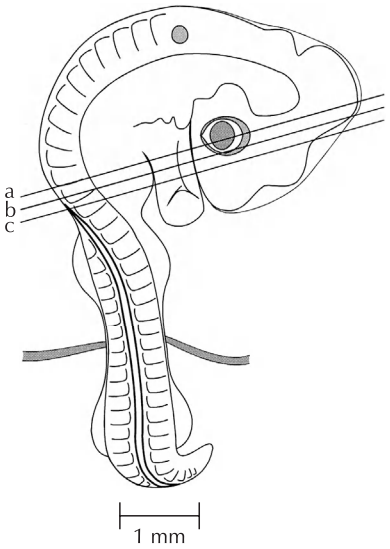

Transverse sections (TS): (a–c) × 45

1. dorsal aorta
2. left anterior cardinal vein
3. left forelimb bud
4. dorsal mesentery
5. duodenum
6. left omphalo-mesenteric vein
7. yolk sac
8. ventricle
9. nasal placode
10. optic cup
11. lens vesicle
12. diocoele
13. prosencephalon
14. bulbus cordis
15. right omphalo-mesenteric vein
16. right forelimb bud
17. splanchnopleure
18. right anterior cardinal vein
19. myotome
20. amniotic cavity
21. chorion
22. extra-embryonic coelom
23. amnion
24. left embryonic coelom
25. diencephalon
26. telencephalon
27. notochord
28. neural tube

Downloaded from Vet-eBooks.com

Plate 101

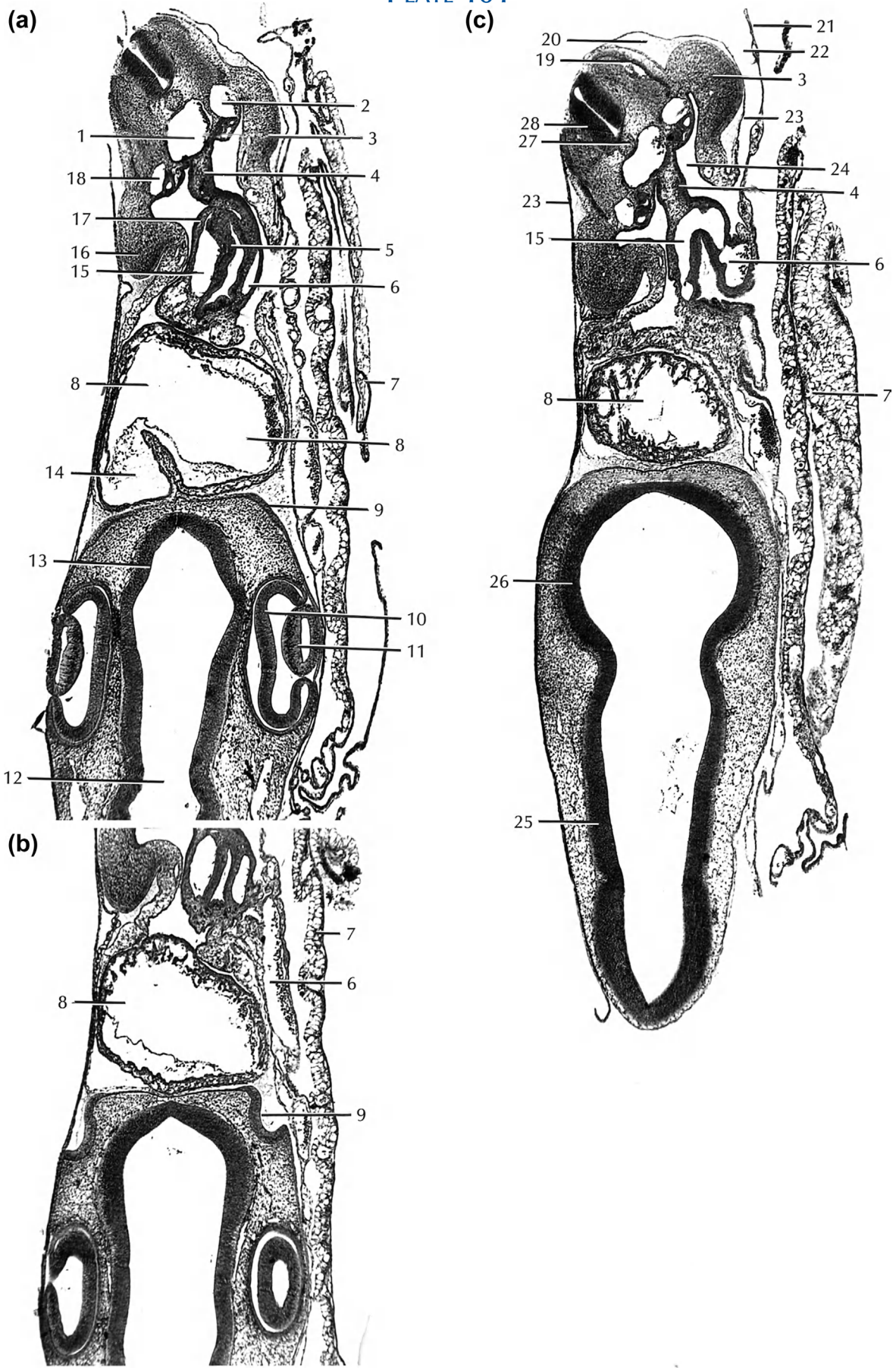

Downloaded from Vet-eBooks.com

Plate 102 Stage 18 (65–69 h) TS

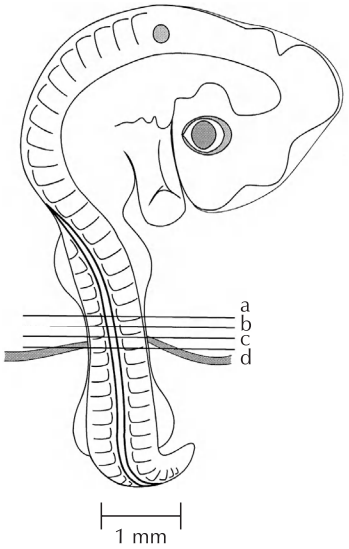

Transverse sections (TS): (a–d) × 90

1. dermatome
2. sclerotome
3. single dorsal aorta
4. left posterior cardinal vein
5. left nephric duct
6. left embryonic coelom
7. neural tube
8. notochord
9. left nephrogenic ridge
10. extra-embryonic coelom
11. right omphalo-mesenteric artery
12. embryonic ectoderm
13. amnion
14. amniotic cavity
15. left dorsal aorta
16. right dorsal aorta
17. left omphalo-mesenteric artery leaving dorsal aorta

Downloaded from Vet-eBooks.com

Plate 102

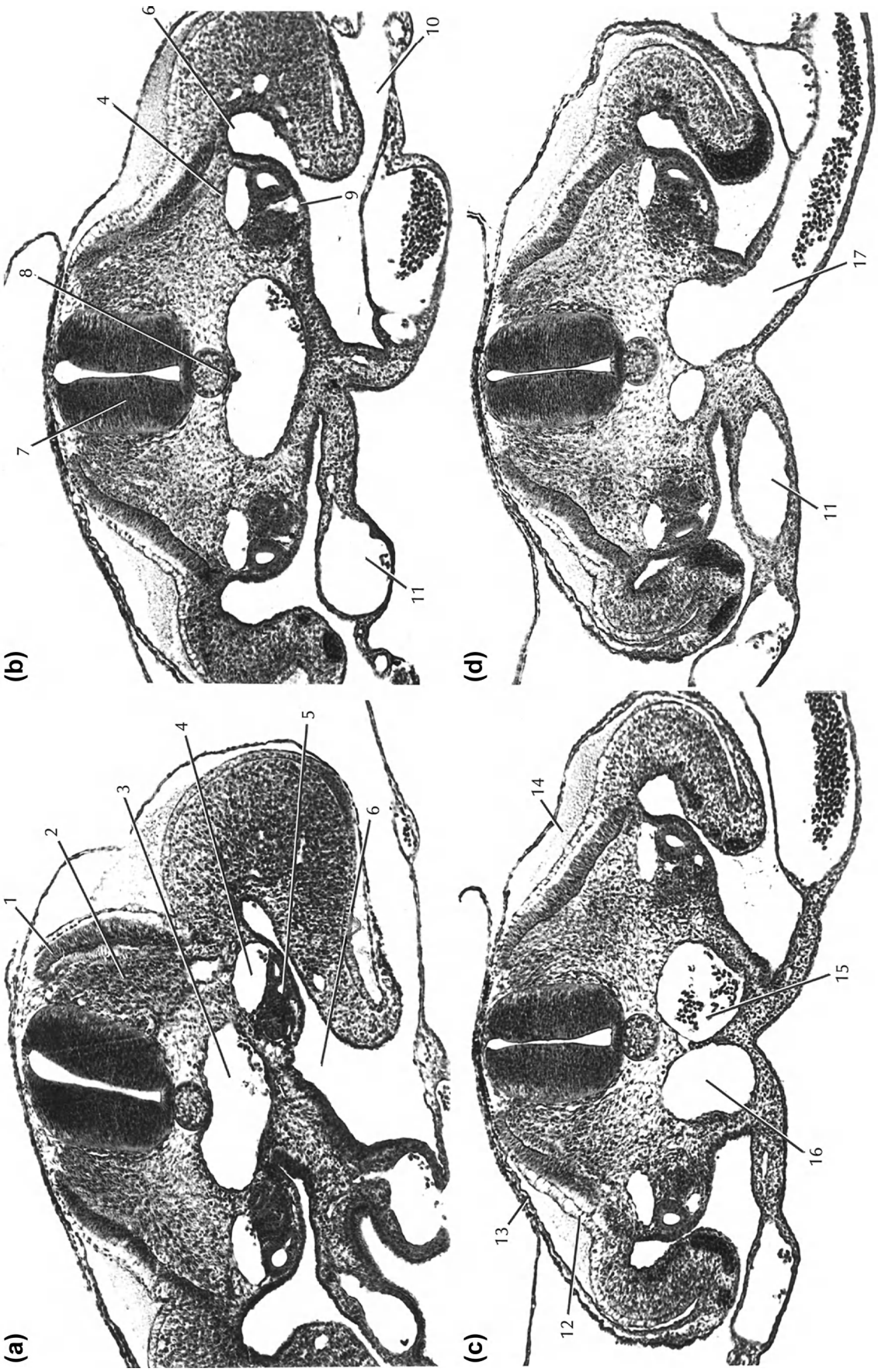

Downloaded From Vet-eBooks.com

Plate 103 Stage 18 (65–69 h) TS

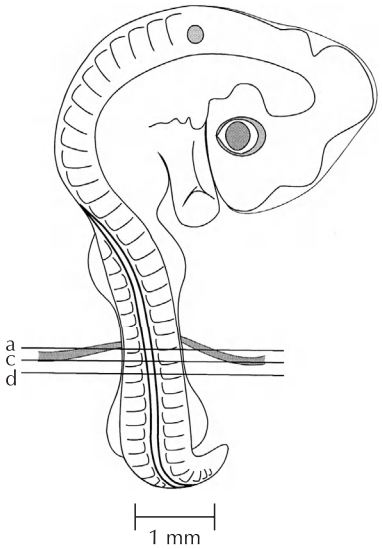

Transverse sections (TS):
(a, c, d) × 120

(b) Enlargement of part of (a) × 400

1. dermatome
2. myotome
3. neural tube
4. notochord
5. sclerotome
6. left posterior cardinal vein
7. left nephrogenous mesenchyme
8. left nephric duct
9. splanchnic mesoderm
10. embryonic endoderm
11. posterior intestinal portal
12. right omphalo-mesenteric artery
13. right embryonic coelom
14. hindgut

Downloaded from Vet-eBooks.com

Plate 103

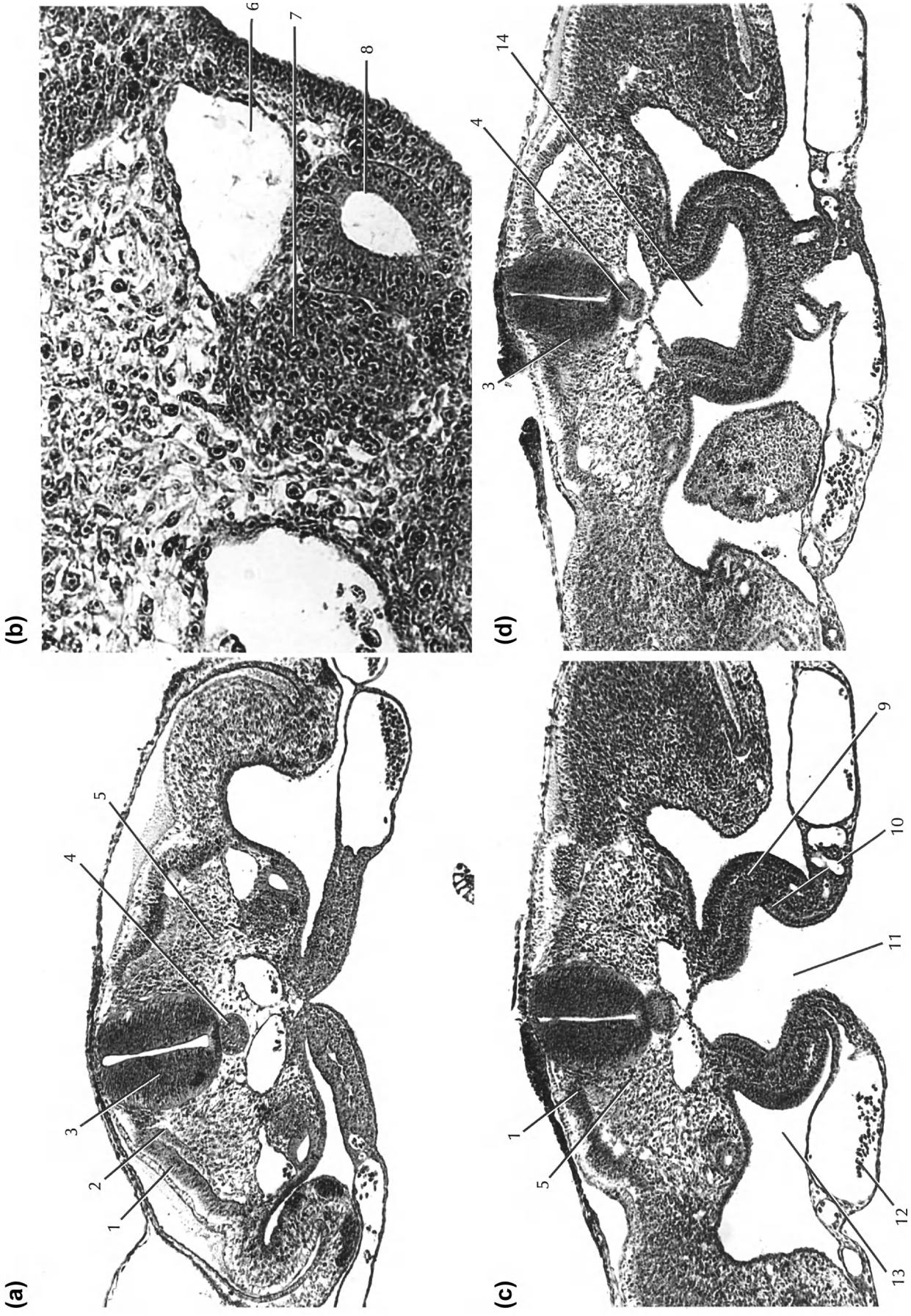

Downloaded From Vet-eBooks.com

Plate 104 Stage 18 (65–69 h) TS

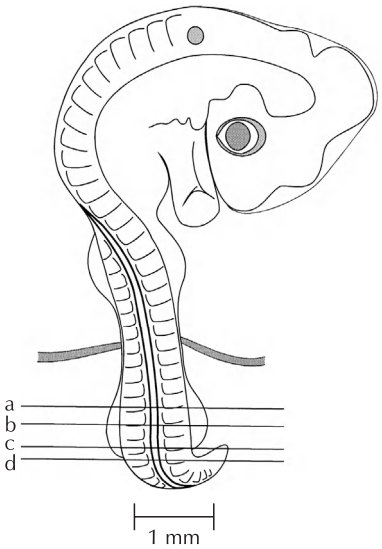

Transverse sections (TS): (a–d) × 120

1. right leg bud
2. embryonic coelom
3. neural tube
4. hindgut
5. subintestinal vein
6. lumen of allantois
7. apical ectodermal ridge of leg bud
8. cloaca
9. yolk sac
10. somatic mesoderm
11. extra-embryonic ectoderm
12. amniotic cavity containing extravasated blood
13. right nephric duct
14. somite
15. embryonic ectoderm
16. cloacal membrane

Downloaded from Vet-eBooks.com

Plate 104

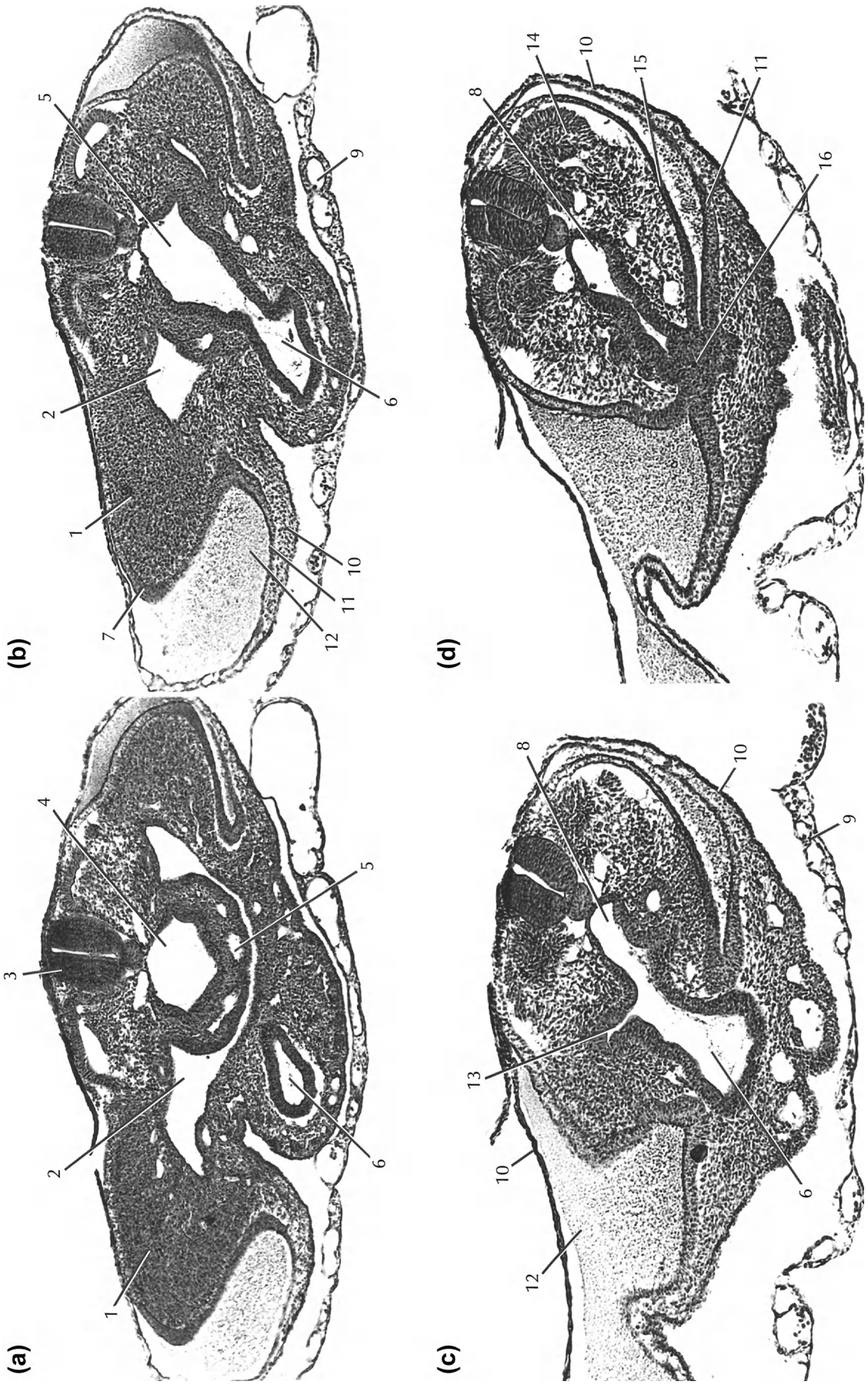

Downloaded From Vet-eBooks.com

Plate 105 Stage 18 (65–69 h) TS

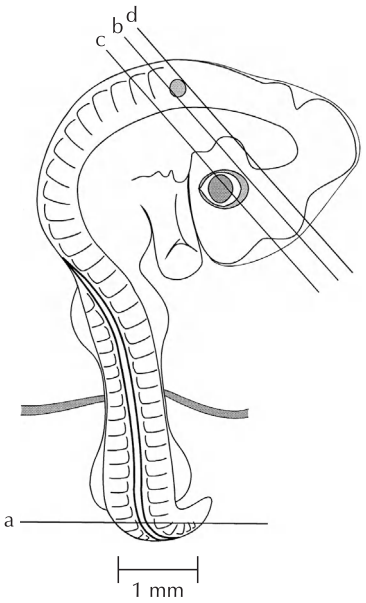

Transverse sections (TS):

(a) Same embryo as in *plates 99-104* × 120

(b–d) A different embryo to illustrate details of the pharyngeal region × 70

1. neural tube
2. amnion
3. somite
4. yolk sac
5. tail gut
6. embryonic ectoderm
7. extravasated blood in amniotic cavity
8. tail mesoderm
9. truncus arteriosus
10. pericardial coelom
11. left second aortic arch
12. left first pharyngeal pouch
13. left first aortic arch
14. left first (mandibular) pharyngeal arch
15. oral cavity
16. left otic vesicle
17. right anterior cardinal vein
18. right first (mandibular) pharyngeal arch
19. right first aortic arch
20. prosencephalon
21. left optic stalk
22. infundibulum
23. Rathke's pouch
24. left first (maxillary) pharyngeal arch
25. myelocoele

Downloaded from Vet-eBooks.com

Plate 105

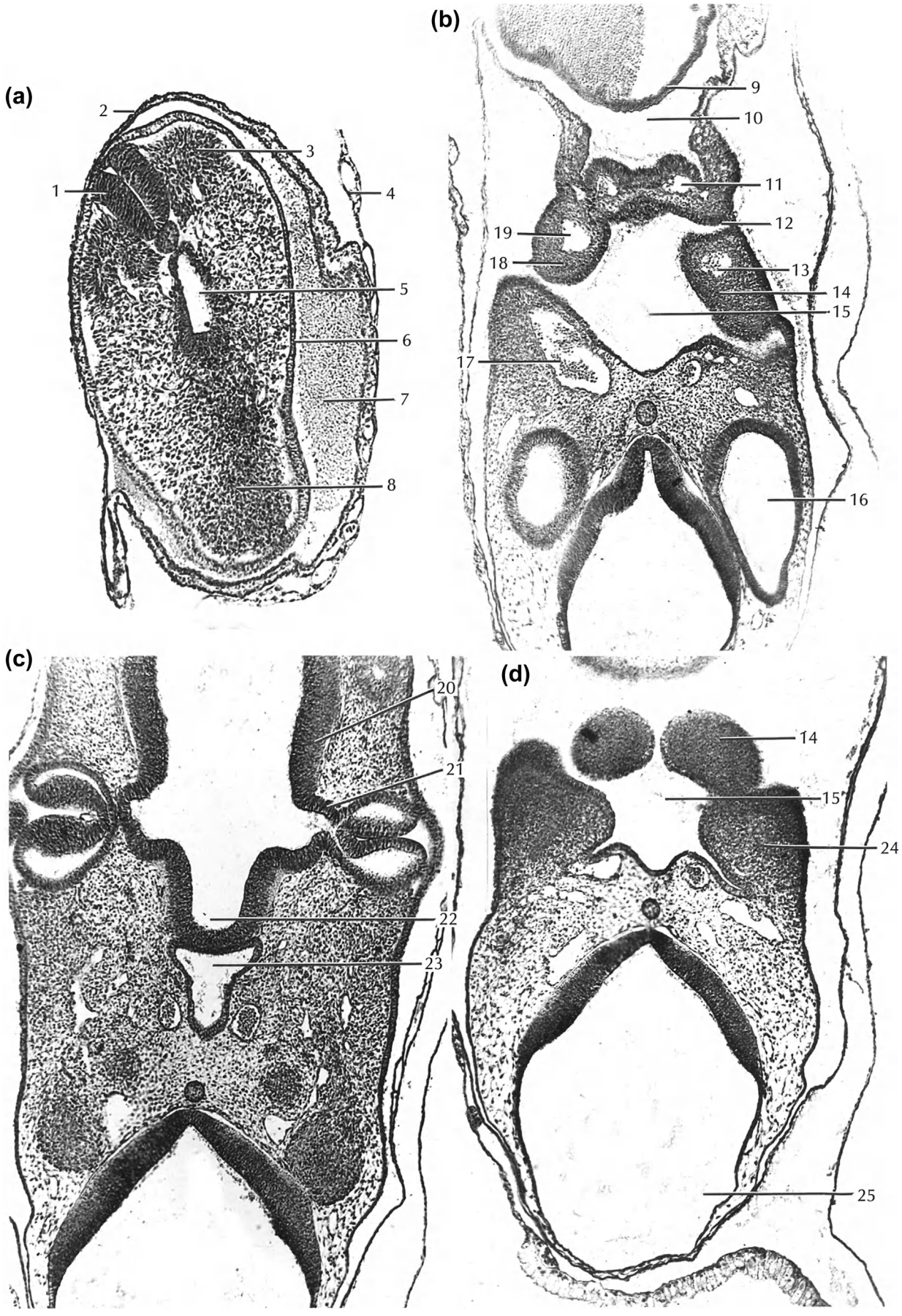

Downloaded from Vet-eBooks.com

Plate 106 Stage 20 (70–72 h)

Whole-mounted embryo viewed from the right side: × 6

1. neural tube
2. heart
3. pharynx
4. myelencephalon
5. metencephalon
6. isthmus in meso-metencephalic fold
7. mesencephalon
8. amnion
9. eye
10. right wing bud
11. right omphalo-mesenteric artery
12. allantois
13. tail bud
14. left leg bud
15. left omphalo-mesenteric artery
16. left wing bud

Downloaded from Vet-eBooks.com

Plate 106

Downloaded from Vet-eBooks.com

Plate 107 Stage 23 (day 4) LS: coronal and sagittal

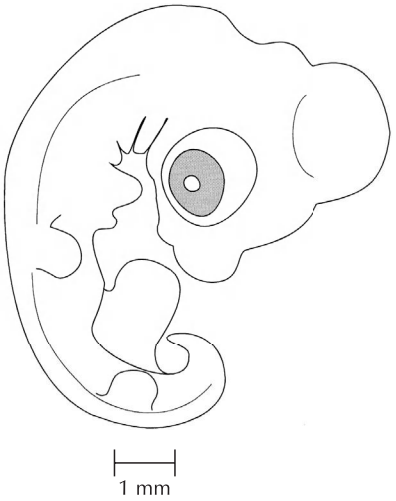

Longitudinal sections in the sagittal plane at the head end and coronal plane at the caudal end due to twisting of specimen during preparation: (a–d) × 12

1. amnion
2. anterior cardinal vein
3. otic vesicle
4. myelocoele
5. maxillary branch of trigeminal (cranial V) nerve
6. head vein
7. ophthalmic branch of trigeminal (cranial V) nerve
8. pigmented layer of retina
9. lumen of optic vesicle
10. 25th right somite
11. lumen of neural tube
12. wall of neural tube
13. geniculate (cranial nerve VII) ganglion
14. first (mandibular) pharyngeal arch
15. choroid fissure
16. left leg bud
17. 31st left somite
18. fourth aortic arch
19. third aortic arch
20. mesocoele
21. infundibulum
22. right wing bud
23. notochord
24. left nephric (Wolffian) duct
25. left wing bud
26. dorsal aorta
27. oral cavity
28. metacoele
29. meso-metencephalic fold isthmus
30. diocoele
31. telocoele
32. truncus arteriosus
33. right mesonephros
34. neural tube of tail region
35. hindgut
36. midgut
37. left mesonephros
38. peritoneal cavity
39. oesophagus

Downloaded from Vet-eBooks.com

Plate 107

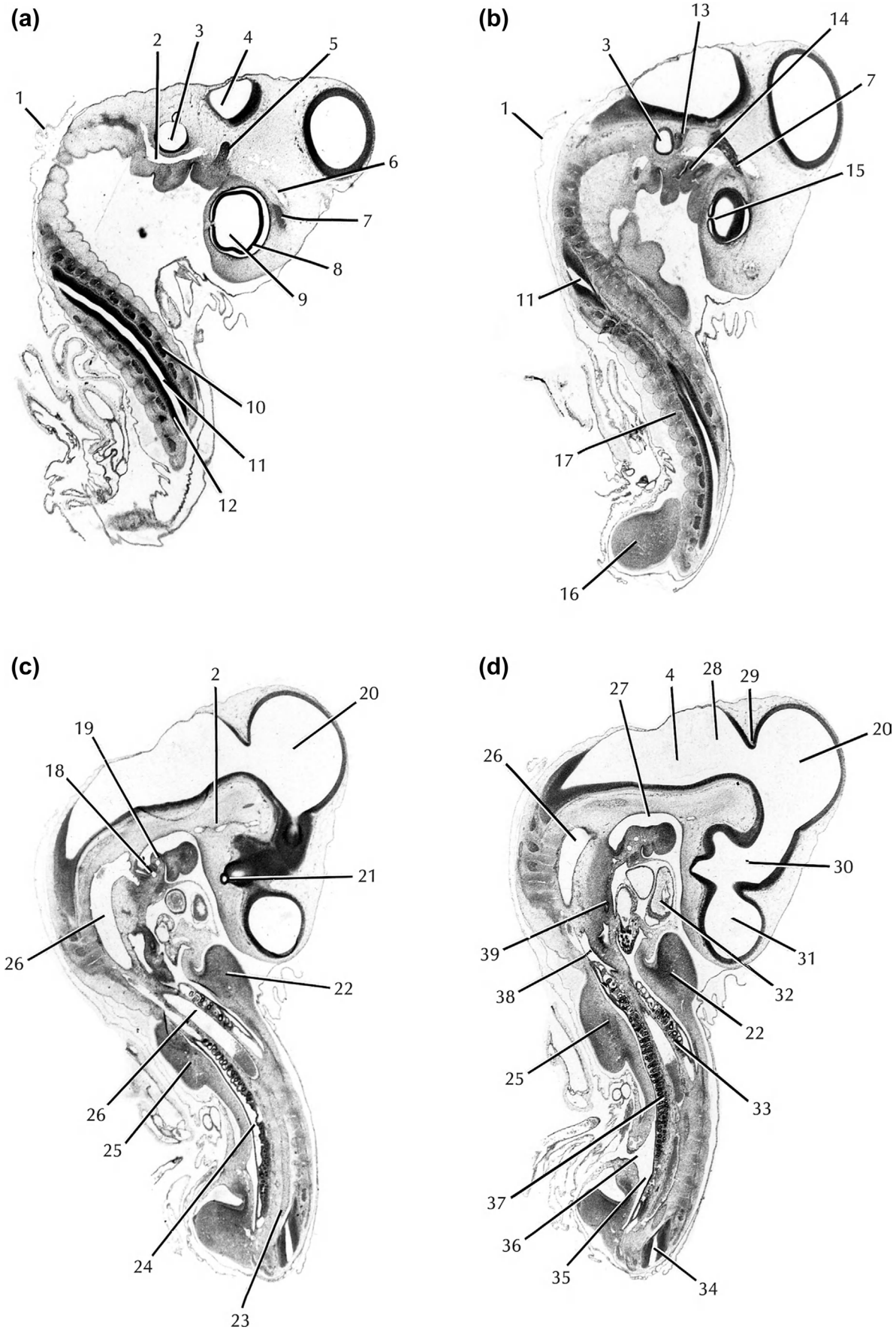

Downloaded from Vet-eBooks.com

Plate 108 Stage 23 (day 4) LS: coronal and sagittal

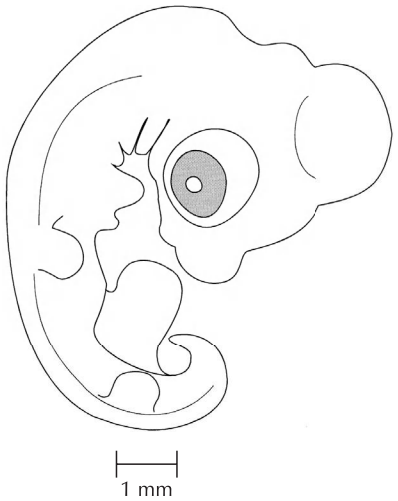

Longitudinal sections in the sagittal plane at the head end and coronal plane at the caudal end due to twisting of specimen during preparation: (a–d) × 12

1. amnion
2. anterior cardinal vein
3. pharynx
4. ventral aorta
5. isthmus in meso-metencephalic fold
6. truncus arteriosus
7. right wing bud
8. posterior cardinal vein
9. nephric duct
10. right mesonephros
11. junction of body wall and amnion
12. left wing bud
13. lesser sac
14. stomach
15. left lung bud
16. coelom
17. sinus venosus
18. atrium
19. trigeminal (cranial nerve V) ganglion
20. myelencephalon
21. metencephalon
22. ventricle
23. neural tube
24. notochord
25. amniotic cavity
26. pericardial cavity
27. otic vesicle
28. geniculate (cranial nerve VII) ganglion
29. myelocoele
30. mesocoele
31. optic recess
32. pineal organ
33. telocoele
34. body wall
35. communication between embryonic and extra-embryonic coeloms
36. cloaca
37. lumen of allantois
38. liver
39. posterior cardinal vein
40. fourth aortic arch
41. third aortic arch
42. second aortic arch
43. superior ganglion of glossopharyngeal (cranial IX) nerve
44. second (hyoid) pharyngeal arch
45. first (mandibular process) pharyngeal arch
46. first (maxillary process) pharyngeal arch
47. trigeminal (cranial V) nerve
48. facial branch of trigeminal (cranial V) nerve
49. diocoele
50. infundibulum
51. right leg bud
52. tail bud

Downloaded from Vet-eBooks.com

Plate 108

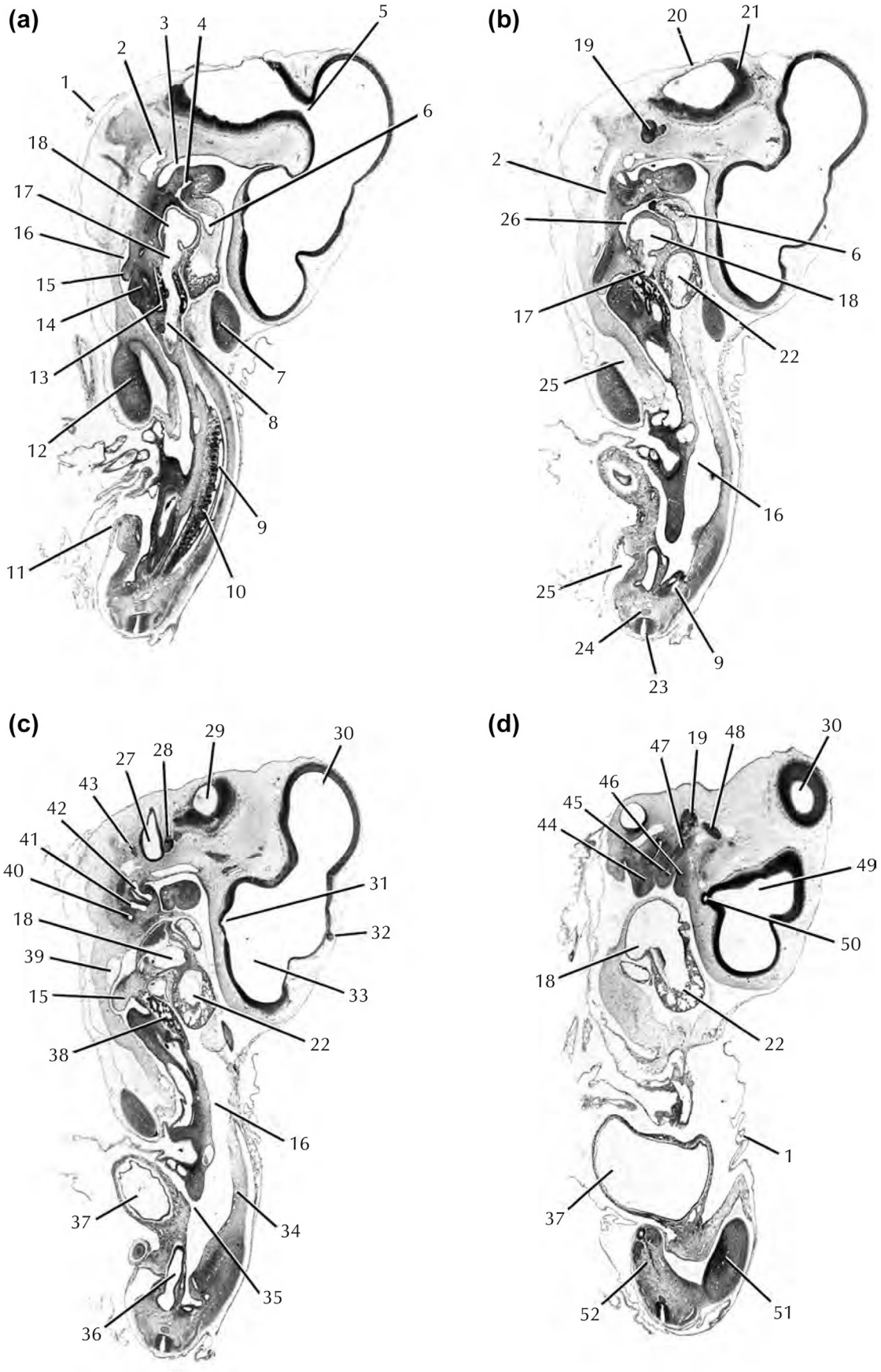

Downloaded from Vet-eBooks.com

Plate 109 Stage 23 (day 4) TS

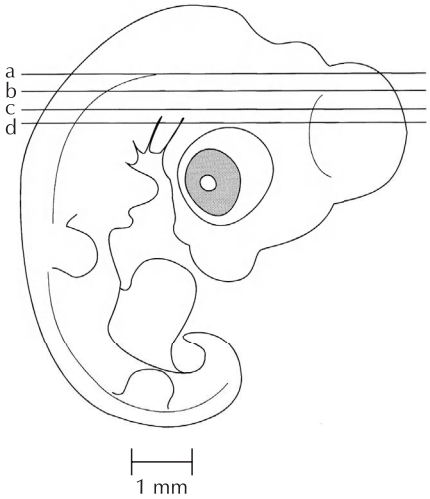

Transverse sections (TS): (a–d) × 22

1. myotome
2. myelencephalon
3. left otic vesicle
4. left acoustico-facialis (cranial nerves VII and VIII) ganglion
5. metacoele
6. diencephalon
7. trigeminal (cranial nerve V) ganglion
8. neuromere
9. left glossopharyngeal (cranial IX) nerve
10. left anterior cardinal vein
11. floor of metencephalon
12. right acoustic (cranial nerve VIII) ganglion
13. right glossopharyngeal (cranial IX) nerve
14. notochord
15. left dorsal aorta
16. left first pharyngeal pouch
17. left trigeminal (cranial V) nerve (maxillary branch)
18. left trigeminal (cranial V) nerve (ophthalmic branch)
19. mesencephalon
20. right trigeminal (cranial V) nerve (ophthalmic branch)
21. right trigeminal (cranial V) nerve (mandibular branch)
22. right first pharyngeal ectodermal groove
23. right second (hyoid) pharyngeal arch
24. right anterior cardinal vein
25. spinal cord
26. left first aortic arch
27. left first (maxillary) pharyngeal arch
28. right first (mandibular) pharyngeal arch

Downloaded from Vet-eBooks.com

Plate 109

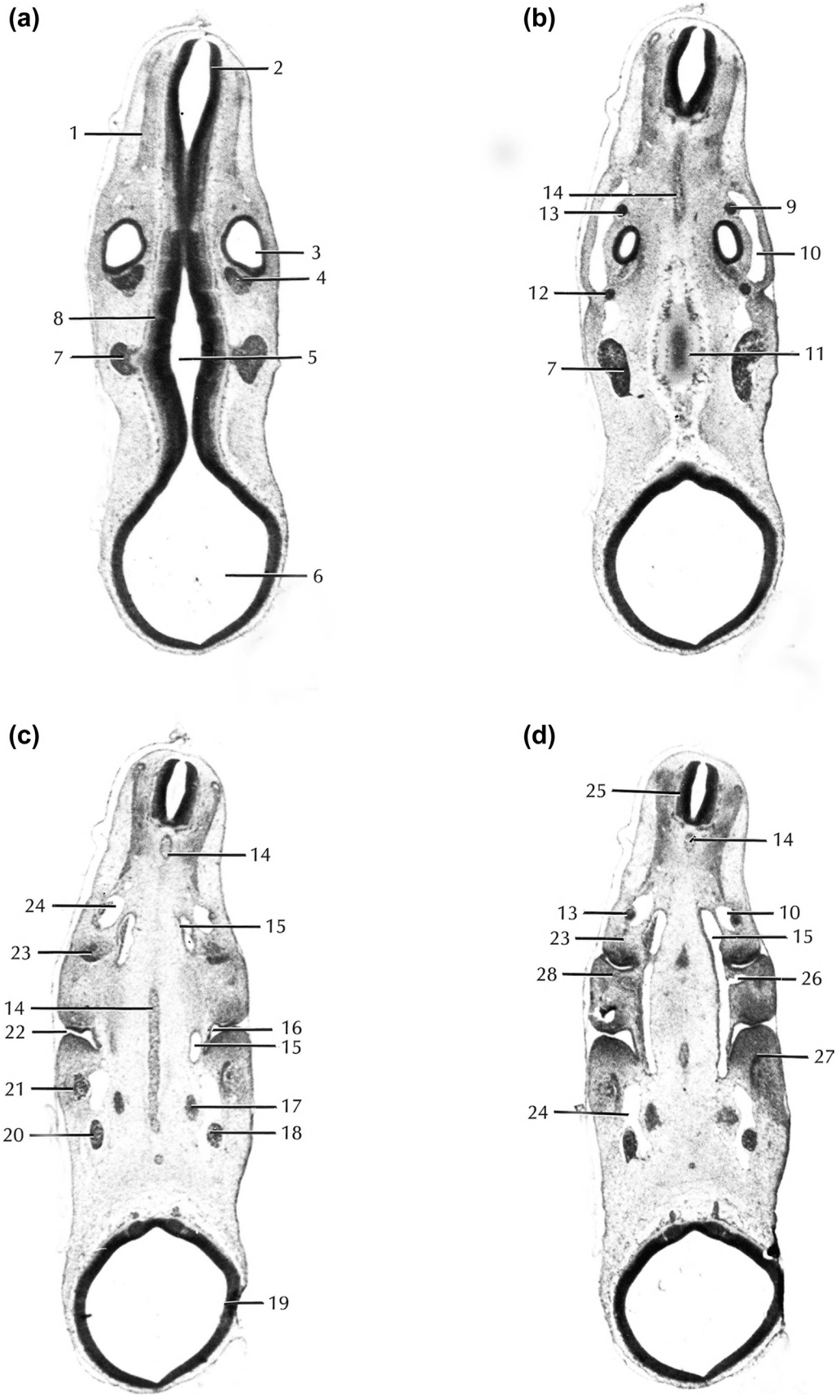

Downloaded from Vet-eBooks.com

Plate 110 Stage 23 (day 4) TS

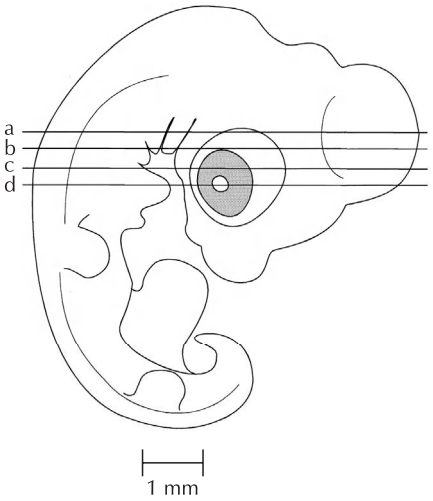

Transverse sections (TS): (a–d) × 22

1. dorsal aorta
2. notochord
3. left fourth aortic arch
4. left third aortic arch
5. thyroid
6. left first (mandibular) pharyngeal arch
7. left first (maxillary) pharyngeal arch
8. Rathke's pouch
9. left eye
10. diocoele
11. infundibulum
12. right oculomotor (cranial III) nerve
13. oral cavity
14. pharynx
15. jugular ganglion of right vagus (cranial X) nerve
16. amnion
17. dorsal root ganglion
18. left anterior cardinal vein
19. ventral aorta
20. left first ectodermal groove
21. diencephalon
22. right eye
23. right first (maxillary) pharyngeal arch
24. right first (mandibular) pharyngeal arch
25. right second (hyoid) arch
26. right fourth aortic arch artery
27. pericardial cavity
28. ventricle
29. nasal placode
30. optic stalk
31. lens
32. sinus venosus
33. laryngo-tracheal groove
34. pharynx
35. oesophagus
36. truncus arteriosus
37. retina
38. atrium
39. trachea

Downloaded from Vet-eBooks.com

Plate 110

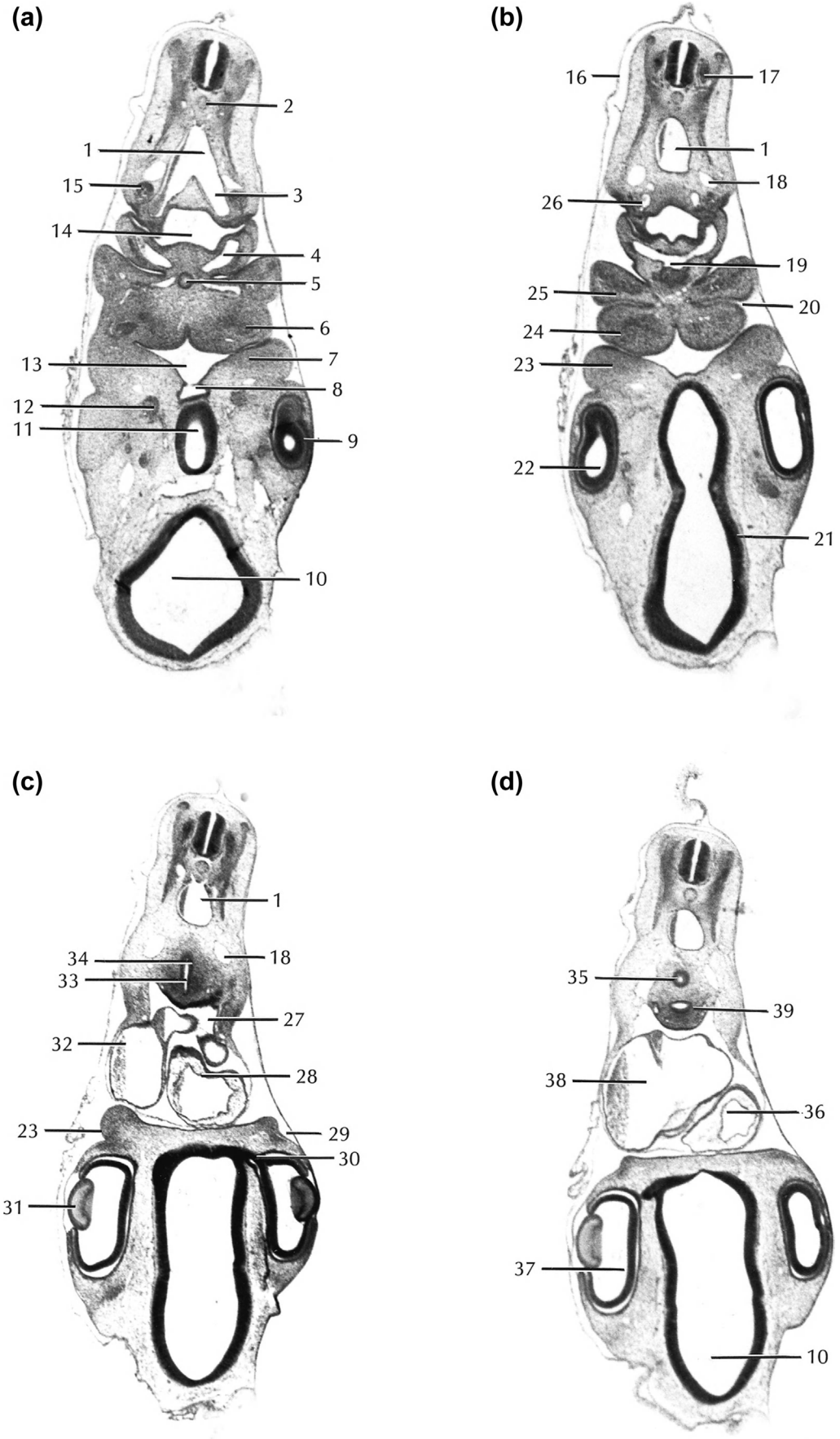

Downloaded from Vet-eBooks.com

Plate 111 Stage 23 (day 4) TS

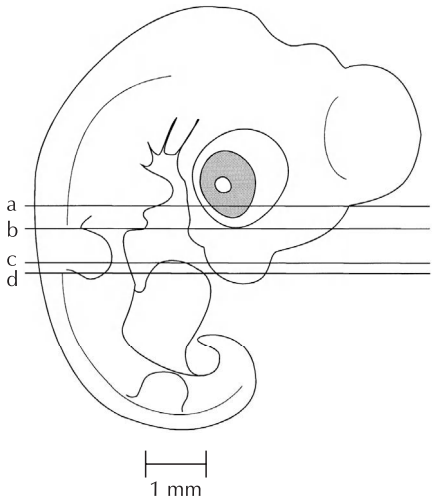

Transverse sections (TS): (a–d) × 22

1. notochord
2. dorsal aorta
3. oesophagus
4. left bronchus
5. left atrium
6. interatrial septum
7. ventricle
8. nasal pit
9. diocoele
10. right eye
11. amnion
12. right atrium
13. right anterior cardinal vein
14. neural tube
15. future pleural cavity
16. ductus venosus
17. liver
18. septum transversum
19. stomach
20. right lung bud
21. left wing bud
22. left lateral telencephalic vesicle
23. lumen of allantois
24. right posterior cardinal vein
25. left nephric duct
26. apical ectodermal ridge of left wing bud
27. left omphalo-mesenteric vein

Downloaded from Vet-eBooks.com

Plate 111

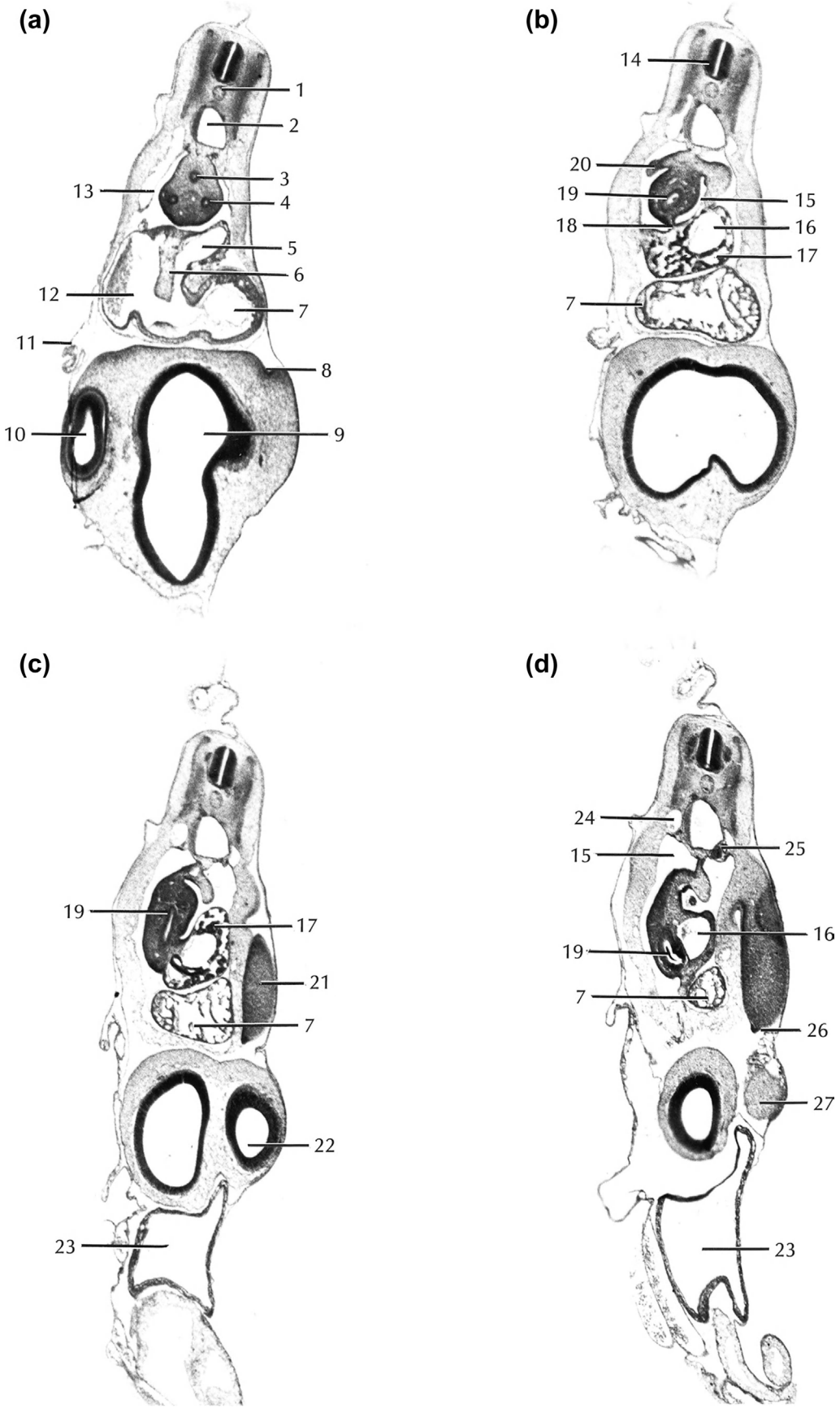

Downloaded from Vet-eBooks.com

Plate 112 Stage 23 (day 4) TS

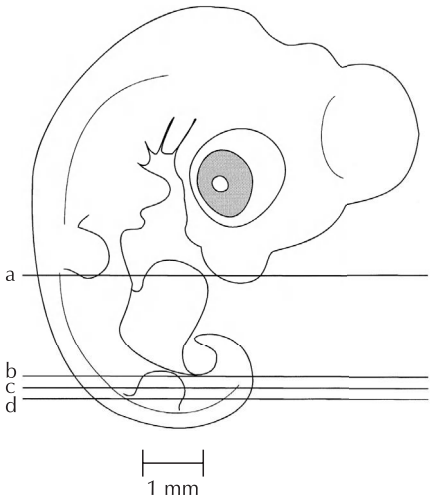

Transverse sections (TS): (a–d) × 22

1. right posterior cardinal vein
2. dorsal aorta
3. left mesonephros
4. left wing bud
5. lumen of allantois
6. yolk sac
7. duodenum
8. right omphalo-mesenteric vein
9. right wing bud
10. right mesonephros
11. amnion
12. left posterior cardinal vein
13. body wall
14. allantois
15. left leg bud
16. spinal cord of tail
17. right leg bud
18. abdominal coelom
19. amniotic cavity
20. spinal cord
21. notochord
22. hindgut
23. left nephric duct
24. dorsal root ganglion
25. prevertebra

Downloaded from Vet-eBooks.com

Plate 112

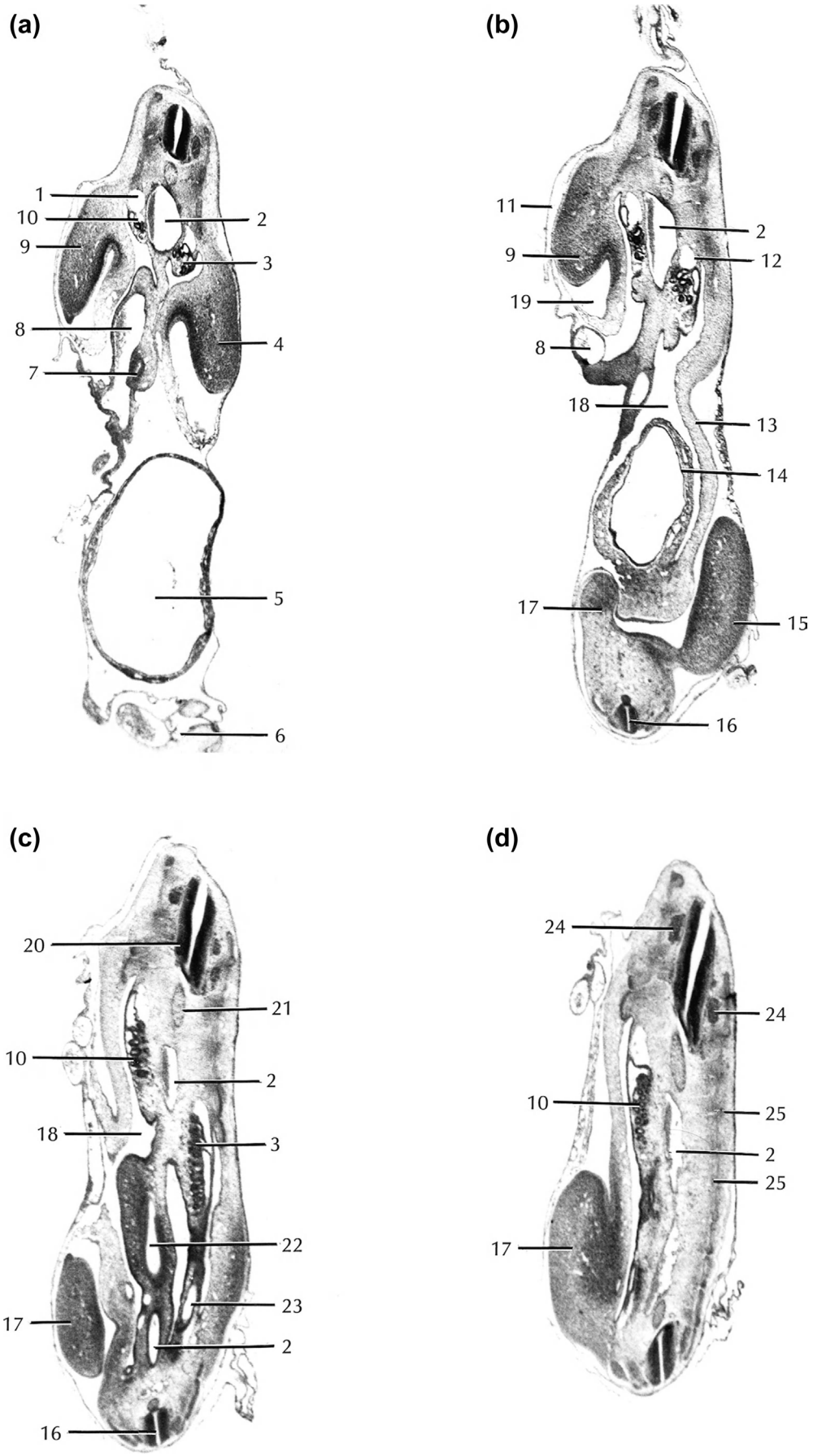

Downloaded from Vet-eBooks.com

Plate 113 Stage 24 (day 4.5) TS

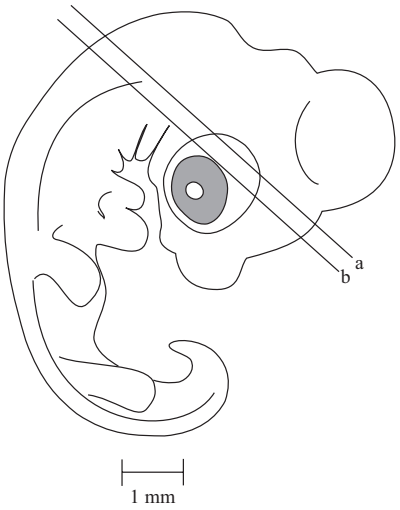

Transverse sections (TS): (a, b) × 20

(a) At level of developing pineal organ.

(b) At level of Rathke's pouch.

1. yolk sac
2. mesocoele
3. left oculomotor (cranial nerve III) ganglion
4. left oculomotor nerve
5. back of left optic cup
6. diocoele
7. epiphysis (pineal organ)
8. ectoderm
9. right optic cup
10. notochord
11. right oculomotor (cranial nerve III) ganglion
12. right otic vesicle
13. retina of left optic cup
14. wall of diencephalon
15. Rathke's pouch

Downloaded from Vet-eBooks.com

Plate 113

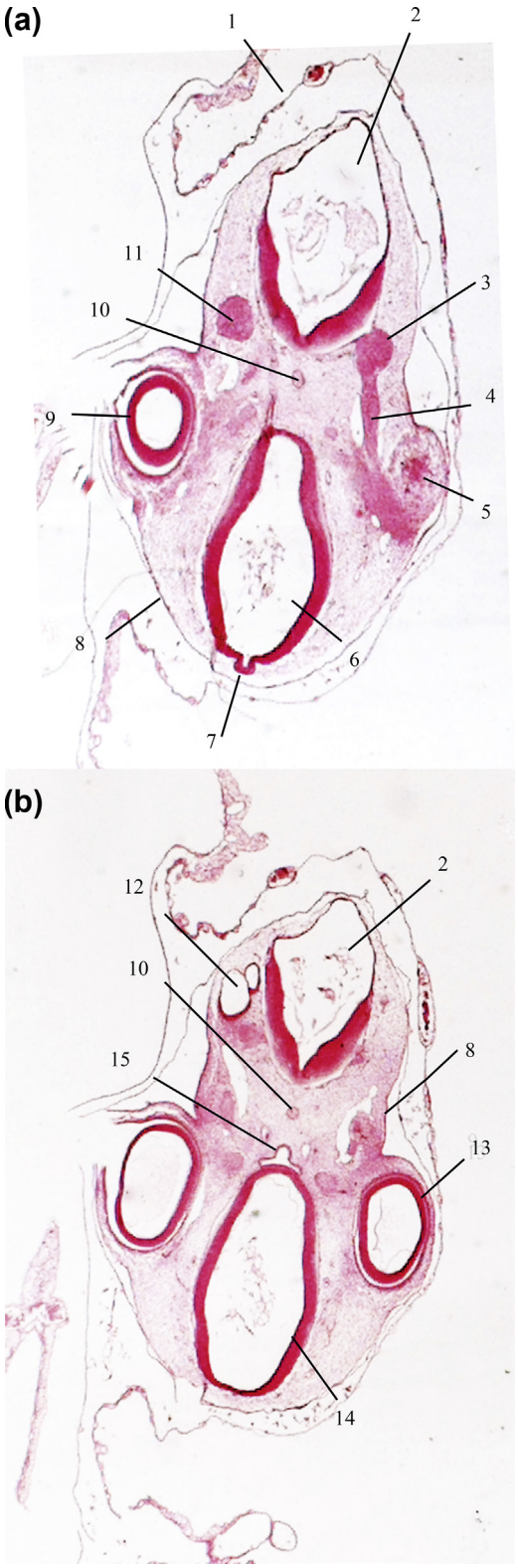

Downloaded from Vet-eBooks.com

Plate 114 Stage 24 (day 4.5) TS

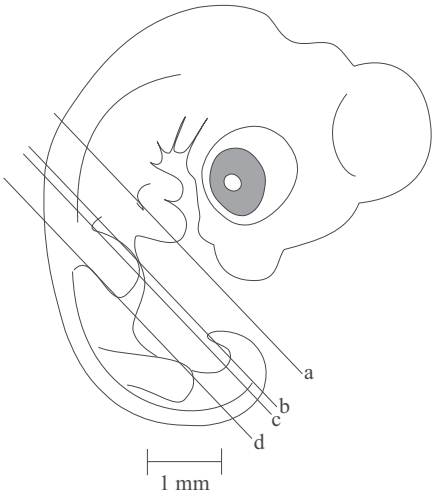

Transverse sections (TS): × 10

1. neural tube
2. notochord
3. dorsal aorta
4. left anterior cardinal vein
5. inter-atrial septum
6. left atrium
7. endoderm of yolk sac
8. right leg bud
9. lumen of allantois
10. right wing bud
11. ventricle
12. right atrium
13. right anterior cardinal vein
14. amnion around cranial end of body
15. left bronchus
16. coelom
17. left anterior cardinal vein close to junction with right anterior cardinal vein
18. liver
19. amnion around caudal end of body
20. left posterior cardinal vein
21. chorion
22. right anterior cardinal vein
23. right trachea
24. oesophagus
25. myotome
26. sinus venosus
27. laryngo-tracheal groove
28. omphalo-mesenteric vein
29. foregut
30. midgut
31. left leg bud
32. hindgut

Downloaded from Vet-eBooks.com

Plate 114

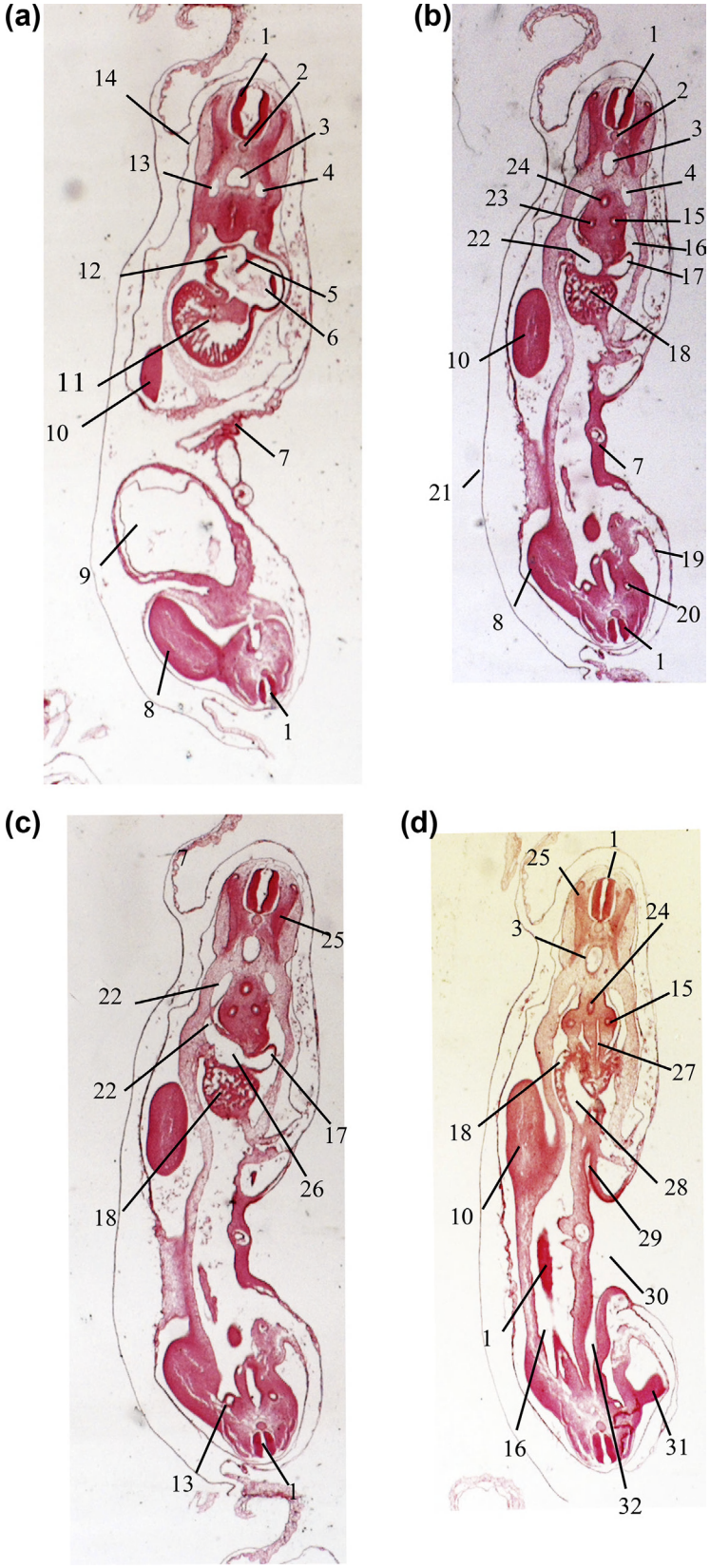

Downloaded from Vet-eBooks.com

Plate 115 Stage 24 (day 4.5) TS

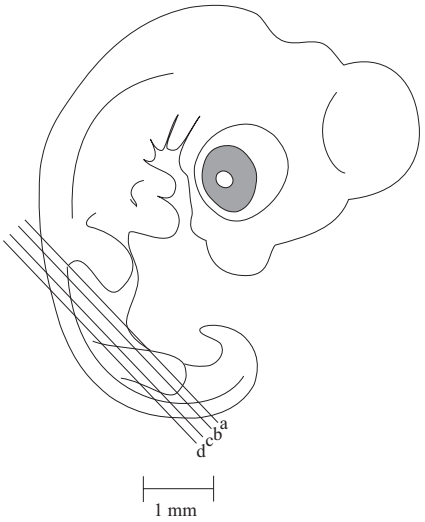

Transverse sections (TS): × 10

1. neural tube
2. myotome
3. dorsal aorta
4. left lung bud
5. stomach wall
6. left leg bud
7. mesonephros
8. coelom
9. dorsal mesentery
10. stomach lumen
11. duodenum
12. omphalo-mesenteric vein
13. ompholo-mesenteric artery
14. liver
15. right lung bud
16. notochord
17. nephric duct

Downloaded from Vet-eBooks.com

Plate 115

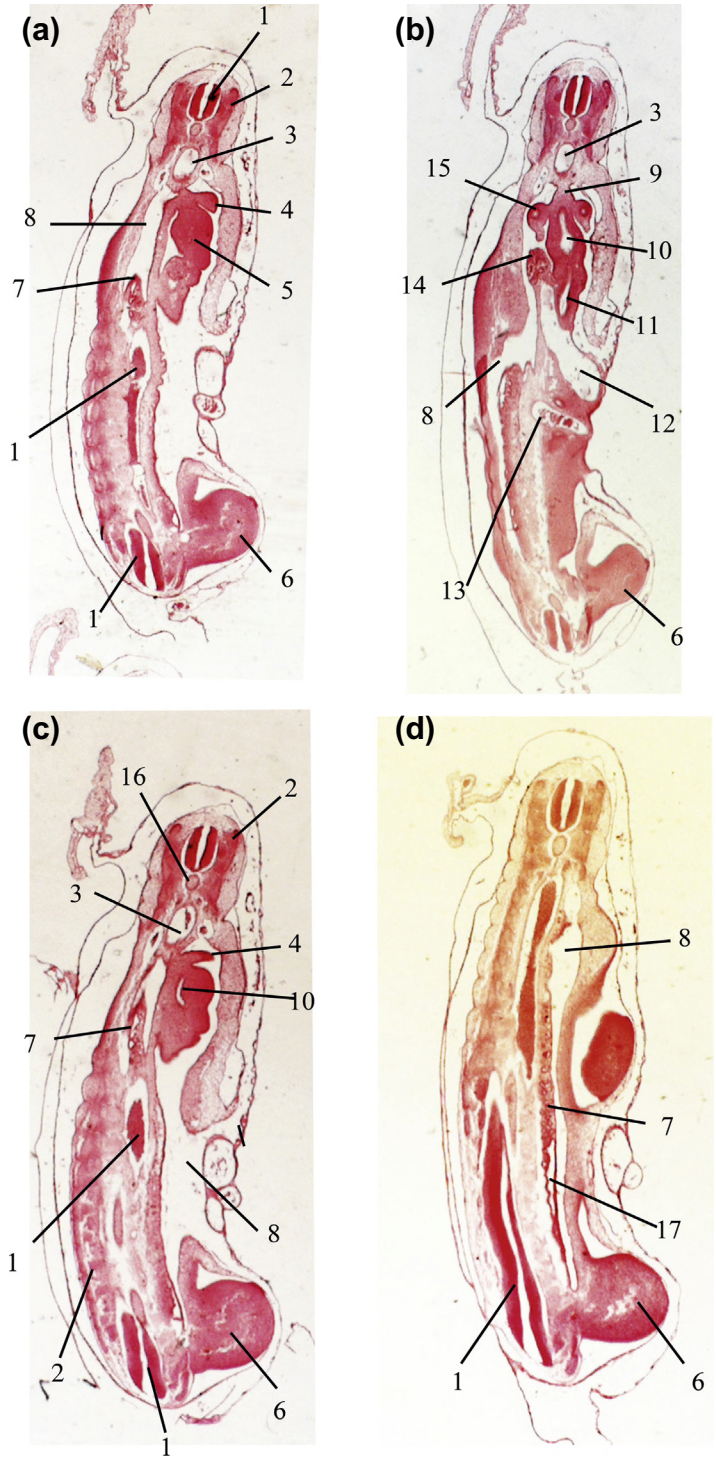

Downloaded from Vet-eBooks.com

Plate 116 Stage 24 (day 4.5) TS

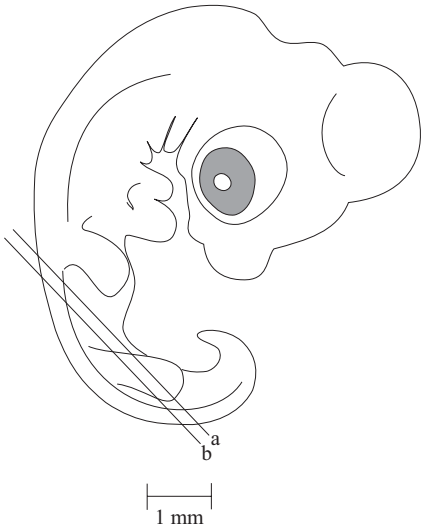

(a) Enlargement of section adjacent to *plate 115b*: × 25

(b) Enlargement of section adjacent to *plate 115c*: × 20

1. right lung bud
2. oesophagus
3. dorsal mesentery
4. left anterior cardinal vein
5. debris surrounding amnion
6. body wall
7. ventral mesentery
8. ductus venosus
9. pharyngeal pouch
10. coelom
11. pulmonary mesoderm
12. stomach
13. amnion
14. oblique septum
15. edge of neural tube
16. myotome
17. mesonephros
18. nephric duct

Downloaded from Vet-eBooks.com

Plate 116

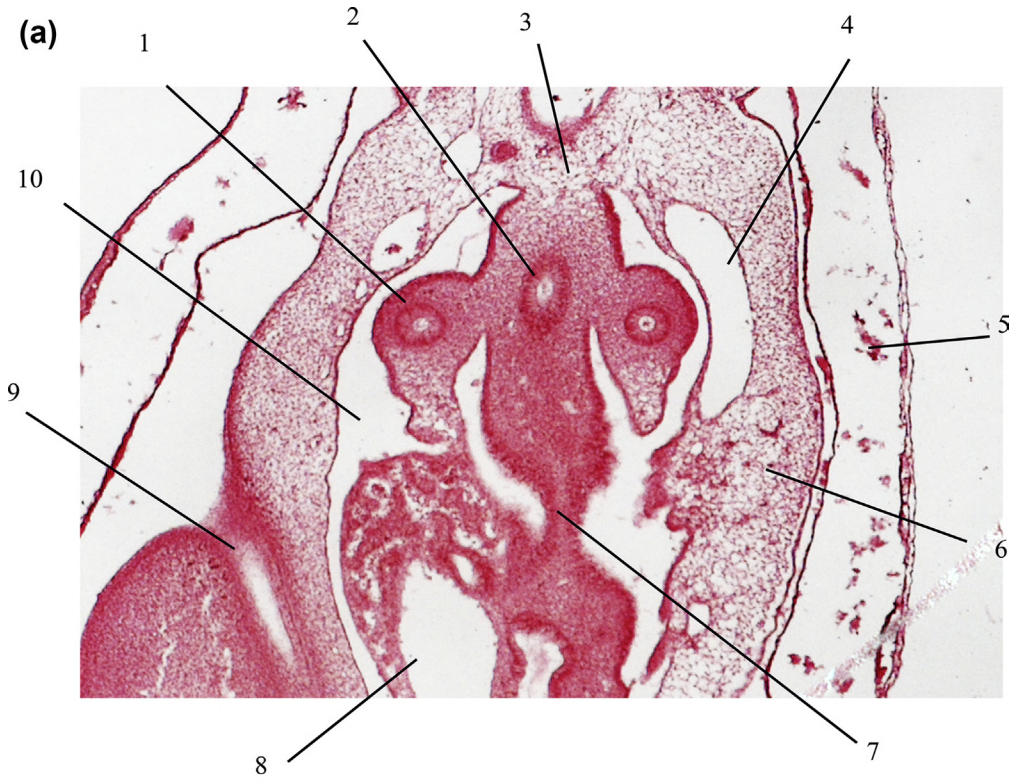

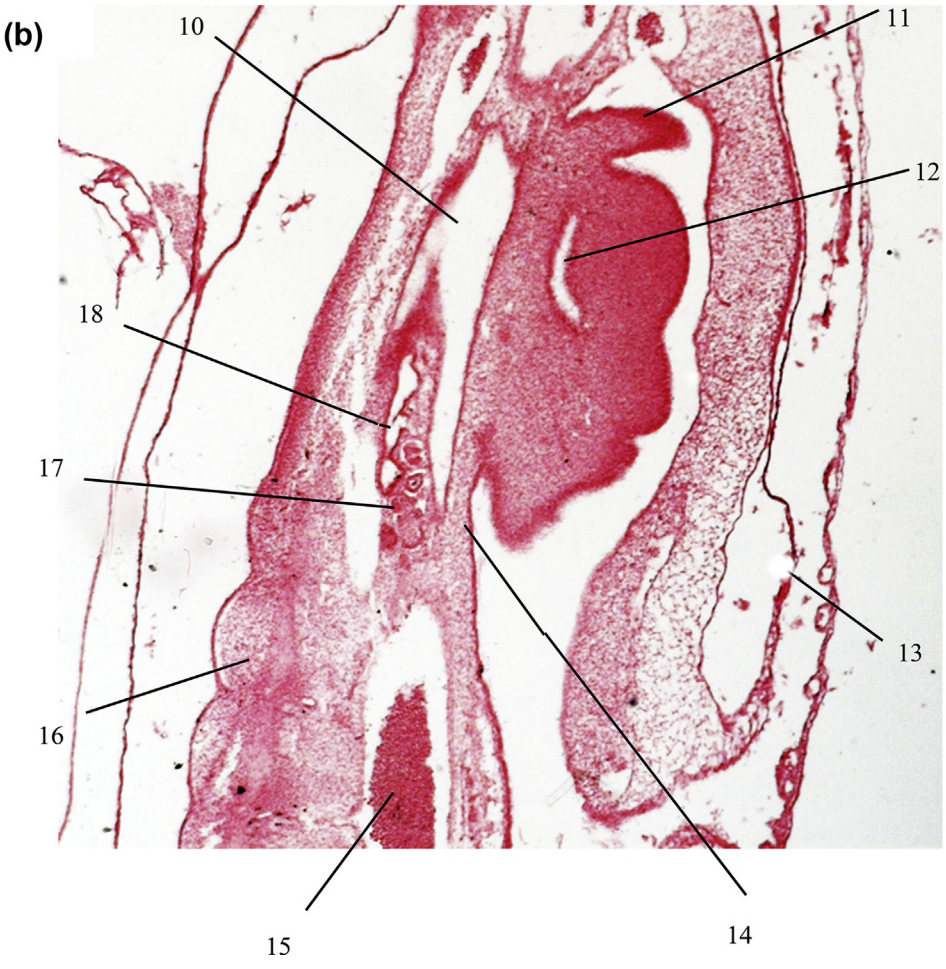

Downloaded from Vet-eBooks.com

Plate 117 Stage 24 (day 4.5) TS

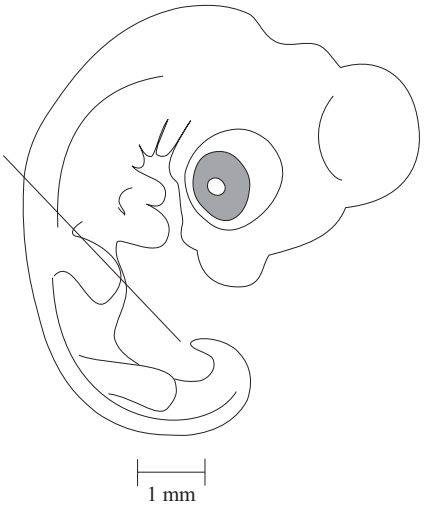

Enlargement of section adjacent to *plate 114b*: × 60

1. pneumo-enteric recess (a pocket in the coelom)
2. right anterior cardinal vein
3. right bronchus
4. oesophagus
5. left bronchus
6. left pulmonary fold
7. ventral mesentery
8. left anterior cardinal vein
9. amnion
10. embryonic coelom (ventral hepatic cavity)
11. yolk sac
12. falciform ligament (ventral mesentery)
13. liver
14. right wing bud
15. body wall
16. right horizontal hepatic ligament
17. common cardinal vein

Downloaded from Vet-eBooks.com

Plate 117

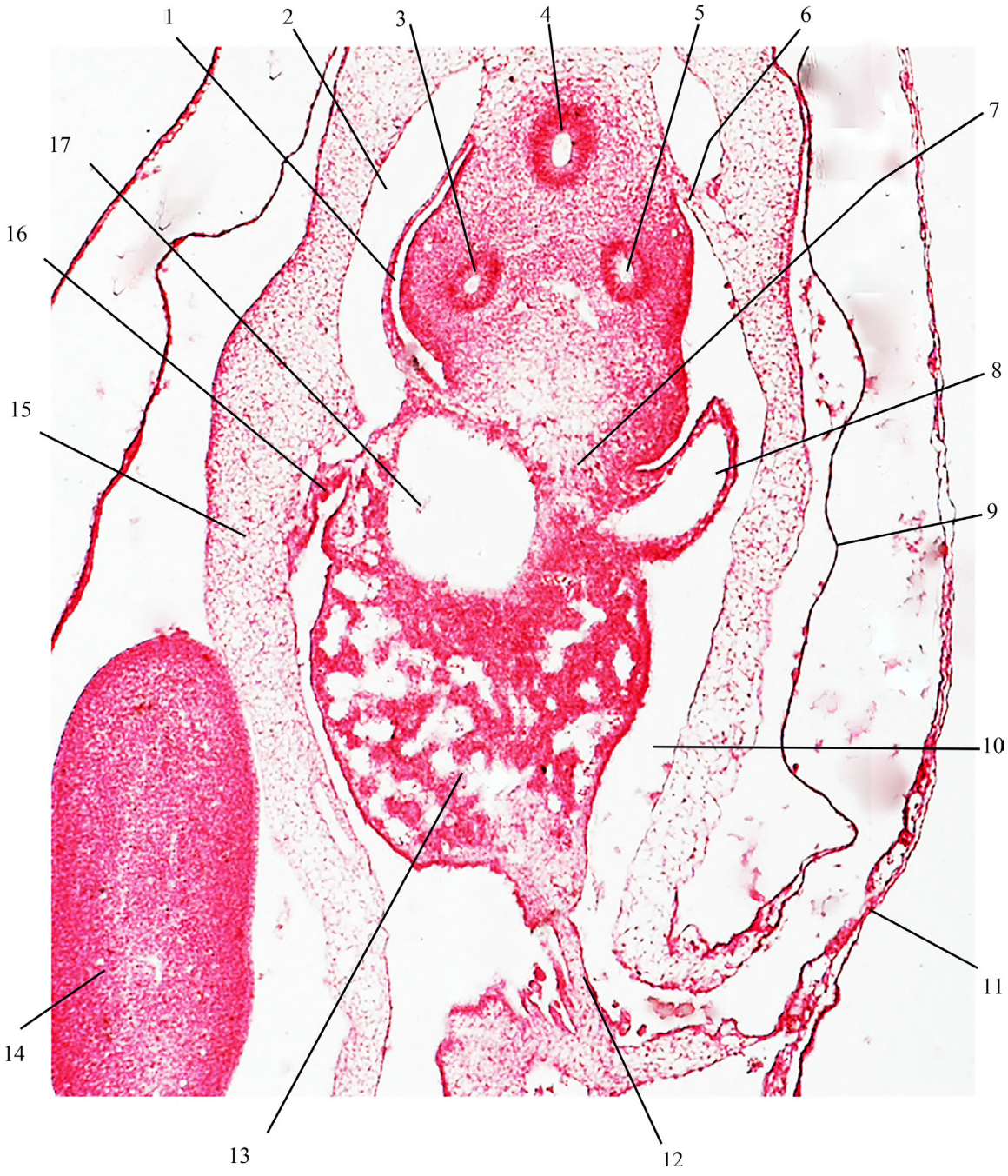

Downloaded from Vet-eBooks.com

Plate 118 Stage 26 (day 5) LS: sagittal

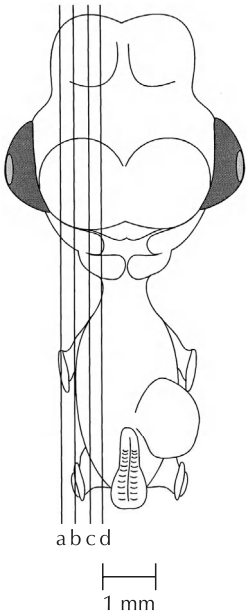

Longitudinal (sagittal) sections: (a–d) × 8

1. spinal cord
2. dorsal root ganglion
3. head vein
4. otic vesicle
5. first pharyngeal pouch
6. pigmented layer of retina
7. amniotic cavity
8. amnion
9. notochord
10. vagus (cranial X) nerve
11. fourth pharyngeal pouch
12. petrosal (cranial nerve IX) ganglion
13. acoustic (cranial nerve VIII) ganglion
14. trigeminal (cranial nerve V) ganglion
15. trigeminal (cranial V) nerve
16. first (mandibular) pharyngeal arch
17. first (maxillary) pharyngeal arch
18. second (hyoid) pharyngeal arch
19. wing bud
20. loop of intestine
21. body of vertebra
22. neural arch of vertebra
23. dorsal aorta
24. fifth aortic arch
25. fourth aortic arch
26. third aortic arch
27. carotid artery
28. mesencephalon (developing optic lobe)
29. atrium
30. pharynx
31. myelocoele
32. peritoneum

Downloaded from Vet-eBooks.com

Plate 118

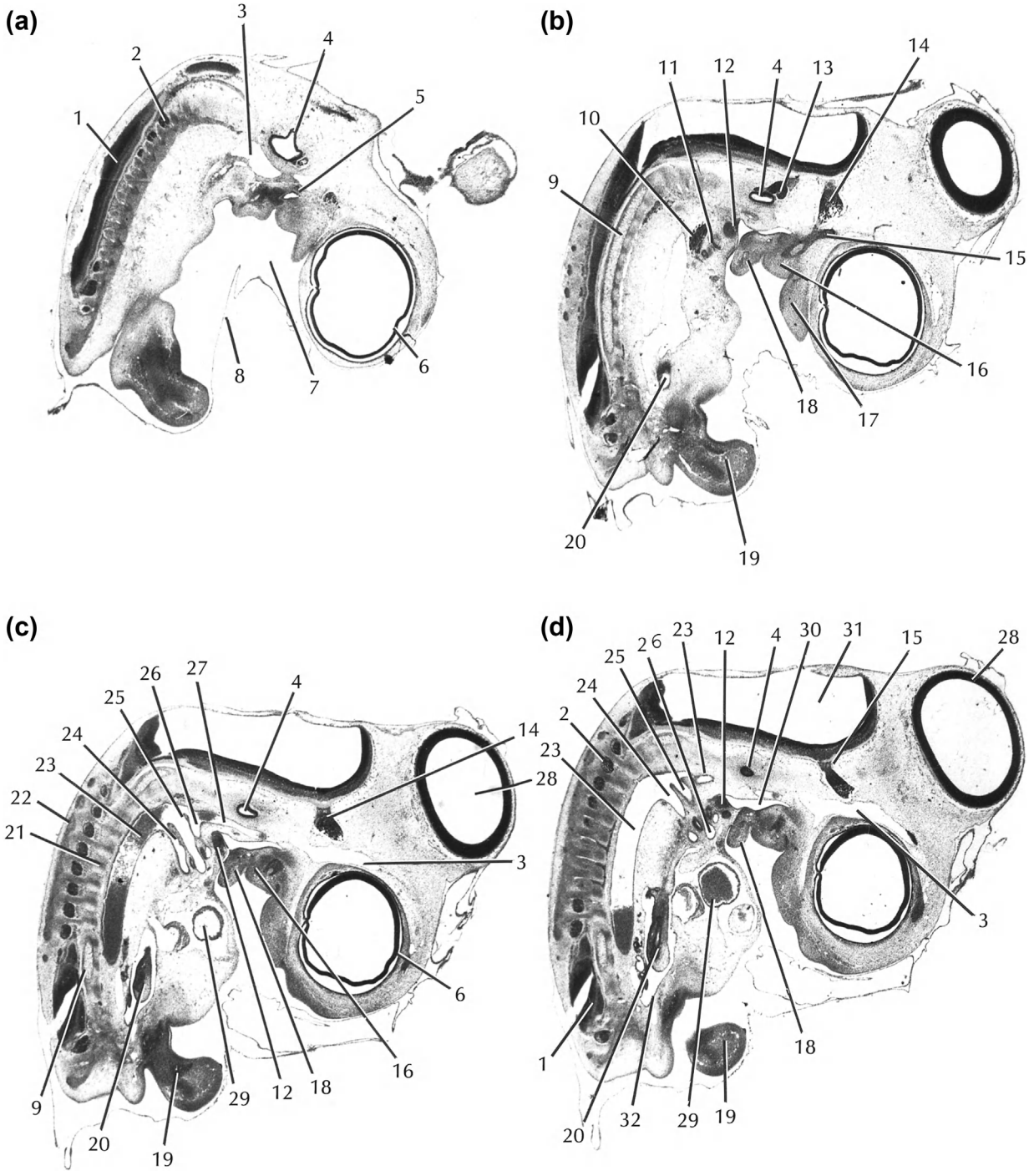

Downloaded from Vet-eBooks.com

Plate 119 Stage 26 (day 5) LS: sagittal

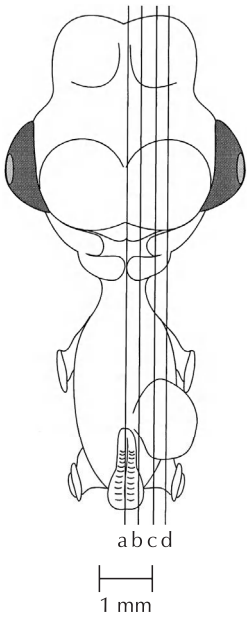

Longitudinal (sagittal) sections: (a–d) × 8

1. fifth aortic arch
2. fourth aortic arch
3. third aortic arch
4. myelocoele
5. trigeminal (cranial V) nerve
6. mesocoele (developing optic lobe)
7. trigeminal (cranial V) nerve (ophthalmic branch)
8. atrium
9. ventricle
10. sinus venosus
11. right allantoic vein
12. liver
13. ductus venosus
14. notochord
15. oesophagus
16. trachea
17. dorsal aorta
18. basal plate of developing chondrocranium
19. first (mandibular) pharyngeal arch
20. nasal pit
21. fronto-nasal process
22. amniotic cavity
23. coelomic cavity
24. left omphalo-mesenteric artery
25. posterior amniotic canal
26. left mesonephros
27. amnion
28. truncus arteriosus
29. otic vesicle
30. Rathke's pouch
31. loop of intestine in mesentery
32. left omphalo-mesenteric artery
33. right oviduct (Mullerian duct)
34. stomach
35. liver in region of falciform ligament
36. pharynx
37. endolymphatic duct
38. acoustic (cranial nerve VIII) ganglion (vestibulo-cochlearis)
39. myelencephalon
40. metencephalon
41. isthmus
42. mesencephalon
43. diocoele
44. telocoele
45. left subcardinal vein
46. posterior cardinal vein
47. right mesonephros
48. second (hyoid) pharyngeal arch

Downloaded from Vet-eBooks.com

Plate 119

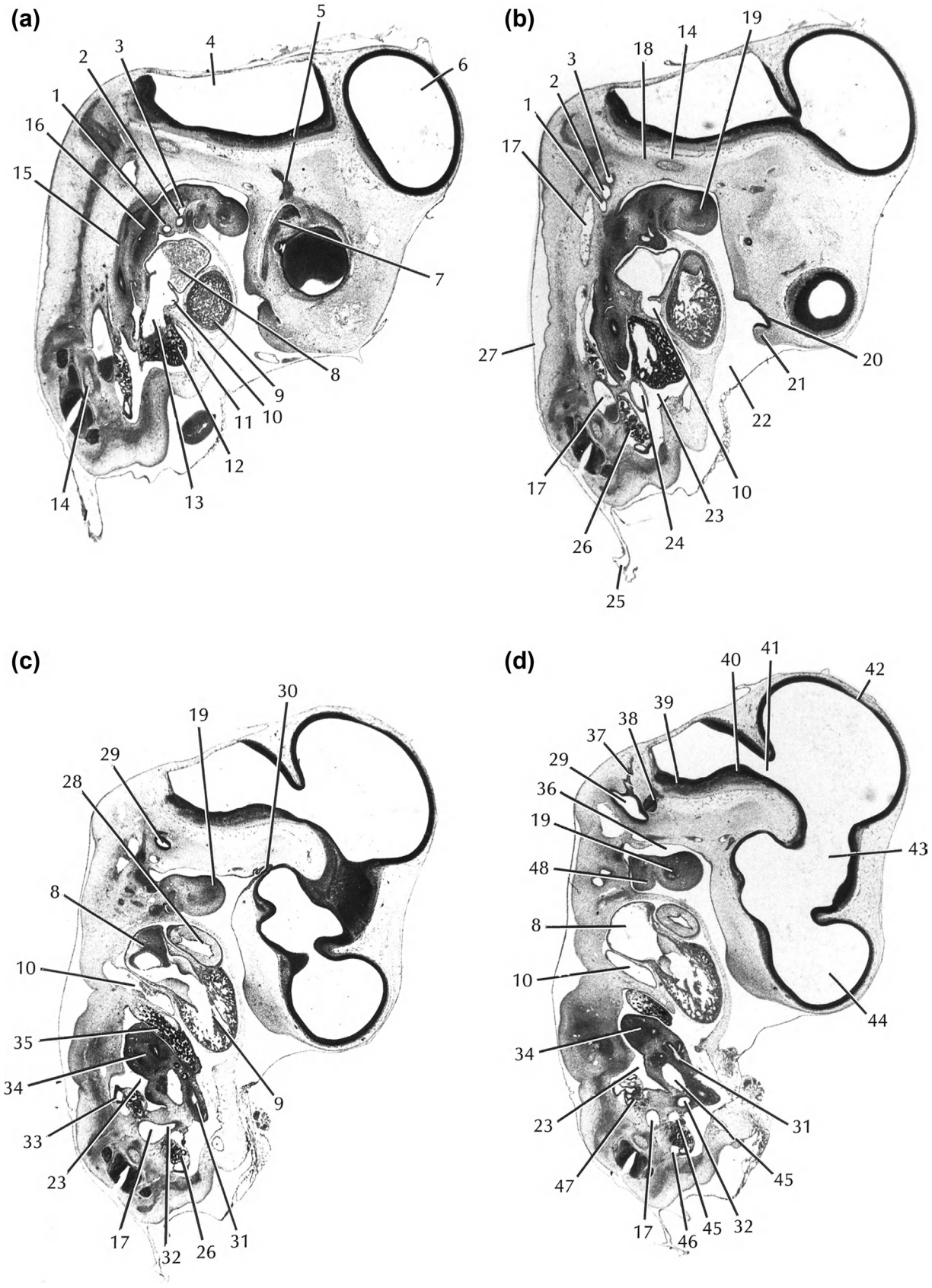

Downloaded from Vet-eBooks.com

Plate 120 Stage 26 (day 5) LS: sagittal

Enlargement of section adjacent to *plate 118b*: × 35

1. floor of myelencephalon
2. otic vesicle
3. acoustic (cranial nerve VIII) ganglion
4. pharynx
5. myelocoele
6. head vein
7. trigeminal (cranial nerve V) ganglion
8. trigeminal nerve
9. pigmented layer of retina
10. first pharyngeal arch (mandibular portion)
11. first pharyngeal arch (maxillary portion)
12. amnion
13. dorsal aorta
14. second (hyoid) pharyngeal arch
15. fifth pharyngeal pouch
16. nodose (cranial nerve X) ganglion
17. petrosal (cranial nerve IX) ganglion

Downloaded from Vet-eBooks.com

Plate 120

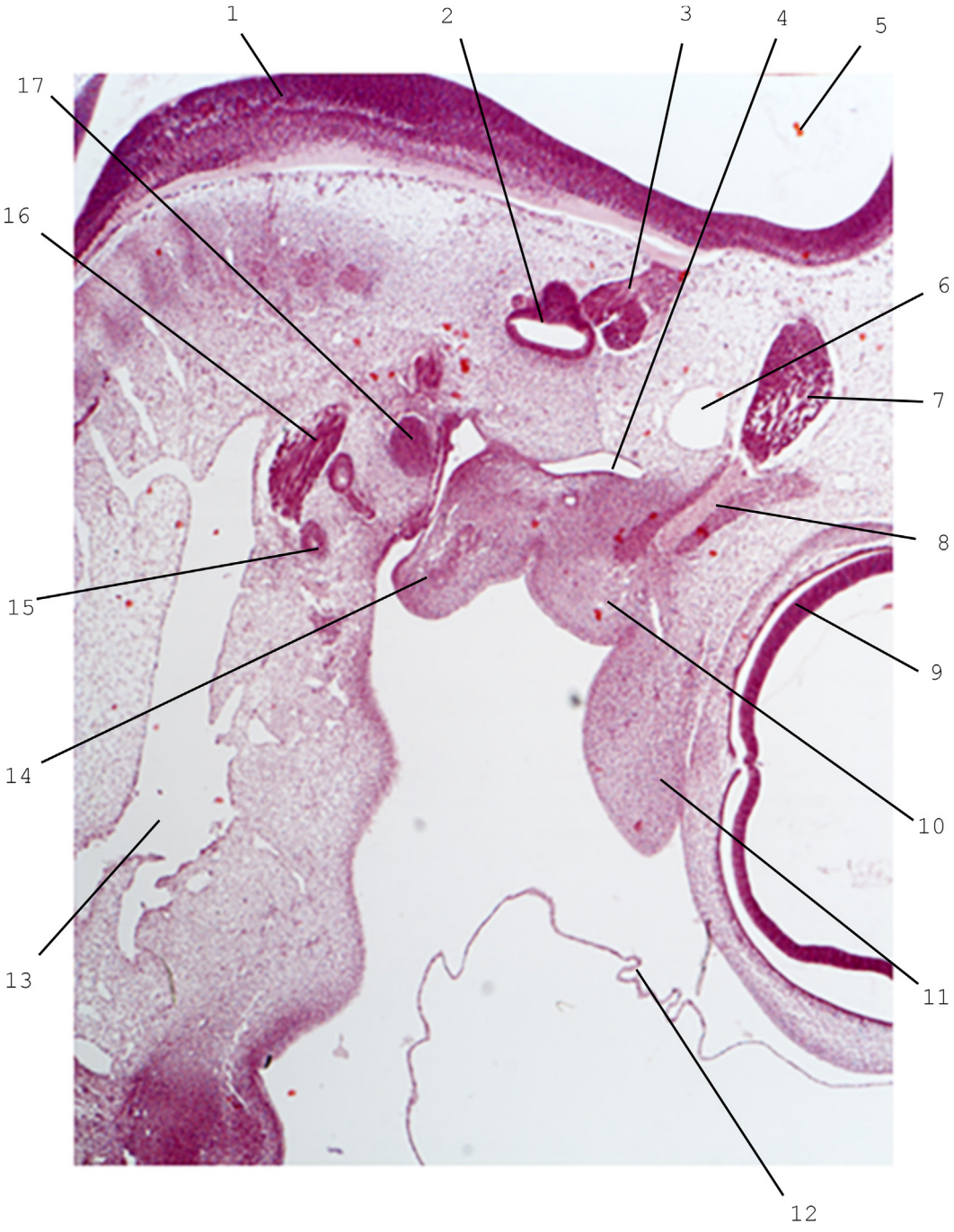

Downloaded from Vet-eBooks.com

Plate 121 Stage 26 (day 5) LS: sagittal

Enlargement of section adjacent to *plate 119a*: × 24

1. otic vesicle
2. fourth aortic arch
3. pharynx
4. third aortic arch
5. anterior body wall
6. atrium
7. ventricle
8. sinus venosus
9. coelom
10. liver
11. ductus venosus
12. dorsal aorta
13. loop of gut in mesentery
14. mesonephros
15. oesophagus
16. fifth aortic arch

Downloaded from Vet-eBooks.com

Plate 121

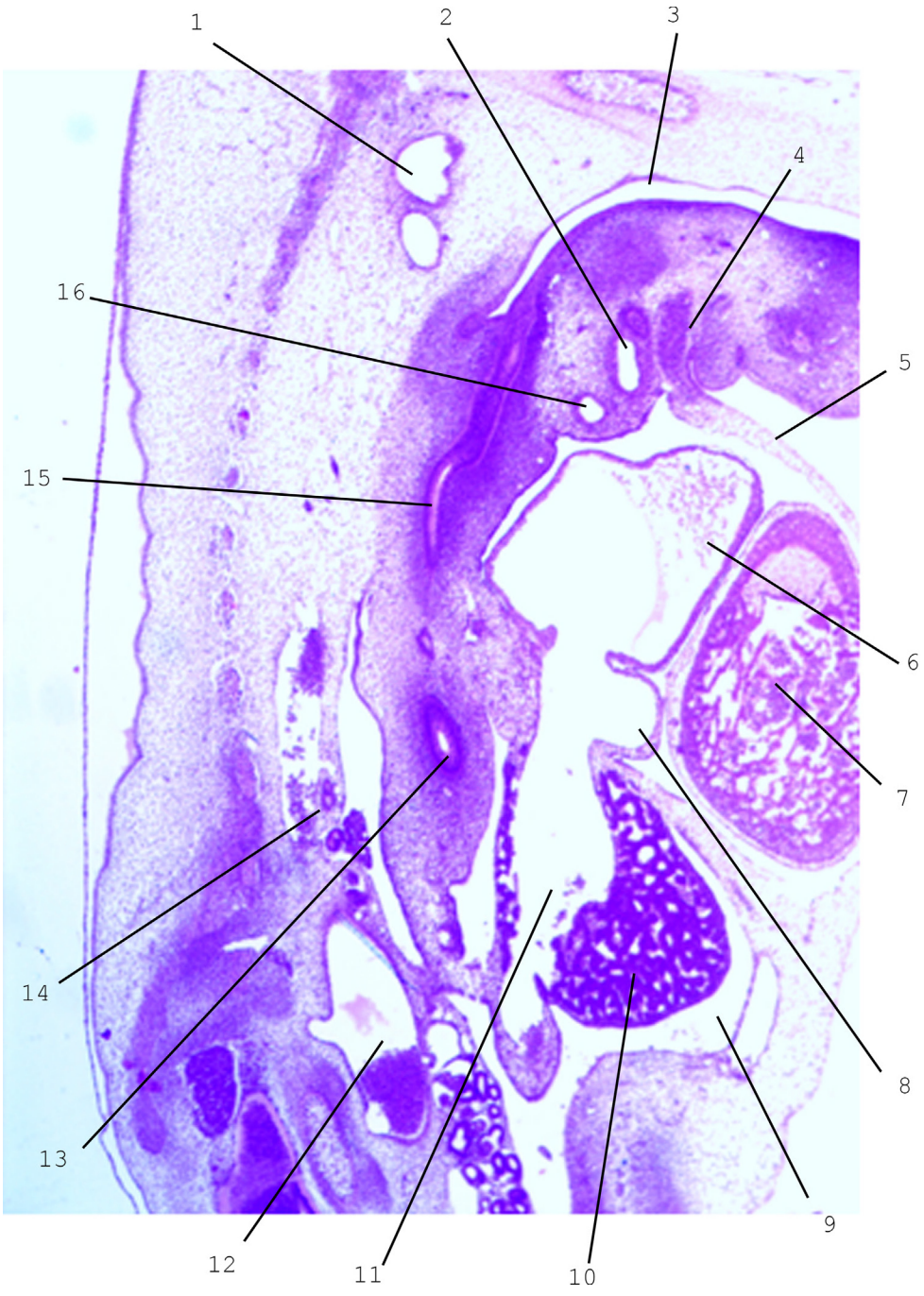

Downloaded from Vet-eBooks.com

Plate 122 Stage 26 (day 5) LS: sagittal

Enlargement of section adjacent to *plate 119c*: × 24

1. sinus venosus
2. atrium
3. truncus arteriosus
4. atrio-ventricular cushion
5. atrio-ventricular canal
6. columna carna of ventricle
7. liver in region of falciform ligament
8. loop of intestine in mesentery
9. left subclavian vein
10. dorsal aorta
11. spinal cord
12. right mesonephros
13. wall of gizzard
14. coelom

Downloaded from Vet-eBooks.com

Plate 122

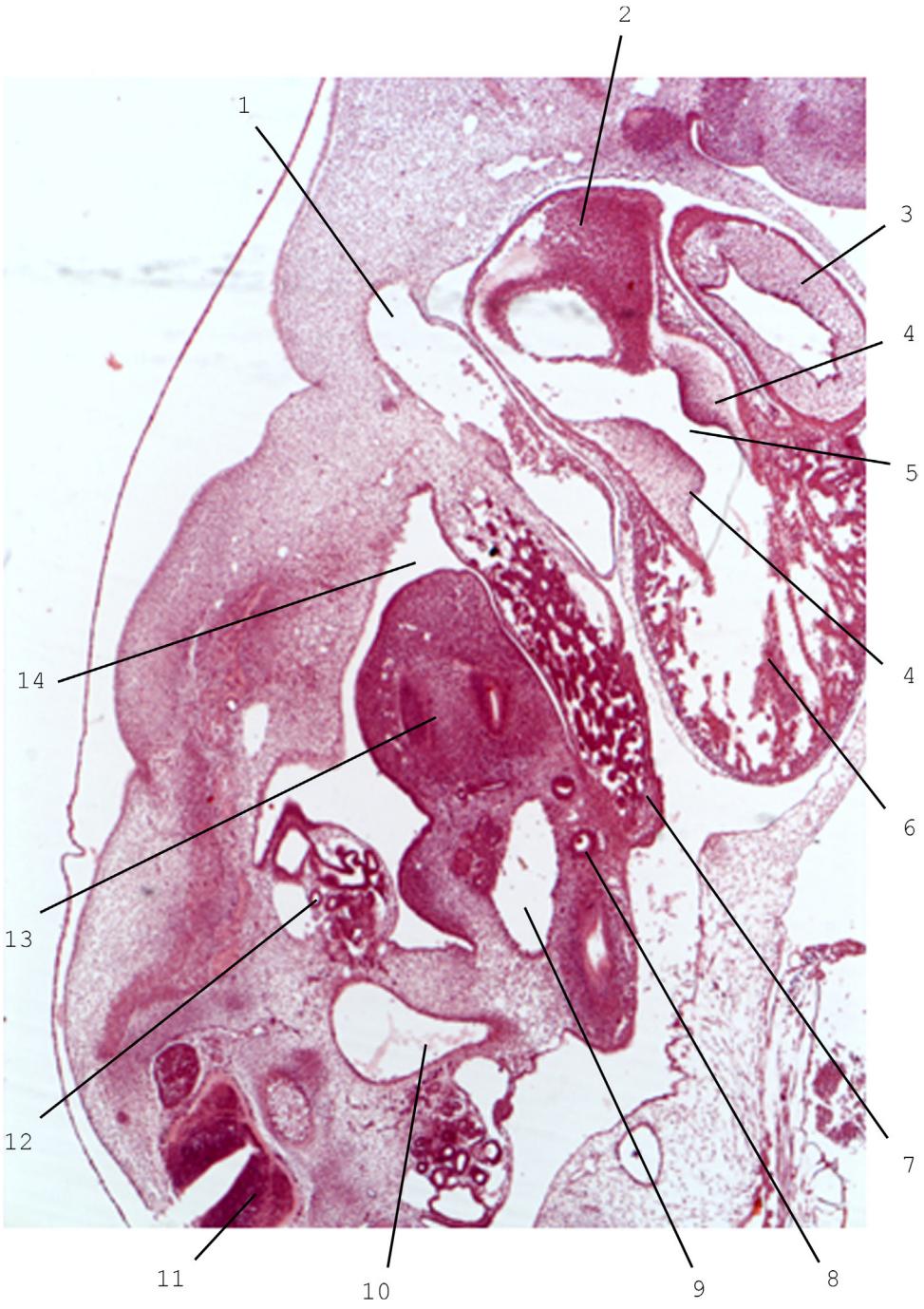

Downloaded from Vet-eBooks.com

Plate 123 Stage 26 (day 5)
LS: sagittal

Enlargement of section in the region of *plate 119c*:
× 30

1. atrium
2. atrio-ventricular canal
3. wall of ventricle
4. hepato-enteric recess
5. ductus venosus
6. coelom
7. post-hepatic septum
8. right nephric duct
9. right mesonephros
10. dorsal root ganglion
11. spinal cord
12. notochord
13. dorsal aorta
14. left mesonephros
15. left anterior cardinal vein
16. left nephric duct
17. gizzard
18. ventral mesentery
19. umbilical vein

Downloaded from Vet-eBooks.com

Plate 123

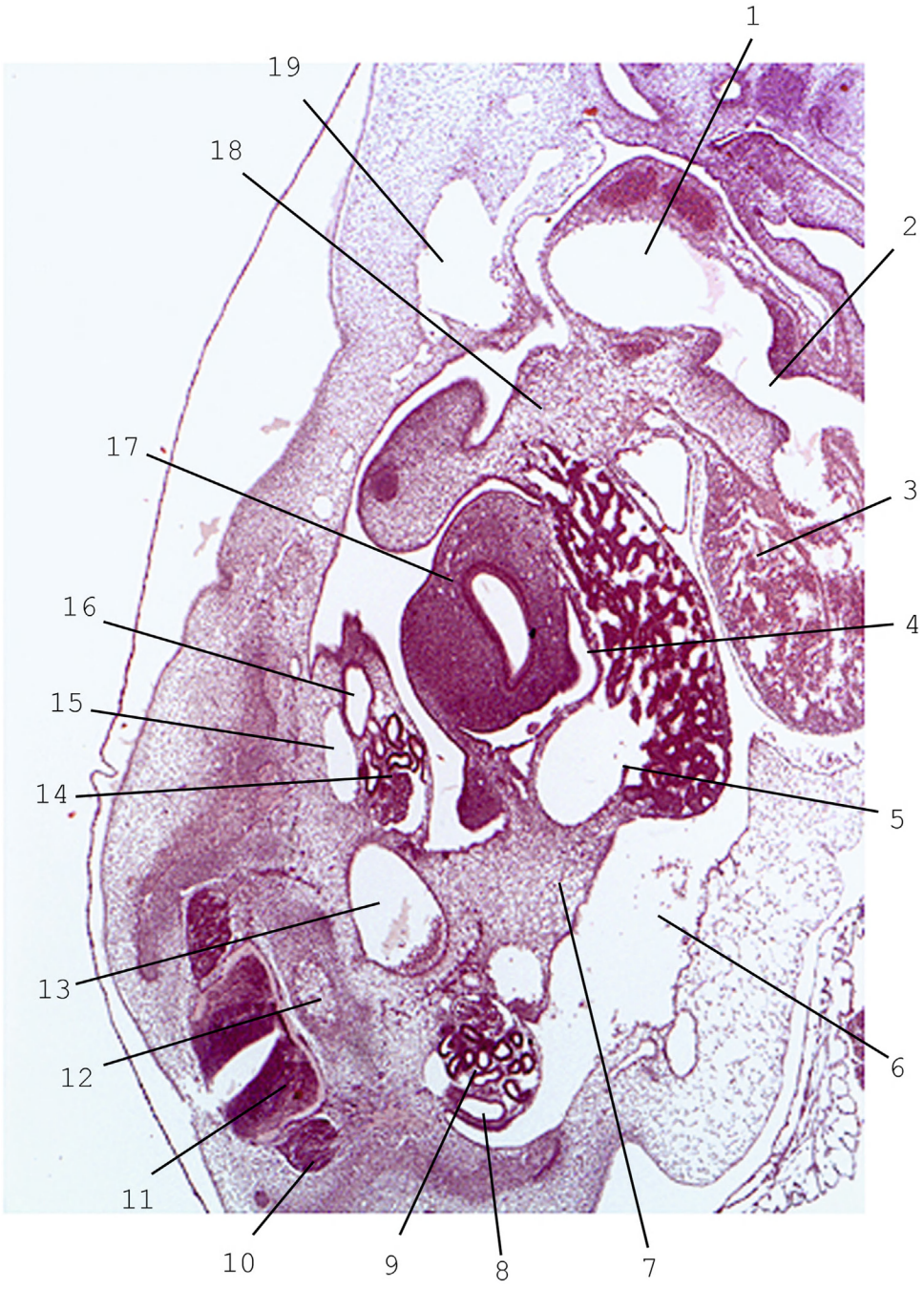

Downloaded from Vet-eBooks.com

Plate 124 Stage 26 (day 5) LS: sagittal

Enlargement of section in the region of *plate 119a*:
× 24

1. fifth aortic arch
2. fourth aortic arch
3. third aortic arch
4. second (hyoid) pharyngeal arch
5. pharynx
6. first (maxillary-mandibulary) pharyngeal arch
7. atrium
8. ventricle
9. amnion
10. sinus venosus
11. body wall
12. coelom
13. mesonephros
14. blood in dorsal aorta
15. loop of intestine in mesentery
16. dorsal aorta

Downloaded from Vet-eBooks.com

Plate 124

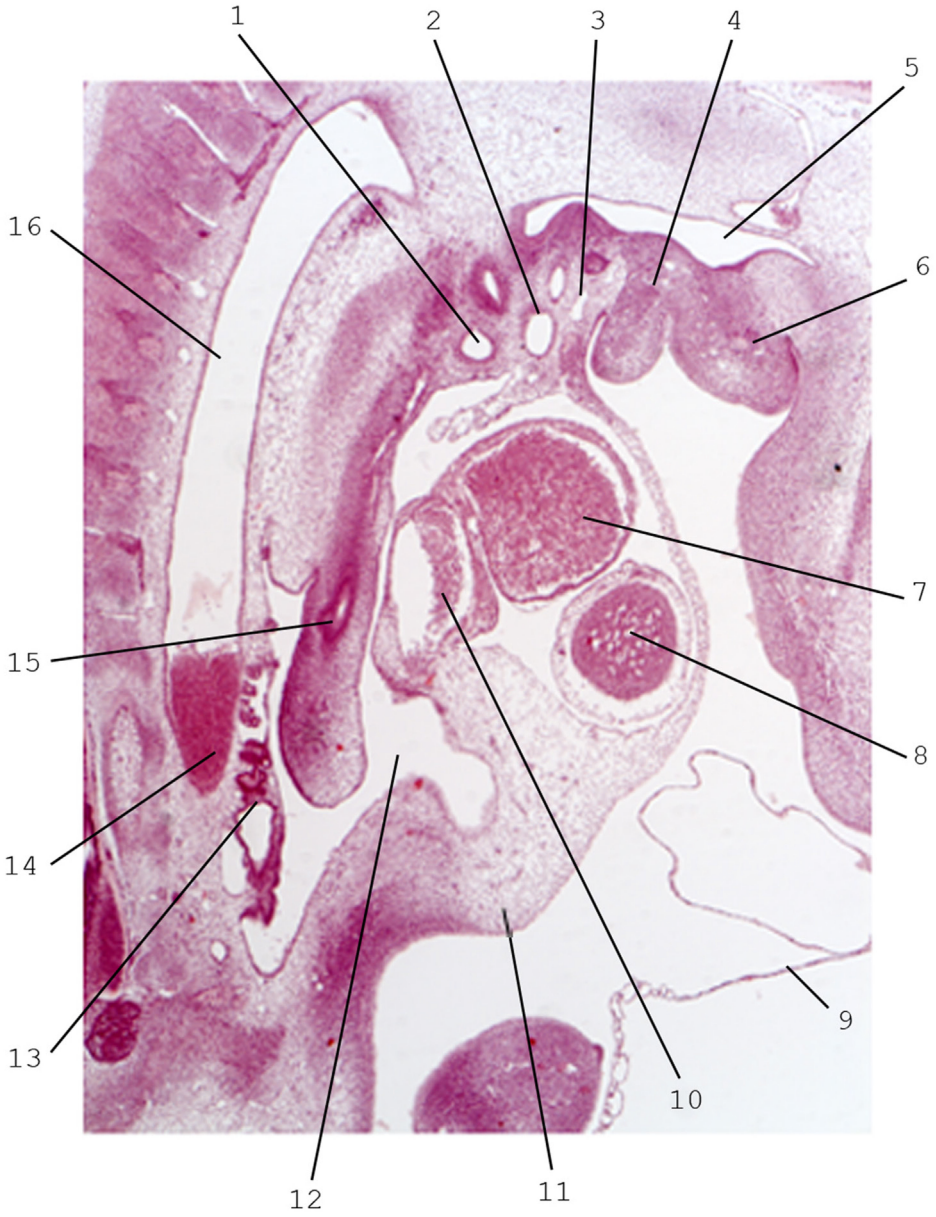

Downloaded from Vet-eBooks.com

Plate 125 Stage 26 (day 5) LS: oblique

Oblique section through the tail region: × 40

1. amnion
2. leg bud
3. amniotic cavity
4. myotomes
5. lumen of spinal cord
6. wall of spinal cord
7. dorsal root ganglion

Downloaded from Vet-eBooks.com

Plate 125

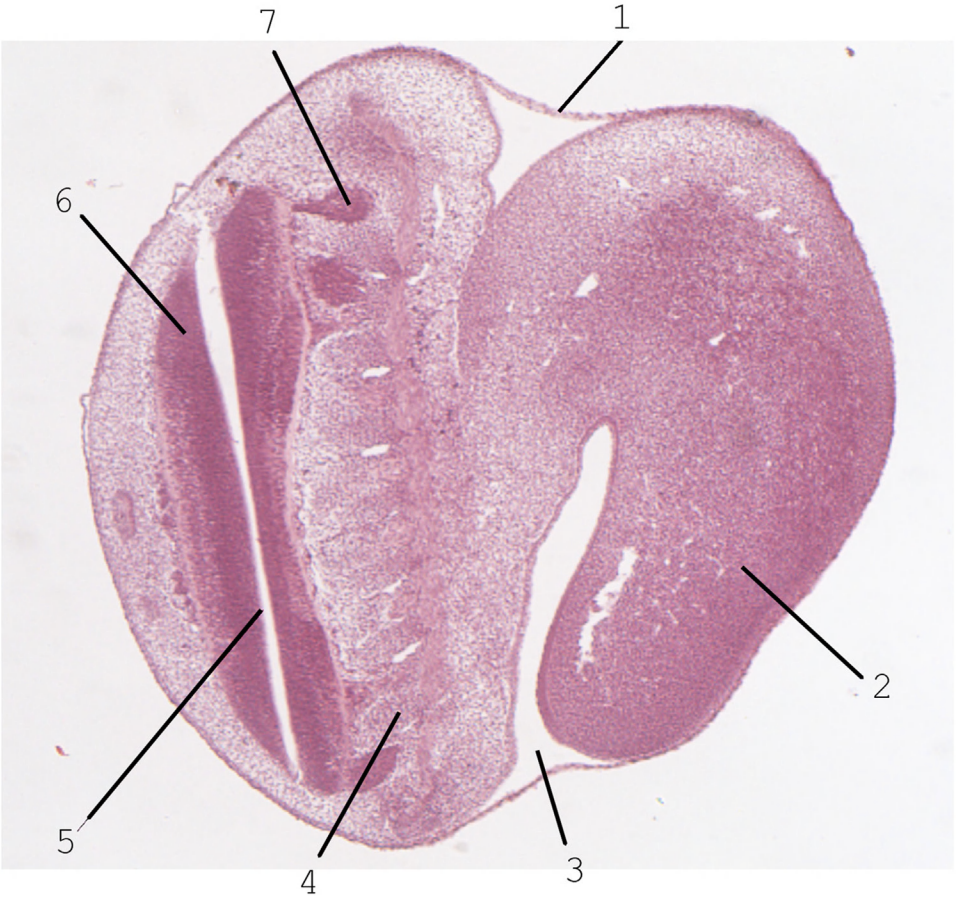

Downloaded from Vet-eBooks.com

Plate 126 Stage 26 (day 5) TS

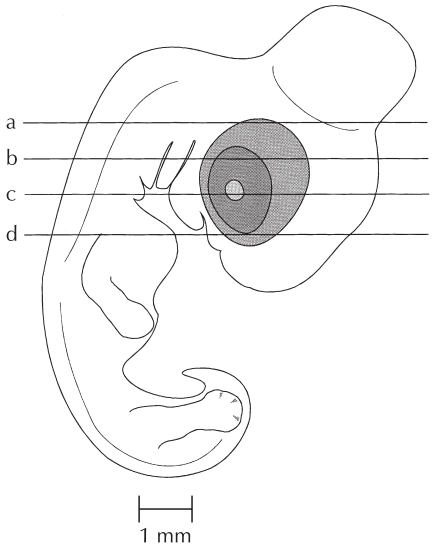

Transverse sections (TS): (a–d) × 15 enlarged on *plate 127a*
Trunk of (c)
Trunk of (d) enlarged on *plate 128a*

1. notochord
2. spinal cord
3. left anterior cardinal vein
4. left carotid artery
5. left second (hyoid) pharyngeal arch
6. first pharyngeal pouch
7. vitreous humour of left eye
8. left ophthalmic vein
9. mesocoele
10. right carotid artery
11. geniculate (cranial nerves VII and VIII) ganglion
12. otic vesicle
13. myotome
14. quadrate cartilage
15. Meckel's cartilage
16. acoustic (cranial VIII) nerve
17. left maxillary (cranial V) nerve
18. lens of left eye
19. dorsal oblique eye muscle
20. dorsal rectus eye muscle
21. mesencephalon
22. trigeminal (cranial nerve V) ganglion
23. lagena of right ear
24. right anterior vena cava
25. right optic nerve
26. oral cavity
27. median nasal eminence
28. retina of left eye
29. wall of left telencephalic vesicle
30. pineal organ
31. diencephalon
32. retina of right eye
33. right lateral nasal eminence
34. fronto-nasal process
35. left nasal pit (external naris)
36. left lateral nasal eminence
37. wall of right telencephalic vesicle
38. vitreous humour of right eye
39. lens of right eye

Downloaded from Vet-eBooks.com

Plate 126

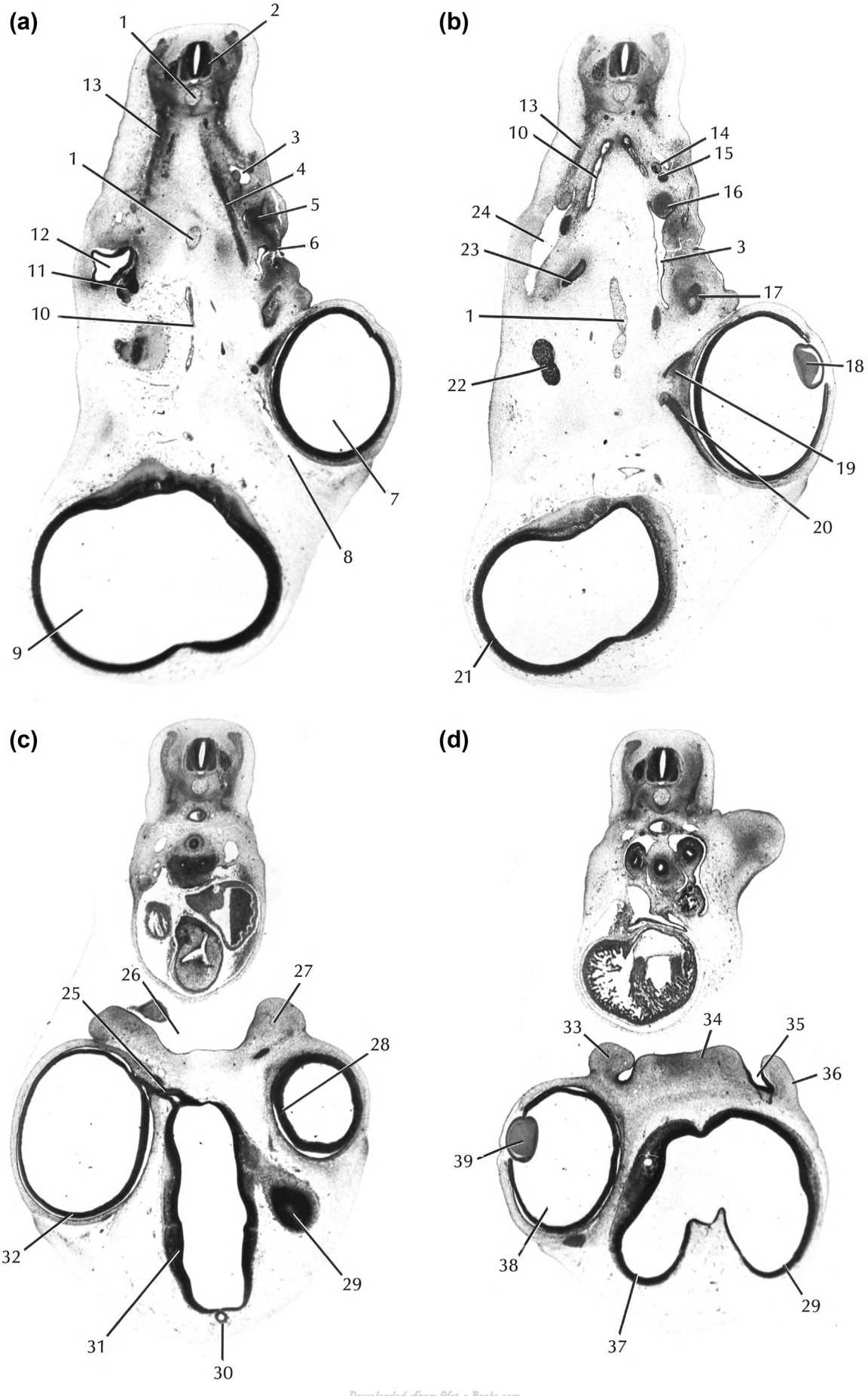

Downloaded from Vet-eBooks.com

Plate 127 Stage 26 (day 5) TS

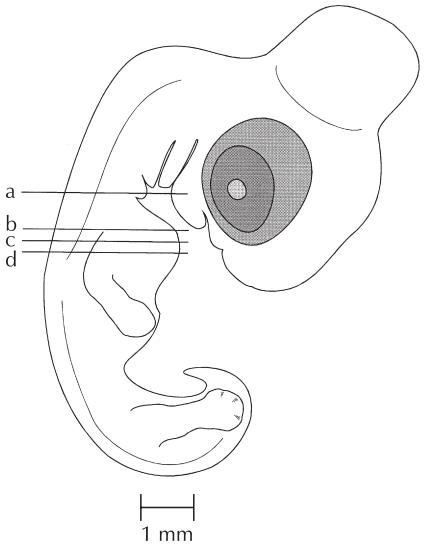

Transverse sections (TS): (a–d) × 30

(a) Enlargement of part of *plate 126c*

1. dorsal aorta
2. neural tube
3. notochord
4. oesophagus
5. left anterior cardinal vein
6. extravasated blood in pericardial cavity
7. left atrium
8. aortico-pulmonary ridges in truncus arteriosus
9. pericardial cavity
10. right atrium
11. right anterior cardinal vein
12. right lung bud
13. ventral body wall
14. truncus arteriosus
15. myotome
16. left lung bud
17. interatrial septum
18. atrio-ventricular cushion
19. edge of pleural cavity
20. right atrio-ventricular canal
21. sinu-atrial valve
22. sinus venosus

Downloaded from Vet-eBooks.com

Plate 127

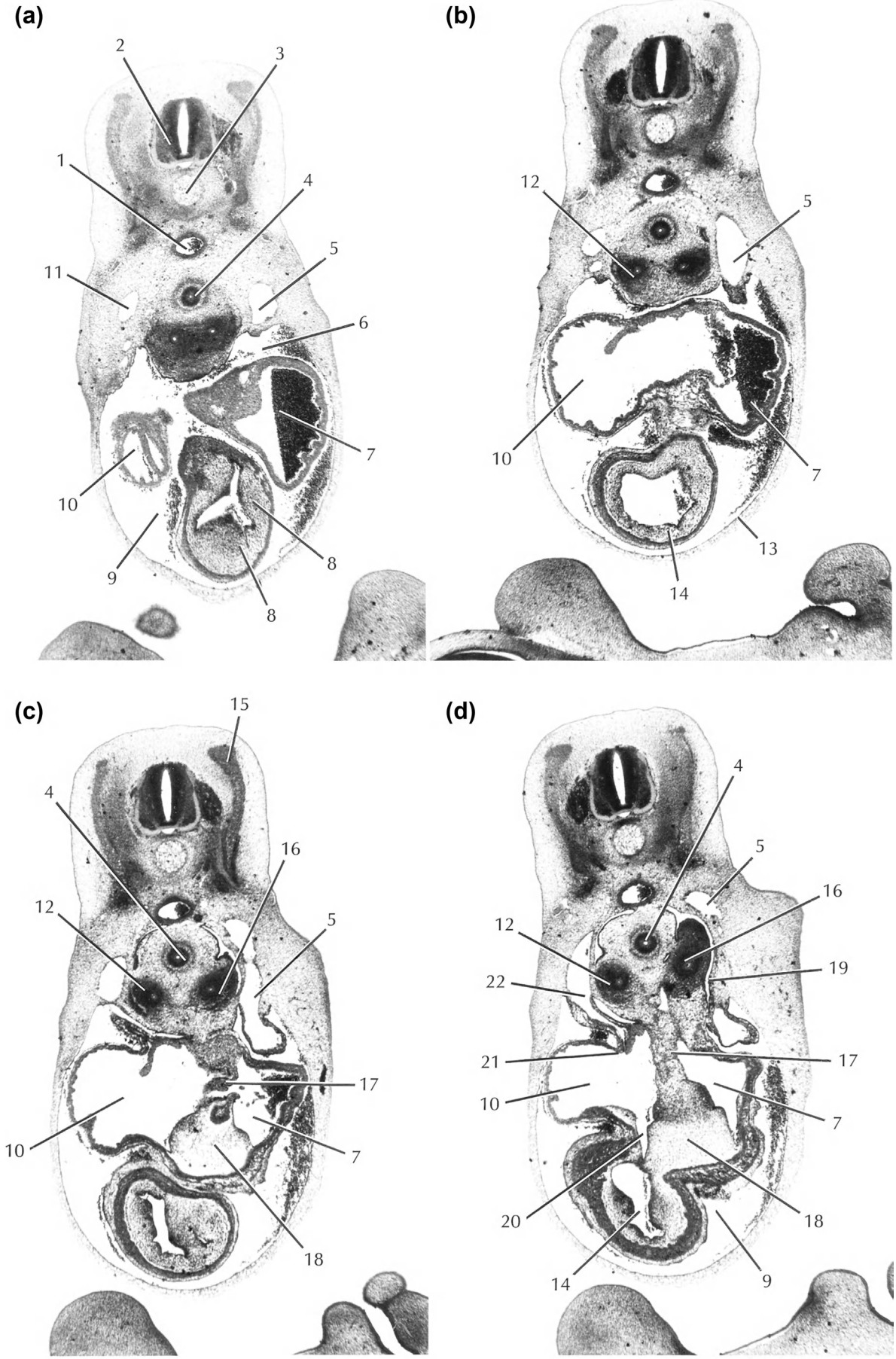

Downloaded from Vet-eBooks.com

Plate 128 Stage 26 (day 5) TS

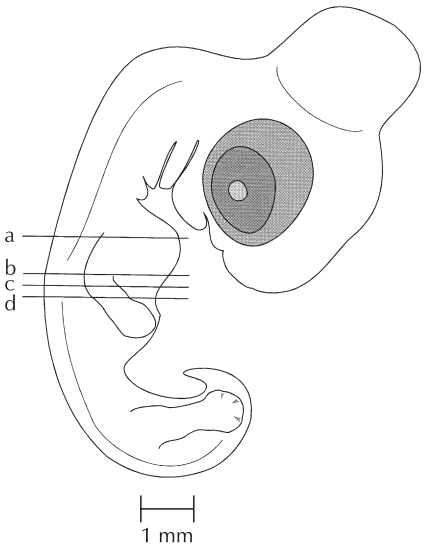

Transverse sections (TS): (a–d) × 30

(a) Enlargement of part of *plate 126d*

1. dorsal root ganglion
2. spinal cord
3. left nephric (pronephric) duct
4. left anterior cardinal vein
5. left wing bud
6. left pleural cavity
7. lesser sac
8. liver
9. ventral mesentery
10. left common cardinal vein
11. atrio-ventricular cushion
12. left ventricle
13. interventricular septum
14. right ventricle
15. sinus venosus
16. crop
17. right lung bud
18. right anterior cardinal vein
19. right nephric (pronephric) duct
20. notochord
21. spinal nerve
22. ramus communicans nerve
23. peritoneal cavity
24. dorsal hepatic cavity
25. ductus venosus
26. right pulmonary fold
27. dorsal mesentery
28. dorsal aorta
29. gizzard
30. left allantoic vein
31. septum transversum
32. left mesonephros
33. right allantoic vein
34. right wing bud

Downloaded from Vet-eBooks.com

Plate 128

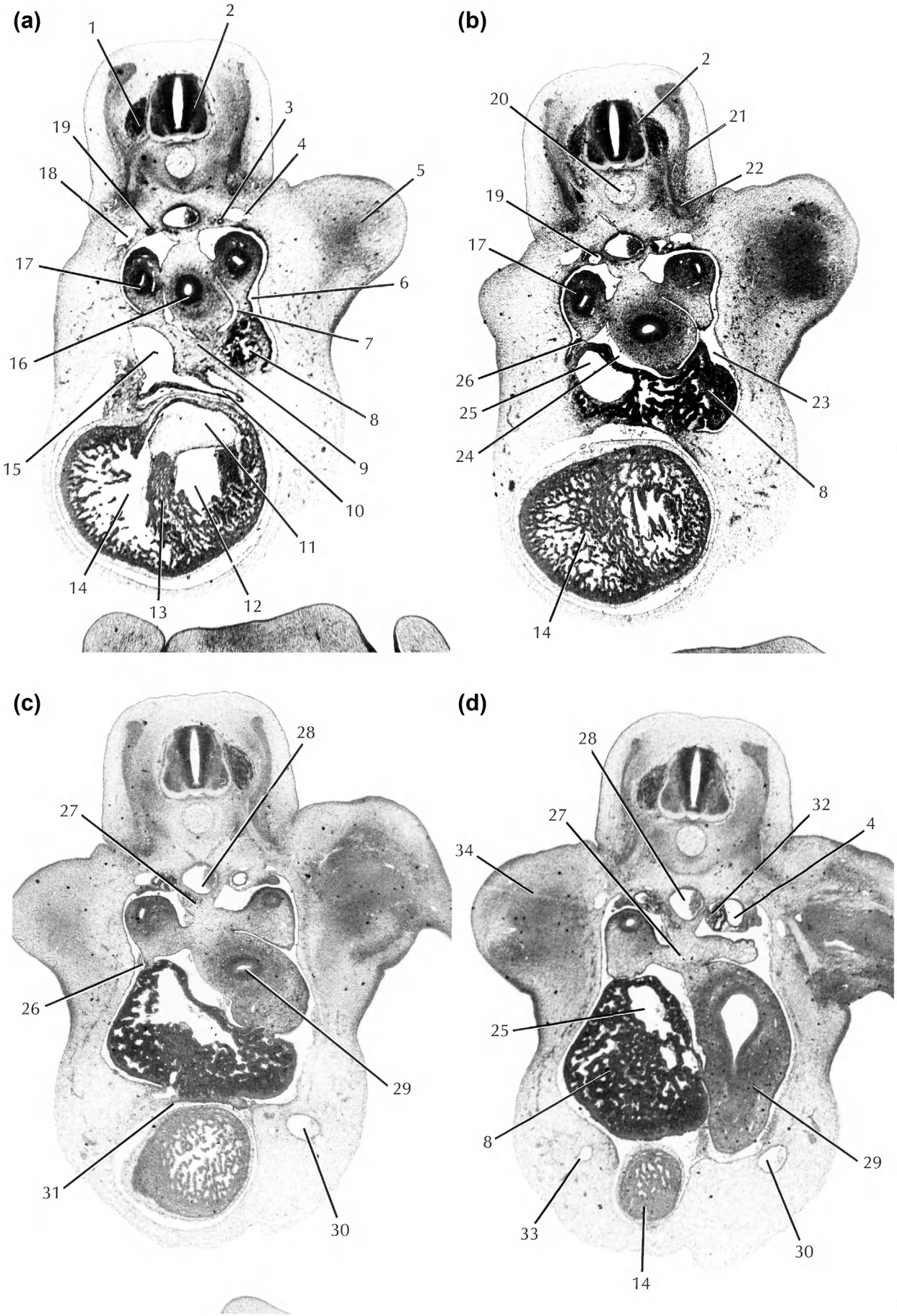

Downloaded from Vet-eBooks.com

Plate 129 Stage 28 (day 6) LS: sagittal

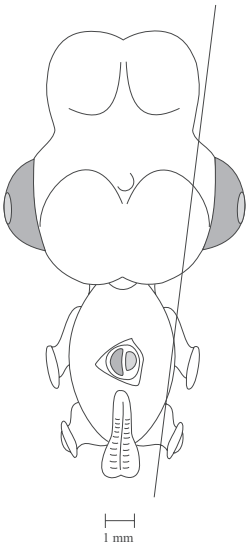

Longitudinal (sagittal) section: × 16

1. left eye
2. quadrate cartilage
3. left otic vesicle
4. left cranial (anterior) vena cava
5. spinal cord
6. anterior median artery
7. left wing
8. left atrium
9. Meckel's cartilage

Downloaded from Vet-eBooks.com

Plate 129

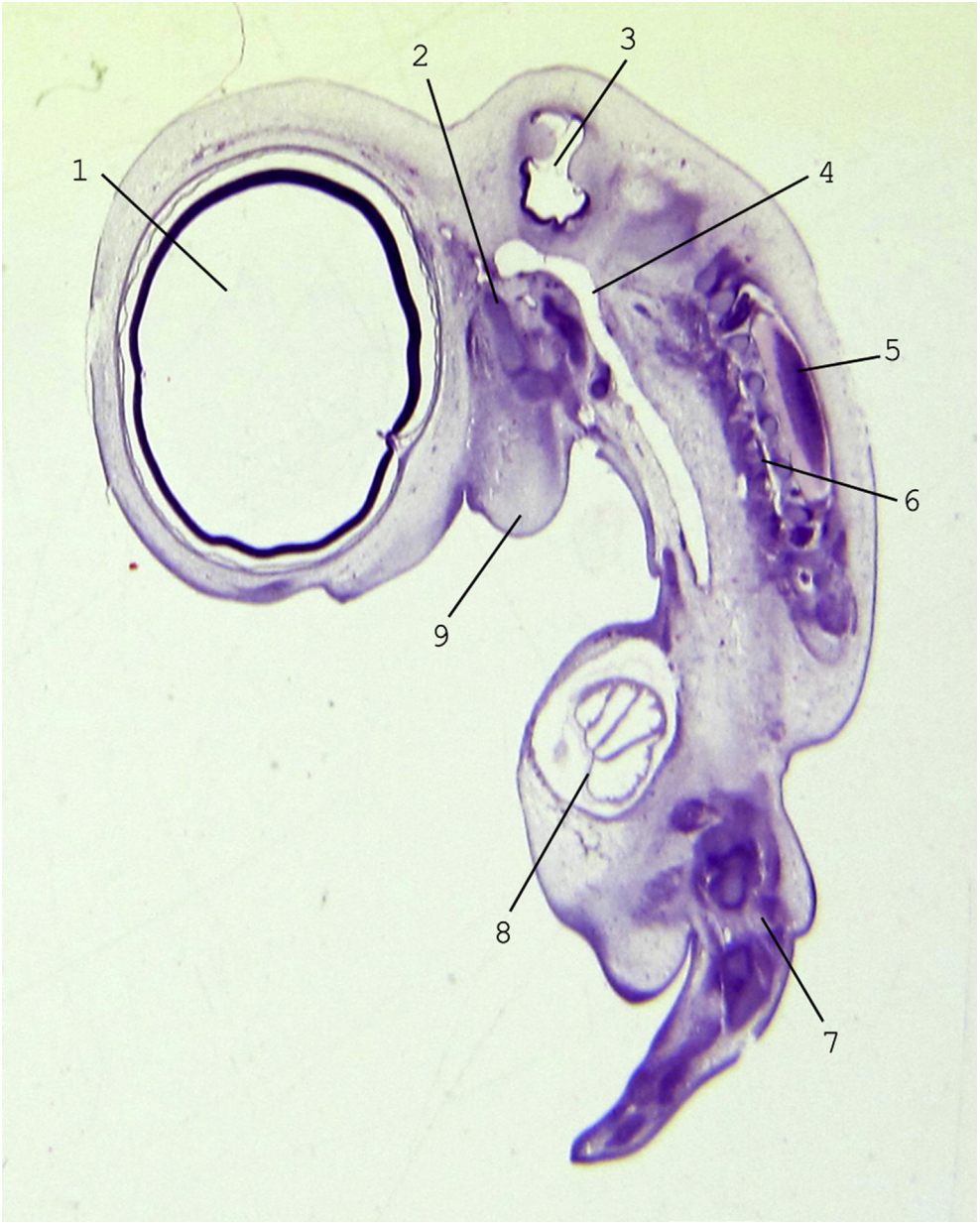

Downloaded from Vet-eBooks.com

Plate 130 Stage 28 (day 6) LS: sagittal

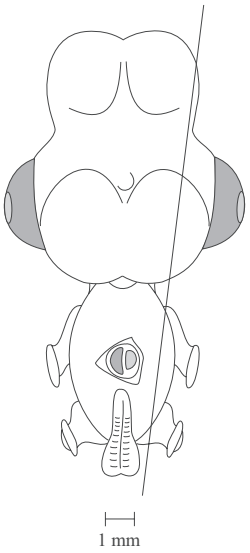

Longitudinal (sagittal) section: × 15

1. wall of left optic lobe
2. lumen of left optic lobe
3. basal plate
4. left trigeminal (cranial nerve V) ganglion
5. thin roof of myelencephalon
6. otic capsule
7. semi-circular canal
8. internal naris
9. floor of myelencephalon
10. atlas vertebra
11. dorsal aorta
12. oesophagus
13. thyroglossal duct
14. trachea
15. intestinal loop
16. notochord
17. spinal cord
18. ventral aorta
19. truncus arteriosus
20. sinus venosus
21. left atrium
22. horizontal septum
23. dorsal hepatic cavity
24. liver
25. left ventricle
26. ventral body wall
27. lower jaw
28. oral cavity
29. external eye muscle
30. optic nerve
31. vitreous body
32. sclera
33. pigmented retina

Downloaded from Vet-eBooks.com

Plate 130

Downloaded from Vet-eBooks.com

Plate 131 Stage 28 (day 6) LS: sagittal

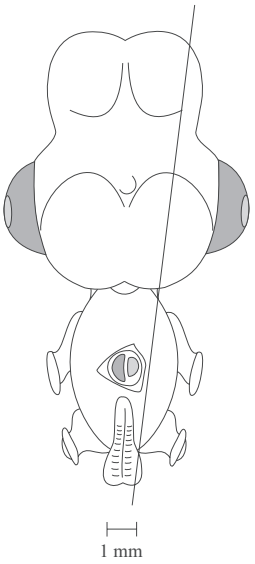

Longitudinal (sagittal) section: × 13

1. damage to section in preparation
2. left optic lobe
3. thin roof of myelencephalon
4. lumen of myelencephalon
5. remnant of notochord in basal plate
6. edge of vertebra
7. spinal ganglion
8. trachea
9. spinal cord
10. notochord
11. loop of intestine
12. spinal nerve
13. trachio-bronchial region
14. left dorsal hepatic cavity
15. gizzard
16. lateral ventral hepatic cavity
17. liver
18. ventricle
19. inter-ventricular septum
20. lower jaw
21. fronto-nasal process
22. left nasal sac
23. pigmented layer of retina
24. left head vein
25. chondrocranium

Downloaded from Vet-eBooks.com

Plate 131

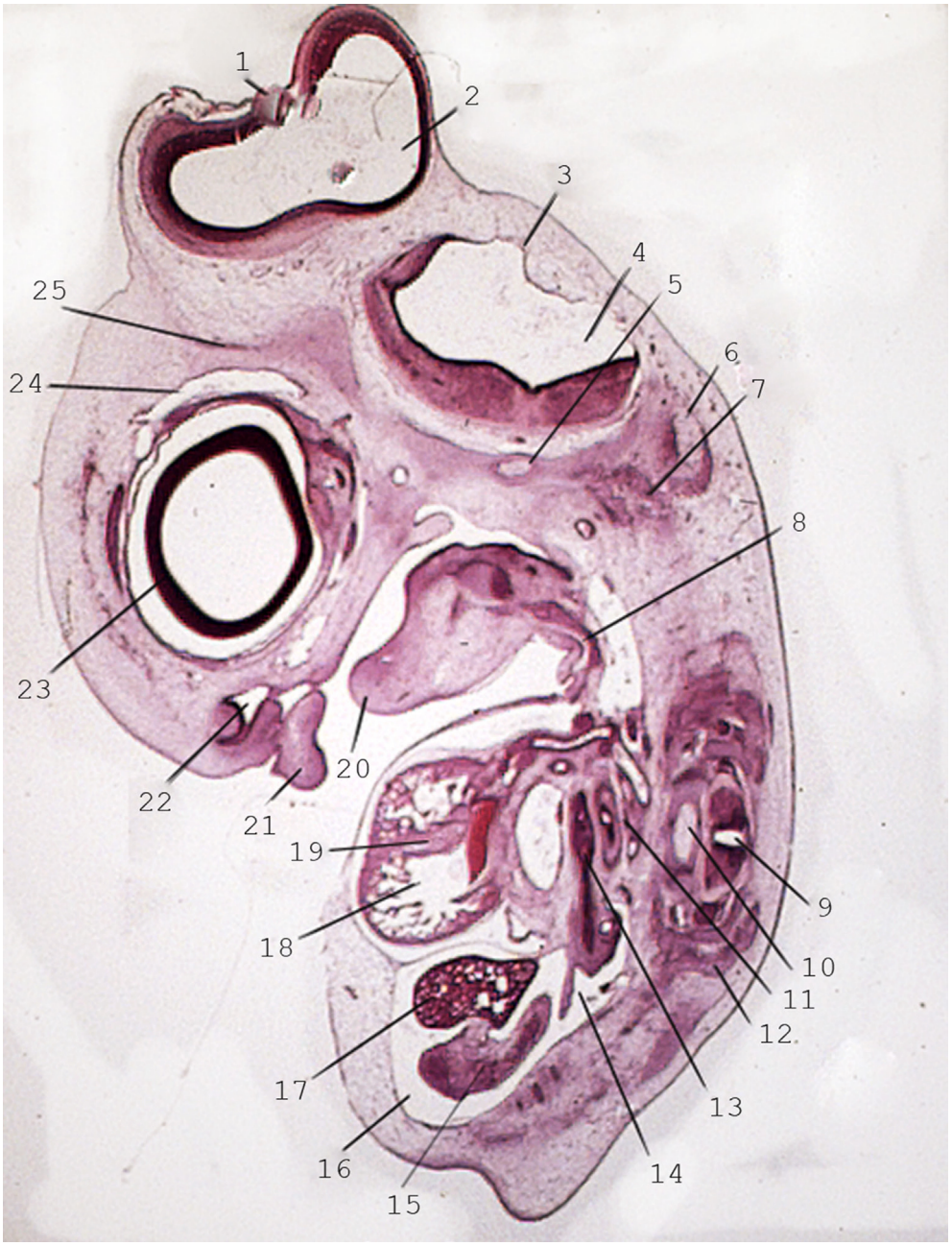

Downloaded from Vet-eBooks.com

Plate 132 Stage 28 (day 6)
LS: sagittal

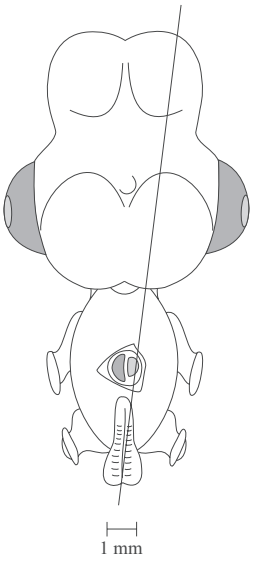

Longitudinal (sagittal) section: × 15

1. wall of left optic lobe (damaged)
2. lumen of left optic lobe
3. myelocoele
4. parachordal cartilage
5. left jugular vein
6. cranial (anterior) vena cava
7. pre-muscle mass
8. left atrium
9. spinal cord
10. notochord
11. dorsal aorta
12. gut
13. left lung
14. gizzard
15. liver
16. pericardial cavity
17. left ventricle
18. Interventricular septum
19. right ventricle
20. left nasal sac
21. left eye
22. external eye muscle

Downloaded from Vet-eBooks.com

Plate 132

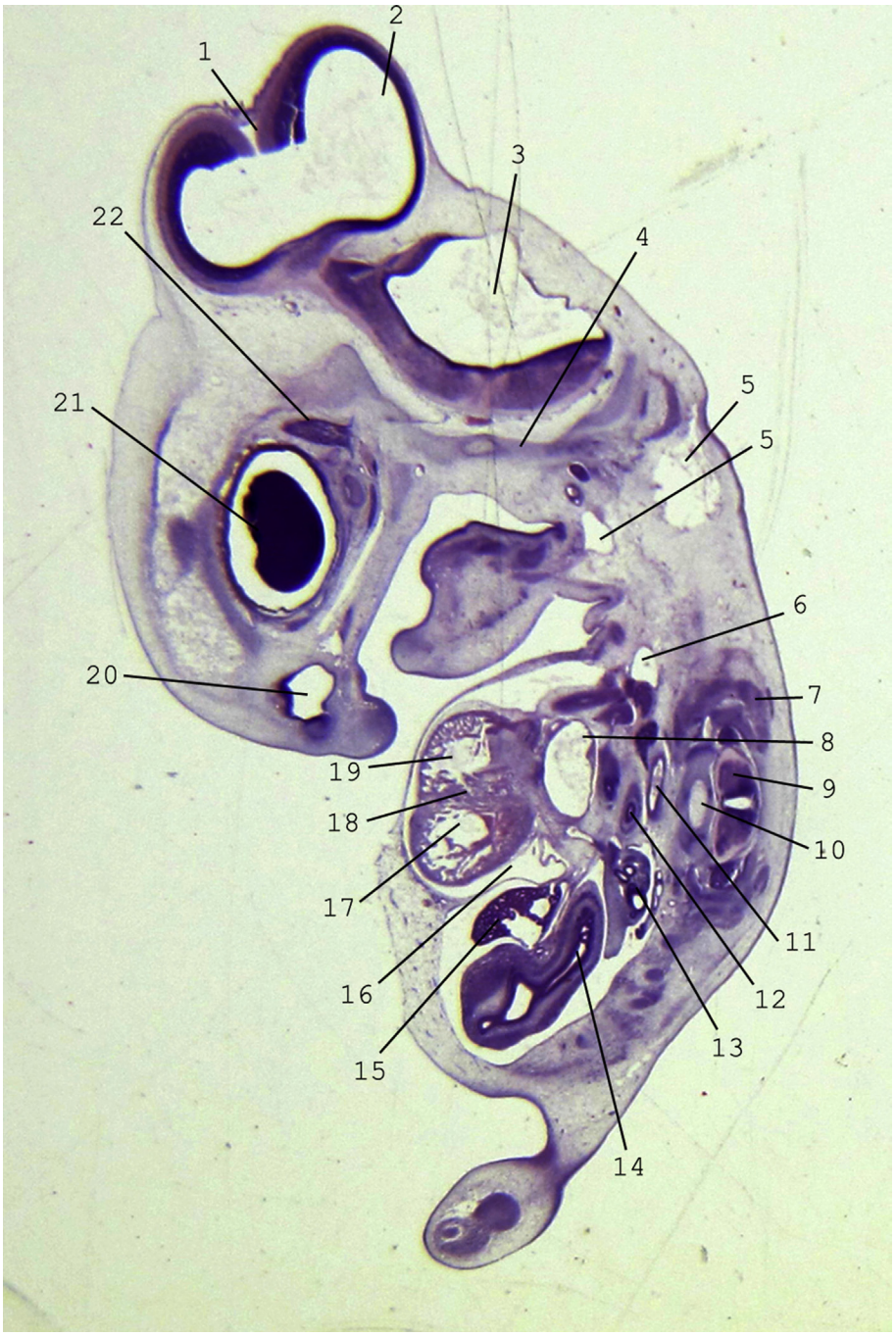

Downloaded from Vet-eBooks.com

Plate 133 Stage 28 (day 6) LS: sagittal

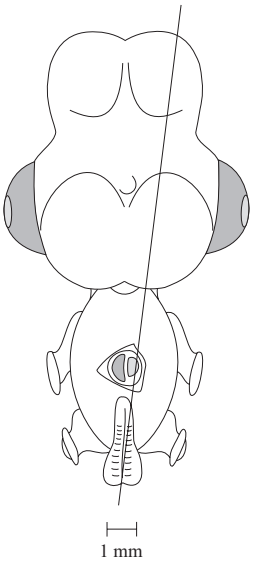

Enlargement of section adjacent to that in *plate 132*:
× 60

1. right spinal nerve
2. right dorsal root ganglion
3. right transverse process of vertebra
4. spinal cord
5. notochord
6. left transverse process of vertebra
7. left dorsal root ganglion
8. left pre-muscle mass
9. left spinal nerve
10. left lung
11. edge of gizzard
12. coelom
13. gut
14. lumen of atrium
15. thin wall of atrium
16. truncus arteriosus
17. deep jugular lymphatic plexus
18. right jugular vein
19. right pre-muscle mass

Downloaded from Vet-eBooks.com

Plate 133

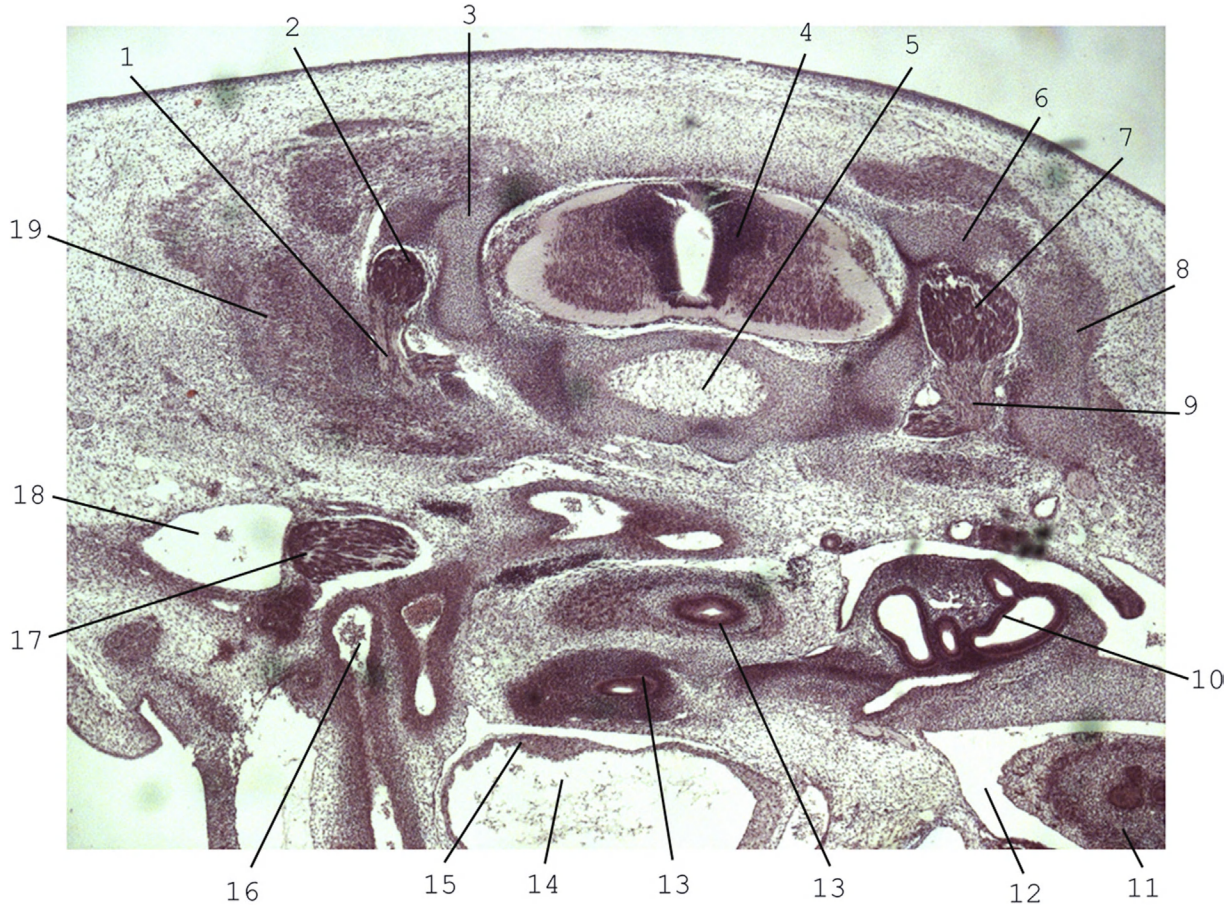

Downloaded from Vet-eBooks.com

Plate 134 Stage 28 (day 6)
LS: sagittal

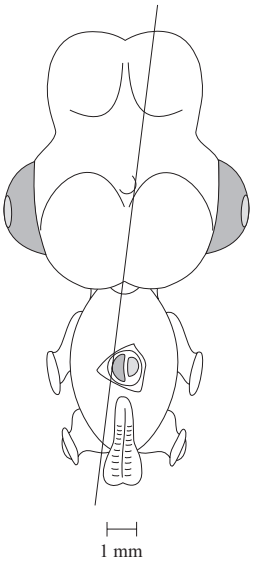

Longitudinal (sagittal) section: × 14

1. optic lobe
2. isthmus
3. myelocoele
4. right carotid artery
5. right otic vesicle
6. right otic tube
7. lower jaw
8. atrium
9. sinus venosus
10. right lung bud
11. dorsal aorta
12. ventral mesentery
13. liver
14. dorsal hepatic cavity
15. left horizontal hepatic septum (not yet extended fully)
16. ventral hepatic cavity
17. gizzard
18. right horizontal hepatic septum
19. pericardial cavity
20. ventricle
21. right cerebral vesicle
22. oral cavity
23. third ventricle (diencephalon)
24. optic thalamus

Downloaded from Vet-eBooks.com

Plate 134

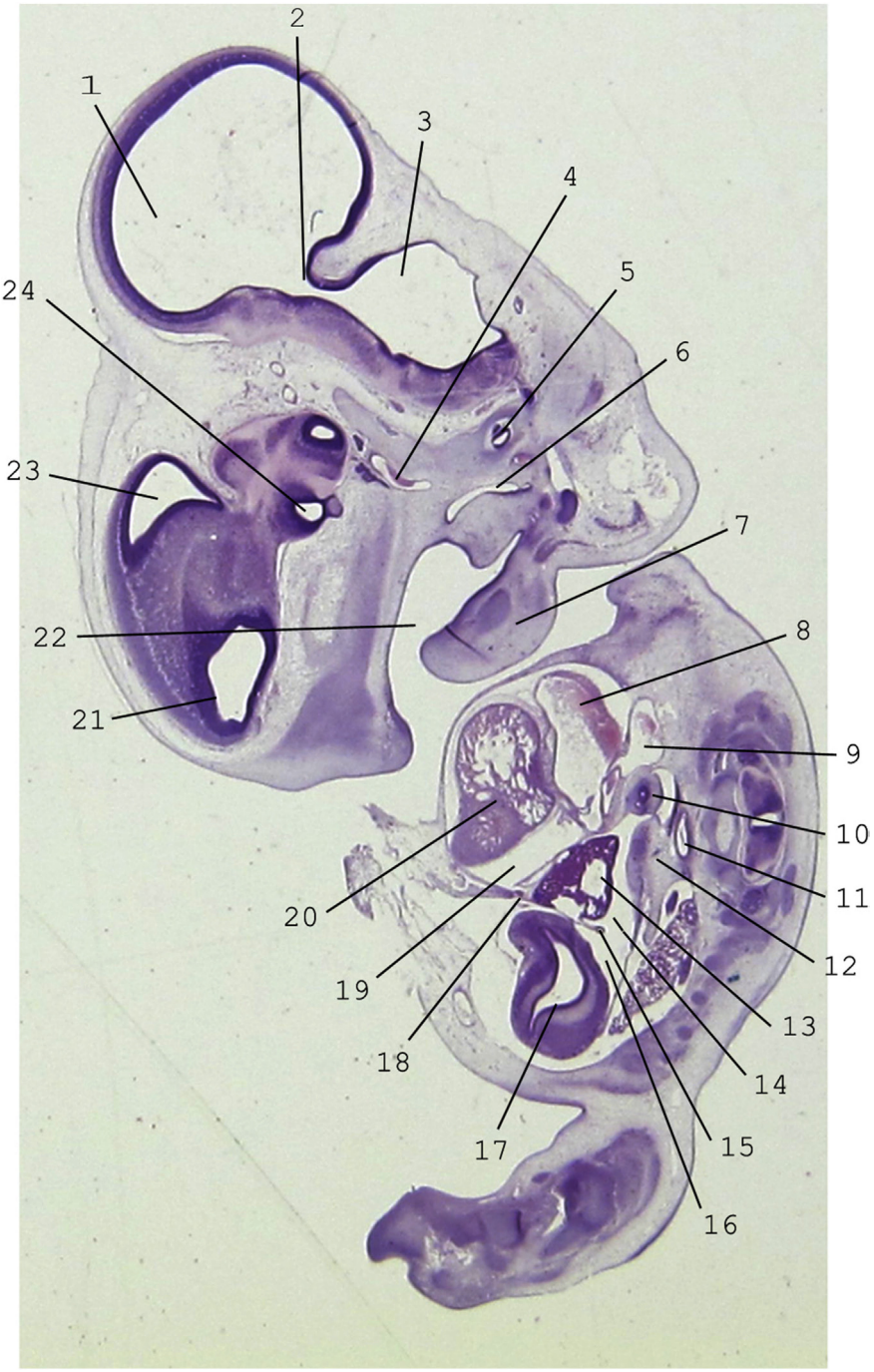

Downloaded from Vet-eBooks.com

Plate 135 Stage 28 (day 6) LS: sagittal

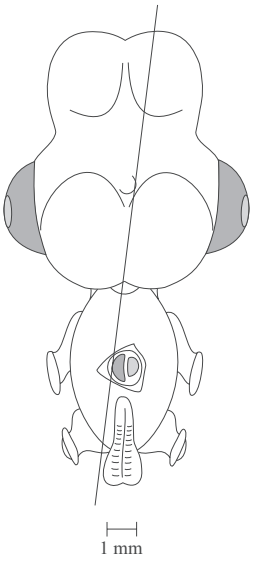

Enlargement of part of *plate 134*: × 50

1. body wall
2. ventricle
3. atrium
4. sinus venosus
5. sinu-atrial valve
6. extravasated blood
7. gut
8. wall of atrium
9. dorsal hepatic cavity
10. hepatic septum partly separating dorsal and ventral hepatic cavities, not yet completed
11. ventral hepatic cavity
12. gizzard
13. pericardial cavity

Downloaded from Vet-eBooks.com

Plate 135

Downloaded from Vet-eBooks.com

Plate 136 Stage 28 (day 6)
LS: sagittal

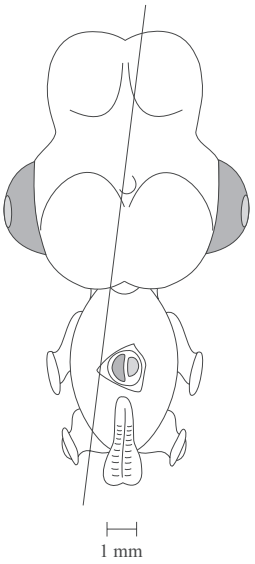

Longitudinal (sagittal) section: × 12

1. optic lobe
2. isthmus
3. myelocoele
4. right Eustachian tube
5. right carotid artery
6. oral cavity
7. lower jaw
8. atrium
9. right lung
10. spinal cord
11. notochord
12. abdominal cavity
13. ductus venosus
14. mesonephros
15. right femur
16. right leg
17. gizzard
18. liver
19. ventricle
20. nasal septum
21. right telocoele
22. optic thalamus

Downloaded from Vet-eBooks.com

Plate 136

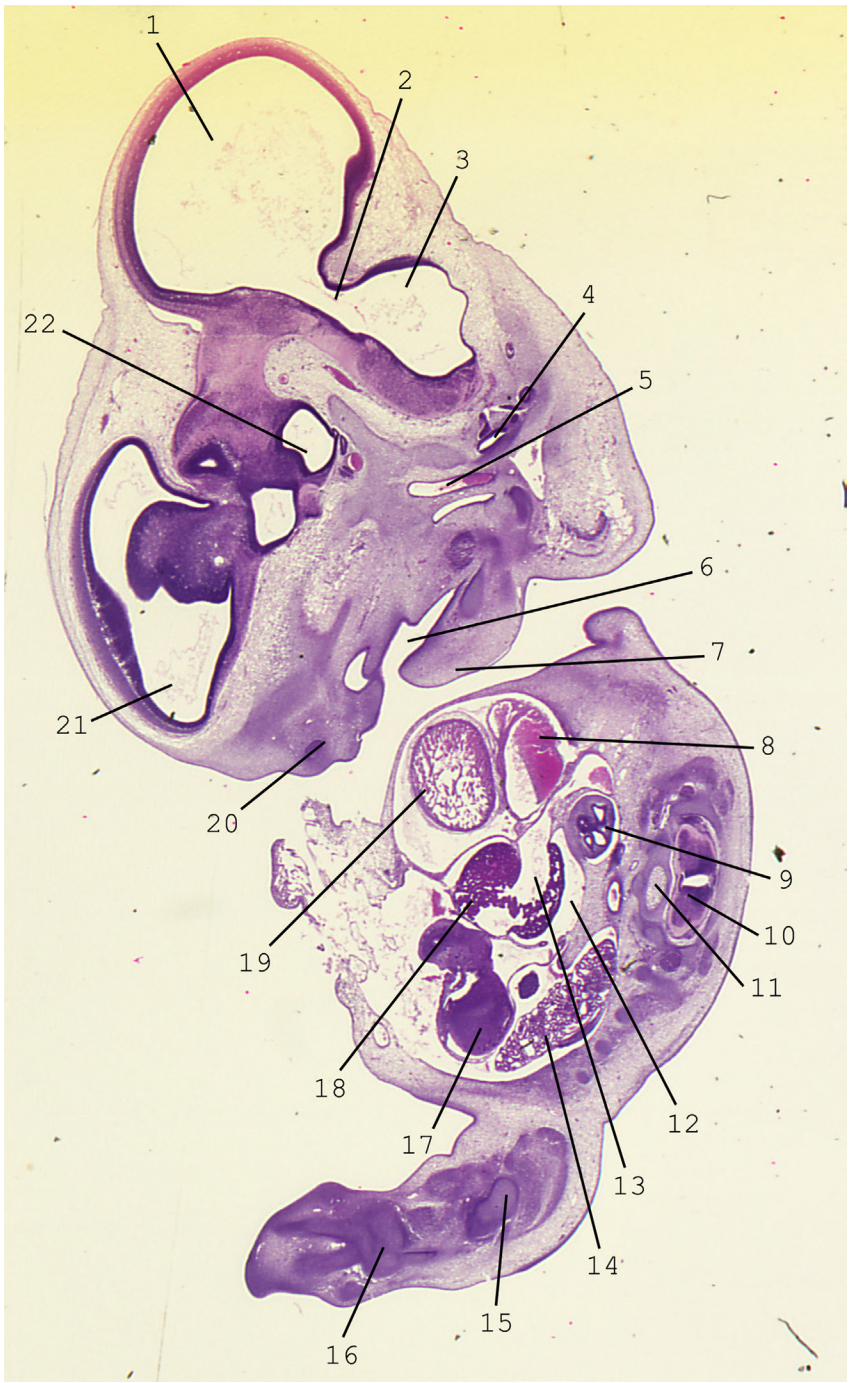

Downloaded from Vet-eBooks.com

Plate 137 Stage 28 (day 6) LS: sagittal

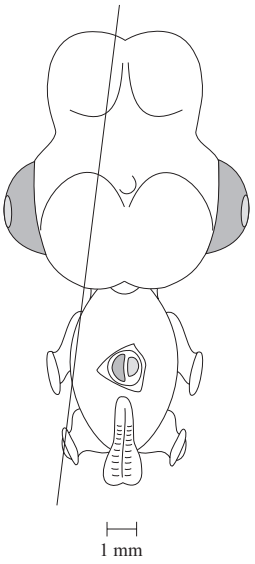

Longitudinal (sagittal) section: × 15

1. optic lobe
2. right trigeminal (cranial nerve V) ganglion
3. right otic vesicle
4. pigmented retina
5. shoulder
6. liver
7. right lung
8. dorsal hepatic cavity
9. horizontal hepatic ligament
10. intestine
11. mesonephros
12. gonad
13. dorsal mesentery
14. posterior loop of gut
15. anterior loop of gut
16. umbilicus
17. nasal sac
18. lamina terminalis
19. lateral telocoele
20. medial telocoele
21. diocoele (third ventricle)

Downloaded from Vet-eBooks.com

Plate 137

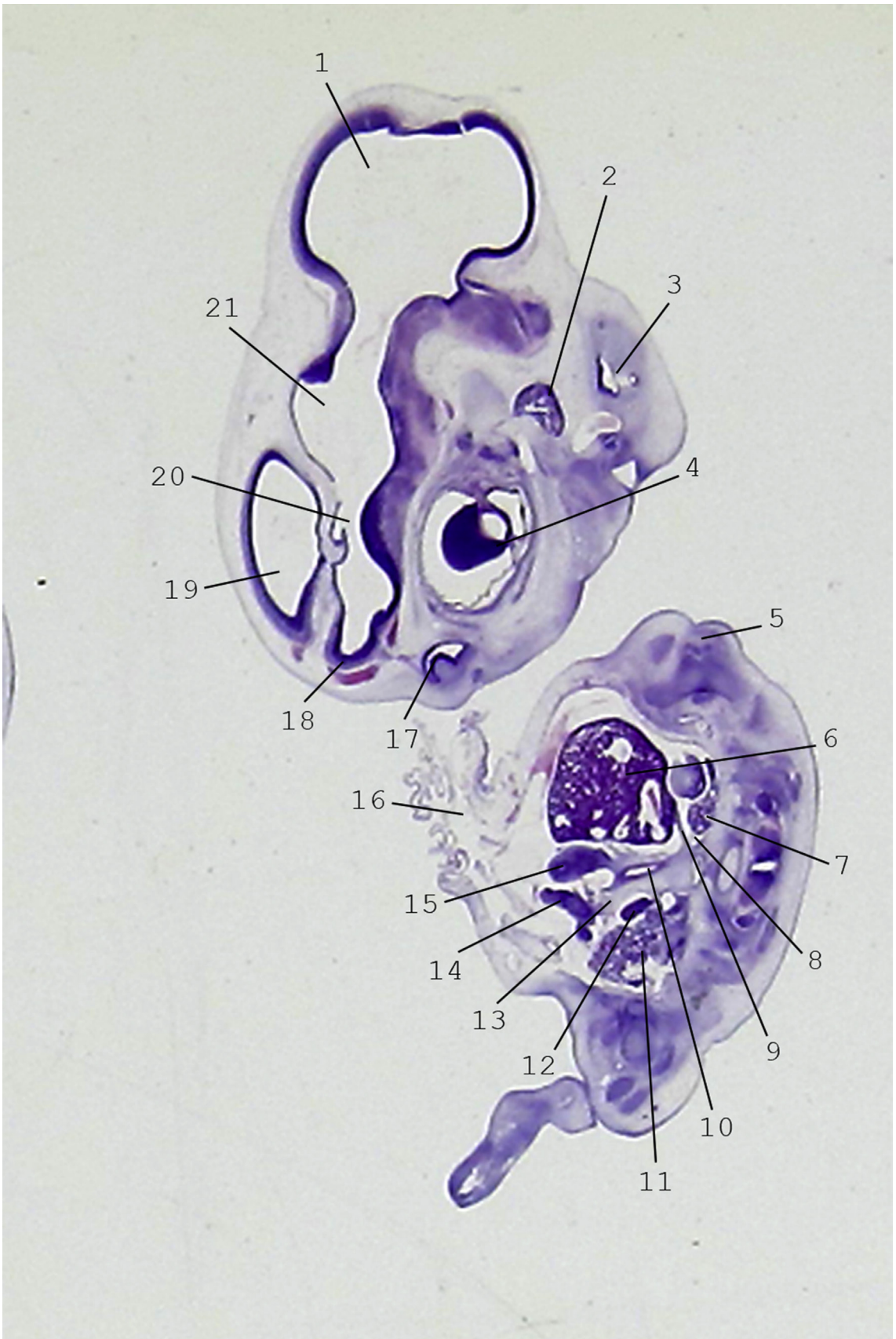

Downloaded from Vet-eBooks.com

Plate 138 Stage 28 (day 6) LS: sagittal

Enlargement of section adjacent to *plate 130*: × 70

1. atrial wall
2. right atrium
3. interatrial septum showing pores
4. left atrium
5. atrio-ventricular canal
6. left ventricle
7. inter-ventricular septum
8. right ventricle
9. ventricular wall
10. truncus arteriosus

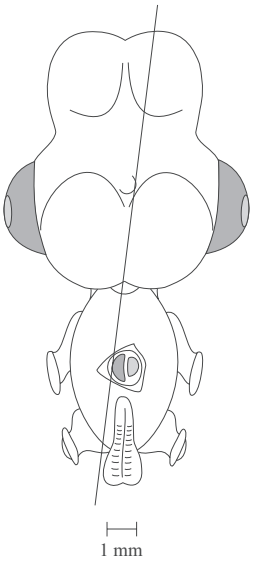

Downloaded from Vet-eBooks.com

Plate 138

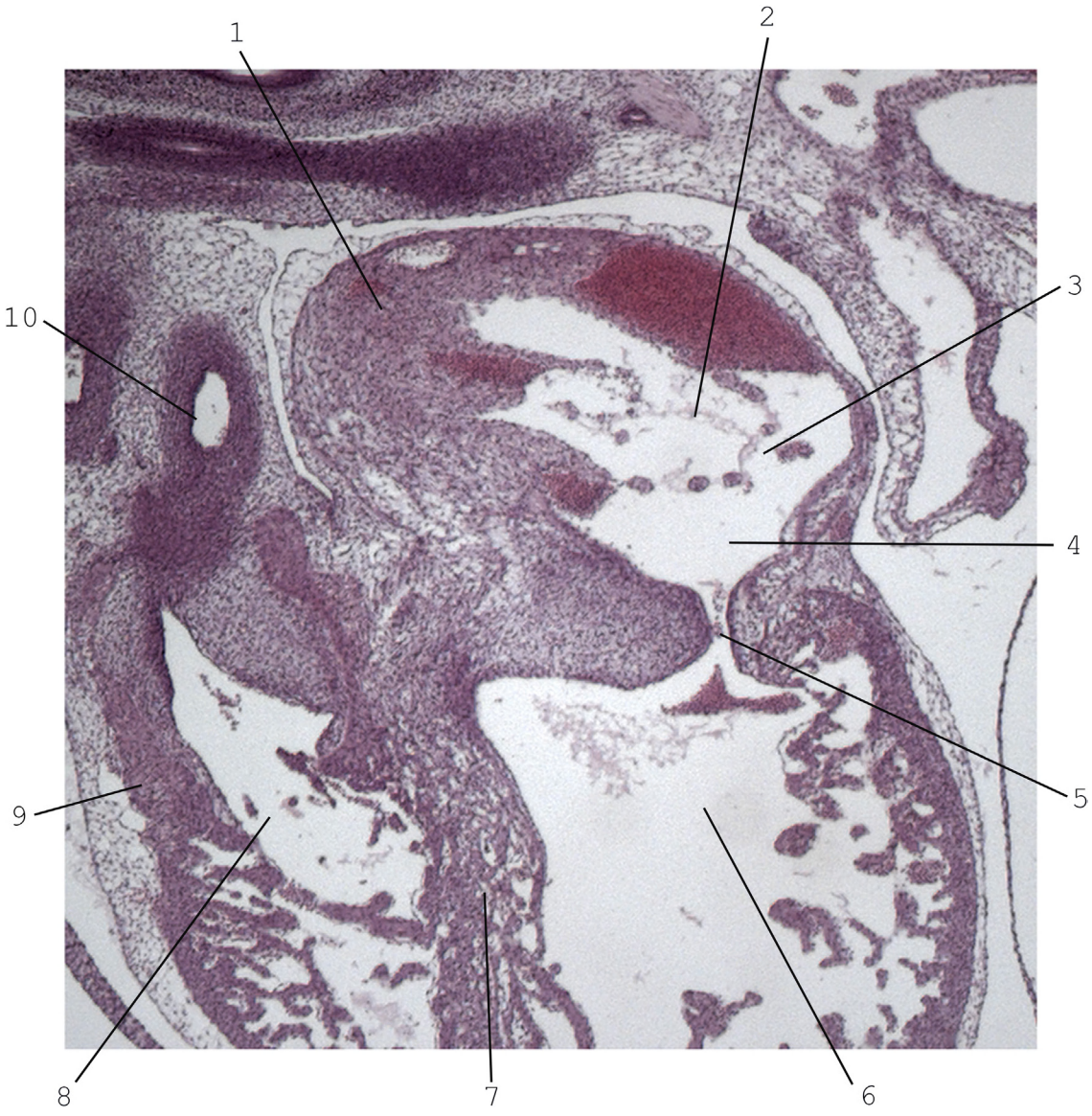

Downloaded from Vet-eBooks.com

Plate 139 Stage 28 (day 6) LS: sagittal

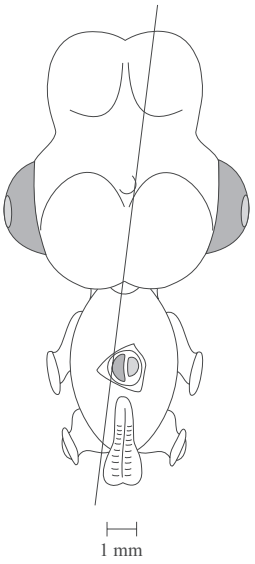

(a) Enlargement of section adjacent to *plate 130*: × 24

(b) Enlargement of section adjacent to *plate 130*: × 30

1. lower jaw
2. oral cavity
3. trigeminal (cranial nerve V) ganglion
4. ossification centre in maxilla
5. internal naris
6. hyoid cartilage
7. oesophagus
8. ventral body wall
9. trachea
10. dorsal aorta
11. spinal cord
12. dorsal root ganglion
13. transverse process of vertebra
14. pre-muscle mass
15. dorsal body wall
16. antero-median artery

Downloaded from Vet-eBooks.com

Plate 139

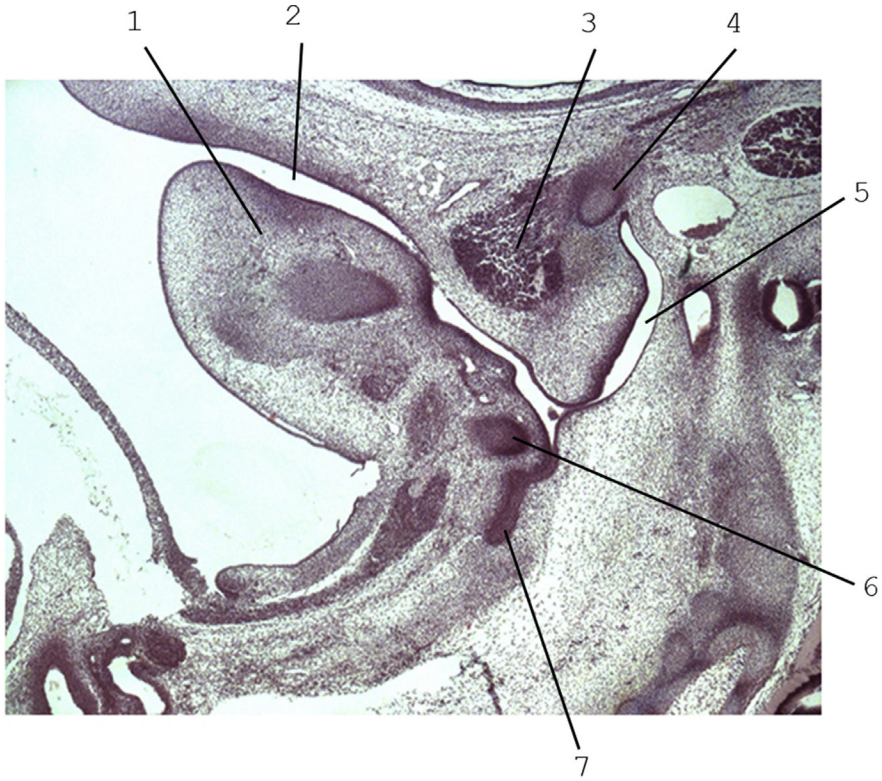

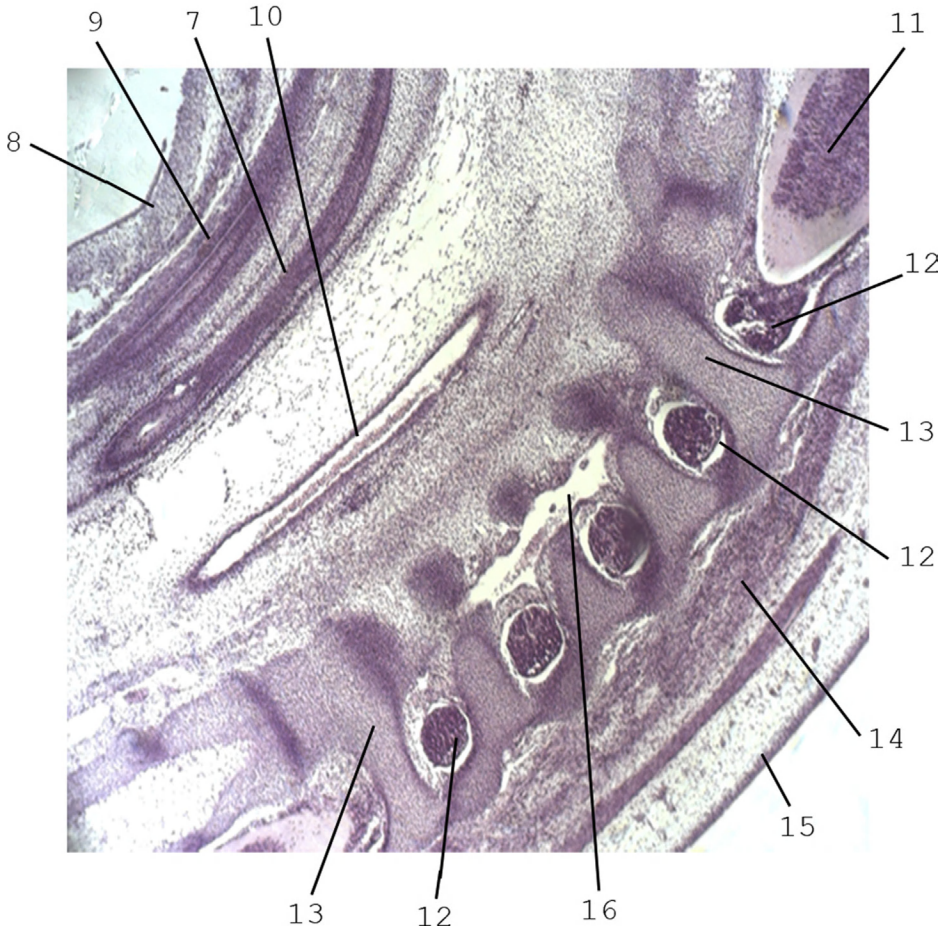

Downloaded from Vet-eBooks.com

Plate 140 Stage 28 (day 6) LS: sagittal

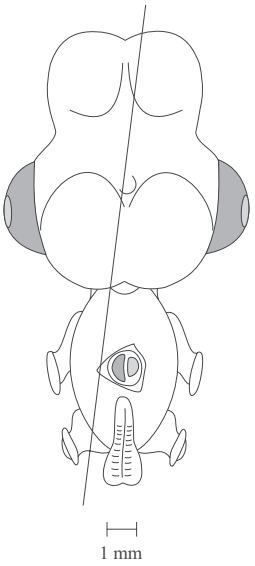

Enlargement of section adjacent to *plate 136*: × 45

1. body wall
2. ventricle
3. atrium
4. sinus venosus
5. lung
6. developing muscle
7. dorsal root ganglion
8. pulmonary coelom
9. spinal cord
10. notochord
11. dorsal hepatic cavity
12. hepatic portal vein
13. ductus venosus
14. liver
15. pericardial cavity

Downloaded from Vet-eBooks.com

Plate 140

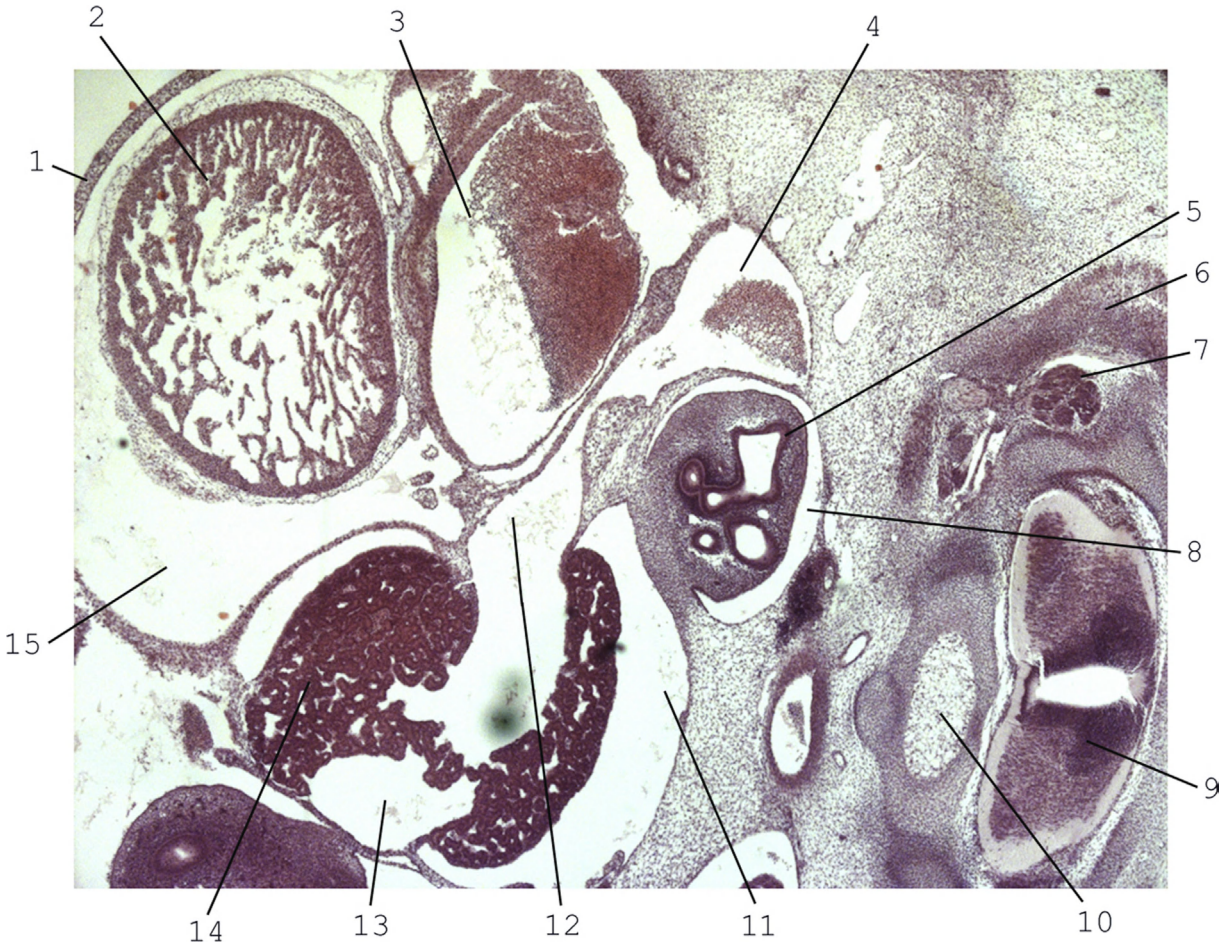

Downloaded from Vet-eBooks.com

Plate 141 Stage 28 (day 6) LS: coronal

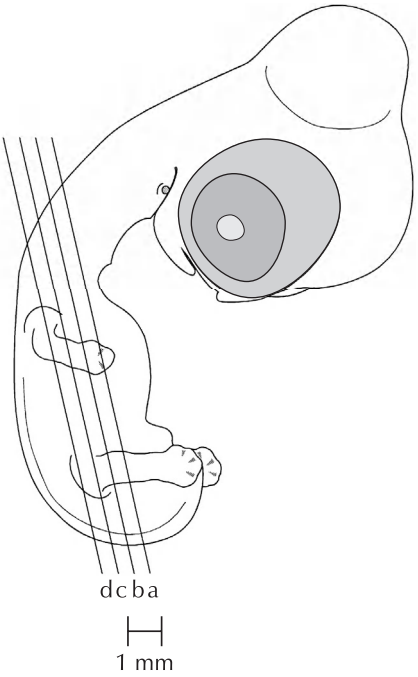

Longitudinal sections in the coronal plane: (a–d) × 15

Enlargements of portions of these sections are shown in *plates 142* and *143*

1. neural tube of trunk
2. dorsal root ganglion
3. sympathetic ganglion in myotome
4. dorsal aorta
5. gizzard
6. left hepatic vein
7. amnion
8. body wall
9. cloaca
10. right leg bud
11. colon
12. small intestine
13. dorsal mesentery
14. liver
15. caudal (posterior) vena cava
16. right lung bud
17. right anterior cardinal vein
18. notochord
19. rib (not yet cartilaginous)
20. head of humerus
21. dorsal premuscle mass of wing bud
22. ventral premuscle mass of wing bud
23. allantoic vein
24. femur
25. dorsal premuscle mass of thigh
26. ventral premuscle mass of thigh
27. neural tube of tail
28. apical ectodermal ridge of right leg bud
29. amniotic cavity
30. coelomic cavity
31. right metanephros
32. left metanephros
33. left mesonephros
34. nephric (Wolffian) duct
35. cloacal membrane
36. rectum
37. right mesonephros
38. right subcardinal vein
39. left gonad
40. cloaca
41. right gonad

Downloaded from Vet-eBooks.com

Plate 141

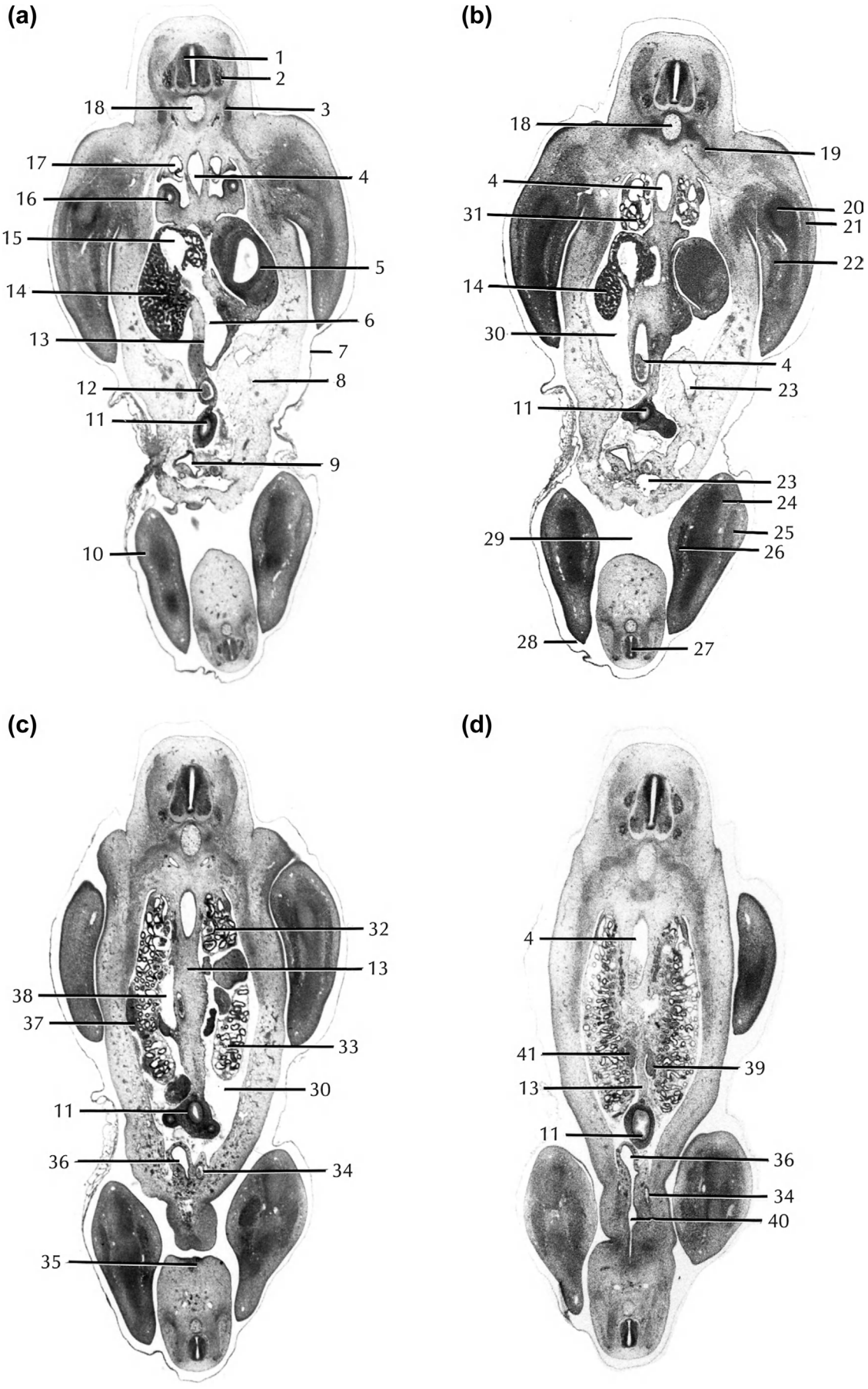

Downloaded from Vet-eBooks.com

Plate 142 Stage 28 (day 6) LS: coronal

Enlargements from *plate 141*: (a–d) × 48

(a) Enlargement of section adjacent to *plate 141c.*

(b) Enlargement of part of *plate 141a.*

(c) Enlargement of part of *plate 141b.*

(d) Enlargement of section adjacent to *plate 141d.*

Downloaded from Vet-eBooks.com

Plate 142

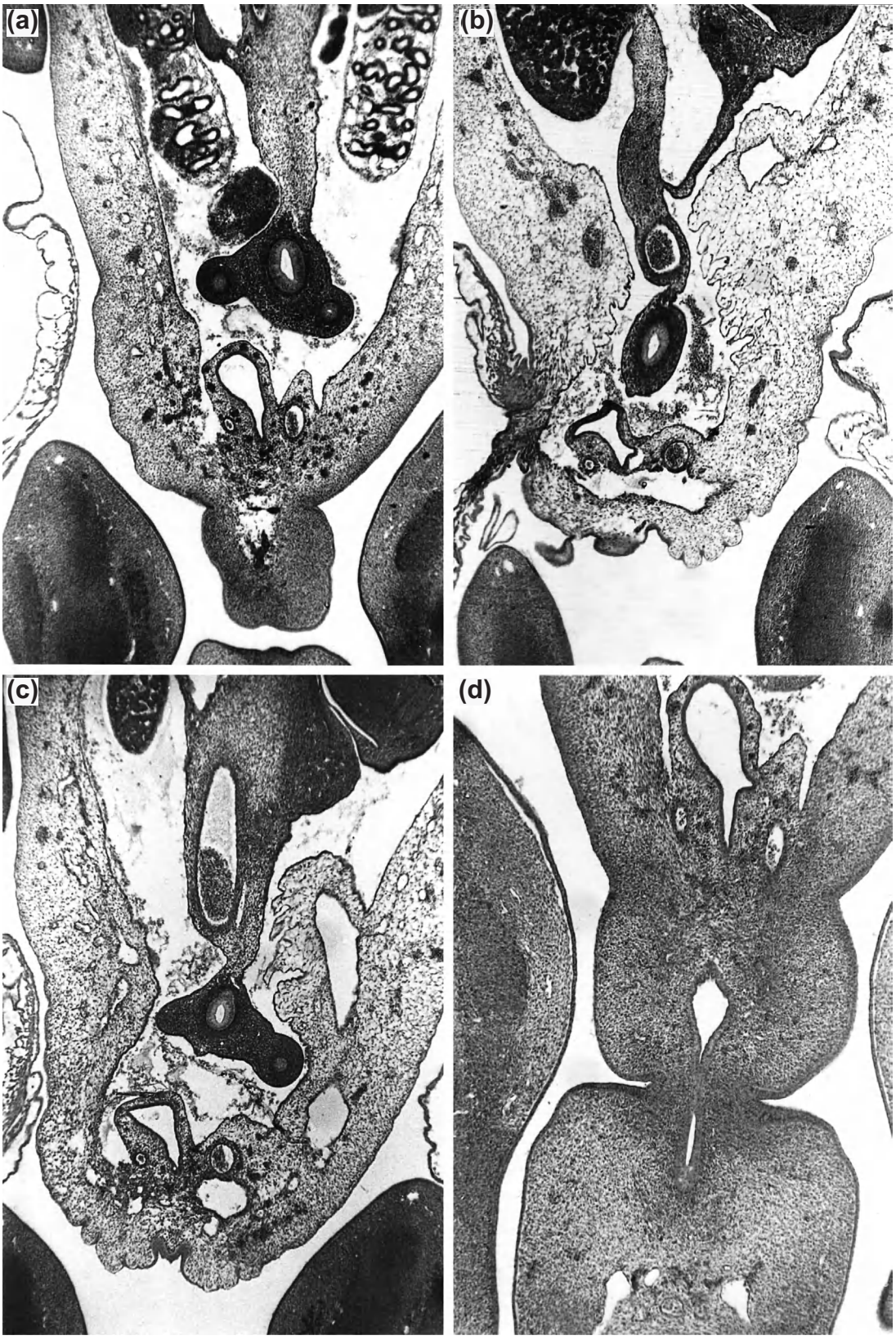

Downloaded from Vet-eBooks.com

Plate 143 Stage 28 (day 6)
LS: coronal

Enlargements from *plate 141*: (a–d) × 48

(a) Enlargement of section adjacent to *plate 141b.*

(b) Enlargement of part of *plate 141c.*

(c) Enlargement of part of *plate 141a.*

(d) Enlargement of section adjacent to *plate 141d.*

Downloaded from Vet-eBooks.com

Plate 143

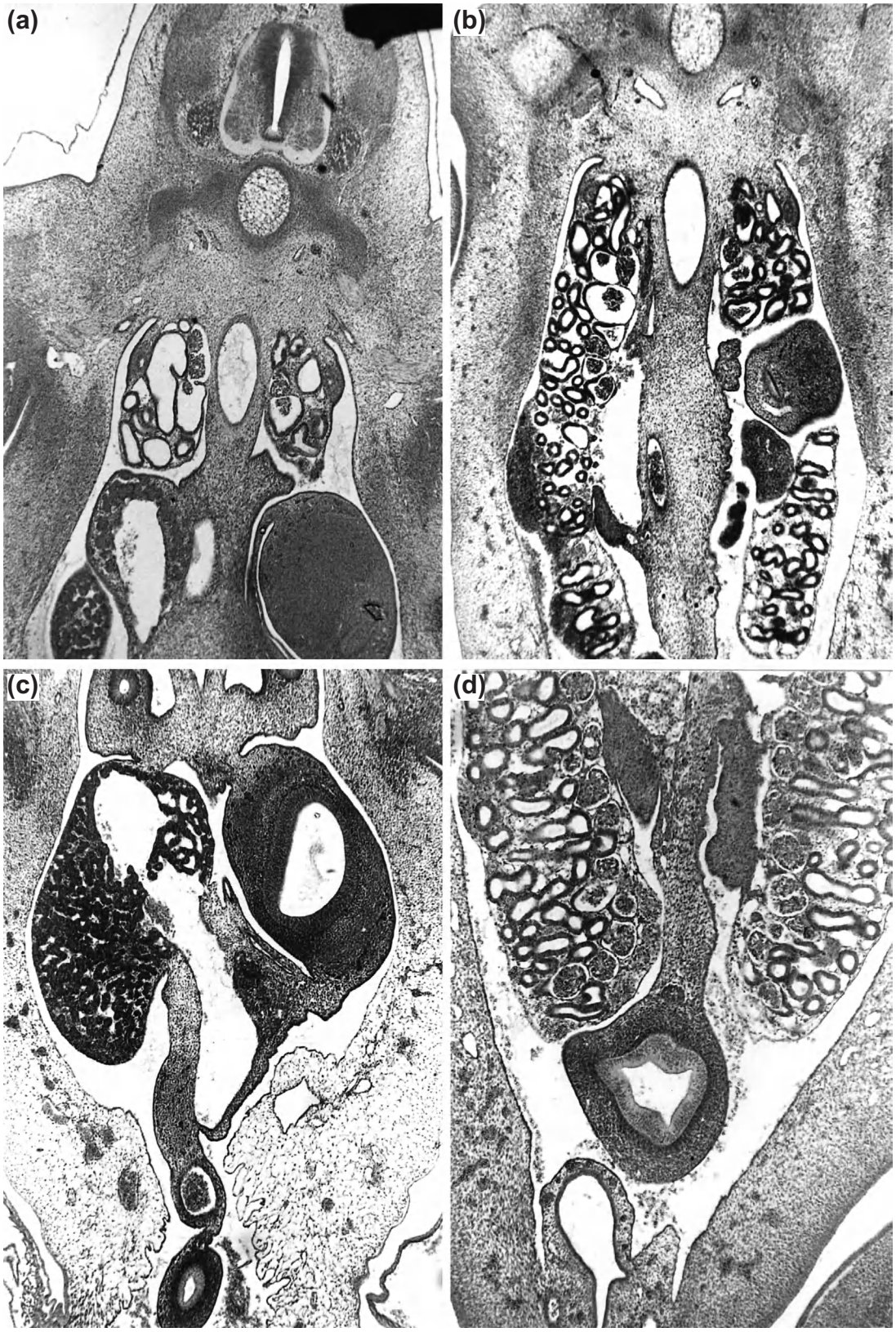

Downloaded from Vet-eBooks.com

Plate 144 Stage 28 (day 6) TS

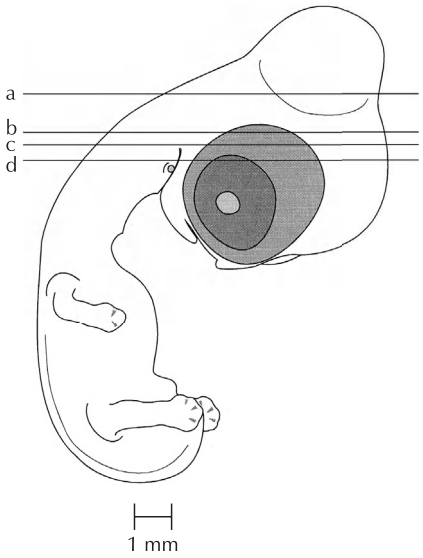

Transverse sections (TS): (a–d) × 14

1. right otic vesicle
2. myelocoele (fourth ventricle)
3. junction between thick-walled metencephalon and thin-walled roof of myelencephalon
4. isthmus
5. lumen of left optic lobe
6. mesocoele (aqueduct of Sylvius)
7. right eye
8. metacoele
9. accessory (cranial XI) nerve
10. thick-walled floor of myelencephalon
11. left otic vesicle
12. floor of diencephalon
13. floor of left optic lobe
14. pineal organ
15. diocoele
16. pigmented retina
17. right trigeminal (cranial nerve V) ganglion
18. spinal cord
19. notochord
20. amnion
21. semicircular canal of left ear
22. occipital artery
23. left trigeminal (cranial nerve V) ganglion
24. cartilage of basal plate of chondrocranium
25. posterior part of left orbital cartilage
26. infundibulum
27. thick lateral wall of diencephalon (optic thalamus)
28. optic recess in diencephalon
29. right optic (cranial II) nerve
30. right jugular vein
31. dorsal root ganglion
32. left jugular vein
33. anastomotic vein (interjugular anastomosis)
34. Rathke's pouch
35. lateral ventricle (telocoele)
36. vitreous chamber
37. lens of right eye

Downloaded from Vet-eBooks.com

Plate 144

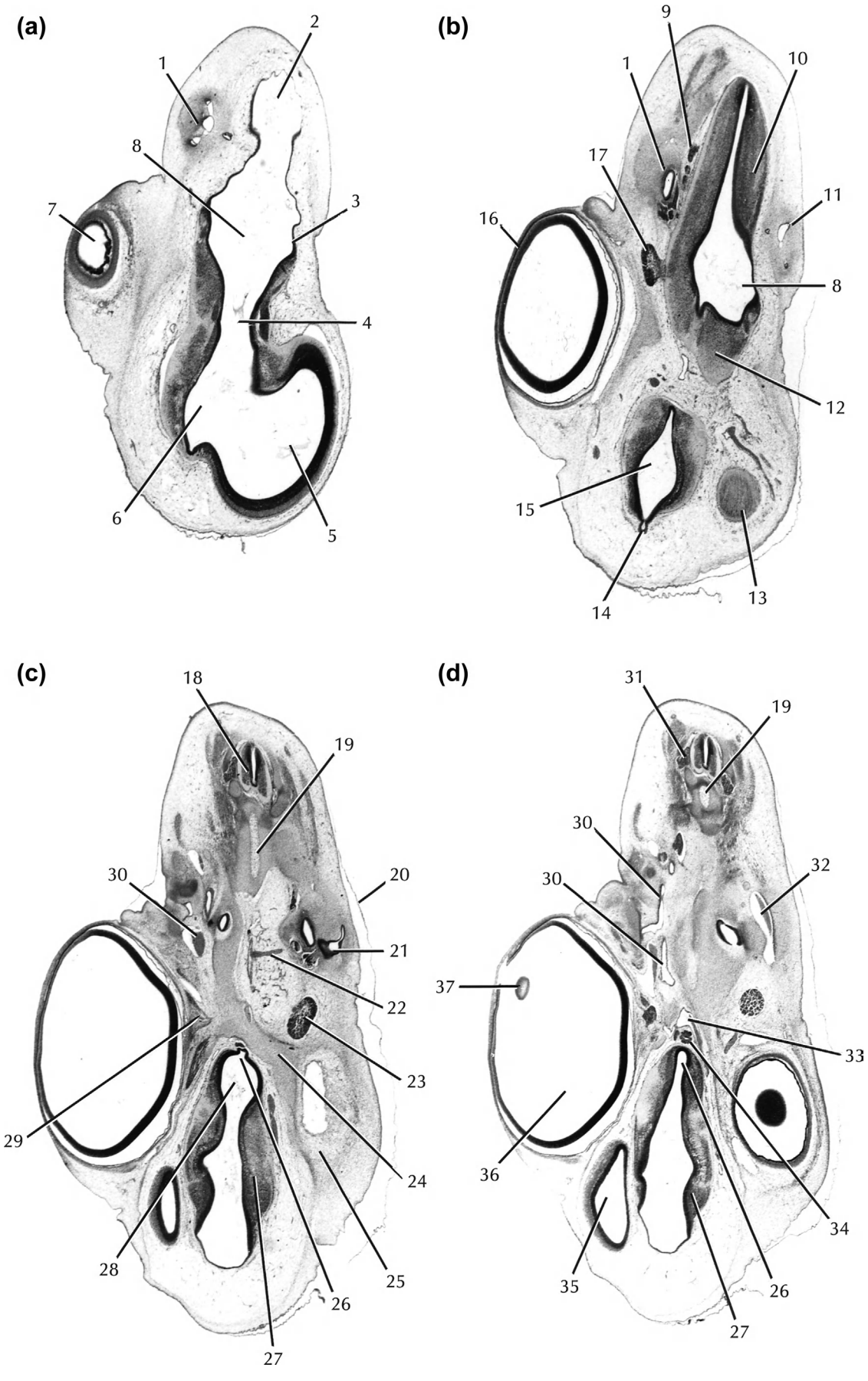

Downloaded from Vet-eBooks.com

Plate 145 Stage 28 (day 6) TS

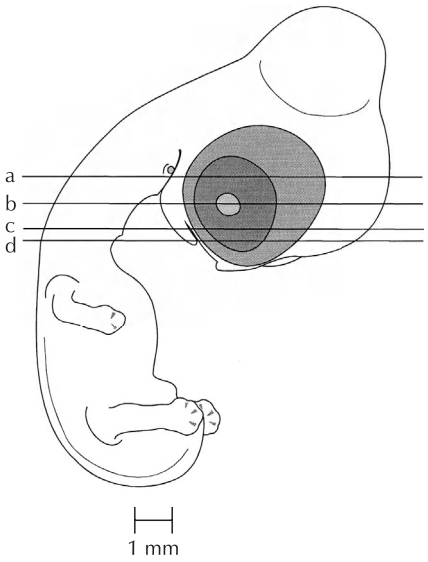

Transverse sections (TS): (a–d) × 14

1. second (hyoid) pharyngeal arch cartilage
2. left carotid artery
3. second pharyngeal pouch
4. first pharyngeal pouch
5. pigmented layer of left retina
6. diocoele
7. left lateral ventricle
8. right lateral ventricle
9. right optic (cranial II) nerve
10. lens
11. pharynx
12. right carotid artery
13. left jugular vein
14. left second (hyoid) pharyngeal arch cartilage
15. left first (mandibular) pharyngeal arch cartilage
16. oral cavity
17. left trabecula cartilage
18. left optic (cranial II) nerve
19. right trabecula cartilage
20. right first (mandibular) pharyngeal arch cartilage
21. myotome
22. right jugular vein
23. oesophagus
24. tongue
25. interorbital septum
26. corpus striatum (wall of cerebral vesicle)
27. choroid plexus
28. foramen of Monro
29. first (maxillary) pharyngeal arch
30. first (mandibular) pharyngeal arch
31. trachea
32. pericardial cavity
33. internal naris

Downloaded from Vet-eBooks.com

Plate 145

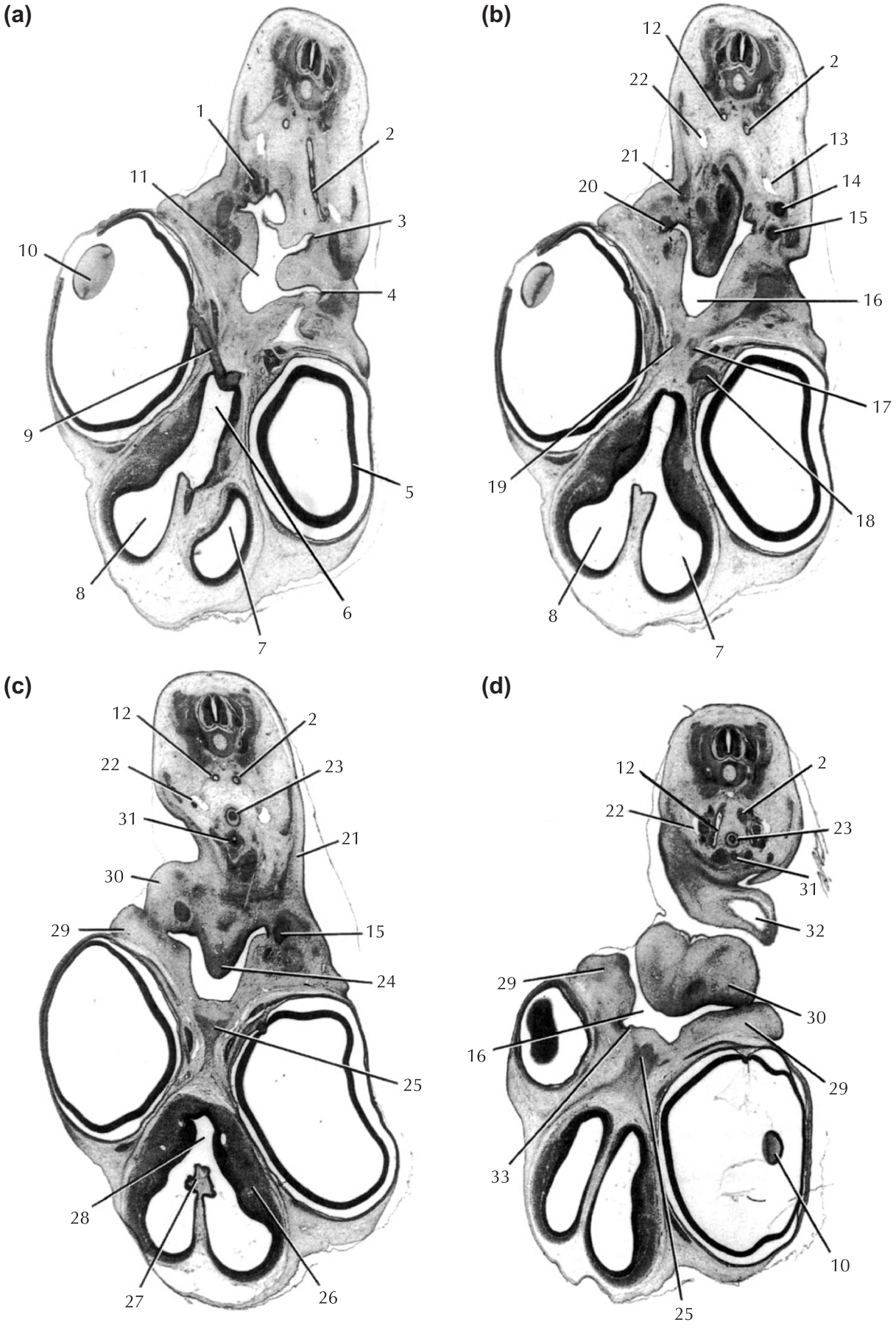

Downloaded from Vet-eBooks.com

Plate 146 Stage 28 (day 6) TS

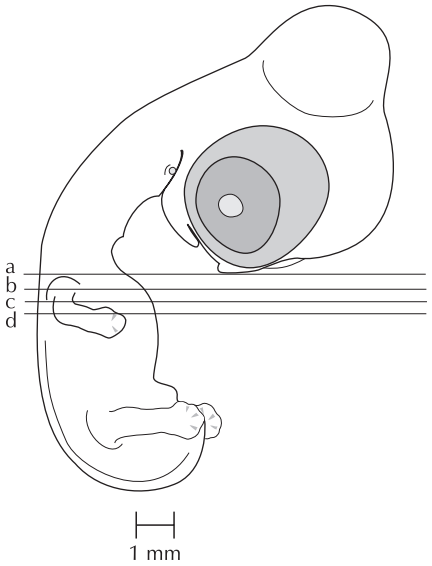

Transverse sections (TS): (a–d) × 18

1. right pleural cavity
2. notochord
3. myotome
4. left anterior cardinal vein
5. left atrium
6. left ventricle
7. sinus venosus
8. right atrium
9. condyle of humerus
10. dorsal root ganglion
11. spinal cord
12. dorsal aorta
13. oesophagus
14. pericardial cavity
15. ventral body wall
16. liver
17. right omphalo-mesenteric vein
18. ventral muscle mass of right wing
19. shaft of humerus
20. dorsal muscle mass of wing
21. right lung bud
22. neural arch
23. body of vertebra
24. left lung bud
25. ventral mesentery
26. pulmonary fold
27. anterior border of right mesonephros
28. dorsal mesentery
29. scapula
30. ischium
31. hepatic ligament of left oblique septum
32. dorsal hepatic cavity
33. crop
34. ductus venosus
35. gizzard
36. right ventral hepatic cavity
37. hepatic ligament of right oblique septum

Downloaded from Vet-eBooks.com

Plate 146

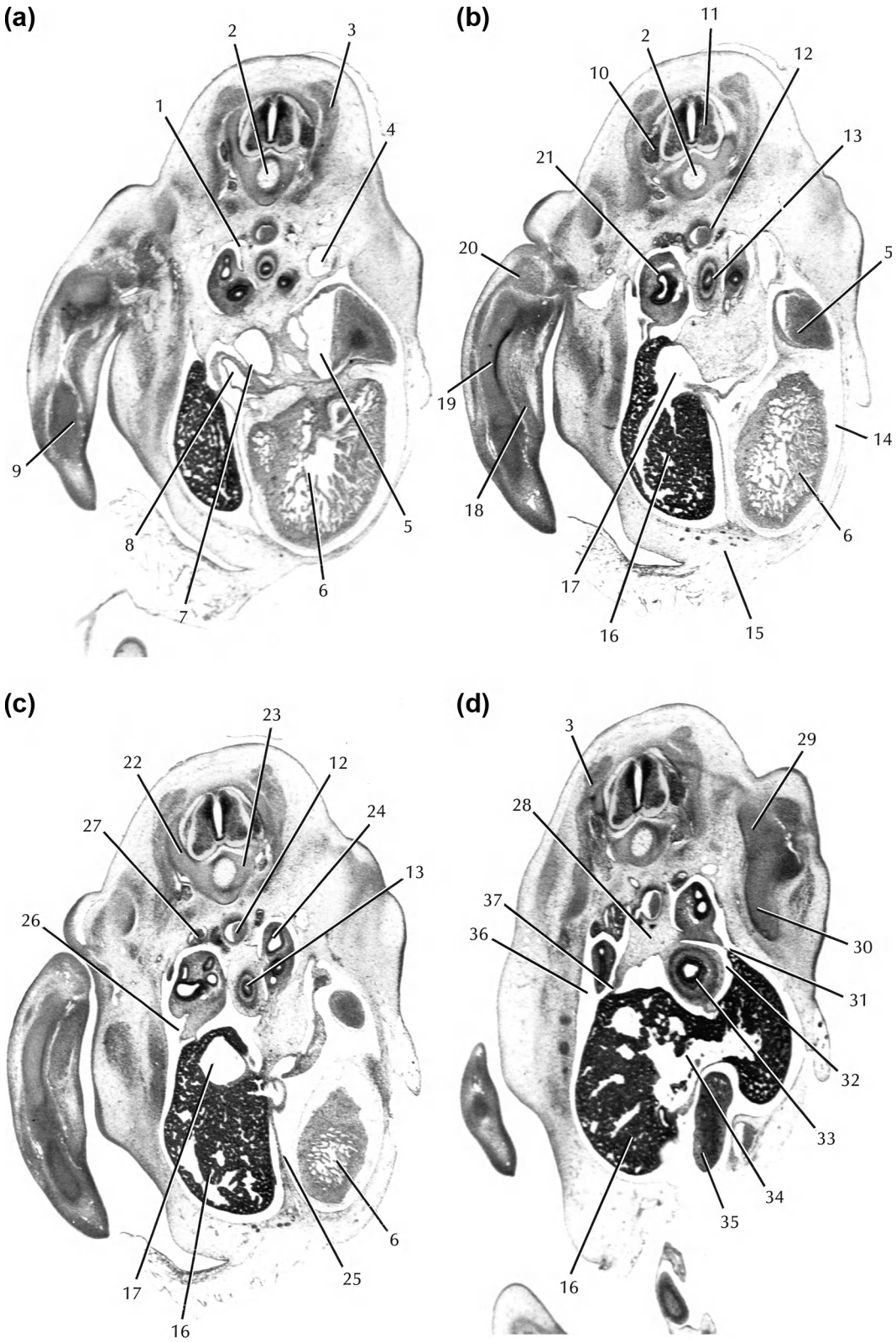

Downloaded from Vet-eBooks.com

Plate 147 Stage 28 (day 6) TS

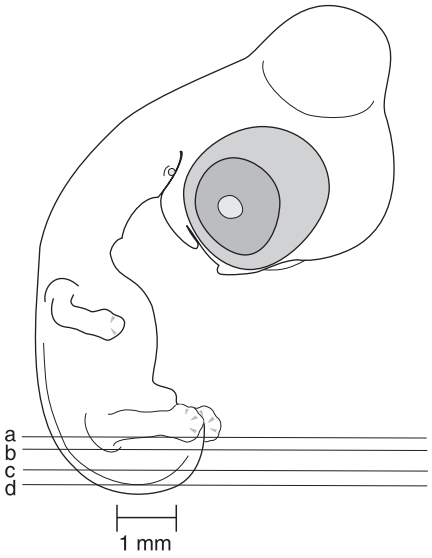

Transverse sections (TS): (a–d) × 18

1. right mesonephros
2. right ventral hepatic cavity
3. dorsal aorta
4. notochord
5. left lung bud
6. junction of crop and gizzard
7. gizzard
8. pancreas
9. hepatic portal vein
10. herniated loop of intestine
11. horizontal hepatic ligament
12. right gonad
13. left mesonephros
14. left femur
15. coeliac artery
16. transverse process of vertebra
17. spinal cord
18. dorsal root ganglion
19. myogenic condensation
20. dorsal muscle mass of left leg
21. ventral muscle mass of left leg
22. post-hepatic septum
23. dorsal mesentery
24. right femur
25. rib
26. cartilaginous precursor of ilium
27. renal artery
28. small intestine
29. ductus venosus

Downloaded from Vet-eBooks.com

Plate 147

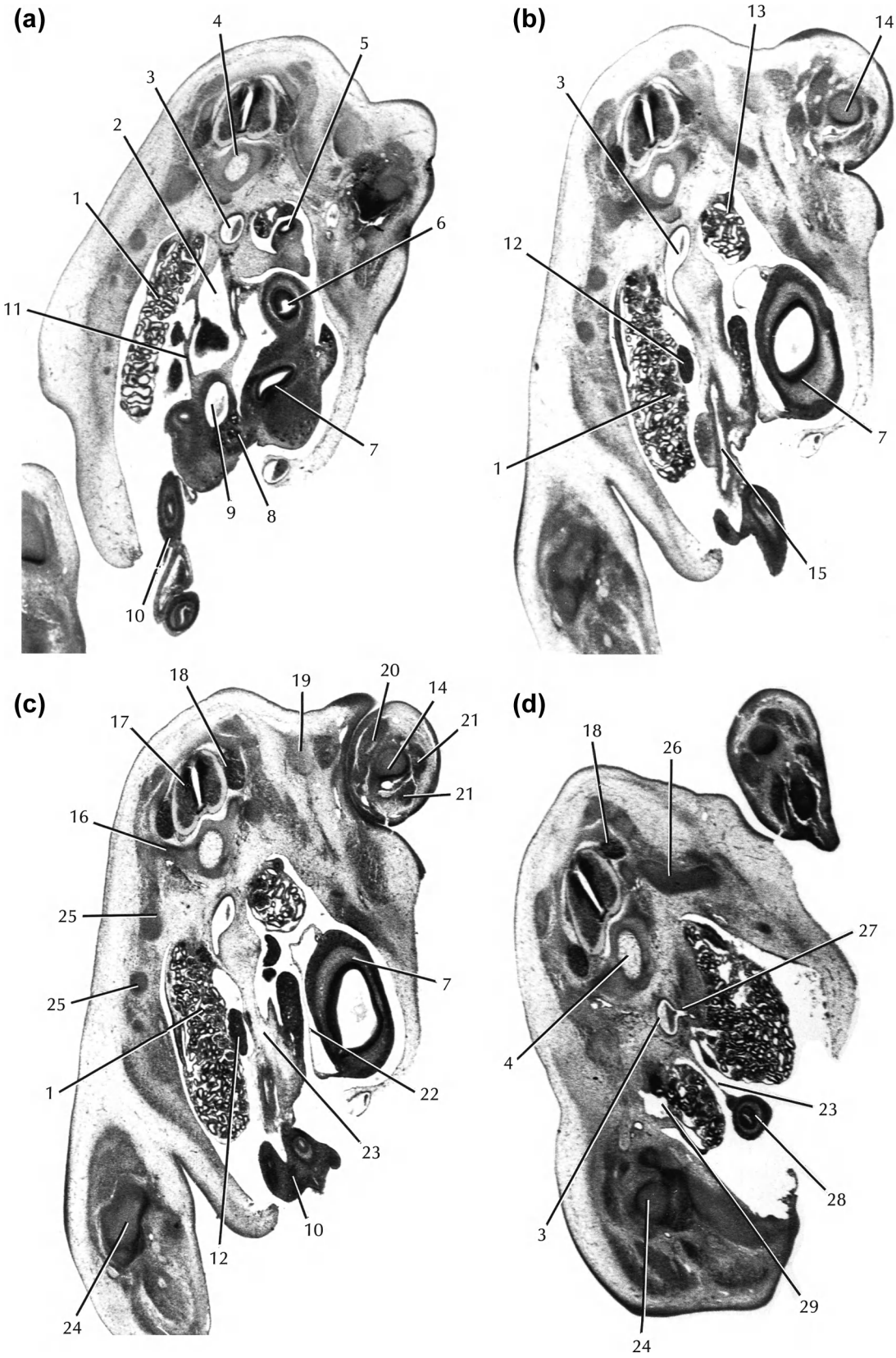

Downloaded from Vet-eBooks.com

Plate 148 Stage 31 (day 7) LS: sagittal

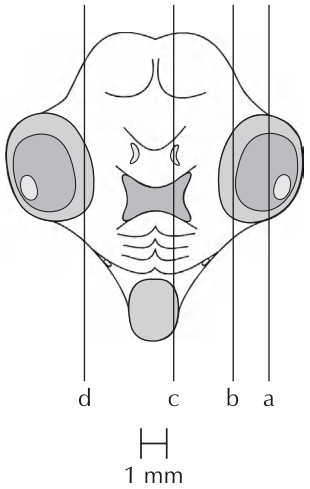

Sagittal sections through the head: (a–d) × 10

Diagram shows view of embryo from ventral side.

1. retinal pigment of left eye
2. left corpus striatum in wall of cerebral hemisphere
3. choroid plexus
4. pallium
5. foramen of Munro
6. pineal organ
7. skin
8. cerebral hemisphere
9. telocoele (lateral ventricle)
10. head mesenchyme
11. diocoele (third ventricle)
12. sulcus parencephalicus transversus
13. metathalamus in posterior commissure
14. optic lobe
15. mesocoele
16. isthmus
17. metencephalon
18. rhombocoele (fourth ventricle)
19. thin roof of myelencephalon
20. thick floor of myelencephalon
21. infundibulum
22. Meckel's cartilage
23. internal naris
24. first (maxillary) pharyngeal arch
25. external naris
26. nostril
27. interorbital septum
28. thick floor of metencephalon
29. roof of metencephalon
30. basal plate of chondrocranium
31. spinal cord
32. cervical vertebra
33. pharynx
34. paraglossal cartilage
35. tongue
36. retinal pigment of right eye
37. semicircular canal
38. basihyal cartilage (copula I)
39. lower jaw
40. oral cavity
41. palatine process

Downloaded from Vet-eBooks.com

Plate 148

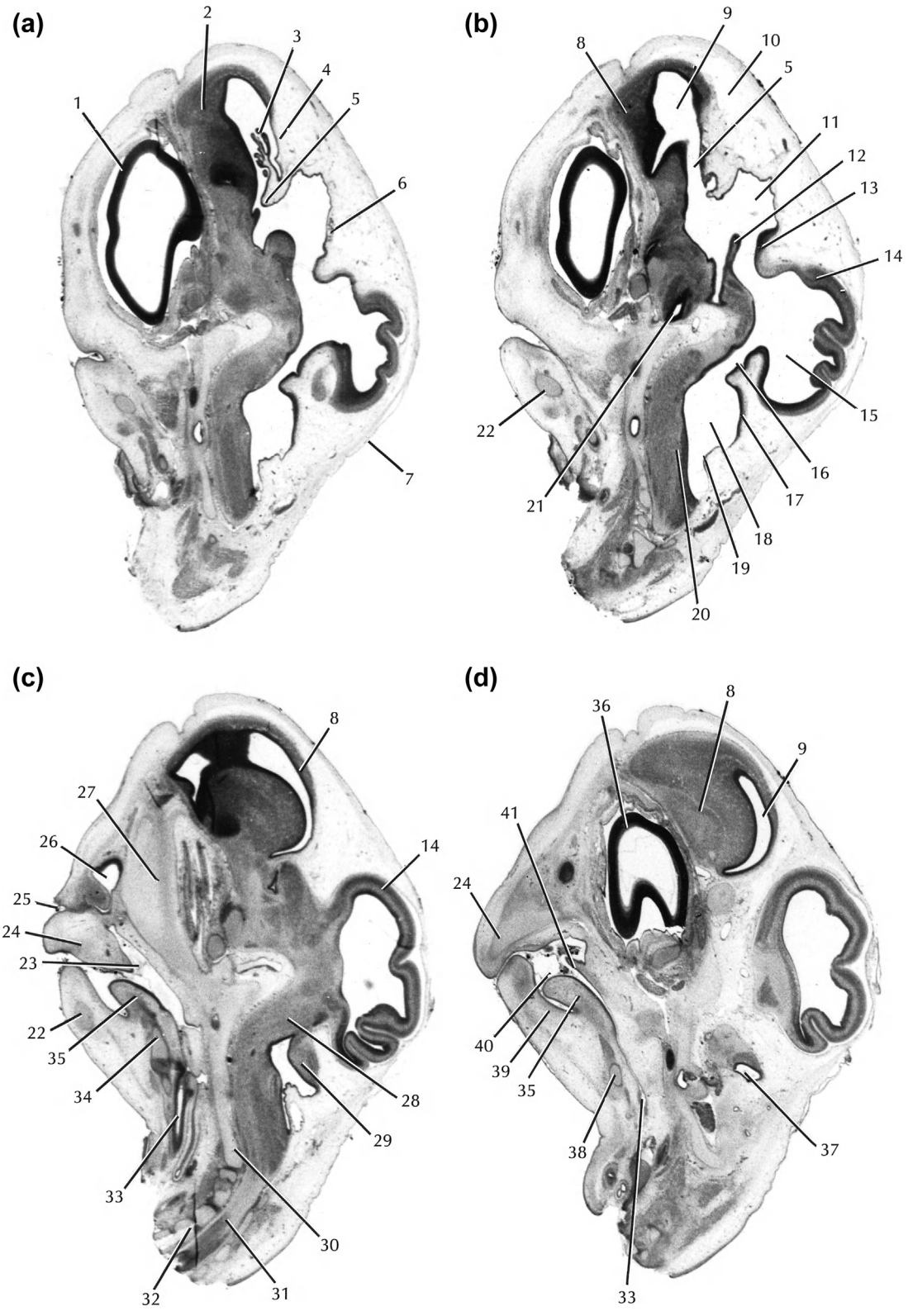

Downloaded from Vet-eBooks.com

Plate 149 Stage 31 (day 7) LS: sagittal

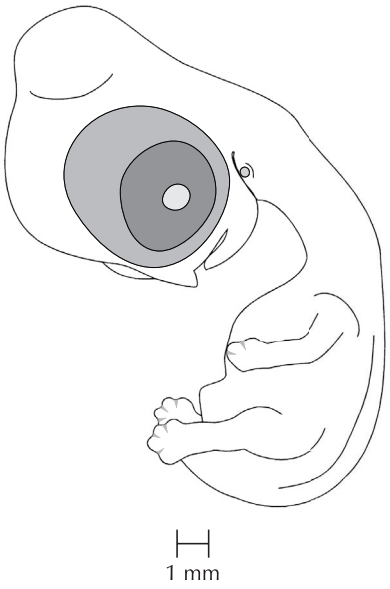

Sagittal sections through the trunk: (a–d) × 20

Sections taken through plane of page.

1. body of vertebra
2. lung bud
3. humerus
4. notochord
5. nephric duct
6. right ovary
7. mesonephros
8. wing bud
9. air sac
10. dorsal aorta
11. dorsal mesentery
12. nephric duct
13. leg
14. subcardinal vein
15. coeliac artery
16. liver
17. transverse process of vertebra
18. ischium
19. allantois
20. coelom
21. left ovary
22. colon
23. posterior abdominal coelom
24. spleen
25. spinal cord grey matter
26. spinal cord white matter
27. dorsal root ganglion
28. ilium
29. head of femur
30. flexor cruris muscle
31. puboischiofemoralis muscle
32. femorotibialis muscle
33. shaft of femur
34. iliotibialis cranialis muscle
35. spinal nerve
36. rib
37. abdominal wall

Downloaded from Vet-eBooks.com

Plate 149

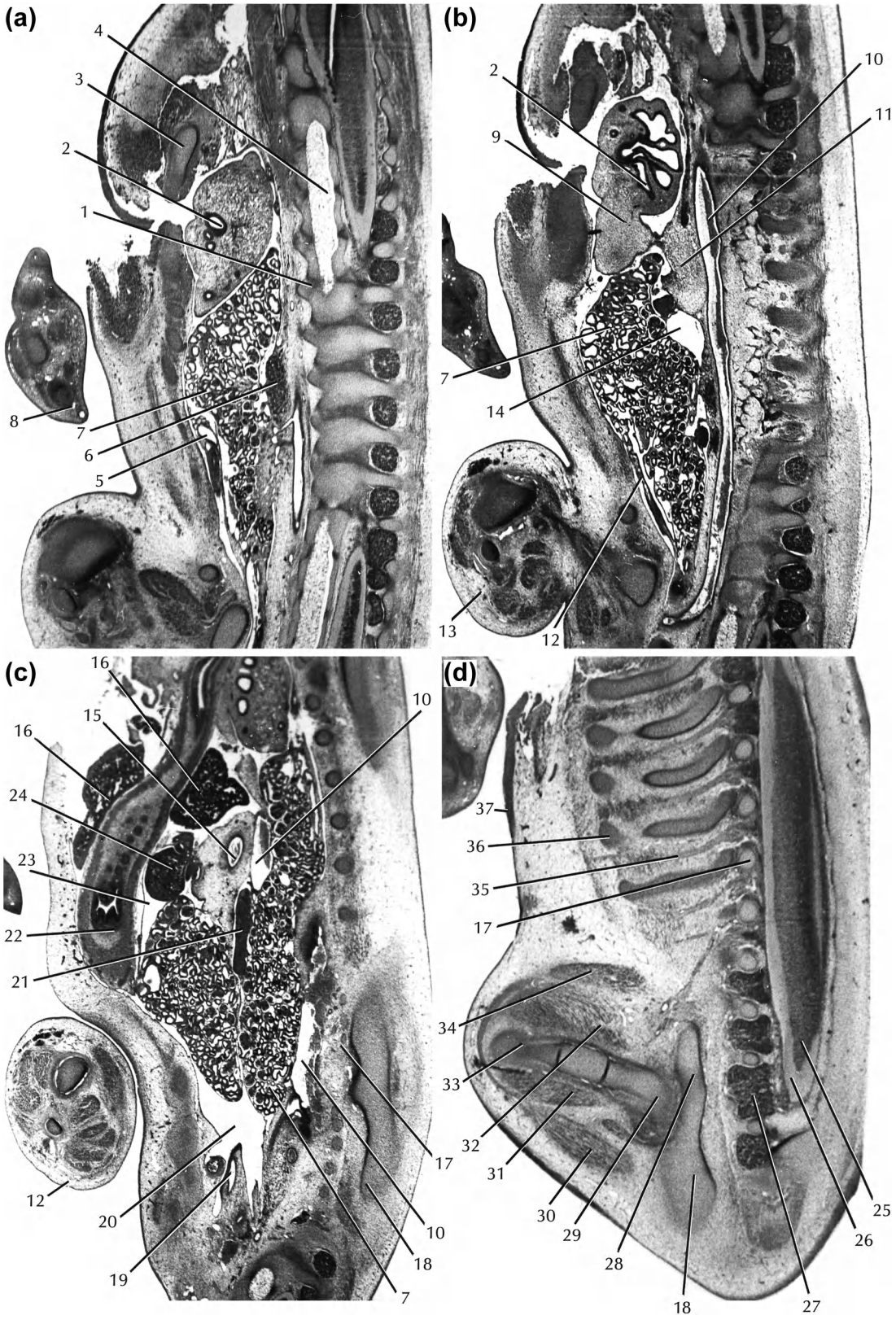

Downloaded from Vet-eBooks.com

Plate 150 Stage 31 (day 7) TS

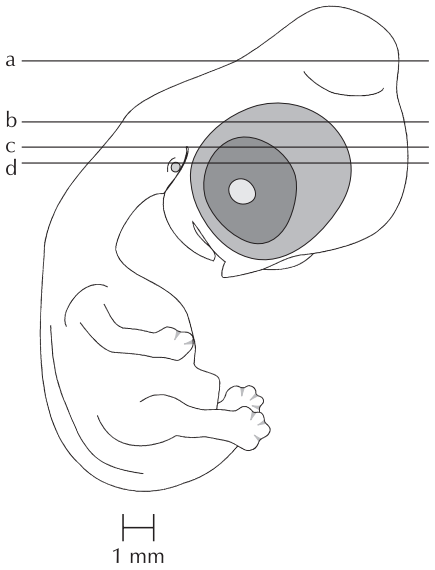

Transverse sections (TS): (a–d) × 12

1. thin roof of myelencephalon
2. metencephalon
3. left optic lobe
4. right optic lobe
5. trigemino-cerebellar fibre tract
6. head mesenchyme
7. myotome
8. thick floor of mesencephalon
9. left accessory (cranial XI) nerve
10. left otic vesicle
11. left ethmoidal artery
12. diencephalon
13. diocoele
14. pigmented retina of right eye
15. vitreous humour of right eye
16. sclera of right eye
17. right trigeminal (cranial nerve V) ganglion
18. right otic vesicle
19. right accessory (cranial XI) nerve
20. spinal cord
21. basal plate of chondrocranium
22. pharyngeal diverticulum
23. left carotid artery
24. left trigeminal (cranial nerve V) ganglion
25. Rathke's pouch
26. infundibulum
27. lateral rectus eye muscle
28. right jugular vein
29. right Meckel's cartilage
30. right carotid artery
31. notochord
32. second pharyngeal pouch
33. left Meckel's cartilage
34. first pharyngeal pouch
35. vitreous humour of left eye
36. choroid plexus
37. right optic (cranial II) nerve
38. lumen of pharynx

Downloaded from Vet-eBooks.com

Plate 150

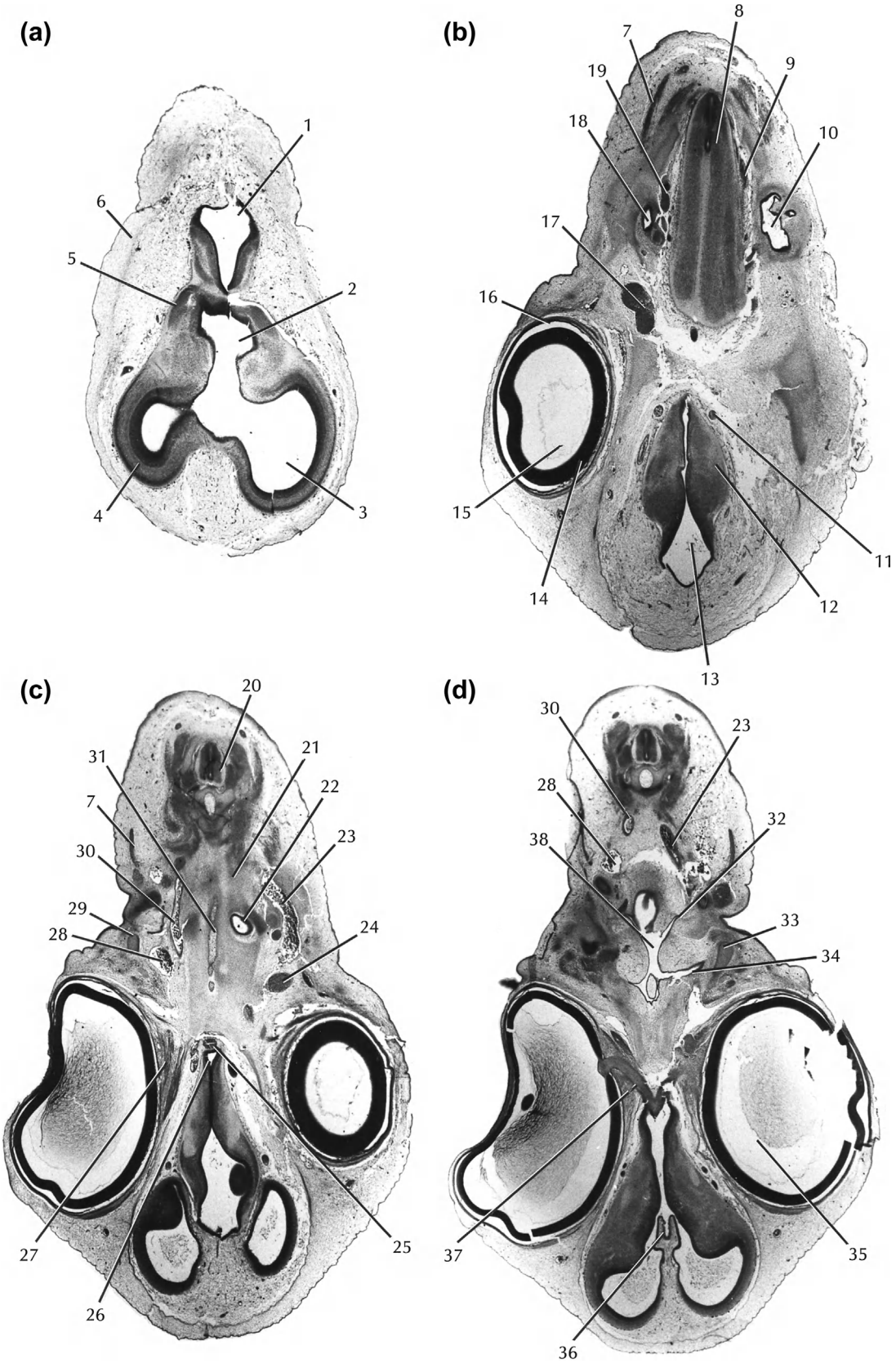

Downloaded from Vet-eBooks.com

Plate 151 Stage 31 (day 7) TS

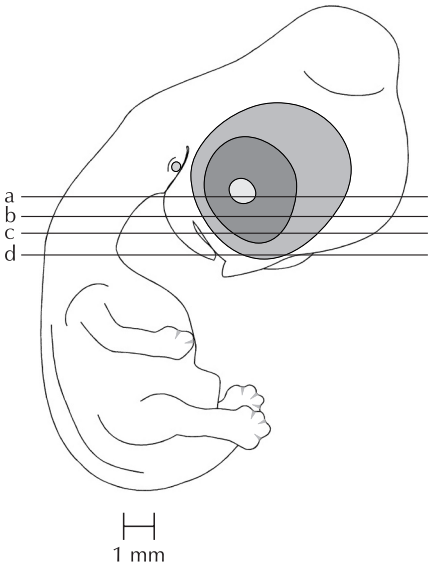

Transverse sections (TS): (a–d) × 12

1. right common carotid artery
2. left common carotid artery
3. oesophagus
4. trachea
5. oral cavity
6. vitreous chamber of left eye
7. lens of right eye
8. interorbital septum
9. right quadrate cartilage
10. right Meckel's cartilage
11. larynx
12. right jugular vein
13. spinal cord
14. primordium of costal process
15. notochord
16. myotome
17. left quadrate cartilage
18. tongue
19. left cerebral vesicle
20. right cerebral vesicle
21. vitreous humour of right eye
22. right first (maxillary) pharyngeal arch
23. lens of left eye
24. pigmented retina of right eye
25. right inferior oblique eye muscle
26. right first (mandibular) pharyngeal arch
27. lumen of left nostril
28. nasal concha
29. lumen of right nostril
30. right internal naris

Downloaded from Vet-eBooks.com

Plate 151

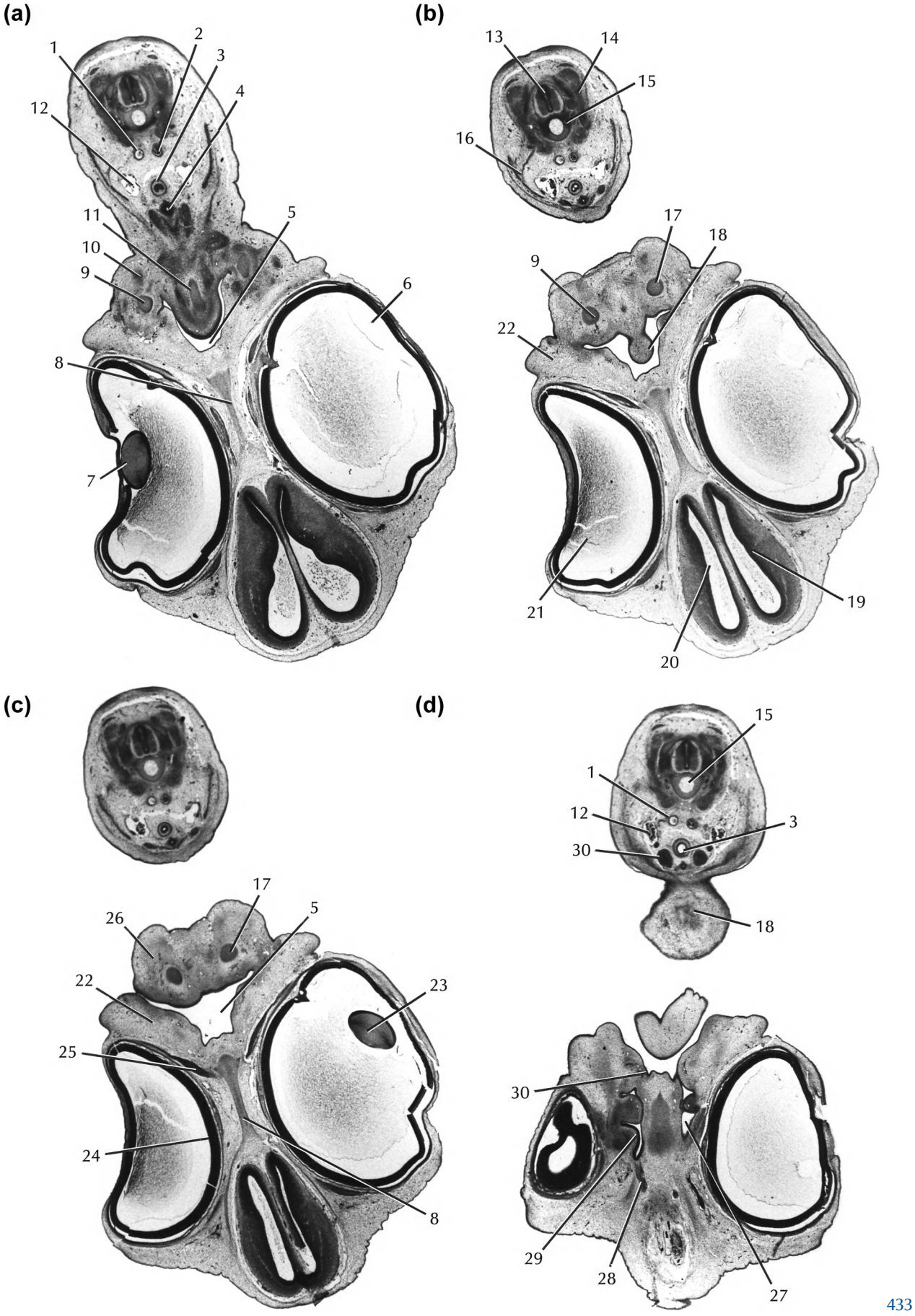

Downloaded from Vet-eBooks.com

Plate 152 Stage 31 (day 7) TS

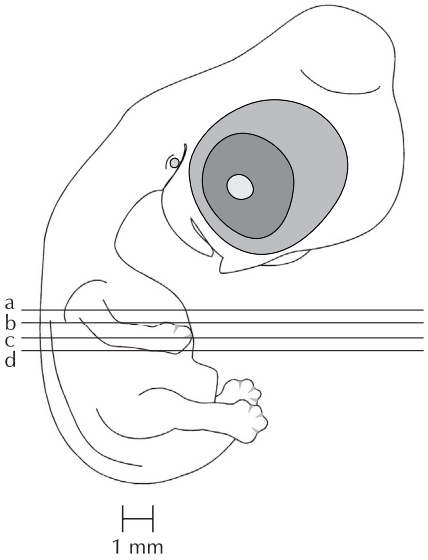

Transverse sections (TS): (a–d) × 20

1. myotome
2. spinal cord
3. notochord
4. oesophagus
5. left dorsal aorta
6. left atrium
7. pericardial cavity
8. body wall
9. ventricle
10. aortico-pulmonary ridge
11. right atrium
12. aortico-pulmonary septum
13. pulmonary artery
14. trachea
15. right dorsal aorta
16. transverse process of vertebra
17. dorsal root ganglion
18. neural arch of vertebra
19. left dorsal aorta just cranial to fusion with right dorsal aorta
20. left cranial (anterior) vena cava
21. left ventricle
22. interventricular septum
23. right ventricle
24. pericardium
25. right atrio-ventricular canal
26. right bronchus
27. ventral muscle mass of wing
28. right cranial (anterior) vena cava
29. humerus
30. dorsal muscle mass of wing
31. scapula
32. perforated interatrial septum (interatrial foramina)
33. coracoid
34. developing muscle
35. median dorsal aorta
36. left bronchus
37. sinus venosus

Downloaded from Vet-eBooks.com

Plate 152

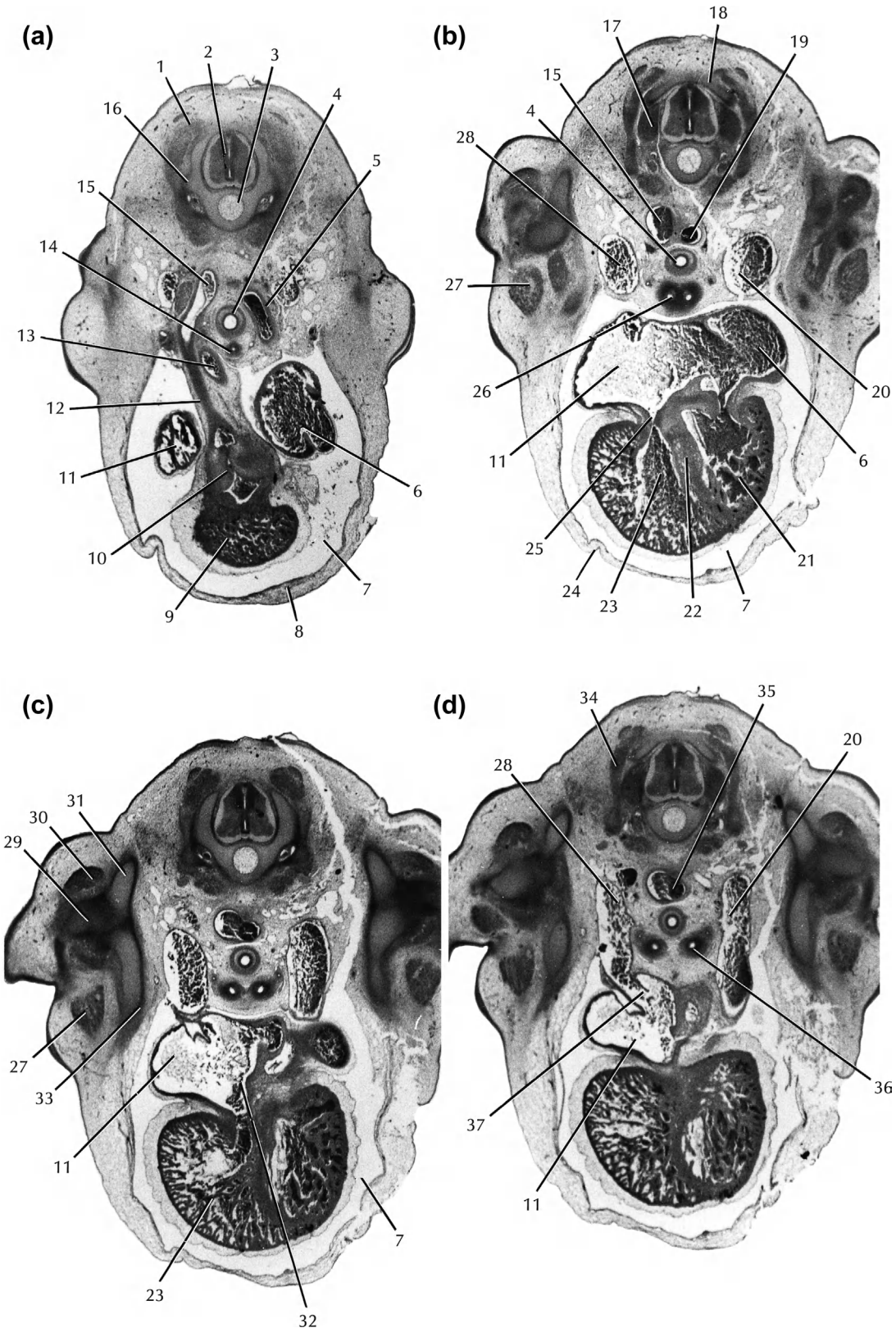

Downloaded from Vet-eBooks.com

Plate 153 Stage 31 (day 7) TS

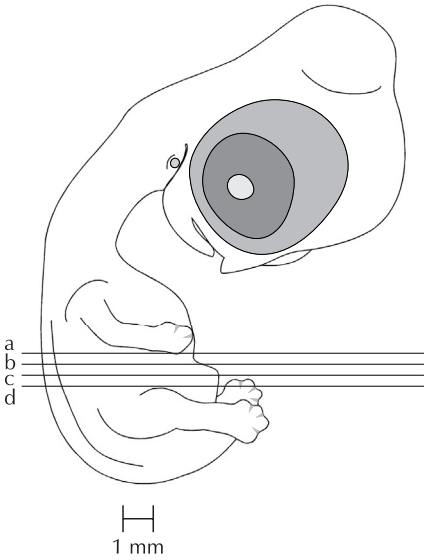

Transverse sections (TS): (a–d) × 20

1. right scapula
2. head of rib
3. crop
4. left lung bud
5. intercostalis externus muscle
6. intercostalis internus muscle
7. left lobe of liver
8. oblique septum
9. ventricle
10. body wall
11. pericardial cavity
12. right cranial (anterior) vena cava
13. right lung bud
14. right oviduct (Mullerian duct)
15. dorsal mesentery
16. dorsal aorta
17. cortical substance of left adrenal gland
18. left subcardinal vein
19. left oviduct (Mullerian duct)
20. proventriculus
21. left allantoic vein
22. ventral mesentery
23. right lobe of liver
24. mesenchyme condensing to form rib
25. dorsal root ganglion
26. coeliac artery
27. gizzard
28. right hepatic vein
29. right dorsal hepatic cavity
30. notochord
31. left gonad
32. left mesonephros
33. spleen
34. intestinal loop
35. right allantoic artery

Downloaded from Vet-eBooks.com

Plate 153

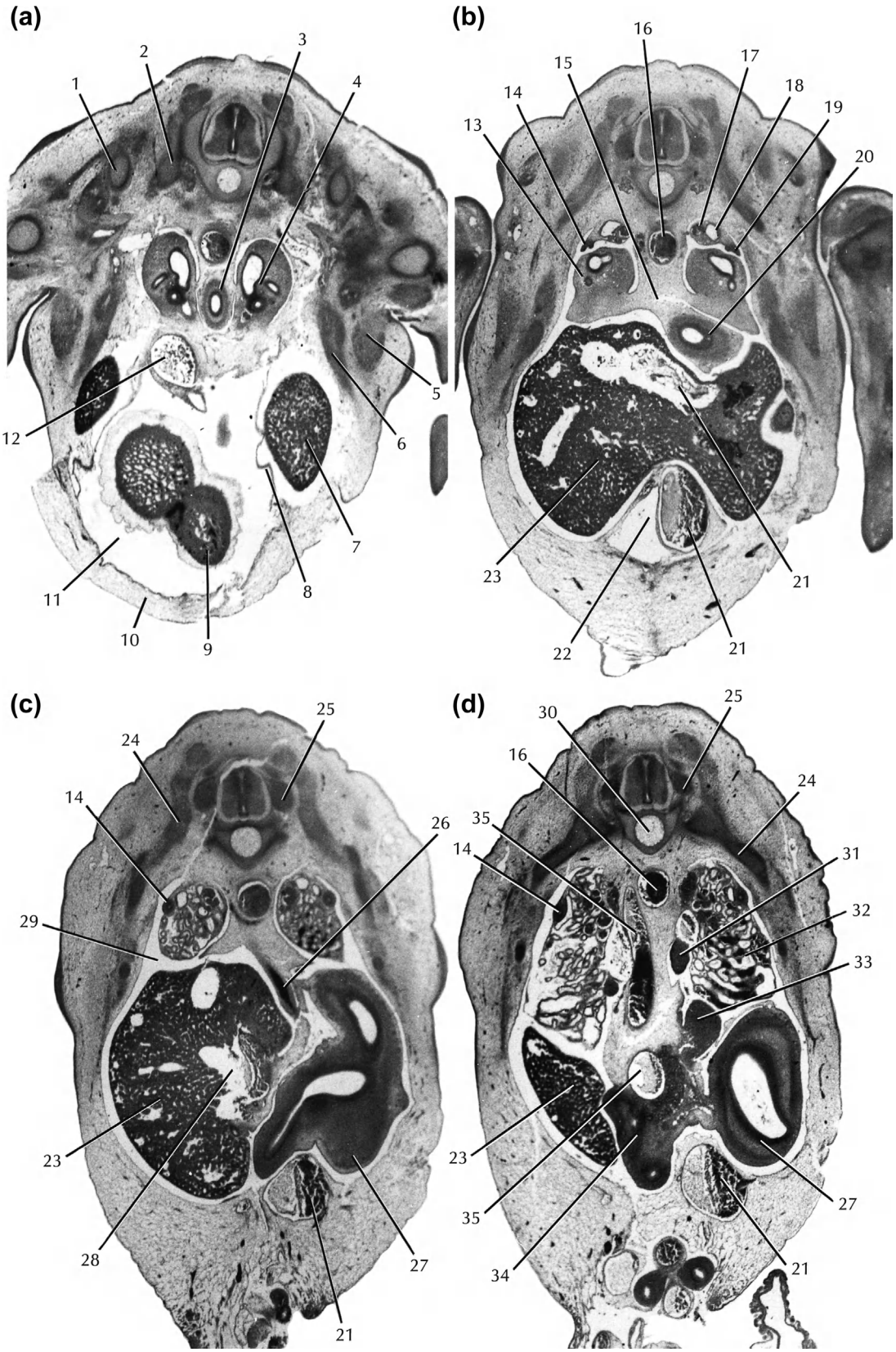

Downloaded from Vet-eBooks.com

Plate 154 Stage 31 (day 7) TS

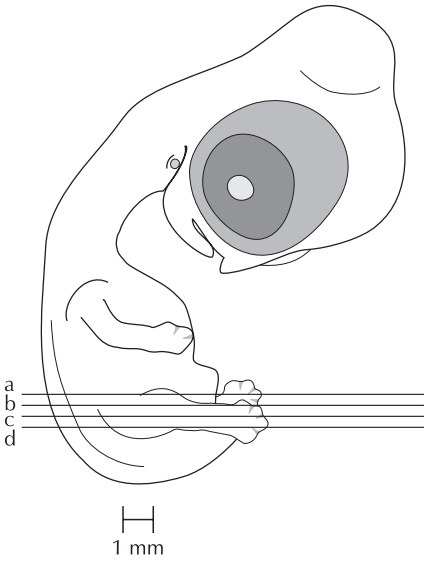

Transverse sections (TS): (a–d) × 20

1. right omphalo-mesenteric (vitelline) artery
2. right oviduct (Mullerian duct)
3. right gonad
4. right metanephros
5. left metanephros
6. left gonad
7. left omphalo-mesenteric (vitelline) artery
8. left mesonephros
9. gizzard
10. peritoneal cavity
11. left allantoic vein
12. yolk sac
13. loop of intestine
14. left omphalo-mesenteric (vitelline) vein
15. right omphalo-mesenteric (vitelline) vein
16. right allantoic vein
17. jejunum
18. right mesonephros
19. dorsal aorta
20. left subcardinal vein
21. left oviduct (Mullerian duct)
22. intestine
23. cloacal fold
24. base of allantois
25. right subcardinal vein
26. right metanephric duct
27. ilium
28. femur
29. dorsal muscle mass of lower leg
30. tibiotarsus
31. ventral muscle mass of lower leg
32. pubis
33. left nephric duct
34. cloaca
35. right nephric duct
36. ventral muscle mass of right thigh
37. dorsal muscle mass of right thigh
38. left metanephric duct
39. genital fold
40. cloacal membrane

Downloaded from Vet-eBooks.com

Plate 154

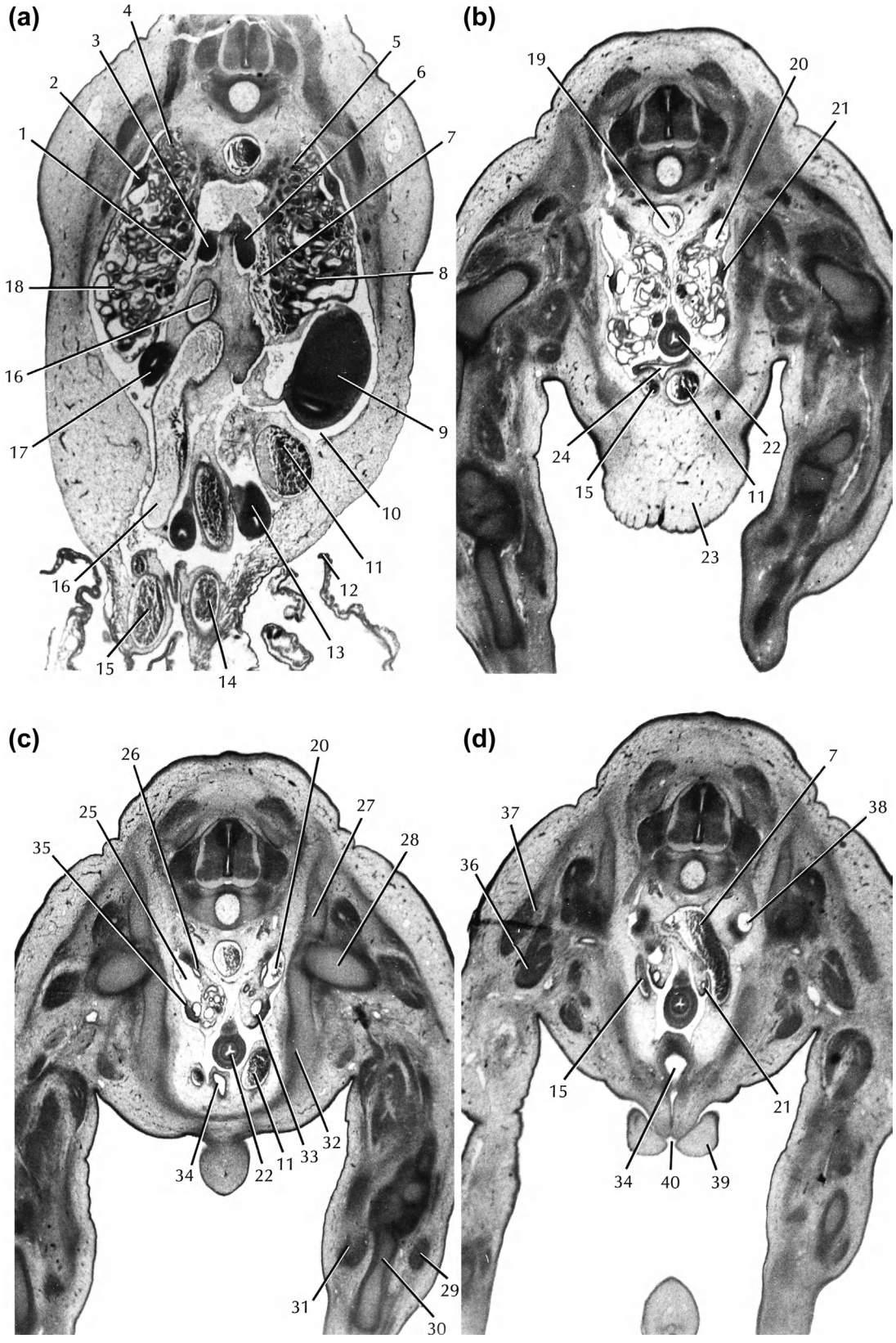

Downloaded from Vet-eBooks.com

Plate 155 Stage 31 (day 7) TS

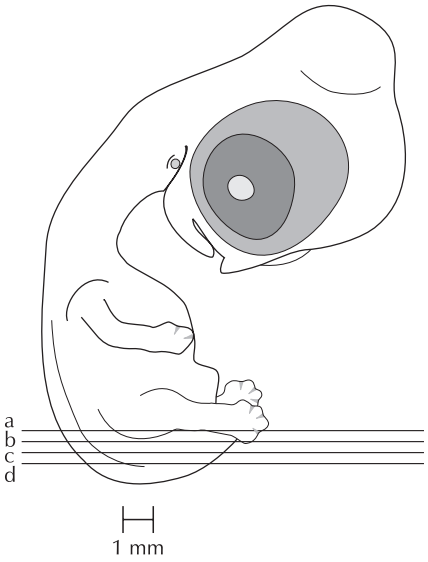

Transverse sections (TS): (a–d) × 20

1. right aorta
2. ilium
3. spinal cord
4. vertebral artery
5. sciatic artery
6. dorsal muscle mass of thigh
7. ventral muscle mass of thigh
8. femur
9. intestinal coelomic cavity
10. colon
11. cloacal fold
12. tail
13. cloacal bursa
14. cloaca
15. mesentery
16. right oviduct (Mullerian duct)
17. right posterior cardinal vein
18. dorsal root ganglion
19. notochord
20. left posterior cardinal vein
21. left metanephric tubule
22. left metanephric (ureteric) duct
23. coelom
24. right metanephric (ureteric) duct
25. derma-myotomal condensation
26. epidermis of tail
27. intersegmental artery
28. sclerotomal condensation for vertebral body

Downloaded from Vet-eBooks.com

Plate 155

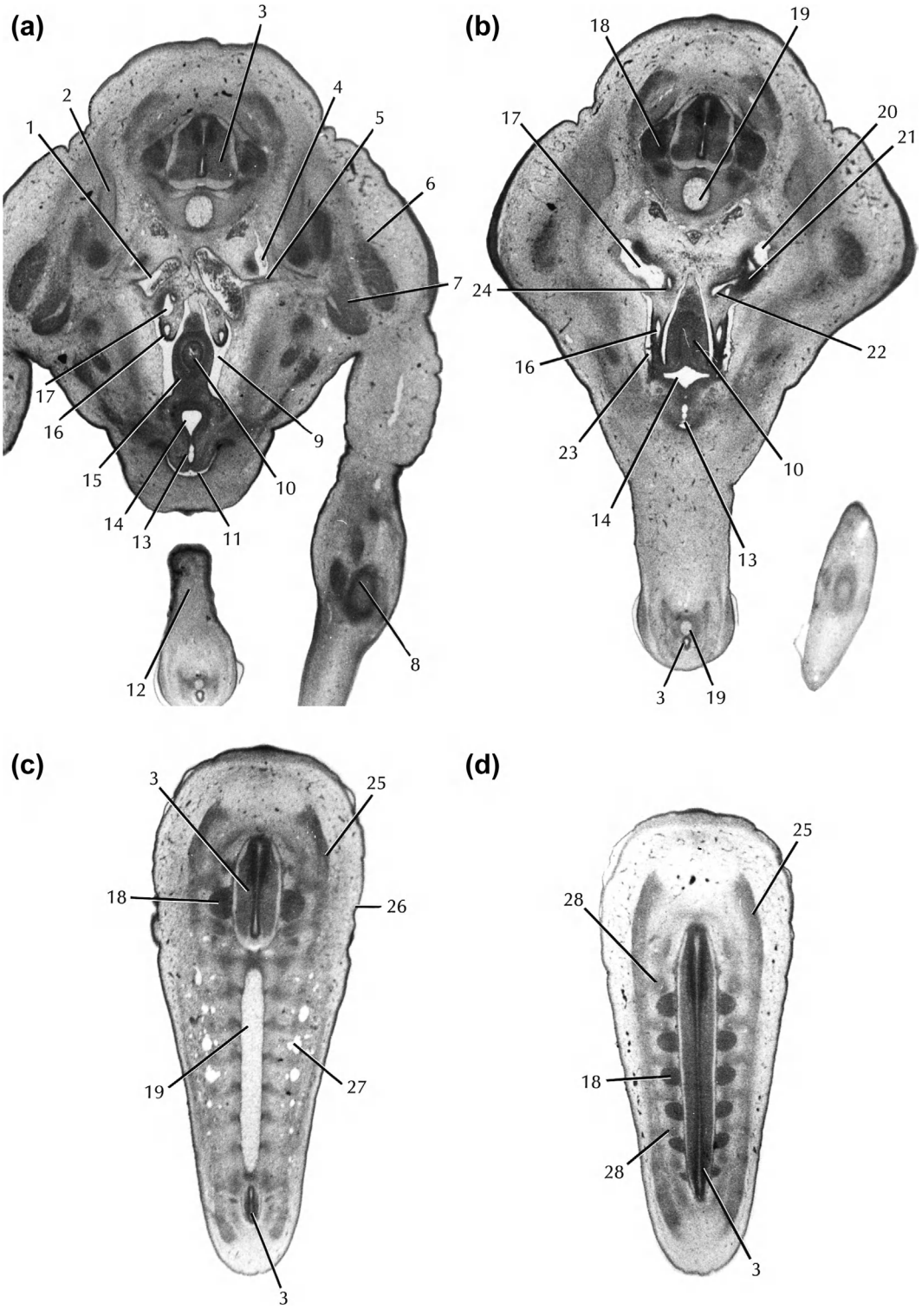

Downloaded from Vet-eBooks.com

Plate 156 Stage 31 (day 7) TS: enlargements

(a) Rathke's pouch (centre top) and infundibulum (centre bottom) from section adjacent to *plate 150c*, × 130.

(b) Oesophagus (top) and trachea (bottom) from section adjacent to *plate 152b*, × 120.

(c) Lung buds and oviduct from section adjacent to *plate 153b*, × 50.

(d) Section through spinal cord region in mid trunk, × 80.

1. right internal carotid artery
2. Rathke's pouch
3. left internal carotid artery
4. infundibulum
5. oesophagus
6. trachea at bifurcation into bronchae
7. right lung bud
8. dorsal aorta
9. ventral horn (motor column)
10. ependyma
11. mantle layer
12. dorsal root ganglion
13. ventral root
14. white matter
15. notochord
16. notochordal sheath

Downloaded from Vet-eBooks.com

Plate 156

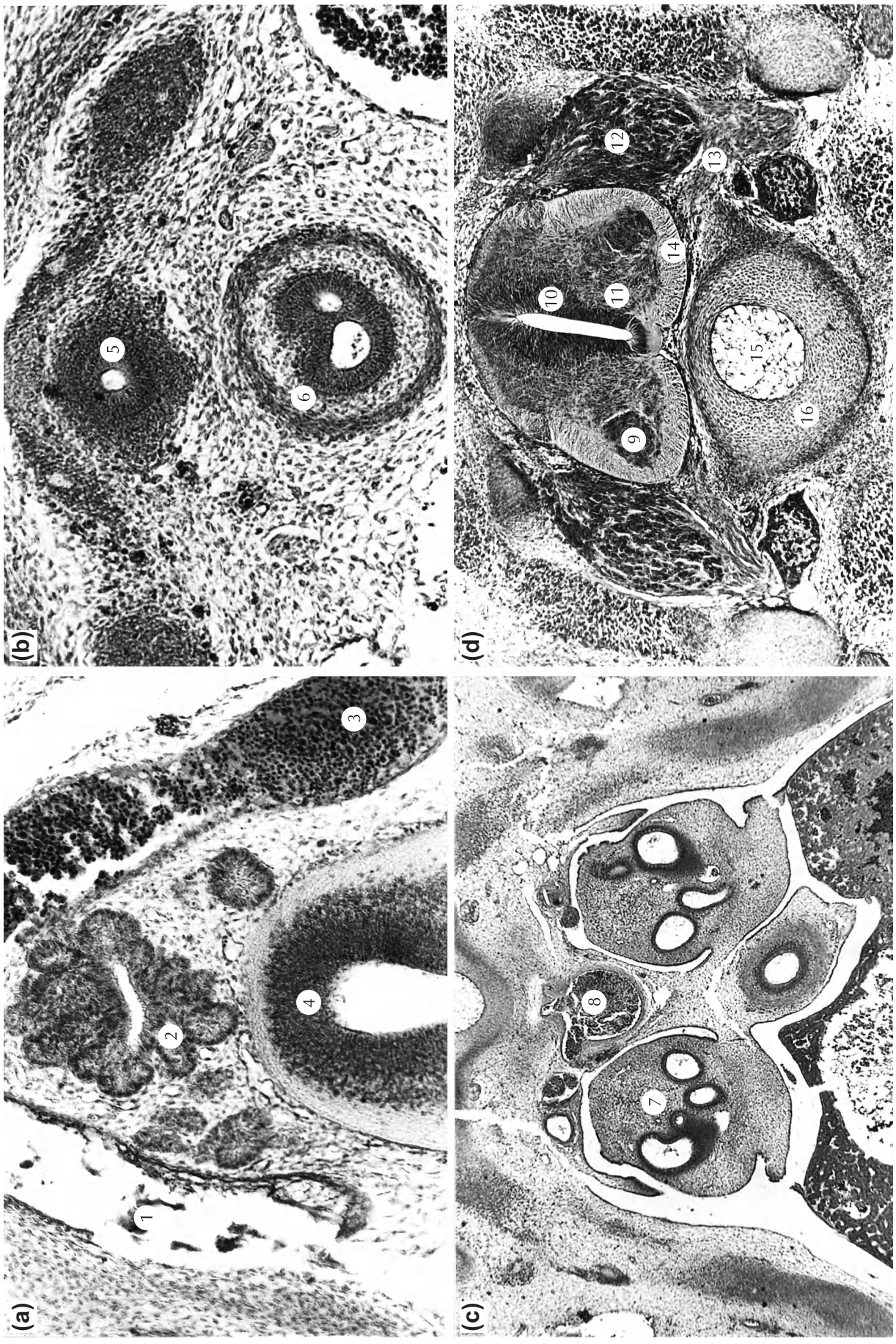

Downloaded from Vet-eBooks.com

Plate 157 Stage 35 (day 9) LS: sagittal

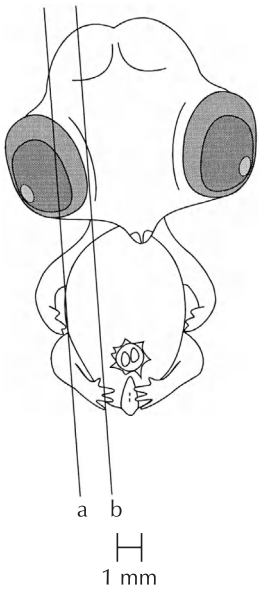

Londitudinal (sagittal) sections: (a, b) × 6

1. optic lobe
2. endolymphatic sac
3. inner ear
4. otic capsule
5. cervical vertebra
6. latissimus dorsi muscle
7. rhomboideus superficialis muscle
8. coracoid
9. dorsal root ganglion
10. lung
11. abdominal air sac
12. mesonephros
13. spinal cord
14. metanephros
15. ilium
16. trochanter of femur
17. flexor cruris medialis muscle
18. biceps femoralis muscle
19. iliotibialis muscle
20. proventriculus
21. thoracic air sac
22. sternal rib
23. pleural cavity
24. flexor carpi ulnaris muscle
25. ulna
26. interosseus dorsalis muscle
27. radius
28. extensor metacarpi radialis muscle
29. eyelid
30. cerebellum
31. metencephalon
32. choroid plexus
33. floor of myelencephalon
34. basal plate of chondrocranium
35. trachea
36. oesophagus
37. carotid artery
38. dorsal aorta
39. left atrium
40. caudal (posterior) vena cava
41. right hepatic vein
42. spleen
43. synsacrum
44. ischiofemoralis muscle
45. metanephric duct
46. renal vein
47. tail spinal cord
48. notochord
49. cloaca
50. small intestine
51. foot
52. gizzard
53. liver
54. ventricle
55. toes
56. wing
57. sternum
58. supracoracoideus muscle
59. pectoralis muscle
60. oral cavity
61. pecten
62. lens
63. collapsed eye
64. pigmented retina
65. cerebral hemisphere

Downloaded from Vet-eBooks.com

Plate 157

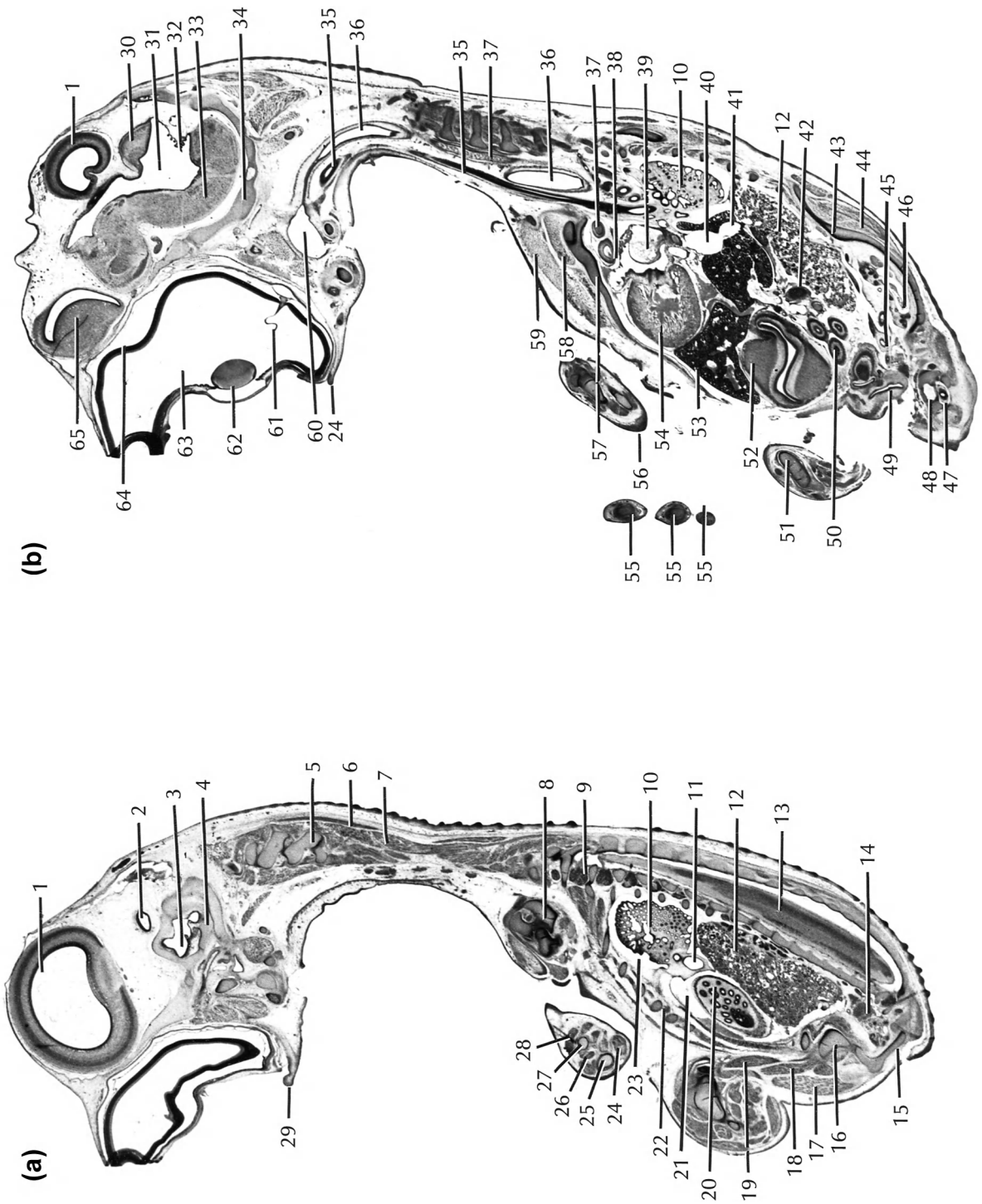

Downloaded from Vet-eBooks.com

Plate 158 Stage 35 (day 9) TS

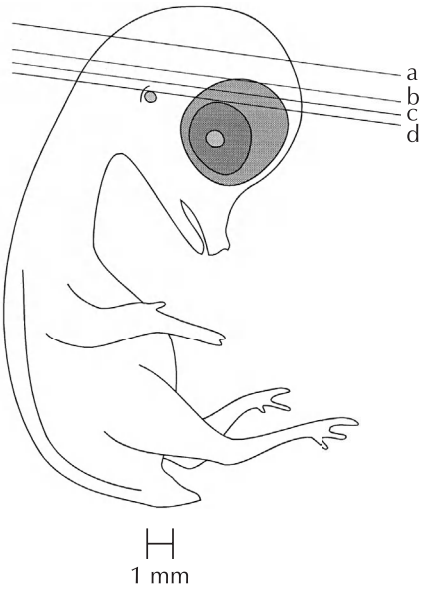

Transverse sections (TS): (a–d) × 9

1. right optic lobe
2. left optic lobe
3. right telencephalon
4. ectoderm of head
5. mesocoele
6. choroid plexus
7. right eye
8. cranial cavity
9. third ventricle
10. thalamus (diencephalon)
11. edge of spinal cord
12. left telencephalon
13. region between the two telencephalic vesicles

Downloaded from Vet-eBooks.com

Plate 158

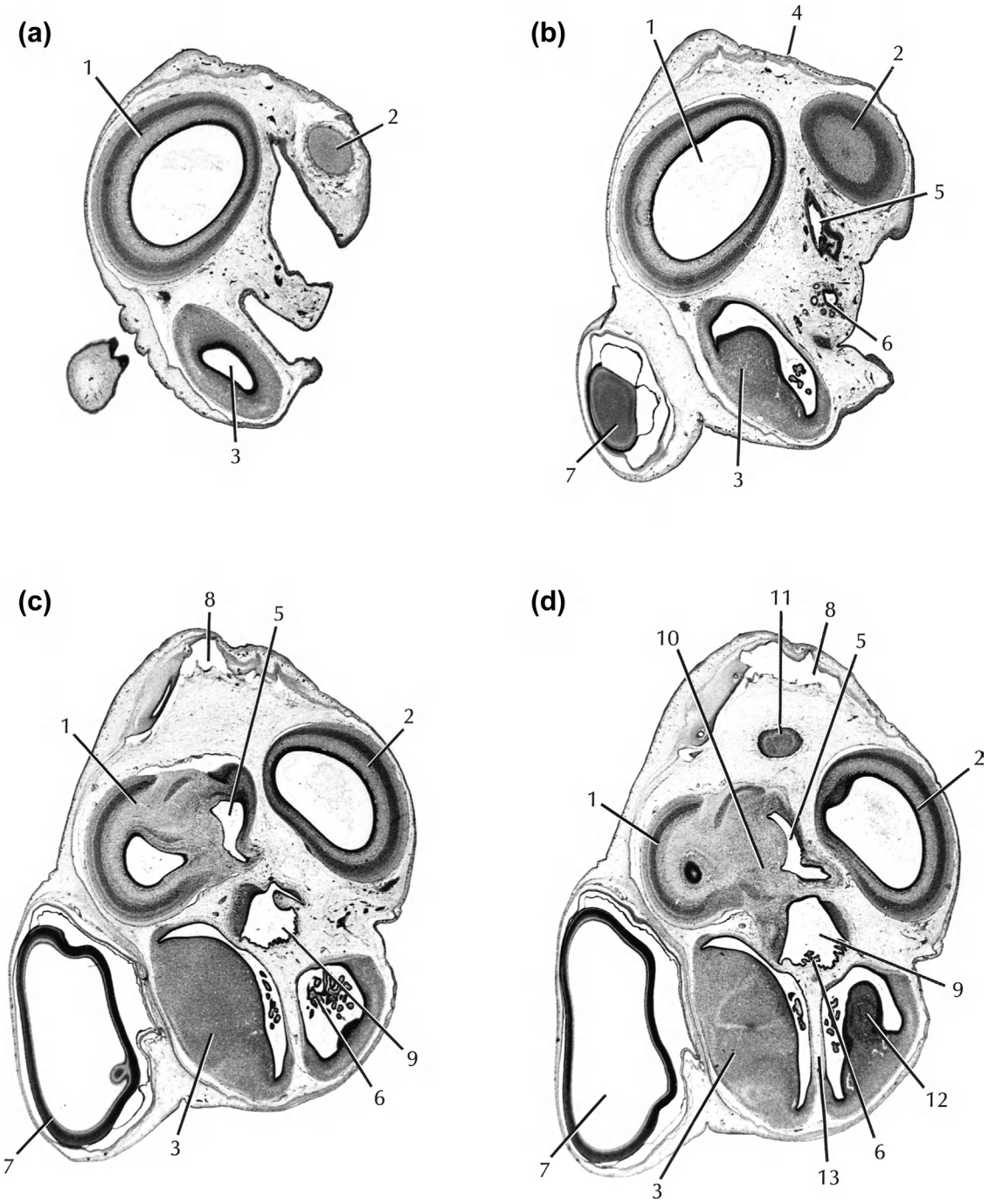

Downloaded from Vet-eBooks.com

Plate 159 Stage 35 (day 9) TS

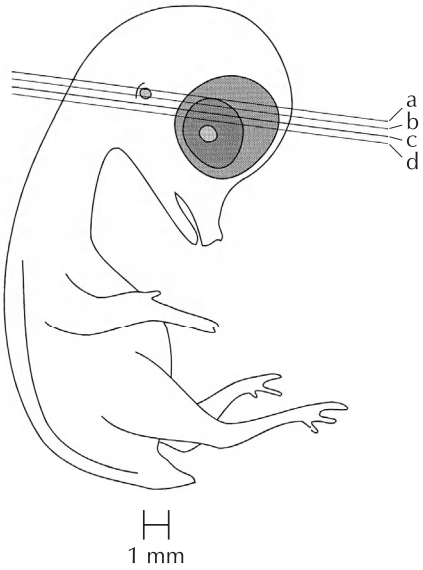

Transverse sections (TS): (a–d) × 9

1. right optic lobe
2. thalamus (diencephalon)
3. foramina of emissaria veins
4. cranial cavity
5. cerebellum
6. fourth ventricle
7. lumen of left optic lobe
8. lateral ventricle
9. telencephalon (cerebral hemisphere)
10. choroid plexus
11. interhemispherical fold
12. head ectoderm
13. right squamosal cartilage
14. semicircular canals
15. wall of medulla oblongata
16. third ventricle
17. cornea
18. postorbital cartilage
19. trigeminal (cranial nerve V) ganglion
20. otic capsule
21. splenius capitis muscle
22. right metotic cartilage
23. right biventer cervicis muscle
24. left optic lobe
25. left eye
26. dorsal oblique eye muscle
27. vitreous chamber of eye
28. lower eyelid
29. adductor mandibulae externus muscle
30. external auditory meatus

Downloaded from Vet-eBooks.com

Plate 159

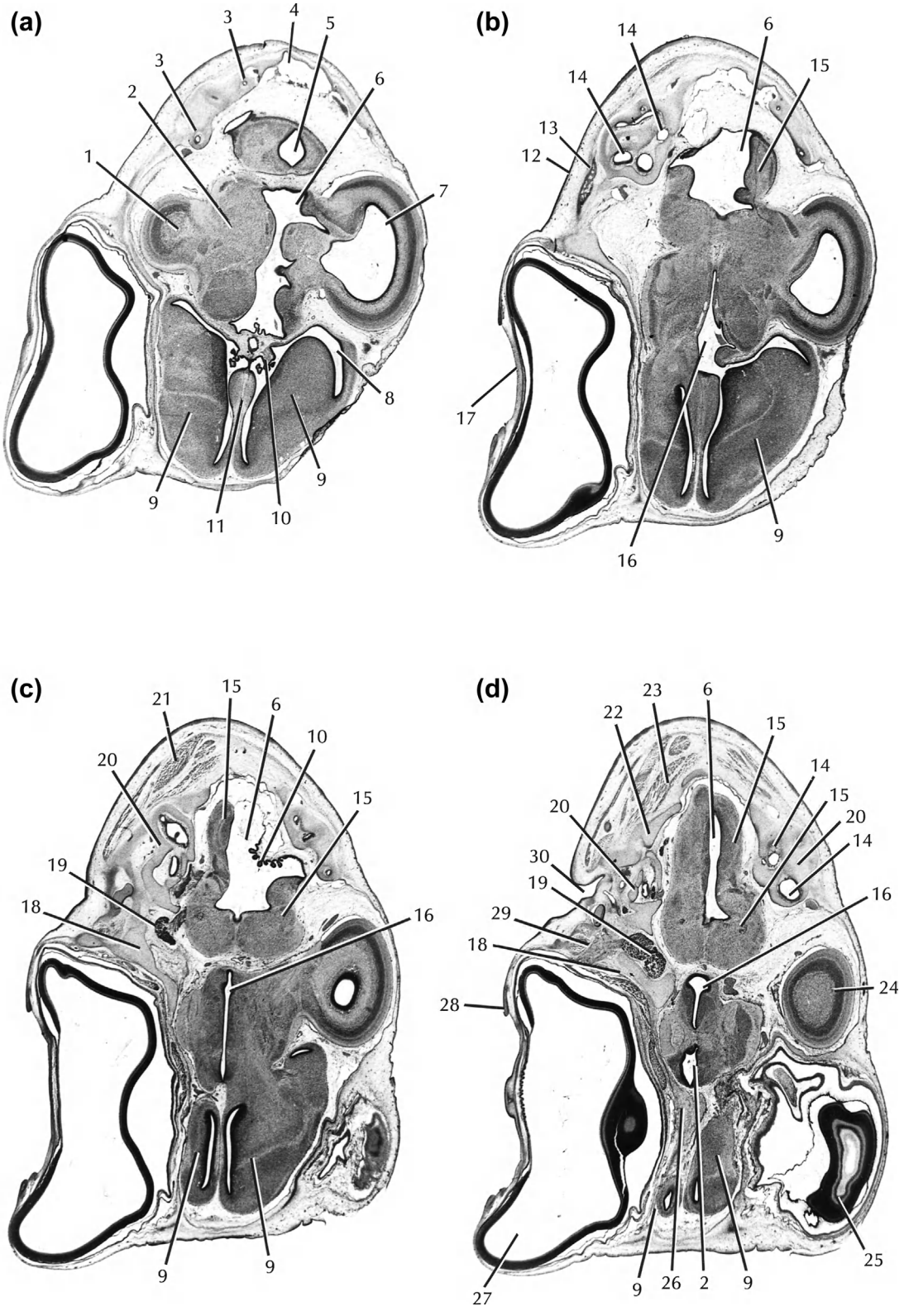

Downloaded from Vet-eBooks.com

Plate 160 Stage 35 (day 9) TS

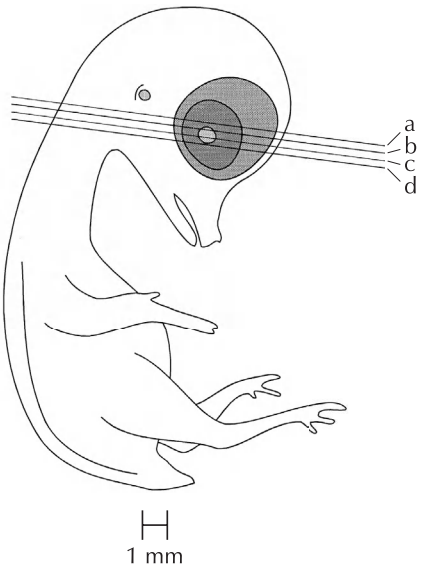

Transverse sections (TS): (a–d) × 9

1. glossopharyngeal (cranial IX) nerve
2. complexus muscle
3. biventer cervis muscle
4. neural arch
5. medulla oblongata
6. cochlea
7. basilar artery
8. diencephalon (and third ventricle)
9. left optic lobe
10. medial rectus muscle of eye
11. telencephalon
12. pigmented retina
13. lateral rectus muscle of eye
14. adductor mandibulae externus muscle
15. external auditory meatus
16. otic capsule
17. right metotic cartilage
18. spinal cord
19. left metotic cartilage
20. trigeminal (cranial nerve V) ganglion
21. optic chiasma
22. interorbital (nasal) septum
23. hypophysis
24. lens
25. epibranchial cartilage
26. depressor mandibulae muscle
27. cochlea canal
28. notochord
29. basal plate
30. artifactual bulge in retina of left eye
31. optic nerve
32. olfactory (cranial I) nerve
33. ventral oblique muscle of eye
34. external ophthalmic vein
35. pecten
36. lower eyelid
37. trabecular cartilage
38. Meckel's cartilage
39. quadrate cartilage
40. columella
41. common carotid artery
42. rectus capitis medialis muscle
43. dorsal root ganglion
44. odontoid process (body of axis)
45. transverse process
46. splenius capitis muscle
47. rectus capitis ventralis muscle
48. rectus capitis lateralis muscle
49. vagus (cranial X) nerve
50. middle ear
51. pterygoid cartilage
52. cranial (anterior) vena cava

Downloaded from Vet-eBooks.com

Plate 160

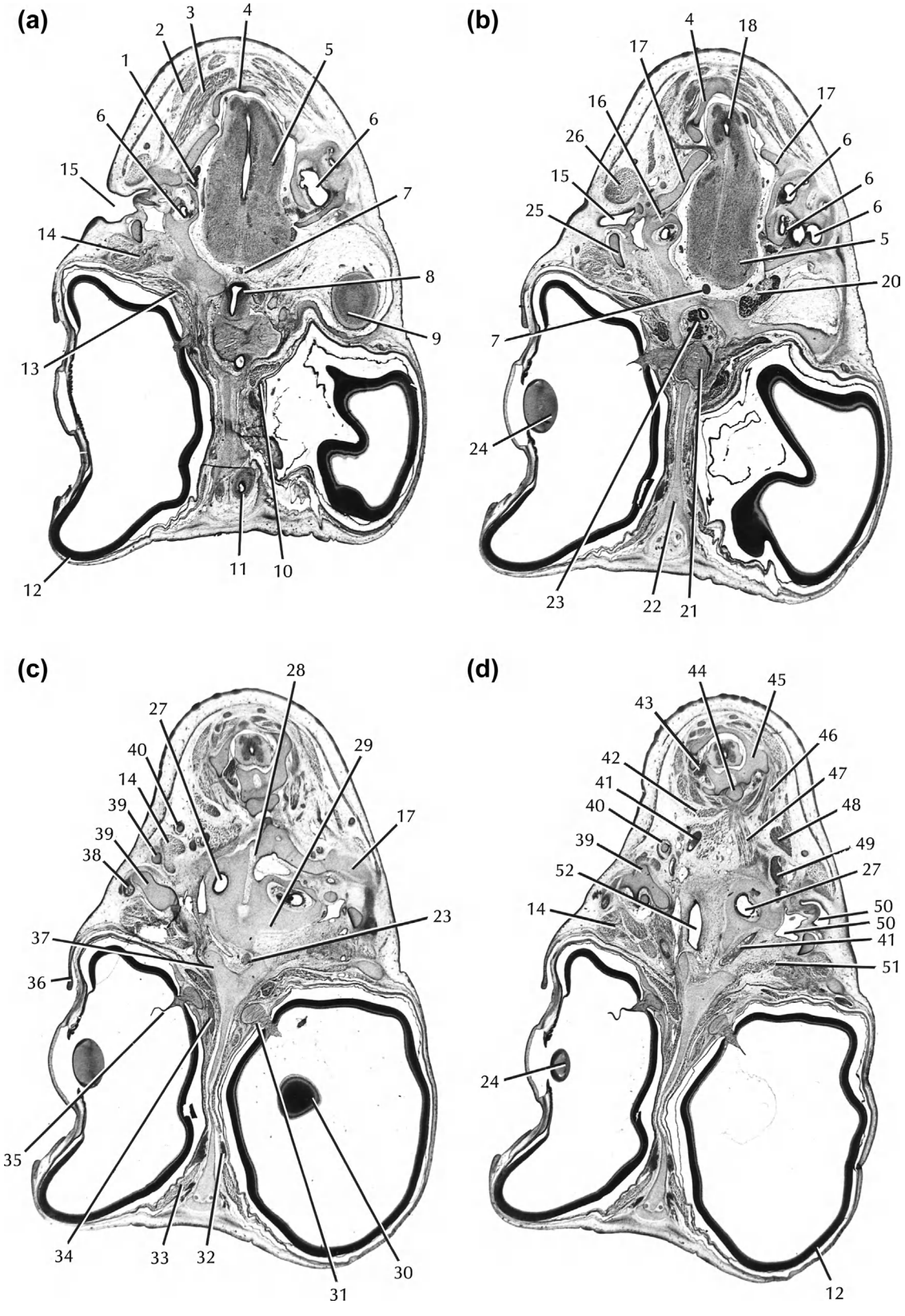

Downloaded from Vet-eBooks.com

Plate 161 Stage 35 (day 9) TS

(a) Enlargement of section adjacent to *plate 159d*: × 45

(b) Enlargement of section adjacent to *plate 160a*: × 45

1. external auditory meatus
2. tympanic membrane
3. middle ear (tympanic cavity)
4. adductor mandibulae externus muscle
5. columella
6. foot plate of columella
7. otic capsule
8. inner ear
9. epibranchial cartilage

Downloaded from Vet-eBooks.com

Plate 161

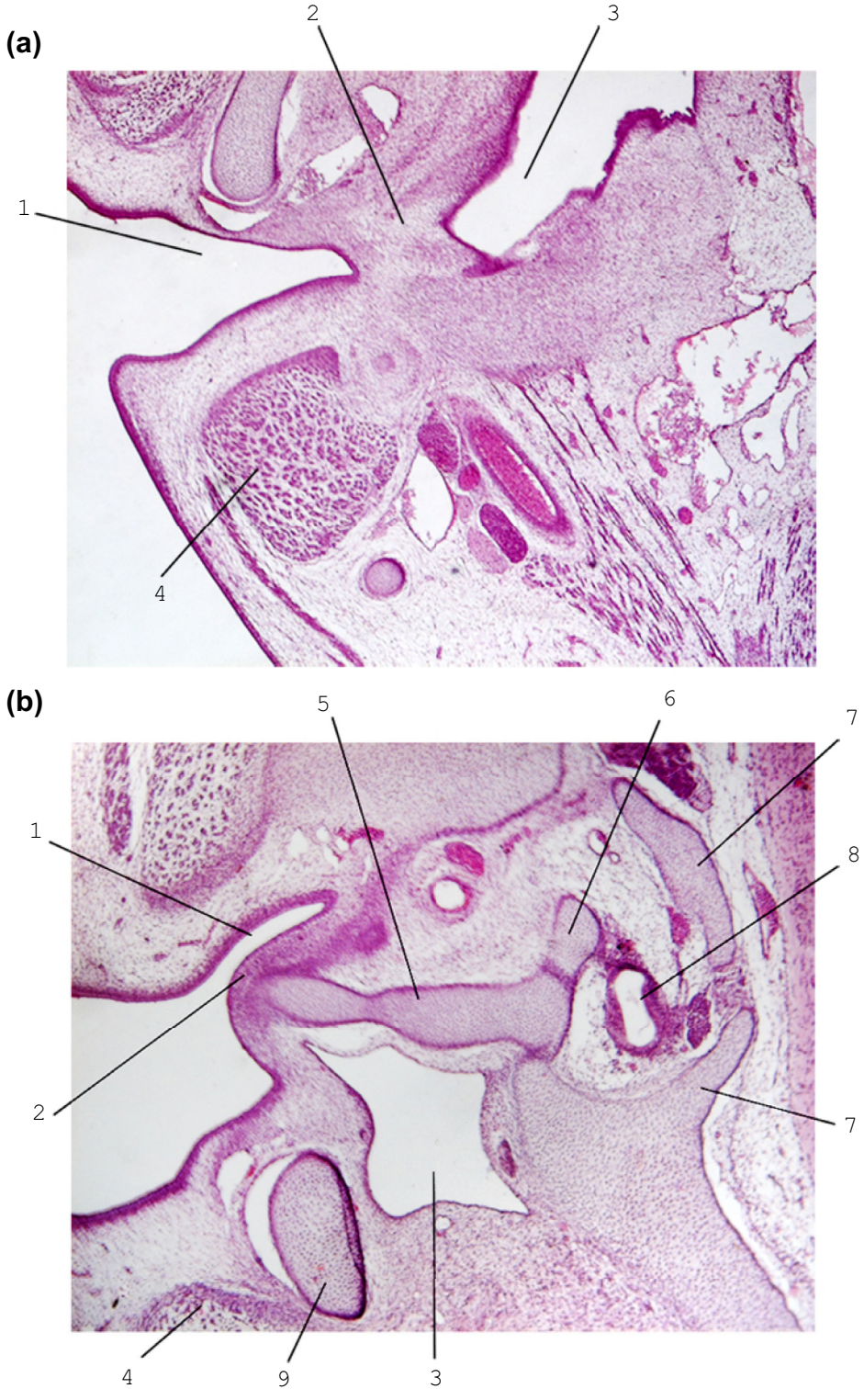

Downloaded from Vet-eBooks.com

Plate 162 Stage 35 (day 9) TS

Enlargements of section adjacent to *plate 160d*: (a, b) × 45

1. quadrate cartilage
2. cranial vena cava
3. semi-circular canal
4. cochlear canal
5. common carotid artery
6. adductor mandibularis muscle
7. dorsal root ganglion
8. neural arch
9. spinal cord
10. remnant of notochord in vertebral body
11. cervical vertebra
12. odontoid process
13. splenius capitis muscle
14. rectus capitis lateralis muscle
15. rectus capitis ventralis muscle
16. rectus capitis centralis muscle
17. zygapophysis of vertebra
18. right longus colli pars caudalis muscle

Downloaded from Vet-eBooks.com

Plate 162

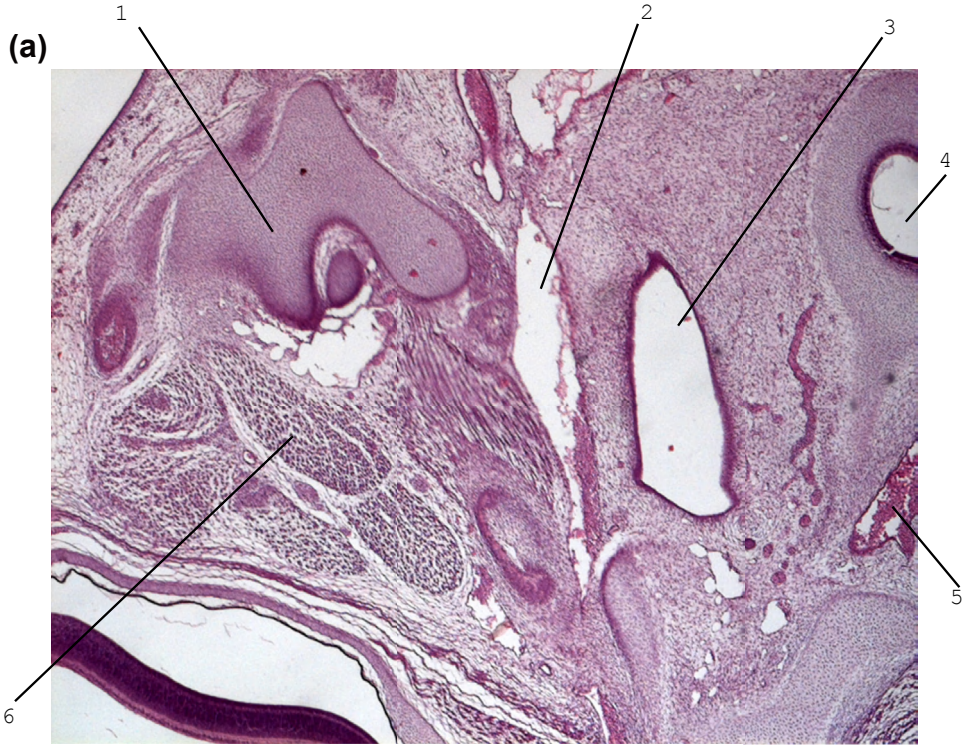

Downloaded from Vet-eBooks.com

Plate 163 Stage 35 (day 9) TS

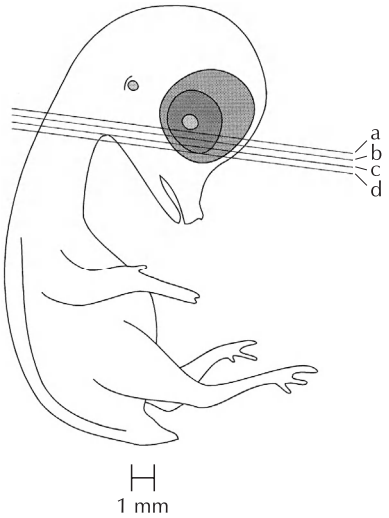

Transverse sections (TS): (a–d) × 9

1. carotid artery
2. rectus capitis lateralis muscle
3. neural arch
4. biventer cervicis muscle
5. splenius capitis muscle
6. rectus capitis ventralis muscle
7. epibranchial cartilage
8. adductor mandibulae externus muscle
9. external auditory meatus
10. pharynx
11. otic process of quadrate cartilage
12. vitreous chamber of eye
13. dorsal oblique eye muscle
14. olfactory (cranial I) nerve
15. palatine artery
16. jugular vein
17. anastomotic vein (interjugular anastomosis)
18. occipital vein
19. trachea
20. spinal cord
21. dorsal root ganglion
22. pterygoid muscle
23. Meckel's cartilage
24. quadrato-jugal cartilage
25. pseudotemporalis superficialis muscle
26. facial vein
27. pseudotemporalis profundus muscle
28. lower eyelid
29. pterygoid condyle of quadrate cartilage
30. extrinsic tracheal muscle
31. feather papilla
32. notochord in body of vertebra
33. intrinsic tracheal muscle
34. pecten
35. interorbital (nasal) process
36. internal naris
37. oral cavity
38. glottis
39. tongue
40. paraglossal cartilage
41. lateral condyle of quadrate cartilage
42. iris
43. lens
44. anterior chamber of eye
45. cornea
46. upper eyelid
47. pigmented retina
48. ectoderm of head
49. nasal cavity
50. nasal concha
51. palatine process

Downloaded from Vet-eBooks.com

Plate 163

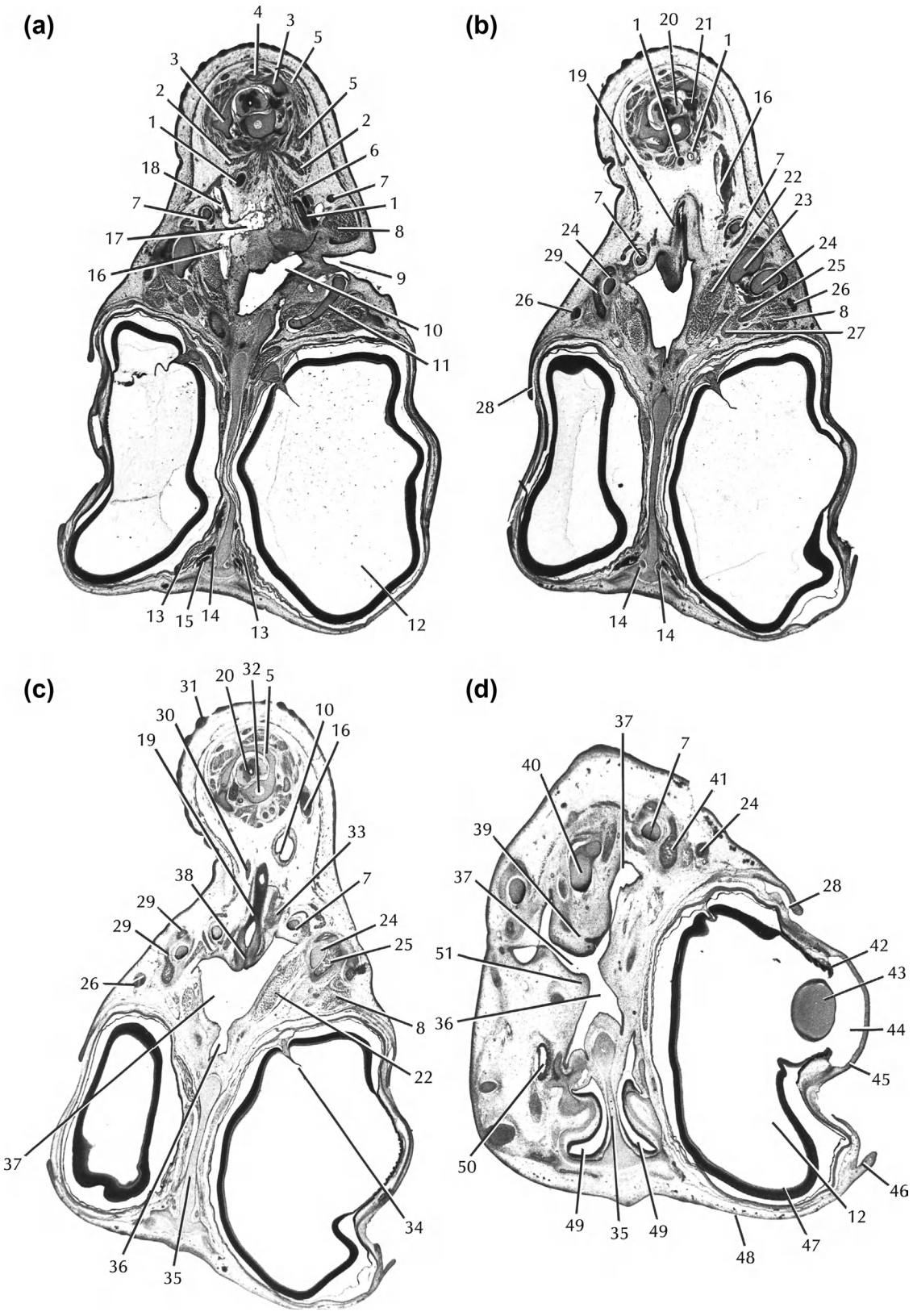

Downloaded from Vet-eBooks.com

Plate 164 Stage 35 (day 9) TS

Enlargement of section adjacent to *plate 163b*: × 35

1. spinal cord
2. left biventer cervicis muscle
3. left longus colli pars dorsali muscle
4. right ascendens cervicis muscle
5. dorsal root ganglion
6. left and right carotid arteries
7. rectus capitis lateralis muscle
8. remnant of notochord in vertebral body
9. right longus colli pars caudalis muscle

Downloaded from Vet-eBooks.com

Plate 164

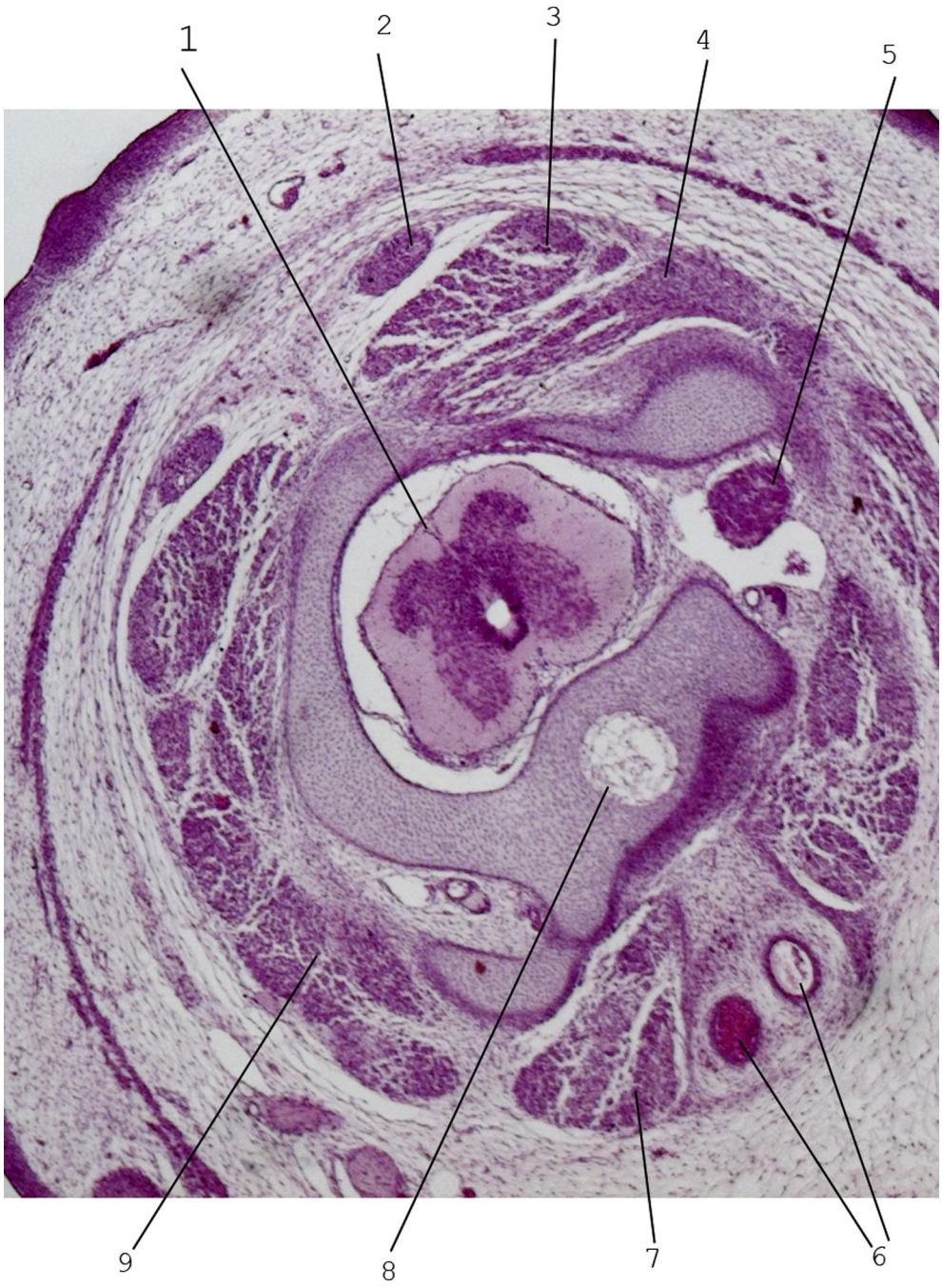

Downloaded From Vet-eBooks.com

Plate 165 Stage 35 (day 9) TS

(a) Enlargement of section adjacent to *plate 163a*: × 70

(b) Enlargement of section adjacent to *plate 163d*: × 30

1. ventral oblique eye muscle
2. optic (cranial II) nerve
3. trabecular cartilage
4. blood vessel
5. choroid
6. pigmented retina underlain by sensory retina
7. vitreous chamber
8. pecten
9. lens
10. iris
11. anterior chamber of eye
12. cornea

Downloaded from Vet-eBooks.com

Plate 165

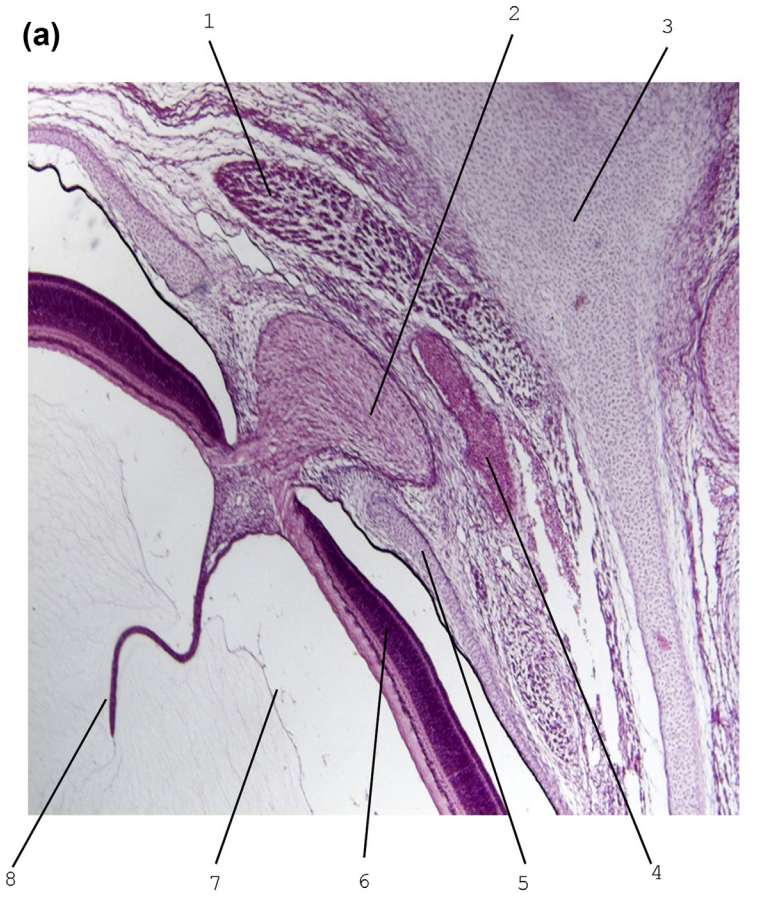

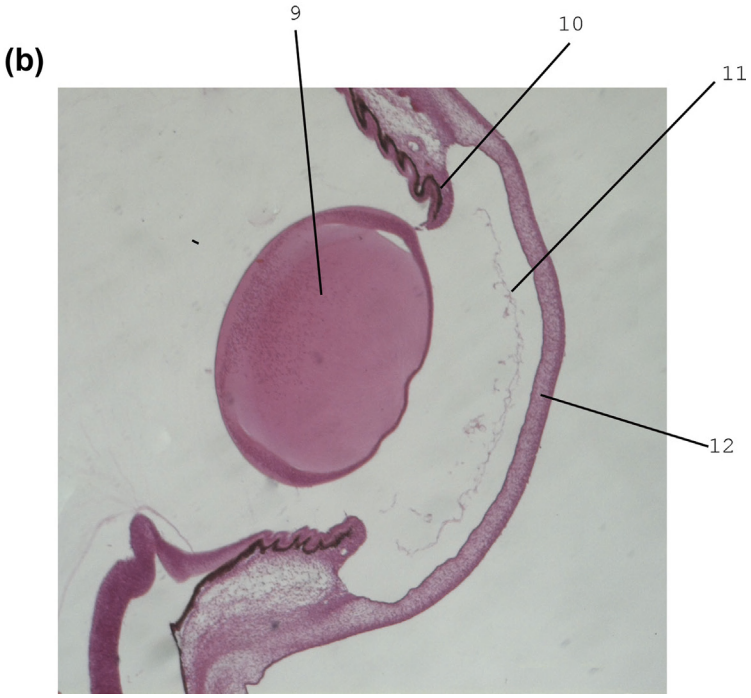

Downloaded from Vet-eBooks.com

Plate 166 Stage 35 (day 9) TS

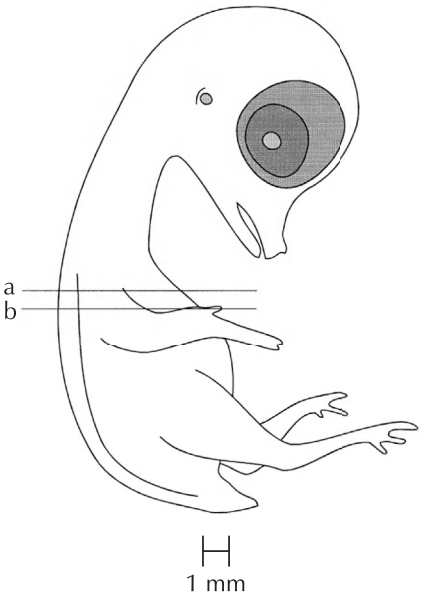

Transverse sections (TS): (a, b) × 20

1. cervical vertebra
2. spinal cord, white matter
3. notochord
4. spinal cord, grey matter
5. feather papilla
6. neural arch of cervical vertebra
7. dorsal root ganglion
8. cervical rib
9. longus colli ventralis muscle
10. scapula
11. deltoid major muscle
12. humerus
13. pectoralis muscle
14. oesophago-tracheo-bronchial artery
15. left common carotid artery
16. coracoid
17. right common carotid artery
18. trachea
19. connective tissue
20. crop
21. apex of sternum
22. costo-sternalis muscle
23. subcoracoideus muscle, minor portion
24. thymus of right side
25. internal jugular vein
26. tensor propatagialis longus muscle
27. spinal nerve
28. branches of latissimus dorsi muscle
29. rhomboideus superficialis muscle
30. sympathetic ganglion
31. part of left brachial plexus
32. thoracic rib
33. thymus of left side
34. cervical air sac
35. supracoracoideus muscle, major portion
36. rim of right wing
37. triceps brachii, pars humerotriceps muscle
38. medial head of triceps muscle
39. serratus superficialis muscle
40. rhomboideus profundus muscle

Downloaded from Vet-eBooks.com

Plate 166

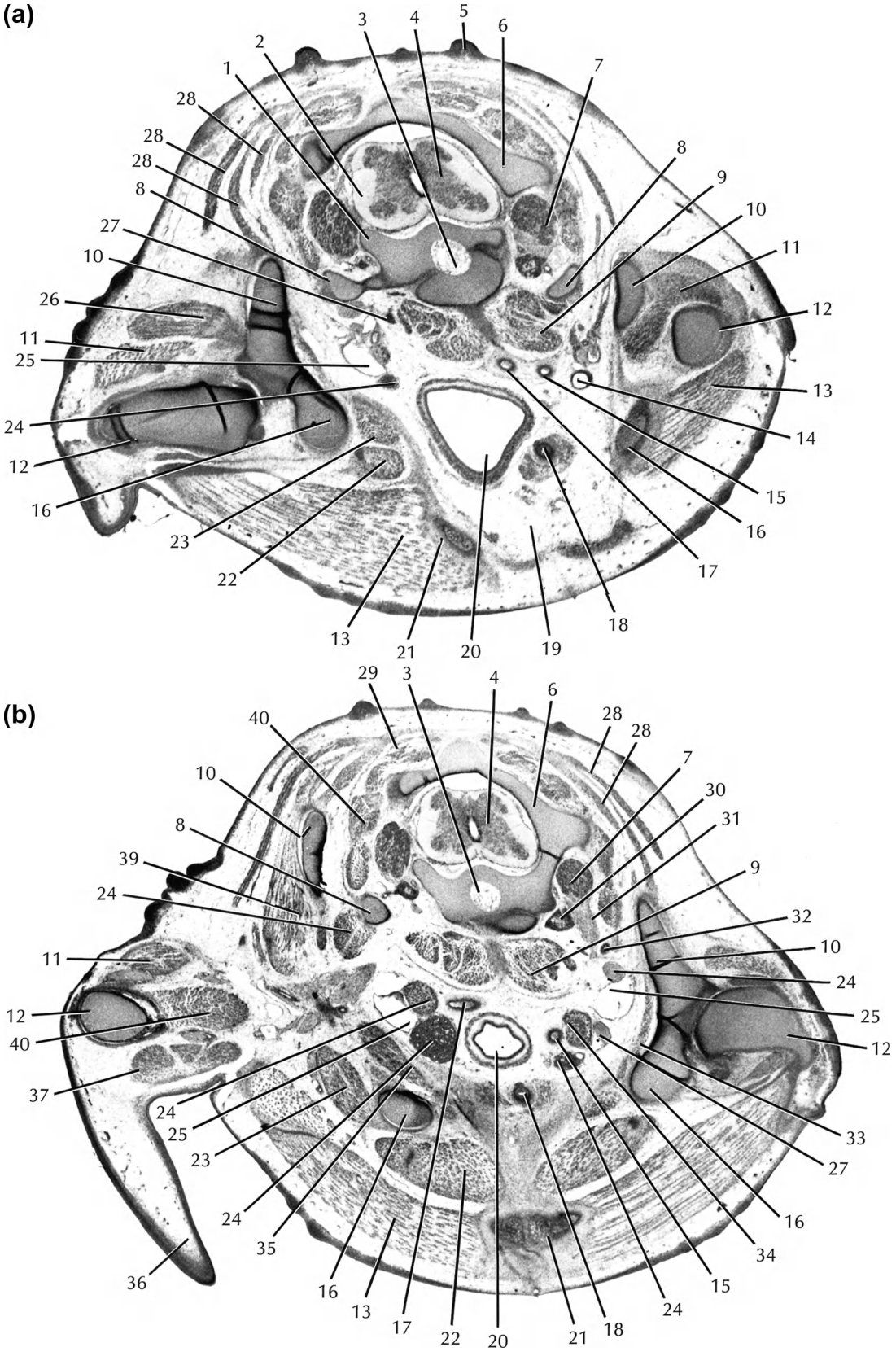

Downloaded from Vet-eBooks.com

Plate 167 Stage 35 (day 9) TS

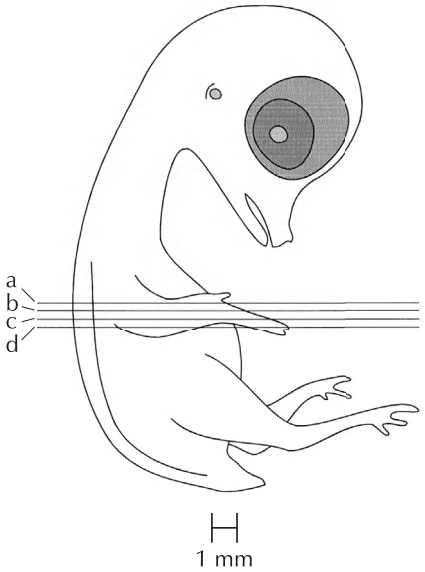

Transverse sections (TS): (a–d) × 14

1. oesophagus
2. head of rib (capitulum)
3. spinal cord, white matter
4. notochord
5. rhomboideus superficialis muscle
6. longus colli ventralis muscle
7. anterior tip of lung
8. scapula
9. intercostal muscle
10. syrinx
11. jugular vein
12. shaft of humerus
13. subclavian vein
14. ventral condyle of humerus
15. coracoid
16. pericardial cavity
17. radius
18. ulna
19. sternum
20. keel of sternum
21. right common carotid artery
22. ulna carpal
23. right internal carotid artery
24. coracobrachialis muscle
25. flexor digitorum profundus muscle
26. extensor digitorum communis muscle
27. extensor metacarpi ulnaris muscle
28. triceps brachii pars humerotriceps muscle
29. pronator profundus muscle
30. right cranial (anterior) vena cava in pleuro-pericardial septum
31. thoracic rib
32. right pleural cavity
33. dorsal condyle of humerus
34. right lung
35. dorsal root ganglion
36. feather papilla
37. left cranial (anterior) vena cava in pleuro-pericardial septum
38. biceps brachii muscle
39. humerus
40. deltoid major muscle
41. extensor indicis longus muscle
42. bronchus
43. left brachiocephalic artery
44. cervical air sac
45. left common carotid artery
46. right common carotid artery
47. right brachiocephalic artery
48. flexor carpi ulnaris muscle
49. pronator muscle
50. head of rib (tuberculum)
51. dispophysis of vertebra
52. pronator superficialis muscle
53. flexor carpi ulnaris muscle
54. trunk of pulmonary arteries
55. trunk of carotid and brachiocephalic arteries
56. right atrium
57. ulnimetacarpalis ventralis muscle
58. bronchus
59. left pleural cavity
60. left atrium
61. interatrial septum (with perforations)
62. semilunar valves of pulmonary trunk
63. aortic arch
64. pleuro-pericardial septum

Downloaded from Vet-eBooks.com

Plate 167

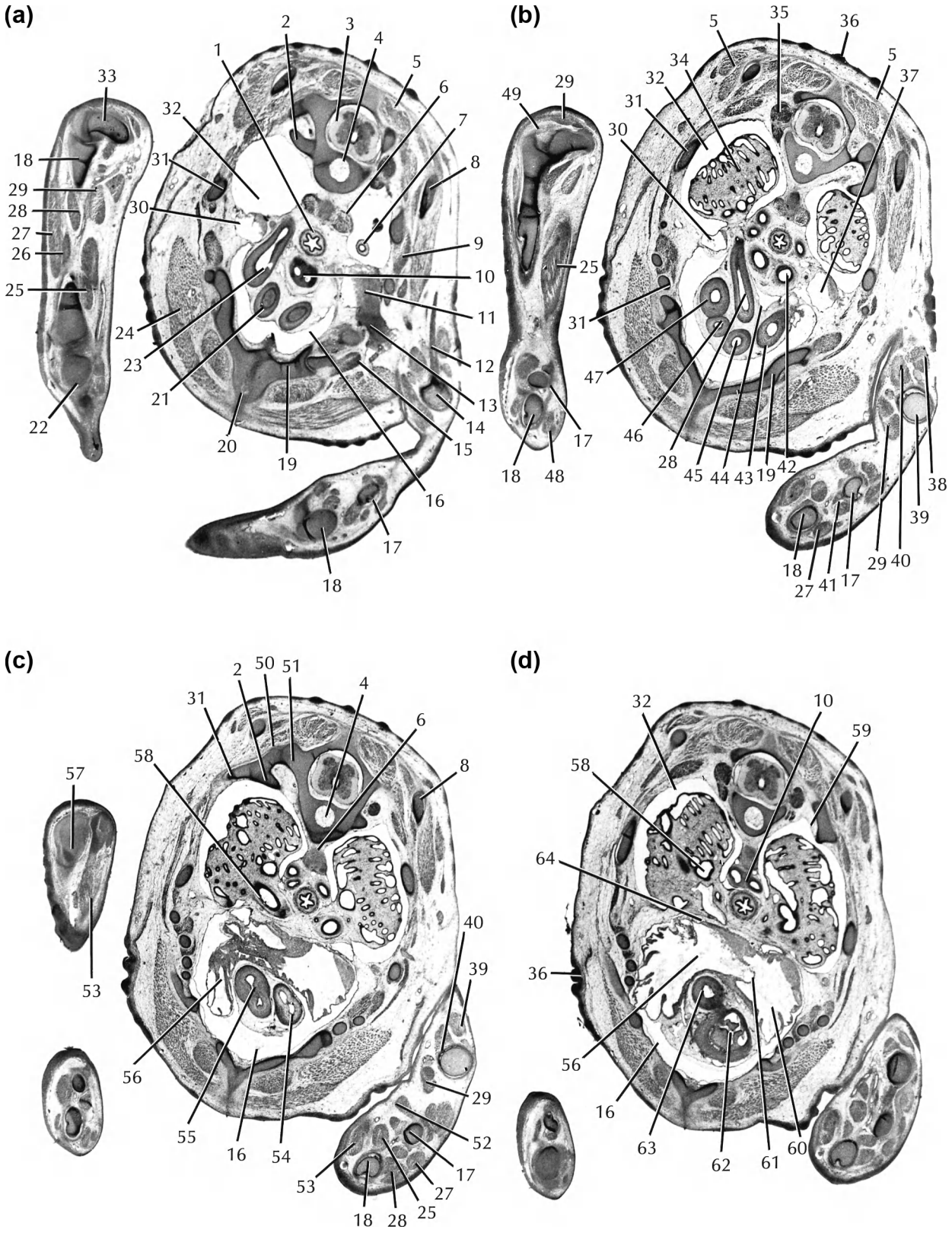

Downloaded from Vet-eBooks.com

Plate 168 Stage 35 (day 9) TS

(a) Enlargement of part of *plate 167a* to show left and right common carotid arteries: × 150

(b) Enlargement of part of *plate 167b* to show interatrial septum: × 100

p = perforations in interatrial septum

Downloaded from Vet-eBooks.com

Plate 168

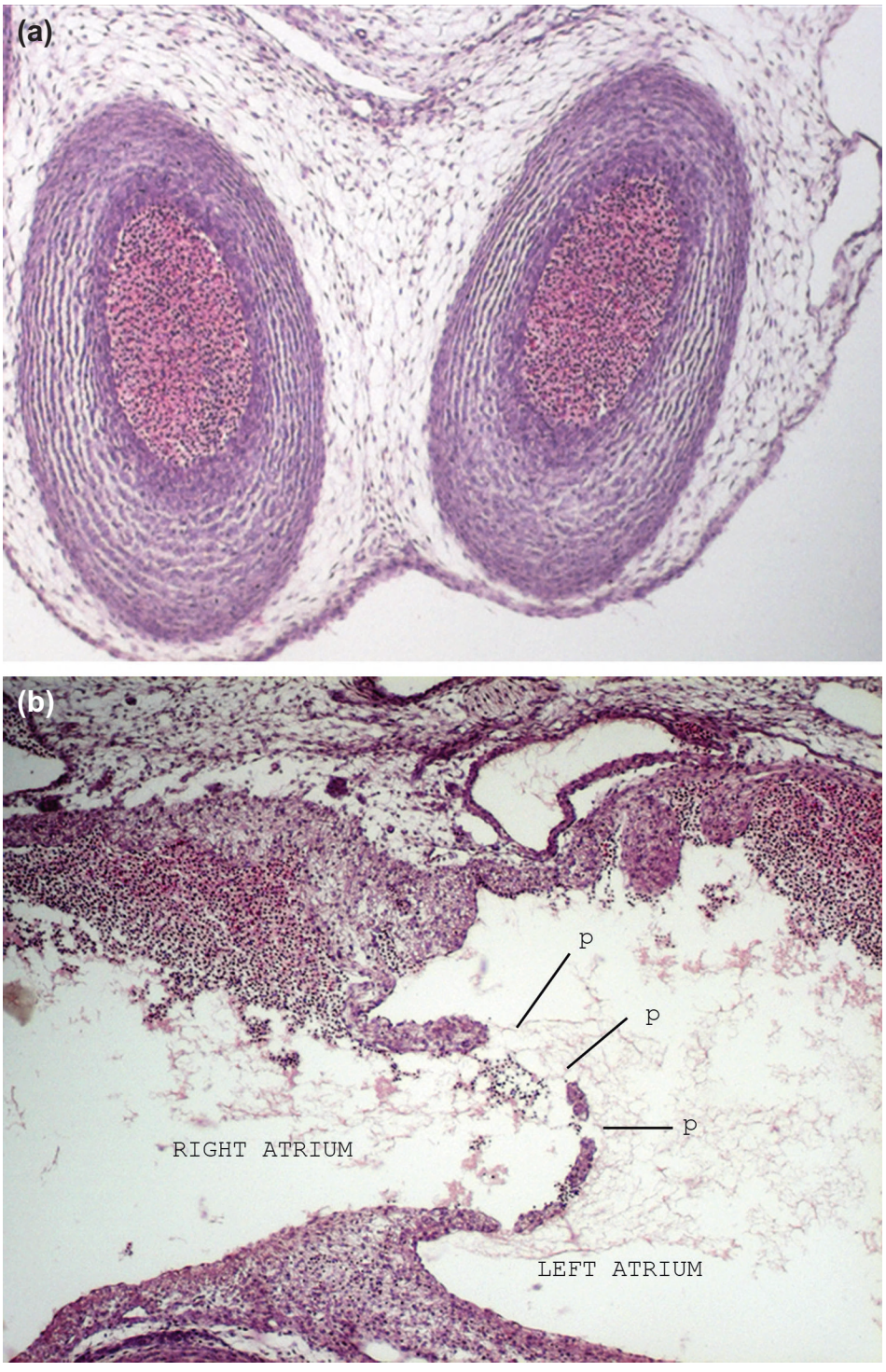

Downloaded from Vet-e-Books.com

Plate 169 Stage 35 (day 9) TS

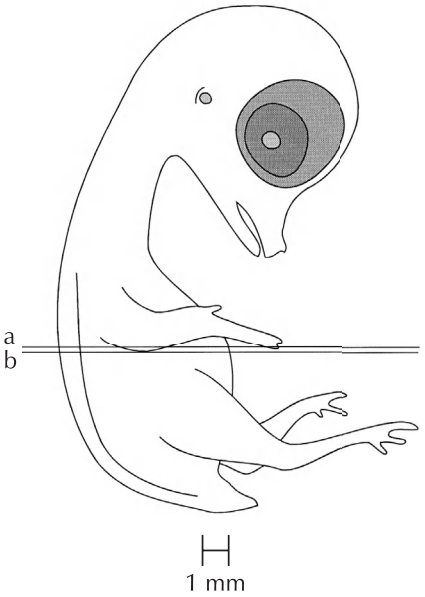

Transverse sections (TS): (a, b) × 18

1. head of vertebral rib
2. rhomboideus superficialis muscle
3. neural arch of vertebra
4. dorsal aorta
5. oesophagus
6. bronchus
7. vertebral rib
8. lung
9. left pleural cavity
10. junction of anterior thoracic air sac and mesobronchus
11. flexor digitorum profundus muscle
12. ulnametacarpalis dorsalis muscle
13. pronator muscle
14. sternal rib
15. left atrium
16. left ventricle
17. sinus venosus
18. pericardial cavity
19. bulbus arteriosus
20. interatrial septum
21. right atrio-ventricular canal
22. right atrium
23. supracoracoideus muscle
24. lobe of right atrium
25. oblique externus abdominis muscle
26. intercostal muscle
27. right pleural cavity
28. dorsal root ganglion
29. sympathetic ganglion
30. pneumo-enteric recess
31. lobulation of left atrium
32. articular surface of ulna
33. interventricular septum
34. right ventral hepatic cavity
35. right lobe of liver
36. pleuro-peritoneal septum
37. omphalo-mesenteric artery

Downloaded from Vet-eBooks.com

Plate 169

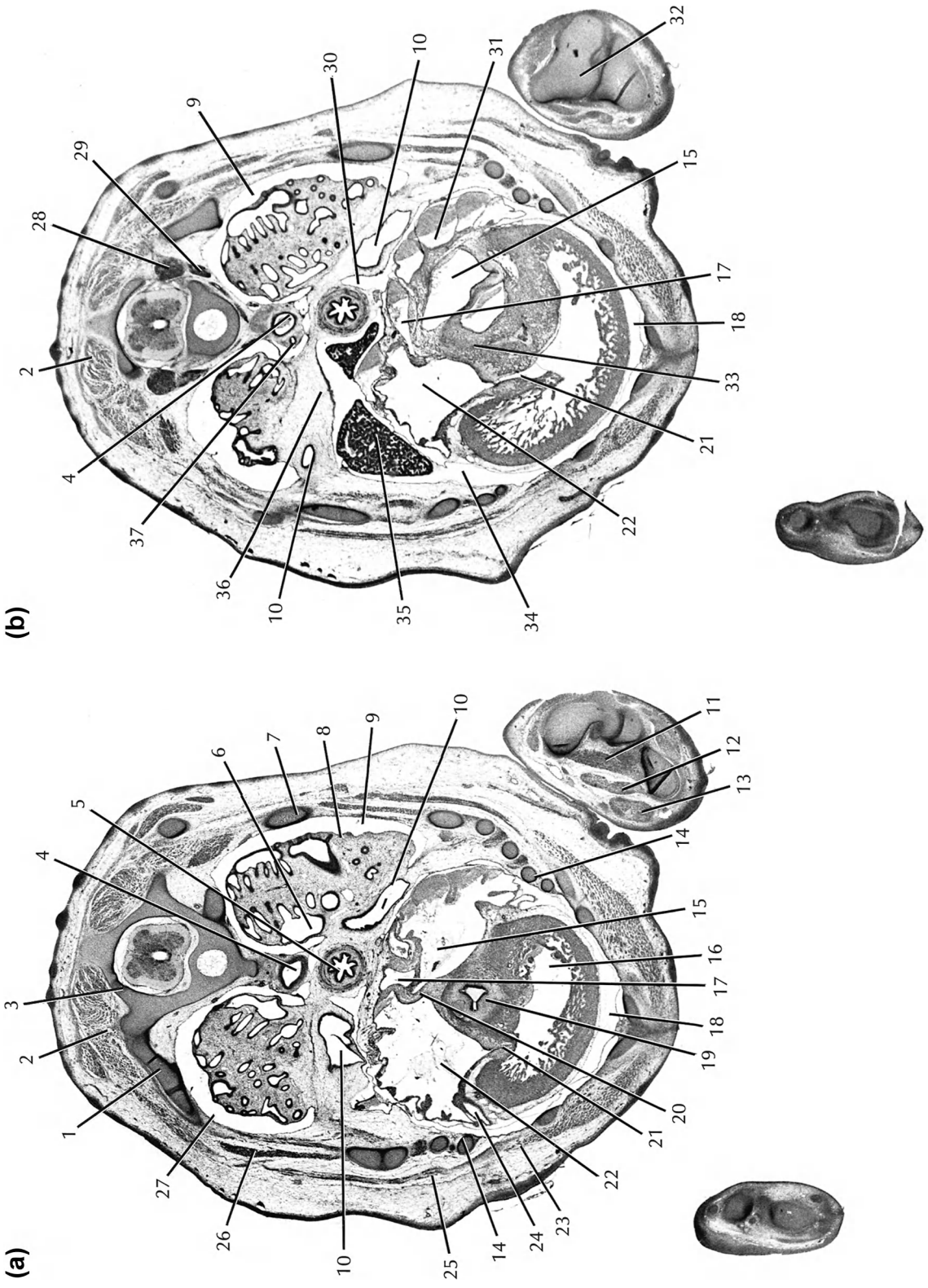

Downloaded from Vet-eBooks.com

Plate 170 Stage 35 (day 9) TS

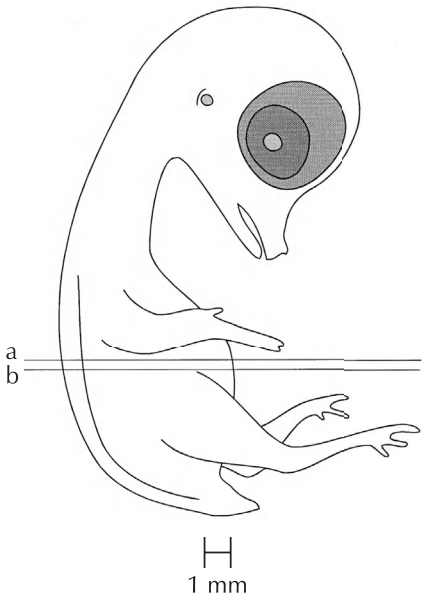

Transverse sections (TS): (a, b) × 18

1. right subcardinal vein
2. omphalo-mesenteric artery
3. dorsal aorta
4. rhomboideus superficialis muscle
5. transverse process of rib
6. coeliac artery
7. pleural cavity
8. oesophagus
9. left lung
10. dorsal hepatic cavity
11. sternal rib
12. lobes of left atrium
13. wing
14. left atrio-ventricular canal
15. left ventricle
16. right ventricle
17. sinus venosus
18. right atrium
19. caudal (posterior) vena cava
20. right lobe of liver
21. ventral hepatic cavity
22. horizontal hepatic ligament
23. right anterior thoracic air sac
24. right oviduct (Mullerian duct)
25. right pleuro-peritoneal septum
26. mesonephros
27. dorsal root ganglion
28. left pleuro-peritoneal septum
29. proventriculus
30. anterior thoracic air sac
31. anterior left lobe of liver
32. pericardium
33. interventricular septum
34. left hepatic vein
35. right hepatic vein
36. femur
37. metanephros
38. right foot

Downloaded from Vet-eBooks.com

Plate 170

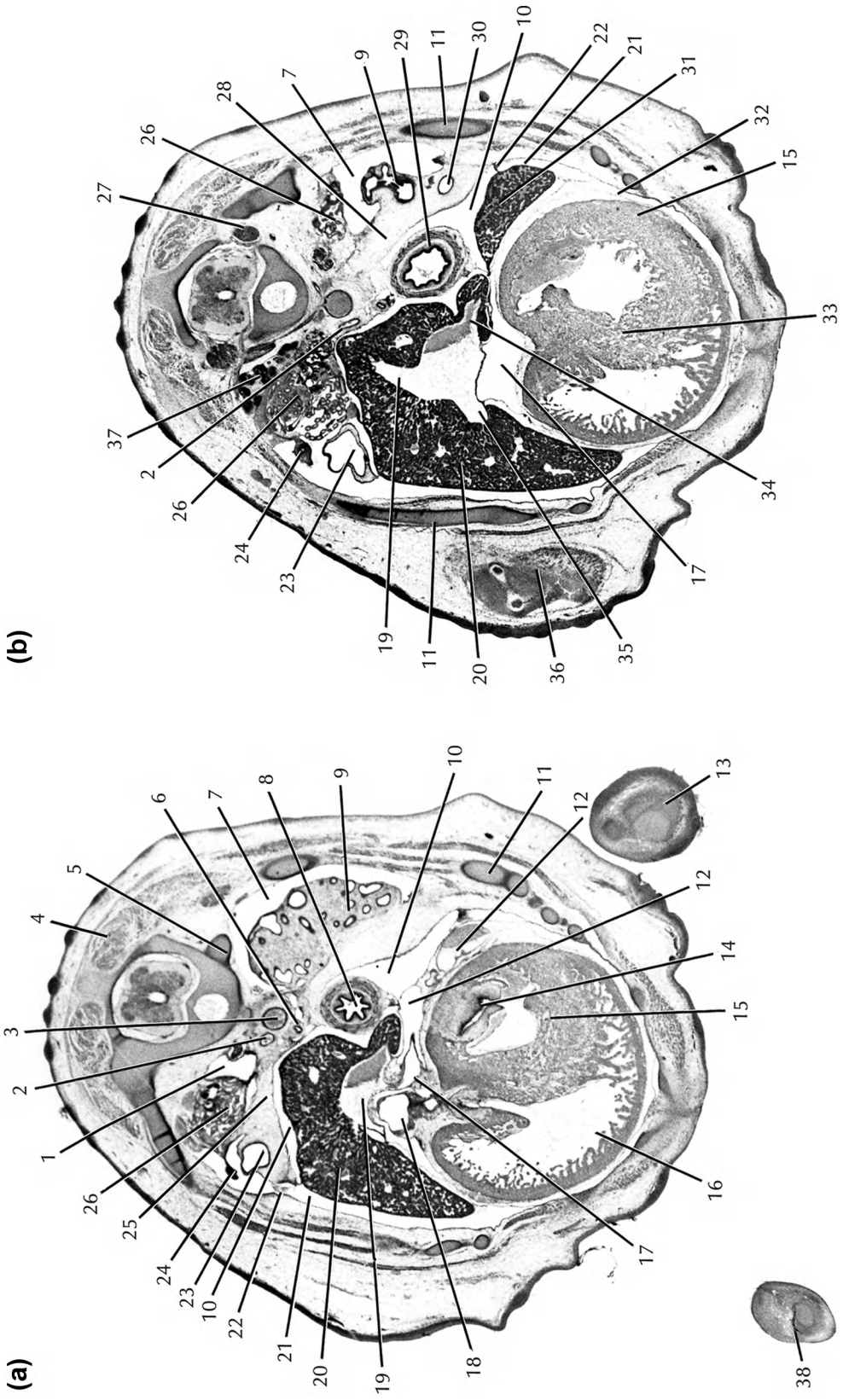

Downloaded from Vet-eBooks.com

Plate 171 Stage 35 (day 9) TS

(a) Enlargement of section adjacent to *plate 170b*: × 150

(b) Enlargement of section adjacent to *plate 176a*: × 100

1. metanephros
2. mesonephros
3. right mesonephric (Wolffian) duct close to mesonephros
4. right metanephric duct
5. descending right mesonephric (Wolffian) duct
6. right oviduct (Mullerian duct)
7. coelom
8. right omphalo-mesenteric artery

Downloaded from Vet-eBooks.com

Plate 171

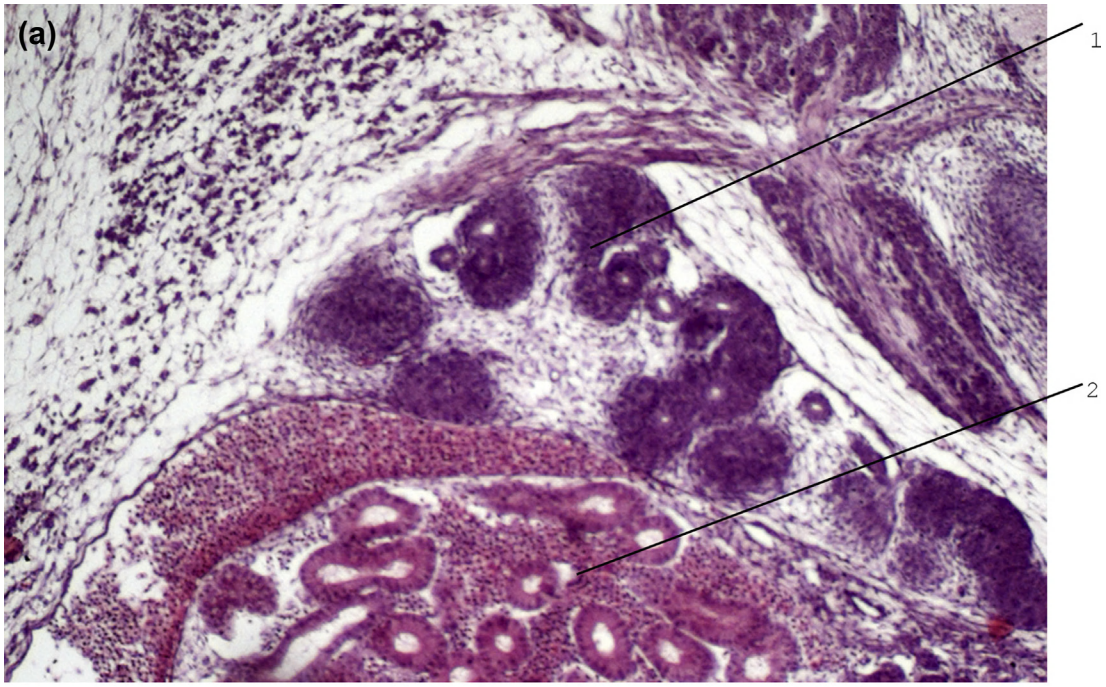

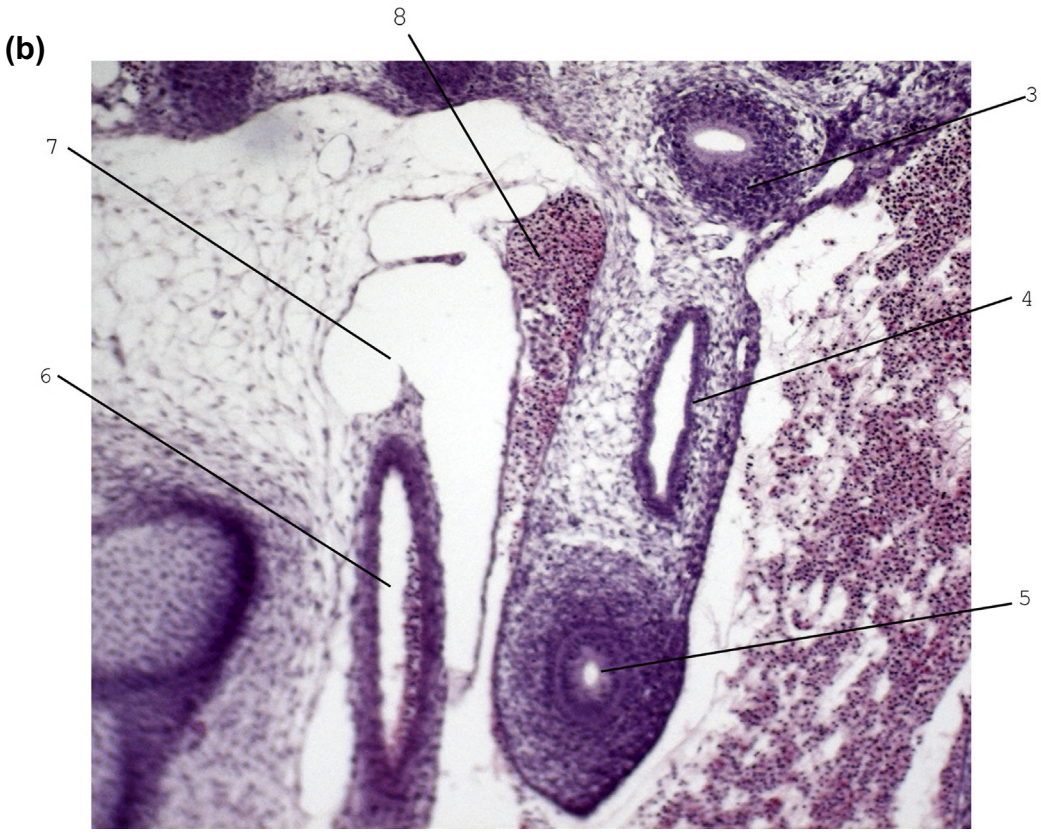

Downloaded from Vet-eBooks.com

Plate 172 Stage 35 (day 9) TS

(a) Enlargement of part of *plate 174a*: × 70

(b) Enlargement of part of *plate 170b*: × 100

(c) Enlargement of part of *plate 174b*: × 130

1. right ovary, mainly medulla
2. coelom
3. left ovary with extensive cortex
4. omphalo-mesenteric artery
5. left mesonephros
6. left oviduct (Mullerian duct)
7. right mesonephros
8. right oviduct (Mullerian duct)

Downloaded from Vet-eBooks.com

Plate 172

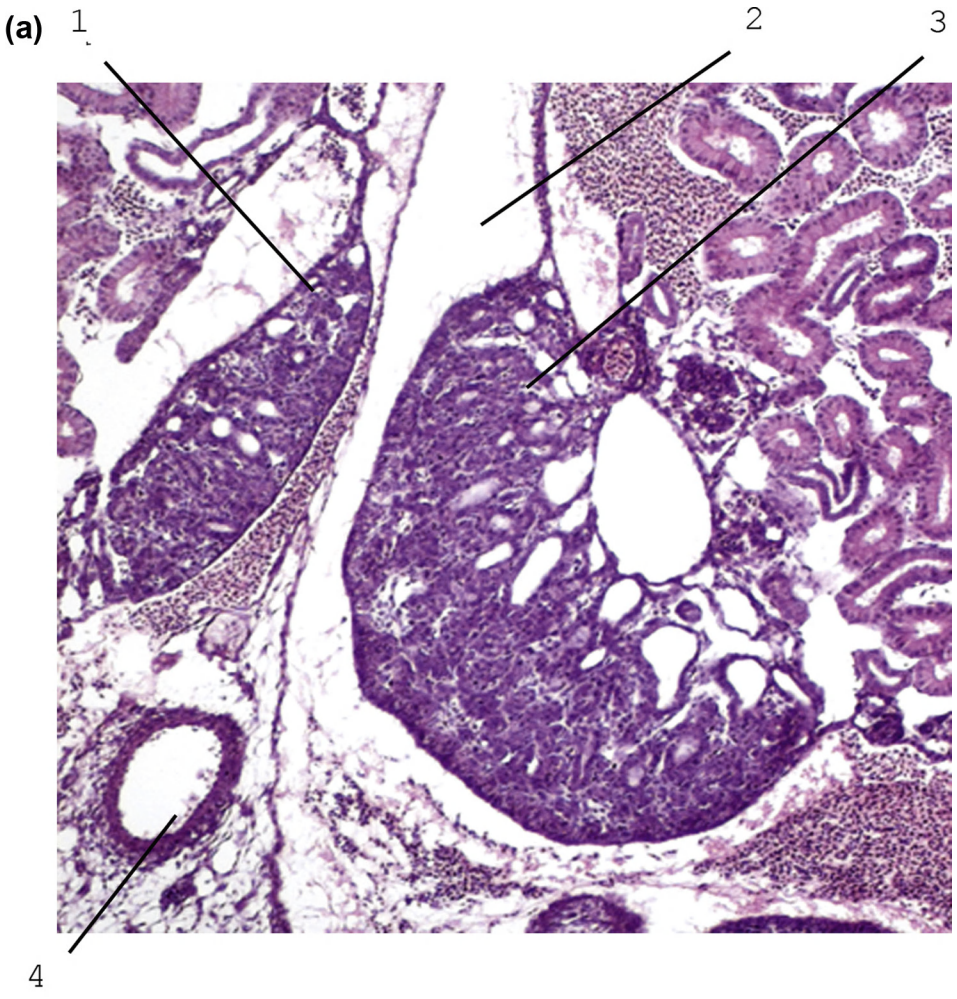

Downloaded from Vet-eBooks.com

Plate 173 Stage 35 (day 9) TS

(a) Enlargement of section adjacent to *plate 170a*: × 125

(b) Enlargement of part of *plate 170b*: × 90

1. omphalo-mesenteric artery
2. left lung
3. dorsal aorta
4. oesophagus
5. right lobe of liver
6. right pleuro-peritoneal septum
7. right pleural cavity
8. proventriculus
9. ventral mesentery
10. dorsal hepatic cavity
11. left anterior lobe of liver
12. wall of left ventricle
13. right anterior lobe of liver
14. hepatic vein

Downloaded from Vet-eBooks.com

Plate 173

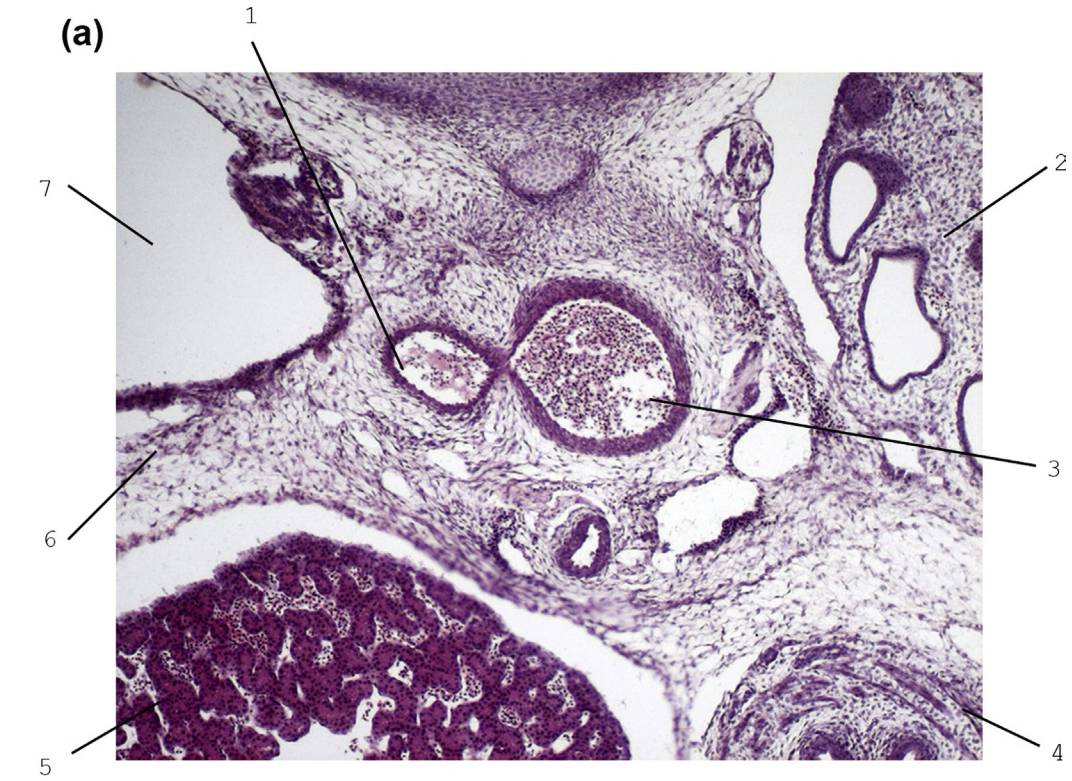

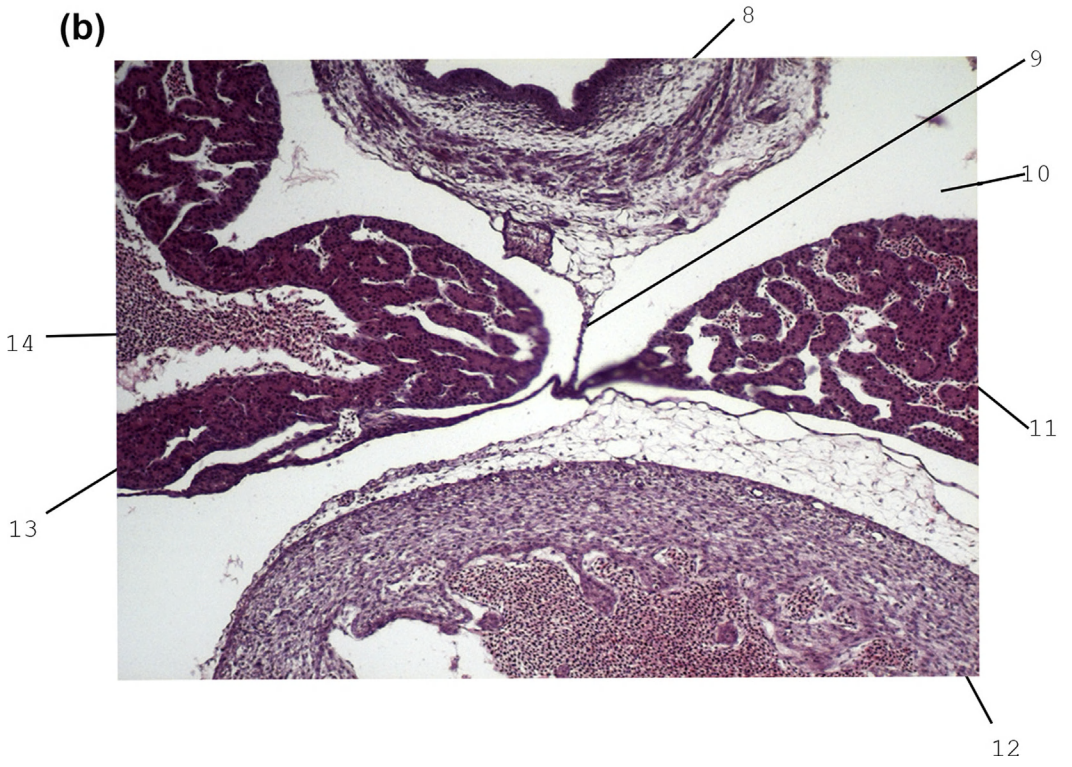

Downloaded from Vet-eBooks.com

Plate 174 Stage 35 (day 9) TS

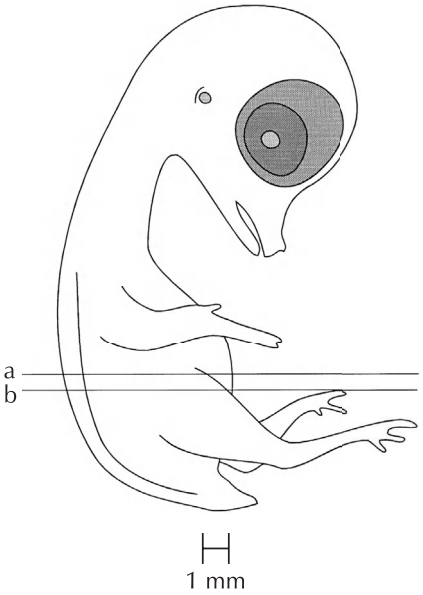

Transverse sections (TS): (a, b) × 18

1. right ovary
2. dorsal aorta
3. ilium
4. left ovary
5. left oviduct (Mullerian duct)
6. mesonephros
7. spleen
8. oblique externus abdominis muscle
9. proventriculus
10. oblique internus abdominis muscle
11. hepatic vein
12. left posterior lobe of liver
13. common bile duct
14. right lobe of liver
15. caudofemoralis muscle
16. femur
17. pancreas
18. trunk of brachial plexus
19. omphalo-mesenteric artery
20. dorsal root ganglion
21. neural arch of vertebra
22. notochord
23. iliotrochantericus cranialis muscle
24. ischiofemoralis muscle
25. iliotibialis lateralis muscle
26. iliotrochantericus caudalis muscle
27. ambiens muscle
28. femorotibialis lateralis muscle
29. puboischiofemoralis muscle
30. femoral artery
31. femorotibialis internus muscle
32. flexor cruris medialis muscle
33. condyle of femur
34. tibiotarsus
35. extensor digitorum longus muscle
36. gastrocnemius muscle
37. coeliac artery
38. duodenum
39. fibula
40. iliofibularis muscle
41. right oviduct (Mullerian duct)

Downloaded from Vet-eBooks.com

Plate 174

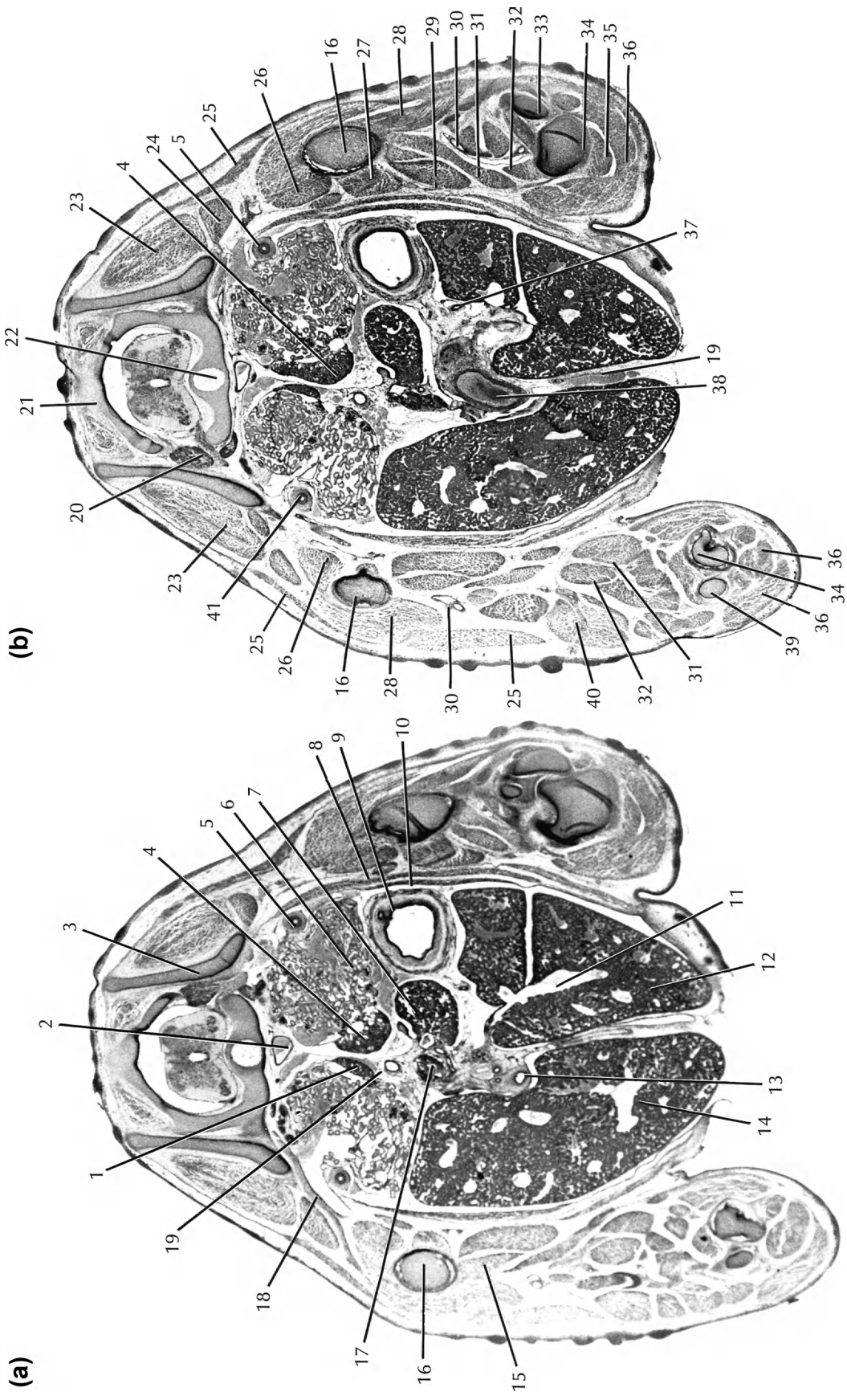

Downloaded from Vet-eBooks.com

Plate 175 Stage 35 (day 9) TS

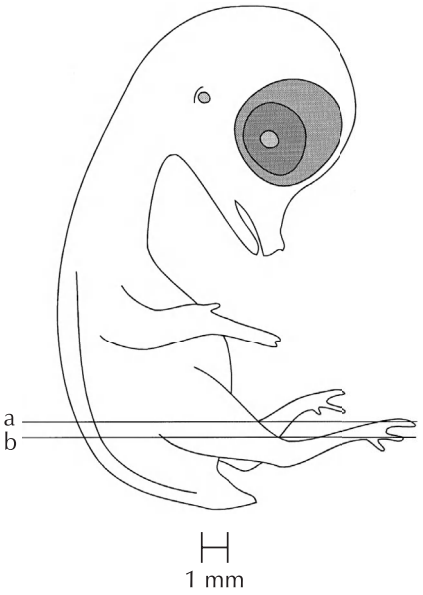

Transverse sections: (a, b) × 18

1. neural arch of vertebra
2. dorsal aorta
3. dorsal root ganglion
4. metanephros
5. oviduct (Mullerian duct)
6. femoral artery
7. mesonephros
8. feather bud
9. cranio-dorsal muscles of gizzard
10. left posterior lobe of liver
11. ventral lateral muscles of gizzard
12. loops of small intestine
13. right lobe of liver
14. duodenum
15. ischium
16. aponeurosis of iliotibialis lateralis muscle
17. femur
18. head of femur
19. ilium
20. iliotrochantericus muscle
21. spinal nerve, part of sacral plexus
22. left renal vein
23. acetabulum
24. trochanter of femur
25. oblique internus abdominus muscle
26. gastrocnemius muscle
27. fibula
28. tibiotarsus
29. tibialis cranialis muscle
30. extensor digitorum longus muscle
31. lumen of gizzard
32. blood extravasated from umbilicus during preparation
33. gastric branch of coeliac artery
34. flexor hallucis brevis muscle
35. peroneus muscle
36. extensor brevis digitorum IV muscle
37. extensor hallucis longus muscle
38. blood extravasated into coelom
39. fibularis nerve
40. ischiofemoralis muscle
41. right renal vein

Downloaded from Vet-eBooks.com

Plate 175

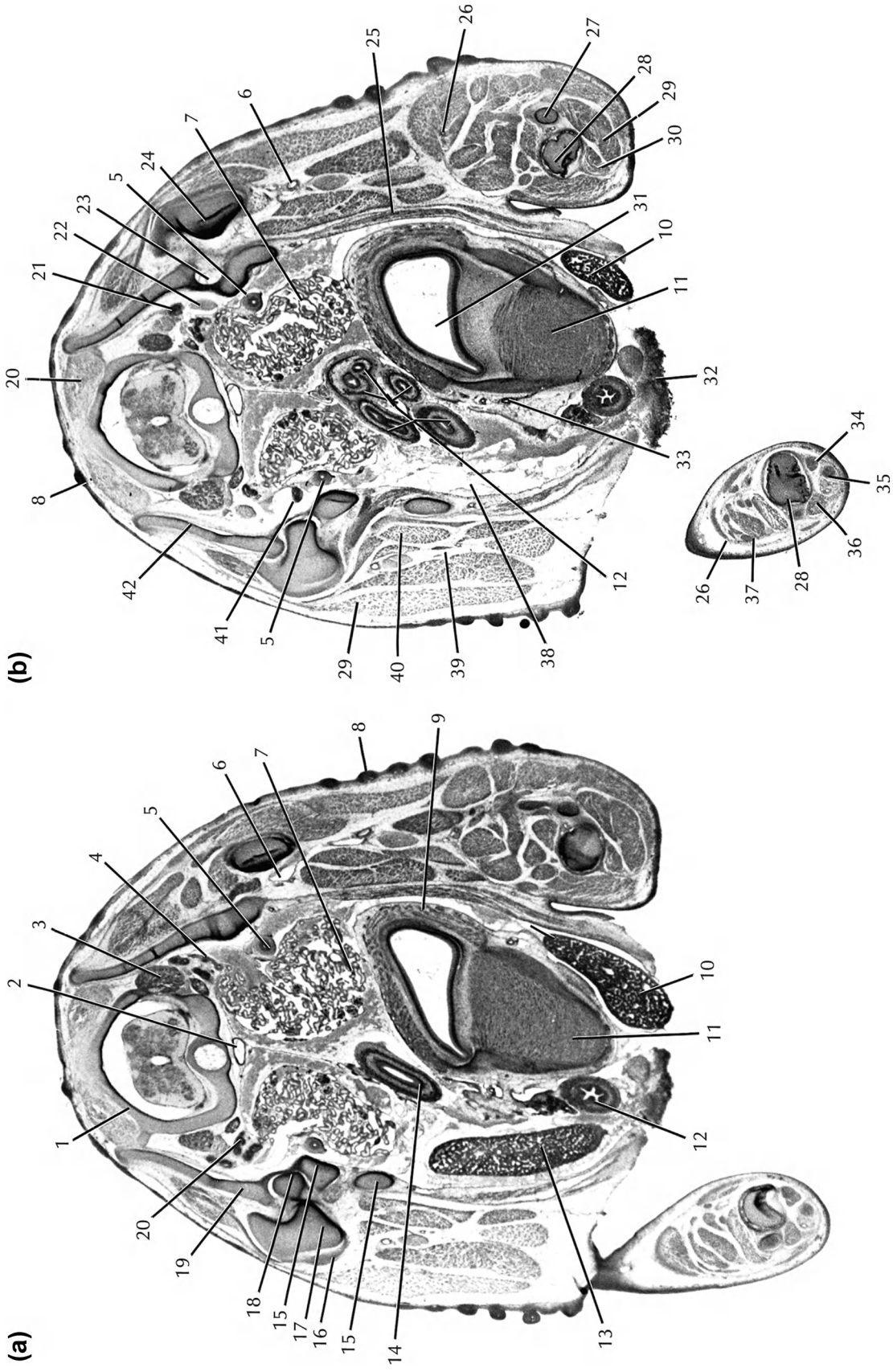

Downloaded from Vet-e-Books.com

Plate 176 Stage 35 (day 9) TS

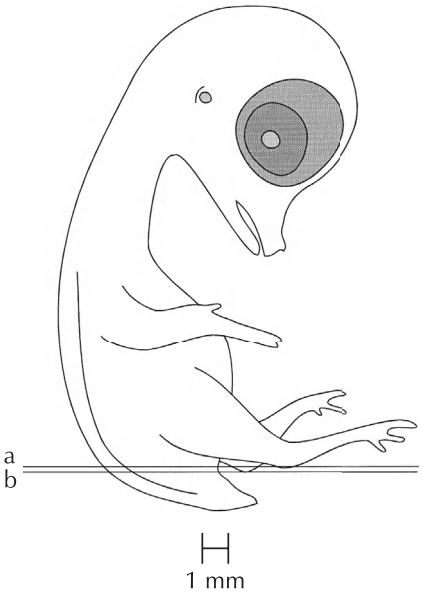

Transverse sections (TS): (a, b) × 20

1. dorsal root ganglion
2. metanephros
3. dorsal aorta
4. metanephric duct
5. left omphalo-mesenteric artery
6. left nephric (mesonephric, Wolffian) duct
7. iliofibularis muscle
8. obturator muscle
9. left oviduct (Mullerian duct)
10. left iliotibialis muscle
11. extravasated blood
12. flexor cruris lateralis muscle
13. rectum
14. pubis
15. yolk sac stalk
16. cloaca
17. right omphalo-mesenteric artery
18. right oviduct (Mullerian duct)
19. right nephric (mesonephric, Wolffian) duct
20. pectineal process
21. right renal vein
22. spinal nerve
23. transverse process of rib
24. tibiotarsus
25. left renal vein
26. ischium

Downloaded from Vet-eBooks.com

Plate 176

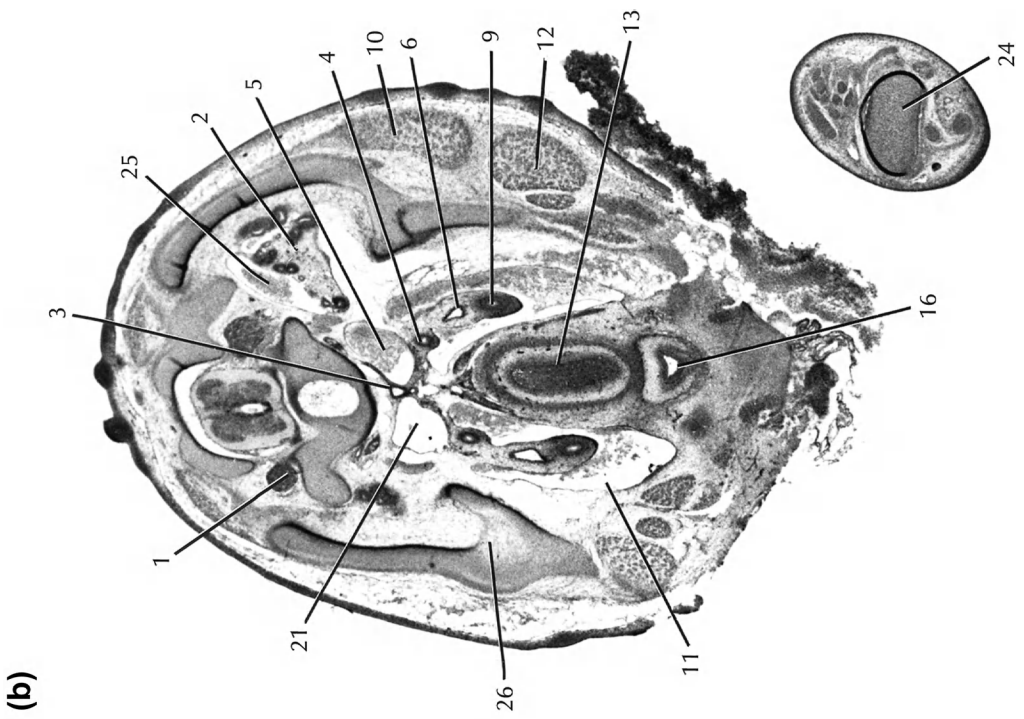

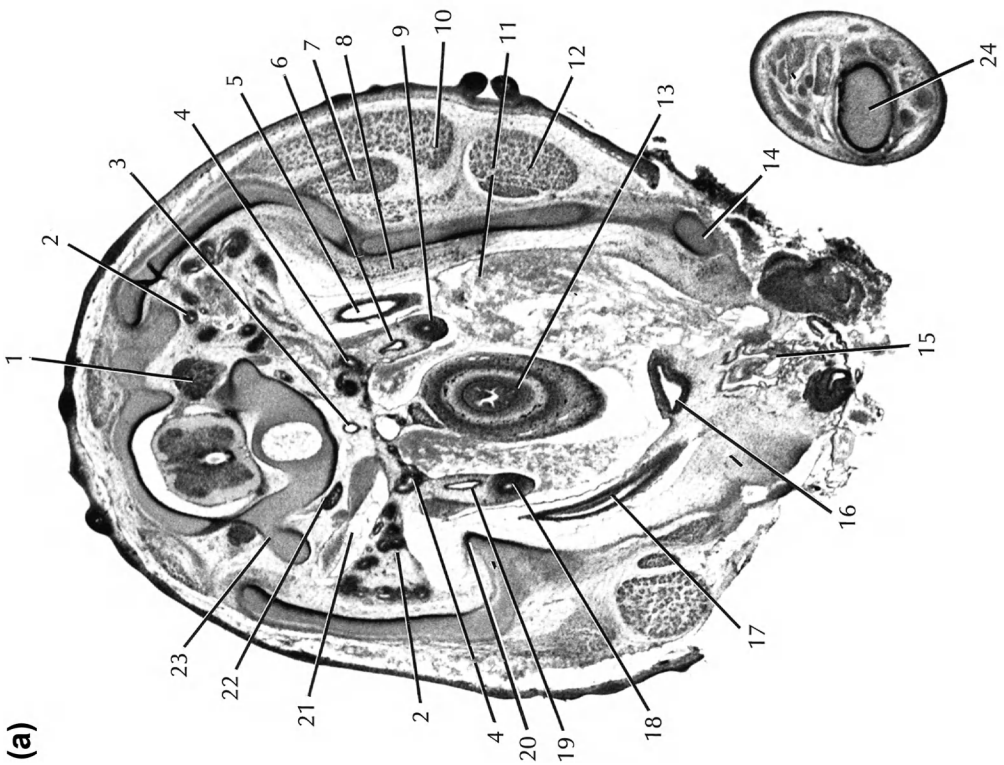

Downloaded from Vet-eBooks.com

Plate 177 Stage 35 (day 9) TS

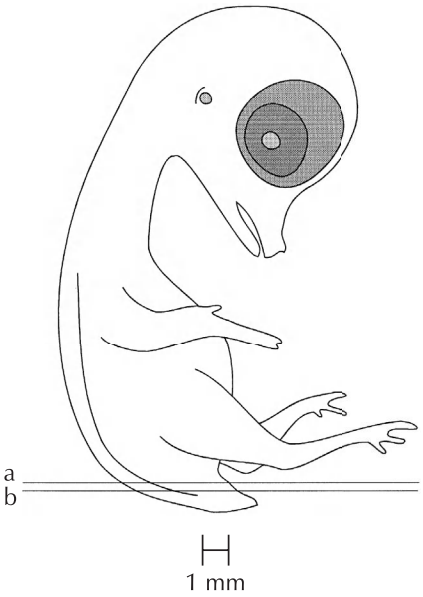

Transverse sections (TS): (a, b) × 20

1. right omphalo-mesenteric artery
2. dorsal aorta
3. left omphalo-mesenteric artery
4. metanephros
5. left metanephric duct
6. renal artery
7. nephric (mesonephric, Wolffian) duct
8. extravasated blood in posterior coelom
9. rectum
10. left oviduct (Mullerian duct)
11. extravasated blood
12. levator cloacae muscle
13. cloaca
14. sphincter cloacae
15. cloacal membrane
16. right oviduct (Mullerian duct)
17. interiliac vein anastomosis
18. right metanephric duct
19. ischium
20. hindlimb
21. iliotibialis lateralis muscle
22. remains of notochord
23. mesenchymal mass connecting vertebra to girdle

24–28. tail muscles

29. lateralis caudae muscle
30. remnant of right posterior cardinal vein

Downloaded from Vet-eBooks.com

Plate 177

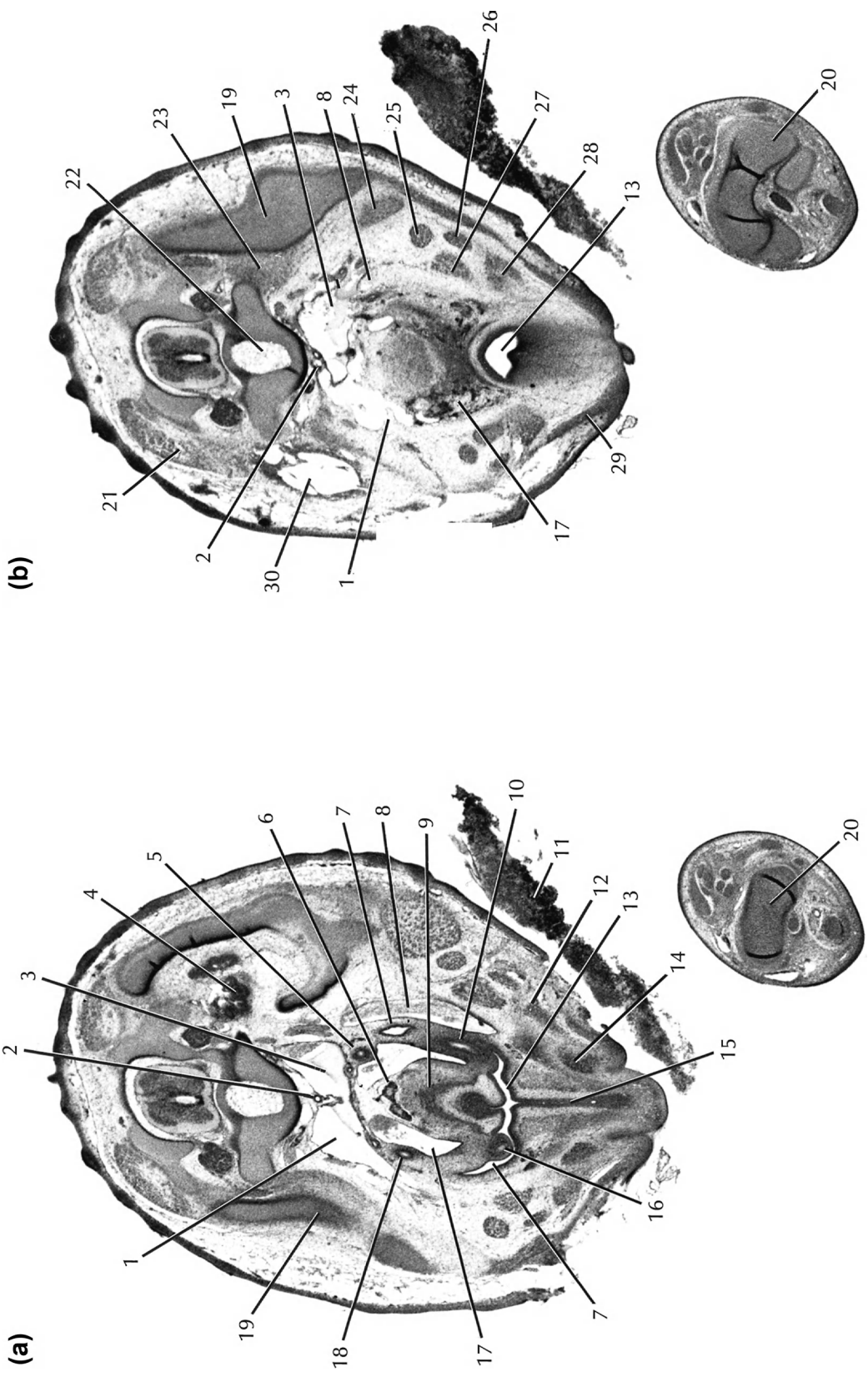

Downloaded from Vet-eBooks.com

Plate 178 Stage 36 (day 10)

Illustrations of a day 10 embryo from Keibel (1900).

(a) Head dissected free from body: × 10

(b) Whole embryo: × 6

1. external nostril
2. future eyelid
3. scleral ossicle
4. external ear
5. lens seen through cornea
6. feather buds
7. umbilicus

Downloaded from Vet-eBooks.com

Plate 178

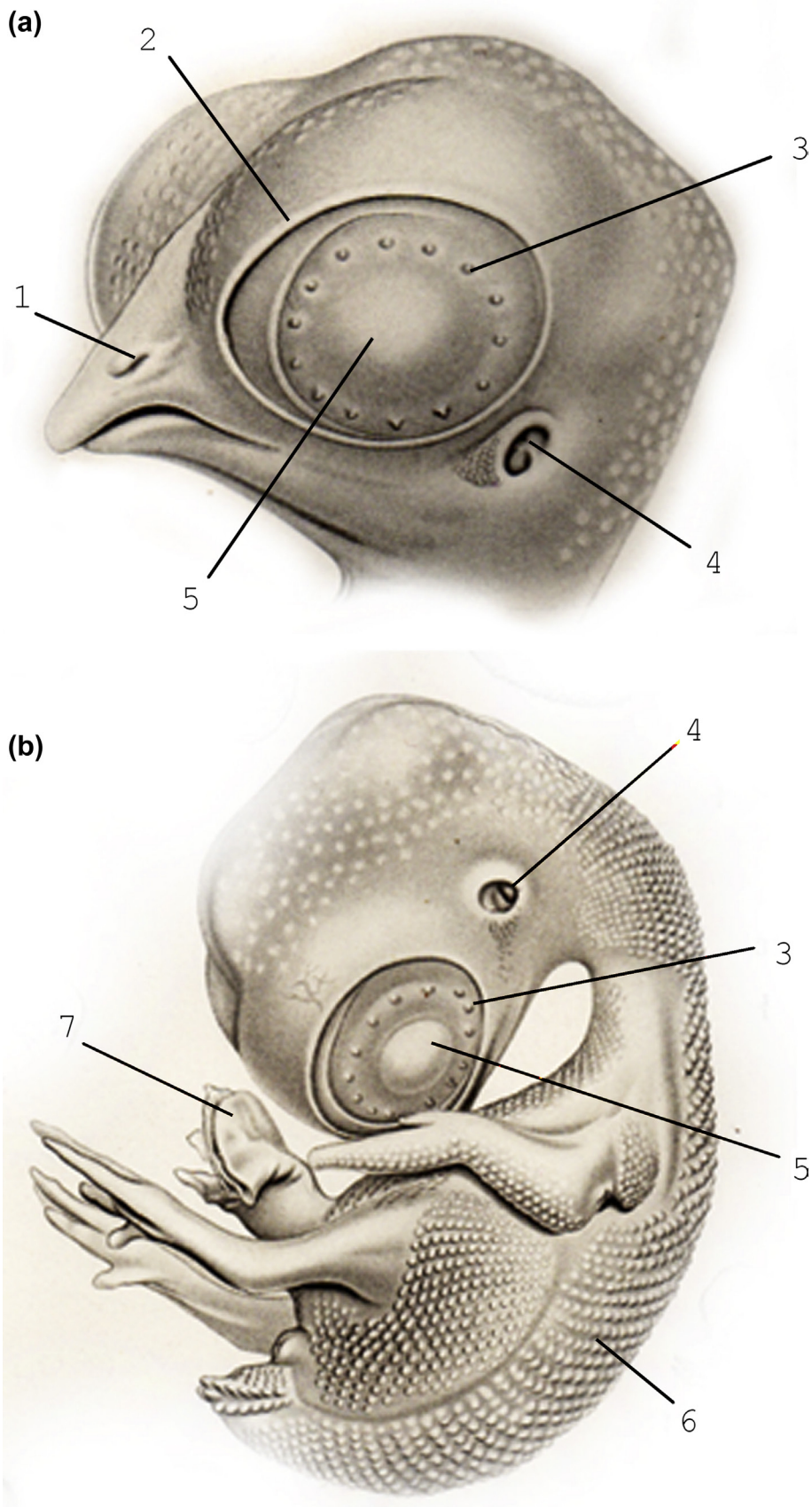

Downloaded from Vet-e-Books.com

Plate 179 Stage 36 (day 10) LS: coronal

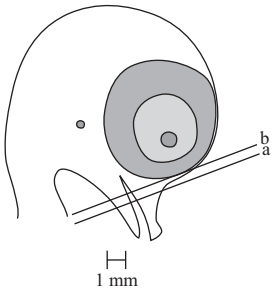

Coronal (frontal) sections through the head:

(a) × 25

(b) × 12

1. nasal glands
2. nasal septum
3. roof of nasal capsule
4. left rostral nasal conchae
5. base of nasal septum
6. palatine bone
7. left Meckel's cartilage
8. oral cavity
9. lower jaw
10. right Meckel's cartilage
11. right maxillary process
12. right rostral nasal conchae
13. left external eye muscle
14. tongue
15. paraglossal (entoglossal) cartilage
16. internal nasal choana
17. nasal cavity
18. eyelid
19. wall of right eye

Downloaded from Vet-eBooks.com

Plate 179

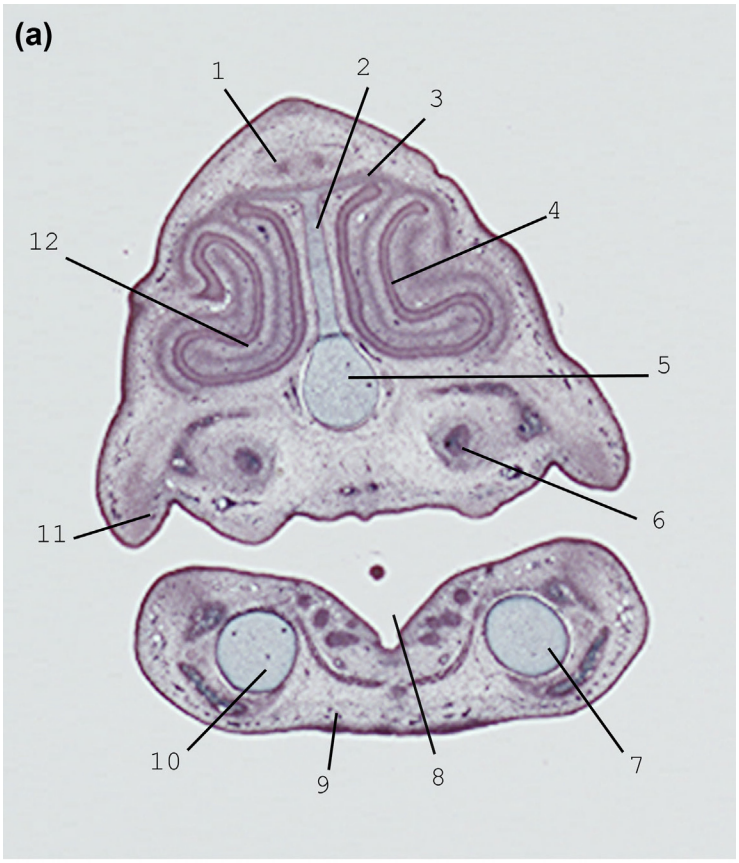

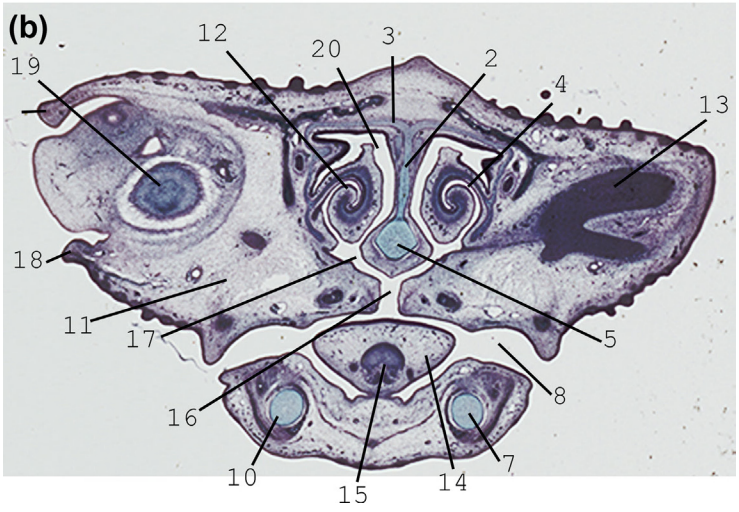

Downloaded from Vet-eBooks.com

Plate 180 Stage 36 (day 10) LS: coronal

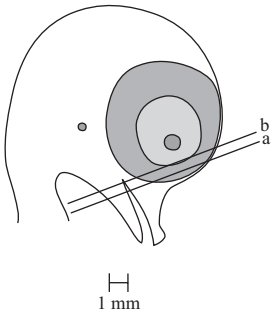

Coronal (frontal) sections through the head:

(a) × 10

(b) × 12

1. base of nasal septum
2. nasal septum
3. nasal cavity
4. left eyelid
5. median nasal concha
6. left palatine bone
7. left mandible
8. left Meckel's cartilage
9. tongue
10. paraglossal (entoglossal) cartilage
11. right hypoglossus obliquus (paraglossus branchialis) muscle
12. median nasal choana
13. oral cavity
14. right eyelid
15. cornea
16. pigmented retina of left eye
17. iris of left eye
18. anterior chamber of left eye
19. cerato-brachial cartilage
20. right palatine bone
21. right mandible
22. vitreous of right eye

Downloaded from Vet-eBooks.com

Plate 180

(a)

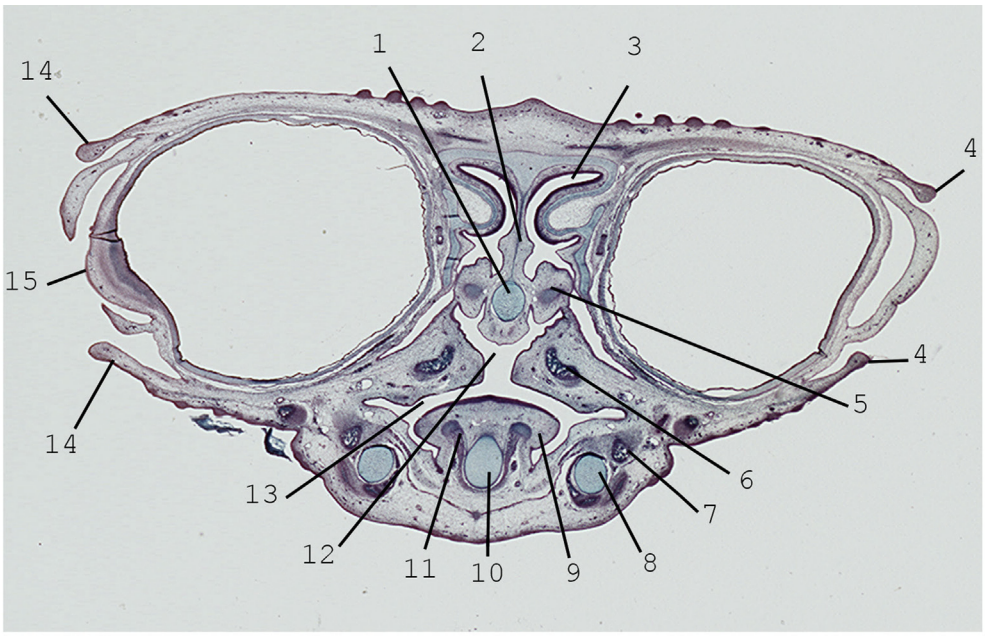

(b)

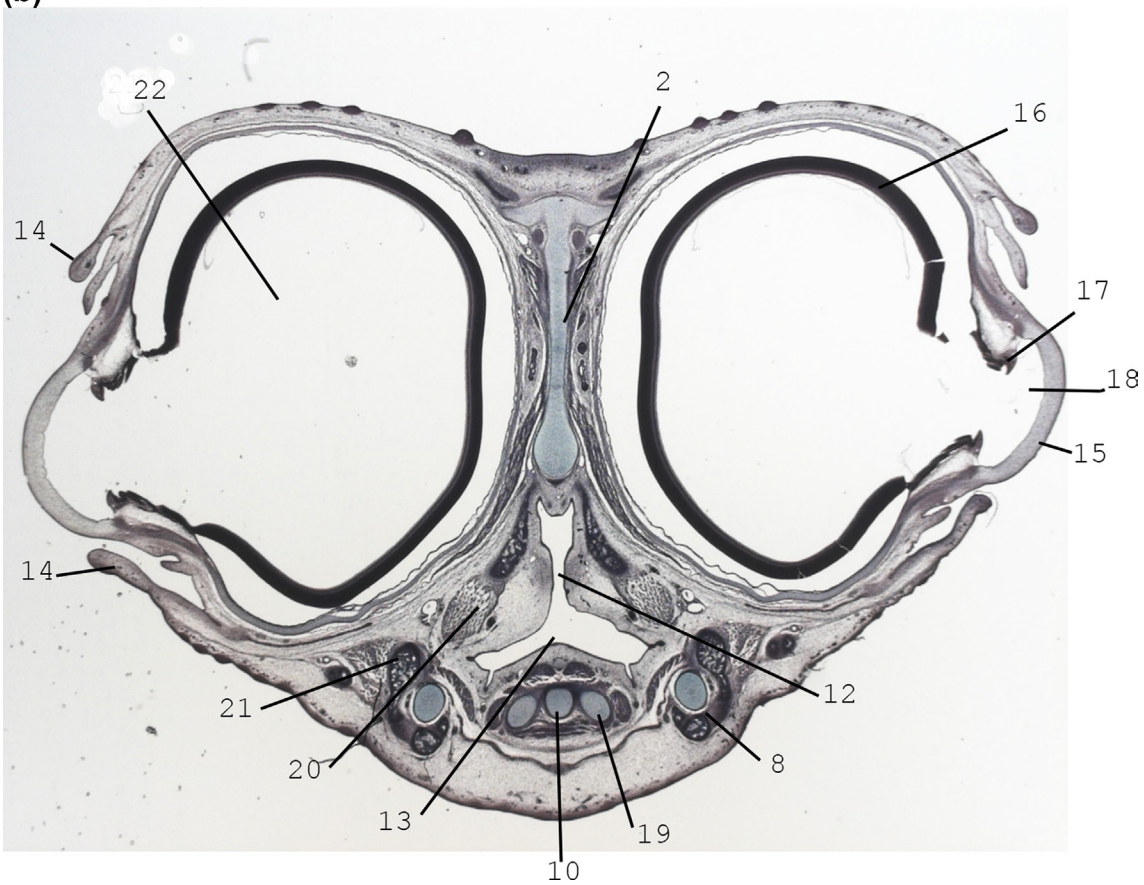

Downloaded From Vet-eBooks.com

Plate 181 Stage 36 (day 10) LS: coronal

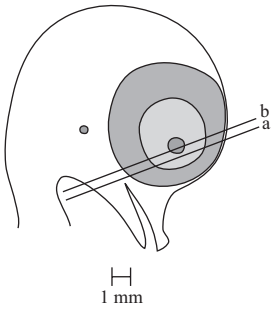

Coronal (frontal) sections through the head:

(a) × 10

(b) × 12

1. vitreous of right eye
2. pyramidalis muscle
3. interorbital septum
4. vitreous of left eye
5. pigmented retina
6. iris
7. cornea
8. left mandible
9. internal nasal choana
10. left Meckel's cartilage
11. pharynx
12. greater horn of left hyoid
13. tongue muscles (hypoglossus obliquus muscle)
14. paraglossal (entoglossal) cartilage
15. greater horn of right hyoid
16. right Meckel's cartilage
17. right mandible
18. parasphenoid rostrum
19. base of interorbital septum
20. anterior chamber of right eye
21. lens of right eye
22. eyelid of right eye
23. lens of left eye (not shown in (a) because lost in preparation)
24. pecten of left eye
25. palatine bone
26. copulo-paraglossal cartilage

Downloaded from Vet-eBooks.com

Plate 181

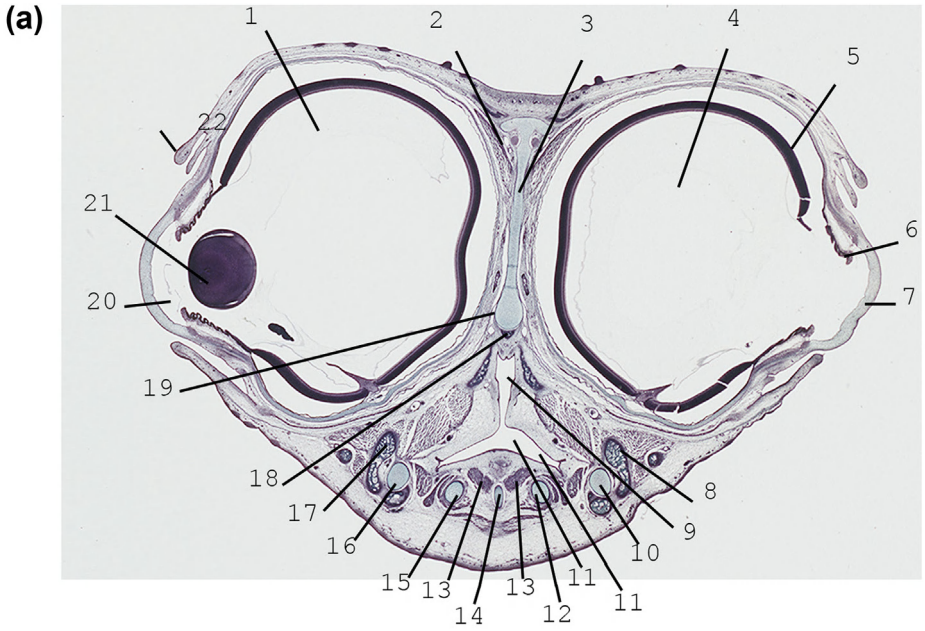

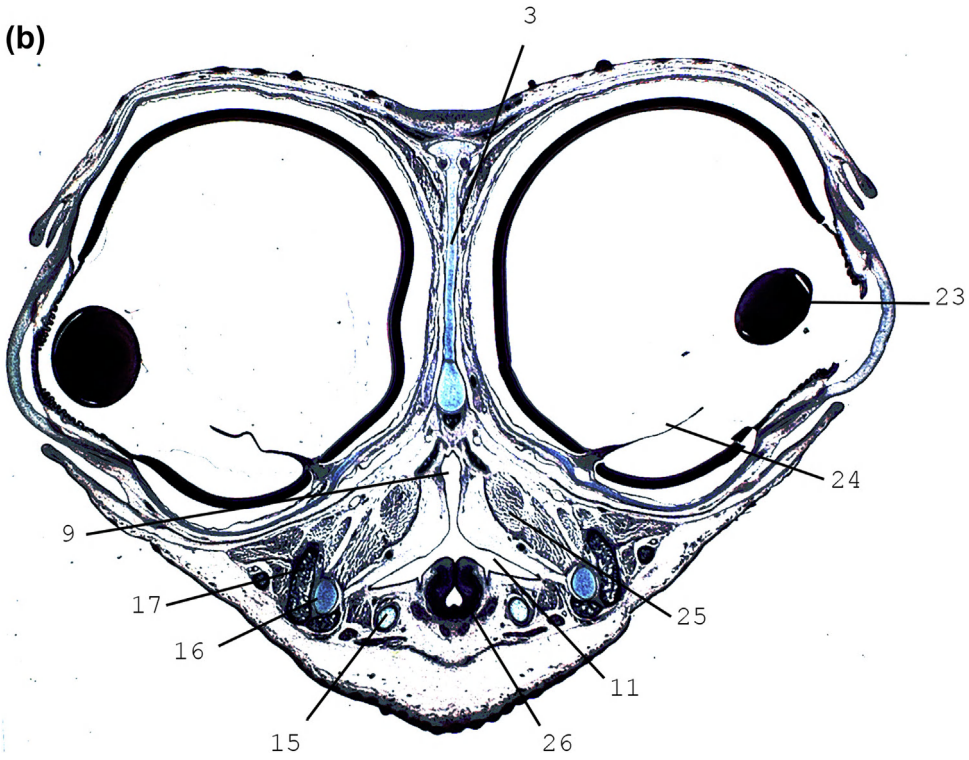

Downloaded from Vet-eBooks.com

Plate 182 Stage 36 (day 10) LS: coronal

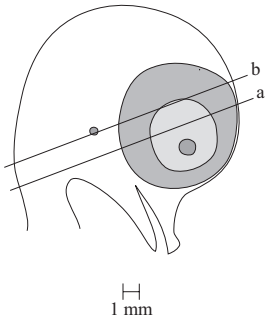

Coronal (frontal) sections through the head: (a, b) × 10

1. Pyramidalis membranae nictitansis muscle
2. right olfactory bulb
3. interorbital septum
4. left olfactory bulb
5. optic chiasma
6. left vitreous chamber
7. intrapolar cartilage
8. left palato-pterygoid cartilage
9. Meckel's cartilage
10. left cerato-branchial cartilage
11. left carotid artery
12. left rectus capitis ventralis muscle
13. right carotid
14. right cerato-branchial cartilage
15. right palato-pterygoid cartilage
16. inferior oblique eye muscle
17. trabecular cartilage
18. right vitreous chamber
19. pigmented retina
20. left cerebral hemisphere
21. parachordal cartilage (future basisphenoid)
22. left tympanic membrane
23. left jaw muscle
24. perilymphatic duct
25. hypophysis in basicranial fenestra
26. odontoid process of axis
27. spinal cord
28. atlas
29. rectus capitis lateralis muscle
30. right jaw muscle
31. right tympanic membrane
32. external auditory meatus
33. right middle ear
34. ventral oblique eye muscle

Downloaded from Vet-eBooks.com

Plate 182

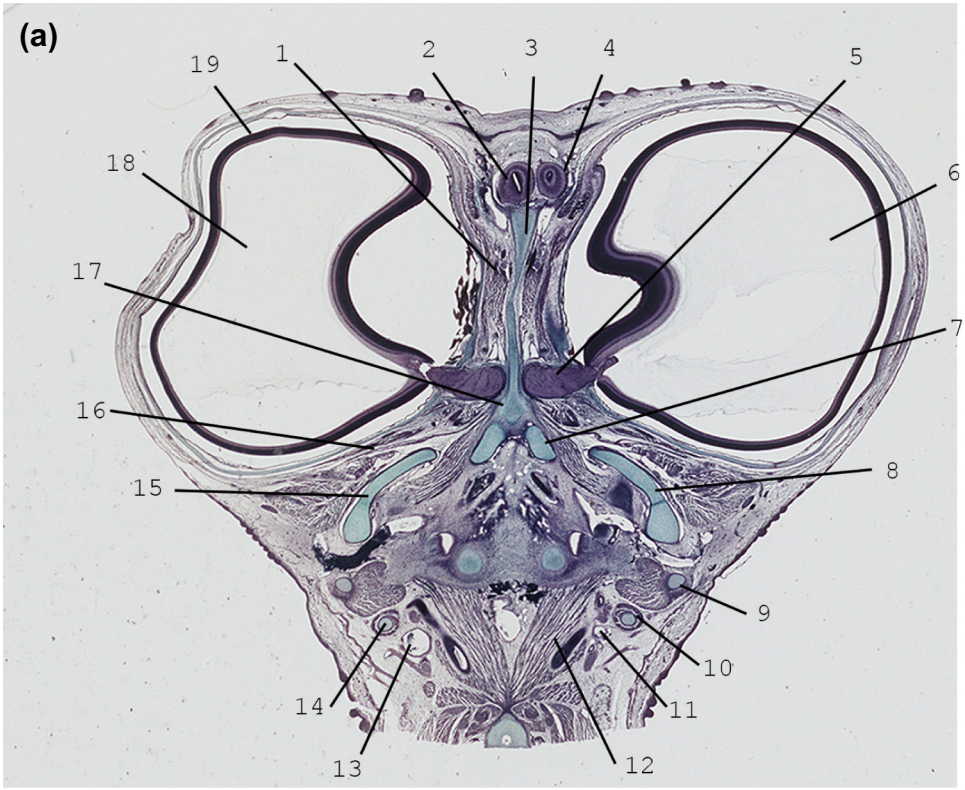

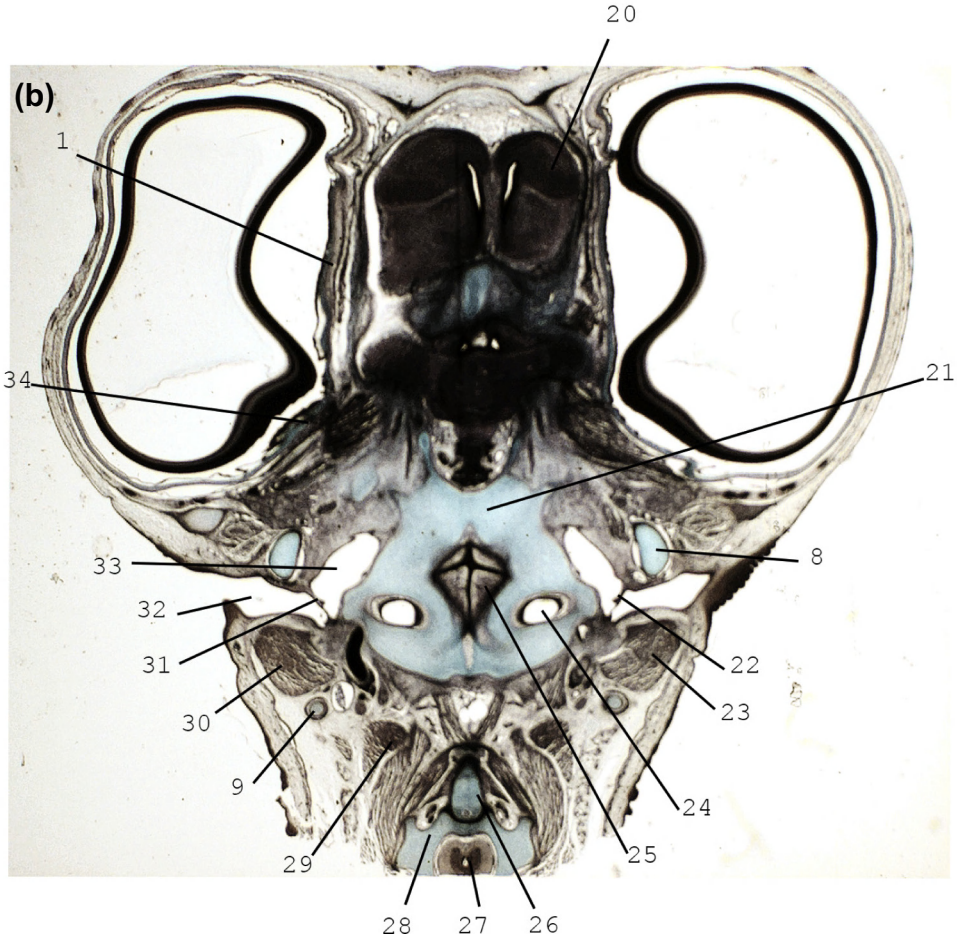

Downloaded from Vet-eBooks.com

Plate 183 Stage 36 (day 10) LS: coronal

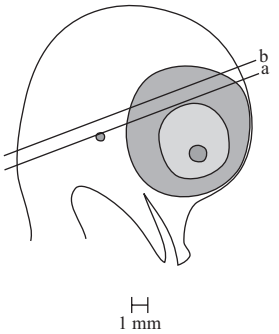

Coronal (frontal) sections through the head: (a, b) × 10

1. right cerebral hemisphere
2. left lateral ventricle
3. third ventricle
4. vitreous chamber
5. left optic lobe
6. trigeminal (cranial nerve V) ganglion
7. post orbital cartilage
8. occipital condyle
9. spinal cord
10. arch of atlas
11. basal plate
12. inner ear
13. medulla oblongata
14. right optic lobe
15. encephalon
16. left lateral ventricle
17. pineal organ
18. left cerebral hemisphere
19. left choroid
20. third ventricle
21. wall of mesencephalon
22. left inner ear
23. vestibulo-cochlearis nerve
24. fourth ventricle
25. thick wall of myelencephalon
26. rectus capitis dorsalis muscle
27. right inner ear
28. otic capsule
29. right choroid
30. feather bud

Downloaded from Vet-eBooks.com

Plate 183

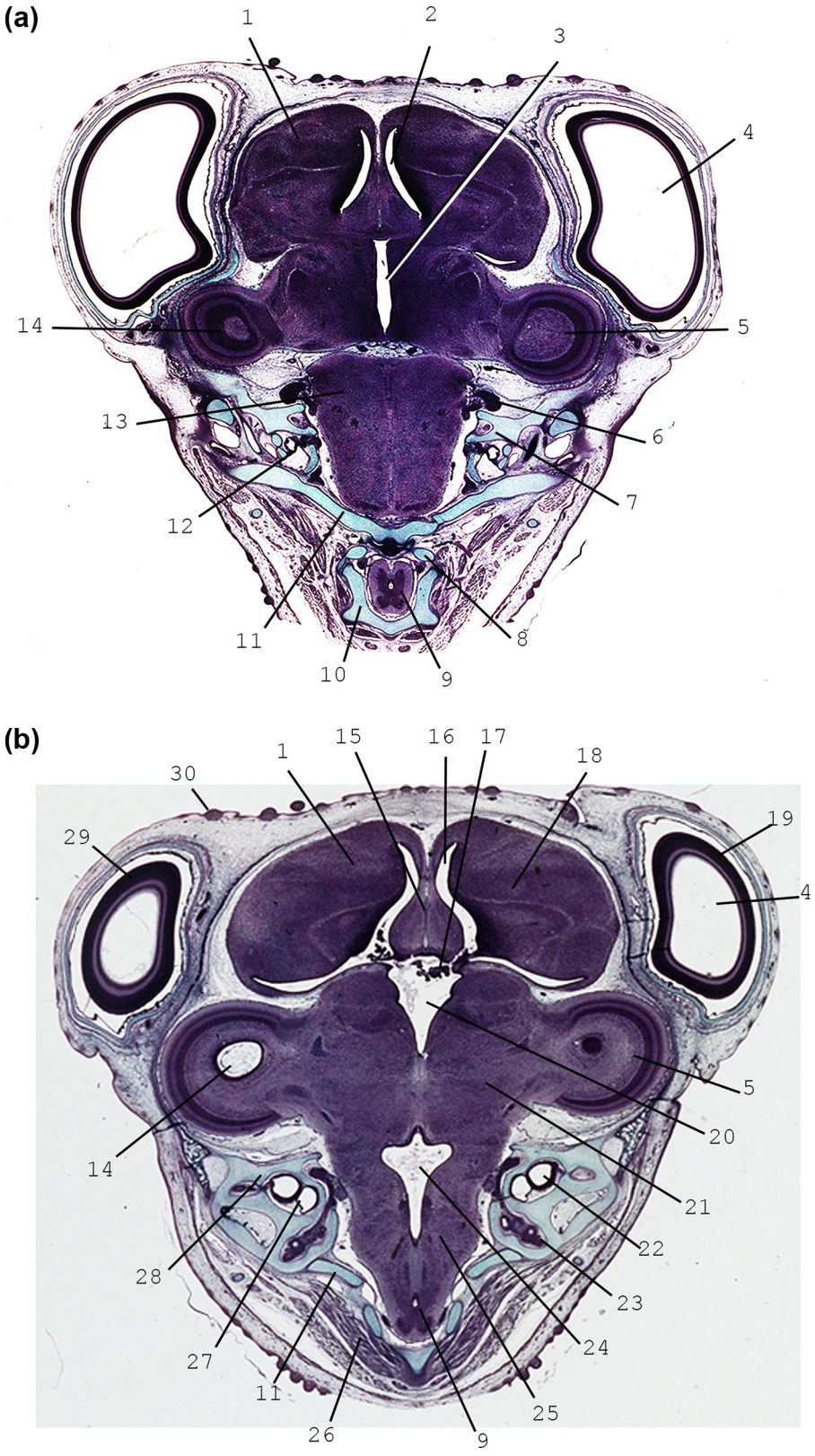

Downloaded from Vet-eBooks.com

Plate 184 Stage 37 (day 11) LS: sagittal

Longitudinal (sagittal) section in plane of diagram: × 5

In this series, plates 184, 187 and 188 show sections near the mid-sagittal plane (see diagram), whilst plates 185, 186, 189 and 190 show sections lateral to this plane.

Sections for plates 184–190 kindly supplied by D A Ede

1. cartilage of orbitosphenoid bone
2. arbor vitae of cerebellum
3. mesencephalon
4. edge of optic lobe
5. feather bud
6. frontal bone
7. cerebral hemisphere (ventricle)
8. dorsal rectus eye muscle
9. ventral rectus eye muscle
10. vitreous chamber of eye
11. dorsal oblique (superior) muscle
12. ventral oblique (inferior) muscle
13. oral cavity
14. nasal conchae
15. tongue
16. maxilla
17. egg tooth
18. dentary
19. trachea
20. pectoralis muscle
21. sternum
22. supracoracoideus muscle
23. truncus arteriosus
24. right atrium
25. right ventricle
26. sterno-cardiac diverticulum of interclavicular air sac
27. pericardial cavity
28. pericardium
29. liver
30. omphalo-mesenteric vein
31. herniated loop of intestine
32. right allantoic vein
33. gizzard wall
34. allantoic stalk
35. genital tubercle
36. cloaca
37. rectum
38. mesentery
39. metanephric kidney
40. dorsal aorta
41. testis
42. caudal (posterior) vena cava
43. intestine
44. spinal cord
45. longus colli ventralis muscle
46. oesophagus
47. feather
48. ninth cervical vertebra
49. rhomboideus supericialis muscle
50. latissimus dorsi muscle
51. adductor mandibulae externus muscle, pars temporalis
52. pontine flexure of medulla oblongata

Downloaded from Vet-eBooks.com

Plate 184

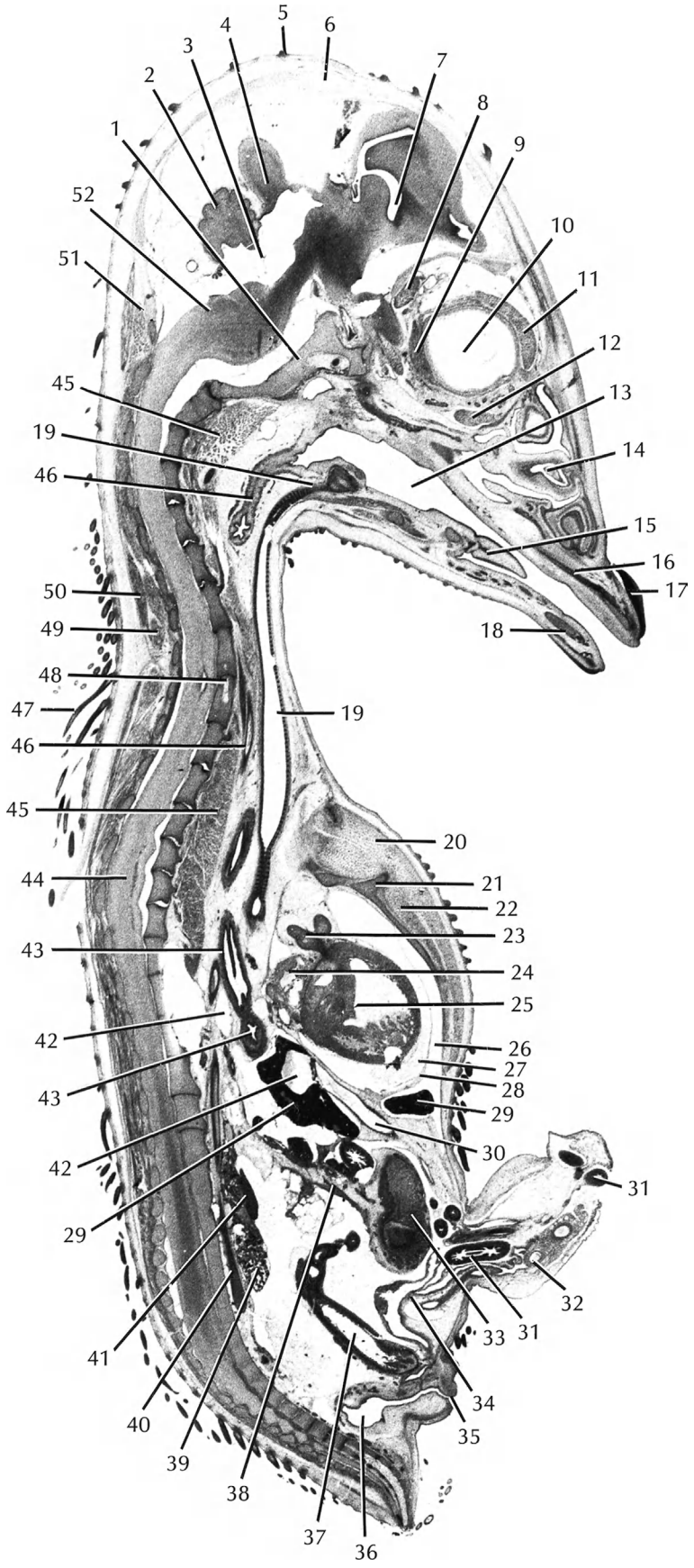

Downloaded from Vet-eBooks.com

Plate 185 Stage 37 (day 11) LS: sagittal

Longitudinal (sagittal) section in plane of diagram: × 7

Stained with alcian blue to show cartilage.

In this series, plates 184, 187 and 188 show sections near the mid-sagittal plane (see diagram), whilst plates 185, 186, 189 and 190 show sections lateral to this plane.

1. utriculus
2. otic capsule
3. optic tectum
4. cerebral hemisphere
5. vitreous body
6. epibranchial cartilage
7. edge of quadrate cartilage
8. ventral rectus eye muscle
9. pterygoid muscle
10. oral opening
11. lower lip (beak)
12. Meckel's cartilage
13. oesophagus
14. pectoralis muscle
15. sternum
16. atrium
17. ventricle
18. liver
19. extra-embryonic coelom
20. herniated gut
21. loop of gut
22. abdominal air sac
23. caudal vertebra
24. spinal cord in caudal region
25. synsacral vertebra
26. mesonephros
27. lung
28. spinal cord in thoracic region
29. thoracic vertebra
30. jugular vein
31. complexus muscle

Downloaded from Vet-eBooks.com

Plate 185

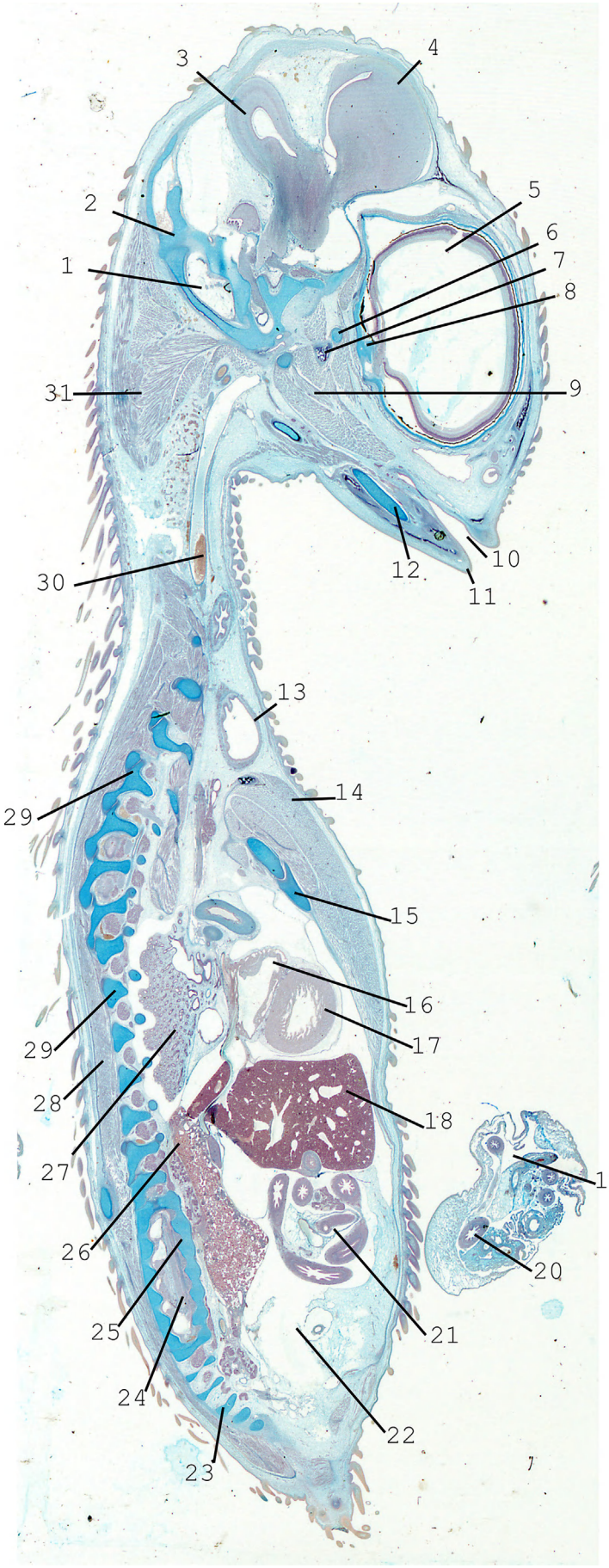

Downloaded from Vet-eBooks.com

Plate 186 Stage 37 (day 11) LS: sagittal

Londitudinal (sagittal) section in plane of diagram: × 6

Stained with alcian blue to show cartilage.

In this series, plates 184, 187 and 188 show sections near the mid-sagittal plane (see diagram), whilst plates 185, 186, 189 and 190 show sections lateral to this plane.

1. cerebellum
2. edge of optic lobe
3. cerebral hemisphere
4. cartilage primordium of orbito-sphenoid bone
5. orbital cartilage
6. jaw muscle
7. vitreous body of eye
8. palatine cartilage
9. Meckel's cartilage
10. oral opening
11. oesophagus
12. thyroid
13. pectoralis muscle
14. sternum
15. ventricle
16. liver
17. herniated gut in umbilical cord
18. retracted section of gut
19. ureteric duct
20. mesonephros
21. gonad
22. lung
23. duodenum
24. vertebral body
25. spinal cord
26. transverse process
27. feather
28. trachea
29. jugular vein
30. longus colli dorsalis muscle
31. cartilage primordium of exoccipital bone
32. foramen for Eustachian tube

Downloaded from Vet-eBooks.com

Plate 186

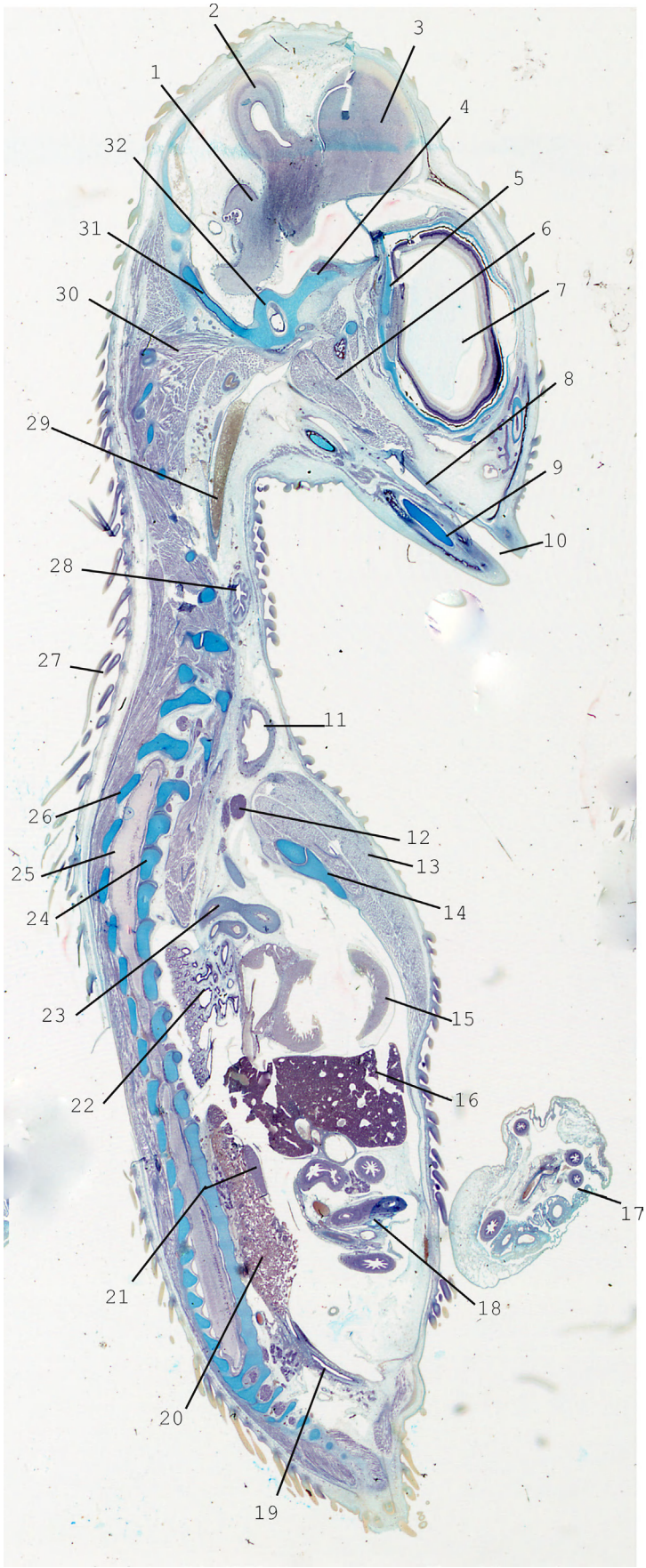

Downloaded from Vet-eBooks.com

Plate 187 Stage 37 (day 11) LS: sagittal

Longitudinal (sagittal) section in plane of diagram: × 7

Stained with alcian blue to show cartilage.

In this series, plates 184, 187 and 188 show sections near the mid-sagittal plane (see diagram), whilst plates 185, 186, 189 and 190 show sections lateral to this plane.

1. basal plate of chondrocranium
2. pituitary
3. cerebral hemisphere
4. nasal and interorbital septum
5. back-growing roof of nasal capsule
6. internal naris
7. nasal concha
8. palate
9. prenasal plate
10. egg tooth
11. Meckel's cartilage in lower beak
12. tongue
13. clavicle
14. ventricle
15. sternum
16. liver
17. herniated gut in umbilical cord
18. allantoic stalk
19. cartilage lining of gizzard
20. cloaca
21. pygostyle
22. caudal vertebra
23. abdominal air sac
24. synsacral vertebra
25. ilium
26. mesonephros
27. spleen
28. lung
29. sulcus caroticus of cervical vertebra
30. arch of cervical vertebra
31. spinal cord
32. oesophagus
33. atlas
34. floor of medulla oblongata
35. arbor vitae of cerebellum

Downloaded from Vet-eBooks.com

Plate 187

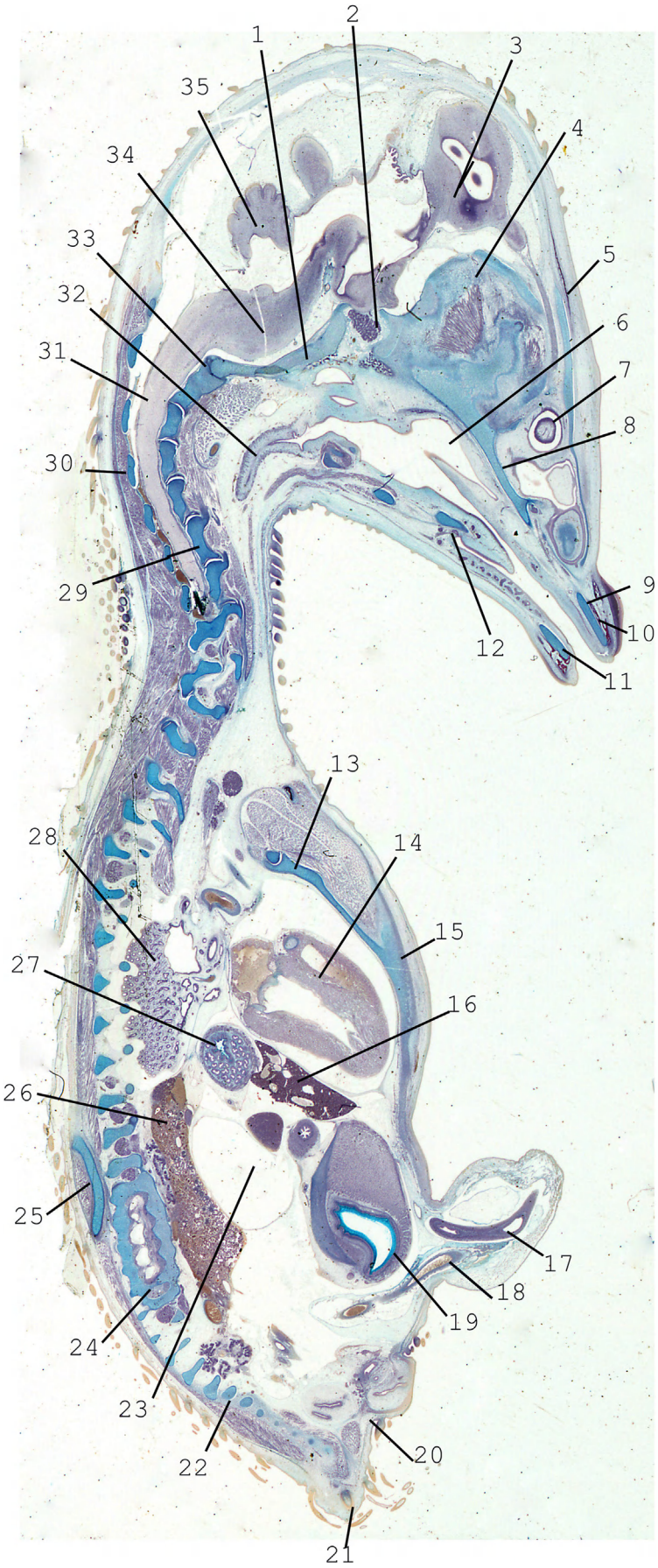

Downloaded from Vet-eBooks.com

Plate 188 Stage 37 (day 11) LS: sagittal

Longitudinal (sagittal) section in plane of diagram: × 10

In this series, plates 184, 187 and 188 show sections near the mid-sagittal plane (see diagram), whilst plates 185, 186, 189 and 190 show sections lateral to this plane.

1. optic lobe
2. mesencephalon
3. cerebral hemisphere
4. basi-occipital plate
5. vitreous body
6. lateral rectus eye muscle
7. dorsal rectus eye muscle
8. ventral oblique eye muscle
9. nasal cavity
10. nasal concha
11. maxilla
12. cornified region of upper beak (future egg tooth)
13. oral opening
14. Meckel's cartilage
15. tongue
16. palatine bone
17. longus capitis muscle
18. trachea
19. longus colli ventralis muscle
20. cervical vertebra
21. axis
22. atlas
23. basal plate of chondrocranium
24. foramen for Eustachian tube
25. medulla oblongata
26. arbor vitae of cerebellum

Downloaded from Vet-eBooks.com

Plate 188

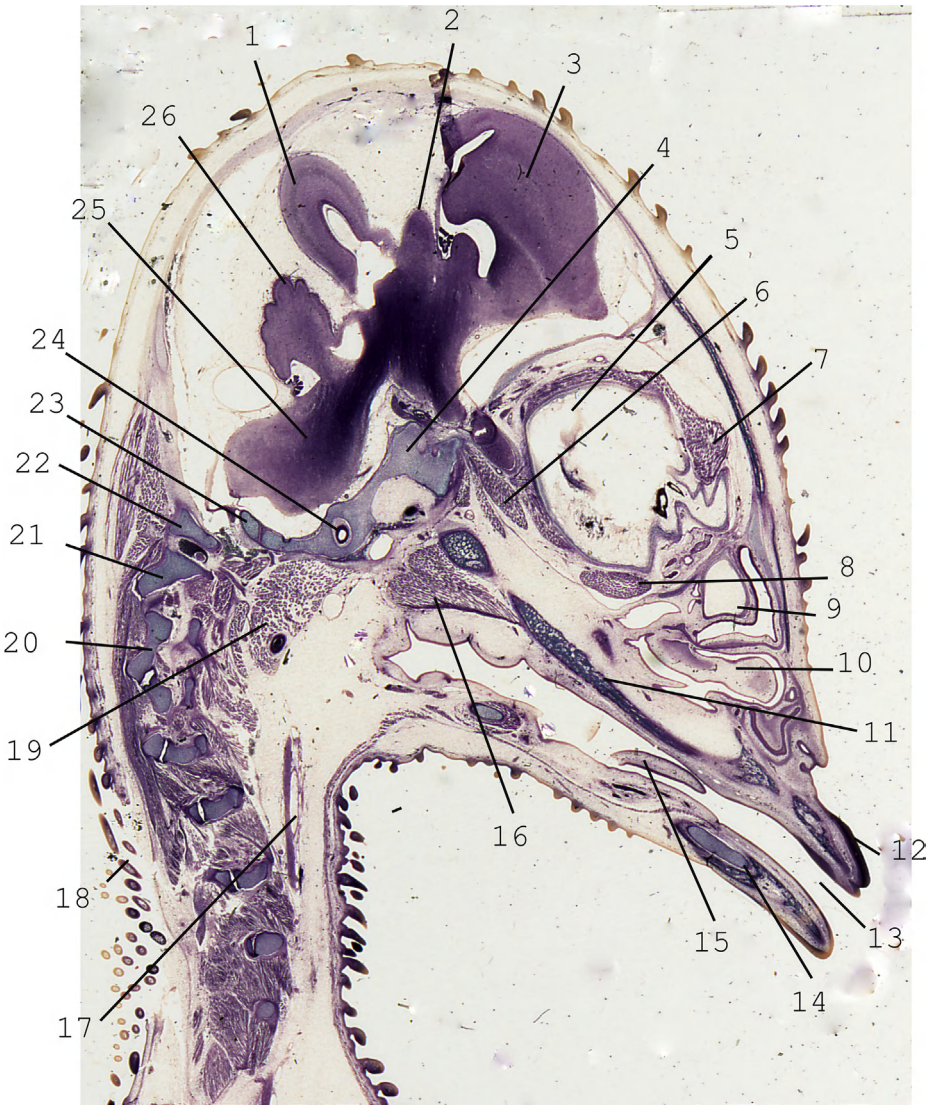

Downloaded from Vet-eBooks.com

Plate 189 Stage 37 (day 11) LS: sagittal

Longitudinal (sagittal) section in plane of diagram: × 6

In this series, plates 184, 187 and 188 show sections near the mid-sagittal plane (see diagram), whilst plates 185, 186, 189 and 190 show sections lateral to this plane.

1. complexus muscle
2. utriculus
3. otic capsule
4. optic tectum
5. cerebral hemisphere
6. vitreous body
7. ventral rectus eye muscle
8. pterygoid muscle
9. proximo-lateral border of upper lip (beak)
10. oral opening
11. lower lip (beak)
12. Meckel's cartilage
13. feather bud
14. pectoralis muscle
15. sternum
16. crop
17. gizzard
18. ischium at junction with ilium
19. lateralis caudi muscle
20. rib
21. lung
22. scapula
23. clavicle

Downloaded from Vet-eBooks.com

Plate 189

Downloaded from Vet-eBooks.com

Plate 190 Stage 37 (day 11) LS: sagittal

Longitudinal (sagittal) sections at the caudal end of embryo: × 7.5

In this series, plates 184, 187 and 188 show sections near the mid-sagittal plane (see diagram), whilst plates 185, 186, 189 and 190 show sections lateral to this plane.

(a) Stained with haematoxylin and eosin.

(b) Stained with alcian blue to show cartilage.

1. rib
2. iliotibialis muscle
3. ischiofemoralis muscle
4. femur
5. iliotrochanter muscle
6. ischium
7. pubis
8. head of femur
9. ilium

Downloaded from Vet-eBooks.com

Plate 190

(a)

(b)

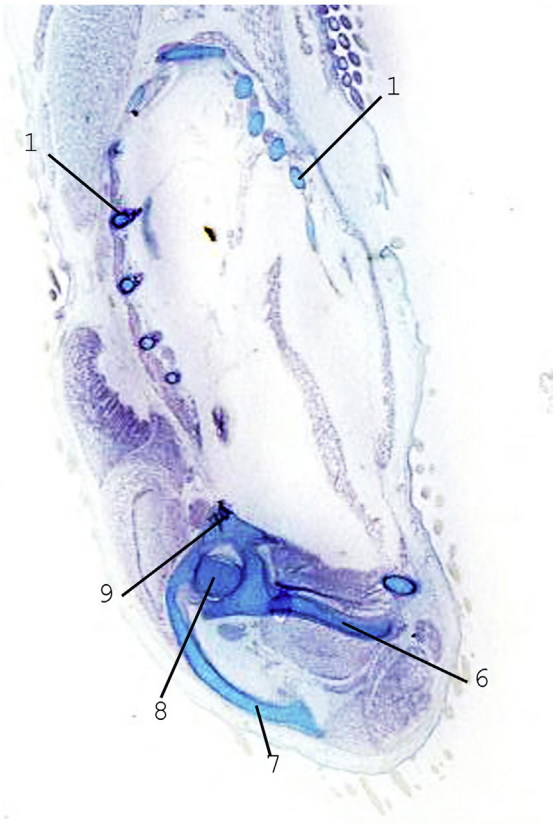

Downloaded from Vet-eBooks.com

Plate 191 Stage 37 (day 11) TS

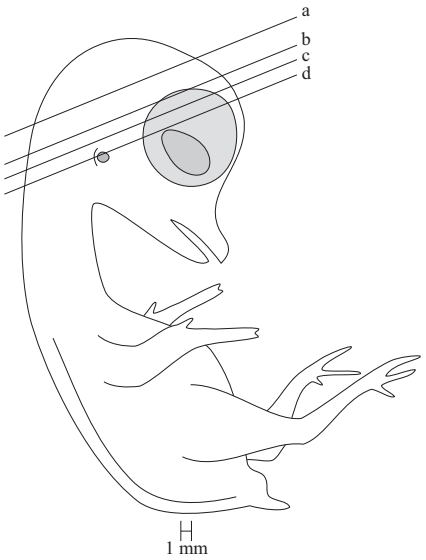

Transverse sections (TS): (a–d) × 12

1. foramina for vena emissaria occipitalis
2. cerebellum
3. cranial cavity
4. fourth ventricle
5. nucleus mesencephalicus lateralis
6. corpus striatum
7. left cerebral hemisphere
8. region of contact of left and right hemispheres
9. anterior horn of right lateral ventricle
10. third ventricle
11. right cerebral hemisphere
12. laminated wall of right optic lobe
13. lumen of optic lobe
14. metencephalon (pons)
15. lateral recess of fourth ventricle
16. utriculus
17. left optic (cranial II) nerve
18. left eye (collapsed in preparation)
19. floor of mesencephalon
20. mesencephalic aqueduct (aqueduct of Sylvius)
21. spinal cord
22. tectum synoticum
23. central canal
24. endolymphatic duct
25. vestibular nerve
26. auditory capsule
27. branches of oculomotor (cranial III) nerve
28. optic thalamus
29. lateral ventricle
30. archistriatum
31. palaeostriatum
32. semicircular canal
33. odontoid process (body of axis)
34. medulla oblongata
35. membranous labyrinth
36. columella
37. middle ear cavity
38. tympanic membrane
39. epibranchial cartilage
40. lobes of trigeminal (cranial nerve V) ganglion
41. retina
42. pigmented layer of retina
43. hypophysial fenestra
44. interorbital septum
45. olfactory bulb
46. dorsal (superior) oblique eye muscle
47. hypophysis
48. postorbital cartilage
49. vestibular ganglion of acoustic (cranial VIII) nerve
50. occipital condyle

Downloaded from Vet-eBooks.com

Plate 191

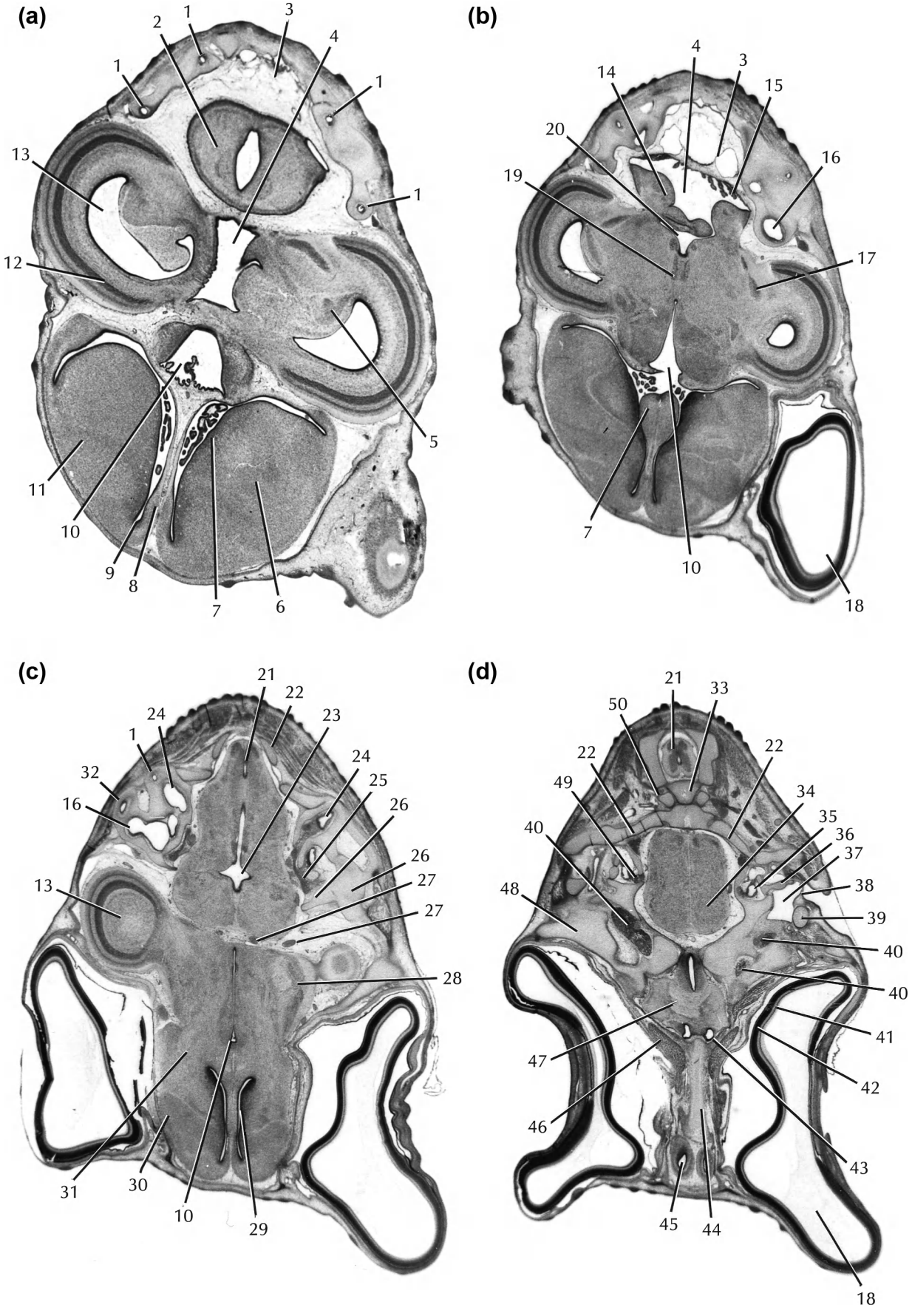

Downloaded from Vet-eBooks.com

Plate 192 Stage 37 (day 11) TS

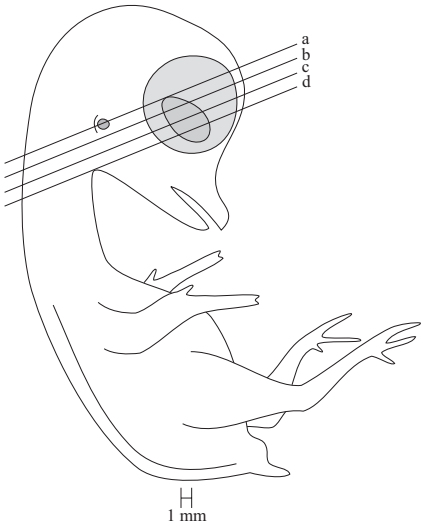

Transverse sections (TS): (a–d) × 10

1. dorsal root ganglion
2. axis
3. complexus muscle
4. odontoid process (body of axis)
5. splenius capitis muscle
6. rectus capitis lateralis muscle
7. vagus (cranial X) nerve
8. foramen magnum
9. stapedial artery
10. depressor mandibulae muscle
11. tympanic membrane
12. middle ear
13. adductor mandibulae externus muscle
14. left dorsal oblique muscle of eye
15. optic (cranial II) nerve
16. lower eyelid
17. ciliary muscle
18. upper eyelid
19. vitreous humour of the eye
20. right dorsal oblique muscle of eye
21. interorbital septum
22. tectal process
23. optic chiasma
24. right internal carotid artery
25. abducens (cranial VI) nerve
26. acrochordal cartilage
27. lagena
28. external auditory meatus
29. acoustic (cranial VIII nerve) ganglion (vestibulocochlearis)
30. medulla oblongata
31. occipital vein
32. occipital artery
33. flexor colli lateralis muscle
34. spinal cord
35. flexor colli medialis muscle
36. epibranchial cartilage of hyoid
37. cochlear canal
38. otic process of quadrate cartilage
39. ciliary ganglion
40. pecten
41. cornea
42. olfactory (cranial I) nerve
43. quadratus muscle
44. hypophysis
45. remains of notochord
46. right rectus capitis ventralis muscle
47. transverse process of cervical vertebra
48. neural arch of cervical vertebra
49. body of vertebra with remnant of notochord
50. connective tissue
51. interjugular anastomosis (anastomotic vein)
52. left head vein
53. Meckel's cartilage
54. quadrate cartilage
55. brachio-mandibular muscle
56. lens
57. ventral rectus eye muscle
58. retro-articular process of Meckel's cartilage
59. angular process of Meckel's cartilage
60. pharynx
61. head vein (jugular)
62. common carotid artery
63. sternotracheal muscle
64. trachea
65. larynx
66. glottis
67. base of choana
68. dentary
69. splenial bone
70. crop

Plate 192

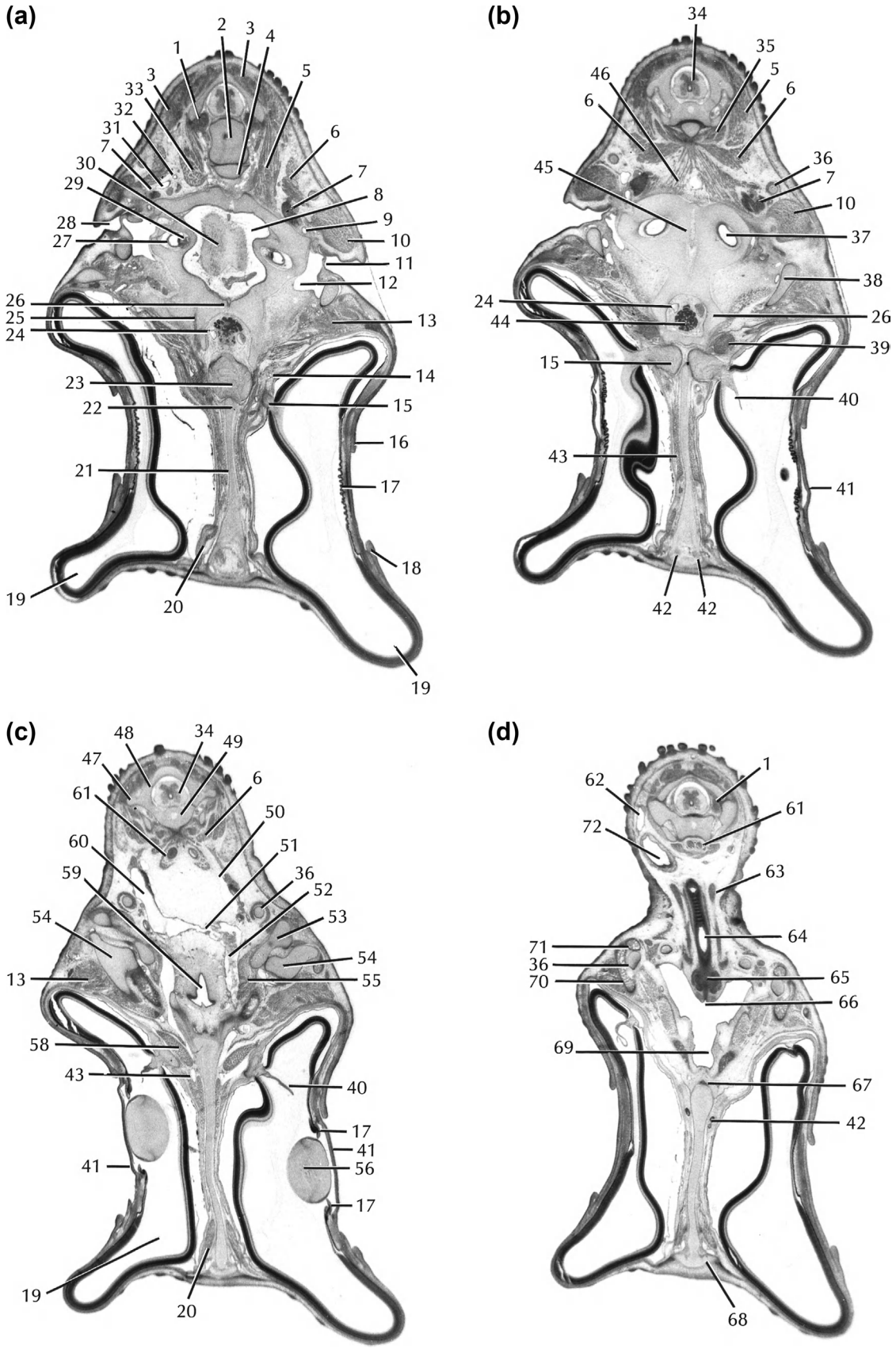
(a)
1
2
3
4
5
6
7
8
9
10
11
12
13
14
15
16
17
18
19
20
21
22
23
24
25
26
27
28
29
30
31
32
33
3
7
6
19
(b)
34
35
5
6
46
6
45
36
7
10
37
38
24
44
26
39
15
40
43
41
42
42
(c)
48
34
49
47
6
61
50
51
60
36
59
52
53
54
54
13
55
58
43
40
17
41
56
41
17
19
20
(d)
1
62
61
72
63
64
71
36
70
65
66
69
67
42
68

Plate 193 Stage 37 (day 11) TS

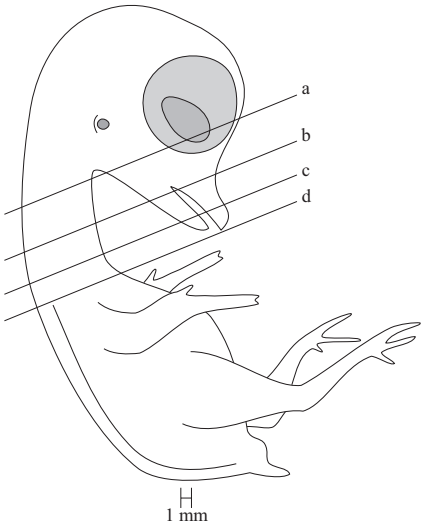

Transverse sections (TS): (a–d) × 12

1. spinal cord, cervical region (white matter)
2. branch of right jugular vein
3. neural arch of cervical vertebra
4. splenius capitis lateralis muscle
5. rectus capitis dorsalis muscle
6. lobe of left thymus
7. vagus (cranial X) nerve
8. left and right common carotid arteries
9. trachea
10. intertransversarii muscle
11. crop
12. right jugular vein
13. quadrate cartilage (otic process)
14. articular cartilage (posterior end of Meckel's cartilage)
15. basihyal (copula I) cartilage
16. paraglosso-ceratobranchial muscle
17. ceratobranchial cartilage
18. hypobranchial muscles
19. oral cavity
20. palatine process
21. maxillary cartilage
22. palatine sinus
23. optic (cranial II) nerve
24. sclera
25. lower eyelid
26. wall of nasal capsule
27. upper eyelid
28. olfactory nerve
29. left nasal meatus
30. orbital cartilage
31. median palatine fissure
32. tongue
33. epidermis
34. hypoglossus oblique lateralis muscle
35. adductor mandibulae muscle
36. Meckel's cartilage
37. paraglossal cartilage
38. wall of lacrimal duct
39. nasal concha
40. interorbital (nasal) septum
41. roof of nasal capsule
42. right nasal meatus
43. premaxilla
44. lumen of lacrimal duct
45. mandibular artery
46. base of nasal septum
47. right vagus nerve and artery
48. cervical rib
49. neural canal
50. ascendens muscle
51. zygapophysis of adjacent vertebra
52. body of cervical vertebra
53. tracheal branch of vagus nerve
54. longus colli ventralis muscle
55. crop branch of vagus nerve
56. crop
57. dorsal root ganglion

Plate 193

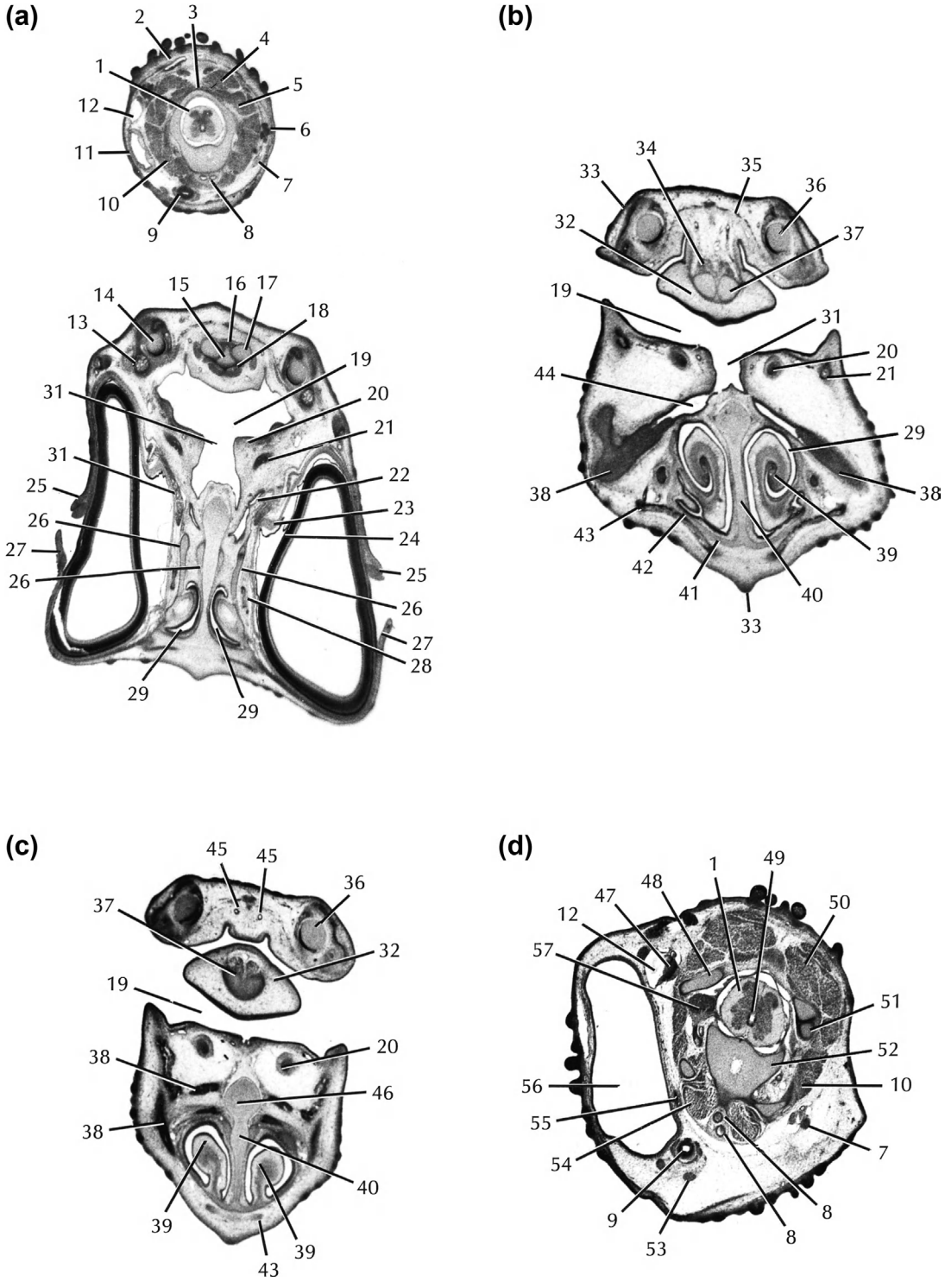
(a)
2
3
4
1
5
12
6
11
7
10
9
8
14
15
16
17
13
18
19
31
20
21
31
22
25
23
26
24
27
25
26
26
27
28
29
29
(b)
34
33
35
36
32
37
19
31
20
44
21
29
38
38
43
39
42
41
40
33
(c)
45
45
36
37
32
19
20
38
46
38
40
39
39
43
(d)
1
49
48
47
50
12
57
51
52
56
10
55
7
54
9
8
53
8

Plate 194 Stage 37 (day 11) TS

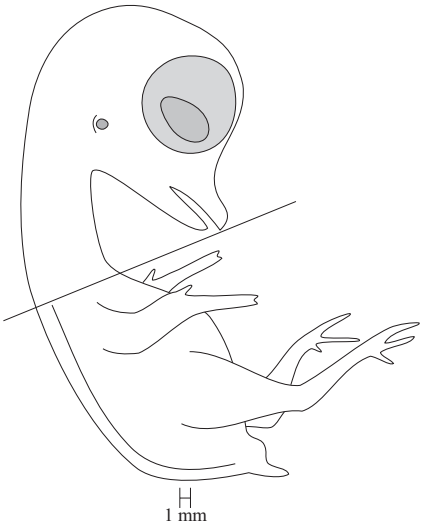

Transverse section through the neck adjacent to part of *plate 193a*: × 36

1. right longus colli dorsalis muscle
2. right biventer cervicis muscle
3. feather bud
4. left biventer cervicis muscle
5. ascendens cervicis muscle
6. left longus colli dorsalis muscle
7. dorsal horn of spinal cord
8. spinal canal
9. left intertransverse muscle
10. zygapophysis of adjacent vertebra
11. dorsal root ganglion
12. left vertebral artery
13. vertebral body
14. nucleus pulposus (remnant of notochord)
15. longus colli ventralis muscle
16. left common carotid artery
17. right common carotid artery
18. right longus colli ventralis muscle
19. trachea
20. right vertebral artery
21. caudal zygapophysis of vertebra
22. crop
23. marginal layer of spinal cord
24. right jugular vein

Plate 194

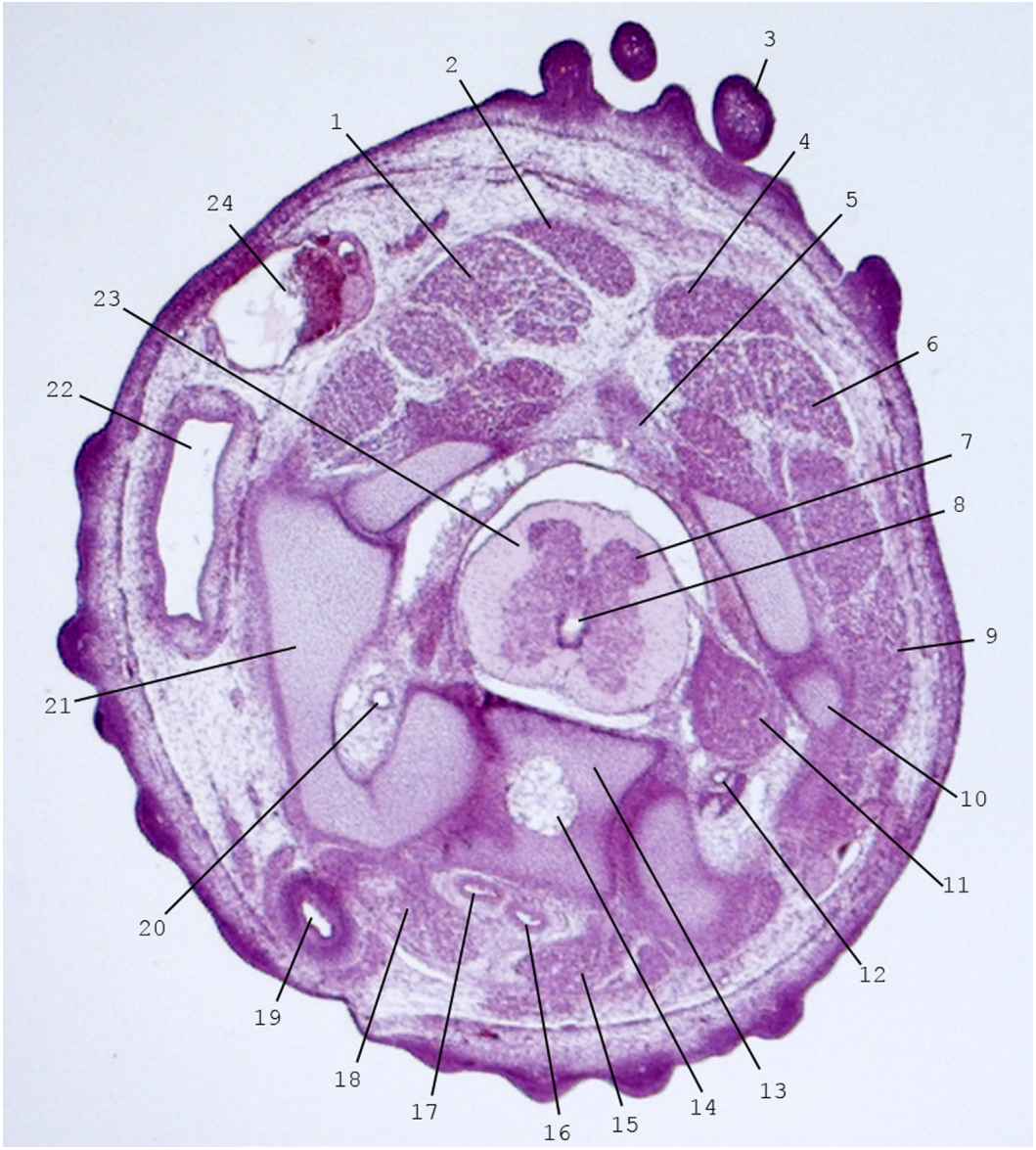

Plate 195 Stage 37 (day 11) TS

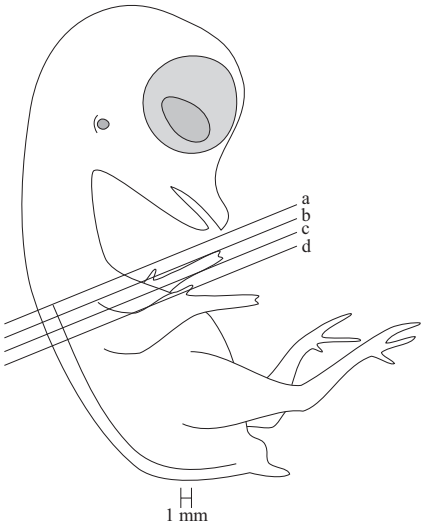

Transverse sections (TS): (a–d) × 12

1. intertransversarii muscle
2. dorsal root ganglion
3. biventer cervicis muscle
4. spinal cord
5. neural arch of cervical vertebra
6. body of vertebra
7. cervical rib
8. humerus
9. coracobrachialis caudalis muscle
10. longus colli ventralis muscle
11. left common carotid artery
12. clavicle
13. trachea
14. oesophagus
15. feather bud
16. pectoralis muscle pars thoracicus
17. transverse process of last cervical vertebra
18. right cranial (anterior) cardinal vein
19. scapula
20. triceps brachii muscle, pars humerotriceps
21. rhomboideus superficialis muscle
22. vertebral artery
23. neural arch of thoracic vertebra
24. spinal cord (white matter)
25. notochord in vertebral body
26. spinal cord (grey matter)
27. left anterior vena cava
28. coracoid
29. right common carotid artery
30. supracoracoid muscle
31. costal process of sternum
32. sternocoracoideus muscle
33. lobes of thymus
34. spinal nerve component of brachial plexus
35. thyroid
36. ulna
37. left ulnacarpal
38. carpo-metacarpus
39. keel of sternum
40. coracoid abutting sternum
41. tip of right phalanx III
42. metacarpal III
43. right ulnacarpal
44. biceps brachii muscle
45. junction of subscapularis muscle and subcoracoideus muscle
46. subscapularis externa muscle
47. ventral ramus of spinal nerve contributing to brachial plexus
48. sympathetic ganglion
49. rostrum of sternum
50. sternum
51. costal process of sternum
52. subclavian artery

Plate 195

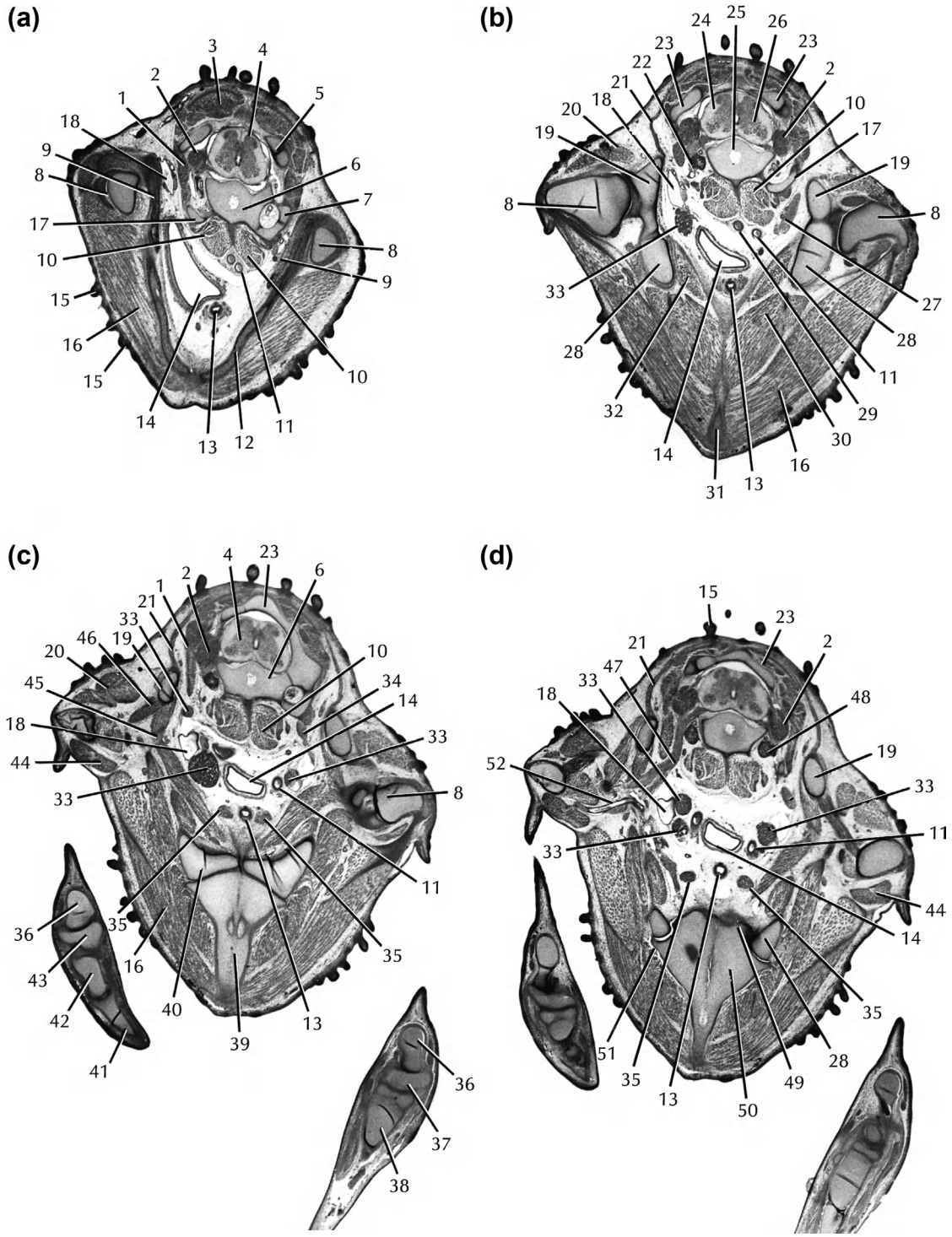
(a)
3
4
2
1
5
18
9
8
6
7
17
10
8
9
15
16
15
10
14
13
12
11
(b)
24
25
26
23
23
22
21
2
20
18
10
19
17
19
8
8
33
27
28
28
11
32
29
14
30
16
31
13
(c)
4
23
6
2
1
21
33
19
46
20
10
34
45
14
18
33
44
33
8
11
36
35
35
16
43
40
42
39
13
41
36
37
38
(d)
15
23
2
21
47
33
18
48
19
52
33
33
11
44
14
35
51
35
28
13
49
50

Plate 196 Stage 37 (day 11) TS

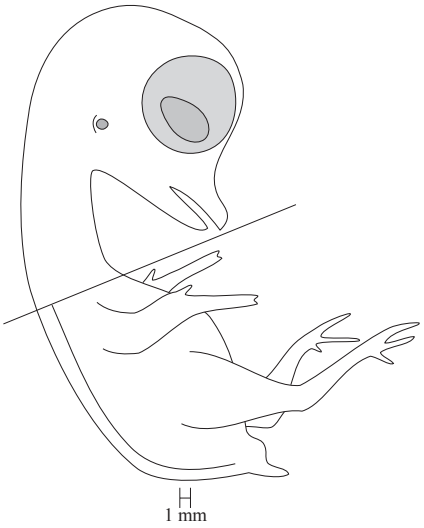

Enlargement of section adjacent to *plate 195a*: × 30

1. right humerus
2. triceps brachii muscle
3. coraco-brachialis cordalis muscle
4. right jugular vein
5. dorsal root ganglion on right side
6. neural arch of thoracic vertebra
7. spinal canal
8. right biventer cervicis muscle
9. spinal cord
10. left biventer cervicis muscle
11. left coracoid
12. dorsal root ganglion on left side
13. body of vertebra
14. vertebral arteries
15. transverse process
16. left humerus
17. left coraco-brachialis muscle
18. left pectoralis muscle
19. left longus colli ventralis muscle
20. left and right carotid arteries
21. clavicle
22. thyroid
23. trachea
24. right longus colli ventralis muscle
25. crop
26. right pectoralis muscle

Plate 196

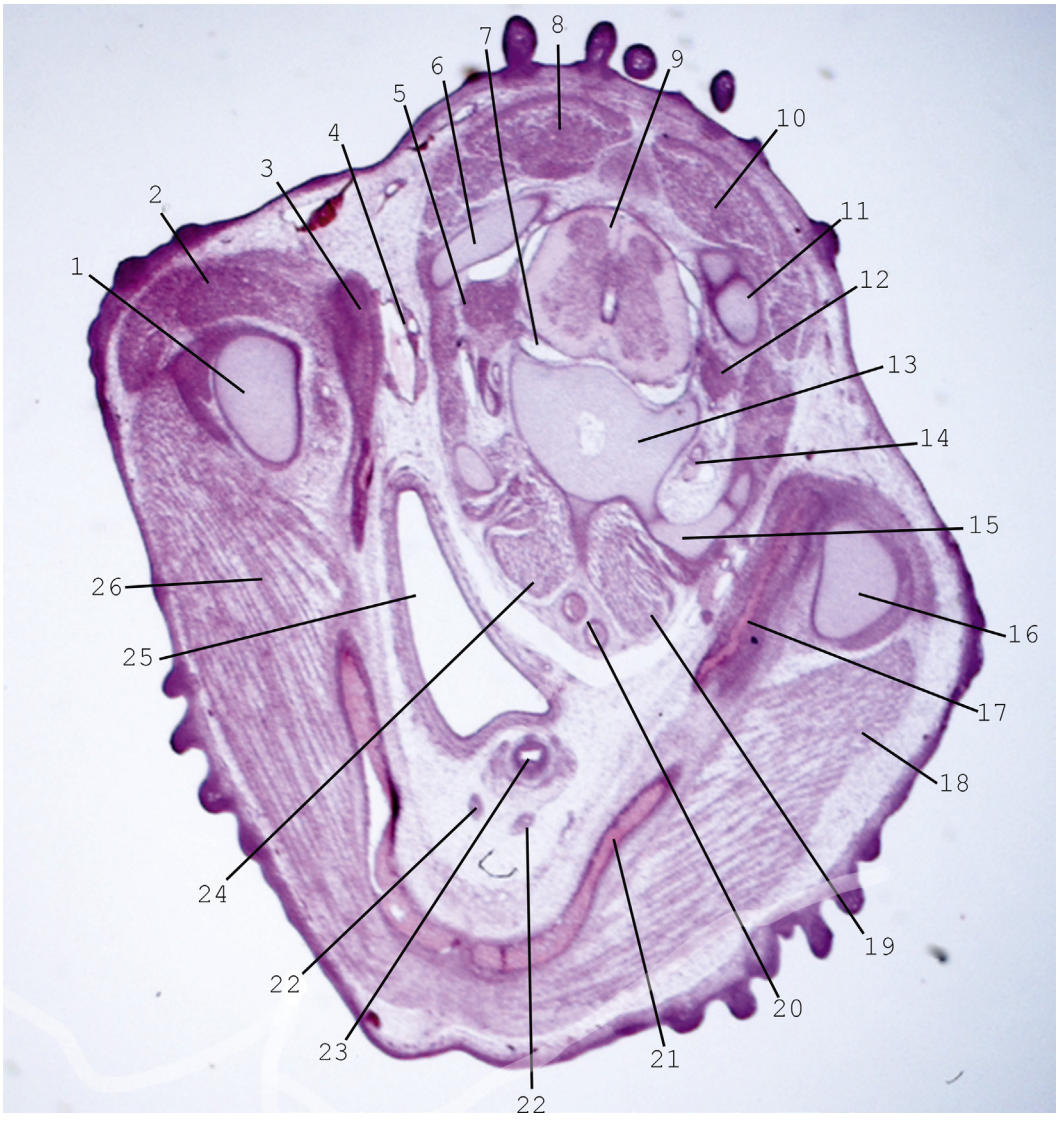

Plate 197 Stage 37 (day 11) TS

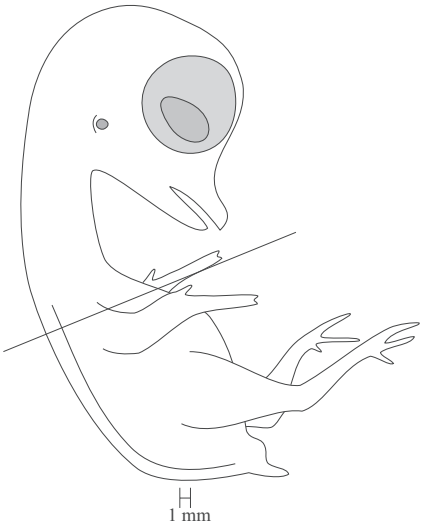

Enlargement of section adjacent to *plate 195c*: × 50

1. right thymus
2. right cranial anterior vena cava
3. right common carotid artery
4. oesophagus
5. longus colli ventralis muscle
6. left common carotid artery
7. coracoids
8. costal process of sternum
9. keel of sternum
10. supra coracoideus muscle
11. pectoralis muscle

Plate 197

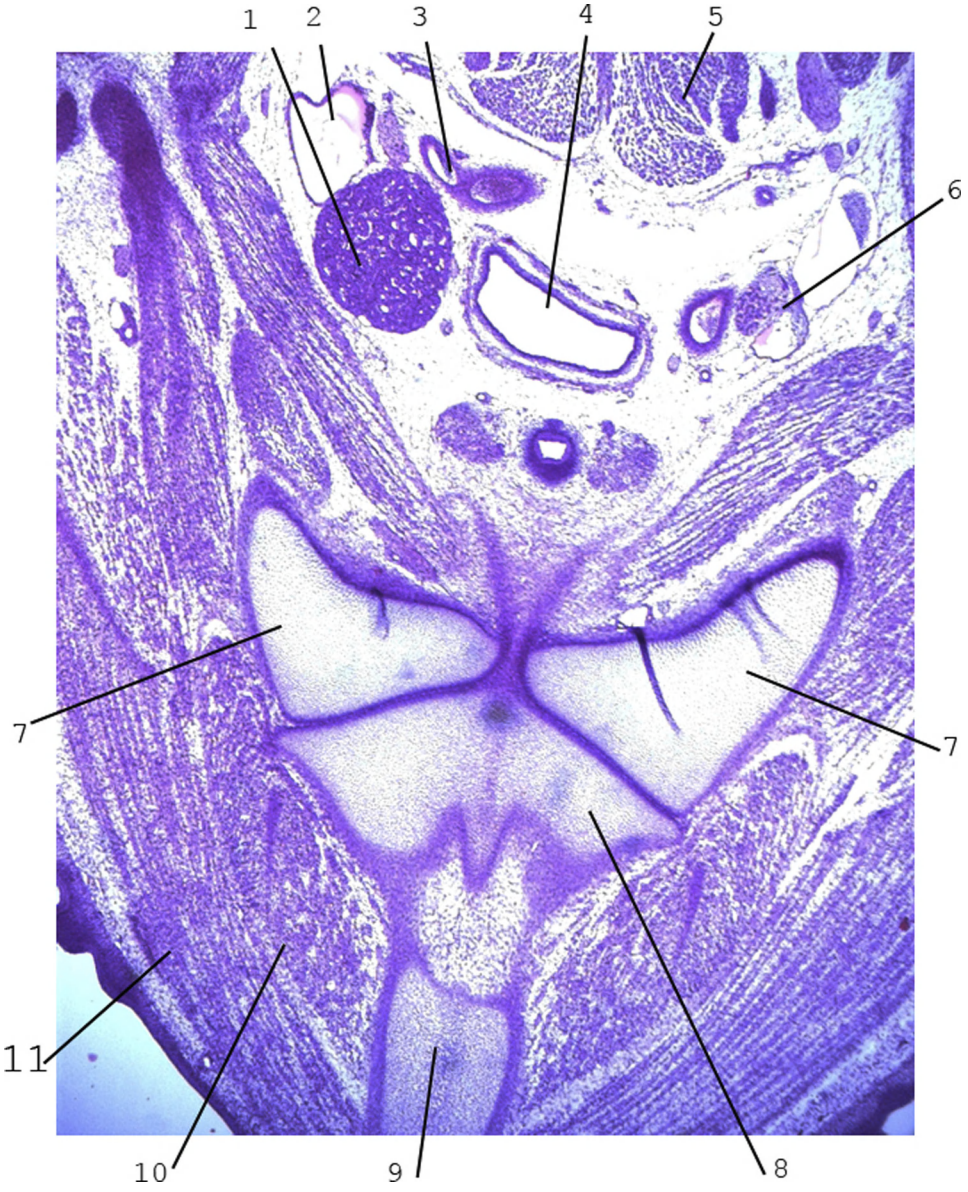

Plate 198 Stage 37 (day 11) TS

Transverse sections (TS): (a, b) × 12

1. dorsal root ganglion
2. capitulum of costa
3. body of vertebra
4. spinal cord (grey matter)
5. notochord
6. neural arch of vertebra
7. spinal cord (white matter)
8. sympathetic ganglion
9. spinal thoracic muscle complex
10. rhomboideus superficialis muscle
11. ventral ramus of spinal nerve 16, contributing to left brachial plexus
12. scapula
13. scapulohumeralis lateralis muscle
14. subscapularis muscle
15. triceps brachii pars humerotriceps muscle
16. left common carotid artery
17. humerus
18. subclavian artery
19. biceps brachii muscle
20. intercostalis externus muscle
21. intercostalis internus muscle
22. thyroid
23. syrinx
24. radius
25. ulna
26. ulnar artery
27. metacarpus
28. extensor medius brevis muscle
29. phalanx
30. digit III
31. feather bud
32. articulation of coroid with sternum
33. supracoracoideus muscle
34. keel of sternum
35. pectoralis muscle pars thoracicus
36. anterior tip of pericardial cavity
37. radial carpal
38. coracoid
39. subclavian artery
40. coracobrachialis muscle
41. subclavian vein
42. deltoid muscle
43. right anterior cardinal vein
44. thymus
45. part of brachial plexus
46. tuberculum of costa (rib)
47. intertransversarii muscle
48. longus colli ventralis muscle
49. thoracic vertebra
50. oesophagus
51. left anterior cardinal vein
52. left tensor propatagialis brevis muscle
53. brachialis muscle
54. flexor digitorum profundus muscle
55. pectoral artery
56. left brachiocephalic artery
57. pericardial cavity
58. right brachiocephalic artery
59. root of subclavian artery
60. jugular vein
61. lobules of thymus

Plate 198

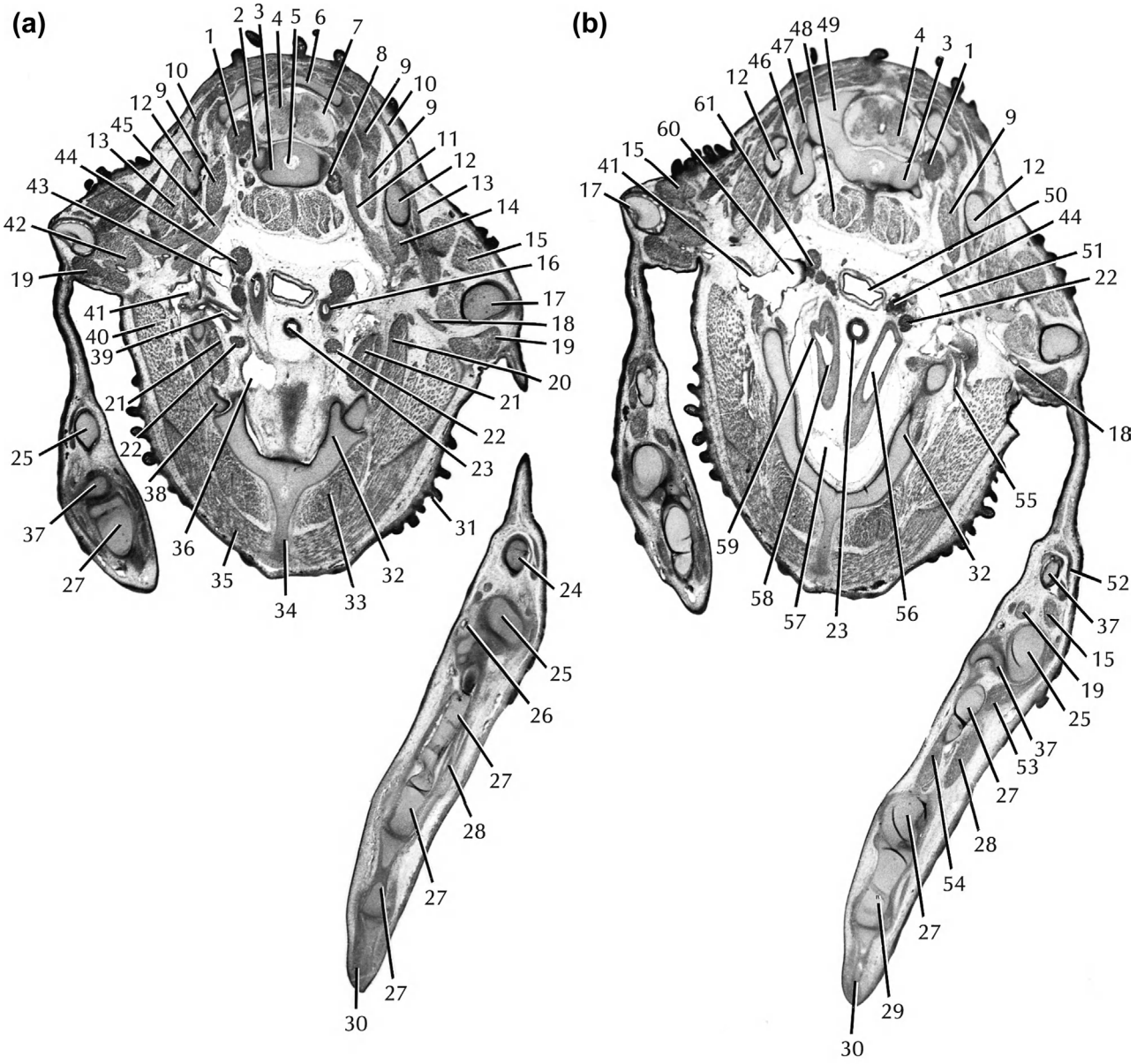

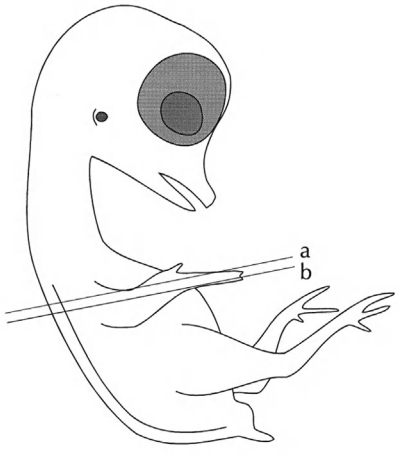

H
1 mm

Plate 199 Stage 37 (day 11) TS

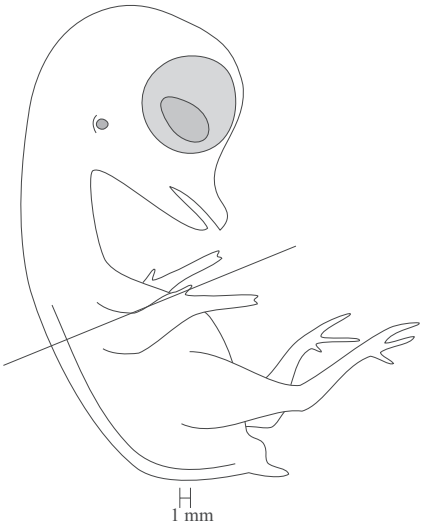

Enlargement of section adjacent to *plate 195d*: × 55

1. body of vertebra
2. sympathetic ganglion
3. dorsal root ganglion
4. rhomboideus superficialis muscle
5. scapula
6. subscapularis muscle
7. triceps brachii pars humerotriceps muscle
8. scapulohumeralis muscle
9. feather bud
10. humerus
11. edge of wing
12. biceps brachii muscle
13. pectoralis muscle
14. serratus superficialis muscle
15. coracoid
16. serratus profundus muscle
17. thymus
18. left common carotid artery
19. oesophagus
20. longus colli ventralis muscle

Plate 199

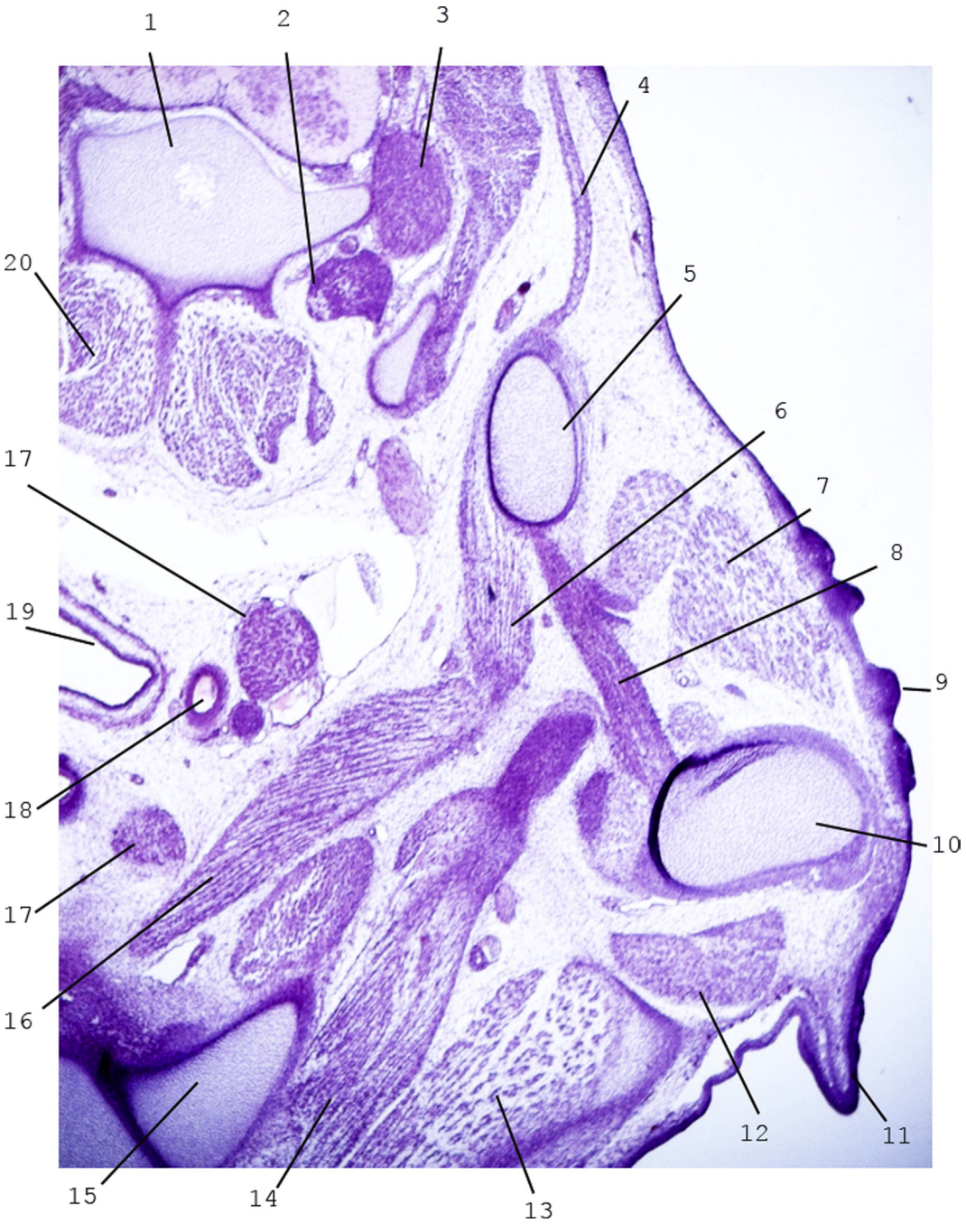

Plate 200 Stage 37 (day 11) TS

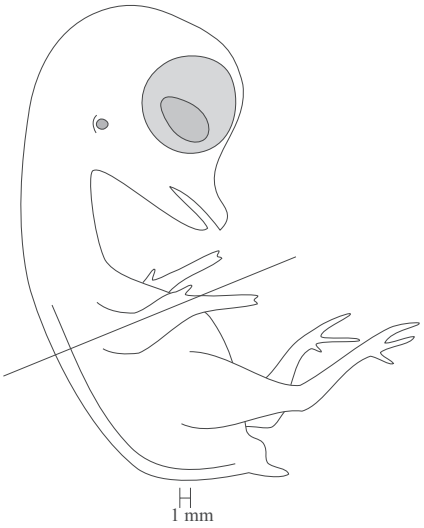

Enlargement of section adjacent to *plate 198b*: × 50

1. right humerus
2. deltoid muscle
3. brachial plexus
4. triceps brachii, pars humerotriceps
5. feather bud
6. serratus profundus muscle
7. subscapularis muscle
8. scapula
9. tuberculum of rib
10. spinal thoracic muscle complex
11. longus colli ventralis muscle
12. right thymus
13. right common carotid
14. oesophagus
15. thyroid
16. syrinx
17. brachiocephalic artery
18. root of subclavian artery
19. pericardial cavity
20. sternum
21. right cranial vena capitis
22. coracobrachialis muscle
23. ulna
24. subclavian vein
25. biceps brachii muscle

Plate 200

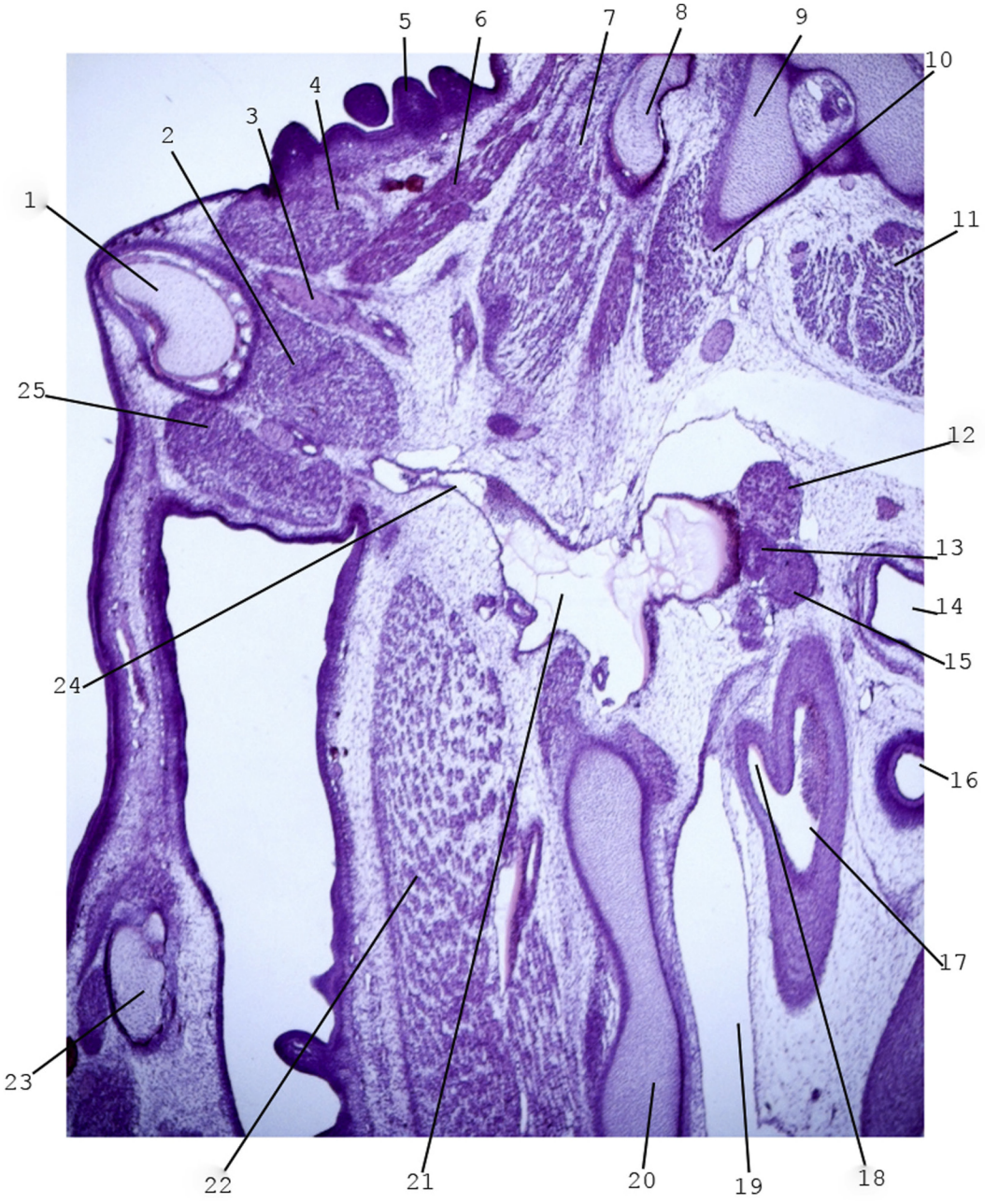

Plate 201 Stage 37 (day 11) TS

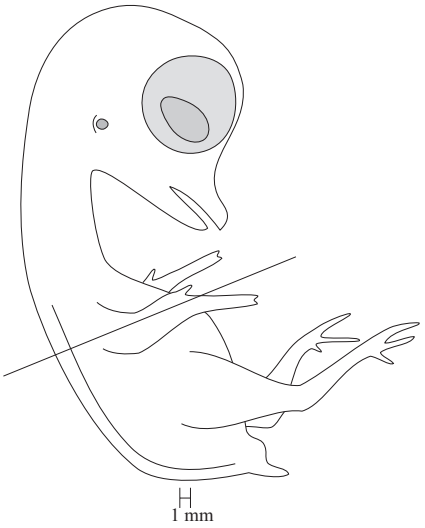

Enlargement of section adjacent to *plate 198b*: × 50

1. interjugular anastomosis
2. right vagus (cranial nerve X)
3. right longus colli ventralis
4. left longus colli ventralis
5. oesophagus
6. left thymus
7. left vagus (cranial nerve X)
8. left jugular vein
9. additional lobule of thymus
10. syrinx
11. left brachiocephalic artery
12. left thyroid
13. pectoral artery
14. left coracoid
15. pericardial cavity
16. right brachiocephalic artery
17. right coracoid
18. right pectoral artery
19. right thymus
20. right subclavian vein
21. right jugular vein

Plate 201

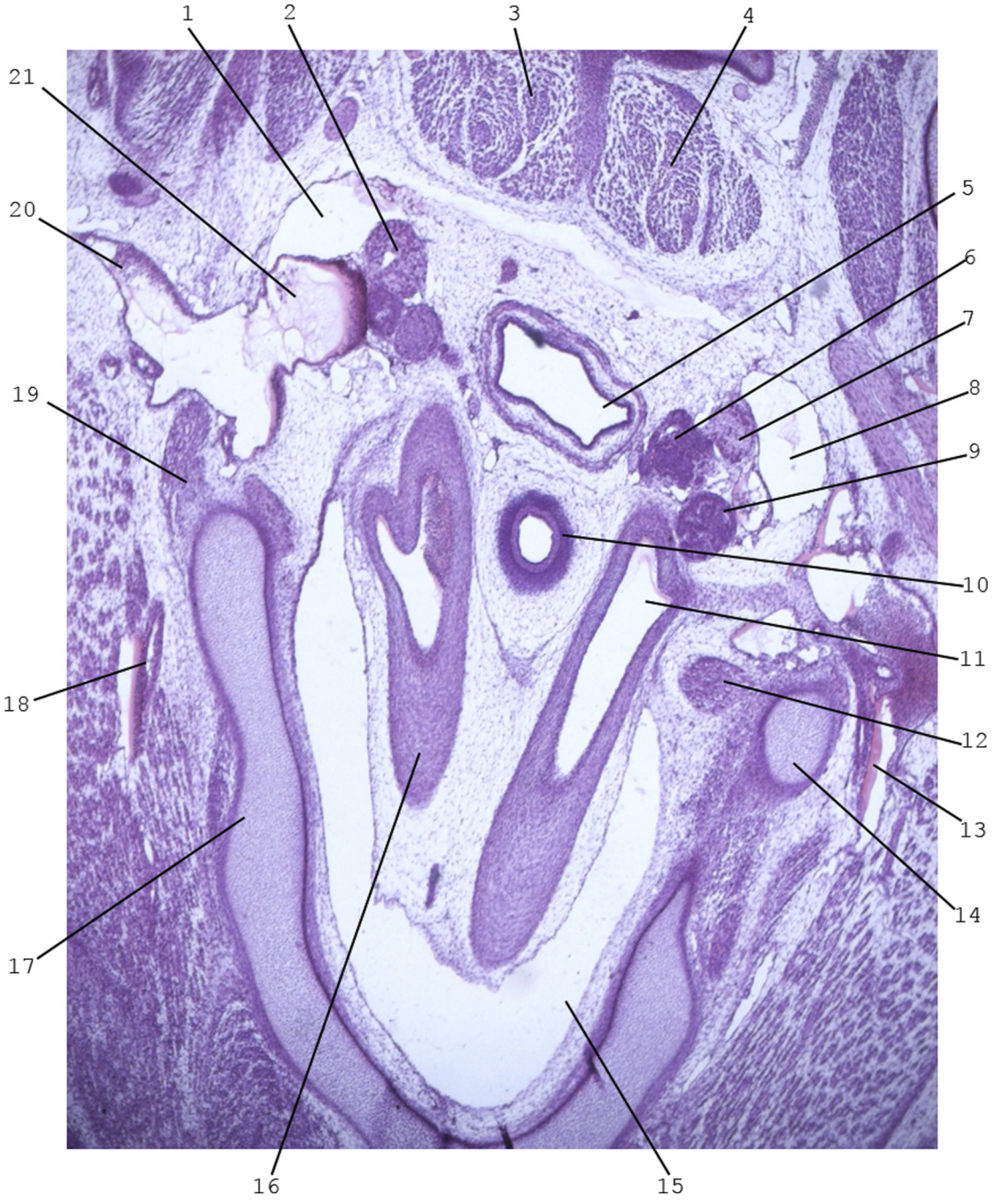

Plate 202 Stage 37 (day 11) TS

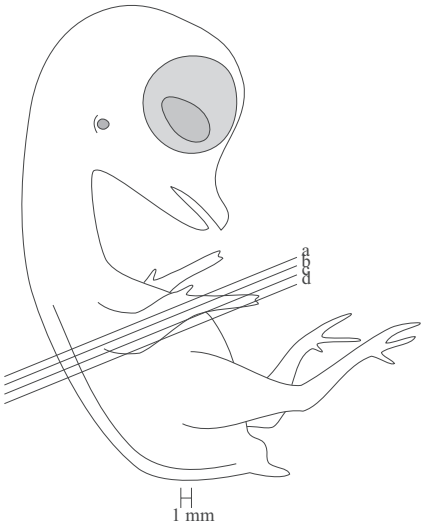

Transverse sections (TS): (a–d) × 12

1. right pleural cavity
2. scapulohumeralis muscle
3. serratus profundus muscle
4. scapula
5. latissimus dorsi muscle
6. body of vertebra
7. spinal cord
8. vertebral arch
9. dorsal root ganglion
10. sympathetic nerve ganglion
11. spinal nerve
12. oesophagus
13. bronchus, immediately posterior to syrinx
14. intercostalis internus muscle
15. intercostalis externus muscle
16. sternum
17. supracoracoideus muscle
18. pulmonary artery
19. left brachiocephalic artery
20. aortic arch
21. right brachiocephalic artery
22. carpo-metacarpus
23. biceps brachii muscle
24. humerus
25. triceps brachialis (anconeus) muscle, pars humerotriceps
26. deltoid muscle
27. pectoral vein
28. right cranial (anterior) vena cava
29. lung
30. longus colli ventralis muscle
31. bronchus
32. left cranial (anterior) vena cava
33. triceps brachialis (anconeus) muscle, pars scapulotriceps
34. brachial artery and median ulna nerve
35. left atrium
36. truncus arteriosus
37. flexor digitorum muscle, profundus tendon
38. superficialis muscle tendon
39. carpo-metacarpus
40. right flexor carpi ulnaris muscle
41. ulnar carpal
42. interosseus dorsalis muscle
43. metacarpiradialis muscle
44. radius
45. ectepicondylo-ulnaris muscle
46. extensor metacarpi ulnaris muscle (attachment to ulna)
47. ulna
48. extensor digitorum communis muscle
49. extensor metacarpi ulnaris muscle
50. rib
51. serratus profundus muscle
52. left pleural cavity
53. rib articulating with sternum
54. left ventricle
55. keel of sternum
56. right common carotid artery
57. left common carotid artery
58. flexor carpi ulnaris muscle
59. ulnimetacarpalis ventralis muscle
60. extensor indicis longus muscle
61. radius
62. flexor digitorum profundus muscle
63. pronator profundus muscle
64. right atrium
65. pericardial cavity

Plate 202

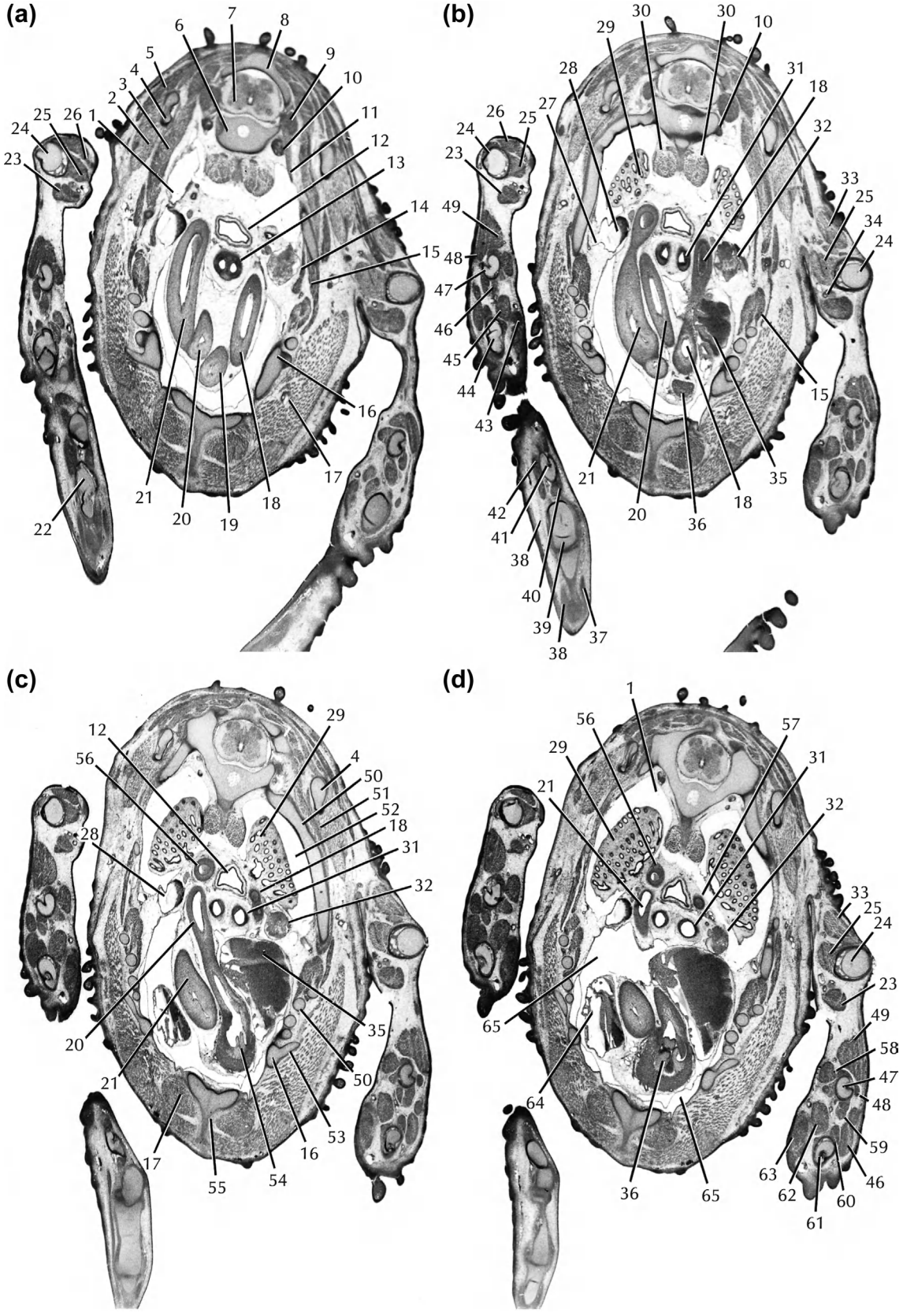

Plate 203 Stage 37 (day 11) TS

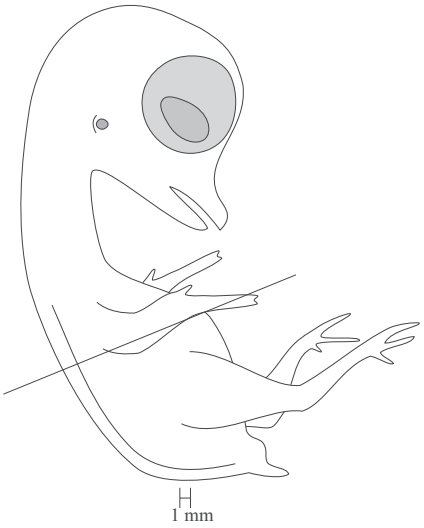

Enlargement of part of *plate 202c*: × 45

1. right cranial (anterior) vena cava
2. right common carotid artery
3. oesophagus
4. left lung
5. left common carotid artery
6. left bronchus
7. left pulmonary vein
8. left cranial anterior vena cava
9. congealed blood in left atrium
10. pericardium
11. left atrium
12. rib
13. pectoralis muscle
14. projections in wall of atrium
15. truncus arteriosus
16. sternum
17. aortic arch
18. right atrium
19. right brachiocephalic artery
20. pericardium
21. pericardial cavity

Plate 203

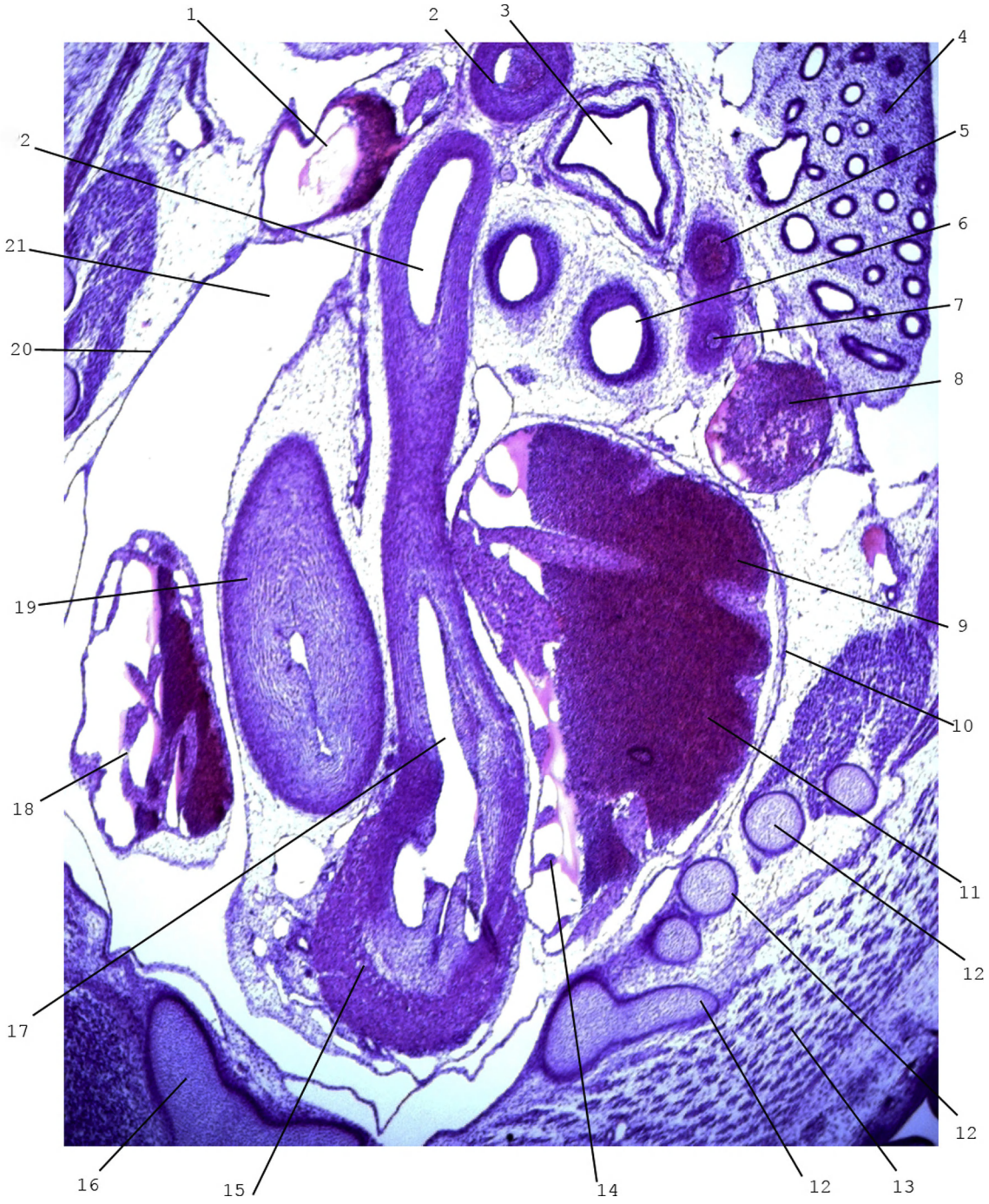

Plate 204 Stage 37 (day 11) TS

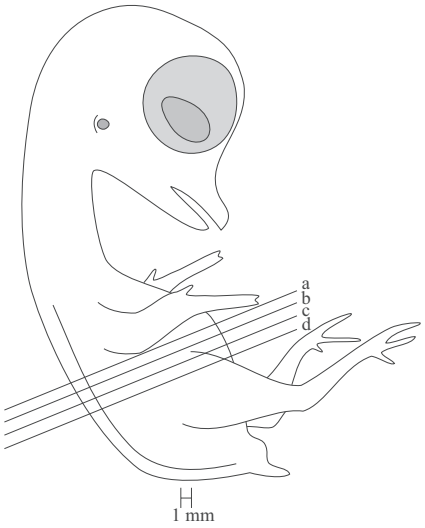

Transverse sections (TS): (a–d) × 12

1. abdominal air sac
2. lung
3. right pleural cavity
4. rib
5. articulation of tuberculum of rib with transverse process
6. dorsal aorta
7. spinal cord (grey matter)
8. spinal process of vertebra
9. rhomboideus superficialis muscle
10. sympathetic nerve trunk
11. capitulum of costa (articulates with transverse process)
12. posterior end of scapula
13. left pleural cavity
14. oesophagus
15. left lateral thoracic air sac
16. left atrium
17. dorsal hepatic cavity
18. oblique septum
19. sternal rib
20. cranial (anterior) vena cava
21. posterior end of pectoralis muscle
22. lumen of left ventricle
23. interventricular septum
24. pericardial cavity
25. atrio-ventricular valve
26. lumen of right ventricle
27. right ventral hepatic cavity
28. lumen of right atrium
29. right lobe of liver
30. sinu-atrial canal
31. sinus venosus
32. horizontal septum
33. dorsal mesentery
34. transverse process of thoracic vertebra
35. proventriculus
36. left horizontal hepatic ligament
37. left lobe of liver
38. wall of left ventricle
39. left umbilical vein
40. caudal (posterior) vena cava
41. right hepatic vein
42. intestinal coelomic cavity
43. mesonephros
44. omphalo-mesenteric artery
45. left ovary
46. coeliac artery
47. rectus abdominis muscle
48. left ventral hepatic cavity
49. ventral mesentery (falciform ligament)
50. right oviduct (Mullerian duct)
51. metanephros
52. adrenal gland
53. dorsal root ganglion
54. left oviduct (Mullerian duct)
55. intercostalis externus muscle
56. hepatic vein
57. tibiotarsus of right leg
58. gastrocnemius muscle

Plate 204

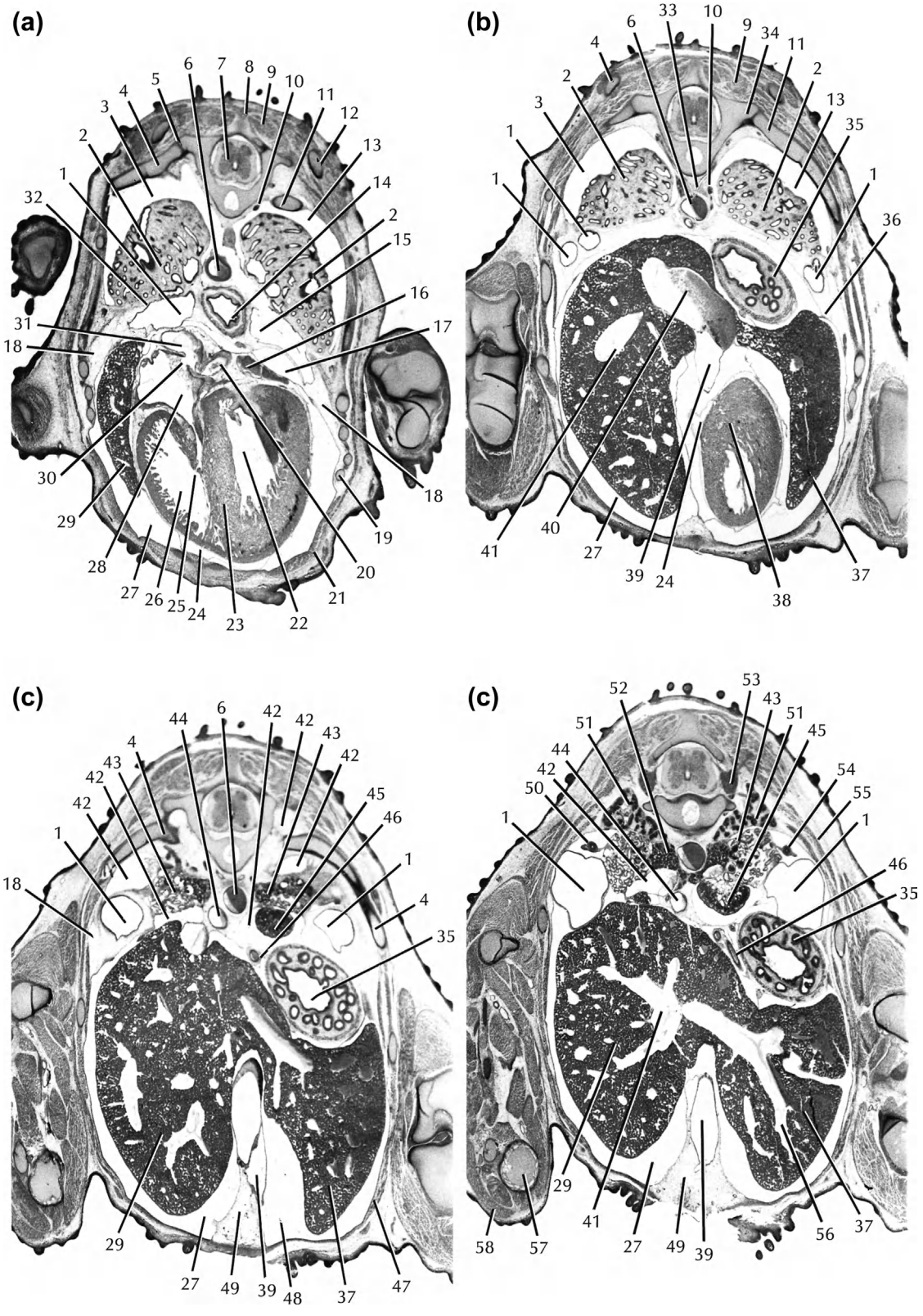

Plate 205 Stage 37 (day 11) TS

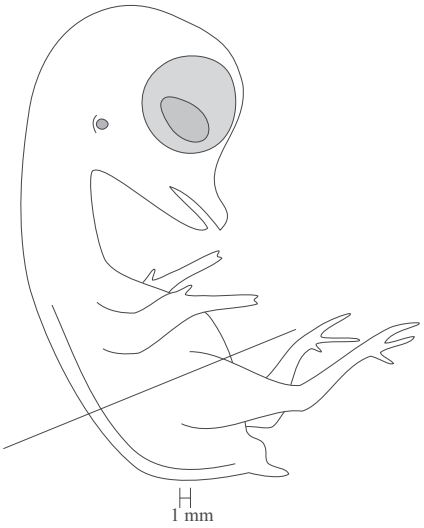

Enlargement of part of *plate 204d*: × 40

1. right oviduct
2. right mesonephros
3. right metanephros
4. right adrenal gland
5. dorsal aorta
6. remains of notochord
7. vertebral body
8. left adrenal gland
9. left metanephros
10. left mesonephros
11. left oviduct
12. left ovary
13. coelomic cavity
14. proventriculus
15. coeliac artery
16. oblique septum
17. omphalo-mesenteric artery
18. liver
19. abdominal air sac

Plate 205

Plate 206 Stage 37 (day 11) TS

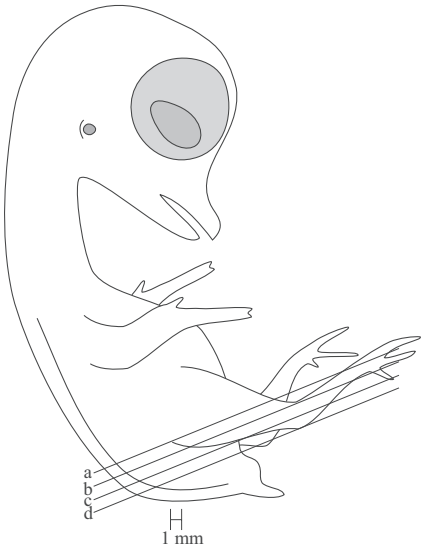

Transverse sections (TS):

(a) × 12; (b) × 10; (c, d) × 15

1. caudal vena cava
2. iliotibialis muscle
3. renal vein
4. dorsal aorta
5. neural arch
6. ilium
7. metanephros
8. left ovary
9. left oviduct (Mullerian duct)
10. abdominal air sac
11. oblique externus abdominis muscle
12. oblique internus abdominis muscle
13. spleen
14. left posterior lobe of liver
15. descending duodenum
16. gizzard
17. dorsal pancreas
18. mesenteric artery
19. descending limb of intestine
20. omphalo-mesenteric vein
21. extraembryonic coelom
22. herniated loop of intestine
23. metatarsus
24. digit IV of right foot
25. digit III of right foot
26. digit II of right foot
27. amniotic covering of umbilical cord
28. ascending limb of intestine
29. common mesenteric vein
30. ventral pancreas
31. ascending duodenum
32. gastropancreaticduodenal vein
33. right lobe of liver
34. right ventral hepatic cavity
35. tibiotarsus
36. fibula
37. branches of ischiatic nerve
38. femoral artery and iliac vein
39. femur
40. posterior tip of right abdominal air sac
41. left metanephric artery
42. remnant of right ovary
43. mesonephros
44. intestine
45. right oviduct (Mullerian duct)
46. head of femur in acetabulum
47. sympathetic nerve
48. body of lumbar vertebra
49. acetabulum
50. trochanter of femur
51. ischium
52. obturator muscle
53. wall of ventral hepatic cavity
54. allantoic stalk
55. yolk sac stalk
56. right metanephric artery
57. renal portal vein
58. right omphalo-mesenteric artery
59. caudal artery (caudal end of dorsal aorta)
60. left omphalo-mesenteric artery
61. spinal nerve
62. sympathetic nerve ganglion
63. nephric (mesonephric, Wolffian) duct
64. foramen of ilioischiadicum
65. iliotibialis muscle
66. flexor cruris lateralis (semitendinosus) muscle
67. left ventral hepatic cavity
68. genital fold
69. cloacal ridge
70. rectum
71. clot of extravasated blood (artefact of preparation)
72. dorsal root ganglion
73. metanephric duct
74. obturator nerve
75. pubocaudalis internus muscle
76. pubocaudalis externus muscle
77. cloaca

Plate 206

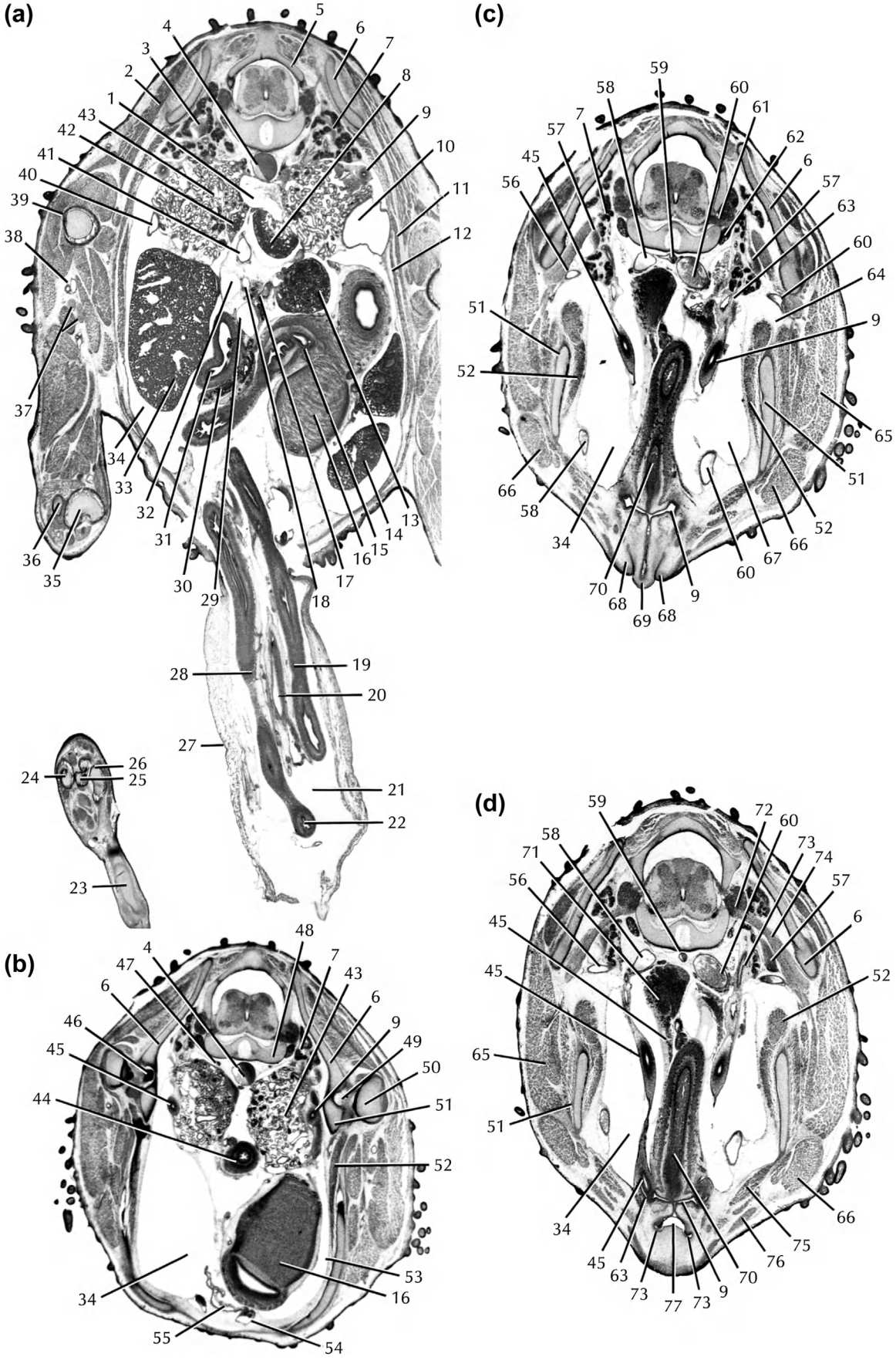

Plate 207 Stage 37 (day 11) TS

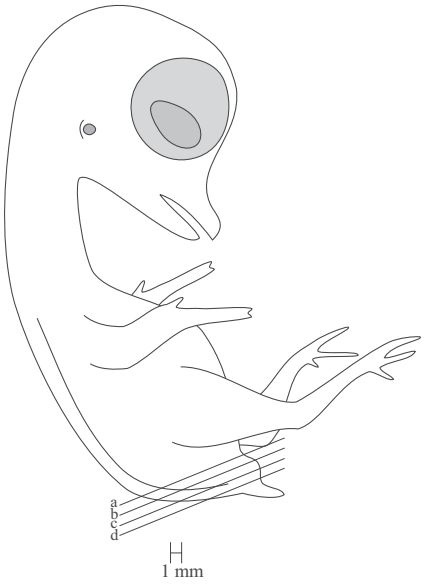

Transverse sections (TS): (a–d) × 15

1. caudal artery
2. transverse process of sacral vertebra fused to ischium, contributing to synsacrum
3. neural arch
4. dorsal root ganglion
5. sympathetic nerve ganglion
6. spinal nerve, part of pudendal plexus
7. caudal renal portal vein
8. left omphalo-mesenteric artery
9. obturator muscle
10. iliotibialis muscle
11. caudofemoralis muscle, pars iliofemoralis
12. pubis
13. metanephric duct (ureter)
14. abdominal air sac
15. left oviduct (Mullerian duct)
16. nephric (mesonephric, Wolffian) duct
17. levator cloacae muscle
18. dorsal mesentery
19. pectineal process
20. right omphalo-mesenteric artery
21. metanephros
22. ilium
23. notochord
24. spinal cord
25. flexor cruris lateralis muscle
26. cloaca
27. peritoneum
28. lateralis caudae muscle
29. coccygeo-mesenteric vein (fused left and right coccygeal veins)
30. cloacal bursa (bursa of Fabricius)
31. caudal renal portal vein
32. body of caudal vertebra
33. levator caudae muscle

Plate 207

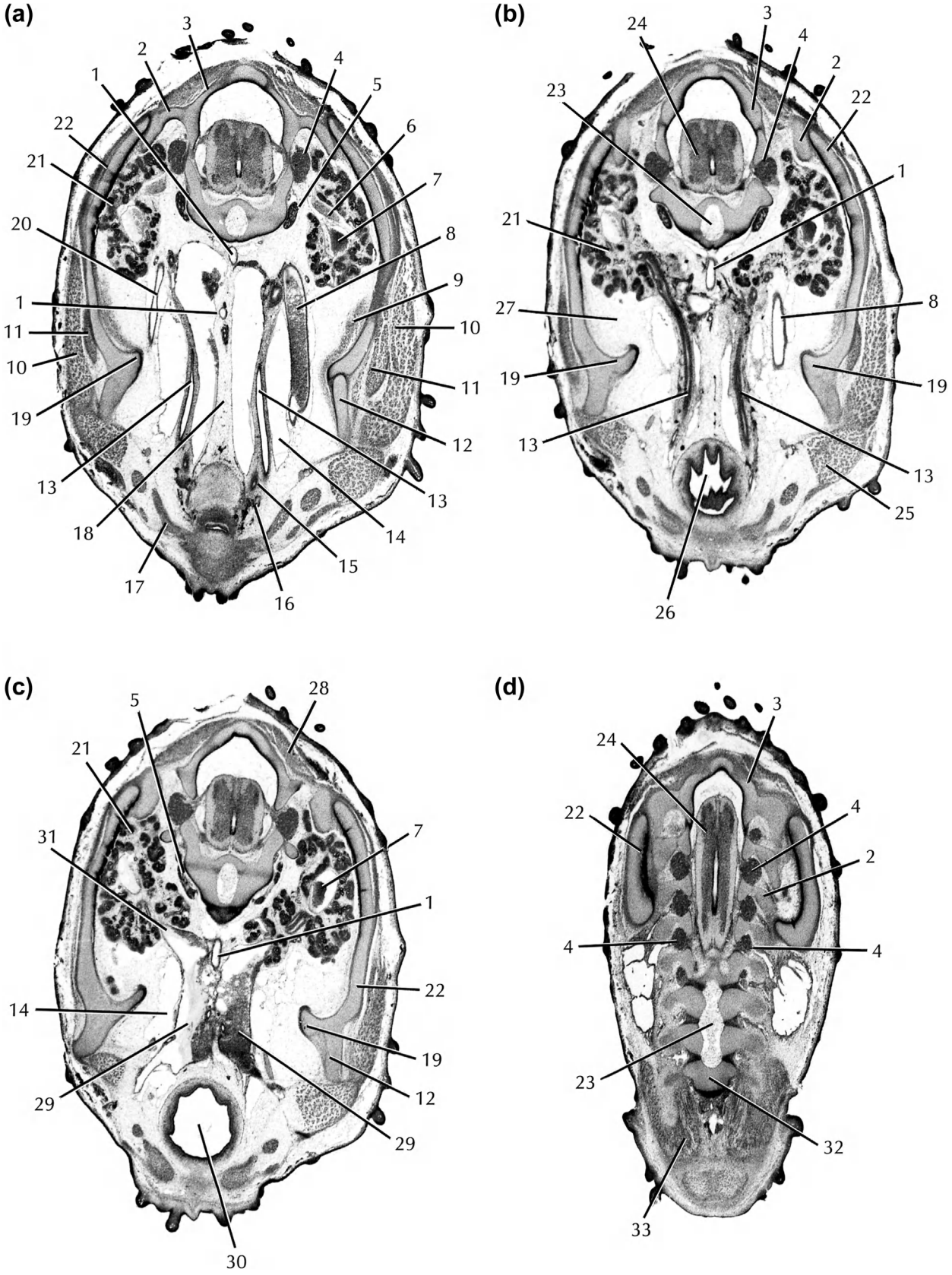
(a)
3
2
1
4
5
22
6
21
7
20
8
1
9
11
10
10
11
19
12
13
13
18
14
15
17
16
(b)
24
3
4
2
23
22
1
21
8
27
19
19
13
13
25
26
(c)
5
28
21
7
31
1
22
14
19
12
29
29
30
(d)
3
24
22
4
2
4
4
23
32
33

Plate 208 Stage 39 (day 13) LS: sagittal

Londitudinal (sagittal) sections taken through plane of page:

(a) Abdomen × 4

(b) Cloacal region × 20

(c) Enlargement of part of (a) × 10

1. cervical muscles
2. spinal cord
3. cervical vertebra
4. spinal nerve
5. left rhomboideus muscle
6. left primary bronchus
7. rib
8. left lung
9. proventriculus
10. left ilium
11. head of left femur
12. ischium
13. oviduct (Mullerian duct)
14. obturator muscle
15. pectineal process
16. pubis
17. cloacal bursa (bursa of Fabricius)
18. coprodaeum
19. loop of intestine
20. gizzard
21. liver
22. ventricle
23. pulmonary artery
24. head of left humerus
25. clavicle
26. trachea
27. oesophagus
28. feather bud
29. cloacal sphincter
30. cloaca
31. left anterior thoracic air sac
32. oblique septum

Plate 208

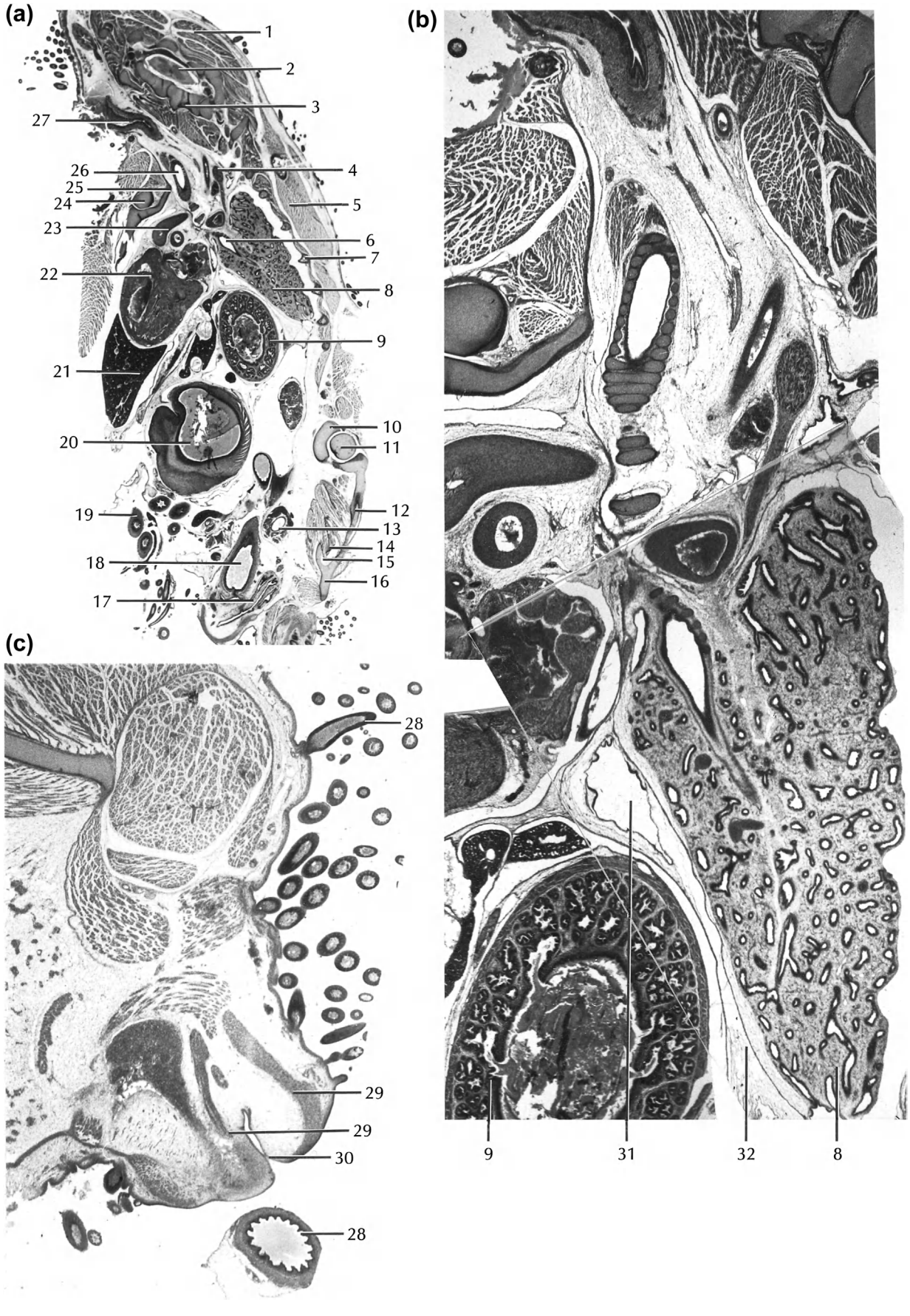
(a)
1
2
3
27
26
4
25
24
5
23
6
7
22
8
9
21
10
20
11
12
19
13
14
18
15
16
17
(b)
9
31
32
8
(c)
28
29
29
30
28

Plate 209 Stage 39 (day 13) LS: coronal and sagittal

(a) Coronal section × 18

(b) Coronal section × 15

(c) Sagittal section through plane of page. Enlargement of part of *plate 208a* × 18

(d) Section adjacent to (c) × 15

1. right mesonephros
2. right metanephros
3. spinal cord
4. caudal vertebra
5. feather papilla
6. feather
7. adductor retricium muscle
8. pubocaudalis internus muscle
9. pubocaudalis lateralis muscle
10. coprodaeum
11. cloacal bursa (bursa of Fabricius)

Plate 209

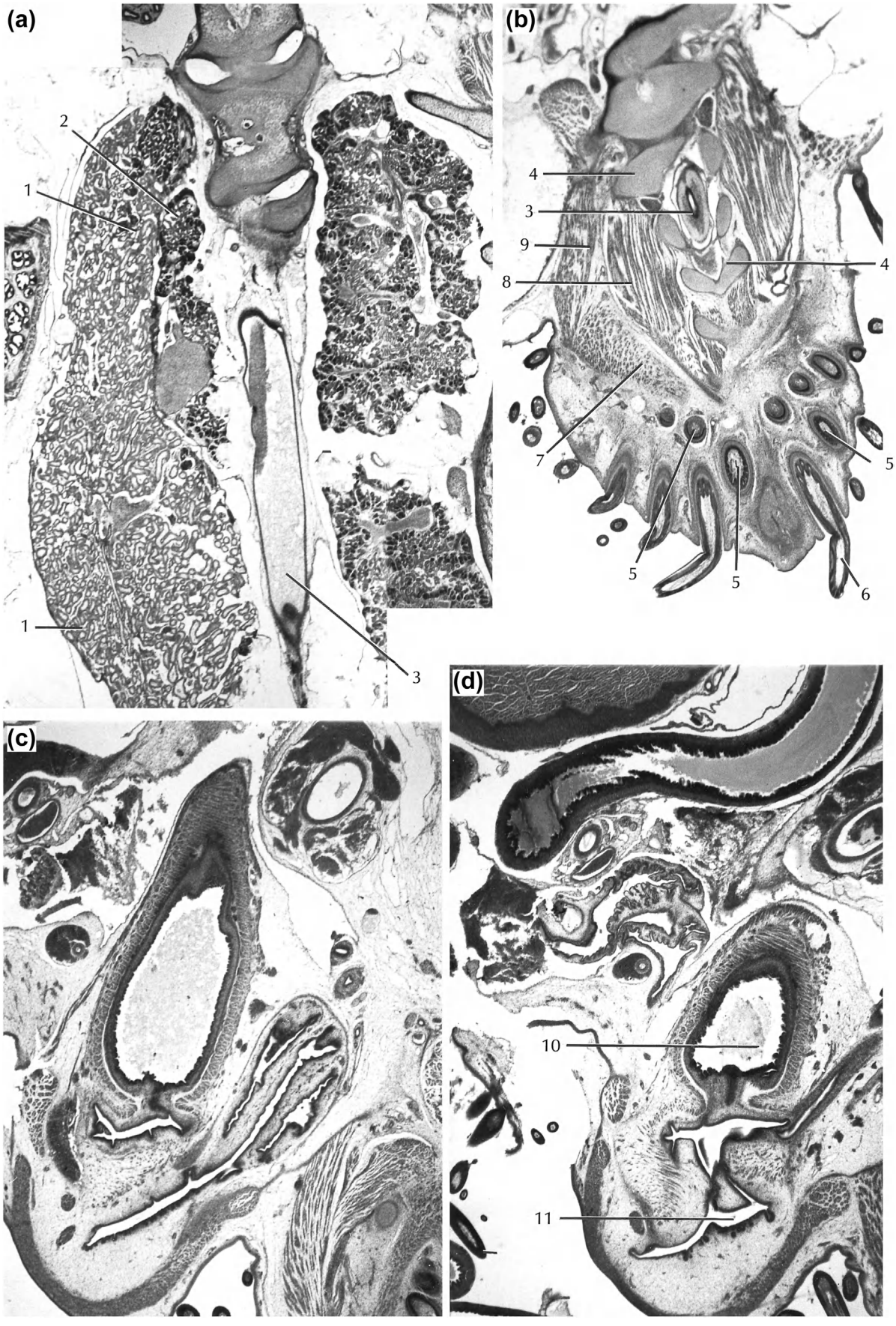

Plate 210 Stage 39 (day 13) TS

Transverse section through the neck: × 10

1. right thymus
2. spinal cord
3. spinalis muscle
4. biventer cervicis muscle
5. spinous process of vertebra
6. spinal canal
7. left thymus
8. transverse process of vertebra
9. left dorsal root ganglion
10. intertransversarii muscle
11. body of vertebra
12. left carotid artery (with right carotid artery adjacent)
13. trachea
14. feathers
15. cervical oesophagus (anterior to crop)
16. right dorsal root ganglion

Plate 210

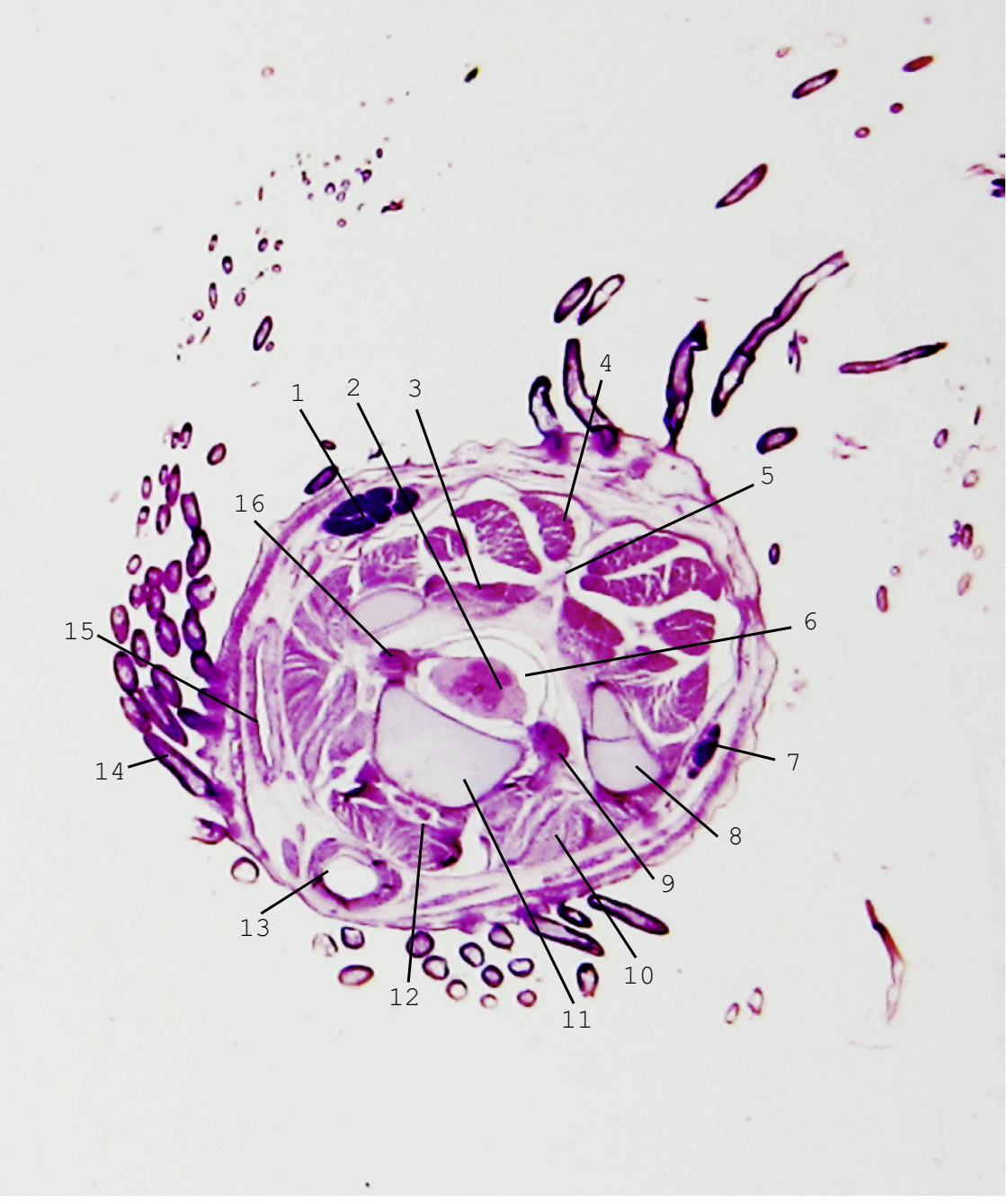

Plate 211 Stage 39 (day 13) TS

Transverse section through the neck: × 13

1. spinal cord
2. spinalis muscle
3. biventer cervicis muscle
4. transverse process of vertebra
5. thymus
6. intertraversii muscle
7. descending vertebral artery
8. longus colli ventralis muscles
9. left and right carotid arteries
10. trachea
11. body of vertebra
12. cervical oesophagus (anterior to crop)
13. neural arch of vertebra

Plate 211

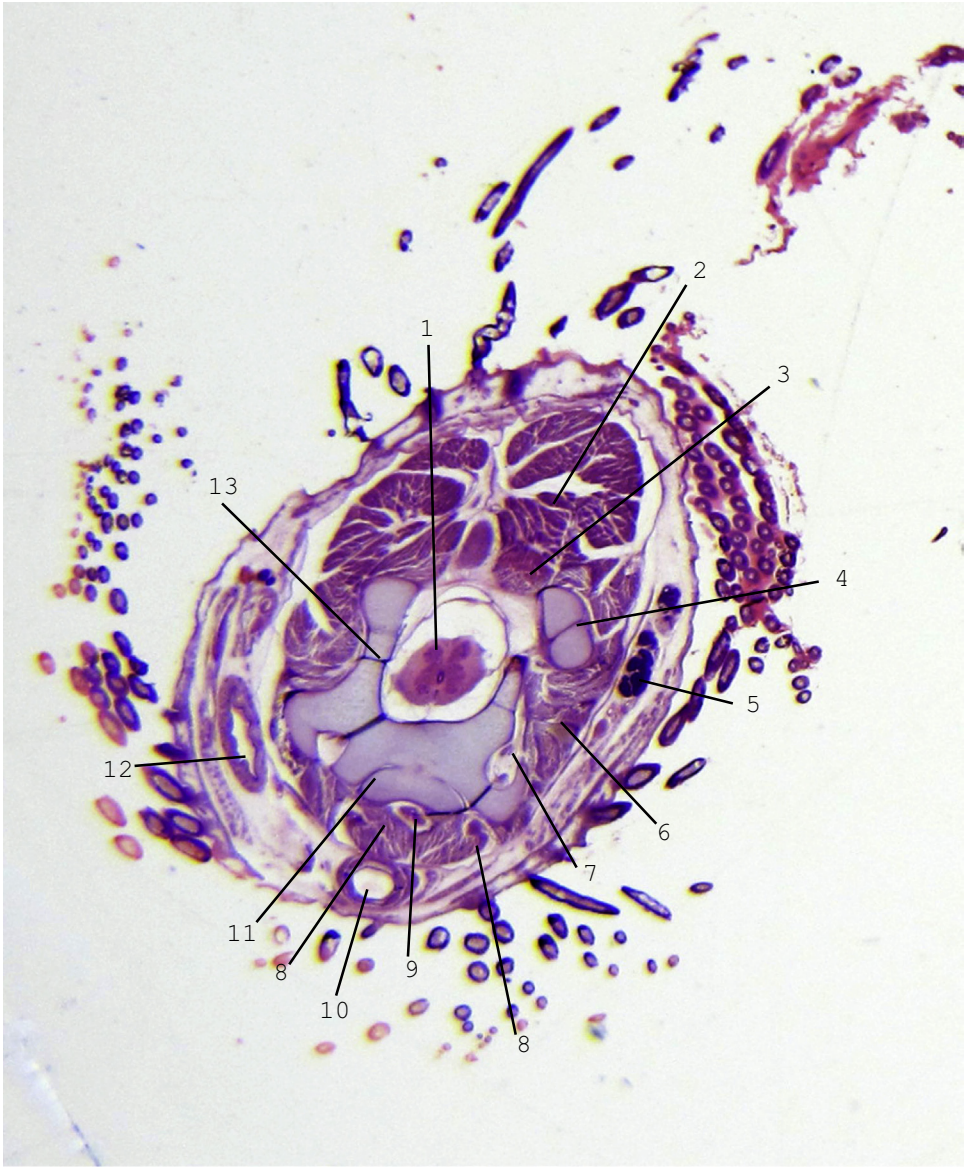

Plate 212 Stage 39 (day 13) TS

Transverse section (TS): × 13

1. spinal cord
2. neural arch
3. dorsal root ganglion
4. left biventer cervicis muscle
5. left scapulohumeralis muscle
6. left humerus
7. left coracoid
8. left internal jugular vein
9. left thymus
10. left longus colli ventralis muscle
11. left carotid artery
12. trachea
13. right carotid artery
14. wall of crop
15. right longus colli ventralis muscle
16. lumen of crop
17. body wall
18. right thymus
19. right pectoralis muscle
20. right coracoid
21. right humerus
22. right internal jugular vein
23. right scapulohumeralis muscle
24. right biventer cervicis muscle
25. right vertebral vein
26. latissimus dorsi muscle
27. right longus colli dorsalis muscle
28. spinous process of vertebra

Plate 212

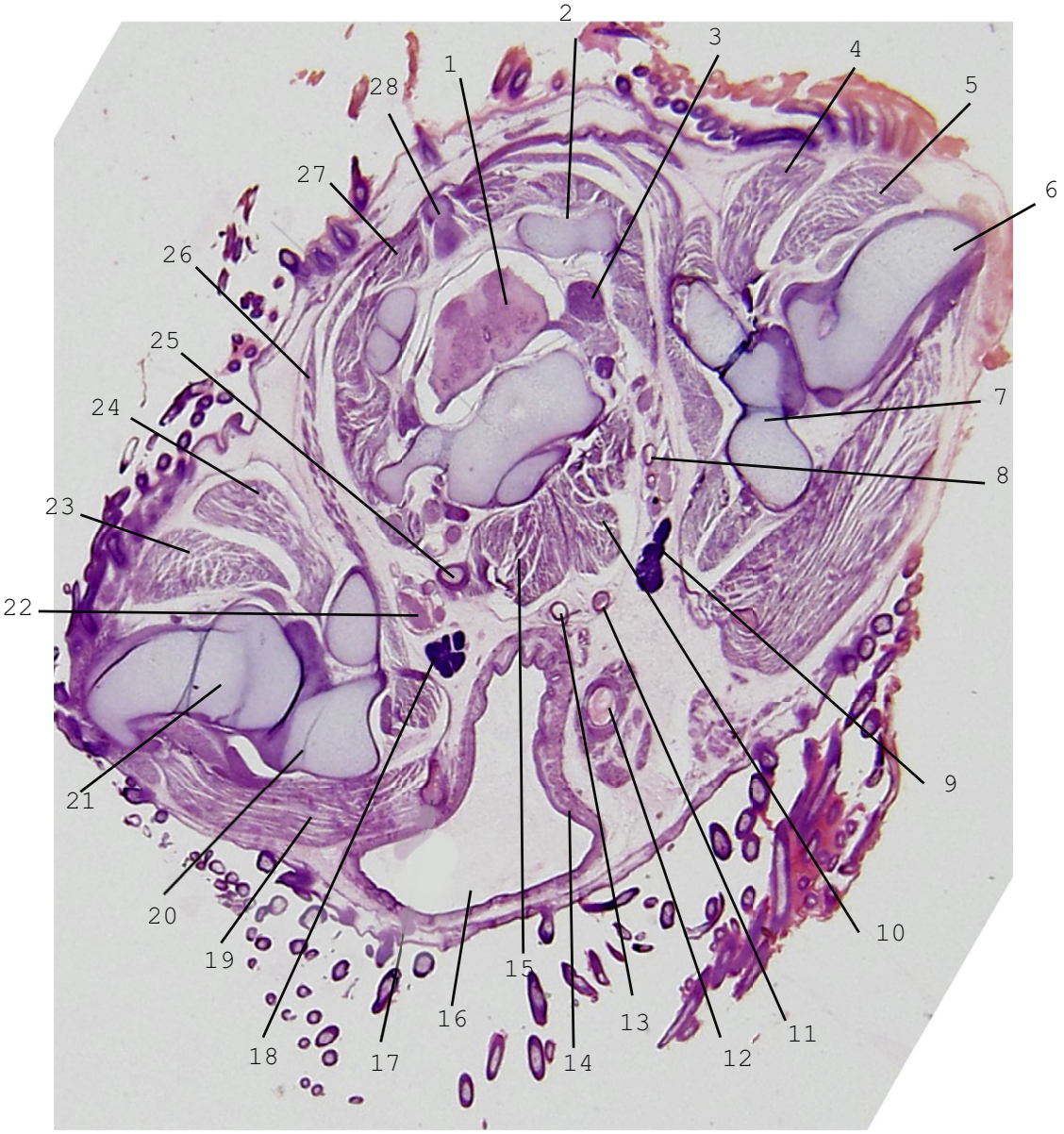

Plate 213 Stage 39 (day 13) TS

Transverse section (TS): × 13

1. body of vertebra
2. neural arch of vertebra
3. right longus colli dorsalis muscle
4. notochord
5. vertebral canal
6. spinal cord
7. left longus colli dorsalis muscle
8. left rhomboideus muscle
9. dorsal root ganglion
10. left spinalis muscle
11. left rhomboideus superficialis muscle
12. left scapula
13. left scapulohumeralis muscle
14. left latissimus dorsi muscle
15. left transverse process of vertebra
16. left deltoid muscle
17. humerus
18. left coracobrachialis muscle
19. left subcoracoideus muscle
20. left coracoid
21. left longus colli ventralis muscle
22. left supracoracoid muscle
23. left lobe of thyroid
24. left pectoralis major muscle
25. left carotid artery
26. trachea
27. fat
28. thoracic oesophagus (posterior to crop)
29. right carotid artery
30. right pectoralis major muscle
31. right longus colli ventralis muscle
32. right lobe of thyroid
33. right internal jugular vein
34. right vagus nerve
35. head of right humerus
36. right scapulohumeralis muscle
37. right scapula
38. right deltoid muscle
39. feathers

Plate 213

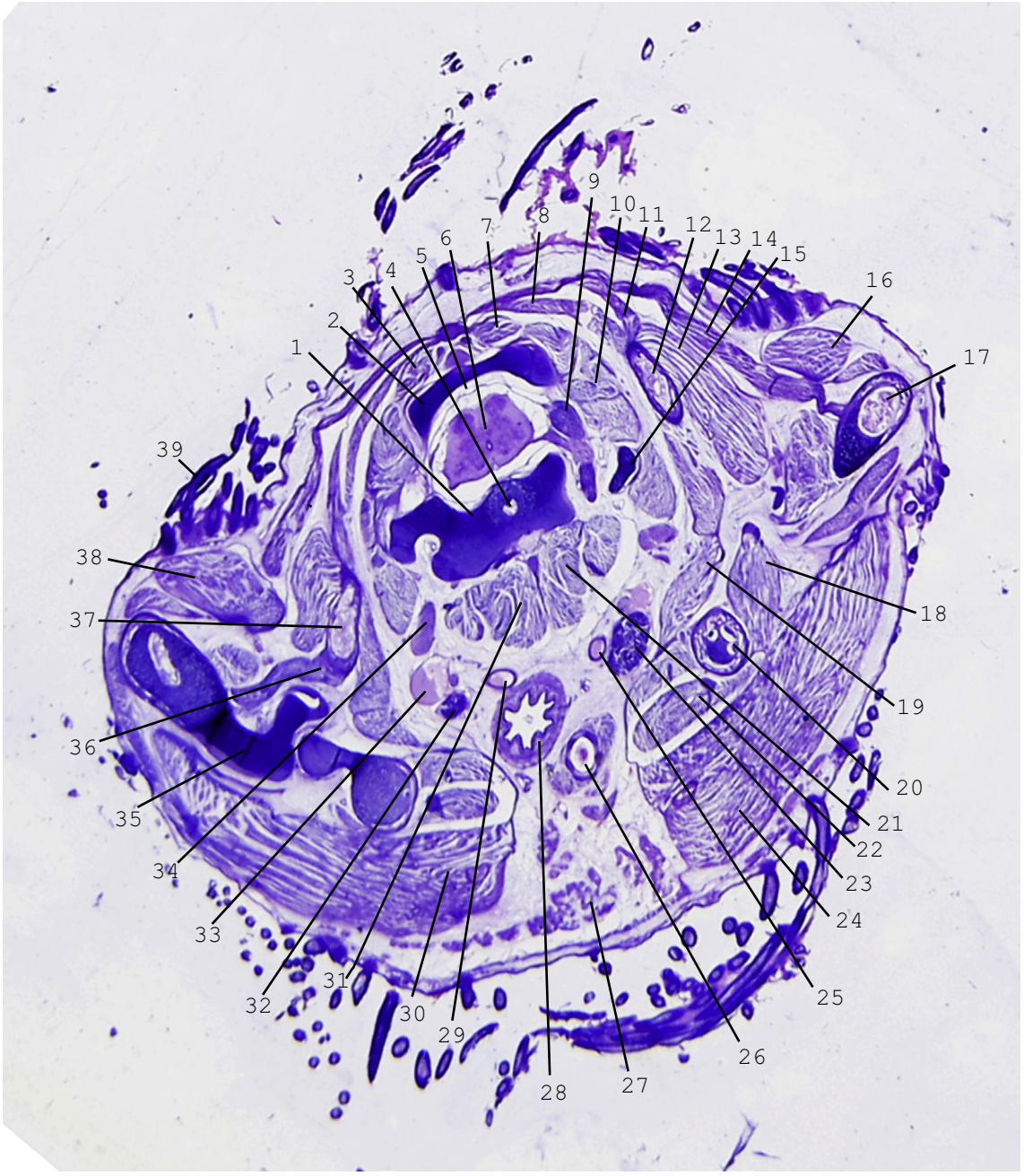
1
2
3
4
5
6
7
8
9
10
11
12
13
14
15
16
17
18
19
20
21
22
23
24
25
26
27
28
29
30
31
32
33
34
35
36
37
38
39

Plate 214 Stage 39 (day 13) TS

Enlargements of parts of *plate 213*:

(a) Fat bodies in neck × 50

(b) Muscle attachments × 70

1. wall of syrinx showing cartilaginous rings and muscle attachments
2. edge of left pectoralis major muscle
3. fat bodies in connective tissue
4. edge of thoracic oesophagus
5. right deltoid muscle
6. right scapula
7. right coracoid
8. junction of right scapulohumeralis muscle and humerus
9. right humerus

Plate 214

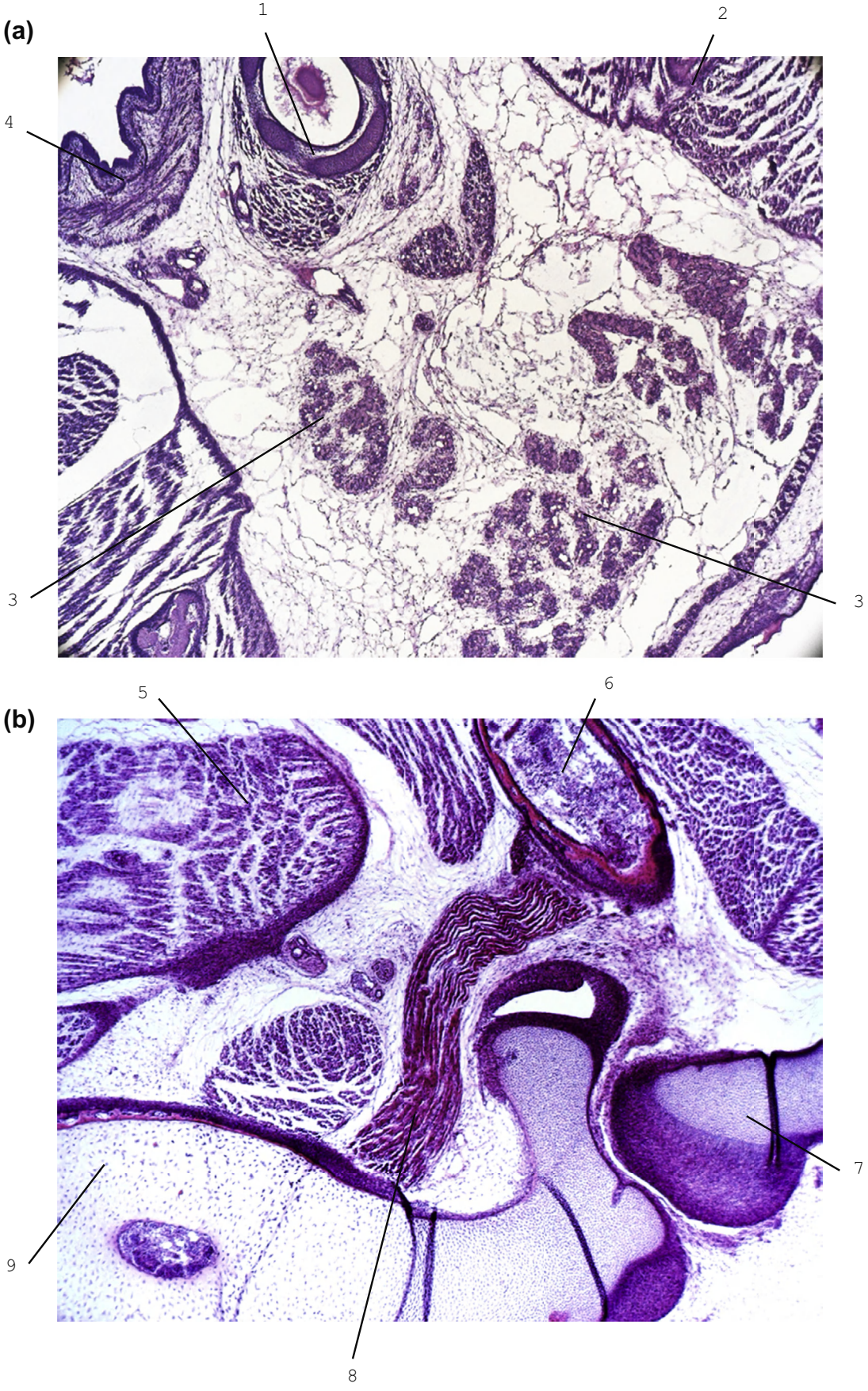

Plate 215 Stage 39 (day 13) TS

Enlargement of part of section adjacent to *plate 216*:
× 45

1. left longus colli ventralis muscle
2. left pulmonary fold
3. left lung
4. left pleural cavity
5. oblique septum
6. rib
7. vertebral rib
8. left subcoracoideus muscle
9. left brachiocephalic artery
10. nerve
11. extrapulmonary bronchus

Plate 215

Plate 216 Stage 39 (day 13) TS

Transverse section (TS): × 15

1. spinal cord
2. spinous process of vertebra
3. left longus colli dorsalis muscle
4. transverse process of vertebra
5. left latissimus dorsi muscle
6. feather
7. scapula
8. pleural cavity
9. left lung
10. triceps brachialis (anconeus) muscle, pars scapula-triceps
11. humerus
12. rib
13. biceps brachii muscle
14. vertebral body
15. left anterior thoracic air sac
16. left longus colli ventralis muscle
17. left brachiocephalic artery
18. left coracoid
19. lumen of syrinx
20. supracoracoideus (pectoralis secundum) muscle
21. hypocledial ligament
22. sternum
23. pectoralis muscle
24. trachea
25. right coracoid
26. right brachiocephalic artery
27. right thymus
28. internal jugular vein
29. right longus colli ventralis muscle
30. right pleural cavity
31. right humerus
32. right lung
33. right scapula
34. dorsal root ganglion
35. notochord

Plate 216

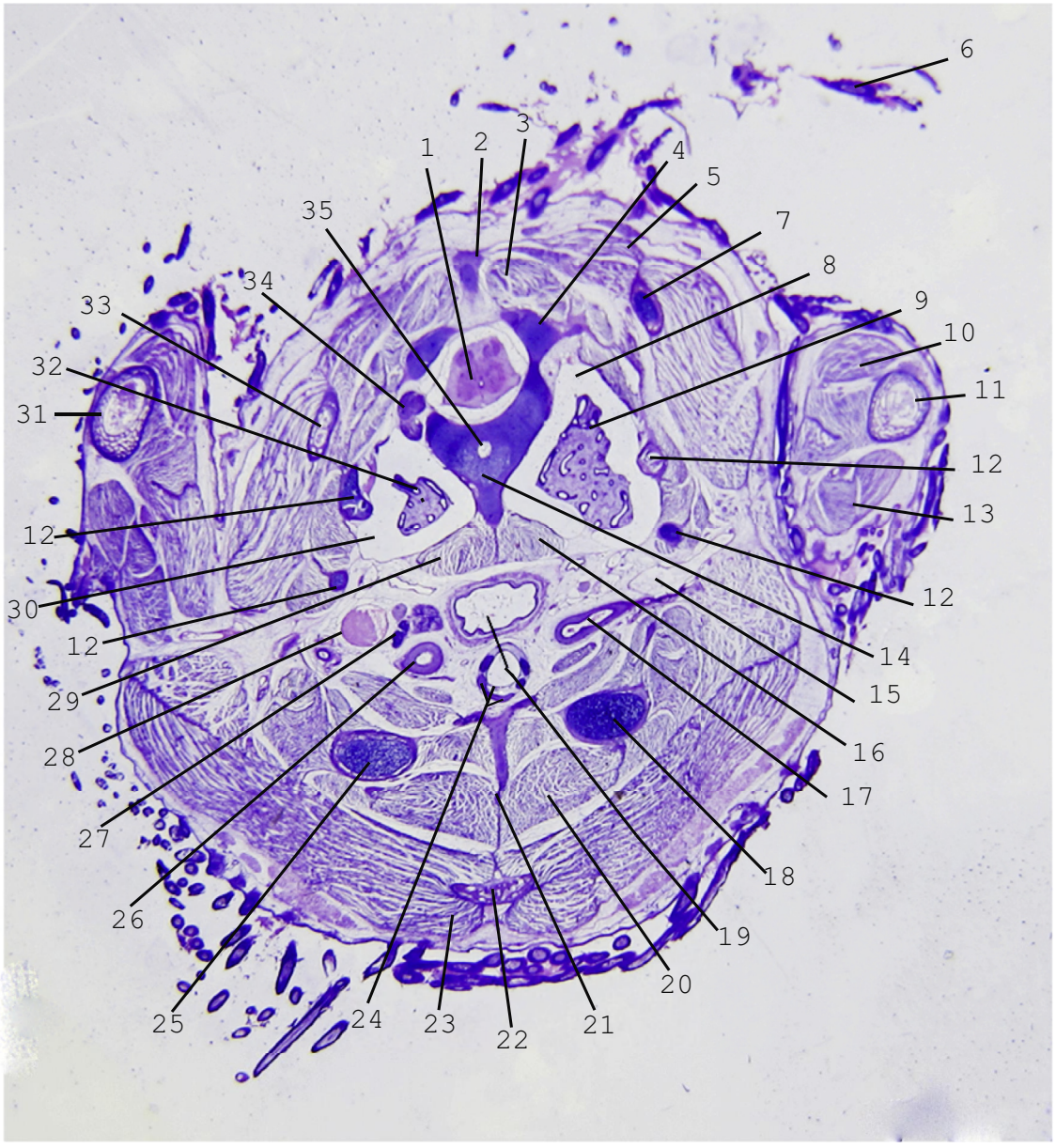
6
1
2
3
4
5
35
7
8
34
33
9
10
32
11
31
12
13
12
30
12
14
29
15
28
16
27
17
18
26
19
20
25
24
23
22
21

Plate 217 Stage 39 (day 13) TS

Transverse section (TS): × 12

1. remains of notochord in vertebral body
2. spinal cord
3. left longus colli dorsalis muscle
4. left latissimus dorsi muscle
5. left pleural cavity
6. left lung
7. left humerus
8. left radius
9. left biceps brachii muscle
10. left carotid artery
11. left wing
12. intercostal muscle
13. peritoneum
14. thoracic oesophagus
15. cranial thoracic air sac
16. sternum
17. left pulmonary artery
18. left brachiocephalic artery
19. hypocledial ligament
20. right brachiocephalic artery
21. aortic arch
22. right pulmonary artery
23. peritoneum
24. right abdominal air sac
25. right pulmonary cavity
26. right bronchus
27. right carotid artery
28. right lung
29. dorsal aorta
30. remnant of dorsal mesentery

Plate 217

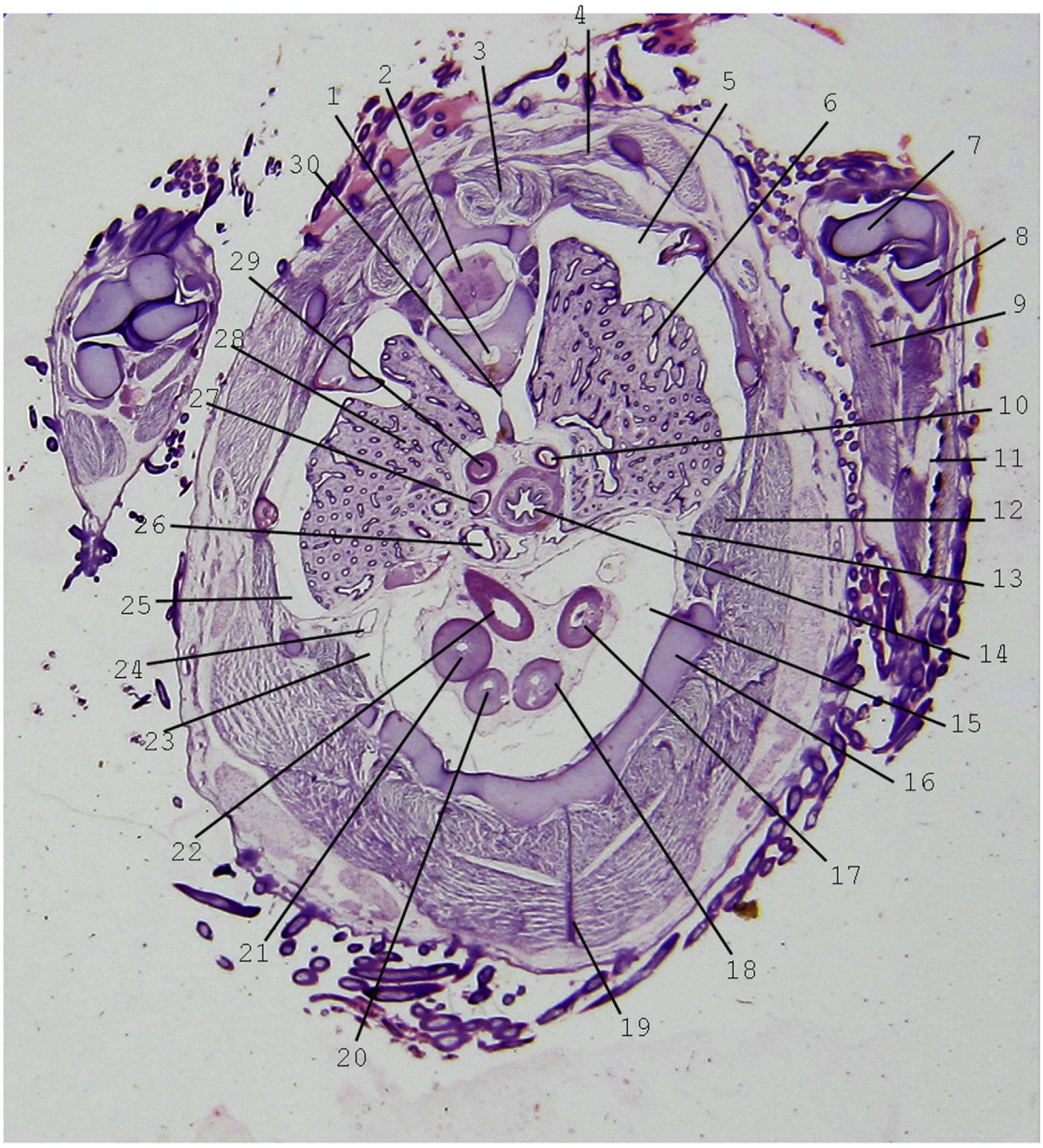
1
2
3
4
5
6
7
8
9
10
11
12
13
14
15
16
17
18
19
20
21
22
23
24
25
26
27
28
29
30

Plate 218 Stage 39 (day 13) TS

Transverse section (TS): × 10

1. spinal cord
2. left longus colli dorsalis muscle
3. vertebral body
4. rib
5. left lung
6. left carotid artery
7. left radius
8. epithelium
9. pulmonary cavity
10. oesophagus
11. oblique septum
12. pericardial cavity
13. thin wall of atrium
14. supracoracoid muscle
15. truncus arteriosus
16. keel of sternum
17. conus arteriosus
18. pectoralis muscle
19. right pulmonary vein
20. right carotid artery
21. right lung
22. right radius
23. right ulna
24. dorsal aorta
25. vertebral arch
26. right longus colli dorsalis

Plate 218

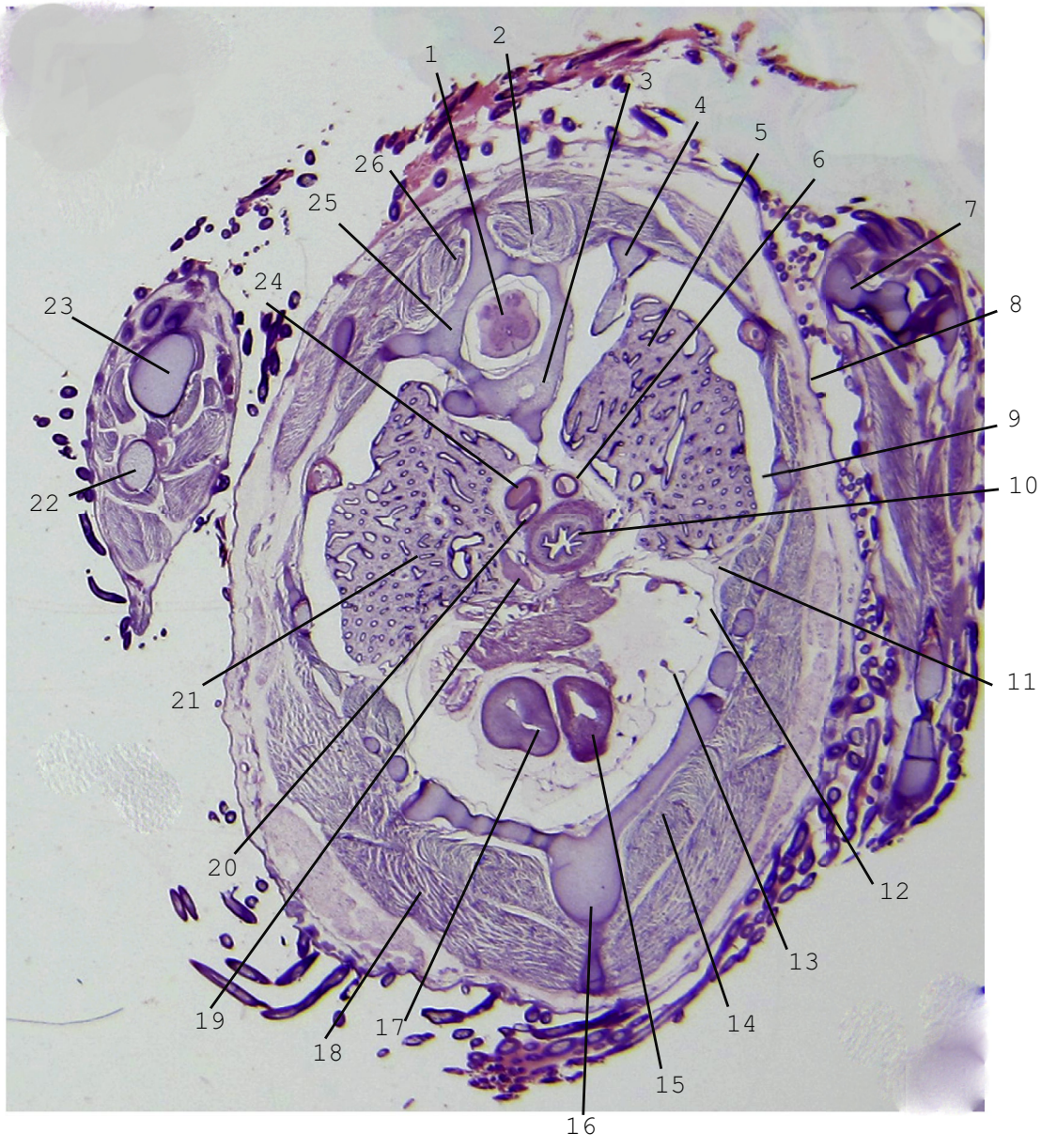

Plate 219 Stage 39 (day 13) TS

Transverse section (TS): × 10

1. spinal cord
2. left longus colli dorsalis muscle
3. rhomboideus superficialis muscle
4. pleural cavity
5. left lung
6. remnant of dorsal mesentery
7. dorsal aorta
8. rib
9. biceps brachii muscle
10. intercostal muscle
11. humerotriceps muscle
12. oesophagus
13. left atrium
14. ulnacarpal
15. pulmonary artery
16. left pectoralis muscle
17. keel of sternum
18. truncus arteriosus
19. pulmonary artery
20. right atrium
21. oblique septum
22. right primary bronchus
23. right lung
24. feathers

Plate 219

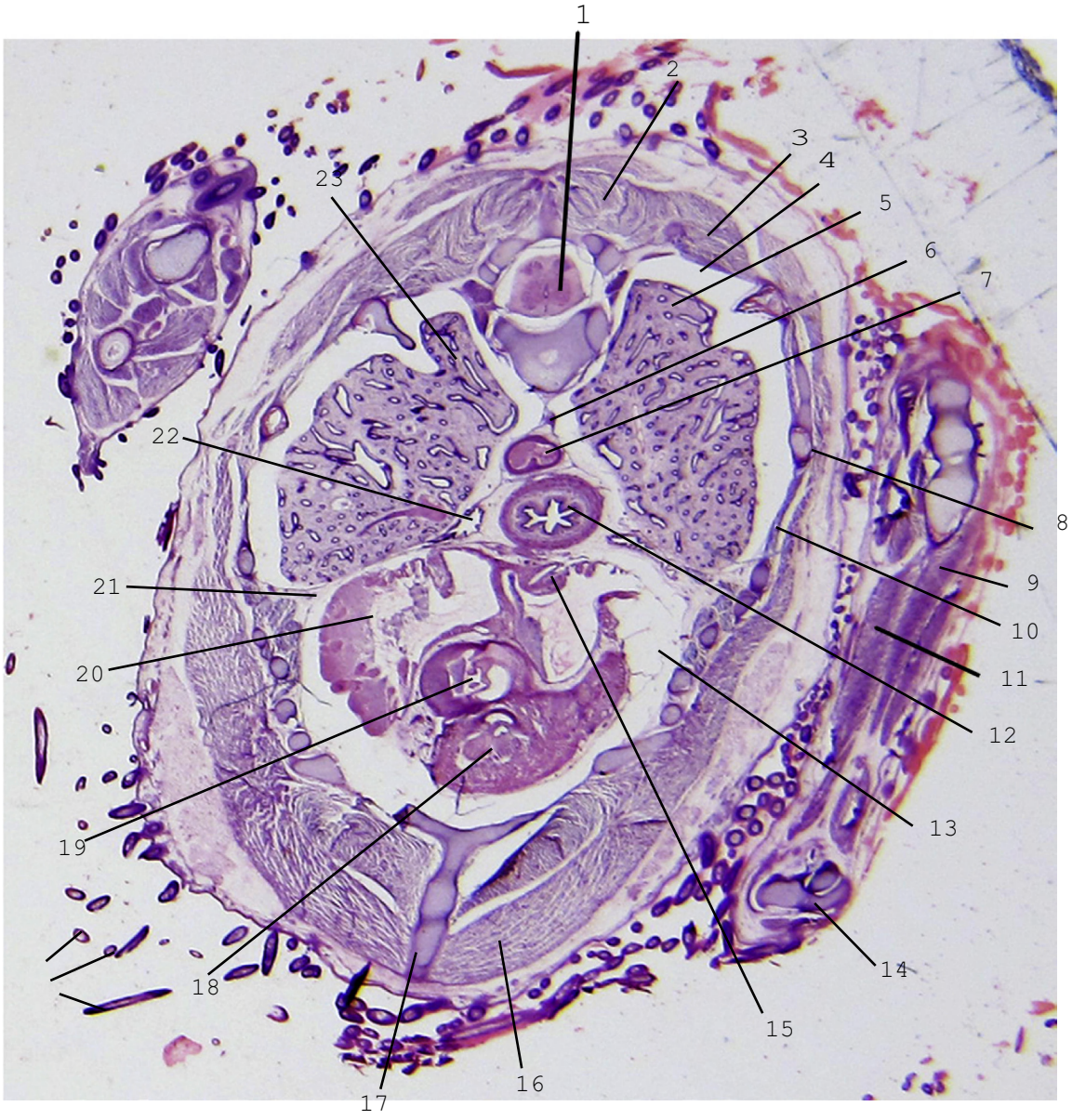

Plate 220 Stage 39 (day 13) TS

Transverse section (TS): × 80

1, 2, 4: valves of pulmonary artery

3: wall of pulmonary artery

5, 7, 8: valves of truncus arteriosus

6: wall of truncus arteriosus

Plate 220

Plate 221 Stage 39 (day 13) TS

Transverse section (TS): × 10

1. spinous process of vertebra
2. spinal cord
3. left ilium
4. left iliofemoralis muscle
5. left metanephros
6. left mesonephros
7. left ovary
8. left dorsal hepatic cavity
9. rib
10. proventriculus
11. left carotid artery
12. crest of left fibula
13. right carotid artery
14. left lobe of liver
15. left ventricle
16. keel of sternum
17. right lobe of liver
18. left patella
19. right dorsal hepatic cavity
20. right mesonephros
21. right metanephros
22. anterior mesenteric artery
23. right ilium
24. dorsal aorta

Plate 221

Plate 222 Stage 39 (day 13) TS

Transverse section (TS): × 10

1. spinal cord
2. vertebral canal
3. neural arch
4. left metanephros
5. left ilium
6. head of left femur
7. left acetabulum
8. left oviduct (Mullerian duct)
9. trochanter of left femur
10. left mesonephros
11. left oblique internus abdominus muscle
12. lumen of gizzard
13. left lobe of liver
14. left femur
15. wall of gizzard
16. duodenum
17. right allantoic artery
18. right lobe of liver
19. right femur
20. condyle of right femur
21. horizontal hepatic ligament
22. anterior mesenteric artery
23. right foot
24. right lateral thoracic air sac
25. trochanter of right femur
26. right mesonephros
27. right metanephros
28. right ilium
29. dorsal aorta
30. remnant of notochord in vertebral body

Plate 222

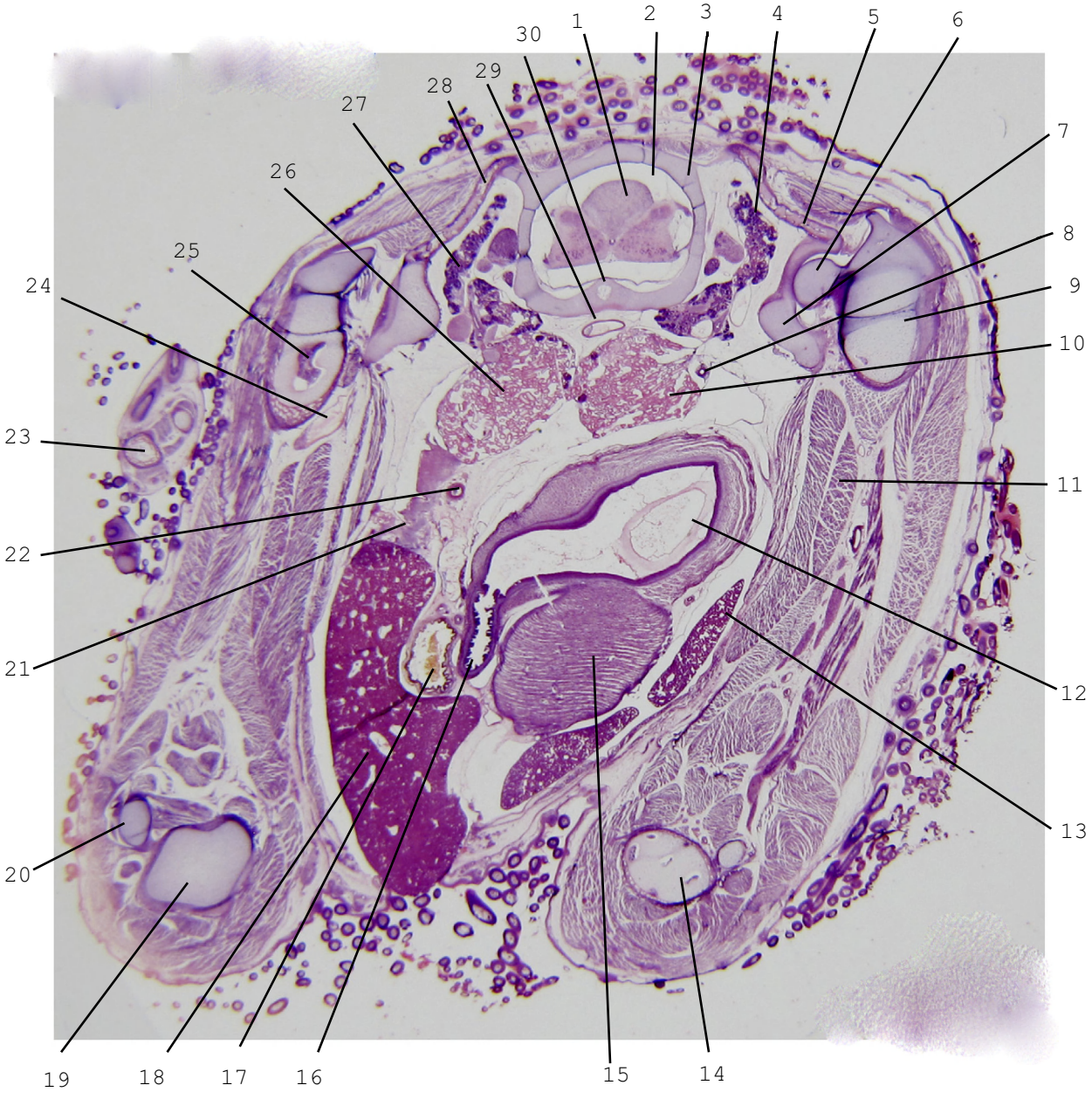
1
2
3
4
5
6
7
8
9
10
11
12
13
14
15
16
17
18
19
20
21
22
23
24
25
26
27
28
29
30

Plate 223 Stage 39 (day 13) TS

Enlargements of parts of *plate 222*:

(a) Mesonephros × 45

(b) Metanephros × 100

1. mesonephric tubules
2. metanephros
3. dorsal root ganglion
4. metanephric tubules
5. sympathetic ganglion
6. vertebral cartilage

Plate 223

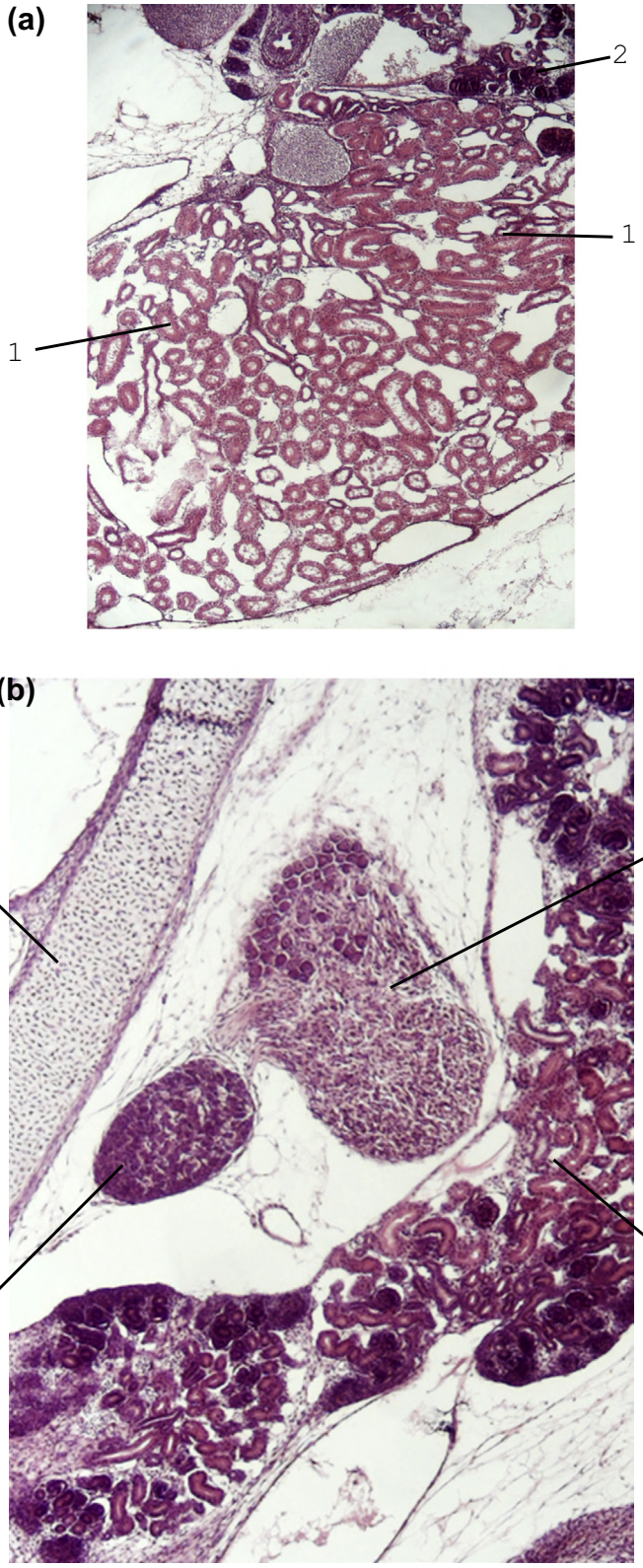

Plate 224 Stage 39 (day 13) TS

(a) Enlargement of part of *plate 226* – loop of herniated gut in umbilicus: × 30

(b) Cloaca and oviducts: × 30

1. embryonic coelom
2. loops of gut in umbilicus
3. remnant of embryonic coelom
4. fatty tissue
5. longitudinal section through a feather
6. extra-embryonic coelom
7. edge of umbilical opening
8. rectum
9. left oviduct (Mullerian duct)
10. cloaca
11. junction of cloaca and rectum
12. right oviduct (Mullerian duct)
13. right pubis

Plate 224

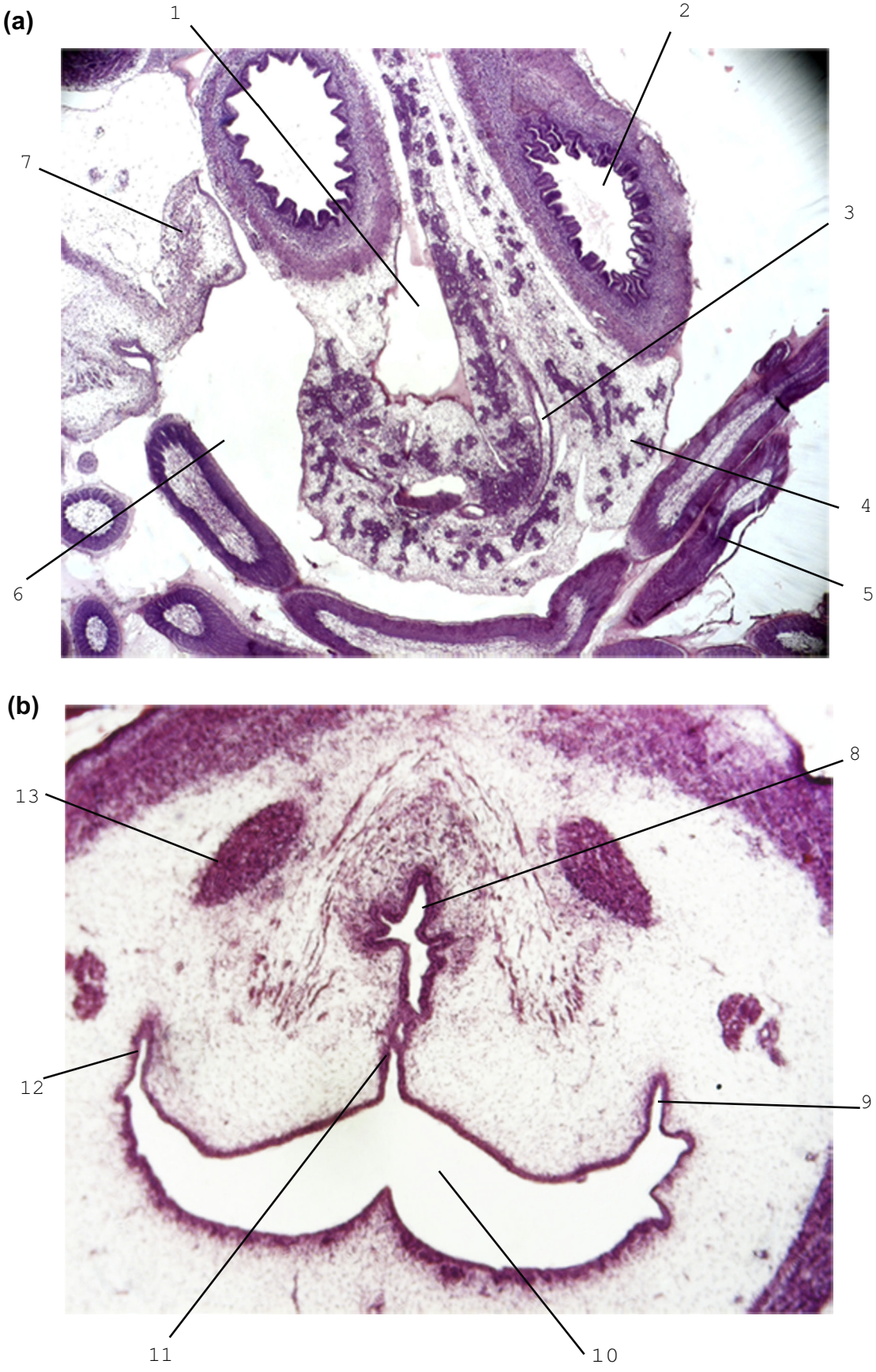

Plate 225 Stage 39 (day 13) TS

Transverse section (TS) through umbilical region: × 13

1. spinal cord
2. notochord
3. neural arch
4. left renal portal vein
5. left metanephros
6. left metanephric duct
7. left ventral gastric artery
8. left ischiofemoralis (obturator externus) muscle
9. iliofibularis muscle
10. acetabulum
11. pubis
12. wall of gizzard
13. feathers
14. lumen of gizzard
15. left fibularis longus muscle
16. left tibiocranialis muscle
17. left tibiotarsus
18. section across large intestine
19. umbilical gap
20. body wall
21. right tibiotarsus
22. right fibula
23. right fibularis longus muscle
24. right flexor cruris medialis muscle
25. right flexor cruris lateralis muscle
26. section across small intestine
27. right foot
28. right pubis
29. right ischium
30. peritoneal cavity
31. right ilium
32. right metanephric duct
33. right metanephros
34. right renal portal vein
35. cloaca

Plate 225

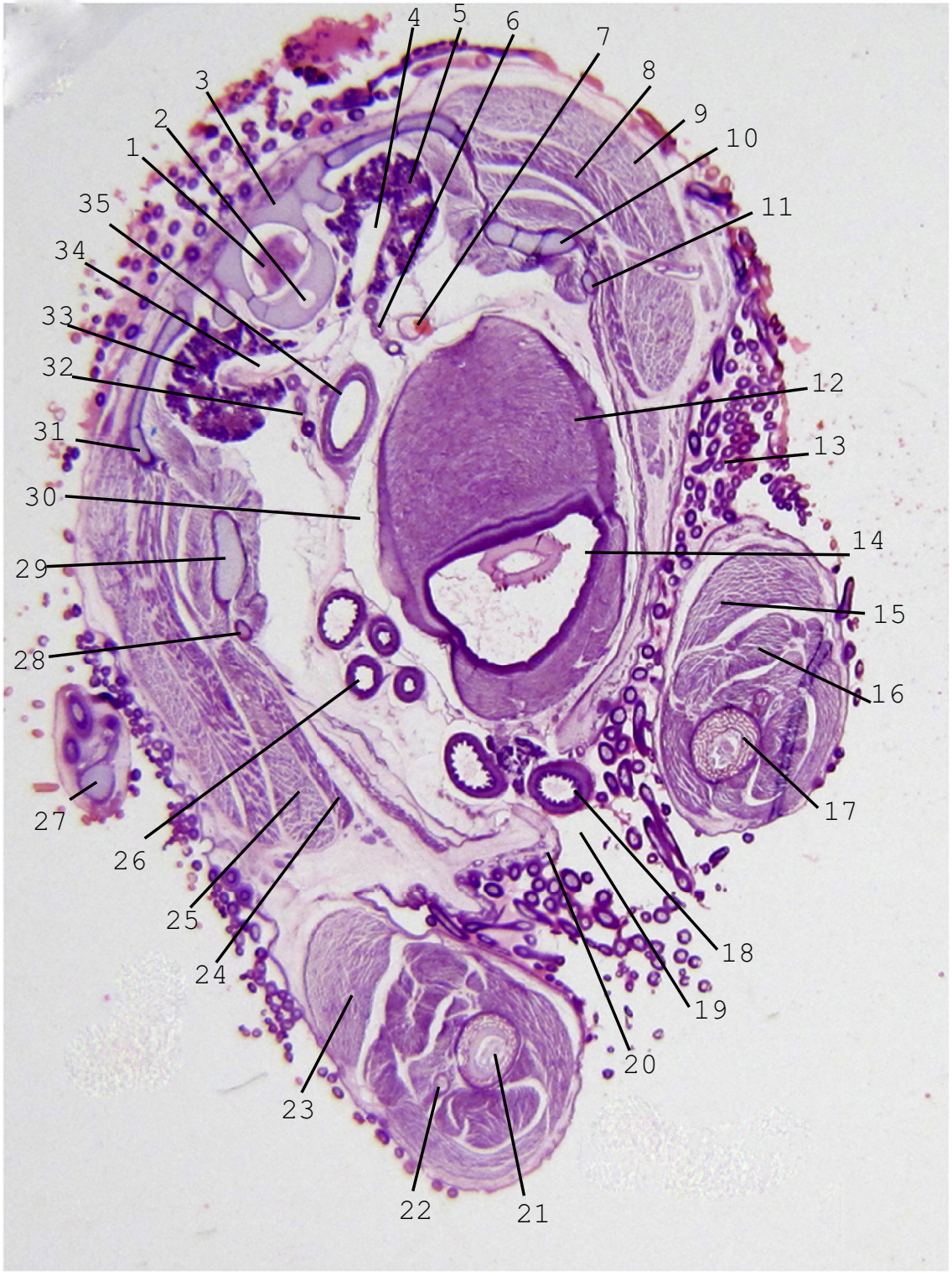
1
2
3
4
5
6
7
8
9
10
11
12
13
14
15
16
17
18
19
20
21
22
23
24
25
26
27
28
29
30
31
32
33
34
35

Plate 226 Stage 39 (day 13) TS

Transverse section (TS) through umbilical region: × 13

1. ventral gastric artery
2. sciatic foramen
3. iliofemoralis muscle
4. left ilium
5. muscular wall of gizzard
6. pubis
7. feathers
8. loop of intestine
9. left abdominal air sac
10. left fibularis longus muscle
11. left femur
12. herniated loop of gut
13. fat
14. right femur
15. right fibularis longus muscle
16. wall of abdominal air sac
17. right abdominal air sac
18. right iliofemoralis muscle
19. oburator medialis muscle
20. right ischium
21. cloaca
22. right oviduct (Mullerian duct)
23. right metanephric duct
24. right nephric (Wolffian) duct
25. right internal iliac vein
26. spinal cord
27. remains of notochord in vertebra
28. right longus colli dorsalis muscle

Plate 226

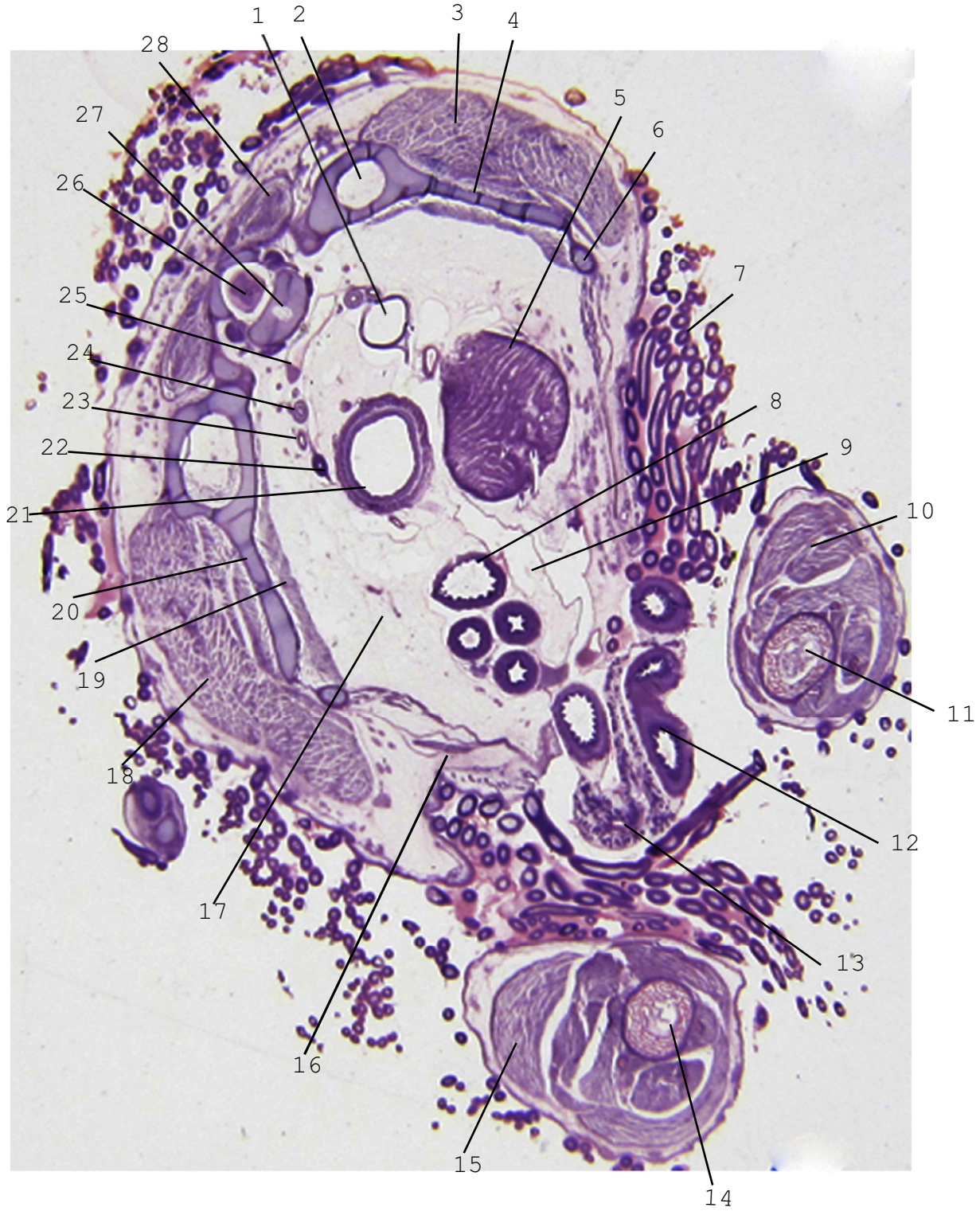

Plate 227 Stage 39 (day 13) TS

Transverse section (TS) through caudal region: × 14

1. rhomboideus superficialis muscle
2. spinal cord
3. left lateral caudalis muscle
4. left pubo-caudalis muscle
5. cloacal bursa (bursa of Fabricius)
6. left internal pubo-caudalis muscle
7. left oviduct (Mullerian duct)
8. body wall
9. cloaca
10. oblique section through loop of intestine
11. left leg
12. allantoic stalk
13. herniated loop of intestine
14. right leg
15. tips of feathers
16. pubis
17. right oviduct (Mullerian duct)
18. vitelline vessels

Plate 227

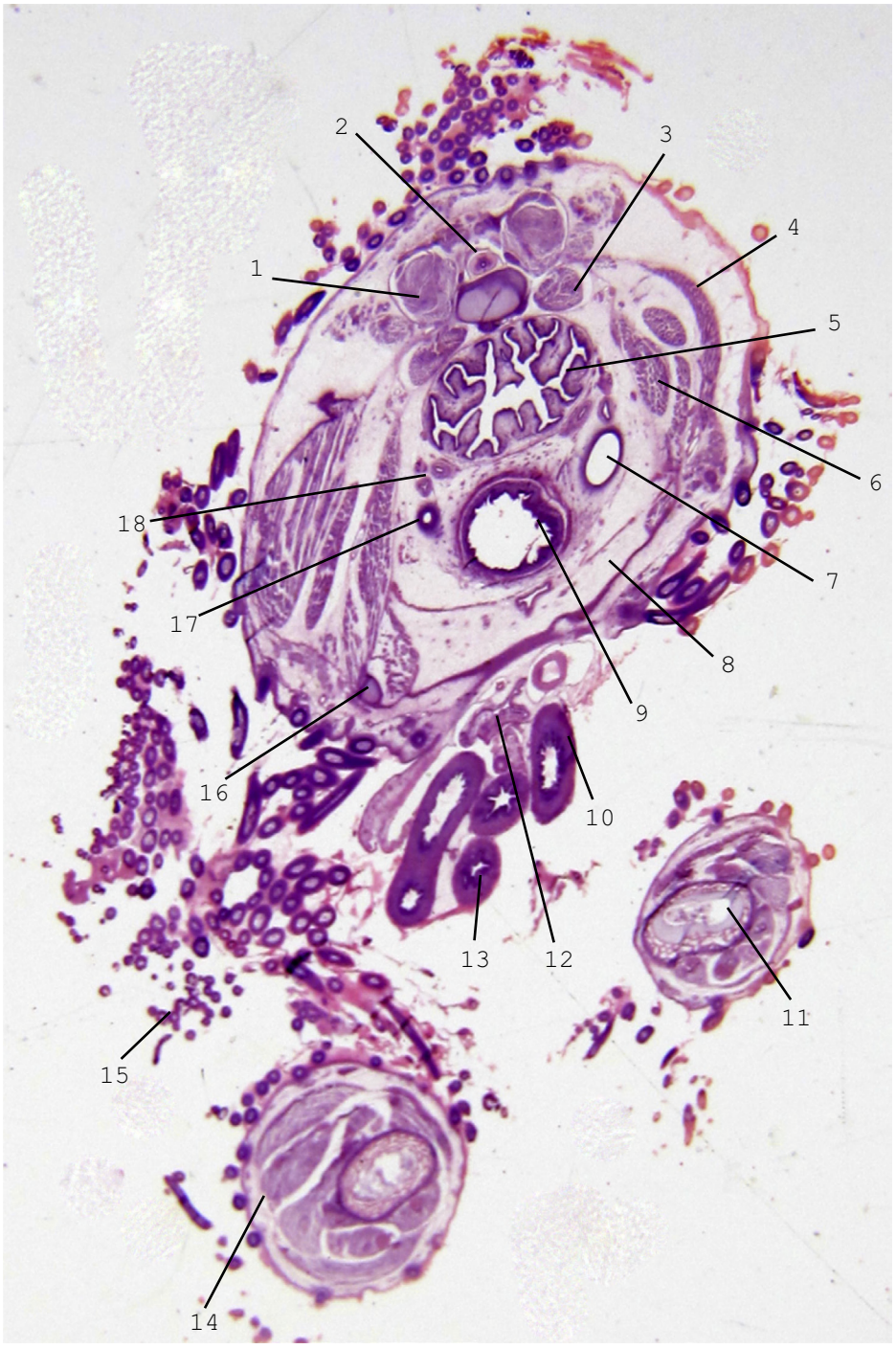

Plate 228 Stage 39 (day 13) TS

Oblique transverse section through the thighs (top), umbilical cord (middle) and tail (bottom): × 13

1. right leg
2. femur
3. left leg
4. left allantoic artery
5. caudal artery
6. herniated loop of intestine in transverse section
7. vitelline vessel
8. allantoic stalk
9. epidermis
10. Wharton's jelly
11. herniated loop of intestine in longitudinal section
12. body of caudal vertebra
13. remnant of notochord
14. left depressor caudal muscle
15. feathers
16. spinal cord
17. feather buds

Plate 228

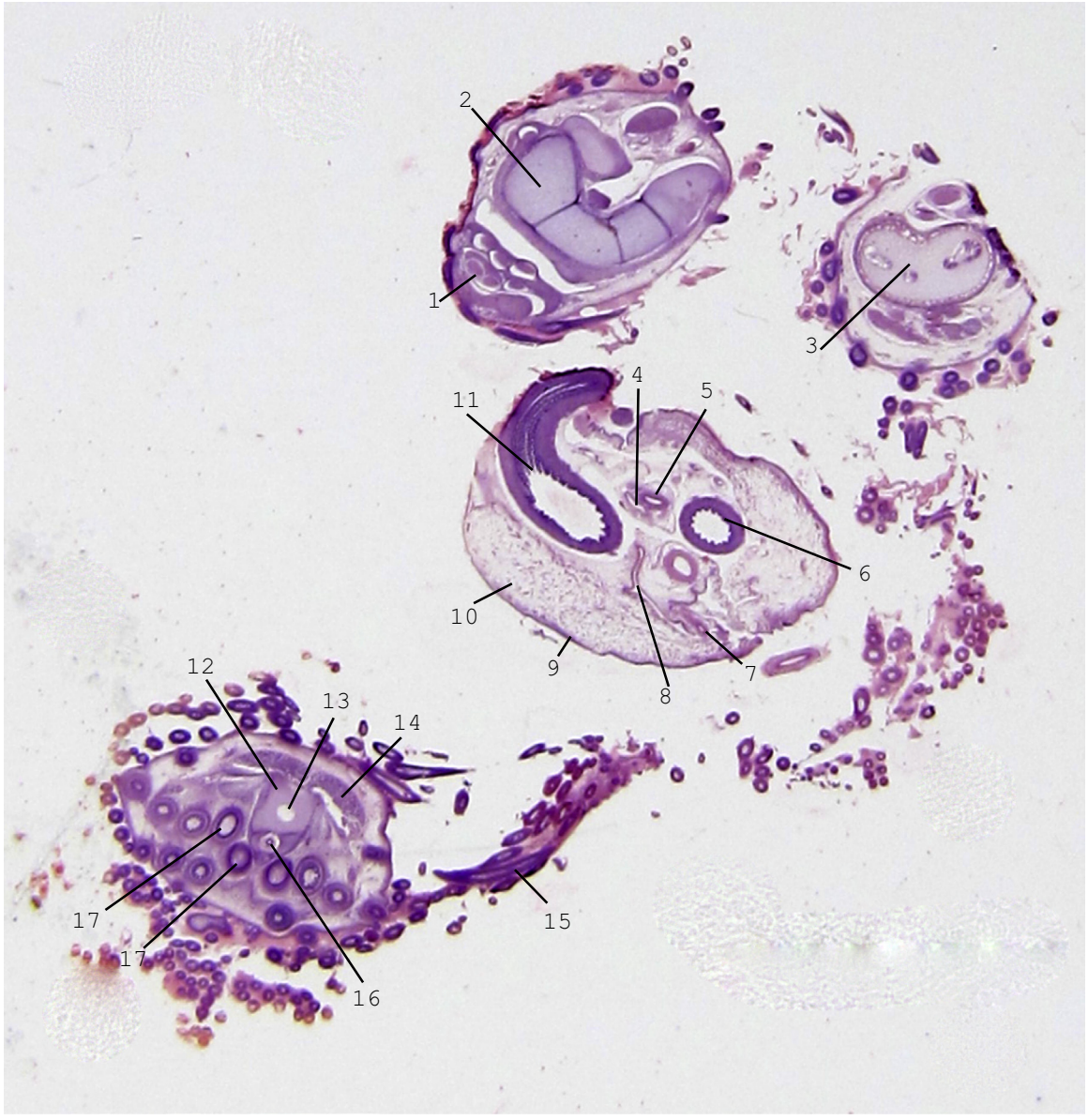

Plate 229 Stage 39 (day 13) TS

Transverse section (TS) through the neural tube and dorsal root ganglion from section adjacent to *plate 212*: × 100

1. vertebral arch
2. vertebral crest
3. spinal canal
4. external limiting membrane
5. dorsal root
6. marginal layer
7. dorsal root ganglion
8. spinal ganglion
9. ventral root
10. ventral horn
11. vertebral body
12. ventral median fissure
13. ventral floor plate
14. ependyma
15. mantle layer
16. dorsal horn
17. dorsal commisure

Plate 229

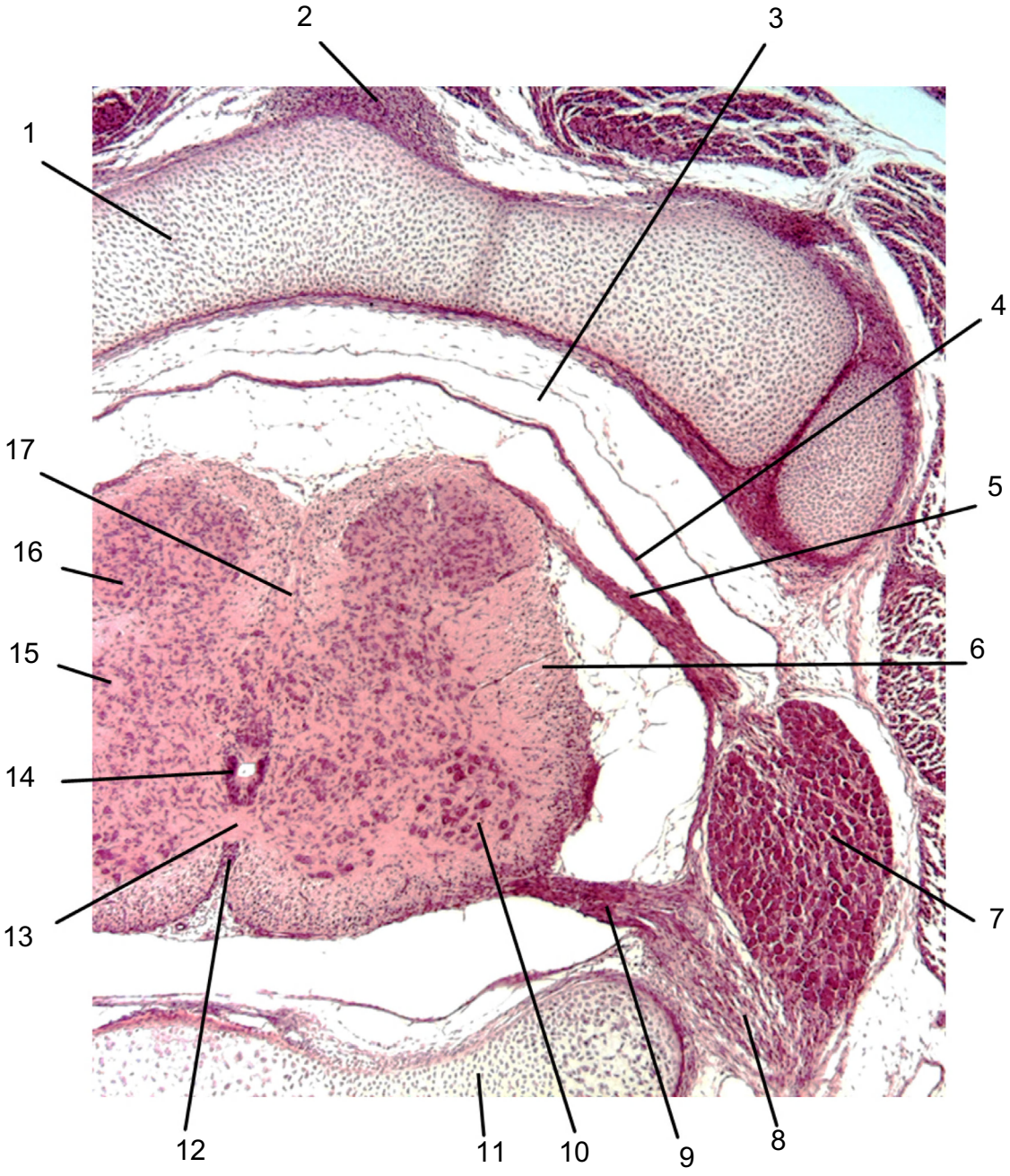

Plate 230 Stage 37 (day 11)

Whole-mount photograph of embryo stained with alizarin red and alcian blue to show skeletal elements. Membranes and cartilages: blue; ossified regions: red.

Ossification has occurred in the quadrate and in the middle of the long bones. Most regions remain unossified. Roman numerals indicate digits: × 6.

Plate 230

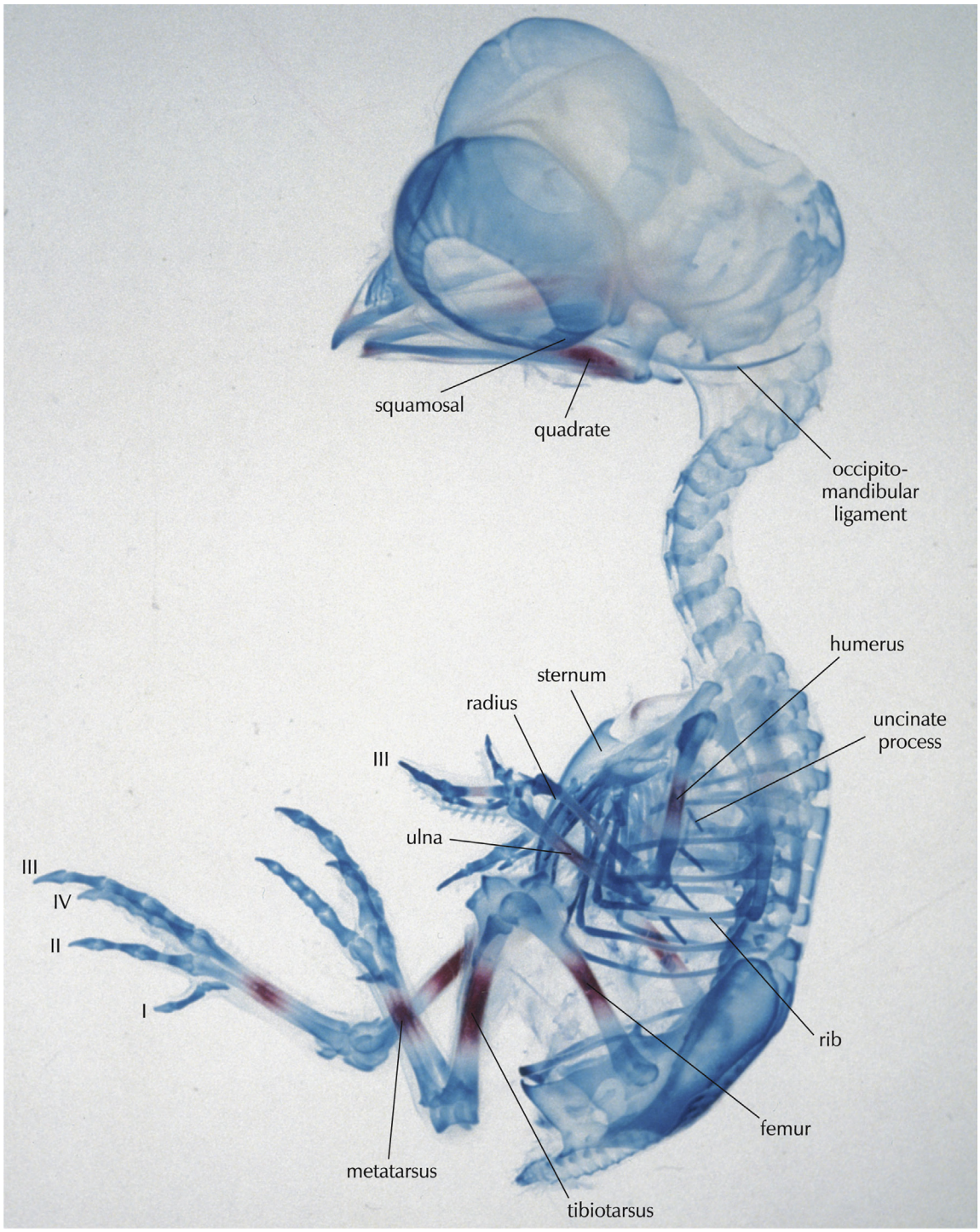
squamosal
quadrate
occipito-
mandibular
ligament
humerus
sternum
radius
uncinate
process
III
ulna
III
IV
II
I
rib
femur
metatarsus
tibiotarsus

Plate 231 Stage 39 (day 13)

Whole-mount photograph of embryo stained with alizarin red and alcian blue to show skeletal elements. Membranes and cartilages: blue; ossified regions: red.

Ossification has occurred in the upper and lower jaws, has increased in the long bones, and is visible in the clavicle, the coracoid, the thoracic ribs and, slightly, in the ilium: × 5.

Plate 231

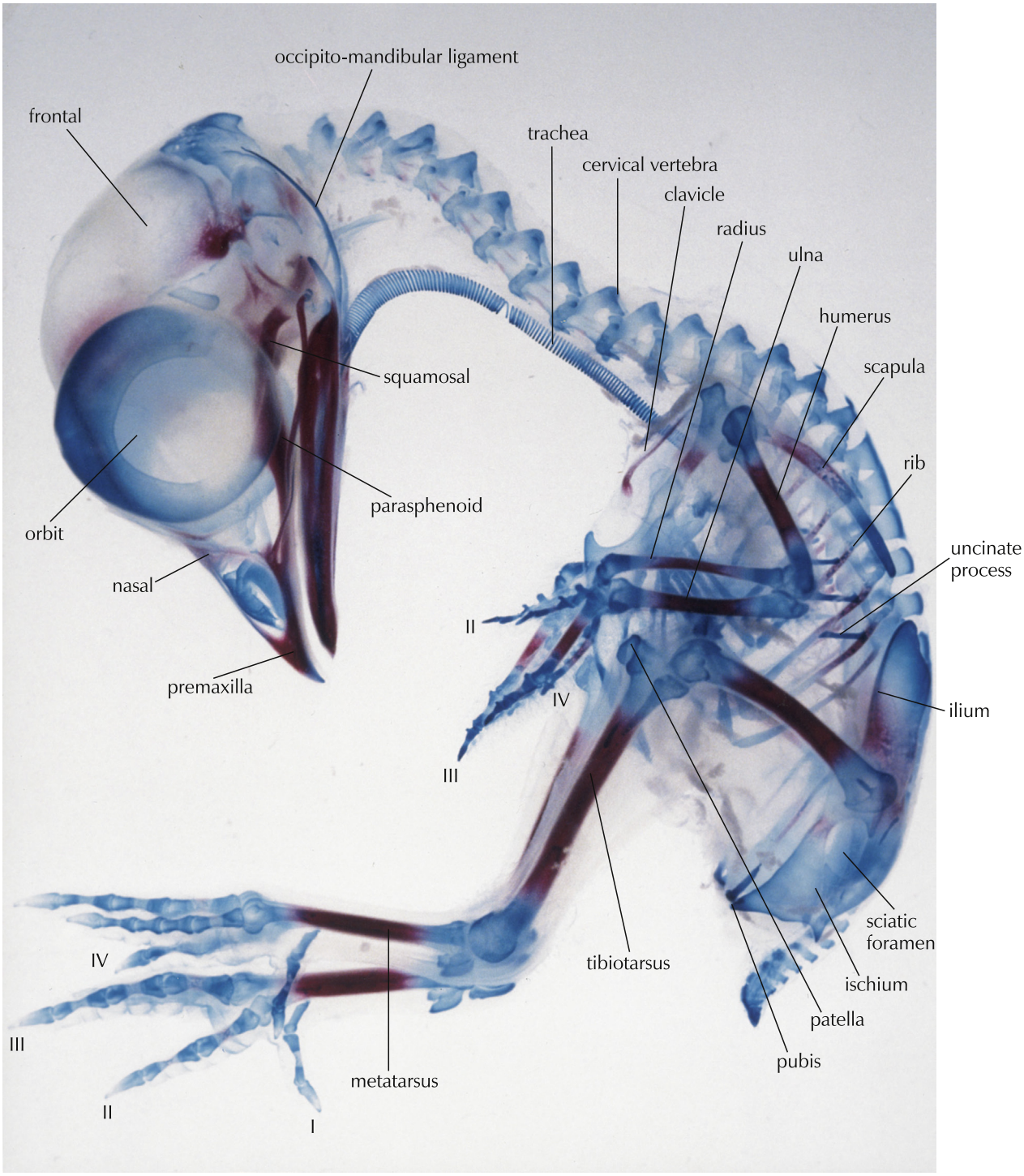
occipito-mandibular ligament
frontal
trachea
cervical vertebra
clavicle
radius
ulna
humerus
scapula
rib
uncinate process
ilium
squamosal
parasphenoid
orbit
nasal
premaxilla
II
IV
III
tibiotarsus
patella
pubis
ischium
sciatic foramen
IV
III
II
I
metatarsus

Plate 232 Stage 45 (Day 19.5)

Whole-mount photograph of embryo stained with alizarin red and alcian blue to show skeletal elements. Membrane and cartilages: blue; ossified regions: red.

The skull shows extensive ossification, especially of the frontal and parietal bones and of the scleral ossicles. Ossification is well advanced in the digits and the vertebrae, though the caudal vertebrae remain largely cartilaginous: × 4.5.

Plate 232

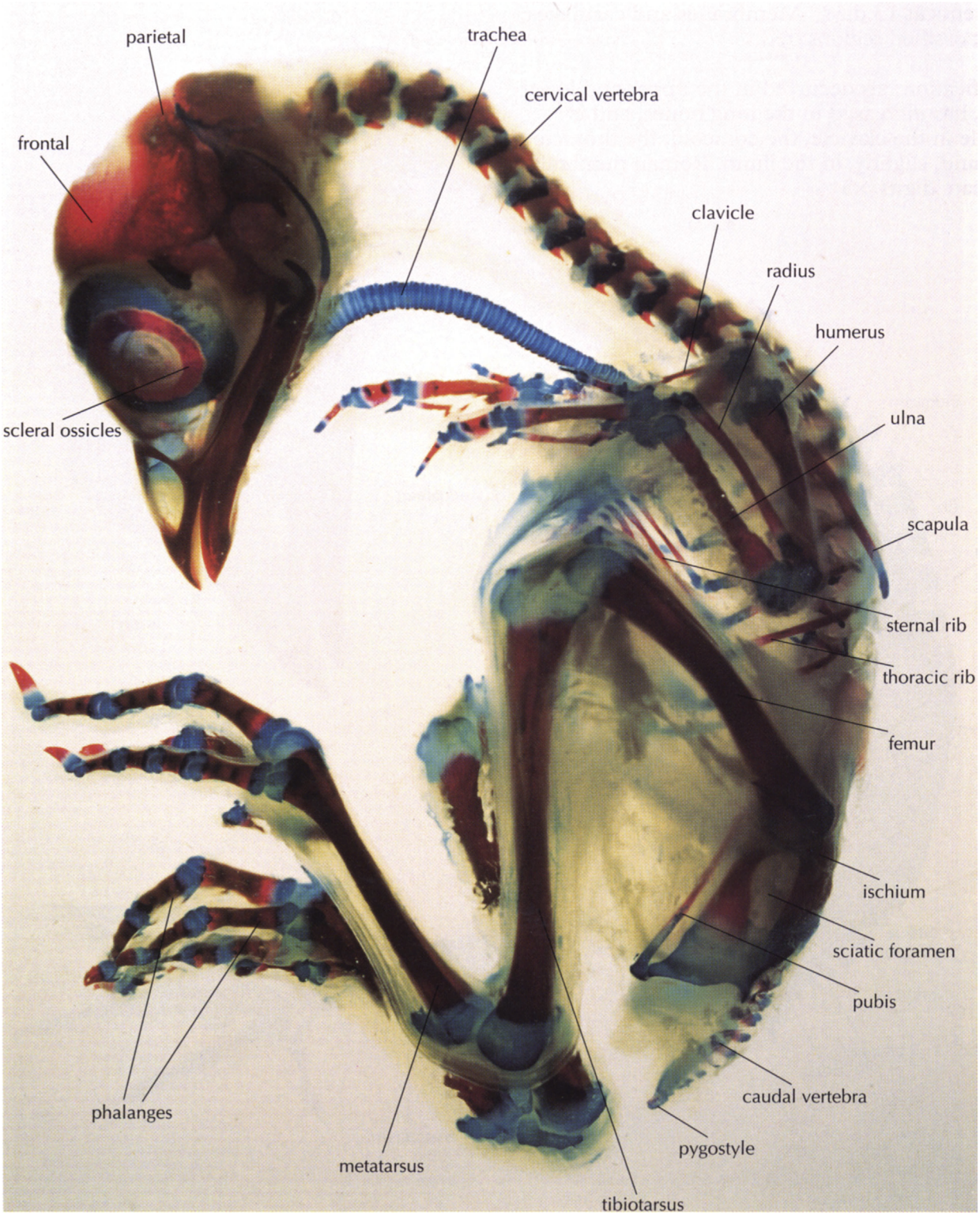
parietal
trachea
cervical vertebra
frontal
clavicle
radius
humerus
scleral ossicles
ulna
scapula
sternal rib
thoracic rib
femur
ischium
sciatic foramen
pubis
caudal vertebra
phalanges
pygostyle
metatarsus
tibiotarsus

Appendices

Normal Tables

Embryologists have long found it convenient to classify normal embryos in a series of developmental stages. Such a classification is called a **normal table.** The most widely used table for the domestic fowl is by Hamburger and Hamilton (1951, reprinted 1992), as reproduced in Appendix II. It is based exclusively on external features and each stage is illustrated by a photograph and accompanied by a brief description. Tables of this sort are of particular value to experimentalists in that they enable the developmental state of an embryo to be assessed and communicated relatively accurately. There are, however, some problems involved in the use of Hamburger and Hamilton's table. The stages from 7 to 14 are based largely on the numbers of somites that have developed, but the rate of differentiation of other structures does not always keep pace with the somites, e.g. stage 8 of the normal table possesses four pairs of somites and a brain that has scarcely begun to bulge, whereas in practice embryos with four pairs of somites may possess a less or more developed head, comparable to those of stages 7 or 9. In later stages the shape of the limb buds is used as the most distinguishing feature for each stage, but again this does not always bear the same relationship to the development of other external features.

Another problem with the Hamburger and Hamilton table is that not enough stages have been allocated for early incubation when development is taking place very rapidly. The primitive streak is fully formed at about 18 hours of incubation, but after a short pause the head process begins to appear, signaling the start of dramatic changes in molecular activity. Hamburger and Hamilton's table failed to distinguish between these two stages, grouping them together as a single stage 4. It is now customary to insert 4- as an additional stage. The problem is compounded by the fact that marked differences occur not only between different batches of eggs but often within the same batch, even though incubation conditions are identical. A supplementary normal table (Appendix I) has therefore been published (Eyal-Giladi and Kochav, 1975) to cover the period from the earliest stages normally to be found in unincubated eggs to the stage when the primitive streak is about half formed. A further table, an elaboration of the stages in wing development (Murray and Wilson, 1994), has not been included in this edition (see Appendix III).

Because the purpose of a normal table is for quick recognition of the stage as indicated by external features, there is no guarantee of a precise correlation with the differentiation of internal organs. For that reason it is often preferable when embryos are older than about 3 days to describe them by the length of incubation time, a practice that has been followed in this book. Nevertheless, it is possible to make some approximations with internal differentiation and these, extracted from the monograph of Freeman and Vince (1974) are inserted into the normal table of Hamburger and Hamilton (Appendix II).

Additional references providing normal tables for chick embryos and those of other domestic birds are listed in Appendix III.

Appendix I

Normal Table of Eyal-Giladi and Kochav (1975)

The following description is slightly modified and abbreviated from the original publication. Reproduced by permission of Academic Press (Elsevier).

CLEAVAGE STAGES

Stage I (0–1 h in shell gland, *Figures 1* and *2).* Each egg was surrounded by viscous albumen and a very flaccid shell membrane. Early cleavage. Germinal disc 3.5–4 mm diameter, (c.fur = cleavage furrows: p.b. = polar body; su.sp. = supernumerary sperm: vac. = large vacuoles).

Stage II (about 2 h in shell gland, *Figures 3* and *4).* About 14–16 laterally closed cells raised above the rest of the germinal disc. Cleavage furrows spread out from the centre.

Stage III (about 3–4 h in shell gland, *Figures 5* and *6).* 80–90 laterally closed blastomeres in the centre. (cl.bl. = closed blastomeres).

Stage IV (about 5 h in shell gland, *Figures 7* and *8).* About 250–300 closed cells in upper layer. About 80–90 closed cells now visible in lower layer. (s.c. = subgerminal cavity).

Stage V (about 8–9 h in shell gland, *Figures 9* and *10).* Cells still bead-like. Subgerminal cavity enlarged.

Stage VI (about 10–11 h in shell gland, *Figures 11* and *12).* Cells now small and flat and have lost bead-like appearance. All cytoplasm now cleaved into true cells (blastomeres).

FORMATION OF AREA PELLUCIDA

Stage VII (about 12–14 h in shell gland, *Figures 13* and *14).* Upper layer cells have become progressively smaller. Lower layer cells have remained large. The first indication of the area pellucida as a thinner region in the embryo where cells have been shed from the underside of the upper layer. (a.p. = area pellucida).

Stage VIII (about 15–17 h in shell gland, *Figures 15* and *16).* The area pellucida has spread but the peripheral region has remained thick and is forming the area opaca (a.o. = area opaca; a.p. = area pellucida; y.l.c. = yolk-laden cells).

Stage IX (about 17–19 h in the shell gland, *Figures 17* and *18).* Further spreading of the area pellucida. Border between area opaca and area pellucida not yet sharply defined. (a.o. = area opaca; a.p. = area pellucida).

Stage X (freshly laid egg, *Figures 19* and *20).* The area pellucida and area opaca are now clearly demarcated from one another. Clusters of small cells lie beneath posterior part of area pellucida except for the extreme posterior region (i.ag. = isolated cell aggregates).

HYPOBLAST FORMATION (EARLY STAGES OF INCUBATION)

Stage XI *(Figures 21* and *22).* A transparent belt-like area (t.b.) at the poster border of the area pellucida and area opaca. Anterior to this region clusters of

cells lie in a horseshoe-shaped arrangement known as Koller's sickle (k.s.).

Stage XII *(Figures 23* and *24).* The hypoblast (hyp) is beginning to form [from Koller's sickle] but is not yet a continuous sheet.

Stage XIII *(Figures 25* and *26).* The hypoblast is now completely formed (as a sheet).

Stage XIV *(Figures 27* and *28).* The anterior border of the hypoblast is now clearly defined. A cellular bridge (pos.br.) begins to link the posterior end of the hypoblast to the area opaca. This bridge is also visible in *Figures 29* and *30,* which correspond with stage 2 of Hamburger and Hamilton (see Appendix II). (p.s. = earliest indication of primitive streak.)

Appendix I Plate 1

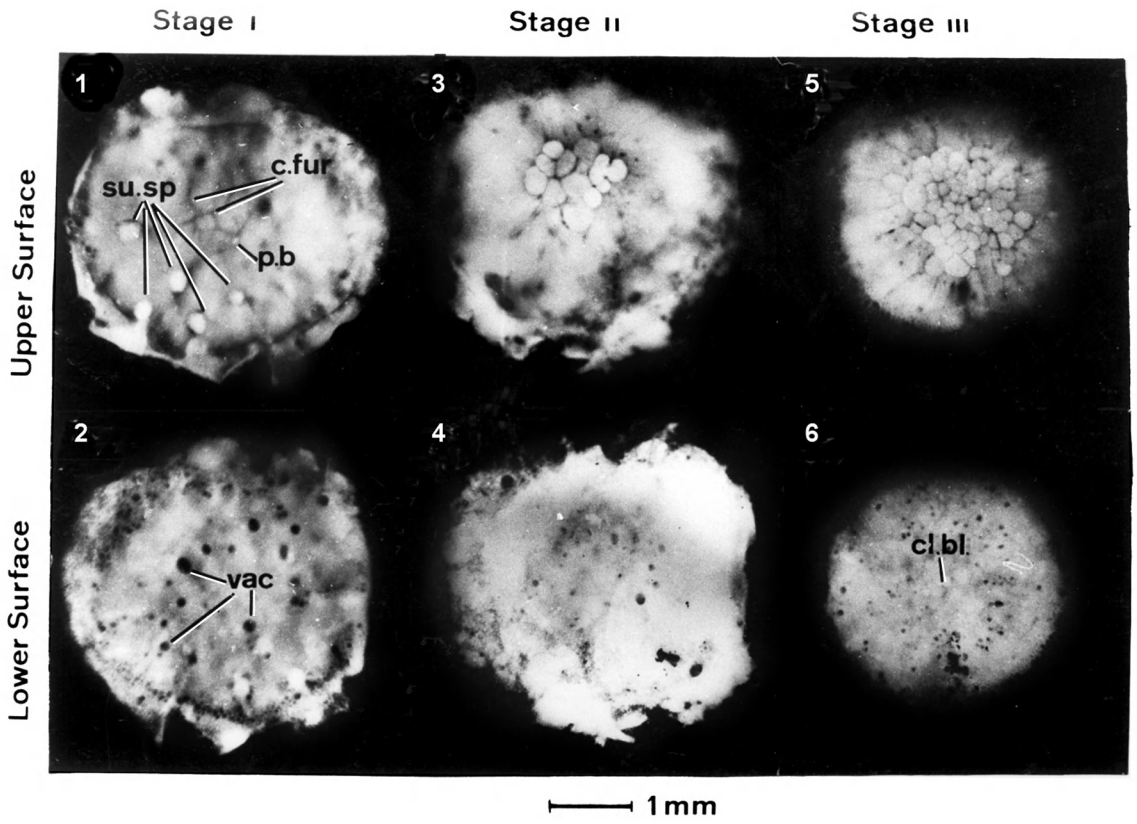

APPENDIX I PLATE 2

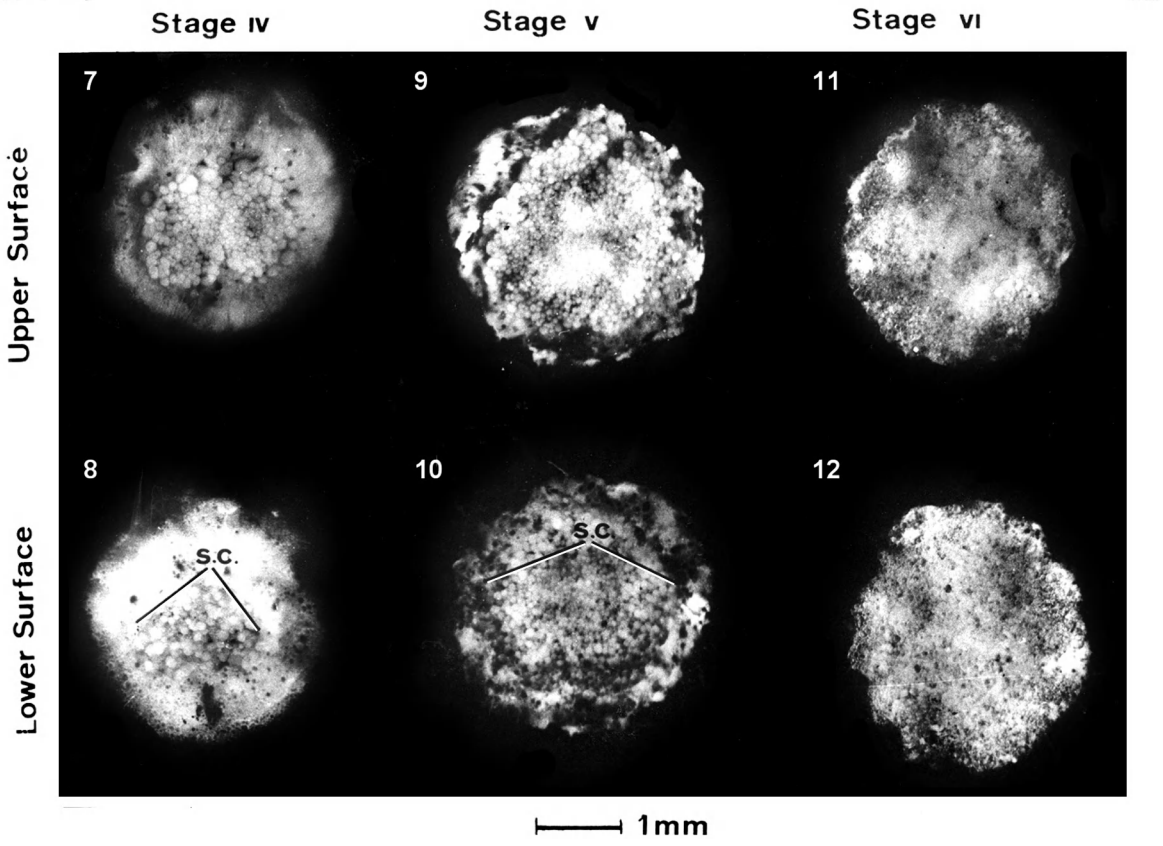

APPENDIX I PLATE 3

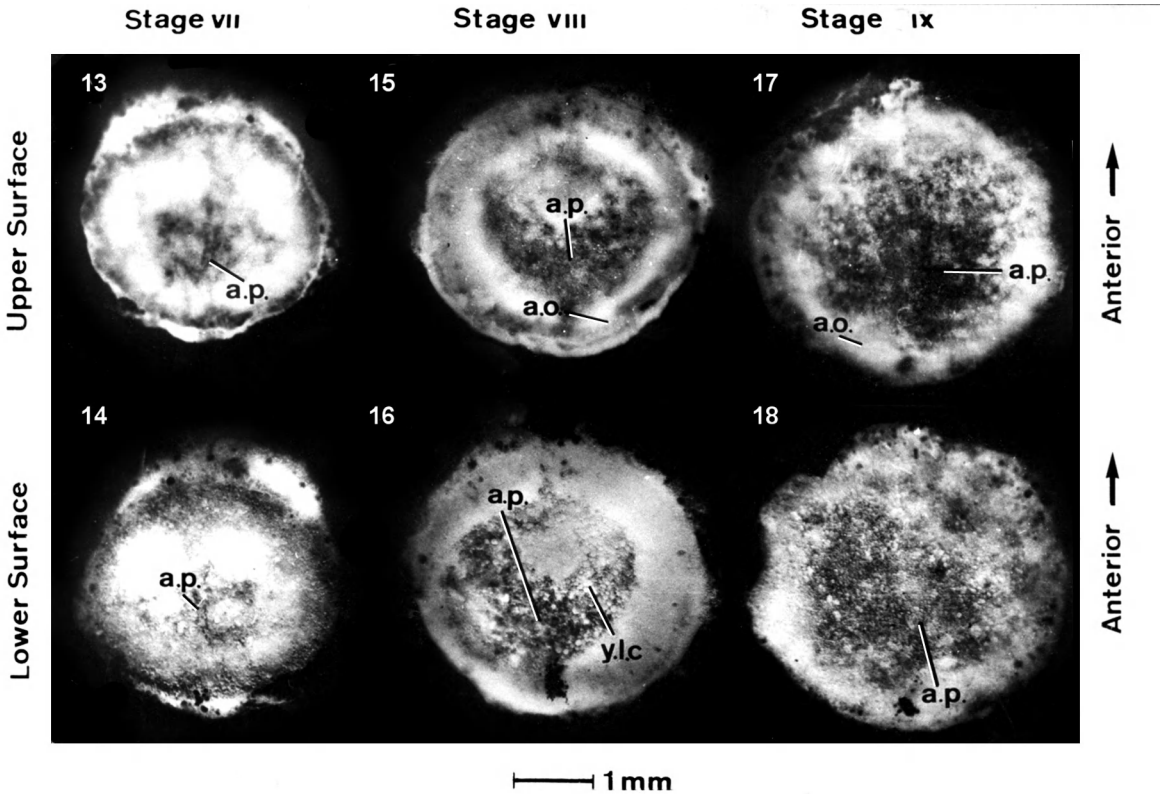

APPENDIX I PLATE 4

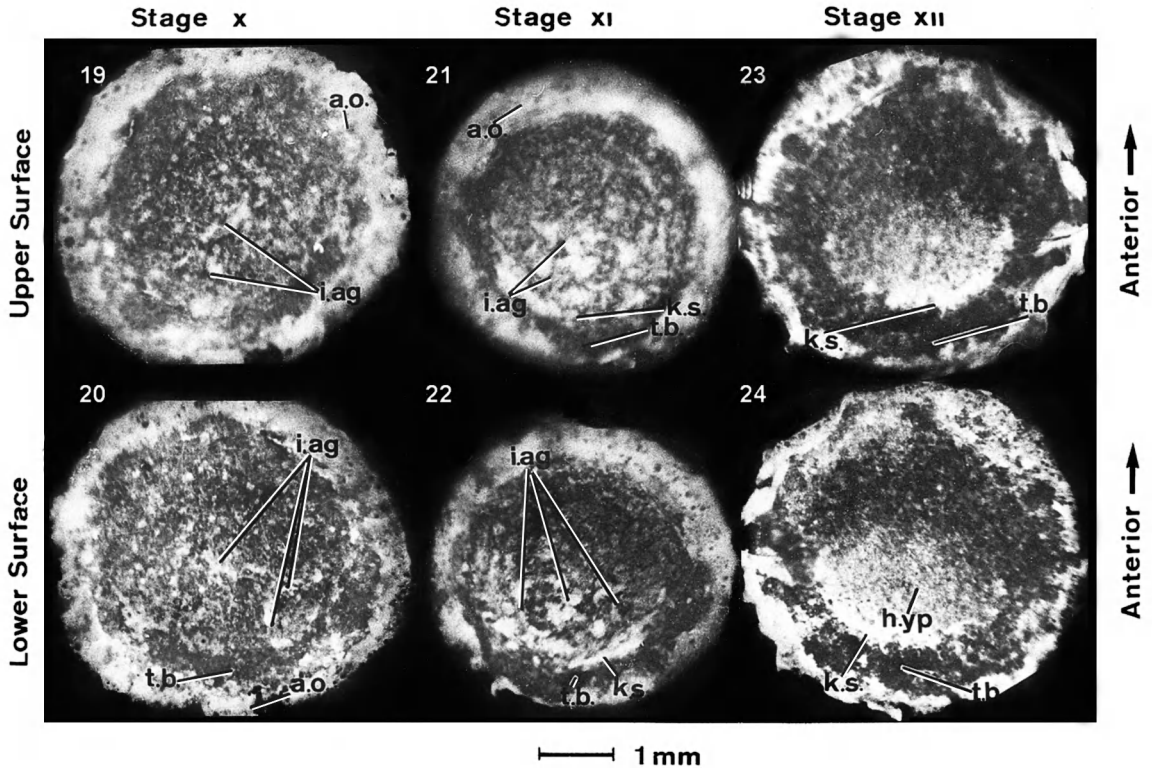

APPENDIX I PLATE 5

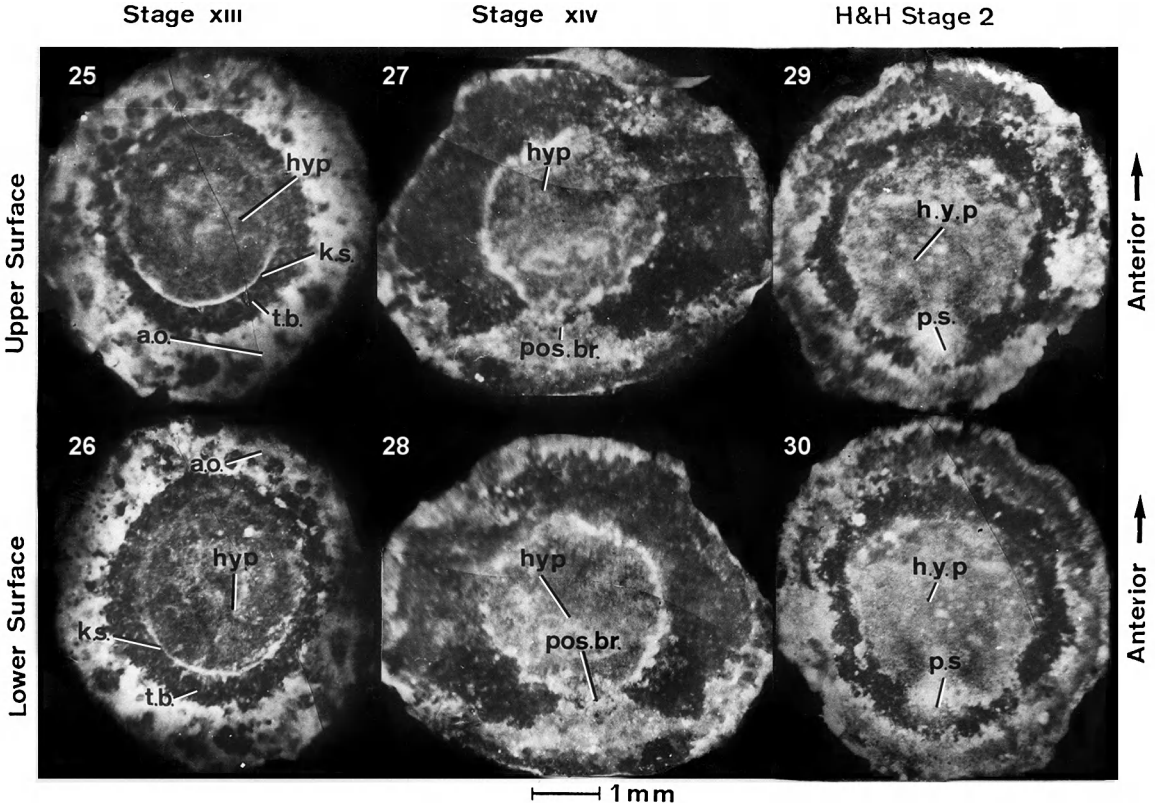

Appendix II

Normal Table of Hamburger and Hamilton (1951; 1992)

(Magnifications are those supplied by Hamburger and Hamilton)

A fuller description of each stage is given in the original publications (1951, reprinted 1992), the following being abbreviated and with minor modifications. Reproduced by permission of John Wiley and Sons, Inc.

Stages 1 and 2 probably correspond to stages XII–XIV of Eyal-Giladi and Kochav (Appendix I). Approximate incubation times are indicated for each stage in parentheses. Notes in italics have been added by the present authors; those in square brackets, derived from the table of Freeman and Vince (1974), describe internal features and their approximate times of appearance.

References to 'HH Plates' refer to plates in this normal table.

Stage 1. ×20 Pre-streak.
An 'embryonic shield' may be visible towards the posterior half of the blastoderm.

Stage 2. ×20 Initial streak (about 6–7 h).
The primitive streak is short and conical (0.3–0.5 mm in length).

Stage 3. ×20 Intermediate streak (12–13 h).
The primitive streak extends to about the centre of the area pellucida.

Stage 3+. This stage was inserted by Hamburger and Hamilton but no description was given.

Stage 4–. This critical stage (illustrated in *Plate 9* of this book) was not included in the Hamburger and Hamilton table. The primitive streak has reached its maximum length and Hensen's node is visible. The distinction between stage 4– and 4 is essential because of changes in cell migration, cell adhesion and gene expression.

Stage 4. ×20 Definitive streak (18–19 h).
The primitive streak has reached its maximum length (about 1.88 mm). The primitive groove, primitive pit and Hensen's node are present. The area pellucida has become pear-shaped and the primitive streak extends over about two-thirds to third-quarters of its length. *(NB: The beginning of the head process is already visible in the photograph as a dark region at the anterior tip of the primitive streak.)*

Stage 5. ×20 Head process (19–22 h).
The head process extends anteriorly from Hensen's node.

Stage 6. ×20 Head fold (23–25 h).
No somites yet visible.

Stages 7–14 are based primarily on the numbers of pairs of somites visible.

Stage 7. ×20 One pair of somites (23–26 h).
This is actually the second somite pair, the first not yet clearly defined. Neural folds are visible in the head region.

Stage 8. ×20 Four pairs of somites (26–29 h).

The neural folds meet at the level of the midbrain. Blood islands are present in the posterior half of the blastoderm.
[Nephric ducts are starting to develop.]

Stage 9. ×20 Seven pairs of somites (29–33 h).
Primary optic vesicles are present. Paired primordia of the heart begin to fuse.
[Inner ear is beginning to form.]

Stage 10. ×12 Ten pairs of somites (33–38 h).
First indication of cranial flexure. Three primary brain vesicles are clearly visible. Heart primordia are fused, bent slightly to right.
[Haemoglobin synthesis begins; thyroid anlage differentiates; pronephros forming.]

Stage 11. ×12 Thirteen pairs of somites (40–45 h).
Slight cranial flexure. Five neuromeres of the hindbrain are distinct. Anterior neuropore is closing. Optic vesicles are constricted at the bases. Heart is bent to the right.
[Rathke's pouch is forming; pronephros degenerates; mesonephros differentiates; amniotic head fold appears; neurohypophysis begins to form.]

Stage 12. ×12 Sixteen pairs of somites (45–49 h).
Head is turning onto the left side. Anterior neuropore is closed. Telencephalon is indicated. Primary optic vesicles and optic stalk are well established. Otic pit is deep but wide open. Heart is slightly S-shaped. Head fold of amnion covers entire region of the forebrain.
[Circulatory system is developing; ductus venosus and liver primordia appear; telencephalon is differentiating; amniotic tail fold.]

Stage 13. ×12 Nineteen pairs of somites (48–52 h).
Head is partly to fully turned onto the left side. Cranial and cervical flexures make broad curves. Enlargement of telencephalon. Atrio-ventricular canal is indicated by constriction. Head fold of the amnion covers forebrain, midbrain and the anterior part of hindbrain.
[Proventriculus and gizzard differentiate; interatrial septum forms; allantoic bud and hindgut develop.]

Stage 14. ×12 Twenty-two pairs of somites (50–53 h).
Cranial flexure: axes of forebrain and hindbrain form almost a right angle. Cervical flexure is a broad curve.
Rotation of body as far back as somites 7–9.
Visceral *(pharyngeal)* arches 1 and 2, and clefts *(grooves)* 1 and 2 are distinct. Optic vesicle begins to invaginate and lens placode is formed. Opening of otic pit is constricted. Rathke's pouch is recognizable. Ventricular loop of the heart is now ventral to the atrio-ventricular canal. Amnion extends to somites 7–10.
[Pancreatic anlage differentiate.]
Beyond stage 14 the number of somites becomes increasingly difficult to determine with accuracy.

Stage 15. ×12 (c. 50–55 h).
Lateral body folds extend to level of somites 15–17.
Limb primordia: inconspicuous condensations of mesoderm for the wing bud. 24–27 pairs of somites.
Amnion extends to level of somites 7–14.
Flexures and rotation: cranial flexure – axes of forebrain and hindbrain form an acute angle. Cervical flexure is a broad curve. Rotation extends to level of somites 11–13.
Optic cup is completely formed.
Visceral (pharyngeal) arches: arch 3 and cleft 1 are distinct.
[Lung primordia differentiate from pharynx.]

Stage 16. ×12 (c. 51–56 h).
Lateral body folds extend to level of somites 17–20, between levels of wings and legs.
Limbs: wings are lifted off the blastoderm. Primordia of the legs are flat.
Somites: 26–28 pairs.
Amnion: extends to level of somites 10–18.
Flexures and rotation: all flexures are more accentuated.
Rotation extends to somites 14–15.
Tail bud: a short, straight cone.
[Epiphysis develops.]

Stage 17. ×12 (c. 52–64 h).
Lateral body folds extend around entire circumference of the body.
Limb buds: both wing and leg buds are lifted off the blastoderm.
Somites: 29–32 pairs.
Amnion: variable in extent.
Rotation: extends to level of somites 17–18.
Tail bud: bent ventrally. Its mesoderm is unsegmented.
Pineal: a distinct knob.
Allantois: not yet formed.

Stage 18. ×12 (c. 65–69 h).
Limb buds enlarged (see *HH Plates 4* and *5*).
Somites: 30–36 pairs.
Amnion: usually closed.
Rotation: now extends to posterior part of the body.
Visceral *(pharyngeal)* arches: maxillary process are absent or inconspicuous. Fourth cleft (groove) is indistinct or absent.
Tail bud: turned to right.

Allantois: short, thick-walled pocket.
[First passive movements can be detected.]

Stage 19. ×12 (c. 68–72 h).
Limb buds: the leg buds are slightly larger than the wing buds (see *HH Plate 5*).
Somites: 37–40 pairs, extend into the tail.
The contour of the posterior part of the trunk is straight to the tail.
Tail bud is curved, the tip pointing forward *(anteriorly).*
Visceral *(pharyngeal)* arches: maxillary process about the same length as mandibular process. The second *(hyoid)* projects slightly over the surface.
Allantois: small pocket of variable size.
Eyes: unpigmented.
[Aortic arches form, the left soon to degenerate; nephric ducts unite with cloaca.]

Stage 20. ×12 (c. 70–72 h).
Limb buds: the wing buds are approximately symmetrical, the leg buds slightly asymmetrical (see *HH Plate 5*).
Somites: 40–43 pairs.
Rotation: completed.
Visceral *(pharyngeal)* arches: maxillary equals or exceeds the mandibular in length. Second *(hyoid)* arch projects over surface. Fourth arch is smaller than the third arch.
Allantois: vesicular, variable size.
Eye pigment: faint grey.
[Pulmonary arch forms; ductus arteriosus; embryo is surrounded by amnion.]

Stage 21. × 12 (*c.* 3.5 days).
Limbs: both wing and leg buds are slightly asymmetrical with proximo-distal axes directed caudally.
Somites: 43–44 pairs.
Visceral *(pharyngeal)* arches: maxillary process is longer than the mandibular. Second *(hyoid)* overlaps the third arch ventrally. Fourth arch is distinct.
Allantois: variable in size, may extend to head.
Eye pigmentation: faint.
[First active movements of the head and neck; earliest motor fibres contact the anterior trunk muscles.]

Stage 22. ×8 (*c.* 3.5 days).
Eye pigmentation: distinct.
Somites: extend to tip of the tail. *(This is incorrect since the mesoderm at the tip of the tail never becomes fully segmented.)*
[Adrenal cortical and medullary cells differentiate; insulin synthesis begins; gonadal anlagen differentiate; amniotic contractions begin; crop differentiates; erythropoiesis in yolk sac begins; oestrogen and oestrodiol-17β synthesis begin.]

Stage 23. ×8 (*c.* 4 days).
Limbs: both wing buds and leg buds are approximately as long as they are wide.
Visceral (*pharyngeal)* arches: see *HH Plates 7* and *8*.
[Pronephros disappears]

Stage 24. ×8 (*c.* 4.5 days).
Limbs: both wing and leg buds are longer than they are wide.
Toe plate in the leg bud is distinct.
Visceral *(pharyngeal)* arches: see *HH Plates 7* and *8*.
[Chorion and allantois fuse to give chorio-allantois; metanephros begins to differentiate; cochlear nucleus becomes visible.]

Stage 25. ×8 (*c.* 4.5–5 days).
Limbs: elbow and knee joints are distinct. Digital plate in the wing is distinct, but no demarcation of the digits.
Visceral *(pharyngeal)* arches: see *HH Plates 7* and *8*.
[Spleen differentiates.]

Stage 26. ×8 (*c.* 5 days).
Limbs: longer. Contour of the digital plate is rounded. Demarcation of the first three toes is distinct.
Visceral *(pharyngeal)* arches: see *HH Plates 8* and *9*.
[Mesonephros becomes functional; production of definitive erythrocytes begins; adult haemoglobin is synthesized; first active movements of trunk; corticosteroid synthesis begins; duodenum begins to differentiate; first mouth movements; bursa of Fabricius begins to differentiate; four-chambered heart is formed; nerves from retina reach the optic lobe; thymus anlagen differentiate.]

Stage 27. ×5 (*c.* 5–5.5 days).
Limbs: grooves between the first, second and third digits of the wing buds are indicated; distinct grooves between the toes.
Visceral *(pharyngeal)* arches: see *HH Plates 8* and *9*.
[Beak is forming; amnion begins to contract rhythmically.]

Stage 28. ×5 (*c.* 5.5–6 days).
Limbs: second digit of wing bud and third toe are longer than the others; three digits and four toes are distinct.

Visceral *(pharyngeal)* arches: see *HH Plates 8* and *9*.
Beak: a distinct outgrowth is visible in profile.
[First reflexes are established.]

Stage 29. ×5 (*c.* 6–6.5 days).
Limbs: wing is bent at the elbow. Shallow grooves between first, second and third digits. Second to fourth toes stand out as ridges separated by grooves and with indications of webs. Rudiments of fifth toes are visible.
Visceral *(pharyngeal)* arches: mandibular process and second arch are broadly fused. Auditory meatus is distinct at the dorsal end of fusion.
Neck has lengthened: see *HH plate 10*.
[Parathyroids differentiate; air sacs begin to differentiate; first eyelid and independent limb movements; ductus venosus is lost.]

Stage 30. ×5 (*c.* 6.5–7 days).
Limbs: the three major segments of limbs are well demarcated. Wing is bent at the elbow and leg is bent at the knee. Distinct grooves between first and second digits.
Neck: lengthened further.
Feather germs: two dorsal rows on either side of the spinal cord at brachial level, three rows at level of the legs.
Scleral papillae: one on either side of the choroid fissure.
Egg tooth: distinct.
[Thyroid concentrates iodine; sexual differentiation begins; testosterone production begins in the male.]

Stage 31. ×4 (*c.* 7–7.5 days).
Limbs: rudiment of the fifth toe is still distinct.
Feather germs: on the dorsal surface, continuous from brachial to lumbo-sacral levels. Approximately seven rows at the lumbo-sacral level. Distinct feather papillae on the thigh.
Scleral papillae: usually six, four on the dorsal side, two on the ventral side.
[Left allantoic blood vessel is lost; first eyeball movements begin; thyroid is able to synthesize monoiodotyrosine; ACTH secretion begins.]

Stage 32. ×4 (*c.* 7.5 days).
Limbs: all digits and four toes have lengthened conspicuously. Webs between digits and toes are thin and their contours concave. Rudiment of the fifth toe has disappeared. Differences in size of individual digits and toes are conspicuous.
Feather germs: eleven rows or more on the dorsal surface at level of the legs. One row on the tail distinct.
Scleral papillae: 6–8 in groups.

Stage 33. x4 (*c.* 7.5–8 days).
Limbs: web on radial margin of the arm and first digit.
Feather germs: three distinct rows in the tail, the middle one considerably larger than the others.
Scleral papillae: 13 present, forming almost a complete circle.
[Mineralization of bone begins; development of the right Mullerian duct ceases in the female and of both left and right in the male]

Stage 34. ×4 (*c.* 8 days).
Limbs: differential growth of the second digit. Third toe is conspicuous.
Feather germs: visible with good illumination over the scapula, ventral side of neck, procoracoid and posterior edge of wing. One row on the inner *(medial)* side of each eye. None around the umbilical cord.
Scleral papillae: 13 or 14.
Nictitating membrane: extends halfway between the outer rim of the eye and scleral papilla.

Stage 35. ×4 (*c.* 8–9 days).
Limbs: webs between the digits and toes are inconspicuous.
Beak: lengthened.
Feather germs: mid-dorsal line stands out distinctly in profile. At least four rows on the inner side of each eye. New feather germs near the mid-ventral line and extending to both sides of the umbilical cord.
Nictitating membrane: approaches the outer scleral papillae.
Eyelids (external to nictitating membrane) have extended towards the beak and begun to overgrow the eyeball.
[Thyroid is able to synthesize diiodotyrosine; male Mullerian ducts regress; chorioallantois becomes fixed in relation to the shell; haemopoietic activity in the bone marrow; fibres of acoustic ganglion enter the cochlear nucleus.]

Stage 36. ×l.2 (*c.* 10 days).
Limbs: tapering primordia of claws just visible on termini of the toes.
Comb: primordium visible as a prominent ridge with slightly serrated edge along the dorsal midline of the beak. Nostril has narrowed to a slit.
Feather germs: flight feathers conspicuous. Feather germs now cover the tibio-fibular portion of the leg. At least nine rows of feather germs between the upper eyelid and dorsal midline. Sternal tracts prominent.
Eyelids: lower lid has grown upward to level of the cornea.

[Whole body movements become jerky and random; thyroid secretes thyroxine; TSH secretion begins; parathormone secretion begins; embryo's position is fixed at right angles to the long axis of the egg; first local proprioceptive muscle reflexes.]

Stage 37. ×l.2 (*c.* 11 days).
Limbs: claws of toes are flattened laterally and curved ventrally. Pads on the plantar surface of the foot. Length of third toe = 7.4 ± 0.3 mm.
Comb: more prominent and clearly serrated.
Feather germs: elongated into long, tapering cones along the back and tail.
Eyelids: lower lid covers one-third to one half of the cornea. Upper lid has reached the dorsal edge of the cornea.
[Metanephros begins to function; first auditory evoked responses from cochlear nuclei.]

Stage 38. ×l.2 (*c.* 12 days).
Limbs: primordia of scales visible as ridges over entire surface of the leg. Length of third toe = 8.4 ± 0.3 mm.
Feather germs: coverts of web of the wing are becoming conical. Sternum is covered with feather germs except along the midline. Upper eyelid is covered with newly formed feather germs.
Lower eyelid covers two-thirds to three-quarters of the cornea.
[Absorption of albumen begins; mesonephros degenerates; Mullerian ducts are lost in the male; calcium absorption from the shell begins; inbibition of amniotic fluid begins.]

Stage 39. ×l.2 (*c.* 13 days).
Limbs: scales overlapping on the superior surface of the leg. Major pads of phalanges are covered with papillae. Length of third toe = 9.8 ± 0.3 mm.
Mandible and maxillae are cornified (opaque) as far back as the proximal level of the egg tooth.
Feather germs: coverts of web of the wing are long, tapering cones.
Eyelids: opening between the lids is reduced to a thin crescent.
[Increased transport of lipids by yolk sac; amniotic contractions cease; sero-amniotic connection ruptures; pituitary–gonad axis is definitely established; neurohypophysis becomes active; gland cells of proventriculus begin secretion.]
Stages 40–44 are based mainly on the length of the beak and on the length of the third (longest) toe, since other external features have lost their diagnostic value.

Stage 40. ×l (*c.* 14 days).
Length of the beak from anterior edge of nostril to tip of the bill = 4.0 mm.
Length of third toe = 12.7 ± 0.5 mm.
[Exocrine pancreas begins maturation; oestriol synthesis begins in the female; maximum sensitivity to sound at 400 Hz; sporadic electrical activity in the cerebrum.]

Stage 41. ×l (*c.* 15 days).
Length of the beak from anterior angle of nostril to tip of the upper bill = 4.5 mm.
Length of third toe = 14.9 ± 0.8 mm.
[Stomach begins to contract; electrical activity in the optic lobes.]

Stage 42. ×l (*c.* 16 days).
Length of the beak from anterior angle of nostril to tip of the upper bill = 4.8 mm.
Length of third toe = 16.7 ± 0.8 mm.
[Embryo capable of respiratory movements; first electrical activity in the cerebellum.]

Stage 43. ×l (*c.* 17 days).
Length of the beak from anterior angle of nostril to tip of the upper bill = 5.0 mm.
Length of third toe = 18.6 ± 0.8 mm.
[Coordinated and stereotyped movements begin.]

Stage 44. ×l (*c.* 18 days).
Length of the beak from anterior angle of nostril to tip of the upper bill = 5.7 mm.
Length of third toe = 20.4 ± 0.8 mm.
[Beak becomes tucked under right wing; maximum sensitivity to sound rises to 800 Hz. Duodenum begins maturation; calcitonin secretion begins; first behavioural responses to light.]

Stage 45. ×l (*c.* 19–20 days).
Beak length is no longer diagnostic because of reduction in length due to sloughing off of the periderm, but it is now shiny.
Length of third toe unchanged (except for certain specialized breeds with a slightly longer incubation period).
Extra-embryonic membranes: yolk sac is half enclosed in the body.
Chorioallantoic membrane is 'sticky' in the living embryo.
[Absorption of the allantoic fluid is completed; hatching muscle matures; hepatic glycogen stores are mobilized; postural reflexes are fully developed; yolk sac withdrawal begins; cerebral auditory

waves attain regularity of those of the hatched chick.]

Day 20: *[Begins to breathe and vocalize; inner shell membrane is pierced; shell is 'pipped'; ductus arteriosus is closed; interatrial foramina are closed; chorioallantoic ectoderm degenerates; chorioallantoic circulation is reduced; withdrawal of the yolk sac is completed.]*

Stage 46. ×l (*c.* 20–21 days). Newly hatched chick.

Appendix II Plates 1

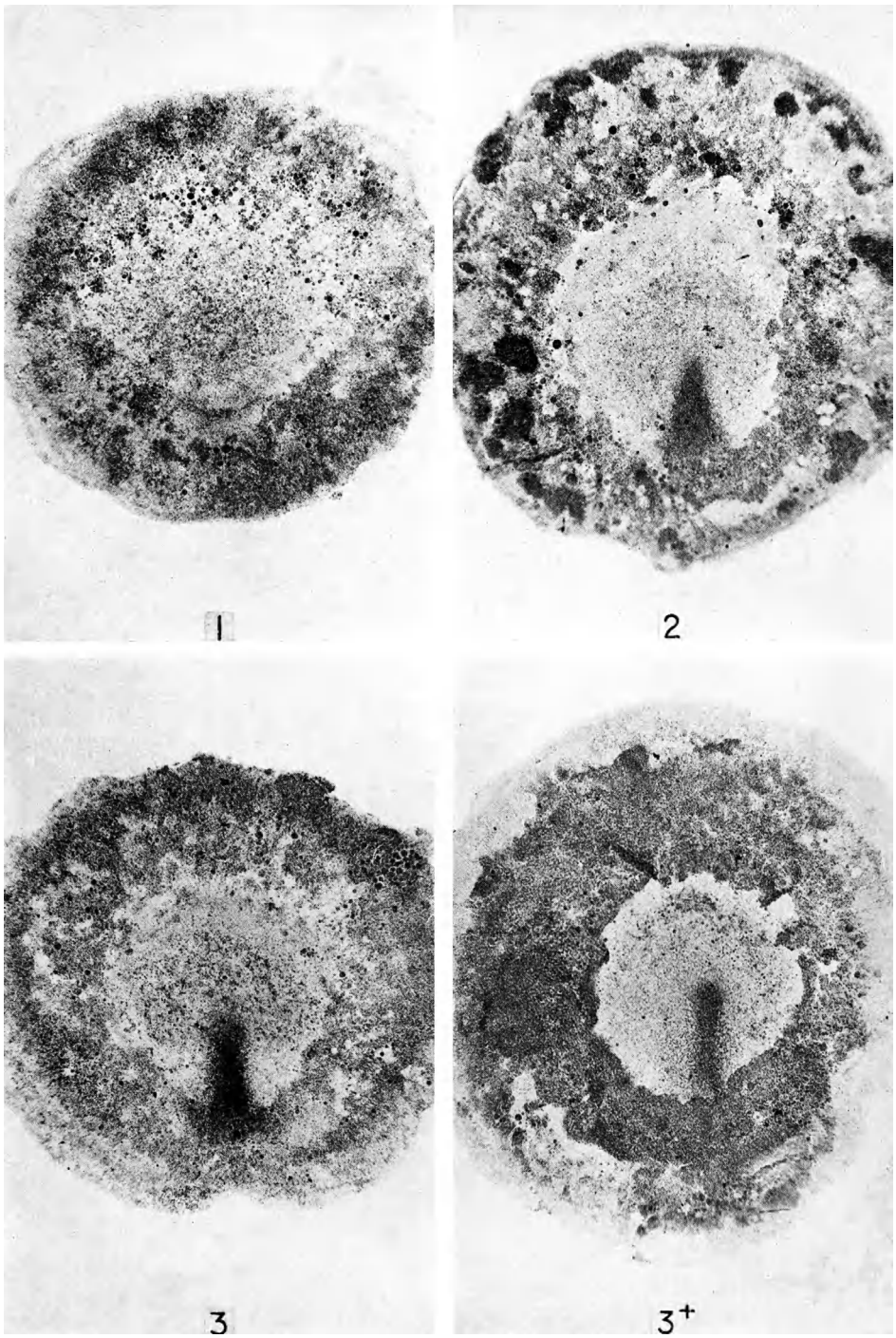

Appendix II Plates 2

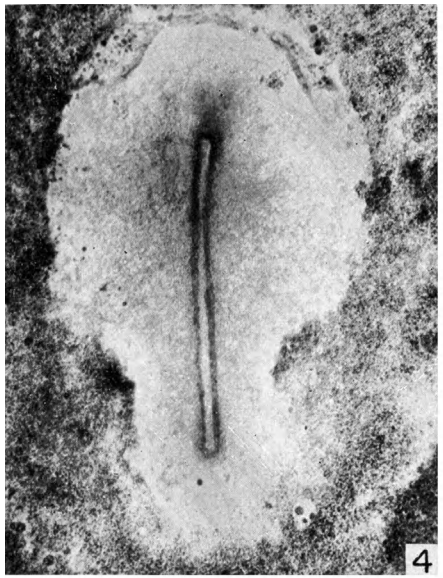

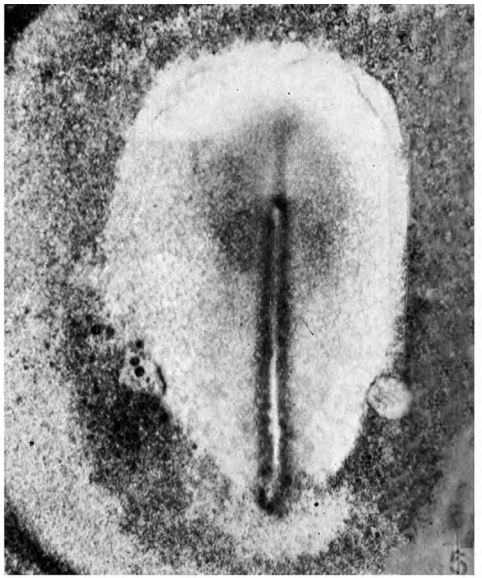

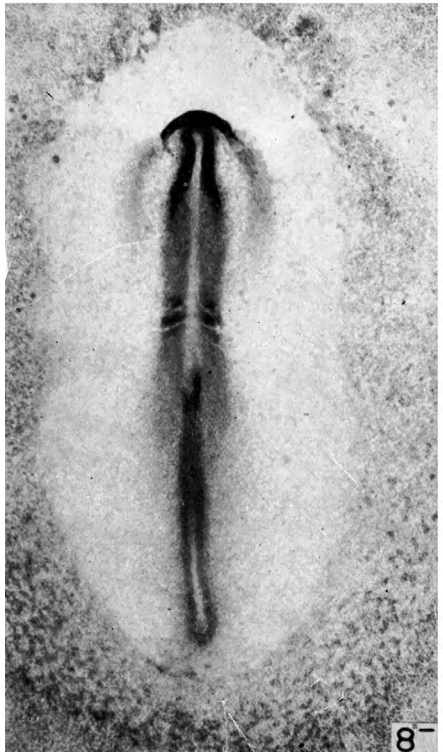

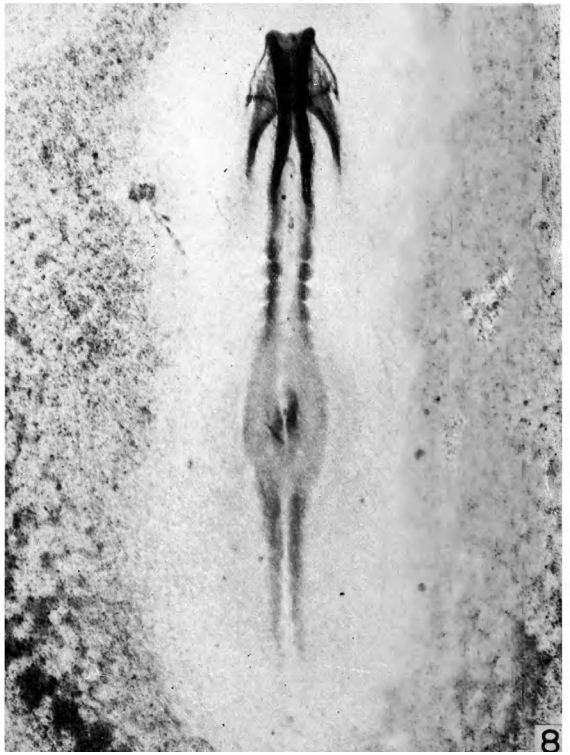

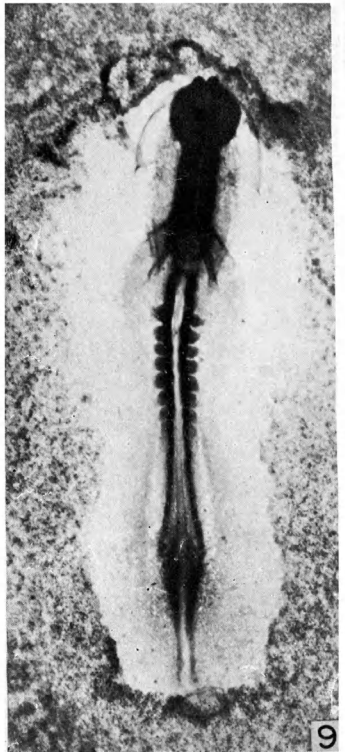

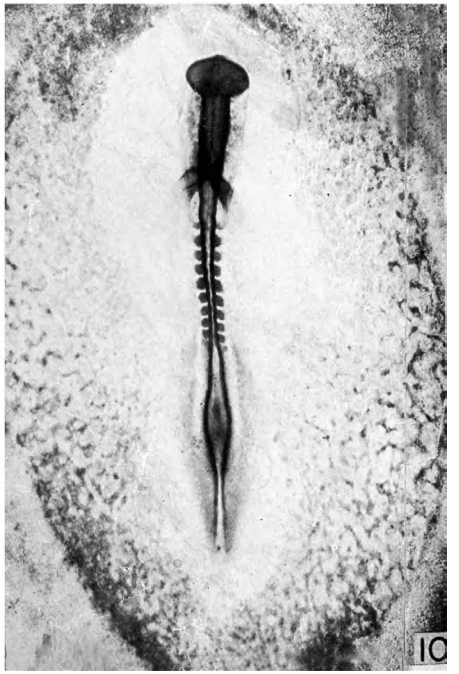

Appendix II Plates 3

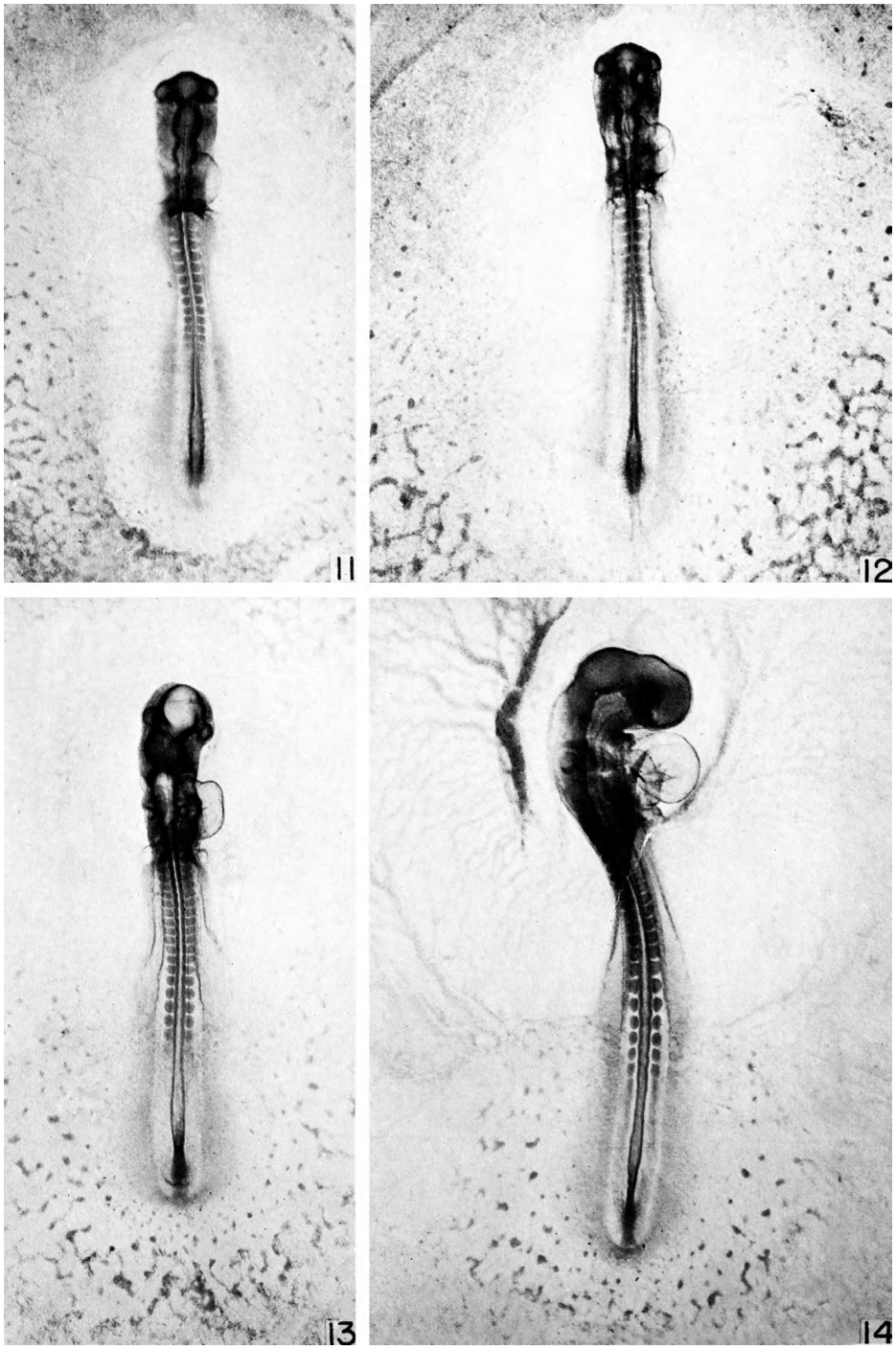

Appendix II Plates 4

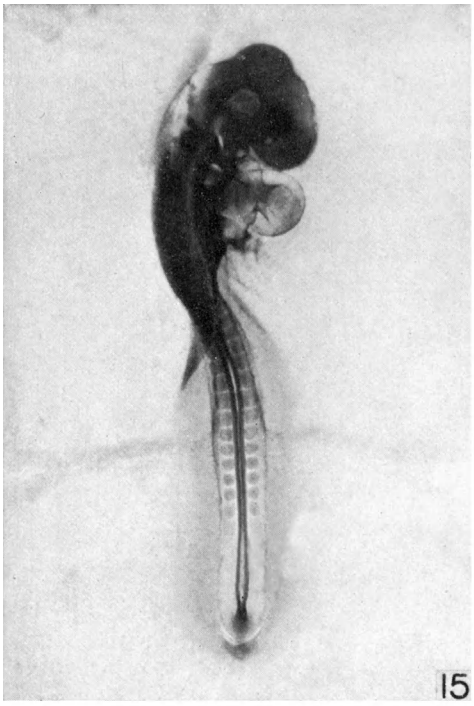

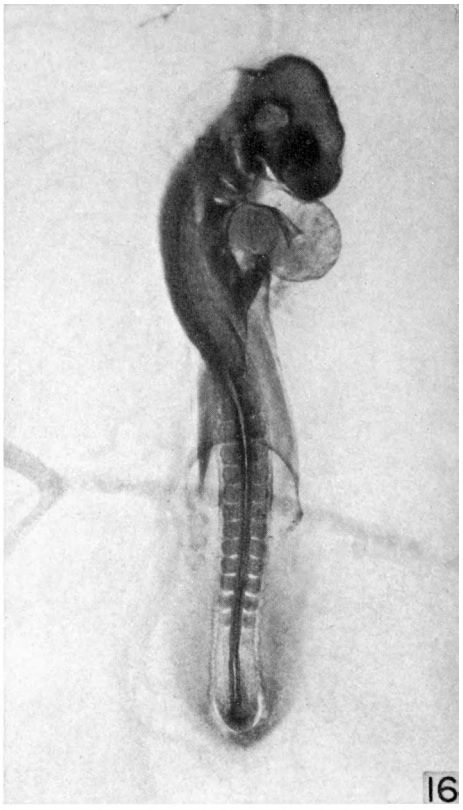

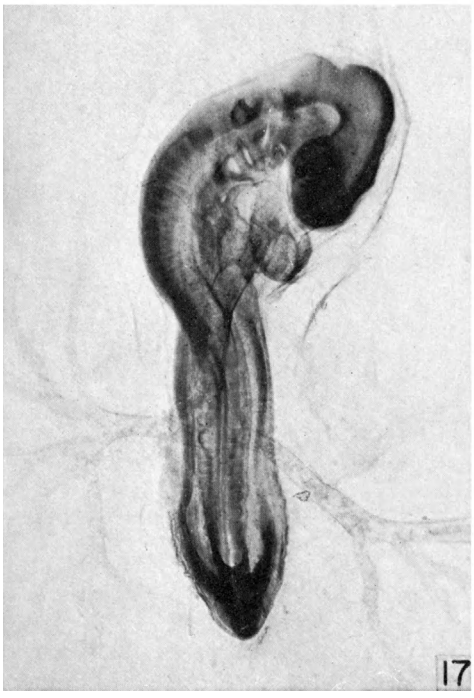

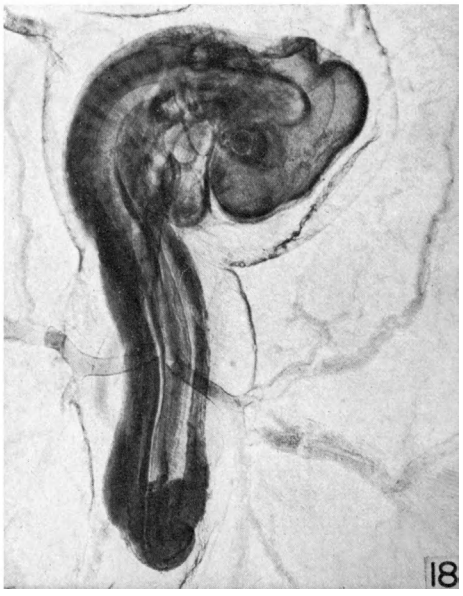

Appendix II Plates 5

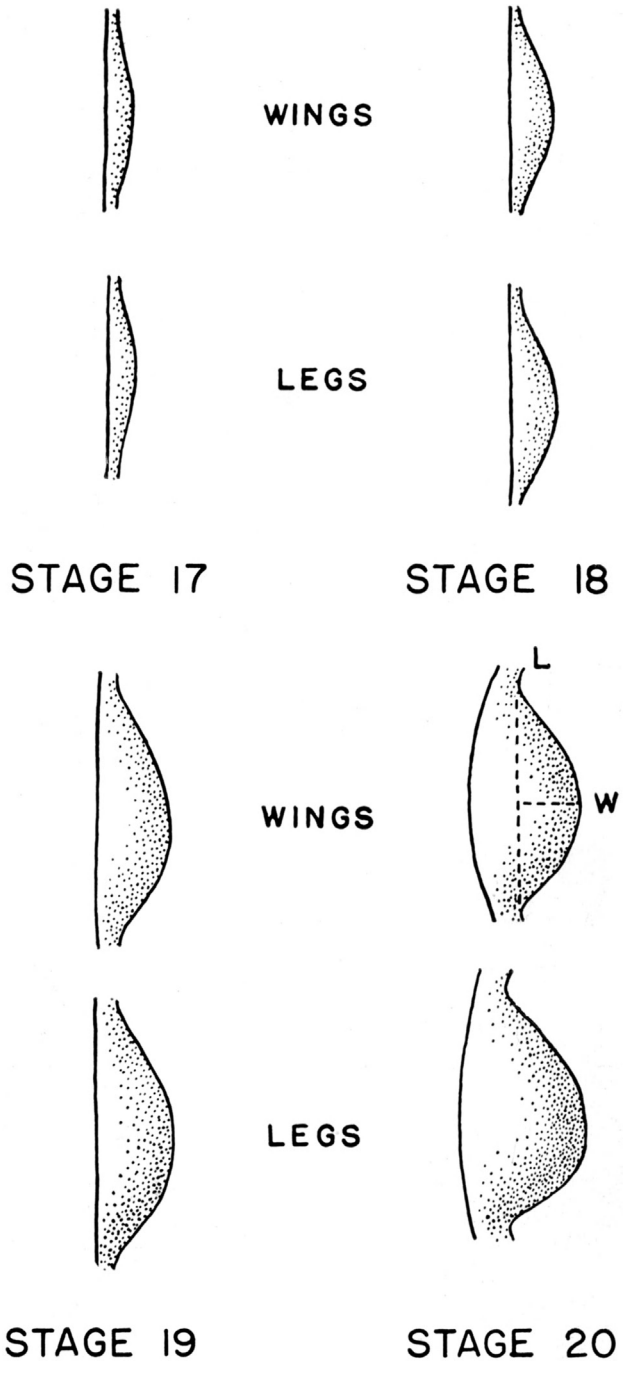

Appendix II Plates 6

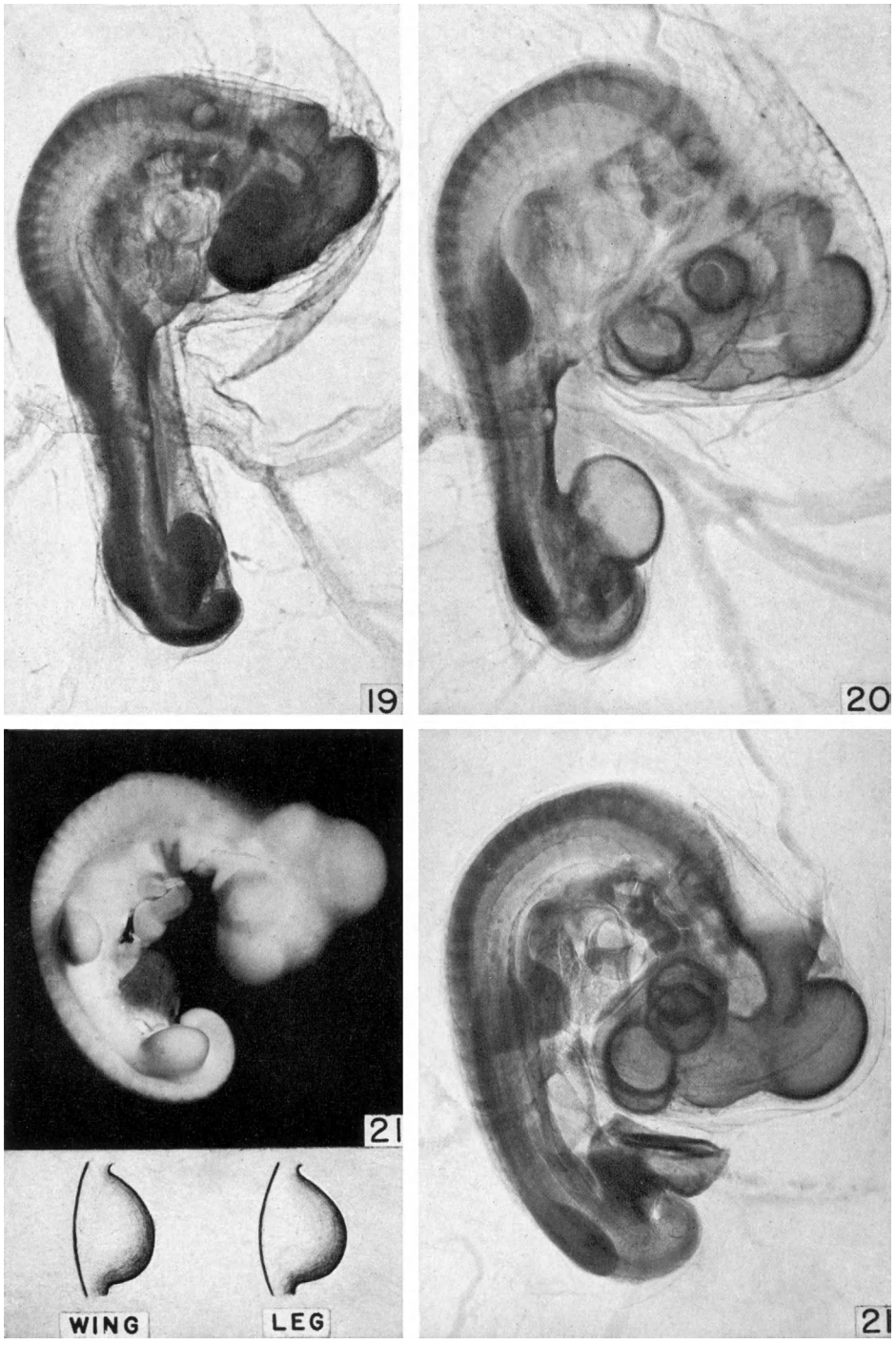

Appendix II Plates 7

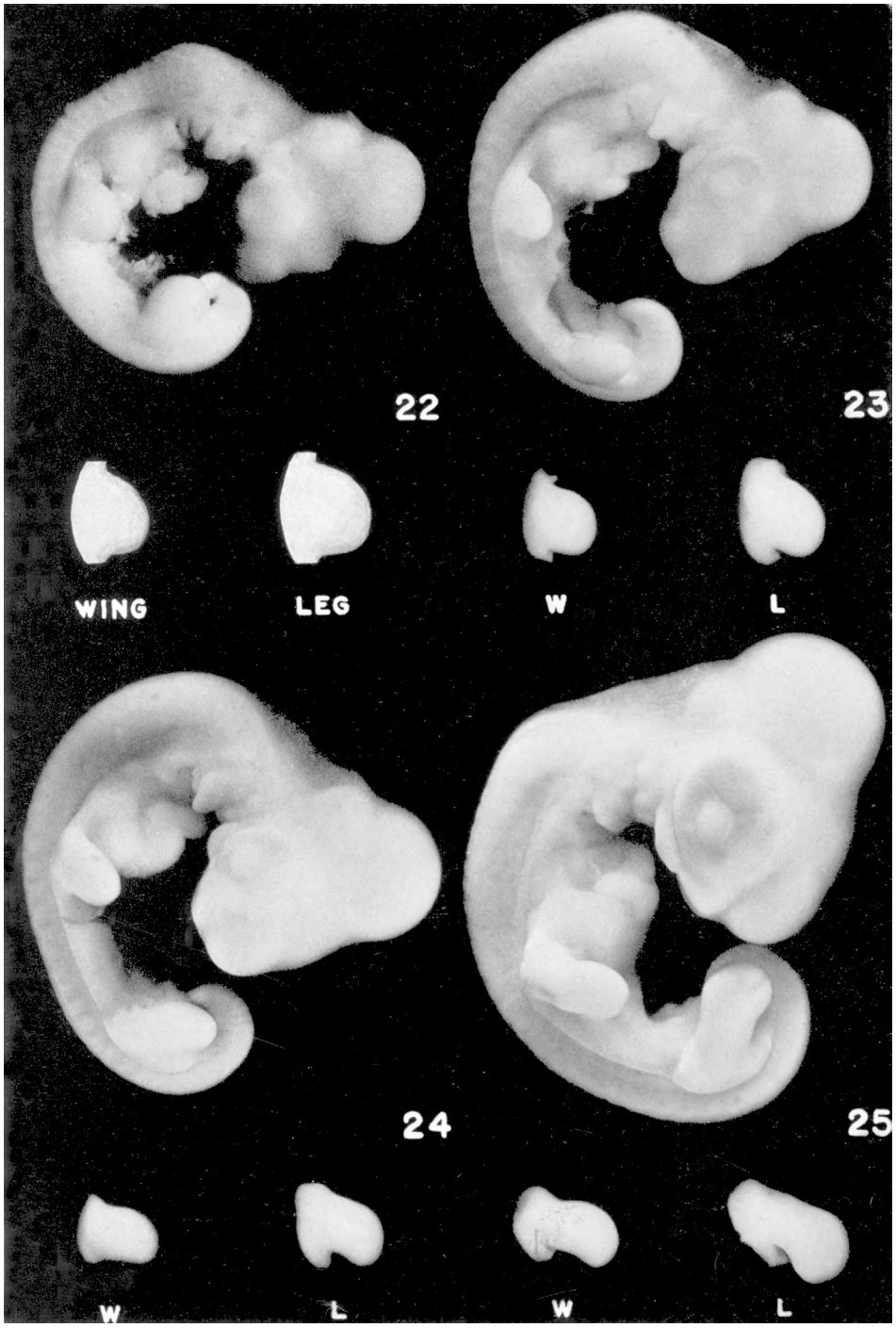

Appendix II Plates 8

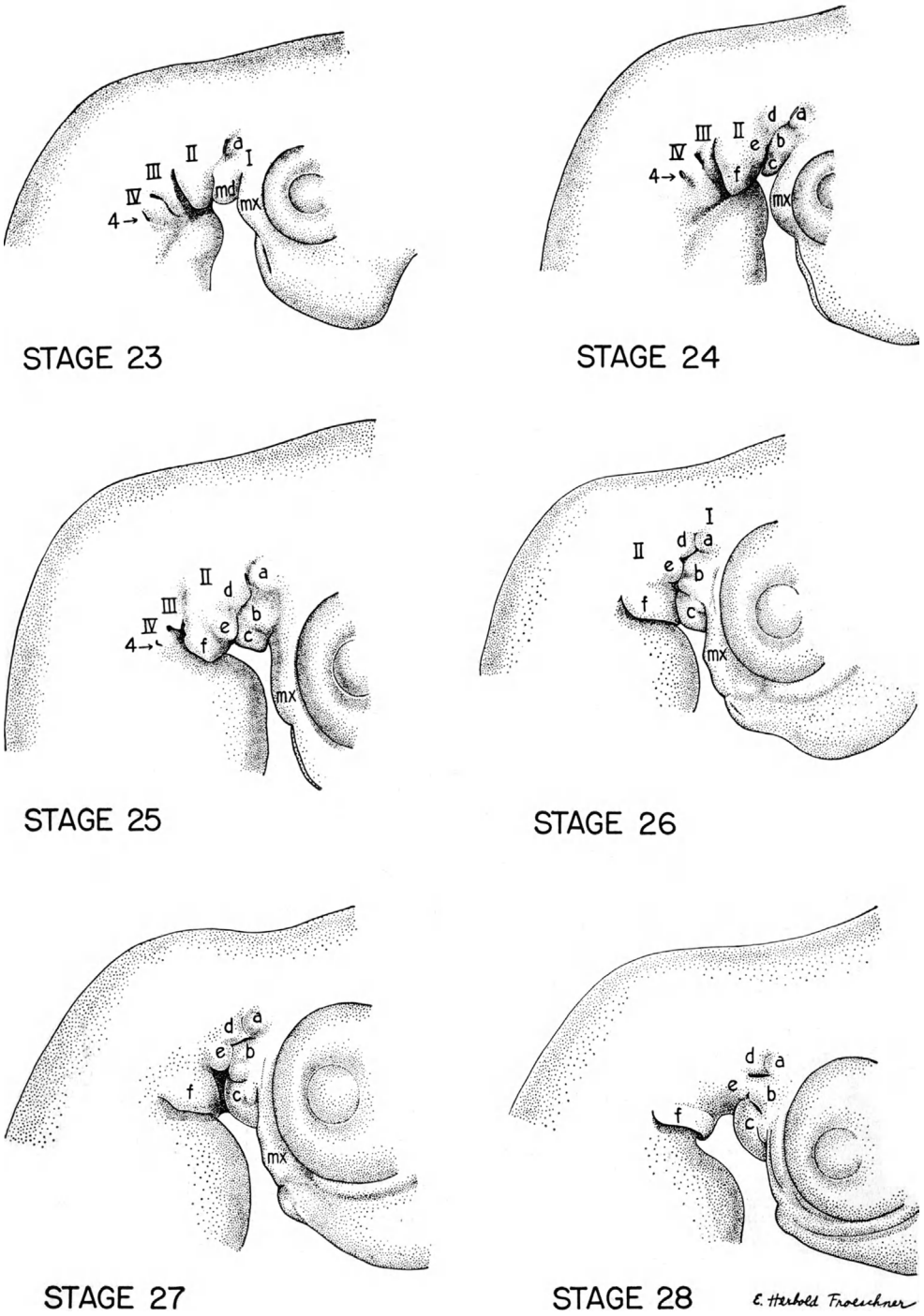

Appendix II Plates 9

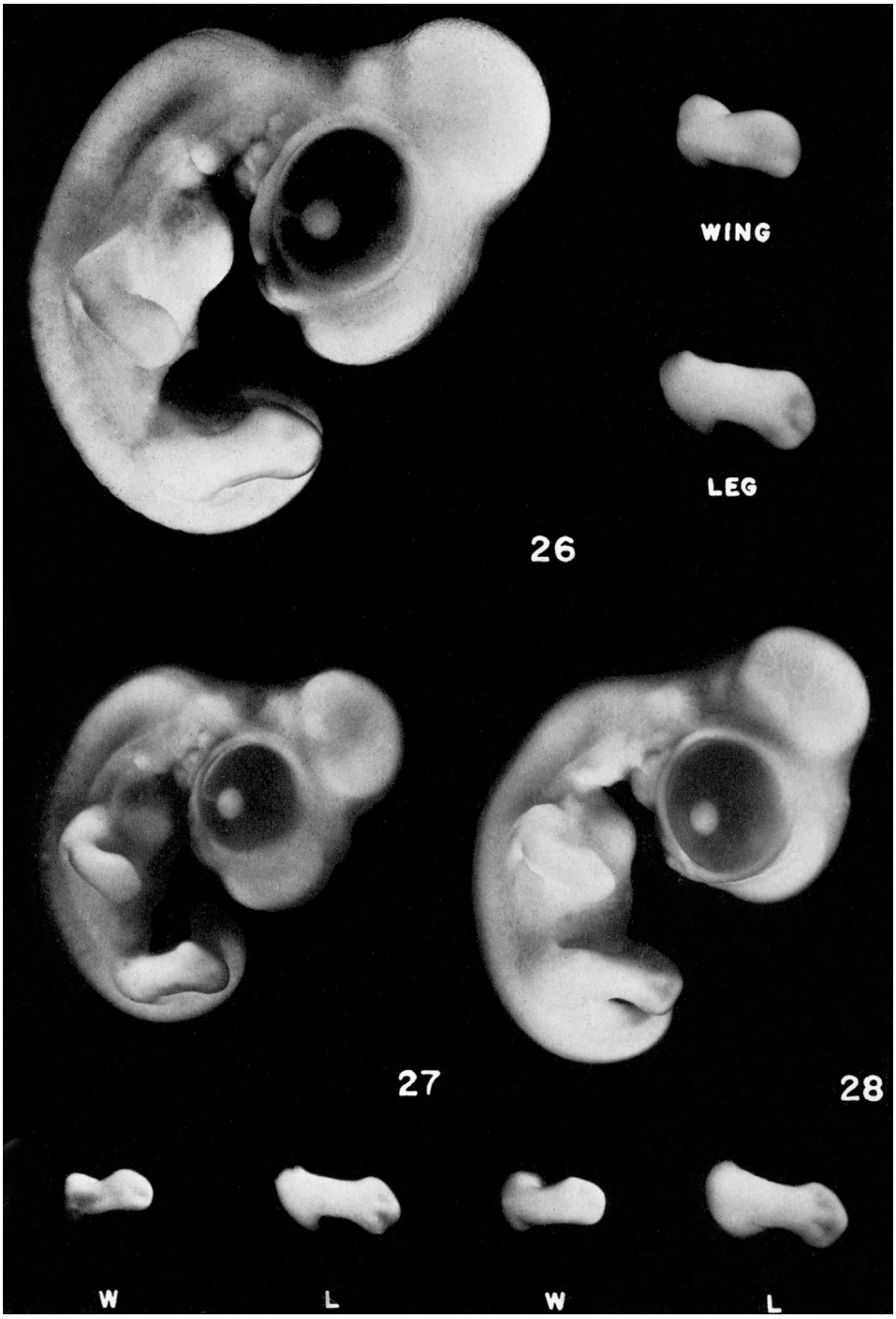

Appendix II Plates 10

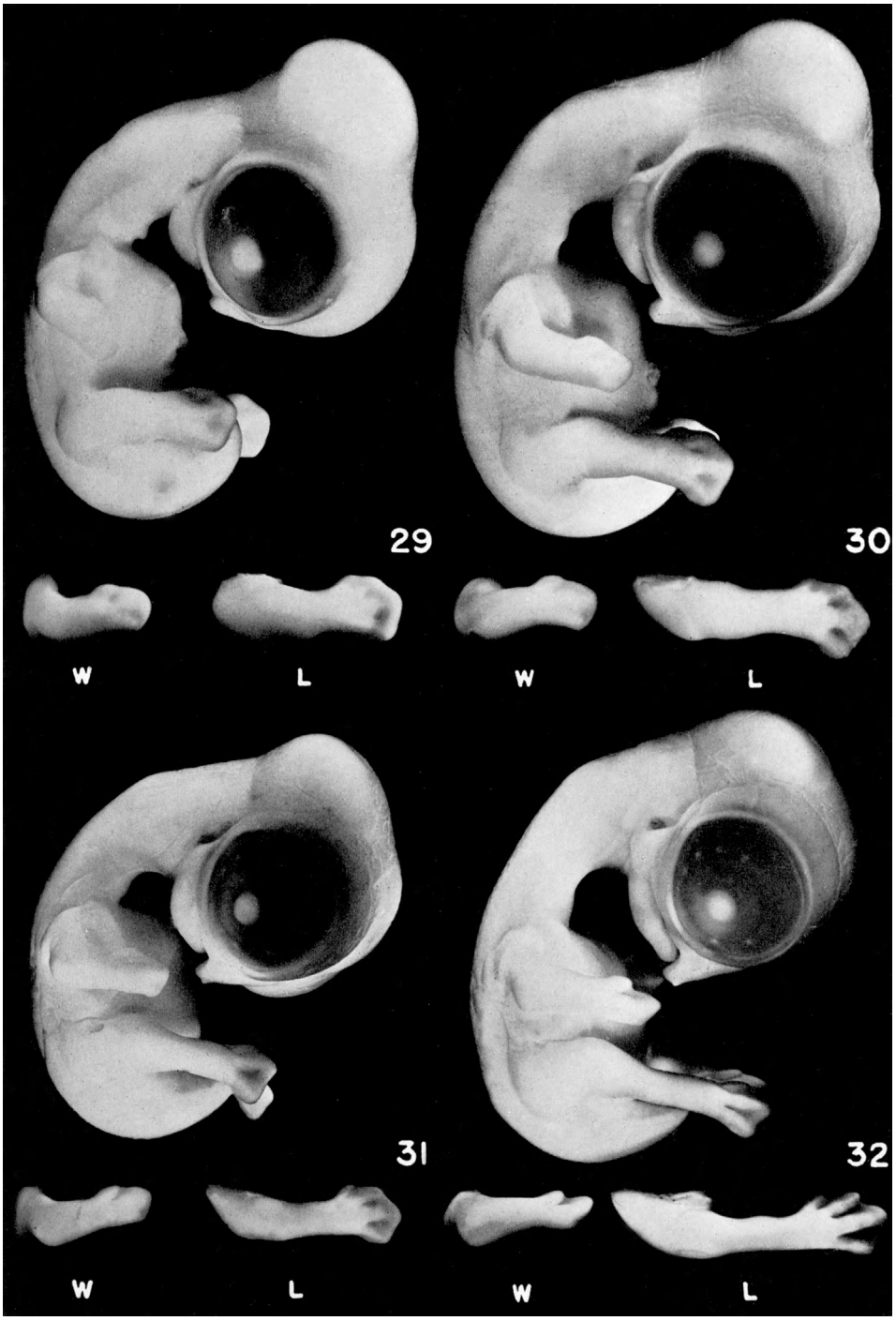

APPENDIX II PLATES 11

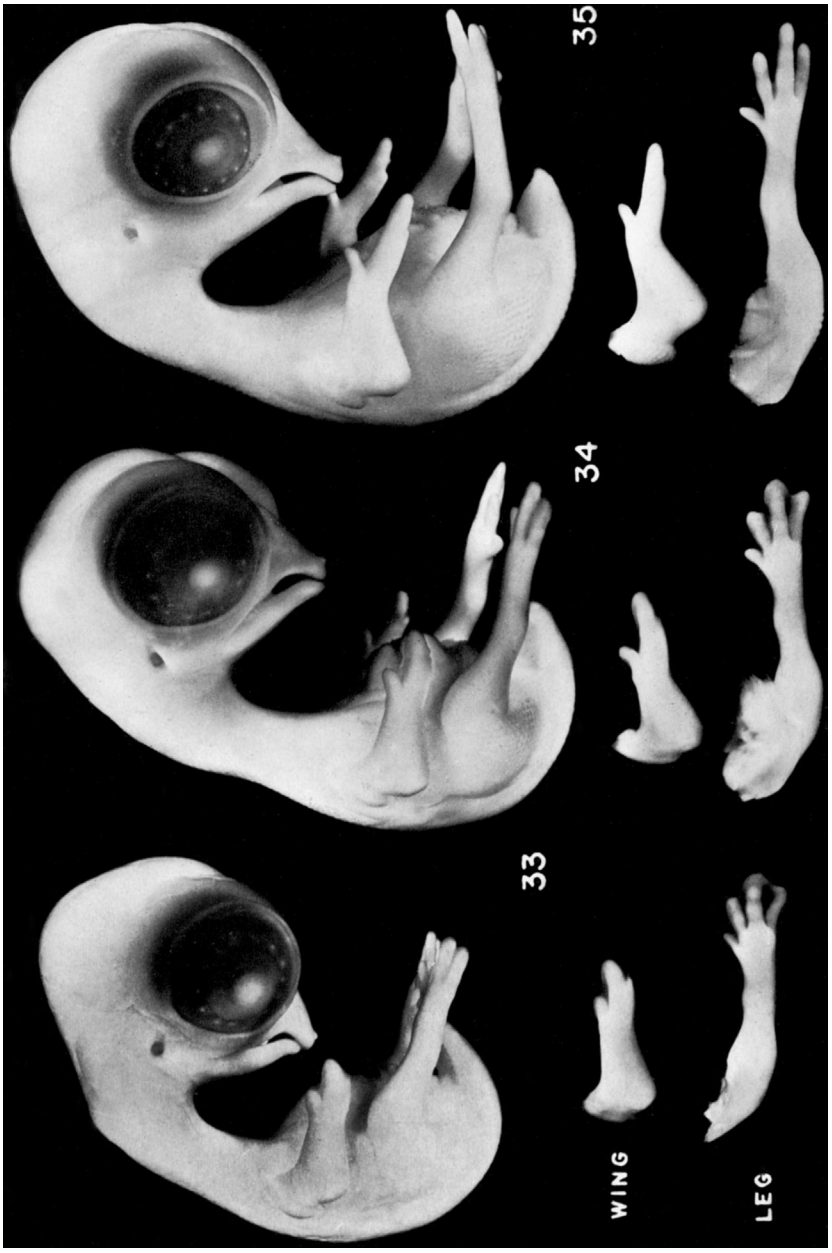

Appendix II Plates 12

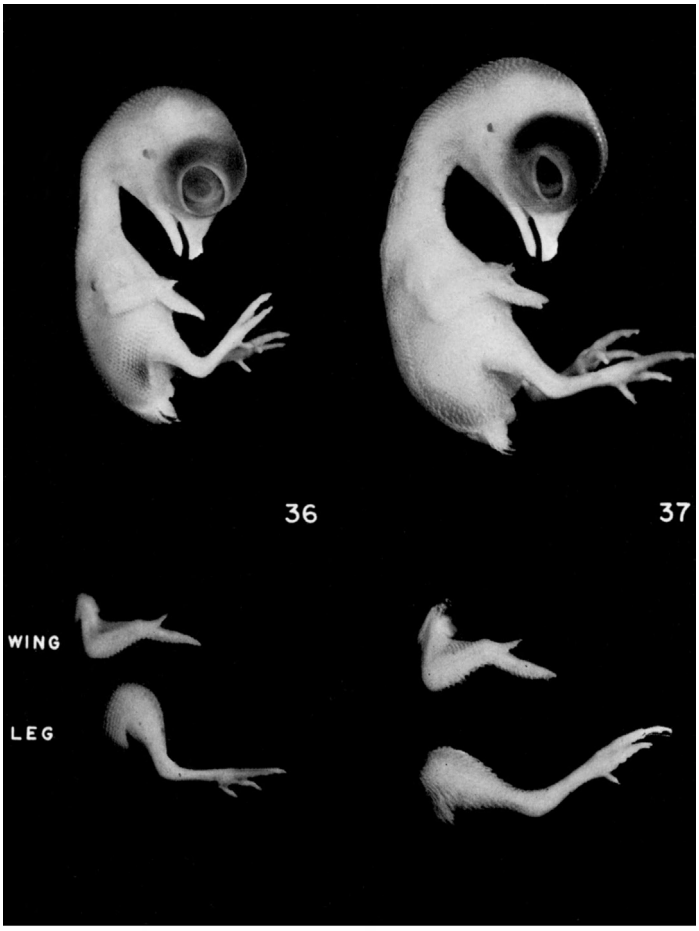

Appendix II Plates 13

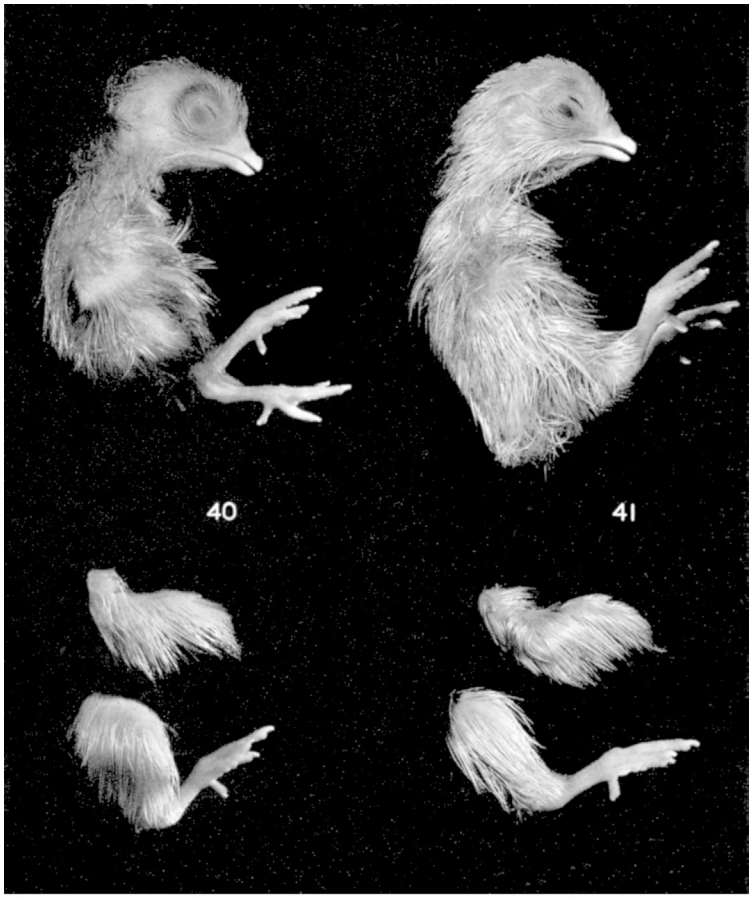

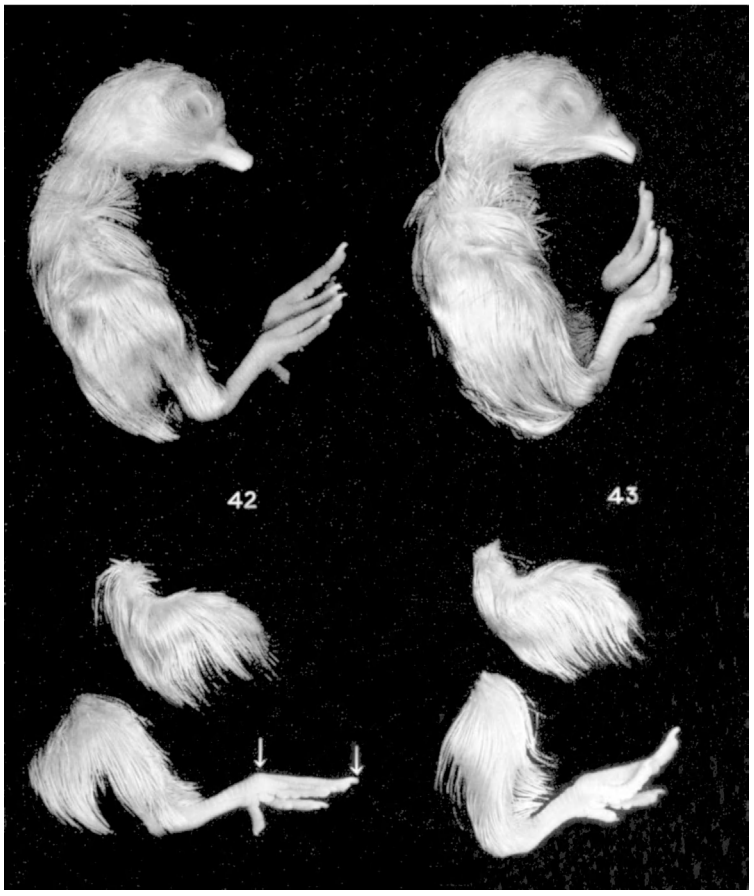

APPENDIX II PLATES 14

Appendix III

Additional Normal Tables

CHICK

Tolhurst, B.E. (1974) Development of the chick embryo in relation to the shell, yolk, albumen and extra-embryonic membranes. *Development of the Avian Embryo,* In (eds. B.M. Freeman, and M.A. Vince) *Chapman and Hall, pp. 277–91.*

Murray, B.M. and Wilson, D.J. (1994) A scanning electron microscopic study of the normal development of the chick wing from stages 19-36. *Anat. Embryol.***89**, 147-58.

DUCK

Dupuy, V., Nersessian, B. and Bakst, M.R. (2002) Embryonic development from first cleavage through seventy-two hours incubation in two strains of pekin duck *(Anas platyrhynchos). Poult. Sci.* **81**, 860–8.

Koecke, H.-U. (1958) Normalstadien der Embryonalentwicklung bei der Hausente *(Anas Boschas domestica). Embryologia* **4**, 55–78.

PHEASANT

Fant, R.J. (1957) Criteria for aging pheasant embryos. *J. Wildlife Management* **21**, 324–8.

QUAIL

Padgett, C.S. and Ivey, W.D. (1960) The normal embryology of the *Coturnix* Quail. *Anat. Rec.* **137**, 1–11.

Zacchei, A.M. (1961) Lo sviluppo embrionale della quaglia giaponese *(Coturnix coturnix japonica). Archo Ital. Anat. Embriol.* **66**, 36–62.

TURKEY

Bakst, M.R., Gupta, S.K. and Akuffo, V. (1997) Comparative development of the turkey and chicken embryo from cleavage through hypoblast formation. *Poult. Sci.* **76**, 83–90.

Phillips, R.E. and Williams, C.S. (1964) External morphology of the turkey during the incubation period. *Poult. Sci.* **23**, 270–77.

References

Abbott, U.K., Pisenti, J.M., 1993. Making the connection: exploring classical concepts in normal and abnormal limb development using contemporary approaches. Prog. Clin. Biol. Res. 383, 99–112.

Abdel-Malek, E.T., 1950. Early development of the urinogenital system in the chick. J. Morph. 86, 599–626.

Abu-Issa, R., Kirby, M.L., 2007. Heart field: from mesoderm to tube. Annu. Rev. Cell Dev. Biol. 23, 45–68.

Abu-Issa, R., Kirby, M.L., 2008. Patterning of the heart field in the chick. Dev. Biol. 319, 223–233.

Abzhanov, A., Rodda, S.J., McMahon, A.P., Tabin, C.J., 2007. Regulation of skeletogenic differentiation in cranial dermal bone. Development 134, 133–144.

Adler, R., Belecky-Adams, T.L., 2002. The role of bone morphogenetic proteins in the differentiation of the optic cup. Development 129, 3161–3171.

Albazerchi, A., Stern, C.D., 2007. A role for hypoblast (AVE) in the initiation of neural induction, independent of its ability to position the primitive streak. Dev. Biol. 301, 489–503.

Albazerchi, A., Cinquin, O., Stern, C.D., 2007. A new method to transfect the hypoblast of the chick embryo reveals conservation of the regulation of an Otx2 enhancer between mouse and chick extraembryonic endoderm. BMC Dev. Biol. 7, 25.

Alfieri, C.M., Cheek, J., Chakraborty, S., Yutzey, K.E., 2010. Wnt signaling in heart valve development and osteogenic gene induction. Dev. Biol. 338, 127–135.

Allen, S.P., Bogardi, J.P., Barlow, A.J., Mir, S.A., Qayyum, S.R., Verbeek, F.J., Anderson, R.H., Francis-West, P.H., Brown, N.A., Richardson, M.K., 2001. Misexpression of noggin leads to septal defects in the outflow tract of the chick heart. Dev. Biol. 235, 98–109.

Alsina, B., Abelló, G., Ulloa, E., Henrique, D., Pujades, C., Giraldez, F., 2004. FGF signaling is required for determination of otic neuroblasts in the chick embryo. Dev. Biol. 267, 119–134.

Amos, A.R., Deeming, D.C., 2009. Roles of water and gas exchange in determining hatchability success. Avian Biol. Res. 2, 61–66.

Anderson-Berry, A., O'Brien, E.A., Bleyl, S.B., Lawson, A., Gundersen, N., Ryssman, D., Sweeley, J., Dahl, M.J., Drake, C.J., Schoenwolff, G.C., Albertine, K.H., 2005. Vasculogenesis drives pulmonary vascular growth in the developing chick embryo.

Andrews, J.E., Smith, C.A., Sinclair, A.H., 1997. Sites of oestrogen receptor and aromatase expression in the chicken embryo. Gen. Comp. Endocrinol. 108, 182–190.

Aoyama, H., Asamoto, K., 2000. The developmental fate of the rostral/caudal half of a somite for vertebra and rib formation: experimental confirmation of the resegmentation theory using chick-quail chimeras. Mech. Develop. 99, 71–82.

Aoyama, H., Mizutani-Koseki, S., Koseki, H., 2005. Three developmental components involved in rib formation. Int. J. Dev. Biol. 49, 325–333.

Arcalis, T., Carretero, A., Navarro, M., Ayuso, E., Ruberte, J., 2002. Vasculogenesis and angiogenesis in the subcardinal venous plexus of quail mesonephros: spatial and temporal morphological analysis. Anat. Embryol. 205, 19–28.

Arguello, C., Alanis, J., Valenzuela, B., 1988. The early development of the atrioventricular node and bundle of His in the embryonic chick heart. An electro-physiological and morphological study. Development 102, 623–637.

Atkins, R.L., Wang, D., Burke, R.D., 2000. Localized electroporation: a method for targeting expression of genes in avian embryos. Biotechniques 28, 94–96.

Aulehla, A., Pourquié, O., 2008. Oscillating signal pathways during embryonic development. Curr. Opin. Cell Biol. 20, 632–637.

Bachvarova, R.F., Skromme, I., Stern, C.D., 1998. Induction of primitive streak and Hensen's node by the posterior marginal zone in the chick embryo. Development 125, 3521–3534.

Bagnall, K.M., 1988. A method to increase the survival rate of early chick embryos in experiments involving surgical intervention. Teratology 38, 75–77.

Bagnall, K.M., Higgins, S.J., Sanders, E.J., 1988. The contribution made by a single somite to the vertebral column: experimental evidence in support of resegmentation using the chick-quail chimaera model. Development 103, 69–85.

Bakst, M.R., 1986. Embryonic development of the chicken external cloaca and phallus. Scanning Electron Micr. II, 653–659.

Bakst, M.R., 1998. Structure of the avian oviduct with emphasis on sperm storage in poultry. J. Exp. Zool. 282, 618–626.

Bakst, M.R., Howarth Jr, B., 1975. The head, neck and midpiece of cock spermatozoa examined with the transmission electron microscope. Biol. Reprod. 12, 632–640.

Bakst, M.R., Howarth Jr., B., 1977. The fine structure of the hen's egg at ovulation. Biol. Reprod. 17, 361–369.
Bakst, M.R., Brillard, J.P., Wishart, G.J., 1994. Sperm selection, transport and storage in the avian oviduct. Poultry Sci. Revs. 5, 143–177.
Bakst, M.R., Vinyard, B., 2002. Oviducal sperm storage in turkeys: spatial distribution of sperm within the utero-vaginal junction sperm-storage tubules. J. Exp. Zool. 292, 206–209.
Baldwin, H.S., Solursh, M., 1989. Degradation of hyaluronic acid does not prevent looping of the mammalian heart *in situ*. Dev. Biol. 136, 555–559.
Bancroft, M., Bellairs, R., 1974. The onset of differentiation in the epiblast of the chick blastoderm. Cell Tiss. Res. 155, 399–418.
Bancroft, M., Bellairs, R., 1975. Differentiation of the neural plate and neural tube in the young chick embryo. Anat. Embryol. 147, 309–335.
Bancroft, M., Bellairs, R., 1976. The neural crest cells of the trunk region of the chick embryo studied by SEM and TEM. Zoon 4, 73–85.
Bancroft, M., Bellairs, R., 1977. Placodes of the chick embryo studied by SEM. Anat. Embryol. 151, 97–109.
Barnes, G.L., Sawyer, P.H., 1995. Histidine rich protein B of embryonic feathers is present in the transient embryonic layers of scutate scales. J. Exp. Zool. 271, 307–314.
Basch, M.L., Selleck, M.A., Bronner-Fraser, M., 2000. Timing and competence of neural crest formation. Dev. Neurosci. 22, 217–227.
Baumel, J.J., King, A.S., Breuzile, J.E., Evans, H.E., Van den Berge, J.C., 1993. Handbook of Avian Anatomy, Nomina Anatomica Avium, second ed. Nuttal Ortholological Club, Cambridge, Mass.
Beebe, D.C., Coates, J.M., 2000. The lens organizes the anterior segment: specification of neural crest cell differentiation in the avian eye. Dev. Biol. 220, 424–431.
Begbie, J., Brunet, J.F., Rubenstein, J.L., Graham, A., 1999. Induction of the epibranchial placodes. Development 126, 895–902.
Belanger, C., Copeland, J., Muirhead, D., Heinz, D., Dzialowski, E.M., 2008. Morphological changes in the chicken ductus arteriosi during closure at hatching. Anat. Rec. Hoboken. 291, 1007–1015.
Bell, D., Streit, A., Gorospe, I., Variela-Nieto, I., Alsina, B., Giraldez, F., 2008. Spatial and temporal segregation of auditory and vestibular neurons. Dev. Biol. 322, 109–120.
Bellairs, R., 1953. Studies on the development of the foregut in the chick blastoderm. J. Embryol. exp. Morph. 1, 369–385.
Bellairs, R., 1961. Cell death in the chick embryo as studied by electron microscopy. J. Anat. 95, 54–60.
Bellairs, R., 1964. Biological aspects of the yolk of the hen's egg. Adv. Morphogen. 4, 217–272.
Bellairs, R., 1967. Aspects of the development of the yolk spheres in the hen's oocyte, studied by electron microscopy. J. Embryol. Exp. Morph. 17, 267–281.
Bellairs, R., 1971. Development Processes in Higher Vertebrates. Logos Press, London.
Bellairs, R., 1979. The mechanism of somite segmentation in the chick embryo. J. Embryol. Exp. Morph. 51, 227–243.
Bellairs, R., 1987. The primitive streak and the neural crest: comparable regions of migration? In: Maderson, P. (Ed.), Developmental and Evolutionary Aspects of the Neural Crest. John Wiley, New York, pp. 123–145.
Bellairs, R., 1993. Fertilization and early development in poultry. Poultry Sci. 72, 874–881.
Bellairs, R., Boyde, A., 1969. Scanning electron microscopy of the shell membranes of the hen's egg. Z. Zellforsch. 96, 237–249.
Bellairs, R., Sanders, E.J., 1986. Somitomeres in the chick tail bud: an SEM study. Anat. Embryol. 175, 235–40.
Bellairs, R., Harkness, M., Harkness, R.D., 1963. The vitelline membrane of the hen's egg: a chemical and electron microscopical study. J. Ultra. Res. 8, 339–359.
Bellairs, R., Bromham, D.R., Wylie, C.C., 1967. The influence of the area opaca on the development of the young chick embryo. J. Embryol. Exp. Morph. 27, 195–212.
Bellairs, R., Boyde, A., Heaysman, J.E.M., 1969. The relationship between the edge of the chick blastoderm and the vitelline membrane. Wilhelm Roux's Arch. Entw. Mech. Org. 163, 113–121.
Bellairs, R., Lorenz, F.W., Dunlap, T., 1978. Cleavage in the chick embryo. J. Embryol. Exp. Morph. 43, 55–69.
Bellairs, R., Lear, P., Yamada, K.M., Rutishauser, U., Lash, J.W., 1995. Posterior extension of the chick nephric (Wolffian) duct: the role of fibronectin and NCAM polysialic acid. Dev. Dyn. 202, 333–342.
Bénazéraf, B., Francois, P., Baker, R.E., Denans, N., Little, C.D., Pourquié, O., 2010. A random cell motility gradient downstream of FGF controls elongation of an amniote embryo. Nature 466, 248–252.
Bénazet, J.-D., Zeller, R., 2009. Vertebrate limb development: moving from classical morphogen gradients to an integrated 4-dimensional patterning system. Cold Spring Har. Perspect Biol. 1a, 1339.
Bereiter-Hahn, J., Matoltsty, A.G., Richards, K.S. (Eds.), 1986. Biology of the Integument, vol. 2. Vertebrates. Springer-Verlag, Berlin.
Beresford, B., 1983. Brachial muscles in the chick embryo: the fate of individual somites. J. Embryol. Exp. Morph. 77, 99–116.
Berger, A.J., 1960. The musculature. In: Marshall, A.J. (Ed.), Biology and Comparative Physiology of Birds, vol. 1. Academic Press, New York and London, pp. 301–344.
Bertocchini, F., Stern, C.D., 2002. The hypoblast of the chick embryo positions the primitive streak by antagonizing node signaling. Dev. Cell 3, 735–744.
Bertocchini, F., Stern, C.D., 2008. Differential screen for genes expressed in the extraembryonic endodermal layer of pre-primitive streak stage chick embryos reveals expression of *Apolipoprotein A1* in hypoblast, endoblast and endoderm. Gene Expr. Patterns 8, 477–480.

Bishop-Calame, S., 1965. Nouvelle recherches concernant le role du canal de Wolff dans la differenciation du mésonéphros de l'embryon de poulet. J. Embryol. Exp. Morph. 14, 239–245.
Bissonette, J.P., Fekete, D.M., 1996. Standard atlas of the gross anatomy of the developing inner ear of the chicken. J. Comp. Neurol. 368, 620–630.
Board, R.G., 1982. Properties of avian egg shells and their adaptive value. Biol. Rev. 57, 1–28.
Board, R.G., Sparks, N.H.C., 1991. Shell structure and formation in avian eggs. In: Deeming, D.C., Ferguson, M.W.J. (Eds.), Egg Incubation: Its Effects on Embryonic Development in Birds and Reptiles. Cambridge University Press, pp. 371–383.
Boettger, T., Knoetgen, H., Wittler, L., Kessel, M., 2001. The avian organizer. Int. J. Dev. Biol. 45, 281–287.
Bohnsack, B.L., Gallina, D., Thompson, H., Kasprick, D.S., Lucarelli, M.J., Dootz, G., Nelson, C., McGonnell, I.M., Kahana, A., 2011. Development of extraocular muscles requires early signals from the periocular neural crest and the developing eye. Arch. Ophthalmol. 129, 1030–1041.
Borghjid, S., Siddiqui, M.A., 2000. Chick homeobox gene cDix expression demarcates the forebrain anlage, indicating the onset of forebrain regional specification at gastrulation. Dev. Neurosci. 22, 183–196.
Bortier, H., Vakaet, L.C.A., 1992. Fate mapping the neural plate and the intraembryonic mesoblast in the upper layer of the chicken blastoderm with xenografting and time-lapse videography. Dev. Suppl. 93–97.
Bortier, H., Callebaut, M., Vakaet, L.C.A., 1996. Time-lapse cinephotomicrography, videography, and videomicrography of the avian blastoderm. Meth. Cell Biol. 51, 331–354.
Borycki, A., Emerson, A.G., 2000. Multiple tissue interactions and signal transduction pathways control somite myogenesis. Curr. Topics Dev. Biol. 48, 165–224.
Bothe, I., Tenin, G., Osenti, A., Dietrich, S., 2011. Dynamic control of head mesoderm patterning. Development 136, 2807–2821.
Boulland, J., Halasi, G., Kasumacic, N., Glover, J.C., 2010. Xenotransplantation of human stem cells into the chicken embryo. J. Vis. Exp. 41, e2071. DOI: 3791/2071.
Boyden, E.A., 1927. Experimental obstruction of the mesonephric ducts. Proc. Soc. Exp. Biol. Med. 24, 572–576.
Boyer, A.S., Runyan, R.B., 2001. TGFβ Type III and TGFβ Type II receptors have distinct activities during epithelial–mesenchymal cell transformation in the embryonic heart. Dev. Dyn. 221, 454–459.
Brand-Saberi, B., Christ, B.B., 1999. Genetic and epigenetic control of muscle development in vertebrates. Cell Tissue Res. 296, 199–212.
Brockman, D.E., Redmond, M.E., Kirby, M.L., 1990. Altered development of pharyngeal arch vessels after neural crest ablation. Ann. N. Y. Acad. Sci. 588, 296–304.
Bronner-Fraser, M. (Ed.), 2008. Avian Embryology, second ed. Methods in Cell Biology, 87, pp. 1–408.
Brown, A.J., Sanders, E.J., 1991. Interactions between mesoderm cells and the extracellular matrix following gastrulation in the chick embryo. J. Cell Sci. 99, 431–441.
Brown, J.M., Robertson, K.E., Wedden, S.E., Tickle, C., 1997. Alterations in Msx1 and Msx 2 expression correlate with inhibition of outgrowth of chick facial primordia induced by retinoic acid. Anat. Embryol. 195, 203–207.
Bryk, S.G., Orlandini, S.Z., Gheri, G., Sgambati, E., 1992. Development of the chick tongue. A scanning electron microscopical investigation. Ann. Anat. 174, 531–534.
Buchtova, M., Kuo, W.P., Nimmagadda, S., Benson, S.L., Poongodi, G.L., Logan, C., Au-Yeung, T., Chiang, E., Fu, K., Richman, J.M., 2010. Whole genome microarray analysis of chick facial prominences. Dev. Dyn. 239, 574–591.
Burke, A.C., 2000. *Hox* genes and the global patterning of the somitic mesoderm. Curr. Topics Dev. Biol. 47, 155–181.
Burke, A.C., Nelson, C.E., Morgan, B.A., Tabin, C., 1995. Hox genes and the evolution of vertebrate axial morphology. Development 121, 333–346.
Burke, W.H., Henry, M.H., 1999. Gonadal development and growth of chickens and turkeys hatched from eggs injected with an aromatase inhibitor. Poultry Sci. 78, 1019–1033.
Burley, R.W., Vadehra, D.V., 1989. The Avian Egg. John Wiley and Sons, New York.
Burns, A.S., Le Douarin, N.M., 2001. Enteric nervous system development: analysis of the selected developmental potentialities of vagal and sacral neural crest cells using quail-chick chimeras. Anat. Rec. 262, 16–28.
Burns, R.K., 1956. Urino-genital system. In: Willier, B.H., Weiss, P.A., Hamburger, V. (Eds.), Analysis of Development. W.B. Saunders, Philadelphia, pp. 462–491.
Butler, J.K., 1952. An experimental analysis of cardiac loop formation of the heart tube in the chick. University of Texas (not seen), MA Thesis.
Callebaut, M., 1987. Ooplasmic localization and segregation in quail germs: fate of the four ooplasms. Arch. Biol. Brux. 98, 441–473.
Callebaut, M., Van Neuten, E., 1994. Rauber's (Koller's) sickle: the early gastrulation organizer of the avian blastoderm. Eur. J. Morph. 32, 35–48.
Callebaut, M., Van Neuten, E., Van Nassauw, L., Bortier, H., Harrisson, F., 1998. Only the endophyll-Rauber's sickle complex and not cells derived from the caudal margin zone induce a primitive streak in the upper layer of avian blastoderms. Reprod. Nutr. Dev. 38, 449–463.
Callebaut, M., Van Neuten, E., Harrisson, F., Van Nassauw, L., Bortier, H., 2000a. Avian junctional endoblast has strong embryo-inducing and dominating potencies. Euro. J. Morphol. 38, 3–16.
Callebaut, M., Van Neuten, E., Harrisson, F., Bortier, H., 2000b. Development of the sickle canal, an unrecognized formation in the avian blastoderm, and its spatial relationship with the first appearing blood islands, induced by Rauber's sickle. Belg. J. Zool. 130, 143–156.
Callebaut, M., Harrisson, F., Bortier, H., 2001. Effect of gravity on the interaction between the avian germ and neighboring ooplasm in inverted egg yolk balls. Eur. J. Morphol. 39, 27–38.

Calvo, J., Boya, J., 1979. Ultrastructural study of the embryonic development of the pineal gland of the chicken *(Gallus gallus)*. Acta. Anat. Basel. 103, 39–73.
Canning, C.A., Lee, L., Luo, S.X., Graham, A., Jones, C.M., 2008. Neural tube derived Wnt signals cooperate with FGF signaling in the formation and differentiation of the trigeminal placodes. Neural Dev. 15, 35.
Canning, D.R., Stern, C.D., 1988. Changes in the expression of the carbohydrate epitope HNK-1 associated with mesoderm induction in the chick embryo. Development 104, 643–655.
Canto-Soler, M.V., Adler, R., 2006. Optic cup and lens development requires Pax6 expression in the early optic vesicle during a narrow time window. Dev. Biol. 294, 119–132.
Caprioli, A., Minko, K., Drevon, C., Eichmann, A., Dieterlen-Lièvre, F., Jaffredo, T., 2001. Hemangio-blast commitment in the avian allantois: cellular and molecular aspects. Dev. Biol. 238, 64–78.
Carretero, A., Ditrich, H., Navarro, M., Splechtna, H., Ruberte, J., 1993. Technical improvements in corrosion casting of small specimens: a study of mesonephric tubules and vessels of chick embryos. Scanning Microsc. 7, 1333–1338.
Carretero, A., Ditrich, H., Perez-Aparicio, F.J., Splechtna, H., Ruberte, J., 1995. Development and degeneration of the arterial system in the mesonephros and metanephros of chicken embryos. Anat. Rec. 243, 120–128.
Carretero, A., Ditrich, H., Navarro, M., Ruberte, J., 1997. Afferent portal venous system in the mesonephros and metanephros of chick embryos: development and degeneration. Anat. Rec. 247, 63–70.
Castro-Quezada, A., Nadal-Ginard, B., De La Cruz, M., 1972. Experimental study of the formation of the bulboventricular loop in the chick. J. Embryol. Exp. Morph. 27, 623–637.
Catala, M., Teillet, M.-A., Le Douarin, N.M., 1995. Organization and development of the tail bud analyzed with the quail-chick chimera system. Mech. Dev. 51, 51–65.
Catala, M., Teillet, M.A., De Robertis, E.M., Le Douarin, N.M., 1996. A spinal cord fate map in the avian embryo: while regressing, Hensen's node lays down the notochord and floor plate thus joining the spinal cord lateral walls. Development 122, 2599–2610.
Chang, W., ten Dijke, P., Wu, D.J., 2002. BMP pathways are involved in otic capsule formation and epithelial-mesenchymal signalling in the developing chicken inner ear. Dev. Biol. 251, 380–394.
Chapman, S.C., Collignon, J., Schoenwolf, G.C., Lumsden, A., 2001. Improved method for chick whole-embryo culture using a filter paper carrier. Dev. Dyn. 220, 284–289.
Chapman, S.C., Matsumoto, K., Cai, Q., Schoenwolf, G.C., 2007. Specification of germ layer identity in the chick gastrula. BMC Dev. Biol. 791, 91.
Charrier, J.B., Teillet, M.A., Lapointe, F., Le Douarin, N.M., 1999. Defining subregions of Hensen's node essential for caudalward movement, midline development and survival. Development 126, 4771–4783.
Charrier, J.B., Lapointe, F., Le Douarin, N.M., Teillet, M.-A., 2001. Anti-apoptotic role of sonic hedgehog protein at the early stages of nervous system organogenesis. Development 128, 4011–4020.
Chernoff, A.E.G., Overton, J., 1979. Scanning electron microscopy of chick epiblast expansion on the vitelline membrane. Dev. Biol. 57, 33–46.
Chernoff, E.A., Clarke, D.O., Wallace-Evers, J.L., Hungate-Muegge, L.P., Smith, R.C., 2001. The effects of collagen synthesis inhibitory drugs on somitogenesis and myogenein expression in cultured chick and mouse embryos. Tissue Cell 23, 97–110.
Chevallier, A., 1975. Role du mésoderme somitique dans la développement de la cage thoracique de l'embryon d'oiseau I. Origine du segment sternal et mécanismes de la différentiation des côtes. JEEM 33, 291–311.
Chevallier, A., 1977. Origines des ceintures scapulaires et pelviennes chez l'embryon d'oiseau. JEEM 423, 275–292.
Chevallier, A., Kieny, M., Mauger, A., 1978. Limb-somite relationship: effect of removal of somitic mesoderm on the wing musculature. J. Embryol. Exp. Morph. 43, 263–278.
Chiba, Y., Khandoker, A.H., Nobuta, M., Moriya, K., Abiyama, R., Tazawa, H., 2002. Development of respiratory rhythms in perinatal chick embryos. Comp. Biochem. Physiol. 131, 817–824.
Chien, Y.C., Hincke, M.T., McKee, M.D., 2009. Ultrastructure of avian eggshell during resorption following egg fertilization. J. Struct. Biol. 168, 527–538.
Chin, K., Kurian, R., Saunders, J.C., 1997. Maturation of tympanic membrane layers and collagen in the embryonic and post-hatch chick (Gallus domesticus). J. Morphol. 223, 257–266.
Chodankar, R., Chang, C.H., Yue, Z., Jiang, T.X., Suksa, S., Burrus, L., Chuong, C.M., Widelitx, R., 2003. Shift of localized growth zones contributes to appendage morphogenesis: role of Wnt/beta catenin pathway. J. Invest. Dermatol. 120, 20–26.
Christ, B., Ordahl, C.P., 1995. Early stages of chick somite development. Anat. Embryol. 191, 381–396.
Christ, B., Wilting, J., 1992. From somites to vertebral column. Ann. Anat. 174, 23–32.
Christ, B., Jacob, H.J., Jacob, M., 1977. Experimental analysis of the origin of the wing musculature in avian embryos. Anat. Embryol. 150, 171–186.
Christ, B., Jacob, M., Jacob, H.J., 1983. On the origin and development of the ventro-lateral trunk musculature in the avian embryo. An experimental and ultrastructural study. Anat. Embryol. 166, 87–101.
Christ, B., Huang, R., Wilting, J., 2000. The development of the avian vertebral column. Anat. Embryol. 202, 179–194.
Chuai, M., Weijer, C.J., 2009. Regulation of cell migration during chick gastrulation. Curr. Opin. Genet. Dev. 19, 343–349.
Chuai, M., Zeng, W., Yang, X., Boychenko, V., Glazier, J.A., Weijer, C.J., 2006. Cell movement during chick primitive streak formation. Dev. Biol. 296, 137–149.

Chuong, C.M., 1993. The making of a feather – homeoproteins, retinoids and adhesion molecules. Bio. Essays 15, 513–522.

Climent, S., Sarasa, M., Villar, J.M., Murillo-Ferrol, N., 1995. Neurogenic cells inhibit the differentiation of cardiogenic cells. Dev. Biol. 171, 130–148.

Cobos, I., Shimamura, K., Rubenstein, J.L.R., Martinez, S., Puelles, L., 2001. Fate map of the avian anterior forebrain at the four-somite stage, based on the analysis of quail-chick chimeras. Dev. Biol. 239, 46–67.

Coco, C.M., Hargis, B.M., Hargis, P.S., 1992. Research note: effect of *in ovo* 17β-estradiol or tamoxifen administration on sexual differentiation of the external genitalia. Poultry Sci. 71, 1947–1951.

Coffin, J.D., Poole, T.J., 1988. Embryonic vascular development: immunohistochemical identification of the origin and subsequent morphogenesis of the major vessel primordia in quail embryos. Development 102, 735–748.

Cohen, G.M., Hersing, W., 1993. Development of the chick's auditory ossicle, the columella. Physiologist 36S, 75–76.

Cohen, Y.E., Hernandez, H.N., Saunders, J.C., 1992. Middle-ear development: II Morphometric changes in the conducting apparatus of the chick. J. Morphol. 212, 257–267.

Cohn, M.J., 2011. Development of the external genitalia: conserved and divergent mechanisms of appendage patterning. Dev. Dyn. 240, 1108–1115.

Colas, J.F., Lawson, A., Schoenwolf, G.C., 2000. Evidence that the translation of smooth muscle alphaactin mRNA is delayed in the chick promyocardium until fusion of the bilateral heart-forming regions. Dev. Dyn. 218, 316–330.

Cook, G.M.W., Bellairs, R., Rutherford, N.G., Stafford, C.A., Alderson, T., 1985. Isolation, characterization and localization of a lectin within the vitelline membrane of the hen's egg. J. Embryol. Exp. Morph. 90, 389–407.

Cooke, J., Zeeman, E.C., 1976. A clock and wave-front model for control of the number of repeated structures during animal morphogenesis. J. Theor. Biol. 58, 455–476.

Cooper, K.L., Hu, J.K., ten Berge, D., Fernandez-Teran, M., Ros, M.A., Tabin, C.J., 2011. Initiation of proximodistal patterning in the vertebrate limb by signals and growth. Science 332, 1083–1086.

Cornish, J.A., Etkin, L.D., 1993. The formation of the pronephric duct in Xenopus involves recruitment of posterior cells by migrating pronephric duct cells. Dev. Biol. 159, 338–345.

Coulombre, A.J., Coulombre, J.L., Mehta, H., 1962. The skeleton of the eye. I. Conjuctival papillae and scleral ossicles. Dev. Biol. 5, 382–401.

Couly, G., Le Douarin, N.M., 1988. The fate map of the cephalic neural primordium at the presomitic to the 3-somite stage in the avian embryo. Development 103 (Suppl.), 101–113.

Couly, G.F., Coltey, P.M., Le Douarin, N.M., 1992. The developmental fate of the cephalic mesoderm in quail-chick chimeras. Development 114, 1–15.

Couly, G.F., Coltey, P.M., Le Douarin, N.M., 1993. The triple origin of skull in higher vertebrates: a study in quail-chick chimeras. Development 117, 409–429.

Creuzet, S., Couly, G., Le Douarin, N.M., 2005. Patterning the neural crest derivatives during development of the vertebrate head; insights from avian studies. J. Anat. 207, 447–459.

Croisille, Y., Le Douarin, N., 1964. Development and regeneration of the liver. In: DeHaan, R.L., Ursprung, H.L. (Eds.), Organogenesis. Holt, Rhinehart and Winston, New York, pp. 421–466.

Croisille, Y., Gumpel-Pinot, M., Martin, C., 1976. Embryologie expérimentale. La différenciation des tubes sécréteurs du rein chez les oiseaux; effets des inducteurs hétérogènes. C. R Acad. Sci. Paris D282, 1987–1990.

Cui, C., Cheuvront, T.J., Lansford, R.D., Moreno-Rodriguez, R.A., Schlutheiss, T.M., Rongish, B.J., 2009. Dynamic positional fate map of the primary heart-forming region. Dev. Biol. 322, 212–222.

Cui, C., Lansford, R., Filla, M.B., Little, C.D., Chevront, T.C., Ronguish, B.J., 2006. Electroporation and EGFP labeling of gastrulating quail embryos. Dev. Dyn. 235, 2802–2810.

Cui, C., Yang, X., Chuai, M., Glazier, J., Weijer, C., 2005. Analysis of tissue flow patterns during primitive streak formation in the chick embryo. Dev. Biol. 284, 37–47.

Czirók, A., Ruppa, P.A., Little, C.D., 2002. Multifield 3D scanning light microscopy of early embryogenesis. J. Microsc. 206, 209–217.

D'Amico-Martel, A., Noden, D.M., 1983. Contributions of placodal and neural crest cells to avian cranial peripheral ganglia. Am. J. Anat. 166, 445–468.

Daniel Jr, J.C., 1955. A simplified method for the preparation of avian embryos. Turtox News 33, 142–143.

Darland, C., D'Amore, 2001. Cell–cell interactions in vascular development. Curr. Top. Dev. Biol. 52, 107–149.

Darnell, D.K., Schoenwolf, G.C., 1997. Modern techniques for cell labelling in avian and murine embryos. In: Daston, G.P. (Ed.), Molecular and Cellular Methods in Developmental Toxicology. CRC Press, New York, pp. 231–272.

Darnell, D.K., Stark, M.R., Schoenwolf, G.C., 1999. Timing and cell interactions underlying neural induction in the chick embryo. Development 126, 2505–2514.

Darras, V.M., Van Herck, S.L., Geysens, S., Reyns, G.E., 2009. Involvement of thyroid hormones in chicken embryonic brain. Gen. Comp. Endocrinol. 163, 58–62.

Das, S.C., Isobe, N., Yoshimura, Y., 2008. Mechanism of prolonged sperm storage and sperm survivability in hen oviduct: a review. Am. J. Reprod. Immunol. 60 (6), 477–481.

Dathe, V., Gamel, A., Männer, J., Brand-Saberi, B., Christ, B., 2003. Morphological left–right symmetry of Hensen's node precedes the asymmetric expression of Shh and Fgf8 in the chick embryo. Anat. Embryol. 205, 342–354.

Davis, E.J., Miller, R.H., 2001. Local sonic hedgehog signalling regulates oligodendrocyte precursor appearance in multiple ventricular zone domains in the chick metencephalon. Dev. Biol. 233, 513–525.

Davis, A.M., Rothenberg, F.G., Shepherd, N., Izatt, J.A., 2008. In vivo spectral domain optical coherence tomography volumetric imaging and spectral Doppler velocimetry of early stage embryonic chicken heart development. JOSA A 25, 3134–3143.

Davey, M.G., Paton, I.R., Yin, Y., Schmidt, M., Bangs, F.K., Morrice, D.R., Smith, T.G., Buxton, P., Stamataki, D., Tanaka, M., 2006. The chick talpid3 gene encodes a novel protein essential for Hedgehog signaling. Genes Dev. 20, 1365–1377.

D'Costa, S., Pardue, S.L., Petitte, J.N., 2001. Comparative development of avian primordial germ cells and production of germ line chimeras. Avian Poultry Biol. Rev. 12, 151–168.

Debby-Brafman, A., Burstyn-Cohen, T., Klar, A., Kalcheim, C., 1999. F-Spondin, expressed in somite regions avoided by neural crest cells, mediates inhibition of distinct somite domains to neural crest migration. Neuron 22, 475–488.

Deeming, D.C., 1989. Characteristics of unturned eggs: critical period, retarded embryonic growth and poor albumen utilisation. Br. Poultry Sci. 30, 239–247.

Deeming, D.C., 2009. The role of egg turning during incubation. Avian Biol. Res. 2, 67–71.

Delaney, M.E., 2004. Genetic variants for chick biology research: from breeds to mutants. Mech. Dev. 121, 1169–1177.

DeFouw, D.O., Rizzo, V.J., Steinfeld, R.N., Feinberg, R.N., 1989. Mapping of the microcirculation in the chick chorioallantoic membrane during normal angiogenesis. Microvasc. Res. 38, 136–147.

De Groef, B., Grommen, S.V.H., Darras, V.M., 2008. The chicken embryo as a model for developmental endocrinology: Development of the thyrotropic, corticotropic and somatotropic axes. Mol. Cell. Endocrinol. 293, 17–24.

DeHaan, R.L., 1959. Cardia bifida and the development of pacemaker function in the early chick heart. Dev. Biol. 1, 586–602.

DeHaan, R.L., 1965. Morphogenesis of the vertebrate heart. In: DeHaan, R.L., Ursprung, H., Holt (Eds.), Organogenesis. Rinehart and Winston, New York, pp. 377–419.

DeHaan, R.L., 1990. The embryonic origin of the heartbeat. In: Hurst, J.W. (Ed.), The Heart, seventh ed. McGraw-Hill, New York, pp. 72–77.

Denetclaw Jr., W.F., Berdougo, E., Venters, S.J., Ordahl, C.P., 2001. Morphogenetic cell movements in the middle region of the dermomyotome dorsomedial lip associated with patterning and growth of the primary epaxial myotome. Development 128, 1745–1755.

DeRuiter, M.C., Gittenberger-de-Groot, A.C., Poelmann, R.E., Van Iperen, L., Mentink, M.M., 1993. Development of the pharyngeal arch system related to the pulmonary and bronchial vessels in the avian embryo. With a concept on system–pulmonary collateral artery formation. Circulation 87, 1306–1309.

De Santa Barbara, P., Roberts, D.J., 2002. Tail gut endoderm and gut/genitourinary/tail development: a new tissue-specific role for Hoxa13. Development 129, 551–561.

Dessimoz, J., Opoka, R., Kordich, J.J., Grapin-Botton, A., Wells, J.M., 2006. FGF signaling is necessary for establishing gut tube domains along the anterior–posterior axis in vivo. Mech. Dev. 123, 42–55.

Dhouailly, D., Olivera-Martinez, I., Fliniaux, I., Missier, S., Viallet, J.P., Thelu, J., 2004. Skin field formation: morphogenetic events. Int. J. Dev. Biol. 48, 85–91.

Dias da Silva, M.R., Tiffin, N., Mima, T., Mikawa, T., Hyer, J., 2007. FGF-mediated induction of ciliary body tissue in the chick eye. Dev. Biol. 304, 272–285.

Diaz, C., Glover, J.C., Puelles, L., Bjaalic, J.G., 2003. The relationship between hodological and cytoarchitectonic organization in the vestibular complex of the 11-day chicken embryo. J. Comp. Neurol. 457, 87–105.

Diaz-Ruiz, C., Perez-Tomas, R., Cullere, X., Domingo, J., 1993. Immunohistochemical localization of transforming growth factor-alpha and epidermal growth factor-receptor in the mesonephros and metanephros of the chicken. Cell Tissue Res. 271, 3–8.

Dickinson, M.E., Selleck, M.A., McMahon, A.P., Bronner-Fraser, M., 1995. Dorsalization of the neural tube by the non-neural ectoderm. Development 121, 2099–2106.

Didier, E., Didier, P., Fargeix, N., Guillot, J., Thiery, J.P., 1990. Expression and distribution of carbohydrate sequences in chick germ cells; a comparative study with lectins and the NC-1/HNK-1 monoclonal antibody. Int. J. Dev. Biol. 34, 421–431.

Dieterlen-Lièvre, F., 1984. Emergence of intra-embryonic blood stem cells in the avian chimeras by means of monoclonal antibodies. Dev. Comp. Immunol. 3, 75–80.

Dieterlen-Lièvre, F., 1997. Intraembryonic hematopoietic stem cells. Hematol. Oncol. Clin. North Am. 11, 1149–1171.

Dieterlen-Lièvre, F., 2005. Commitment of hematopoietic stem cells in avian and mammalian embryos: an ongoing story. Int. J. Dev. Biol. 49, 125–130.

Dietrich, S., Schubert, F.R., Healy, C., Sharpe, P.T., Lumsden, A., 1998. Specification of the hypaxial musculature. Development 125, 2235–2249.

Dingerkus, G., Uhler, L., 1977. Enzyme clearing of alcian blue stained whole small vertebrates for demonstration of cartilage. Stain Technol. 52, 229–232.

Djonov, V.G., Galli, A.B., Burri, P.H., 2000. Intussusceptic arborization contributes to vascular tree formation in the chick chorio-allantoic membrane. Anat. Embryol. 202, 347–357.

Dockter, J.L., 2000. Sclerotome induction and differentiation. Curr. Topics Develop. Biol. 48, 77–127.

Dockter, J., Ordahl, C.P., 2000. Dorsoventral axis determination in the somites: a re-examination. Development 127, 2201–2206.

Dormann, D., Weijer, C.J., 2006. Imaging of cell migration. Embo. J. 25, 3480–3493.
Drushel, R.F., Caplan, A.I., 1991. Three-dimensional reconstruction and cross-sectional anatomy of the thigh musculature of the developing chick embryo *(Gallus gallus)*. J. Morph. 208, 293–309.
Dudley, J., 1942. The development of the ultimobranchial body of the fowl, *Gallus domesticus*. Am. J. Anat. 71, 65–97.
Dunn, B.E., 1991. Methods for shell-less and semi-shell-less culture of avian and reptilian embryos. In: Deeming, D.C., Ferguson, M.W.J. (Eds.), Egg Incubation: Its Effects on Embryonic Development in Birds and Reptiles. Cambridge University Press, pp. 409–418.
Dupin, E., Glavieux, C., Vaigot, P., Le Douarin, N.M., 2000. Endothelin3 induces the reversion of melanocytes to glia through a neural crest-derived glial-melanocytic progenitor. Proc. Natl. Acad. Sci. USA 97, 7882–7887.
Duval, M., 1889. Atlas d'Embryologie. Masson et Cie, Paris.
Easton, H.S., Bellairs, R., Lash, J.W., 1990. Is chemotaxis a factor in the migration of precardiac mesoderm in the chick? Anat. Emb. 181, 461–468.
Ebensperger, C., Wilting, J., Brand-Saberi, B., Mizutani, Y., Christ, B., Balling, R., Koseki, H., 1995. Pax-1, a regulator of sclerotome development is induced by notochord and floorplate signals in avian embryos. Anat. Emb. 191, 297–310.
Ede, D.A., 1964. Bird Structure: An Approach Through Evolution, Development and Function in the Fowl. Hutchinson Educational.
Egawa, C., Kameda, Y., 1995. Innervation of the chicken parathyroid glands; Immunohistochemical study with the Tu J1, galanin, VIP, substance P, CGRP and tyrosine hydroxylase antibodies. Anat. Embryol. 191, 445–450.
Eichmann, A., Yuan, L., Moyen, D., Lenoble, F., Pardanaud, L., Bréant, C., 2005. Vascular development: from precursor cells to branched arterial and venous networks. Int. J. Dev. Biol. 49, 259–267.
El-Ghali, N., Rabadi, M., Ezin, M., de Bellard, M.E., 2010. New methods for chick embryo manipulations. Microsc. Res. Tech. 73 (1), 58–66.
Ellestad, L.E., Saliba, J., Porter, T.E., 2011. Ontogenic characterization of gene expression in the developing neuroendocrine system of the chick. Gen. Comp. Endocrinol. 171, 82–93.
Erickson, C.A., Goins, T.L., 1995. Avian neural crest cells can migrate in the dorsolateral path only if they are specified as melanocytes. Development 121, 915–924.
Etches, R.J., 1996. Reproduction in Poultry. CAB International, Oxford.
Etches, R.J., Carsience, R.S., Clark, M.E., Fraser, R.A., Toner, A., Verrinder Gibbins, A.M., 1993. Chimeric chickens and their use in manipulation of the chicken genome. Poult. Sci. 72, 882–889.
Eyal-Giladi, H., 1991. The early development of the chick as an epigenetic process. Crit. Rev. Poult. Biol. 3, 143–146.
Eyal-Giladi, H., Fabian, B., 1980. Axis determination in uterine chick blastodiscs under changing spatial positions during the sensitive period of polarity. Dev. Biol. 77, 228–232.
Eyal-Giladi, H., Kochav, S., 1975. From cleavage to primitive streak formation; a complementary Normal table and a new look at the first stages of the development of the chick. I. General morphology. Dev. Biol. 49, 321–337.
Ezin, A.M., Fraser, S.E., Bronner-Fraser, M., 2009. Fate map and morphogenesis of presumptive neural crest and dorsal neural tube. Dev. Biol. 330, 221–236.
Fabian, B., Eyal-Giladi, H., 1981. A SEM study of cell shedding during the formation of the area pellucida in the chicken embryo. J. Embryol. Exp. Morph. 64, 11–22.
Fairman, C.L., Clagett-Dame, M., Lennon, V.A., Epstein, M.L., 1995. Appearance of neurons in the chick gut. Dev. Dyn. 204, 192–201.
Faraco, C.D., Vaz, S.A., Pastor, M.V., Erickson, C.A., 2001. Hyperpigmentation in the Silkie fowl correlates with abnormal migration of fate-restricted melanoblasts and loss of environmental barrier molecules. Dev. Dyn. 220, 215–225.
Fasenko, G.M., Robinson, F.E., Whelan, A.I., Kremeniuk, K.M., Walker, J.A., 2001. Prestorage incubation of long-term stored broiler breeder eggs: 1. Effects on hatchability. Poult. Sci. 80, 1406–1411.
Faucounau, N., Ichas, F., Stoll, R., Maraud, R., 1995. Action of testosterone on the estradiol-induced feminization of the male chick embryo. Anat. Embryol. 191, 377–379.
Fernandez-Teran, M., Ros, M.A., 2008. The apical ectodermal ridge: morphological aspects and signaling pathways. Int. J. Dev. Biol. 52, 857–871.
Filas, B.A., Varner, V.D., Voronov, D.A., Tabor, L.A., 2011. Tracking morphogenetic tissue deformations in the early chick embryo. J. Vis. Exp. 56, 3129.
Filla, M.B., Czirók, A., Zamir, E.A., Little, C.D., Cheuvront, T.J., Rongish, B.J., 2004. Dynamic imaging of cell, extracellular matrix, and tissue movements during avian vertebral axis patterning. Birth Defects Res. C. Embryo. Today 72, 267–276.
Fisher, J.R., Eakin, R.E., 1957. Nitrogen excretion in developing chick embryos. J. Embryol. Exp. Morph. 5, 215–224.
Fisher, M.A., Downie, H., Welton, M.C.M., Delgado, I., Bain, A., Planzer, T., Sherman, A., Sang, H., Tickle, C., 2011. Comparative analysis of 3D expression patterns of transcription factor genes and digital fate maps in the developing chick wing. PLoS One 6 (4), e18661.
Flamme, I., 1987. Edge cell migration in the extra-embryonic mesoderm of the chick embryo. Anat. Embryol. 176, 477–491.
Flynn, M.E., Pikalow, A.S., Kimmelman, R.S., Searls, R.L., 1991. The mechanism of cervical flexure formation in the chick. Anat. Embryol. 184, 411–420.
Foley, A., Skromme, I., Stern, C.D., 2000. Reconciling different models of forebrain induction and patterning: a dual role for the hypoblast. Development 127, 3839–3854.

Fontaine, J., Le Douarin, N.M., 1977. Analysis of endoderm formation in the chick blastoderm by the use of quail-chick chimeras. The problem of the neuroectodermal origin of the APUD series. J. Embryo. Exp. Morphol. 41, 208–222.

Francis-West, P.H., Tatla, T., Brickell, P.M., 1994. Expression patterns of the bone morphogenetic proteins Bmp-4 and Bmp-2 in the developing chick face suggest a role in outgrowth of the primordia. Dev. Dyn. 201, 168–178.

Franz-Odendaal, T.A., 2008. Toward understanding the development of scleral ossicles in the chicken, Gallus gallus. Dev. Dyn. 237, 3240–3251.

Freedman, S.L., Akuffo, V.G., Bakst, M.R., 2001. Evidence for the innervation of sperm storage tubules in the oviduct of the turkey *(Melleagri gallopavo)*. Reproduction 121, 809–814.

Freeman, B.M., Vince, M.A., 1974. Development of the Avian Embryo. Chapman and Hall, London.

Freund, R., Döfler, D., Popp, W., Wachtler, F., 1996. The metameric pattern of the head – does it exist? Anat. Embryol. 193, 73–80.

Froman, D., 2003. Deduction of a model for sperm storage in the oviduct of the domestic fowl (*Gallus domesticus*). Biol. Reprod. Org. 69, 248–253.

Fukuda, K., Yasugi, S., 2002. Versatile roles for sonic hedgehog in gut development. J. Gastroenterol. 37, 239–246.

Fukui, Y., 1988. Cell proliferation during bud formation of the quail uropygial gland. Dev. Growth Diff. 30, 501–514.

Fukui, Y., 1989. Cell proliferation in the quail uropygial gland during placode stage to lumen formation. Anat. Embryol. 179, 347–351.

Funayama, N., Sato, Y., Matsumoto, K., Ogura, T., Takahashi, Y., 1999. Coelom formation: binary decision of the lateral plate mesoderm is controlled by the ectoderm. Development 126, 129–138.

Gambaryan, S.P., 1992. Development of the metanephros in the chick: maturation of glomerular size and nephron size. Anat. Embryol. 185, 291–297.

Gammill, L.S., Bronner-Fraser, M., 2002. Genomic analysis of neural crest induction. Development 129, 5731–5741.

Gao, J., Yuan, F., Tang, X., Han, H., Sha, J., Yuan, J., Shao, Y., Jin, X., Liu, H., Rui, L., Li, Z., 2011. Contribution of blastoderm cells to Japanese quail (Coturnix coturnix japonica)-Peking duck (Anas platyrhynchos) chimeras. Anim. Sci. J. 82, 729–734.

Garcia-Martinez, V., Schoenwolf, G., 1992. Positional control of mesoderm movement and fate during avian gastrulation and neurulation. Dev. Dyn. 193, 249–256.

Garcia-Martinez, V., Schoenwolf, G.C., 1993. Primitive-streak origin of the cardiovascular system in avian embryos. Dev. Biol. 159, 706–719.

Garcia-Martinez, V., Alvarez, I.S., Schoenwolf, G.C., 1993. Locations of the ectodermal and neurectodermal subdivisions of the epiblast at stages 3 and 4 of avian gastrulation and neurulation. J. Exp. Zool. 267, 431–446.

Garda, A.L., Puelles, L., Rubenstein, J.L., Medina, L., 2002. Expression patterns of Wnt8b and Wnt7b in chicken embryogenic brain suggest a correlation with chicken forebrain patterning centers and morphogenesis. Neuroscience 113, 689–698.

Garic-Stankovic, A., Hernandez, M., Flentke, G.R., Zile, M.H., Smith, S.M., 2008. A ryanodine receptor-dependent Ca(i)(2+) asymmetry at Hensen's node mediates avian lateral identity. Development 135, 3271–3280.

Gasc, J.M., 1991. Distribution and regulation of progesterone receptor in the urinogenital tract of the chick embryo. An immunohistochemical study. Anat. Embryol. 183, 415–426.

George, L., Kasemeier-Kulesa, J., Nelson, B.R., Koyano-Nakagawa, N., Lefcort, F., 2010. Patterned assembly and neurogenesis in the chick dorsal root ganglion. J. Comp. Neurol. 518, 405–422.

Gerlach, L.M., Hutson, M.R., Germiller, J.A., Nguyen-L., Luu, D., Victor, J.C., Barald, K.F., 2000. Addition of BMP4 antagonist, noggin, disrupts avian inner ear development. Development 27, 45–54.

Gheri, G., Gheri-Bryk, S., 1987. Computerised morphometric analysis of the chick embryo ileum organogenesis. Z. Mikrosk. Anat. Forsch. 101, 1011–1022.

Gheri-Bryk, S., Gheri, G., Pacini, P., 1990. The development of the chick embryo gall bladder studied by scanning electron microscope. Anat. Anz. 171, 297–305.

Gheri, G., Bryk, S.G., Gloria, L., Audino, S., 1992. The development of the caeca in the chick embryo ileum organogenesis. Arch. Ital. Anat. Embryol. 97, 89–107.

Gheri-Bryk, S., Gheri, G., Sgambati, E., 1993. Computerised morphometric analysis of the chick embryo oesophagus. Arch. Ital. Anat. Embryol. 98, 1–11.

Gil, J., Murillo, N.L., Gimeno, M., 1992. Measurement of mechanical forces acting on the area pellucida of the early chick embryo. Anat. Histol. Embryol. 21, 160–174.

Gilbert, A.B., 1971. The egg: its physical and chemical aspects. In: Bell, D.J., Freeman, D.M. (Eds.), The Physiology of the Domestic Fowl, vol. 3. Academic Press, London, pp. 1379–1409.

Gilbert, S.F., 2000. Developmental Biology, sixth ed. Sinauer Associates, Sunderland. Mass, p. 749.

Ginsburg, M., 1997. Primordial germ cell development in avians. Poult. Sci. 76, 91–95.

Gleiberman, A.S., Fedtsova, N.G., Rosenfeld, M.G., 1999. Tissue interactions in the induction of anterior pituitary: role of the ventral diencephalons, mesenchyme, and notochord. Dev. Biol. 213, 340–353.

Glick, B., Olah, I., 1993. Bursal secretory dendritic-like cell: a microenvironment issue. Poult. Sci. 72, 1262–1266.

Goetinck, P.F., Sekellic, M.J., 1972. Observations on collagen synthesis, lattice formation and morphology of scaleless and normal embryonic skin. Dev. Biol. 28, 636–648.

Goldschneider, I., Barton, R.W., 1976. Development and differentiation of lymphocytes. In: Poste, G., Nicolson, G.L. (Eds.), The Cell Surface in Animal Embryogenesis and Development. North Holland, Amsterdam, pp. 599–695.

Goldstein, R.S., Avivi, C., Geffen, R., 1995. Initial axial level-dependent differences in size of avian dorsal root ganglia are imposed by the sclerotome. Dev. Biol. 168, 214–222.
Gomez, C., Pourquié, O., 2009. Developmental control of somite numbers in vertebrates. J. Exp. Zool. B. Mol. Dev. Evol. 312, 533–544.
Gomperts, M., Wylie, C., Heasman, J., 1994. Primordial germ cell migration. Ciba Found. Symp. 182, 121–134.
Gonzalez-Morán, M.G., 2011. Histological and stereological changes in growing and regressing chicken ovaries during development. Anat. Rec. 294, 893–904.
Gonzalez-Sanchez, A., Bader, D., 1990. *In vitro* analysis of cardiac progenitor cell differentiation. Dev. Biol. 139, 197–209.
Goodrum, G.R., Jacobson, A.G., 1981. Cephalic flexure formation in the chick embryo. J. Exp. Zool. 216, 399–408.
Gordon, J., Bennett, A.P., Blackburn, C.C., Manley, N.R., 2001. Gcm2 and Foxn1 mark early parathyroid- and thymus-specific domains in the developing third pharyngeal pouch. Mech. Dev. 103, 141–143.
Gräper, L., 1929. Die Methodik der stereokinematographischen Untersuchung der lebenden vitalfärbten Hühnerembryos. Arch. Entw. Mech. Org. 115, 523–543.
Grapin-Botton, A., 2005. Antero-posterior patterning of the vertebrate digestive tract: 40 years after Nicole Le Douarin's PhD thesis. Int. J. Dev. Biol. 49, 335–347.
Grapin-Botton, A., Majithia, A.R., Melton, D.A., 2001. Key events of pancreas formation are triggered in gut endoderm by ectopic expression of pancreatic regulatory genes. Genes Dev. 15, 444–454.
Graw, J., 2010. Eye development. Curr. Top. Dev. Biol. 90, 343–386.
Grenier, J., Teillet, M.A., Grifone, R., Kelly, R.G., Duprez, D., 2009. Relationship between neural crest cells and cranial mesoderm during head muscle development. PLoS One 4 (2), e4381.
Grevellec, A., Graham, A., Tucker, A.S., 2011. Shh signalling restricts the expression of Gcm2 and controls the position of the developing parathyroids. Dev. Biol. 353, 194–205.
Griffith, C.M., Sanders, E.J., 1991. Effects of extracellular matrix components on the differentiation of chick embryo tail bud mesenchyme in culture. Differentiation 47, 61–68.
Griffith, C.M., Wiley, M.J., Sanders, E.J., 1992. The vertebrate tail bud: three germ layers from one tissue. Anat. Embryol. 185, 101–113.
Grim, M., Halata, Z., 2000. Developmental origin of avian Merkel cells. Anat. Embryol. 202, 401–410.
Groenendijk-Huijbers, M.M., 1967. Experimental studies concerning the compensatory growth of the rudimantary right ovary of sinistrally castrated chick embryos. Verh. Anat. Ges. 62, 321–325.
Gros, J., Hugh, J.K., Vinegoni, C., Feruglio, P.F., Weissleder, R., Tabin, C.J., 2010. WNT5A/JNK and FGF/MAPK pathways regulate the cellular events shaping the vertebrate limb bud. Curr Biol. 20, 1993–2002.
Gruenwald, P., 1941. The relation of the growing tip of the Mullerian duct to the Wolffian duct and its importance for the genesis of malformations. Anat. Rec. 81, 1–19.
Guioli, S., Lovell-Badge, R., 2007a. PITX2 controls asymmetric gonadal development in both sexes of the chick and can rescue the degeneration of the right ovary. Development 134, 4199–4208.
Guioli, S., Lovell-Badge, R., 2007b. The origin of the Mullerian duct in chick and mouse. Dev. Biol. 302, 389–398.
Guioli, S., Nandi, S., Zhao, D., Burgess-Shannon, J., Lovell-Badge, R., Clinton, M., 2014. Gonadal asymmetry and sex determination in birds. Sex. Dev. published on-line: February 27, 2014.
Gumpel-Pinot, M., 1984. Muscle and skeleton of limbs and body wall. In: Le Douarin, N.L., McClaren, A. (Eds.), Chimeras in Developmental Biology. Academic Press, London, pp. 281–310.
Gunhaga, L., Jessell, T.M., Edlund, T., 2000. Sonic hedgehog signalling at gastrula stages specifies ventral telencephalic cells in the chick embryo. Development 127, 3283–3293.
Guzmán, L.V., Mayoral, P.V., Valencia, J.P., Pine, S.S., Gómez, C.S., 2010. Developmental pattern of the right atrioventricular septal valve leaflet and tendinous cords. Anat. Rec. Hoboken 293, 55–61.
Hacker, A., Guthrie, S., 1998. A distinct developmental programme for the cranial paraxial mesoderm in the chick embryo. Development 126, 3461–3472.
Halata, Z., Grim, M., 1993. Sensory nerve ending in the back skin of the Japanese quail. Anat. Embryol. 187, 131–138.
Halata, Z., Grim, M., Christ, B., 1990. Origin of spinal meninges, sheaths of peripheral nerves, and cutaneous receptors including Merkel cells. Anat. Embryol. 182, 529–537.
Hall, B.K., 1981. Specificity in the differentiation and morphogenesis of neural crest-derived scleral ossicles and of epithelial scleral papillae in the eye of the embryonic chick. J. Embryol. Exp. Morph. 66, 175–190.
Hall, B.K., 1999. The Neural Crest Development. Springer-Verlag, New York.
Hall, B.K., 2001. Development of the clavicles in birds and mammals. J. Exp. Zool. 289, 153–161.
Hall, B.K., Höstadius, S., 1988. The Neural Crest. Oxford University Press, London.
Hamburger, V., 1947. A Manual of Experimental Embryology. University of Chicago Press, Chicago, Ill.
Hamburger, V., Hamilton, H.L., 1951. A series of normal stages in the development of the chick embryo. J.Morph. 88, 49–92 (Reprinted 1992 Dev. Dyn. 195, 229-230.).
Han, L., Monné, M., Okumura, M., Schwend, T., Cherry, A.L., Flot, D., Matsuda, T., Jovine, L., 2010. Insights into egg coat assembly and egg-sperm interaction from the X-ray structure of full-length ZP3. Cell 143, 404–415.
Hardy, K.M., Garriock, R.J., Yatskievych, T.A., D'Agostino, S.L., Antin, P.B., Krieg, P.A., 2008. Non-canonical Wnt signaling through Wnt5a/b and a novel Wnt11 gene, Wnt11b, regulates cell migration during avian gastrulation. Dev. Biol. 320, 391–401.

Harfe, B.D., 2011. Keeping up with the zone of polarizing activity: new roles for an old signaling center. Dev. Dyn. 240, 915–919.
Harris, M.L., Erickson, C.A., 2007. Lineage specification in neural crest cell pathfinding. Dev. Dyn. 236, 1–19.
Harris, M.P., Fallon, J.F., Prum, R.O., 2002. Shh-Bmp2 signalling module and the evolutionary origin and diversification of feathers. J. Exp. Zool. 294, 160–176.
Harrison, T.A., Stadt, H.A., Kumiski, D., Kirby, M.L., 1995. Compensatory responses and development of nodose ganglion following ablation of placode precursors in the embryonic chick (Gallus domesticus). Cell Tissue Res. 281, 379–385.
Harrisson, F., Andries, L., Vakaet, L., 1988. The chicken blastoderm: current views on cell biological events guiding intercellular communication. Cell Differ. 22, 1–23.
Harvey, S., Johnson, C.D., Sanders, E.J., 2000. Extrapituitary growth hormone in peripheral tissues of early chick embryos. J. Endocrinol. 166, 489–502.
Hasson, P., 2011. 'Soft tissue' patterning: muscles and tendons of the limb take their form. Dev. Dyn. 240, 1100–1107.
Hatada, Y., Stern, C.D., 1994. A fate map of the epiblast of the early chick embryo. Development 120, 2879–2890.
Haworth, K.E., Healy, C., Morgan, P., Sharpe, P.T., 2004. Regionalisation of early head ectoderm is regulated by endoderm and prepatterns the orofacial epithelium. Development 131, 4797–4806.
Haworth, K.E., Wilson, J.M., Grevellec, A., Cobourne, M.T., Healy, C., Helms, J.A., Sharpe, P.T., Tucker, A.S., 2007. Sonic hedgehog in the pharyngeal endoderm controls arch pattern via regulation of FGF8 in head ectoderm. Dev. Biol. 303, 244–258.
Hebrock, M., Kim, S.K., Melton, D.A., 1998. Notochord repression of endodermal Sonic hedgehog permits pancreas development. Genes Dev. 12, 1705–1713.
Herzog, Y., Kalcheim, C., Kahane, N., Reshef, R., Neufeld, G., 2001. Differential expression of neuropilin-2 in arteries and veins. Mech. Dev. 109, 115–119.
Hilfer, S.R., 1964. Follicle formation in the embryonic chick thyroid. I. Early morphogenesis. J. Morph. 115, 135–151.
Hirakow, R., Hiruma, T., 1981. Scanning electron microscopic study on the development of primitive blood vessels in chick embryos at the early somite stage. Anat. Embryol. 163, 290–306.
Hirata, M., Hall, B.K., 2000. Temporospatial patterns of apoptosis in chick embryos during the morphogenetic period of development. Int. J. Dev. Biol. 44, 757–768.
Hirota, A., Kamino, K., Komuro, H., 1987. Mapping of early development of electrical activity in the embryonic chick heart using multiple-site optical recording. J. Physiol. 383, 711–728.
Hirsinger, E., Jouve, C., Malapert, P., Pourquié, O., 1998. Role of growth factors in shaping the developing somite. J. Mol. Cell Endocrinol. 25, 83–87.
Hiruma, T., Hirakow, R., 1985. An ultrastructural topographic study on myofibrillogenesis in the heart of the chick embryo during pulsation onset period. Anat. Embryol. 172, 325–329.
Hiruma, T., Hirakow, R., 1995. Formation of the pharyngeal arch arteries in the chick embryo. Observations of corrosion casts by scanning electron microscopy. Anat. Embryol. 191, 415–423.
Hiruma, T., Nakamura, H., 2003. Origin and development of the pronephros in the chick embryo. J. Anat. 203, 539–552.
Hofmann, C., Drossopoulou, G., McMahon, A., Balling, R., Tickle, C., 1998. Inhibitory action of BMPs on *Pax1* expression and on shoulder girdle formation during limb development. Dev. Dyn. 213, 199–206.
Höhn, E.O., 1961. Endocrine glands, thymus and pineal body. In: Marshall, A.J. (Ed.), Biology and Comparative Physiology of Birds. Academic Press, London, pp. 87–114.
Holm, L., Ekwall, H., Wishart, G.J., Ridderstrale, Y., 2000. Localization of calcium and zinc in the sperm storage tubules of chicken and turkey using X-ray microanalysis. J. Reprod. Fertil. 118, 331–336.
Horder, T.J., Witowski, J.A., Wylie, C.C. (Eds.), 1986. A History of Embryology. Cambridge University Press.
Horrocks, A.J., Stewart, S., Jackson, L., Wishart, G.J., 2000. Induction of acrosomal exocytosis in chicken spermatozoa by inner perivitelline-derived N-linked glycans. Biochem. Biophys. Res. 278, 84–89.
Hu, D., Marcucio, R.S., 2009a. Unique organization of the frontonasal ectodermal zone in birds and mammals. Dev. Biol. 325, 200–210.
Hu, D., Marcucio, R.S., 2009b. A SHH-responsive signaling center in the forebrain regulates craniofacial morphogenesis via the facial ectoderm. Development 136, 107–116.
Hu, D., Marcucio, R.S., Helms, J.A., 2003. A zone of frontonasal ectoderm regulates patterning and growth in the face. Development 130, 1749–1758.
Hu, N., Christensen, D.A., Agrawal, A.K., Beaumont, C., Clark, E.B., Hawkins, J.A., 2009. Dependence of aortic arch morphogenesis on intracardiac blood flow in the left atrial ligated chick embryo. Anat. Rec. 292, 652–660.
Huang, R., Brand-Saberi, B., Christ, B., 2000a. New experimental evidence for somite resegmentation. Anat. Embryol. 202, 195–200.
Huang, R., Christ, B., Patel, K., 2006. Regulation of scapula development. Anat. Embryol. Berl 211 (Suppl. 1), 65–71.
Huang, R., Lang, E.R., Otto, W.R., Christ, B., Patel, K., 2001. Molecular and cellular analysis of embryonic avian tongue development. Anat. Embryol. 204, 179–187.
Huang, R., Zhi, Q., Wilting, J., Christ, B., 1994. The fate of somitocoele cells in avian embryos. Anat. Embryol. 190, 243–250.
Huang, R., Zhi, Q., Izpisua-Belmonte, J.-C., Christ, B., Patel, K., 1999. Origin and development of the avian tongue muscles. Anat. Embryol. 200, 137–152.

Huang, R., Zhi, Q., Patel, K., Wilting, J., Christ, B., 2000b. Dual origin and segmental organisation of the avian scapula. Development 127, 378–394.
Huang, R., Zhi, Q., Patel, K., Wilting, J., Christ, B., 2000c. Contribution of single somites to the skeleton and muscles of the occipital and cervical regions in avian embryos. Anat. Embryol. 202, 375–383.
Huang, R., Zhi, Q., Schmidt, C., Wilting, J., Brand-Saberi, B., Christ, B., 2000d. Sclerotomal origin of the ribs. Development 127, 527–532.
Huang, R., Zhi, Q., Christ, B., 2003. The relationship between limb muscle and endothelial cells migrating from a single somite. Anat. Embryol. 206, 283–289.
Hughes, A.F.W., 1934. On the development of the blood vessels in the head of the chick. Phil. Trans. Roy. Soc. Lond. Ser. B 224, 75–129.
Hughes, A.F.W., 1937. Studies on the area vasculosa of the embryo chick. II The influence of the circulation on the diameter of the vessels. J. Anat. 72, 1–17.
Hume, C.R., Dodd, J., 1993. A novel Wnt gene with a potential role in primitive streak formation and hind-brain organization. Development 119, 1147–1160.
Hutson, J.M., Donahoe, P.K., 1984. Improved histology for chick-quail chimeras. Stain Technol. 59, 105–111.
Icardo, J.M., 1989. Changes in the endocardial cushion morphology during the development of the endocardial cushions. Anat. Embryol. 179, 443–448.
Icardo, J.M., 1990. Development of the outflow tract. A study of hearts with *situs solitus* and *situs inversus*. Ann. N.Y. Acad. Sci. 588, 26–40.
Iimura, T., Pourquié, O., 2008. Manipulation and electroporation of the avian segmental plate and somites in vitro. Methods Cell Biol. 87, 257–270.
Iimura, T., Yang, X., Weijer, C.J., Pourquié, O., 2007. Dual mode of paraxial mesoderm formation during chick gastrulation. Proc. Nat. Acad. Sci. USA 2007, 2744–2749.
Iimura, T., Denans, N., Pourquié, O., 2009. Establishment of Hox vertebral identities in the embryonic spine precursors. Curr. Top. Dev. Biol. 88, 201–234.
Inagaki, T., Garcia-Martinez, V., Schoenwolf, G.C., 1993. Regulative ability of the prospective cardiogenic and vasculogenic areas of the primitive streak during avian gastrulation. Dev. Dyn. 197, 57–68.
Ishimaru, Y., Komatsu, T., Kasahara, M., Katoh-Fukui, Y., Ogawa, H., Toyama, Y., Maekawa, M., Toshimori, K., Chandraratna, R.A.S., Morohashi, K.-I., Yoshioka, H., 2008. Mechanisms of asymmetric development in chick embryos. Development 135, 677–685.
Itasaki, N., Nakamura, H., Sumida, H., Yasuda, M., 1991. Actin bundles on the right side in the caudal part of the heart play a role in dextro-looping in the embryonic chick heart. Anat. Embryol. 183, 29–39.
Ito, K., Nakamura, H., Watanabe, Y., 2011. Protogenin mediates cell adhesion for ingression and re-epithelialization of paraxial mesodermal cells. Dev. Biol. 351, 13–24.
Izpisúa-Belmonte, J.C., De Robertis, E.M., Storey, K.G., Stern, C.D., 1993. The homeobox gene *goosecoid* and the origin of organizer cells in the early chick blastoderm. Cell 74, 645–659.
Jacob, H.J., Christ, B., 1978. Experimental investigations on the excretion apparatus of young chick embryos. XIXth Morphological Congress Symposia, Charles University, Prague. 219–35.
Jacob, M., Christ, B., Jacob, H.J., 1979. The migration of myogenic cells from the somites into the leg region of avian embryos. Anat. Embryol. 157, 291–309.
Jacob, M., Jacob, H.J., Wachtler, F., Christ, B., 1984. Ontogeny of avian extrinsic ocular muscles. I Light and electronmicroscopic study. Cell Tiss. Res. 234, 549–557.
Jacob, M., Konrad, K., Jacob, H.J., 1999. Early development of the Mullerian duct in avian embryos with reference to the human. An ultrastructural and immunohistochemical study. Cells Tissues Organs 164, 63–81.
Jacobson, A.G., Miyamoto, D.M., Mai, S.H., 1979. Rathke's pouch morphogenesis in the chick embryo. J. Exp. Zool. 207, 351–366.
Jaffredo, T., Bollerot, K., Sugiyama, D., Gautier, R., Drevon, C., 2005. Tracing the hemangioblast during embryogenesis: developmental relationships between endothelial and hematopoietic cells. Int. J. Dev. Biol. 49, 269–277.
James, R.G., Schultheiss, T.M., 2003. Patterning of the avian intermediate mesoderm by lateral plate and axial tissues. Dev. Biol. 253, 109–124.
Jarzem, J., Meier, S.P., 1987. A scanning electron microscope survey of the origin of the primordial pronephric duct cells in the avian embryo. Anat. Rec. 218, 175–181.
Jaskoll, T.F., Maderson, P.F., 1978. A histological study of the development of the avium middle ear and tympanum. Anat. Rec. 190, 177–199.
Jeffs, P., Osmond, M., 1992. A segmented pattern of cell death during development of the chick embryo. Anat. Embryol. 185, 589–598.
Jiang, T.-X., Tuan, T.L., Wu, P., Widelitz, R.B., Chuong, C.M., 2011. From buds to follicles: matrix metalloproteinases in developmental tissue remodeling during feather morphogenesis. Differentiation 81, 307–314.
Jin, E.J., Erickson, C.A., Takada, S., Burrus, L.W., 2001. Wnt and Bmp signalling govern lineage segregation of melanocytes in the avian embryo. Dev. Biol. 223, 22–37.
Jirkovská, M., Náprstková, I., Janáček, J., Kučera, T., Macášek, J., Karen, P., Kubínová, L., 2005. Three-dimensional reconstructions from non-deparaffinized tissue sections. Anat. Embryol. 210, 163–173.
Johnson, R.L., Tabin, C.J., 1997. Molecular models for vertebrate limb development. Cell 90, 979–990.
Johnston, S.D., Orgeig, S., Lopatko, O.V., Daniels, C.B., 2000. Development of the pulmonary surfactant system in two oviparous vertebrates. Am. J. Physiol. Regul. Integr. Comp. Physiol. 278, 486–493.
Jordanov, J., Georgiev, I., Boyadjieva-Mihailova, A., 1966. Physicochemical and electron microscopical investigations on the vitelline membrane of the hen's egg with a view to its permeability to macromolecules. C. R. Acad. Bulg. Sci. 19, 153–156.

Jourdeuil, K., Franz-Odendaal, T.A., 2012. Vasculogenesis and the induction of skeletogenic condensations in the vain eye. Anat. Rec. Adv. Integr Anatomy Evo. Biol. 295, 691–698.

Kagami, H., Clark, M.E., Verrinder Gibbins, A.M., Etches, R.J., 1995. Sexual differentiation of chimeric chickens containing ZZ and ZW cells in the germline. Mol. Reprod. Dev. 42, 379–387.

Kageyama, R., Masamizu, Y., Niwa, Y., 2007. Oscillator mechanism of notch pathway in the segmentation clock. Dev. Dyn. 236, 1403–1409.

Kajiwara, E., Shigeta, A., Horiuchi, H., Matsuda, H., Furusawa, S., 2003. Development of Peyer's patch and cecal tonsil in gut-associated lymphoid tissues in the chicken embryo. J. Vet. Med. Sci. 65, 607–614.

Kameda, Y., 1984. Ontogeny of chicken ultimobranchial glands studied by an immunoperoxidase method using calcitonin, somatostatin and 19S-thyroglobulin antisera. Anat. Embryol. 170, 139–144.

Kameda, Y., 1990. Ontogeny of the carotid body and glomus cells distributed in the wall of the common carotid artery and its branches in the chicken. Cell Tissue Res. 261, 525–537.

Kameda, Y., 1993. Electron microscopic study on the development of the chicken ultimobranchial glands, with special reference to the innervation of C-cells. Anat. Embryol. 188, 561–570.

Kameda, Y., Miura, M., Ohno, S., 2000. Expression of the common alpha-subunit mRNA of glycoprotein hormones during the chick pituitary organogenesis, with special reference to the pars tuberalis. Cell Tissue Res. 299, 71–80.

Kamei, C.N., Kempf, H., Yelin, R., Daoud, G., James, R.G., Lassar, A.B., Tabin, C.J., Schultheiss, T.M., 2011. Promotion of avian endothelial cell differentiation by GATA transcription factors. Dev. Biol. 353, 29–37.

Karabagli, H., Karabagli, P., Ladher, R.K., Schoenwolf, G.C., 2002. Comparison of the expression patterns of several fibroblast growth factors during chick gastrulation and neurulation. Anat. Embryol. 205, 365–370.

Karagenc, L., Cinnamon, Y., Ginsburg, M., Petitte, J.N., 1996. Origin of primordial germ cells in the prestreak chick embryo. Dev. Genet. 19, 290–301.

Kato, N., Ayoyama, H., 1998. Dermomyotomal origin of the ribs as revealed by extirpation and transplantation experiments in chick and quail embryos. Development 125, 3437–3443.

Katsu, K., Tatsumi, N., Niki, D., Yamamura, K., Yokouchi, Y., 2013. Multimodal effects on BMP signalling expression in the lateral plate mesoderm during left–right axis formation in the chick embryo. Dev. Biol. 374, 71–84.

Katsu, K., Tokumori, D., Tatsumi, N., Suzuki, A., Yokouchi, Y., 2011. BMP inhibition in Hensen's node is a critical step for the establishment of left–right asymmetry in the chick embryo. Dev. Biol. 363, 15–26.

Katsumoto, K., Fukuda, K., Kimura, W., Shimamura, K., Yasugi, S., Kume, S., 2009. Origin of pancreatic precursors in the chicken embryo and the mechanism of endoderm regionalization. Mech. Dev. 126, 539–551.

Kawakami, Y., Capadevilla, J., Buscher, D., Itoh, T., Esteban, C., Izpisua Belmonte, J.C., 2001. Wnt signals control FGF-dependent limb initiation and ART induction in the chick embryo. Cell 23, 891–900.

Keller, B.B., Hu, N., Clark, E.B., 1990. Correlation of ventricular area, perimeter, and conotruncal diameter with ventricular mass and function in the chick embryo from stages 12 to 24. Circ Res. 66, 109–114.

Kelly, R.G., Buckingham, M.E., 2002. The anterior heart-forming field: voyage to the arterial pole of the heart. Trends Genet. 18, 210–216.

Kent, J., Wheatley, S.C., Andrews, J.E., Sinclair, A.H., Koopman, P., 1996. A male-specific role for SOX9 in vertebrate sex determination. Development 122, 2813–2822.

Kerr, J.G., 1919. Text-Book of Embryology, with the Exception of Mammals, vol. 2, Vertebrata, Macmillan, London.

Kessel, J., Fabian, B.C., 1985. Graded morphogenetic patterns during the development of the extraembryonic blood system and coelom of the chick blastoderm: a scanning electron microscope and light microscope study. Amer. J. Anat. 173, 99–112.

Keyes, W.M., Sanders, E.J., 1999. Cell death in the endocardial cushions of the developing heart. J. Mol. Cell Cardiol. 31, 1015–1023.

Keyes, W.M., Logan, C., Parker, E., Sanders, E.J., 2003. Expression and function of bone morphogenetic proteins in the development of the embryonic endocardial cushions. Anat. Emb. 207, 135–147.

Keynes, R.J., Stern, C.D., 1984. Segmentation in the vertebrate nervous system. Nat. Lond. 310, 786–789.

Keynes, R.J., Stern, C.D., 1988. Mechanisms of vertebrate segmentation. Development 103, 413–429.

Khalil, M., Sultana, S.Z., Rahman, M., Mannan, S., Ahmed, S., Azra, Z.G., Sultana, Z.R., Chowdhurry, A.A., 2009. Study of prenatal and postnatal development of spleen of *Gallus domesticus* (deshi chicken). Mymensingh Med. J. 18, 169–174.

Khaner, O., 1995. The rotated hypoblast of the chicken embryo does not initiate an ectopic axis in the epiblast. Proc. Natl. Acad. Sci. USA 92, 10733–10737.

Khaner, O., 1998. The ability to initiate an axis in the avian blastula is concentrated mainly at a posterior site. Dev. Biol. 194, 256–266.

Kido, S., Janado, M., Nunoura, H., 1976. Macromolecular components of the vitelline membrane of hen's eggs. II Physicochemical properties of glycoprotein II. J. Biochem. 79, 1351–1356.

Kieny, M., Mauger, A., Sengel, P., 1972. Early regionalization of the somitic mesoderm as studied by the development of the axial skeleton of the chick embryo. Dev. Biol. 28, 142–161.

Kim, J.S., Min, J., Recknagel, A.K., Riccio, M., Butcher, J.T., 2011. Quantitative three-dimensional analysis of embryonic chick morphogenesis via microcomputed tomography. Anat. Rec. 294, 1–10.
Kimura, W., Yasugi, S., Stern, C.D., Fukuda, K., 2006. Fate and plasticity of the endoderm in the early chick embryo. Dev. Biol. 289, 283–295.
Kimura, W., Yasugi, S., Fukuda, K., 2007. Regional specification of the endoderm in the early chick embryo. Develop. Growth Differ. 49, 365–372.
King, A.S., McLelland, J., 1979. Form and Function in Birds, vol. 1. Academic Press, London.
King, A.S., McLelland, J., 1979–1989. Form and Function in Birds, 4 vols. Academic Press, London.
King, D.B., May, J.D., 1984. Thyroidal influence on body growth. J. Exp. Zool. 232, 453–460.
Kirby, M.L., 1990. Alteration of cardiogenesis after neural crest ablation. Ann. N.Y. Acad. Sci. 588, 289–295.
Kirby, M.L., Hutson, M.R., 2010. Factors controlling cardiac neural crest cell migration. Cell Adh Migr. 4, 609–621.
Kirunda, D.F., McKee, S.R., 2000. Relating quality characteristics of aged eggs and fresh eggs to vitelline membrane strength as determined by a texture analyser. Poultry Sci. 79, 1189–1193.
Knezevic, V., de Santo, R., Mackem, S., 1998. Continuing organizer function during chick tail development. Development 125, 1791–1801.
Knospe, C., Seichert, V., Rychter, Z., 1991. The topogenesis of the thyroid in chick embryos. Eur. J. Morphol. 29, 291–296.
Koda, I., Nakamura, H., Watanabe, Y., 2010. Protogenin mediates cell adhesion for ingression and re-epithelialization of paraxial mesodermal cells. Dev. Biol. 351, 13–24.
Kolesova, H., Roelink, H., Grim, M., 2008. Sonic hedgehog is required for the assembly and remodeling of branchial arch blood vessels. Dev. Dyn. 237, 1923–1934.
Kosaka, Y., Akimoto, Y., Obinata, A., Hirano, H., 2000. Localization of HB9 homeobox gene mRNA and protein during the early stages of chick feather development. Biochem. Biophys. Res. 276, 1112–1117.
Krull, C.E., 2004. A primer on using in ovo electroporation to analyze gene function. Dev. Dyn. 229, 433–439.
Krull, C.E., 2010. Neural crest cells and motor axons in avians. Cell Adh. Migr. 4, 631–634.
Kucera, P., Burnand, M.-B., 1987a. Routine teratogenicity test that uses chick embryos *in vitro*. Teratogen. Carcinogen. Mutagen. 7, 427–447.
Kucera, P., Burnand, M.B., 1987b. Mechanical tension and movement in the chick blastoderm as studied by real-time image analysis. J. Exp. Zool. (Suppl. 1), 329–339.
Kucera, P., Abriel, H., Katz, U., 1994. Ion transport across the early chick embryo: electrical measurements, ionic fluxes and regional heterogeneity. J. Membr. Biol. 141, 149–157.
Kulesa, P.M., 2004. Developmental Imaging: insights into the avian embryo. Birth Res. Defects Res. Part C Embryo Today: Rev. 72, 260–266.
Kulesa, P.M., Schnell, S., Rudloff, S., Baker, R., Maini, P.K., 2007. From segment to somite: segmentation to epithelialization analyzed within quantitative frameworks. Dev. Dyn. 236, 1392–1402.
Kulesa, P.M., Bailey, C.M., Cooper, C., Fraser, S.E., 2010. In ovo live imaging of avian embryos. Cold Spring Harb Protoc. 5446.
Kumar, M., Jordan, N., Melton, D., Grapin-Botton, A., 2003. Signals from lateral plate mesoderm instruct endoderm toward a pancreatic fate. Dev. Biol. 259, 109–122.
Kume, S., 2005. The molecular basis and prospects in pancreatic development. Dev. Growth Differentiation. 47, 367–374.
Kuo, B.R., Erickson, C.A., 2010. Regional differences in neural crest morphogenesis. Cell Adh. Migr. 4, 567–585.
Kuratani, S., Kirby, M.L., 1991. Initial migration and distribution of the cardiac neural crest in the avian embryo: an introduction to the concept of the circumpharyngeal crest. Am. J. Anat. 191, 215–227.
Kuratani, S., Tanaka, S., 1990. Peripheral development of the avian vagus nerve with special reference to the morphological innervation of heart and lung. Anat. Embryol. 182, 435–445.
Kuwana, T., Rogulska, T., 1999. Migratory mechanisms of chick primordial germ cells toward gonadal anlage. Cell Mol. Biol. Noisy-le-grand 45, 725–736.
Kuwana, T., Maeda-Suga, H., Fujimoto, T., 1986. Attraction of chick primordial germ cells by gonadal anlage in vitro. Anat. Rec. 215, 403–406.
Lambson, R., 1970. An electron microscopical study of the endodermal cells of the yolk sac of the chick during incubation and after hatching. Am. J. Anat. 129, 1–20.
Lance-Jones, C., 1988. The somitic level of origin of embryonic chick hindlimb muscles. Dev. Biol. 126, 394–407.
Lance-Jones, C., 1990. Pathfinding by motoneurons in the limb of the avian embryo. In: Le Douarin, N., Dierterlen-Lièvre, F., Smith, J. (Eds.), The Avian Model in Developmental Biology: From Organism to Genes. Editions du CNRS, Paris, pp. 129–138.
Landauer, W., 1967. The Hatchability of Chicken Eggs as influenced by Environment and Heredity. Monograph 1 (revised) of Storrs Agri. Dev. Station, Storrs, Conn.
Lapao, C., Gama, L.T., Soares, M.C., 1999. Effects of broiler breeder age and length of early storage on albumen characteristics and hatchability. Poultry Sci. 78, 640–645.
Lash, J.W., Seitz, A.W., Cheney, C.M., Ostrovsky, D., 1984. On the role of fibronectin during the compaction stage of somitogenesis in the chick embryo. J. Exp. Zool. 232, 197–206.
Lash, J.W., Linask, K.K., Yamada, K.M., 1987. Synthetic peptides that mimic the adhesion recognition signal of fibronectin. Differential effects on cell–cell and cell–substratum adhesion in embryonic chick cells. Dev. Biol. 123, 411–420.

Lash, J.W., Gosfield III, E., Ostrovsky, D., Bellairs, R., 1990. Migration of chick blastoderm under the vitelline membrane: the role of fibronectin. Dev. Biol. 139, 407–416.

Latter, G.V., Baggott, G.K., 1996. Effect of egg turning and fertility upon the sodium concentration of albumen of the Japanese quail. Br. Poult. Sci. 37, 301–308.

Lavial, F., Pain, B., 2010. Chicken embryonic stem cells as a non-mammalian embryonic stem cell model. (92010). Dev. Growth Diff. 52, 101–114.

Lawson, A., Schoenwolf, G.C., 2001. New insights into critical events of avian gastrulation. Anat. Embryol. 262, 238–252.

Lawson, A., Schoenwolf, G.C., 2003. Epiblast and primitive streak origins of the endoderm in the gastrulating chick embryo. Development 130, 3491–3501.

Le, A.C., Musil, L.S., 2001. FGF signalling in chick lens development. Dev. Biol. 233, 394–411.

Le, S.H., Fu, K.K., Hui, J.N., Richman, J.M., 2001. Noggin and retinoic acid transform the identity of avian facial prominences. Nat. Lond. 414, 909–912.

Le Douarin, N., 1969. Particularités du noyaux interphasique chez la caille japonaise (*Coturnic coturnix* japonica). Utilisation de ses particularitiés comme 'marquage biologique' dans les recherches sur les interactions tissulaires et les migrations cellulaires au cours de l'ontogenèse. Bull. Biol. Fr. Belg. 103, 435–452.

Le Douarin, N.M., 1988. On the origin of pancreatic endocrine cells. Cell 53, 169–171.

Le Douarin, N.M., 2001. Early neurogenesis in amniote vertebrates. Int. J. Dev. Biol. 45, 373–378.

Le Douarin, N.M., Jotereau, F.V., 1975. Tracing of cells of the avian thymus through embryonic life in interspecific chimeras. J. Exp. Med. 142, 17–40.

Le Douarin, N.M., Kalcheim, C., 1999. The Neural Crest, second ed. Cambridge University Press, Cambridge.

Le Douarin, N.M., Jotereau, F.V., Houssaint, E., Thiery, J.-P., 1984a. Primary lymphoid organ ontogeny in birds. In: Le Douarin, N., McLaren, A. (Eds.), Chimeras in Developmental Biology. Academic Press, London, pp. 179–216.

Le Douarin, N.M., Teillet, M.A., Fontaine-Perus, J., 1984b. Chimeras in the study of the peripheral nervous system in birds. In: Le Douarin, N.M., McClaren, A. (Eds.), Chimeras in Developmental Biology. Academic Press, London, pp. 313–352.

Le Douarin, N.B., Dieterlen-Lièvre, F., Creuzet, S., Teillet, M.A., 2008. Quail-chick transplantations. Methods Cell Biol. 87, 19–58.

Le Douarin, N.M., Couly, G., Creuzet, S.E., 2012. The neural crest is a powerful regulator of pre-otic brain development. Dev. Biol. 366, 74–82.

Lear, P.V., 1993. Nephrogenesis in the chick embryo. PhD Thesis. University of London.

Lee, S.H., Bédard, O., Buchtová, M., Fu, K., Richman, J.M., 2004. A new origin for the maxillary jaw. Dev. Biol. 276, 207–224.

Lee, J.Y., Lee, S.J., 2010. Hemodynamics of the omphalomesenteric arteries in stage 18 chicken embryos and 'flow-structure' relations for microcirculation. Microvascular Res. 80, 402–411.

Levin, M., 2005. Left–right asymmetry in embryonic development. Mech. Dev. 122, 3–25.

Levin, M., Johnson, R.L., Stern, C.D., Kuehn, M., Tabin, C., 1995. A molecular pathway determining left-right asymmetry in chick embryogenesis. Cell 82, 803–814.

Levin, M., Pagan, S., Roberts, D.J., Cooke, J., Kuehn, M.R., Tabin, C.J., 1997. Left/right patterning signals and the independent regulation of different aspects of situs in the chick embryo. Dev. Biol. 189, 57–67.

Levy, V., Khaner, O., 1998. Limited left-right cell migration across the midline of the gastrulating avian embryo. Dev. Genet. 23, 175–184.

Li, Z., Song, Y., Ma, Y., Wei, H., Liu, C., Huang, J., Wan, N., Sha, J., Sakurai, F., 2002. Influence of simulated microgravity on avian primordial germ cell migration and reproductive capacity. J. Exp. Zool. 292, 672–676.

Liang, J., Bok, J., W, D.K., 2010. Distinct contributions from the hindbrain and mesenchyme to inner ear morphogenesis. Dev. Biol. 337, 324–334.

Liem, K.F., Jessel, T.M., Briscoe, J., 2000. Regulation of the neural patterning activity of sonic hedgehog by secreted BMP inhibitors expressed by notochord and somites. Development 127, 4855–4866.

Lillie, F.R., 1952. Development of the Chick: An Introduction to Embryology. In: Hamilton, H.L. (Ed.), third ed. Henry Holt, New York.

Linask, K.K., Lash, J.W., 1986. Precardiac cell migration: fibronectin localization at mesoderm: endoderm interface during directional migration. Dev. Biol. 114, 87–101.

Liu, G.Q., Zhu, J.J., Wang, Z.Y., Jiang, X.P., Dafalla, M.M., 2008. Analysis of sperm storage ability using duration of fertility in hens. Br. Poult. Sc. 49, 770–775.

Locy, W.A., Larsell, O., 1916. The embryology of the bird's lung based on observations of the domestic fowl. Am. J. Anat. 19, 447–504. and 20, 1–44.

Lopez-Sanchez, C., Garcia-Martinez, V., Schoenwolf, G.C., 2001. Localization of cells of the prospective neural plate, heart and somites within the primitive streak and epiblast of avian embryos at intermediate primitive-streak stages. Cells Tissues Organs 169, 334–346.

Lopez-Sanchez, C., Garcia-Masa, N., Gaňan, C.M., Garcia-Martinez, V., 2009. Movement and commitment of primitive streak precardiac cells during cardiogenesis. Int. J. Dev. Biol. 53, 1445–1455.

Lough, J., Sugi, Y., 2000. Endoderm and heart development. Dev. Dyn. 217, 327–342.

Loveless, W., Bellairs, R., Thorpe, S.J., Page, M., Feizi, T., 1990. Developmental patterning of the carbohydrate antigen FC10.2 during early embryogenesis in the chick. Development 108, 97–106.

Lucas, A.M., Stettenheim, P.R., 1972. Avian Anatomy – Integument. 2 vols. U.S. Department of Agriculture.

Lumsden, A., 2004. Segmentation and compartition in the early avian hindbrain. Mech. Dev. 121, 1081–1088.
Lunn, J.S., Fishwick, K.J., Halley, P.A., Storey, K.G., 2007. A spatial and temporal map of FGF/Erk1/2 activity and response repertoise in the early chick embryo. Dev. Biol. 277, 536–552.
Lwigale, P., Schneider, A.A., 2008. Other chimeras: quail-duck and mouse-chick, second ed. In: Bronner-Fraser, M. (Ed.), Methods in Avian Embryology, vol. 87, pp. 59–74.
Maderson, P.F.A., 1985. Some developmental problems of the reptilian integument. In: Gans, C., Billett, F., Maderson, P.F.A. (Eds.), Biology of the Reptilia, vol. 14. Wiley, New York, pp. 523–598.
Mahler, G., Gould, R., Butcher, J., 2010. Isolation and culture of avian embryonic valvular progenitor cells. J. Vis. Exp. 44, 2159.
Mahowald, A.P., 1971. Polar granules of *Drosophila.* III The continuity of polar granules during the life cycle of *Drosophila*. J. Exp. Zool. 176, 329–343.
Maina, J.N., 2003. Developmental dynamics of the bronchial (airway) and air/sac systems of the avian respiratory system from day 3 to day 26 of life: a scanning electron microscopic study of the domestic fowl, *Gallus gallus* variant domesticus. Anat. Embryol. 2007, 119–134.
Makanya, A.N., Djonov, V., 2008. Development and spatial organization of the air conduits in the lung of the domestic fowl, *Gallus gallus* variant domesticus. Microsc. Res. Tech. 71, 689–702.
Makanaya, A.N., Djonov, V., 2009. Parabranchial angioarchitecture in developing and adult chickens. J. Applied Physiol. 106, 1959–1969.
Makanaya, A.N., Stauffer, D., Ribatt, D., Burri, P.H., Djonov, V., 2005. Microsc. Res. Tech. 66, 275–288.
Malashichev, Y., Christ, B., Pröls, F., 2008. Avian pelvis originates from lateral plate mesoderm and its development requires signals from both ectoderm and paraxial mesoderm. Cell Tissue Res. 331, 595–604.
Malago Jr., W., Franco, H.M., Matheucci Jr., E., Medaglia, A., Henrique-Silva, F., 2002. Large scale sex typing of ostriches using DNA extracted from feathers. BMC Biotechnol. 2, 19.
Mandler, M., Neubüser, A., 2004. FGF signaling is required for initiation of feather placode development. Development 131, 3333–3343.
Männer, J., 1993. Experimental study on the formation of the epicardium in chick embryos. Anat. Embryol. 187, 281–289.
Männer, J., 2000. Cardiac looping in the chick embryo: a morphological review with special reference to terminological and biomechanical aspects of the looping process. Anat. Rec. 259, 248–262.
Männer, J., 2009. The anatomy of cardiac looping: a step towards the understanding of the morphogenesis of several forms of congenital malformations. Clin. Anat. 22, 21–35.
Männer, J., Merkel, N. 2007. Early morphogenesis of the sinuatrial region of the chick heart. A contribution to the understanding of the pathogenesis of direct pulmonary venous connections to the right atrium and atrial septal defects with right isomerism of the atrial appendages. Anat Rec. 290, 168–180.
Männer, J., Seidl, W., Steding, G., 1989. The role of extracardiac factors in normal and abnormal development of the chick embryo heart: cranial flexures and ventral thoracic wall. Anat. Embryol. 191, 61–72.
Männer, J., Seidl, W., Steding, G., 1993. Correlation between embryonic head flexures and cardiac development. An experimental study in chick embryos. Anat. Embryol. 188, 269–285.
Männer, J., Perez-Pomares, J.M., Macias, D., Muñoz-Chápuli, R., 2001. The origin, formation and developmental significance of the epicardium: a review. Cells Tissues Organs 169, 69–103.
Mareel, M., Bellairs, R., De Bruyne, G., Van Peteghem, M.C., 1984. Effect of microtubule inhibitors on the expansion of hypoblast and margin of over-growth of chick blastoderms. J. Embryol. Exp. Morph. 81, 273–286.
Martin, C., 1971. Contribution du canal de Wolff et de ses dérivés à l'édification des tubed urinaires du mésonéphros chez l'embryon d'oiseaux. C. R. Acad. Sc. Paris, série D 272, 1305–1307.
Martin, C., 1972. Technique d'explantation *in ovo* blastodermes d'embryons d'oiseaux. C.R. Soc. Biol. 116, 283.
Martin, C., 1990. Quail chick chimeras, a tool for developmental immunology. In: Le Douarin, N., Dieterlen-Lièvre, F., Smith, J. (Eds.), The Avian Model in Developmental Biology: From Organisms to Genes, pp. 207–217(Editions du CNRS), Paris.
Marvin, M.J., Di Rocco, G., Gardiner, A., Bush, S.M., Lassar, A.B., 2001. Inhibition of Wnt activity induces heart formation from posterior mesoderm. Genes Dev. 15, 316–327.
Matsumoto, K., Miki, R., Nakayama, M., Tatsumi, N., Yokouchi, Y., 2008. Wnt9a secreted from the walls of hepatic sinusoids is essential for morphogenesis, proliferation, and glycogen accumulation of chick hepatic epithelium. Dev. Biol. 319, 234–247.
Matsuda, S., Baluk, P., Shimizu, D., Fujiwara, F., 1996. Dorsal root ganglion neuron development in chick and rat. Anat. Embryol. 193, 475–480.
Matsushita, S., 1995. Fate mapping study of the splanchnopleural mesoderm of the 1.5-day-old chick embryo. Roux's Arch. Dev. Biol. 204, 392–399.
Matsushita, S., 1996. Fate mapping study of the endoderm of the 1.5-day-old chick embryo. Roux's Arch. Dev. Biol. 205, 225–231.
Matsushita, S., 1998. Developmental changes in mucosubstances revealed by immunostaining with antimucus monoclonal antibodies and lectin staining in the epithelium lining the segment from gizzard to duodenum of the chick embryo. J. Anat. 193, 587–597.
Matsushita, S., 1999. Fate mapping study of the endoderm in the posterior part of the 1.5-day-old chick embryo. Develop. Growth Differ. 41, 313–319.

Matsushita, S., Ishii, Y., Scotting, P.J., Kuroiwa, A., Yasugi, S., 2002. Pregut endoderm of chick embryos is regionalised by 1.5 days of development. Dev. Dyn. 223, 33–47.
Matulionis, D.H., 1970. Morphology of the down feathers of chick embryos. A descriptive study at the ultrastructural level of differentiation and keratinization. Z. Anat. Entw. 132, 107–157.
Mauch, T.J., Yang, G., Wright, M., Smith, D., Schoenwolf, G.C., 2000. Signals from trunk paraxial mesoderm induce pronephros formation in chick imtermediate mesoderm. Dev. Biol. 220, 62–75.
Mayer, A.W., 1939. The Rise of Embryology. Stamford University Press.
Mayerson, P.L., Fallon, J.F., 1985. The spatial pattern and temporal sequence in which feather germs arise in the White Leghorn chick embryo. Dev. Biol. 109, 259–267.
McCabe, K.L., Bronner-Fraser, M., 2009. Molecular and tissue interactions governing induction of cranial ectodermal placodes. Dev. Biol. 332, 189–195.
McCann, J.P., Owens, P.D.A., Wilson, D.J., 1991. Chick frontonasal process excision significantly affects midfacial development. Anat. Embryol. 184, 171–178.
McGonnell, I.M., Clarke, J.D.W., Tickle, C., 1998. Fate map of the developing chick face: analysis of expansion of facial primordia and establishment of the primary palate. Dev. Dyn. 212, 102–118.
McGonnell, I.M., McKay, I.J., Graham, A., 2001. A population of caudally migrating cranial neural crest cells: functional and evolutionary implications. Dev. Biol. 236, 354–363.
McGrew, M.J., Sherman, A., Lillico, S.G., Ellard, F.M., Radcliffe, P.A., Gilhooley, H.J., Mitrophanous, K.A., Cambray, N., Wilson, V., Sang, H., 2008. Localised axial progenitor cell populations in the avian tail bud are not committed to a posterior Hox identity. Development 155, 2289–2299.
McLaren, A., 1981. Germ cell lineages. In: Chimeras in Developmental Biology. Academic Press, London, pp. 111–129.
McLelland, J., 1979. Digestive system. In: King, A.S., McLelland, J. (Eds.), Form and Function in Birds, vol. 1. Academic Press, London, pp. 69–181.
McLelland, J., King, A.S., 1970. The gross anatomy of the peritoneal coelomic cavities of *Gallus domesticus*. Anat. Anz. 127, 480–490.
McLelland, J., King, A.S., 1975. Aves coelomic cavities and mesenteries. In: Getty, R. (Ed.), Sisson and Grossman's 'The Anatomy of the Domestic Animals'. W.B. Saunders, Philadelphia, London, Toronto, pp. 1849–1856.
McNabb, F.M.A., 2006. Avian thyroid development and adaptive plasticity. Gen. Comp. Endocrinol. 147, 93–101.
Meier, S., 1979. Development of the chick mesoblast. Formation of the embryonic axis and establishment of the metameric pattern. Dev. Biol. 73, 25–45.
Meier, S., 1981. Development of the chick embryo mesoblast: morphogenesis of the prechordal plate and cranial segments. Dev. Biol. 83, 49–61.
Mekki-Dauriac, S., Agius, E., Kan, P., Cochard, P., 2002. Bone morphogenetic proteins negatively coat oligodendrocyte precursor specification in the chick spinal cord. Development 129, 5117–5130.
Méndez, M.C., Ramirez, M., Varela, A.R., Chavez, B., Pedernera, E., 2003. Follicle-stimulating hormone increases cell proliferation in the ovary and the testis of the chick embryo. Gen. Comp. Endocrinol. 133, 181–188.
Menna, T.M., Mortola, J.P., 2002. Metabolic control of pulmonary ventilation in developing chick embryo. Respir. Physiol. Neurobiol. 130, 43–55.
Menon, G.K., Aggarwal, S.K., Lukas, A.M., 1981. Evidence for the holocrine nature of lipoid secretion by avian epidermal cells: a histochemical and ultra-structural study of rictus and the uropygial gland. J. Morphol. 167, 185–199.
Merido-Velasco, J.A., Sanchez-Montesinos, I., Espin, J., Garcia-Garcia, J.D., Roldan-Schilling, V., 1996. Grafts of the third branchial arch in chick embryo. Acta Anat. Basel 155, 73–80.
Merino, R., Gavan, Y., Macias, D., Economides, A.N., Sampath, K.T., Hurle, J.M., 1999a. Morphogenesis of digits in the avian limb is controlled by FGFs, TGFβs and noggin through BMP signalling. Dev. Biol. 200, 35–45.
Merino, R., Macias, D., Ganan, Y., Rodriguez-Leon, J., Economides, A.N., Rodriguez-Esteban, C., Izpisua-Belmonte, J.C., Hurle, J.M., 1999b. Control of digit formation by activin signalling. Development 126, 2161–2170.
Metzger, R., Wachowiak, R., Kluth, D., 2011. Embryology of the early foregut. Semin. Pediatr. Surg. 20, 136–144.
Meyer, D.B., 1964. The migration of the primordial germ cells in the chick embryo. Dev. Biol. 10, 154–190.
Michaille, J.J., Kanzler, B., Blanchet, S., Garnier, J.M., Dhouailly, D., 1995. Characterization of cDNAs encoding two chick retinoic acid receptor alpha isoforms and distribution of retinoic acid receptor alpha, beta and gamma transcripts during chick skin development. Int. J. Dev. Biol. 39, 587–596.
Milgrom-Hoffman, M., Harrelson, Z., Ferrarer, N., Zelzer, E., Evans, S.M., Tzahor, E., 2011. The heart endocardium is derived from vascular endothelial progenitors. Development 138, 4777–4787.
Miller, A.M., 1903. The development of the postcaval vein in birds. Am. J. Anat. 2, 283–298.
Miller, S.A., 1982. Differential proliferation in morphogenesis of lateral body folds. J. Exp. Zool. 221, 205–211.
Miller, S.A., Briglin, A., 1996. Apoptosis removes chick embryo tail gut and remnant of the primitive streak. Dev. Dyn. 206, 212–218.
Miller, S.A., Bresee, K.L., Michaelson, C.L., Tyrell, D.A., 1994. Domains of differential cell proliferation and formation of amnion folds in chick embryo ectoderm. Anat. Rec. 238, 225–236.
Mills, C.L., Bellairs, R., 1989. Mitosis and cell death in the tail of the chick embryo. Anat. Embryol. 180, 301–308.

Mills, C.L., Ariyo, O., Yamada, K.M., Lash, J.W., Bellairs, R., 1990. Evidence for the involvement of receptors for fibronectin in the promotion of chick til segmentation. Anat. Embryol. 182, 425–434.
Mitrani, E., 1982. Primitive streak-forming cells of the chick invaginate through a basement membrane. Wilhelm Roux's Arch. 191, 320–324.
Mittapalli, V.R., Huang, R., Patel, K., Christ, B., Scaal, M., 2005. Arthrotome: a specific joint forming compartment in the avian somite. Dev. Dyn. 234, 48–53.
Mjaatvedt, C.H., Nakoaka, T., Moreno-Rodriguez, R., Norris, R.A., Kern, M.J., Eisenberg, C.A., Turner, D., Markwald, R.R., 2001. The outflow tract of the heart is recruited from a novel heart-forming area. Dev. Biol. 238, 97–109.
Mobbs, I.G., McMillan, D.B., 1981. Transport across endodermal cells of the chick yolk sac during early stages of development. Am. J. Anat. 160, 285–308.
Monnet-Tschudi, F., Kucera, P., 1988. Myosin, tubulin and laminin immunoreactivity in the ectoderm of the growing area opaca of the chick embryo. Anat. Embryol. 179, 157–164.
Monsoro-Burq, A.H., Bontoux, M., Teillet, M.A., Le Douarin, N.M., 1994. Heterogeneity in the development of the vertebra. Proc. Natl. Acad. Sci. USA 91, 10435–10439.
Moore, M.A.S., 2004. The role of cell migration in the ontogeny of the lymphoid system. Stem Cells Dev. 13, 1–21.
Morais da Silva, S., Hacker, A., Harley, V., Goodfellow, P., Swain, A., Lovell-Badge, R., 1996. *Sox9* expression during gonadal development implies a conserved role for the gene in testis differentiation in mammals and birds. Nat. Genet. 14, 62–68.
Moran Jr, E.T., 2007. Nutrition of the developing embryo and hatchling. Poult. Sci. 86, 1043–1049.
Moro-Balbás, J.A., Gato, A., Alonso, M.I., Martin, P., de la Mano, A., 2000. Basal heparan sulphate proteoglycan is involved in otic invagination in chick embryos. Anat. Embryol. 202, 333–343.
Moury, J.D., Schoenwolf, G.C., 1995. Cooperative model of epithelial shaping and bending during avian neurulation: autonomous movements of the neural plate, autonomous movements of the epidermis, and interactions in the neural plate/epidermis transition zone. Dev. Dyn. 204, 323–337.
Müller, E., Schneider, M., Rickenbacher, J., 1983. Metabolic pathways in chick amnion muscle. Acta Anat. 115, 272–281.
Münsterberg, A., Yue, Q., 2008. Cardiac progenitor migration and specification. Cell Adhes. Migration. 2, 74–76.
Muroyama, Y., Fujihara, M., Ikeya, M., Kondoh, Takada, S., 2002. Wnt signalling plays an essential role in neuronal specification of the dorsal spinal cord. Genes Dev. 16, 548–553.
Murray, B.M., Wilson, D.J., 1994. A scanning electron microscopic study of the normal development of the chick wing from stages 19–36. Anat. Embryol. 89, 147–158.
Murillo, G.L., Gimeno, M., 1992. Measurement of mechanical forces acting on the area pellucida of the early chick embryo. Anat. Histol. Embryol. 21, 160–174.
Nacher, V., Carretero, A., Navarro, M., Armengol, C., Liombart, C., Rodruigez, A., Herrero-Fresneda, I., Avuso, E., Ruberts, J., 2006. The quail mesonephros: a new model for renal senescence? J. Vasc. Res. 43, 581–586.
Nafstad, P.H.J., 1986. On the avian Merkel cells. J. Anat. 145, 25–33.
Nagai, H., Sheng, G., 2008. Definitive erythropoiesis in chicken yolk sac. Dev. Dyn. 237, 3332–3341.
Nagy, N., Oláh, I., 2010. Experimental evidence for the ectoderal origin of the epithelial anlage of the chicken bursa of Fabricius. Development 137, 3019–3023.
Nagy, N., Magyar, M., Tóthy, M., Oláh, I., 2004. Origin of the bursal secretory dendritic cell. Anat. Emb. 208, 99–107.
Naito, M., Nirasawa, K., Oishi, T., 1991a. Development in culture of the chick embryo from fertilized ovum to hatching. J. Exp. Zool. 254, 322–326.
Naito, M., Watanabe, M., Kinutani, M., Nirasawa, K., Oishi, T., 1991b. Production of quail-chick chimaeras by blastoderm cell transfer. Br. Poult. Sci. 32, 79–86.
Nakabayashi, O., Kikuchi, H., Kikuchi, T., Mizuno, S., 1998. Differential expression of genes for aromatase and oestrogen receptor during gonadal development in chicken embryos. J. Mol. Endocrinol. 20, 193–202.
Nakamura, Y., Kagami, H., Tagami, T., 2013. Development, differentiation and manipulation of chicken germ cells. Dev. Growth Differ. 55, 20–40.
Nakamura, A., Kulikowski, R.R., Lacktis, J.W., Manasek, D.M.D., 1980. Heart looping: a regulated response to deforming forces. In: Van Pragh, R. (Ed.), Etiology and Morphogenesis of Congenital Heart Disease. Futura, New York, pp. 81–98.
Nakamura, Y., Yamamoto, Y., Usui, F., Mushika, T., Ono, T., Setioko, A.R., Takeda, K., Nirasawa, K., Kagami, H., Tagami, T., 2007. Migration and proliferation of primordial germ cells in the early chick embryo. Poultry Sci. 86, 2182–2193.
Nakaya, Y., Sheng, G., 2009. An amicable separation. Chick's way of doing EMT. Cell Adh. Migr. 3, 160–163.
Nakaya, Y., Sukowati, E.W., Alev, C., Nakazawa, F., Sheng, G., 2011. Involvement of *dystroglycan* in epithelial-mesenchymal transition during chick gastrulation. Cells, Tissues, Organs 193, 64–73. *Blood* 108, 3335-43.
Nakazawa, F., Alev, C., Jakt, L.M., Sheng, G., 2011. Yolk sac endoderm is the major source of serum proteins and lipids and is involved in the regulation of vascular integrity in early chick development. Dev. Dyn. 240, 2002–2010.
Nakazawa, F., Nagai, H., Shin, M., Sheng, G., 2006. Negative regulation of primitive hematopoiesis by the FGF signaling pathway. Blood 108, 3335.

Narabara, K., Abe, A., Gerilechaogetu, Hanieh, H., Kondo, Y., 2009. B cell differentiation in the bursa of Fabricius and spleen of embryos and chicks immediately after hatching. Animal Sc. J. 80, 669–677.

Narita, T., Saitoh, K., Kameda, T., Kuroiwa, A., Mizutani, M., Koike, C., Iba, H., Yasugi, S., 2000. BMPs are necessary for stomach gland formation in the chick embryo: a study using virally induced NMP-2 and noggin expression. Development 127, 981–988.

Nechaeva, M.V., Turpaev, T.M., 2002. Rhythmic contractions in chick amnio-yolk sac and snake amnion during embryogenesis. Comp. Biochem. Physiol. A. Mol. Integr. Physiol. 131, 861–870.

Needham, J., 1934. A History of Embryology, second ed. Cambridge University Press.

Nellemann, C., de Bellard, M.E., Barembaum, M., Laufer, E., Bronner-Fraser, M., 2001. Excess lunatic fringe causes cranial neural crest over-proliferation. Dev. Biol. 235, 121–130.

Neves, H., Dupin, E., Parreira, L., Le Douarin, N.L., 2012. Modulation of BMP4 signalling in the epithelial-mesenchymal interactions that take place in early thymus and parathyroid development in avian embryos. Dev. Biol. 361, 208–219.

New, D.A.T., 1955. A new technique for the cultivation of the chick embryo *in vitro*. J. Embryol. Exp. Morph. 3, 326–331.

New, D.A.T., 1956. The formation of sub-blastodermic fluid in hens' eggs. J. Embryol. Exp. Morph. 4, 221–227.

New, D.A.T., 1959. The adhesive properties and expansion of the chick blastoderm. J. Embryol. Exp. Morph. 7, 146–164.

New, D.A.T., 1966. The Culture of Avian Embryos. Logos Press, London.

Newgreen, D.F., Scheel, M., Kaster, V., 1986. Morphogenesis of sclerotome and neural crest cells in avian embryos. In vivo and in vitro studies on the role of notochordal extracellular material. Cell Tiss. Res. 244, 299–313.

Newman, H.H., 1917. The Biology of Twins. University of Chicago Press. Ill.

Nicolet, G., Gallera, J., 1963. Dans quelles conditions l'amnios de l'embryon de poulet peut-il se former en culture *in vitro?* Experientia 19, 165–166.

Niedorf, H.R., Wolters, B., 1978. Development of the Harderian gland in the chicken: light and electron microscopic investigations. Invest. Cell Pathol. 1, 205–215.

Nieuwkoop, P.D., Satasurya, L.A., 1979. Primordial Germ Cells in the Chordates. Cambridge University Press.

Noden, D.M., 1983a. The embryonic origins of avian cephalic and cervical muscles and associated connective tissues. Am. J. Anat. 168, 257–276.

Noden, D.M., 1983b. The role of the neural crest in patterning of avian cranial, skeletal, connective and muscle tissue. Dev. Biol. 96, 144–165.

Noden, D.M., 1986. Patterning of avian craniofacial muscles. Dev. Biol. 116, 347–356.

Noden, D.M., 1987. Interactions between cephalic neural crest and mesodermal populations. In: Maderson, P.F.A. (Ed.), Developmental and Evolutionary Aspects of the Neural Crest. Wiley, New York, pp. 89–119.

Noden, D.W., 1988. Interactions and fates of craniofacial mesenchyme. Development 103, 121–140.

Noden, D.W., 1990. Origin and assembly of avian embryonic blood vessels. Ann. N.Y. Acad. Sci. 588, 236–249.

Noden, D.M., 1992. Morphogenetic movements of avian prechordal mesoderm. Anat. Rec. 232, 65a.

Noden, D.M., DeLahunta, A., 1985. The Embryology of Domestic Animals: Devlopmental Mechanisms and Malformations. Williams and Wilkins, Baltimore.

Noden, D.M., Marcucio, R., Borycki, A.G., Emerson Jr, C.P., 1999. Differentiation of avian craniofacial muscles: 1. Patterns of early regulatory gene expression and myosin heavy chain synthesis. Dev. Dyn. 216, 96–112.

Noden, D.M., Trainor, P.A., 2005. Relations and interactions between cranial mesoderm and neural crest populations. J. Anat. 207, 575–601.

Noveen, A., Jiang, T.X., Ting-Bereth, S.A., Chuong, C.M., 1995. Homeobox genes Msx-1 and Msx-2 are associated with the induction and growth of skin appendages. J. Invest. Dermatol. 104, 711–719.

Nowicki, J.L., Burke, A.C., 1999. Testing *Hox* genes by surgical manipulation. Dev. Biol. 210, 228.

Noy, Y., Sklan, D., 1998. Yolk utilisation in the newly hatched poult. Br. Poult. Sci. 39, 446–451.

Ohashi, H., Takewaki, T., Uno, T., Komori, S., 1993. Development of vagal innervation to the muscles of the avian gizzard. J. Auton. Nerv. Syst. 42, 233–240.

Okaba, M., Graham, A., 2004. The origin of the parathyroid gland. P. N. A. S. 101, 17716–17719.

Ohta, K., Lupo, G., Kuriyama, S., Keynes, R., Holt, C.E., Harris, W.A., Tanaka, H., Ohnuma, S., 2004. Tsukushi functions as an organizer inducer by inhibition of BMP activity in cooperation with chordin. Dev. Cell 7, 347–358.

Ohta, S., Suzuki, K., Tachibana, K., Tanaka, H., Yamada, G., 2007. Cessation of gastrulation is mediated by suppression of epithelial-mesenchymal transition at the ventral ectodermal ridge. Development 134, 4315–4324.

Ohta, S., Schoenwolf, G.C., Yamada, G., 2010. The cessation of gastrulation; BMP signalling and EMT during and at the end of gastrulation. Cell Adhes. Migration 43, 440–446.

Oldfield, S.F., Evans, D.J.R., 2003. Tendon morphogenesis in the developing avian limb: plasticity of fetal tendon fibroblasts. J. Anat. 202, 153–164.

Olivera-Martinez, I., Coltey, M., Dhouailly, D., Pourquié, O., 2000. Mediolateral somitic origin of ribs and dermis determined by quail-chick chimeras. Development 127, 4611–4617.

Olivera-Martinez, I., Thelu, J., Teillet, M.A., Dhouailly, D., 2001. Dorsal dermis development depends on a signal from the dorsal neural tube which can be substituted by Wnt-1. Mech. Dev. 100, 233–244.

Olsen, M.W., 1962. Polyembryony in unfertilized turkey eggs. J. Hered. 53, 125–129.

Olsson, J.E., Kamachi, Y., Penning, S., Muscat, G.E., Kondoh, H., Koopman, P., 2001. Sox18 expression in blood vessels and feathers during chicken embryogenesis. Gene 271, 151–158.
Olszanska, B., Stepinska, U., 2008. Molecular aspects of avian oogenesis and fertilization. Int. J. Dev. Biol. 52 (2), 187–194.
Ooi, V.E.C., Sanders, E.J., Bellairs, R., 1986. The contribution of the primitive streak to the somites in the avian embryo. J. Embryol. Exp. Morph. 92, 192–206.
Oppenheim, R.W., Homma, S., Marti, E., Prevette, D., Wang, S., Yaginuma, H., McMahon, A.P., 1999. Modulation of early but not later stages of programmed cell death in embryonic avian spinal cord by sonic hedgehog. Mol. Cell Neurosci. 13, 348–361.
Oppenheimer, J., 1955. Problems, concepts and history. In: Willier, B.H., Weiss, P.A., Hamburger, V. (Eds.), Analysis of Development. W.B. Saunders, Philadelphia, pp. 1–24.
Ordahl, C.P., 1993. Myogenic lineages within the developing somite. In: Molecular Basis of Morphogenesis. Liss, New York, pp. 165–176.
Ordahl, C.P., Le Douarin, N.M., 1992. Two myogenic lineages within the developing somite. Development 114, 339–353.
Ordahl, C.P., Berdougo, E., Venters, S.J., Denetclaw Jr, W., 2001. The dermomyotome dorsomedial lip drives growth and morphogenesis of both the primary myotome and dermomyotome epithelium. Development 128, 1731–1744.
Oreal, E., Pieau, C., Mattei, M.G., Josso, N., Picard, J.Y., Carre-Eusebe, D., Magre, S., 1998. Early expression of AMH in chicken embryonic gonads precedes testicular *SOX9* expression. Dev. Dyn. 212, 522–532.
Orosz, S.E., Ensley, P.K., Haynes, C.J., 1992. Avian Surgical Anatomy. Thoracic and Pelvic Limbs. W.R. Saunders Co., Phladelphia.
Orts-Llorca, F., Collado, J.J., 1970. The development of heterologous grafts of the cardiac area (labelled with thymidine-3H) to the caudal area of the chick blastoderm. Arch. Anat. Histol. Embryol. 53, 113–124.
Osmond, M.K., Butler, A.J., Voon, F.C.T., Bellairs, R., 1991. The effects of retinoic acid on heart formation in the early chick embryo. Development 113, 1405–1417.
Osório, L., Teillet, M.A., Palmerim, I., Catala, M., 2009. Neural crest ontogeny during secondary neurulation: a gene expression pattern study in the chick embryo. Int. J. Dev. Biol. 53, 641–648.
Overton, J., 1989. Fusion of epithelial sheets as seen in formation of the chick amnion. Cell Tissue Res. 257, 141–147.
Packard, D.S., Meier, S., 1983. An experimental study of the somitomeric organization of the avian segmental plate. Dev. Biol. 97, 191–202.
Paganelli, C.V., 1991. The avian eggshell as a mediating barrier: respiratory gas fluxes and pressure during development. In: Deeming, D.C., Ferguson, M.W.J. (Eds.), Egg Incubation: Its Effects on Embryonic Development in Birds and Reptiles. Cambridge University Press, Cambridge, pp. 261–276.
Panman, L., Zeller, R., 2003. Patterning the limb before and after SHH signalling. J. Anat. 202, 3–12.
Pannett, C.A., Compton, A., 1924. The cultivation of tissues in saline-embryonic juice. Lancet 1, 381–384.
Pardenaud, L., Dieterlen-Lièvre, F., 1993. Emergence of endothelial and hemopoietic cells in the avian embryo. Anat. Embryol. 187, 107–114.
Pardenaud, L., Dieterlen-Lièvre, F., 1999. Manipulation of the angiopoietic/hemangiopoietic commitment in the avian embryo. Development 126, 617–627.
Pardenaud, L., Buck, C., Dieterlen-Lièvre, F., 1987. Early germ cell segregation and distribution in the quail blastodisc. Cell Diff. 22, 47–60.
Parker, H.M., McDaniel, C.D., 2009. Parthenogenesis in unfertilized eggs of *Coturnix chinensis*, the Chinese painted quail, and the effect of egg clutch position on embryonic development. Poultry Sci. 88, 784–790.
Parker, W.K., Bettany, G.T., 1877. The Morphology of the Skull. Macmillan, London.
Pasteels, J., 1937. Etudes sur la gastrulation du vertebrés meroblastiques. III Oiseaux. Arch. Biol. 48, 381–488.
Patel, K., Makarenkova, H., Jung, H.S., 1999. The role of long range, local and direct signal molecules during chick feather bud development involving the BMPs, follistatin and the Eph receptor tyrosine kinase Eph-A4. Mech. Dev. 86, 51–62. 399–415.
Patten, B.M., 1922. The formation of the cardiac loop in the chick. Am. J. Anat. 30, 373–397.
Patten, B.M., 1950. Early Embryology of the Chick, fourth ed. H.K. Lewis, London.
Patten, I., Placzek, M., 2002. Opponent activities of Shh and BMP signaling during floor plate induction in vivo. Curr. Biol. 12, 47–52.
Patterson, S.B., Minkoff, R., 1985. Morphometric and autoradiographic analysis of frontonasal development in the chick embryo. Anat. Rec. 212, 90–99.
Paul, E.R., Ngai, P.K., Walsh, M.P., Groschel-Stewart, U., 1995. Embryonic chicken gizzard: expression of the smooth muscle regulatory proteins caldesmon and myosin light chain kinase. Cell Tissue Res. 279, 331–337.
Paulsen, D.F., 1994. Retinoic acid in limb-bud outgrowth: review and hypothesis. Anat. Embryol. 190, 399–415.
Pearse II, R.V., Tabin, C.J., 1998. The molecular ZPA. J. Exp. Zool. 282, 677–690.
Pearson, C.A., Ohyama, K., Manning, L., 2011. FGF-dependent midline-derived progenitor cells in hypothalamic infundibular development. Development 138, 2613–2624.
Pedernera, E., Solis, L., Peralta, I., Vel Markazquez, P.N., 1999. Proliferative and steroidogenic effects of follicle-stimulating hormone during chick embryo gonadal hormone. Gen. Comp. Endocrinol. 116, 213–220.
Peebles, F., 1898. Some experiments on the primitive streak of the chick. Arch. Entw. Mech. Org. 7, 405–429.

Perriton, C.L., Powles, N., Chiang, C., Maconochie, M.I., Cohn, M.J., 2002. Sonic hedgehog signalling from the urethral epithelium controls external genital development. Dev. Biol. 247, 26–46.

Perry, M.M., 1988. A complete culture system for the chick embryo. Nature, Lond. 331, 70–72.

Petitte, J.N., Clark, M.E., Liu, G., Verrinder Gibbins, A.M., Etches, R.J., 1990. Production of somatic and germline chimeras in the chicken by transfer of early blastodermal cells. Development 108, 185–189.

Pfeffer, P.L., De Robertis, E.M., Izpisua-Belmonte, J.C., 1997. Crescent, a novel chick gene encoding a frizzled-like cysteine-rich domain, is expressed in anterior regions during early embryogenesis. Int. J. Dev. Biol. 41, 449–458.

Pikalow, A.S., Flynn, M.E., Searls, R.L., 1994. Development of the cranial flexure and Rathke's pouch in the chick embryo. Anat. Rec. 238, 407–414.

Pinho, S., Simonsson, P.R., Trevers, K.E., Stower, M.J., Sherlock, W.T., Khan, M., Streit, A., Sheng, G., Stern, C.D., 2011. Distinct steps of neural induction revealed by Asterix, Obelix and TrkC genes induced by different signals from the organizer. PLoS One 6 (4), e19157.

Pinot, M., 1969. Etude expérimentale de la morphogenèse de la cage thoracique chez l'embryon de poulet: mécanismes et origine du matérial. J. Embryol. Exp. Morph. 21, 149–164.

Pombero, A., Martinez, S., 2008. Telencephalic morphogenesis during the process of neurulation: an experimental study using quail-chick chimeras. J. Comp. Neurol. 512, 784–797.

Poole, T.J., Steinberg, M.S., 1982. Evidence for the guidance of pronephric duct migration by a craniocaudally travelling adhesion gradient. Dev. Biol. 92, 144–158.

Poole, T.J., Finkelstein, E.B., Cox, C.M., 2001. The role of FGF and VEGF in angioblast induction and migration during vascular development. Dev. Dyn. 220, 1–17.

Pourquié, O., 2001. Vertebrate somitogenesis. Annu. Rev. Cell Dev. Biol. 17, 311–350.

Pownall, M.E., Strunk, K.E., Emerson Jr, C.J., 1996. Notochord signals control the transcriptional cascade of myogenic bHLH genes in somites of quail embryos. Development 122, 1475–1488.

Prin, F., Dhouailly, D., 2004. How and when the regional competence of chick epidermis is established: feathers *vs.* scutate and reticulate scales, a problem *en route* to a solution. Int. J. Dev. Biol. 48, 137–148.

Psychoyos, J., Stern, C.D., 1996. Fates and migratory routes of primitive streak cells in the chick embryo. Development 122, 1523–1534.

Quay, W.B., 1986. The skin of birds – uropygial gland. In: Bereiter-Hahn, J., Matoltsty, A., Richards, K.S. (Eds.), Biology of the Integument, vol. 2. Vertebrates Springer-Verlag, Berlin and New York, pp. 248–254.

Quinlan, R., Martin, P., Graham, A., 2004. The role of actin cables in directing the morphogenesis of the pharyngeal pouches. Development 131, 593–599.

Quiring, D.P., 1933. The development of the sino-atrial region of the chick heart. J. Morph. 55, 81–118.

Rautenfeld, D.B.V., 1993. Systema lymphaticum et spleen. In Handbook of Avian Anatomy: Nomina Anatomia Avium, second ed. In: Baumel, J.J., King, A.S., Breazile, J.E., Evans, H.E., Vanden Berge, J.C., (Eds.), Nuttal Ornithological Club. Cambridge, Mass, pp. 477–491.

Rawdon, B.B., 1998. Morphogenesis and differentiation of the avian endocrine pancreas, with particular reference to experimental studies on the chick embryo. Microsc. Res. Tech. 15, 292–305.

Rawdon, B.B., Andrew, A., 1999. Gut endocrine cells in birds: an overview, with particular reference to the chemistry of gut peptides and the distribution, ontogeny, embryonic origin and differentiation of the endocrine cells. Prog. Histochem. Cytochem. 34, 3–82.

Rawdon, B.B., Larsson, L.I., 2000. Development of hormonal peptides and processing enzymes in the embryonic avian pancreas with special reference to co-localisation. Histochem. Cell Biol. 114, 105–112.

Rawles, M., 1943. The heart-forming areas of the early chick blastoderm. Physiol. Zool. 16, 22–24.

Redkar, A., Montgomery, M., Litvin, J., 2001. Fate map of early avian cardiac progenitor cells. Development 128, 2269–2279.

Reizis, A., Hammel, I., Arl, A., 2005. Regional and developmental variations of blood vessel morphometry in the chick embryo chorioallantoic membrane. J. Exp. Biol. 208, 2483–2488.

Richman, J.M., Tickle, C., 1989. Epithelia are interchangeable between facial primordia of chick embryos and morphogenesis is controlled by the mesenchyme. Dev. Biol. 136, 201–210.

Richman, J.M., Herbert, M., Matinovic, E., Walin, J., 1997. Effect of fibroblast growth factors on outgrowth of facial mesenchyme. Dev. Biol. 189, 135–147.

Riddle, R.D., Johnson, R.L., Lauter, E., Tabin, C., 1993. *Sonic hedgehog* mediates the polarizing activity of the ZPA. Cell 75, 1401–1416.

Risau, W., Flamme, I., 1995. Vasculogenesis. Annu. Rev. Cell Biol. 11, 73–91.

Roberts, D.J., Johnson, R.L., Burke, A.C., Nelson, C.E., Morgan, B.A., Tabin, C., 1995. *Sonic hedgehog* is an endodermal signal inducing *Bmp-4* and *Hox* genes during induction and regionalization of the chick hindgut. Development 121, 3163–3174.

Robertson, C.P., Gibbs, S.M., Roelink, H., 2001. cGMP enhances the sonic hedgehog response and neural plate cells. Dev. Biol. 238, 157–167.

Robertson, L., Wishart, G.J., Horrocks, A.J., 2000. Identification of perivitelline N-linked glycan as mediators of sperm-egg interaction in chickens. J. Reprod. Fertil. 120, 397–403.

Rodler, D., Sasanami, T., Sinowatz, F., 2012. Assembly of the inner perivitelline layer, a homolog of the mammalian zona pellucida: and immunohistochemical and ultrastructural study. Cells Tissues Organs 195, 330–339.

Rodriguez-Estaban, C., Capdevila, J., Kawakami, Y., Belmonte, J.C.I., 2001. Wnt signalling and PKA control Nodal exprsion and left-right determination in the chick embryo. Development 128, 3189–3196.

Rodriguez-León, J., Rodriguez-Esteban, C., Martí, M., Santiago-Josefat, B., Dubova, I., Rubiralta, X., Ipsúa Belmonte, J.C., 2008. Pitx2 regulates gonad morphogenesis. Proc Natl. Acad. Sci. USA. 105, 11242–11247.

Romano, L.A., Runyan, R.B., 2000. Slug is an essential target of TGFβ2 signaling in the developing chicken heart. Dev. Biol. 223, 91–102.

Romanoff, A.L., 1960. The Avian Embryo. Structure and Functional Development. MacMillan, New York.

Romanoff, A.L., Romanoff, A.J., 1949. The Avian Egg. Wiley, New York.

Romer, A.S., 1927. The development of the thigh musculature of the chick. J. Morph. 43, 347–386.

Ros, M.A., Rivero, F.B., Hinchliffe, J.R., Hurle, J.M., 1995. Immunohistochemical and ultrastructural study of the developing tendons of the avian foot. Anat. Embryol. 192, 483–496.

Rosenquist, G.C., 1966. A radioautographic study of labelled grafts in the chick blastoderm: development from primitive streak to stage 12. Contr. Embryol. Carneg. Inst. 38, 71–110.

Rosenquist, G.C., 1971. The location of pregut endoderm in the chick embryo at the primitive streak stage as determined by radioautographic mapping. Dev. Biol. 26, 323–335.

Rothenberg, F., Hitomi, M., Fisher, S., Watanabe, M., 2003. Initiation of apoptosis in the developing avian outflow tract myocardium. Dev. Dyn. 223, 469–482.

Rowlett, K., Simkiss, K., 1987. Explanted embryo culture: in vitro and in ovo techniques for domestic fowl. Br. Poultry Sci. 28, 91–101.

Ruffins, S., Bronner-Fraser, M., 2000. A critical period for conversion of ectodermal cells to a neural crest fate. Dev. Biol. 218, 13–20.

Ruiz I Altaba, A., Placzek, M., Baldassare, M., Dodd, J., Jessell, T.M., 1995. Early stages of notochord and floor plate development in the chick embryo defined by normal and induced expression of HNF-3 beta. Dev. Biol. 170, 299–313.

Saber, G.M., Parker, S.B., Mintoff, R., 1989. Influence of epithelial-mesenchymal interaction on the viability of facial mesenchyme in vitro. Anat. Rec. 225, 56–66.

Sakiyama, J., Yokouchi, Y., Kuroiwa, A., 2000. Coordinated expression of Hoxb genes and signalling molecules during development of the chick respiratory tract. Dev. Biol. 227, 12–27.

Sánchez-Bringas, G., Salazar, O., Pedernera, E., Méndez, C., 2006. Follicle-stimulating hormone treatment reverses the effect of hypophysectomy on cell proliferation in the chicken embryo ovary. Gen. Comp. Endocrinol. 149, 134–140.

Sanders, E.J., 1989. The Cell Surface in Embryogenesis and Carcinogenesis. The Telford Press, New Jersey.

Sanders, E.J., 1991. Embryonic cell invasiveness: an *in vitro* study of chick gastrulation. J. Cell Sci. 98, 403–407.

Sanders, E.J., 1997. Cell death in the avian sclerotome. Dev. Biol. 192, 551–563.

Sanders, E.J., Parker, E., 2001. Ablation of axial structures activates apoptotic pathways in somite cells of the chick embryo. Anat. Embryol. 204, 389–398.

Sanders, E.J., Prasad, S., 1991. Possible roles for TGFβ1 in the gastrulating chick embryo. J. Cell Sci. 99, 617–626.

Sanders, E.J., Bellairs, R., Portch, P.A., 1978. *In vivo* and *in vitro* studies on the hypoblast and definitive endoblast of avian embryos. J. Embryol. Exp. Morph. 46, 187–205.

Sanders, E.J., Khare, M.K., Ooi, V.C., Bellairs, R., 1986. An experimental and morphological analysis of tail bud mesenchyme of the chick embryo. Anat. Embryol. 174, 179–185.

Sanders, E.J., Varedi, M., French, A.S., 1993. Cell proliferation in the gastrulating chick embryo: a study using Brd U incorporation and PCNA localization. Development 118, 389–399.

Sanders, E.J., Torkkeli, P.H., French, A.S., 1997. Patterns of cell death during gastrulation in chick and mouse embryos. Anat. Embryol. 195, 147–154.

Sang, H., 2004. Prospects for transgenesis in the chick. Mech. Dev. 121, 1179–1186.

Sanz-Ezquerro, J.J., Tickle, C., 2003. Digital development and morphogenesis. J. Anat. 202, 51–58.

Sasaki, F., Doshita, A., Matsumoto, Y., Kuwahara, S., Tsukamoto, Y., Ogawa, K., 2003. Embryonic development of the pituitary gland in the chick. Cells Tissues Organs 173, 65–74.

Sasanami, T., Murata, T., Ohtsuki, M., Matsushima, K., Hiyama, G., Kansaku, N., Mori, M., 2007. Induction of sperm acrosome reaction by perivitelline membrane glycoprotein ZP1 in Japanese quail (Coturnix japonica). Reproduction 133 (1), 41–49.

Sato, K., Mochida, H., Yazawa, I., Sasaki, S., Momose-Sato, Y., 2002. Optical approaches to functional organization of glossopharyngeal and vagal motor nuclei in the embryonic chick hindbrain. J. Neurophysiol. 88, 383–393.

Sato, Y., Takahashi, Y., 2005. A novel signal induces a segmentation fissure by acting in a ventral to dorsal direction in the presomitic mesoderm. Dev. Biol. 9, 735–744.

Sauka-Spengler, T., Barenbaum, M., 2008. Gain and loss of function approaches in the chick embryo. Methods Cell Biol. 87, 237–256.

Saunders Jr., J.W., Cairns, J.M., Gasseling, M.T., 1957. The role of the apical ridge of ectoderm in the differentiation of the morphological structure and inductive specificity of limb parts of the chick. J. Morphol. 101, 57–88.

Sawada, K., Aoyama, H., 1999. Fate maps of the primitive streak in chick and quail embryo: ingression timing of progenitor cells of each rostro-caudal axial level of somites. Int. J. Dev. Biol. 43, 809–815.

Sawyer, R.H., 1972. Avian scale development. I. Histogenesis and morphogenesis of the epidermis and dermis during formation of the scale ridge. J. Exp. Zool. 181, 365–384.
Sawyer, R.H., Knapp, L.W., O'Guin, W.M., 1986. The skin of birds: epidermis, dermis and appendages. In: Bereiter-Hahn, J., Matoltsty, A., Richards, K.S. (Eds.), Biology of the Integument, vol. 2 Vertebrates. Springer-Verlag, Berlin and New York, pp. 194–238.
Saxod, R., 1980. Development of Merkel corpuscles and so-called 'transitional' cells in the white leghorn chicken. Am. J. Anat. 151, 453–474.
Saxod, R., 1996. Ontogeny of the cutaneous sensory organs. Micr. Res. Tech. 34, 313–333.
Scaal, M., Prols, F., Fuchtbauer, E.M., Patel, K., Hornik, C., Kohler, T., Christ, B., Brand-Saberri, B., 2002. BMPs induce dermal markers and ectopic feather tracts. Mech. Dev. 110, 51–60.
Scanes, C.G., Hart, L.E., Decuypere, E., Kuhn, E.R., 1987. Endocrinology of the avian embryo: an overview. J. Exp. Zool. (Suppl. 1), 253–264.
Schellpfeffer, M.A., Kuhlmann, R.S., Bolender, D.L., Ruffalo, C.G., Kolesari, G.L., 2005. Preliminary investigation of the use of high frequency ultrasound imaging in the chick embryo. Birth Defects Res. Clin. Mol. Teratol. 73, 39–49.
Schepelmann, K., 1990. Erythropoietic bone marrow in the pigeon: development of its distribution and volume during growth and pneumatization of bones. J. Morph. 203, 21–34.
Schlueter, J., Brand, T., 2009. A right-sided pathway involving FGF8/Snail1 controls asymmetric development of the proepicardium in the chick embryo. Proc. Natl. Acad. Sci. USA 106, 7485–7490.
Schmidt, C., Christ, B., Maden, M., Brand-Saberi, B., Patel, K., 2001. Regulation of Epha-4 expression in paraxial and lateral plate mesoderm by ectoderm-derived signals. Dev. Dyn. 220, 377–386.
Schneider, R.A., 2005. Developmental mechanisms facilitating the evolution of bills and quills. J. Anat. 207, 563–573.
Schneider, R.A., Hu, D., Rubenstein, J.L., Maden, M., Helms, J.A., 2001. Local retinoid signalling coordinates forebrain and facial morphogenesis by maintaining FGF8 and SHH. Development 128, 2755–2767.
Schoenwolf, G.C., Singh, U., 1981. Changes in the surface morphologies of the cells in the bursa cloacalis (bursa of Fabricius) during ontogeny of the chick embryo. Anat. Rec. 201, 303–316.
Schoenwolf, G.C., Smith, J.L., 1990. Mechanisms of neurulation: traditional viewpoint and recent advances. Development 109, 243–270.
Schoenwolf, G.C., Watterson, R.L., 1989. Laboratory Studies of Chick, Pig, and Frog Embryos. Guide and Atlas of Vertebrate Development, sixth ed. Macmillan, New York.
Schöfer, C., Frei, K., Weipoltshammer, K., Wachtler, F., 2001. The apical ectodermal ridge, fibroblast growth factors (FGF-2 and FGF-4) and insulin-like growth factor I (IGF-I) control the migration of epidermal melanoblasts in chicken wing buds. Anat. Embryol. 203, 137–146.
Schramm, C., Solursh, M., 1990. The formation of premuscle masses during chick wing bud development. Anat. Embryol. 182, 235–247.
Schreiner, K.E., 1902. Über die Entwicklung der Amniotenniere. Zeit. wiss. Zool. 71, 1–188.
Schweitzer, R., Chyung, J.H., Murtaugh, L.C., Brent, A., Rosen, V., Olson, E.N., Lassar, A., Tabin, C.J., 2001. Analysis of the tendon cell fate using Scleraxis, a specific marker for tendons and ligaments. Development 128, 3855–3866.
Searls, R.L., 1986. A description of caudal migration leading to the formation of pericardial and pleural coeloms, to caudal migration of the arches and to development of the shoulder. Am. J. Anat. 177, 271–283.
Seidl, W., Steding, G., 1978. Topogenesis of the anterior intestinal portal. Anat. Embryol. 155, 37–45.
Sekido, R., Lovell-Badge, R., 2007. Mechanisms of gonadal morphogenesis are not conserved between chick and mouse. Dev. Biol. 302, 132–142.
Sekine, K., Ohuchi, H., Fujiwara, M., Yamasaki, M., Yoshizawa, T., Sato, T., Yagishita, N., Matsui, D., Koga, Y., Itoh, N., Kato, S., 1999. FGF10 is essential for limb and lung formation. Nat. Genet. 21, 138–141.
Sela-Donenfeld, D., Kalcheim, C., 2000. Inhibition of noggin expression in the dorsal neural tube by somitogenesis: a mechanism for coordinating the timing of neural crest emigration. Development 127, 4845–4854.
Selleck, M.A.J., Bronner-Fraser, M., 1995. Origins of the avian neural crest: the role of neural plate-epidermal interactions. Development 121, 525–538.
Selleck, M.A., Bronner-Fraser, M., 2000. Avian neural crest cell fate decisions: a diffusible signal mediates inductions of neural crest by the ectoderm. Int. J. Dev. Neurosci. 18, 621–627.
Selleck, M.A.J., Stern, C.D., 1991. Fate mapping and cell lineage analysis of Hensen's node in the chick embryo. Development 112, 615–616.
Selleck, M.A.J., Stern, C.D., 1992. Commitment of mesoderm cells in Hensen's node of the chick embryo to notochord and somite. Development 114, 403–415.
Sengel, P., 1976. Morphogenesis of Skin. Cambridge University Press, London.
Sengel, P., 1986. Epidermal-dermal interaction. In: Bereiter-Hahn, J., Matoltsty, A., Richards, K.S. (Eds.), Biology of the Integument, vol. 2 Vertebrates. Springer-Verlag, Berlin, pp. 374–408.
Shah, S.B., Skromme, I., Hume, C.R., Kessler, D.S., Lee, K.J., Stern, C.D., Dodd, J., 1997. Misexpression of chick Vg1 in the marginal zone induces primitive streak formation. Development 124, 5127–5138.
Shapiro, F., 1992. Vertebral development of the chick embryo during days 3–19 of incubation. J. Morph. 213, 317–333.
Sharpe, J., 2003. Optical projection tomography as a new tool for studying embryo anatomy. J. Anatomy 202, 175–181.

Shearman, R.M., Tulenko, F.J., Burke, A.C., 2011. 3D reconstructions of quail-chick chimeras provide a new fate map of the avian scapula. Dev. Biol. 355, 1–11.
Shen, X., Steyrer, E., Retzek, H., Sanders, E.J., Schneider, W., 1993. Chicken oocyte growth: receptor-mediated yolk deposition. Cell Tissue Res. 272, 459–471.
Sheng, G., 2010. Primitive and definitive erythropoiesis in the yolk sac: a bird's eye view. Int. J. Dev. Biol. 54, 1033–1043.
Sheng, G., Stern, C.D., 1999. *Gata2* and *Gata*3: novel markers for early embryonic polarity and for non-neural ectoderm in the chick embryo. Mech. Dev. 87, 213–216.
Shigetani, Y., Nobusada, Y., Kuratani, S., 2000. Ectodermally derived FGF8 defines the maxillomandibular region in the early chick embryo: epithelial–mesenchymal interactions in the specification of the craniofacial ectomesenchyme. Dev. Biol. 228, 73–85.
Shimade, Y., Ho, E., 1980. Scanning electron microscopy of the chick heart: formation of the epicardium and surface structure of the four heterotypic cells that constitute the embryonic heart. In: Van Pragh, R. (Ed.), Etiology and Morphogenesis of Cardiac Heart Disease. Futura, pp. 63–80.
Shimokita, E., Takahashi, Y., 2011. Secondary neurulation: Fate mapping and gene manipulation of the neural tube in tail bud. Dev. Growth Differ. 53, 401–410.
Shin, M., Noji, S., Neubüser, A., Yasugi, S., 2006. FGF10 is required for cell proliferation and gland formation in the stomach epithelium of the chicken embryo. Dev. Biol. 294, 11–23.
Simkiss, K., 1967. Calcium in Reproductive Physiology. Chapman and Hall, London.
Simkiss, K., 1991. Fluxes during embryogenesis. In: Deeming, D.C., Ferguson, M.W.J. (Eds.), Egg Incubation: Its Effects on Embryonic Development in Birds and Reptiles. Cambridge University Press, Cambridge, pp. 47–52.
Simkiss, K., Tyler, C., 1971. Shell formation. In: Bell, R.F., Freeman, D.J. (Eds.), Biochemistry and Physiology of the Domestic Fowl, vol. 1. Academic Press, London, pp. 1331–1343.
Sjödal, M., Gunhaga, L., 2008. Expression patterns of *Shh, PTc2, Raldh3, Pitx2, Isl1, Lim3* and *Pax6* in the developing chick hypophyseal placode and Rathke's pouch. Gene Expr. Patterns 8, 481–485.
Skieresz-Szewczyk, K., Prozorowska, E., Jackowiak, H., 2012. The development of the tongue of the domestic goose from 9th to 25th day of incubation as seen by scanning electron microscopy. Microsp. Res. Tech. 75, 1564–1570.
Skromne, I., Stern, C.D., 2001. Interactions between Wnt and Vg1 signalling pathways initiate primitive streak formation in the chick embryo. Development 128, 2915–2927.
Skromne, I., Stern, C.D., 2002. A hierarchy of gene expression accompanying induction of the primitive streak by Vg1 in the chick embryo. Mech. Dev. 114, 115–118.
Smith, C.A., 2007. Sex determination in birds: HINTs from the W sex chromosome? Sex Dev. 1, 279–285.
Smith, C.A., Smith, M.J., Sinclair, A.H., 1999. Expression of chicken steroidogenic factor-1 during gonadal sex differentiation. Gen. Comp. Endocrinol. 113, 187–196.
Smith, C.A., Roeszler, K.N., Ohnesorg, T., Cummins, D.M., Farlie, P.G., Doran, T.J., Sinclair, A.H., 2009. The avian Z-linked gene DMRT1 is required for male sex determination in the chicken. Nature 461, 267–271.
Smith, D.M., Tabin, C.J., 1999. BMP signalling specifies the pyloric sphincter. Nature 402, 748–749.
Smith, D.M., Tabin, C.J., 2000. Clonally related cells are restricted to organ boundaries early in the development of the chicken gut to form compartment boundaries. Dev. Biol. 227, 422–431.
Smith, D.M., Grasty, R.C., Theodosiou, N.A., Tabin, C.J., Nascone-Yoder, N.M., 2000a. Evolutionary relationships between the amphibian, avian, and mammalian stomachs. Evol. Dev. 2, 348–359.
Smith, D.M., Nielsen, C., Tabin, C.J., Roberts, D.J., 2000b. Roles of BMP signalling and Nkx2.5 in patterning at the chick midgut-foregut boundary. Development 127, 3671–3681.
Sosic, D., Brand-Saberi, B., Schmidt, C., Christ, B., Olson, E.N., 1997. Regulation of paraxis expression and somite formation by ectoderm- and neural tube-derived signals. Dev. Biol. 185, 229–243.
Southwell, B.R., 2006. Staging of intestinal development in the chick. Anat. Rec. Part A. 288A, 909–920.
Sparks, N.H.C., 2009. Shell formation and function and its role in incubation. Avian Biol. Res. 2, 47–53.
Spemann, H., 1938. Embryonic Development and Induction. Yale University Press, New Haven, Conn.
Spratt Jr, N.T., 1963. Role of the substratum, supra-cellular continuity and differential growth in morphogenetic cell movements. Dev. Biol. 7, 51–63.
Stabellini, G., Locci, P., Calvitti, M., Evangelisti, R., Marinucci, L., Bodo, M., Caruso, A., Canaider, S., Carinci, P., 2001. Epithelial-mesenchymal interactions and lung branching morphogenesis. Role of polyamine and transforming growth factor beta 1. Eur. J. Histochem. 45, 151–162.
Stalsberg, H., 1969. The origins of heart asymmetry: right and left contributions to the early chick embryo heart. Dev. Biol. 19, 100–127.
Stark, M.R., Rao, M.S., Schoenwolf, G.C., Yang, G., Smith, D., Mauch, T.J., 2000. *Frizzled-4* expression during chick kidney development. Mech. Dev. 98, 121–125.
Stéphan, F., 1949. Les suppléances obtenue expérimentalement dans le systeme des arcs aortiques de l'embryon d'oiseau. C. Rend. Assoc. Anat. 36, 647–651.
Stephens, T.D., Sanders, D.D., Yap, C.Y.F., 1992. Visual demonstration of the limb-forming zone in the chick embryo lateral plate. J. Morph. 213, 305–316.
Stepinska, U., Olszanska, B., 1983. Cell multiplication and blastoderm development in relation to egg envelope formation during uterine development of quail (*Coturnix coturnix*) embryo. J. Exp. Zool. 228, 505–510.

Stern, C.D., 1990. The marginal zone and its contribution to the hypoblast and primitive streak of the chick embryo. Development 109, 667–682.
Stern, C.D., 1993a. Transplantation in avian embryos. In: Stern, C.D., Holland, P.W.H. (Eds.), Essential Developmental Biology, a Practical Approach. IRL Press at Oxford University Press, pp. 111–118.
Stern, C.D., 1993b. Avian embryos. In: Stern, C.D., Holland, P.W.H. (Eds.), Essential Developmental Biology, A Practical Approach. IRL Press at Oxford University Press, pp. 45–54.
Stern, C.D., 2005. Neural induction: old problem, new findings, yet more questions. Development 132, 2007–2021.
Stern, C.D., 2005. The chick: a great model system becomes even greater. Developmental Cell. 8, 9–17.
Stern, C.D., 2008. Grafting Hensen's node. Methods Mol. Biol., 265–276.
Stern, C.D., Canning, D.R., 1988. Changes in the expression of the carbohydrate epitope HNK-1 associated with mesoderm induction in the chick embryo. Development 104, 643–655.
Stern, C.D., Canning, D.R., 1990. Origin of cells giving rise to mesoderm and endoderm in chick embryo. Nature Lond. 343, 273–275.
Stern, C.D., Holland, P.W.H., 1993. Essential Developmental Biology, A Practical Approach. IRL Press at Oxford University Press.
Stern, C.D., Ireland, G.W., 1981. An integrated experimental study of endoderm formation in avian embryos. Anat. Embryol. 163, 245–263.
Stockdale, F.E., Nikovits, J.R., Christ, B., 2000. Molecular and cellular biology of avian somite development. Dev. Dyn. 219, 304–321.
Stoll, R., Ichas, F., Fancounan, N., Maraud, R., 1993. Action of estradiol and tamoxifen on the testis-inducing activity of the chick embryonic testis grafted to the female embryo. Anat. Embryol. 188, 587–592.
Storey, K.G., Crossley, J.M., De Robertis, E.M., Norris, W.E., Stern, C.D., 1992. Neural induction and regionalisation in the chick embryo. Development 114, 729–741.
Storey, K.G., Selleck, M.A.J., Stern, C.D., 1995. Neural induction and regionalisation by different subpopulations of cells in Hensen's node. Development 121, 417–428.
Streit, A., Stern, C.D., 1999. Establishment and maintenance of the border of the neural plate in the chick: involvement of FGF and BMP activity. Mech. Develop. 82, 51–66.
Streit, A., Stern, C.D., 2008. Operations on primitive streak stage embryos. In: Bronner-Fraser, M. (Ed.), Methods in Cell Biology, 87, pp. 3–17.
Sudo, H., Takahashi, Y., Tonegawa, A., Arase, Y., Ayoyama, H., Mizutani-Koseki, Y., Moriya, H., Wilting, J., Christ, B., Koseki, H., 2001. Inductive signals from the somatopleure mediated by bone morphogenetic proteins are essential for the formation of the sternal component of avian ribs. Dev. Biol. 232, 284–300.
Sullivan, G.E., 1962. Anatomy and embryology of the wing musculature of the domestic fowl (*Gallus*). Aust. J. Zool. 10, 458–518.
Sullivan, L.C., Orgeig, S., 2001. Dexamethasone and epinephrine stimulate surfactant secretion in type II cells of embryonic chicks. Am. J. Physiol. Regul. Integr. Comp. Physiol. 281, R770–R777.
Sun, D., Baur, S., Hay, E.D., 2000. Epithelial–mesenchymal transformation is the mechanism for fusion of the craniofacial primordia involved in morphogenesis of the chicken lip. Dev. Biol. 228, 337–349.
Sweetman, D., Wagstaff, L., Cooper, O., Weijer, C., Münsterberg, A., 2008. The migration of paraxial and lateral plate mesoderm cells emerging from the late primitive streak is controlled by Wnt signals. BMC Dev. Biol. 8, 63.
Szabo-Rogers, H.L., Geetha-Loganathan, P., Nimmagadda, S., Fu, K.K., Richman, J.M., 2008. FGF signals from the nasl pit are necessary for normal facial morphogenesis. Dev. Biol. 318, 289–302.
Tajima, A., Hayashi, H., Kamizumi, A., Ogura, J., Kuwana, T., Chikamune, T., 1999. Study on the concentration of circulating primordial germ cells (cPGCs) in early chick embryos. J. Exp. Zool. 284, 759–764.
Takagi, H., Nagashima, K., Inoue, M., Sakata, I., Sakai, T., 2008. Detailed analysis of formation of chicken pituitary primordium in early embryonic development. Cell Tissue Res. 333, 417–426.
Tan, H., Junor, L., Price, R.L., Norris, R.A., Potts, J.D., Goodwin, R.L., 2011. Expression and deposition of fibrous extracellular matrix proteins in cardiac valves during chick development. Microsc. Microanal. 17, 91–100.
Tao, H., Yoshimoto, Y., Yoshioka, H., Nohno, T., Noji, S., Ohuchi, H., 2002. FGF10 is a mesenchymally derived stimulator of epidermal development in the chick embryonic skin. Mech. Dev. 116, 39–49.
Teillet, M., Watanabe, Y., Jeffs, P., Duprez, D., Lapointe, F., Le Douarin, N.M., 2004. Sonic hedgehog is required for survival of both myogenic and chondrogenic somatic lineages. Development 125, 2019–2030.
Tenin, G., Wright, D., Ferjentsik, Z., Bone, R., McGrew, M.J., Maroto, M., 2010. The chick somitogenesis oscillator is arrested before all paraxial mesoderm is segmented into somites. BMC Dev. Biol. 25, 10–24.
Theis, S., Patel, K., Valasek, P., Otto, A., Pu, Q., Harel, I., Tzahor, E., Tajbakhsh, S., Christ, B., Huang, R., 2010. The occipital lateral plate mesoderm is a novel source for vertebrate neck musculature. Development 137, 2961–2971.
Thommes, R.C., 1987. Ontogenesis of thyroid function and regulation in the developing chick embryo. J. Exp. Zool. (Suppl. 1), 273–280.
Thurston, R.J., Hess, R.A., 1987. Ultrastructure of spermatozoa from domesticated birds: comparative study of turkey, chicken and guinea fowl. Scanning Microsc. 1, 1829–1838.
Tickle, C., 1991. Retinoic acid and chick limb bud development. Development (Suppl. 1), 123–130.

Tickle, C., 1993. Chick limb buds. In: Stern, C.D., Holland, P.W.H. (Eds.), Essential Developmental Biology. A Practical Approach. IRL Press at Oxford University Press, pp. 119–125.

Tickle, C., Munsterberg, A., 2001. Vertebrate limb development. Curr. Opin. Genet. 11, 476–481.

Tipping, N., Wilson, D., 2011. Chick amniogenesis is mediated by an actin cable. Anat. Rec. 294, 1143–1149.

Torrey, T.W., 1965. Morphogenesis of the vertebrate kidney. In: DeHaan, R.L., Ursprung, H., Holt (Eds.), Organogenesis. Rinehart and Winston, New York, pp. 559–579.

Toyoshima, K., Seta, Y., Shimamura, A., 1993. Fine structure of Merkel corpuscles in the lingual mucosa of Japanese quail, *Coturnix coturnix japonica*. Arch. Oral. Biol. 38, 1009–1012.

Trousse, F., Esteve, P., Bovolenta, P., 2001. Bmp4 mediates apoptotic cell death in the developing chick eye. J. Neurosci. 21, 1292–1301.

Tsunekawa, N., Naito, M., Sakai, Y., Nishida, T., Noce, T., 2000. Isolation of chicken vasa homolog gene and tracing the origin of primordial germ cells. Development 127, 2741–2750.

Tuan, R.S., Ono, T., Akins, R.E., Koide, M., 1991. Experimental studies on cultured, shell-less fowl embryos: calcium transport, skeletal development and cardio-vascular functions. In: Deeming, D.C., Ferguson, M.J. (Eds.), Egg Incubation: Its Effects on Embryonic Development in Birds and Reptiles. Cambridge University Press, pp. 419–433.

Uehara, M., Oomori, S., Kitagawa, H., Ueshima, T., 1990. The development of the pectin oculi in the chick. Nihon Juigaku Zasshi 52, 503–512 (not seen).

Ukeshima, A., Fujimoto, T., 1991. A fine morphological study of germ cells in asymmetrically developing right and left ovaries of the chick. Anat. Rec. 230, 378–386.

Ukeshima, A., Kudo, M., Fujimoto, T., 1987. Relationship between genital ridge formation and settlement site of primordial germ cells in chick embryos. Anat. Rec. 219, 311–314.

Vakaet, L.C., 1962. Some new data concerning the formation of the definitive endoblast in the chick embryo. J. Embryol. Exp. Morph. 10, 38–57.

Vakaet, L., 1970. Cinephotomicrographic investigations of gastrulation in the chick blastoderm. Arch. Biol. 81, 387–426.

Vakaet, L., 1984. Early development in birds. In: Le Douarin, N., McLaren, A. (Eds.), Chimeras in Developmental Biology. Academic Press, London, pp. 71–88.

Vakaet, L., Vanroelen, Chr., Andries, L., 1980. An embryological model of non-malignant invasion or ingression. In: de Brabander, M. (Ed.), Cell Movement and Neoplasia. Pergamon Press, Oxford, pp. 65–75.

Valasek, P., Theis, S., DeLaurier, A., Hinits, Y., Luke, G.N., Otto, A.M., Minchin, J., He, L., Christ, B., Brooks, G., Sang, H., Evans, D.J., Logan, M., Huang, R., Patel, K., 2011. Cellular and molecular investigations into the development of the pectoral girdle. Dev. Biol. 357, 108–116.

Van den Berg, G., Moorman, A.F.M., 2011. Development of the pulmonary vein and the systemic venous sinus: an interactive 3D overview. PLoS One 6 (7), e22055.

Vanden Berge, J.C., Zweers, G.A., 1993. Myologia. In: Baumel, J.J., King, A.S., Breazile, J.E., Evans, H.E., Vanden Berge, J.C. (Eds.), Handbook of Avian Anatomy: Nomina Anatomica Avium, second ed. Nuttall Ornithological Club, Cambridge, MA, pp. 189–250.

Varner, V., Voronov, D.A., Taber, L.A., 2010. Mechanics of head fold formation: investigating tissue-level forces during early development. Development 137, 3801–3811.

Veini, M., Bellairs, R., 1990. Early mesoderm differentiation in the chick embryo. Anat. Embryol. 183, 143–149.

Vendrell, V., Carnicero, E., Giraldez, F., Alonso, M.T., Schimmang, T., 2000. Induction of inner ear fate. Development 127, 2011–2019.

Verbout, A.J., 1985. The development of the vertebral column. Adv. Anat. Embryol. Cell Biol. 89, 1–122.

Vesque, C., Ellis, S., Lee, A., Szabo, M., Thomas, P., Beddington, R., Placzek, M., 2000. Development of chick axial mesoderm: specification of prechordal mesoderm by anterior endoderm-derived TGFbeta family signalling. Development 127, 2795–2809.

Viallet, J.P., Prin, F., Olovera-Martinez, I., Hirsinger, E., Pourquié, O., Dhouailly, D., 1998. Chick Delta-1 gene expression and the formation of the feather primordial. Mech. Dev. 72, 159–168.

Villalpando, I., Sanchez-Bringas, G., Sanchez-Varga, I., Pedernera, E., Villafa-Monroy, H., 2000. The *P450 aromatase (P450arom)* gene is asymmetrically expressed in a critical period for gonadal sexual differentiation in the chick. Gen. Comp. Endocrinol. 117, 325–334.

Virágh, S., Gittenberger-de Groot, A.C., Poelmann, R.E., Kálmán, F., 1993. Early development of quail heart epicardium and associated vascular and glandular structures. Anat. Embryol. 188, 381–393.

Voiculescu, O., Bertocchini, F., Wolpert, L., Keller, R., Stern, C.D., 2007. The amniote embryo primitive streak is defined by epithelial cell intercalation before gastrulation. Nature 449, 1049–1052 (25 Oct).

Voiculescu, O., Papanayotou, C., Stern, C.D., 2008. Spatially and temporally controlled electroporation of early chick embryos. Nat. Protocols 3, 419–426.

Vogel-Hopker, A., Momose, T., Rohrer, H., Yasuda, K., Ishihara, L., Rapaport, D.H., 2000. Multiple functions of fibroblast growth factor 8 (FGF-8) in chick eye development. Mech. Dev. 94, 25–36.

Vorster, W., 1989. The development of the chondrocranium of Gallus gallus. Adv. Anat. Embryol. Cell Biol. 113, 1–77.
Wada, N., Nohno, T., Kuratani, S., 2011. Dual origins of the perichordal cranium in the chicken embryo. Dev. Biol. 356, 528–540.
Waddington, C.H., 1932. Experiments on the development of chick and duck embryos cultivated *in vitro*. Phil. Trans. B221, 179–230.
Waddington, C.H., 1952. The Epigenetics of Birds. Cambridge University Press, Cambridge.
Waddington, C.H., Schmidt, G.A., 1933. Induction by heteroplastic grafts of the primitive streak in birds. Arch. Entw. Mech. Org. 128, 522–563.
Waddington, D., Gribbin, C., Sterling, R.J., Sang, H., Perry, M.M., 1998. Chronology of events in the first cell cycle of the polyspermic egg of the domestic fowl (*Gallus domesticus*). Int. J. Dev. Biol. 42, 625–628.
Wagner, J., Schmidt, C., Nikowits Jr., W., Christ, B., 2000. Compartmentalization of the somite and myogenesis in chick embryos are influenced by wnt expression. Dev. Biol. 228, 86–94.
Wagstaff, L.J., Bellatt, G., Mogensen, M.M., Münsterberg, A., 2008. Multicellular rosette formation during cell ngression in the avian primitive streak. Develop. Dynam. 237, 91–96.
Waldo, K.L., Kumiski, D.H., Wallis, K.T., Stadt, H.A., Hutson, M.R., Platt, D.H., Kirby, M.L., 2001. Conotruncal myocardium arises from a secondary heart field. Development 128, 3179–3188.
Waldo, K.L., Hutson, M.R., Stadt, H.A., Zdanowicz, M., Zdanowicz, J., Kirby, M.L., 2005a. Cardiac neural crest is necessary for the normal addition of the myocardium to the arterial pole from the secondary heart field. Dev. Biol. 281, 66–77.
Waldo, K.L., Hutson, M.R., Ward, C.C., Zdanowicz, M., Stadt, H.A., Kumiski, D., Abu-Issa, R., Kirby, M.L., 2005b. Secondary heart field contributes myocardium and smooth muscle to the arterial pole of the developing heart. Dev. Biol. 281, 78–90.
Walsh, C., McLelland, J., 1978. The development of the epithelium and its innervation in the avian extra-pulmonary respiratory tract. J. Anat. 125, 171–182.
Wang, B., Pu, Q., De, R., Patel, K., Christ, B., Wilting, B., Huang, R., 2010. Commitment of chondrogenic precursors of the avian scapula takes place after epithelial–mesenchymal transition of the dermomyotome. BMC Dev. Biol. 10, 91.
Wang, Y., Dur, O., Patrick, M.J., Tinney, J.P., Tobita, K., Keller, B.B., Pekkan, K., 2009. Aortic arch morphogenesis and flow modeling in the chick embryo. Ann. Biomed. Eng. 37, 1069–1081.
Ware, M., Schubert, F.R., 2011. Development of the early axon scaffold in the rostral brain of the chick embryo. J Anat. 219, 203–216.
Watanabe, M., Kinutani, M., Naito, M., Ochi, O., Takashima, Y., 1992. Distribution analysis of transferred donor cells in avian blastodermal chimeras. Development 114, 331–338.
Watanabe, Y., Duprez, D., Monsoro-Burq, A.H., Vincent, C., Le Douarin, N.M., 1998. Two domains in vertebrate development: antagonistic regulation by SHH and BMP4 proteins. Development 125, 2631–2639.
Webb, S., Brown, N.A., Anderson, R.H., Richardson, M.K., 2000. Relationship in the chick of the developing pulmonary vein to the embryonic systemic venous sinus. Anat. Rec. 259, 67–75.
Wei, Y., Mikawa, T., 2000. Fate diversity of primitive streak cells during heart field formation in ovo. Dev. Dyn. 219, 505–513.
Weismann, A., 1885. Die Continuität des Keimplasma's als Grundlage einer Theorie des Vererbung. Fischer Verlag, Jena.
Weninger, W.J., Maurer, B., Zendron, B., Dorfmeister, K., Geyer, S.H., 2009. Measurements of the *diameters* of the great arteries and semi-lunar valves of chick and mouse embryos. J. Microsc. 234, 173–190.
Wenner, P., O'Donovan, M.J., 2001. Mechanisms that initiate spontaneous network activity in the chick spinal cord. J. Neurophysiol. 86, 1481–1498.
West, N.H., Langille, B.L., Jones, D.R., 1981. In: King, A.S., McLelland, J. (Eds.), Form and Function in Birds, vol. 2. Academic Press, London, pp. 235–339.
Willier, B.H., 1937. Experimentally produced sterile gonads and the problem of the origin of the germ cells in the chick embryo. Anat. Rec. 70, 89–112.
Wilson, L., Maden, M., 2005. The mechanism of dorsoventral patterning in the vertebrate neural tube. Dev. Biol. 282, 1–13.
Wilson, V., Olivera-Martinez, I., Storey, K.G., 2009. Stem cells, signals and vertebrate body axis extension. Develop. 136, 1591–1604.
Wilt, F.H., Wessels, N.K., 1967. Methods in Developmental Biology. Thomas Y. Crowell Co., New York.
Wilting, J., Papoutsi, M., Othman-Hassan, K., Rodriguez-Niedenfuhr, M., Prols, F., Tomarev, S.I., Eichmann, A., 2001. Development of the avian lymphatic system. Microsc. Res. Tech. 55, 81–91.
Wilting, J., Buttler, K., Schulte, I., Papoutsi, M., Schweigerer, l., Männer, J., 2007. The proepicardium delivers hemangioblasts but not lymphangioblasts to the developing heart. Dev. Biol. 305, 451–459.
Wishart, G., Horrocks, A.J., 2000. Fertilization in birds. In: Tarina, J.J., Cano, A. (Eds.), Fertilization in Protozoa and Metazoan Animals. Springer-Verlag, Heidelberg, pp. 193–222.
Withington, S., Beddington, R., Cooke, J., 2001. Foregut endoderm is required at head process stages for anteriormost neural patterning in chick. Development 128, 309–320.
Wittler, L., Kessel, M., 2004. The acquisition of neural fate in the chick. Mech. Dev. 121, 1031–1042.
Wolff, E., 1953. Le role des hormones embryonnaires dans la differenciation sexuelle des oiseaux. Arch. Anat. Microscop. Morphol. Exptl. 39, 426–450.

Wood, J.L., Hughes, A.J., Mercer, K.J., chapman, S.C., 2010. Analysis of chick (*Gallus gallus)* middle ear columella formation. BMC Dev. Biol. 10, 16.

Woods, J.E., 1987. Maturation of the hypothalamo–adenohypophyseal-gonadal (HAG) axes in the chick embryo. J. Exp. Zool. (Suppl. 1), 265–272.

Wolpert, L., 2002. Principles of Development, second ed. Oxford University Press.

Wortham, R.A., 1948. The development of the muscles and tendons in the lower leg and foot of chick embryos. J. Morph. 83, 105–148.

Wu, P., Jiang, T.-X., Shen, J.-Y., Widelitz, R.B., Chuong, C.-M., 2006. Morphoregulation of avian beaks: Comparative mapping of growth zone activities and morphological evolution. Dev. Dyn. 235, 1400–1412.

Wyngaarden, L.A., Vogeli, K.M., Ciruna, B.G., Wells, M., Hadjantonakis, A.K., Hopyan, S., 2010. Oriented cell motility and division underlie early limb bud morphogenesis. Development 137, 2551–2558.

Yadgary, aal, Uni, Z., 2012. Yolk sac carbohydrate levels and gene expression of key gluconeogenic and glycogenic enzymes during chick embryonic development. Poultry Sci. 91, 444–453.

Yanagawa, N., Sakabe, M., Sakata, H., Yamagishi, T., Nakajima, T., 2011. Nodal signal is required for morphogenetic movements of epiblast layer in the pre-streak chick blastoderm. Dev. Growth Differ. 53, 366–377.

Yander, G., Searle, R.L., 1980. A scanning electron microscopic study of the development of the shoulder, visceral arches, and the region ventral to the cervical somites of the chick embryo. Am. J. Anat. 157, 27–39.

Yang, A., Siegel, P.B., 1997. Late embryonic and early posthatch growth of heart and lung in White Leghorn lines of chickens. Growth Dev. Aging 61, 119–126.

Yang, X., Chrisman, H., Weijer, C.J., 2008. PDGF signaling controls the migration of mesoderm cells during gastrulation by regulating N-cadherin expression. Development 135, 3521–3530.

Yassine, F., Feddeka-Brunner, B., Dieterlen-Lièvre, F., 1989. The ontogeny of the chick embryo spleen; a cytological study. Cell Differ. Dev. 27, 29–45.

Yasugi, S., Mizuno, T., 2008. Molecular analysis of endoderm regionalization. Dev. Growth Diff 50 (Suppl. 1), S79–S96.

Yee, G.W., Abbott, U.K., 1978. Facial development in normal and mutant chick embryos. I Scanning electron microscopy of primary palate formation. J. Exp. Zool. 206, 307–321.

Yew, D.T., 1978. The origin and initial development of the pecten oculi. Anat. Anz. 143, 383–387.

Yin, Y., Bangs, F., Paton, I.R., Precott, A., James, J., Davey, M.G., Whitley, P., Genikhovich, G., Technau, U., Burt, D.W., Tickle, C., 2009. The Talpid3 gene (KIAA0586) encodes a centrosomal protein that is essential for primary cila formation. Development 136, 655–664.

Young, R.L., Bever, G.S., Wang, Z., Wagner, G.P., 2011. Identity of the avian wing digits: problems resolved and unsolved. Dev. Dyn. 240, 1042–1053.

Yu, M., Yue, Z., Wu, D.-Y., Mayer, J.-A., Medina, M., Widelitz, R.B., Jang, T.-X., Chuong, C.-M., 2004. The developmental biology of feather follicles. Int. J. Dev. Biol. 48, 181–191.

Yu, X., St Amand, T.R., Wang, S., Li, G., Zhang, Y., Hu, Y.P., Nguyen, L., Qiu, M.S., Chen, Y.P., 2001. Differential expression and functional analysis of *Pitx2* isoforms in regulation of heart looping in the chick. Development 128, 1005–1013.

Yutzey, K.E., Kirby, M.L., 2002. Wherefore heart thou? Embryonic origins of cardiogenesis mesoderm. Dev. Dyn. 223, 307–320.

Zaccanti, F., Vallisneri, M., Quagia, A., 1990. Early aspects of sex differentiation in the gonads of chick embryos. Differentiation 43, 71–80.

Zamir, E.A., Czirók, A., Cui, C., Little, C.D., Rongish, B.J., 2006. Mesodermal cell displacements during avian gastrulation are due to both individual cell-autonomous and convective tissue movements. Proc. Natl. Acad. Sci. USA 103, 19806–19811.

Zamir, E.A., Rongish, B.J., Little, C.D., 2008. The ECM moves during primitive streak formation – computation of ECM versus cellular motion. PLOS Biol. Oct. 14, 6 (10), e247.

Zehavi, N., Reich, V., Khaner, O., 1998. High proliferation rate characterizes the site of axis formation in the avian blastula-stage embryo. Int. J. Dev. Biol. 42, 95–98.

Zemanova, Z., Ujec, E., 2002. Transepithelial potential in mesonephric nephrons of 7-day-old chick embryos in relation to the histochemically detected sodium pump. Physiol. Res. 51, 43–48.

Zhang, G., Boyle, D.L., Zhang, Y., Rogers, A.R., Conrad, G.W., 2012. Development and mineralization of embryonic avian scleral ossicles. Mol. Vis. 18, 348–361.

Zhang, Y., Levin, M., 2009. Left-right asymmetry in the chick embryo requires core planar cell polarity protein Vang12. Genesis 47, 719–728.

Zhi, Q., Huang, R., Christ, B., Brand-Sabieri, B., 1996. Participation of individual brachial somites in skeletal muscles of the avian forearm and hand. Anat. Embryol. 194, 327–339.

Zimmermann, A., Haina, A., Groschel-Stewart, U., 1995. Neural and smooth muscle development in the chicken gizzard. Roux's Arch. Dev. Biol. 204, 271–274.

Zwaan, J., Ikeda, A., 1966. Studies of the differentiation of the chicken lens with the fluorescent antibody technique. Anat. Rec. 154, 447.

Zwilling, E., 1949. The role of epithelial components in the developmental origin of the 'wingless' syndrome of chick embryos. J. Exp. Zool. 111, 175–188.

Index

Note: Bold: text and text-figures; italics: glossary; standard text: plates.

A
Abnormalities, **13**, **14**
Acetabulum, 480, 542, 574, 580
Acrosome, xix, **16**
Activation, xix, **16**
Adenohypophysis, **36**, 123
ADMP, **29**
Adrenal gland, **125**, 437, 538, 540
Adreno-medullary cells, **125**
Air sacs, **88**, **89**, 103, 428
  Abdominal, 444, 500, 504, 538, 542, 544, 564, 582
  Cervical, 462, 464
  anterior thoracic, **88**, 444, 468, 470, 564
  interclavicular, **88**, 498
  lateral thoracic, 538, 574
  thoracic, 444
Albumen (egg white), *xix*, **1**, **3–5**
Allantoic stalk, *xix*, 318, 384, 504, 542
Allanto-chorion, 129, 290, 358. *See also* chorio-allantois
Allantois, *xix*, **84**, **85**, **129**, 319, 347, 353, 355, 428
  circulation. *See* Allantoic Arteries and Allantoic Veins
  diverticulum, **79**
Amnio-cardiac vesicle, *xix*, **52**, **53**, 154, 250
Amnion, *xix*, **127**, **128**, 162, 248, 295, 301, 350, 358
Amniotic
  Cavity, 128, 292, 294, 364, 366
  Ectoderm, 166, 278
  Fluid, *xix*, **128**
  Fold, *xix*, **128**, 250, 288, 296, 300, 306
  Umbilicus, **128**
Angiogenesis, *xix*, **57**, **58**
Animal pole, *xix*
Anterior chamber of eye, **98**, **99**, 456, 490, 460
Anterior intestinal portal, *xix*, 196, 256, 260, 266, 278, 280, 300
Anterior necrotic zone (ANZ), *xx*, **49**
Anterior neuropore, *xx*, 166, 167, 250, 256
Aortic arches, **60**, **61**, 214, 215, 328, 340, 350, 366, 368, 378, 464. *See also* Ductus Arteriosus
Aortico-pulmonary
  ridges, 384, 434
  septum, **55**, **56**, 200, 434
Apical ectodermal ridge, *xx*, **47**, 338, 412
Apoptosis, *xx*, **49**
Aqueduct of Sylvius (mesencephalic aqueduct), 418, 512
Arbor vitae of cerebellum, 506
Archistriatum, 512
Arcualia, 104
Area opaca, *xx*, **18**, 134, 146, 148, 162, 163
Area pellucid, *xx*, **18–22**, 144, 146, 148, 158, 250
Area vasculosa, *xx*, ***59***, ***127***, 250, 284
Area vitellina, *xx*, **127**, 282, 284
AROM (aromatose gene), 72
Arteries
  allantoic (umbilical), **59–64**, 224, 574, 586
  anterior mesenteric, 222, 226, 586
  aortic arches (arterial arches), **60–63**, **81**, 196, 197, 221, 223, 292, 294, 308, 324, 346
  aortic sac, 292, 298, 500
  basilar, 450
  brachial, 534
  brachiocephalic, 214, 464, 526, 530, 532, 562, 564
  carotid, 223, 324, 366, 398, 430, 450, 462, 514, 550, 566
  caudal, **62**, **64**, 224, 542, 544, 586
  cerebral, **61**
  celiac, 214, 222, 424, 428, 470, 478, 480, 538
  dorsal aorta, **60–64**, 164, 214, 216, 220, 226, 270, 280, 294, 296, 332, 394, 434, 572
  ductus arteriosus, **60**
  ethmoidal, 430
  femoral, 478, 542
  gastric, 530
  head and neck, **61**
  iliac, **64**, 224
  inter-somitic/intersegmental, **62**, 216
  mesenteric, **62**, 226, 542
  mesonephric, **62**, 226
  metanephric, 440, 542
  occipital, 418, 514
  oesophago-tracheo-bronchial, 462
  omphalo-mesenteric (vitelline), **59**, **64**, 214, 284, 290, 306, 334, 342, 468, 484, 538, 542, 585
  palatine, 456
  parabronchial, 244
  pectoral, **526**, **532**
  pharyngeal arch arteries, 220, 222
  pulmonary, **56**, **60**, 214, 220, 222, 434, 464, 534, 546, 564, 568
  renal, 424
  sciatic, **64**, 224
  stapedial, 222, 226, 514
  subclavian, **60**, 222, 520, 526
  truncus arteriosus, **56**, **63**, 196, 200, 220, 272, 288, 310, 330, 350, 368, 390, 566, 570
  ulnar, 526
  vagus, 516
  ventral aorta, **60**, 258, 270, 298, 390
  ventral gastric, 582
  vertebral, 518, 520, 522, 552
  vitelline. *See* omphalo-mesenteric
Atrio-ventricular
  Canal, *xx*, 210, 374, 376, 384, 406, 434, 468, 470
  cushions, **56**, 374, 384, 386
  valves, 538
Atrium of heart, **56**, 162, 196, 210, 286, 310, 328, 352, 368, 372, 464
Auditory (otic) tube (Eustachian), 402
Auerbach's plexus, **82**
Axial mesoderm, *xx*
Axis of body, *xx*

B
Balbiani body, xiv, **75**, 132
Basal plate of chondrocranium, **111**, 368, 390, 426, 430, 444, 450, 496
Beak, **89**, **110**, **120**, 500, 506, 508

Bilaminar embryo, *xx*
Bile duct, 478
Blastoderm, *xx*, **1**, **9**, **28**
Blood islands, *xx*, **57**
Blood vessels. *See also* arteries and veins
BMPs (bone morphogenetic proteins), **34**, **37**, **40**, **46**, **78**, **82**, **101**, **112**
Body folds and flexures, *xxi*, **45**, **46**, 288
Branchial arches. *See* Pharyngeal arches
Bronchus, 352, 358, 364, 434, 464, 468, 534, 536, 560
Bucco-pharyngeal membrane, *xxi*
Bulbus (conus, cordis) arteriosus, 258, 326, 330, 468, 566

C
Caeca, **84**
Candling, *xxi*
Cardiac jelly, 280
Cardio-hepatic regions, **82**
Carpals, **107**
Cartilages, 418. *See also* other structures individually listed
  acrochordal, 514
  alisphenoid, **111**
  articular, 516
  basibranchial, **112**
  basihyal (copula. I), **112**, 426, 516
  biventer cervicis, 448, 458
  carpo-metacarpus, 520
  ceratobranchial, 490, 494, 516
  ceratohyal, **112**
  chordin, **29**
  columella, **81**, **112**, 450, 512
  copula. *See* basihyal
  copulo-paraglossal, 492
  coracoid, **106**, **107**, 526, 528, 532
  entoglossal, **112**
  epibranchial, **112**, 450, 452, 456, 500, 512
  ethmoidal (nasal), **97**, **98**, 111
  hyoid, **81**, 420
  infrapolar, 494
  mandibular, 420
  maxillary, 516
  Meckel's, **112**, 382, 388, 426, 430, 432, 450, 456, 488, 494, 500, 514
  metacarpus, 526
  metatarsus, 393
  metotic, 448, 450
  orbital, 418, 516
  otic capsule. *See* Otic
  orbitosphenoid, 498, 502
  palato-quadrate, **112**, 494
  palatine, 502
  parachordal, **111**, 494
  paraglossal, 426, 456, 488, 490, 516
  parasphenoid, 492, 593
  pharyngeal cartilages. *See* pharyngeal arches
  postorbital, 448, 496, 512
  pterygoid condyle of quadrate, 450
  quadrate, 382, 388, 432, 450, 452, 456, 514, 590
  quadrato-jugal, 456
  scapula. *See* Scapula
  squamosal, 448, 593
  trabecular, **111**, 420, 450, 494
  tracheal, **88**
CDix, **36**
Cell death. *See* Apoptosis
Cell numbers and proliferation, **17**
Central nervous system, **91**
Cerebellum, **92**, 444, 448, 494
Cerebral hemispheres, cerebral vesicles, 398, 426, 432, 444, 448, 494, 496, 506, 512
Cervical flexure. *See* Body Folds
Chalazae, *xxi*, **1**, **5**
Chick/quail chimeras, *xxi*, **8**
Choana. *See* Internal Naris
Chondrogenesis, *xxi*
Chordin, **34**
Chorioallantois, chorioallantoic membrane, *xxi*, **89**, **128**, 218
Chorion, *xxi*, **128**, 298, 332, 358
Choroid, **99**, 300, 496
  fissure, **98**, 344
  plexus, 420, 426, 430, 444, 446
Clavicle, **106**, 504, 508, 520, 546, 592
Claws, **120**
Cleavage, *xx*i, **16**, **17**
Cleidoic egg, *xxi*
Cloaca, **70**, **85**, 240, 412, 444, 482, 498, 542, 578. *See also* Proctodaeal
Cloacal bursa (bursa of Fabricius), *xxi*, **85**, *544*, *548*, *584*
Cloacal fold (ridge), *542*
Cloacal membrane (proctodaeal membrane), 338, 346, 412
Cloacal sphincter, 484, 546
Cochlea/cochleal canal, 450, 454, 514
Coelom(embryonic), xxi, **86**, 272, 300, 302, 314, 316, 332
  dorsal hepatic cavity, **87**, 386, 392, 400, 404, 422, 470, 538, 572
  intestinal (peritoneal) cavity, 344, 386, 580
  pericardial, **64**, **86**, 278, 292, 346, 350, 384, 394, 398, 420, 422, 434, 498, 526
  pleural/pulmonary, **87**, 352, 410, 420, 444, 464, 468, 534, 538, 568
  posterior abdominal, 428
  ventral hepatic cavity, **87**, 364, 398, 400, 424, 468, 470, 538
Coelom (extra-embryonic), 164, 288, 300, 302, 316, 332, 346, 500, 579
Colon, 412, 428
Columella, **101**. *See* Cartilages
Comb, **121**
Commitment (determination), *xxi*
Common abnormalities, **13**
Conchae (turbinals), **101**. *See* Nasal
Conus arteriosus. *See* Bulbus arteriosus
Coprodaeum, 546
Coracoid, 444, 462, 464, 520, 556, 562, 592
Cornea, 448, 460, 490, 492, 514
Corpus striatum, 420, 512
Costa. *See* Rib
Coturnix coturnix japonica, *xxi*, **623**
Cranial cavity, 446, 512
Cranial flexure, **46**, **47**. *See also* Body folds
Cranial nerves and ganglia, **95**
  I olfactory, 450, 456, 514, 516
  II optic, 418, 420, 430, 512, 516
  III oculomotor, 350, 356, 512
    ciliary ganglion, **96**
  IV trochlear, **96**
  V trigeminal, 308, 324, 348, 366, 368, 382
    facial branch, *346*
    maxillary branch, 344, 348
    mandibular branch, 348
    ophthalmic branch, 328, 344, 348, 368
    trigeminal (Gasserian, Semi-lunar) ganglion (V), 366, 390, 496
  VI abducens, 514
  VII facial, 308, 348
    geniculate ganglion, 344, 346, 382
  VIII acoustic or vestibulo-cochlearis, 308, 348
    vestibular (acoustic) ganglion, 348, 366, 368, 382, 512
  IX glossopharyngeal, 324, 348, 450
    petrosal ganglion, 366, 370
    superior ganglion, 346
  X Vagus, 366, 450, 514, 516, 532, 556
    jugular ganglion, 350
    nodose ganglion, 370
  XI spinal accessory, 418, 430
  XII hypoglossal
Clavicle, **106**, **107**, 593, 595
Cochlea, **100**
Cochlea canal (cochlea duct), **101**, 450, 514
Creeper mutation, **81**, **82**
Crop, **81**, **82**, 386, 422, 424, 462, 514, 516, 554
Crystallins, **99**
Culture techniques, **9–11**

D
Decemet's membrane, **99**
Definitive (gut) endoderm, **20**. *See also* **Lower Layer**
Delamination, *xxi*
Deltoid crest, **108**
Dentary bone, 498, 514
Dermatome, 176, 314, 322, 334
Derma-myotome, xv, 266, 272, 300, 303
Dermis, *xxii*, **117**
Determination, *xxii*
Diencephalon (thalamus), **91**, **93**, 292, 294, 332, 350, 418, 446
Diocoele (lumen of diencephalon, IIIrd ventricle), 292, 298, 314, 404

Differentiation, *xxii*
Digits. *See* Phalanges
Diplocardia, 54
Dorsal aorta. *See* Arteries
Dorsal mesentery, *xxii*. *See* mesenteries
Dorsal mesocardium, **53**, 266, 267
Dorsal root ganglia, 350, 354, 424, 576, 588
Duck, **75**, 623
Ductus choledochus, **83**
Duplications, **48**, 136, 190
Duodenum, **84**, 208, 478, 502, 542, 574

E
Ear, 444. *See also* Otic
Ectoderm, *xxii*, **22**, **34**. *See also* Epiblast
  extra-embryonic, *270*
Edge cells (margin of overgrowth), **28**
Egg tooth, *xxii*, 236, 498, 504
Eggs, storage, **7**
Embryonic disc, *xxii*
Encephalon, 496
Endoblast, *xxii*, **20**
Endocardial cushions, **57**
Endocardium, **54**
Endoderm, xxii, **18**, **21**, 146, 148, 150, 272, 288, 294, 296, 336
  extra-embryonic endoderm. *See also* area opaca
Endolymphatic duct/sac, **100**, 368, 444, 512
Endophyll cells, *xxii*, **18**, **21**, **75**
Endothelial cells of heart, **55**, **65**
Ependyma, xxii, **93**
EphA4, **40**
Epiblast, *xxii*, **20**, **22**, 144
Epiboly, *xxii*, **28**
Epicardium, **54**, 266
Epidermis, **117**, 322
Epimyocardium, 272, 300
Epiphysis. *See* Pineal organ
Epithelial-mesenchymal interactions, *xxii*
ERNI (early response gene for neural induction), **34**
Erythrocytes, **65**
Eustachian tube, 502, 506. *See* auditory tube
Explanted embryos, grafting and transplants, **9–11**
External auditory meatus, **101**, 448, 452, 456, 494, 514
External genitalia, **74**, 238, 240
External naris. *See* Nasal
Extra-embryonic membranes, 127
Eye, **98**, **99**, 162, 318, 498. *See also* Muscles, Eye
Eyelid, **98**, **99**, 444, 448, 450, 456, 492, 516

F
Fabricius, Bursa of. *See* Cloacal Bursa
Face, **46**, **110**, 236
Falciform ligament, **87**, 364
Fate maps, **19**, **26**, **30**
Feather, **117**, **119**, 498, 568, 580
  bud, 496
  induction, **118**
  muscles, **120**, 456
  papilla, **118**, 462
Femur, **106**, **108**, 412, 424, 428, 444, 470, 478, 542, 574, 595
Fertilization, **15**, **16**
FGFs (fibroblast growth factors), **29**, **46**, **48**, **58**
Fibronectin, **25**, **28**, **38**, **52**
Fibula, **108**, 478, 480, 542, 572, 580
Fixatives, **13**
Flexures, *xxiii*, **46**
Follicles (ovarian), **1**, 132
Foot, **48**, **108**
Footplate of columella, 444, 574
Foramen caecum, 328
Foramen magnum, 514
Foramen of Monro, 420, 426
Foramen triosseum, **107**
Forebrain (prosencephalon), 258, 326
Foregut, *xxiii*. *See* Gut
Forelimb, *xxiii*, 332. *See also* wing
Fourth ventricle, 448, 512. *See* Metocoele and Myelocoele
Frizzled-4, **68**
Frontal bone, 498
Fronto-nasal process, **46**, **48**, **80**, 236, 368, 382, 392

G
Gall bladder, **82**
Ganglia, sympathetic, **42**
GANF, **35**
Gastrula, *xxiv*
Gastrulation, *xxiv*, **22–24**
Gata-2, **50**
Genital folds, *xxiv*, **74**, 438, 542
Genital (nephrogenic) ridges, **71**
Genital system, **67–71**
Genital tubercle, **74**, 238, 498
Germinal crescent, *xxiv*, **74**, 148
Germinal disc, *xxiv*, 1
Germ plasm, **74**
Gizzard, **82**, **84**, 210, 374, 386, 422, 444, 480, 542, 546, 574, 580
Glomeruli, **69**, **70**, 234
Glottis, 456, 514
Gonad, 234, 412, 424. *See also* Ovary and Testis
Gonadotrophins, **3**
Goosecoid (g.s.c.), **29**
Growth, **49**
Gut/intestine, **77**, 314
  Foregut, **21**, **77**, 264, 252, 292, 358
  herniated, 404, 500, 502, 582. *See also* Intestine looping
  hindgut, **78**, 296, 322, 336, 344, 358
  midgut, **78**, 302, 316, 344, 358
  tail, 340

H
Haemopoietic cells, haematopoiesis, *xxiv*, **58**
Handplate, 108
Harderian gland, **99**
Hatching, **56**, **89**
Head
  fold, *xxiv*, **80**, 146, 160, 256, 264
  mesenchyme, *xxiv*, 264, 270, 430
  process, *xxiv*, **31**, 146, 154, 156, 158
  vein. *See* Veins; jugular
Heart, **51–57**, 194–206, 266, 272, 290
  atrium, 164, 214, 297
  cardiac crescent, **52**
  cardiac jelly, 280
  endocardial tubes, **53**
  formation of, **53**, 194, 256
  beat, **57**
  looping/looped, **45**, **54**, **55**, 196, 198, 282, 284
  neural crest contribution, **51**, **52**
  position in body, **57**
  primary and secondary heart fields, **51**, **52**
  pro-epicardial serosa, 202
  septation, **55**
Hensen's (primitive) node, *xxiv*, **18**, **20**, **21**, **25**, **26**, **29**, **30**, **31**, **33**, 146, 148, 156, 160, 256, 260, 268, 282, 294
Hepatic. *See also* Liver
  cavities, **87**, **88**, 390. *See also* coelom
  endoderm, **83**
  enteric recess, 376
  ligament (horizontal hepatic ligament), 364, 404, 422, 424, 470, 538, 574
  septum, 398, 400
Herbst corpuscles, **122**
Heterogametic sex, *xxiv*
Hindbrain, 260. *See also* Rhombencephalon
Hindgut, *xxv*. *See* Gut
Homeobox genes/Hox genes, *xxv*, **17**
Horizontal hepatic ligament, **87**, 538
Horizontal septum, **87**, 390, 398, 538
Humerus, **106**, 412, 422, 434, 462, 522, 558, 593
Hypoblast, *xxv*, **18**, **21**
Hypocledial ligament, *564*
Hypophyseal fenestra, *512*
Hypophysis, 450, 494, 512, 514
Hypothalamus, **92**

I
Ilium, **107**, 424, 428, 440, 444, 478, 504, 510, 542, 544, 572, 574, 593
Imaging, **13**
Incubation, **7**
Indifferent gonad, *xxv*, **72**
Induction, embryonic, *xxv*
Infundibulum, *xxv*
  of brain, **93**, **123**, 344, 418, 426, 430
  of oviduct, **2**

Ingression, *xxv*, **26**
Injection techniques, **12**
In ovo techniques, **11**
Integument, **117**
Interatrial
  foramina (perforations), **56**, 464, 466
  septum (with perforations), **56**, 164, 204, 352, 358, 384, 406, 464
Intermediate mesoderm, *xxv*, **40**, **67**, **68**, **71**, 268
Internal naris (choana). *See* Nasal
Interorbital septum, 420, 426, 432, 450, 456, 494, 512. *See also* Nasal septum
Interventricular septum, 210, 386, 392, 394, 434, 468, 470, 538
Intervertebral discs, **105**
Intestine
  small, **84**, 412, 424
  looping, **84**, **85**, 378, 390, 392, 424, 480, 498, 542, 578, 586
Intracoelomic grafting, **12**
Invagination, *xviii*
Iris, 456, 460, 490
Ischium, **107**, 422, 426, 428, 482, 484, 546, 580, 582, 593, 595
Isthmus
  of brain, **91**, 322, 342, 344, 346, 368, 398, 418
  of oviduct, **2**, **3**

J

Jejunum, 438
Junctional endoblast, **20**, **21**

K

Kidneys. *See* Mesonephros, Metanephros and Pronephros
Koller's sickle (Rauber's sickle), *xxv*, **19**, **20**, **22**, **26**, **29**

L

Labile determination, *xxv*
Lacrimal duct, *516*
Lagena, 382, 514
Large intestines, **84**, 186, 543, 580
Laryngo-tracheal groove, **88**, 310, 350
Larynx, **88**, 432, 514
Latebra, **1**
Lateral body folds, 300, 306. *See also* Body Folds
Lateral lingual ridges, **80**
Lateral mesocardial folds
Lateral plate mesoderm, **40**, 216, 260, 280, 300
  somatic and somatopleure, *252*, *260*, *274*, *302*
  splanchnic and splanchnopleure, *252*, *260*, *272*, *274*, *288*
Lateral ventricles. *See* Telocoele
Lefty, **50**
Leg/leg bud, 162, 306, 318, 322, 338, 342, 358
Lens, 310, 350, 382, 420, 432, 450, 456, 514
Lens placode, 186
Lens vesicle, **98**, 292, 330
Lesser sac, *346*, *386*
Limbs/limb buds, **47**, **538**, 542, 574, 591–595. *See also* Leg
Liver, **63**, 210, 212, 290, 346, 352, 358, 368, 386, 412, 422, 476, 498, 542
Lower layer (hypoblast), *xx*
Lung/Lung buds, **81**, **88**, 206, 242, 244, 322, 328, 346, 352, 360, 384, 396, 412, 502, 566
Lymphatics, **65**

M

Magnum, **2**
Mammillary knobs, *xxv*
Mandible, 490
Mantle layer of spinal cord, **94**, 588
Margin of overgrowth, *xxv*
Marginal layer of spinal cord, *xxvi*, **93**, **94**, 588
Marginal zone, **18**
Maxilla, 506
Maxillary and mandibulary processes, **46**, 200, 488. *See also* Pharyngeal Arches
Median palatine fissure, **101**
Median rostral choana. *See* Nasal
Medulla oblongata, 448, 450, 496, 504, 506, 512
Meissner's plexus, **82**
Melanin, **121**
Melanocytes, **121**
Merkel cells, 122
Mesencephalon (midbrain), **91**, 262, 272, 276, 282, 504
Mesenchyme, *xxvi*
Mesendoderm, *xxvi*
Mesentery. *See also* Mesocardia
  dorsal, **55**, **86**, 260, 314, 324, 330, 360, 412, 428, 538, 564
  ventral, **86**, **87**, 164, 260, 314, 324, 330, 364, 398, 422, 476, 538. *See also* Falciform ligament
Mesobronchus, 468
Mesocardia, dorsal and ventral, 266, 272
Mesoderm, *xxvi*, 148, 150
  Secondary, 274
Mesocoele (lumen of mesencephalon, Aqueduct of Sylvius), 286, 298
Mesonephric duct. *See* Nephric duct
Mesonephros (mesonephric kidney), **67–71**, *224*, *232*, *234*, *316*, *322*, *354*, *368*, *374*, *424*, *428*, *444*, *540*, *576*
Metacarpals, **108**
Metacoele, **93**, 322
Metanephric (ureteric) duct (ureter), 444, 472, 482, 484, 582
Metanephros (metanephric kidney), *xxvi*, **67–71**, 412, 444, 470, 484, 538, 540, 576
Metatarsus, 542, 593, 595
Metathalamus in posterior commisure, *426*
Metencephalon, **91**, 162, 282, 306, 444, 512
Midbrain, **91**. *See* Mesencephalon
Midgut, *xxvi*. *See* Gut
"Milking hens", **7**
Morphogenetic (gastrulation) movements, **23–31**
Mullerian duct, *xxvi*, **73**, **84**. *See also* Oviduct
Muscle mass, *xxvi*. *See* pre-muscle mass
Muscles, general, **112**
  head and neck, **115**, 546
  heart, **116**
  limbs and girdles, **112**, **114**
  thorax and abdomen, **14**
Muscles, specific
  adductor mandibulae externus, *448, 450, 454, 456, 498, 514, 516*
  adductor retricium, 548
  ambiens, 478
  ascendens, 458, 516, 518
  biceps brachii, 464, 520, 528, 530, 534
  biceps femoralis, 444
  biventer cervicis, 450, 456, 518, 520, 522, 550, 554, 568
  brachialis, *526*
  brachiomandibular, 514
  caudofemoralis, 478, 544
  ciliary, 514
  cloacal sphincter, 546
  complexus, 450, 500, 508, 514
  coracobrachialis, 464, 520, 522, 526, 530, 556
  costosternalis, 462
  deltoid, 462, 464, 526, 530, 534, 556
  depressor mandibulae, 450, 514
  depressor cauda, 586
  ectoepicondylo-ulnaris, 534
  extensor brevis digitorum, 464, 480
  extensor digitorum communis, 534
  extensor digitorum longus, 478, 480
  extensor hallucis longus, 480
  extensor indicis longus, 464
  extensor medius brevis, *526*
  extensor metacarpi radialis, *444*
  extensor metacarpi ulnaris, *464*, *534*
  external eye muscles, *394*
    dorsal (superior) oblique, 382, 448, 456, 498, 506, 512
    dorsal (superior) rectus, 382, 498
    lateral rectus, *430*, 450, 506
    medial rectus, 450
    Ventral (inferior) oblique, 432, 450, 460, 494, 498, 506
    Ventral (inferior) rectus, 484, 514
  extrinsic tracheal, 456
  femorotibialis internus and lateralis, 428, 478

fibularis longus, 580, 582. *See also* peroneus
flexor carpi ulnaris, 444, 464, 534
flexor colli lateralis, 514, 542
flexor colli medialis, 514
flexor cruris lateralis (semi-tendinous), 444, 482, 542, 544, 580
flexor cruris medialis, 428, 478, 580
flexor digitorum profundus, 464, 468, 526, 534
flexor hallucis brevis, 480
gastrocnemius, 478, 480, 538
hypobranchial, 516
hyoglossus, 516
iliofemoralis, 572, 582
iliofibularis, 478, 482, 580
iliotibialis, 444, 478, 480, 482, 542, 544
  cranialis, 428
  lateralis, 484
iliotrochantericus cranialis, 478, 480
iliotrochantericus caudalis, *510*
intercostalis internus and externus
interosseus dorsalis, *436*, *444*, *468*, *526*, *534*, *538*, *568*
interosseum dorsalis, 444, 534
intertransversarii, 516, 518, 526, 550
intrinsic tracheal, 456
ischiofemoralis, 444, 478, 480, 510, 580
lateralis caudae, 484, 508, 544, 584
latissimus dorsi, 444, 462, 498, 534, 554, 562
levator caudae, 544
levator cloacae, 484, 544
longus capitis, 506
longus colli dorsali, 458, 502, 518, 554, 556, 562, 564, 568
longus colli ventralis, 462, 464, 498, 506, 516, 520, 524, 530, 534, 554, 562
masseter, **100**
metacarpiradialis, 534
oblique external abdominal, 468, 478, 542
oblique internal abdominal, 478, 480, 542, 574
obturator, 482, 542, 544, 546, 582
paraglossocerato-branchial, 516
pectoralis, 444, 462, 498, 500, 502, 520, 526, 544, 566, 568
peroneus, 480. *See also* fibularis
pronator profundus, 464
pronator superficialis, 464
pseudotemporalis profundus, 456
pseudotemporalis superficialis, 456
pterygoid, 456, 500, 508
puboischiofemoralis, 428
pubocaudalis externus and lateralis, 478, 542
pyramidalis membranae nictitansis, 494
quadrates, 514
rectus abdominis, 538
rectus capitis, 450, 454
  dorsalis (superior), 496, 516
  lateralis, 454, 456, 458, 494, 514
  ventralis (inferior), 450, 454, 494, 514, 556
rhomboideus superficialis, 444, 462, 464, 468, 470, 498, 520, 528
rhomboideus profundus, 462
scapulo-humeralis, 526, 528, 534, 554, 556
serratus profundus, 528, 530, 534
serratus superficialis, 462
sphincter cloacae, 484
spinal thoracic complex, 526, 530
spinalis, 556
splenius capitis, 448, 450, 454, 456, 514
sterno-trachealis, 514
sternocoracoideus, 520, 556
subscapularis, 520, 526, 528, 530
supracoracoideus (pectoralis secundus), 444, 462, 468, 498, 520, 526, 534, 566
tail muscles, 355
tensor propatagialis brevis, 426, 526
tibialis cranialis (anterior), 480, 580
tibiotarsus, 580
tongue, **115**
triceps brachii, 462, 522
  pars humerotriceps, 464, 520, 526, 530, 534, 568
  pars scapulotriceps, 534, 562
ulnimetacarpalis dorsalis, 468
ulnimetacarpalis ventralis, 464, 534
Myelencephalon, 276, 282, 292, 296, 300, 368, 390, 418, 426
Myelocoele (lumen of myelencephalon, IVth. ventricle), **93**, 286. *See also* Metacoele
Myocardium, **54**
Myogenesis, *xxvi*
Myotome, 286, 306, 308, 328, 358, 362

N

Nasal (olfactory)
  capsule, 488, 504, 516
  cavity, 490, 506
  conchae (turbinals), **101**, 432, 456, 488, 490, 498, 504, 516
  eminence, 382
  glands, **101**, 488
  meatus, 516
  naris, internal (choana) and external, 390, 420, 426, 456, 488, 492, 504
  pit, **101**, 162, 352, 382
  placode, *xxvii*, **101**, 184, 314, 350
  sac, 392, 404
  septum (interorbital *septum*), 488, 490, 516
Nephric (pronephric, mesonephric, Wolffian) duct, *xxvi*, **67–70**, **73**, 174, 230, 232, 336, 338, 344, 360, 386, 428, 472, 542
Nephric primordium, 304
Nephrogenic (nephric) ridge, *xxvi*
Nephrogenous mesenchymen, **69**, 336
Nephrostome, **69**
Nerves. *See also* Cranial nerves and ganglia
  autonomic, **97**
  brachial plexus, 462, 478, 520, 526, 530
  deltoid, 556
  fibularis, 480
  intercostals, 534
  ischiatic, 542
  obturator, 542
  ramus communicans, *386*
  spinal, **94**, 482, 534, 544
  sympathetic, 538
  sympathetic ganglia, **96**, 462, 526, 534, 542, 544
  vestibulocochlearis/vestibular, 496, 512
  wing, **113**
Neural arch, xxvi, 422, 434, 450, 462
Neural crest, *xxvi*, **37**, **38**, **40–43**
Neural folds, 146, 164, 252
Neural induction, **33**, **34**
Neural plate, **34**, **35**, 164, 152
Neural tube, **35**, 164, 302, 310, 312
Neurulation, secondary, **35**, **36**
Neuromere, **348**
Neuropore
  anterior, 146, 164
  posterior, **35**
New technique, **9**, **10**
Nictitating membrane, **99**
Nodal, **24**, **29**, **50**
Noggin, **29**, **34**, **40**
Normal Tables. *See* Appendices I, II and III
Notch, ***34***, ***35***
Notochord, *xxvi*, **26**, **35**, **36**, **80**, **103**, 168, 170, 258, 260, 288, 292, 294, 312, 332, 356, 382, 392, 422, 430, 450
Notochordal sheath, *xxvi*
Nucleus mesencephalicus lateralis, 512
Nucleus of Pander, **1**, **5**

O

Oblique septum, **87**, 362, 422, 538, 546, 566, 568
Occipital condyle, 512
Occipitomandibular ligament, 593
Optic lobe, **93**, 390
Oesophagus, **81**, **82**, 296, 310, 328, 330, 350, 358, 364, 464, 520, 532, 546, 550
Olfactory
  bulb, 494, 512
  nerve. *See* Cranial nerves
  placode. *See* Nasal placode
Omphalo-mesenteric vessels, *xxvii*. *See also* Arteries and Veins

Oocytes, *xxvii*, **1**
Open cells, *xxvii*, **17**
Optic chiasma, 450, 494, 514
Optic cup, **98**, 282, 292, 356
Optic lobe, 394, 398, 418, 430, 444, 446
Optic recess, 322, 418
Optic stalk, 292, 298, 310, 350
Optic tectum, 500, 508
Optic thalamus, 398, 418, 512
Optic vesicle, 262, 264, 278
Oral cavity, 258, 292, 330, 344, 382, 408
Organ of Jacobson, **101**
Organiser, *xxviii*, **23**
Orientation. *See* polarity
Oscillating genes, **3**
Ostium of oviduct, **2**
Otic (auditory)
  capsule, 444, 448, 450, 452, 496, 500, 508, 512
  pit, 160, 182
  placode, **100**, 182, 266, 276, 286
  vesicle (otocyst), xxvii, 282, 286, 306, 328, 340, 344, 404, 418
Otx2, **29**, **36**
Ovary, **2**, **73**, 428, 474, 478, 538, 542
Oviduct (Mullerian duct), 228, 234, 368, 470, 474, 478, 480, 538, 540, 542, 546, 578
Ovulation, *xxvii*, **2**

P
Palaeostriatum, 512
  bone, 488, 490, 492, 506, 516
  process, 426, 456
Palate, 504
Pallium, 426
Pancreas, **83**, **84**, 125
Pander, *xxvii*, 142
Parachordal mesoderm, 260
Parathyroid glands, **81**, **124**
Paraxial mesoderm, *xxvii*
Parthenogenesis, **16**
Patella, 572, 593
Pax, **98**
Pecten, **99**, 444, 450, 460, 492, 514
Pectineal process, 482, 544, 546
Pectoral girdle, **106**, **107**
Pelvic girdle, **106**, **107**
Periblast, **17**
Pericardial cavity. *See* Coelom
Pericardium. *See* Coelom
Periderm, *xxvii*, **120**
Perilymphatic duct, 494
Peritoneal cavity. *See* Coelom
Peritoneum, **86**, 366, 544, 564
Phalanges, **108**, 520, 526, 593, 595
Phallus, **74**
Pharyngeal arches, *xxvii*, **80**, 214, 220–222, 236, 294, 296, 308, 320, 324, 348, 378
  mandibular (I), 220, 310, 344, 346, 350, 366
  maxillary (I), 330, 346, 348, 350, 366, 420, 498
  hyoid (II), 220, 308, 348, 350, 366, 382
  pouches, **80**, 294, 296, 310, 366, 420
Pharynx, **80**, 258, 264, 272, 318, 346, 456, 492
Pigmentation, **121**
Pineal gland/organ, **92**, **93**, 346, 356, 382, 426, 496
Pituitary gland, **123**, 504
  control of egg laying, **3**
Pitx2gene, **50**, **55**
Placodes, *xxvii*
  ectodermal, **95**
  lens. *See* Lens
  nasal, olfactory. *See* Nasal
  otic. *See* Otic
Pleural cavity. *See* Coelom
Pleuro-pericardial membrane/septum, 464
Pleuro-peritoneal membrane/septum, 468, 470, 476
Pneumo-enteric recess, 364, 468
Polarity and bilaterality, *xxvii*, **17**, **45**, **49**
Polarizing zone, *xxvii*, **108**
Polyinvaginated cells, **19**
Positional information (PI), *xxvii*
Posterior necrotic zone (PNZ),
Post-hepatic septum, 376, 424
Posterior abdominal coelom. *See* Coelom
Posterior cardinal vein. *See* Veins
Posterior intestinal portal, *xxviii*, 296, 336
Posterior marginal zone, xxviii, **18**, **23**
Precardiac mesoderm, **116**, 252
Pre-chordal plate/mesoderm, **116**, 252
Premaxilla, 598
Premuscle (muscle) mass, **115**, 394, 396, 408, 412, 422, 424
Prenasal plate, 504
Pronephros, **67**, **68**
Prevertebra, 354
Primary and secondary neural tube. *See* Neurulation
Primitive groove, 148, 152, 158
Primitive streak, *xxviii*, **18**, **22–25**, **30**, 148, 152, 154, 158, 256, 268
Primordial germ cells, *xxviii*, **21**, **72–75**
Pro-amnion, 158
Proctodaeal plate/membrane, **85**
Proepicardial serosa, *xxviii*, **54**
Pronephros (pronephric kidney), *xxviii*, **67**
Prosencephalon (diencephalon, telencephalon), **91**, 262, 264, 266, 276, 330, 340. *See also* Forebrain.
Proventriculus, **78**, **82**, 444, 470, 476, 478, 538, 540, 546, 572
Pubis, **106**, 482, 544, 546, 580, 582
Pulmonary fold, 386, 560
Pygostyle, 504
Pyloric sphincter, 71, 73

Q
Quail, **8**, 623

R
Radius, **107**, 444, 526, 534, 566, 592
Rathke's pouch, **45**, **123**, **124**, 292, 294, 308, 322, 330, 356, 418
Rectum, 412, 482, 484, 542, 579
Regression, *xxviii*, **31**, **32**
Regulation, *xxviii*
Reproductive tract of hen, 2, 3
Resegmentation, 92
Respiratory tract, 78
Retina, **99**, 330, 344, 350, 366, 382, 450, 490
Retinoic acid/retinoids, **19**
Rhombencephalon, **92**, **91**
Rhombocoele (lumen of rhombencephalon), 426
Rib (Costa), **104–106**
  capitulum, 526
  cervical, 462, 516
  sterna, 444, 468, 470, 538, 595
  thoracic, 462, 592, 595
  vertebral, 468
Rotation of gut, **84**

S
Saccule, **101**
Saline used in experiments, **9**
Scales, **120**
Scapula, **106**, **107**, 422, 434, 462, 464, 508, 520, 534, 538, 566, 593, 595
Schwann cells, **42**
Sciatic foramen, 592, 594
Sclera, **99**, 390, 430, 436, 516
Scleral ossicles, **112**, 486, 595
Scleraxis, 91, 101
Sclerotome, *xxviii*, **39**, **104**, 168, 302, 306, 316
Segmental plate mesoderm, *xxviii*, **37**, **38**, 172, 256, 262, 274, 294
Segmentation of somites, *xxviii*, **38**, **39**
Semi-circular canals, **100**, 390, 418, 426, 448, 454, 512
Semi-lunar valves, 464, 570
Septum transversum, 352, 386
Serial sections, *xxix*
Sero-amniotic connection, *xxix*
Sertoli cells, **72**
Sex cords, **72**
Sex ducts, **73**
Shell, **1**, **5**
Shell gland, **2**, **3**
Shell-less culture, **11**
Shell membranes, **1**, **3**, 134
Sinu-atrial
  canal/openings, 538
  valve, 384, 400

Sinus terminalis, **59**
Sinus venosus. *See* Veins
Skeleton, **105**
Skin, **117**, 426
Slug gene, **40**
Somatic cells, *xxix*
Somatopleure, *xxix*
Somites, *xxix*, **32**, **33**, **36**, **38**, **39**, **111**, 160, 172, 174, 176, 216, 256, 294, 296
Somitocoele (lumen in somite), 264, 280
Somitomeres, *xxix*
Sonic hedgehog, **29**, **35**, **36**, **40**, **48**, **50**, **74**, **78**, **80**, **93**, **103**
Sox, **34**, **36**
Specification, *xxix*
Spemann, Hans, xxix
Spermatozoa, **15**, **16**
Sphenoid bone, **96**
Splanchnic mesoderm, 164, 266
Splanchnopleure, *xxix*, 302
Spinal cord, **93**, 366, 374, 392, 424, 428, 498, 500, 514, 526
Spleen, **82**, 428, 444, 504, 542
Squamosal bone, 591, 593
Staging of development, **8**
Sternum, **106**, 444, 462, 464, 498, 500, 520, 562, 572
Stomach, **82**, 352, 360, 368. *See also* proventriculus and gizzard
Stomatodaeum/Stomatodaeal plate, *xxix*, **79**, 258, 266, 270
Sub-blastodermal fluid, **4**
Sub blastodermal (germinal) cavity, *xxix*, 140, 142
Sub-cephalic pocket, 270
Sulcus parencephalicus transverses, 426
Symmetry. *See also* Polarity and bilaterality
Sympathetic nerves/ganglia, **96**, 412, 468, 520, 526, 576
Synsacrum, **103**, **105**, 444
Syrinx, 464, 526, 530, 558, 562

T
Tail, **31–33**, 344, 412, 444
  bud, *xxix*, 162, 192, 274
  fold, **45**, **79**, 346
  gut, *xxix*, **85**
  mesoderm, 296, 304
  muscles, 484
Talpid mutant, *xxix*, **108**, 188
Tarsus and metatarsus, 108
Tectal process, 514
Tectum, 512
Telencephalon/telencephalic vesicles, **93**, 332, 352, 382, 446
Telocoele (lumen of telencephalon) lateral ventricle), 314, 31, 402, 404, 418, 420, 426, 448, 496
Temperature of incubation, **7**
Tendons, 113
Testis, **72**
TGFβ (transforming growth factor), **37**, **108**
Thalamus. *See* Diencephalon
Third ventricle, 446. *See also* diocoele
Thymus, **81**, 462, 516, 520, 526, 530, 548, 550, 562
Thyroglossal duct, **81**, **124**, 390
Thyroid, **124**, 328, 350, 502, 520, 526, 530, 556
Tibiotarsus, **108**, 438, 478, 480, 482, 538, 542, 593, 595
Toes, 444
Tongue, **80**, **115**, 420, 426, 432, 456, 488, 498, 506
Trachea, 350, 358, 390, 392, 444, 456, 592
Tubo-tympanic recess, **81**, 160
Tuberculum impar, **80**
Turkeys, **623**
Twinning/twinned axes, **17**, 136
Tympanic membrane, **100**, **101**, 452, 494, 512, 514

U
Ulna, **107**, 444, 464, 468, 520, 526, 566, 593
Ulna carpal, 464, 520, 534, 568
Ultimo-branchial bodies, **81**
Umbilical cord, 404, 542, 578
Uncinate process, **105**, 591
Ureter. *See* Metanephric duct
Ureteric bud, **68**
Urinogenital (urogenital) ridge, xxii. *See* Nephrogenic ridge
Urinary system, **67**
Uropygial gland, **121**
Utricle, 500, 508, 512

V
Vagina, **2**
Valvulae venosae, **57**
Veins
  allantoic (umbilical), **63**, 368, 386, 412, 498, 538
  anastomotic, 418, 456
  anterior cardinals, 196, 278, 280, 292, 294, 314, 330, 352, 358, 422
  anterior metanephric portal, 226
  coccygeal, **64**
  coccygeo-mesenteric, *544*
  common cardinal, **62**, **63**, 278, 286
  cranial (anterior) vena cava, **62**, **63**, 394, 464, 520, 524, 526, 534
  caudal (posterior) vena cava, **62–64**, 542
  ductus venosus, **62**, **63**, 352, 372, 386, 402
  emissaria, 448
  facial, 456
  gastropancreaticduodenal, 542
  head veins (vena capitis), **63**, 276, 320, 344, 366, 514, 530
  hepatic portal, **62**, 410, 424
  hepatic, 412, 444, 470, 476, 538
  iliac, **64**, 226, 542
  interiliac anastomosis, 484
  inter-jugular anastomosis, **63**, 514, 532. *See* anastomotic vein
  jugular, 394, 396, 418, 420, 430, 432, 456, 462, 502, 516, 526, 532
  mesonephric (renal portal), **62**, 544
  occipital, 456, 514
  omphalo-mesenteric (vitelline), **59**, **62**, **63**, **87**, 138, 284, 316, 352, 498, 585
  ophthalmic, 382, 450
  parabronchial, 244
  pectoral, 534
  posterior cardinals, **64**, 224, 334, 346
  posterior mesonephric portal, 224, 226
  posterior (caudal) vena cava, **64**, 174, 294, 336, 346, 358, 412, 444, 470, 498
  pulmonary, **63**, 536, 566
  renal, **64**, 444, 480, 482, 542
  renal portal, 542, 544, 580
  sciatic, **64**
  segmental, 174
  sinus terminalis, **127**, 284, 368
  sinus venosus, **54**, 204, 296, 350, 372, 384, 398, 468, 538
  subcardinals, **62–64**, **69**, 226, 412, 428, 470
  subclavians, **62**, **64**, 228, 374, 464, 530, 532
  subintestinal, 338
  umbilical. *See* allantoic
VEGFR (vascular endothelial growth factor), **51**
Ventricle (heart), 162, 210, 214, 272, 314, 320, 358, 372, 468, 470
Ventricle (cerebral hemisphere), 498
Vertebrae
  arch, 478, 504, 520. *See also* neural arch
  atlas, 390, 494, 496, 504, 506
  axis, 494, 506, 514
  body of vertebra, 366, 422, 428, 454, 502
  caudal, 500, 504, 544, 546, 595
  cervical, 426, 444, 454, 462, 498, 504, 514, 546
  dispophysis, 464
  number, **103**
  odontoid process, 350, 454, 494, 512
  pygostyle, 595
  sacral/synsacral, 500, 504, 544
  spinous process, *538*
  thoracic, 500, 526
  transverse process, 396, 408, 424, 428, 434, 450, 502
  vertebrarterial canal, 574
  zygapophysis, 454

Vertebral column, **104**, **105**
Vg, *121*
Vitelline membrane (perivitelline layer), **1**, **2**, **49**, 134, 142
Vitreous chamber of eye, **98**, 390, 448, 460, 494
Vitreous humour, **100**, 382, 490, 492, 498
Von Baer, *xxx*
Von Ebner's fissure, **40**, **104**

W
Waddington, CH, *xxx*
Wattle, **121**
White Leghorns, **121**
Wing bud(s), **47**, **48**, 190, 220, 342, 346, 428, 444, 470
Wing skeleton, **107**, **108**
Wnt, **31**, **40**, **48**, **78**, **121**
Wolff, Caspar Friedrich, *xxx*
Wolffian ducts, *xxx*, **73**. *See* nephric ducts

X
Xenoplastic grafting, *xxx*

Y
Yolk, **1**, **5**, **6**
Yolk sac, *xxx*, **58**, **127**, 276, 288
Yolk sac stalk, **78**, **84**, 482, 542

Z
ZPA (zone of polarising activity), *xxx*, **48**